AVS Quantum Science Workshop and Panel on Quantum Industry & Workforce Development
Room 123 - Session AQS-SuA

AVS Quantum Science (AQS) Workshop and Panel on Quantum Industry & Workforce Development (INVITED SESSION)

Moderators: Charles R. Eddy, Jr., Office of Naval Research Global - London, **Dave Pappas**, Rigetti Computing, **Andre Schleife**, University of Illinois at Urbana-Champaign, **Sean Jones**, Argonne National Laboratory

3:30pm **AQS-SuA-3 Review of AVS Educational Outreach Activities in the Context of an Evolving Quantum Industry and its Related Workforce Development Needs**, *Timothy Gessert*, AVS Education Committee Chair
INVITED

The AVS has provided various types of education opportunities to its members and others since the mid 1960's. One important component of these activities has been public and private short courses on topics consistent with the needs of various high-technology sectors. Indeed, for many technologists, engineers, and scientists now working in these high-tech industries, their initial exposure to areas such as basic vacuum technology, vacuum-process development, and characterization, often began with an AVS short course. In the mid 1980's, AVS education outreach expanded to include training high-school teachers through the *AVS Science Educators Workshop* (SEW). Through this activity, many hundreds of high-school teachers throughout the U.S. have now received not only basic vacuum training, but also a working vacuum system designed for the needs of a high-school classroom. In addition to the SEW helping these teachers convey the extensive uses of vacuum processes in many industries, another goal of the SEW has always been to possibly help "spark" student interest in considering post-secondary education (i.e., college), and possibly even toward an STEM career involving vacuum technology. Recently, and encouraged by the realities of COVID, many AVS education outreach activities now also include the option for virtual training, including virtual short courses, webinars, and You-Tube videos that can often align better with changing workplace and workforce needs. Additionally, in partnership with the American Institute of Physics (AIP), the AVS is now actively exploring how to better provide this type of education outreach to communities that have been historically underrepresented in the high-technology sectors.

In this presentation, the ~60 years of AVS experience with educational outreach will be briefly reviewed, emphasizing how these ongoing activities and experiences might be leveraged to benefit the workforce needs of a rapidly evolving Quantum Industry. It will also be discussed how, while the workforce of the Quantum Industry will certainly require many skilled individuals with advanced academic degrees, (and similar to the needs of the existing semiconductor industry) the workforce of the new Quantum Industry will also require many individuals with hands-on technology skills in areas such as process development/optimization and equipment operation/maintenance. Because of the long-term AVS experience with training involving all these different workforce sectors, it is believed that much of the established AVS education outreach activities can significant benefit the evolving Quantum Industry.

4:00pm **AQS-SuA-5 Broadening Participation in Quantum Information Science and Engineering as a Generator of Qualified Workforce**, *Tomasz Durakiewicz*, National Science Foundation
INVITED

The highly specialized area of Quantum Information Science and Engineering (QISE) is composed of several convergent disciplinary areas from computer sciences to materials sciences, chemistry, engineering, mathematics and physics. The ongoing explosion of interest in QISE includes new industrial opportunities and preparing for future markets, but also involves a heavy component of fundamental research characteristic to our early and evolving ability to translate QISE discoveries into practical solutions. Within this landscape, the government, industrial partners, academics and educators together express the need for qualified workforce generation. I propose that novel approaches to broadening participation in QISE, including special attention to diversity and inclusion, offer a solution to insufficient workforce while also providing direct benefit to taxpayer by expanding the STEM research and education base across the nation. This point will be illustrated using examples of actual need and corresponding programs, with identification of gaps and areas of future focus.

4:45pm **AQS-SuA-8 The Quantum Industry: Status and Gaps**, *Jonathan Felbinger*, SRI
INVITED

This talk presents a snapshot of the quantum industry: economic trends, perspective on near-term use cases for quantum technologies, the importance of benchmarking quantum solutions, and the need for a diverse workforce. The mission of the Quantum Economic Development Consortium (QED-C®) is to grow the quantum economy via community-building, collaboration, and commercialization. QED-C's approximately 250 member organizations enable the real-world application of quantum technology and, in turn, grow a robust commercial industry and supply chain. QED-C is managed by SRI, an independent nonprofit research institute.

5:15pm **AQS-SuA-10 Alternating Bias Assisted Annealing of Amorphous Oxide Tunnel Junctions**, *Josh Mutus*, Rigetti Computing, Canada*; Dave Pappas, Mark Field, Cameron Kopas*, Rigetti Computing*; Lin Zhou*, Ames Laboratory*; Xiqiao Wang*, Rigetti Computing*; Jinsu Oh*, Ames Laboratory
INVITED

We demonstrated a novel method for tuning the tunnel barrier of a Joshephson junction by applying a series of alternating bias pulses. While this process allows for significant tuning at room temperature, the rate of resistance change increases with temperature, at 80C we achieve a resistance change of over 70%. The technique was also applied to transmon qubit junctions. The results align with the Ambegaokar-Baratoff relation, indicating a correlation between shifted resistance and critical current. Moreover, the treated junctions exhibited reduced losses and fewer defects compared to untreated samples. Observation through high-resolution TEM imaging, showed a more uniform distribution of aluminum coordination across the barrier. This innovation is anticipated to have broad applications in devices using amorphous aluminum oxide and similar metal-insulator-metal structures in modern electronics.

5:45pm **AQS-SuA-12 Progress Towards Merged-Element Transmons with Si Fins – the Si FinMet**, *Chris Palmstrøm*, University of California, Santa Barbara
INVITED

A merged-element transmon (MET) device combines the capacitor and the Josephson Junction in a superconducting transmon qubit into a single device, which can reduce the size of a qubit by several orders of magnitude[1,2]. We have utilized anisotropic etching of Si(111) relative to Si(110) to define atomically flat, high aspect ratio Si tunnel barriers with superconductor contacts on the parallel side-wall surfaces. By utilizing low-loss, intrinsic float-zone single crystal Si as the barrier material rather than commonly used, amorphous Al_2O_3, the Si FinMET is expected to overcome problems with standard transmons by (1) reducing dielectric losses; (2) minimizing the formation of two-level system spectral features; (3) potentially exhibiting greater control over barrier thickness and qubit frequency spread, (4) reducing the footprint, and (5) allowing scalable fabrication.

We havefabricated and demonstrated low loss Si fin capacitors on Si(110) substrates with shadow-deposited Al electrodes[3]. Lumped element resonators using ~300nm thick fin capacitors have Qi >5×10^5 at low power at 30mK. By adding a Josephson Junction in parallel, transmon devices have been fabricated with T1 times ~20 μs. Recent efforts have been made to make fins thin enough to exhibit tunneling. Preliminary tunneling measurement yield I_cR_n values ~900μV. These results indicate great progress towards the development of Si FinMet devices.

In this presentation, the process and progress in developing a Si fin based merged element transmon – the FinMET, will be discussed.

1R. Zhao, et al., Phys. Rev. Appl. **14**, 064006 (2020).

2H. J. Mamin, et al., Phys. Rev. Appl. **16**, 024023 (2021).

3A. Goswami, et al., Applied Physics Letters **121**, 064001 (2022).

This work has been done in collaboration with T.A.J. van Schijndel, J. K. Nangoi, W. Yánez-Parreño, J.T. Dong, and C. G. Van de Walle at UCSB, A. Goswami at MIT, and A.P. McFadden and R. Simmonds at NIST. The work was supported by ARO W911NF2210052 and UCSB NSF Quantum Foundry funded via the Q-AMASE-i program under award DMR-1906325

Sunday Afternoon, November 3, 2024

Biomaterials Plenary

Room 117 - Session BP-SuA

Biomaterials Plenary Session (INVITED SESSION)

Moderators: Kenan Fears, U.S. Naval Research Laboratory, **Christopher So**, Naval Research Laboratory

4:15pm **BP-SuA-6 Biomimetic Chemistry from Sea Creatures for Making Sustainable Adhesives**, *Jonathan Wilker,* Purdue University   **INVITED**
Adhesives are wonderful materials, holding together our electronics, furniture, and packaging. However, most of these glues are petroleum-based, do not degrade, and prevent substrate separation, thereby meaning that most consumer products end up in landfills for centuries. These glues and the materials held together contribute to land-based and ocean microplastics. Given the amount of adhesive use, impact in the marketplace will arrive only when alternative adhesives are high performance, low cost, easy to make, and the components are already available at large scales. In order to begin down this path of adhesive sustainability, we have turned to sea creatures for design cues. Mussels, barnacles, and oysters all bond to rocks using chemistry not found in commercial glues. Characterization insights on biological materials have provided a starting point for adhesive design. Here we report new materials based upon epoxidized soy oil. Cross-linking with bio-based, multifunctional alcohols and acids was examined. Plant-based compounds such as malic acid reacted with the soy oil. However, catechol-like chemistry, found in marine mussel glue, was required to bring about the extreme degree of cross-linking needed for curing into viable adhesives. In the best of cases, bond strengths could be of quite high strength, similar to epoxies. Spectroscopic characterization showed that all components, including tannic acid, cross-linked with each other, although some reactions were more prominent than others. Water resistance studies showed a middle ground of being able to withstand being submerged for a short period of time while enabling debonding at later time points. Bulk scale costs worked out to be a modest ~1/3 premium over incumbent materials. Preliminary calculations indicate that, considering sourcing, manufacturing, and curing, this new adhesive system is, overall, carbon negative. By making new adhesives from bio-based components and demonstrating high bonding performance we hope that, soon, several environmental problems may be solvable.

4:45pm **BP-SuA-8 Interfacial Bonding in Underwater Adhesion**, *Joelle Frechette,* UC Berkeley   **INVITED**
Underwater environments are particularly challenging for adhesives, as water weakens the interfacial bonds that underlying adhesion. A promising strategy for improving underwater adhesion is the incorporation of multidentate Hydrogen bonding groups. However, it remains challenging to quantitatively relate the macroscale adhesive strength to cooperative hydrogen-bonding interactions at the interface, limiting our understanding of the bonding mechanisms. This presentation will discuss efforts to understand how the presence of multidentate hydrogen bonding groups leads to strong underwater adhesion. To do so we show a relationship between the bond activation energy to the macroscale adhesive strength and how this relationship can be employed in self-arresting crack measurements. We will also report on measurements using the Surface Forces Apparatus to show that epoxies modified with tridentate hydrogen bonding groups exhibit robust adhesion to both mica and ultra-smooth aluminum substrates in water. These results inform our understanding of how molecular debonding mechanisms impact macroscale adhesion, aiding our ability to connect adhesive chemistry to performance.

Nanoscale Science and Technology Plenary Session (INVITED SESSION)

Room 114 - Session NSP-SuP

Nanoscale Science and Technology Plenary Session (INVITED SESSION)

Moderator: Nikolai Klimov, NIST

3:00pm **NSP-SuP-1 NSTD Nanotechnology Recognition Award Talk: The Energy Challenge from a Materials Perspective**, *Federico Rosei*[1], Institut National de la Recherche Scientifique, Centre Énergie, Matériaux et Télécommunications, Canada   **INVITED**
Sustainability is the overarching challenge of modern times. In this context, replacing fossil fuels with renewables is urgent and critical. This presentation focuses on next generation (solar) energy technologies from a materials perspective. We study structure property/relationships in advanced materials, emphasizing multifunctional systems that exhibit several functionalities. Such systems are then used as building blocks for the fabrication of various emerging technologies. In particular, nanostructured materials synthesized via the bottom–up approach present an opportunity for future generation low cost and low energy intensive manufacturing of devices. We focus in particular on recent developments in solar technologies, including third generation photovoltaics, solar hydrogen production, luminescent solar concentrators and other optoelectronic devices. [1-20].

References

[1] Appl. Cat. B 264, 118526 (2020); [2] Adv. Func. Mater. 30, 1908467 (2020); [3] J. Mater. Chem. A 8, 20698 (2020); [4] Nano Energy 79, 105416 (2021); [5] Nano Energy 81, 105626 (2021); [6] Small Meth. 8, 2300133 (2024); [7] ACS Appl. Mater. Int. 15, 56413 (2023); [8] J. Mater. Chem. A 11, 23821 (2023); Chem. Eng. J. 474, 145830 (2023); [9] ACS Appl. Mater. Int. 15, 34797 (2023); [10] Nano Energy 111, 108438 (2023); [11] Small 19, 2300606 (2023); [12] ACS Appl. Mat. Int. 14, 54790 (2022); [13] Nano Energy 100, 107524 (2022); [14] Chem. Eng. J. 446, 137312 (2022); [15] Small 18, 2201815 (2022); [16] Small Meth. 6, 2101470 (2022); [17] Chem. Eng. J. 435, 135037 (2022); [18] Chem. Eng. J. 429, 132425 (2022); [19] Small 20 [https://onlinelibrary.wiley.com/toc/16136829/2024/20/22], 2306203 (2024); [20] J. Mater. Chem. A 12, 11644 (2024).

---

[1] NSTD Nanotechnology Recognition Award

Atomic Scale Processing Mini-Symposium
Room 116 - Session AP+EM+PS+TF-MoM

Area Selective Deposition (ASD) I

Moderators: Eric Joseph, IBM T.J. Watson Research Center, **Adrie Mackus**, Eindhoven University, Netherlands

8:15am **AP+EM+PS+TF-MoM-1 Unlocking the Atomic Canvas: Applications and Challenges of Area Selective Deposition in Next-Generation Memory Devices**, *Ebony Mays,* Micron Technology   **INVITED**

The semiconductor industry is on the cusp of an AI-driven revolution, propelling scaling and density trends for integrated circuit devices. As we delve deeper into a 3D transformation in circuit architecture, we are driven to find solutions to memory and storage bottlenecks and capacity demands. This necessity is fueling a new wave of architectural, material, and process technology innovations that meet power, performance, and cost demands. The push to control material deposition and removal at the atomic scale over extremely high aspect ratios is more critical than ever. In this context, area selective deposition (ASD) emerges as a powerful tool to meet these evolving challenges. With the application of new materials at higher aspect ratios, we must continue to expand our toolbox with new precursor and deposition technologies for ASD. This talk will address some of the ensuing challenges and hurdles for the use of ASD in manufacturing applications for memory devices. It will also highlight opportunities for innovation and collaboration in these areas, emphasizing the need for future technology innovation. The future of the semiconductor industry hinges on our ability to innovate and collaborate in these critical areas.

8:45am **AP+EM+PS+TF-MoM-3 Area-Selective Atomic Layer Deposition by Sputter Yield Amplification**, *Arthur de Jong, Manosch Bär, Marc Merkx, Erwin Kessels, Adrie Mackus,* Eindhoven University of Technology, Netherlands

Area-selective deposition (ASD) is an emerging technique in device fabrication that can bypass lithography-based fabrication of certain layers in a device stack that require perfect alignment. The distinction between growth and non-growth areas is commonly attained through chemical differences, such as selective precursor or inhibitor adsorption [1]. To expand the ASD toolbox, this study explores a physical approach that integrates (non-selective) atomic layer deposition (ALD) with area-selective sputter etching by ions of the undesired material deposited on the non-growth area. Sputter yield amplification occurs if a non-growth area contains an element with significantly larger mass than the incoming ion [2]. When an ion collides with such atom, the momentum is more effectively redirected upward compared to a collision with a lighter atom. This enhanced redirection augments the energy transfer to the deposited material on the non-growth area, thereby increasing the likelihood of etching. Conversely, the growth area should lack heavy elements, resulting in a considerably lower etch rate of the film that is deposited on top.

Selective sputter etching was investigated for SiO_2 and TiN films. On various substrates, a thin SiO_2 overlayer deposited by ALD was exposed to low-energy Ar ions (33-50 eV). The amount of SiO_2 removed depends significantly on the substrate (Al_2O_3, TiO_2, Nb_2O_5, MoO_3, HfO_2, Ta_2O_5, and WO_3 were investigated here). In general, the heavier the mass of the metal atoms in the substrate, the less SiO_2 is observed after the ion exposure. TiN was selectively deposited on Al_2O_3 with respect to a HfO_2 non-growth area by repeating supercycles of six TiN ALD cycles and Ar ion exposure from a plasma. Approximately 7.0 nm of selective growth is achieved on Al_2O_3 with only 0.15 nm on HfO_2 (giving 96% selectivity). The key benefit of (selective) sputter etching lies in its relative insensitivity to temperature and ALD chemistry. This proof-of-concept shows that exploiting sputter yield amplification can enable ASD processes that are complementary to the existing chemical approaches.

[1] A. J. M. Mackus et al., Chemistry of Materials 31, 2 (2019).

[2] S. Berg et al., Journal of Vacuum Science & Technology A: Vacuum, Surfaces, and Films 10, 1592 (1992).

9:00am **AP+EM+PS+TF-MoM-4 Effectiveness of SiO₂ Functionalization with Methyl versus Silyl Groups to Enable Area-Selective Atomic Layer Deposition of Al₂O₃**, *Andrew Kaye,* Colorado School of Mines; *Sumit Agarwal,* Colorado School of Mines, USA; *Haripin Chandra, Ronald Pearlstein, Xinjian Lei, Agnes Derecskei,* EMD Electronics, USA; *Bhushan Zope,* Intermolecular, Inc.

Plasma-deposited SiO_2 films are extensively used in semiconductor manufacturing. Area-selective atomic layer deposition (AS-ALD) of a dielectric, such as Al_2O_3, on a target surface with SiO_2 as a non-growth surface, can simplify device processing. Gas-phase functionalization of SiO_2 using aminosilanes as small molecule inhibitors has been previously reported. Most studies show that growth nucleation during ALD occurs on the functionalized SiO_2 surface after just a few nanometers of deposition on the growth surface. It is speculated that nucleation on the SiO_2 surface occurs due to the availability of unreacted surface –SiOH groups. We tested this hypothesis by functionalizing the SiO_2 surfaces with different densities of surface –SiOH groups with two aminosilanes that offer a different degree of steric hindrance. Specifically, we functionalized of the plasma-deposited SiO_2 surface with N,N-dimethylaminotrimethylsilane (DMATMS) and di-sec-butylaminosilane (DSBAS). *In situ* infrared spectroscopy shows that DMATMS and DSBAS react with isolated surface –SiOH groups resulting in –$Si(CH_3)_3$ and –SiH_3 terminated surfaces, respectively. Due to steric hindrance from the bulky di-sec-butylamino ligand, ~50% of the surface –SiOH groups remained unreacted after functionalization of the as-deposited SiO_2 surface: these –SiOH groups became available for reaction with dimethylaluminum isopropoxide (DMAI) during Al_2O_3 ALD. In contrast, *in situ* 4-wavelength ellipsometry shows that functionalization of the as-deposited SiO_2 surface with DMATMS resulted in a nucleation delay of ~20 ALD cycles due to the much higher surface ligand coverage, which we attribute to a much smaller reactive leaving group. Next, we pre-annealed the as-deposited SiO_2 films at 500 °C, which lowered the surface –SiOH density by ~72%. After annealing, both inhibitors had nearly equal surface coverage, and reacted with most of the available surface –SiOH groups. However, surface functionalization with DMATMS still provided a nucleation delay of ~20 ALD cycles, while DSBAS did not provide any nucleation delay. On the pre-annealed surface, both DMAI and H_2O did not react with surface –SiH_3 or –$Si(CH_3)_3$ groups. Instead, we show that DMAI can strongly absorb onto surface Si–O–Si sites to initiate film growth. Since DMATMS provides a higher degree of steric blocking due to the bulkier –$Si(CH_3)_3$ ligand, there is a still a nucleation delay on the pre-annealed SiO_2 surface even though the surface density of the ligands is much lower compared to the as-deposited surface.

9:15am **AP+EM+PS+TF-MoM-5 Progress Towards a New Class of Area Selective Deposition Using Photoassisted Chemical Vapor Deposition on Thermally Sensitive Substrates**, *Bishwa Das, Rashmi Rashmi,* University of Florida; *Bryan Salazar, Christopher Brewer,* University of Texas at Dallas; *Lisa McElwee-White,* University of Florida; *Amy Walker,* University of Texas at Dallas

Area selective deposition (ASD) has been successfully realized in microelectronics using high-temperature processes, but continued performance and scaling, new materials, and future device fabrication schemes require new low-temperature (<400 °C) ASD methods for metals, dielectrics and other films. In this talk we describe progress towards a new low (near room) temperature ASD method in which reactive functionalized self-assembled monolayers direct Ru film deposition using novel photoassisted chemical vapor deposition (PACVD) processes. The ideal precursor for photoassisted low temperature CVD is a volatile complex with a high quantum yield for ligand loss, which provides an empty coordination site for surface attachment. The surface-bound primary photoproduct then undergoes facile decomposition to the target material and for ASD selectively reacts with the functionalized SAM terminal groups. Our initial proof-of-concept studies employed (η^3-allyl)Ru(CO)$_3$X (X = Cl, Br, I) precursors. Three SAMs were employed with –CH_3, –OH or –COOH terminal groups. Under UV light using (η^3-allyl)Ru(CO)$_3$Br we showed that Ru(0) and RuO_x selectively deposits on –CH_3 and –OH terminated SAMs but not on –COOH terminated SAMs. We attribute this behavior to the formation of Ru-carboxylate complexes which block deposition. We further show that using (η^3-allyl)Ru(CO)$_3$X (X = Cl, I) precursors only lead to molecular deposition and DFT calculations indicate that this is not due to the primary photoprocess but the energy required to lose a second carbonyl. Most recently we have studied a series of (η^4-diene)Ru(CO)$_3$ (diene = butadiene, isoprene, 1,3-cyclohexadiene or cyclobutadiene) to further investigate the role of polyhapto carbon ligands and the metal oxidation state. We have already demonstrated that these complexes undergo photochemical loss of CO and/or the diene and that exhaustive photolysis of the complexes in solution leads to the formation of colloidal Ru. In agreement with our observations using (η^3-allyl)Ru(CO)$_3$Br we show that the primary photoprocess and the metal oxidation state are not the most important reaction variable for Ru metal deposition but rather the energy required to lose further ligands. Further we show that Ru selectively deposits on –COOH terminated SAMs and not on –CH_3 and –OH terminated SAMs.

9:30am AP+EM+PS+TF-MoM-6 Atomic and Molecular Monolayers on Silicon as Resists for Area-Selective Deposition, *Andrew Teplyakov*, University of Delaware

As the size of the components in electronic devices decreases, new approaches and chemical modification schemes are needed to produce nanometer-size features with bottom-up manufacturing. Atomic and molecular layers can be used as effective resists to block the growth of materials on non-growth substrates in area-selective deposition methods. However, in order for these monolayers to be useful, it is imperative to know the initial structure and reactivity of these modified surfaces and also to understand what happens when the selectivity is lost. This talk will summarize recent developments in our search for effective resists based on chlorination and bromination of silicon surfaces performed by solution and gas-phase modification methods and preparation of organic monolayers starting with these surfaces. The structure, stability, and reactivity of the modified surfaces will be evaluated with spectroscopic and microscopic techniques, and their performance as potential resists in ALD of titanium dioxide will be discussed. The TiO_2 deposition is performed using thermal ALD with tetrakisdimethylamidotitanium (TDMAT) or $TiCl_4$ as the source of titanium and water as the co-reactant. The selectivity of the process will be compared to that of unmodified (oxidized) silicon surfaces (prototypical growth surface) and of the H-covered silicon surfaces (prototypical non-growth surface).

9:45am AP+EM+PS+TF-MoM-7 Selective Deposition of Low k SiCOH and Surface Sialylation Repair of Low K Dielectrics for Nano Cu Interconnects, *Son Nguyen, H Shobha, A. Jog, Huai Huang, Brown Peethala, Juntao Li, James Demarest, Yiping Yao,* IBM Research Division, Albany, NY

In this paper, we demonstrate the integrated surface sialylation, low-k repair, and selective SiCOH deposition on 32 nm pitch Cu-SiCOH damascene structures to form a 5-6 nm raised SiCOH for the Fully Aligned Via (FAV) integration. Initially, the nominally damaged patterned SiCOH dielectric surface was repaired by UV sialylation process with carbonsiloxane to reduce the typical RIE patterning damage and cyclic selective deposition of Cobalt [4] by replenishing the surface carbon with UV/Thermal assisted carbonsilane precursor repair. The time-of-flight secondary ion mass spectrometry (ToF SIMS) analysis indicates nominal amount of carbon replenished on the SICOH surface (see Figure 2). This surface sialylation repair reduces the capacitance and significantly improves the TDDB as shown in Figure 1. FTIR analysis also indicates an increased Si-CH_3 bonding in SiCOH surface after sialylation suggesting the replenishment of carbon on the SiCOH surface. After the initial one cycle SiCOH surface sialylation repair with Carbo-Siloxane precursor, additional selective SiC(O) films were deposited using multi step cyclic deposition and treatment processing steps as illustrated in Figure 3. The average selective deposition/H2 plasma treatment steps per each cycle is about 6A. Electrical measurement on blanket MIS wafers yields a k = 4.1 ± 0.1 for the selective SiCO layer which is 1.8 times lower compared to selectively deposited of AlOx with k ~ 7.5 for FAV applications [2-3]. Figure 4 shows the various analyses for sialylation and SiC(O) selective deposition on SiCOH_Co capped Cu patterned surface. Clearly, sialylation repair penetrates to SiCOH and selective growth of 6 nm SiC(O) after cyclic processing steps. Figure 5 shows representative image of 32/36 nm pitch FAV structure fabricated after integrated sialylation and selective deposition of 4 nm SiC(O) with UV/Thermal Assisted Vapor Processing. Overall, the integrated Sialylation and selective provide a simpler the low k SiCOH dielectric repairs and selective dep of lower k SiC(O) dielectrics film for FAV and other planar surface applications in electronic device fabrication without the need of SAM that normally required in selective deposition.

REFERENCES

[1] B. D. Briggs et al., " IEDM Tech. Dig., Dec. 2017 pp. 338-341

[2] S. Van Nguyen et al., " Proc. IEEE Int. Interconnect Technol. Conf., paper S7-4, Jul. 2021 Kyoto, Japan.

[3] H.P. Chen, et al. , International Electron Device Meeting 2021, paper 22.1, San Francisco, CA, USA

[4] C.C.Yang, B. Li, H. Shobha, S. Nguyen, A. Grill, J. Aubuchon, M. Shek and D. Edelstein. IEEE Electron Device Letter, Vol 33, No, 4, pp.588-560 (2012).

* Figures 1-5 are in supplement

10:30am AP+EM+PS+TF-MoM-10 Selectivity Loss During Area-Selective Deposition Processes: The Role of Chemical Passivation and Steric Shielding, *Marc J. M. Merkx, Pengmei Yu, Ilker Tezsevin, Adriaan J. M. Mackus,* Eindhoven University of Technology, Dept. Applied Physics, Netherlands*; Tania E. Sandoval[1],* Universidad Técnica Federico Santa María, Dept. Chemical and Environmental Engineering, Chile **INVITED**

Area-selective deposition (ASD) processes have been an extensive area of research for the past few decades. Strategies to achieve selectivity include the use of self-assembled monolayers, inherent selectivity of precursor molecules, and most recently, the use of small molecule inhibitors (SMIs). All these different approaches require a fundamental understanding of the mechanism at every step of the process, and more importantly, what determines selectivity loss. In the case of SMIs, there are several challenges related to their vapor phase dosing to be overcome to improve selectivity, such as, reaching high packing, chemical passivation, and steric shielding.[1-2]

This study explores the connection between chemical passivation and steric shielding with selectivity loss using SMIs. Specifically, how the adsorption of the SMI acetylacetone influences the nucleation of trimethylaluminum (TMA), dimethylaluminum isopropoxide (DMAI), and tris(dimethylamino)aluminum (TDMAA) on the non-growth area through displacement reactions.

Through a combination of experimental and theoretical characterization, we found that the observed changes to the non-growth area during ASD are related to the reactivity of the precursor towards the inhibition layer. Infrared spectroscopy reveals that 23% of TMA adsorbs on the non-growth area after SMI adsorption, exceeding DMAI and TDMAA by more than an order of magnitude. Density functional theory calculations are used to explore the role of chemical passivation by calculating adsorption energies of SMI and precursor, as well as displacement energies. We found that differences in reactivity across precursors and SMI are an important metric to determine displacement.

In addition, we carried out molecular dynamics to characterize the role of steric shielding by looking at the inertness of the non-growth area after SMI adsorption, and the different pathways of the precursor to reach the surface. These results show that the adsorption configurations of acetylacetone provide different degrees of steric shielding, where the most weakly adduct promotes precursor adsorption.[3] Moreover, they also show how the small size of TMA is detrimental to blocking as it can easily reach the surface, while TDMAA is more hindered from adsorption. Overall, this study provides important insights into the mechanism for selectivity loss, and highlights the different contributions to precursor blocking, providing a thorough understanding of inhibition in ASD processes.

[1] J. Li, et al. J. Vac. Sci. Technol. A 40, 062409, 2022

[2] P. Yu, et al. Appl. Surf. Sci. J.apsusc.2024.160141, 2024

[3] M.J.M. Merkx, et al. Chem. Matter. 32, 3335-3345, 2020

11:00am AP+EM+PS+TF-MoM-12 Computational Screening of Small Molecule Inhibitor Candidates for Area-Selective Atomic Layer Deposition, *Joost Maas, Ilker Tezsevin, Pengmei Yu, Marc Merkx,* TU / Eindhoven, Netherlands*; Tania Sandoval,* Universidad Tecnica Federico Santa Maria, Chile*; Adriaan Mackus,* TU / Eindhoven, Netherlands

Area-selective atomic layer deposition using small molecule inhibitors (SMIs) represents a promising avenue to facilitate the downscaling of nanoelectronics. SMIs eliminate challenges such as alignment errors by enabling bottom-up selective growth using vapor-phase processing. Two main factors play a role in the viability of SMI candidates: (*i*) the inhibitor molecules must adsorb strongly and selectively on the non-growth area and (*ii*) these molecules must pack densely once adsorbed. In this contribution, these two factors are investigated using density functional theory (DFT) and random sequential adsorption (RSA) simulations respectively.[1] RSA simulations mimic the adsorption of molecules as they arrive one-by-one in gas-phase and are used to determine the chemical passivation (by means of coverage and surface density) and steric shielding (by means of the fraction of covered area) performance of the SMIs.[2] RSA is computationally lightweight and easily scalable.

A four tier simulation approach is followed to screen SMI candidates: (1) DFT on small clusters to determine whether adsorption is energetically favorable and to determine the adsorption configuration. The adsorption configuration is then used to create a 2D footprint of the molecule, such that it can be used in (2) initial RSA simulations of the candidate SMIs,

yielding the coverage and fraction of covered area. (3) Based on this initial screening, the most promising candidates are further tested using periodic DFT to improve the accuracy of our approximation, and (4) RSA is re-run using the updated geometry. By narrowing down the list of candidates within each step, time is spent more efficiently on more complex simulations. A list of 30+ candidates is screened for Al_2O_3, SiO_2, AlN, and Si_3N_4 using this method; surfaces chosen for their applications in semiconductor industry (AlN was included for a comparison between oxides and nitrides). The list of candidates is comprised of carboxylic acids and diketones, a selection inspired on the experimental performance of (among others) Hacac and acetic acid. Further divisions are made to investigate the effect of the carbon chain length (up to 5 for valeric acid), halides in the SMI, and reactive atoms (O/N/S). In line with simulation results, experimental results indicate that acetic acid performs well as an SMI, lending credence to the screening approach. Our analysis suggests that formic acid, acetamide, valeric acid, acetadiimidine, and imidodicarbonic diamide are promising candidates to be use as SMIs for ASD processes.

1. J. Li; et. al. *JVST A* **2022**, 40 (6), 062409
2. Mameli, A.; et. al. *ACS Nano* **2017**, 11 (9), 9303–9311.

11:15am AP+EM+PS+TF-MoM-13 Ordering of Small Molecule Inhibitors to Block Precursor Adsorption on Cu During Area-Selective Atomic Layer Deposition: A Computational Study, *Ilker Tezsevin, Joost F. W. Maas, Marc J. M. Merkx,* Eindhoven University of Technology, Netherlands*; Scott Semproni, Jiun-Ruey Chen,* Intel Corporation*; Tania E. Sandoval,* Universidad Técnica Federico Santa Mariá, Chile*; Adriaan J. M. Mackus,* Eindhoven University of Technology, Netherlands

Thanks to their industrial compatibility, small molecule inhibitors (SMIs) offer a promising route for achieving area-selective atomic layer deposition (ASALD) in semiconductor fabrication. Cu is widely used in integrated circuits as an interconnect material and is a target non-growth area for many ASD applications. This study explores the adsorption and packing of SMIs on the Cu surface to achieve ASALD considering Cu as the non-growth area.

SMIs are dosed in the vapor phase and arrive one-by-one on random surface sites. Therefore, SMIs typically cannot form a dense ordered layer, leaving some surface sites uncovered and available for precursor adsorption.[1,2] To promote the packing on the surface, an SMI favoring lateral interactions and surface mobility on the non-growth area is required such that a self-assembled monolayer (SAM)-like packing can be achieved. Our screening for effective SMIs using density functional theory (DFT) calculations led to the discovery of the great potential of pyridazine ($C_4H_4N_2$), which exhibits strong adsorption on Cu via its nitrogen atoms. Random sequential adsorption simulations[3] of pyridazine on Cu show that it can densely pack on the surface with a surface density of more than 2.4 molecules per nm^2 such that precursors with a radius larger than 0.3 nm cannot reach the surface. Furthermore, detailed DFT and molecular dynamics studies suggest that pyridazine molecules show ordering on the Cu surface. Due to its unique adsorption configuration, pyridazine molecules favor lateral interactions resulting in a SAM-like ordering. Additionally, the pyridazine adsorption configuration allows for diffusion or rotation of the inhibitor on Cu with an activation barrier of less than 0.22 eV, enabling denser packing on the surface. In summary, the pyridazine molecule exhibits exceptional adsorption energetics on the Cu surface promoting a densified inhibitor layer on the non-growth area. Hence the unique properties of pyridazine may bridge the gap between the industrial applicability of SMIs and the efficiency of SAMs, making it a promising candidate for ASALD applications targeting Cu non-growth areas.

(1) Merkx, M. J. M.; et. al. *Chem. Mater.* **2020**, *32* (18), 7788–7795.

(2) Tezsevin, I.; et. al. *Langmuir* **2023**, *39* (12), 4265–4273.

(3) Li, J.; et. al. *J. Vac. Sci. Technol. A* **2022**, *40* (6), 062409.

11:30am AP+EM+PS+TF-MoM-14 Revealing the Mechanisms for Loss of Selectivity in Area-Selective ALD Using in-Situ Infrared Spectroscopy, *Eric H. K. Wong, Marc J. M. Merkx, Joost F. W. Maas, Ilker Tezsevin, Wilhelmus M. M. Kessels,* Eindhoven University of Technology, The Netherlands*; Tania E. Sandoval,* Universidad Tecnica Federico Santa Maria, Chile*; Adriaan J. M. Mackus,* Eindhoven University of Technology, The Netherlands

To fulfil the needs for self-aligned fabrication in sub-5 nm technology nodes in nanoelectronics, much research efforts have been devoted to the development of area-selective atomic layer deposition (AS-ALD). The use of small-molecule inhibitors (SMIs) is considered to be an industrially-compatible option due to its vapor-phase dosing. Our previous works have provided mechanistic insights into the first cycle of AS-ALD of SiO_2 as a model system for understanding blocking by SMIs [1, 2]. However, the mechanisms for loss of selectivity in AS-ALD remain unexplored which is critical to improving the selectivity. In this work, we performed in-situ reflection-absorption infrared spectroscopy (RAIRS) measurements as a function of the number of cycles to reveal the mechanisms of the selectivity loss.

Twenty cycles of an ABDC-type process [3] comprising an acetylacetone (Hacac) inhibitor dose (step A), a bis(diethylamino)silane (BDEAS) precursor dose (step B), and subsequently two plasma (H_2 and O_2) exposure (steps D and C) were carried out on the non-growth area Al_2O_3. RAIRS spectra were taken after the steps A, B, and DC. We learned in previous work that the adsorption of Hacac on Al_2O_3 results in a mixture of chelate and monodentate adsorption configurations, with the chelate configuration being the effective form for precursor blocking [2]. Our results from the current study indicate that the precursor-blocking by the inhibitor layer decreases as a function of cycles. In addition, the mixture of inhibitor adsorption configuration changes to a higher chelate-to-monodentate ratio. DFT calculations indicate that the SiO_2 defects formed due to the partial loss of selectivity prevent the successful re-application of the inhibitor molecules in the subsequent cycles. In summary, our results suggest that the change of chemical character of the non-growth area due to the formation of defects escalates the loss of selectivity. Furthermore, this work demonstrates a general approach for inspecting the mechanisms for loss of selectivity that can be extended to other AS-ALD systems.

[1] A. Mameli *et al.*, *ACS Nano*. **11**, 9303–9311 (2017).

[2] M. J. M. Merkx *et al.*, *Chem. Mater.* **32**, 3335–3345 (2020).

[3] M. J. M. Merkx *et al.*, *Journal of Vacuum Science & Technology A*. **39**, 012402 (2020).

11:45am AP+EM+PS+TF-MoM-15 Use of Sulfide Inhibitors for Multi-Surface Passivation and Area Selective Deposition, *Summal Zoha, Bonwook Gu,* Incheon National University, Republic of Korea*; Fabian Pieck, Ralf Tonner Zeck,* Leipzig University, Germany*; Han-Bo-Ram Lee,* Incheon National University, Republic of Korea

In recent years, the area-selective atomic layer deposition (AS-ALD) process has excelled over conventional methods for precise and area-selective thin film deposition. This area selective deposition (ASD) method has displayed promising capability for 2D and 3D nanoscale patterning. With the help of inhibitor molecules capable of tailoring the surface properties, thin films can be deposited only on desired growth surfaces using AS-ALD without any unwanted growth on non-growth surfaces. In this regard, small molecule inhibitors (SMIs) have recently gained a lot of attention for their inhibiting capabilities despite having small sizes. The choice of surface inhibitor is crucial in determining the growth, non-growth surface, and the degree of surface passivation. In this study, three organosulfide inhibitors have been utilized for AS-ALD on metal, oxide, and nitride surfaces, Cu, SiO_2, and TiN, respectively. These inhibitors display selective adsorption on the Cu surface and in some cases on the SiO_2 surface, while the TiN surface remains unaffected by the inhibitors. The density functional theory (DFT) study revealed that the inhibitors are capable of decomposing to assist the adsorption of their constituents on the Cu and SiO_2 substrates, thereby simultaneously inhibiting two surfaces through a single inhibitor. A comparison between the organosulfide inhibitors was performed to comprehend blocking behavior. Blocking results of HfO_2 ALD revealed that the longer straight-chained organosulfide inhibitor was able to uphold better blocking properties than compared to the shorter and branched organosulfide inhibitor. This concept of multi-surface inhibition by a single inhibitor can be an essential approach for Si device fabrication where several surfaces are exposed under AS-ALD processes.

Biomaterial Interfaces
Room 117 - Session BI1-MoM

Biomolecules and Biophysics at Interfaces

Moderators: Christopher So, Naval Research Laboratory, **Markus Valtiner**, Vienna University of Technology, Austria

8:15am BI1-MoM-1 Molecular Modeling of Peptide and Protein-Based Materials: Role of Surface and Interface on Structure and Function, *Yaroslava Yingling,* North Carolina State University **INVITED**
Borrowing the structure and function of proteins to design novel multifunctional materials offers a potential solution for pressing technological needs and various applications. However, integration of proteins or peptides with synthetic materials requires a deeper understanding of properties and processes at the bio-material interfaces. We use molecular modeling for the detailed examination of proteins or peptides as they interact with material surfaces or interfaces revealing critical insights into binding dynamics, structural changes, orientation shifts, and conformational alterations. These molecular interactions are key to engineering materials that are not only stable and biocompatible but also capable of retaining specific biological functions. We specifically examine the interaction of proteins and peptides with heterogeneous material interfaces, such as graphene oxide and silica, elucidating how these interactions impact the protein structure. We also incorporated functional peptides into supramolecular structures, such as micelles, that would mimic protein functions from natural metalloproteins and phosphate-binding functionalities and explore the role of core-corona interface by altering the chemical nature of the core on the retention of protein function and structure, the influence of molecular tails on properties and secondary structures, and the adsorption behaviors of phosphate and zinc ions. Overall, we show that atomic-level understanding of the properties and processes at the protein-material interface is crucial for designing advanced materials that enhance functionality and performance across diverse applications.

8:45am BI1-MoM-3 Crowding Accelerates Molecular Aging in Protein Droplets, *Mateusz Brzezinski, Pablo Argudo, Jasper Michels,* Max Planck Institute for Polymer Research, Germany*; Sapun Parekh,* University of Texas at Austin
Protein liquid-liquid phase separation (LLPS) is a process in which a homogeneous mixture of proteins in a solvent self-assembles, upon certain stimuli, into a protein-rich and protein-depleted phase. In a simple two-component system, the protein-rich phase is called a protein condensate or droplet phase, and the protein-depleted phase is the continuous phase. Recent work has shown that many intrinsically disordered proteins (IDPs) undergo two-component phase separation in vitro due to a myriad of weak interactions. LLPS can be further enhanced by crowding agents. Crowders help to tune effective volume fractions to more "convenient" ratios, which results in a broader window of suitable parameters for obtaining phase separation. Moreover, with use of crowding agents, LLPS has been shown to occur not only for IDPs, but also for folded proteins. So, how do crowding agents affect LLPS of proteins? Depending on the affinity of the crowder for the protein, segregative and associative phase separation can be distinguished. In the following work, we present a systematic approach to quantifying LLPS influenced by crowding agents for an IDP and folded protein. We use fluorescence recovery after photobleaching (FRAP) to quantify material properties and coherent anti-Stokes Raman spectroscopy (CARS) to quantify molecular composition and secondary structure, and theory to demonstrate molecular aging in crowded condensates. We find that crowding accelerates aging in condensates and that folded proteins can phase separate and show molecular aging as well. These results have implication for studying transitions from condensates to fibrils over time.

9:00am BI1-MoM-4 Self-Healing Nanotubes Consisting of Cyclic Peptides Conjugated by Azobenzene Derivatives, *Olufolasade Atoyebi, Maryssa Beasley, William Maza, Matthew Thum, Cynthia Pyles, Sara Tuck, Adam Dunkelberger, Manoj Kolel-Veetil, Kenan Fears,* US Naval Research Laboratory
Cyclic peptides are capable of self-assembling into supramolecular peptide nanotube structures, via hydrogen bonding along the backbone of the peptide rings. Research from our lab has improved upon the synthesis of the self-assembled peptide nanotubes by covalently linking the cyclic peptides into a linear polymer chain that transitions from the unfolded structure to the peptide nanotube by varying the pH of the solution. Here we present an alternate way to control the self-assembly from the linear polymer chain to the rigid peptide nanotube via photo-isomerization. We

capitalize on azobenzene's photo-actuable nature using a di-carboxylic acid azobenzene to covalently crosslink the cyclic peptide rings (KVVKVV) via the two primary amines displayed by each ring. When the azobenzene crosslinker is in its thermally-relaxed, *trans* conformation, the cyclic peptide polymer adopts a rigid, nanotube conformation. When excited by UV light (320 nm), the *trans* to *cis* transition of the azobenzene crosslinker disrupts hydrogen bonding between adjacent rings, causing the polymer to unfold. Atomic force microscopy (AFM) shows that the polymer chain re-fold into rigid nanotube when the azobenzene crosslinkers return to the trans conformation, either by stimulation by visible light (420 nm) or thermal relaxation. This work introduces a novel class of intrinsically self-healing nanomaterials that can be used as reinforcement agents for a wide variety of industrial and biological materials.

9:15am BI1-MoM-5 Anti-Biofouling Polymer Coatings with Statistical Amphiphilicity and Improved Environmental Sustainability, *Rong Yang[1],* Cornell University **INVITED**
Biofouling caused by bacterial biofilms is found in nearly every ecosystem on earth, ranging from ship hulls to membranes for separations and to bioimplants and live tissues (e.g., auditory bullae). It drives up energy consumption and causes dangerous infections. The need for economical, safe, and environmentally sustainable anti-biofouling coatings has motivated our recent investigations into a new class of copolymers with statistical amphiphilicity, demonstrating exceptional biofouling deterrence. Such amphiphilic copolymers simultaneously present hydrophilic and hydrophobic moieties mixed at a molecular level. As such, they are uniquely positioned to reduce biofouling at the air-liquid-solid three-phase interface, where bacterial biofilms are rampant via facile side-chain reorientation. However, their synthesis has challenged common solution-based techniques due to the need for a common solvent for the precursors that present disparate solubility. To overcome that challenge, my group has leveraged an all-dry polymer synthesis technique, namely initiated Chemical Vapor Deposition (iCVD), which has led to several synthesis pathways toward anti-biofouling coatings with statistical amphiphilicity. Our recent effort has focused on improving the environmental sustainability of this class of polymers by replacing the fluorine-bearing hydrophobic side chains with siloxanes or antimicrobial enzymes, which led to improved fouling deterrence. The iCVD method enables polymer synthesis and coating formation in a single step and on virtually any substrate. It has been scaled up to produce functional polymer coatings in a roll-to-roll configuration, pointing to rapid translation of the amphiphilic coatings to reduce the environmental and economic impact of biofouling.

9:45am BI1-MoM-7 Aqueous Underwater Adhesives Made from Multiple Agricultural Proteins, *Zachary Lamberty, Christopher So,* U.S. Naval Research Laboratory
Underwater adhesion, *i.e.* binding to wet surfaces, is a major challenge for medical adhesives, marine repair, and for the durability of shoreside structures. The majority of industrial and academic solutions utilize hydrophobic solvents or polymers to exclude water from the bond area with the goal of obtaining a dry-like contact.However, many organisms have evolved methods of adhering in adverse underwater environments using water-borne protein adhesives. Not only are aqueous adhesives generally less toxic than their organic counterparts, but the water-soluble precursor components are believed capable of diffusing through interfacial water layers, vastly increasing the true contact area of the bond. Inspired by the tenaciously sticky barnacle, we have designed an aqueous two-part adhesive from common agricultural byproduct proteins. Upon mixing, the protein will denature and aggregate, forming a hydrogel. Overtime these proteins rearrange into β-sheet rich amyloid fibers, lending the material strength and allowing it to remain water-insoluble for long periods. We have previously demonstrated this adhesive system using Bovine Serum Albumin (BSA) proteins, with underwater-deposited bond strengths of 0.6 – 0.8 MPa on metal oxide or polymer substrates. Here I will demonstrate that similar principles can be applied to make underwater adhesives from bovine α-lactalbumin (αLa), an abundant milk protein. αLa adhesives can be deposited underwater like BSA adhesives, with bond strengths of 0.52 - 0.09 MPa on polycarbonate after 1 week aging in artificial sea water. Interestingly, unfolded αLa proteins are stabilized by the denaturant urea, remaining liquid for hours in air but rapidly solidifying when deposited in solution as the denaturant diffuses away. This offers unique advantages, including greatly reduced sag and the ability to densify the material to improve cohesive strength. By understanding and controlling the aggregation and densification process we aim to develop tunable, easily

---

[1] **BID Early Career Researchers Award**

deployable underwater adhesives made from non-toxic, domestically sourced agricultural proteins.

10:00am BI1-MoM-8 How Is the Hydrophobic Force Modified by an Oscillation Frequency in Saline Conditions?, *Chiara Wagner, Paul Stöcher, Markus Valtiner, **Laura Mears,*** Vienna University of Technology, Austria

Hydrophobic interactions can occur in many biorelevant systems, including hydrophobic side chains as part of many amino acids, drug molecules and surfaces used to support and control the adhesion of cells. Several of Stephanie Allen's works involve such hydrophobic amino acids [1] or surfaces [2] and their characterisation with atomic force microscopy (AFM). In this contribution we set our work on the hydrophobic force in the context of biointerfaces. There have been many investigations over the years regarding the mechanism behind the hydrophobic force and over how long a range it can be felt [3]. We present a detailed set of AFM force measurements of hydrophobic SAM modified surfaces, with varying salt concentration and oscillation frequency (0-2kHz). We observe dynamic changes in the force curve characteristics with both salt concentration and oscillation frequency. The changes lead to a reduction of the average force with increasing applied frequency, while multiple distinct characteristic curves are present and enhanced by certain conditions. We also notice changes in the range of the force away from the surface. Altogether, the results we will present bring new insight into the mechanism of hydrophobic interactions. Further they open the opportunity for discussion of how the addition of oscillations could, perhaps, be used in biorelevant applications to modify the hydrophobic forces directly.

[1] L. Niu, Xi. Chen, S. Allen, and S. J. B. Tendler, *Langmuir*, **2007**, 23, 14, 7443–7446.[2] S. Allen, S.D.A. Connell, X. Chen, J. Davies, M.C. Davies, A.C. Dawkes, C.J. Roberts, S.J.B. Tendler, P.M. Williams, *Journal of Colloid and Interface Science*, **2001**, 242, 2, 470-476.[3] W. A. Ducker and D. Mastropietro, Current Opinion in Colloid & Interface Science, **2016**, 22, 51–58.

Biomaterial Interfaces
Room 117 - Session BI2-MoM

Functional Materials

Moderators: Kenan Fears, U.S. Naval Research Laboratory, **Rong Yang**, Cornell University

10:30am BI2-MoM-10 Customizing Naturally-Derived Polymers Using Plasma-Enhanced Chemical Vapor Deposition, *Morgan Hawker,* California State University, Fresno

Naturally-derived polymers are the fastest-growing biomaterials because they are non-immunogenic and are able to recapitulate a range of biological tissues through bulk mechanical property tuning. This remarkable materials class includes silk, collagen and cellulose, all of which have high potential for use as tissue engineering implants, biosensors, and drug delivery devices. One drawback is that naturally-derived polymers are bioinert, exhibiting non-specific interactions with proteins, cells, bacteria, enzymes, and other biological species. Another possible drawback in some applications includes fixed degradation kinetics which may not match the rate required for a given application. Plasma-enhanced chemical vapor deposition (PECVD) is a useful strategy to address both drawbacks, providing a chemically customizable coating that can control interfacial interactions while also modulating degradation.

This talk will highlight our recent work on plasma-enhanced chemical vapor deposition approaches to modify different naturally-derived polymers. First, an acrylic acid and pentane plasma copolymerization strategy has been developed to control silk film wettability. We demonstrate that silk film wettability decreases with increasing pentane in the feedgas, with impressive static water contact angle tunability between 50° and 100°. High-resolution XPS findings provided additional insight into changes in surface chemical composition for coatings deposited with varying proportions of monomers in the feedgas. Second, PECVD coatings were deposited on commercially-available cellulosic wound dressings using a 1,8-cineole precursor. Pulsed and continuous power conditions were utilized with the goal of preserving the 1,8-cineole monomer structure because of the molecule's well-documented antibacterial properties. Although surface analysis revealed minimal difference between films deposited under different powers, films unexpectedly exhibited differing performance when interfaced with *Streptococcus pneumoniae*. Last, novel PECVD systems currently under development in our lab will be presented. One goal of employing new precursors is to develop additional antibacterial coating systems that are stable in aqueous environments. Each of these systems is poised to enhance naturally-derived polymer utility in biomedical contexts through controlling interfacial interactions.

10:45am BI2-MoM-11 Vascularized Polymers: Optimizing Support Systems for Biotic/Abiotic Living Materials, *Evan Leonard, Sandro Zier, **Caitlin Howell,*** University of Maine

Large-scale detection of and active response to changing conditions at interfaces is a promising pathway to facilitating the long-term growth and stability of the biotic component of biotic/abiotic living materials. In Nature, one method of both detecting and actively responding to environmental changes is by using vascular networks as intermediaries that transport signals and materials from one location to another. In this work, we explore various methods of embedding vascular networks into abiotic polymeric matrices that use widely available fused filament deposition model (FDM) 3D printing. We test each method for the efficacy of diffusion to and from the interface, as well as how well it can be used in both hydrophobic and hydrophilic abiotic polymers. Our goal is to create detection-and/or-response systems to support the growth of biotic systems located at abiotic polymer interfaces in a low-cost, easily scalable manner, paving the way for the creation of durable and adaptable biotic/abiotic living materials.

11:00am BI2-MoM-12 Preserving the Hydrophilicity of Biodegradable Films Post-Plasma Treatment: Impact of Aging Environment on Hydrophobic Recovery, *Mina Abdelmessih, Morgan Hawker,* California State University, Fresno

Polylactic acid (PLA) and chitosan (CS) are biopolymers with vast potential in the biomedical field. Their biodegradability and non-toxicity *in vivo* makes them useful as tissue engineering scaffolds. The slower degradability of PLA is suitable for slower-healing bone tissues, while the faster degradability of CS is suitable for faster-healing soft tissues. Nevertheless, both polymers are inherently hydrophobic, which would potentially restrict the cell adhesion desirable for tissue engineering applications. There is some evidence that hydrophilic surfaces are preferable for cell adhesion and growth. Previous studies display the promise of utilizing radio-frequency nitrogen plasma treatment in increasing the surface hydrophilicity of PLA and CS. In addition, nitrogen plasma treatment polymers have been shown to exhibit improved surface cell adhesion properties. Many plasma treated polymers, including PLA and CS exhibit a phenomenon known as hydrophobic recovery, where the polymers partially retain their original hydrophobic properties with age. Hydrophilicity loss in treated PLA and CS is detrimental, especially in applications that require cell adhesion. Methods of preventing this phenomenon in PLA and CS are widely unexplored.

This work explored the impact of various aging conditions (storage in vacuum, cold temperature, and air) on the surface hydrophilicity of nitrogen-plasma-treated PLA and CS following treatment. Films were prepared as model substrates using the solvent-casting method. The films were treated in a RF plasma reactor under optimized parameters (power, pressure, and treatment time). After treatment, the films were aged in the different aging environments for two weeks. Throughout the aging period, multiple surface analyses were conducted on samples exposed to the various preservation environments, including untreated samples as controls. Surface wettability analysis utilizing water contact angle goniometry displayed that vacuum aged samples possess the least hydrophobic recovery in comparison to the other aging conditions. Additionally, surface chemical composition was examined using x-ray photoelectron spectroscopy. Expanding these treatment preservation methods to PLA and CS has potential to positively impact their use as scaffolds in the biomedical field.

11:15am BI2-MoM-13 3-D Atomic Layer Infiltrated Metal Oxide Barriers for Thin-Film Active Microelectrode Arrays, *Martin Niemiec, Kyungjin Kim,* University of Connecticut

A recent trend in neural interfaces is a shift away from rigid devices comprised of materials such as silicon and metals toward thin and flexible material classes such as polymers. While such devices show more favorable biointegration over chronic timescales, they are often plagued by issues of reliability, stemming from poorer resistance to the permeation of moisture and ions as compared to traditional materials. As such, the incorporation of ultrathin barrier layers of inorganic materials deposited by atomic layer deposition (ALD) or chemical vapor deposition (CVD) is an area of interest. Most ALD and CVD processes incorporate wafer-grown inorganic barriers,

depositing metal oxides above and below the polymeric layers, followed by via opening using established microfabrication techniques. However, the etching step can leave unprotected polymer sidewalls, leaving a significant path for permeation, and the high stiffness mismatch between the polymer and inorganic film often leads to interfacial delamination.

Herein, we describe a technique and its advantages for the fabrication of mechanically reliable thin-film barrier encapsulated polymeric active microelectrode arrays with three-dimensional all-side atomic layer infiltration using a modified liftoff process. Unlike barriers grown on-wafer, the metal oxides infiltrate all sides of the polymer array at once and leave no exposed sidewalls vulnerable to moisture. Secondly, the gradual stiffness transition at the polymer-inorganic barrier interface can reduce delamination and improve flexibility. Finally, the modified liftoff process allows ALD via opening on freestanding devices. We have demonstrated such devices previously in a completely encapsulated form, without active microelectrodes. Here, the combination of active electrodes with our three-dimensional coating is achieved via a modified liftoff process utilizing ultrasonication to remove the metal oxide over the microelectrodes, without removing it elsewhere. Because the inorganic barrier is deposited after insulation via opening, our devices feature the additional benefit of via sidewall encapsulation with a protective barrier, thereby decreasing the chances of side-permeation and delamination initiation at the microelectrode. The encapsulation (~10nm Al_2O_3, ~25nmTiO_2) can provide water vapor transmission rates less than 1 mg m-2day-1 at 85% RH (see supplement). Ongoing accelerated aging tests will offer insights as to the effectiveness of our encapsulation on preserving functionality under implanted conditions, with initial trials showing functionality up to ~20 days at 87°C (roughly 640 days at 37°C).

11:30am **BI2-MoM-14 Injectable Siloxane Sponges for on-Site Treatment and Rapid Hemostasis**, *Pritha Sarkar*, **Kausik Mukhopadhyay**, University of Central Florida

Hemorrhage is one of the main causes of preventable civilian death and on the battlefield. According to a report by the USAMRDC in 2022, nearly 50% of combat deaths have been due to exsanguinating hemorrhage. Of those, about half could have been saved if timely, appropriate care had been available. This underscores the need to develop appropriate FDA-approved hemostatic treatments. While external wound injury can be treated mostly by visual inspection, internal hemorrhages are often much more intractable. The need to treat trauma wounds requires an immediate solution that can be applied by individual soldiers in the field swiftly and efficiently. In our current study, we report a silicone-based hemostatic bandage system that is both antibacterial and self-expanding. The two-component hemostatic system chemically reacts in situ to form a stretchable foam that generates autogenous pressure on the wound to control bleeding. It can be easily administered with a dual-syringe device, and when the components interact on delivery, hydrogen peroxide decomposition is catalyzed by silver oxide, releasing oxygen to expand the siloxane matrix into a rigid 'foam' within seconds. This foam or sponge then acts as a 'tamponade' arresting further bleeding. The adhesive properties of the foam render them optimal for wound-dressing applications and the presence of silver oxide imparts antibacterial effects against both Gram-positive and Gram-negative strains of bacteria. Optimization of the constituents allows control over system temperature and porosity. Support data include studies on rheology, adhesion, and in-vitro assays. To further assess the efficacy of the foam, a unique mannequin system capable of simulating a deep abdominal wound has been employed. The objective of this novel hemostatic agent is to provide the injured party with a means to rapidly stagnate or arrest bleeding from external and internal wounds in a manner superior to those currently available. This unique formulation presents an easy and economical approach to a hemostatic bandage system with spontaneous self-expanding properties, capable of remaining functional in inclement weather conditions.

CHIPS Act Mini-Symposium
Room 122 - Session CPS-MoM

CHIPS Act Mini-Symposium

Moderators: Alain Diebold, University at Albany-SUNY, **Erica Douglas**, Sandia National Laboratories, **Timothy Gessert**, Gessert Consulting

8:15am **CPS-MoM-1 Midwest Semiconductor Collaborative Network for Work Force Training (MSN Force)**, *Gozde Tutuncuoglu*, **Alireza Moazzeni**, Wayne State University

The U.S. semiconductor industry's workforce is expected to grow by nearly 115,000 jobs by 2030, increasing from approximately 345,000 jobs today to about 460,000—representing a 33% rise. In response to this demand, the Midwest Semiconductor Collaborative Network for Workforce Training (MSN Force), funded by the National Science Foundation (NSF), aims to address the urgent need for highly skilled workers in the semiconductor sector, particularly within the Midwest. With a broader long-term vision of meeting national workforce development and R&D needs in semiconductor and microelectronics, MSN Force seeks to promote U.S. leadership in this critical industry.

Led by Wayne State University, MSN Force brings together a consortium of key academic institutions including Ohio State University, University of Michigan, Purdue University, Lorain Community College, and Youngstown State University. Our industrial and research partners, spanning organizations such as Synopsys, Intel, Mercedes Benz, NASA Glenn Research Center, SMART Microsystems, and the Semi Foundation, play a vital role in this initiative.

MSN Force focuses on co-developing training activities through close academia-industry partnerships, with an emphasis on experiential learning and robust industry engagement. The program integrates hands-on learning across all phases of semiconductor production, from device simulation and chip design to packaging, assembly, and testing. The ultimate goal is to create a comprehensive, state-of-the-art workforce training program that equips trainees with the skills needed to meet the evolving demands of the semiconductor industry.

8:30am **CPS-MoM-2 Opportunities and Challenges for Interdisciplinary Research and Education in Microelectronics**, *Ashok Kumar,* University of South Florida

As evident from the 2022 CHIPS and Science Act and the 2020 National AI Initiative Act, there is an acute need for talented and trained workforce in semiconductor manufacturing and Artificial Intelligence (AI)/Machine Learning (ML) areas. Recent NSF NRT (National Research Traineeship) grant has provided support to develop and implement a comprehensive and experiential learning-based education, research, training, and skills development program in semiconductor design, manufacturing, and packaging. This talk will provide interdisciplinary semiconductor concepts and emerging technologies that will be integrated in existing courses with novel experiential lab training in Class 1000 cleanroom environment.Students will be involved with industrial partners to define research problems using a convergence approach to design and develop application-driven semiconductor systems and devices. This program is innovatively designed such that the students on completion will gain essential competencies, namely, transdisciplinary knowledge, communication, teamwork, experimental & computational skills, informed decision making, entrepreneurship skills, project management, ethics, leadership, and safe and sustainable manufacturing. Students with entrepreneurial interest will have the opportunity to complete NSF I-Corps site training. In summary, this presentation will provide on-going development and implementation of a new interdisciplinary curriculum, featuring novel courses in fundamentals of materials, processing, metrology, device fabrication with specific applications to semi-conductor technology development.

8:45am **CPS-MoM-3 Strategic Roadmapping for Information and Communication Technologies**, *Victor Zhirnov*, Semiconductor Research Corporation*; Victor Zhirnov,* SRC **INVITED**

Information and Communication Technologies (ICT) is the social-economic growth engine of the modern world. This electronic processing and transmission of information includes the explosion of sensing for real-world applications in many market segments, such as automotive, industrial manufacturing and automation, robotics, health, environmental, etc. The use of ICT continues to grow without bounds driven by the exponential creation of data that must be moved, stored, computed, and communicated. Ever-rising energy demands for information and

communication technologies versus global energy production are creating new risks. Therefore, new paradigms need to be discovered in order to dramatically improve energy efficiency of ICT.

In the past, the role of strategic planning for semiconductor industry was met by the International Technology Roadmap for Semiconductors (ITRS), serving as a master plan that provided manufacturers, designers, and equipment suppliers with direction years in advance. By providing a common framework for coordination across semiconductor industry stakeholders, technology development efforts were efficient and aligned. However, the dissolution of the ITRS in 2015 left a void, leading to years of disjointed efforts. Recognizing the need for unified guidance, the industry rallied for the creation of new strategic plans, which yielded the 2030 Decadal Plan for Semiconductors (identifies the "What") and the Microelectronics and Advanced Packaging Technologies (MAPT) Roadmap (identifies the "How") were developed. These comprehensive plans outline ambitious goals for the industry's future.

Inventing the next hardware/software ICT paradigm is a tall order. However, it is achievable if the right questions are asked and the right resources are put in place. These steps are outlined in the Decadal Plan and in the MAPT Roadmap, which emphasize the need for radical new solutions for future ICT, including sustainability and workforce development.

9:15am CPS-MoM-5 Challenges and Opportunities in Characterization and Metrology for the Microelectronics and Advanced Packaging Technologies (MAPT) Roadmap, *Markus Kuhn,* Rigaku*; Alain Diebold,* SUNY Polytechnic Institute, Albany **INVITED**
The recently released Microelectronics and Advanced Packaging Technologies (MAPT) Roadmap represents the collective efforts of hundreds of individuals representing >100 organizations from government, academia, and industry. The MAPT Roadmap directly supports the Chips and Science Act, led by the U.S. Department of Commerce, in efforts to develop a robust domestic semiconductor ecosystem.

The metrology chapter describes the characterization and metrology requirements for all areas of the MAPT Roadmap including Materials and Devices through Advanced Packaging and Heterogeneous Integration and Systems.Metrology measurements enable all aspects of semiconductor materials and device research, development, and manufacturing, therefore making support for this area critical to meeting technology objectives.

This talk will highlight the importance of continued metrology development and assess the key challenges facing this segment for the next 10+ years. Some of the key challenges and initiatives are highlighted below.

- Manufacturing-ready 3D metrology.
- Lab to fab transition to introduce new capabilities into manufacturing.
- Accelerating lab metrology output (wafer coverage, precision, throughput).
- Enabling and incorporating DFM (design for metrology,) ML/AI, hybrid metrology concepts as part of a holistic process, test, and simulation ecosystem.

9:45am CPS-MoM-7 CHIPs Act and Optoelectronics, Devices, and AI/ML, *Volker Sorger,* University of Florida **INVITED**
What is the CHIPS ACt?The bipartisan CHIPS and Science Act signed into action in 2022 was a seminal action; for the first time since World War II (i.e. the Manhattan project) an economic stimulus package for a single industry was signed. The federal focus to re-shore manufacturing capabilities ($39B) along with R&D and workforce stimulus packages ($11B) is joined by matching funds from the States and the private sector (i.e. corporations, SMEs, venture capital), thus adding multiplication factors to the semiconductor ecosystem.

Why now? Chips having been invented in the U.S. some sixty years ago, have been off-shored since the 2000's to far Asia, mainly due to economic factors. The resulting technological- and supply chain independence became all-too evident during the COVID years. With semiconductors (i.e. chips) being a critical part of modern businesses in virtually all economic sectors, securing and re-vitalizing manufacturing capabilities along with critical R&D projects are timely and, thankfully underway.

What is the Role of Photonics in Chips?Optics provides synergistic and performance extending capabilities in two major ways: a) data interconnects and b) special purpose computing. Optical Interconnects and Advanced Packaging: Starting with the former, the bosonic nature and 1,000x wavefunction difference between photons and matter offers optics

to provide low-loss long-distance data links. Unlike fibers, new to the CHIPS activities are that photonics is now considered inside board and even insider the package; the latter stems from the desire to blur-the-lines between what is in the package vs. what is on the board in advanced packaging. In addition to 2.5D interposer (e.g. active optical interposer) packaging strategies, 3D heterogenous integration (3DHI) solutions are anticipated to provide not just 100x interconnect performance gains (e.g. in units of [Gbps/mm/pJ/bit]), but also enable best-of-both world co-design and optimization 'options' (i.e. 'known-best-die'). In regard to Special Purpose Computing, photonic chips offers some interesting benefits but also challenges: the benefits resolve around the ability to i) executing mathematical functions in the optical domain at zero energy, ii) processing data at full bit resolution in their natural domain (no analog-to-digital conversion past the sensor), iii) allowing for high degrees of signal fan-out (e.g. for neuromorphic computing), and iv) enabling real-time computing in the 10's of picosecond range per device (minus RC delays from the optoelectronic components).

10:30am CPS-MoM-10 Bridging Opportunities and Challenges: Examining a Community College's Role in Preparing Technicians for the Semiconductor Industry, *Nancy Louwagie,* Normandale Community College **INVITED**
Community colleges offer the potential to take on a crucial role in preparing the technician workforce for the semiconductor industry. This presentation aims to showcase a vacuum technology program offered at Normandale Community College (Bloomington, MN) as a case study, illustrating how such institutions can serve as hubs for workforce development. Furthermore, it delves into the obstacles faced by community colleges in establishing and sustaining high-tech programs of study.

Opportunities:

1. Affordability: Community colleges are recognized as the most cost-effective option in higher education, offering accessible pathways to technical education.
2. Accessibility: With campuses spread across states, community colleges ensure geographical inclusivity, providing equitable access to post-secondary education.
3. Localized Programming: Community colleges have the flexibility to tailor programs to meet the specific workforce demands of their regions.
4. Industry Collaboration: Increasingly, local employers are partnering with community colleges to provide internship and apprenticeship opportunities that enhance students' practical skills and employability prospects.

Challenges:

1. Financial Sustainability: Community colleges grapple with financial instability, particularly small programs, which are at constant risk of closure, threatening the continuity of any technician training program.
2. Faculty Recruitment: Technical programs require specialized faculty, but community colleges often struggle to attract and retain qualified instructors.
3. Equipment Procurement: Maintaining up-to-date equipment for hands-on learning is essential in technical education, yet community colleges face challenges acquiring and maintaining this equipment.
4. Pandemic Impact on Disadvantaged Students: COVID-19 exacerbated existing disparities, disproportionately affecting students from disadvantaged backgrounds. Academic setbacks pose challenges to program retention and completion rates.

Conclusion: Community colleges can fulfill a critical role in meeting the substantial technician development demands of the semiconductor industry. They are known for delivering affordable, accessible, and regionally tailored programs. However, sustaining and enhancing these initiatives requires addressing financial constraints, faculty shortages, equipment needs, and supporting students, particularly those facing pandemic-related setbacks. Collaborative efforts between educational institutions, industry partners, and policymakers are essential in navigating these challenges and maximizing the potential of community colleges in preparing the semiconductor workforce of tomorrow.

11:00am CPS-MoM-12 CHIPS Act and the Future of the Semiconductor Industry Panel Discussion, *Erica Douglas,* Sandia National Lab
Leading experts will participate in CHIPs Act panel session chaired by Erica Douglas. The panel session will explore aspects of the new initiatives in the semiconductor industry funded by the CHIPs Act. Participants will include the invited speakers for the Chips Act Session.

Light Sources Enabled Science Mini-Symposium
Room 121 - Session LS-MoM

Light Sources Enabled Science Mini-Symposium
Moderators: Slavomir Nemsak, Advanced Light Source, Lawrence Berkeley National Laboratory, **Jessica McChesney**, Argonne National Laboratory

8:15am LS-MoM-1 Microsecond Dynamics of Surface Reactions Studied by the Time-resolved Ambient Pressure XPS with Chemical Perturbations, *Calley Eads, Weijia Wang,* Max IV Laboratory, Sweden; *Ulrike Kust, Julia Prumbs,* Lund University, Sweden; *Robert Temperton,* max iv Laboratory, Sweden; *Mattia Scardamaglia,* max iv laboratory, Sweden; *Jan Knudsen,* Lund University, Sweden; **Andrey Shavorskiy,** Max IV Laboratory, Sweden
INVITED

Recently,a new time-resolved Ambient Pressure X-ray Photoelectron Spectroscopy (APXPS) method based on chemical perturbations has been developed for studying dynamic processes with microsecond time resolution. The method uses the rapid change in the gas pressure/composition as a perturbation that drives the system away from equilibrium [1,2]. In the experiment, a sharp and strong gradient in chemical potential is created by modulating the gas composition over the catalyst via a fast valve. Such gas pulse has internal pressure in the mbar range and a rising edge of a few hundred microseconds. A time-sensitive delayline detector is synchronized with the valve operation to measure X-ray photoemission spectra with nano- to microsecond time resolution. We will present several experiments characterizing the setup's performance, including the CO oxidation reaction over Pt (111) to demonstrate the capability of the setup to correlate the gas phase composition with that of the surface during the transient supply of CO gas into an O2 stream [3]. These experiments demonstrate that under CO pressure modulation conditions, the system remains active (i.e. producing CO2) at temperatures below the CO lift-off temperature under the flow conditions. We will also demonstrate that little chemisorbed oxygen is observed during the active phase of the catalytic cycle when the Pt(111) surface is saturated with the oxide. This points out a much higher activity of the O_chemisorbed towards CO oxidation than O_oxide, resolving the ongoing debate about the role of the Platnum surface oxide in the reaction.

[1] J. Knudsen *et al. Nat Commun* **12**, 6117 (2021). doi:10.1038/s41467-021-26372-y

[2] A. Shavorskiy et al. *ACS APPLIED MATERIALS & INTERFACES* **13**, 47629 (2021). doi: 10.1021/acsami.1c13590

[3] C. Eads et al. *in preparation*

8:45am LS-MoM-3 HAXPES at PETRA III and IV: Electronic Structure, Operando Devices and In-situ Catalysis, *Christoph Schlueter,* Desy, Deutsches Elektronen-Synchrotron, Germany
The P22 beamline at PETRA III is a cutting-edge facility dedicated to hard X-ray photoelectron spectroscopy (HAXPES) techniques, featuring four specialized experimental end stations for high-resolution studies of electronic and chemical structures in various complex materials, device-like structures, and catalytic interfaces.

- HAXPES Hemisphere: Known as the "workhorse" instrument, this setup offers extensive opportunities for operando device characterization, depth profiling, and chemical analysis.
- POLARIS (Ambient Pressure XPS System): This system is tailored for investigating the catalytic properties of surfaces under industrially relevant conditions, making it crucial for practical catalysis research.
- HarMoMic (Hard X-ray Momentum Microscope): This novel microscope explores electronic and atomic structures through wide-field imaging of band dispersions and electron diffraction patterns.
- HAXPEEM (Hard X-ray Photoemission Electron Microscopy): Dedicated to studying laterally resolved chemical and elemental structures.

These instruments are fully operational and used in close collaboration with external user groups, reflecting the wide range of scientific fields engaged by the P22 beamline community. The P22 beamline first received light in November 2017 and conducted its first user experiments in June 2018. Since then, it has contributed to over 100 publications.

In this contribution, I will briefly present the experimental capabilities of the P22 beamline, provide an overview of the most prominent scientific results, and present an outlook towards HAXPES at PETRA IV.

9:00am LS-MoM-4 Hard X-Ray Photoelectron Spectroscopy and Its Application to the Bonding and Electronic Structure of Metal Dihydrides, *Anna Regoutz,* University College London, UK
Metal hydrides hold significant promise in various hydrogen-related technologies, encompassing energy storage, hydrogen compression, and hydrogen sensing. Although metal hydrides appear simple compared to many other energy materials, understanding the electronic structure and chemical environment of hydrogen within them remains a key challenge. This work presents a new analytical pathway to explore these aspects in technologically relevant systems using Hard X-ray Photoelectron Spectroscopy (HAXPES) on thin films of two prototypical metal dihydrides: YH2−δ and TiH2−δ.[1,2] By taking advantage of the tunability of synchrotron radiation, a non-destructive depth profile of the chemical states is obtained using core-level spectra. Combining experimental valence band spectra collected at varying photon energies with theoretical insights from density functional theory (DFT) calculations, a description of the bonding nature and the role of d versus sp contributions to states near the Fermi energy are provided. Moreover, a reliable determination of the enthalpy of formation is proposed by using experimental values of the energy position of metal s band features close to the Fermi energy in the HAXPES valence band spectra.

[1] C. Kalha, L. E. Ratcliff, G. Colombi, C. Schlueter, B. Dam, A. Gloskovskii, T.-L. Lee, P. K. Thakur, P. Bhatt, Y. Zhu, J. Osterwalder, F. Offi, G. Panaccione, A. Regoutz, "Revealing the Bonding Nature and Electronic Structure of Early-Transition-Metal Dihydrides", PRX Energy, 3, 013003, 2024, https://doi.org/10.1103/PRXEnergy.3.013003.

[2] C. Kalha, N. K. Fernando, P. Bhatt, F. O. L. Johansson, A. Lindblad, H. Rensmo, L. Zendejas Medina, R. Lindblad, S. Siol, L. P. H. Jeurgens, C. Cancellieri, K. Rossnagel, K. Medjanik, G. Schönhense, M. Simon, A. X. Gray, S. Nemšák, P. Lömker, C. Schlueter, and A. Regoutz, "Hard X-ray Photoelectron Spectroscopy – A Snapshot of the State-of-the-Art in 2020", J. Phys. Condens. Matter, 33, 233001, 2021, https://doi.org/10.1088/1361-648X/abeacd.

9:15am LS-MoM-5 The Electric Double Layer at Ultra-Thin Film Electrodes and How to Experimentally Assess It, *Maximilian Jaugstetter,* LBNL; *Lorenz Falling,* Technical University Munich, Germany; *Slavomir Nemsak, Miguel Salmeron,* LBNL
Understanding the structure of the electric double layer (EDL) is fundamental for the development of improved heterogeneous catalysts, batteries, and membranes for the sustainable accumulation of key materials and, generally, any process that involves a solid-liquid interface.Due to their hidden nature, the difficulty of spectroscopic detection, and the difficulty of formulating holistic molecular dynamics simulations, knowledge of the properties of these interfaces is sparse and focuses on a few example systems.

In order to obtain a better understanding of the effects of solvated ions on the interfacial water structure, local pH, and reactant adsorption, we employ soft X-ray techniques to spectroscopically investigate the atomic composition of the first few nanometers behind an X-ray transmissive electrode. For these experiments, we utilize interface-sensitive techniques such as X-ray absorption spectroscopy/total electron yield (XAS/TEY) and X-ray photoelectron spectroscopy (XPS) in combination with nano-electrochemistry as well as nanofabrication of ultra-thin free-standing films of graphene and graphene-like 2D materials.

With these methods, we are able to demonstrate the huge implications of different electrolytes and electrode materials on the structure of the EDL as well as the contributions of individual species to its formation. A quantification of dissolved species at the interface by XPS allows us to directly relate their presence to EDL properties.

By understanding the dependence of these properties, we are one step closer to fine-tuning them to support favorable transition states in electrocatalysis or decrease inhomogeneous growth processes in energy storage.

10:30am LS-MoM-10 In situ Synchrotron Characterization of Materials Synthesis and Electrochemical Interfaces, *Katherine Harmon,* Stanford University; *F. Joseph Heremans, Stephan Hruszkewycz, Matthew J. Highland,* Argonne National Laboratory
INVITED
Advanced X-ray characterization tools exploiting the high coherent flux of 4th generation synchrotrons (e.g., the upgraded Advanced Photon Source) and X-ray free electron lasers promise to revolutionize our understanding of material synthesis, catalysis, and many other physiochemical processes. I will present our recent work investigating the synthesis of silicon carbide, a

quintessential "polytypic" material. SiC is a versatile wide bandgap semiconductor host of optically active point defects (color centers) that may be exploited for quantum sensing and communications. SiC has also been reported to occur in over 200 polytypes, with mixed polytype inclusions being common in nominally single-polytype materials. Color centers are extremely sensitive to such heteropolytypic inclusions. Yet, the thermodynamic and kinetic drivers of polytype transformations during growth remain speculative due to a lack of characterization tools able to probe the growth process in real time. We developed a hard X-ray compatible chemical vapor deposition (CVD) reactor for the characterization of silicon carbide (SiC) polytype transformations during synthesis. Preliminary *in situ* crystal truncation rod measurements obtained using our new reactor at the Advanced Photon Source (APS) demonstrate the sensitivity to different polytypes in SiC. Notably, these measurements were carried out prior to the APS upgrade (APS-U) and did not exploit the coherent flux of the beam, which was not sufficiently high at the photon energies required to penetrate the CVD reactor walls (E > 24 keV). The APS-U will provide a two order of magnitude increase in the coherent flux of the beam across the energy spectrum, enabling advanced coherent X-ray measurements, namely, X-ray photon correlation spectroscopy (XPCS), at the requisite X-ray photon energies for SiC synthesis characterization. I will outline the principles of XPCS and discuss the upcoming opportunities at the APS-U not only for characterizing and controlling polytype transformations in SiC but also more broadly for understanding material processing in cases requiring complex sample environments that were previously inaccessible.

11:00am LS-MoM-12 Direct Imaging of Local Orbitals in Quantum Materials, *Martin Sundermann,* Max Planck Institute for Chemical Physics of Solids, Germany*; Hasan Yavas,* PETRA III, Deutsches Electron Synchrotron, DESY, Germany*; Paulius Dolmantas, Chun-Fu Chang,* Max Planck Institute for Chemical Physics of Solids, Germany*; Hlynur Gretarsson,* PETRA III, Deutsches Elektron Synchrotron, DESY, Germany*; Alexander Komarek,* Max Planck Institute for Chemical Physics of Solids, Germany*; Andrea Severing,* Universität zu Köln, Germany*; Maurits Haverkort,* Universität Heidelberg, Germany*; Liu Hao Tjeng,* Max Planck Institute for Chemical Physics of Solids, Germany

The search for new quantum materials with novel properties is often focused on materials containing transition-metal, rare-earth and/or actinide elements. The presence of the atomic-like d or f orbitals provides a fruitful playground to generate novel phenomena. The intricate interplay of band formation with the local electron correlation and atomic multiplet effects leads to phases that are nearly iso-energetic, making materials' properties highly tunable by doping, temperature, pressure or magnetic field. Understanding the behavior of the d and f electrons is essential for designing and controlling novel quantum materials. Therefore, identifying the d or f orbitals that actively participate in the formation of the ground state is crucial. So far, these orbitals have mostly been deduced from optical, X-ray and neutron spectroscopies in which spectra must be analyzed using theory or modelling. This, however, is also a challenge by itself, since *ab-initio* calculations hit their limits due to the many-body nature of the problem.

Here we developed a new experimental method that circumvents the need for involved analysis and instead provides the information as measured. With this technique, we can make a direct image of the active orbital and determine what the atomic-like object looks like in the real solid. The method, X-Ray Raman spectroscopy or non-resonant inelastic X-ray scattering using an s-core level (s-NIXS), relies on high momentum transfer in the inelastic scattering process, which is necessary for dipole-forbidden terms to gain spectral weight. To demonstrate the strength of the technique, we imaged the (text-book example) ground-state $x^2-y^2/3x^2-r^2$ hole orbital of the Ni^{2+} ion in NiO single crystal [1] We will present the basic principles of s-NIXS and details of its experimental implementation. We will show how we can apply this technique to unveil the active orbitals in a wide range of quantum materials [2,3], including those that undergo complex metal-insulator transitions.

[1] H. Yavaş, M. Sundermann, K. Chen, A. Amorese, A. Severing, H. Gretarsson, M.W. Haverkort, L.H. Tjeng, **Nature Physics** 15, 559 (2019)

[2] B. Leedahl, M. Sundermann, A. Amorese, A. Severing, H. Gretarsson, L. Zhang, A.C. Komarek, A. Maignan, M.W. Haverkort, and L.H. Tjeng, **Nature Commun.** 10, 5447 (2019).

[3] A. Amorese, B. Leedahl, M. Sundermann, H. Gretarsson, Z. Hu, H.-J. Lin, C.T. Chen, M. Schmidt, H. Borrmann, Yu. Grin, A. Severing, M.W. Haverkort, and L.H. Tjeng, **Phys. Rev. X** 11, 011002 (2021).

11:15am LS-MoM-13 Bismuth-Trimer Adlayer and Thin Film Growth on In- and Sb-Terminated InSb(111) Surfaces, *Rohit Yadav, ShengPeng Huang, Sina Ritter, Rainer Timm,* Lund University, Sweden

Bismuth-semiconductor interfaces are important from both fundamental and application point of view. For example, a monolayer of bismuth on compound semiconductors like SiC and GaAs is predicted to be a 2D topological insulator with a quantum spin hall phase.[1,2] Similarly, Bi-induced trimers on Si(111) have been reported for giant Rashba splitting.[3] Here, we investigate Bi incorporation on InSb(111)A and B surfaces due to their large spin-orbit coupling and the small lattice mismatch.[4] Furthermore, individual Bi-based compounds like InBi and $Sb_{1-x}Bi_x$ have been predicted to induce non-trivial topological states.[5,6] We are focusing on the initial deposition, from less than a monolayer up to a few monolayers of Bi.

We have employed scanning tunneling microscopy/spectroscopy (STM/S) and synchrotron-based angle-resolved photoemission spectroscopy (ARPES) and XPS to investigate surface topography, electronic properties, and chemical composition. STM topography of oxide-free InSb(111)A shows (2X2) reconstructions with In-trimers. Upon Bi incorporation, Bi mainly forms a homogeneous periodic hexagonal bilayer, highlighting the formation of large-scale Bi-induced (2X2) reconstruction, along with some areas of $(2\sqrt{3}X2\sqrt{3})$–R30° reconstruction. A bias-dependent STM study shows that the Bi-film is decorated with Bi-trimers. STS on these trimers show metallic character and discrete surface states in the InSb bandgap, indicating possible band engineering upon Bi incorporation. Discrete Bi-induced surface states are further confirmed by ARPES measurement. However, Bi-incorporation into InSb(111)B results in mixed surface topography of Bi-trimers and Bi-monomer structures. Bi 5d core-level XPS for both InSb(111)A and B reveals that Bi-incorporation results in mainly Bi-Sb bonding and minor metallic Bi-Bi bonds. Interestingly, the Bi-Sb layer thickness remains self-limiting in the case of Bi/InSb(111)B, when deposited at elevated temperature. Thus, the amount of Bi-Sb remains unchanged, regardless of the number of deposition cycles.

Here, we discuss Bi-induced electronic band engineering and the formation of several 2D structures on InSb. This research highlights the metallic behaviour of decorated Bi-trimers and self-limiting BiSb film thickness in InSb(111)A and B substrates, respectively, which is highly versatile from an application point of view

References:

[1] F. Reis et al., Science 357, 287−290 (2017)

[2] Y. Liu et al., ACS Nano 17, 5047−5058 (2023)

[3] I. Gierz et al., PRL 103, 046803 (2009)

[4] H .S. Inbar et al., arXiv:2302.00803 (2023)

[5] D. Hsieh et al., Nature 452, 970 (2008)

[6] H. Huang et al., Phys. Rev. B 90, 195105 (2014)

11:30am LS-MoM-14 Innovative High Energy X-Ray Characterization of Interfaces for Quantum Application, *Andrea Sartori, Jakub Drnec,* ESRF, France

Small layered junctions, integral to quantum applications, typically comprise thin films, often conductors or superconductors, separated by thin oxide layers. These junctions play critical roles in various quantum devices, including Josephson junctions, thermionic devices and parametric amplifiers. However, characterizing these structures poses significant challenges due to their small dimensions and complex compositions. Traditional techniques like cross-sectional SEM and TEM offer limited insights and may be destructive. While X-ray Reflectivity (XRR) provides valuable out-of-plane electron density profile information for these junctions, it lacks the in-plane spatial resolution required for detailed analysis. Here we introduce a novel approach utilizing High Energy XRR Tomography (HEXRR-Tomo). Unlike conventional XRR, HEXRR-Tomo enables spatial mapping of the entire surface, allowing for the potential reconstruction of a high-resolution 3D electron density map of the junction. This technique promises to offer easily accessible and non-destructive insights into the thickness, density, and roughness of individual layers within the junction, thereby advancing our understanding of their structure and properties.

In this contribution, we will present preliminary examples of the technique, demonstrating our ability to visualize the morphology and key features of various devices with specific applications. For instance, one example involves a thermoionic junction comprising complex layers of Si, SiO_2, Al, and V (Fig. 1), which is utilized as a cooling device for cryogenic temperatures. Another example features $NbAlAlO_xAlNb$ films and NbTiN

structures on a Si wafer, which serve as Josephson junctions for quantum computing and as parametric amplifiers, respectively. Further analysis will provide information about the roughness and thickness of each individual layer.

Nanoscale Science and Technology
Room 114 - Session NS1-MoM

Water and Ionic Transport at the Nanoscale
Moderator: Mark Hersam, Northwestern University

8:45am **NS1-MoM-3 Phase Separation and Oxygen Diffusion in Resistive Memory**, *Yiyang Li,* University of Michigan **INVITED**
Resistive memory is a promising technology that conducts memory and computation through the migration of oxygen in transition metal oxide. Understanding the mechanisms of oxygen migraiton is critical towards understanding the functionality of resistive memory devices. In this talk, we present our recent research on the materials thermodynamics and kinetics principles that govern ion motion in oxide-based resistive memory. Using a combination of device measurements, materials characterization, and multiscale physical modeling, we find that oxygen vacancies do not obey Fick's First Law of diffusion as conventionally believed, but instead undergo composition phase separation, which enables diffusion against the concentration gradient. This work yields design rules for nonvolatile memory devices based on composition phase separation.

9:15am **NS1-MoM-5 Advanced Aqueous Separations Using Membranes with Tailored 1D and 2D Confinement**, *Seth Darling,* Argonne National Laboratory
Solute transport in confined environments is a subject of profound interest and ongoing exploration, with recent advancements pointing toward transformative possibilities. Traditional hindered transport theory, a longstanding framework for understanding solute movement through cylindrical pores, underscores the significance of convective and diffusive hindrance in impeding solute permeation, thereby limiting sharp solute separations by membranes. However, breakthroughs in membrane technology, particularly the utilization of near-perfect isoporous membranes, offer new avenues to surmount these limitations. By leveraging nanofabricated, defect-free silicon nitride membranes and employing recirculated feed strategies to enhance solute-membrane interactions, we have achieved encouraging solute rejections, effectively barring solutes larger than the pore size while facilitating the passage of smaller solutes. This advancement not only represents a departure from historical constraints but also holds promise for unprecedented membrane separations through meticulous process design and tight pore-size distributions. Concurrently, the integration of two-dimensional (2D) materials into membranes introduces a distinct paradigm for ion transport and separation applications. These membranes exploit interlayer galleries to drive separation and selectivity, with specific transport properties shaped by chemical and structural modifications within the interlayers. A novel approach involving exfoliated and restacked phyllosilicate minerals with molecular crosslinkers allows precise control over interlayer spacing, influencing ion diffusivities in the resulting crosslinked 2D membranes. These membranes, characterized by tunable ion diffusivities, provide a platform for systematic studies of confined ionic transport, offering insights into fundamental mechanisms governing solute movement in nanoconfinement and paving the way for synergistic advancements in membrane-based separation technologies.

9:30am **NS1-MoM-6 Radioactive Tracer Diffusion through TPT-CNMs**, *Andre Beyer*, *Neita Khayya, Armin Gölzhäuser,* Bielefeld University, Germany
In recent years, Carbon Nanomembranes (CNMs) have emerged as an innovative class of 2D materials known for their exceptional combination of high selectivity and permeation properties, with a particular emphasis on p-[1,1',4',1"]-terphenyl-4-thiol (TPT)-CNM with a thickness of about 1 nm. Such CNMs combine a rapid water permeation with ultrahigh ionic exclusion in aqueous solution [1]. Here, we report permeation measurements of carbon dioxide and water through TPT-CNMs, which were conducted with concentration-gradient-driven transport of radioactive tracer molecules, specifically [3H] H_2O, [14C] $NaHCO_3$, and [32P] H_3PO_4. Our investigation explores the impact of the pH value on the diffusion process. The equilibrium ratio of carbon dioxide and the corresponding anions change with the pH value. Therewith, an independent characterisation of the diffusion of carbon dioxide and its anionic forms appears to be feasible.

Considering concentration polarization and outgassing effects, our results align with previously obtained radioactive diffusion data for a neutral pH value of 7 [2]. Interestingly, despite the electrostatic barrier associated with TPT-CNM in neutral aqueous environments, our observations indicate enhanced permeation of anions in the basic range of pH.

[1] Y. Yang et al., ACS Nano 12, 4695 (2018); Y. Yang et al., Adv. Mater. 32, 1907850 (2020).

[2] R. Dalpke, A. Dreyer, R. Korzetz, K. J. Dietz, and A. Beyer, J. Phys. Chem. Lett. 11, 6737 (2020).

9:45am **NS1-MoM-7 Molecular-Resolution Elucidation of Ice Defects Formed by Liquid Water Crystallization**, *Jingshan Du,* Pacific Northwest National Laboratory; *Suvo Banik,* University of Illinois - Chicago; *Henry Chan,* Argonne National Laboratory; *Birk Fritsch,* Helmholtz Institute Erlangen-Nürnberg for Renewable Energy, Germany; *Ying Xia,* University of Washington; *Andreas Hutzler,* Helmholtz Institute Erlangen-Nürnberg for Renewable Energy, Germany; *Subramanian Sankaranarayanan,* University of Illinois - Chicago; *James De Yoreo,* Pacific Northwest National Laboratory
Despite the ubiquity of ice, defects in ice formed by water crystallization have never been directly observed on the molecular scale. Here, we report the stabilization and Ångstrom-resolution electron imaging of ice I_h crystallized from liquid water. Combining lattice mapping and molecular dynamics simulations, we show that ice is highly tolerant to nanoscale defects such as misoriented subdomains and trapped gas bubbles, which are stabilized by molecular-scale structural motifs. We discovered subdomain-rich regions near the defective crystal edges despite the structure appearing single-crystalline according to diffraction criteria. These subdomains connect via low-angle grain boundaries with flat energy landscapes as a function of tilt angles, showing the high tolerance of ice to defect structures. Furthermore, bubble surfaces adopt low-energy nanofacets and create negligible strain fields in the surrounding crystal. These bubbles can dynamically nucleate, grow, migrate, dissolve, and coalesce under electron irradiation and be monitored in situ near a steady state. This work opens the door to understanding water crystallization behaviors at an unprecedented spatial resolution and provides new research paradigms to the theory, modeling, and forecasting of ice crystallization and melting in environmental, biological, and material systems.

10:00am **NS1-MoM-8 Reduce Liquid Waste and Improve Throughput in CVD and ALD Processing**, *Kathleen Erickson,* MSP - A Division of TSI
Liquid Flow Controllers (LFCs) are routinely used with vaporizers in gas-phase processing to improve process repeatability, precision and adjustability. In the microelectronic industry LFCs are used to vaporize liquid precursors for Chemical Vapor Deposition (CVD) or Atomic Layer Deposition (ALD). Due to high precision requirements and long LFC flow control response/stabilization times (time to reach and maintain ±1% of set-point), liquid or vapor divert schemes are often used in CVD and ALD. In this scenario, the liquid or vapor is diverted to exhaust until the LFC is able to reach and stably maintain the setpoint. Legacy LFCs can have response times on the order of 4-9 seconds. These long stabilization times, result in significant time sending vapor/liquid to the diverter line – meaning more liquid waste. More liquid is consumed, pumps are exposed to more liquid, and remediation systems have a higher load. Increased liquid waste negatively impacts cost of ownership in increased liquid precursor source cost, reduced pump lifetime, and increased maintenance requirements.Additionally, it worsens the environmental impact of these semiconductor processes. As more and more semi processes run short processing times, this long response time is becoming increasing problematic to throughput as well. For long processes, LFC response times have a relatively small impact on throughput; in a 150 second process, a 3 second liquid flow stabilization time only adds 2% to the processing time - still significant, but perhaps not intolerable. However, for short process times, like short pulse CVD or ALD, the stabilization time of the LFC can become a much larger percentage of the processing time.For example, in a 6 second short pulse CVD process, a 3 second response time increases deposition times by 50%.

This presentation will introduce a new Liquid Flow Controller (Turbo LFC) designed specifically for semiconductor processing. The Turbo LFC can reach ±1% of set-point within 0.3s – a significant improvement over conventional LFCs. The fast response time is a result of a high-speed sensor, which can also provide advantages in process control. A fast sensor enables a faster feedback control loop which can result in tighter control. This high-speed LFC also opens the possibility for measuring the delivered mass of vapor pulses (0.05 – 1+s), providing an alternative to ALD valves, which

provide no feedback on mass flow rates and are affected by line pressure and temperature. Details on Turbo LFC design and performance data will be reviewed, including the accuracy, repeatability and response time, and the impact of ambient temperature and line pressure on performance.

Nanoscale Science and Technology
Room 114 - Session NS2-MoM

Imaging at the Nanoscale including Focused Ion Beam and Electron Microscopy
Moderator: Mausumi Mahapatra, Loyola University Chicago

10:30am NS2-MoM-10 3D Reconstructions of Dislocation Networks via Focused Ion Beam Electron Channeling Contrast Imaging, *Julia Deitz, Andrew Polonsky, Timothy Ruggles, Luis Jauregui, Andrew Allerman,* Sandia National Laboratories   **INVITED**
Electron Channeling Contrast Imaging (ECCI) performed in a scanning electron microscope (SEM) serves as a rapid method for structural defect characterization in a wide array of crystalline materials such as metals and semiconductor materials/devices. Largely due to ease associated with sample preparation, much of this characterization has been performed in plan-view. The ability to instead perform ECCI cross-sectionally is advantageous for characterization of defects below 150 nm of the surface, sometimes at buried interfaces. Additionally, cross-sectional ECCI would demonstrate the potential to achieve three-dimensional (3D) analysis of dislocation networks, giving more detail on dislocation-dislocation interactions. With increases in serial sectioning implementations in the focused ion beam (FIB) SEM, automation routines are well positioned to obtain 3D dislocation network reconstructions. In this contribution, we demonstrate a 3D reconstruction of a dislocation network in an AlGaN via ECCI performed in the FIB-SEM and discuss practical challenges to collecting this data.

Sandia National Laboratories is a multi-mission laboratory managed and operated by National Technology and Engineering Solutions of Sandia, LLC., a wholly owned subsidiary of Honeywell International, Inc., for the U.S. Department of Energy's National Nuclear Security Administration under contract DE-NA0003525.

11:00am NS2-MoM-12 Transmission Electron Microscopy Investigation of Carbon Nanotube Growth on Stainless Steel Substrates, *Joshua Hancock, Richard Vanfleet,* Brigham Young University
Carbon nanotubes (CNT) are a unique nanomaterial with a wide variety of research applications. One of the most common chemical vapor deposition (CVD) methods to grow CNTs is via the thermal decomposition of a hydrocarbon precursor gas by a metallic catalyst. This is usually done using an iron catalyst deposited on a "noble" or nonreactive substrate, such as alumina. In this setup, the foreign iron is treated to form nanoparticles on the substrate that act as the active sites for CNT growth. Stainless steel is a novel substrate because it does not require the addition of a foreign catalyst to grow carbon nanotubes. Instead, the substrate itself can be treated to become catalytic for CNT growth.

We investigate the effects of CNT growth on stainless steel and form a model for how nanotube growth occurs on the substrate. 316 stainless steel chips are first exposed to a flow of air at high temperature to oxidize the surface. The gas flow is then switched to ethylene to reduce the oxide layer and initialize CNT growth. The active temperature and exposure time of these steps are varied between samples to understand how each affects the growth and how the growth process evolves over time.

To better understand the growth mechanisms, we investigate the CNT-substrate interface at the base of the nanotubes. Focused ion beam (FIB) processing was used to create cross-sections of the CNTs and substrate. To protect the original material from ion beam damage and to contrast redeposited material, samples were coated in a thin layer of alumina using atomic layer deposition (ALD) prior to FIB processing. The final cross-sections were analyzed in a scanning transmission electron microscope (STEM) to allow for high resolution imaging and energy dispersive x-ray spectroscopy (EDX).

Results from STEM and EDX analysis have allowed us to form a basic model for CNT growth on stainless steel. CNTs were seen to grow out of iron-rich metallic nanoparticles embedded in the oxide layer. The oxide layer was also seen to lose iron over time, suggesting that these iron nanoparticles were reduced out of the oxide by the hydrocarbon precursor gas. The base particles were seen to sink into the oxide, leaving a hole when CNTs were removed. The diameters of the nanotubes were also seen to grow over time, suggesting that carbon infiltration is actively coating our CNTs. The effects of the sinking particle and infiltration quickly isolate the catalyst, leading to very short CNTs (1-10 microns).

11:15am NS2-MoM-13 Focused Ion Beam Species Affect Beam Chemistry Applications, *Gavin Mitchson,* Thermo Fisher Scientific
Some modern plasma focused ion beam (PFIB) systems offer the capability to switch between multiple ion species. Each ion species (typically xenon, argon, oxygen, or nitrogen) can exhibit unique strengths and weaknesses for specific materials or applications. For example, oxygen often performs exceptionally well for cross sectioning resin-embedded samples and polymeric materials [1-3]. Low energy argon polishing can provide enhanced TEM image quality [4, 5]. However, signification portions of the parameter space remain unexplored and fundamental questions around limits of performance remain unanswered.

Beam chemistry is a critical component for many applications and to-date the effect of ion species in this space remains unexplored. For example, high quality protective caps are critical for most cross-sectioning and TEM lamella preparation processes. These protective caps are typically formed using at least one of a metallic precursor, a non-metallic carbonaceous precursor, or an insulating silicate-based precursor. In other situations, etchant precursors provide either selective material removal, enhanced material removal rates, or improved surface finish quality [6]. Since the initial PFIB system development and release, most workflows have relied on the Xe^+ ion species for beam chemistry processes. Critical knowledge around how other ion species perform with different beam chemistry precursors is missing.

We report the results of an extensive survey of different ion species and beam chemistry precursor combinations. All the ion species are capable of depositing various materials, although there are differences in the density of the deposited material and typical growth rates. Materials deposited using lighter ion species (argon, oxygen, and nitrogen) typically exhibit significant porosity and bubble formation when the ion beam energy exceeds some threshold, typically between 2-5 keV, which can obfuscate the relative yield comparisons (see Figure 1). For xenon, higher beam energies (below about 12 keV) are typically adequate for dense non-porous depositions. We also observed some interesting differences in etch rate as a function of halogenated etchant gas flow rate for argon and xenon ion species when milling silicon and aluminum substrates. For aluminum, the etch rate suppression or enhancement depends on the ion species, beam energy, and etchant precursor (Figure 2). We speculate that the different interaction volume sizes affect the relative kinetics of the possible gas-sample interaction pathways.

11:30am NS2-MoM-14 Detection Efficiency Enhancement for Deterministic Single Ion Implantation, *Kristian Stockbridge,* Ionoptika, Ltd., UK*; David Cox,* University of Surrey, UK*; Gianfranco Aresta,* Ionoptika, Ltd., UK*; Roger Webb, Steven Clowes, Ben Murdin,* University of Surrey, UK
Techniques for deterministic implantation of single ions are currently of high interest for quantum tech-nology applications such as single photon emitters[1,2] and solid-state qubits[3]. Here we present our capabilities for single ion implantation over a range of ion species into different target materials at different implant energies (<100keV) using a liquid metal alloy ion source (LMAIS) Ionoptika Q-ONE single ion implanter.

For some systems their low secondary electron (SE) yield can limit our ability to efficiently detect single ion implantation, and this therefore limits the number of error-free deterministic implants we can ex-pect to achieve. We present on-chip ion beam induced charge (IBIC) detection for 25keV Bi+ and 50keV Bi2+ implantation into a Si device. The detection efficiency using IBIC is increased close to 100%. Alt-hough coincident SE detection was performed, the active substrate suppressed the emission of SEs such that the on-chip detection dominated.

$SiO2$ appears to be the target which gives consistently the best secondary electron detection efficiency. We therefore also investigate implantation through thin films of atomic layer deposited (ALD) $SiO2$ to enhance the detection efficiency of targets where on-chip detection may be incompatible.

[1] T. Herzig et al., Diamond for Quantum Applications Part 2, Semiconductors and Semimetals, Elsevir, 2021, Vol. 104, Chapter 1, pp 1-30

[2] K. Groot-Berning et al., 'Deterministic Single-Ion Implantation of Rare-Earth Ions for Nanometer-Resolution Color-Center Generation', Phys. Rev. Lett., vol. 123, p. 106802 (2019).

[3] M.T. Mądzik et al. 'Conditional quantum operation of two exchange-coupled single-donor spin qubits in a MOS-compatible silicon device', Nat Commun, vol. 12, p. 181 (2021).

Plasma Science and Technology
Room 124 - Session PS1-MoM

Plasma Processes for Advanced Logic

Moderators: John Arnold, IBM Research Division, Albany, NY, **Angelique Raley**, TEL Technology Center America

8:15am **PS1-MoM-1 Mechanism of Formation of Roughness During Ru Direct Etching**, *Miyako Matsui,* Hitachi Ltd., Japan*; Makoto Miura, Kenichi Kuwahara,* Hitachi High-Tech Corp., Japan

Scaling of logic devices is still mainly driven by fabricating three-dimensional structures. As device scaling continues, alternative metal interconnects are required to replace Cu that enable reduction of metal pitch at the back end of the line. Ru is a candidate for an alternative interconnect material with metal pitch of 20 nm and beyond because a Ru interconnect is expected to have lower effective resistance than that of a Cu interconnect at such small pitches. Ru is expected to be etched directly, which leads to new scaling boosters such as semi-damascene patterning. In addition, to reduce interconnect resistance, roughness or other damage should be suppressed. In our previous study, we investigated the mechanism of Ru etching and the effects of protection layers formed on the sidewall of a line-and-space Ru pattern etched using Cl_2/O_2-based plasma. In this study, we investigated the mechanism of formation of line-width-roughness (LWR) of a Ru pattern with 32-nm pitch by using Cl_2/O_2-based plasma. We also investigated the influence of mask-pattern roughness and Ru line grain-boundaries on LWR.

We investigated the influence of the roughness of the Si_3N_4 mask pattern on that of the Ru pattern. Before and after Ru etching, LWR was measured by a high voltage CD-SEM, namely, critical-dimension-scanning electron microscope using an incident electron beam at energy of 45 keV. The high voltage CD-SEM was used to simultaneously measure both LWR of the mask-pattern and that of the Ru line. LWR of the mask pattern was measured from the image formed by the secondary electrons and that of the Ru line was measured from the image formed by the backscattering electrons (BSE). These measurements showed that after the Ru etching, LWR of the Si_3N_4 mask pattern and that of the Ru line depend on ion flux, which was adjusted by changing the duty cycle of wafer bias power. When wafer bias power was applied continuously, width of the Si_3N_4 mask became larger and LWR became smaller because the Si_3N_4 mask was widened by the re-deposition of the Si containing by-product. On the contrary, LWR of the Ru line remained mostly constant even when the ion flux was reduced. According to these results, it is necessary to measure LWR of the Ru line from BSE images because LWR of the mask after etching and that of the Ru line are not necessarily correlated.

We also investigated the effect of the grain boundary of Ru on LWR formed at the edge of the Ru line pattern. It was found that sidewall etching tends to proceed from the grain boundary. Accordingly, it is important to prevent the grain boundary from being etched by forming uniform passivation layers on the sidewall.

8:30am **PS1-MoM-2 Enabling Advanced Beol Interconnect Scaling Through Ruthenium Subtractive Etch Patterning**, *Shravana kumar Katakam,* IBM Research Division, Albany, NY*; Nicholas Joy, Dayun Yan,* TEL Technology Center, America, LLC, Albany, NY*; Christopher Penny, Chanro Park, Koichi Motoyama, Hosadurga Shobha, Yann Mignot, Joe Lee,* IBM Research Division, Albany, NY

With the ever-increasing demand to shrink the critical dimensions (CDs) for advanced technology complementary metal–oxide–semiconductor (CMOS) nodes, the demand to shrink the backend-of-the-line (BEOL) metal line pitch is also increasing. Traditionally, the copper (Cu) damascene process has been the main candidate, but modeling results indicate that it may be difficult to scale Cu damascene processes beyond 20nm pitch due to increase in-line resistance. In this regard, ruthenium (Ru) metal is a potential candidate for replacing copper for tighter pitch nodes beyond 20nm pitch. This is attributed to its superior electrical performance compared to traditional copper resistance at these line widths. Ru patterning is through subtractive etch as opposed to damascene process for Cu metals and it has been established that Ru can be patterned easily using chlorine (Cl_2) and oxygen gas (O_2) chemistries due to formation of volatile by products for relaxed pitches, but we run into difficulties as the pitch becomes tighter than 20nm pitch (P20).

The unique challenges during patterning at P20 or less are attributed to significant hardmask swelling from HM re-deposition during the etching process resulting in incomplete Ru etch at the regions affected by HM swelling. Additionally, the oxide re-deposition also results in severe RIE lag demanding a significant amount of over etch compromising pattern fidelity at min pitch structures.

In this work, we have systematically analyzed the changes to the plasma as the etch progresses and identified a possible mechanism for the HM swelling. With the understanding of these mechanisms, we were able to tune the plasma parameters to successfully reduce the HM swelling significantly to the levels that can be tolerated at the tighter pitches of P18 and beyond. We will also enlist some possible approaches to reduce swelling in the context of scaling the Ru etch for even tighter pitches of P16 and beyond.

8:45am **PS1-MoM-3 Atomic Level Control of Plasma Etching Using Various Pulsing and Cyclic Technologies for Leading-edge LSI**, *Masaru Izawa,* Hitachi High-Tech Corp., Japan **INVITED**

The cell size of logic LSI has been reduced by adopting Design-Technology Co-Optimization (DTCO) and pitch scaling using double patterning or EUV lithography. Recently, Gate-All-Around (GAA) FETs are being developed for the production of advanced nodes. For the fabrication of leading-edge devices, not only high selective vertical etching but also lateral etching is required. In terms of vertical etching, various pulsing technologies have been investigated, including gas switching using microwave ECR (M-ECR) plasma. For lateral etching, DCR (dry chemical removal) with IR lamp has been applied. This paper discusses some etching challenges in leading-edge devices, particularly related to EUV, DTCO, and GAA.

In EUV tri-layer etching, a mask reconstruction process (MRP) has been developed [1], where area-selective deposition is applied to reduce line-width roughness (LWR) and protect the EUV resist. In Si/SiGe fin etching, an atomic layer etching (ALE) function that includes source, wafer RF bias, and gas pulsing is adopted to achieve a vertical profile with high selectivity. Additionally, hydrogen gas is added to suppress etch depth and CD differences between Si and SiGe fin profiles [2]. In WFM (work function metal) patterning, DC pulse technology is applied to minimize fin damage [3]. The erosion of the fin top is reduced by 57% using this technique, and charging effects are also mitigated by using DC pulses. Furthermore, lateral etching processes using the DCR tool have been studied [4]. For example, etching a 2.5 nm space in Si_3N_4 film using a thermal cyclic ALE scheme was achieved without microloading. Lateral etching of SiO_2 and W has also been investigated.

[1] A. Amend, PS+TF-MoM-10 in AVS 69 (2023).

[2] Y. Ishii *et al.*, Jpn. J. Appl. Phys. **57**, 06JC04 (2018).

[3] R. Ochiai *et al*, JSAP spring meeting, 2021, 19a-P04-9.

[4] K. Shinoda *et al.*, J. Phys. D **50**, 194001 (2017).

9:15am **PS1-MoM-5 Investigating Plasma Interaction with Ultrathin Polymethylmethacrylate Films for EUV Lithography**, *Shikhar Arvind, Esben Witting Larsen, Philippe Bezard, John Petersen, Stefan De Gendt,* IMEC, Belgium

State-of-the-art extreme ultraviolet (EUV) lithographic scanners can now pattern with 12 nm half pitch resolution. To enable this high-resolution patterning requires the use of ultrathin (sub-50 nm) photoresists (or resists). This is due to pattern stability concerns of high aspect ratio structures, as well as the exceptionally short depth of focus of high numerical aperture (NA) scanners[1]. But the use of ultrathin resists further complicates pattern transfer as unintended plasma-induced effects during dry etching are more pronounced. The vacuum ultraviolet (VUV) photons generated in plasma are of particular interest for us as they can cause considerable resist modification. A better understanding of the interaction of plasma species, particularly of VUV photons with ultrathin resists is critical for enabling pattern transfer of sub-10 nm features.

Here, we study the impact of VUV photons, argon ions, and argon plasma on a 40 nm thick polymethylmethacrylate (PMMA) film[2]. Using a deuterium lamp, an industrial ion beam etch tool, and an industrial inductively coupled plasma etch tool, we exposed the polymer to VUV photons, ions,

and plasma, respectively. The exposed samples were then analyzed for chemical and physical changes using multiple characterization techniques. We observe that the thin resist thickness caused the vacuum ultraviolet photons interact with the entire bulk of the PMMA film, while the ions only affect the surface and near surface region. The photon exposed samples formed smaller polymer fragments at low exposure doses and further started to crosslink at high doses. In contrast, the ion modification led to carbonization of only the top few nanometers of the polymer film, leaving the bottom bulk intact. The plasma exposed sample showed changes characteristic to both vacuum ultraviolet photons and ions, and their synergism. It was stratified with a 1.34 ± 0 .03 nm thick ion-caused carbonized layer on top of 13.25 ± 0.12 nm photon-induced crosslinked layer. By studying the impact of the individual plasma constituents on ultrathin PMMA, we thus establish a baseline testing methodology for plasma-resist interactions on a simple model system, which we will further deploy on novel resists for EUV lithography.

References:

1. A. Burov, A. Vaglio Pret, and R. Gronheid, "Depth of focus in high-NA EUV lithography: a simulation study," in SPIE Photomask Technology 2022.
2. Shikhar Arvind, Esben W. Larsen, Philippe Bezard, John Petersen, Stefan De Gendt; Impact of vacuum ultraviolet photons on ultrathin polymethylmethacrylate during plasma etching. *J. Vac. Sci. Technol. A* 1 May 2024; 42 (3): 033009. https://doi.org/10.1116/6.0003541

9:30am **PS1-MoM-6 In situ Hard Mask Growth for Break Healing in Ultra-Thin Layers Patterning**, *Rémi Vallat, Philippe Bézard, Bhavishya Chowrira,* IMEC, Belgium*; Atefeh Fathzadeh,* ku Leuven and Imec, Belgium*; Konstantina Filippidou, Laurent Souriau, Kurt Ronse,* IMEC, Belgium

One of the challenges introduced by High NA EUV lithography include defectivity management, particularly when working with (ultra-)thin resists and low EUV exposure doses[1]. Reducing the bridges and breaks density is thus a major point of focus when patterning Line/Space[2]. Traditionally, a descum step is used to remove bridges, resulting in a reduced resist budget for underlayer patterning and leading to the creation of breaks. Therefore, recovering breaks is a strategic capability for defect reduction.

The method consists of patterning an underlayer of suitable thickness for thin resists and run an in situ PECVD process onto this underlayer, selectively to the material below in order to prevent and recover breaks[3]. This way, the hard-mask budget is increased in-situ during the etch process to prevent the formation of breaks while patterning from a thin underlayer (~10nm). This approach is presented in Fig1. Moreover, this method offers a reduced environmental footprint compared to conventional one as thinner ULs need fewer Global Warming Potential gases (GWP)[4]. Patterning of such ultra-thin layers (≤5nm) may come with high bridge/ break density which can be addressed by using this break healing strategy, thanks to in-situ selective HM growth.

In this work, the selectivity of deposition has been achieved, along with a notable decrease in break density and these results are shown in Fig2 and Fig3. However, the presence of additional deposited material brings new challenges. The focus of this work is to investigate the etch mechanisms which occur at the amorphous Carbon layer level, as well as to ensure the pattern transfer uniformity. Preliminary defectivity measurements will also be explored. Applications for both resist types, CAR and MoR, will be discussed. MoR is expected to induce more breaks, particularly problematic for low dose strategies. In addressing this issue, our break healing strategy emerges as a potential candidate for further exploration.

[1] L. Meliet al,*Proc. SPIE*11609, 116090P (2021)

[2] P. De Bisschop, *J. Micro/Nanolithogr. MEMS MOEMS*16, 041013 (2017)

[3] R. Vallat et al, *AVS69*, (PS+NS+FrM-3) (2023)

[4] P. Bézard et al. *Advanced Etch Technology and Process Integration for Nanopatterning XIII*. SPIE (2024)

9:45am **PS1-MoM-7 Plasma Etching of Low K Materials from Room Temperature to -40ºC in Different Fluorine-Based Chemistries**, *Daniel Santos, Christophe Vallee,* University at Albany-SUNY

Plasma etching of ultra-low-k materials at aggressive back end of line (BEOL) nodes has become increasingly challenging as plasma induced damage becomes a significant challenge to overcome. Conventional reactive ion etching (RIE) processes usually occur at a temperature near room temperature or higher in which diffusion of radicals will damage low-k materials surface. Alternatively, to limit diffusion mechanisms and prevent damage, cryogenic cooling of a substrate sub <-100 C can be used.

However, cooling substrates and controlling surface exposed to plasma to temperature down to -110C in 300 mm etching chamber is a technical challenge. This is why alternative solutions can be found using a low temperature process (down to -60ºC) that behaves like a cryogenic process. For this work we propose to study the plasma etching of low k materials exposed to different fluorine precursors with a substrate temperature going from room temperature to -40ºC. For this purpose, we use a 300 mm dual frequency CCP chamber equipped with a low-temperature electrostatic chuck to conduct our experiments. A shadowing methodology is used to study the plasma/surface reactions with surfaces exposed to radicals only and surfaces exposed simultaneously to radicals and ions. By way of comparison, we chose to use two precursors with very different properties:

1. a fluorocarbon precursor with a high triple point temperature favoring condensation mechanisms, for which we observed a switch from an etching regime to a deposition regime in RIE mode at T = -20ºC. However, the shadowing mask study shows that when the surface is only exposed to radicals, the regime is always the same, deposition.
2. NF_3 gas which has a very low triple point temperature that should not do any deposition. When lowering the temperature, not only is the etching regime not suppressed, but its speed is also increased. This result is explained by the increases of surface coverage by F etching radicals. Using the shadowing methodology, we observed that the etching is highly suppressed at -40ºC compared to room temperature in the absence of ions

Patterned damascene structure are also tested to observe the benefits of low temperature etching. Furthermore, we propose to add hydrogen to NF_3 plasma to promote HF formation and study its impact on low k etching when going from room temperature to -40ºC.

10:00am **PS1-MoM-8 Mitigating Plasma-Induced Damage in Low-K SiCOH Thin Films by Cryogenic Etching Process**, *Rajib Chowdhury, Thomas Poché, Seonhee Jang, Yonatan Tesfamariam,* University of Louisiana at Lafayette

The integration of semiconductor chips to enhance their performance has led to the widespread use of low-dielectric-constant materials with a relative dielectric constant of k ≤ 3.5, particularly as intermetal dielectric (IMD) materials within multilevel interconnects. This choice aims to minimize resistance-capacitance delays associated with microchip operation. Plasma etching of low-k materials presents a significant challenge due to plasma-induced damage (PID), which can increase the k-value and degrade its quality. This degradation is attributed to factors such as the formation of polar bonds, losing surface hydrophobicity, and carbon depletion.

To mitigate PID damage, this research focuses on reducing the degradation of low-k films during etching by employing a cryogenic process. Cryogenic conditions offer a promising strategy to alleviate PID damage, as etching by-products condense within the pores of the materials, protecting them from plasma-active radicals. By incorporating cryogenic etching process, significant reductions in dielectric degradation can be achieved.

Low-k SiCOH thin films were fabricated using plasma-enhanced chemical vapor deposition (PECVD) of the tetrakis(trimethylsilyloxy)silane precursor at room temperature. Dry etching process was conducted using CF_4, SF_6, CHF_3, and C_4F_8 gases at both room temperature and cryogenic temperatures (up to -120 °C) in an inductively coupled plasma-reactive ion etching (ICP-RIE) system. Tetraethyl orthosilicate (TEOS) oxide was used as a reference material for calculating etch rates and etch selectivity. The etch selectivity of the SiCOH film over the TEOS was compared between regular and cryogenic etching processes.

Fourier transform infrared (FTIR) spectroscopy identified four prominent bonds in the films which were C–H_x stretching, Si–CH_3 bending, Si–O–Si stretching, and Si–$(CH_3)_x$ bending vibration modes. The equivalent damage layer (EDL) was calculated based on the variation in the peak area of Si–CH_3 bending and Si–O–Si stretching peaks, with SF_6 gas causing the highest amount of EDL compared to other gases. However, all gases showed a decreasing trend in EDL value when etching was performed at cryogenic temperatures, indicating reduced PID damage.

Electrical properties such as the k-value, leakage current density, breakdown field, and time-dependent dielectric breakdown (TDDB) were also measured to evaluate an improvement in their electrical performance under cryogenic etching confirming reduced PID damage. These findings highlight the potential of cryogenic etching as a promising approach to mitigate PID damage and improve the quality of low-k films.

10:30am **PS1-MoM-10 Investigation of Cryogenic Fluorine-Based Etching of TaN with Selectivity to SiOCH Low-κ**, *Ivo Otto IV*, *Christophe Vallée*, University at Albany College of Nanotechnology, Science, and Engineering (CNSE)

The industry shift from silicon dioxide and aluminum as the respective dielectric and conductor within the back-end-of-the-line (BEOL) interconnect superstructure to SiOCH low-κ dielectric (ULK) and copper improved key metrics such as RC delay, but had inherent integration challenges, one of which was copper diffusion into the ULK film. The solution was the use of diffusion barriers, which are required in current integration schemes to prevent copper diffusion. TaN is a key diffusion barrier candidate because of strong dielectric adhesion and low in-plane resistivity properties at 2-3 nm thicknesses. Creation of the BEOL interconnect superstructure is completed in cycles to create each metal level, requiring the repeated selective removal of not only copper, but the TaN diffusion barrier, selective to the ULK.

ULK films attain dielectric constant values of between 2-3 by incorporating non-polar bonds (Si-CH$_3$) and pores into their structure, making ULK sensitive to abrasive processes like CMP and physical, ion-assisted etching. Radical-dominated, fluorine etching of TaN with respect to ULK also comes with challenges because of the high volatility of SiF$_2$, SiF$_4$, and CF$_x$ ULK etch byproducts. We have previously explored methods to accomplish radical fluorine etching of TaN with selectivity to ULK as an alternative landing process on the ULK, for BEOL integration. Selective deposition of an SiOF film on the ULK film compared to the TaN, while etching the TaN, allowed the selective etching of TaN with respect to ULK. In this work, we explore the use of radical NF$_3$/SiF$_4$ discharges, without O$_2$ addition (1), at sub-zero sample temperatures ranging from -45 °C to 0 °C (2). In this investigation, we seek to reduce the possibility of ULK damage by (1) removal of radical and atomic O interaction with the ULK film and (2) reduce the diffusion path for F to limit F diffusion through any SiF$_x$ deposition on the ULK, and to limit F diffusion within the SiOCH structure itself. *Ex-situ* spectroscopic ellipsometry is utilized to characterize film thickness changes after processing in addition to characterization of changes in film refractive index. *Ex-situ* X-ray photoelectron spectroscopy is used to probe the sample surface to characterize surface film properties, while *ex-situ* Fourier-transform infrared spectroscopy is used to analyze bulk changes in the SiOCH ULK bonding structure. Though this multi-modal investigation, we gain insight in the mitigation of SiOCH ULK damage using an O$_2$-free, sub-zero process to selectively remove TaN.

10:45am **PS1-MoM-11 Overview of Mutually Compatible Approaches for Sustainable Patterning Process Development**, *Philippe BEZARD*, IMEC Belgium; *Atefeh Fathzadeh,* KU Leuven and Imec, Belgium; *Remi Vallat, Konstantina Filippidou, Emily Gallagher,* IMEC Belgium; *Stefan De Gendt,* KU Leuven and Imec, Belgium; *Frank Holsteyns,* IMEC Belgium

Various approaches can be employed to ensure the sustainability of a process. One option is to utilize new molecules as reactants, aiming to reduce the quantities and/or the impact of emitted fragments in the atmosphere. If suitable candidate molecules are not available, materials that require environmentally harmful gases could be replaced with others that do not rely on such chemistries, for example, replacing a sacrificial SiO2 hard-mask with amorphous carbon. Alternatively, the process flow can be adjusted to avoid the need for these materials altogether.

When changing materials is not feasible, there are several ways to further minimize gas consumption. One approach is to increase throughput without increasing gas flows, often achieved by using higher RF powers or pressures. Thinning down the layer is another option, but this increases the selectivity requirements of patterning steps. In such cases, in-situ reconstruction of the hard-mask, as demonstrated by Vallat et al., can provide thicker, usable hard-masks at the expense of patterning a much thinner problematic layer [1].

To regulate the selectivity of hard-mask deposition and subsequent patterning steps, Transient Assisted Plasma Processing (TAPP) [2] can be employed to significantly reduce gas consumption while maintaining excellent patterning performance and compatibility with High-Volume Manufacturing throughput. Combining these hard-masks with etch processes based on TAPP is particularly appealing because it offers better control over the precursor's fragmentation, resulting in improved deposition selectivity at low substrate temperatures.

In a transient-assisted plasma etching process, these hard-masks can serve as a passivation source by carefully managing their sputtering while allowing the etch to proceed, eliminating the need for often problematic passivating gases. Furthermore, to further eliminate the requirement for environmentally harmful passivation gases, low-density plasmas can be utilized in conjunction with low partial pressure of reactants and overall gas flows. The scarcity of neutral species in such plasmas reduces the risks of bowing and undercutting, requiring minimal passivation to achieve the necessary patterning performance.

This paper will present an overview of the characteristics of these various approaches and illustrate how they can be combined to significantly reduce the consumption of environmentally harmful gases.

[1] Rémi Vallat, "Break healing and LER mitigation for low dose EUV exposure," in *AVS 69th , November 5-10,*(AVS 69th, Portland, OR, 2023).

[2] A. Fathzadeh, *J. Vac. Sci. Technol. A* 42, 033006 (2024), https://doi.org/10.1116/6.0003380

Plasma Science and Technology
Room 124 - Session PS2-MoM

Atmospheric Plasma Processing
Moderator: Michael Gordon, University of California at Santa Barbara

11:00am **PS2-MoM-12 Adapting Atmospheric Pressure Plasma Sources to Fit Diverse Applications**, *Michael Johnson,* Naval Research Laboratory, USA
INVITED

Atmospheric pressure plasma technology offers the potential to utilize plasmas in applications occurring outside the confines of a vacuum chamber, opening many new, exciting opportunities. However, generating a plasma at atmospheric pressure comes with challenges that limit its viability. In particular, large electric fields are needed to break down air (~30 kV/cm) while the generated plasma volumes are comparatively small, and energy can be quickly lost to gas heating. This presentation describes novel approaches to nonthermal plasma generation at atmospheric pressure that address these key hurdles to their wider adoption. Piezoelectric transformers are solid-state transformers that create large voltages via electromechanical conversion, providing a small form factor, high gain alternative for generating atmospheric-pressure plasma jets. These transformers enable the production of plasma jets with characteristics similar to those driven by standard high voltage power supplies while only requiring tens of volts. Given the low input voltages, multiple jets can be operated in parallel to facilitate a synergistic increase in plasma volume and enhanced control over species production. Alternatively, gas management can be used to expand the functional volume of jets without an increase in applied power. Additionally, nanosecond pulsed power approaches improve the energy efficiency of plasma production, which can be advantageously used to improve water remediation in a plasma-liquid reactor. Example systems will be discussed and described through a variety of plasma diagnostics to illustrate how the approaches to applied power and plasma generation impact the plasma properties and applications, with an eye on developing more sustainable and versatile plasma sources.

11:30am **PS2-MoM-14 Atmospheric Plasma Deposition of Bio-Based Composite Coatings for Enhanced Functional Properties of Paper**, *Kamal Baba, François Loyer, Nicolas Boscher, Patrick Choquet,* Luxembourg Institute of Science and Technology (LIST), Luxembourg; *Indira Husić, Arunjunai Raj Mahendran, Judith Sinic, Christoph Jocham, Herfried Lammer,* Wood K plus - Kompetenzzentrum Holz GmbH, Austria

Functional coatings on paper surfaces often rely on low-recyclable synthetic feedstock and wet chemistry techniques, leading to extended processing times and increased material usage. In this work, we address these challenges by the development of functional bio-based composite coatings reinforced with sustainable fillers using atmospheric pressure plasma as sustainability-oriented coating technology.

Various low viscosity acrylated biobased monomer, including Vanillyl Alcohol Methacrylate (VAM), Eugenyl Methacrylate (EM) and Isosorbide Methacrylate (IM), were used as resin to form the polymeric coating. while seashell particles (SS) or cellulose nanocrystals (CNC) were used as sustainable additives. The targeted applications of these formulations are the enhancement of release function, water vapor barrier and antimicrobial properties of paper substrates.

The polymerization of these different monomers was possible thanks to a liquid assisted dielectric barrier discharge approach with either Argon or

Nitrogen as plasma gases, and ultrasonic nebulization as monomer injection method. The plasma polymerization of coatings with a thickness ranging from 0.5 to 2 µm on Si wafers, Glassine and Barrier 60g paper was evidenced by FTIR, showing a successful conversion of vinyl double bonds. . The degree of conversion was calculated from the FTIR spectra to assess the effect of the plasma parameters on the polymerization and coating properties. Notably, the polymerization degree increases with the applied plasma power yielding longer polymer chains, as evidenced by high resolution mass spectrometry analyses. This technique revealed the possibility of favoring the formation of polymer compositions rich in organic mono- or di-methacrylate chains in a plasma-polymer matrix by adjusting the plasma power. SEM imaging confirmed the homogeneity of the coatings and a uniform distribution of the particles.The addition of SS and CNC particles to the VAM or EM coating affects both hydrophobicity and surface energy, likely impacting the release properties of the coated surface. The VAM composite coating exhibited the best release function for coated Glassine paper (<250cN/25mm according to Finat10/TESA 7475 test), whereas the lowest water vapor transmission rate for barrier paper was achieved with the EM composite coating (<50g/m^{2}day/bar).

On the other hand, antibacterial properties were achieved through plasma coating with isosorbide methacrylate alone, effectively targeting the E. Coli bacterial strain without the incorporation of any additional additives.

11:45am PS2-MoM-15 Atmospheric Air Plasma Pre-treatment of Plastics, *Aunic Goodin,* North Carolina State University*; Roxanne Walker, Jesus Alcala,* University of Michigan, Ann Arbor*; Tridip Das,* California Institute of Technology*; Shashwata Chakraborty, Sujoy Bepari, Debasish Kuila,* North Carolina A&T State University*; William Goddard,* California Institute of Technology*; John Foster,* University of Michigan, Ann Arbor*; Steven Shannon,* North Carolina State University

In 2018 almost 36 million tons of plastic waste was produced in the US with only 9% recycled that year. One of the limiting factors for reusing or recycling plastic waste is the difficulty of conversion into usable products. One potential solution for this is a plasma pretreatment followed by a catalytic deconstruction into C2-C4 olefins. Catalytic deconstruction of plastics is a viable method for using plastic waste. Atmospheric plasma is investigated primarily for cost-effective pretreatment of the plastics. The oxidation of the plastics through the plasma treatment provides a potential avenue for the catalyst to more easily break down the material. The initial concept is shown with a pin-to-plate discharge within vials for analysis of the gas by-products as well as material analysis. The combination of VUV, UV, electron, and ion bombardment modifies the surface of the polymer for oxygen absorption both during and after treatment from the oxygen in normal air. This oxidation will be measured and quantified through XPS, contact angle measurements, FTIR spectroscopy, and RAMAN spectroscopy. The analysis of the gas products through mass spectroscopy is compared to molecular dynamics and reactive force-field simulations to understand the mechanism of the process. The plastics polypropylene and polyethylene are treated as powders, beads, and sheets of varying particle size/thickness, molecular weight, and density. The variation of the samples gives an indication of the material shape and characteristics for future processing and also allows for different analyses depending on the material's shape and thickness. These plastics are also treated in liquid plasma for comparison of the surface modifications. Analysis of the products of the catalytic deconstruction is done by GC/MS to characterize potential value-adding C2-C4 olefins and compare the process with and without plasma treatment.

Quantum Science and Technology Mini-Symposium
Room 123 - Session QS1+VT-MoM

Vacuum Systems for Quantum Applications

Moderators: Freek Molkenboer, TNO Science and Industry, the Netherlands, **David Pappas**, Rigetti Computing

8:15am QS1+VT-MoM-1 High-Precision, Four-Way Comparison of Three Cold Atom Vacuum Standards and an Orifice Flow Standard, *Stephen Eckel, Daniel Barker, James Fedchak, Julia Scherschligt,* National Institute of Standards and Technology (NIST)

The cold atom vacuum standard (CAVS) is the first primary standard and sensor for vacuum in the ultra-high vacuum regime and below. By measuring the loss rate of ultra-cold atoms from a conservative magnetic trap, the CAVS infers the pressure of the surrounding vacuum from first principles calculations of the scattering cross section. Various CAVSs have been constructed or are under construction, with different sensor atoms, sizes, and technical capabilities. In 2023, we reported the first comparison of two CAVSs – a laboratory-sized version based on ^{87}Rb and a portable version based on ^{7}Li – to a traditional vacuum metrology apparatus, an orifice flow standard. This initial experiment showed agreement between all three at roughly the 2 % uncertainty level. Here, we report a comparison between three different CAVSs – a laboratory-sized version that can use either ^{7}Li or ^{87}Rb and a portable version that uses ^{7}Li – and our orifice flow standard. We anticipate our new comparison will have total uncertainties < 1 %. In combination with other studies, our results represent a stringent test of quantum mechanical scattering theory.

8:30am QS1+VT-MoM-2 Vacuum Based Quantum Technology with Aluminum Alloys for Space Applications, *Klaus Bergner, Florian Löwinger, Chris Gruber, Lara Gerlach, Sebastian Hüttl, Lukas Axtmann, Andreas Trützschler, Jan Hertel,* VACOM, Germany*; Jörg Schneider, Lars Kanzenbach, Torsten Schmidt, Sebastian Wieland, Daniel Richter,* Fraunhofer Institute for Machine Tools and Forming Technology IWU, Germany*; Jens Grosse, Marvin Warner, Michael Elsen,* ZARM Center of Applied Space Technology and Microgravity, Germany

The advancement of quantum technologies has opened new horizons for space applications with capabilities in communication and metrology. This talk explores the potential of vacuum-based quantum technology utilizing aluminum as a pivotal material to enabling access to a wide range of robust and miniaturized turn-key solutions. Vacuum systems used in these quantum physics package solutions often require low form factors, low weight as well as robust and economic design combined with a low magnetic susceptibility and low outgassing rates. But current first demonstrators mainly rely on expensive, bulky, fragile, and unique solutions.

To overcome these limitations, these systems demand the miniaturization as well as increased reliability of used vacuum systems. Optimization and up-scaling of manufacturing processes is key to distinguish competitive technologies for use in commercial applications. One key factor of this approach could be the use of aluminum alloys as base material of vacuum systems. An advantage of aluminum is simpler processing during manufacturing and the associated simpler miniaturization approach. However, the use of aluminum-based ultra-high vacuum (UHV) systems for space applications has not been qualified, nor have the effects of static and dynamic mechanical loads and temperature fluctuations been researched. Due to the complexity of this qualification work, in this joint paper we present the effects of mechanical and thermal influences on the critical system components - the releasable ConFlat (CF) sealing technologies.

The mechanical load of aluminum UHV CF sealing was characterized within a cooperation between Center of Applied Space Technology and Microgravity in Bremen and VACOM. The talk shows results of leakage rate due to static loads. In addition, a disadvantage of aluminum is the temperature limitation of only 120 °C. Within the cooperation between Fraunhofer Institute IWU in Chemnitz and VACOM it was possible to raise this limit up to 200 °C with our newly developed aluminum UHV CF sealing technology. Both results demonstrate the high temperature and mechanical stability of aluminum related CF sealing technology. In summary, this talk is intended to understand the demands of quantum space technology for vacuum systems and allows to develop a proper design of space suitable commercially viable solutions.

8:45am QS1+VT-MoM-3 Compact UHV Technology for Quantum, *Alex Kato,* IonQ   **INVITED**
UHV systems for quantum technology (E.g. sensors, computing) can be made smaller by moving away from conventional vacuum parts. I will review several ways in which size, weight, and power can be significantly reduced without sacrificing on desired system performance. This requires moving away from conventional vacuum components, such as off the shelf conflat flanges and windows, feedthroughs, and gauges.

9:15am QS1+VT-MoM-5 Quantum-Based Sensors and Standards with the NIST on a Chip Program, *Jay Hendricks,* NIST*; Barbara Goldstein,* NIST-Gaithersburg
The NIST on a Chip program (NOAC) is briefly introduced as a forward-looking vision of the future of measurement science.The world-wide redefinition of units that occurred on May 20th, 2019, has opened new ways

to think about metrology under a "zero-chain-traceability" paradigm.Next generation quantum-based sensors and standards, based on physical constants of nature, are briefly introduced, for pressure, vacuum, mass and more.The re-definition of the SI units enables new ways to realize the units for the kelvin, mass, and therefore the pascal. A new way to realize the pascal is exciting for vacuum technology (VT), will lead to other exciting applications. These quantum-based systems; however exciting, do raise new challenges and several important questions: Can these new realizations enable the size and scale of the sensor to be miniaturized to the point where it can be imbedded into everyday products?What will be the role of metrology institutes in this new ecosystem of measurement?Where will these new quantum-based systems go and what will they do? This talk will begin to explore these important questions.

9:30am QS1+VT-MoM-6 3D Printed Ion Traps for Quantum Computation, *Kristin Beck*, Lawrence Livermore National Laboratory   **INVITED**
Trapped atomic ions are one of the leading qubit candidates for quantum computing. The fidelity of quantum gates and the noise performance of a quantum processor built on this platform depends on the degree of isolation between the classical environment and the ions. One leading noise source is electric field noise. Additive manufacturing has introduced the possibility of generating accurate, replicable and scalable ion traps with geometries that promise to reduce sensitivity to this noise source. In this talk, I will describe miniaturized RF Paul traps that we have fabricated at LLNL using high-resolution 3D printing approach based on two-photon polymerization and share the results of initial tests.

Quantum Science and Technology Mini-Symposium
Room 123 - Session QS2-MoM

Quantum Simulations: Materials, Power Distribution, Computing, and Machine Learning Applications

Moderators: Andre Schleife, University of Illinois at Urbana-Champaign, **Sisira Kanhirathingal**, Rigetti Computing

10:30am QS2-MoM-10 Power System Dynamic Simulation with Generalized Quantum Carleman Linearization, *Jianing Chen, Yan Li,* The Pennsylvania State University   **INVITED**
The dynamics of power systems are described by a set of nonlinear differential-algebraic equations (DAEs). Over the past few decades, the expansion of the power system scale has led to a notable increase in the dimension of DAEs, posing a substantial challenge for conventional numerical integration methods to simulate power system dynamics. Herein, we introduce a novel generalized quantum Carleman linearization method to tackle dynamic simulation of large-scale power systems, substantially mitigating computational complexity compared to conventional methods. In light of the characteristics of nonlinear power system DAEs, they are transformed into 4th order inhomogeneous polynomial DAEs through a diffeomorphic transformation. By iteratively employing high-dimensional hyperplanes for approximating nonlinear algebraic equations, the classical ordinary differential equation solver, Carleman linearization, can be extended to solving the high-order DAEs of power systems. Consequently, the proposed method can yield a quantum state proportional to the solution of the DAEs in time $O(\log (n))$, exponentially smaller than the linear complexity of Euler's method. Numerical results demonstrate that the proposed method can successfully obtain the trajectory of dynamic simulation of power systems with small errors under various scenarios.

11:00am QS2-MoM-12 Quantum Computer Simulation of Near-Surface Oxygen Vacancies in α-Al$_2$O$_3$ (0001), *Vijaya Begum-Hudde, Yi-Ting Lee,* University of Illinois at Urbana-Champaign*; Barbara Jones,* IBM*; André Schleife,* University of Illinois at Urbana-Champaign
Aluminum oxide is a technologically-relevant material as it is employed in a wide range of applications such as catalysis, quantum devices, aviation, and ship industry, among others. Corrosion is a naturally-occurring process in this material, and due to its detrimental effect on the optimal performance, initiation and propagation of corrosion is an area of active research. The near-surface vacancy in the most stable phase, α-Al$_2$O$_3$, plays an important role in corrosion, and an improved understanding of the electronic structure is necessary to describe these processes.

We employ first-principles calculations and quantum simulations for an in-depth study of the near-surface O vacancies in α-Al$_2$O$_3$ (0001). The geometry of the relaxed Al-terminated pristine (0001) surface obtained with the hybrid exchange-correlation functional (HSE06) are consistent with X-ray diffraction results. Upon introducing an O vacancy, a shallow in-gap electronic defect state. Its band-decomposed charge density and that of the second unoccupied state reveal a strong charge localization near the O vacancy and the adjacent surface Al atom. We study these vacancy states with quantum-defect embedding theory (QDET) calculations to unravel their ground- and excited-state properties. We define an active space consisting of strongly localized states near the defect and treat the remainder as environment. An effective Hamiltonian is solved for the active space which includes the effective screening from the environment within the random phase approximation to obtain the eigenvalues with full configuration interaction (FCI).

Furthermore, we solve the effective Hamiltonian on a quantum computer by employing a model consisting of an active space of one occupied and one unoccupied band from the QDET calculation. On a four-qubit circuit with a Unitary coupled-cluster (UCC-3) ansatz, we calculate the ground-state energy for the active space with the variational quantum eigensolver (VQE). On the noiseless simulator, we achieve excellent agreement with the reference FCI values. Upon introducing noise with a noise model from hardware, the simulator renders an error of 0.19±0.03 eV. We use zero-noise extrapolation with global folding for error mitigation, and successfully reduce the error to 0.01±0.04 eV. Also, a subspace-search VQE implementation to calculate the excited-state eigenvalues for the minimum model results in very good agreement with the first and second excited FCI values.

11:15am QS2-MoM-13 Quantum Inception Score: A Quality Measure of Quantum Generative Models, *Akira Sone,* University of Massachusetts Boston
This presentation is based on our recent work [arXiv:2311.12163]. One of the most significant areas in quantum machine learning is quantum generative models. These models are a leading strategy for unsupervised learning, which focuses on uncovering hidden patterns in unlabeled data sets and classifying them. The primary goal of generative models is to train a generator to produce data with high accuracy and substantial diversity from a large amount of unlabeled data, reflecting their quality. Here, we focus on the quantum generative models where both the generators and classifiers are fully quantum. We introduce a novel quality measure called the quantum inception score, linking the classical capacity of the quantum channel playing a role as a quantum classifier. We demonstrate that the entanglement output generated by the quantum generator could contribute to further quality enhancement due to the potential superadditivity of the classical capacity. Also, we demonstrate that the quality degradation due to the quantum decoherence can be captured by using the quantum fluctuation theorems. We also show the application of the quantum inception score in the quantum phase classification in the one-dimensional spin-1/2 chain system. Our results underscore the importance of exploring quantum foundations and communication approaches in studying quantum machine learning protocols.

Advanced Surface Engineering
Room 125 - Session SE-MoM

Plasma-Assisted Surface Modification and Deposition Processes/Nanostructured and Multifunctional Coatings

Moderator: Diana Berman, University of North Texas

8:15am SE-MoM-1 Materials Design in Surface Engineering, *Johanna Rosen*, Linköping University, IFM, Sweden   **INVITED**
MAX phases are a family of atomically laminated ceramics where M is a transition metal, A is a group A element, and X is C or N. These materials are a playground for design of both three- and two-dimensional (3D/2D) phases, for diverse applications. MAX phases are to date primarily synthesized in powder form, but we present epitaxial thin films of Ti$_3$AlC$_2$ and Ti$_3$SiC$_2$ on sapphire through magnetron sputtering from three elemental targets. We show that Ti$_3$AlC$_2$ can be converted to 2D Ti$_3$C$_2$ MXene through selective etching of Al in hydrofloric acid (HF), while Ti$_3$SiC$_2$

can be transformed into 3D Ti_3AuC_2, $Ti_3Au_2C_2$ and Ti_3IrC_2 by noble metal substitution reaction, the latter forming high-temperature-stable Ohmic contacts to SiC. Evidence is also presented for synthesis of single-atom thick layers of gold by selective removal of Ti_3C_2 from Ti_3AuC_2 by Murakami's reagent. Insight into these 3D and 2D materials and the methods by which they are formed is given through a combination of first principles simulations and electron microscopy, which suggest additional pathways for design of new phases.

8:45am SE-MoM-3 Development of Texture in Ta₂C Thin Films Sputter-Deposited on Free-Standing Graphene, *Suneel Kodambaka,* Virginia Tech; *Koichi Tanaka,* University of Chicago

Thin crystalline films are commonly deposited on bulk solids and the development of texture (preferred orientation) in such thin films is reasonably well understood.[1] Efforts to grow highly crystalline thin films have included, for example, the use of low-energy ion irradiation[2] and van der Waals (vdW) epitaxy.[3] Exciting developments based on vdW epitaxy include the use of vdW buffer layers (e.g., graphene, and hBN) on crystalline substrates to grow highly oriented MoS_2 and $(VNbTaMoW)S_2$ thin films.[4, 5] Recently, Koichi *et al.*[6] reported that Ta_2C thin films sputter-deposited on hBN/Ta_2C surfaces are more highly oriented than those grown using the same deposition parameters on bare Ta_2C. These results led us to question the need for a bulk substrate and if crystalline thin films can be directly deposited on *free-standing* vdW layers instead.

Here, we present results obtained from sputter-deposition of Ta_2C films on monolayer-thick graphene substrates and on relatively thicker (~8 nm) amorphous silicon nitride (a-SiN_x) membranes supported by transmission electron microscopy (TEM) grids. Using plan-view TEM and selected area electron diffraction, we compare and contrast the microstructures of the Ta_2C films on graphene and a-SiN_x. We find that the Ta_2C layers deposited on a-SiN_x are composed of a mixture of nanoscale crystallites and non-crystalline phases, while the Ta_2C film on graphene is polycrystalline with grains that are oriented in-plane as $[2\text{-}1\text{-}10]_{film} || [10\text{-}10]_{graphene}$. These results indicate that even a single-atom-thick crystal can promote crystalline and oriented growth.

References

1. J. E. Greene, Critical Reviews in Solid State and Materials Sciences **11** (3), 189-227 (1983).
2. T. Lee, H. Seo, H. Hwang, B. Howe, S. Kodambaka, J. E. Greene and I. Petrov, Thin Solid Films **518** (18), 5169-5172 (2010).
3. A. Koma, K. Sunouchi and T. Miyajima, Microelectronic Engineering **2** (1), 129-136 (1984).
4. A. Deshpande, K. Hojo, K. Tanaka, P. Arias, H. Zaid, M. Liao, M. Goorsky and S. K. Kodambaka, ACS Applied Nano Materials **6** (4), 2908-2916 (2023).
5. K. Tanaka, H. Zaid, T. Aoki, A. Deshpande, K. Hojo, C. V. Ciobanu and S. Kodambaka, Nano Lett. **24** (1), 493-500 (2024).
6. K. Tanaka, P. Arias, K. Hojo, T. Watanabe, M. E. Liao, A. Aleman, H. Zaid, M. S. Goorsky and S. K. Kodambaka, Nano Lett. **23** (10), 4304-4310 (2023).

9:00am SE-MoM-4 Manufacture and Microstructure of Tantalum Nitride Films by Radio Frequency and High Power Impulse Magnetrom Sputtering Techniques, *Yu-Rou Chiang, Yun-Chi Chang, Fan-Bean Wu,* National United University, Taiwan; *Jyh-Wei Lee,* Ming Chi University of Technology, Taiwan

Tantalum nitride, TaN, film attracted attension for decades due to its merits in thermal, mechanical, tribological, electrical properties and had been employed in versatile applications, including microelectronics, seiconductor, protective layer and so on. However, the TaN films frequently deposited through sputtering process in vacuum possessed various microstructural features according to deposition conditions, leading to the evolution in characteristics. A comparative study focused on the control on fabrication parameters of inlet gas ratio, input power types, including radio frequency, and high power impulse magnetron sputtering, i.e. RFMS and HiPIMS, respectively, and the duty cycle modulation of the HiPIMS technique was conducted. An amorphous/nanocrystalline microstructure feature could be deduced under a low RF power, while a higher level of RF power enhanced the crystallization of the TaN films. The even higher power density upto 0.5 kW by the HiPIMS technique triggered a multiphase microstructure comprised of TaN, Ta_2N, and TaN_2 phases. Under such high power density, a strong columnar feature was obtained regardless of the duty cycle. In addition, under a higher Ar/N_2 gas ratio of 18/2 with limited nitrogen the TaN showed a stoichiometry of Ta_2N, while an elemental ratio Ta:N=1:1 was achieved with a ratio of Ar/N_2=15/5. Recent findings on

microstructure evolution and related characteristics of the TaN coatings were discussed.

9:15am SE-MoM-5 In-Situ Laser Diagnostics of Plasma Surface Interactions by Fs-TALIF, *Mruthunjaya Uddi,* Advanced Cooling Technologies; *Gerardo Urdaneta, Arthur Dogariu,* Texas A&M University

Plasma surface interaction has been a critical area of research for many applications such as Plasma-Enhanced Atomic Layer Etching (PEALE). To meet the demanding needs of more advanced atomically controlled microfabrication methods, the physics of PEALE needs to be better understood to enable high quality, repeatable and controllable deposition process. Several challenges that need to be addressed regarding PEALE include damage to the substrate from highly energetic species and UV radiation, need for precise amorphous/crystalline modulated selective layer deposition, conformality in coating non-uniform substrates, achieving an aspect ratio of >100, repeatability and controllability of the finish. To address these challenges, we are developing laser diagnostics methods to measure species over substrates by advanced laser diagnostics such as femtosecond- Two-Photon Absorption Laser Induced Fluorescence (fs-TALIF) to image atomic species over substrates. Here we present measurements of N, O atom densities over a substrate with high spatial (< 10 microns) and temporal resolution (<1 ns) using fs-TALIF at pressures of 5-150 mTorr. Temperature was measured over a substrate surface using NO 2-line LIF using femtosecond laser excitation.

9:30am SE-MoM-6 Interlayer Optimization for Nitrogen-Incorporated Tetrahedral Amorphous Carbon Thin Film Optically Transparent Electrode, *Nina Baule, Davit Galstyan, Lars Haubold,* Fraunhofer USA Center Midwest

While several studies around the usage of nitrogen-incorporated tetrahedral amorphous carbon (ta-C:N) in electroanalysis have been published, they mainly focus on ta-C:N films deposited on conductive substrates. This is due to the relatively high resistivity of ta-C:N compared to other carbon and metal-based electrodes: without the electrically conducting substrate, there are high ohmic losses in the ta-C:N when subjected to an electrical current. This limits the use of ta-C:N in optically transparent electrodes (OTEs), which must be deposited on optically transparent (typically electrically insulating) substrates such as quartz. In this study we deposited 50 nm of ta-C:N by laser controlled pulsed cathodic vacuum arc (Laser-Arc) onto insulating quartz substrates to investigate the electrochemical response compared to the same film deposited on conductive silicon. To test the responses of the films, we performed electrochemical oxidation/reduction of potassium ferrocyanide during cyclic voltammetry (CV). Here we find that no oxidation or reduction during CV could be observed at the ta-C:N electrode deposited on quartz. To address this and to maintain optical transparency over the visible wavelength range, we then introduced a 5 nm chromium (Cr) interlayer deposited by magnetron sputtering between the ta-C:N and quartz. While this electrode configuration led to clear cathodic and anodic CV peaks of potassium ferrocyanide, the peak separation compared to the ta-C:N deposited on conductive silicon was increased. That finding indicates that the electrode has a higher resistance. However, we further improved ta-C:N's electrode functionality on quartz by optimizing the Cr sputtering conditions and introducing a plasma pretreatment by a single-beam ion source. Atomic force microscopy revealed that these changes caused an improved Cr growth homogeneity, which led to the enhanced electrical conductivity. These results show that ta-C:N's potential as an OTE is not precluded by its high ohmic losses on insulating substrates. In fact, the promise of mechanically stable and electrochemically active ta-C:N requires only that a conductive interlayer be used, and these films could impact the realms of optical materials, flexible electronics, sensors, and more.

9:45am SE-MoM-7 Highly-Ordered Metallic Nanostructure Arrays: Strategies, Status, and Challenges, *Jinn P. Chu,* National Taiwan University of Science and Technology, Taiwan

This presentation reports on the wafer-scale fabrication of metallic nanostructure arrays with highly ordered periodicity. With the semiconductor-based lithography and sputter deposition, various metallic arrays including metallic nanotube array, metal mesh, and metallic pillar array are fabricated. The array structure is manufactured by sputtering metals onto a contact-hole array template created in the photoresist by photolithography. Following sputter deposition, the photoresist and any excess top-layer coating were removed using acetone, leaving behind the nanotube array on the substrate. The efforts were recognized with the American Chemical Society (ACS) Award at the nano tech 2018 International Nanotechnology Exhibition & Conference in Tokyo, Japan. We utilized both ferrous (stainless steel) and nonferrous alloys (Cu-, Ni-, Al-,

and Ti-based), elemental metals (Cu, Ag, and Au), as well as various oxides to form these array structures. The proposed arrays can be fabricated over a wide range of heights and diameters (from a few hundred nm to 20 µm) and in various shapes, including tall cylinders, dishes, triangles and rhombuses. Furthermore, when combined with other nanomaterials (e.g., ZnO nanowires, graphene oxide, or Au nanoparticles), arrays become nanohybrids suitable for many applications. These applications include thermal emitters, triboelectric nanogenerators, SERS-active biosensors, and anti-icing devices.

10:00am SE-MoM-8 Refining Deposition and Thermal Processes for High-Quality Bi-Mo-O Thin Films, *Ricardo Gonzalez-Campuzano, Agileo Hernandez-Gordillo,* **Sandra Elizabeth Rodil,** Instituto de Investigaciones en Materiales, Universidad Nacional Autónoma de México

Bismuth molybdates, a family of Bi-Mo-O materials with diverse elemental compositions and crystalline structures, have been extensively investigated for their excellent catalytic properties in the oxidation of lower olefins. These properties facilitate the synthesis of organic chemicals widely used in the plastic industry. Their photocatalytic activity under visible light has recently been demonstrated in micro and nano powder samples. However, there has been limited research on the deposition and characterization of Bi-Mo-O materials as thin films. Since 2016, Matova et al. have shown that sputtering deposition using Bi and Mo targets in an Ar+O_2 atmosphere is feasible, demonstrating the visible-light photocatalytic degradation of dyes in water. Despite these promising results, the broader application of this bismuth-based photocatalyst has seen limited advancement. To address this gap, our research group has renewed the investigation of Bi-Mo-O semiconductors for photocatalytic degradation of recalcitrant pollutants, leveraging their active response to visible light. In this study, we report on the thin-film deposition of Bi-Mo-O samples using a co-sputtering system with Bi_2O_3 and Mo targets. The direct current power applied to the Mo target varied from 20 to 60 W, while the RF power applied to the Bi_2O_3 target was fixed at 30 W, allowing us to achieve films with different Bi/Mo ratios. The substrate was pre-heated to 420 K and rotated at approximately 10 RPM to ensure film uniformity. Our results indicated that the films transitioned from crystalline to amorphous as the Mo content increased. Annealing experiments using rapid thermal processing equipment, introducing air into the chamber, performed at 773.15, 873.15, and 973.15 K for 20 minutes for each sample, aiming to obtain various Bi-Mo-O crystalline structures. The structure variations, optical band gap, and bonding-composition analysis are presented. Mo-rich samples presented high optical absorption with band gaps below 0.5 eV, but most samples presented band gaps in the visible-range. Pure phase Bi-Mo-O films and heterostructures containing MoO_x phases were obtained and tested for the degradation of the indigo carmine dye under visible light.

10:30am SE-MoM-10 Low-Temperature Synthesis of Stress-Free, Ceramics Thin Films Using Metal-Ion Irradiation, *Ivan Petrov,* Univerisity of Illinois at Urbana-Champaign*; Lars Hultman, Greg Greczynski,* Linköping University, IFM, Sweden

Ion irradiation is a key tool for controlling epitaxy-to-nanostructure, phase content, and physical properties of refractory ceramic thin films grown by magnetron sputtering. Until recently, thin film growth relied on enhancing adatom mobility in the surface region by inert and/or reactive gas ion irradiation to obtain dense layers at low deposition temperatures. Development of high-power pulsed magnetron sputtering (HiPIMS), which provides metal-ion plasmas with tunable degree of ionization, enabled systematic studies of the effects of metal-ion irradiation on properties of refractory ceramic thin films. A motivation for the use of metal-ions stems is that they are film constituents, hence they can provide the benefits of ion-mixing without causing the high compressive stresses associated with trapping of gas ions at interstitial sites.

This presentation reviews growth experiments of transition metal nitride model systems including TiAlN, TiSiN, VAlN, TiTaN, TiAlTaN, and TiAlWN. Film synthesis is carried out in a hybrid configuration with one target powered by HiPIMS and other operated in direct current magnetron sputtering (DCMS) mode.A substrate bias potential V_s is synchronized with the metal-ion-rich portion of the HiPIMS pulses to control the metal-ion energy. The time-resolved mass spectrometry analyses performed at the substrate position enables us to suppress the role of gas ion irradiation and select intense

Irradiation with lower-mass metal-ions (Al^+ or Si^+) results in near-surface implantation with the depth controlled by V_s amplitude. This enables synthesis of *metastable* ternary cubic Me_1Me_2N solid solutions far above the Me_1N concentration range achieved by DCMS. At the other end,

bombardment of the growing film surface with pulsed high-mass metal ion fluxes (W^+ or Ta^+)during hybrid HiPIMS/DCMS high-rate deposition of dilute $Ti_{1-x}Ta_xN$, $Ti_{1-x-y}Al_xTa_yN$, and $Ti_{1-x-y}Al_xW_yN$ alloys provides high fluxes of low energy recoils and results in fully-dense, low-stress, hard and superhard coatings without external substrate heating (temperature ≤130 ºC).

10:45am SE-MoM-11 ASED Young Investigator Award Finalist Talk: Understanding Ceramics Under Extreme Mechanical Loads via Machine-Learning Potential Molecular Dynamics, *Nikola Koutna*[1], *Shuyao Lin,* TU Wien, Austria*; Lars Hultman, Davide Sangiovanni,* Linköping Univ., IFM, Thin Film Physics Div., Sweden*; Paul Mayrhofer,* TU Wien, Austria

Inherent brittleness and easy crack formation are serious challenges for applications of hard ceramic films. Prior to the development and targeted testing of a specific material, data-driven ab initio and machine-learning techniques can facilitate efficient and relatively inexpensive screening of the relevant chemical space with desired structure–property constraints. Furthermore, theoretical approaches can aid experiment in providing atomic-to-nanoscale understanding of deformation and crack initiation processes under well-defined loading conditions. In this talk I will discuss the exciting and rapidly growing field of machine-learning interatomic potentials (MLIPs) for molecular dynamics and how these can be used to study boron-based ceramics under extreme mechanical loads, highly relevant for applications of these materials. Transition metal diborides (TiB_2, TaB_2, WB_2) and MAB phases (nanolaminates alternating ceramic-like, Ti–B, Ta–B, W–B, and metallic-like, Al, layers) will be used to exemplify a possible MLIP training strategy as well as to discuss challenges upon up-scaling beyond ab initio length scales. Uniaxial tensile tests as well as compression tests with a surface pre-crack will be simulated for supercells with up to 10^6 atoms, previously inaccessible to both ab initio as well as molecular dynamics calculations due to the size limitations (ab initio) and due to the fact that only few interatomic potentials for ceramics exist (molecular dynamics) and basically none has been properly tested for large-scale simulations including severe mechanical loads. Equipped with the newly developed machine-learning interatomic potentials, I will further discuss strain-induced nucleation of extended defects MAB phases and relate them to relevant experimental observations.

11:00am SE-MoM-12 ASED Rising Star Talk: Coupling CdS/g-C_3N_4 Heterojunctions with Remarkably Transfers Process: Impact of Stacking Grade of g-C_3N_4 Micro-flakes, *Karen Valencia García*[2], *Agileo Henández Gordillo, Sandra Elizabeth Rodil Posada,* National Autonomous University of Mexico

In this work, heterojunction materials of cadmium sulfide (CdS) with carbon nitride (g-C_3N_4) were prepared and the photocatalytic activity in hydrogen (H_2) production was studied using an ethanol-water solution. The influence of ammonia (NH_3) on the physicochemical and photocatalytic properties of g-C_3N_4 was investigated. It was evaluated in the photocatalytic H_2 production, obtaining a null response, but the g-C_3N_4 exhibit activity in the photodegradation of the indigo carmine dye (*IC*) solution using blue LED light. From the analysis of the results, a parameter defined as SA/(WCA*gap) (**surface area** (SA); **water contact angle** (WCA) and photon absorption (**band gap**)) is proposed to show how the different **surface parameters** in the photocatalytic response. Subsequently, the effect of the amount of g-C_3N_4 on the heterojunction formed with the CdS nanofibers, which were synthesized in the solvent mixture of ethylenediamine and butanol, was studied. The heterojunction of CdS/g-C_3N_4 was carried out using the g-C_3N_4 synthesized by polymerization with 1 mL of hydrazine (UH1, the g-C_3N_4 with the maximum value of **SA/(WCA*gap)** and with the g-C_3N_4 synthesized with 2 mL of hydrazine (UH2, the g-C_3N_4 that presented the greatest physical-chemical and optoelectronic modification). The CdS heterojunctions with the modified g-C_3N_4 exhibited a high H_2 production rate of (5258 µmol $h^{-1}g^{-1}$) ~2.0 times higher than the unmodified CdS nanofibers. The increase in H_2 production rates of the heterojunctions was related to the coupling of the CdS nanofibers on the surface of g-C_3N_4 lamellar plate: (1) result of a better capacity to absorb visible light; (2) the lower resistance to charge transfer, decreasing the recombination of the e^-/h^+ pairs. For the heterojunctions, the increase in photocatalytic activity suggests that the coupling of the CdS materials with g-C_3N_4 was satisfactorily achieved, observing a synergy of CdS with g-C_3N_4. Physical mixtures equivalent to heterounions were made, and they presented a low rate in the evolution of H_2, the low activity is due to the fact that there is no coupling between the CdS nanofibers and g-C_3N_4.

---

[1] **ASED Young Investigator Award Finalist**
[2] **AVS Rising Star**

Keywords: heterojunctions, hydrogen production, photocatalysis.

11:15am SE-MoM-13 ASED Young Investigator Award Finalist Talk: Advanced EMI Shielding with Quantum Dots and 2D Nanomaterial Enhanced Dual-Polymer Fiber Films, *Lihua Lou*[1], Florida International University; *Ghaleb Al-Duhni,* Florida International University, Jordan; *Omar Cruz,* Florida International University, Nicaragua; *John Volakis, Markondeyaraj Pulugurtha, Arvind Agarwal,* Florida International University

An ultra-thin, lightweight, and highly flexible nanocomposite film is developed by synergistically integrating iron oxide quantum dots (FeQDs) and graphene nanoplatelets (GNPs), specifically targeting electromagnetic interference (EMI) shielding applications. To enhance the electrical conductivity of the resulting thin film, a dual-faceted strategy is employed: utilizing a hybrid polymer system as the matrix and constructing a QDs/2D nanomaterial-integrated multilayer network within the film's architecture. This intricate design approach facilitates a robust investigation into the fiber-based thin films' structural, chemical properties, electrical conductivity, and EMI shielding capabilities, including characterization and simulation methodologies. Findings reveal that the electrospun fibers of 10GNP-1QDs exhibit an average diameter of ~613 ± 192 nm, presenting a significantly higher surface roughness than the pristine PAN fibers. This morphological variance is attributed to the intricate particle-polymer interactions. Raman spectroscopy analysis confirms the successful incorporation of GNPs and FeQDs into the fiber matrix, as evidenced by slight shifts in peak positions, indicative of atomic and molecular interactions between the composite's organic and inorganic constituents. Electrical conductivity measurements underscore a remarkable figure of 350,000 S/m, a characteristic partially ascribed to GNPs and FeQDs' facilitative role in enhancing the polymer matrix's conductive pathways. The magnetic SE within the frequency range of 250 to 1000 MHz spans between 30 to 35 dB, surpassing the performance of all other thin films, including control samples fabricated through coating and casting methodologies. This enhanced performance is linked to the improved electron mobility afforded by FeQDs. Additionally, within the low-frequency range of 0 to 1 MHz, the film exhibits an SE ranging from 40 to 50 dB, markedly outperforming Al and Cu films of equivalent thickness. Notably, within the high-frequency X-band spectrum of 8 to 12 GHz, the SE reaches levels up to 170 dB, ~30 dB higher than that of Al and Cu films. Furthermore, across the far-field frequency range of 100 MHz to 12 GHz, the film demonstrates an SE between 65 to 100 dB. The predominant shielding mechanisms contributing to these outcomes include absorption, multi-reflection, reflection, hysteresis loss, and polarization loss, collectively ensuring the nanocomposite's superior performance in EMI shielding applications. This exploration significantly advances the field by demonstrating the exceptional capabilities of 1D/2D nanomaterial-integrated thin films across a wide frequency spectrum.

11:30am SE-MoM-14 Microstructural, Nanomechanical, and Tribological Properties of Thin Dense Chromium Coatings, *Esteban Broitman, Adwait Jahagirdar,* SKF Research and Technology Development, Netherlands; *Ehsam Rahimi,* Delft University of Technology, Netherlands; *Ralph Meeuwenoord,* SKF Research and Technology Development, Netherlands; *Arjan Mol,* Delft University of Technology, Netherlands

Nowadays, Thin Dense Chromium (TDC) coatings are being industrially used in rolling bearings applications due to their claimed advantages such as high hardness, low wear, and good corrosion resistance. However, despite their broad commercial use, very little has been published in the open scientific literature regarding their microstructure, nanomechanical and tribological properties.

In this presentation, TDC coatings with a thickness of about 5 μm were deposited by a customized electrochemical process on 100Cr6 bearing steel substrates. Surface microstructure and chemical composition analysis of the TDC coatings was carried out by X-ray Diffraction, Scanning Electron Microscopy coupled with Energy Dispersive Spectroscopy, and Atomic Force Microscopy. The results revealed a coating with a dense, nodular, and polycrystalline microstructure. Unlike standard electrodeposited "Hard Chromium" coatings, TDC coatings show no presence of micro/nano-cracks, likely contributing to their superior corrosion resistance. The nanomechanical behavior, studied by nanoindentation as a function of penetration depths exhibits a pronounced size effect near the coating surface, that can be linked to the nodular microstructure. A hard surface with hardness H_{IT} ~ 25 GPa and reduced Young's modulus E_{IT} ~ 300 GPa at 150 nm depth from the surface was observed. Tribological characterization

was performed by two single-contact tribometers using coated and uncoated steel balls against flat steel substrates. An in-house fretting wear rig was used to measure the lubricated friction coefficient in pure sliding conditions, whilst the friction performance in rolling/sliding lubricated conditions was evaluated using a WAM test rig. In pure sliding, both steel/steel and TDC/TDC show similar friction coefficients. However, under rolling/sliding conditions with 5% sliding, the traction coefficient of TDC/TDC coating contact was 22% lower than that for steel/steel contact. The tribological results obtained in various contact conditions demonstrate the benefits of applying TDC coatings to reduce bearing friction.

Surface Science
Room 120 - Session SS+AMS-MoM

Dynamics and Mechanisms in Heterogeneous Catalysis
Moderators: Abner de Siervo, University of Campinas (UNICAMP), **Arthur Utz**, Tufts University

8:15am SS+AMS-MoM-1 Accurate Dynamical Modelling of Vibrationally Enhanced N$_2$ Dissociation on Ru(0001) – Implications (Not Only) for Plasma Catalysis, *Floris van den Bosch, Nick Gerrits, Jörg Meyer,* Leiden University, Netherlands **INVITED**

Pioneering work of Mehta et al. [1] has quantified the efficiency of plasma-enhanced over conventional (temperature-driven) heterogeneous catalysis - nurturing hopes for a future more sustainable alternative that can be easily upscaled. The focus has been on ammonia synthesis and vibrationally excited states available in the plasma, because the dissociative chemisorption of N$_2$ molecules on a metal catalyst is usually the rate-limiting step. Prevalent micro-kinetic modeling based on transition state theory (TST) for the reaction rates needs to be extended by introducing vibrational-state-dependent rate constants. To do so, Mehta et al. have postulated that the computationally convenient Fridman-Macheret model often used for reactions in the gas phase [2] also works for surface reactions.

Using N$_2$ on Ru(0001) as a representative showcase, we scrutinize the effect of vibrational excitations of N$_2$ on its surface reactivity by using explicit molecular dynamics on an accurate potential energy surface using the quasi-classical trajectory method [3,4]. We compute the dissociative chemisorption probabilities as a function of the initial vibrational state ranging from 0 to 10 vibrational quanta. These calculations yield vibrational efficacies of about 1.8, i.e., vibrational excitations are more considerably more effective for promoting dissociative chemisorption reactions than equivalent amounts of translation energy. We compare our findings to TST-based models and carefully analyze why they cannot capture the vibrationally enhanced dissociation correctly. Finally, we discuss these findings in the context of thermal and plasma-enabled catalysis by critically investigating which molecules dominate the reactivity.

1. P. Mehta, P. Barboun, F. A. Herrera, J. Kim, P. Rumbach, D. B. Go, J. C. Hicks, and W. F. Schneider, Overcoming Ammonia Synthesis Scaling Relations with Plasma-Enabled Catalysis, Nat. Catal. 1, 269 (2018). DOI: 10.1038/s41929-018-0045-1
2. A. Fridman, Plasma Chemistry, Cambridge University Press, Cambridge, 2008.
3. K. Shakouri, J. Behler, J. Meyer, and G.-J. Kroes, Accurate Neural Network Description of Surface Phonons in Reactive Gas–Surface Dynamics: N2 + Ru(0001), J. Phys. Chem. Lett. 8, 2131 (2017). DOI: 10.1021/acs.jpclett.7b00784
4. P. Spiering, K. Shakouri, J. Behler, G.-J. Kroes, and J. Meyer, Orbital-Dependent Electronic Friction Significantly Affects the Description of Reactive Scattering of N$_2$ from Ru(0001), J. Phys. Chem. Lett. 10, 2957 (2019). DOI: 10.1021/acs.jpclett.9b00523

8:45am SS+AMS-MoM-3 SSD Morton S. Traum Award Finalist Talk: A Priori Designed NiAg Single-Atom Alloys for Selective Epoxidation Reactions, *Elizabeth E. Happel*[2], Tufts University; *Anika Jalil,* University of California at Santa Barbara; *Sarah Stratton,* Tulane University; *Laura Cramer,* Tufts University; *Phillip Christopher,* University of California at Santa Barbara; *Matthew M. Montemore,* Tulane University; *E. Charles H. Sykes,* Tufts University

Ethylene oxide, produced via the partial oxidation of ethylene, is among the largest volume chemicals produced by the chemical industry and has one of the largest carbon footprints. Using Ag catalysts, the reaction can achieve

high selectivity ~90%, but only with a combination of promoters including Cl, Cs, and Re, and must be run at low conversions (< 15%) to avoid the total combustion of ethylene to carbon dioxide. Herein, we report a theory guided investigation demonstrating that the addition of low concentrations of Ni to Ag(111) lowers the barrier for O_2 dissociation and enables spillover of oxygen atoms to sites on the Ag surface. Temperature programmed desorption experiments quantify the facile dissociation, spillover and desorption of O_2 from NiAg(111) and demonstrate that, unlike all previous studies, Ni addition enables the population of the Ag(111) surface with atomic oxygen in near UHV pressure without having to atomize oxygen or introduce species like NO_2 or O_3. Furthermore, ambient pressure X-ray photoelectron spectroscopy reveals that Ni not only aids in activation and spillover, but also stabilizes nucleophilic oxygen which is thought to be selective towards total oxidation. These results informed the synthesis and testing of supported catalysts which demonstrated that NiAg single-atom alloy nanoparticles produce ethylene oxide both with greater selectivity and conversation than Ag without the need for a co-flow of Cl and other promoters.

9:00am SS+AMS-MoM-4 Effect of Surface Diffusion of Methoxy Intermediates on Methanol Decomposition on Pt/TiO$_2$(110), *Can Liu, Bang Lu,* Hokkaido University, Japan*; Hiroko Ariga-Miwa,* The University of Electro-Communications (UEC-Tokyo), Japan*; Shohei Ogura,* Tokyo Denki University, Japan*; Katsuyuki Fukutani,* The University of Tokyo, Japan*; Min Gao, Jun-ya Hasegawa, Ken-ichi Shimizu,* Hokkaido University, Japan*; Kiyotaka Asakura,* Ritsumeikan University, Japan*; **Satoru Takakusagi,** Hokkaido University, Japan

In oxide-supported metal catalysts, atomic-level understanding of dynamic behavior of intermediate adsorbates such as diffusion, spillover, and reverse spillover is crucial to unravel the origins of catalytic activity and product selectivity. Our previous *in situ* STM study on methanol adsorption process on a Pt/TiO$_2$(110) surface revealed that methoxy intermediates were formed on five-fold coordinated Ti^{4+} (Ti$_{5c}$) sites by dissociative adsorption of methanol on the Pt nanoparticles, followed by spillover to the TiO$_2$(110) substrate.[1] They were mobile at room temperature. In this study, diffusion and thermal decomposition of the methoxy intermediates were examined by STM, density functional theory (DFT) calculation and temperature programmed desorption (TPD), in order to reveal how their diffusion affect activity and product selectivity in the methoxy decomposition on the Pt/TiO$_2$(110) surface.[2] The TPD measurements showed that the methoxy intermediates were thermally decomposed at >350 K on the Pt sites to produce CO (dehydrogenation) and CH$_4$ (C-O bond scission) through their reverse spillover. We have found that activity and product selectivity for the methoxy decomposition was much dependent on the particle density, suggesting that it was controlled by diffusion of the methoxy intermediates. Decrease of the Pt nanoparticle density significantly enhanced the selectivity to CH$_4$, and thus we propose that Pt-TiO$_2$ interfacial sites are active for CH$_4$ formation while the other Pt sites for CO formation.

[1] S. Takakusagi, K. Fukui, R. Tero, K. Asakura, Y. Iwasawa, *Langmuir* 2010, **26**, 16392.

[2] C. Liu, B. Lu, H. Ariga-Miwa, S. Ogura, T. Ozawa, K. Fukutani, M. Gao, J. Hasegawa, K. Shimizu, K. Asakura, S. Takakusagi, *J. Am. Chem. Soc.* 2023, **145**, 19953.

9:15am SS+AMS-MoM-5 Simultaneous Tracking of Ultrafast Surface and Gas-Phase Dynamics in Solid-Gas Interfacial Reactions, *Keith Blackman, Eric Segrest, George Turner, Kai Machamer, Aakash Gupta, Md Afjal Pathan,* University of Central Florida, Department of Physics*; Novia Berriel,* University of Central Florida, Department of Material Science and Engineering*; Parag Banerjee,* University of Central Florida, Department of Material Science and Engineering, Renewable Energy and Chemical Transformations Cluster (REACT)*; Mihai Vaida,* University of Central Florida, Department of Physics, Renewable Energy and Chemical Transformations Cluster (REACT)
ABSTRACT

Real-time detection of intermediate species and final products at the surface and near-surface in interfacial solid-gas reactions is critical for an accurate understanding of heterogeneous reaction mechanisms. In this contribution, an experimental method that can simultaneously monitor the ultrafast dynamics at the surface and above the surface in photoinduced heterogeneous reactions is presented. The method relies on a combination of mass spectrometry and femtosecond pump-probe spectroscopy. As a model system, the photoinduced reaction of methyl iodide on and above a cerium oxide surface is investigated. The species that are simultaneously

detected from the surface and gas-phase present distinct features in the mass spectra, such as a sharp peak followed by an adjacent broad shoulder. The sharp peak is attributed to the species detected from the surface while the broad shoulder is due to the detection of gas-phase species above the surface, as confirmed by multiple experiments. By monitoring the evolution of the sharp peak and broad shoulder as a function of the pump-probe time delay, transient signals are obtained that describe the ultrafast photoinduced reaction dynamics of methyl iodide on the surface and in gas-phase. Finally, SimION simulations are performed to confirm the origin of the ions produced on the surface and gas-phase.

9:30am SS+AMS-MoM-6 Controlling Surface Sites on CuO Nanoparticles by Annealing Treatments after Synthesis, *Sergio Rodriguez Bonet,* Instituto de Desarrollo Tecnológico para la Industria Química (CONICET-UNL), Argentina*; Kazi Hanium Maria,* University of Dhaka, Bangladesh*; Marta V. Bosco,* Universidad Nacional del Litoral, Argentina*; **Florencia C. Calaza,** Instituto de Desarrollo Tecnológico para la Industria Química (CONICET-UNL), Argentina

In recent years, transition metal oxides thin films have gained a great attention from material scientists and engineers due to their different properties which in turn provide promising applications in various fields of technology. Cu$_x$O has beenidentified as promising materials for solar energy conversion and heterogeneous catalysis. In addition to their favorable band gap energies that allow for the utilization of visible light, the low cost, earth abundance, and non-toxicity of Cu are additional advantages for developing Cu-based materials. The performance of the copper oxide thin films can be enhanced by improving the crystal quality and surface morphology of the material. Among different synthesis strategies for thin film fabrications, solution-processed methods, such as hydrothermal and electrophoretic deposition, are attractive in terms of their scalability, financial advantages and eco-friendliness. In this work the synthesis of Cu$_x$O nanoparticles by solution-processed methods followed by annealing treatments, shows the stabilization of different available surface sites. In summary, results will be presented for CuO nanoparticle synthesis where the materials were calcined at different temperatures ranging from 300 to 500 C, showing mainly CuO chemical composition and structure in the bulk, but a hint to the presence of Cu$_2$O on the surface is observed by CO IR titration experiments at ambient conditions.

9:45am SS+AMS-MoM-7 Velocity Map Imaging of Desorbing Oxygen from sub-Surface States of Single Crystals, *Arved C. Dorst, Rasika E. A. Dissanayake,* Georg-August Universität, Göttingen, Germany*; Daniel R. Killelea,* Loyola University Chicago*; **Tim Schäfer,** Georg-August Universität, Göttingen, Germany

We combine velocity map imaging (VMI) with temperature-programmed desorption (TPD) and molecular beam surface scattering experiments to record the angular-resolved velocity distributions of recombinatively-desorbing oxygen from single crystal surfaces. We assign the velocity distributions to desorption from specific surface and sub-surface states by matching the recorded distributions to the desorption temperature. These results provide insight into the recombinative desorption mechanisms and the availability of oxygen for surface-catalyzed reactions. We use concepts of detailed balance to analyze translational energy distributions of O_2 when shifted towards hyperthermal energies. These distribution indicate desorption from intermediate activated molecular chemisorption states.

10:00am SS+AMS-MoM-8 Kinetic Monte Carlo Modelling of Hydrogen Oxidation on Pt/Pd Surfaces, *Alexander Kandratsenka,* MPI for Multidisciplinary Sciences, Germany
Recent velocity-resolved kinetics measurements of water production from gas-phase H_2 and O_2 at Pt and Pd surfaces revealed the complex dependence of reaction rates on the oxygen coverage and step density. We aim to clarify the detailed mechanisms of these oxidation reactions by means of Kinetic Monte Carlo approach with adsorption energies, reaction barriers and transition state geometries determined from *ab initio* calculations, and rate constants derived from the Transition State Theory.

10:30am SS+AMS-MoM-10 Designing the Local Environment of Single Atom Catalysts for Product Selectivity: Theory Meets Experiment, *Talat Shahnaz Rahman,* University of Central Florida **INVITED**
Singly dispersed transition metal atoms on oxide surfaces, the so-called single atom catalyst (SAC) have recently been shown to attain chemical activity and selectivity for several technologically important reactions that surpass those of Pt single crystal surfaces, the prototype exemplary catalyst but with a large price tag. Apart from being cost-effective, single atom catalyst offer excellent opportunities for tuning their local environment and

thereby their oxidation state, local coordination, and electronic structure. In this talk, I will present results of collaborative work with several experimental groups on singly-dispersed transition metal atoms anchored on metal oxide surfaces, with and without ligands, that have the potential to be cost-effective catalysts with high activity and product selectivity. Examples will include Pd and Pt atoms anchored on ZnO that form a bimetallic local environment consisting of one Pd and three Zn atoms with high catalytic activity for generation of H_2 through methanol partial oxidation (MPO) [1] and Pt atoms stabilized in specific fine-tuned local coordination environments that exhibit strikingly distinct catalytic behaviors in reactions as varied as CO oxidation and NH_3 oxidation [2]. I will also pay attention to the special role played by ligands (1,10-phenanthroline-5,6-dione (PDO)) in emergent catalytic properties of Pd single atoms stabilized on ceria surfaces [3]. I will also draw attention to some factors that control the emerging functionalities of the above systems in controlled confinement.

[1] Y. Tang, et al., Nano Lett. 20, 6255 (2020); T.B. Rawal, et al., ACS Catalysis 8, 5553-5569 (2018).

[2] W. Tan, *et al.*, Nat Commun. **13**, 7070 (2022)

[3] E. Wasim, N. Ud Din, D. Le, et al., J. Catalysis 413, 81 (2022)

11:00am SS+AMS-MoM-12 Stabilizing and Characterizing Single-Atom Catalysts: Rhodium on Titania, *Faith J Lewis, Moritz Eder, Johanna I Hütner, David Rath, Jan Balajka, Jiri Pavelec, Gareth S Parkinson,* TU Wien, Austria

Single-atom catalysis (SAC) aims to minimize the amount of precious metals in catalysts while maintaining catalytic activity. SAC often uses oxide supports to stabilize individual transition metals as isolated active sites. A multi-technique surface science approach allows characterization of these sites to determine their coordination structure. In this work, rhodium adatoms, stabilized by carbon monoxide, were studied on a rutile titania (r-TiO_2(110)) surface.

In idealized SAC systems, metal atoms are assumed to stay isolated on oxide surfaces. In reality, this is not always the case. On titania, rhodium adatoms readily sinter into larger clusters above cryogenic temperatures. It has been suggested that adding ligands stabilizes single rhodium atoms on the surface; carbon monoxide has been proposed to form a geminal dicarbonyl ($Rh(CO)_2$) structure to stabilize the individual rhodium atoms on r-TiO_2(110).[1]

The rhodium gem-dicarbonyl infrared (IR) stretch has been used to signify single rhodium atoms on titania surfaces since the turn of the century, but no scanning probe images have been published of this $Rh(CO)_2$/r-TiO_2(110) system. Using a newly integrated infrared reflection absorption spectroscopy (IRAS) system, a protocol for forming the $Rh(CO)_2$ species on r-TiO_2(110) in UHV was established. In this talk, I will present scanning tunneling microscopy (STM) and non-contact atomic force microcopy (nc-AFM) images of the rhodium gem-dicarbonyl system after annealing to various temperatures with complementary IRAS and X-ray photoelectron spectroscopy (XPS) data. The images show two distinct double-lobed species, one parallel to the [001] direction and one perpendicular, at a low coverage (0.005 ML). Contradictory to theoretical predictions,[2] the images show an asymmetry of the two lobes in both confirmations. Our results illustrate that the surface science approach provides unique information about single atom catalysts and is a prerequisite for their accurate theoretical description.

1. Frank, M.; Bäumer, M.; Kühnemuth, R.; Freund, H.-J., Metal Atoms and Particles on Oxide Supports: Probing Structure and Charge by Infrared Spectroscopy. *The Journal of Physical Chemistry B, 8569-8576* (2001).
2. Tang, Y., Asokan, C., Xu, M. *et al.,* Rh single atoms on TiO_2 dynamically respond to reaction conditions by adapting their site. *Nature Communications*, 4488 (2019).

11:15am SS+AMS-MoM-13 In-Situ Observation of the Effects of Oxygen-Containing Compounds on MoS_2-Based Catalysts Using Near-Ambient Pressure Scanning Tunnelling Microscopy, *Kerry Hazeldine, Martin Hedevang,* Aarhus University, Denmark*; Lars Mohrhusen,* Carl von Ossietzky University of Oldenburg, Germany*; Jeppe Vang Lauritsen,* Aarhus University, Denmark

More than 20% of greenhouse gas emissions in the European Union are produced by the heavy transport and aviation sector. Pyrolysis oil derived from biomass is a promising replacement for fossil fuels for aviation and heavy transport applications and is one of the technologies being researched for the generation of green aviation fuel. Fast pyrolysis is a process of decomposing biomass into pyrolysis oil by rapidly heating it in an oxygen-free atmosphere. An advantage of pyrolysis oil derived from biomass is that it is compatible with the existing infrastructure that is used in the catalysis and distillation of jet fuels and diesel. However, the oxygen content in pyrolysis oil derived from biomass is unacceptably high (up to 50%) and can lead to corrosion and instability [1].

To reduce the oxygen content and produce useful and efficient hydrocarbons from the pyrolysis oil, a pre-treatment and hydrodeoxygenation (HDO) step is required to be added to the refining process. Molybdenum disulphide (MoS_2) has previously demonstrated its effectiveness as a catalyst in hydrodesulphurisation (HDS) and has further shown to be a promising candidate as a catalyst in HDO and is therefore the primary material of interest in this study [2].

To develop atomistic structure determination of the catalyst and elucidate to the reaction pathways for oxygen-containing molecules during HDO, model studies are required. In this study, the model system based on MoS_2 growth on Au(111), has been exposed to oxygen-containing molecules and characterised in-situ using the surface-sensitive techniques, near-ambient pressure scanning tunnelling microscopy (NAP-STM), and near-ambient pressure X-ray photoelectron spectroscopy (NAP-XPS). By using a gold substrate, the oxygen uptake can be evaluated without background from the oxide support. NAP-XPS shows evidence of O exchange on the sulphide phase, consistent with current theoretical models, whilst the corresponding NAP-STM shows structural changes to the particle shape and size of the sulphide phase. For example, preliminary work shows restructuring in the MoS_2 clusters when exposed to elevated pressures of methanol vapour. By using these complementary techniques, we can gain insight into both the chemical and physical changes of MoS_2 upon exposure to oxygen-containing compounds.

[1] Cao J, Zhang Y, Wang L, Zhang C, Zhou C. Unsupported MoS_2-Based Catalysts for Bio-Oil Hydrodeoxygenation: Recent Advances and Future Perspectives. *Front Chem*. 10, 928806 (2022).

[2] Salazar, N., Rangarajan, S., Rodríguez-Fernández, J. *et al.* Site-dependent reactivity of MoS_2 nanoparticles in hydrodesulfurization of thiophene. *Nat Commun*.11, 4369 (2020).

11:30am SS+AMS-MoM-14 Revealing Local Coordination of Ag Single Atom Catalyst Supported on CeO_2(110) and ZrO_2(-111), *Syeda Sherazi, Duy Le, Kailong Ye, Shaohua Xie, Fudong Liu, Talat Rahman,* University of Central Florida

Single atom catalyst (SAC) supported on metal oxide surfaces is a promising candidate for various reactions as it possesses high temperature stability and potentially high selectivity. Determining the local atomic coordination and geometric structure of the SAC is important for the understanding of its catalytic performance. In this work, we apply the ab initio thermodynamics approach to investigate the coordination environment of Ag SAC supported on CeO_2(110) and ZrO_2(-111), so chosen as accompanying experimental observations find the former to be a more viable support than the latter. We find that the Ag SAC structure in which Ag is embedded in the CeO_2 lattice with one surface oxygen vacancy nearby is the most favorable on the CeO_2(110) surface while the structure in which Ag embeds in the ZrO_2(-111) lattice without any oxygen vacancy nearby is the most favorable on the ZrO_2(-111) surface. Our results also show that it is easier to create oxygen vacancy near the Ag atom when the support is CeO_2(110) than ZrO_2(-111). We compare the trends in the energetics of NH_3 adsorption and dissociation on Ag SAC supported on CeO_2(110) with those on ZrO_2(-111) to compare with accompanying experimental observations that find the ceria-supported Ag SAC to exhibit a pronounced selectivity in ammonia oxidation. We will report experimental data to compare with our finding and comment on their implications for the catalytic performance of the Ag SAC.

11:45am SS+AMS-MoM-15 Trends for Predicting Adhesion Energies of Catalytic Late Transition Metal Nanoparticles on Oxide Supports, *Nida Janulaitis,* The University of Washington*; Kun Zhao, Charles Campbell,* University of Washington

Understanding the energetics of late transition metal nanoparticles dispersed on oxide-based catalyst support materials is important for the

development of high-performance catalysts. Metal/support adhesion energies, which are used to estimate the metal chemical potential as a function of metal nanoparticle size, which in turn correlates with the surface reactivity and sintering kinetics of the metal nanoparticles. Single crystal adsorption calorimetry (SCAC) was used to directly measure Cu vapor adsorption energies and Cu chemical potential as a function of Cu coverage on the clean rutile-TiO_2(100) surface, while He^+ low-energy ion scattering (LEIS) was used to measure the average size of the Cu nanoparticles. By fitting these data to a theoretical model, we extracted the adhesion energy of Cu nanoparticles on rutile-TiO_2(100). By comparing to earlier results for Ag, we find that the adhesion energies of metals on the rutile-TiO_2(100) surface correlate proportionally to the oxophilicity of the metal element. Similar proportional correlations for the adhesion energy of metals to MgO(100) and CeO_2(111) surfaces as a function metal oxophilicity have been previously published. Expanding upon these existing oxide adhesion energy trends with the new rutile-TiO_2(100) data clarifies the structure-function relationship between the physical properties of the oxide supports and their metal adhesion energetics. The ability to predict the adhesion energy, and thus the metal chemical potential versus size, of late transition metal nanoparticles across oxides streamlines development of optimal catalysts.

Thin Films
Room 115 - Session TF1-MoM

Thin Films for Energy Applications I: Green Fuels and Photovoltaics

Moderators: Alexander Kozen, University of Vermont, **Blake Nuwayhid**, Naval Research Laboratory

8:45am **TF1-MoM-3 Stability of $CsPbBr_3$ Employing an Ultrathin Al_2O_3 Protective Layer**, *Fernando Quintero-Borbon,* Centro de Investigación en Materiales Avanzados SC, Unidad Monterrey, Mexico*; Joy Roy, Leunam Izquierdo-Fernandez,, Robert M. Wallace, Manuel A. Quevedo-Lopez,* Department of Material Science and Engineering, University of Texas at Dallas*; Francisco S. Aguirre-Tostado,* Centro de Investigación en Materiales Avanzados SC, Unidad Monterrey, Mexico

Lead halide perovskite nanocrystals, such as $CsPbBr_3$, have gathered significant interest due to their attractive optical properties and cost-effective production. However, their environmental stability remains a major challenge, hindering practical applications and scalability for commercialization. In this study, we propose an effective method to enhance the stability of $CsPbBr_3$ by depositing an ultrathin Al_2O_3 film using atomic layer deposition (ALD). The $CsPbBr_3$ was deposited on a glass substrate using closed space sublimation (CSS) from a 1:1 molarratio of PbBr2 and CsBr previusly mix powders. The $Al_2O_3$was deposited from a TMA and H_2O suources using thermal ALD. This unique single layer protection structure significantly improves their resistance to moisture, and polar solvents. Notably, the modified surface exhibits chemical stability and stable photoluminescence (PL) intensity compared to the ordinary $CsPbBr_3$ surface. Additionally, Xray photoelectron spectroscopy analysis shows a chemically abrupt Al_2O_3/$CsPbBr_3$ interface with high stability with respect to the water-soaked $CsPbBr_3$ surface. This research presents a promising approach for developing stable perovskite thin films with enhanced performance in various optoelectronic devices.

9:00am **TF1-MoM-4 Deposition of Yb-doped Double Halide Perovskite $Cs_2AgBiCl_6$ for High-Efficiency Downconversion of Ultraviolet Photons**, *Pulkita Jain, Minh Tran, Iver Cleveland, Yukun Liu, Seda Sarp, Eray Aydil,* New York University

Halide perovskites, particularly those containing lead such as $CsPbX_3$ (X=Cl, Br, I), have emerged as a new class of materials for applications in optoelectronics. However, the toxicity of lead necessitates the pursuit of lead-free alternatives. Bismuth-based halide double perovskite $Cs_2AgBiCl_6$ has emerged as a promising candidate, but there are still conflicting reports and interpretations regarding this material's optical properties, such as its bandgap and the origin of its characteristic high-intensity visible orange emission. Here, we report on synthesizing $Cs_2AgBiCl_6$ thin films through reactive thermal evaporation and address these discrepancies. Specifically, we deposited $Cs_2AgBiCl_6$ thin films by co-evaporating CsCl, $BiCl_3$, and AgCl onto glass substrates, which, upon reaction on the substrate, yielded polycrystalline thin films. Film thickness and stoichiometry were controlled by controlling the evaporation fluxes of the precursors using quartz crystal microbalances. Typical film thicknesses were 100-400 nm. Optical

characterization analysis of the thin films reveals a bandgap of 2.77 eV. X-ray diffraction (XRD) and Raman spectroscopy were used to verify the phase purity and structure of the perovskite as well as impurity phases when present. Steady-state and time-resolved photoluminescence (TRPL) measurement of emission lifetime gave insights into the origin of the orange visible emission. We propose a mathematical model of emission kinetics considering both defect and self-trapped exciton emissions. The high-fidelity fitting of the data with only a few adjustable kinetic parameters suggests both defect and self-trapped exciton emissions may be present, and their contributions may depend on the synthesis conditions, possibly settling the debate in the literature. We also doped the $Cs_2AgBiCl_6$ perovskite with Yb by co-evaporating $YbCl_3$ during film deposition to explore the possibility of downconversion and quantum cutting, the generation of two near-infrared photons from one ultraviolet (UV) photon. The perovskite host absorbs the UV photon and transfers its energy to Yb, which then relaxes ($^2F_{5/2} \rightarrow {}^2F_{7/2}$) and emits photons (1.25 eV) in the near-infrared. Doping with Yb resulted in a photoluminescence quantum yield (PLQY) of 50%, the highest reported in the literature for $Cs_2AgBiCl_6$. We investigated various post-deposition treatments, such as annealing in air versus in a nitrogen-filled environment, and concluded that annealing in air, in the presence of moisture, results in the formation of bismuth oxychloride (BiOCl), confirmed by XRD and Raman spectroscopy. We hypothesize that BiOCl passivates non-radiative defects, aiding in achieving high PLQY.

9:15am **TF1-MoM-5 Low-cost Grown a-Si:H Using Trisilane and its Application to Post Deposition Processes**, *Benedikt Fischer, Maurice Nuys, Stefan Haas, Uwe Rau,* Forschungszentrum Jülich GmbH, Germany

Hydrogenated amorphous silicon (a-Si:H) films are used in a wide range of semiconductor devices. Especially in the current highly efficient solar cell techniques named silicon heterojunction (SHJ) solar cells and tunnel oxide passivated contact (TopCon) solar cells, they are used directly as passivation layer or as a precursor for recrystallized silicon films, respectively. However, for the growth of the a-Si:H films, techniques like plasma enhanced chemical vapor deposition or electronic beam evaporation with expensive vacuum technology are used. Here we show a new setup for the deposition of a-Si:H by atmospheric pressure chemical vapor deposition using liquid trisilane allowing a fast and cost-effective deposition process. By varying the deposition temperature, time and precursor amount we could set the H-content of the films to 0 – 10 %$_{vol}$ and achieved a maximum photosensitivity of 10^4 with a photoconductivity of 10^{-7} S/cm. By applying post deposition H treatments, a photoconductivity of 5×10^{-6} S/cm could be achieved, leading to a photosensitivity of almost 10^5. The low H-content of the films allows annealing without blistering of the samples, especially for the films grown at a substrate temperature of ≥ 500°C. Therefore, we applied rapid thermal annealing to the films and achieved recrystallized silicon with conductivities up to 10^{-1} S/cm. The results show that the as deposited thermally grown films already have a high film quality, indicated by the high photosensitivity. The application of post H-treatment can further improve the film quality, approaching the photosensitivity of high quality PECVD films. Both photoconductivity and photosensitivity can be further increased by improving the hydrogenation process, which was not optimized yet. In addition, the high conductivity achieved by the rapid thermal annealing experiments in comparison with state-of-the-art films show the applicability in TopCon solar cells. Further investigations regarding film doping and application of the polysilicon films for the passivation in combination with a tunnel oxide are in progress. These results, and the fact that the films were produced by a low-cost deposition system, make them highly promising for an industrial application in solar cells.

9:30am **TF1-MoM-6 Optimization of DC Reactive Sputtering of NiOx Transport Layer and Effects of Annealing Conditions on NiOx film for Perovskite Solar Cells**, *Firdos Ali, Subhadra Gupta,* University of Alabama

DC reactively sputtered NiO_x was optimized as a hole transport layer for perovskite solar cell applications. We introduced the reactively sputtered NiO_x hole transport layer over a spin-coated NiO_x layer in solution-processed perovskite (MeO-2PACZ/MAPBI3-XClx) solar cells. The typical reactive hysteresis effects were not observed on the cathode voltage while varying the reactive gas flow during deposition, and this case may be explained by Berg's hysteresis model. We have investigated the unusual hysteresis behavior of the cathode voltage as a function of oxygen flow rate in argon, and correlated this with the deposition rate. The NiOx films were infrared lamp annealed at various temperatures at high vacuum. Perovskite solar cells were fabricated using a solution processing method. A parallel set of devices were fabricated using hot-plate annealing of the NiO_x hole transport layer in atmosphere. The NiO_x thin films were structurally characterized using a variety of techniques: scanning electron microscopy

(SEM), X-ray reflectivity (XRR), and X-ray diffraction. SEM studies were carried out to observe the surface morphology of the NiO_x film. A continuous film of NiO_x was observed at higher oxygen flows and lower deposition rates. XRD analysis on ITO/NiO_x thin films sputtered with various oxygen flows was carried out to study the crystal orientation and crystallinity. The effects of sputtered NiO_x deposition rate, film thickness, as well as annealing conditions on the solar cell efficiency were investigated. The power conversion efficiency was improved from 5% to 13.5 % .

9:45am **TF1-MoM-7 Tunable Sn_xS_y Deposition onto Functionalized Alkanethiolate Self-Assembled Monolayers by Chemical Bath Deposition**, *Christopher Brewer, Reed Woolard, Tania Estrada, Amy Walker,* University of Texas at Dallas

Tin sulfides (Sn_xS_y) are non-toxic and inexpensive materials with low band gaps, making them suitable for semiconductor applications and photovoltaic materials, such as solar cells.Sn_xS_y has three naturally occurring compositions, SnS, Sn_2S_3, and SnS_2, each with different properties.The ability to control the stoichiometry of a Sn_xS_y deposit is of interest for devices like SnS solar cells, where Sn_2S_3 contamination reduces the device efficiency.Chemical bath deposition (CBD) is a low cost and scalable technique that can be used under ambient conditions to deposit Sn_xS_y onto a variety of substrates, including organic substrates.Alkanethiolate self-assembled monolayers (SAMs), functionalized with $-CH_3$, $-OH$, and $-COOH$ terminal groups, are a readily available system, which can be used as a model organic substrate for deposition of Sn_xS_y by CBD.A CBD bath has multiple tunable components, including the solution pH, complexing agent, bases used, and sulfur source as the most common.Modification of any of the bath components, as well as the SAM functionalization, can control the deposit's major composition and phase.Using a mechanism based approach, we have been able to tune the bath chemistry to yield pure SnS deposits.

Thin Films
Room 115 - Session TF2-MoM

Thin Films Special Session: Remembering Dr. Paul Holloway I

Moderators: James Fitz-Gerald, University of Virginia, **Sean Jones**, Argonne National Laboratory, **Robert Grubbs**, IMEC Belgium

10:30am **TF2-MoM-10 Fundamental Aspects of Focused Nanoscale Electron-Ion- and Photon-Beam Induced Processing and Recent Advances in Editing Transition Metal Dichalcogenide Materials and Devices**, *Philip Rack,* Department of Materials Science and Engineering, University of Tennessee, Knoxville **INVITED**

I graduated from Paul Hollloway's group at the University of Florida in 1997 where I studied luminescent materials for electroluminescent displays.If the saying is true that "imitation is the sincerest form of flattery," then my career path captures the admiration for the man I had the privilege to call my Phd advisor.In this talk, I will briefly discuss some of the luminescent materials research that my group has performed and overview my serendipitous journey to focused nanoscale electron beam induced processing, highlighting how it has been an eerily mirror image to Dr. Holloway's path. The scientific portion of my talk will review topics near and dear to Dr. Holloway's heart, electron(ion, photon)-gas-solid interactions, and illustrate that appropriate understanding of these interactions can result in directed growth/etching at the nanoscale.I will overview a Monte Carlo simulation we developed to illustrate some of the critical electron(ion, photon)-gas-solid interactions that can rate and resolution limit nanoscale focused beam induced processing.Finally, I will review our recent work in focused electron beam induced etching of MoS_2 multi- and single-layer devices.

11:00am **TF2-MoM-12 Stability of Phosphor Thin Films During Cathodoluminescence and Upconversion**, *Hendrik Swart,* University of the Free State, South Africa **INVITED**

Surface characterization and optical characterization techniques play a vital role in the complete understanding of the luminescent properties of phosphor nanomaterials and thin films. Auger electron spectroscopy (AES), X-ray photo electron spectroscopy (XPS), time of flight scanning ion mass spectrometry (TOF SIMS), Photoluminescence (PL) and cathodoluminescence (CL) are used to characterize these different phosphor materials and thin films. The crystal field that is determined by the environment in the host material in combination with the various dopant ions with the correct valence state can be used to obtain emissions from the Ultraviolet (UV) to the infra-red (IR) wavelength ranges. Phosphor materials have been successfully used to improve the efficiency of various applications. Nanoparticles both undoped and doped with different rare earth elements were synthesized by several synthesized techniques. The defects incorporated into the bulk material play an important role in the emission efficiency and colour scheme. XPS in combination with PL can be used to identify some of these defects in the material. Thin films of different phosphors have been deposited using the Pulsed laser deposition (PLD) and spin coating techniques. Degradation of the different phosphors during prolonged electron/photon bombardment also played a vital role in their possible applications. The combination of CL, PL, AES and XPS techniques helps to determine the mechanisms behind the degradation. A small number of impurities in the chemicals used during synthesis can play a large role in the final emission intensity and colour of the phosphor materials. TOF SIMS can point out these impurities. It is also important to test the suitability of phosphors powders and thin films during prolonged upconversion photoluminescence. Examples of different phosphor materials with different applications such as Solid-State Lighting will be shown.

11:30am **TF2-MoM-14 Extracting Diffusing Parameters for Indium Segregating form Copper using TOF-SIMS**, *Jacobus Johannes Terblans, Lehlohonolo Makoloane, Shaun Cronje, Hendrik C. Swart,* University of the Free State, South Africa

Time-of-Flight Secondary Ion Mass Spectrometry (TOF-SIMS), with its superior concentration detection limit (in the parts per million (ppm) range) and its ability to operate in static mode (where only the top 1-2 monolayers contribute to the measuring signal), makes TOF-SIMS a technique that is widely used for surface characterisation. This makes TOF-SIMS particularly suitable for studying surface segregation.However, concentration calculations are significantly influenced by the matrix effect, which makes it difficult to perform quantitative measurements.To investigate the segregation of indium with TOF-SIMS, the concentration quantification was addressed by utilising a set of Cu/In thin films of varying concentrations to calibrate the TOF-SIMS system by determining the In sensitivity factor relative to a Cu matrix. The Cu/In thin films used for the calibration were prepared using the Electron Beam Physical Vapor Deposition (EBPVD) co-evaporation method, and the composition of the films was controlled by varying the deposition rates of In and Cu.

To study indium segregation from copper, a polycrystalline Cu crystal was doped with 0.5 at% In by evaporating In onto a polycrystalline Cu crystal and annealing it at 1173 K for 23 days. Indium segregation was stimulated by heating the In-doped polycrystalline Cu crystal linearly from 323 K to 873 K with a heating rate of 0.1 K/s.At the same time, the surface concentration of In was recorded with TOF-SIMS as a function of temperature.The recorded segregation profile was fitted with the modified Fick semi-infinite, the Langmuir-McLean, and modified Darken models.The semi-infinite Fick model successfully extracted the pre-exponential factor (D_0) and activation energy (Q) of 1.44×10^{-5} m^2s^{-1} and 183.3 kJ/mol, respectively, from the kinetic region of the segregation data.With the Langmuir-McLean model, fitted to the equilibrium region, a segregation energy of -64.6 kJ/mol was obtained.The modified Darken model was fitted to the segregation profile, and the segregation parameters were determined as $D_0 = 0.50 \times 10^{-5}$ m^2s^{-1}, Q = 176.0 kJ/mol, and ΔG = -64.4 kJ/mol.These diffusion parameters were in good agreement with the segregation parameters obtained using Auger electron spectroscopy measurements.

Atomic Scale Processing Mini-Symposium
Room 116 - Session AP1+EM+PS+TF-MoA

Area Selective Deposition (ASD) II

Moderators: Satoshi Hamaguchi, Osaka University, Japan, **Richard Vanfleet**, Brigham Young University

2:30pm AP1+EM+PS+TF-MoA-5 Area Selective Deposition: Advances, Challenges and Future Technology Enablement, *Kandabara Tapily, Jeffrey Smith, Anton deVilliers, Gert Leusink,* TEL Technology Center, America, LLC
INVITED

K. Tapily, J. Smith, A. deVilliers, G. Leusink

TEL Technology Center, America, LLC, 255 Fuller Road, suite 214, Albany, NY 12203

To achieve higher performance, higher density, and lower cost, for decades the semiconductor industry has relied on aggressive scaling of the device feature size using top-down lithography. Additionally, scaling is driving the need for new materials introduction, new processes and new device architectures increasing the integration complexity. As a result, the industry has introduced several scaling boosters such as high k / metal gate, stress engineering, air gaps and recently area selective deposition to meet the power performance area cost or PPAC requirement.

Advanced device architectures such as gate-all-around (GAA) and complimentary field-effective transistors (CFET) require additional design / technology co-optimized (DTCO) solutions to continue the device scaling roadmap.Selective deposition of materials is fundamental not only for the reduced cost and complexity of manufacturing these advanced devices, but also as fundamental solutions to promote power / performance / CPP scaling of these advanced device architectures.

Surface engineering iskey in successfully realizing defect free area selective deposition. Surface sensitive and reaction driven processes such atomic layer processes (deposition and etch) will be key enabler in some of the required selective deposition processes (1).

This talk will discuss the status and approaches of area selective deposition technology and challenges the industry is facing in implementing future technology nodes. We will go over multiple examples of how novel selective deposition processes can accelerate the industry roadmap in terms of PPAC scaling.

References:

1. G. N Parsons, R. D Clark, *Chem. Mater.,* 32(12), 4920 (2020).

3:00pm AP1+EM+PS+TF-MoA-7 Examining UV-Induced Functional Group Formation on 2D Nanomaterials for Patterned ALD, *Azeez O. Musa, Andreas Werbrouck, Nikhila C. Paranamana, Matthew R. Maschmann, Matthias J. Young,* University of Missouri-Columbia

In our previous work, we employed a focused electron beam (e-beam) within an environmental scanning electron microscope (eSEM) to break down water vapor, allowing for the precise creation of hydroxylated patterns on highly oriented pyrolytic graphite (HOPG) surfaces. These patterns facilitated subsequent atomic layer deposition (ALD) in patterned areas, offering exceptional control over spatial resolution (exceeding 42 nm), and surface selectivity (ranging from 69.9% to 99.7%). However, despite its precision, the use of an e-beam is time-consuming and lacks industrial scalability due to the limited functionalization area on the substrate. In this study, we aim to explore the feasibility of patterning large areas of 2D material using UV irradiation in the presence of water vapor. Specifically, we seek to understand the impact of the direct UV ionization of water vs. ionization of water from secondary emitted electrons. Our experimental setup utilizes a custom-built hot-walled viscous-flow ALD reactor equipped with a vacuum ultraviolet (VUV) source unit with a peak emitted wavelength of 160 nm. This UV source incorporates a compact deuterium lamp with a MgF2 window and UV photons are focused onto the sample using a convex MgF2 lens to enhance photon flux density. We posit that the UV irradiation induces the formation of hydroxyl defects on the HOPG surface. To verify this, we employ spectroscopy including X-ray photoelectron spectroscopy (XPS), Fourier transform infrared spectroscopy (FTIR), and Raman spectroscopy (RS), assessing the formation of functional groups on 2D material surfaces. We also examine the impact of UV-functionalization on ALD nucleation and growth onto 2D materials. Our studies inform the applicability of this method for patterned thin-film deposition for semiconductor manufacturing.

3:15pm AP1+EM+PS+TF-MoA-8 ASD of Low Temperature Cu Capping Layers for Polymers-Based 3D Technologies, *Silvia Armini,* IMEC Belgium*; Anita Brady Boyd,* Aberystwyth University, UK*; Emmanuel Chery,* IMEC Belgium

With the constant increase of complexity in integrated systems, more and more connections are required between adjacent chips. Advanced packaging technologies using heterogeneous integration rely heavily on the interconnects redistribution layer (RDL) for this routing.

The most promising option to further reduce the interconnect dimensions relies on a dual-damascene process using photo-sensitive polymers as dielectric.

Unfortunately, using a polymer as a dielectric presents serious reliability challenges as polymers are generally unable to block the diffusion of oxygen, resulting in copper oxidation even at temperatures below 200 °C. Additionally, copper oxidation is not self-limiting.

As the critical dimensions of the lines are scaled down, high rates of oxidation are therefore a major reliability concern.

Recently the possibility of protecting the copper lines from oxidation through very thin ALD layers was demonstrated. For example, HfO_2 films as thin as 9 nm have been shown to effectively prevent copper oxidation during aggressive corrosion stress tests. Nevertheless, despite their minimal thickness, these dense films, deposited on the full surface of the wafer, are known to lead to mechanical stress. Ultimately, this stress can result in delamination and fracture during the next process steps.

To overcome this issue, area-selective deposition of TiO_2 and Al2O3 capping layers on Cu with respect to polymers are studied and their reliability performance investigated

3:30pm AP1+EM+PS+TF-MoA-9 SiO_2 Fluorination/Passivation for Area-Selective Deposition of TiO_2, ZnO, and Polymer on Metal and SiN_x vs. SiO_2, *Jeremy Thelven, Hwan Oh, Hannah Margavio, Gregory Parsons,* North Carolina State University

Challenges related to nanoscale pattern alignment are motivating research in chemically-directed patterning by Area-Selective Deposition (ASD) for future 3D devices. Recently, we have begun to explore the growth and inhibition mechanisms of metal oxide ALD materials (Al_2O_3, ZnO, and TiO_2) on hydroxylated and fluorinated SiO_2, and hydroxylated and fluorinated silicon nitride, SiNx, The ability to selectively react and deposit on an oxide vs nitride surface is recognized as a key problem due to the wide use of SiO_2 and SiNx in electronic device processing, and because of the chemical similarity of these surfaces. To explore ASD on SiNx and SiO_2, we exposed blanket SiNx and SiO_2 wafers to multiple doses of molybdenum hexafluoride, MoF_6, at low temperature (~200°C). Based on XPS analysis, the MoF_6 exposure leads to fluorination of both surfaces. Then, we performed polypyrrole (PPy) oxidative-CVD using pyrrole monomer and $SbCl_5$ as a surface oxidant. For the oxidative CVD process, 15 seconds of CVD produced ~50 nm of deposition on receptive surfaces. We found that PPy deposited readily on SiNx surface after some nucleation delay, but on SiO_2, only isolated nuclei were formed. Control experiments using SiNx and SiO_2 substrates without the MoF_6 exposure step showed uniform deposition on both substrates. To extend this demonstration of ASD of SiNx vs SiO_2 to other materials and substrates, we tested ALD of TiO_2, ZnO, and Al_2O_3 SiO_2, SiNx and Mo metal after exposure to MoF_6. We find that this selective fluorination passivation of the SiO_2 surface allows for selective growth of TiO_2 and ZnO on Mo vs SiO_2, whereas ALD Al_2O_3 using TMA/H_2O showed uniform, non-selective deposition. Moreover, after exposing SiO_2 and SiNx to MoF_6, TiO_2 ALD using $TiCl_4/H_2O$ deposited on SiNx after some delay, whereas a much longer delay was observed on SiO_2. The mechanisms behind selectivity, and the extent of metal-fluoride exposure needed to achieve passivation is currently under investigation. Direct comparisons between metal oxide ALD nucleation on SiO_2, SiNx and metal after exposure to MoF_6 will give insight into mechanisms necessary to achieve high selectivity, as well as provide options for advanced multi-material ASD schemes.

Atomic Scale Processing Mini-Symposium
Room 116 - Session AP2+EM+PS+TF-MoA

Modeling and Simulations of Atomic Layer Processing

Moderator: Satoshi Hamaguchi, Osaka University, Japan

4:00pm AP2+EM+PS+TF-MoA-11 Atomistic Simulations on the Fundamental Aspects of Atomic Layer Processing (ALP), *Bonggeun Shong*, Hongik University, Republic of Korea **INVITED**

As size of electronic devices are miniaturized to nanoscale, the precision of their fabrication processes is becoming extremely demanding. Atomic layer deposition (ALD) is a vapor phase thin film deposition technique based on sequential, self-limiting surface reactions. Through ALD, high conformality on high-aspect ratio substrates, thickness control at the Angstrom level, and tunable film composition are achievable. Furthermore, area-selective ALD (AS-ALD) has recently emerged as a possible alternative bottom-up approach for nanoscale patterning. With these advantages, ALD is gaining interest as a powerful tool for many industrial and research applications, especially in microelectronic fabrication. Furthermore, atomic layer etching (ALE) is emerging as a novel technique that can provide atomically controlled etching of materials. These technologies with atomic layer precision are often altogether referred to as atomic layer processing (ALP). Ideally, the entire ALP processes are based only on the surface chemistry of the substrates. Thus, it is important to understand their surface reaction mechanisms in order to improve the process conditions and material quality, and even to design novel materials and processes. With development of modern simulation tools, utilization of atomistic calculations is becoming increasingly useful toward deeper understanding and design of such chemical reactions. However, ALD processes often face limitations toward fabrication of next-generation semiconductor devices due to their size scale and structural complexity; furthermore, such problems are often convoluted with challenges toward realistic simulations of surface chemical processes. In this talk, analysis of fundamental surface chemistry of various ALP based on computational chemistry methods, as well as development of new processes and materials based on chemical simulations will be presented.

4:30pm AP2+EM+PS+TF-MoA-13 Understanding Process Parameters in High-Aspect-Ratio ALD via Transport Modeling , *Victor Vogt,* University of Michigan*; Andrew Gayle,* National Institute of Standards and Technology (NIST)*; Andres Miranda Manon, Andrej Lenert, Neil Dasgupta,* University of Michigan

Atomic layer deposition (ALD) is a powerful tool to modify ultra-high-aspect-ratio structures with unparalleled conformality. We have recently demonstrated the ability of ALD to modify silica aerogels with aspect ratios greater than 60,000:1 and improve their thermal stability from ~600°C to ~800°C, for applications in concentrating solar thermal energy generation.[1] To facilitate conformal ALD modifications on these extreme aspect ratios, a reaction-diffusion model was developed to precisely predict infiltration into the aerogel as a function of exposure time and number of doses, enabling tunable control of the infiltration depth.[2]

In this study, we have built upon our previous reaction-diffusion model to explore the effects of exposure time, precursor temperature, and number of aerogels coated on process time and precursor utilization. We analyze process parameter trends in terms of the governing reaction-diffusion mechanism and relevant equations. These trends are then validated experimentally via energy dispersive x-ray spectroscopy (EDS) mapping of the infiltration depth. Additionally, we explore the relationship between number of aerogels coated and reactor volume, and we analyze the impacts of this on ALD reactor design for high-aspect-ratio substrates. Finally, we demonstrate that ALD can be used to tune the mechanical strength and stiffness of silica aerogels, a key limitation of these materials in practical applications. This work will enable a greater understanding of high-aspect-ratio ALD processing as well as its potential applications in the modification of porous materials.

References:

[1] Z.J. Berquist, A.J. Gayle, N.P. Dasgupta, and A. Lenert, Transparent Refractory Aerogels for Efficient Spectral Control in High-Temperature Solar Power Generation. *Adv. Funct. Mater.* **2022** *32*, 2108774.

[2] A.J. Gayle, Z.J. Berquist, Y. Chen, A.J. Hill, J.Y. Hoffman, A.R. Bielinski, A. Lenert, and N.P. Dasgupta, Tunable Atomic Layer Deposition into Ultra-High-Aspect-Ratio (>60000:1) Aerogel Monoliths Enabled by Transport Modeling, *Chem. Mater.* **2021** *33* (14), 5572-5583.

4:45pm AP2+EM+PS+TF-MoA-14 Modeling Remote Inductively Coupled Plasmas for Plasma-Enhanced Atomic Layer Deposition, *Mackenzie Meyer, David Boris, Michael Johnson, Jeffrey Woodward, Virginia Wheeler,* US Naval Research Laboratory*; Mark Kushner,* University of Michigan, Ann Arbor*; Scott Walton,* US Naval Research Laboratory

Plasma-enhanced atomic layer deposition (PEALD) uses a plasma step to generate the necessary reactive species, allowing atomic layer deposition (ALD) processes to occur at lower temperatures and with additional reaction chemistries compared to thermal ALD. Remote inductively coupled plasma (ICP) sources are often used in PEALD as they limit electrons and ions at the growth substrate while providing radicals from the plasma. However, remote ICP systems, particularly downstream of the source, are not fully understood. Modeling of remote ICPs can contribute to an understanding of these systems. In this work, modeling of remote ICPs is performed using the 2D Hybrid Plasma Equipment Model (HPEM). The remote ICPs are based on the Veeco Fiji G1 and G2 sources operating in an N_2/Ar mixture. Both inductively and capacitively coupled power contribute to the power deposited into the plasma. The results of the model are compared to experimental measurements reported, including atomic N density in the plasma source and electron density and plasma potential downstream in the spatial afterglow of the ICP. The model is also used to examine the production of species that are not measured, including metastable N_2, as well as the absolute and relative fluxes of reactive species to the substrate, for a range of operating conditions. The results are then linked to the growth of nitride films in an effort to quantify the relative importance of different operating modes and reactive species. This work is partially supported by the Naval Research Laboratory base program.

5:00pm AP2+EM+PS+TF-MoA-15 Prediction of Plasma-induced Changes in Surface Morphology and Composition during Atomic Layer Deposition: A Combined Ab-Initio and Monte Carlo Approach, *Gyeong Hwang, **Ting-Ya Wang**,* University of Texas at Austin

Atomic layer deposition (ALD) has emerged as a method offering enhanced precision and control in comparison to traditional chemical vapor deposition. It operates through alternating cycles of two half-cycle reactions, ensuring sequential and self-limiting deposition. However, thermal ALD necessitates high deposition temperatures (> 400 °C), particularly for nitridation. Although employing plasma can reduce these surface temperatures, plasma can have detrimental effects on materials too, including modification of the chemical composition and densification, which profoundly impact crucial material properties such as dielectric constant.

Therefore, understanding the plasma-induced changes in surface morphology and composition is crucial. However, existing experimental techniques encounter limitations in surface analysis. Non-polar bonds, such as N_2 dimer, are inactive under infrared (IR) spectroscopy. X-ray photoelectron spectroscopy causes surface damage to a certain extent. Moreover, overlapping signals may render the analysis uncertain and challenging. Theoretical methods have their own set of limitations. Molecular dynamics (MD) simulations allow the study of dynamic processes but are constrained by limitations in both length and time scales, which make it unsuitable for ALD systems, where primary reactions fall into the category of rare events.

The integration of kinetic Monte Carlo (kMC) with density functional theory (DFT) presents a promising simulation approach for ALD. However, a notable challenge lies within kMC, specifically the requirement for a predefined list of permissible events. Traditionally, researchers identify a set of reactions considered most significant. Yet, given the numerous potential events occurring on a surface and the criticality of rare events in ALD, outcomes derived from a manually compiled list may sometimes lack authenticity.

We developed an atomistic, off-lattice, and three-dimensional simulator that integrates kMC and DFT, and employed a strategic approach to formulate a comprehensive event list, with the goal of encompassing a wide range of potential surface reactions. Our investigation centered on assessing the effects of N_2, H_2, and NH_3 plasmas on SiCN material, including examination of the roles played by radicals and ion bombardment. Furthermore, we also studied the influence of process conditions, including temperature and pressure, while also analyzing the influence of oxygen exposure.

5:15pm AP2+EM+PS+TF-MoA-16 Modelling and Simulation of Plasma-Enhanced Atomic Layer Deposition of Silicon Nitride Over Sidewall Surfaces of a Closing Narrow-Gap Trench, *Jomar Tercero, Kazumasa Ikuse, Satoshi Hamaguchi,* Osaka University, Japan

Molecular dynamics (MD) simulations were performed to study the transport mechanisms of chlorine (Cl) atoms during the plasma-enhanced atomic layer deposition (PE-ALD) of silicon nitride (SiN). PE-ALD is a technique to deposit highly precise and uniform thin films required for nanoscale semiconductor devices. The typical PE-ALD process involves sequential and self-limiting surface reactions, facilitating the formation of monolayers in a layer-by-layer manner.[1] In the case of SiN PE-ALD, chlorosilanes such as SiH_2Cl_2 are commonly used as Si-containing gas precursors. During the first half-cycle, Si atoms of the precursors adsorb on the surface, whose surface atoms are then terminated by Cl atoms. Subsequently, the surface is exposed to nitrogen (N) and hydrogen (H)-containing plasmas. During this second half-cycle, H atoms react and capture Cl atoms on the surface, forming volatile hydrogen chloride (HCl) molecules.[2] In this study, our focus is PE-ALD of SiN over a trench structure when the gap is closing and the two facing sidewalls are approaching each other. In the desorption/nitridation half-cycle, Cl atoms must be removed from the extremely narrow gap by Cl or HCl diffusion if the gap is closing. The diffusion coefficients of Cl atoms in such narrow gaps were evaluated from molecular dynamics (MD) simulations, under different conditions for the surface temperature (700, 800, and 900 K), gap distance (0.6, 1, and 2 nm), and H density. The MD simulations revealed that, without H atoms, Cl diffusion was highly restricted. H atoms were observed to capture Cl atoms, assisting their transport in the narrow gap. Additionally, we observed the formation of H_2 molecules, some of which penetrated the SiN bulk and diffused. The results indicate that, as the two facing SiN sidewalls approach each other and the gap diminishes, the transport of atoms and molecules in the gap becomes restricted and therefore the ALE process slows down, eventually forming a seam between the two facing sidewalls.

References

[1] K. Arts, S. Hamaguchi, T. Ito, K. Karahashi, H. C. M. Knoops, A. J. M. Mackus, and W. M.
M. E. Kessels, "Foundations of atomic-level plasma processing in nanoelectronics," Plasma
Sources Science and Technology, 31, 103002 (2022).

[2] R. A. Ovanesyan, E. A. Filatova, S. D. Elliott, D. M. Hausmann, D. C. Smith, and S. Agarwal, "Atomic layer deposition of silicon-based dielectrics for semiconductor manufacturing: Current status and future outlook", Journal of Vacuum Science and Technology A, 37, 060904 (2019).

Applied Surface Science
Room 116 - Session AS-MoA

Chemical Processes at Surfaces

Moderators: Jordan Lerach, PPG Industries, **Alexander Shard**, National Physical Laboratory

1:45pm AS-MoA-2 SiO$_2$ Surfaces Sputtering Profiles: Experimental and Numerical Study, *Camil Bocaniciu, Julian Pichler, Alper Celebi,* TU Wien, Austria*; Markus Ostermann,* CEST GmbH, Austria*; Markus Valtiner,* TU Wien, Austria

Silicon dioxide (SiO_2) crystals serve as a relevant material in sputtering processes for their well-defined properties and broad applications in material science. The material offers a stable, reproducible target, aiding in the accurate calibration of sputtering equipment and standardizing experimental conditions. This stability is crucial for developing thin films, coatings, and semiconductor devices, where precise material control is essential [1].

The objective of this study is to explore the atomic layer structure and the composition of SiO_2 surfaces at different thicknesses from both experimental and numerical point of views. We first measure depth profiles of different thicknesses of SiO_2 using Low Energy Ion Spectroscopy (LEIS) at various energies. LEIS is a highly surface sensitive technique which probes only the top atomic layer of a material surface [2]. Our findings indicate that combining sputtering with LEIS is an effective technique for probing the in-depth structure of SiO_2 crystals grown on Si substrates. Distinct profile variations were observed for different surface oxidation processes, including O_2 plasma, thermal oxide, and native oxide, particularly for oxide thicknesses varying between 1.2 to 2 nm. In contrast, for thicker oxides

between 30 and 60 nm, the profiles converged, showing minimal dependence on the oxidation method employed.

To provide additional physical insights into the obtained depth profiles by LEIS measurements, we subsequently perform sputtering simulations using SDTrimSP [3]. Sputtering simulations calculate the interaction between incident ions and surface atoms and describe sputtering, as well as surface degradation and ion implantation in the target material. For Ar^+, simulations demonstrate preferential sputtering of oxygen compared to silicon and suggest a layer intermixing in SiO_2 of 1.2 nm for 0.5 keV incident ion energy and 3.2 nm for 2 keV incident ion energy. Our simulations further show that simulated sputtering depth profiles correlate well with the depth profiles obtained by the LEIS measurements. Ultimately, the well-established stoichiometry of SiO_2 will be used as a reference for oxygen content by integrating experimental measurements with simulation results. This method will enable quantification with LEIS for any material surface that contains oxygen

[1]Kelly, J. J. (2003) "SiO2: A Versatile Reference Material for Sputtering and Thin Film Research." Journal of Vacuum Science & Technology A, vol. 21, no. 4.

[2]Brongersma, H. H., Draxler, M. (2007). Surface composition analysis by low-energy ion scattering. Surface Science Reports, 62(3), 63-109.

[3]Mutzke, A. et al. (2019) "SDTrimSP Version 6.00"

Biomaterial Interfaces
Room 117 - Session BI-MoA

Microbes at Interfaces

Moderators: Axel Rosenhahn, Ruhr-University Bochum, **Rong Yang**, Cornell University

1:30pm BI-MoA-1 The Role of Surface/Interface Phenomena in The Antibacterial Action of Nano- and Microscale Gallium Oxide and Gallium Hydroxide, *Yuri M. Strzhemechny, Dustin A. Johnson, John H. Brannon,* Texas Christian University*; Pavan Ahluwalia,* Harmony School of Innovation Fort Worth*; Tiffany Y. McHenry, Madeline M. Smit, Devansh Kalluholematham,* Texas Christian University*; Zachary Rabine,* Wayne State University*; Parmeet Jodhka,* Tarrant County College Northwest

Worldwide trend of increasing antibiotic resistance has spun interest in alternative antibacterial agents such as metal oxide particles. Whereas the antibacterial action of many such oxides is well established, the mechanism of this activity is largely unknown. Cytotoxicity could be mediated via such mechanisms as production of reactive oxygen species, release of toxic cations, interactions disrupting cell walls and causing osmotic stress. Targeted applications of oxide antibacterials are also hindered by a lack of understanding of the role and nature of the local bacterial environment in mediating/hindering antibacterial interactions. Surface defects in nano- and micro-crystals strongly affect performance of metal oxides in applications, necessitating elucidation and control of those defects. The beta polymorph of gallium oxide (β-Ga$_2$O$_3$) in nano- and microcrystalline form is attracting a significant research interest due to potential applications in biological therapeutics, optoelectronics, and catalysis. In our studies, we employ nano- and microparticles of β-Ga$_2$O$_3$ synthesized via a simple bottom-up hydrothermal method, which yields, as a first step, a GaOOH precursor, which then undergoes calcination to bear the final product. Such growth method, through variation of growth parameters, allows production of particles with tunable morphology and controllable relative abundances of surfaces with desired polarities. To address the nature of interactions between β-Ga$_2$O$_3$ and GaOOH crystal surfaces, cellular membranes and bacterial growth media we perform detailed systematic studies of the optoelectronic and physicochemical properties of both GaOOH and β-Ga$_2$O$_3$ samples and then evaluate their impact of on the antibacterial action of these samples. We are especially interested in the influence of surface defects and particle morphologies on the antimicrobial efficiency of the studied oxides. The biological assays with *Escherichia coli* and *Staphylococcus aureus* are used to examine the antibacterial action and also to run pre- and post-assay comparative studies of the oxide specimens themselves. For the latter we employ a variety of characterization techniques, such as electron microscopy, energy-dispersive X-ray spectroscopy, time and wavelength dependent surface photovoltage, temperature-dependent photoluminescence spectroscopy, Fourier-transform infrared spectroscopy, etc. We find in our samples a strong correlation between the growth parameters, particle morphologies, crystal surface characteristics, and antimicrobial properties.

Monday Afternoon, November 4, 2024

1:45pm BI-MoA-2 Microbially-Induced Corrosion of Synthetic Granite and Dike Glass by Paenibacillus Polymyxa SCE2 Using ToF-SIMS, *Gabriel Parker,* University of Illinois Chicago*; Andrew Plymale, Jacqueline Hager, Jeffery Dhas, Zihua Zhu,* PNNL*; Luke Hanley,* University of Illinois - Chicago*; Xiao-Ying Yu,* ORNL

Microbially-induced corrosion (MIC) is an important topic that focuses on material degradations over extended periods. Soil microbes are often associated with MIC of foreign objects interacting within the rhizosphere. *Paenibacillus polymyxa* SCE2 is a facultative anaerobic microbe found in soil. Time-of-flight secondary ion mass spectrometry (ToF-SIMS) is a powerful mass spectrometry imaging technique that provides insights into the surface characteristics by its spectral, two-dimensional (2D) imaging, and depth profiling capabilities of biointerphases. Herein, ToF-SIMS was used to detect surface changes on synthetic granite and synthetic dike glass coupons that were treated with *Paenibacillus polymyxa* SCE2 over extensive periods of time. Confocal laser scanning microscopy (CLSM) was used to verify bacterial coverage across the granite and dike glass surfaces after three and seven months' growth in a static cell. ToF-SIMS spectral analysis shows detection of glass component related ions, such as m/z 276.84, 380.81, 418.77, 607.62, 693.48, and 721.51. Also, ions that are indicative of extracellular polymeric substance (EPS) components were observed, such as m/z 241.22, 255.23, 269.25, 297.15, 311.16, and 325.18.Clusters of un-identified peaks are detected in the biofilm treated glass coupons, which are speculated to reflect EPS components as they incorporated into the glass to form colonies, resulting in MIC. ToF-SIMS analysis results show that granite glass has more "corrosion related" peaks than the dike glass.The observed surface compositional and morphological differences between the two types of glass are hypothesized to be related to the glass surface hydrophobicity and ultimately its affinity to biofilms.

2:00pm BI-MoA-3 Titanium Oxynitride Thin Films Deposited in a Custom-Built ALD Reactor with Real-Time Residual Gas Probing to Enhance the Photocatalytic Activity of Polymethylmethacrylate (PMMA) and Induce Antimicrobial Activity on Its Surface, *Harshdeep Bhatia,* University of Illinois - Chicago*; Bruna Nagay, Valentim Barão,* University of Campinas (UNICAMP), Brazil*; Gregory Jursich, Cortino Sukotjo, Christos Takoudis,* University of Illinois - Chicago

Titanium oxynitride is a novel material researched for its visible light photocatalytic activity (PCA). Polymethylmethacrylate (PMMA) is a common organic biomaterial used in the dental industry which is used in conditions where they are highly susceptible to microbial biofilm formation. In this study, Atomic Layer Deposition (ALD) was used to deposit a thin layer of titanium oxynitride on 3D printed PMMA disks. The reactor used tetrakis(dimethylamino) titanium(IV) as the titanium precursor and ammonia (NH_3) as the nitriding agent; the system was custom-designed and controlled using a Python program. A common single board computer controlled the solenoid valves connected to the pneumatic valves. The Python program could deposit a single or a bilayer of oxide and nitride and control the ALD valves manually. A Chemical Vapor Deposition (CVD) mode is also possible for faster film growth. In addition, a residual gas analyzer (RGA) was connected to the downstream to study the outgassed products from the reactor in real time. The operating pressure for the ALD reactor was 1.6 Torr while for the RGA was 1×10^{-6} Torr. After deposition, thickness was measured on the reference silicon sample using Spectroscopic Ellipsometry while the composition was measured using X-ray Photoelectron Spectroscopy. Post-deposition, PCA of the PMMA surfaces were also determined using the degradation of a standard methylene blue solution after irradiation by three different light sources. A similar approach was used to test the antibacterial and antifungal effect under light irradiation. Cell viability tests were also performed to test the biocompatibility of the film.

2:15pm BI-MoA-4 Isolation and Identification of Copper-Tolerant Fouling Communities, *Sara Tuck, Melissa Kardish,* US Naval Research Laboratory*; Beatriz Orihuela,* Duke University*; Gary Vora,* US Naval Research Laboratory*; Katherine Franz,* Duke University*; Kenan Fears,* US Naval Research Laboratory

Biofouling, the accumulation of unwanted organisms on submerged assets, is a fundamental problem in maritime transport and human health. Biofouling build-up increases fuel consumption, exhaust emissions, and operational costs in addition to facilitating the transfer of environmental and pathogenic bacteria from one location to another. Conventionally, biofouling is inhibited by the application of antifouling coatings, the most popular of which are copper based. In biological systems, copper is tightly regulated and, in an attempt, to exploit this, antifouling coatings contain up to 75% CuO by weight. Despite these high loadings, the efficacy of these coatings is rapidly declining with the emergence and spread of copper-tolerant species. Microbial communities resistant to copper have been found to form mature biofilms on these coatings, which could be altering the interfacial properties to create more favorable conditions for the settlement of a broader biofouling community. To gain an understanding of the mechanisms responsible for the loss of antifouling performance, coated and uncoated polyvinyl chloride panels were submerged at estuarine and marine field test sites and microbial communities were isolated. Biofouling communities were harvested from three test sites and individual species were cultured, isolated, and identified. Copper tolerance was assessed by re-exposing these cells to copper-containing coatings and traditional broth microdilutions.

2:30pm BI-MoA-5 Surface-Cleaning Mechanisms Used by Acorn Barnacles (Amphibalanus Amphitrite) to Prevent Microbial Colonization at Their Adhesive Interface, *Qin Lu, Eric McGhee, William Hervey, Dasha Leary, Christopher Spillmann, Kenan Fears,* US Naval Research Laboratory

Barnacles have long been admired, or hated, for their robust underwater adhesives that allow them to tenaciously adhere to surfaces and endure harsh marine environments. Previously, we revealed that acorn barnacles evolved a remarkable surface cleaning fluid that removes microorganisms ahead of expansion of their base and the deposition of a new ring of cement. This process involves the secretion of a lipidaceous material that phase separates in seawater, into a phenolic laden gelatinous phase that presents a phase rich in lipids and reactive oxygen species to the seawater interface. Biofilms in close proximity to this material rapidly oxidize and lift off the surface as the secretion advances. Proteomics analysis of the adhesive interface reveals the presence of a haloperoxidase, a class of enzyme known to participate in the innate immune response of a wide variety of organisms, which converts chlorine ions to hypochlorite ions (bleach) in the presence of hydrogen peroxide. We performed agar well diffusion assays the assess the susceptibility of marine and terrestrial micro-organisms to hydrogen peroxide with and without the presence of a haloperoxidase. While yeast cells (*P. larentii*) where shown to be quite susceptible to hypochlorite ions at low doses, the oxidation of biofilms of marine bacterium (*V. natrigens* and *M. atlanticus*) by hypochlorite ions did not result in significant cell death. Confocal microscopy of different barnacle species revealed that the surface cleaning mechanisms employed by acorn barnacles is not ubiquitous to all barnacle species. Microbial colonies were present in the basal region of barnacle species in which the secretion of this surface cleaning fluid was not observed, in stark contrast to barnacle with this surface cleaning fluid. Knowledge of these processes could enhance the efficiency of synthetic underwater adhesives and lead to novel environmentally benign antifouling technologies.

2:45pm BI-MoA-6 BioSAXS - a Tool to Enrich and De-Risk Antimicrobial Drug Development, *Axel Rosenhahn, Christoph Rumancev, Andreas Gräfenstein,* Ruhr University Bochum, Germany*; Kai Hilpert,* University of London, UK **INVITED**

Antimicrobial resistance is a worldwide threat to modern health care. Low-profit margin and high risk of cross-resistance resulted in a loss of interest in big pharma, contributing to the increasing threat. Strategies to address the problem are starting to emerge. Novel antimicrobial compounds with novel modes of action are especially valued because they have a lower risk of cross-resistance. Up to now determining the mode of action has been very time and resource consuming and will be performed once drug candidates were already progressed in preclinical development. BioSAXS is emerging as a new method to test up to thousands of compounds to classify them into groups based on ultra-structural changes that correlate to their modes of action. BioSAXS experiments in gram-negative E. coli and a correlation with transmission electron microscopy have demonstrated that using conventional and experimental antimicrobials a classification of compounds according to their mode of action was possible. Further work showed that the approach can also be used for gram-positive bacteria (S. aureus) and the effects of novel antimicrobial peptides on both types of bacteria were studied. Preliminary experiments will be presented that show that BioSAXS can also be used to classify antifungal drugs, demonstrated on Candida albicans. The data will be discussed in view of the perspective of how BioSAXS can accelerate and enrich the discovery of antimicrobial compounds from screening projects with a novel mode of action and hence de-risk the development of urgently needed antimicrobial drugs.

Nanoscale Science and Technology
Room 114 - Session NS1+2D+QS-MoA

Functionality in 2D Nanostructures and Devices
Moderators: Nikolai Klimov, NIST, **Andy Mannix**, Stanford University

1:30pm **NS1+2D+QS-MoA-1 Low-Dimensional Neuromorphic Electronic Materials and Applications**, *Mark Hersam,* Northwestern University **INVITED**

The exponentially improving performance of digital computers has recently slowed due to the speed and power consumption issues resulting from the von Neumann bottleneck. In contrast, neuromorphic computing aims to circumvent these limitations by spatially co-locating logic and memory in a manner analogous to biological neuronal networks [1]. Beyond reducing power consumption, neuromorphic devices provide efficient architectures for image recognition, machine learning, and artificial intelligence [2]. This talk will explore how low-dimensional nanoelectronic materials enable gate-tunable neuromorphic devices [3]. For example, by utilizing self-aligned, atomically thin heterojunctions, dual-gated Gaussian transistors have been realized, which show tunable anti-ambipolarity for artificial neurons, competitive learning, spiking circuits, and mixed-kernel support vector machines [4,5]. In addition, field-driven defect motion in polycrystalline monolayer MoS_2 enables gate-tunable memristive phenomena that serve as the basis of hybrid memristor/transistor devices (i.e., 'memtransistors') that concurrently provide logic and data storage functions [6]. The planar geometry of memtransistors further allows multiple contacts and dual gating that mimic the behavior of biological systems such as heterosynaptic responses [7]. Moreover, control over polycrystalline grain structure enhances the tunability of potentiation and depression, which enables unsupervised continuous learning in spiking neural networks [8]. Finally, the moiré potential in asymmetric twisted bilayer graphene/hexagonal boron nitride heterostructures gives rise to robust electronic ratchet states. The resulting hysteretic, non-volatile injection of charge carriers enables room-temperature operation of moiré synaptic transistors with diverse bio-realistic neuromorphic functionalities and efficient compute-in-memory designs for low-power artificial intelligence and machine learning hardware [9].

[1] V. K. Sangwan, *et al.*, *Matter*, **5**, 4133 (2022).

[2] V. K. Sangwan, *et al.*, *Nature Nanotechnology,* **15**, 517 (2020).

[3] M. E. Beck, *et al.*, *ACS Nano*, **14**, 6498 (2020).

[4] M. E. Beck, *et al.*, *Nature Communications*, **11**, 1565 (2020).

[5] X. Yan, *et al.*, *Nature Electronics*, **6**, 862 (2023).

[6] X. Yan, *et al.*, *Advanced Materials*, **34**, 2108025 (2022).

[7] H.-S. Lee, *et al.*, *Advanced Functional Materials*, **30**, 2003683 (2020).

[8] J. Yuan, *et al.*, *Nano Letters*, **21**, 6432 (2021).

[9] X. Yan, *et al.*, *Nature*, **624**, 551 (2023).

2:00pm **NS1+2D+QS-MoA-3 Defect Manipulation in van der Waals Heterostructures and its Applications**, *Son Le,* Laboratory for Physical Sciences*; Thuc Mai, Maria Munoz, Angela Hight Walker, Curt Richter,* 100 Bureau Dr.*; Aubrey Hanbicki, Adam Friedman,* 8050 Greenmead Dr. **INVITED**
Reliable and accurate spatial doping of 2-dimensional (2D) materials is important for future applications using this novel class of materials. Here, we present our work on photo-doping of an h-BN/Graphene/h-BN heterostructure. Natural defect states in bulk h-BN can remotely dope graphene and can be optically activated or deactivated. In this way, we can modify both the carrier density and type in graphene accurately and reversibly by several orders of magnitude. Using a spatially-resolved light source, we can activate photo-dopants in selected areas of the sample, and by laterally modulating the doping, we have created PNP junction (PNPJ) devices. *In-situ* quantum Hall measurements were used to demonstrate the effectiveness of this doping technique and characterize the electrostatic profile of the PNPJ. Doping and undoping the heterostructure in a specific sequence, we were able to introduce and destroy correlation among the dopants. Defect correlation greatly enhances carrier mobility while the destruction of this correlated state significantly degrades the carrier mobility in the graphene, effectively creating a mobility switch. An elegant demonstration of this mobility switch is the observation of spin and valley-resolved Landau levels of the graphene in the quantum Hall regime with high-mobility, dopant correlated states, and spin and valley -degenerate Landau levels in the low-mobility, dopant uncorrelated states. I will discuss ongoing studies to better understanding the nature of these defects with photo-doping measurements of different hBN thicknesses as well as hBN

from different sources. This doping technique opens up the possibility to engineer novel device and expand the applications of 2D heterostructures.

2:30pm **NS1+2D+QS-MoA-5 Extraordinary Tunnel Electroresistance in Layer-by-Layer Engineered Van Der Waals Ferroelectric Tunnel Junctions**, *Qinqin Wang,* Department of Electrical and Computer Engineering and Quantum Technology Center, University of Maryland, College Park
The ability to engineer potential profiles of multilayered materials is critical for designing high-performance tunneling devices such as ferroelectric tunnel junctions (FTJs). FTJs comprise asymmetric electrodes and a ferroelectric spacer, promising semiconductor platform-compatible logic and memory devices. However, the traditional FTJs consisting of metal/oxide/metal multilayer heterostructures can only exhibit modest tunneling electroresistance (TER, usually $<10^6$), which is fundamentally undermined by the unavoidable defect states and interfacial trap states. Here, we constructed van der Waals (vdW) FTJs by a layered ferroelectric $CuInP_2S_6$ (CIPS) and graphene. Owing to the gigantic ferroelectric modulation of the chemical potentials in graphene by as large as ~1 eV, we demonstrated a giant TER of 10^9. While inserting just a monolayer MoS_2 between CIPS/graphene, the off state is further suppressed, leading to $>10^{10}$ TER. Our discovery opens a new solid-state paradigm where potential profiles can be unprecedentedly engineered in a layer-by-layer fashion, fundamentally strengthening the ability to manipulate electrons' tunneling behaviors and design advanced tunneling devices.

Keywords: 2d materials, ferroelectric tunnel junctions, tunneling electroresistance

2:45pm **NS1+2D+QS-MoA-6 Scanning Tunneling Microscopy Studies of Twisted Transition Metal Dichalcogenides**, *Adina Luican-Mayer,* STEM 150 Louis Pasteur Private, Canada
Material systems, devices, and circuits, based on the manipulation of individual charges, spins, and photons in solid-state platforms are key for quantum technologies. Two-dimensional (2D) materials present an emerging opportunity for the development of novel quantum technologies, while also pushing the boundaries of fundamental understanding of materials. Our laboratory aims to create quantum functionality in 2D systems by combining fabrication and assembly techniques of 2D layers with atomically precise microscopy.

In this talk, I will focus on experimental observations of novel phenomena in moiré structures created by twisting 2D layers using scanning tunnelling microscopy and spectroscopy. I will discuss the demonstration of reversible local response of domain wall networks using scanning tunneling microscopy in ferroelectric interfaces of marginally twisted WS_2 bilayers. Moreover, in the case of twisted WS_2 bilayers close to 60°, we observe signatures of flat bands and study the influence of atomic relaxation on their band structure.

Nanoscale Science and Technology
Room 114 - Session NS2-MoA

Light-Matter Interactions at the Nanoscale
Moderator: Nikolai Klimov, NIST

4:00pm **NS2-MoA-11 Time-Resolved Photoemission Electron Microscopy Imaging of the Near-Field Dynamics in Silver Nanowires Excited by Few-Cycle Short-Wave Infrared Pulses**, *Nelia Zaiats,* Lund University, Sweden
Ultrafast photoemission electron microscopy (PEEM) is a powerful technique for studying the dynamics of surface plasmons and other electronic excitations, allowing space and time coherent imaging of plasmonic phenomena at the sample, irradiated by pulsed light with high temporal and spatial resolution [1].

Short-wave infrared (SWIR) light is used for optical communication as well as in a wide range of sensor applications [2]. Femtosecond SWIR sources can also be used for generating high-order harmonics in the water window [3]. Silver nanowires, which can be synthesized with high crystal perfection [4], present a pronounced plasmonic resonance in the SWIR range, allowing them to act as efficient light concentrators. While detailed interferometric time-resolved photoemission electron microscopy (ITR-PEEM) measurements have been carried out on Ag nanoparticles in the visible and near-infrared range [5,6], few such PEEM studies have been reported in the SWIR range [1].

Here, we investigate the near-field dynamics in Ag nanowires excited by SWIR pulses with a duration of ~17 fs (2.3 optical cycles) and wavelengths in the 1600-2400 nm range using ITR-PEEM. We study the nanowire

response for different light polarizations and intensities as well as for different orientations and geometrical shapes of the wires. We excite the dipolar longitudinal plasmon mode of the nanowire and investigate the near-field dynamics on the femtosecond time scale using two SWIR pump-probe pulses separated in time. The study shows the use of ITR-PEEM in the SWIR wavelength regime, revealing the dynamics of a model plasmonic system.

References

[1] E. Mårsell, et al. Photoemission electron microscopy of localized surface plasmons in silver nanostructures at telecommunication wavelengths, J. of Appl. Phys. 117, 083104 (2015).

[2] M. P. Hansen and D. S. Malchow "Overview of SWIR detectors, cameras, and applications", Proc. SPIE 6939, Thermosense XXX, 69390I (2008).

[3] J. Li, J. Lu, A. Chew, et al. Attosecond science based on high harmonic generation from gases and solids. Nat Commun 11, 2748 (2020).

[4] M. Mayer, et al. Controlled Living Nanowire Growth: Precise Control over the Morphology and Optical Properties of AgAuAg Bimetallic Nanowires. Nano Lett 15(8), 5427 (2015).

[5] D. Bayer, et al. Time and Space Resolved Studies on Metallic Nanoparticles. In: D.T. Cat, A. Pucci, K. Wandelt. (eds) Physics and Engineering of New Materials. Springer Proceedings in Physics 127. Springer, Berlin, Heidelberg (2009).

[6] E. Mårsell, et al. Nanoscale imaging of local few-femtosecond near-field dynamics within a single plasmonic nanoantenna, Nano Lett 15(10), 6601 (2015).

4:15pm NS2-MoA-12 AFM-IR of EHD-Printed PbS Quantum Dots: Quantifying Ligand Exchange at the Nanoscale, *Lorenzo Ferraresi, Goekhan Kara,* Empa, Swiss Federal Laboratories for Materials Science and Technology, Switzerland*; **Nancy Burnham,** Worcester Polytechnic Institute; Roman Furrer, Dmitry Dirin, Fabio La Mattinia, Maksym Kovalenko, Michel Calame, Ivan Shorubalko,* Empa, Swiss Federal Laboratories for Materials Science and Technology, Switzerland

Colloidal quantum dots (cQDs) recently emerged as building blocks for semiconductor materials with tuneable properties. Electro-hydrodynamic printing can be used to obtain sub-micrometre patterns of cQDs without elaborate and aggressive photolithography steps. Post-deposition ligand exchange is necessary for the introduction of new functionalities into cQD solids. However, achieving a complete bulk exchange is challenging and conventional infrared spectroscopy lacks the required spatial resolution for its analysis. Infrared nanospectroscopy (AFM-IR) enables quantitative analysis of the evolution of vibrational signals and structural topography on the nanometre scale upon ligand substitution on lead sulphide (PbS) cQDs. A solution of ethane-dithiol in acetonitrile demonstrated rapid (~60 s) and controllable exchange of more than 80% of the ligands, encompassing structures up to ~800 nm in thickness. Prolonged exposures (>1 h) led to the degradation of the microstructures, with a systematic removal of cQDs regulated by surface-to-bulk ratios and solvent interactions. This study establishes a method for the development of devices through a combination of tuneable photoactive materials, additive manufacturing of microstructures, and their quantitative nanometre-scale analysis.

4:30pm NS2-MoA-13 AVS National Student Awardee Talk: Slow and Fast Timescale Effects of Photoinduced Surface Oxygen Vacancies on the Charge Carrier Dynamics of TiO₂, *Bugrahan Guner*[1]*, Omur E. Dagdeviren,* École de technologie supérieure, University of Quebec, Canada

The migration of charge carriers (*e.g.,* electrons, holes) in metal oxides, such as TiO_2, plays a vital role in (photo)catalytic applications [1]. Nevertheless, photoinduced surface oxygen vacancies (PI-SOV) scan significantly alter the dynamics of charge carriers [2-4]. Here, we study the effect of PI-SOVs (prompted by high-energy ultraviolet irradiation) on fast (*i.e.,* electrons) and slow (*i.e.,* holes) charge carriers via time-resolved atomic force microscopy (TR-AFM) measurements, while simultaneously exploring the effect of gold nanoparticles (Au-NPs). We conducted our measurements on Au-NP-deposited titanium dioxide, *i.e.,* TiO_2. Our measurements illustrate that the induced oxygen vacancy (V_O) defects result in a decrease in time constants associated with the migration of electrons. In addition, we quantified the effect of induced defectson the migration barrier of slow charge carriers, *i.e.,* holes. Our respective measurements show that PI-SOVs lower the migration barrier of holes for both the TiO_2 and TiO_2/Au-NP interface. We believe that the observed statistical difference is caused by the effect of defects over the

recombination and trapping mechanisms of fast and slow charge carriers. Our results express the important effect of V_O on charge migration dynamics, which underlines the need for further studies of defects under realistic conditions.

[1] Bugrahan Guner, Orcun Dincer, and Omur E. Dagdeviren, ACS Applied Energy Materials **7** (6), 2292 (2024).

[2] Bugrahan Guner, Simon Laflamme, and Omur E. Dagdeviren, Review of Scientific Instruments **94** (6) (2023).

[3] Bugrahan Guner and Omur E. Dagdeviren, ACS Applied Electronic Materials **4** (8), 4085 (2022).

[4] Orcun Dincer, Bugrahan Guner, and Omur E. Dagdeviren, APL Materials **12** (2) (2024).

4:45pm NS2-MoA-14 Improving the Shape and Optical Stabilities of Plasmonic Au Nanobipyramids by Metal Shell Deposition, *Thomas Egan, Gang Chen,* University of Central Florida

Anisotropic plasmonic metal nanoparticles show significant promise as light-sensitizing components in the design of advanced optical materials. Their plasmon resonances can be tuned across the visible and near-IR regions by adjusting their aspect ratio, allowing them to harvest solar energy well below the bandgaps of conventional semiconductors. However, their processing and applications under environmental conditions often involve elevated temperatures, which may cause restructuring and shape change of the anisotropic plasmonic metal nanoparticles and lead to a shift of their plasmon resonances. Therefore, it is necessary to improve their thermal stability for robust applications. Here, using anisotropic Au nanobipyramids (NBPs) immobilized on a TiO_2 support as a model system, we demonstrate that the deposition of thin shells of different metals (Au@M NBPs, M = Ag, Pd, Pt) can alter and drastically increase their thermal stability. For pure Au NBPs and Au@Ag NBPs, their tips are observed to progressively blunt and their plasmon resonances begin to blue-shift when annealed at 100 ℃ for 1 hour, while the shapes and plasmon resonances of Au@Pd and Au@Pt NBPs are well-maintained up to 200 ℃ and 250 ℃, respectively. Notably, we also find that the thermal stability of Au@Pd and Au@Pt NBPs is unaffected by annealing up to 4 hours, suggesting that this method can be used to protect metal nanoparticles under various operating conditions. We further use energy-dispersive X-ray (EDX) spectroscopy to map the alloying processes of these core@shell NBPs, which reveal that the onset temperature of alloying increases as the lattice mismatch between core and shell metals increases.

5:00pm NS2-MoA-15 Photonic Chip Packaging for Extreme Environments, *Nikolai N Klimov, Sarah M Robinson,* National Institute for Science and Technology (NIST)*; Ashutosh S Rao,* National Institute for Science and Technology (NIST); University of Maryland*; Daniel S Barker, Fred B Bateman, Glenn E Holland, Daron A Westly,* National Institute for Science and Technology (NIST)

Integrated photonic sensors have advanced significantly in the past decade, driven by a combination of the inherent scalability of integrated photonics combined with precision nanofabrication as well as an ever-increasing range of applications. Such integrated sensors offer advantages in size, weight, and power compared to traditional sensor form-factors. While photonic packaging is well established for many applications, robust and ruggedized photonic packaging is indispensable to field-deployable photonic sensors that must operate under extreme environments. Here, we demonstrate a method for photonic packaging that can operate at cryogenic temperatures as well as in high radiation environments. We also assess the feasibility of the bonding method for high-temperature applications. Using low temperature hydroxide catalysis bonding and a custom packaging station to actively align and attach optical fiber v-groove arrays to a silicon photonic chip, we characterize the packaged chip across a wide temperature range from 360 K down to 3.8 K, confirming suitability for cryogenic operation, and observe < 1 dB variation per grating coupler across a 50 nm wavelength range. Moreover, we expose our packaged chip to an electron beam corresponding to an accumulative radiation dose of 1.1 MGray and observe no degradation in insertion loss across 1510 nm to 1630 nm wavelength range. Finally, we bond several dies and confirm the high temperature compatibility of our bonding approach by observing no

---

[1] **AVS National Student Awardee**

change in mechanical bond strength before and after annealing at 973 K. Our packaging methodology can be readily adapted to different photonics applications, ranging from cryogenic circuits to deployable extreme-environment sensors.

5:15pm NS2-MoA-16 Periodic and Quasi-Periodic Plasmonic Architectures for Strong Light-Matter Interaction, *Marzia Ferrera, Vincenzo Aglieri, Jacopo Stefano Pelli Cresi,* Istituto Italiano di Tecnologia, Italy; *Elena Ghidorsi,* Istituto Italiano di Tecnologia, Dipartimento di Fisica, Università degli Studi di Genova, Italy; *Andrea Toma,* Istituto Italiano di Tecnologia, Italy

Light-matter interaction pervades our everyday life and typically involves an energy exchange between an external electromagnetic field and a photon emitter (dye molecules, quantum dots, etc.). Usually, this interaction is rather weak and such that only the spontaneous emission rate is modified. However, the engineering of nanohybrid architectures can promote an energy exchange rate between light and matter faster than any relaxation process. Under these conditions, the system can enter the strong-coupling regime and new hybrid light-matter states, called polaritons, are formed, with potential interest in various fields spanning from photocatalysis to optoelectronic and quantum technologies [1].

For the realization of functional polaritonic devices, particular interest has been devoted towards the integration of quantum emitters with periodic structures supporting collective modes, such as surface plasmon polariton Bloch waves or surface lattice resonances. These resonance features can be properly controlled by acting on the design of the photonic architecture. Among the various possibilities, the exploitation of photonic metamaterials lacking periodic translational order (e.g. quasicrystals) can significantly increase the design degrees of freedom of the photonic component thus offering interesting perspectives in the development of novel hybrid platforms [2]. Here, the focus is on strongly-coupled systems in which quantum emitters are integrated with both periodic and quasi-periodic two-dimensional plasmonic crystals. The radiative properties of the heterostructures along with their intrinsic photophysics were investigated by means of both steady-state and time-resolved optical spectroscopies [3,4]. This work is stimulating toward a further exploration on the symmetry-dependent properties of long-range ordered 2D arrays, with a particular focus on their peculiar near-field distribution. More in general, the presented results can set the stage for the realization of novel polaritonic devices with tailored properties for specific applications, such as photocatalysis.

Acknowledgement

This work is part of the REPLY project that received funding from the European Research Council (ERC) under the European Union's Horizon 2020 research and innovation program (grant agreement No 101002422).

References

[1] F. J. Garcia-Vidal, *et al.* Science 373, eabd0336 (2021); [2] S. Yu, *et al.* Nat. Rev. Mater. 6, 226 (2020); [3] H. Wang, *et al.* Adv. Opt. Mater. 5, 1600857 (2017); [4] H. Wang, *et al.* Adv. Funct. Mater. 28, 1801761 (2018).

Plasma Science and Technology
Room 124 - Session PS1-MoA

Plasma Surface Interactions

Moderators: Sumit Agarwal, Colorado School of Mines, **Tetsuya Tatsumi**, Sony Semiconductor Solutions Corporation

1:30pm PS1-MoA-1 Advanced Semiconductor Plasma Processes Pioneered by Understanding and Controlling Plasma-Surface Interactions, *Masaru Hori, Makoto Sekine, Takayoshi Tsutsumi, Kenji Ishikawa,* Nagoya University, Japan **INVITED**

Plasma processes were introduced into semiconductor manufacturing more than 50 years ago, leading to today's nanoscale, three-dimensional integrated circuit manufacturing and explosive scientific and industrial advances. One of the core technologies is reactive ion etching (RIE). Initially, the focus of basic science was on why RIE occurs, with many reports and discussions on fast etching, material-to-material selectivity and fine shape control reactions resulting from the interaction of ions and radicals from the plasma with diverse materials, forming a unified understanding of RIE principles. However, the current demand for microfabrication technologies aimed at fabricating devices of 2 nm or smaller requires further understanding of nanometer reaction regions called surface modified layers, mixed layers, condensed layers, and damaged layers resulting from

ion, radical and solid interactions. Here, we would like to name this reaction region the meta-layer due to the need for a unified understanding and definition as a science. In addition to pioneering atomic layer etching and self-organized growth processes of three-dimensional nanomaterials by measuring and controlling the meta-layer, wet-like etching techniques have recently been produced by utilizing the interaction between plasma and liquid phase. The identification and control of this meta-layer is the key to the core science and applications for future advances in advanced plasma processing. In this talk, the importance of identifying and controlling the plasma-induced meta-layer in plasma processes used to fabricate logic and memory devices will be explained. The relationship between the reaction dynamics occurring in the meta-layer and the etching mechanism will then be discussed based on *in-situ* FT-IR, *in-situ* XPS and *in-situ* ellipsometry observations of chemical reactions occurring in the meta-layer induced by the plasma process. Furthermore, based on the analysis of meta-layer structures formed in various plasma processes using TOF-SIMS and *in-situ* TEM-EELS, the evolution of state-of-the-art semiconductor manufacturing processes produced by meta-layer science and the precise control of non-equilibrium reaction fields in which active species and solids and liquids work together will be mentioned.

2:00pm PS1-MoA-3 Concurrent Thin Film Deposition in Fluorocarbon Plasmas as a Function of Gas Phase and Surface Reactions, *Austin Krauss,* University at Albany; *Qi Wang, Nicholas Smieszek, Sergey Voronin, Akiteru Ko,* Tokyo Electron America; *Shigeru Tahara,* Tokyo Electron Ltd., Japan; *Christophe Vallee,* University at Albany

High aspect ratio (HAR) etching in fluorocarbon plasmas has presented challenges in the pursuit of continuous shrinking of the integrated circuit technological node. With increasing aspect ratios of etched features, maintaining a constant channel critical dimension (CD) requires precise control of the plasma species involved. As such, the advancement of existing plasma processing techniques depends on a complete understanding of transport and surface interactions of electrically charged and neutral species (i.e. radicals) within HAR channels.

For better understanding of such mechanisms and better control over neutral species delivery and distribution inside etch channels, we characterized the transport of radical species in the process chamber as a function of the distance from the plasma source, as well as their transport through capillary plates with different aspect ratios. The experiments were performed in an inductively coupled $C_4F_8/O_2/Ar$ discharge at 20 mTorr to minimize collisions between the molecules inside of the micrometer-scale capillary via holes. The plasma phase chemistry composition and the nature of the radicals transported to the substrate were controlled by adjusting of the O_2 flow rate; the experimental films were grown on SiO_2 substrates, attached to the rear side of the capillary plates. In addition, the composition of the radicals diffusing toward the substrate was controlled through variation in sample distance from the plasma source and was monitored in-situ by spatially-resolved optical emission spectroscopy (OES) and spatially-resolved mass spectrometry. The composition and deposition rates of the films were determined as a function of AR via X-ray photoelectron spectroscopy (XPS) and atomic force microscopy (AFM), respectively.

Surface analysis indicated significant reduction in the film deposition rate and a lower carbon content with increase of the channel length, which could be addressed to higher consumption of CF and CF_2 species (compared to CF_3) on the via wall. Addition of O_2 to the plasma has shown a decrease of the CF_x species with higher carbon content in the plasma phase and carbon concentration in the film, which can be used as a knob for deposition uniformity control inside of a via. Additional characterization of the radical flux, its composition at different distances from the plasma source, and its impact on the film properties will be discussed.

2:15pm PS1-MoA-4 Investigation of Highly Diffusive Point Defects During Si Plasma Etching, *Nobuyuki Kuboi, Koichiro Saga, Masafumi Miyoshi, Takashi Hamano, Shoji Kobayashi, Tetsuya Tatsumi,* Sony Semiconductor Solutions Corporation, Japan; *Koji Eriguchi,* Kyoto University, Japan; *Yoshiya Hagimoto, Hayato Iwamoto,* Sony Semiconductor Solutions Corporation, Japan

The quantitative prediction and precise control of plasma-induced damage during Si etching for detailing the regions of amorphous, dangling bonds, and point defects are essential for optimizing the performance of CMOS devices. Particularly, regions of two formers with concentrations of 10^{18}-10^{19} atoms/cm^3 have been studied and modeled extensively [1][2][3]. Insights obtained from these studies are used for suppressing damage to these layers to realize plasma processes with low damage. To enhance the

performance of advanced CMOS devices with complex structures, understanding the mechanisms of formation and distributions of points defects with less than 10^{17} /cm^3 is crucial. However, limited studies have focused on the effects of point defects generated during Si etching.

Therefore, we focused on point defects as Si etching damage and proposed simulation modeling for Si interstitials (I). These interstitials are highly diffused and interact with nearby interstitials and incident hydrogens from plasma to form clusters (I_m). Considering the energy balance between an incident ion and sum of forming energy of each cluster during Si trench etching, I_3 or I_4 cluster can be formed at most. In the proposed model, this transient phenomenon was included depending on the substrate temperature.

To confirm the validity of the damage model, we analyzed photoluminescence (PL) data after Si trench etching with or without hydrogen irradiation and revealed that the model assumptions are reasonable for the variations of the observed PL intensities originating from point defects. Furthermore, we performed in-situ XPS on the B1s spectrum in the highly Boron-doped Si substrate after Ar$^+$ ion irradiation as damage with a temperature variation of 25, -50, and -120 °C. At 1.5-nm depth from the surface corresponding to the a-Si region, the B1s intensity did not vary, but the intensity at the 6-nm region increased with the decrease in the temperature (i.e., -50 and -120 °C) and decreased when the substrate temperature of -120 °C was back to 25 °C. This experimental result revealed various phenomena with the depth on the nanometer scale and supports the proposed formulation as the diffusion phenomena of Si interstitials.

Consequently, we revealed that the diffusion of Si interstitials induced by plasma irradiation can be suppressed by extremely low temperature. Furthermore, cryo etching exhibits considerable potential for not only improving etched profile with high selectivity but also suppressing plasma-induced Si damage.

[1] K. Eriguchi, JJAP **56**, 06HA01 (2017).

[2] T. Tatsumi, JJAP **61**, SA0804 (2022).

[3] N. Kuboi *et al.*, JJAP **55**, 07LA02 (2016).

2:30pm PS1-MoA-5 Effect of Bias Voltage and H₂ Addition on the Formation of Ammonium Salt Layer during RIE of SiN$_x$ in a CH₂F₂/Ar Plasma, *Xue Wang*, Colorado School of Mines; *Prabhat Kumar, Thorsten Lill, Harmeet Singh, Mingmei Wang, Taner Ozel,* Lam Research Corporation; *Sumit Agarwal,* Colorado School of Mines

During the etch of SiO₂ and SiN$_x$ in a fluorocarbon plasma, the selective etch is believed to be realized by the accumulation of a fluorine-deficient graphitic carbon layer on the SiN$_x$ surface. While the hydrofluorocarbon gases are also widely used in the selective etch of SiO₂ to SiN$_x$, the mechanism of SiN$_x$ retardation is still unclear. It has been hypothesized that in addition to the graphitic carbon layer, another blocking layer—ammonium fluoride or ammonium fluorosilicate—may form on the SiN$_x$ surface. These layers can retard or even fully stop the etching of SiN$_x$. The formation of an ammonium salt layer has been reported in some atomic layer etching and reactive ion etching (RIE) processes. However, the mechanism of formation of these ammonium salts, their thermal stability, and stability under directional ion bombardment are not fully understood.

In this work, we investigate the effect of temperature, bias voltage, and H₂ addition on the formation of an ammonium salt layer during RIE of plasma-deposited SiN$_x$ in a CH₂F₂/Ar plasma. Using *in situ* attenuated total reflection Fourier-transform infrared spectroscopy (ATR-FTIR) spectroscopy, we monitored the surface bonding changes of SiN$_x$ film during RIE over a temperature range of 25-150 °C at bias voltages over the range of 100-300 V. As expected, the etch rate was lower at a lower bias voltage (see Figure 1), and the etch stopped with rapid accumulation of ammonium salt layer (NH₄ bending mode at ~1430 cm^{-1} and NH₄ stretching mode at ~ 3000–3300 cm^{-1} in Figure 2) and graphitic hydrofluorocarbon layer (C=C stretching mode at ~1600 cm^{-1} in Figure 2). Interestingly, no salt or graphitic carbon layers formed when we decoupled the RIE process into a CH₂F₂/Ar plasma deposition step and an Ar plasma activation step with a bias voltage of -240 V. This implies that the formation of ammonium salt and graphitic carbon layers requires the participation of etch byproducts and plasma species. We also observed that, after adding H₂ into feed gas, the SiN$_x$ etch at room temperature and under bias voltage of -240 V proceeded linearly with no accumulation of ammonium salt and graphitic carbon layers. We speculate that the graphitic carbon layer was efficiently removed with H₂ addition,

making the ammonium salt layer unstable when it was exposed to high-energy ion bombardment. We anticipate that SiN$_x$ etching with HF plasma may provide further insights into the formation mechanism of ammonium salt layer by eliminating the graphitic carbon layer that forms on the SiN$_x$ surface prior to an etch stop.

2:45pm PS1-MoA-6 Plasma-Induced Oxidation in Micron-Sized Droplets: Evaluating Transport Limitations, *Dongxuan Xu, Peter Bruggeman,* University of Minnesota

Cold plasmas interacting with liquids at ambient conditions provides a unique chemical reactive environment and so have been studied extensively for a broad range of applications - material synthesis, wastewater treatment, and disinfection. The plasma-liquid interface, a thin liquid region bridging plasma gas phase and bulk liquid phase, is crucial for reactive chemistry in the liquid phase. Typically, highly reactive plasma gas phase species (i.e., e$^-$ and OH) are injected into the liquid phase and readily react with solutes at this interface. As the redox processes in this interface occur on timescales of ns to µs while the transport of reactive gas phase species and liquid solutes occurs on timescales of tens of µs to seconds, the rate of conversion is in many cases not limited by the speed of the reaction but by transport. Specifically, conversion yields for a plasma-liquid system can be limited by both the gas phase reactive species flux into the liquid and the diffusion/convection of solutes from the bulk liquid to the interface where reactions occur.

In this study, we evaluate the effect of these transport limitations on OH-driven oxidation processes in an RF-driven diffuse glow discharge at atmospheric pressure. A droplet generator enables the generation of a train of droplets (40 µm diameter) passing through the homogeneous plasma allowing us to study the interaction of a micron-sized droplet with a plasma at a well-defined droplet residence time (10 ms). Here, the dominant liquid phase transport within the droplet is diffusion of the bulk liquid solute towards the plasma-liquid interface.

Firstly, we treated the redox couple ferri/ferrocyanide in the plasma-droplet system to confirm oxidation is the dominant reaction. Next, various solutes were treated at different initial concentrations, and we observed two trends: 1) an initial linear increase in solvent conversion with increasing solvent concentration consistent with solute diffusion limited conversion, 2) and a saturation of the solvent conversion independent of the solvent concentration consistent with a conversion that is limited by the gas phase reactive species flux into the liquid. We show that these results can be described by a 1D reaction-diffusion model which also allows us to determine the gas phase OH flux into the droplet. Finally, we compared these derived OH fluxes with calculated estimates of OH fluxes in the gas phase independently determined with measured bulk gas phase OH densities as boundary condition. The results are in excellent agreement and show that for molecules that readily react with OH radicals, conversion can be described by OH-driven plasma-induced chemistry.

3:00pm PS1-MoA-7 Effects of Si/N Ratio on Plasma-induced Damage Creation in Silicon Nitride Films, *Takahiro Goya, Keiichiro Urabe, Koji Eriguchi,* Kyoto University, Japan

Various properties of SiN films have been designed by optimizing the stoichiometry (Si/N ratio). For example, Si-rich SiN films with their superior mechanical property such as high hardness [1] are one of the promising candidates for an anti-plasma erosion layer called a "hard" mask. It is widely known that plasma exposure results in the creation of defects in SiN films, leading to the change of the designed properties by Si—N network modification. Thus, the property degradation during plasma process (plasma-induced damage: PID) [2] is considered to be a critical issue for SiN film design and/or plasma process optimization. In this study, we investigated the effects of PID on the mechanical property change in SiN films with various Si/N ratios, in combination with optical analysis. The SiN films were prepared using PECVD on Si substrates. The thicknesses were approximately 200 nm and the refractive index n showed 1.9 ~ 2.2 depending on the Si/N ratio. All samples were exposed to inductively coupled Ar plasma. DC self-bias voltage was −200 V and the exposure time was 60 s. For mechanical property analysis, a nanoindentation technique was employed. We adopted the contact stiffness S (obtained from the slope of an unloading curve) as a measure of the mechanical property [3]. Since it turned out that a single loading/unloading process could not reveal a clear change in S by plasma exposure due to stochastic variation etc., we performed cyclic (time-dependent) loading/unloading measurements with an iteration time N = 75. An increase in S with an increase in Si/N ratio was found for Si-rich SiN films (n > 2.05), while no apparent increase was seen for N-rich SiN films (n < 2.05). To clarify the Si/N ratio effects, the change in

the extinction coefficient k estimated by spectroscopic ellipsometry was investigated. A decrease in k was observed for the Si-rich SiN films after plasma exposure. Since the optical bandgap is narrower and the S value is larger in SiN films, compared to SiO_2 films, we anticipate that the change is attributed to the surface oxidation [4] of the damaged layer. The present findings imply that Si-rich SiN films are more significantly subject to PID, leading to the degradation of the anti-plasma feature (hard mask property) during plasma processing steps.

[1] H. Huang et al., Mater. Sci. Eng. A **435**, 453 (2006).

[2] K. Eriguchi, Jpn. J. Appl. Phys **60**, 040101 (2021).

[3] T. Goya et al., Proc. Symp. Dry Process, 2021, p 35.

[4] T. Kuyama et al., Jpn. J. Appl. Phys. **57**, 06JD03 (2018).

3:15pm PS1-MoA-8 Highly Selective Sin Etching by HF Plasma, *Megan Manos,* Hitachi High-Tech America, Inc.*; Yosuke Kurosaki,* Hitachi High-Tech America, Inc., Japan*; Jeff Ditto,* Hitachi High-Tech America, Inc.*; Takahiko Maeda, Takashi Hattori,* Hitachi High-Tech, Corp., Japan*; Masaki Yamada,* Hitachi, Ltd., Japan*; Yohei Ishii,* Hitachi High-Tech America, Inc.*; Hiroto Ohtake,* Hitachi High-Tech, Corp., Japan*; Kenji Maeda,* Hitachi High-Tech Corp., Japan

Recently, it has been found that combination of H and F is critical for highly selective SiN etching over SiO in dry etching. HF is suggested to work for SiN etching as a catalyst by lowering the activation energy of F migration, while NO is well known to promote SiN etching as well [1]. In addition, HF is a promising etching gas with low GWP (Global Warming Potentials) and has capability of SiN etching by reactive ion etching or evaporating ammonium salts by ion bombardment [2,3].

In this study, we investigated isotropic etching of SiN by HF remote plasma and found high selectivity to SiO of over 100. HF plasma was generated by an inductively coupled plasma source and radicals were supplied to the wafer through an ion shield plate. LPCVD-SiN and thermally oxidized SiO were used for checking the etching capability.

Highly diluted Ar/HF plasma (Ar/HF = 20) showed continuous SiN etching while SiO and poly-Si with native oxide layer were hardly etched. Once HF flow was increased, poly-Si started to be etched and SiO showed slight etching. Selective SiN etching over SiO was still observed due to increasing SiN etching rate. Note that SiN etching was observed with small amounts of F radicals as suggested by using dilute HF gas and optical emission spectroscopy (OES). OES showed small signals of fluorine in HF plasma when compared a conventional gas such as SF_6. In fact, small addition of H_2 suppressed SiN etching due to scavenger effects. When tuning process pressure, the etching rate had a maximum at around 100 Pa while the OES signals of fluorine monotonically decreased. These results indicate that HF assists to enable SiN etching even with small number of etchants while achieving the extremely high selectivity over SiO. Addition of SF_6 slightly reduced SiN etching rate while poly-Si etching rate rapidly increased, supporting the mechanism that the reduction of HF partial pressure suppressed SiN etching. No clear XPS signal of ammonium salt was observed after etching on SiN samples and the etching rate has a maximum at around 0°C. These results suggest that SiN etching occurs not through the formation of ammonium fluorosilicate (AFS), which is well known to promote SiN etching, since the boiling point of AFS is over 100°C. In the structure of SiN/SiO multilayers, Ar/HF plasma showed lateral etching of SiN tiers without specific loss of SiO tiers.

[1] Y. V. Barsukov et al., J. Vac. Sci. Technol. A **36**, 061301 (2018)

[2] Y. Kihara et al., VLSI symposium T3-2 (2023)

[3] S-N Hsiao et al., ACS Appl. Electron. Mat. **5**, 6797 (2023)

3:30pm PS1-MoA-9 Dense-Amorphous-Carbon (DAC) Formation from Ion bombardment of Plasma Deposited FCH Films: Temperature and Precursor Dependence, *Sang-Jin Chung,* University of Maryland, College Park*; Pingshan Luan, Minjoon Park,* TEL Technology Center America*; Gottlieb S. Oehrlein,* University of Maryland, College Park

The passivation layer deposited during high-aspect-ratio-contact (HARC) etching is important for protecting the sidewall from forming various etch defects. The etch resistance of these often-carbon-based films plays a crucial role in effective profile control. Ion bombardment of polymeric films creates bond scissioning in the surface layer, which often results in the formation of a thin and dense amorphous carbon (DAC) layer above the bulk.[1]

In this work, we evaluate the mechanisms of DAC layer formation on plasma-deposited (hydro)fluorocarbon (FCH, FC) films and their etch resistance at various ion energies. Various HARC etching precursors (Ar/C_4F_6, Ar/C_4F_8, Ar/CHF_3, Ar/CH_2F_2, or Ar/CH_3F) were used to deposit FCH/FC on Si, oxide, or nitride materials, on both blanket as well as in trench-like HAR structures[2, 3]. After film deposition, the chamber was cleaned, and DAC film was formed using ion bombardment from noble gas (Ar) plasma under self-bias. With various ion energies (25, 50, 75, 100, and 125 eV) and substrate temperatures, the thickness and composition of films were monitored in real-time using *in-situ* ellipsometry. Initial results show that the DAC film formation from FCH deposited by higher -H containing precursors show greater changes, indicated by higher refractive index of the DAC layer compared to the deposited bulk layer, which is due to ion driven depletion of F from the FCH films. During the initial phase of Ar ion bombardment, the etch rate (ER) is very high as there is no DAC layer. The ER gradually reaches a steady state as the DAC layer forms. At higher ion energies the DAC layer thickness is greater, and after a certain thickness the DAC layer greatly inhibits the bulk etch rate. When treating the film with sequentially higher ion energies, we found that the DAC thickness increases, and the ER reaches a peak at ~75 eV after which the ER decreases. When reversing the ion energy, we found that both the DAC thickness and ER decreases . Depending on the film chemistry, higher overall ER could be achieved with optimized ion energy up-ramp (F rich FC films) or down-ramp (F poor FCH films), which highlights the importance of the DAC layer thickness and chemistry to the ER. When comparing DAC layers formed at -20 °C or 10 °C, we found that the refractive index is smaller at -20 °C and the DAC layer is less dense, which allowed for a higher etch rate. The formation and properties of DAC films will also be studied at -60 °C substrate temperature. Chemical composition of the films before and after Ar plasma treatment will be reported.

Plasma Science and Technology
Room 124 - Session PS2-MoA

Plasma Chemistry and Catalysis I
Moderators: Michael Gordon, University of California at Santa Barbara, **Mohan Sankaran**, University of Illinois at Urbana-Champaign

4:00pm PS2-MoA-11 Stress Reduction of Hydrogenated Amorphous Carbon Films by Controlling Incorporation of Carbon Nanoparticles, *Kazunori Koga, Shinjiro Ono, Takamasa Okumura, Kunihiro Kamataki, Masaharu Shiratani,* Kyushu University, Japan   **INVITED**

Stress reduction of hydrogenated amorphous carbon (a-C:H) films has been an important topic in improving the performance of the protective coating, which has been employed for the masking of dry etching, automotive parts, and electrodes of batteries [1,2]. Metal nanoparticle incorporation into the films has been one conventional method to reduce stress [3,4]. However, it led to metal contamination of the films, resulting in the deterioration of the semiconductor device performance. In this study, inspired by the insertion of the metal nanoparticles, we aimed to relieve the stress by incorporating the carbon nanoparticles (CNPs) into the a-C:H films. As the first step, we have successfully controlled the size of nanoparticles by plasma chemical vapor deposition (CVD) [5,6]. Then, we succeeded in controlling the coverage of carbon nanoparticles (CNPs) deposited on substrates using capacitively coupled plasma chemical vapor deposition (CVD), which has been widely employed in large-area deposition. From TEM images, deposited CNPs were classified into two size groups. The mean size of the smaller CNP group is around 5 nm, and that of the larger CNP group is around 25 nm. We succeeded in controlling the coverage Cp of CNPs with discharge duration without unexpected agglomeration. Based on the results, we fabricated a-C:H/CNP/a-C:H sandwich-like films using the parallel plate plasma CVD reactor. Ar and CH4 mixture gas was introduced from the top of chamber at 19 sccm and 2.6 sccm, respectively. The total pressure was kept at 0.3 Torr. The gas flow rate and the pressure were same as those for the CNP deposition. The mass density of deposited a-C:H films is 1.88 g/cm3. The dependence of the film stress on the Cp. With increasing the Cp, the stress decreases from 1.59 GPa at Cp= 0 % to 1.02 GPa at Cp= 8.9 %. It shows same value for Cp= 15.9 %. The reduction rate is 35.8 %. On the other hand, the films' thickness and refractive index were kept at approximately 320 nm and 2 regardless of the Cp. The results indicate that a small amount of CNP incorporation can reduce the film stress.

[1] N. Hiwasa, et al., Jpn. J. Appl. Phys. Express 15, 106002 (2022). [2] C. Y. Ho, et al., Thin Solid Films 518(21), pp.6076-6079 (2010). [3] M. Constantinou, et al., Nanomaterials 8(4), pp.209-229 (2018). [4] R. Paul, et al., Appl. Surf. Sci. 257(24), pp.10451-10458 (2011). [5] S. H. Hwang, et al., Diam. Relat. Mater. 109, 108050 (2020). [6] S. H. Hwang, et al., Plasma and Fusion Research: Regular Articles 14, 4406115 (2019).

4:30pm PS2-MoA-13 Is Plasma Electrochemistry Just Electrochemistry at Plasma-Liquid Interfaces? Learnings from Organic Reactions, *Casey Bloomquist*, Eray Aydil, Miguel Modestino, New York University

In plasma electrochemical synthesis, one of the electrodes of a traditional electrochemical cell is replaced by plasma. Recent work has focused on using plasma-generated solvated electrons to perform reductive chemistry in aqueous solutions. In this study, we explored the use of plasma electrochemistry for the largest industrial organic electrosynthesis process, the electrohydrodimerization of acrylonitrile (AN) to adiponitrile (ADN), a precursor to Nylon 6,6. We used a DC pin-to-liquid Ar plasma to study both negative polarity and positive polarity plasma interactions with aqueous AN. Interestingly, we did not produce ADN, which was expected to be created through radical coupling in a negative polarity plasma. However, we did produce H_2, H_2O_2, propionitrile (PN), O_2, CO_2, C_2, and C_3 hydrocarbons and AN-derived polymers with amounts depending on the AN concentration, current, and polarity. H_2 was produced in amounts 10 – 20 times that expected from Faradaic currents, highlighting the importance of non-electrochemical reactions. PN, a competing reaction in traditional ADN electrosynthesis, was produced at rates commensurate with Faradaic currents under negative potentials. However, under positive potentials, PN production was much higher than predicted by Faradaic currents, suggesting that PN production under either polarity may be produced via non-electrochemical pathways. Clearly, there is more to plasma electrochemistry than just electrochemistry.

4:45pm PS2-MoA-14 Nonequilibrium Plasma Aerotaxy of $In_xGa_{1-x}N$ Nanocrystals, *Dillon Moher, Elijah Thimsen*, Washington University in St. Louis

Semiconductors with good stability in harsh chemical environments, tunable band gap, and non-toxicity are sought after for solar energy conversion and solid-state light sources. The solid solution of InN and GaN ($In_xGa_{1-x}N$) is a good candidate material whose band gap depends on the mole fraction of InN in the GaN (x). Full control over the composition can provide photon absorption and emission from the ultraviolet to the infrared. However, homogeneous thin film $In_xGa_{1-x}N$ with intermediate x is plagued by strain-induced threading dislocations and phase segregation due to the miscibility gap. High material quality and tunability may be achieved in freestanding $In_xGa_{1-x}N$ nanocrystals, absent of epitaxial growth and having distinct mixing behavior due to nanoscale effects. Moreover, nanocrystals may have 3D quantum confinement effects, high specific surface area, and compatibility with solution processing. Yet, their synthesis is underdeveloped. In this work, the synthesis of $In_xGa_{1-x}N$ nanocrystals by nonequilibrium plasma aerotaxy was demonstrated. STEM-EDS observation showed that individual nanocrystals consisted of a mixture of InN and GaN. The nanocrystals, deposited into thin films, had a composition-dependent band gap demonstrated by UV-Vis extinction spectroscopy. Annealing procedures were pursued to improve the crystallinity and photoluminescence of the nanocrystal films. Decomposition of the nanocrystals, which occurred at temperatures of 600 °C and above, was suppressed when the nanocrystals were first coated with Al_2O_3 deposited by atomic layer deposition. Furthermore, the photoluminescence of the nanocrystals increased by an order of magnitude. This new synthesis strategy for $In_xGa_{1-x}N$ nanocrystals is a step towards advanced optoelectronic applications, paving the way for further research into material property optimization and integration into devices.

5:00pm PS2-MoA-15 Plasma-Based Reforming of LNG?, *Norleakvisoth Lim, Michael Gordon*, UC Santa Barbara

Developing novel reacting systems for more sustainable use of our natural resources is central to both reducing the risks associated with CO_2 emissions and making the long-term transition to a more circular, sustainable, and electrified economy. Moreover, developing technologies to leverage and reform the energy density of global commodities such as liquified natural gas (LNG), to produce clean H_2, olefins, and solid carbon without producing CO_2, could be game changing. Toward this end, we have been exploring how plasmas might be directly excited in liquid methane at cryogenic conditions to create value-added products.

This talk will highlight our preliminary work on striking and sustaining low (60 Hz) and high (~20 kHz) frequency, as well as pulsed, plasma discharges directly in liquid methane at ~100K (**Figure 1**), with emphasis on (i) the reactor configuration (i.e., with rotating electrodes to prevent carbon buildup), (ii) yield of H_2 and other (solid) hydrocarbon products, (iii) energy efficiency, and (iv) management and characterization (SEM/TEM) of the solid carbon product (**Figure 2**). Although the four-phase reaction

environment encountered at cryogenic conditions – namely, plasma, gaseous H_2, slurry of frozen C_2+ hydrocarbons, and solid carbon - presents many challenges, it is still possible to generate H_2, some C_2 olefins, and a graphite-like carbon product.

Various aspects of this unorthodox cryogenic reaction environment will be discussed including: what might be going on in the discharge?, is the plasma thermal or nonthermal?, does the input energy vaporize the methane?, how can the carbon be managed?, what products are formed under different plasma conditions?, what is the H_2 production rate and SER?, and might this process be a better or more useful way to re-gasify and reform LNG?

5:15pm PS2-MoA-16 Hydrogen Production from Nebulized Ethanol in a Nanosecond Pulsed Discharge, *Linus Nyssen, Thomas Fontaine, David Petitjean,* Université libre de Bruxelles, Belgium*; Nathalie De Geyter,* Ghent University, Belgium*; François Reniers,* Université libre de Bruxelles, Belgium

Means of energy production that don't emit greenhouse gases (GHG) are highly sought after. H_2 is a great candidate, as it could serve as fuel as well as energy storage for intermittent sources. For certain industrial sectors such as the steel industry, it is often the only viable alternative mentioned. Today H_2 is mainly produced by the Steam Methane Reforming process, emitting GHG in the process. The only alternative at the moment is water electrolysis but is highly demanding in energy: $\Delta_r H° = 285.83\ kJ/mol_{H2}$.

We investigate other sources to produce H_2 through plasma reforming. As an alternative to gas feedstocks in a plasma discharge, we use liquids such as ethanol, because it yields a high H/C ratio while staying liquid at room temperature. By spraying this ethanol inside an Ar discharge, we produce a high contact surface between the plasma and liquid phase compared to plasmas at the surface of a liquid. While aerosols in a plasma discharge are more often used for film deposition, we investigate the use of the method at atmospheric pressure for liquid conversion to H_2. To ignite the discharge, a nanosecond pulsed plasma is used, yielding high electric fields and allowing for high energy reactions while keeping the reactor at room temperature.

In this work, the conversion of ethanol to H_2 is investigated while varying parameters such as the pulse width, the voltage and the gap between electrodes and establishing their influence. We monitor conversion, selectivity and consumed power to extract the energy cost to produce H_2. The pin-to-rod reactor used has 6 pins at high voltage surrounding a central rod at ground potential. This conformation makes for a plasma section through which the gas and aerosols flow perpendicularly. The pulses are triggered 4000 times a second, so that each pulse is triggered in a new batch of gas & liquid, given the flow. Pulse widths of 50, 250 and 450 ns are used, at gaps of 2 and 6 mm, while using 10, 14 and 18 kV to trigger the discharge, giving a pulse energy ranging from 0.25 – 1.00 mJ/pulse. The conversion ranges from 3.96 to 21.01 % with the best conversion obtained at an energy of 1.00 mJ/pulse (obtained at 450 ns), yielding an energy cost of 287.65 kJ/mol H_2. For all conditions, the highest conversions and pulse energy were obtained for the larger gap. Interestingly, the selectivity for CO rises significantly (3.33 % to 7.60 % on average) when the gap is larger. These first results suggest an efficient way of producing H_2 at an interesting energy cost.

Quantum Science and Technology Mini-Symposium
Room 123 - Session QS1+EM+MN+PS-MoA

Materials + Devices for Quantum Systems

Moderators: Somil Rathi, Arizona State University, **Jaesung Lee**, University of Central Florida

1:30pm QS1+EM+MN+PS-MoA-1 Elastic Layered Quantum Materials, *Jiun-Haw Chu,* University of Washington **INVITED**

Recently elastic strain has emerged as a powerful tool for probing and controlling quantum materials. By changing chemical bond lengths, elastic strain can modulate electronic structure up to very high energy scale. Additionally, as a second rank tensor, strain enables access to various instabilities associated with different symmetry channels. In this talk, I will discuss several examples of the application of strain to unconventional electronic orderings in van der Waals layered materials, including zigzag antiferromagnetism, charge density waves and excitonic insulators.

Monday Afternoon, November 4, 2024

2:00pm QS1+EM+MN+PS-MoA-3 Controllable Extended Defect States in Topological Insulators and Weyl Semimetals, *Eklavya Thareja, Jacob Gayles,* University of South Florida; *Ilya Vekhter,* Louisiana State University
Over the past decade study of topological materials has emerged as one of the most active areas in condensed matter physics, owing to a wide range of their proposed applications ranging from quantum computing to spintronics. What sets them apart from the materials currently used to build information technology is their robustness to disorder. However, in addition to the immunity of their electronic states against disorder, one needs ways to control the properties of these electronic states in these materials. We show that extended defects such as line defects and planar defects host localized states in Topological Insulators and Weyl Semimetals, which are two common topological materials. These localized states can be manipulated by controlling the scattering at the defects, for example, by using an external magnetic field. This leads to controllable spin accumulation and non-dissipative currents near the defects, due spin-momentum locking. These results bring us closer to functional applications.

2:15pm QS1+EM+MN+PS-MoA-4 Topological Interfacial State in One-Dimensional h-BN Phononic Waveguide, *Yanan Wang, Sanchaya Pandit,* University of Nebraska - Lincoln
Artificial topological structures have gained considerable research attention in the fields of photonics, electronics, mechanics, acoustics, and many others, as they promise robust propagation without loss along the edges and interfaces. In this work, we explored the topological states in one-dimensional (1D) phononic waveguides empowered by hexagonal boron nitride (h-BN), a hallmark two-dimensional (2D) material with robust mechanical properties that can support phonon propagation in high frequency regime. First, degenerate trivial and nontrivial topological structures were designed based on the Su-Schrieffer-Heeger (SSH) model. The dispersion engineering was then performed to match the passbands and bandgaps for these two topological structures through optimizing the geometric parameters of the unit cells. An interfacial state emerged when connecting these two sets of unit cells together and forming the 1D waveguide. The topological nature of this interfacial state, immune to structural and material parameter perturbation, was verified with the variation of strain and thickness in the waveguide. The phononic topological state studied here can be further coupled with defect-related quantum emitters in h-BN, opening the door for next-generation hybrid optomechanical circuits.

2:30pm QS1+EM+MN+PS-MoA-5 Scanning Nano-Optical Imaging of Quantum Materials, *Guangxin Ni,* Florida State University
Scanning near-field Nano-Optical imaging is an invaluable resource for exploring new physics of novel quantum materials. Surface plasmon polaritons and other forms of hybrid light-matter polaritons provide new opportunities for advancing this line of inquiry. In particular, nano-polaritonic images obtained with modern scanning nano-infrared tools grant us access into regions of the dispersion relations of various excitations beyond what is attainable with conventional optics. I will discuss this emerging direction of research with two examples from 2D layered quantum materials.

2:45pm QS1+EM+MN+PS-MoA-6 Engineering of Erbium-Implanted Lithium Niobate Films for Integrated Quantum Applications, *Souryaya Dutta,* College of Nanotechnology, Science, and Engineering (CNSE), University at Albany; *Alex Kaloyeros, Spyros Gallis,* College of Nanotechnology, Science, and Engineering (CNSE), University at Albany (UAlbany)
Rare-earth-doped materials have garnered significant attention as material platforms in emerging quantum information and integrated photonic technologies. Concurrently, advances in its nanofabrication processes have unleashed thin film lithium niobate (LN), $LiNbO_3$, as a leading force of research in these technologies, encompassing many outstanding properties in a single material. Leveraging the scalability of ion implantation to integrate rare-earth erbium (Er^{3+}), which emits at 1532 nm, into thin film lithium niobate can enable a plethora of exciting photonic and quantum technologies operating in the telecom C-band. Many of these technologies also rely on coupling via polarization-sensitive photonic structures such as waveguides and optical nanocavities, necessitating fundamental material studies.

Toward this goal, we have conducted an extensive study on the role of implantation and post-implantation processing in minimizing implantation-induced defectivity in *x*-cut thin film LN. By leveraging this, we have demonstrated an ensemble optical linewidth of ~140 GHz of the Er emission at 77 K. Our demonstration showcases the effectiveness of our ion implantation engineering in producing cutting-edge Er emission linewidth in thin film LN at higher temperatures compared to values reported for diffusion-doped bulk materials at liquid helium temperatures (~3 K). Furthermore, we show that the Er photoluminescence (PL) is highly polarized perpendicular to the *x*-cut LN *c*-axis through a systematic and combinational PL and high-resolution transmission electron microscopy (HRTEM) study. These results indicate that using Er rare-earth emitters in thin film LN, along with their polarization characteristics and related ion implantation engineering, presents a promising opportunity to produce highly luminescent Er-doped LN integrated photonic devices for nanophotonic and quantum applications at telecom wavelengths.

3:00pm QS1+EM+MN+PS-MoA-7 MBE Grown InAs/GaAs Quantum Dot Platforms with Spatial and Spectral Control for Quantum Devices, *Nazifa Tasnim Arony,* University of Delaware; *Lauren McCabe,* University of Delaware- Now at Yale University; *Joshya Rajagopal, Lan Mai, Lottie Murray, Prashant Ramesh, Townsend Long, Matthew Doty, Joshua Zide,* University of Delaware
Epitaxially grown semiconductor quantum dots (QDs) have been well studied in the past few decades and have shown great promise as single photon emitters, and as a basis for potential qubits. These features of quantum dots grown on a semiconductor matrix make it a desirable platform/building block for quantum devices which has a wide-range of applications in quantum information, quantum sensing and quantum computing. For a complete epitaxially grown quantum device, spatial, spectral and structural homogeneity, optical tunability, and scalability are the key requirements. Recent work from our group has shown a method for site controlled QD growth where InAs QDs are grown on site-templated GaAs substrates with arrays of nano-pits.[1] However, achieving spectral homogeneity and good optical quality to ensure scalability is still a big challenge due to the size distribution of the QDs during growth, and impurities introduced in the regrowth surface from the fabrication processes respectively. This work addresses these challenges and explores three different objectives, first one being the domain of quantum dot columns (QDCs) as a buffer layer for the top QD-arrays of interest while burying defects/impurities underneath the QDCs. Additionally, initial experiments on spectral control of InAs/GaAs QDs by an in-situ method called 'cap and flush' are discussed, and the concept of quantum dot molecules (QDMs) is introduced for optical tunability in site-templated scalable device platforms.

[1] J. Vac. Sci. Technol. B 38, 022803 (2020).

3:15pm QS1+EM+MN+PS-MoA-8 High Bandwidth Al-Based Single Electron Transistors for Silicon Quantum Dot Charge Sensing, *Runze Li,* University of Maryland, College Park; *Pradeep Namboodiri, Joshua Pomeroy,* NIST-Gaithersburg
We have reduced the resistance of all-metal-based single electron transistors (SETs) for a 10 to 15 times higher operation current. This will provide more bandwidth and less noise to the SETs for eventual use as quantum dot charge sensors. People want to use the gate layer integrated all-metal-based SETs as charge sensors for quantum computing, but the long-remaining problem was the instability of readout due to the charge offset drift. Our group has developed stable aluminum-based SETs using plasma oxidation techniques, solving the instability problem. However, the devices we made are limited by the output current, typically <10 pA level when working in the single electron regime. The limitation on the current is due to the AlOx tunnel junctions' high resistance. Our goal is to bring up the output current up to ~100 pA level. We have been working on reducing the resistance of the AlOx thin film by reducing the plasma oxidation time and increasing the thin film area. We have seen a 10 to 15 times reduction in the resistance by varying plasma parameters. And we have also seen an obvious decrease in the resistance when increasing the tunnel junction area. We are continuing to develop data to study the quantitative relationship between the oxidation time/area and resistance. We are expecting to report the results of the reduced resistance in this talk.

Quantum Science and Technology Mini-Symposium
Room 123 - Session QS2+PS-MoA

Advanced Fabrication and Plasma Techniques for Quantum Applications

Moderators: **Angelique Raley**, TEL Technology Center America, **Sebastian Engelmann**, IBM T.J. Watson Research Center, **David Pappas**, Rigetti Computing

4:00pm **QS2+PS-MoA-11 High-Rate (>50 nm/hour) Plasma-Enhanced ALD of Superconducting NbxTi1-xN with Substrate Biasing for Quantum Technologies**, *Silke Peeters, Lisa Nelissen,* Eindhoven University of Technology, Netherlands*; Dmytro Besprozvannyy,* Oxford Instruments Plasma Technology, UK*; Nidhi Choudhary,* University of Glasgow, UK*; Ciaran Lennon,* Oxford Instruments Plasma Technology, UK*; Marcel Verheijen,* Eindhoven University of Technology, Netherlands*; Michael Powell, Louise Bailey,* Oxford Instruments Plasma Technology, UK*; Robert Hadfield,* University of Glasgow, UK*; Erwin Kessels,* Eindhoven University of Technology, Netherlands*; Harm Knoops,* Oxford Instruments Plasma Technology, UK

The advancement of a wide range of quantum technologies hinges on improvements in materials and their interfaces. Plasma-enhanced atomic layer deposition (PEALD) enables the growth of high-quality superconducting thin films with atomic-scale control. Scalable integration of PEALD in the diverse field of superconducting quantum device fabrication requires the development of versatile, high-throughput processes.

We demonstrate PEALD of superconducting $Nb_xTi_{1-x}N$ films at a high rate of > 50 nm/hour on the Oxford Instruments PlasmaPro ASP system. The RF-driven remote capacitively coupled plasma (CCP) ALD system with small chamber volume allows for low-damage conditions and short cycle times. The CCP source is combined with RF substrate bias functionality allowing for ion-energy control. The depositions consist of NbN and TiN supercycles using the TBTDEN and TDMAT precursors and an $Ar/H_2/N_2$ plasma at a table temperature of 320 °C.

$Nb_xTi_{1-x}N$ films are prepared with film thicknesses ranging from 5 to 100 nm with < 5 % non-uniformity on a 150 mm diameter wafer. Four-point probe measurements yield low room-temperature resistivities increasing with Nb content from 160 μΩ cm (41 nm TiN) to 284 μΩ cm (25 nm NbN). The films are stoichiometric with a low ~2 at.% O impurity content. Accurate $Nb_xTi_{1-x}N$ composition control through supercycling is demonstrated from x=0 to x=1, with the C content increasing from 10 at.% to 19 at.% and the N content correspondingly decreasing from 40 at.% to 26 at.%. EDX mapping confirms homogeneous mixing of Ti and Nb and XRD reveals all prepared films are fcc polycrystalline. The crystallinity and conductivity of the films can be tuned by RF substrate biasing. TEM imaging of the most conductive 50 nm $Nb_{0.5}Ti_{0.5}N$ film prepared with 90 V bias reveals a disordered polycrystalline film in agreement with XRD, which shows peak broadening beyond 50 V bias.

$Nb_{0.5}Ti_{0.5}N$ films of 5 nm to 100 nm thickness display superconducting transitions at critical temperatures of 3.5 K to 10 K. A high sheet kinetic inductance of 470 pH/sq is found for the 5 nm film prepared with 90 V bias. Superconductivity is also confirmed for all explored compositions and substrate bias voltages. As a result, the film properties can be tailored whilst maintaining the high quality required for quantum applications. The novel ALD configuration negates the need for long plasma exposures to achieve this quality. This tunability and high rate of the $Nb_xTi_{1-x}N$ deposition process puts forward PEALD as a promising technique to tackle material challenges in a wide range of quantum technologies.

4:15pm **QS2+PS-MoA-12 Plasma etch study of NbTiN/αSi/NbTiN Josephson Junctions for Superconducting Digital Loic**, *Yann Canvel, Shreya Kundu, Vincent renaud, Ankit Pokhrel, Daniel Lozano, Diziana Vangoidsenhoven, Bart Kennens, Amey Walke,* IMEC Belgium*; Anna Herr,* IMEC

In the development of next-generation logic devices, an attractive complement to CMOS technology would be to leverage the superconducting technology which operate at a low temperature. Superconducting Digital Logic (SDL) devices are attractive as they are inherently faster and have much less power dissipation than their CMOS counterpart. Although SDL devices have existed for decades now, there have been fundamental challenges to scale down its main components and related interconnects. To provide groundwork for exploring SDL device integration, and a possible hybrid integration of SDL/CMOS circuits, one of the key patterning challenges is the Josephson Junction (JJ) device

fabrication. JJ devices are the active devices of SDL technology that can potentially provide computational density, energy efficiency and interconnect bandwidth beyond conventional electronics.

In this communication, an in-depth plasma etch investigation is reported to demonstrate the patterning of high-density junctions with diameters between 210-500nm and CD control of <2% across the 300mm wafer. Using the Reactive Ion etching (RIE) technique, the study has firstly consisted of developing a non-standard NbTiN etch process which enables to pattern the JJ pillars through the Top Electrode (TE) and the αSi barrier, down to the Bottom Electrode (BE) with a precise etch landing control. Subsequent etch processes have then required successive engineering optimization to build up the final device. Some of the main challenges to tackle were the etch residues mitigation, the reduction of oxidized NbTiN interfaces and the final electrical contact with the Top metal. The successful fabrication of high density NbTiN/αSi/NbTiN junctions has offered the first demonstration of a Josephson Junction compatible with CMOS BEOL. Some electrical measurements at room and cryogenic temperatures will complete the investigation by showing high critical current, high speed and device stability up to 420°C.

Pokhrel, A *et al.,* First Demonstration of High Density NbTiN/αSi/NbTiN Josephson Junctions. *IEEE Symposium on VLSI Technology & Circuits (VLSI), (2024).*

Pokhrel, A. *et al.* Towards Enabling Two Metal Level Semi-Damascene Interconnects for Superconducting Digital Logic: Fabrication, Characterization and Electrical Measurements of Superconducting $Nb_xTi_{(1-x)}N$. *IEEE International Interconnect Technology Conference (IITC),* (2023).

Holmes, D. S. *et al.* Energy-Efficient Superconducting Computing - Power Budgets and Requirements. *IEEE Transactions on Applied Superconductivity* **23**, 1701610–1701610 (2013).

Herr, Q. P. *et al.* Ultra-low-power superconductor logic. *Journal of Applied Physics* **109**, 103903 (2011).

4:30pm **QS2+PS-MoA-13 Patterning Improvements and Oxidation Mitigation of $Nb_xTi_{(1-x)}N$ Metal Lines Processes for Superconducting Digital Logic**, *Vincent Renaud, Yann Canvel, Ankit Pokhrel, Sara Iraci, Min-Soo Kim, Benjamin Huet, Jean-Philippe Soulie, Sujan Sarkar, Quentin Herr, Anna Herr, Zsolt Tokei,* IMEC, Belgium

One promising alternative to standard CMOS technology is Superconducting Digital Logic (SDL) which enables computing at cryogenic temperature and, thus, performs faster at a reduced cost and power. Recently, it was demonstrated that a two-metal level BEOL unit process using $Nb_xTi_{(1-x)}N$ for the metal lines with a critical dimension of 50nm could be achieved on 300mm wafers. Cryogenic temperature electrical measurement showed that the lines and via of the device have a critical temperature of 12-13.4 K and a critical current density of 80-113 mA/μm². It was also highlighted that one of the crucial challenge in the making of this technology was the oxidation of the $Nb_xTi_{(1-x)}N$ metal lines during the direct metal etch process of the material itself and/or during the conception of the full device. This oxidation negatively impacts the electrical performance of the wire and could become a serious showstopper for the scalability of the device.

The goal of this study is to discuss different approaches for constructing and patterning the $Nb_xTi_{(1-x)}N$ metal lines while mitigating the oxidation of the device during the process. Different Hard-Mask (HM) materials have been investigated, as well as alternative HM removal processes. Finally, an in-situ encapsulation of the $Nb_xTi_{(1-x)}N$ metal lines post-etch process has been experimented to mitigate the oxidation the device when exposed to the air or during the sub-sequent dielectric gap-fill. These experiments were coupled with electrical measurements at room and cryogenic temperature with the aim of validating the best fabrication process for the $Nb_xTi_{(1-x)}N$ metal lines for SDL devices.

Pokhrel, A. *et al.* Towards Enabling Two Metal Level Semi-Damascene Interconnects for Superconducting Digital Logic: Fabrication, Characterization and Electrical Measurements of Superconducting $Nb_xTi_{(1-x)}N$. *IEEE International Interconnect Technology Conference (IITC),* (2023).

Holmes, D. S. *et al.* Energy-Efficient Superconducting Computing - Power Budgets and Requirements. *IEEE Transactions on Applied Superconductivity* **23**, 1701610–1701610 (2013).

Herr, Q. P. *et al.* Ultra-low-power superconductor logic. *Journal of Applied Physics* **109**, 103903 (2011).

4:45pm QS2+PS-MoA-14 Patterning of TiN and TaN for advanced superconducting BEOL, *Thibaut Chêne,* CEA-LETI, France*; Roselyne Segaud, Fabrice Nemouchi, Stéphane Minoret,* CEA-Leti, France*; Frédéric Gustavo,* CEA INP Grenoble, IRIG, France*; Julien Garrione, Thierry Chevolleau,* CEA-Leti, France

The development of new quantum technologies based on superconducting Qubits or spin Qubits becomes a major subject of interest for applications in communication and data computing. Such technology operating at low temperature requires a superconducting rooting development.

The superconducting materials have been selected based on their superconducting properties and their integration capabilities in an industrial process flow. The integration is based on a top down approach by patterning successively both metals with a selective etch process to define lines and vias.

To develop the patterning process, a 40 nm thick film of TiN or TaN is deposited by PVD on a SiO_2 layer over 300 mm silicon wafers. Then the lithography is performed on a 193nm stepper to achieve 150 nm line and via critical dimension (CD). Etching developments are carried out on a 300 mm industrial ICP chamber using Cl_2 chemistry with or without HBr or CH_4 addition. A parametric study of Cl_2 based chemistries is performed to achieve a straight profile with low CDbias and also to determine the selectivity of TaN over TiN. Optical Emission Spectroscopy (OES) and quasi in-situ Xray Photo-electon Spectroscopy (XPS) are conducted to better understand the etching mechanisms.

Regarding the TiN, straight profiles and good CD control are achieved with Cl_2/HBr chemistries but micromasking is observed. The micromasking phenomenon will be further discussed in terms of plasma/surface interaction based on the quasi in-situ XPS analyses. The addition of CH_4 instead of HBr prevents the micromasking while keeping a rather straight profile with an etch rate of 70 nm/min. For the TaN, whatever the etching chemistries, lower etch rates are observed in comparison with TiN. This trend is attributed to a higher Ta-N binding energy and lower etch by-product volatility. The Cl_2/HBr and Cl_2/Ar plasma chemistries lead both to CD loss and tapered profile mainly due to a lack of selectivity with the PR. Oppositely, the Cl_2/CH_4 chemistry allows achieving straight TaN profile by adjusting the amount of CH_4. The patterning of 80 nm vias for both TiN and TaN are obtained by combining resist trimming and the etching processes previously optimized for the narrow lines. After this patterning process optimization, the T_c of 150 nm CD structures is measured using a specific test vehicle for both TiN and TaN thin films. We will then leverage the TiN:TaN etching selectivity of 4.6 achieved by tuning the Cl_2/CH_4 amount to integrate TiN vias on TaN lines.

5:00pm QS2+PS-MoA-15 Optimization of Superconducting Transition Metal Nitride Films Deposited by Reactive High-Power Impulse Magnetron Sputtering, *Hudson Horne, Collin Hugo, Brandon Reid, Daniel Santavicca,* University of North Florida

Ultra-thin films of transition metal nitrides are used to create superconducting devices such as superconducting nanowire single-photon detectors, kinetic inductance detectors, and parametric amplifiers. Nanowires made from such materials also have applications in quantum computing, for example as high-impedance, low-dissipation shunts to suppress charge noise in superconducting qubits. In this work, we explore the use of high-power impulse magnetron sputtering (HiPIMS) to optimize the superconducting properties of transition metal nitride thin films for such device applications.

Initial work has focused on niobium nitride deposited using a reactive process in which a niobium target is sputtered in the presence of nitrogen gas. We compare films deposited on silicon substrates via HiPIMS and conventional DC sputtering, and we find that HiPIMS can produce films of the same thickness with a higher critical temperature and a lower normal-state resistivity. Film composition and structure are characterized with scanning electron microscopy, wavelength-dispersive x-ray spectroscopy, and x-ray diffraction, and these results are correlated with the electrical properties of both unpatterned films and nanowires. These characterizations suggest that the improved superconducting properties of the HiPIMS films is the result of optimizing the stoichiometry in the desired δ crystal phase. We show that further improvement in the critical temperature is possible through the use of an aluminum nitride buffer layer and through substrate heating.

We have begun extending these studies to other materials such as titanium nitride and hafnium nitride. This work seeks to systematically explore the HiPIMS process for optimizing transition metal nitride films with an emphasis on ultra-thin films for quantum device applications.

Advanced Surface Engineering
Room 125 - Session SE-MoA

Surface Engineering Solutions for Sustainable Development
Moderators: Jyh-Wei Lee, Ming Chi University of Technology, **Ivan Petrov**, University of Illinois at Urbana-Champaign

1:30pm SE-MoA-1 Towards Responsible Surface Engineering Based on PVD Technology, *Marcus Hans, Jochen Schneider,* RWTH Aachen University, Germany*; Allan Matthews,* The University of Manchester, UK*; Christian Mitterer,* Montanuniversität Leoben, Austria **INVITED**

The sustainable development goal (SDG) 12 'Responsible Consumption and Production' of the United Nations deals with the necessary change of consumption and production patterns towards a more sustainable future. Plasma-assisted physical vapor deposition (PVD) is increasingly employed to address global challenges, such as energy efficiency and reduction of CO_2 emissions. Two important questions are critically evaluated in this context:

1) How sustainable are state-of-the-art PVD processes and materials?

2) Which pathways are needed for future responsible surface engineering?

While our modern world and human life benefit from surface engineering, the consideration of energy and mass balances demonstrates that state-of-the-art PVD processes and products are not necessarily sustainable, leaving space for innovation. Responsible surface engineering comprises pathways to enhance the sustainability of processes as well as materials. Impurities will be discussed with respect to tolerable levels and even exploitation of 'impurities', which can be beneficial for the performance of a coating. Moreover, the microstructural design of chemically simple coatings offers opportunities to avoid economically and ecologically expensive elements. Prospective product cycles of emerging technologies and future products will enable the evaluation of ecological, economical as well as societal costs and benefits. Finally, responsible surface engineering involves a change in mindset of materials scientists, process engineers and of all stakeholders involved in garnering innovation.

2:00pm SE-MoA-3 ASED Rising Star Talk: Unprecedented B Solubility in Cubic (Hf,Ta,Ti,v,Zr)B-C-N Coatings, *Andreas Kretschmer*[1], TU Wien, Austria*; Alexander Kirnbauer,* TU Wien, Institute of Materials Science and Technology, Austria*; Robert Frost, Daniel Primetzhofer,* Uppsala University, Sweden*; Marcus Hans, Jochen Schneider,* RWTH Aachen University, Germany*; Paul Mayrhofer,* TU Wien, Institute of Materials Science and Technology, Austria

In the past, we have studied the system (Hf,Ta,Ti,V,Zr)B-N with exceptional hardness and thermal stability, but the coatings contained a significant amount of C impurities, which may have influenced the properties [1]. To investigate the impact of C in this system, we have deposited new coatings with a TiN target, on which we placed diboride and/or carbide pieces of the metals Hf, Ta, V, and Zr. We have varied the composition by using either only diborides, only carbides, or different mixtures of the two material types to make 5 coatings containing either N and B, N and C, or all three. The B concentration varies between 42 and 0 at%, the C content between 25 and 0 at%, and the N content is stable at around 30 at% in all coatings. The Ti makes up roughly 20 at%, while the other metals are in the range between 2 and 5 at%. X-ray diffraction (XRD) shows a weakly textured single-phase fcc solid solution in all coatings. The FWHM of the 200 reflex ranges from 2 ° in the C-free coating down to 0.5 ° in the B-free coating, indicating different grain sizes. This is confirmed by transmission electron microscopy, revealing fine columnar growth in the 2.3 to 3.2 μm thick coatings, with especially fine grains in the B-richer coatings. Electron diffraction confirms that no secondary phases are present. We annealed the coatings in a vacuum furnace at 1000, 1200, and 1400 °C for 10 min, followed by XRD and nanoindentation. The coatings stay stable up to 1200 °C and start decomposing at 1400 °C. The as-deposited hardness of all coatings lies between 36 and 38 GPa, and is maintained after annealing at

---

[1] **AVS Rising Star**

1000 °C. After annealing at 1200 °C, the coatings containing only C or only B both soften to ~34 GPa, while the coatings with both C and B do not lose any hardness at this temperature. Only after annealing at 1400 °C does the hardness of all coatings drop below 30 GPa. We confirmed the thermal stability by atom probe tomography on the most promising sample, hereby we show that despite the high B content of 22 at%, decomposition into a diboride phase initiates only after annealing at 1400 °C. We further investigated the fracture-toughness by in-situ micromechanical cantilever bending. The best performing coating yields 4.0±0.5 MPa*m^(1/2), thus surpassing other similar coatings not only in hardness and thermal stability, but also fracture toughness.

[1] Kretschmer, A., et al. (2022). *Materials & Design*, *218*, 110695. https://doi.org/10.1016/j.matdes.2022.110695

2:15pm SE-MoA-4 ASED Rising Star Talk: High Temperature Behavior of $Ti_{0.12}Al_{0.21}B_{0.67}$ Coatings Investigated by High-Resolution Transmission Electron Microscopy and DFT Calculations, *Sebastian Lellig*[1], RWTH Aachen University, Germany, Switzerland; *Amir Hossein Navidi Kashani,* RWTH Aachen University, Germany; *Peter Schweizer,* Empa, Swiss Federal Laboratories for Materials Science and Technology, Thun, Switzerland; *Marcus Hans, Ganesh Nayak,* RWTH Aachen University, Germany; *Johann Michler,* Empa, Swiss Federal Laboratories for Materials Science and Technology, Thun, Switzerland; *Jochen M. Schneider,* RWTH Aachen University, Germany

The oxidation behavior of stoichiometric $Ti_{0.12}Al_{0.21}B_{0.67}$ coatings is investigated by high resolution Transmission Electron Microscopy (TEM) after oxidizing for 1, 4 and 8 h at 700 °C and at 800 and 900 °C.

In the as deposited state, a ~ 4 nm thick, native, amorphous oxide layer covers the surface of the coating while the magnitude of incorporated O along the column boundaries decreases with depth. During oxidation, the formation of scale layers consisting predominantly of Al, O and B is observed that appear to be amorphous at 700 °C in which, after oxidation at 900 °C for 8h, nanocrystalline $Al_5(BO_3)O_6$ regions form. Concurrently, underneath the scale, the formation of Al- and Ti-rich boride regions, consistent with spinodal decomposition, is observed. Chemical environment dependent DFT predictions of the energies required for mass transport on the metal sublattice indicate that that Al diffusion is initiated before Ti. Hence, as the temperature is increased, the migration of Al is initiated first, leading to the formation of the oxide scale observed already after oxidation at 700 °C after 1 h. Below the oxidized region, the formation of Al-rich and Ti-rich regions by spinodal decomposition require the concurrent migration of Al and Ti. The fact that decomposition takes place at 900 °C and hence at larger temperatures than the Al diffusion mediate scale formation is consistent with DFT predictions as the averages of the predicted energies required for both, vacancy formation and migration for Ti are larger than for Al.

2:30pm SE-MoA-5 ASED Rising Star Talk: Friction and Wear of MXene/MoS2 Nanocomposite Coating Under Dry and Hydrocarbon-Lubricated Conditions, *Ali Zayaan Macknojia*[2], *Andrey Voevodin, Samir Aouadi,* University of North Texas; *Stephen Berkebile,* Army Research Laboratory; *Diana Berman,* University of North Texas

Friction and wear-related failures remain the greatest problems in moving mechanical assemblies operating under various conditions. This study demonstrate lubricity achieved by spray-coating solution-processed multilayer Ti3C2Tx-MoS2 blends onto rough 52100-grade steel surfaces. Blends exhibited lower frictional performance for individual pristine materials, MoS_2 and $Ti_3C_2T_x$, under high pressure, sliding speed. Study investigated the processing, structure, and property correlation to gain a deeper understanding of the underlying phenomena. Raman spectroscopy, scanning electron microscopy, and transmission electron microscopy results revealed the formation of an in-situ robust tribolayer responsible for the outstanding performance observed at high contact pressures and sliding speeds. This study has broad implications for the development of solid lubricants that can operate under extreme conditions and low viscosity fuel environment, inspiring further research and development in this field.

2:45pm SE-MoA-6 ASED Rising Star Talk: Tunable Tribochemical Behavior of Pt-Au Thin Film Alloys Using High-Throughput Testing, *Tomas Babuska*[3], *Frank DelRio, Justin Hall, Brad Boyce, David Adams, Joyce Custer, Manish Jain,* Sandia National Laboratories; *Jason Killgore,* NIST-Boulder; *Filippo Mangolini, Camille Edwards,* University of Texas at Austin; *John Curry,* Sandia National Laboratories

Binary alloy systems such as Pt-Au have been shown to exhibit ultra-low wear and high hardness enabled by its intrinsically thermally stable nanocrystalline microstructure making them suitable candidates for electrical contact materials. When the unique mechanical properties are combined with the catalytic behavior of platinum under cyclic shearing in inert environments, adventitious carbon can be mechano-chemically transformed into lubricious surface films (μ < 0.05). While ideal for solid lubrication applications, carbon deposits can inhibit electrified interfaces and compromise end-use performance. By balancing the catalytic and mechanical properties of Pt-Au thin films, the friction behavior and surface film morphology can be controlled to either promote/prevent lubricious carbon film formation.In this work, we explore 448 compositions of sputter deposited Pt and Au thin films spanning 0-100 at% and the intertwined role of hardness and composition on the resulting friction and wear behavior. We highlight the use of custom high-throughput tribological platforms with robotic automation to rapidly test large material spaces and for the creation of in-depth structure-property relationships that will play a crucial role in the development of next-generation tribological coatings. SNL is managed and operated by NTESS under DOE NNSA contract DE-NA0003525.

3:00pm SE-MoA-7 ASED Rising Star Talk: Advanced Hipims Nanocrystalline and Metallic-Glass High Z Coatings for Interaction with Liquid Metals, *Davide Vavassori*[4], *Luigi Bana, Marco Bugatti, Maria Sole Galli De Magistris,* Politecnico di Milano, Italy; *Matteo Iafrati,* Department of Fusion and Technology for Nuclear Safety and Security, ENEA, Italy; *David Dellasega, Matteo Passoni,* Politecnico di Milano, Italy

Liquid metals (LMs) are of interest for the development of several applications related to the energy sector. However, the presence of LMs creates concerns about the compatibility with standard structural materials since, generally, LMs affects their integrity and mechanical properties through different phenomena [1]. Therefore, the mitigation of LM corrosion emerges as a crucial step. This especially applies if the aim is the integration of LMs in a nuclear energy system which, being characterized by high temperatures and strong radiation fields, introduces constraints on the choice of possible structural materials.

The deposition of nanocrystalline or metallic-glass protective coating is an appealing approach to engineer the structural material surface and, consequently, to control the interaction with LMs. In this respect, the fine tailoring of the coating properties at the nanoscale represents a key aspect to optimize its performances in the harsh LM environment. To this end, the use of an of advanced Physical Vapor Deposition methods such as High Power Impulse Magnetron Sputtering (HiPIMS) [2] can play a key role to produce films with controlled properties.

In this framework, a notable example is represented by the magnetic confinement fusion research area where innovative divertor designs based on liquid tin (Sn) are under investigation [3,4]. Nevertheless, the action of liquid Sn in detrimental for many structural materials typically used in fusion systems. Specifically, liquid Sn heavily corrodes the heath-sink components which are constituted by CuCrZr alloy to satisfy the thermomechanical and cooling requirements imposed by the fusion power flux.

This works aims at investigating the corrosion resistance of tungsten (W)-based coatings produced by HiPIMS when in contact with liquid Sn. To this end, two different strategies have been studied to grow the metallic coating on CuCrZr substrates. On the one hand, the application of different pulsed substrate bias voltages synchronized with the HiPIMS pulse were considered to produce pure W coatings. On the other hand, the co-sputtering from a W target and an aluminium (Al) target, both working in HiPIMS mode, was examined to realize a multilayer coating. The produced samples were tested in corrosion experiments carried out at 400 °C for relatively short periods of time (150 or 600 minutes). The characterization of the samples before and after the exposure allowed to evaluate how coatings properties determined their effectiveness as protective layer and, thus, to retrieve preliminary information about their ability to withstand the typical operation condition expected in a LM-based divertor.

3:15pm SE-MoA-8 Eliminating Surface Charging in X-Ray Photoelectron Spectroscopy of Insulators for Reliable Bonding Assignments, *Grzegorz (Greg) Greczynski,* Linkoping University, Sweden

Sample charging during X-ray photoelectron spectroscopy (XPS) analyses of electrically insulating samples is a widely recognized challenge of this essential technique. If the electron loss caused by the photoelectric effect is not compensated due to specimens' poor electrical conductivity, the positive charge building up in the surface region results in an uncontrolled shift of detected core level peaks to higher binding energy (BE). This seriously complicates chemical bonding assignment, which is based on measured peak positions, and accounts for a large spread in reported core level BE values. Here, we show that peaks from several industry-relevant oxides, serving as model insulators, typically displaced by several eV due to charging, shift back to positions characteristic of electrically-neutral samples following *ex-situ* capping with a few nm thick metallic layer with low affinity to oxygen. The effect is present only if the capping layers contain sufficiently large non-oxidized volume that provides long-range conduction paths to grounded Cu clamps, while being thin enough to allow for recording high quality spectra from the underlying insulators. The versatility of the charging elimination is demonstrated for different oxides/cap combinations and air exposure times. The method is robust and easy to apply.

4:00pm SE-MoA-11 STrengthening Mechanisms for High Entropy Alloy Coatings Fabricated by Magnetron Sputtering, *Jyh-Wei Lee,* Ming Chi University of Technology, Taiwan, Republic of China*; Bih-Show Lou,* Chang Gung University, Taiwan

Prof. Yeh has been developing high entropy alloys (HEAs) for twenty years. The research on bulk HEA materials has attracted much attention due to their unique properties being better than those of traditional alloys. On the other hand, the HEA coatings fabricated by magnetron sputtering methods have been ensured for improving substrate materials' mechanical properties, corrosion resistance, oxidation resistance, and wear resistance. In this work, several strengthening mechanisms, including nitridation, carburization, solid solution hardening, and grain refinement,were adopted to study their effects on the mechanical properties improvements of VNbMoTaW, VNbMoTaWAl, VNbMoTaWCr, TiZrNbTaFe, TiZrNbTaFeB, and ZrTiNbSiFe high entropy alloy coatings grown by magnetron sputtering technique. The chemical compositions, phase structures, microstructures, and surface roughness of these HEA coatings were examined. The nanohardness, reduced elastic modulus, and wear resistance of HEA coatings were measured by nanoindenter and pin-on-disk wear tester, respectively.

We can conclude that good mechanical properties, including higher hardness and lower wear rate, can be obtained for those HEA coatings through the proper selection of strengthening mechanisms and the addition of several constituents, such as nitrogen, carbon, TiB_2, and Cr elements. This work evaluated some strengthening mechanisms and promising results of HEA coatings that can be used as protective coatings in harsh environments.

4:15pm SE-MoA-12 ASED Rising Star Talk: Multifunctional Optical Surfaces for Displays: From Antireflective to Self-Cleaning and Antimicrobial Functionalities, *Iliyan Karadzhov*[1], *Christina Graham, Alessia Mezzadrelli,* ICFO-Institut de Ciencies Fotoniques, Spain*; Wageesha Senaratne, Karl W. Koch, Prantik Mazumder,* Corning Research and Development Corporation*; Valerio Pruneri,* ICFO-Institut de Ciencies Fotoniques, Spain

Glass is an indispensable part of display technologies, and knowing how to incorporate multiple useful properties into a single optical surface will enhance their performance. For example, nature-inspired designs can deliver high transparency and clarity, broadband and omnidirectional optical response, self-cleaning capabilities, and mechanical resistance. However, fabricating these surfaces with the desired properties can be complex, often requiring multistep lithography methods, which are costly and not easy to scale. In this talk, we discuss our team's recent developments in utilizing thermal dewetting of ultrathin metal films (Cu, Ag, Ni) as a lithography-free method to create durable, nanostructured optical surfaces with tailored multifunctional features.

In the first part, we demonstrate a transparent anti-microbial coating on glass surface based on dewetted copper (Cu) nanoparticles encapsulated by conformal SiO_2 and fluorosilane functional layers. The coatings kill more than 99.9% of *Staphylococcus aureus* within 2 hours due to the released Cu ions and can maintain their anti-microbial properties after wiping tests. The

relatively flat transmission of 70-80% in the 380-750 nm range along with color neutrality and non-conductivity make them suitable for high-touch surfaces in medical and public settings where hygiene is important.

The second part focuses on a simplified method to create abrasion-resistant antireflective glass surfaces by creating randomly arranged subwavelength nanoholes. The fabrication process involves three main steps. First, silver nanoparticles are obtained by quickly thermally annealing an ultra-thin silver film on the glass substrate. These particles then serve as a base for a secondary etch mask, created by depositing a thin nickel layer over the silver nanoparticles and performing selective chemical wet etching. Finally, this mask is used in a dry etching process to carve nanoholes of varying depths into the glass surfaces. We achieve a transmission above 99% across a broad wavelength range with minimal scattering, where maximum spectral performance can be tuned to either the visible or near-infrared range by adjusting the lateral arrangement of the silver nanoparticles and the depths of the nanoholes. After undergoing an abrasion test of 10,000 passes with cheesecloth under constant load, the nanoholes remain structurally intact due to the redistribution of shearing mechanical forces.

4:30pm SE-MoA-13 Effect of Europium and Gadolinium Alloying Elements on the Tribological Response of Low Hydrogen Content Amorphous Carbon, *Camille Edwards, Hsu-Ming Lien, Nicolás Molina,* *Filippo Mangolini,* The University of Texas at Austin

Dopants and alloying elements are commonly introduced in amorphous carbon (a-C) materials to tailor their mechanical and tribological properties. While most published studies have focused on doping and/or alloying a-C coatings with metals or metalloids, doping a-C films with rare-earth elements has only recently been explored. Notably, our understanding of the shear-induced structural changes occurring in rare-earth element-containing a-C films is still elusive, even in the absence of any liquid lubricants. Here, the friction response of Eu- and Gd-containing a-C films with low hydrogen content deposited by high-power impulse magnetron sputtering (HiPIMS) on silicon was evaluated in open air and at room temperature. The load-dependent friction measurements indicated that the introduction of Gd ((2.3 ± 0.1) at.%) and Eu ((2.4 ± 0.1) at.%) into the a-C matrix results in a significant reduction of the shear strength of the sliding interfaces ((41 ± 2) MPa for a-C, (16 ± 1) MPa for a-C:Gd2.3 at.%, and (11 ± 2) MPa for a-C:Eu2.4 at.%.). Near-edge X-ray absorption fine structure (NEXAFS) spectromicroscopy experiments provided evidence that no stress-assisted sp3-to-sp2 rehybridization of carbon atoms was induced by the sliding process in the near-surface region of undoped a-C, while the amount of sp2-bonded carbon progressively increased in a-C:Gd2.3 at.% and a-C:Eu2.4 at.% upon increasing the applied normal load in tribological tests. The formation of an sp2-bonded carbon-rich surface layer in a-C:Gd2.3 at.% and a-C:Eu2.4 at.% films was not only proposed to be the origin for the reduced duration of the running-in period in tribological tests, but was also postulated to induce shear localization within the sp2-carbon rich layer and the transfer film formed on the countersurface, thus decreasing the interfacial shear strength. These findings open the path for the use of Gd- and Eu-containing a-C even under critical conditions for nearly hydrogen-free a-C films (i.e., humid air).

4:45pm SE-MoA-14 Importance of the Near-Infrared Optical Properties of Thermal Barrier Coatings, *Francis Blanchard, Mathieu Bruzzese, Bill Baloukas, Jolanta Klemberg-Sapieha,* *Ludvik Martinu,* Polytechnique Montreal, Canada

As aircraft engine operating temperatures increase, so must the thermal insulation capabilities of the thermal barrier coatings (TBCs) used to shield metallic components in the combustion chamber and high-temperature turbine areas. Heat transfer from the hot gases to the engine components occurs through two main mechanisms: conduction and radiation. Considerable efforts have been deployed over the years to ensure TBCs have low thermal conductivity, thanks to a porous microstructure generally achieved by thermal spray or EB-PVD techniques. The radiative component of heat transfer, however, has been largely ignored in TBC design. This aspect is however very important due to an exponential increase in radiative heat transfer for higher gas temperature. While TBCs are naturally reflective of radiative heat due to light scattering, this property is very vulnerable to degradation.

Degradation of TBCs over their lifetime is related to microstructural change mainly due to high temperature exposure and CMAS (Calcium-Magnesium-Alumino-Silicate) attack. Basic understanding of the underlying mechanism is an important aspect of the design and development of high performance TBCs. In this work, the effects of high temperature cycling and CMAS infiltration on the optical performance of Yttria-stabilized zirconia (YSZ)

---

[1] **AVS Rising Star**

coatings prepared by atmospheric plasma spray (APS) were systematically investigated. Optical absorption and scattering coefficients have been extracted from spectrophotometry using integrating sphere measurements in a novel way via the inverse adding-doubling (IAD) method. The microstructure was analyzed using scanning electron microscopy (SEM) and mercury infiltration porosimetry (MIP) in an attempt to establish a relationship between the evolving microstructure and the optical properties. Both were found to have a significant impact on performance, with CMAS infiltration having the biggest effect. To further study the evolution of their performance as the pores are filled, atomic layer deposition (ALD) is used to mimic CMAS infiltration in a controllable fashion. The results show that most of the performance loss occurs with very little material inserted into the pores and that a saturation point is quickly reached. In addition, a finite-difference time-domain (FDTD) model was developed to predict the optical performance of TBCs before and after degradation with good agreement with experimental data. This model can now be applied to investigate ways to mitigate the degradation processes.

5:00pm SE-MoA-15 Assessing the Feasibility of Laser Ablation Coating Removal (LACR) on Legacy Bridge Steel: Coating Removal and Adhesion, and Effects on Mechanical Properties, *W.P. Moffat,* University of Virginia*; S. Sharp, J. Provines,* Virginia Transportation Research Council*; S.R. Agnew, J.M. Fitz-Gerald,* University of Virginia

The application of protective organic coatings is one of the most effective and commonly used corrosion mitigation strategies. To maintain the protective nature of coatings on long-term-exposed surfaces such as steel bridge components, coatings must be periodically removed and reapplied. A relatively new method called laser ablation coating removal (LACR), which incorporates a high energy nanosecond pulsed laser beam (1 kW, 1064 nm, Nd:YAG) in combination with a high efficiency filtration system, allows for safe and effective removal of coatings and contamination from metal surfaces and provides excellent re-coating adhesion.

LACR cleaning has been applied to legacy bridge steel components to investigate its effect on substrate cleanliness, adhesion, and steel mechanical properties. Legacy bridges were never grit blasted and contain a 20–100 μm thick mill-scale layer (Fe_3O_4, Fe_2O_3, FeO) below several coating layers (including lead-rich coatings). The surface oxide layer thermally insulates the underlying steel, preventing melting of the metallic substrate. Characterization of the LACR surfaces with electron microscopy, hardness, tensile, and fatigue testing has shown that LACR does not cause any measurable detrimental effects to the bulk mechanical properties of the bridge steel.

Re-coating LACR surfaces was found to have the same or higher adhesion values in comparison with the state of the art grit blasted surfaces, despite a three-fold decrease in surface roughness. Detailed analysis and adhesion testing of both zinc rich organic and inorganic (OZ and IOZ respectively) coating systems show that LACR cleaning provides excellent adhesion. OZ coatings show exclusively cohesive failures during adhesion testing, whereas IOZ coatings show a mix of both cohesive and adhesive failures.

Surface Science
Room 120 - Session SS+AMS-MoA

Surface Chemistry and Reactivity on Oxide Surfaces
Moderators: Ashleigh Baber, James Madison University, **Florencia C. Calaza**, Instituto de Desarrollo Tecnológico para la Industria Química

1:30pm SS+AMS-MoA-1 Dynamic Formation of Gem-Dicarbonyl on Rh Decorated $Fe_3O_4(001)$, *Jiří Pavelec, Chunlei Wang, Panukorn Sombut, Lena Puntscher, Moritz Eder,* Vienna University of Technology, Austria*; Zdeněk Jakub,* CEITEC, Czechia*; Roland Bliem,* Advanced Research Center for Nanolithography, Netherlands*; Michael Schmid, Ulrike Diebold,* Vienna University of Technology, Austria*; Cesare Franchini,* University of Vienna, Austria*; Matthias Meier, Gareth Parkinson,* Vienna University of Technology, Austria

Single atom catalysts (SACs) have the potential to reduce the amount of precious materials needed in catalytic reactions. Understanding and utilizing SACs requires studying the coordination of adatoms to their supports, as well as their coordination to reactants. This coordination can change during reactions, and intermediate dynamic steps may be invisible to conventional spectroscopy.

In this study [1], we employ scanning tunneling microscopy (STM) in combination with theory to investigate a model SAC: Rhodium decorated $Fe_3O_4(001)$. Our results demonstrate that the formation of dicarbonyl on

Rh_1 requires the initial presence of Rh_2 on the surface, a finding corroborated by detailed density functional theory (DFT) studies.

CO adsorption at Rh_1 sites at room temperature results exclusively in stable Rh_1CO monocarbonyls, as the Rh atom adapts its coordination to form a stable pseudo-square planar environment. $Rh_1(CO)_2$ gem-dicarbonyl species are also observed, but they form exclusively through the brake up of Rh_2 dimers via an unstable $Rh_2(CO)_3$ intermediate. Identification of this intermediate step would be challenging without a multi-technique approach.

These results are compared to the Rh decorated TiO_2 model SAC using temperature-programmed desorption (TPD), infrared reflection absorption spectroscopy (IRAS) [2], nc-AFM, and X-ray photoelectron spectroscopy (XPS).

[1] Wang, C.; Sombut, P.; Puntscher, L.; Jakub, Z.; Meier, M.; Pavelec, J.; Bliem, R.; Schmid, M.; Diebold, U.; Franchini, C.; Parkinson, G. S., Angewandte Chemie **2024**, 63 (16).

[2] Rath D.; Mikerásek V., Wang C.; Eder M.; Schmid M.; Diebold U.; Parkinson G.S., Pavelec J. **2024**, *submitted*

1:45pm SS+AMS-MoA-2 Water-Gas Shift Reaction Mechanisms on Ligand Coordinated Pt Single Atom Catalyst: Insights from DFT & Microkinetics, *Dave Austin,* Duy Le, Talat Rahman, University of Central Florida

Hydrogen is a promising renewable and environmentally friendly fuel to meet future global energy needs. An important reaction to produce hydrogen is the water-gas shift (WGS) reaction, ($CO+H_2O \rightarrow CO_2+H_2$; ΔH=-41.1 KJ/mol). Interest in the use of single-atom catalysts (SACs) for facilitating these reactions has grown. This project explores a new strategy that can create a metal-ligand coordinated SAC on metal oxide (Titanium oxide) support. 1,10-phenanthroline-5,6-dione (PDO), was chosen as the ligand for its oxidative potential for stabilizing metal cations in two bidentate sites. Our experimental collaborators Fereshteh Rezvani and Steve Tait from Indiana University were able to characterize the single-atom nature of the Pt with EXAFS, XPS, XRD, DRIFTS, and TEM. They evaluated for the WGS reaction, and it was discovered that Pt-ligand SAC supported on defective TiO_2 shows higher inherent catalytic activity than Pt NPs with significantly lower activation energy which is generally desirable for the redox mechanism.

First, the structure of the Pt-PDO molecule had to be determined, this is because the ligand has two bidentate sites. Experimental results that this complex has a ratio of 2:1 for the ligand to Pt, giving three different potential structures. After the molecule was determined, we had to understand the role of vacancies on the TiO_2 surface. The Pt-PDO complexes (all three configurations) were adsorbed onto to TiO_2 surface that was either clean, or had an oxygen, titanium, or oxygen and a titanium vacancy. We showed that the vacancies were important to activate the Pt-PDO complex, on the clean surface there is only van der Waals interaction between the surface and the complex. The electronic structure of these systems also shows the activation of the Pt atom from vacancies, as the Pt becomes more reactive and has its frontier orbitals pushed closer to the Fermi level. The WGS reaction has two different proposed mechanisms. They are the Redox and the associative mechanisms. They differ by which point the reactants are adsorbed. These two mechanisms' pathways were simulated on the Pt-PDO complex and to understand the role of ligands the Redox mechanism was also studied on a single Pt atom. The DFT calculations confirmed that the redox mechanism has a lower energy barrier than the associative mechanism for Pt-ligand SAC. A microkinetic study was also performed to obtain the theoretical turnover frequency for all three reactions. The microkinetic study shows that the Redox mechanism has a higher turnover frequency than that of the associative and single Pt atom reactions.

2:00pm SS+AMS-MoA-3 Surface Chemistry and Catalysis of $IrO_2(110)$, *Jason Weaver,* University of Florida*; Aravind Asthagiri,* Ohio State University*; Minkyu Kim,* Yeungnam University, Republic of Korea*; Jovenal Jamir, Connor Pope,* University of Florida*; Jungwon Yun,* Ohio State University*; Suriya Ramasubramanian,* University of Florida **INVITED**

Developing more efficient catalytic processes to oxidize light-alkanes partially or completely is important for various applications, including power generation, exhaust gas remediation and chemical synthesis. In this talk, I will discuss investigations of alkane oxidation on the $IrO_2(110)$ surface, and emphasize how mechanistic insights obtained from UHV surface science experiments and DFT calculations have been used to inform our understanding of rates and species coverages measured during alkane oxidation under catalytic conditions. I will discuss the development of a

first-principles microkinetic model that accurately reproduces key aspects of the kinetics of methane oxidation on $IrO_2(110)$ and identifies how different surface species, observed using operando spectroscopy, affect the catalytic kinetics. I will also discuss recent results which clarify how gaseous H_2O influences the catalytic oxidation of ethane on $IrO_2(110)$ and the surface species that develop under reaction conditions. Our studies demonstrate how fundamental knowledge gained from surface science and DFT calculations can play a critical role in interpreting operando measurements and identifying the mechanisms of complex, catalytic reactions.

2:30pm SS+AMS-MoA-5 Room Temperature Activation of Methane and Its Dry Reforming by MgO Nanostructures Embedded in CuO_X on Cu(111), *Arephin Islam, Kasala Prabhakar Reddy,* Brookhaven National Laboratory; *Yi Tian,* Stony Brook University/Brookhaven National Laboratory; *José A. Rodriguez,* Brookhaven National Laboratory

Natural gas, primarily methane, is valued for its versatility and potential in sustainable energy production through reforming or partial oxidation reactions. The investigation stems from the need for efficient technologies to utilize natural gas for sustainable syn gas or hydrogen production while simultaneously addressing carbon dioxide (CO_2) utilization and conversion challenges. MgO nanostructures show promise for methane activation due to their unique surface properties, while Cu-based catalysts are explored for selective methane oxidation at lower temperatures.This study investigates the growth and reactivity of MgO nanostructures on a $Cu_2O/Cu(111)$ substrate, employing scanning tunneling microscopy (STM) and synchrotron-based ambient-pressure X-ray photoelectron spectroscopy (AP-XPS). Deposition of Mg atoms on the "29" structured copper oxide film induces oxygen transfer from the $Cu_2O/Cu(111)$ substrate to the deposited Mg, forming MgO and CuO_x. Diverse morphologies are observed, including structured copper oxide films with embedded MgO clusters (1-3 Mg atoms) and randomly dispersed MgO nanoparticles. Reactivity studies reveal that MgO nanostructures smaller than 1 nm in width activate methane at room temperature, dissociating it into CH_x species. CO_2 dissociates into CO and C species instead of forming plain carbonates. The size and morphology of MgO nanostructures significantly influence their reactivity, enabling dry reforming of methane (MDR) by CO_2 into syn gas. Specifically, MgO nanostructures with a coverage of 0.04-0.11 ML activate methane at room temperature, leading to its dissociation into CH_x species. Additionally, smaller MgO clusters (0.2-0.5 nm in width, 0.4-0.6 Å in height) at lower coverages exhibit distinct reactivity towards CO_2, dissociating it into CO and C species. This investigation underscores the size- and morphology-dependent reactivity of MgO nanostructures, showcasing a behavior distinct from bulk MgO. The catalytic performance observed is attributed to the unique magnesia-copper interface, featuring multifunctional sites comprising magnesium cations, oxygen, and copper cations, which facilitate methane activation and drive the MDR processes forward at around 500K.

2:45pm SS+AMS-MoA-6 Mixed $IrO_2/RuO_2(110)$ Thin Films: Distinct Surface Chemical Properties of the Single-Layer Oxides, *Suriya Narayanan Ramasubramanian, Chethana Sudarshan, Jisu Shin, Christopher Lee,* University of Florida, Gainesville; *Craig Plaisance,* Louisiana State University; *David Hibbitts, Jason F. Weaver,* University of Florida, Gainesville

Mixed metal-oxides of IrO_2 and RuO_2 have potential to serve as efficient catalysts for promoting the partial or complete oxidation of alkanes, due to the unusual ability of IrO_2 to activate light alkanes at low temperature as well as the possibility that the mixed oxides exhibit distinct surface chemical properties compared with the pure oxides. In this talk, I will discuss our recent studies of the growth and surface chemical properties of layered structures of $IrO_2(110)$ and $RuO_2(110)$ thin films as well as mixed IrO_2-$RuO_2(110)$ films prepared in UHV. We find that single-layers (SL) of $IrO_2(110)$ on $RuO_2(110)$ and vice versa exhibit distinct binding properties toward adsorbed molecules compared with the corresponding multilayer (ML), bulk-like oxides. TPD shows that the binding of N_2 and O is stronger on SL-$RuO_2(110)$ on ML-$IrO_2(110)$ relative to ML-$RuO_2(110)$, whereas these species bind more weakly on SL-$IrO_2(110)$ on ML-$RuO_2(110)$ relative to ML-$IrO_2(110)$. These differences are especially pronounced for oxygen in that the binding energy of an adsorbed O-atom on top of a surface metal site increases in the order, SL-IrO_2 < ML-RuO_2 < ML-IrO_2 < SL-RuO_2, with the binding energy differing by ~50 kJ/mol between each single vs. multiple layer structure. I will discuss DFT calculations which show that these differences originate from a trans-ligand effect, wherein the bonding properties of surface metal atoms are strongly influenced by the bonding of sub-surface O-atoms to the second layer oxide. Lastly, I will discuss recent results showing that well-mixed $Ir_xRu_yO_2(110)$ thin films can be generated in UHV and will discuss their surface chemical properties. The significant

differences between the surface chemical properties of single vs. multiple layer oxide structures may have broad implications for understanding the catalytic behavior of mixed IrO_2/RuO_2 systems.

3:00pm SS+AMS-MoA-7 Active Sites for Oxidation Reactions on Cu_2O Surfaces, *Dario Stacchiola,* Brookhaven National Laboratory

Cu-based catalysts are active for partial and full oxidation reactions. Copper can be oxidized under moderate oxidant pressures and temperature to Cu_2O, and further to CuO under typical catalytic reaction conditions. We present here model systems using both copper oxide thin films and single crystals used to interrogate the effect of modifiers on the stability of exposed active Cu sites. *In situ* experiments allow the observation of dynamic processes and phases under reaction conditions.

References

[1] "Oxidation of CO on a reconstructed Cu_2O surface", (submitted)

[2] "Stabilization of Cu_2O through site-selective formation of a Co_1Cu hybrid single-atom catalyst", *Chem. Mat.* **34**,2313(2022)

[3] "Potassium-Promoted Reduction of $Cu_2O/Cu(111)$ by CO",*J. Phys. Chem. C* **123**, 8057–8066 (2019)

[4] "Redox Properties of $Cu_2O(100)$ and (111) Surfaces", *J. Phys. Chem. C* **122**, 28684–28691 (2018)

3:15pm SS+AMS-MoA-8 Tracking Elementary Steps in Conversion of Carboxylic Acids on Single Crystalline and Nanofaceted $TiO_2(101)$, *Xingyu Wang,* Pacific Northwest National Lab; *William Debenedetti,* Los alamos National Laboratory; *Christopher O'Connor,* Harvard University; *Zdenek Dohnalek, Greg Kimmel,* Pacific Northwest National Lab

Ketonization of carboxylic acid used to be a method to produce acetone in industry. Recent interest has focused on this C-C coupling reaction due to its potential for upgrading biomass. The production of acetone from acetic acid was only observed in high pressure reactors on anatase nanoparticles. However, on anatase $TiO_2(101)$ single crystals in ultra-high vacuum (UHV), acetone production from acetic acid has not been observed. This is an example of the material gap in surface science studies. The mechanism of ketonization is also under debate; the two most commonly proposed pathways are ß-keto acid pathway and ketene pathway.

In this study, we introduced well-defined nanoparticles (NPs) with mostly (101) surfaces into a UHV chamber to elucidate the ketonization mechanism and bridge the material and pressure gaps in this system. A combined experimental approach of temperature programmed desorption (TPD), scanning tunneling microscopy (STM), X-ray photoelectron spectroscopy (XPS), and reflection absorption infrared spectroscopy (RAIRS) was used, along with theoretical studies. Our finding is that on single crystals, the ketene produced desorbs from the surface without encountering another acetate. In contrast, ketene desorbing from a given NP within a layer of NPs can subsequently react with an acetate on another NP, leading to acetone production. To demonstrate this, we prepared three samples with varying thickness of anatase NP layers, with mostly (101) facets, in an UHV system. We then compared the reaction of acetic acid on these NP layers with its reaction on an anatase(101) single crystal. We found that the production of acetone starts from 10ML of acetic acid exposure, and the yield correlates with the depth of acetic acid absorption into the nanoparticle beds. Along with theoretical studies, we identified a mechanism through a key intermediate, α-enolate acetic acid, which forms through the reaction of gas phase ketene with surface-bound acetate species. Further studies, which involve dosing ketene through a homemade heated quartz tube ketene source onto an acetic acid pre-dosed single crystal surface, are currently underway to confirm this reaction mechanism.

3:30pm SS+AMS-MoA-9 Developing First-principles Microkinetic Models for Selective Ethane Oxidation on Cl-substituted IrO2(110), *Jungwon Yun,* The Ohio State University; *Dasol Bae, No-Kuk Park,* Yeungnam University, Republic of Korea; *Jason Weaver,* University of Florida; *Minkyu Kim,* Yeungnam University, Republic of Korea; *Aravind Asthagiri,* The Ohio State University

In this study, we investigated the role of Cl doping on ethylene selectivity for ethane oxidation on IrO2(110) using a combination of density functional theory (DFT) and microkinetic modeling (MKM). Catalytic oxidative dehydrogenation (ODH) of ethane is an attractive route to produce value-added products such as ethylene. Our previous research demonstrated that stoichiometric IrO2(110) exhibits significant potential for ethylene production at low temperature (~ 400 K) due to the low activation energy for initial C-H bond cleavage of light alkanes. Temperature programmed reaction spectroscopy (TPRS) experiments showed that surface HO groups

promote ethylene selectivity in ethane ODH. Given Cl is isoelectronic to surface HO groups and has been experimentally shown to be able to substitute bridge O atoms on RuO2(110) surfaces, we explored Cl substitution effects on ethylene selectivity on IrO2(110). DFT calculations indicated that the presence of bridge Cl on the IrO2(110) surface destabilizes adjacent adsorbed ethane and ethylene but has minimal impact on the reaction barriers of C2Hx species with adjacent oxygen. This suggests that limited Cl substitution would still allow the IrO2(110) surface to convert C2H6 to C2H4, but subsequently start to constrain further dehydrogenation and oxidation steps due to the lack of bridge O atoms. A DFT-based MKM was developed to understand the relationship between product yields (C2H6, C2H4, CO/COx) on degree of Cl substitution. The MKM modeled TPRS confirms that ethylene yield is increased by Cl substitution but eventually reaches a maximum where there is a drop due to the deactivation of the surface. This maximum in ethylene yield is dependent on initial C2H6 coverage since dehydrogenative oxidation steps produce surface HO groups that, when combined with bridge Cl, deactivate the surface. We will discuss ongoing work to extend the MKM simulations to reaction conditions where activity and selectivity are examined as a function of partial pressures of C2H6 and O2 along with percent Cl substitution.

4:00pm SS+AMS-MoA-11 Small Alcohol Reactivity Over TiO2/Au(111) Inverse Model Catalysts, *Ashleigh Baber,* James Madison University

Gold-based catalysts have received tremendous attention as supports and nanoparticles for heterogeneous catalysis, in part due to the ability of nanoscale Au to catalyze reactions at low temperatures in oxidative environments. Surface defects are known active sites for low temperature Au chemistry, so a full understanding of the interplay between intermolecular interactions and surface morphology is essential to an advanced understanding of catalytic behavior and efficiency. Our undergraduate research lab uses ultrahigh vacuum temperature programmed desorption (UHV-TPD) to investigate the fundamental interactions between small alcohols on Au(111) and the reactivity of TiO2/Au(111) inverse model catalysts on small alcohol redox behavior. In a systematic study to better understand the adsorption and intermolecular behavior of small alcohols (C1-C4) on Au(111) defect sites, coverage studies of methanol, ethanol, 1-propanol, 1-butanol, 2-butanol, and isobutanol have been conducted on Au(111). These small alcohols molecularly adsorb on the Au(111) surface and high resolution experiments reveal distinct terrace, step edge, and kink adsorption features for each molecule. The desorption energy of small primary alcohols was shown to trend linearly with increasing C1-C4 carbon chain length, indicating that the H-bonded molecular packing of 1-butanol resembles that of methanol, ethanol, and 1-propanol, while isobutanol and 2-butanol deviate from the trend. These energy insights are particularly interesting when studying the redox behavior of small alcohols over TiO2/Au(111).Depending on the surface preparation conditions, Au(111) supported TiO2 nanoparticles react with small alcohols to form either reduced and oxidized products. The reactivity of the surface for ethanol oxidation was altered by controlling the oxidation state of TiO_x (x<2) and coverage of TiO_2. Low coverages of fully oxidized TiO_2 nanoparticles on Au(111) are active for the selective oxidation of ethanol to form acetaldehyde, but not all small alcohols behave similarly.

4:15pm SS+AMS-MoA-12 Partial Chlorination of IrO₂(110) for Selective Ethane Chemistry, *Connor Pope,* University of Florida, Gainesville; *Jungwon Yun,* Ohio State University; *Rishikishore Reddy, Jovenal Jamir,* University of Florida, Gainesville; *Minkyu Kim,* Yeungnam University, Republic of Korea; *Aravind Asthagiri,* Ohio State University; *Jason F. Weaver,* University of Florida, Gainesville

Developing more efficient catalytic processes to convert ethane to ethylene is important for improving hydrocarbon-to-chemicals processing and transitioning to carbon-neutral technologies. Our prior work demonstrates that C_2H_6 dehydrogenation on the IrO_2(110) surface produces C_2H_4 between ~350 and 450 K during temperature programmed reaction spectroscopy (TPRS), and that the C_2H_4 selectivity can be increased by pre-hydrogenating the oxide surface to deactivate a fraction of the surface oxygen sites. In this talk, I will discuss recent work in which we controllably replaced surface O-atoms of IrO_2(110) with Cl-atoms through the oxidation of gaseous HCl in ultrahigh vacuum. We find that the stepwise adsorption of HCl on IrO_2(110) with heating to 650 K causes H_2O desorption, and generates Cl atoms on bridging and on-top sites in about a 1:1 ratio, with the total Cl coverage saturating near 0.7 ML. Measurements using TPRS and XPS further demonstrate that the partitioning of Cl-atoms between bridging and on-top sites can be altered by exposing the surfaces to reducing vs. oxidizing

conditions. Lastly, I will discuss how partial chlorination affects the surface reactivity toward CO and C_2H_6, and produces a nearly two-fold increase in the selectivity of C_2H_6 dehydrogenation to C_2H_4 during TPRS. Our findings demonstrate the potential of controlled surface deactivation for improving the selectivity of IrO_2(110) for partial alkane oxidation.

4:30pm SS+AMS-MoA-13 Insights into CO₂ Hydrogenation on the InOx/Cu (111) and InOx/Au (111) Surfaces: Surface Electronic Structure and Reaction Mechanistic Studies, *Prabhakar Reddy Kasala, Jose Rodriguez,* Brookhaven National Laboratory

In CO_2 hydrogenation, In_2O_3 catalysts are known for their higher CH_3OH selectivity, primarily attributed to their oxygen vacancies. Subsequent studies explored depositing metals on In_2O_3 to enhance CO_2 conversion and oxygen vacancy formation.[1-2] Besides metal supported on In_2O_3-based catalysts, intermetallic In-M (M= Pd, Cu) compounds have also shown good performance for CO_2 hydrogenation to methanol synthesis.[3-4] Despite extensive research on metal (M) supported In_2O_3 catalysts, the role of In-M alloy and M/In_2O_3 interfaces in CO_2 activation and methanol selectivity remains unclear. Our surface electronic structural studies using APXPS reveal that during CO_2 hydrogenation, very low coverage (~0.035 ML) InO_x/Cu(111) undergoes structural changes at/above 500 K, forming a Cu-In intermetallic alloy at the surface. Further increase in Indium coverage (0.325 ML) results in InOx/Cu(111) at the surface, while the interface remains an In-Cu alloy. Carbon 1s core level spectra of the InO_x/Cu (111) regions of the surface under 1 Torr of CO_2 + H_2 (1:3 ratio) show the formate (HCOO*) and H_xCO* species, with H_xCO having the higher concentration at 500 K in 0.035 ML, while the 0.325 ML Indium oxide has shown the carbonate (CO_3*) at 300 K and decreased with an increase in temperature to 500 K. Our results clearly demonstrate the promotional effects of In_2O_3 for CO_2 hydrogenation. Furthermore, we extended our studies on InO_x/Au(111) and InO_x/TiO_2 (001) surfaces to understand the role of Oxide/Metal, Alloy, Oxide/Oxide roles in methanol selectivity. Our preliminary STM and XPS results on InO_x/Au (111) established the preparation of In/Au (111) and InO_x/Au (111) surfaces. We are making progress on indium-based catalysts for CO_2 hydrogenation to establish the role of possible alloys/intermetallic and metal-support interfaces in CO_2 activation and CO_2 hydrogenation to methanol under reaction conditions.

References:

1. Cao et. al., *ACS Catal.* 2021, *11*, 1780-1786

2. Rui et. al., *ACS Catal.* 2020, *10*, 11307-11317

3. Shi et. al., *J. Catal.* 2019, *379*, 78-89

4. Chen et. al., *ACS Catal.* 2019, *9*, 8785-8797

4:45pm SS+AMS-MoA-14 Structural-Electronic Property Evolution of LiCoO₂ (001) Under Varied Oxygen Chemical Potentials, *Yuchen Niu, Janice Reutt-Robey,* University of Maryland College Park

Since its discovery as an intercalation Li-ion battery electrode in 1980, $LiCoO_2$ remains a popular cathode material for portable devices. Its surfaces also provide an unexplored opportunity to tune the structure and charge-transport properties for emergent electronic applications. In this study, we report on the evolution of $LiCoO_2$ (001) surfaces, specifically their structural and electronic property response to processing under low/high O_2 chemical potential extremes via scanning probe microscopy (SPM), low energy electron diffraction (LEED), X-ray photoelectron spectroscopy (XPS) and Raman spectroscopy.

Under a traditional UHV regimen at low O_2 chemical potentials, $LiCoO_2$ (100) persistently displays a diffused (1x1) LEED pattern after many cycles of Ar^+ sputtering- thermal annealing, suggestive of nanoscale disorder without major atomic surface reconstruction. UHV-STM imaging reveals the singular surface terminated by shallow grains of ~2 nm width, which coarsen to ~30 nm grains under prolonged processing. Atomically resolved images of local regions show ($\sqrt{7}$x$\sqrt{7}$) R 19.1° ordering, which could be attributed to local Li ordering on Li-terminated layers. The electronic properties of this surface are further mapped with UHV scanning tunneling spectroscopy. Electronic band gaps derived from I-V spectroscopy are reported. This is corroborated by in situ XPS measurements of the surface chemical composition and valence band structures during the Ar^+ sputtering- thermal annealing cycles.

Under high O_2 chemical potentials (160~ 760 torr O_2), dramatic changes in surface structures are observed, indicating more efficient surface mass transport. In contrast to the nanograin features observed at low O_2 chemical potentials, high O_2 chemical potential treatments generate expansive atomically flat (100) terraces of ~ 1 µm width, step edges and

quasi-hexagonal islands. Partial surface decomposition to Co_3O_4 due to Li loss is also observed.

Thin Films
Room 115 - Session TF+AP-MoA

Thin Films Special Session: Remembering Dr. Paul Holloway II & Reception

Moderators: Sean Jones, Argonne National Laboratory, **Philip Rack**, University of Tennessee

1:30pm TF+AP-MoA-1 A Surface Science Approach to Advancing Area-Selective Deposition and Atomic Layer Etching, *Adrie Mackus,* Eindhoven University of Technology, Netherlands **INVITED**
With future nanoelectronics relying on the vertical stacking of devices, selective deposition and etching techniques are essential for enabling self-aligned processing of materials on such 3-dimensional devices structures. Similar to the research approach of dr. Paul. H. Holloway, in this work surface science methods are employed to obtain understanding of thin film processing. A combination of in-situ experiments and simulations is carried out to study the mechanisms of selectivity and inhibition.

Our work on area-selective atomic layer deposition (ALD) involves the use of small molecule inhibitors (SMIs) in three-step ALD cycles.[1] For example, diketone molecules can be used to inhibit the growth on various oxides surfaces. In-situ infrared spectroscopy studies previously revealed that the diketone acetylacetone (Hacac) can adsorb on an Al_2O_3 surface in chelate and monodentate adsorption configurations.[2] Inspired on these insights, we recently developed atomic layer etching (ALE) processes based on etching by diketone dosing (e.g., hexafluoroacetylacetone) and plasma cleaning steps. Infrared spectroscopy and simulation studies suggest that the mechanism of etching with diketones involves a competition between etching and inhibition reactions. In this presentation, I will discuss how inhibition reactions can be exploited for achieving either area-selective ALD or ALE, and highlight how surface science methods are crucial for understanding the underlying mechanisms.

1. Mackus *et al., Chem. Mater.* **31**, 2 (2019)
2. Merkx *et al., Chem. Mater.* **32**, 3335 (2020)

2:00pm TF+AP-MoA-3 Tuning Surface Radical Species for Area-Selective Initiated Chemical Vapor Deposition of Polymer Thin Films, *Junjie Zhao,* Zhejiang University, China **INVITED**
Self-aligned bottom-up growth of polymer thin films is desired for non-lithographic patterning in applications ranging from nanostructure fabrication to device integration. Aiming at achieving area-selectivity for initiated chemical vapor deposition (iCVD), we developed a toolkit to tune the local concentration of radicals and thus the surface polymerization kinetics. We found that the radical concentration can be promoted locally by (1) generation on targeted surfaces, (2) trapping through gradient forces, and (3) retainment *via* reversible dormant species. *In-situ* quartz crystal microbalance was employed to investigate the reaction mechanisms involved in these area-selective iCVD processes. Cross-sectional imaging and spectroscopic microscopy confirmed the high selective of polymer deposition on the growth areas. Finally, we will show that these strategies are generally effective for area-selective deposition of poly(glycidyl methacrylate), poly(divinylbenzene) and cyclosiloxane polymers.

2:30pm TF+AP-MoA-5 Recent Trends in Thermal ALD Chemistry, *Markku Leskelä, Georgi Popov, Miika Mattinen, Anton Vihervaara, Mikko Ritala,* University of Helsinki, Finland
A review published in 2013 listed all the two-precursor ALD processes reported by the end of 2010 [1]. Since then, many new materials have been deposited by ALD and new processes have been developed for earlier known ALD materials. The recently published ALD database aims to provide a crowdsourced up-to-date collection of ALD processes [2]. In this presentation, we highlight the new precursor and thermal process chemistries published after 2010 based on the ALD database.

The data base contains 1725 unique thermal ALD processes for 548 thin film materials published between 1975 and 2023. The boom in ALD started around 1995 and the number of new processes reported annually increased from 20 in early 1990s to 60 in 2008. Since then, the number of new processes has remained at 60-80 each year. Since 2010, 991 new processes have been published for 441 materials from which 316 materials did not earlier have any ALD process.

Oxide processes form more than 50 % of all the published processes but their share has slightly decreased after 2010. Processes for chalcogenides, pnictides and elements are next in the list. Binary compounds clearly dominate the materials but after 2010 ternary and quaternary compounds as well as elements have increased their share. The number of new ternary processes is roughly double compared to new binary processes. From the ternary and quaternary compounds about 75 % are oxides. Before 2010 the five most common ligands used in metal precursors were halides, alkoxides, alkyls, β-diketonates and amides/imides. The order changes after 2010 to amides/imides, cyclopentadienyls, halides, alkoxides, and alkyls. Heteroleptic complexes have increased their share during the last decade. In non-metal precursors, reducing agents increased importance because of the increased interest to metal deposition.

New elements added to the ALD portfolio since 2010 are alkali metals (Na, K, Rb, Cs), Be, Re, Os, Au and Sb, the first five as oxides and latter four as elements. Reductive processes for transition metals are sought and first thermal processes have been reported for tin and chromium.

86 new binary materials were deposited by ALD since 2010 the biggest group being chalcogenides (29), halides (15) and oxides (15). These materials are linked to broader material and application trends, including perovskite solar (halides) and 2D materials (chalcogenides). Disulfide processes have been reported for Zr, Hf, Mo, Nb, Sn, Re and diselenides for Mo and W.

References
[1] V. Miikkulainen, M. Leskelä, M. Ritala, R.L. Puurunen, J. Appl. Phys. 113, (2013) 021301.
[2] https://www.atomiclimits.com/alddatabase/

2:45pm TF+AP-MoA-6 Ultrathin Polymers Films: Smart Materials and Functionality, *Rigoberto Advincula,* University of Tennessee Knoxville
Nanostructuring involves the application of materials and processing methods to achieve unique dimensional structures at the nanoscale. Soft matter looks at polymers and the self-assembly and directed assembly of macromolecules that results in a unique function, e.g. sensors, electronic actuators, microfluidics, etc.. The research and development of smart or intelligent surfaces and coatings capable of stimuli-response or Omni behavior represent an essential development for coatings in any major application. The ability to control wetting through nanostructuring and choice of chemical functionality can be supplemented by the right deposition methods or application of both lithographic and non-lithographic printing methods. In particular, we have used: 1) polymer grafting, 2) polyelectrolyte layer-by-layer deposition, 3) molecular imprinting of polymers, 4) electro-nanopatterning method using conducting AFM and 5) colloidally templated arrays. Until now, colloidal template 2D electropolymerization remains largely an unexplored method, and there are only a few accounts on colloidal template electropolymerization techniques for micropatterning polymer films. But combined with electropolymerization and polymer brushes it is possible to have functional polymer films that can have sensing and controlled wettability. We will be reporting on the use of stereolithographic lithography (SLA) to create functional superhydrophobic surfaces and nanoreactors.

3:00pm TF+AP-MoA-7 Growing Polymers Molecule by Molecule Through Vapor Deposition, *Matthias J. Young,* University of Missouri-Columbia*; Nikhila C. Paranamana, Mahya Mehregan, Shima Mehregan, Amit K. Datta,* University of Missouri, Columbia **INVITED**
Controlling the sequence of monomers within a copolymer is challenging. Solid-phase peptide synthesis provides molecular sequence control of amino acids by employing solution-phase synthesis with removable protecting groups. This technique was awarded a Nobel prize in 1984 and has spawned a revolution in molecular biology and biochemistry over the last fifty years. However, this approach for peptide synthesis is not readily transferrable to other classes of polymers. Here, we summarize our efforts over the last five years to provide molecular sequence control in polymers formed by oxidative polymerization by employing self-limiting vapor-phase surface reactions through a process termed oxidative molecular layer deposition, or oMLD. We describe insights into the mechanism of oMLD growth that facilitates molecular sequence control, and we examine how molecular sequence impacts redox activity and electronic conductivity. We discuss the various oMLD homopolymer and copolymer chemistries that have been developed to date, expanding from the first oMLD homopolymer chemistry in 2014 to seven oMLD homopolymer chemistries in 2024, and the outlook for oMLD growth of hundreds of potential homopolymer chemistries and a factorial number of copolymer chemistries. We demonstrate the ability to form ultrathin conformal polymer coatings by

oMLD and we discuss the application of these thin film coatings to electrochemical energy storage and ion sensors. We also discuss opportunities for improving on current oMLD synthesis techniques and how the knowledge we have gained about oMLD growth may inform the development of other layer-by-layer vapor-phase polymerization chemistries.

3:30pm TF+AP-MoA-9 Solar Cells, Sensors, and Sensorimotor Neural Prosthetics: My Branch of the Holloway Tree, *Loren Rieth,* West Virginia University **INVITED**

Professor Paul Holloway was my PhD mentor from 1994 to 2001. "Doc's" combination of down-to-earth practicality, erudite knowledge of fundamental materials science, absence of hubris, and mischievous sense of humor resonated with me then and now. His passion for science and engineering was clear from the hours he kept (his modest car was always one of the first to arrive in the morning), his joy when learning something new, and the sustained research productivity he achieved. He balanced this with helping Bette run the family farm, hunting gators, and a love for the Florida outdoors. It was an honor, privilege, and joy to have him as a mentor. The exemplary training I received in the Holloway group on thin film semiconducting materials for solar cell included vicarious learning about luminescent and optical materials and Ohmic semiconductor contacts. This led to my research in metal oxide gas sensors, harsh environment MEMS, and ultimately neural interface microelectrode research and development, the focus of my technical talk.

My neural interface research focuses on penetrating neural electrodes based on micromachined silicon, and flexible neural interfaces based on polyimide microfabrication. Rapid progress is being made in technologies to record, stimulate, and modulate the nervous system. These advancements are being made both to treat diseases with new medical device technologies, and also as tools for basic neuroscience research. Treatments enabled by neural interfaces include controlling bionic limbs for patients with amputations or paralysis, restoring senses (hearing, vision, and touch), treating inflammatory diseases, controlling metabolic diseases, helping to restore mental health, and many others. Currently, successful devices such as cochlear implants, deep brain stimulators, and vagus nerve stimulators, rely on macro-electrodes fabricated using bulk materials. This limits their ability to scale towards interfacing the billions of neurons that comprise the nervous system. Materials science plays a critical role in the development penetrating and flexible micro-electrode technologies. I'll highlight development and use of Utah Slanted Electrode Arrays in the peripheral and central nervous system, and their associated materials challenges. Additionally, recent developments regarding advanced polyimide-based flexible electrodes and optical neural interfaces for small (e.g. 100 μm diameter) peripheral nerves will be presented. An important example is the vagus nerve of murine models, which can be modulated to regulate the autonomic nervous system, a technique called bioelectronic medicine.

Vacuum Technology
Room 121 - Session VT1-MoA

History of Vacuum Technology

Moderators: Marcy Stutzman, Jefferson Lab, **Alan Van Drie**, TAE Technologies

1:30pm VT1-MoA-1 Advancements Through the Ages: The Evolution of Vacuum Technology, *Kurt Lesker IV,* Kurt J. Lesker Company*; Gary Vergason,* Vergason Technology **INVITED**

In this informative presentation, **Kurt J. Lesker IV** and **Gary Vergason** delve into the fascinating journey of vacuum technology. From its humble beginnings to cutting-edge innovations, they explore the pivotal role vacuum science plays in diverse fields. With historical milestones of time, technology, and industry, they discuss how vacuum technology has shaped semiconductor manufacturing, aerospace research, and sustainable energy production. Join them as they unravel the secrets behind vacuum technology and the companies that laid the foundation. Please join us!

Vacuum Technology
Room 121 - Session VT2-MoA

Measurement, Partial Pressure, and Gas Analysis

Moderators: Marcy Stutzman, Jefferson Lab, **Alan Van Drie**, TAE Technologies

2:00pm VT2-MoA-3 Monitoring Chamber Health with an Optical Plasma Gauge, *Martin Wüest, Stefan Kaiser,* INFICON AG, Liechtenstein

Leak testing is a common task in the daily laboratory routine. There are simple but lengthy procedures available to test for leaks, for example the rate-of-rise method. To check if a gas such as water or oxygen is below a certain concentration is often done just by waiting for a time that has been determined by experience. More powerful methods are also available such as mass spectrometers, in particular residual gas analyzers, or dedicated leak detectors. However, they tend to be expensive, are often not very easy to operate, and operate at low pressures. Alternative methods exist such as optical emission spectrometer. They tend to be bulky and extracting robust information is not that easy and below a certain pressure there is not enough light available to analyze.

We have now developed a compact optical plasma gauge to address the questions and shortcomings mentioned above. It combines a gas type monitoring optical plasma sensor with a total pressure sensor. Its design is optimized to allow a gas detection measurement in the range between 10^{-7} and 5 hPa. The gauge allows for the detection of gases such as oxygen, nitrogen, hydrogen or argon in–situ or in a rate of rise leak testing. Above 20 hPa the plasma generation is switched off in order to prevent plasma damage in the sensor. The total pressure sensor operates from 10^{-5} Pa to atmosphere. Discharge pressure is known to play a substantial role in the various competing collisional excitation and de-excitation processes that occur in the plasma. The measured optical spectrum is convoluted with the independent total pressure data to provide higher accuracy. The intelligence implemented directly on the gauge automatically configures the optimal measurement setting in order to ensure easy integration and optimized signal-to-noise ratio. Impurities > 10 ppm can be detected.

2:15pm VT2-MoA-4 Design and Construction of a Fixed Length Optical Cavity (FLOC) Pressure Calibration Standard for Calibration of Military and Commercial Aircraft, *Jacob Ricker, Kevin Douglass, Jay Hendricks, Thinh Bui,* NIST

NIST has constructed several Fixed Length Optical Cavity (FLOC) pressure standards based on gas refractivity and shown that they are effective at measuring absolute pressure [1]. The US Air Force has recently funded development of these standards for the support of their Air Data Calibration Systems. These Air Data Systems provide calibration for altimeters and air speed indicators and traceability of these sensors is crucial for all operational military and commercial aircraft. The current US airspace requirements dictate every aircraft be calibrated at least every 2 years with a device that has an accuracy of pressure reading around 0.03% at pressures around 1/10th of atmosphere.

The air force maintains hundreds of portable standards, working standards, and secondary standards worldwide to achieve that goal. Additionally, the Air Force also maintains other high-pressure standards to meet the operational requirements to provide calibration of pressures up to 10,000 kPa. The air force desires a high accuracy, portable standard that operates over the full pressure range using direct traceability via gas refractivity. A portable standard that is based on fundamental constants rather than frequent recalibration can be forward deployed and will save significant time and money for all civilian and military aircraft operators. With a redesigned FLOC, NIST believes it can meet all the requirements with one portable unit. This presentation will describe the design and construction of a new lower cost/robust/portable calibration system capable of calibrating gas pressure sensors over the entire range of 1 Pa to 10 MPa.

References:

[1] https://doi.org/10.1016/j.measen.2021.100286.

2:30pm VT2-MoA-5 Analysis and Adaptability of the ITER Diagnostic Residual Gas Analyzer Vacuum System, *Brendan Quinlan, Chris Marcus, Jonathan Perry, Charles Smith III, C. Chris Klepper, Theodore Biewer,* Oak Ridge National Laboratory **INVITED**

The composition of exhaust gases in the divertor region is a critical measurement for long pulse devices like ITER. This measurement will provide important information for areas such as fuel-cycle processing and plasma heating [1]. The ITER Diagnostic Residual Gas Analyzer (DRGA) is well suited to make these measurements because it is a multi-sensor

diagnostic system capable of resolving isotopic compositions of hydrogen and helium as well as other heavier elements and compounds [1]. The DRGA will sample a slip stream of gas from the cryogenic pump duct via a sampling pipe that is approximately 7 meters in length and 70-100 millimeters in diameter. At the sampling pipe entrance, an orifice is present which creates molecular flow conditions in the entire length of the sample pipe. The sampling pipe has recently been updated to reflect necessary changes in the ITER port cell area. To provide measurements on timescales that are relevant, the DRGA vacuum system conductance must be revisited from [2] to ensure the appropriate response time and pressure can still be achieved. In this work, Molflow+, which is a Test Particle Monte Carlo (TPMC) simulation code, is used to simulate the conductance and assess the impact of the revised pipe routing. In addition to the new pipe routing, a new pumping scheme has been proposed in previous work and will provide the ability for variable pump speed [3, 4], while overcoming limitations of using an inter-stage port for the optical gas analysis [5]. In the event the orifice is restricted over time, the variable pump speed provides the added benefit of adaptability to ensure the appropriate conductance can be maintained. The restricted orifice is simulated using Molflow+ and compared to test data collected from an in-lab prototype. This study provides important guidance for the design of the ITER DRGA and confirm key operational parameters.

[1] C.C. Klepper et al., 2022 *IEEETPS*, 50 (12) 4970-4979

[2] C.C. Klepper et al., 2021 *Fusion Science and Technology*, DOI 10.1080/15361055.2021.1898867

[3] C. Marcus et al., 2024 SVC TechCon, Pending

[4] B.R. Quinlan et al., 2024 *IEEETPS*, DOI 10.1109/TPS.2024.3387443

[5] C.C. Klepper et al., 2017 JINST 12 C10012

The views and opinions expressed herein do not necessarily reflect those of the ITER Organization.

3:00pm VT2-MoA-7 Effect of Thermal Transpiration on Calibration of Sapphire-Based Capacitance Manometer, *Kimihiro Sato,* Azbil Corporation, Japan

In semiconductor manufacturing, capacitance manometers are generally used for measuring the pressure during deposition or etching. These process gases are highly reactive and often corrosive and the manometers are often heated to 100 to 300 ℃ to prevent byproduct depositions inside them. Therefore, they are required to have high corrosion resistance and operate at these high temperatures. In order to meet these requirements, we have developed capacitance manometers equipped with a MEMS (Micro-Electro-Mechanical Systems) sensor chip based on sapphire, which has the excellent chemical corrosion resistance and thermostability [1].

Since manometers are often used at high temperatures, they must be calibrated at similar temperature at production. These products are heated to various temperatures depending on the target process, while the reference gauge is kept at a constant temperature (near room temperature) for the production efficiency. In this case, the pressure may be different between the product side and the reference side by thermal transpiration. It occurs when two vessels with different temperatures are connected by a narrow tube and the gas flow is in molecular or intermediate flow regime. Therefore, the difference must be compensated in the calibration process and we correct it based on the formula [2,3].

Conventionally, the instrumental error between the product and the reference gauge had been a typical specification (accuracy) that indicates the performance. In addition, the ISO standard [3] requires that the uncertainty be considered. It improves reliability of measurements and brings benefits to the users. In order to comply the standard, it is essential to consider thermal transpiration which is one of the uncertainty factors.

Since the uncertainty of the formula [2,3] is unknown, we studied the effect in the productional facility by comparing experimental and simulated results. In the experiment, the pressure difference between the product side and the reference gauge side was measured. In the simulation, the temperature distribution of each part in the environment was obtained by thermal analysis, and the pressure distribution was obtained by Monte Carlo direct simulation (DSMC-Direct Simulation Monte Carlo). We show the results and consideration of the two efforts.

[1] T. Ishihara, Upgrading a sapphire-based capacitance manometer for reduced size and enhanced anti-deposition characteristics, azbil Technical Review, April 2023.

[2] T. Takaisi and Y. Sensui: Trans. Faraday Soc., 59 (1963) 2503.

[3] ISO 20146:2019, Vacuum technology — Vacuum gauges — Specifications, calibration and measurement uncertainties for capacitance diaphragm gauges.

3:15pm VT2-MoA-8 Measurements of Electrode Temperatures in the Standardized Ion Reference Gauge, *Janez Setina,* Institute of Metals and Technology, Slovenia

A consortium of European National metrology institutes and industrial partners has recently developed a new type of reference ionization vacuum gauge. It is distinguished by its well-known sensitivity and excellent temporal stability, which is the result of straight electron trajectories. Electrons flying through the ionization volume have practically the same path lengths, so the probability of ionization of gas molecules is almost the same for all electrons [1]. The novel Ion Reference Gauge is on its way to standardization of electrode system configuration in ISO TS 6737.

The source of electrons in the gauge is the thermionic cathode, which heats the surrounding surfaces with thermal radiation. Therefore, the ionization cell has a higher temperature than the temperature of the vacuum system in which we want to accurately measure the gas pressure. In non-isothermal systems at low pressures (in the molecular regime), due to the so-called phenomenon of thermal transpiration, the pressure in parts with different temperatures is not the same.

In our research, we measured the temperatures of individual electrodes in the vicinity of the thermionic cathode with the aim of evaluating the influence of the phenomenon of thermal transpiration on the sensitivity of the gauge. In this talk, we will present the experimental setup and the obtained results.

[1] Jousten K, et all, Electrons on a straight path: A novel ionisation vacuum gauge suitable as reference standard, Vacuum 189, (2021), 110239

3:30pm VT2-MoA-9 Calibrations of Spinning Rotor Gauges Towards International Comparison of Vacuum Standards, *Yoshinori Takei,* Hajime Yoshida, AIST, Japan

With the advancement of the semiconductor industry and the transition to a hydrogen energy society, the demand for vacuum measurement has surged. In such circumstances, the spinning rotor gauges (SRG) has garnered attention as one of the most accurate vacuum gauges capable of measuring the vacuum pressure range from 0.1 mPa to 1 Pa. In metrology field, the SRGs have been used as a reference standard for many years.

In national metrology institutes around the world, several vacuum standards such as static expansion system, optical pressure standard and orifice-flow method system are managed for the calibration of vacuum gauges like SRGs, diaphragm gauges, and ion gauges. These standards are based on physical principles, and their uncertainties are evaluated in each metrology institute. For instance, the static expansion system in Japan calibrates SRGs with a relative expansion uncertainty of 0.28% (k=2) [1]. Furthermore, this uncertainty is expected to improve further by combining static expansion system with the optical pressure standard [2]. To verify the consistency of uncertainty, national metrology institutes compare their vacuum standards. Since transporting the vacuum standards themselves for direct comparison is challenging, the same vacuum gauge (SRG) is transported. The calibration results for the same gauge with the vacuum standard of each country are compared. However, the reproducibility of SRG poses a challenge in this process. While SRGs are excellent vacuum gauges, their values may change by about 1 % during transportation, limiting the comparison accuracy of vacuum standards. Therefore, for enhancing the accuracy of international comparison of vacuum standards in the future, careful selection of superior SRGs and in-depth understanding of calibration conditions are essential.

Until recently, only one manufacturer produced SRGs. However, another company has recently entered the market, manufacturing and selling SRGs. There are some differences in the specifications of these SRGs. In this study, we experimentally confirmed the differences when using the SRGs for metrological purposes. Additionally, with the recent publication of ISO 24477 concerning the calibration of SRGs, which describes two calibration methods, we experimentally confirmed the differences. We also conducted calibrations by varying conditions such as the rotation frequency of the rotor, the rotor itself, and the mounting angle of the flange. These experimental results are shown in this presentation.

[1] Yoshinori Takei et.al., Vacuum, 187, 110034, (2021).

[2] Yoshinori Takei et.al., Measurement: Sensors, 22, 100371, (2022).

4:00pm VT2-MoA-11 Vacrysim - Modeling Noise from Residual Gas for Cryogenic Interferometry, *Henk Jan Bulten,* Nikhef, Netherlands*; Vera Erends,* High Voltage Engineering Europa, Netherlands*; Berend Munneke,* Nikhef, Netherlands **INVITED**

Since 2015, gravitational waves (small ripples in the fabric of spacetime) that arose from the mergers of black holes and/or neutron stars have been measured with the large, ultra-precise interferometers of LIGO and Virgo. Einstein Telescope (Fig. 1) is a plan for a next-generation gravitational-wave observatory with a strain sensitivity of 10^{-25}, allowing for precision tests of general relativity, cosmology and astrophysics. In order to reduce thermal noise, Einstein Telescope will operate with mirrors at cryogenic temperatures. This poses new stringent criteria on the vacuum system. Residual gas introduces noise via optical path length changes in the arms, Brownian motion of the mirrors, and ice build-up on the mirror coatings. Einstein Telescope requires residual gas pressures of below 10^{-10} hPa in the (10-km long) arms, and better around the cryogenic mirrors.

The design of the Einstein telescope requires accurate modeling of migration of molecules through the vacuum system, which contains complicated metal support structures and thermal shields, electronic devices with polymer cable mantles, silicon mirrors, etc. We want to model the outgassing and incident particle rate of all components as a function of time. This outgassing is strongly dependent on the history and on the applied temperatures.

Generally, heat flow and molecular flow predictions in finite-element based toolkits like Molflow or Comsol are calculated for steady-state;:adsorption/desorption from the surfaces is taken as constant. However, to numerically calculate the time evolution of the system and see where the molecules deposit/evaporate one needs millions of time steps in which the coupled equations are solved. We developed a simulation toolkit, vacrysim, that is capable of this feat thanks to separating the time-independent tracking information from the time-dependent material properties information. Vacrysim can track thermal radiation and molecular paths and subsequently solve for conductive and radiative heat flow, and adsorption/desorption. Using vacrysim one can model the performance of cryogenic designs in terms of cool-down times, ice build-up and pump-down times. For instance one can predict the ice build-up on the mirror, and the time-dependence of the water distribution in a kapton-coated cable, after venting and evacuating a part of the vacuum system.

In this presentation we will address vacuum requirements for cryogenic interferometry and discuss the vacrysim toolkit.

Vacuum Technology
Room 121 - Session VT3-MoA

Leaks, Flows, and Material Outgassing

Moderators: Marcy Stutzman, Jefferson Lab, **Alan Van Drie**, TAE Technologies

4:30pm VT3-MoA-13 Practical Considerations When Using Low Carbon Steel for Extreme High Vacuum Applications, *Aiman Al-Allaq,* Old Dominion University*; Md Abdullah Mamun, Matthew Poelker,* Thomas Jefferson National Accelerator Facility*; Abdelmageed Elmustafa,* Old Dominion University

The very low outgassing rate of low-carbon steel – of the order 1000 times smaller than degassed stainless steel - suggests this material could provide the means to routinely achieve significantly better vacuum, well into the extreme high vacuum range. At Jefferson Lab, low carbon steel will be used for the construction of a new spin-polarized electron source. The improved vacuum we expect to achieve will ensure reliable and long-lasting beam delivery at milliampere beam currents, which is roughly one hundred times more current than today's state-of-the-art spin-polarized electron sources provide. However, reaping the full benefit of low-carbon steel depends on practical matters, namely, limiting the surface area of all non-low-carbon steel materials required to build a functional photogun. For example, the pressure reduction expected in a photogun with a surface area composed of just 10% stainless steel (e.g., the surface area contribution from an all-metal gate valve leading to the accelerator beamline) would be just a factor of ten, and not the factor of 1000 suggested by the ratio of outgassing rates. This submission describes outgassing rate measurements of chambers built using low-carbon steel and stainless steel and the ultimate pressures achieved for vacuum systems composed of low-carbon steel and stainless steel and pumped using a non-evaporable getter and ion pump. A factor of ten pressure reduction was observed in the system with a surface area dominated by low-carbon steel, consistent with MolFLow+ predictions based on measured outgassing rates. Lower pressures are expected when more thoughtful steps are taken to limit the amount of surface area of non-low carbon steel material.

4:45pm VT3-MoA-14 Systematic Approach for Ultra-Clean Vacuum, *Freek Molkenboer,* TNO Science and Industry, the Netherlands

The demand for smaller, faster, higher accuracy and lower noise levels continues in the scientific field and applications i.e. microchip manufacturing. Contamination concerns that use to be not a concern now suddenly are. This also applies for the vacuum environment. To ensure the desired cleanliness a systematic approach is advised.

During the definition phase of a system, it is important to clearly define the needs of the system. A common methodology within systems engineering is using the v-model. After defining the needs of the system, the design and realisation phase of the system starts. The v-model ends with the validation that the needs are satisfied.

With the increasing cleanliness demands adding cleanliness needs or requirements during the definition phase will increase the successful outcome and will save overall cost.

In my presentation I will show the increase of complexity of a product when cleanliness is key for performance. For this I will use the design of a reflectometer that will be used to measure EUV reflection as a real life example.

5:00pm VT3-MoA-15 Optimal Load Lock Pressure Measurement Technology?, *Tim Swinney, Gerardo Brucker,* MKS Instruments, Inc., Pressure and Vacuum Measurement Group*; Cindy Merida,* MKS Instruments, Inc., Pressure and Vacuum Measurement Group, USA **INVITED**

Transferring silicon wafers from ambient atmosphere into a semiconductor manufacturing cluster tool is a critical step that must be carefully sequenced and controlled. Every wafer must be (1) individually loaded into a load lock chamber through a loading port, (2) sealed against ambient pressure, (3) pumped down to a target pressure level and (4) transferred into a buffer chamber through a transfer port. Once at vacuum, the wafer can then be cycled across multiple process chambers. The same Load Lock chamber is then accessed, operated in a venting sequence, to return the wafer to ambient pressure conditions.

Careful control of differential pressures-i.e. ambient-to-load lock and load lock-to-buffer chamber, during pump-down and venting processes is critical to assure not only the compatibility of pressure levels between chambers and also to minimize the lifting and transport of damaging particles into the tool. Load lock pressure gauges, specifically designed to monitor and control both pump down and vent operations, are preferred pressure sensors for the Semiconductor industry. Load lock pressure gauges provide both differential and absolute pressure readings with accuracy levels required to ensure particles are not disturbed during wafer-load, -pump down, -transfer and -venting processes. Particle control has become critical as feature dimensions continue to drop.

MKS Instruments, Inc. offers multiple pressure measurement instruments that can assist Load Lock operation; however, its exclusive line of compact gauges delivering simultaneous absolute and differential pressure monitoring capabilities has rapidly become a new industry standard. With MEMS technology, two-sensor combination-Differential Piezo resistive diaphragm (PRD) plus Pirani sensor- and proprietary pressure calculation algorithms these sensors can provide accurate differential measurements between ambient and load lock chambers unmatched by any other multi-sensor combination in the market. Their ability to track ambient as well as chamber pressures allows particle-safe pump-downs and vents even after sudden changes in ambient pressure. The pressure measurement technologies in these device as well as planned future enhancements will be discussed. Interface options, calibration routines and control algorithms built into the load-lock sensors will also be described in detail.

Monday Evening, November 4, 2024

Plenary Lecture
Room Ballroom B - Session PL-MoE

Plenary Lecture
Moderator: Mark Engelhard, Pacific Northwest National Laboratory

5:30pm **PL-MoE-1 Advancing Measurement Science for Microelectronics: CHIPS R&D Metrology Program**, *Marla Dowell,* NIST CHIPS Metrology Program   **INVITED**

Metrology plays a key role in semiconductor manufacturing. As devices become more complex, smaller, and multi-layered, the ability to measure, monitor, predict, and ensure quality in manufacturing becomes much more difficult and uncertain. For example, modern chips may contain over 100 billion complex nanodevices that are less than 50 atoms across—all must work nearly identically for the chip to function. Today, the semiconductor industry faces some of these metrology challenges with workarounds and inadequate tools, limiting production yields, impacting quality, and increasing costs. As greater demands are put on semiconductor device performance and material requirements, these challenges will continue to intensify.

The 2022 NIST Report *Strategic Opportunities for U.S. Semiconductor Manufacturing* identified seven grand challenges that if overcome will support increased production, innovation, and competitiveness in the domestic semiconductor industry. The CHIPS Metrology Program has aligned its R&D portfolio with these grand challenges, emphasizing measurements that are accurate, precise, and fit-for-purpose to produce microelectronic materials, devices, circuits, and systems.

This work leverages NIST's proven measurement science expertise, foundational communications and computing research capabilities, standards development contributions, and stakeholder engagement practices to address the highest priority metrology challenges identified across industry, academia, and government agencies. This talk will highlight research activities that support measurements for materials, processing and interfaces of interest to the semiconductor research and manufacturing communities.

2D Materials
Room 122 - Session 2D+AP+EM+QS+SS+TF-TuM

2D Materials: Synthesis and Processing

Moderators: Jyoti Katoch, Carnegie Mellon University, **Huamin Li**, University at Buffalo-SUNY

8:00am 2D+AP+EM+QS+SS+TF-TuM-1 Tailored Growth of Transition Metal Dichalcogenides Monolayers and Their Heterostructures, *Andrey Turchanin*, Friedrich Schiller University Jena, Germany   **INVITED**
Two-dimensional materials (2D), their van der Waals and lateral heterostructures possess a manifold of unique electronic, optoelectronic and photonic properties which make them highly interesting for fundamental studies and technological applications. To realize this potential, their tailored growth as well as understanding of the role of their intrinsic defects and 2D-material/substrate interactions are decisive. In this talk, I will present an overview of our recent progress on the synthesis by chemical vapor deposition (CVD), material characterization and studying of fundamental electronic and photonic properties of 2D transition metal dichalcogenide (TMDs) including some applications in electronic and optoelectronic device as well as observing of new excitonic phenomena. A particular focus will be on the lateral heterostructures of TMD monolayers with atomically sharp boundaries and Janus TMDs.

References

[1] A. George et al. *J. Phys. Mater.* **2**, 016001, 2019.

[2] S. Shree et al. *2D Mater.* **7**, 015011, 2020.

[3] I. Paradeisanos et al. *Nat. Commun.* **11**, 2391 (2020).

[4] G. Q. Ngo et al., *Adv. Mater.* **32**, 2003826 (2020).

[5] A. George et al. *npj 2D Mater. Appl.* **5**, 15 (2021).

[6] S. B. Kalkan et al., *npj 2D Mater. Appl.* **5**, 92 (2021).

[7] E. Najafidehaghani et al. *Adv. Funct. Mater.* **31**, 2101086 (2021).

[8] Z. Gan et al. *Adv. Mater.* **34**, 2205226 (2022).

[9] Z. Gan et al. *Small Methods* **6**, 2200300 (2022).

[10] D. Beret et al., *npj 2D Mater. Appl.* **6**, 84 (2022).

[11] G. Q. Ngo et al. *Nat. Photonics* **16** 769-776 (2022)

[12] S.B. Kalkan, *Adv. Opt. Mater.* **11**, 2201653 (2023).

[13] R. Rosati et al., *Nat. Commun.* **14**, 2438 (2023).

[14] H. Lamsaadi et al., *Nat. Commun.* **14**, 5881 (2023).

[15] J. Picker et al., *Nanoscale Adv.* **6**, 92-101 (2024).

8:30am 2D+AP+EM+QS+SS+TF-TuM-3 High-Coverage MoS_2 Growth by Two-Step Annealing Process, *Shinichi Tanabe, Hitoshi Miura,* Tokyo Electron Ltd., Japan*; Naoya Okada, Toshifumi Irisawa,* AIST, Japan*; Yu min Huang, Hisashi Warashina, Atsuki Fukazawa, Hiroki Maehara,* Tokyo Electron Ltd., Japan
Continuation of Moore's Law scaling requires thin channels in nanosheet field-effect transistor architecture. In this respect, transition-metal dichalcogenides (TMDs) are candidates for the channel material because TMDs are expected to show higher mobility than Si when thickness of the channel is extremely thin. Compatibility to Si nanosheet field-effect transistor fabrication process requires TMD/buffer multilayer film. To obtain such film, alternative preparation of TMD and buffer layers is necessary. Although high-quality TMD can be obtained on a buffer layer by transferring TMD from other substrates, development of a reliable transferring method is challenging. Thus, direct growth of a TMD on a buffer layer is preferable.

We report on a successful growth of high-coverage MoS_2 on SiO_2/Si substrate. The process starts with growing an initial film on SiO_2/Si substrate. Here, a continuous initial film can be easily grown by this process with high growth rate. Next, the initial film is sulfurized by a first annealing step followed by crystallization of the film by a second annealing step. The obtained film is a continuous layered film which was confirmed by cross-sectional TEM images. In addition, typical Raman spectra consisted of E_{2g} and A_{1g} peaks are observed in entire substrate which shows that MoS_2 is grown with high coverage. The difference of E_{2g} and A_{1g} peaks is about 21 cm^{-1}. These results indicate that the two-step annealing process is suitable for obtaining MoS_2 in large area.

8:45am 2D+AP+EM+QS+SS+TF-TuM-4 Anomalous Isotope Effect on the Optical Bandgap in a Monolayer Transition Metal Dichalcogenide Semiconductor, *Kai Xiao,* Center for Nanophase and Materials Sciences Oak Ridge National Laboratory*; Yiling Yu,* School of Physics and Technology, Wuhan University, China*; Volodymyr Turkowski,* Department of Physics, University of Central Florida*; Jordan Hachtel,* Center for nanophase and Materials Sciences Oak Ridge National Laboratory*; Alexander Puretzky, Anton Ievlev, Christopher Rouleau, David Geohegan,* Center for Nanophase and Materials Sciences Oak Ridge National Laboratory
Isotope effects on optical properties of atomically thin 2D materials have rarely been studied to date due to significant challenges posed by sample-to-sample variations resulting from defects, strain, and substrate interactions, complicating the interpretation of optical spectroscopic results. Here, we report a novel two-step chemical vapor deposition method to synthesize isotopic lateral junctions of MoS2, comprising monolayer single crystals with distinct isotopic regions. This method allowed the minimization of shifts in photoluminescence due to synthetic heterogeneities necessary to confirm the intrinsic isotope effect on the optical band gap of 2D materials. Raman measurements and temperature-dependent photoluminescence spectra revealed an unusual 13 (± 7) meV redshift as the Mo isotope mass increased in monolayer MoS2. This shift is distinct from the trend observed in conventional semiconductors and quantum wells (Si, GaAs, diamond, hBN, etc.). Our experimental characterization, along with time-dependent density-functional theory (TDDFT) and many-body second-order perturbation theory, disclosed that this anomalous shift in the optical band gap in 2D MoS2resulted from significant changes in the exciton binding energy induced by strong exciton-phonon scattering. This study provides fundamental insights into understanding the effect of exciton-phonon scattering on the optoelectronic properties of atomically thin 2D materials.

9:00am 2D+AP+EM+QS+SS+TF-TuM-5 CVD Growth and Characterization of High-Quality Janus SeMoS and SeWS Monolayers, *Julian Picker,* Friedrich Schiller University Jena, Germany*; Mahdi Ghorbani-Asl,* Helmholtz Zentrum Dresden-Rossendorf, Germany*; Maximilian Schaal, Oliver Meißner, Felix Otto, Marco Gruenewald, Christof Neumann, Antony George,* Friedrich Schiller University Jena, Germany*; Silvan Kretschmer,* Helmholtz Zentrum Dresden-Rossendorf, Germany*; Torsten Fritz,* Friedrich Schiller University Jena, Germany*; Arkady Krasheninnikov,* Helmholtz Zentrum Dresden-Rossendorf, Germany*; Andrey Turchanin,* Friedrich Schiller University Jena, Germany
Structural symmetry breaking of two dimensional (2D) materials leads to novel physical phenomena. For 2D transition metal dichalcogenides (TMDs) such symmetry breaking can be achieved by exchange of one chalcogen layer with another one. The resulting, so-called Janus TMD structure exhibits an intrinsic dipole moment due to the different electronegativity values of the top and bottom chalcogen layers. Since Janus TMDs do not exist as bulk crystals, they cannot be obtained by exfoliation and need to be synthesized. Recently, we developed a route to grow Janus SeMoS monolayers (MLs) by chemical vapor deposition (CVD). [1] In this approach $MoSe_2$ monolayers are firstly grown on Au foils and then sulfurized to exchange the bottom selenium layer with sulfur atoms. The formation of high-quality Janus SeMoS MLs and the growth mechanism are proven by Raman and X-ray photoelectron spectroscopy (XPS), photoluminescence measurements, transmission electron microscopy and density functional theory (DFT). Here we present an investigation down to the atomic scale of Janus SeMoS MLs grown on Au(111). From low-energy electron diffraction (LEED) and scanning tunneling microscopy (STM) measurements we determine experimentally the lattice parameters of Janus SeMoS for the first time. The obtained results are in good agreement with the respective DFT calculation. Based on the angle-resolved ultraviolet photoelectron spectroscopy (ARUPS) study, we also obtain the spin-orbit splitting value of the valence band at the K point. Moreover, applying the same approach, we grow and characterize Janus SeWS MLs and provide a comparative analysis with the Janus SeMoS system.

[1] Z. Gan, I. Paradisanos, A. Estrada-Real, J. Picker, C. Neumann, A. Turchanin *et al.*, *Chemical Vapor Deposition of High-Optical-Quality Large-Area Monolayer Janus Transition Metal Dichalcogenides*, Adv. Mater. **34**, 2205226 (2022).

9:15am 2D+AP+EM+QS+SS+TF-TuM-6 Location-Selective CVD Synthesis of Circular MoS$_2$ Flakes with Ultrahigh Field-Effect Mobility, *Chu-Te Chen, Anthony Cabanillas, Asma Ahmed, Anthony Butler, Yu Fu, Haolei Hui, Anindita Chakravarty, Hao Zeng,* University at Buffalo-SUNY; *Ajay Yadav,* Applied Materials, Inc.*; Huamin Li,* University at Buffalo-SUNY; *Keith Wong,* Applied Materials, Inc.*; Fei Yao,* University at Buffalo-SUNY

Two-dimensional (2D) semiconducting transition metal dichalcogenides (TMDs) have been considered as promising channel material candidates for future nanoelectronics. The device performance has been significantly improved over the years due to the advancements in understanding of TMD materials, device design, and fabrication process. Despite the early success in demonstrating proof-of-concept devices, scalable and single-crystal growth of TMD films on suitable substrates remains a formidable roadblock to the development of commercially viable TMD-based nanoelectronics. To mitigate this problem, we exploit a controlled growth of high-quality TMD layers at desired locations and demonstrate excellent and consistent electronic properties in transistor device architectures. Taking MoS2 as an example, we develop a precursor-seeded growth strategy for the direct and site-specific synthesis on SiO2 substrates using chemical vapor deposition (CVD). By employing electron-beam lithography to pattern seed layers, precise nucleation and growth at designated positions are achieved. Through systematic exploration of CVD synthesis parameters, ordered arrays of circular MoS2 flakes are successfully grown with the MoO3 seeds serving as the nucleation sites. A comprehensive suite of microscopic/spectroscopic characterizations along with electrical measurements is utilized to analyze the microstructural and transport properties of the as-grown MoS2 flakes. The tri-layer circular MoS2 arrays possess an adjustable and uniform size and exhibit a consistent field-effect mobility up to ~20 cm2/V·s with Bi/Au electrode contacts. These findings showcase a technological breakthrough to 2D material synthesis and hold great promise for future integration of 2D materials in the next generation nanoelectronics.

9:30am 2D+AP+EM+QS+SS+TF-TuM-7 Optoelectronic Properties of Exfoliated and CVD Grown TMD Heterostructures, *Elycia Wright, Kedar Johnson, Selena Coye, M.K. Indika Senevirathna, Michael D. Williams,* Clark Atlanta University

Transition metal dichalcogenides (TMDs) have attracted significant attention due to their distinctive electronic band structures, which result in intriguing optoelectronic and magnetic properties such as direct bandgap in the visible-infrared range, large exciton binding energies and the presence of two intrinsic valley-contrasting quantities-the Berry curvature and the orbital magnetic moment. Researchers have recently shown interest in studying heterostructures made from different TMD materials. The idea is to combine these materials to create synergistic effects, which can result in even more exciting properties than those found in individual TMDs. For instance, MoS$_2$/WS$_2$ heterostructure can exhibit novel and enhanced optoelectronic performances, including bipolar doping and photovoltaic properties. TMD-based heterostructures may open many possibilities for discovering new physics and developing novel applications. While the science of TMDs and TMD-based heterostructures has made significant strides over the past decade, the field has not yet matured. Numerous challenges, particularly in realizing TMD-based practical applications, remain unresolved. This underscores the importance of our collective efforts in pushing the boundaries of this field.

Exfoliation is a common method for assembling TMD heterostructures, but it has limitations in producing TMD heterostructures on a large scale. The chemical vapor deposition (CVD) method can be used to grow TMD heterostructures on a large scale, which is required in massive device production. However, there are numerous challenges in growing high-quality TMD heterostructures with large areas by CVD, which need to be solved before TMD-based practical applications can be achieved. Our research will focus on the growth of heterostructures (MoS$_2$/WS$_2$) on various substrates (such as sapphire and SiO$_2$/Si) using chemical vapor deposition (CVD). We will explore different mechanisms to achieve large area heterostructures and compare the resulting optoelectronic properties with exfoliated heterostructures. The properties will be characterized using Raman and Fourier Transform infra-red (FTIR) spectroscopy and confocal laser optical microscopy.

9:45am 2D+AP+EM+QS+SS+TF-TuM-8 Pulsed Laser Deposited Amorphous Boron Nitride for 2D Materials Encapsulation, *Daniel T. Yimam, Sumner B. Harris, Alexander Puretzky, Ivan Vlassiouk, Gyula Eres, Kai Xiao, David B. Geohegan,* Oak Ridge National Laboratory, USA

Recent advancements in 2D materials have opened new avenues in optoelectronics and microelectronics. However, their integration is hindered by challenges related to materials stability and degradation. Realizing the full potential of 2D materials requires synthesizing and functionalizing an encapsulation layer with desired properties. Recently amorphous boron nitride (aBN) has attracted attention as an ideal low-k material suitable for 2D electronics due to its effectiveness as a protective encapsulation layer.Unlike hexagonal boron nitride (h-BN), which requires high temperatures for deposition and poses challenges for large-area synthesis and integration, aBN can be deposited at significantly lower temperatures. This property makes aBN highly attractive and compatible for back-end-of-line (BEOL) processes in the semiconductor industry.

In this work, we demonstrate that pulsed laser deposition (PLD) enables the deposition of aBN with precise kinetic energy control of precursors, facilitating direct deposition onto 2D materials without significant defect formation. Various in situ plume diagnostics and monitoring tools during deposition were utilized to identify optimal deposition conditions, ensuring ideal kinetic energy ranges and accurate thickness control. This enhances the aBN as an effective encapsulation and barrier against 2D materials thermal degradation, while improving photoluminescence of encapsulated 2D materials. We believe our work significantly impacts future microelectronics by providing low thermal budget method for encapsulating 2D materials and understanding strain and defect evolution. Our work not only advances the practical applications of 2D materials but also paves the way for in situ experimental analysis and diagnostics in the field of material science.

11:00am 2D+AP+EM+QS+SS+TF-TuM-13 Topotaxy for Compositional Variations of Transition Metal Dichalcogenides, *Matthias Batzill,* University of South Florida

Topotaxy is a kind of solid-state reaction in which the product crystal is crystallographically related to the initial crystal. In 2D materials the initial crystal could be a single sheet or a few layers that are being reacted with same or dissimilar elements to produce novel 2D materials that may not exist in the bulk. Here we investigate such topotactical reactions for transition metal dichalcogenides (TMDs) by reacting them with vapor deposited transition metals. This can result in phase transformations of know layered materials, such as PtTe$_2$ +Pt => Pt$_2$Te$_2$ [1], new phases such as mirror twin grain boundary networks in MoSe$_2$ or MoTe$_2$ [2], or covalently linking bi-layer TMDs by intercalants of the same or different TMs [3]. The studies are performed on MBE grown TMDs and are further modified by post-growth reaction with TM. The resulting structures are characterized by surface probes, such as STM, photoemission, and LEED. In general, the open structure of many 2D materials make them ideal for topotaxy and provide an approach for modifying their composition and induce new properties. Moreover, it allows to locally modify an extended 2D sheet and thus produce in-plane heterojunctions between 'original' and modified 2D domains in a first step to create in-plane device structures.

[1] P.M. Coelho, H.P. Komsa, H. Coy Diaz, Y. Ma, A.V. Krasheninnikov, M. Batzill.

Post-Synthesis Modifications of Two-Dimensional MoSe2 or MoTe2 by Incorporation of Excess Metal Atoms into the Crystal Structure.

ACS Nano 12, 3975-3984 (2018)

[2] K. Lasek, J. Li, M. Ghorbani-Asl, S. Khatun, O. Alanwoko, V. Pathirage, A.V. Krasheninnikov, M. Batzill.

Formation of In-Plane Semiconductor–Metal Contacts in 2D Platinum Telluride by Converting PtTe2 to Pt2Te2.

Nano Letters 22, 9571-9577 (2022)

[3] V. Pathirage, S. Khatun, S. Lisenkov, K. Lasek, J. Li, S. Kolekar, M. Valvidares, P. Gargiani, Y. Xin, I. Ponomareva, M. Batzill.

2D Materials by Design: Intercalation of Cr or Mn between two VSe2 van der Waals Layers.

Nano Letters 23, 9579-9586 (2023)

11:15am **2D+AP+EM+QS+SS+TF-TuM-14 Solid State Reaction Epitaxy to Create van der Waals Heterostructures between Topological Insulators and Transition Metal Chalcogenides**, *Salma Khatun, Onyedikachi Alanwoko, Vimukthi Pathirage, Matthias Batzill,* University of South Florida

Van der Waals (vdW) heterostructures have emerged as a promising avenue for exploring various quantum phenomena. However, the formation of these heterostructures directly is complicated, as individual materials could have different growth temperatures, and alloying can occur at the interface. We present an alternative process akin to a solid-state reaction to modify the surface layer of quantum materials and introduce new properties. Specifically, we used vapor-deposited transition metals (TMs), Cr and Mn, with the goal to react with Bi_2Se_3 and transform the surface layer into XBi_2Se_4 (X = Cr, Mn). Our results demonstrate that the TMs have a high selenium affinity that drives Se diffusion toward the TM. We found that when a monolayer of Cr is evaporated, the surface Bi_2Se_3 is reduced to Bi_2-layer, and a stable (pseudo) 2D $Cr_{1+\delta}Se_2$ layer is formed, whereas $MnBi_2Se_4$ phase is formed with a mild annealing for monolayer amount of Mn deposition.[1] However, this phase only occurs for a precise amount of initial Mn deposition. Sub-monolayer amounts dissolve into the bulk, and multilayers form stable MnSe adlayers. Our study highlights the delicate energy balance between adlayers and desired surface-modified layers that govern the interface reactions.[1] The success of obtaining the $MnBi_2Se_4$ septuple layer manifests a promising approach for engineering other multicomponent vdW materials by surface reactions.

REFERENCE

[1] S. Khatun, O. Alanwoko, V. Pathirage, C. C. de Oliveira, R. M. Tromer, P. A. S. Autreto, D. S. Galvao, and M. Batzill, *Adv. Funct. Mater.* **2024**, 2315112

11:30am **2D+AP+EM+QS+SS+TF-TuM-15 AVS National Student Awardee Talk: Quasi-Van Der Waals Epitaxial Growth of Thin γ'-Gase Films**, *Mingyu Yu[1]*, University of Delaware*; Stephanie Law,* Pennsylvania State University

As an advanced two-dimensional (2D) layered semiconductor, GaSe has various appealing properties, such as rare intrinsic p-type conductivity, nonlinear optical behavior, high transparency in 650-180000nm, and a shift from an indirect-bandgap single-layer film to a direct-bandgap bulk material. These features make GaSe rich in potential in quantum photonic devices, field-effect transistors, photodetectors, etc. GaSe has a hexagonal crystal structure composed of Se-Ga-Ga-Se quadruple layers (QLs). Each QL is bonded by weak van der Waals (vdW) forces, enabling multiple polymorphs: ε-(2H), β-(2R), δ-(4H), and γ-(3R). They have identical non-centrosymmetric QL with a D_{3h} space group. Besides the four extensively explored polymorphs, a new polymorph, γ'-(3-R) GaSe, was proposed for the first time in 2018. γ'-GaSe is unique for its centrosymmetric D_{3d} QL (Fig. S1), for which γ'-GaSe is predicted to show intriguing properties compared to other polymorphs. However, there are few existing reports on the observation of γ'-GaSe due to its less-favorable formation energy. Moreover, the wafer-scale production of pure GaSe single crystal thin films remains challenging because of the coexistence of stable multiphases and polymorphs.

We developed a quasi-vdW epitaxial growth method to obtain high-quality pure γ'-GaSe nanometer-thick films on GaAs(111)B at a wafer scale. It results in GaSe thin films exhibiting a smooth surface with a root-mean-square roughness as low as 7.2 Å (Fig. S2a) and a strong epitaxial relationship with the substrate (Fig. S2b). More interestingly, we observed a pure γ'-polymorph using scanning transmission electron microscopy (Fig. S2c,d). Through density-functional theory analysis (Fig. S3), γ'-GaSe can be stabilized by Ga vacancies since its formation enthalpy tends to become lower than that of other polymorphs when Ga vacancies increase. We also observed that, unlike other GaSe polymorphs, γ'-GaSe is inactive in room-temperature photoluminescence tests. This may be related to its centrosymmetric QL structure, which we are exploring further. Meanwhile, we systematically studied the growth window for GaSe with high structural quality and identified that GaAs(111)B is more suitable than c-sapphire as a substrate for GaSe growth. Overall, this study advances the wafer-scale production of γ'-GaSe films, and elucidates a method for direct epitaxial growth of hybrid 2D/3D heterostructures with atomically sharp interfaces, facilitating the development of heterogeneous integration. In the future, we will focus on developing the properties and applications of γ'-GaSe, and delving into the understanding of the epitaxial growth mechanism.

11:45am **2D+AP+EM+QS+SS+TF-TuM-16 Investigation of Dry Transfer of Epitaxial Graphene from SiC(0001)**, *Jenifer Hajzus, Daniel Pennachio, Shawn Mack, Rachael Myers-Ward,* U.S. Naval Research Laboratory

Transfer of high-quality graphene from its growth substrate to substrates of technological interest can be necessary to enable its use in certain applications, however it remains challenging to achieve large-area transfer of graphene that is clean and intact. This work utilizes a dry transfer technique in which an adhesive metal stressor film is used to exfoliate epitaxial graphene (EG) from SiC(0001) [1]. In this method, the strain energy in the metal film must be high enough to allow for uniform exfoliation, but low enough such that self-exfoliation of graphene does not occur.

We investigate the dry transfer of monolayer EG (MEG) and hydrogen-intercalated, quasi-freestanding bilayer graphene (QFBEG) grown by sublimation of Si from nominally on-axis 6H-SiC(0001) in a CVD reactor in Ar ambient. A magnetron sputtered Ni stressor layer is used to exfoliate EG and transfer to GaAs, glass, and SiO_2/Si substrates. The Ar pressure during sputtering is found to impact the stress, film density, and roughness of the Ni film, as determined from wafer curvature and X-ray reflectivity (XRR) measurements. By using appropriate sputtering conditions, the Ni/graphene film exfoliates from the entire area of the SiC substrate with use of thermal release tape. Atomic force microscopy (AFM), scanning electron microscopy, Raman spectroscopy, x-ray photoelectron spectroscopy (XPS), and Nomarski microscopy are used to characterize the graphene. The Ni 2p peak was not detected in XPS of the transferred graphene after removal of the Ni film by etching in acid. Additionally, XPS revealed minimal oxide present at the graphene-GaAs interface, consistent with previous reports for this dry transfer method [2].

Raman spectroscopy mapping showed that predominately monolayer graphene is transferred from MEG, while predominately bilayer graphene is transferred from QFBEG. Raman spectroscopy of the SiC substrate after MEG exfoliation shows the $6\sqrt{3}$ buffer layer that forms during growth on SiC(0001) remains on the SiC substrate. Consequently, if there are regions of exposed $6\sqrt{3}$ buffer layer in the as-grown MEG on SiC, AFM shows that there are corresponding gaps in the transferred graphene film where the areas of exposed buffer layer do not transfer. The $6\sqrt{3}$ buffer layer is not present in QFBEG due to the hydrogen-intercalation process. It is found that the same Ni sputtering conditions that led to uniform exfoliation and transfer of MEG result in micron-scale tears in the Ni/QFBEG film. By lowering the strain energy in the sputtered Ni film, these tears can be reduced or eliminated.

[1] Kim, J., *et al.*, Science, 342, 833 (2013).

[2] Kim, H., *et al.*, ACS Nano, 15, 10587 (2021).

12:00pm **2D+AP+EM+QS+SS+TF-TuM-17 Nickel Foams Enable Space-Confined Chemical Vapor Deposition (CVD) Synthesis of High-Quality MoS2 Films**, *Taylor Currie, Laurene Tetard, Titel Jurca,* University of Central Florida

Space-confined chemical vapor deposition (CVD) is a variation on traditional CVD syntheses in which the space between the substrate and precursor is restricted, which can lead to more consistent growth of high-quality two-dimensional (2D) materials. Space-confinement can be achieved by, for example, (1) using a shorter tube of smaller diameter inside the reactor tube, or (2) placing the substrate and precursor very close to each other. In both cases the concentration of reactants reaching the substrate is limited, which prevents excessive and rapid (lateral) growth and instead favors 2D film growth. In our approach, a growth substrate (c-plane sapphire wafer) was placed directly on top of nickel foam (NF) pre-loaded with molybdenum oxide (MoO_x/NF). A quartz boat containing sulfur powder was placed upstream in a 275 °C temperature zone, and a second boat containing the substrate and MoO_x/NF was placed in a separately controlled temperature zone at 850, 900, or 950 °C. Using this approach, high-quality MoS_2 monolayers were grown at 1, 5, or 15 min, as confirmed by optical microscopy, Raman and photoluminescence spectroscopies, energy-dispersive x-ray spectroscopy, and atomic force microscopy. We determined that the quality and thickness (i.e. monolayer, few layer, multilayer, bulk) of the MoS_2 films were dependent on temperature and hold time used for the growth, with trials at 850 °C for 15 min, 900 °C for 15 min, and 950 °C for 5 min resulting in the best films. The use of a readily available metal foam with inherent porosity enhances the ease and accessibility of this space-confined CVD approach. This provides many more opportunities for modifications (e.g. varying the metal precursor used to decorate NF, surface coverage of precursor on NF, porosity of NF, and/or distance between substrate and NF).

---

[1] **AVS National Student Awardee**

Tuesday Morning, November 5, 2024

Atomic Scale Processing Mini-Symposium
Room 116 - Session AP1+EM+PS+TF-TuM

Atomic Layer Etching I: Thermal Processes

Moderators: **Steven M. George**, University of Colorado at Boulder, **Austin Minnich**, California Institute of Technology

8:00am **AP1+EM+PS+TF-TuM-1 Highly Selective and Isotropic Atomic Layer Etching using Dry Chemical Removal**, *Nobuya Miyoshi*, Hitachi High-Tech America, Inc. **INVITED**

As semiconductor devices shrink to sub-10 nm dimensions, the introduction of new device structures, integration schemes, and materials brings many challenges to device manufacturing processes. A new structure with gate-all-around (GAA) nanosheets has been introduced to reduce the power consumption of transistors and achieve higher transistor integration density. For advanced semiconductor memory devices, 3D NAND flash has been introduced to achieve higher bit densities. Fabricating these three-dimensional (3D) devices requires isotropic etching of thin films with atomic layer control, high selectivity to underlying materials, and high uniformity over high-aspect-ratio 3D structures. Thermal atomic layer etching (ALE) is a promising method for isotropic etching with atomic-level precision and high conformality over three-dimensional structures. We developed a dry chemical removal (DCR) tool with an infrared (IR) wafer annealing and quick cooling system to perform highly selective thermal ALE for various materials. Thermal ALE was demonstrated for Si_3N_4 and SiO_2 films using the formation and desorption of $(NH_4)_2SiF_6$-based surface-modified layers. Thermal ALE processes for W and TiN films were also demonstrated by the formation and desorption of halogenated surface-modified layers. These ALE processes show a self-limiting formation of modified layers, enabling conformal and precisely controlled etching. In addition, spontaneous and highly selective etching of SiO_2 was demonstrated on the DCR tools using HF/CH_3OH vapor. SiO_2 films can be etched spontaneously with high selectivity to SiN films when the temperature of the substrate is lower than −20⁰C.

8:30am **AP1+EM+PS+TF-TuM-3 Selective Si or Ge Dry, Thermal Spontaneous Etching Using HF Vapor**, *Marcel Junige, Troy Colleran, Steven M. George*, University of Colorado Boulder

Advanced 3D structures in microelectronics require novel self-aligned techniques. For example, selective etching may remove one specific material while leaving intact others in proximity. This multi-color challenge gets particularly difficult for selectivity between Si-based materials, as well as between Si and Ge. Instead of plasma activation, this work focused on developing gas-phase spontaneous etch pathways based on thermal chemistry using anhydrous hydrogen fluoride (HF) vapor.

In situ spectroscopic ellipsometry experiments discovered substantial spontaneous etching of Si by HF at 275℃. The Si etch rate was 12.2 Å/min at an HF pressure of 3 Torr. The Si etch rate increased further with higher HF pressures. In addition, Si etched selectively with an exceptionally high selectivity factor of >1,000:1 versus the retention of SiO_2 and stoichiometric Si_3N_4.

Temperature-programmed quadrupole mass spectrometry (QMS) experiments confirmed the spontaneous etching of crystalline Si nano-powder by HF. SiF_4 and H_2 were observed as the main volatile etch products. QMS detected the SiF_4 product with a gradual onset above ~175℃. This temperature dependency indicated that the etch reaction may be limited by SiF_4 desorption from the Si surface. SiF_4 desorption from fluorinated Si surfaces has been reported to occur at >125℃.

Additional QMS experiments also observed the spontaneous etching of Ge nano-powder by HF. GeF_4 and H_2 were revealed as the main volatile etch products. QMS detected GeF_4 already at 25℃. The GeF_3^+ signal intensity increased with elevating temperature and exhibited a maximum at ~80-85℃. Subsequently, the GeF_3^+ signal decreased below the noise level above ~125℃.

These results suggest that Si etching could be achieved selectively over Ge retention at >175℃. Likewise, Ge etching could be accomplished selectively over Si retention at <125℃. This reciprocal selectivity between Si and Ge etching will depend on the influence of proximity effects resulting from the volatile etch products when Si and Ge are both present in the reactor.

8:45am **AP1+EM+PS+TF-TuM-4 Theoretically Designed Thermal Atomic Layer Etching Processes for Interconnect Metals**, *Miso Kim, Hyeon Cho,* Hongik University, Republic of Korea; *Dongjun Lee, Jeongbin Lee, Jung Tae Kim, Woo-Hee Kim,* Hanyang University, Republic of Korea; *Bonggeun Shong,* Hongik University, Republic of Korea

Atomic layer etching (ALE) is emerging as a key technology for the precise and selective removal of materials at the atomic level, especially for manufacturing of nanoscale three-dimensional semiconductor devices. Previously known thermal ALE processes often involve two-step sequence of surface chemical reactions: surface modification of the substrate such as halogenation, followed by volatilization using another etchant. For example, a recent study reported a thermal ALE process for Ni, employing SO_2Cl_2 for halogenation and $P(CH_3)_3$ for volatilization via ligand addition [1]. Since ALE process is based on self-limiting surface chemical reactions, it is desirable to design ALE processes by understanding their surface reactions. However, the mechanistic aspects of such thermal ALE reactions remain significantly underexplored. In this work, we employed neural network potential (NNP) calculations to screen for suitable process conditions for thermal ALE process of metals, especially those considered as materials for nanoscale interconnects. Our findings demonstrate that several metals are capable of forming energetically stable volatile compounds via halogenation and ligand addition of thermal molecular etchants. Several novel thermal ALE processes that were theoretically predicted are experimentally demonstrated with varying etch rates and selectivity between the substrates. Overall our study show the applicability of theoretical analysis of the surface chemical reactions toward design of novel ALE processes.

References. (1) Murdzek, J. A.; Lii-Rosales, A.; George, S. M. Chem. Mater. 2021, 33 (23), 9174–9183.

Acknowledgments. This work was supported by Samsung Electronics.

9:00am **AP1+EM+PS+TF-TuM-5 X-ray Photoelectron Studies of Removal of Sputter Damage from InGaP Surfaces Using Thermal Atomic Layer Etching**, *Ross Edel,* University of Colorado Boulder; *Ezra Alexander,* MIT; *Andrew Cavanagh,* University of Colorado Boulder; *Taewook Nam,* Soonchunhyang University, Republic of Korea; *Troy Van Voorhis,* MIT; *Steven George,* University of Colorado Boulder

InGaP is widely used for red LED devices. Surface defects on LED devices can lead to non-radiative electron/hole pair recombination that reduces their light output. This light quenching effect is more severe for smaller µLEDs that have high surface-to-volume ratios. The surface defects are believed to be formed by energetic ion species during plasma processing that forms the µLEDs. Thermal ALE may provide a method to remove these defects.

To quantify the removal of surface damage, x-ray photoelectron (XPS) studies employed InGaP samples sputtered with argon as a model system. These InGaP samples simulate the µLED sidewalls that are exposed to energetic species during plasma processing. Thermal InGaP ALE was then performed using static, sequential HF and dimethylaluminum chloride (DMAC) exposures. This procedure yielded etch rates of 0.5–1.0 Å/cycle at temperatures from 300–330 °C, respectively. This work was conducted using a new apparatus that combines a hot wall ALD/ALE reactor with *in vacuo* Auger spectroscopy to allow sample characterization without exposure to air.

InGaP samples damaged by Ar^+ ion sputtering were analyzed using *ex situ* X-ray photoelectron spectroscopy (XPS) before and after thermal ALE by tracking the shifted components in the P 2p XPS region that correspond to sputter damage. An *ex situ* XPS scan of a sputtered InGaP sample displayed two shifted doublets (Figure 1a) while an unsputtered sample showed only a bulk doublet (similar to Figure 1b). DFT simulations identified the higher energy doublet as phosphorus directly bound to three-coordinate indium or gallium and the lower energy doublet as three-coordinate phosphorus (Figure 2a). In contrast, the DFT simulations showed only a bulk doublet for InGaP without under-coordinated surface atoms (Figure 2b).

InGaP ALE can then remove the XPS features associated with the damaged lattice. A bulk-like XPS spectrum showing minimal damage was recovered after 50 ALE cycles for a sample initially exposed to 500 eV sputtering (Figure 1b). By contrast, annealing for 72 hours at 300 C without etching was not sufficient to eliminate the damage. AES analysis similarly showed that the argon implanted in the sample by sputtering was removed after etching but not annealing. Increasing the sputtering ion energy to 2 keV required more extensive etching to remove the sputter damage. In this case, 100 ALE cycles were able to largely remove the surface defects. The corresponding AES data showed a linear decrease in implanted argon and

reached zero after 100 ALE cycles. The etch depth consistent with 100 ALE cycles indicates a damaged material depth of ~4 nm.

9:15am AP1+EM+PS+TF-TuM-6 Chemical Vapor Etching or Atomic Layer Etching of ZnO? in Situ Ellipsometry and Mass Spectrometric Studies, *Terrick McNealy-James*, *S. Novia Berriel, Brian Butkus, Parag Banerjee*, University of Central Florida

"Atomic layer etching (ALE) stands out as a remarkable technique for precise Angstrom-level control for material removal. With a growing demand in the semiconductor and nanotechnology sectors, ALE becomes a promising solution to address evolving challenges in patterning and in the shrinking of device dimensions. For ideal ALE, processes must demonstrate self-limiting, dose independent etch behavior with well-defined temperature windows. These set of criteria are a challenge for many recently demonstrated metal oxide films.[1]

Here we present the etching characteristics of zinc oxide (ZnO) films, using Hacac and O_2 plasma[2]. We comprehensively map the etch rates using *in situ* spectroscopic ellipsometry. The chemistry of the etching process is verified using mass spectrometry. Etch rate per cycle (EPC) is optimized within a temperature window of 220 – 280 °C. However, it is found that the etch rates are dose dependent and are not only governed by the Hacac pulse times but also by a subsequent "hold" step which continues to etch the ZnO film with no signs of self-limiting behavior. In this context, the Hacac + O_2 plasma process appears to be a controllable chemical vapor etch process.

The impact of inserting etch stop layers in ZnO is explored. While a single monolayer of Al_2O_3 slows the EPC, 3 monolayers of Al_2O_3 are sufficient to completely block further etching. These results point to the non self-limiting behavior of Hacac etching of ZnO and strategies which may provide EPC control and selectivity with ZnO composition tuning.

References:

(1) Jonathan L. Partridge, Jessica A. Murdzek, Virginia L. Johnson, Andrew S. Cavanagh, Andreas Fischer, Thorsten Lill, Sandeep Sharma, and Steven M. George
Chemistry of Materials 2023 35 (5), 2058-2068

(2) A. Mameli, M. A. Verheijen, A. J. M. Mackus, W. M. M.Kessels, and F. Roozeboom, ACS Appl. Mater. Interfaces, vol. 10, 38588, (2018).

9:30am AP1+EM+PS+TF-TuM-7 Examination of Atomic Layer Etch Mechanisms by Nuclear Magnetic Resonance Spectroscopy, *Taylor G. Smith*, *Jane P. Chang,* University of California, Los Angeles **INVITED**
As atomic layer etching (ALE) becomes more widespread, there is a need to better understand the underlying mechanisms by which it operates. Of particular interest is the removal half-cycle of thermal ALE wherein a vapor-solid reaction leads to the formation of a volatile etch product. Solid state magic angle spinning nuclear magnetic resonance (MAS-NMR) can provide a wealth of structural and chemical information, but it has not yet been used to examine ALE reaction mechanisms. In this work, MAS-NMR of CuO etched in solution phase formic acid (FA) is demonstrated and compared with prior density functional theory results[1]. Although it may seem a simple system, the paramagnetic nature of CuO and the formation of many products with slightly different structures both lead to complicated NMR spectra. The issue of significant peak broadening by paramagnetic relaxation can be alleviated in part by spinning at very fast speeds (>30kHz). From the resulting spectra, confirmation of $Cu(HCOO)_2 \cdot 4H_2O$ as a product is possible by comparison to a commercial reference powder. However, assignment of other peaks requires correlation spectroscopy showing ^{13}C-^{13}C and ^1H-^{13}C correlations to deduce the structures of the various products, illuminating the reaction landscape of CuO with FA. To extend these findings to the vapor-solid interactions present in ALE, a special heterogeneous NMR rotor can be used that was originally designed for use with high pressure gases. To adapt this rotor use with lower pressure FA vapor, a novel rotor packing method that separates the FA from the CuO prior to vaporization is presented.

Atomic Scale Processing Mini-Symposium
Room 116 - Session AP2+EM+PS+TF-TuM

Atomic Layer Etching II: Energy-Enhanced Processes
Moderators: Steven M. George, University of Colorado at Boulder, **Austin Minnich**, California Institute of Technology

11:00am AP2+EM+PS+TF-TuM-13 Atomic Layer Etching of Lithium Niobate for Quantum Photonics, *Austin Minnich,* California Institute of Technology
INVITED
Lithium niobate (LiNbO3, LN) is a ferroelectric crystal of interest for integrated photonics owing to its large second-order optical nonlinearity and the ability to impart periodic poling via an external electric field. However, on-chip device performance based on thin-film lithium niobate (TFLN) is presently limited by optical loss arising from corrugations between poled regions and sidewall surface roughness. Atomic layer etching (ALE) could potentially smooth these features and thereby increase photonic performance, but no ALE process has been reported for LN. Here, we report a directional ALE process for x-cut MgO-doped LN using sequential exposures of H_2 and SF_6/Ar plasmas. We observe etch rates up to 1.01 +/- 0.05 nm/cycle with a synergy of 94\%. We also demonstrate ALE can be achieved with SF_6/O_2 or Cl_2/BCl_3 plasma exposures in place of the SF_6/Ar plasma step with synergies above 90%. When combined with a wet post-process to remove redeposited compounds, the process yields a 50\% decrease in surface roughness. With additional optimization to reduce the quantity of redeposited compounds, these processes could be used to smoothen surfaces of TFLN waveguides etched by physical Ar+ milling, thereby increasing the performance of TFLN nanophotonic devices or enabling new integrated photonic capabilities.

11:30am AP2+EM+PS+TF-TuM-15 Tunable Electron Enhanced Etching of β-Ga₂O₃ Using HCl Reactive Background Gas and Positive Sample Voltage, *Michael Collings,* University of Colorado Boulder*; Jacob Steele, Darrell Schlom, Huili (Grace) Xing,* Cornell University*; Steven George,* University of Colorado Boulder
Crystalline β-Ga_2O_3 is an ultra-wide band gap material with important applications for high power electronics. High precision etching is required for β-Ga_2O_3 device fabrication. Previous thermal atomic layer etching (ALE) attempts to etch β-Ga_2O_3 have not been successful. Plasma etching of β-Ga_2O_3 using Cl-containing gases is difficult for Ångstrom-level etching control and can leave surface damage. In this work, electron-enhanced etching of β-Ga_2O_3 is performed using a HCl reactive background gas (RBG) and positive sample bias. The β-Ga_2O_3 is a -oriented epitaxial film grown by suboxide molecular-beam epitaxy on a single-crystal (0001) Al_2O_3 substrate. The ~100 eV primary electrons from a hollow cathode plasma electron source (HC-PES) are incident on the β-Ga_2O_3 sample. The HC-PES is a chemically robust electron source capable of delivering >200 mA over an area >10 cm². The HCl reactive background gas (RBG) is present at ~1 mTorr. A small positive voltage of <50 V is applied to the sample stage.

The β-Ga_2O_3 film thicknesswas monitored using in situ spectroscopic ellipsometry during electron exposure. Figure 1 shows that the etching of β-Ga_2O_3 is tunable from 1-50 Å/min by varying the stage voltage from 0 to +40 V, respectively. No etching was monitored from electron exposures without the HCl RBG. Negligible etching was observed without a positive sample stage. The following mechanism can explain these results: (1) The primary electrons at ~100 eV can generate secondary electrons from the substrate. (2) The lower energy secondary electrons can attach to the HCl gas in the reactor. (3) The electron attachment then dissociates HCl into H + Cl^- through dissociative electron attachment ionization. (4) The Cl^- negative ions are attracted to the sample by the positive sample stage voltage. (5) The incoming Cl^- flux leads to an enhancement in etch rate resulting from the formation of volatile chloride species. An illustration of this proposed mechanism is shown in Figure 2.

The β-Ga_2O_3 etching was reproducible and only weakly dependent on the primary electron energy from 100-150 eV. The electron current going to ground through the sample also increased with positive sample voltages as expected if the secondary electrons are pulled back to the sample. Surface morphology of the β-Ga_2O_3 was also investigated after the electron enhanced etching. The RMS roughness decreased after etching. The RMS roughness decreased from 1.88 nm to 1.58 nm after the etching process removed 10 nm at +10 V stage voltage. In contrast, the surface roughness did not change after only electron exposures in the absence of HCl RBG.

11:45am AP2+EM+PS+TF-TuM-16 Bias-Pulsed Atomic Layer Etching, *Julian Michaels,* University of Illinois at Urbana-Champaign; *Nazar Delegan,* Argonne National Laboratory, USA; *Yeghishe Tsaturyan,* University of Chicago; *Russ Renzas,* University of Nevada Reno; *Gary Eden,* University of Illinois at Urbana-Champaign; *David Awschalom,* University of Chicago; *Joseph Heremans,* Argonne National Laboratory, USA

Atomic layer etching (ALE) is a binary cyclical process noted for its ability to controllably remove atomic monolayers for nanotechnological device fabrication; however, its relatively slow effective etch rate, often less than a monolayer each minute (tenths of an Angstrom per second), limits its applicability to niche devices that necessitate unmatched precision. If the process were slightly faster, semiconductor, optical, and quantum devices would be regularly implementing ALE because it can reach critical dimensions more consistently while simultaneously offering a smoother post-etch surface, both of which deliver superior device performance regardless of the application.

ALE is slow because the chemical reagent gas(es) is purged in and out of the chamber during each cycle. This is standard practice so that the binary steps, chemical and physical, are fully separated, but purge steps also tend to be the most time-consuming components of any ALE process. Thus, if shortening the cycle duration (speeding up the effective etch rate) is the aim, minimizing purge step duration is a sensible first pursuit.

Bias-pulsed atomic layer etching (BP-ALE) is the execution of the above goal with plasma etching in perhaps the simplest way possible. While traditional plasma ALE often pulses gas flows, plasma DC bias, chamber pressure, substrate temperature, and other parameters, BP-ALE achieves atomic precision by pulsing merely the plasma DC bias, hence "bias-pulsed" indicates that the plasma DC bias is the only parameter that distinguishes the steps, and the purge step duration is absolutely minimized as there is no gas purging whatsoever.

As of now, BP-ALE has been demonstrated in both 4H-SiC and diamond, where the usual ALE cycle duration that often exceeds a minute is superseded by the 6-second cycles of BP-ALE, and smoothing to subangstrom RMS surface roughness is achieved for both after etch treatment. This talk seeks to outline the main differences between BP-ALE in execution and potential applications, explain the material and chemistry characteristics needed for a viable BP-ALE method, and predict material/chemistry systems that are suitable for BP-ALE processing.

12:00pm AP2+EM+PS+TF-TuM-17 Atomic Layer Etching of 2D Transition Metal Dichalcogenides Semiconductors and Its 2D Device Application, *Jeongmin Kim, Jihyun Kim,* Seoul National University, Republic of Korea

Transition metal dichalcogenides (TMDs), a class of 2D materials, possess a layered structure with individual layers bound by van der Waals forces. TMDs exhibit excellent electrical properties and have potential applications in various fields due to their low surface defect density. Moreover, TMDs possess a unique property where the bandgap varies with the number of layers, leading to changes in electrical characteristics depending on the thickness. Therefore, precise control of TMD thickness is crucial. Conventional etching methods, such as reactive ion etching, suffer from plasma-induced damage or difficulties in precise thickness control, making them unsuitable for accurate thickness control of TMDs. Consequently, atomic layer etching (ALE) utilizing self-limiting reactions has been devised to achieve precise thickness control at the atomic level.

We developed an ALE process for TMDs utilizing the adsorption of SF_6 gas, which exhibits minimal reactivity at room temperature. In a capacitively coupled plasma system, an etching with constant-thickness for each cycle was achieved by adsorbing SF_6 followed by Ar^+ ion bombardment at an appropriate radio frequency (RF) power. The etch rate was controllable, and no change in the etching rate was observed within a specific RF power range. This was realized by the self-limiting reaction induced by the decomposition of SF_6 under Ar^+ ion bombardment where further sputtering does not occur once all of the adsorbed SF_6 molecules are consumed. Using our ALE process, TMD-based recessed-channel FETs were fabricated. The electrical characteristics and device performance were evaluated, showing a decrease in off-current with reduced channel thickness and no significant deterioration in device performance. This ALE method enables precise thickness control while maintaining the crystallinity of the channel in TMD-based electronic devices, contributing to device performance enhancement. The ALE technology developed in this study paves the way of the advanced application with the TMD-based electronic devices.

This work was supported by the Korea Research Institute for defense Technology planning and advancement (KRIT) grant funded by Defense Acquisition Program Administration (DAPA) (KRIT-CT-21-034)

Biomaterial Interfaces
Room 117 - Session BI1-TuM

Characterization of Biological and Biomaterial Surfaces I: Celebration of Stephanie Allen

Moderators: Morgan Hawker, California State University, Fresno, **Sapun Parekh**, University of Texas at Austin

8:00am BI1-TuM-1 Biointerfacial Characterisation of Implanted Medical Devices with OrbiSIMS, *Morgan Alexander,* University of Nottingham, UK

The 3DOrbiSIMS hyphenation of ToF SIMS with an OrbiTrap™ makes meaningful analysis the molecules in complex biological samples and bio-interfaces formed on materials feasible. [1,2] Critically, the mass resolving power and mass accuracy has rendered routine peak assignment with deviations below 2 ppm. The large spectral data files with thousands of peaks that arise from biological samples requires automated untargeted analysis to make the most of this information. These have been enabled by the methodology for molecular formula prediction (MFP) assignment adapted to SIMS by Edney et al. [3]

I will illustrate how this enables us to investigate the bio-interface for implanted medical devices, to shed light on their failure mechanisms. The importance of the lipids and other metabolites is revealed in the analysis of tissue sections. Subsequent analysis of the bio interfacial deposit at the surface of extracted devices sheds light on the complexity of this process. [4,5] Understanding medical implant fibrosis by biointerfacial OrbiSIMS analysis [Bin Sabri unpublished]

References

1. Mass spectrometry and informatics: distribution of molecules in the PubChem database and general requirements for mass accuracy in surface analysis. FM Green, IS Gilmore, MP Seah (2011) *Analytical Chemistry*.
2. The 3D OrbiSIMS: Label-free metabolic imaging with subcellular lateral resolution and high mass-resolving power. Passarelli et al. (2017) *Nature Methods*.
3. Molecular formula prediction for chemical filtering of 3D OrbiSIMS Datasets. Edney et al (2022) *Anal Chem.*
4. Single-cell metabolic profiling of macrophages using 3D OrbiSIMS: Correlations with phenotype. Suvannapruk et al. (2022) *Anal Chem*
5. Spatially resolved molecular analysis of host response to medical device implantation using the 3D OrbiSIMS highlights a critical role for lipids. Suvannapruk et al. (2024) *Advanced Science*.

8:15am BI1-TuM-2 Insights into the Chemistry of Wheat Leaves and their Uptake of Agrochemicals using OrbiSIMS, *Mohammed Khan,* University of Nottingham, UK; *Conor Whitehouse, Tim Powell,* Syngenta, UK; *Clive Roberts, David Scurr,* University of Nottingham, UK

The estimated size of the global agrochemicals market in 2022 amounted to USD 227.9 billion with a projected increase to USD 234.27 billion in 2023 [Market Analysis Report 2018-2022]. The notable increase in agrochemical usage observed worldwide can be attributed to the economic benefits that to farmers through the safeguarding of crops against invasive species, including the improvement in quality and quantity of harvests. Limited knowledge of the *in-situ* chemical composition of wheat leaves and the permeation mechanisms of pesticides into skin and leaf tissues constrains research and development of new products.

OrbiSIMS has been recently demonstrated as a powerful tool for skin research, providing label-free insight into the 3D permeation profiles of endogenous and exogenous compounds. Previous work [Starr et. al., *PNAS*, 2022] investigated the molecular composition of the *stratum corneum* and tracking the permeation of an active agent. Our study expands the use of OrbiSIMS to investigate the native chemistry of wheat leaves, particularly the plant cuticle as the primary diffusion barrier. The study reveals the distribution of a fungicide formulation through both wheat leaves and skin, offering insights into its diffusion in relevant biological matrices.

The molecular architecture of wheat leaves was first probed, with a focus on the cuticle. *In-situ* analysis provided novel insights into the localisation of endogenous species, including fatty acids, aldehydes, phospholipids, flavones and vitamins. Depth profiling revealed depth-dependent variations in leaf structure, with fatty acids and aldehydes associated with the cuticle and epicuticular waxes exhibiting a prominent concentration at the leaf surface. Conversely, flavones and vitamins were predominant in the epidermis.

Exogenous compounds were identified in skin and wheat leaves, alongside endogenous species. The investigation focused on the impact of exposure time and concentration on agrochemical permeation across skin and wheat leaves. *In-situ* analysis provided the detection and tracking of the entire formulation, even at 100 ppm. Cyproconazol exhibited enhanced permeation with prolonged exposure time and higher concentrations in both matrices. Co-formulants showed varied localization patterns, with carrier solvents resembling the permeation of cyproconazole and emulsifiers remained primarily at the surface.

8:30am **BI1-TuM-3 Imaging 3D Cell Culture Systems** , *Sally McArthur,* Deakin University, Australia

Imaging three dimensional cell and tissue systems is central to our fundamental understanding of tissue engineered materials. We need to be able to look at the cell morphology, scaffold architecture and their specific interactions. By combining a range of tools we have explored how biomaterials and cells interact in 3D and the reproducibility of 3D cell culture systems. This talk is submitted as part of the celebration of Prof Stephanie Allen's career.

8:45am **BI1-TuM-4 SIMS for Label-Free in situ Analysis of Glycosaminoglycans**, *Li Jennifer Lu,* University of Nottingham, UK*; Joseph Hippensteel,* University of Colorado - Anschutz Medical Center*; Kay Grobe,* University of Münster, Germany*; Christian Gorzelanny,* University Medical Center Hamburg - Eppendorf, Germany*; Anna M. Kotowska, David J. Scurr, Andrew L. Hook,* University of Nottingham, UK

Glycosaminoglycans (GAGs) are linear polysaccharide chains with many varied roles in physiology, including embryonic patterning and modulation of blood vessel permeability. Despite their biological importance, their *in-situ* analysis is limited by a lack of analytical tools with which to study their complex structure. Here we present the development of secondary ion mass spectrometry (SIMS) for *in-situ* GAG analysis [1], allowing for simultaneous spatial and compositional analysis. Initially, a list of characteristic ions for different GAG types was identified using high mass resolution analysis using an Orbi-trap mass analyser of a library of reference GAGs. These GAG-derived ions were validated using a range of biosynthetic enzyme knockout cellular models. This approach has been used to spatially assess the distribution of varied GAG types within complex tissues, including a sepsis model and to explore embryogenesis within *Drosophila*. Additionally, the depth profiling capability of SIMS enables 3D imaging of GAG ions within samples. This demonstrated ToF-SIMS as a powerful analytical tool to spatially analyse (at near optical resolution) GAG type and composition within a single analysis across multiple biological sample types.

References

1. Hook, A.L., Hogwood, J., Gray, E. et al. High sensitivity analysis of nanogram quantities of glycosaminoglycans using ToF-SIMS. Commun Chem 4, 67 (2021).

9:00am **BI1-TuM-5 Tribochemical Nanolithography – Fast, Simple Biomolecular Nanopatterning with 23 nm Resolution at Speeds of up to 1 mm s-1**, *Oscar Siles-Brugge, Camery Ma, Anthony Meijer,* **Graham Leggett**, University of Sheffield, UK

Films formed by the adsorption of (methoxyheptaethylene glycol) nitrophenylethoxycarbonyl-protected aminopropyltriethoxysilane (OEG-NPEOC-APTES) on silica are highly resistant to the adsorption of proteins. On exposure to UV light, the photocleavable protecting group is removed allowing the immobilization of biomolecules.

We have discovered that the same result can be achieved using an AFM probe at a load of ca. 100 nN in the absence of UV light. A FWHM of 23 nm can be achieved at a writing rate of 1 mm s-1. The FWHM increases with load, reaching 90 nm at a load of 10 μN. At larger loads than this an abrupt transition occurs to a regime dominated by mechanical abrasion, yielding broader features. However, for control films that do not contain photo-removable protecting groups, lithographic modification was not observed at loads below 10 μN.

We hypothesize that at low loads the AFM probe causes selective cleavage of the same C-N bond in the carbamate group that is cleaved during UV irradiation. Consistent with this, we found that patterned surfaces can be derivatized with nitrilotriacetic acid (NTA) functional groups, enabling coupling of His-tagged green fluorescent protein (GFP) to the surface. Confocal fluorescence microscopy confirms that GFP attaches to nanolines, but is released when the samples are treated with imidazole, which disrupts the interaction between NTA and the His tag on the protein, consistent with site-specific binding.

The effect of compression on the nitrophenyl protecting group was explored using density functional theory (DFT). Our results indicate that compression of the nitrophenyl group causes substantial changes in its electronic structure. In particular, the energy of the main energetic barrier in the photodeprotection scheme, the initial S_0 to S_1 transition, is greatly reduced, so that deprotection may occur at near IR wavelengths. Hence, application of the AFM probe facilitates deprotection by low energy photons, while UV photons are required in the absence of a mechanical deformation.

The methodology may also be applied to the fabrication of polymer nanostructures. Tribochemical nanolithography of nitrophenylpropyloxyoxycarbonyl protected aminopropyl triethoxysilane (NPPOC-APTES) films yields amine-functionalised nanolines that are functionalized with bromine initiators and used to grow surface-grafted polymer brushes. Polymer chains grafted to the smallest nanolines are collapsed, because they have a high free volume and because adsorption to the surrounding surface is energetically favourable. However, as wider structures are formed, the chains repel each other and begin to swell away from the surface.

9:15am **BI1-TuM-6 Nanoprobe X-Ray Fluorescence Analysis of Frozen-Hydrated Biological Samples - from 2D to 3D**, *Axel Rosenhahn, Christoph Rumancev, Lejla Jusifagic, Andreas Gräfenstein,* Ruhr University Bochum, Germany

The accumulation of metals and the homeostasis of ions in biological cells and tissue is of fundamental relevance for a wide range of environmental, biological, and medical processes. Synchrotron-based nanoprobe X-ray fluorescence analysis provides a unique combination of metal analysis with high spatial resolution, a high penetration depth, and high sensitivity down to trace concentrations. In the last years we developed several endstations for the analysis of cryogenically prepared biological samples at the P06 beamline at Petra III. Cryopreservation is the gold standard if cells are meant to be analyzed in a preserved state that is as close as possible to their natural, hydrated state. In particular for highly soluble ions, such as potassium, cryopreservation is the only way to obtain accurate concentrations. The new technique has been used to analyze the stress response of cells to the presence of Huntingtin aggregates, which are currently hypothesized to be responsible for the consequences of the corresponding disease. Also, the intracellular distribution of different metal-based cytostatic compounds has been analyzed and compared to the cellular stress response as reflected by changes in the intracellular potassium level. In addition to the 2D imaging experiments, a new tomography setup has been developed that allows cross-sectional imaging of biological samples to image metal distributions. A novel self-absorption correction during the tomographic reconstruction has been implemented that compensates artefacts especially for light elements due to the limited photon-escape depth.

Biomaterial Interfaces
Room 117 - Session BI2-TuM

Characterization of Biological and Biomaterial Surfaces II
Moderators: Morgan Hawker, California State University, Fresno, **Sapun Parekh**, University of Texas at Austin

11:15am **BI2-TuM-14 Native Supported Lipid Bilayers: A Bioanalytical Tool to Study and Detect Viruses**, *Marta Bally, Hudson Pace,* Umea University, Sweden **INVITED**

Cellular membranes are complex dynamic structures consisting of a lipid bilayer containing a multitude of biomolecules, including a variety of lipids, proteins and carbohydrates. Systematic investigations of biomolecular processes at the cell surface call for the development of bioanalytical platforms capable to recapitulate, in vitro and under well-controlled experimental conditions, this compositional complexity while maintaining the membrane´s basic physico-chemical properties (e.g. membrane fluidity). In this context, we present native supported lipid bilayers (nSLBs), two-dimensional fluid planar bilayers produced from purified cellular plasma membranes and mounted on a solid support as a promising tool. [1,2] These cell-free systems provide the compositional complexity of nature, yet they are free from metabolic feedback loops. They are a snapshot of the membrane's composition at the moment of cell lysis, providing hundreds of experiments with the exact same membrane

composition. They further allow for optimal instrumental accessibility, being compatible with a broad range of surface-sensitive biosensing tools.

In our work, we take advantage of nSLBs to characterize virus- membrane interactions [2]. The combination of nSLBs with total internal reflection fluorescence microscopy allows us to quantitatively assess the attachment, detachment, and diffusion behavior of individual virus particles at the cell membrane and to address a variety of fundamental questions related to viral attachment and entry. Specifically, this experimental approach was used to (i) study how SARS-CoV-2 changes its interaction with the plasma membrane when evolving and mutating [3], (ii) investigate the role of a cellular factor in modulating HSV-1 interactions at the cell surface [4] and (iii) to study how different carbohydrate moieties modulate the dynamics of norovirus-membrane interactions [5].

Taken together, our research contributes to a better understanding of the mechanisms regulating the interaction between a virus and the surface of its host. Such insights will without a doubt facilitate the design of more efficient antiviral drugs or vaccines.

[1] Pace at al., Analytical Chemistry, **87(18)** (2015)

[2] Peerboom, N. et al., ACS Infect. Dis. **4 (6)**, (2018)

[3] Conca, D. et al., Biorxiv (2024), https://doi.org/10.1101/2024.01.10.574981

[4] Liu, L. et al., Biorxiv (2023)¸ https://doi.org/10.1101/2023.02.10.526562

[5] Pace, et al., In manuscript.

11:45am BI2-TuM-16 Force Probe Techniques for Probing Biologic and Lipid Bilayer Interactions Under Physiological Conditions, *Markus Valtiner, Laura Mears, Iago Peters,* TU Wien, Austria

Quantification of biologic interactions - from single molecular to macroscopic interfaces - is essential for understanding function in living systems. We will provide a short overview of force probe techniques (AFM, SFA, and optical tweezers) and will then discuss lipid bilayer interactions, and single molecular interaction measurements (under potential control) in detail. These are essential to a vast range of biological functions, such as intracellular transport mechanisms. Surface charging mediated by concentration dependent ion adsorption and desorption on lipid headgroups alters electric double layers as well as van der Waals and steric hydration forces of interacting bilayer and molecules. Two examples will be discussed:

First, we characterized the interaction between single hydrophobic molecules quantitatively using atomic force microscopy, and demonstrated that single molecular hydrophobic interaction free energies are dominated by the area of the smallest interacting hydrophobe. The interaction free energy amounts to 3–4 kT per hydrophobic unit. Also, we find that the transition state of the hydrophobic interactions is located at 3 Å with respect to the ground state, based on Bell–Evans theory.

Further, we directly measure bilayer interactions during charge modulation in a symmetrically polarized electrochemical three-mirror interferometer surface forces apparatus. We quantify polarization and concentration dependent hydration and electric double layer forces due to cation adsorption/desorption. Results demonstrate that exponential hydration layer interactions effectively describe surface potential dependent surface forces due to cation adsorption at high salt concentrations. Hence, electric double layers of lipid bilayers are exclusively dominated by inner Helmholtz charge regulation under physiological conditions. These results are important for rationalizing bilayer behavior under physiological conditions, where charge and concentration modulation may act as biological triggers for function and signaling.

We will finally provide an outlook on combining all force probe techniques with electrochemical potential modulation.

MEMS and NEMS
Room 125 - Session MN1-TuM

RF and Magnetic MEMS

Moderators: Robert Davis, Brigham Young University, **Vikrant Gokhale**, Naval Research Laboratory

8:30am **MN1-TuM-3 Acoustoelectric Devices on Thin-Film Piezoelectric on Substrate Platform: Harnessing the Potential of Phonon-Electron Coupling**, *Reza Abdolvand,* University of Central Florida **INVITED**
MEMS devices based on the thin-film piezoelectric on substrate (TPoS) platform, such as resonators, have demonstrated exceptional characteristics including low loss, high power handling, and low noise, enabling the creation of high-performance filters, clocks, and sensors. The TPoS platform also facilitates strong energy coupling between acoustic phonons and electrons, which can be harnessed for key radio frequency (RF) components in the micro-acoustic domain. This talk will review the advancements in utilizing the TPoS platform to achieve amplification, non-reciprocal transmission, and phonon mixing in a compact and energy-efficient manner. These innovations can simplify and miniaturize RF frontend modules, transitioning from passive RF filters to active amplifiers, isolators, and mixers, potentially reducing or eliminating the need for their electronic and magnetic counterparts. Despite the phonon-electron coupling, known as the "acoustoelectric effect," being understood for over sixty years, only recent advancements in thin-film processing technology have enabled the development of scalable and manufacturable platforms with strong phonon-electron coupling. Heterostructures like thin-film lithium niobate on silicon, tailored to support specific acoustic waves with high electromechanical coupling and optimized electronic properties, offer a promising platform for scalable fabrication of miniaturized and energy-efficient "acoustoelectric" devices.

9:00am **MN1-TuM-5 Enhanced Performance of Thin-Film Lithium Niobate RF Acoustic Devices through Novel Material Process**, *Tito Busani, **Arjun Aryal**,* University of New Mexico*; Sidhant Tiwari, Darren W. Branch, Aleem Siddiqui,* Sandia National Laboratories, USA
Advancements in RF acoustic devices for telecommunications are significantly enhanced by the novel application of thin-film lithium niobate (LiNbO3), favored for its high electromechanical coupling. A persistent challenge in utilizing this material has been its compatibility with Si process manufacturing which results in poor quality device manufacturing. Moreover, the various spurious resonances present in those devices degrades the resonator efficient in storing energy, thus degrading quality factor Q and the electromechanical coupling coefficient k_t^2. This can be overcome typically by device design or by material processing, such as controlling the side walls roughness and their verticality. In this work we demonstrate how, comparing different edge treatments, i.e. different etching processes, we can both suppress spurious modes and increase the coupling coefficient at the main mode.

Unlike conventional methods, our innovative approach involves adjusting the surface roughness of the resonator's edges. In this study, resonators with specifically engineered roughened edges exhibited significant reduction and elimination of spurious resonances below 500 MHz frequency. This effect is more pronounced for a surface roughness of approximately 110 nm. Further explorations in this work demonstrate that varying the degree of roughness allows for controlled suppression behavior not only in the lower frequency range, but also potentially across broader frequency spectra. This method opens new opportunities for optimizing the performance of lithium niobate RF devices. Future investigations will focus on quantifying the effects of both higher and lower roughness levels to develop a comprehensive understanding of their impact on device performance across all operating frequencies.

Figure 1. (b) compares the resonant behavior between two resonators of same architecture with two different edged roughness. Several spurious modes, respectively at 50 MHz, 150 MHz, and 365 MHz are completely removed by the edge treatment process, while the peaks at 175 MHz and 250 MHz are greatly suppressed. The observed phenomenon is attributed to the ability of the roughened edges to scatter short-wavelength spurious modes, preventing the establishment of strong resonances.

9:15am **MN1-TuM-6 Garnet Based Integrated GHz Thin Film Inductors With High Quality Factor and High Inductance Density**, *Rafael Puig, Daniel Hedlund, Piotr Kulik,* University of Central Florida
Demand for lighter and smaller devices is increasing, and thus the interest in thin film inductors (TFI) is rising. Inductors are key components in

electronics and are used for e.g. power delivery and filters. Especially TFIs that can be heterogeneously integrated with e.g. existing silicon processing steps for integrated circuits. Furthermore, the inductor should be easy to fabricate. TFI need magnetic layer(s) and to magnetically bias the devices to be effective.

The magnetic material in a TFI should have a large permeability (μ) in the operating frequency (f_0). This can be achieved through the relationship $\mu \approx 4\pi M_s/H_a$, where M_s is the saturation magnetization and H_a is the magnetic anisotropy field. Kittel's formula [1] of ferromagnetic resonance (FMR)

$$f_{FMR} = \gamma(4\pi M_s H_a)^{1/2}$$

where γ is the gyromagnetic gives rise to Snoek's limit [2], where to achieve high μ, M_s/H_a should be large, whereas to achieve high FMR frequency $M_s H_a$ should be large. Frequencies near and above f_{FMR} yields that μ is mainly imaginary, i.e. a high magnetic loss tangent $\tan(\delta)$, in this regime the inductor starts working resistively. In addition, the material should have low FMR linewidths, as this is related to dissipation processes, such as eddy currents in the material, which are mostly reduced with electrical insulation. This can be mitigated by using magnetic materials that are electrically insulated, such as ferrites in inductors.

The first published magnetic TFI dates back more than 50 years [3] and demonstrated a quality factor (Q) of 18 at an f_0 of 10 MHz. Major advancements in thin-film inductors were made 10 years later when Soohoo [4] presented a thorough analysis on the requirements of the magnetic material and how high-performing TFI could be produced. It is rare to find thin film inductors operating in the GHz range with high Q, even though major advancements has been made in recent years [5–11].

In this work, we used Ansys Maxwell to model and design a $Y_3Fe_5O_{12}$ (YIG)-integrated TFI that has a f_0 in the GHz range, Q of 8, and an inductance density of 4300 nH/mm^2 when approaching magnetic saturation. We applied the magnetic field both in-plane and out-of-plane. The thin film stack used composed of 500 μm thick gadolinium gallium garnet substrate coated with a 10 μm thick YIG layer with M_s of 140 kA/m (1750 G), to which we placed a spiral inductor composed of 1 μm thick Cu wires with 270 μm spacing. This design was a compromise for rapid prototyping. We used YIG because it shows highμ [12] in the GHz range, with very few losses associated with dissipative processes. Future work will involve fabricating several designs to improve performance and incorporating with MEMS.

9:30am **MN1-TuM-7 Fabrication of Strip Line Micro Inductors Using Nickel-Iron Oxide Nanocomposite for Power-Supply on Chip Applications**, *Sai Pranesh Amirisetti, David P. Arnold,* University of Florida, Gainesville
The demand for miniaturized, more power efficient electronics has spurred the need for power supply solutions using novel magnetic materials that offer high permeability, operate at high frequencies, and minimize losses [1]. This study introduces a microfabrication technique for strip line inductors using nickel-iron oxide nanocomposite cores with an area of 0.07 mm^2, offering a significant advancement over traditional air-core or other magnetic-core microinductors.

Electro-infiltration, a process where a magnetic composite is formed by electroplating a metal through a deposited nanoparticle layer, yields a nickel-iron oxide nanocomposite with high relative permeability (~20) up to 300 MHz and low loss tangent [2,3]. The fabrication process, as shown in figure 1, involves deposition of the magnetic nanocomposite over patterned molds on a silicon substrate, followed by planarization, insulation layer deposition, seed layer deposition for copper electroplating, and finally a second deposition of the magnetic nanocomposite layer.

While there are relatively large device-to-device variations in this early-stage fabrication process, the experimental findings demonstrate that these nickel-iron oxide nanocomposite microinductors exhibit inductance between 0.5-1 nH and with a max quality factor between 4-6 at 100 MHz Furthermore, the compatibility of the fabrication process with semiconductor manufacturing techniques enables seamless integration for power system on chip (PwrSoC) applications.

This research contributes to the advancement of micro inductor technology for PwrSoC applications, shedding light on the potential of nickel-iron oxide magnetic nanocomposites as promising materials for high-performance on-chip power supply solutions.

References:

[1] Mathúna, Cian Ó., et al. "Review of integrated magnetics for power supply on chip (PwrSoC)." IEEE Transactions on Power Electronics 27.11 (2012): 4799-4816.

[2] Smith, Connor S., et al. "Electro-infiltrated nickel/iron-oxide and permalloy/iron-oxide nanocomposites for integrated power inductors." *Journal of Magnetism and Magnetic Materials* 493 (2020): 165718.

[3] Mills, Sara C., et al. "Method for the fabrication of thick multilayered nickel/iron oxide nanoparticle magnetic nanocomposites." *Journal of Magnetism and Magnetic Materials* 542 (2022): 168578.

9:45am **MN1-TuM-8 Rapid Fabrication of Tunable Resonators on Garnet based Magnetic Thin-Films**, *Nicholas Gagnon, Michael Franz, Michael Gamez, Daniel Hedlund, Reza Abdolvand, Piotr Kulik,* University of Central Florida
Current MEMS-based resonators are limited in frequency tunability by providing a narrow operational frequency range or requiring complex architectures. These challenges impose practical limitations for tunable devices operating over desired large frequency ranges (>5%). For the first time, an Al/YIG/GGG (aluminum, yttrium iron garnet, and gadolinium gallium garnet) tunable resonator was fabricated using rapid laser lithography. This tunable resonator requires zero static power and leverages a permanent magnet to provide a magnetic field bias (H_{ex}). YIG is a promising material for tunability due to high permeability (μ), low losses and low Gilbert damping [1–6]. The ferromagnetic resonance frequency, the shift in frequency due to a H_{ex}, can be calculated using Kittel's equation (eq. 1) [7],

$$f_{FMR} = \gamma(4\pi M_s H_a)^{1/2}, (eq.\ 1)$$

where M_s, H_a, γ is the saturation magnetization, magnetic anisotropy field and gyromagnetic ratio respectively. The H_{ex} applied by the permanent magnet shifts the operational frequency of the device, hence providing tunability. Using finite element method (FEM) simulations, we have designed a device that can operate between 0.5 and 2 GHz with a quality factor (Q) of 200. Q is calculated using eq. 2,

$$Q = f_{res}/(\Delta f_{3db}), (eq.\ 2)$$

where f_{res} is the resonance frequency and Δf_{3db} is the 3-dB bandwidth. The results of the FEM simulations can be seen in Figure 1(A) together with the model in Figure 1(C). Compared to conventional lithography our method can prototype devices in *seconds* on any garnet material stack. The resonator presented here was manufactured in <10s and shows tunability of 33%. Figure 1(C) shows the tunability, and the resonator can be seen in Figure 1(D). The Q factor of the fabricated resonator operating near 1 GHz is 130. For a rapid prototyping method, that eliminates conventional lithography, a Q factor that is more than 50 % of expected from simulations is promising.

Future efforts will delve into investigating means to improve our fabrication method, i.e. smaller feature sizes as it is applicable to a wide range of devices. Additionally, we are focusing on concentrating H_{ex} using flux-based techniques providing additional tunability. The thin-film resonator presented here shows great potential to compete with commercially available sphere based YIG-resonators, with much smaller size and ease of manufacturing.

MEMS and NEMS
Room 125 - Session MN2-TuM

Heterogeneous Integration and Packaging
Moderators: Robert Davis, Brigham Young University, **Vikrant Gokhale**, Naval Research Laboratory

11:00am **MN2-TuM-13 Advanced Packaging Driven Heterogeneous Integration**, *Robert Patti,* NHanced Semiconductors Inc **INVITED**
Introduction

Semiconductors are an amazing success story. Since their introduction in 1959 they have found their way into every segment of our lives – transportation, entertainment, medicine, communication, weaponry, etc.At each step the chips became smaller, faster, cheaper, and more powerful, in a progression known as Moore's Law.

Today, Moore's Law is slowing and the industry's path forward is less well defined.This paper introduces a new concept, Foundry 2.0™, that offers fresh solutions for the future.

Current Challenges

Scaling

Shrinking the transistors no longer produces inevitable gains. Each new node is more difficult and expensive to achieve and some elements, notably

capacitors, actually perform more poorly at smaller sizes. Meanwhile, wiring is approaching its physical limits, consuming a larger share of the power and signal time and generating problematic capacitance.

Size and Yield

One solution to the scaling problem is to cram more functionality onto each chip. The resulting system-on-chip (SoC) dies are powerful but physically larger, which translates directly to poorer yield. In addition, all functionality is necessarily built in the same processes, which imposes compromises.

Cost vs. Innovation

The cost and complexity of today's leading-edge chips dictates that they be manufactured in vast quantities to achieve economies of scale. Customization is out of the question and innovation is greatly constrained.

Foundry 2.0™ Solutions

Foundry 2.0™ is a manufacturing model that takes dies and chiplets from high-volume foundries and applies advanced packaging (AP) and other back-end-of-line (BEoL) processes to create specialized devices at lower volumes. Foundry 2.0 does not attempt to replace the existing industry, but to transform it. It does not compete with the high-volume leading-edge foundries; it works with them to penetrate the smaller markets where customization is prized.

As a neutral party, the Foundry 2.0 manufacturer can source its dies from any major foundry. Best-of-class components can be selected regardless of node, substrate, manufacturing process, or source, and then combined in 3D stacks or 2.5D assemblies that precisely fill the needs of specific markets.

By avoiding the high cost of building transistors Foundry 2.0 can economically produce smaller lots. Its high-mix low-volume model addresses markets that high-volume fabs simply cannot afford to accommodate. Foundry 2.0 makes innovation profitable again.

11:30am **MN2-TuM-15 Advances in Reliability Monitoring and Failure Analysis in Three-Dimensional Microsystems**, *Matthew B. Jordan, Matthew Bahr, Luca Basso, Andrew Mounce, Andrew Ferris, Jessica McDow, Joel Christiansen, Jeremy Walraven, William Mook,* Sandia National Laboratories; *Jaesung Lee,* University of Central Florida; *Amun Jarzembski, Wyatt Hodges, Jay Carroll, Benjamin Young, Gregory Pickrell, Luke Yates, Jason Neely,* Sandia National Laboratories

Three-dimensional, heterogeneous integration of microsystems has introduced new failure mechanisms while making it more difficult to screen and diagnose those failures. High-consequence applications require accurate reliability estimates; thus, we have developed *in-situ* reliability monitors for continuous surveillance. Furthermore, when components fail, we need to locate and characterize the failure mechanisms. To that end, we have adapted and developed novel failure analysis techniques for use in 3D microsystems.

In this manuscript we present two reliability monitors designed to provide granular detail on the state of health of a 3D microsystem. The first generalizes daisy-chain analysis methods based on network flow. The individual 3D interconnects are treated as vertices in a network where when they are cut it alters the maximum flow through the network. In this way, data on the failure rate of individual interconnects can be accurately determined with a smaller set of tests than a standard daisy chain where the network is severed after a single failure. The second reliability monitor is an *in-situ* strain gauge based on the Si piezoresistive effect allowing for localized measurement of the fatigue of 3D microsystems.

Secondly, we will discuss some methods used to localize and characterize failures in 3D microsystems. As we cannot access the surface of the components as we would in a planar system, we must rely on subsurface probing methods. The first of these methods is frequency domain thermoreflectance (FDTR), which utilizes a pump/probe laser system to characterize the thermal interfaces of a 3D microsystem. We find with FDTR that after sufficient sample preparation, small changes in microbumps can be resolved based on their thermal transport properties. Secondly, EM field analysis as nitrogen-vacancy in diamond based magnetic field measurements and scanning electric field measurements have been utilized to determine short-circuit and open circuit defects. Lastly, electrical frequency has been used to characterize components as they age (power spectrum analysis).

Guaranteeing the reliability of 3D microsystems is crucial for high-consequence systems. Monitoring system reliability and effectively localizing and analyzing failures are essential for providing this guarantee.

Nanoscale Science and Technology
Room 114 - Session NS1-TuM

Synthesis and Visualization of Nanostructures I
Moderator: Aubrey Todd Hanibiki, Laboratory for Physical Sciences

8:00am **NS1-TuM-1 Fabrication of High Aspect Ratio Gan and AlN Nanopillar Arrays with M-Oriented Sidewalls by Combining Dry and Wet Processes for the Next Generation of Deep Ultraviolet Light-Emitting Diodes**, *Lucas Jaloustre, Saron-Rosy Sales de mello,* CNRS-LTM, France; *Lucie Valera,* CEA, France; *Sébastien Labau, Camille Petit-Etienne,* CNRS-LTM, France; *Gwénolé Jacopin,* CNRS, France; *Christophe Durand,* CEA, France; *Erwine Pargon,* CNRS-LTM, France

III-N materials have emerged as promising candidates for ultraviolet (UV) light-emitting diodes (LEDs) due to their wide band gap [1]. However, the current planar architecture of III-N LEDs has demonstrated unsatisfactory efficiency, particularly for wavelengths below 250 nm where the external quantum efficiency drops below 0.1%. One strategy to address this challenge is the transition from a planar to a core-shell geometry [2], which offers many advantages (reduced defects, larger emissive area, better light extraction). This approach involves patterning organized arrays of AlN or GaN nanowires with a high aspect ratio (AR>10) and ideally *m*-plane sidewalls using plasma etching. Metalorganic Chemical Vapor Deposition (MOCVD) is then used to radially grow emissive quantum wells.

In this work, the authors developed an Inductively Coupled Plasma etching process using a Cl_2 chemistry and a hard mark, suitable for the realization of highly anisotropic and smooth GaN and AlN pillars with an aspect ratio up to 16. They demonstrate that the III-N etching using Cl_2 plasma is driven by crystallographic orientation preferential etching and ultimately leads to the formation of *a*-plane sidewalls (Fig. 1-a), and not to the desired *m*-faceting [3].

Post-etching chemical treatments have been explored to improve sidewall roughness and to favour the appearance of the *m*-planes. The authors demonstrate the feasibility of such *m*-faceting on III-N pillars with KOH wet etching and highlight two key parameters for this process[4]: 1) The presence of a HM with a suitable shape during the wet to prevent top pillar erosion and drives the etching, allowing the transfer of the HM shape onto the pillars (Fig. 1-b and 1-c). 2) A tapered pillar profile, which is mandatory to ensure the HM shape transfer.

The wet mechanisms leading to this faceting, and the significant impact of KOH concentration on the etching dynamics (Fig. 2), will be discussed.

This work provides a promising path for achieving pillar arrays that serve as the first building block for highly efficient UV core-shell LEDs. The fabrication of straight and smooth GaN and AlN pillar arrays with the desired crystalline *m*-planes sidewalls (Fig 1-d) was achieved through a two-step process combining Cl_2 plasma etching and KOH wet etching. Finally, successful MOCVD growth of AlGaN/AlN MQWs has been achieved through a collaboration with CEA-PHELIQS, demonstrating UV-C emission on such structures (Fig. 3).

1. M. Kneissl, *et al. Nat. Photonics* **13**,233–244 (2019).
2. J. Kim, *et al. scientific reports **8**, 935 (2018)*
3. L. Jaloustre, *et al. Mater. Sci. Semicond. Process* **165**, (2023)
4. L. Jaloustre, *et al. Mater. Sci. Semicond. Process* **173**, (2024)

8:15am **NS1-TuM-2 Exploring Large PAH in "Stardust" by HR-AFM**, *Percy Zahl,* Brookhaven National Laboratory; *Martha L. Chacon-Patino, Joseph Frye-Jones,* National High Magnetic Field Laboratory

Meteorites provide a glimpse into the past of the solar system by preserving snapshots of the universe for millions to billions of years. (1) Organic material, i.e. Polycyclic Aromatic Hydrocarbons (PAH), forms over this time, creating common molecules seen on Earth such as carboxylic acids, aromatic and aliphatic hydrocarbons, and most importantly for life, amino acids. (1–4) Organic material formed in such a way is often revealed as ultra-complex mixtures, similar to fossil fuels and natural dissolved organic matter seen on Earth.

However, these ultra-complex organic mixtures require ultrahigh-resolution analytical techniques to achieve comprehensive molecular-level characterization.

Tuesday Morning, November 5, 2024

Very little work has been done so far using High Resolution non-contact Atomic Force Microscopy (HR-AFM) (5). Here we analyze highly enriched PAH meteorite sample extracts using our preliminary extraction method similar to that used for fossil fuels. Acetone assists in the extraction of highly aromatic compounds out of a powdered form of meteorite specimens that have already been extracted in a polarity gradient from methanol to toluene. The resulting fraction is enriched in highly aromatic/hydrogen-deficient compounds, as suggested by ultrahigh resolution FT-ICR mass spectrometry.

Comparison with a fraction extracted with chloroform demonstrates a drop in the H/C ratio (a measure of aromaticity) from an average 1.6 for chloroform species down to 0.6 for acetone-extracted compounds. This correlates with the images observed in HR-AFM, where more aliphatic species were observed in the chloroform extract compared to the highly aromatic compounds observed in the acetone fraction. The selected motifs observed highlight the highly aromatic composition of species from the acetone fraction, containing complex ring systems.

References:

[1] Sephton, M. A.,Phil. Trans. R. Soc. A: Mathematical, Phys. and Eng. Sci., 363(1837), 2729–2742 (2005)

[2]Pizzarello, S.; Cooper, G. W.; Flynn, G. J.,Meteorites and the Early Solar System II,625–651 (2006)

[3] Pizzarello, S.,Acc Chem Res, 39(4), 231–237 (2006)

[4] Pizzarello, S.; Shock,Cold Spring Harb Perspect Biol, 2(3), 1–19 (2010)

[5] Kaiser K.;Meteoritics & Planetary Science 57, Nr 3, 644–656 (2022)

8:30am NS1-TuM-3 Direct Atomic Manipulation of a Buried Graphene Interface, *Marek Kolmer,* Ames National Laboratory*; Joseph Hall,* Iowa State University*; Shen Chen,* Ames National Laboratory*; Samuel Roberts, Zhe Fei,* Iowa State University*; Yong Han,* Ames National Laboratory*; Michael C. Tringides,* Iowa State University

Controlling the two-dimensional (2-d) materials via interlayer interactions is a promising strategy for synthesizing novel electronic and topological phases. These interactions may be tuned locally via atomic-scale manipulations using scanning tunneling microscopes (STMs). However, the practical application of STM manipulation encounters fundamental problems in protecting the designer structures formed atop the surface. We will present a material platform and experimental protocol for precisely manipulating the buried epitaxial graphene interface, which can serve as a template for further targeted synthesis. The covalent bonds between a graphene buffer layer and the silicon carbide substrate may be reversibly broken and restored using the electric field from the STM tip. The charge separation resulting from covalent bond redistribution is used to pull or push the interface atoms by controlling the polarity of the tip-sample bias voltage. The reported effect propagates to the top graphene layer to form a pattern of nanoprotrusions with lateral precision, reaching the dimension of a single unit cell of the interface moiré lattice (~1.8 nm).

Local and reversible electric-field-induced patterning of the epitaxial graphene heterostructures from the bottom interface presents an alternative architecture to synthesize metastable configurations at the interface. The decoupled interface could be locally arranged in ordered superstructures, creating a new 2-d phase with long-range periodic potential experienced by the Dirac electrons in the top graphene layer(s). The location of the voltage pulses controls the period of these superstructures. It allows exploring novel, rich 2-d quantum phases with low-energy electronic excitations of tailored superlattice minibands. This band structure control is realized directly within the epitaxial graphene-based tunable heterostructures on the technologically relevant silicon carbide substrate.

8:45am NS1-TuM-4 Effect of Methanol and Photoinduced Surface Oxygen Vacancies on the Charge Carrier Dynamics in TiO₂, *Bugrahan Guner, Omur E. Dagdeviren,* École de technologie supérieure, University of Quebec, Canada

The migration of holes in metal oxides such as TiO_2 plays a vital role in (photo)catalytic applications. The dynamics of charge carriers under operation conditions can be influenced by both methanol addition and photoinduced surface oxygen vacancies (PI-SOVs) [1]. Nevertheless, the existing knowledge of the effect of methanol as a function of PI-SOVs solely concentrates on the chemical reduction process. For this reason, the fundamental understanding of the time-dependent charge carrier-vacancy interactions with the presence of methanol is impaired. To overcome this challenge, we performed time-resolved atomic force microscopy measurements to quantitatively disclose the dynamics of charge carriers in a rutile-terminated, single-crystal TiO_2 (100) sample under the influence of methanol as a function of high-energy ultraviolet (UV) surface irradiation [2-4]. We have three major experimental findings: (I) The addition of methanol decreased the time constant, and hence, the mobility of the charge carriers. (II) The energy barrier within the system was decreased by UV irradiation; however, the presence of methanol did not alter the corresponding barrier. (III) The reversibility of the charge carrier dynamics was observed upon the termination of UV irradiation. Our analysis of methanol's role in hole mobility as a function of surface irradiation contributes to the understanding of surface interactions and charge carrier dynamics, offering valuable insights for (photo)catalytic applications.

[1] Orcun Dincer, Bugrahan Guner, and Omur E. Dagdeviren, APL Materials **12** (2) (2024).

[2] Bugrahan Guner, Simon Laflamme, and Omur E. Dagdeviren, Review of Scientific Instruments **94** (6) (2023).

[3] Bugrahan Guner and Omur E. Dagdeviren, ACS Applied Electronic Materials **4** (8), 4085 (2022).

[4] Bugrahan Guner, Orcun Dincer, and Omur E. Dagdeviren, ACS Applied Energy Materials **7** (6), 2292 (2024).

9:00am NS1-TuM-5 Single Nanofabrication Step of Low Series Resistance Silicon Nanowire-Based Devices for Giant Piezoresistance Characterization, *Kung Shao Chi, Lucas Spejo,* University of Campinas (UNICAMP), Brazil*; Renato Minamisawa,* Institut für Mathematik und Naturwissenschaften Fachhochschule, Switzerland*; José Diniz, **Marcos Puydinger,** University of Campinas (UNICAMP), Brazil

Strained silicon nanowires (NWs) are essential in sensor applications and in the microelectronics industry, as they exhibit giant piezoresistance and variable carrier mobility as a function of stress. In this work, individual NWs were fabricated from strained silicon-on-insulator (sSOI) thin films with 0.8% biaxial strain. After a lithographic step, the buried oxide (BOX) was removed from the SOI film, thus suspending the NWs. The new boundary condition induces mechanical stress amplification, now uniaxial in the NW longitudinal direction (Fig. 1a). Finite element method simulations show that before the removal of SiO2, the nanowires exhibit predominantly uniaxial strain of around 0.8%, while the peripheral pads show a 0.8% biaxial strain. In this sense, the proposal is to stress the NWs to levels higher than those employed in industry.

The solutions proposed in the literature usually require external actuators or complex multi-step nanofabrication infrastructure [1], [2]. Here, we present a method for prototyping sSiNWs without external actuators and measuring their piezoresistance directly in a 2-probe setup (Figs. 1b and 1c) without further lithographic or metal deposition steps for the electrical contacts. We were able to simplify the steps involved in the fabrication, thus making fast prototyping of strained NWs possible using a single-step protocol and electrical characterization with optimized contact resistance.

In addition, Raman spectroscopy was used to measure the NW uniaxial stress. Figure 2 shows an example of the fabricated suspended sSiNW and its spectrum. We have measured the uniaxial mechanical stresses of around 2.9 GPa for 200 nm-wide sSiNWs, which vary depending on the NW dimension. Parameter optimization can further result in the fabrication of MOSFETs based on a single ultra-strained NW in gate-all-around (GAA) topology, as well as chemical and physical sensors for various technological applications.

[1] F. Ureña-Begara et al. J Appl Phys, vol. 124 (9), 2018.

[2] H. Ando and T. Namazu. J. Vac. Sci. Technol. B, vol. 41 (6), 2023.

9:15am NS1-TuM-6 Size-Dependent Oxidation of Supported Pd and Pd-Pt Nano-Catalysts Under Methane Oxidation Conditions, *Alexander I. Large,* Diamond Light Source, UK*; Henry Hoddinott, Richard E. Palmer,* University of Swansea, UK*; **Georg Held,** Diamond Light Source, UK

The importance of cluster size effects in heterogeneous catalysis has been recognized for some time and numerous studies have addressed this issue.

XPS is awell-established technique to study changes in the chemical composition and electronic structure of catalyst nanoparticles. However, as XPS is an averaging technique and based on the detection of electrons, experiments require a narrow distribution of cluster size and a conducting homogeneous support in order to avoid sample charging, which would prevent accurate measurements of chemical shifts. Traditional methods of catalyst synthesis by impregnation/calcination of support powders lead to very large particle size distributions (typically ±50 %) and insulating samples, which fail on both the above criteria. Here we present an operando XPS study of Al_2O_3-supported Pd and Pd-Pt nanoparticles under various dry and wet reaction conditions for methane oxidation ($CH_4 + O_2$ [+ H_2O]). In order to create a system as close to industrial catalysts as possible, the support consists of 5-10 nm thick alumina films electrochemically grown on Al foil. The nanoparticles (1 to 10,000 atoms) were produced by gas condensation and size-selected within 4-5%. TEM confirms the narrow size distribution. The XPS spectra of the clusters before the reaction show clear chemical shifts as function of particle size. Under dry reaction conditions larger clusters tend to oxidize fully (Pd II) whereas smaller particles show a mix of oxidation states (Pd 0-II).The situation is less clear under wet conditions, which could be due to sintering.

9:30am NS1-TuM-7 Evidence from Molecular Force Microscopy of Magnetic Monopole-Like Behavior in Chiral Molecule-Coated Superparamagnetic Nanoparticles , *Sidney Cohen, Qirong Zhu,* Weizmann Institute of Science, Israel*; Jonas Fransson,* Uppsala University, Sweden*; Olga Brontvein, Ron Naaman,* Weizmann Institute of Science, Israel

Ever since Dirac's proposition[1] nearly a century ago that magnetic monopoles should exist, experimentalists have searched for them without success. A flurry of work starting about 50 years ago eventually showed magnetic *monopole-like* behavior in very limited and extreme conditions. The potential for tunable energy storage and stable information storage makes such structures interesting technologically. Here, we use atomic force microscope (AFM)-based molecular force microscopy to show that superparamagnetic iron oxide nanoparticles (SPIONs) coated with an amino acids of opposing chirality (D and L-cysteine) exhibit monopole magnetic behavior whose polarity depends on the chirality of the molecular entity. The effect is governed by the chiral-induced spin selectivity effect (see for instance references 2-4). Attractive magnetic forces were measured between a magnetized Ni film and an SPION attached to the AFM tip through a polyethylene glycol linker. Experiments were performed in a phosphate-buffered saline solution. A thin Ti (oxide) layer covered the Ni to prevent chemical interaction between the cysteine thiol and Ni. The direction of the field was changed between up and down by flipping a magnet held under the substrate. The magnetic force is comprised of spin-exchange interactions (short range) and magnetic monopole interactions (longer range). The interaction force was observed to vary with chirality of the molecule and magnetic field direction. A significant difference was measured in the pulling force for the D vs. L cysteine and up/down magnet orientations when the Ti (oxide) layer was about 2 nm thick. Thicker layers (of Ti oxide or aluminum oxide) result in significant reduction of the magnetic force, allowing estimation of the range of the force interaction.

REFERENCES

[1] Dirac, P. A. M. Quantised singularities in the electromagnetic field. *Proc. Roy. Soc. Lond.* **A133,** 60–72 (1931).

[2] Naaman, R., Paltiel, Y., Waldeck, D.H. Chiral induced spin selectivity gives a new twist on spin control in chemistry *J. Phys. Chem. Lett.* **11**, *11*, 3660-3666 (2020).

[3] Banerjee-Ghosh, K. et al. Separation of enantiomers by their enantiospecific interaction with achiral magnetic substrates *Science* **360**, 1331-1334 (2018).

[4] Adhikari, Y., et al. Interplay of structural chirality, electron spin and topological orbital in chiral molecular spin valves *Nat. Commun.* **14**, 5163 (2023).

9:45am NS1-TuM-8 Mapping the Slow-Decay of End States in a Laterally Extended Graphene Nanoribbon, *Umamahesh Thupakula,* CEMES-CNRS, France

End states (ESs) of quasi one-dimensional (1D) graphene nanoribbons (GNRs) have become a central focus in recent years because of their inclusion into the classification of topological tailor-made quantum systems.[1] So far, the topological phases of the GNRs are solely characterized by an integer parameter, called Z_2 invariant originating from the Zak phase, which takes values of 0 or 1 corresponding to topologically trivial or nontrivial configurations, respectively.[1] In these calculations, an infinite nanoribbon is always considered after defining the unit cells structure long the ribbon.[2] However, finite length nanoribbons are mainly observed and characterized experimentally. The tracking of the step-by-step building-up of ESs from a few unit cells to the formation of desired 1D/quasi-1D GNR molecular wire electronic band structure remains elusive. Combining picometer scale precision scanning tunneling microscopy, dI/dV spectroscopy mapping (STM and STS) with topological Hückel molecular orbital (HMO) calculations, we explain how topological quantum states are emerging or not with respect to the length 'N' (number of repeating molecular units) of the GNR starting from the basic polyene to the 1D polyacetylene chain and by a step-by-step enlargement of the nanoribbon width.

References

[1] Ting Cao, Fangzhou Zhao, & Steven G. Louie, Phys. Rev. Lett. 119, 076401 (2017)

[2] Daniel J. Rizzo, Gregory Veber, Ting Cao, Christopher Bronner, Ting Chen, Fangzhou Zhao, Henry Rodriguez, Steven G. Louie, Michael F. Crommie & Felix R. Fischer, *Nature* **560**, 204-208 (2018)

Nanoscale Science and Technology
Room 114 - Session NS2-TuM

Novel Imaging Techniques at the Nanoscale
Moderator: Adina Luican-Mayer, University of Ottawa, Canada

11:30am NS2-TuM-15 Silicon-Containing Poly(Phthalaldehyde) Resists for Nanofrazor Applications – Direct Patterning of Hard Mask Materials by Thermal Scanning Probe Lithography, *Nicholas Hendricks, Emine Çağin,* Heidelberg Instruments Nano AG, Switzerland

Thermal scanning probe lithography (t-SPL), enabled by the NanoFrazor technology, is establishing itself as a mature and reliable direct-write nanolithography technique for generating nanoscale structures [1-5]. The NanoFrazor technology offers an alternative or complementary process for conventional lithography techniques of electron-beam lithography (EBL) or focused-ion beam (FIB). t-SPL generates patterns by scanning an ultrasharp tip over a sample surface to induce local changes with a thermal stimulus. By using thermal energy as the stimulus, it is possible to perform various modifications to the sample via removal, conversion, or addition of/to the sample surface. Along with an ultrasharp tip, the t-SPL cantilever contains several other important functions such as an integrated thermal height sensor and an integrated heating element both of which are advantageous for fabricating devices for nanoelectronics, photonics, molecular sensing, and quantum computing.

The main thermal imaging resists used in t-SPL are poly(phthalaldehyde) (PPA) based materials that are commercially available from Allresist or Polymer Solutions. PPA is an all-organic based resist capable of undergoing direct sublimation when exposed to temperatures greater than the decomposition temperature, ~180°C, by a localized endothermic depolymerization reaction. With such characteristics, PPA has been able to produce sub-10 nm lateral dimensions while providing sub-nm vertical resolution and having an etch selectivity of 3 to 1 for a trifluoromethane-based reactive ion etch of silicon dioxide, a standard hard mask material. With a flexible synthesis, PPA can undergo an efficient and effective copolymerization to allow for the direct incorporation of silicon-containing functionalities into the thermal imaging resist. Such a strategy allows for the direct patterning of the silicon-containing hard mask for high-resolution and grayscale patterning with a simplified film stack.

Within this presentation, the background and workings of t-SPL will be introduced as well as the nanolithography and processing capabilities of silicon-containing PPA will be shown. There will be a focus on patterning high-resolution, e.g. sub-40 nm features, from a bi-layer stack of silicon-containing PPA and organic transfer layer (OTL) into a silicon substrate.

[1] S. Howell et al., Microsystems & Nanoengineering, 6, 21 (2020)

[2] V. Levati et al., Adv. Mater. Technol. 8, 2300166 (2023)

[3] O. J. Barker et al., Appl. Phys. Lett., 124, 112411 (2024)

[4] B. Erbas et al., Microsystems & Nanoengineering, 10, 28 (2024)

[5] L. Shani et al., Nanotechnology, 35, 255302 (2024)

11:45am NS2-TuM-16 Atomic Force Microscopy-Based Nanoscale Mechanics as a Function of Temperature, *Gheorghe Stan,* National Institute for Science and Technology (NIST)*; Cristian Ciobanu,* Colorado School of Mines

In the last decades, Atomic Force Microscopy (AFM)-based nanoscale mechanics underwent significant developments in terms of measurements and analytics.The measured relative contrast between stiff and compliant materials can now be resolved quantitatively through either relevant models or numerical modeling to reveal the true mechanical properties of materials and structures tested. In comparison, the temperature dependence of the mechanical response has not been sufficiently investigated. The AFM modules for thermomechanical applications are just starting to be added on commercial instruments and the theoretical framework for such measurements is still in its infancy. In this work, we analyze AFM-based quasistatic and dynamic measurements from room temperature up to 250 C on few test materials to probe the reliability of these measurements for nanoscale mechanical properties. The temperature dependence of the tip-sample contact mechanics in these measurements was analyzed both analytically and numerically. This analysis consistently reproduced the experimental response and was used to extract the temperature dependence of the elastic modulus of materials tested.

12:00pm NS2-TuM-17 Cryogenic Scattering Near-Field Optical Microscopy for Probing Optical Properties with 20nm Spatial Resolution at Temperatures < 10k, *Tobias Gokus,* attocube systems AG, Germany*; Artem Danilov,* attocube systems AG*; Richard Hentrich, Andreas Huber,* attocube systems AG, Germany

Near-field microscopy and spectroscopy has matured as a key technology for modern optics, combining the resolving power of atomic force (AFM) based measurements with the analytical capabilities of optical microscopy and spectroscopy.

Scattering-type near-field microscopy (s-SNOM) has already proven itself vital for probing local optical material properties of modern nanomaterials by enabling applications such as chemical identification [1], free-carrier profiling [2], or the direct mapping and measurement of the dispersion relation of propagating plasmon [3,4], phonon [5], and exciton polaritons [6] in layered materials.

Transferring these near-field measurement capabilities to cryogenic temperatures opens up new avenues for nanoscale-resolved optical characterization of novel materials and their fundamental properties. Until recently, cryogenic s-SNOM measurements were only available to a few experts utilizing home-built microscopes [7].

By integrating a scattering-type near-field optical microscope (s-SNOM) into an ultra-stable, vibrationally damped and automated closed-cycle cryostat system we developed the first commercial cryogenic s-SNOM microscope. It uniquely supports near-field amplitude and phase resolved imaging and spectroscopy in the visible to THZ spectral range and operates in a variable temperature range between < 10K to room temperature.

We will demonstrate infrared and visiblenear-fieldimaging with deep subwavelength spatial resolution, visualizing phonon polariton modes in hBNand exciton polariton waveguide modes in MoS₂ at temperatures < 10K.

Furthermore, we will present recent researchresults onspatially resolved measurements of the spectral response of a2D electron gas and its impact on the surface phonon polariton of LaAlO₃/SrTiO₃ heterostructure systems by utilizing s-SNOM based mid-infrared spectroscopy at variable temperatures [8,9].

1. I. Amenabar et al., *Nat. Commun.* **8** (2017), p. 14402. https://doi.org/10.1038/ncomms14402

2. J. M. Stiegler et al., *Nano Lett.* **10** (2010), p. 1387. https://doi.org/10.1021/nl100145d

3. J. Chen et al., *Nature* **487** (2012), p. 77. https://doi.org/10.1038/nature11254

4. Z. Fei et al., *Nature* **487** (2012), p. 82. https://doi.org/10.1038/nature11253

5. E. Yoxall et al., *Nat. Photon.* **9** (2015), p. 674. https://doi.org/10.1038/nphoton.2015.166

6. F. Hu et al., *Nat. Photon.* **11** (2017), p. 356. https://doi.org/10.1038/nphoton.2017.65

7. A. S. McLeod et al., *Nat. Phys.* **13** (2017), p. 80. https://doi.org/10.1038/nphys3882.

8. Y. Zhou et al., *Nat. Commun.* **14** (2023), p. 7686. https://doi.org/10.1038/s41467-023-43464-z

9. J. Barnett et al., *arXiv:2311.08354* (2024). https://doi.org/10.48550/arXiv.2311.07354

Plasma Science and Technology
Room 124 - Session PS1-TuM

Plasma Processes for Advanced Memory

Moderators: John Arnold, IBM Research Division, Albany, NY, **Jeffrey Shearer**, TEL

8:00am PS1-TuM-1 Control of High Aspect Ratio Dielectric Etch Profile using Additive Etching Gases, *Hyun Woo Tak, Chan Hyuk Choi, Myeong Ho Park, Jun Soo Lee, Bong Sun Kim, Jun Ki Jang, Eun Koo Kim, Dong Woo Kim, Geun Young Yeom,* Sungkyunkwan University (SKKU), Republic of Korea

To form high-density memory devices, high aspect ratio contact (HARC) etching is critical as it determines the integration density of memory devices. Given that there is no standardized definition of "high" in high aspect ratio, it is crucial to continuously improve the HARC etching capability to meet the requirements of next generation memory devices. In this study, the effects of various additive etching gases added with only a few standard cubic centimeters per minute (sccm) flow rates on etch characteristics of HARC structures were investigated. It is found that, by using a few sccm of various fluorine, sulfur and metal containing gases added to the process gases, etch characteristics such as etch selectivity, etch profile, and pattern charging can be controlled during the HARC etching. Detailed results on the effects of these gases such as etch rates, selectivity, and profiles, assessed through scanning electron microscopy (SEM) analyses will be provided in the presentation. Moreover, to understand the etch mechanism, the plasma and surface characteristics after addition of the additive gases were investigated by optical emission spectroscopy (OES), quadrupole mass spectrometry (QMS), and X-ray photoelectron spectroscopy (XPS). This research demonstrates that small additive gases in addition to main etch gases can significantly affect next-generation HARC etching processes, paving the way for advanced memory device fabrication.

8:15am PS1-TuM-2 Experimental and Molecular Dynamics Simulation Study of W and WSi Hard-Mask Etching by Fluorocarbon Plasmas, *Hojun Kang,* Osaka University, Japan, Republic of Korea*; Shunta Kawabata,* Osaka University, Japan*; Nicolas A. Mauchamp,* Osaka University, Japan, France*; Erin Joy Capdos Tinacba,* Osaka University, Japan, Philippines*; Tomoko Ito,* Osaka University, Japan*; Song-yun Kang, Dongkyu Lee, Jiwon Son,* Samsung Electronics, Republic of Korea*; Kazuhiro Karahashi, Satoshi Hamaguchi,* Osaka University, Japan

In response to the growing demand for high-density memory devices, driven by the advancement of smartphones, data centers, and AI technologies, the development of efficient fabrication techniques for complex structures of DRAM and 3D NAND devices has become increasingly critical. This necessitates the enhancement of plasma etching capabilities with high-energy ions, especially the development of mask materials with little erosion under high-energy ion irradiation. This study aims to clarify the etching characteristics of W-based hard masks under SiO₂ etching conditions with fluorocarbon plasmas. W-based hard masks are among the candidate materials to replace conventional Si or C-based hard masks. With a mass-selected ion beam system[1], W and WSi sample surfaces were irradiated with high-energy Ar⁺ and CF₃⁺ ions ranging from 500 to 4000 eV, with an ion dose of $1\sim2\times10^{17}$ ions/cm². After ion irradiation, etched depths were measured with a surface profiler, and the etching yields were evaluated. Changes in the surface atomic compositions and chemical bonding were assessed through ex situ X-ray photoelectron spectroscopy (XPS). The depth profiles of the atomic composition below the etched surfaces were also measured with XPS employing 1,000 eV Ar⁺ ion etching. Our findings indicate that, below 1,000 eV, CF₃⁺ ions exhibit lower etching yields on W-Si masks compared to Ar⁺ ions; however, this trend reverses at energies exceeding 2000 eV. At lower energies, the formation of a W-C mixed layer inhibits the etching yield. Molecular dynamics (MD) simulations were also performed to evaluate the beam-surface interactions. The simulations used an embedded atom method (EAM) interatomic potential functions for W-W interactions [2], and Stillinger-Weber (SW)-type interatomic potential functions for W-C and W-Si interactions developed in this study. The study found good agreements between the experimental findings and simulated data. The force fields developed in this study allow further MD simulation of challenging etching scenarios that are hard to investigate by experiments only, such as etching with high incident angles, various ion energies, and high-aspect-ratio (HAR) etching with sidewall

effects. This study underscores the potential of W-based hard masks in next-generation memory fabrication, offering critical insights into the surface reactions essential for optimizing the etching processes, supported by both experimental and simulation data.

References

[1] K. Karahashi, et al., J. Phys. D: Appl. Phys. **47**, 224008 (2014)

[2] D. R. Mason, et al., J. Phys.: Condens. Matter **29** 505501 (2017)

8:30am PS1-TuM-3 3D NAND Dielectric Etch Technology Challenges and Breakthrough, *Youn-Jin Oh, Thorsten Lill, Mark Wilcoxson, Tae Won Kim, Harmeet Singh,* Lam Research Corporation   **INVITED**

Three-dimensional NAND technology has revolutionized the landscape of memory storage, enabled higher capacities and improved performance in semiconductor devices. However, the fabrication of 3D NAND structures presents unique challenges, particularly in the plasma etching. This presentation explores the challenges of plasma etching encountered and the indispensable role of new chemistries in cryogenic etch processes.

In 3D NAND device manufacturing, the vertical stacking of memory cells increases continuously, and lateral scaling has been tightened simultaneously, which brings more challenges to plasma etch process. The introduction of cryogenic etch has been able to breakthrough the critical challenges of vertical etch rate, mask selectivity, and critical dimension (CD) control, which enable us to scale up continuously.

In the cryogenic etch process, the role of chemical interactions on surfaces emerges as pivotal. In this presentation, the process breakthrough with various new chemistries will be discussed on the high aspect ratio SiO_2/Si_3N_4 (O/N) stacks in a capacitively coupled plasma (CCP) etcher which has high power, dual frequency, and high conductance capabilities. How cryogenic process performance is optimized with the synergy between new chemistries and advanced plasma modulation techniques will also be presented.

9:00am PS1-TuM-5 Patterning Challenges of Thick Tungsten Carbide Hard Mask Layers, *Daniel Montero, Kostantine Katcko, Frederic Lazzarino,* IMEC, Belgium

Newer technology nodes are increasingly demanding the patterning and integration of High aspect ratio vias (HAR) with increasing aspect ratios (AR) to meet stricter chip design requirements. For some fields, as in memory applications, it comes at the cost of increasing the stack height to accommodate more memory layers, while in logic patterning, a reduction in the via critical dimension (CD) may also be necessary. High AR vias are challenging structures to pattern from the plasma etch point of view, as it requires a precise control of the plasma parameters to pattern straight HAR vias, while reducing the bowing, undercut and hard mask consumption. For most applications using HAR vias, the target layers to pattern are dielectrics, which require the use of a long plasma etch process, and hence a highly selective hard mask (HM) layer able to resist this process. Most hard mask layers may lack enough selectivity to achieve the desired dielectric HAR via patterning quality in terms of selectivity, bowing and uniformity.

Our previous work [1] demonstrated that Tungsten Carbide (WCx) HM layer may exhibit higher selectivity than other HM in Back End of Line applications. However, the results derived in [1] cover the development of thin WCx layers (up to 15 nm thick) for line-space patterns. In this work, we extend and detail the etch development of thick WCx layers, up to 350 nm thick, in the context of HAR via 3DNAND memhole patterning applications. Our test vehicle uses immersion lithography at 193 nm to pattern staggered vias at 480 nm pitch into a 1 μm thick silicon oxide layer, with expected AR of 8.0 and 5.3 for 60 and 90 nm CD vias respectively.

In a first approach, we used Continuous Wave (CW) plasma, derived from [1], with an adapted etch time to pattern the 350 nm thick WCx layer, but it showed limited performance. Hence, a redevelopment of the plasma etch process was needed to guarantee uniform, straight, and complete opening of the thick WCx HM layer. Different passivation and etching methods, as well as the use of Synchronized Pulsed Plasma, are proposed to improve the patterning performance of WCx layers. Then, the 300 mm wafers continue processing towards the oxide etch, and selectivity to WCx HM is evaluated. The results are then compared to the reference HM of the test vehicle, Amorphous Carbon Layer (ACL). WCx HM showed better selectivity and lower corner erosion than the ACL reference layer, proving that WCx layers may be a valuable candidate for HAR via patterning in 3DNAND memhole applications.

Refences: [1] D. Montero et al, *Exploring the use of Tungsten-based Hard Masks in BEOL interconnects for 3nm node and beyond.* AVS68 2022.

9:15am PS1-TuM-6 Sheath Uniformity with Pulsed Low Frequency Biases for High Aspect Ratio Plasma Etching, *Evan Litch, Mark J. Kushner,* University of Michigan

Current roadmaps for microelectronics fabrication place focus on fabrication of 3-dimensional devices for higher functionality requiring increasing high aspect ratio (HAR) features. 3D-NAND memory structures containing hundreds of alternating layers of SiO_2 and Si_3N_4 require etching of vias having aspect ratios (ARs) exceeding 100. Deep trench isolation (DTI) for electrical isolation have similar HAR challenges. DTI etching of conductive substrates using halogen gas mixtures (e.g. HBr/Cl_2) is typically performed in inductively coupled plasmas (ICPs) with a substrate bias to facilitate highly anisotropic etching.

Plasma etching of HAR features requires ion energy and angular distributions (IEADs) that are high in energy, more than several keV, and narrow angular distribution. These requirements motivate the use of very low frequency biases (VLF) – 100s kHz. Concurrently, there is a transition to using pulsed biases to optimize the ratio of radical to ion fluxes. One of the motivations for pulsing is to gain the advantages of high peak power that produces higher energy ions with narrow angle distribution while lowering the average power deposition. However, pulsing at higher voltages thicken the sheath while low frequencies charge focus rings (FR), that can lead to significant sheath curvature at substrate boundary thereby modifying IEADs away from desired characteristics.

In this presentation, results will be discussed from a computational investigation of IEADs incident onto wafers and remediation of edge exclusion when using pulsed VLF biases in ICPs for etching of trenches for DTI and TSVs (through silicon vias). Simulations were conducted using the Hybrid Plasma Equipment Model (HPEM). Operating conditions are tens of mTorr mixtures of $Ar/Cl_2/O_2$ with bias frequencies from 250 kHz to 5 MHz. Bias voltages are up to a few kV with pulse repetition frequencies of up to 10s kHz. The consequences of these operating conditions on etching DTI and TSV features were evaluated using the Monte Carlo Feature Profile Model (MCFPM). When using continuous wave biases, the charging of the FR is sensitive to frequency, and this charging produces sheath curvature at the edge of the wafer, which perturbs IEADs. With pulsed biasing, the FR is transiently charged both during the VLF cycle and during the pulsed cycle, adding additional challenges to minimizing edge exclusion. Comparisons for different reactor/FR properties will be discussed.

9:30am PS1-TuM-7 Study of Electrode Material Effects on High Aspect Ratio SiO₂ Etching in CCP Etch Systems, *Chanhyuk Choi, Hyunwoo Tak, Seongbae Kim, Myeongho Park, Junsoo Lee, Bongsun Kim, Junki Jang, Eunkoo Kim, Dongwoo Kim, Geunyoung Yeom,* Sungkyunkwan University (SKKU), Republic of Korea

In semiconductor memory device manufacturing, plasma etching, particularly for high aspect ratio contact (HARC), has become increasingly crucial. A significant challenge is the uneven polymer deposition on the sidewalls of structures, leading to ion tilting, charging effects, and pattern distortion. Recent advancements have focused on integrating conductive materials, especially tungsten (W) by using WF_6 as an additive gas. WF_6 gas addition to the process gases has been effective in forming conductive polymers that resist etching, improving etch profiles, thus enhancing precision in etching. This study examines the use of a different showerhead material in addition to Si showerhead as an upper electrode with DC voltage for etching, comparing it to the traditional showerhead made of Si to assess their impacts on etching properties.

The SiO_2 etch rate was increased for all showerheads used in the experiment with increasing DC voltage, while the amorphous carbon layer (ACL) etch rate was remaining constant, indicating enhanced selectivity. The Si showerhead showed minimal improvement in removing charging with increased voltage, whereas the other showerhead significantly enhanced the bottom etch profile due to improved charge related issues. That is, Si showerhead showed bottom hole distortion, and which was not improved with increasing DC voltage to the showerhead while the other showerhead showed improved bottom hole shapes and profiles at higher DC voltages indicating improved charging related issues. XPS also showed a higher showerhead material atomic percent (at%) on the substrate for the -600V process compared to the 0V process when using the other showerhead, indicating more conductive polymer formation during the etching.

The etching with the other showerhead showed more anisotropic and undistorted etch profiles of ACL masked SiO_2 holes compared to the etching with Si showerhead due to lower charging related issues during the SiO_2 etching with polymer forming fluorocarbon gases due to the formation of more conductive polymer on the substrate during the etching. This research provides new insights into the role of electrode material reactivity in advanced etching processes of high aspect ratios in CCP systems.

9:45am PS1-TuM-8 Low GWP and Low Emission Gases for High Aspect Ratio Etching Application, *Scott Biltek*, *Nathan Stafford, Phong Nguyen, Fan Qin,* Air Liquide; *Pierre Forest,* Air Liquide, France

Over the past few years, numerous countries and semiconductor manufacturing entities have unveiled their commitments to achieving net-zero carbon emissions by 2050 or even sooner. When it comes to manufacturing chips, plasma etch processes contribute significantly to emissions, especially in dielectric etching. High aspect ratio structures are commonly used in both memory (3D NAND and DRAM) as well as logic chip manufacturing processes. These structures are traditionally etched using fluorocarbon and hydrofluorocarbon gases to etch very challenging dielectric structures. Unfortunately these gases, such as C4F8, CH2F2, CHF3, CF4, etc have very high Global warming potentials (GWP) along with other gases like C4F6 and CH3F which have low input GWP but potentially high GHG emissions.

However, while there has been a significant amount of work over the years to develop alternative low GWP etching gases, it is not only difficult to incorporate these chemistries in such very challenging etch processes but also understanding the emitted species from the plasma into the exhaust is rather limited. As the plasma dry etching is an extremely complex process involving chemical bond dissociation, recombination, side reactions, etc it is difficult to predict with any accuracy the post plasma exhaust stream and thus the CO2 equivalence of the plasma byproducts.

In this work we will present novel low GWP etching gases to replace traditional high GWP gases such as C4F8 and CHF3/CH2F2 that not only give improved etching performance but reduce the CO2 equivalent (CO2 eq) emissions from the etch chamber exhaust. This work utilizes Fourier Transform Infrared Spectroscopy (FTIR) to measure the exhaust stream of a 300mm CCP plasma etch chamber. Finally, we will present an etching recipe exclusively composed of low GWP etching gases.

Plasma Science and Technology
Room 124 - Session PS2-TuM

Plasma Processing at Cryogenic Temperatures

Moderators: Phillipe Bezard, IMEC Belgium, **Harutyun Melikyan**, Micron Technology

11:00am PS2-TuM-13 Plasma Prize Award Talk: The Evolution of Cryogenic Etching Plasma Processes Since Their Introduction 35 Years Ago, *Remi Dussart[1]*, GREMI CNRS/Université d'Orléans, France **INVITED**

Cryoetching was first introduced in 1988 by Tachi's team to selectively etch silicon and form anisotropic trench profiles [1]. Since these very first experiments, etching at very low substrate temperature has been developed and studied. In particular, a passivation mechanism involving both fluorine and oxygen was found and characterized by in-situ diagnostics. [2] Cryogenic etching was also studied for other materials than silicon: metal and dielectric material cryoetching was also investigated. Due to the enhanced physisorption of some radicals on cold surfaces, it is possible to foster some reactions and modify the composition of the deposited layer at the sidewalls. One of the advantages relies on the low contamination of the reactor walls since deposition in cryoetching is efficient on low temperature surfaces only. Cryoetching was successfully used for porous ultra-low-k materials [3]. Experiments on cryo-Atomic Layer Etching were also carried out and self limiting etching was shown. [4] More recently, cryoetching was used to etch 3D NAND very high aspect ratio structures composed of thin SiO_2 and Si_3N_4 repetitively stacked layers. [5] A different chemistry involving HF was used and a new etching mechanism was proposed for both dielectrics.

The presentation will be focused on the evolution of the cryogenic etching process from its introduction to the most advanced developments that have been recently disclosed.

[1] S. Tachi, K. Tsujimoto, and S. Okudaira, Appl. Phys. Lett. 52, 616 (1988).

[2] R. Dussart, T. Tillocher, P. Lefaucheux, and M. Boufnichel, J. Phys. D: Appl. Phys. 47, 123001 (2014).

[3] R. Chanson, L. Zhang, S. Naumov, Yu. A. Mankelevich, T. Tillocher, P. Lefaucheux, R. Dussart, S. De Gendt, J.-F. de Marneffe, Sci. Rep. 8:1886 (2018).

[4] G. Antoun, P. Lefaucheux, T. Tillocher, R. Dussart, K. Yamazaki, K. Yatsuda, J. Faguet, and K. Maekawa, Appl. Phys. Lett., 115, 153109 (2019).

[5] Y. Kihara, M. Tomura, W. Sakamoto, M. Honda and M. Kojima, 2023 IEEE Symposium on VLSI Technology and Circuits (VLSI Technology and Circuits), Kyoto, Japan, 1-2 (2023).

echnology and Circuits), Kyoto, Japan, 1-2 (2023).

11:30am PS2-TuM-15 The Role of PF₃ on Etching Characteristics of SiO₂ and SiN Using HF-Based Cryogenic Plasma Etching Analyzed with in situ Monitoring Techniques, *Shih-Nan Hsiao*, *Makoto Sekine,* Nagoya University, Japan; *Yuki Iijima, Ryutaro Suda, Masahiko Yokoi, Yoshihide Kihara,* Tokyo Electron Ltd. Miyagi, Japan; *Masaru Hori,* Nagoya University, Japan

Since the introduction of 3D architecture in NAND Flash Memory technology in 2014, the areal density has significantly increased. With the stacking of more layers to enhance data capability, the fabrication of memory channel holes with very high aspect ratios becomes a major challenge. One of the most demanding etch processes for fabricating advanced 3D NAND structures is the high-aspect-ratio contact (HARC) hole etch. Recently, cryogenic plasma etching containing hydrogen fluoride (HF)-contained species has been reported to mitigate surface charging effects while significantly increasing the throughput of SiO_2 etching [1, 2]. Furthermore, a significant enhancement of ONON etching by adding PF_3 to HF plasma has also been reported [3]. To understand the role of PF_3 in surface reactions and etching mechanisms, cryogenic etching of SiO_2 and SiN using HF diluted with PF_3 was investigated. A quasi-atomic layer etching (quasi-ALE) of SiO_2 and SiN film was conducted by using $HF/PF_3/O_2$ plasma for surface modification, followed by an Ar plasma for etching. *In situ* monitoring techniques, including spectroscopic ellipsometry and attenuated total reflectance Fourier transformation infrared spectroscopy (ATR-FTIR), were used to analyze the surface structure and etching characteristics. The substrate temperature (T_s) was controlled from 20 to -60 °C by circulating a coolant through the bottom electrode. At -20 °C, real-time thickness variation versus Ar sputter time exhibited a greater etched depth per cycle (EPC) after the Ar ion sputtering, compared to that at 20 °C. (see supplemental document for details). Surface structure observation using *in situ* ATR-FTIR revealed an increase in surface-adsorbed HF due to the presence of H_3PO_4 at -20 °C during the surface modification step, consistent with the results of density function theory simulations. This observation explains the increase in etched depth of SiO_2 attributed to the increased amount of surface-adsorbed HF. Conversely, the EPC vs T_s for the SiN exhibited an opposite tendency. Although more surface-adsorbed HF was also confirmed on the SiN surface using the plasma with PF_3 addition, the EPC was lower compared to pure HF. The surface structure observations reveal that the presence of P_3N_5 phase on the SiN surface, which might hinder the etching.

[1] S.N. Hsiao et al., Appl. Phys. Lett., 123 (2023) 212106.

[2] S.N. Hsiao et al., Small methods (Under review).

[3] Y. Kihara et al., VLSI symposium T3-2 (2023).

11:45am PS2-TuM-16 MD Simulations of Cryogenic Etching of SiO₂ by HF Plasmas, *Nicolas Mauchamp,* Osaka University, Japan; *Thorsten Lill, Mingmei Wang, Harmeet Singh,* Lam Research Corporation; *Satoshi Hamaguchi,* Osaka University, Japan

Plasma etching is a key technology for the manufacturing of semiconductor devices. Cryogenic etching, first introduced in 1988 by Tachi *et al.*, is an etching process at a very low material temperature (-50ºC or lower). The extremely low surface temperature typically contributes to faster etching, a better control of etched profiles, and reduced contamination from the chamber walls. However, there seems an optimal temperature for the best etching results and too low a temperature can impede the desired etching process. This study attempts to clarify the surface reaction mechanisms of cryogenic etching of silicon dioxides (SiO_2) by hydrogen fluoride (HF) plasmas with molecular dynamics (MD) simulations. In the MD simulations, a SiO_2 material surface was thermalized at 200 K (-73.15ºC) to emulate cryogenic conditions. Under such conditions, a relatively thick layer of gaseous species (HF molecules in our case) is formed on the material surface due to condensation. The surface is then exposed to highly energetic ions of Ar⁺ (or other ions from HF plasmas) with an incident

energy of 1 keV or higher, together with a large flux of gaseous HF molecules that continue to condense on the material surface. The MD simulation results showed that the energetic ion impact caused the mixing of F and H atoms from the condensed layer in the material's subsurface layer and lead to efficient reactive ion etching of SiO_2. The material surface chemical composition, the sputtering yields, and desorbed species were analyzed under different etching conditions. It was found that, with an increasing flux ratio of HF molecules to incident ions, more F atoms accumulated in the material's subsurface layer and the sputtering yield of SiO_2 increased.

12:00pm PS2-TuM-17 Mechanisms for Cryogenic Plasma Etching, *Yeon Geun Yook, **Mark J. Kushner**,* University of Michigan

The increasing demands for high-aspect-ratio (HAR) plasma etching for 3-dimensional devices has produced a resurgence in innovations in cryogenic etching. Cryogenic plasma etching (CPE) is a process in which the substrate in an otherwise conventional capacitively coupled plasma is cooled temperatures as low as –90 C. The lower substrate temperature is thought to increase the rate of adsorption of precursor species to the degree of having a thin condensed layer. CPE of dielectric materials have produced etch rates of up to several times that of conventional etching for aspect ratios exceeding 100 though the mechanisms for this performance are unclear. Recipes for CPE of SiO_2 range from fluorocarbon gases with H_2 additives to Ar/HF mixtures. A common feature of such mixtures is production of HF and H_2O (the latter by either gas phase or surface processes) which is hypothesized to produce a condensed hydrofluoric acid-like layer at the surface which would normally produce isotropic etching. The lower temperature reduces the rate of isotropic etching, which then enables anisotropic etching by ion-bombardment. The use of additives such as PF_3 suggests that there may also be a catalytic component to the process. In gas mixtures that do not contain, for example, fluorocarbon species there is not a natural source of passivation for sidewall control, which suggests that passivation is in the form of etch products.

In this presentation, results will be discussed from a computational investigation of CPE of SiO_2 on reactor and feature scales using the Hybrid Plasma Equipment Model (HPEM) and Monte Carlo Feature Profile Model (MCFPM). The processing conditions are single- and dual-frequency capacitively coupled plasmas of tens of mTorr pressure. An investigation of surface kinetics during CPE was first performed while artificially specifying reactive fluxes to the wafer for Ar/HF gas mixtures. The consequences of adsorption probabilities, redeposition of etch products and enhanced yield on etch rate and profile control will be discussed. Results for coupled reactor and feature scale simulations for CPE of SiO_2 using CF_4/H_2 and Ar/HF mixtures will then be discussed with the goal of determining whether these proposed mechanisms are consistent with practice in high volume manufacturing.

Quantum Science and Technology Mini-Symposium
Room 123 - Session QS-TuM

Superconducting Qubits and Surface Engineering for Quantum Applications

Moderators: David Pappas, Rigetti Computing, **Sisira Kanhirathingal**, Rigetti Computing

8:00am QS-TuM-1 Cryogenic Growth of Tantalum on Silicon and the Effect of Substrate Preparation on Superconducting Circuit Performance, *Teun van Schijndel*, University of California Santa Barbara; *Anthony McFadden*, NIST-Boulder; *Wilson Yánez-Parreño, Jason Dong*, University of California Santa Barbara; *Raymond Simmonds*, NIST-Boulder; *Christopher Palmstrøm*, University of California Santa Barbara

Recent advances in superconducting quantum information systems show the effectiveness of tantalum as a superconducting material, with qubits reaching coherence times up to 0.5 ms[1,2]. The growth of alpha-Ta is required for the realization of desirable superconducting properties. However, challenges persist as various sources of energy losses arise from material-related factors. One of the potential sources comes from the substrate-superconductor interface. Here, we demonstrate cryogenic growth (< 20 K) of polycrystalline alpha-Ta on silicon substrates. First, we show the ability to grow alpha-Ta on different substrate orientations and confirm with X-ray diffraction and transport that we form a similar polycrystalline-oriented film regardless of the substrate orientation. Furthermore, we explore different substrate preparation techniques such as HF etching and *in-situ* Atomic Hydrogen Annealing. We will study the silicon

substrates before growth by *in-situ* Scanning Tunneling Microscopy (STM). Next, we perform microwave measurements on fabricated CPW resonator circuits and 2D Transmon qubits and compare the performance of different surface orientations and substrate preparation techniques. We aim to correlate the findings in the microwave measurements with our observations in STM.

1) Place, A.P.M., *et al.*, *Nat Commun* **12**, 1779 (2021).

2) Wang, C., *et al.*, *npj Quantum Inf* **8**, 3 (2022).

8:15am QS-TuM-2 Thin Film Growth of Alpha- and Beta-Ta on Low-Loss Oxides for Superconducting Resonator Development, *Nate Price, Carter Wade, Lakshan Don Manuwelge Don,* Miami University; *Sushant Padhye, Huma Yusuf, Evgeny Mikheev,* University of Cincinnati; ***Joseph Perry Corbett**,* Miami University

Superconducting qubits are one of the leading candidates for creating quantum computers with the potential to surpass modern supercomputers in solving specific problems. Steady progress over the last 20 years has occurred, increasing the lifetime of quantum states and the number of qubits. A popular method to create a 2-level quantum system for quantum computation is to pattern a low-loss insulator/superconductor heterostructure into circuits. A recent new discovery in the qubit community is the fabrication of qubits from α-Ta thin films with improved coherence times of 0.5 ms! Despite recent success, an impetus for fundamental material science on insulator/superconductor heterostructure is well-recognized in the QISE community. We perform a systematic investigation of the nucleation and thin film microstructure of alpha- and beta-Ta grown on several low-dissipation insulating oxide substrates alongside identifying essential growth conditions that result in material conditions that adversely affect the sharpness of superconducting transition and Q-factor. Utilizing a combination of coil-assisted sputtering epitaxy, electron and scanning probe microscopy, alongside millikelvin microwave transport measurements, we uncovered the nucleation and thin film microstructure of alpha, beta, and mixed Ta films. We correlated this with impacts on transition temperature and Q-factor.

8:30am QS-TuM-3 Quantum Engineering of Superconducting Qubits, ***William D. Oliver**,* MIT   **INVITED**

Superconducting qubits are coherent artificial atoms assembled from electrical circuit elements and microwave optical components. Their lithographic scalability, compatibility with microwave control, and operability at nanosecond time scales all converge to make the superconducting qubit a highly attractive candidate for the constituent logical elements of a quantum information processor. Over the past decade, spectacular improvements in the manufacturing and control of these devices have moved the superconducting qubit modality from the realm of scientific curiosity to the threshold of technical reality. In this talk, we present recent progress, challenges, and opportunities ahead in the engineering of larger scale processors based on superconducting qubits.

9:15am QS-TuM-6 Characterization of Hydroxyls in Surface Oxides of Tantalum and Their Mitigation for Superconducting Qubits, ***Ekta Bhatia**, Nicholas Pieniazek, Aleksandra Biedron, Sandra Schujman,* NY CREATES; *Hunter Frost,* Tokyo Electron Ltd. Technology Center America (TTCA) LLC; *Zhihao Xiao, Stephen Olson, Jakub Nalaskowski, Kevin Musick, Thomas Murray, Corbet Johnson, Satyavolu Papa Rao,* NY CREATES

Recently, Ta has attracted more attention [1] in the superconducting quantum community due to the high coherence times in superconducting qubits when it replaces Nb in the capacitor pads [2]. The surface oxides of superconducting metals have been demonstrated to be a major contributor to microwave loss mechanisms [3], and hence to decoherence in superconducting qubits. In this study, we quantify the concentration of hydroxyls [OH], and their variation with depth in various surface oxides of Ta. We also demonstrate, for the first time, that it is possible to modulate the extent to which such tantalum hydroxyls are present by replacing the native oxide of Ta with a chemically-formed surface oxide. Using Time-of-Flight Secondary Ion Mass Spectrometry (ToF-SIMS) analysis, we were able to quantitatively determine the concentrations of TaOH as a function of depth, for both the native oxide of Ta, as well as for the surface oxide that is formed during chemical mechanical planarization of Ta. The effect of fiber texture in the deposited Ta film on the oxidation and the incorporation of [TaOH] was also studied. Angle-resolved X-ray photoelectron spectroscopy was used to study the composition of the surface oxide – specifically, the prevalence of Ta_2O_5 on the surface, with suboxides of Ta closer to the

interface with metallic Ta, with thickness information obtained from transmission electron microscopy. It has been hypothesized [3] that TLS are not uniformly distributed throughout the oxide - our observations not only substantiate that hypothesis but indicate that hydroxyls are a possible molecular origin for such TLS. In a fashion analogous to studies of aluminum oxide [4], where the rotational freedom of the [OH] bond is suggested to be a source of the TLS, it is possible that [OH] plays a similar role in tantalum oxides as well. We also explore ways to modulate TaOH using nitridization on the Ta surface. Our findings provide ways to mitigate the effects of two-level systems in superconducting quantum devices.

[1] S. Papa Rao *et al.*, *Electrochem. Soc. Trans.* **85** (6), 151 (2018).

[2] N.P. de Leon *et al.*, *Science* **372**, eabb2823 (2021).

[3] K. D. Crowley *et al.*, *Phys. Rev. X* **13**, 4 (2023).

[4] L. Gordon *et al.*, *Sci. Rep.* **4**, 7590 (2014).

9:30am **QS-TuM-7 Identifying and Mitigating Sources of Loss in Superconducting Qubits**, *Akshay Murthy, Mustafa Bal, Francesco Crisa, Shaojiang Zhu, Daniel Bafia, Jaeyel Lee, Alex Romanenko, Anna Grassellino,* Fermilab **INVITED**

Advances in our understanding of materials has played a crucial role driving recent increases in achievable coherence times and gate fidelities in superconducting transmon qubits. This includes identifying defects, impurities, interfaces, and surfaces present within the device geometry as well as implementing new strategies to mitigate the deleterious effects introduced by these disordered regions. As part of the Superconducting Quantum Materials and Systems (SQMS) center, we have deployed a wide variety of unique materials characterization techniques in tandem with microwave measurements to examine sources of loss in these devices. These include materials characterization techniques such as scanning/transmission electron microscopy, x-ray diffraction/reflectivity, scanning probe microscopy, secondary ion mass spectrometry, and atom probe tomography performed at both room temperature and cryogenic temperatures in addition to microwave loss measurements leveraging high quality factor superconducting radiofrequency (SRF) cavities. Through this effort, researchers have identified a wide variety of defective structures that serve as sources of two-level systems (TLS) or non-TLS dissipation as well as estimate their relative impacts to build a hierarchy of losses.

In this talk, I will discuss our results demonstrating that the surface oxide associated with superconducting niobium metal serves as a major source of microwave loss and that this loss scales with oxygen vacancies present in this oxide region. Based on this insight, we encapsulate the surface of niobium with various metal and dielectric layers that eliminate and prevent the formation of this lossy niobium surface oxide upon exposure to air and systematically achieve coherence times on the order of hundreds of microseconds. In order to continue to extend coherence times such that they reproducibly exceed beyond a millisecond, the loss hierarchy we have developed indicates that additional materials development to eliminate loss associated with the underlying substrate as well as the Josephson junction is needed. During the second half of my talk, I will discuss ongoing efforts in this area as well as the progression along our Quantum Technology roadmap that will move us from individual qubits to scalable, high coherence, multi-qubit platforms.

11:00am **QS-TuM-13 Dielectric Loss and Two-Level Systems in Superconducting Qubits**, *Chen Wang,* University of Massachusetts **INVITED**

Superconducting circuits are one of the leading technology platforms for the development of a practical quantum computer.In superconducting quantum circuits, qubits are typically constructed from Al/AlOx/Al Josephson tunnel junctions and patterned superconducting thin films such as Al, Nb, Ta on crystalline Si or sapphire substrate, and operated with external microwave pulses.Superconducting qubits enjoy advantages in their circuit design flexibilities, lithographic scalability, and operational clock speed, but must overcome decoherence and parameter variability and fluctuations from the solid-state environment.In particular, microwave noise from dielectric materials, including the Josephson junction, the bulk substrate, and various interfaces, have increasingly stood out as a limiting factor for both the lifetime and frequency stability of superconducting qubits.Such dielectric dissipation and fluctuation have been attributed to the omni-presence of a large number of discrete microscopic two-level systems (TLS) over an extremely broad frequency ranges (from kHz to GHz).Various improvements in qubit design and materials processing have led to substantial improvement of qubit coherence over the past decade through the mitigation of the TLS problem, but any atomistic understanding of these TLS in relevant materials remains elusive.In this talk, I will give a

birds-eye view of the phenomenological studies of dielectric loss and two-level systems in superconducting circuits, and explain how the dream of building a quantum computer has been intertwined with so-far the most sensitive probe and the most demanding quest of traditional but pristine materials.

11:30am **QS-TuM-15 Measuring Loss Tangents of Substrates for Superconducting Qubits with Part per Billion Precision**, *Daniel Bafia, Akshay Murthy, Andrei Lunin, Geev Nahal, Adam Clairmont, Mustafa Bal, Alexander Romanenko, Anna Grassellino,* Fermi National Accelerator Laboratory

This talk will present a comparative study on the dielectric loss tangent of various substrates measured with an ultra-high quality factor niobium SRF cavity at the low electric fields and mK temperatures relevant for superconducting quantum computing architectures. We study the loss tangent evolution of c-plane sapphire post various treatments and correlate the resulting performance with materials analysis including time-of-flight secondary ion mass spectrometry and atomic force microscopy and report on key findings.

This material is based upon work supported by the U.S. Department of Energy, Office of Science, National Quantum Information Science Research Centers, Superconducting Quantum Materials and Systems Center (SQMS) under contract number DE-AC02-07CH11359.

11:45am **QS-TuM-16 Enhanced Qubit Frequency Targeting and Quantum Gate Fidelities in a 25-Qubit Superconducting Quantum Processor**, *Amr Osman, Liangyu Chen, Hang-Xi Li, Andreas Nylander, Marcus Rommel, Stefan Hill, Eleftherios Moschandreou, Daryoush Shiri, Michele Faucci Giannelli, Anita Fadavi Roudsari, Giovanna Tancredi, Jonas Bylander,* Chalmers University of Technology, Gothenburg, Sweden **INVITED**

Crosstalk poses a significant challenge to the scalability of superconducting quantum processors. This issue can be mitigated by implementing a careful frequency crowding scheme that ensures sufficient separation between neighboring quantum gate frequencies. Nevertheless, deviations in the fabrication process from the design parameters can undermine this scheme, leading to reduced qubit-gate fidelities. In this study, we designed and fabricated a 25-qubit quantum processor in a flip-chip geometry using a specially tailored frequency allocation scheme for parametric-gate architectures [1]. We present an extensive characterization of parameter targeting in this quantum processor, exploring the uncertainties introduced by the flip-chip bonding, and discussing the implications for crosstalk and quantum-gate fidelities.

[1] A. Osman, J. Fernandez-Pendas, C. Warren, S. Kosen, M. Scigliuzzo, A. Frisk Kockum, G. Tancredi, A. Fadavi Roudsari, and J. Bylander, "Mitigation of frequency collisions in superconducting quantum processors," Phys. Rev. Res. 5, 043001 (2023).

Surface Science
Room 120 - Session SS+CA+LS-TuM

Electrochemical Transformations on Surfaces
Moderators: Florencia C. Calaza, Instituto de Desarrollo Tecnológico para la Industria Química, **Zhuanghe Ren**, University of Central Florida

8:00am **SS+CA+LS-TuM-1 Beyond Static Models: Chemical Dynamics in Energy Conversion Electrocatalysts**, *Beatriz Roldan Cuenya,* Fritz-Haber-Institut der Max-Planck-Gesellschaft, Germany **INVITED**

Environmentally friendly technologies for green energy generation and storage in the form of chemical bonds are being urgently sought in order to minimize the future consequences of climate change. The latter includes developing more efficient and durable materials for green H_2 production from water splitting as well as for the re-utilization of CO_2 via its electrocatalytic reduction into value-added chemicals and fuels. Nonetheless, in order to tailor the performance of such energy conversion catalysts, fundamental insight must be gained on their evolving structure and surface composition under reaction conditions.

This talk will illustrate how morphologically and chemically well-defined pre-catalysts experience drastic modifications under operation. Examples for the electrocatalytic reduction of CO_2 as well as the oxygen evolution reaction in water splitting will be given. The model pre-catalysts studied range from size and shape-controlled nanoparticles (Co_3O_4, Fe/Co_3O_4, Fe/NiO, Cu_2O, ZnO/Cu_2O, Au/Cu_2O), thin films (NiO_x, $CoFe_2O_4$, Co_3O_4, Fe_3O_4) to single crystals (differently-oriented Cu surfaces). The need of a

synergistic multi-technique *operando* microscopy, spectroscopy and diffraction approach will be evidenced in order to follow the active state formation of complex catalytic materials. Correlations between the dynamically evolving structure and composition of the catalysts and their activity, selectivity and durability will be featured.

8:30am SS+CA+LS-TuM-3 Sulfur-Doped Carbon Support Boosts CO2RR Activity of Ag Electrocatalysts, *Xingyi Deng, Dominic Alfonso, Thuy-Duong Nguyen-Phan, Douglas Kauffman,* National Energy Technology Laboratory

In this work, we show that the activity of Ag electrocatalysts for electrochemical CO_2 to CO conversion is improved when supported on sulfur-doped (S-doped) carbon materials. S-doped carbon support was created by treating the heavily sputtered, highly oriented pyrolytic graphite (HOPG) in H_2S at elevated temperatures, as confirmed by the S 2p X-ray photoelectron spectroscopy (XPS) peak. Scanning tunneling microscopy (STM) images indicated that Ag nanoparticles supported on S-doped HOPG had similar size distributions as those supported on sulfur-free (S-free) HOPG. While both catalysts reached > 90% CO Faradaic efficiency (FE_{CO}) at E = -1.3 V vs. the reversible hydrogen electrode (RHE) in the CO_2 reduction reaction (CO_2RR), Ag catalysts supported on S-doped HOPG demonstrated 70% higher CO turnover frequency (TOF_{CO} = 3.4 $CO/atom_{Ag}/s$) than those supported on S-free HOPG (TOF_{CO} = 2.0 $CO/atom_{Ag}/s$). Preliminary calculations based on density functional theory (DFT) indicated a more favorable energetic pathway of CO_2-to-CO at the C-S-Ag interface, tentatively consistent with experiments. These results hint at a new approach to design active and selective electrocatalysts for CO_2 conversion.

8:45am SS+CA+LS-TuM-4 Non-Metal Cations for Enhancing CO2 Electroreduction on Bismuth Electrode, *Theodoros Panagiotakopoulos, Kaige Shi, Duy Le, Xiaofeng Feng,* University of Central Fllorida; *Talat Rahman,* University of Central Florida

In exploring the effectiveness of non-metal cations in CO_2 electroreduction, we have carried out a comparative examination of the mechanisms for CO_2 electroreduction to formate (HCOO–) and CO on the Bi(111) electrode in the presence of cations, Na+ and NH_4^+, using grand canonical density functional theory. Our results reveal that the reduction of CO2 to formate is driven by the direct hydrogenation of aqueous CO_2 with a hydrogen atom adsorbed on the electrode (H*), i.e., $CO_2(aq) + H^* \rightarrow HCOO^-$. The activation barrier for this process is found to be small, less than 100 meV, in the presence of both cations. Furthermore, our results show that the adsorbed intermediate COOH* is formed via a proton shuttling process, i.e., H* moves from the Bi(111) electrode to a H_2O molecule and one of its H atoms is then transferred to a CO2*. The activation energy barrier for this step was determined to be 0.77 eV and 0.75 eV in the presence of Na^+ and NH_4^+, respectively. CO is formed via the dissociation of COOH* species with an activation energy barrier of 0.62 eV and 0.01 eV in the presence of Na^+ and NH_4^+, respectively. These findings lead to two important conclusions: 1) the non-metal cation NH_4^+ can be equally effective as the alkali metal cation Na^+ in promoting the CO_2 electroreduction to formate; 2) NH_4^+ is actually more effective than Na^+ in promoting the CO_2 electroreduction to CO on the Bi(111) electrode, in excellent agreement with experimental observations [1].

[1]K. Shi, D. Le, T. Panagiotakopoulos, T. S. Rahman, and X. Feng, Effect of Quaternary Ammonium Cations on CO_2 Electroreduction (Submitted, 2024).

This work is supported in part by the U.S. Department of Energy under grant DE-SC0024083.

9:00am SS+CA+LS-TuM-5 AVS Russell and Sigurd Varian Awardee Talk/SSD Morton S. Traum Award Finalist Talk: How do Cations Promote CO2 Reduction at the Electrode-Electrolyte Interface, *Kaige Shi[1][2], Duy Le, Theodoros Panagiotakopoulos, Talat Rahman, Xiaofeng Feng,* University of Central Florida

Electrochemical CO2 reduction reaction (CO2RR) can enable a promising path towards sustainable fuel production and closing the carbon cycle. Despite the reports of numerous electrocatalysts, the mechanism of CO2RR at the electrode-electrolyte interface remains to be elucidated, particularly on the role of electrolyte cations in the reaction. While most studies of CO2RR focused on alkali metal cations, we investigate CO2RR using quaternary ammonium cations, which provide unique tunability in size, shape, and charge distribution to elucidate the cation effect. For the CO2RR on a Bi catalyst that produces both CO and formate, we find that the cations are essential for both products. Furthermore, we observe a significant impact of the cation identity and concentration on CO production but a minor one on formate production. Our computational studies reveal that cations are required to stabilize adsorbed *CO2 on Bi surface via electrostatic interaction, and the quaternary ammonium cations have a more profound effect on the CO2 adsorption characteristics and CO2RR activity than metal cations. The adsorbed *CO2 is an essential step for CO production, but not necessary for formate production due to the pathway with direct reaction of aqueous CO2 with surface *H species. Based on the understanding, we employ the substitute ammonium cations to enhance CO2 electrolysis in a gas-diffusion-electrode (GDE) flow cell, which achieves multi-fold improvement of the activity for CO2RR to CO on Bi and other metal catalysts, as compared to that using alkali metal cations. Our work elucidates the critical effect of cations on the CO2RR at the electrode-electrolyte interface and demonstrates a strategy to enhance electrocatalysis by optimizing electrolyte composition.This work is supported by the U.S. Department of Energy, Office of Science, Office of Basic Energy Sciences Catalysis Science program under Award Number DE-SC0024083.

9:15am SS+CA+LS-TuM-6 Atomistic Simulations on the Triple-Phase Boundary in Proton-Exchange Membrane Fuel Cells, *Juan Jimenez, German Soldano, Esteban Francesichini,* Facultad de Ciencias Quimicas UNC, Argentina; *Marcelo Mariscal,* Universidad Nacional de Cordoba, Argentina
INVITED

In this work, we use molecular dynamics simulations and electrochemical experiments on a Nafion/Pt/C system. We perform a systematic analysis, at an atomistic level, to evaluate the effect of several fundamental factors and their intercorrelation in the ECSA (electrochemical surface area) of the catalysts. Besides, we evaluate the diffusion and structuring processes of water at different system interfaces. Overall, this investigation allows us to rationalize how the catalyst utilization is affected, which is an important step in establishing the relationship between the environment and the effectiveness and durability of the PEMFC system. It is important to consider that when experimentally analyzing the changes originating from the different experimental parameters in the operation of a fuel cell, only the average effect of the catalyst, flow field and membrane as a whole can be measured, and it is not possible to separate the corresponding contributions, even less from a region as complex as the TPB. Thus, computational studies provide the appropriate tools for studying each of the parameters separately and in sufficient detail to understand the effects found experimentally.

Proton Exchange Membrane Fuel Cells (PEMFCs), are a well-developed technology aimed at providing cleaner and more sustainable energy solutions. They offer a promising alternative to traditional fossil fuel systems that produce harmful emissions. However, the success of these cells depends greatly on the Three-Phase Boundary (TPB), a critial region composed by the ionomer (liquid, usually Nafion), catalyst (solid, usually platinum) and fuel (H_2 gaseous) interact and is the most important region in a fuel cell, as it is where the electrochemical reaction occurs with the adsorption of the fuel (or oxygen) on the catalyst surface, electron transfer to form H^+ and subsequent conduction of the generated ions to the ionomer for transport across the membrane. This is because experimentally only a few very general parameters, such as temperature, humidity or fuel flow rate, can be modified, and each of these parameters affects all components of the fuel cell and not just the three-phase region so it is impossible to separate the contributions corresponding to the three-phase boundary from the effects occurring, for example, in the membrane or from the kinetic effects in catalysis. Therefore, understanding, characterizing, and optimizing the variety of factors that affect the TPB content in fuel cells provide excellent opportunities for performance enhancement.

9:45am SS+CA+LS-TuM-8 Mechanism of Activity Decrease in Orr on Nitrogen-Doped Carbon Catalysts Based on Acid-Base Equilibrium, *Kenji Hayashida, Rei Shimizu,* Tsukuba University, Japan; *Junji Nakamura, Miho Isegawa,* Kyushu University, Japan; *Kotaro Takeyasu,* Hokkaido University, Japan

Fuel cells, which use the energy carrier hydrogen directly as a fuel, are important devices for achieving carbon neutrality. However, current fuel cell catalysts use a large amount of platinum, therefore a fuel cell catalyst that can replace platinum in the future is essential. A plausible candidate is nitrogen-doped carbon catalysts, which are durable and abundantly available. However, their activity is very low in acidic media, a practical condition, and this is the biggest challenge to overcome. In this study, we focused on the acid-base equilibrium of pyridinic nitrogen (pyri-N), the active site of nitrogen-doped carbon-based catalysts, to elucidate the

---

[1] **AVS National Student Awardee**
[2] **SSD Morton S. Traum Award Finalist**

reaction mechanism and clarify the mechanism of reduced activity in acidic media. Using a model catalyst with pyri-N-containing molecules adsorbed on a carbon support, we observed the change in electronic state upon immersion in electrolyte and application of potential, and analyzed the kinetics of the activities. It was found that the pyri-N, which is the active site, becomes protonated and hydration-stabilized in the acidic electrolyte, resulting in a decrease in activity. In particular, kinetic analysis showed that the 2 or 2+2 electron pathway via H_2O_2 proceeds independently of the acid-base equilibrium. X-ray photoelectron spectroscopy revealed that the potential for the formation of pyri-NH, associated with oxygen adsorption, an important reaction intermediate, is 0.4 V lower in acidic than in basic conditions. This is due to the formation of pyri-NH+, in which pyri-N is protonated by acid-base equilibrium and its stabilization by hydration lowers the pyri-NH formation potential, resulting in lower activity in acidic conditions. Therefore, to improve catalytic activity in acidic conditions, it is important to increase the redox potential of this pyri-NH formation. A possible guideline is to decrease the pK_a and impart hydrophobicity.

11:00am SS+CA+LS-TuM-13 Particle Size Effect of Ru Nanocatalyst for Nitrate Electroreduction, *Zhen Meng, Kaige Shi, Zhuanghe Ren, Xiaofeng Feng,* University of Central Florida

Electrochemical nitrate reduction reaction (NO_3RR) shows great promise for the recycling of nitrate from wastewater sources for the denitrification of wastewater and sustainable NH_3 production. Among various catalytic materials, Ru shows a high activity and selectivity for the NO_3RR to NH_3, while the effect of Ru atomic structure and active sites on the NO_3RR activity and selectivity remains ambiguous. Here, we prepare size-controlled Ru nanoparticles ranging from 2.2 to 7.1 nm and investigate the dependence of the NO_3RR on the Ru particle size. The activity (current density) decreases along with the increase of Ru particle size, mainly due to the more Ru surface area for the smaller particles, given the same Ru loading. In contrast, the specific (Ru-surface-area-normalized) activity for the NO_3RR exhibits a volcano-shaped dependence on the particle size, with 4.9-nm Ru nanoparticles showing the highest activity, which should reflect their intrinsic activity and active sites. On the other hand, the specific activity for the competing hydrogen evolution reaction (HER) increases with the particle size, so that an optimal selectivity for NO_3RR to NH_3 is also reached on the 4.9-nm Ru nanoparticles. Looking into the size-dependent ratio of Ru surface sites, we find that the superior activity of 4.9-nm Ru nanoparticles correlates with the surface population of the D_5 step site, which favors the adsorption of NO_3RR reaction intermediate as compared to other surface sites. This work is supported by the National Science Foundation (NSF) Chemical Catalysis Program under Grant No. 1943732.

11:15am SS+CA+LS-TuM-14 Probing Solvation with Liquid Jet Photoelectron Spectroscopy, *Jared Bruce, Stephen Faussett, Rebecca Woods,* University of Nevada, Las Vegas*; Kimberly Zhang,* MIT*; Amanda Haines, Filipp Furche,* University of California Irvine*; Robert Seidel,* Helmholtz Zentrum Berlin, Germany*; Bernd Winter,* Fritz-Haber-Institut der Max-Planck-Gesellschaft, Germany*; John Hemminger,* University of California Irvine

The local chemical structure around solutes in aqueous solution is challenging to characterize on a molecular scale given the amount of hydrogen bonding interactions that occur in solution. Liquid jet photoelectron spectroscopy (LJ-XPS) can be a critical tool providing valuable chemical information both near the surface and in the bulk of the solution.

In this talk I will discuss how a combination of liquid jet photoelectron spectroscopy and electronic structure calculations were used to investigate the local chemical solvation of two systems – Fe^{2+} and acetic acid aqueous solutions. Each system has specific interfacial behavior that was investigated with liquid jet photoelectron spectroscopy. Fe showed coordination events with small anions like Cl^- alter the relative concentration of both species near the interface, whereas acetic acid shows alterations to its local solvation environment as a function of both the proximity to the interface and the pH of the bulk solution. Each will be discussed in detail and recent work from the lab at UNLV will be highlighted.

Thin Films
Room 115 - Session TF1-TuM

Thin Films: Controlling Crystalline Phases
Moderators: Lauren Garten, Georgia Institute of Technology, **April Jewell**, Jet Propulsion Laboratory

8:00am TF1-TuM-1 Peter Mark Memorial Award Talk: Strain-Induced Magnetism and Superconductivity in Single-Crystalline Heusler Membranes, *Jason Kawasaki[1],* University of Wisconsin - Madison **INVITED**
Single-crystalline membranes of functional materials enable the tuning of properties via extreme strain states; however, conventional routes for producing membranes require the use of sacrificial layers and chemical etchants, which can both damage the membrane and limit the ability to make them ultrathin. I will describe how the growth of thin films on graphene-terminated substrates enables synthesis of single crystalline, mechanically exfoliatable membranes [1,2]. Using rippled membranes of the Heusler compound GdPtSb, we demonstrate the first experimental example of flexomagnetism, that is, ferro/ferri-magnetism induced by strain gradients [3]. I will also describe evidence of superconductivity induced in another Heusler membrane via strain. More broadly, Heusler membranes provide highly tunable platform for tuning ferroic order, topological states, and correlations [4].

[1] S. Manzo, et. al., Nature Commun., 13, 4014 (2022). https://doi.org/10.1038/s41467-022-31610-y

[2] D. Du et. al., Nano Lett. 22, 21, 8647 (2022). https://doi.org/10.1021/acs.nanolett.2c03187

[3] D. Du, et. al., Nature Commun., 12, 2494 (2021). https://doi.org/10.1038/s41467-021-22784-y

[4] D. Du, e. al. APL, 122, 170501 (2023). https://doi.org/10.1063/5.0146553

8:30am TF1-TuM-3 Stabilization of P63cm ScFeO₃ on (111) Pt Mediated via an Fe₃O₄ Interlayer, *Marshall Frye, Jonathan Chin,* Georgia Institute of Technology*; Nicholas Parker, Matthew Barone,* Cornell University*; Lauren Garten,* Georgia Institute of Technology

Marshall Frye1, Jonathan Chin1, Nicholas Parker2, Matthew Barone3, Lauren M. Garten1

1. School of Materials Science and Engineering, Georgia Institute of Technology, Atlanta, Georgia 30332, USA
2. Department of Materials Science and Engineering, Cornell University, Ithaca, New York 14850, USA
3. Platform for the Accelerated Realization, Analysis, and Discovery of Interface Materials (PARADIM), Cornell University, Ithaca, New York 14853, USA

Ferroelectric photovoltaics are an emerging renewable energy technology where charge separation occurs in a single layer and the open-circuit voltage can be larger than the bandgap. The metastable $P6_3cm$ phase of $ScFeO_3$ (h-$ScFeO_3$) is an ideal candidate for ferroelectric photovoltaics due to its polar crystal structure and narrow bandgap (1.2 eV). While h-$ScFeO_3$ can be grown on Al_2O_3 using a layered approach,[1] on conductive substrates, such as (111) Pt, only the ground state bixbyite phase of $ScFeO_3$ is stable. h-$ScFeO_3$ growth on a substrate with high conductivity and low epitaxial strain is critically needed for photovoltaic device fabrication.

In this work we grew h-$ScFeO_3$ on (111) platinum via molecular beam epitaxy (MBE). The stabilization of the h-$ScFeO_3$ phase was enabled by an Fe_3O_4 interlayer. This approach is adapted from reports of growth of hexagonal $LuFeO_3$ on oriented Fe_3O_4 via MBE.[2] Epitaxial (111) Pt which was deposited on c-Al_2O_3 was found to have a narrow (~0.005°) full width at half maximum (FWHM) rocking curve about the (111) peak, indicating a highly crystalline film. After depositing (111) Pt, a Fe_3O_4 layer was deposited. $ScFeO_3$ was then deposited on the Fe_3O_4 film with alternating depositions of Sc and Fe.[1] The films are solely (000$2l$) oriented of h-$ScFeO_3$ with clear Laue oscillations. Furthermore, rocking curves about the (0004) hexagonal $ScFeO_3$ peak have a FWHM of 0.07°, indicating a highly crystalline film. Films grown on conductive substrates then enabled measurements of the carrier mobility and dielectric response of the h-$ScFeO_3$. Overcoming the challenge of growing h-$ScFeO_3$ on conductive substrates will allow us to utilize these materials advantageous properties for high-efficiency photovoltaics.

---

[1] **Peter Mark Memorial Award Winner**

1. Garten, L. M.*et al.* Stromataxic Stabilization of a Metastable Layered ScFeO₃ Polymorph. *Chem. Mater.* **33**, 7423–7431 (2021).

1. Zhang, X. *et al.* Effect of interface on epitaxy and magnetism in h-RFeO₃/Fe₃O₄/Al₂O₃ films (R = Lu, Yb). *J. Phys. Condens. Matter* **29**, 164001 (2017).

8:45am TF1-TuM-4 Optimizing Sputter Deposition of Bi₂Te₃ and Sb₂Te₃ for Photolithographic Device Fabrication, *Rumana Zahir,* University of Central Florida*; F. Javier Gonzalez,* Truventic LLC*; Darian Smalley, Akash Hari Bharath, Edgar Nino, Kalpathy Sundaram, Masahiro Ishigami, Robert Peale,* University of Central Fllorida

Antenna-coupled thermoelectric junctions have potential for THz and mm-wave detection and energy harvesting. These require patterned deposition of thermoelectric materials with a junction at the feed of a suitable antenna, where the junction is heated by the received radiation. Sb₂Te₃ and Bi₂Te₃ thin films have ideal thermoelectric properties for this application, and deposition over patterned photoresist on suitable substrate followed by lift-off is the simplest patterning approach. Our optimization study of unpatterned sputtered films on heated substrates required temperatures exceeding 175 °C to obtain ideal thermoelectric performance. Such temperatures tend to carbonize photoresists, complicating the subsequent lift-off. Here we report the results of a new optimization study using lower substrate temperatures during sputtering followed by annealing. Our approach considers three factors in a two-level full factorial optimization experiment. The three factors are substrate temperature during sputtering, subsequent vacuum annealing temperature, and annealing time. High and low values are selected for each factor giving 8 possible combinations. A mid-point tests for curvature in the main effects. The nine depositions per material were performed on glass substrates in randomized order. Graphs of the response (Seebeck coefficient) averaged over two of the factors plotted vs the third reveal the main effects of varying each factor. Graphs of the response averaged over one of the factors and plotted vs a second factor for each value of the third factor reveal interactions between factors. Examples of device fabrication following the optimized recipe, characterization, and simulation will be presented.

9:00am TF1-TuM-5 Hybrid Pulsed Laser Deposition Growth of Epitaxial Chalcogenides, *Mythili Surendran,* USC

Chalcogenides such as transition metal dichalcogenides (TMDC) and chalcogenide perovskites (CP) have garnered attention for their electronic and photonic properties. Despite their promising potential for electronic applications, the epitaxial growth of these materials is still in its nascent stages. Adding to the complexity, a most of the emerging chalcogenides are vapor pressure mismatched transition metal compounds. The stark differences in vapor pressures between transition metal cations and chalcogen anions present a great challenge during epitaxial growth. This challenge is particularly pronounced in sulfide thin film growth and exacerbated in CPs due to their complex stoichiometries. Addressing these complexities demands innovative strategies to achieve precise flux control and maintain stoichiometric integrity during epitaxial growth.

Sulfides have been mostly grown using CVD, although MBE, MOCVD, pulsed laser deposition (PLD)and several other techniques have been exploited. However, large area and high-quality growth with precise and uniform thickness control and low defect densities still remain a challenge due to a large cation-sulfur vapor pressure mismatch, corrosive and reactive nature of most chalcogen precursors, high synthesis temperatures and the propensity to oxidize easily in the presence of oxygen at these high temperatures. Most growth techniques utilize H2S as the sulfur source. However, H₂S is a toxic, hazardous, and flammable gas and require high temperatures for efficient decomposition and sulfurization, resulting in high defect densities.

Here, we discuss epitaxial growth of CPs and TMDCs (specifically sulfides) using a novel hybrid PLD (*Adv. Mater* 2024) approach wherein we employed organo-sulfur precursors as the sulfur source. Large area epitaxial thin films of Group IV 2D chalcogenides such as TiS₂ (metallic) and ZrS₂ (semiconducting) and CPs such as BaZrS₃ and BaTiS₃ were successfully grown. This novel method utilizes precursors with optimum vapor pressures and they decompose at a lower temperatures (~250-400℃) to provide dissociated sulfur species. Structural and electrical characterization, along with low temperature transport studies reveal low defect densities and high carrier mobilities in these films. This work emphasizes on low temperature growth of high mobility refractory metal-based sulfides, especially with BEOL compatibility. Although slightly elevated temperatures were required for CPs, the interfacial roughness and optoelectronic performance were improved. The potential of these chalcogenides as candidates for transparent and conducting layers in chalcogenide-based optoelectronic devices will be discussed.

9:15am TF1-TuM-6 Atomic Layer Deposition of Entropy Stabilized ZrₓTaᵧOz, *Shane Witsell, Jessica Haglund,* **John Conley,** Oregon State University

High entropy oxides (HEOs) can exhibit enhanced mechanical, refractory, catalytic, cryogenic, and dielectric properties over conventional materials [1]. The classic understanding of HEOs is founded on a high degree of configurational disorder as well as a positive enthalpy of formation. It has been thought that five discrete elements were necessary to cause this high degree of disorder (S_{config} >1.6R,J/mol*K). However, it has recently been shown that A₆B₂O₁₇ perovskites, where A = Zr or Hf and B = Nb or Ta can demonstrate an exceptionally high degree of disorder (S_{config} of 4.50R, J/mol*K) [2]. Though these materials have been synthesized by powder sintering [5] and ternary ZrTaO has been demonstrated with atomic layer deposition (ALD) [3], entropy stabilized ZrₓTaᵧOz has yet to be achieved via ALD. Herein we report the successful transformation of ALD ZrₓTaᵧOz into the entropy-stabilized form.

ZrO₂ and Ta₂O₅ were synthesized via ALD using tantalum ethoxide (Ta(OEt)₅) and zirconium chloride (ZrCl₄), respectively, with O₃ [3]. ZrₓTaᵧOz was deposited using modulated ZrCl₄/N₂/Ta(OEt)₅/N₂/O₃/N₂ super cycles [4]. Films were deposited on Si substrates and were amorphous as-deposited. Following annealing at 800℃ for 30 minutes in N₂, x-ray diffractometry (XRD) spectra (Fig. 1) show a strong overlap between annealed ALD Zr₆Ta₂O₁₇ and the expected peaks for HEO stabilized A₆B₂O₁₇ [5], and no overlap with binary ZrO₂ or Ta₂O₅.

Metal/insulator/Si (MIS) electrical devices were fabricated using Ag top electrodes. 800 °C annealed entropy stabilized ZrₓTaᵧOz devices exhibited unipolar threshold voltage switching when illuminated, with a ON/OFF current ratio of 7x10³ and a ~ +0.56 MV/cm SET voltage. Switching did not occur in the dark. Unannealed amorphous ZrₓTaᵧOz devices did not exhibit switching in this voltage range but required a +1.8 MV/cm SET voltage and had an ON/OFF ration of only ~10². Switching under illumination is still under investigation and was possibly due to the formation of oxygen vacancies in the entropy stabilized matrix as opposed to the un-annealed amorphous form [6].

1. Aamlid, S. *et al.* J. Am. Chem. Soc. **145** (2023).
2. Voskanyan, A. *et al.* Scritpa Materiala **204** (2021).
3. Kukli, K. *et al.* AIP Advances **7** (2017).
4. Nguyen, C. *et al.* Chem. Mater. **33** (2021).
5. Spurling, R. *et al.* J. Mater. Sci **85** (2023).
6. Li, H. *et al.* Coatings **11** (2021)

9:30am TF1-TuM-7 Stabilizing Oriented Barium Nickelate Thin Films, *Ian Graham, Marshall Frye, Lauren Garten,* Georgia Institute of Technology

Oxygen evolution reaction (OER) is the rate limiting step inhibiting the production of fuel from water.[1,2] Barium nickelate (BaNiO₃) is a potential candidate for OER catalysis because it has an order of magnitude higher catalytic activity for the OER compared to the current benchmark iridium oxide (IrO₂).[1] Understanding the impact of crystallographic orientation and oxygen vacancy concentration on OER catalytic activity is critical to enabling BaNiO₃ catalysts. [1,2]

In this work, we demonstrate the growth of oriented BaNiO₃ films via pulsed laser deposition (PLD). Films were deposited from a BaNiO₂.₃₆ target onto (0001) Al₂O₃ substrates over a range of deposition temperatures, laser fluences, and oxygen partial pressures. X-ray diffraction shows that the orientation of BaNiO₃ is dependent on the deposition temperature. The (11-20) orientation of BaNiO₃ grows at temperatures below 500 °C, whereas increasing the deposition temperature from 400 °C to 500 °C leads to (10-10) BaNiO₃. Further increasing the deposition temperature to 700 °C changes the orientation of the film to predominately (0002) oriented. X-ray photoelectron spectroscopy shows the oxidation state of films deposited under different deposition oxygen partial pressures. Reducing deposition pO₂ from 1.65 x 10⁻² mbar to 1.27 x 10⁻² mbar shows a 4% decrease in oxygen atomic percentage. Atomic force microscopy shows that decreasing the laser fluence and oxygen partial pressure decreases the root mean square surface roughness of the deposited films. Reducing the laser fluence from 3.5 J/cm² to 2.5 J/cm² shows a 3 nm decrease in the root mean square surface roughness, while decreasing the oxygen partial pressure from 9.1 x 10⁻² mbar to 1.65 x 10⁻² mbar shows a 1 nm decrease in root mean square surface roughness. Co-planar top electrodes enabled impedance spectroscopy and dielectric measurements. Impedance data shows the migration of oxygen vacancies which play an important role in OER. Elucidating the impact of crystallographic orientation on oxygen vacancy

migration gives insight into how crystallographic orientation affects OER catalytic activity.

References

1. Lee, J. G. *et al.* A New Family of Perovskite Catalysts for Oxygen-Evolution Reaction in Alkaline Media: BaNiO $_3$ and BaNi $_{0.83}$ O $_{2.5}$. *J. Am. Chem. Soc.* **138**, 3541–3547 (2016).
2. Plevová, M., Hnát, J. & Bouzek, K. Electrocatalysts for the oxygen evolution reaction in alkaline and neutral media. A comparative review. *Journal of Power Sources* **507**, 230072 (2021).

Thin Films
Room 115 - Session TF2-TuM

Thin Films for Extreme Environments

Moderators: April Jewell, Jet Propulsion Laboratory, **Lauren Garten**, Georgia Institute of Technology

11:00am **TF2-TuM-13 Nanoscale Metasurfaces for UV Spectropolarimetric Applications**, *Tobias Wenger, Deacon Nemchick, Daniel Wilson, Richard Muller, Kenneth Manatt, Frank Winiberg, William Johnson,* Jet Propulsion Laboratory (NASA/JPL)*; Hui-Hsin Hsiao,* National Taiwan University, Taiwan*; Brian Drouin,* Jet Propulsion Laboratory (NASA/JPL)   **INVITED**
In this talk I will describe our efforts to develop optical metasurfaces for applications in the ultraviolet part of the spectrum. Metasurfaces are made from subwavelength elements that can be thought of as imprinting a phase on incident wavefronts, thereby allowing precise control over light by use of micro-fabrication methods. Here, I will focus on our work on UV spectropolarimetric gratings intended for vertical ozone profiling within Earth's planetary boundary layer. Particular emphasis will be on the fabrication of metasurface nanostructures with high aspect ratios and feature sizes well below 100 nm. To accomplish this, we utilize low-temperature atomic layer deposition on resist preform structures fabricated using electron-beam lithography. To date we have used this method to fabricate metasurfaces from a variety of materials, e.g., hafnium oxide.

11:30am **TF2-TuM-15 Amorphous Boron Carbide-Amorphous Silicon Heterojunction Devices for Neutron Voltaic Application**, *Vojislav Medic, Natale Ianno,* University of Nebraska - Lincoln
Amorphous hydrogenated boron carbide (a-BC:H) has been extensively researched as a semiconductor for neutron voltaic device fabrication. Previous work on a-BC:H devices investigated the fabrication of homojunction, heterojunction and heteroisomeric devices from the polymeric precursors ortho-carborane (p-type) and meta-carborane (n-type) using plasma enhanced chemical vapor deposition (PECVD).

The p-type single crystal silicon (c-Si) with n-type a-BC:H grown from meta-carborane has been previously studied and shown to produce the most optimal device performance compared to different a-BC:H device structures (Figure 1). However, as c-Si degrades over time due to radiation induced damage to its crystalline structure, p+ type hydrogenated amorphous silicon (a-Si:H) was identified as a viable layer for development of the a-BC:H heterojunction device.

Characterization via 4-wire current-voltage measurements, X-ray Photoelectron Spectroscopy (XPS) and ellipsometry of a-BC:H/c-Si and a-BC:H/a-Si:H devices was done, and the a-BC:H/a-Si:H device shows potential in fabricating a novel neutron voltaic device. Utilizing well known material and electronic properties of c-Si, Kraut's method for calculating valence band offset (VBO) at the interface junction via XPS (Equation 1) was used to produce a band structure of both c-Si/a-BC:H and a-Si:H/a-BC:H p-n heterojunction devices (Figures 2-5).

Equation 1: $VBO = \Delta E_v = (CL\text{-}VBM)_{Si} - (CL\text{-}VBM)_{BC} + (CL_{BC}\text{-}CL_{Si})_{int}$

Additionally, the metal contact formation with a-BC:H has not been previously studied with respect to its possible effects on device performance. The metal/a-BC:H contact investigation was performed, identifying Ti as an Ohmic contact with n-type a-BC:H (Figure 3).

11:45am **TF2-TuM-16 Investigating the Practical Limits of Delta Doping by Low-temperature Silicon Molecular Beam Epitaxy**, *April Jewell, Michael Hoenk,* Jet Propulsion Laboratory
Silicon-based photodetectors and imaging arrays are used in nearly every space-based mission, including those for astrophysics, heliophysics, planetary science, and Earth science. In order to achieve the highest sensitivity and stability, silicon detectors must be properly passivated; JPL's approach to surface passivation uses low-temperature molecular beam epitaxy (MBE) to embed an atomically thin (i.e. <monolayer) delta layer of dopant atoms with nanometers of the silicon surface. The delta doping process allows for nanometer-scale control of the near surface band structure, which can be fine-tuned through dopant concentration, number of delta layers, layer separation, and depth. Most scientific silicon imaging arrays—including charge coupled devices (CCDs) and complementary metal oxide semiconductor (CMOS) image sensors—are backside illuminated to maximize efficiency, and the delta-doped layers are deposited on the back surface. In all of JPL's work on development and deployment of delta-doped detectors, our fabrication process has required heating the substrate surface to at least 400 °C to prepare the hydrogen-terminated surface for epitaxial growth. However, the same hydrogen chemistry that enables epitaxial growth can also lead to depassivation of the Si-SiO$_2$ interface in frontside MOS gate structures; furthermore, the 400°C temperature may result in thermal stresses at the interfaces or through-silicon-vias in 3D stacked detectors. Here we report on recent work to investigate the practical limits of low temperature MBE in an effort reduce the minimum substrate temperature required to achieve epitaxial growth and good dopant activation in delta-doped detectors.

12:00pm **TF2-TuM-17 Improvement of Coating Uniformity on Non-Planar, Non-Stationary Substrates Through a Combined Experiment-Simulation Approach**, *Sean Hayes, Salmaan Baxamusa, Juergen Biener, Xavier Lepro-Chavez, Jean-Babtiste Forien, Tom Parham, Tom Braun, Liam Sohngen,* Lawrence Livermore National Laboratory*; Christoph Wild, Tobias Fehrenbach,* Diamond Materials GmbH, Germany
Laser inertial confinement fusion (ICF) has come into worldwide focus after the historic experiment on December 4th, 2022 which achieved a target gain >1 for the first time at the National Ignition Facility.ICF experiments on NIF utilize ultrathick(~80-95μm) hollow spherical CVD diamond capsules that must have a coating with >99.8% thickness uniformity to efficiently convert laser energy to compression energy. The CVD diamond is coated on a spherical substrate that is agitated during deposition to ensure even coating. This work provides a framework for understanding the combined effects of instantaneous coating non-uniformity (ICNU) and substrate reorientation on coating uniformity.ICNU measurements on characteristic ensembles of shells in controlled settings were used to understand the effect of the number of nearest neighbors (coordination number, CN). These measurements were used as inputs for Monte Carlo simulations and tested against dynamic batch coatings to determine the effects of CN and FWHM of overall coating non-uniformity, and to infer reorientation times. Such an approach allows us to connect physical processes and dynamics to coater hardware configurations.

Vacuum Technology
Room 121 - Session VT1-TuM

Vacuum Technology for Semiconductor

Moderators: Sol Omolayo, Lawrence Berkeley National Laboratory, **Jacob Ricker**, NIST

8:00am **VT1-TuM-1 Optimizing Electron Emitter Module Geometry for Improved Lifetime through Test-Particle Monte Carlo (TPMC) Simulation**, *Naga Chennuri, Nick Petrone, Lawrence Muray,* KLA Corporation
Thermal field emitters (TFEs) are the most common electron sources used in scanning electron microscopes (SEMs) due to their stable emission and long lifetime (>10,000 hrs). To maintain long lifetime, TFE's must operate at pressures less than ≤5x10-9 Torr, in ultra high vacuum (UHV). The TFE's consist of a cylindrical suppressor cap which is mounted a few hundred microns above the SEM lens stack. This narrow gap between the emitter and the top of lens is a region where there is potential for an increased local pressure due to low vacuum conductance. In this work, we used advanced vacuum modeling to simulate the local pressure increase around TFE tips and use this knowledge to optimize the geometry of TFE emitter (suppressor cap) module to increase conductance and improve lifetime. The model consists of a base vacuum chamber, emitter mount, emitter module and lens. For the emitter module (suppressor cap), four different geometries have been modelled and compared. A total pumping speed of 20L/s and tabulated material outgassing values for the components were employed, and MolFlow+ was used to perform vacuum simulations. The

background pressure in the chamber was simulated across all four geometries, as shown in Fig. 1, and was verified to be consistent, at 1.5x10-9 torr. The cylindrical emitter module (baseline) showed a peak local pressure of 1.5x10-8 torr. The two beveled cylinders, with minor diameters 4.7mm and 3mm, showed notable improvements with local peak pressures of 7.5x10-9 torr and 6x10-9 torr respectively. The rounded design demonstrated the greatest reduction in peak pressure, with a local high of 4x10-9 torr which falls well within the acceptable operational limits, thereby preserving lifetime. Machine downtime is a critical factor for SEM tools used for wafer inspection and metrology making it essential to preserve and extend the lifetime of TFE's to maintain optimal service intervals. The results from study were used to determine an optimized suppressor cap geometry for TFE modules, allowing for high conductance, and ultimately improved TFE stability and lifetime.

8:15am **VT1-TuM-2 New Advanced Home-Built Reactor for in-Situ Studies of ALD and ALE**, *Cristian van Helvoirt*, Caspar van Bommel, Marc Merkx, Janneke Zeebregts, Freek van Uittert, Erwin Kessels, Adrie Mackus, Eindhoven University of Technology, Netherlands

In the field of nanotechnology atomic scale processing is getting more and more advanced and requires in-depth understanding of the reaction mechanisms of deposition and etching processes. In-situ diagnostics are essential for accomplishing this. Within our group a reactor is designed and installed capable for in-depth study of atomic layer deposition (ALD) and atomic layer etching (ALE) surface reactions, with the focus on infrared spectroscopy (IR) at sub-monolayer sensitivity.

In-situ IR spectroscopy has proven itself to be a powerful tool to study the mechanism of ALD and ALE. [1,2]. To improve sensitivity into the sub-monolayer regime, the technique becomes dependent on the substrate material. Solutions can be found using pressed powder, ATR (attenuated total reflection) for dielectrics or grazing incidence RAIRS (Reflection Absorption Infra-Red Spectroscopy) for metals. The wish to be able to perform this type of diagnostics in one tool made us design a new reactor with the capability for in-situ transmission and reflection IR spectroscopy. For this versatility the back flange is designed to be able to load samples vertically (for transmission) and horizontally (for reflection).

Based on the experiences within our group and the field, the system has a hot wall reactor that is equipped with a loadlock, has the capability to bias the substrate for ion energy control and has a cabinet to mount up to eight different precursor/inhibitor bubblers. The system is pumped down using a turbo-molecular pump backed with roughening pump, to be able to reach high vacuum levels. As an extra feature the setup has the option to install up to four plasma, light or particle sources at a 45-degree angle which is to expand the research in the field of surface science and plasma physics. These ports also give the capability for extra in-situ diagnostics, e.g. optical emission spectroscopy (OES), quadrupole mass spectroscopy (QMS), quartz crystal microbalance (QCM). This contribution will outline the background, design, and capabilities of this next generation home-built reactor.

[1] Goldstein *et al., J. Phys. Chem. C* **112**, 19530 (2008)

[2] Mameli *et al., ACS Appl. Mater. Interfaces* **10**, 38588 (2018)

8:30am **VT1-TuM-3 Improved Thermal Uniformity in Pedestal Heaters Through the Integration of Thermal Pyrolytic Graphite (TPG®)**, *Matt Gallaugher*, Ismail Nas, Anand Murugaiah, Jefferson Troha, David Sabens, Momentive Technologies

Thermal uniformity is a critical metric for pedestal heaters used in semiconductor thin film processing, particularly in chemical vapor deposition (CVD) and atomic layer deposition (ALD). Heaters made of aluminum alloys have a reasonable inherent thermal conductivity (~150 W/mK), but thermal conductivities of stainless-steels and nickel alloys used in higher temperature applications are much poorer (~10-20 W/mK). As a result, stainless steel and nickel alloy heaters have poorer thermal uniformity, unless complex engineering solutions such as multiple heating zones are implemented. A simple alternative is possible: embedding a high thermal conductivity material, such as Thermal Pyrolytic Graphite (TPG®), inside a billet of stainless-steel to passively improve the thermal uniformity of the heater. The unique properties of the TPG® (~1700 W/mK in-plane, ~10 W/mK out of plane thermal conductivity) serve to distribute the heat across the surface of the heater for greater temperature uniformity. The advantage of this "thermally conductive billet" approach is that it can be flexibly integrated into different heater designs, enabling machining on both its bottom surface (heating coils and/or cooling loops) and its top surface (mesas, backside gas, etc.). A simplified schematic of this design is shown in Figure 1. To demonstrate the concept, a stainless-steel billet with embedded TPG® was made into a single zone, 8" heater to reveal the thermal uniformity improvement. Greater than 2x improvement in uniformity was realized, as shown by the variation (standard deviation / average) measured via a thermal camera (Figure 2). In addition, local azimuthal variations were eliminated, leading to a more symmetric profile. These real-world results were used to create a thermal-mechanical model, which was scaled up to conceptual 12" stainless-steel heater designs with both one and two heating zones. The models demonstrated improved thermal uniformity changes in all cases: >2x improvement. Although this work sought to optimize the heater temperature uniformity, the thermally conductive billet and/or the heating pattern could be designed to optimize the wafer thermal uniformity as well, including using two zone temperature control with superior intra-zone thermal uniformity.The integration of TPG® is a key technological path for passively improving the thermal uniformity of pedestal heaters used in more demanding applications.

Vacuum Technology
Room 121 - Session VT2-TuM

Sustainable Energy Production
Moderators: Sol Omolayo, Lawrence Berkeley National Laboratory, **Jacob Ricker**, NIST

8:45am **VT2-TuM-4 Photochemistry and Photocatalysis of Alcohols – Vacuum Technology for Sustainable Chemistry**, *Moritz Eder,* TU Wien, Austria; *Philip Petzoldt, Clara Aletsee, Martin Tschurl,* Technical University of Munich, Germany; *Jiri Pavelec, Gareth Parkinson,* TU Wien, Austria; *Ulrich Heiz,* Technical University of Munich, Germany   **INVITED**

In photocatalysis, light is harvested by semiconductors to utilize its energy for chemical reactions. Despite being highly promising for sustainable chemistry driven by (sun)-light, large-scale applications are still nonexistent due to the low efficiency of these photocatalysts. Screening for more efficient photocatalysts by mixing different powder materials has so far not led to the desired breakthrough.

With a more recent approach based on vacuum technology, photocatalysts can be optimized by observing the chemical and physical processes at the atomic level. To this end, single-crystalline semiconductors with atomically defined surfaces are investigated with different analytical techniques in ultra-high vacuum (UHV) during illumination with light. Since this is a comparably young topic in vacuum technology as well as physical chemistry, I will show the different approaches to the problem as well as the technological requirements and developments which go along with them.

While the investigation of a broad range of semiconductor materials for the bigger picture is still lacking, titania (TiO_2) has been investigated thoroughly as a photocatalyst in the last years. Among other substrates, alcohols have often been used as reactants with very unexpected results. While structurally more complex than common model substrates such as CO or water, alcohols provide a very versatile chemistry. Furthermore, molecular hydrogen can be produced selectively and efficiently by alcohol photocatalysis.

Using alcohols on the TiO_2(110) surface as an example, I will present the tools which have been developed and utilized in UHV to elucidate the photocatalytic processes. I will show the learning process of how photocatalysis on titania works at the atomic level over the last decade. Finally, I will discuss the most recent developments, which aim at designing devices for (near) ambient pressure photocatalysis. The goal is to close the so-called pressure gap between model systems and applied catalysts. This way, one can utilize vacuum technology for the rational design of photocatalytic materials and pave the way for sustainable, light-driven chemistry.

Tuesday Morning, November 5, 2024

Vacuum Technology
Room 121 - Session VT3-TuM

Novel Vacuum Instrumentation

Moderators: Sol Omolayo, Lawrence Berkeley National Laboratory, **Jacob Ricker**, NIST

9:15am VT3-TuM-6 Enabling Vacuum Process Monitoring with Time-of-Flight Spectroscopy, *Marco John, Klaus Bergner, Sebastian Hüttl, Kristian Kirsch, Andreas Trützschler,* VACOM Vakuum Komponenten & Messtechnik GmbH, Germany

As the complexity of industrial vacuum processes increases, detailed knowledge of the vacuum itself becomes even more important. A crucial aspect to manage this challenge is the importance of fast in-situ monitoring and control of process parameters such as pressure and residual gas composition. Improving process control in this way minimizes production errors, avoids damage to process equipment and ensures longer operating times. The capabilities of hot cathodes and quadrupole mass spectrometers are limited for this complex task, as they can only measure either the total pressure or the gas composition. One answer to this challenge is our novel ion source NOVION®, which combines the well-known technology of time-of-flight spectroscopy with our patented ion trap to an industrially available gas analyzing application.

In this talk we present the fundamental physical principles of the novel ion source and explain the compact combination of time-of-flight spectroscopy with our own patented ion trap. On the one hand we demonstrate the capability of precise total pressure measurements over a wide pressure range. On the other hand, we show the available possibilities to use the novel ion source in partial pressure measurement mode, leak detection and detection of air leaks.

We discuss the advantages and limits in different applications as well as best practices in the field and show the capability to push the principle to its limits at high pressures without compromising the performance or lifetime of the filaments. In addition, we demonstrate a special signal enhancement method to improve the resolution in the near signal-to-noise range.

Vacuum Technology
Room 121 - Session VT4-TuM

Accelerators and Large Vacuum Systems

Moderators: Sol Omolayo, Lawrence Berkeley National Laboratory, **Jacob Ricker**, NIST

11:00am VT4-TuM-13 Vacuum System for the High Magnetic Field Beamline at Cornell High Energy Synchrotron Sources, *Yulin Li,* Cornell University

After a very successful CHESS-U upgrade in 2019, a special new X-ray beamline is currently under development at CLASSE. The new beamline, the High Magnetic Field (HMF) beamline, enables users to study samples under up to 20-Tesla magnetic field, with 4X larger optic access, a factor of 10e4 in the photon flux at photon energy >20 keV. The design and fabrication of vacuum components for the HMF beamline is presented in this talk, including the storage ring modification, the front ends, and a very large end station vacuum system.

11:15am VT4-TuM-14 Leveraging SLAC Facilities and Expertise to Optimize Vacuum Beamline for LCLS-II Accelerator, *Giulia Lanza,* SLAC National Accelerator Laboratory

The success of the Linac Coherent Light Source II (LCLS-II) accelerator critically hinges on the efficient operation of its vacuum beamline, demanding the presence of technical facilities and skilled personnel. This presentation showcases the resources available at SLAC National Accelerator Laboratory (SLAC) tailored to support the vacuum beamline of the LCLS-II accelerator.

The plating shop provides vital support for the cleanliness of components. The brazing and welding expertise at SLAC allows the construction and repair of vacuum beamline infrastructure, fostering resilience and longevity in the face of demanding operational conditions. Multiple bake stations facilitate processing of different components in parallel, ensuring optimal vacuum conditions. Moreover, SLAC's array of cleanrooms tailored to diverse particle-free requirements guarantees the integrity and purity of vacuum components, essential for maintaining operational efficiency and minimizing contamination risks. Rounding out SLAC's capabilities are

systems specific for outgassing tests and residual gas analysis, providing the possibilities to test non-standard material and composites.

This presentation illuminates how the integration of SLAC's facilities and skilled workforce supports the vacuum beamline of the LCLS-II accelerator, underpinning its mission to push the boundaries of scientific exploration.

11:30am VT4-TuM-15 Factors Affecting XHV Polarized Electron Source Lifetime, *Marcy Stutzman,* Jefferson Lab*; Joshua Yoskowitz,* Jefferson Lab, Los Alamos National Lab

The Jefferson Lab polarized electron source utilizes a combination of ion pumps, NEG pumps, and NEG coating to achieve pressures as low as 2×10^{-12} Torr. Operational lifetime is primarily limited by residual gas in the system being ionized by the electron beam and accelerating into the photocathode, which is susceptible to ion implantation damage. Recent upgrades to the injector vacuum system include additional pumping in the first 15 meters downstream of the electron gun. Additionally, the anode in the gun has been biased to reduce ion impingement from gas ionized downstream of the anode. We will present a study of the effect of these upgrades, and our efforts to distinguish improvements due to the biased anode from those due to the improved beamline vacuum, including comparison of beamline vacuum modeling and ion implantation simulations.

11:45am VT4-TuM-16 Vacuum Technology Developments at Daresbury Laboratory for Modern Accelerators, *Keith J. Middleman, C. Benjamin, J. Conlon, R. Luff, O.B. Malyshev, E. Marshall, O. Poynton, D. Seal, L. Smith, R. Valizadeh, S. Wilde,* STFC Daresbury Laboratory, UK

The Vacuum Solutions group at the STFC Daresbury Laboratory has a unique position in that it has the capability to operate and design the vacuum systems for new accelerators whilst maintaining a very active research laboratory looking at many new facets of vacuum design for accelerators.This gives the group the opportunity to develop ideas in the laboratory before implementing them on the accelerator.This paper will present some of the latest accelerator ideas and machines at Daresbury and provide an insight into how some of our laboratory developments are helping improve the vacuum design.

A range of topics will be covered such as:

1. Machine developments – CLARA, FEBE and the vacuum challenge of plasma-wakefield experiments
2. NEG coatings – our latest research
3. Thin films – SRF coating developments
4. Photocathode research – metal and semiconductor cathode developments
5. New cleaning solutions for UHV and XHV
6. In-Kind contributions to major projects, ESS, Hi-Lumi LHC and PIP-II

Exhibitor Technology Spotlight Sessions
Room West Hall - Session EW-TuL

Exhibitor Technology Spotlight Session
Moderator: Christopher Moffitt, Kratos Analytical Inc

12:30pm EW-TuL-3 New Developments for Surface Analysis from Thermo Fisher Scientific, *Tim Nunney, Paul Mack, Robin Simpson, Hsiang-Han Tseng,* Thermo Fisher Scientific, UK

In this presentation we will present the latest innovations in instrumentation for Surface analysis and materials analysis from Thermo Fisher Scientific.

12:45pm EW-TuL-4 Physical Electronics Spotlight Session: Driving Discoveries Through Surface Analysis: New Methods for Thin Film Characterization, *Amy Ferryman,* Physical Electronics

Physical Electronics (PHI) innovative technology offers the world's only complete portfolio of powerful surface analysis instruments, including X-ray photoelectron spectroscopy (XPS), Auger electron spectroscopy (AES) and time-of-flight secondary ion mass spectrometry (TOF-SIMS). This presentation will highlight recent developments in methodologies for thin film characterization utilizing our fully automated *Genesis*. The multi-technique XPS platform offers an array of optional excitation sources, from valence and conduction bands with ultraviolet photoelectron spectroscopy (UPS) and low energy inverse photoemission spectroscopy (LEIPS) to core level excitation with hard X-ray photoelectron spectroscopy (HAXPES). The *Strata*PHI software package can be paired with the latter to calculate the thickness of advanced multilayer thin film structures.

1:00pm EW-TuL-5 Kratos Spotlight Session: Kratos Axis Supra+ -- Automated XPS analysis, including HAXPES and operando measurements, *Chris Moffitt,* Kratos Analytical Inc.

The automation of modern instrumentation allows for broader access to more robust analysis over larger sample sets with advanced approaches.Kratos Axis Supra+ incorporates automated sample handling with automated analysis of XPS, UPS, depth profiling and others, including higher energy Ag-Lα generated, quantitative HAXPES, for increased depth analysis.

The Axis Supra+ allows more samples to be analyzed with the full capabilities of the highest-performing XPS instrument, without intervention.Once samples are physically loaded, analyses are submitted through the computer interface, utilizing multiple cameras for location identification, which can be done remotely.This follows on for utilizing the HAXPES mono source, so that analysis by standard Al-Ka monochromatic x-rays can be automatically followed by analysis with the higher energy Ag-La monochromatic source and the results automatically processed and quantified using new Data Dependent Acquisition software features.

The Axis Supra+ is uncompromised in its ability to analyze the wide range of new advanced materials, including operando surface analysis measurement of battery materials while biasing or flowing current and heating.The multi-contact stage in the Axis Supra⁺ spectrometer accommodates the specialized holders for the operando analysis, supplying 4 electrical contacts to be used for these analyses, while still accepting all the standard sample platens for high throughput analysis. An inert sample transfer version of these multi-contact holders has also been developed, which allows the sample to be loaded and electrical connections made in a glove box and then loaded into the spectrometer without exposure to atmosphere.Cryo-cooling of battery and other materials has been shown to minimize degradation and chemical bonding damage that can be caused by x-ray exposure at room temperature, and Kratos offers new sample holder options that allow cooling of sample to cryogenic temperatures to mitigate chemical changes during XPS measurement.

Soft materials analysis has greatly expanded in the last several years since the introduction of argon gas cluster ion sources (GCIS), with the Kratos dual mode cluster source also able to perform traditional monoatomic argon profiling of hard inorganic materials.The cluster mode is able to profile light ion materials without the artifacts inherent in monoatomic sputter-etching of these materials.

Additional analytical techniques, such as Ag-Lα HAXPES, ISS, UPS, AES, REELS and IPES are all possible on the Supra⁺, and additional sample preparation chambers can be easily added, such as a station for deposition or the high-pressure, high-temperature gas reaction cell for catalysis experiments and measurement.

1:15pm EW-TuL-6 Enviroesca II: An Evolution in Surface Chemical Analysis Under Environmental Conditions, *Stefan Böttcher, Francesca Mirabella, Paul Dietrich, Andreas Thissen,* SPECS Surface Nano Analysis GmbH, Germany

EnviroESCA elevated chemical surface analysis into a new era, bringing operando chemical studies and easily accessible near ambient pressure XPS from fundamental research into applied surface science and standard analytical laboratories. For the recent focus of XPS applications on renewable energies, UHV incompatible specimen and advanced electrochemical studies now it is time for the next step. EnviroESCA II significantly enhances surface analysis capabilities under environmental conditions.

As an evolution from the successful first release, EnviroESCA II keeps the unique operational concept for chemical and dynamical analysis, expanding into bulk, electronic structure and atomic structure analysis, with seamless infrastructure integration and higher operational performance. Using the newly released SPECS AEOLOS 150 AD-CMOS electron analyzer and the µFOCUS 450 multiline X-ray monochromator source EnviroESCA II allows for unrivaled automated routine analysis under environmental conditions with adjustable surface to bulk sensitivity.

1:30pm EW-TuL-7 Impedans Spotlight Session: Advancing Plasma Understanding and Control: Cutting-Edge Solutions from Impedans Ltd., *Angus McCarter, A. Verma, T. Gilmore,* Impedans Ltd., Ireland

Impedans Ltd. is a leading provider of advanced plasma and RF sensors and plasma control applications, dedicated to enhancing the understanding of plasma processes. Our comprehensive range of products caters to diverse needs in fundamental research, equipment design, calibration and testing, process development, and process control.

We serve a wide array of industries, including semiconductor manufacturing, vacuum coating, medical device production, and aerospace, among many others. Our expertise in plasma diagnostics is recognized globally, with our instruments renowned for their high-resolution and high-speed data capture capabilities.

In this presentation, we will provide an overview of our innovative products and their applications. Our product lineup includes:

1. Bulk Plasma Sensors: Langmuir Probes are designed to measure critical plasma parameters such as electron density, electron temperature, electron energy distribution function, plasma potential etc in any kind of DC/RF/Microwave plasma source with time average and time resolved modes.

2. Substrate Level Sensors: These sensors are crucial for understanding interactions at the substrate level in various plasma processes. The advanced range of retarding field energy analysers provide accurate measurements of ion energy distribution functions, ion flux and also reports live etch/deposition rates during plasma processes.

3. RF Sensors: These VI probes are specialized to measure key RF parameters including voltage, current, phase, impedance, power, and harmonics in both continuous and pulsed applications. Advance sensors allow to measure the same parameters for up to 15 harmonics of the fundamental frequency as well as recreate the RF waveform and predict the ion flux of your plasma.

Our state-of-the-art techniques offer real-time process monitoring, ensuring precise control and optimization of plasma processes. By leveraging our advanced sensors and control solutions, users can achieve greater accuracy and efficiency in their plasma-related research and industrial applications, driving innovation and excellence in their respective fields.

1:45pm EW-TuL-8 Vital Materials Spotlight Session: Film Properties of LTC V2 - A Low Process Temperature TCO, *Rajiv Pethe, S.W. Yoon,* Vital Chemicals

Vital Materials is a global company providing materials across many industries including displays, photovoltaics, semiconductors etc.We provide materials such as metals, ceramics, semiconductors, and transparent conductive oxides.As the photovoltaic industry moves towards higher efficiencies and low cost processes, this requires innovation of novel transparent conductive oxides that can be processed at low temperatures while maintaining low sheet resistance and high transmission.Having good broadband transmission across the 300-1200nm while maintaining low resistance values would be an added value.Traditional ITO requires high processing temperatures to achieve low resistance. However low resistance also results in lower transmission above 800nm.Vital Materials has been

working towards development of such transparent conductive oxides one of which is LTC V2.This presentation will cover Vital Materials core products and film properties to a new novel material LTC V2 that provides low resistance combined with high transmission across the 300-1200nm wavelength range.

2:00pm **EW-TuL-9 Using VSim to Predict Magnetron Performance Through Multiscale Computations**, *Daniel Main,* Tech-X Corporation

Magnetron sputtering is the most common device for Physical Vapor Deposition (PVD) and is widely used for its many advantages over other thermal methods and other PVD devices.Even within the design of magnetron sputtering devices, there is a wide range of design parameters including the applied voltages, background gases, magnet placement, and chamber design.A Computer-Aided Engineering (CAE) approach of designing these devices *in silico*, instead of the traditional empirical approach, offers the ability to optimize devices like never before.However, the physics of the plasmas produced in these devices, including their important sheath region, makes designing these devices challenging.A particular challenge is the time scale of the underlying physics involved.In this talk, we demonstrate the use of VSim to meet this challenge.

VSim is a 1D, 2D, and 3D multi-physics simulation suite that contains plasma modeling capabilities including surface processes, and collision models. Using VSim, you can design your complete magnetron sputtering setup by correctly modeling the plasma discharge region and the sheath near the cathode and thereby correctly computing the ion flux and ion energy distribution onto the cathode. This detailed understanding is necessary to correctly compute the sputtering yield from the cathode. VSim allows you to design your entire magnetron sputtering setup by (1) computing the external magnetic field based on your permanent magnet configuration, (2) predicting the cathode current and voltage, (3) computing the deposition profile onto the substrate and (4) computing the erosion profile on the cathode. We discuss this workflow and show that the high accuracy VSim provides gives a better and more intuitive approach to optimizing magnetron sputtering devices.

2D Materials
Room 122 - Session 2D+LS+NS+SS-TuA

Electronics Properties

Moderators: Masa Ishigami, University of Central Florida, **Slavomir Nemsak**, Advanced Light Source, Lawrence Berkeley National Laboratory

2:15pm 2D+LS+NS+SS-TuA-1 NanoARPES for the Study of 2D Materials, *Aaron Bostwick*, Advanced Light Source, Lawrence Berkeley National Laboratory **INVITED**

Angle-resolved photoemission spectroscopy (ARPES) is the premier technique for the determination of the electronic bandstructure of solids, and has found wide application for manyclasses of materials, such as oxides, semiconductors, metals, and low-dimensional materials and surfaces. Among the important topics it addresses are the underlying many-body interactions that determine the ground and excited state functionalities of all materials. Recently the development of nanoARPES using microfocused x-ray beams has opened ARPES to a wider class of samples and enabled the measurement of 2D devices *in-situ* with applied electric fields, currents, strain and femtosecond laser pulses to the samples. In this talk I will give an introduction to the ARPES technique, the MAESTRO facility and share some our recent work on the bandstructure and many-body interactions in 2D heterostructuresof chalcogenides, graphene, and boron nitride and light induced metastable phases in 1T-TaS$_2$.

2:45pm 2D+LS+NS+SS-TuA-3 Observation of Interlayer Plasmon Polaron in Graphene/WS$_2$ Heterostructures, *Soren Ulstrup,* Aarhus University, Denmark*; Yannn in 't Veld,* Radboud University, Netherlands*; Jill Miwa, Alfred J ones,* Aarhus University, Denmark*; Kathleen M. McCreary, Jeremy T. Robinson, Berend T. Jonker,* Naval Research Laboratory*; Simranjeet Singh,* Carnegie Mellon University, USA*; Roland Koch, Eli Rotenberg, Aaron Bostwick, Chris Jozwiak,* Advanced Light Source, Lawrence Berkeley National Laboratory*; Malte Rosner,* Radboud University, Netherlands*; **Jyoti Katoch**,* Carnegie Mellon University, USA

Van der Waals heterostructures offer us exciting opportunity to create materials with novel properties and exotic phenomena such as superconductivity, bound quasiparticles, topological states as well as magnetic phases. In this talk, I will present our work on directly visualizing the electronic structure of graphene/WS$_2$/hBN heterostructure using micro-focused angle-resolved photoemission spectroscopy (microARPES). Upon electron doping via potassium deposition, we observe the formation of quasiparticle interlayer plasmon polarons in graphene/WS$_2$ heterostructure due to many-body interactions. I will discuss that such low-energy quasiparticle excitation is important to consider as they can have huge implications on the electronic and optical properties of heterostructures based on 2D transition metal dichalcogenides.

3:00pm 2D+LS+NS+SS-TuA-4 Harnessing the Synergy of X-ray Photoelectron Spectroscopy (XPS) and Argon Cluster Etching for Profound Analysis of MoS$_2$ and Graphene, *Jonathan Counsell*, Kratos Analytical Limited, UK*; Chris Moffitt, David Surman,* Kratos Analytical Inc.*; Liam Soomary, Khadisha Zahra,* Kratos Analytical Limited, UK

Understanding the intricate properties of two-dimensional (2D) materials such as MoS2 and graphene is pivotal for advancing their applications across diverse fields. However, achieving comprehensive characterization at the nanoscale requires advanced analytical techniques. This study explores the synergistic potential of X-ray Photoelectron Spectroscopy (XPS) coupled with Gas Cluster Ion Source (GCIS) etching and depth profiling to delve deeper into the structural and electronic intricacies of MoS2 and graphene.

By integrating XPS with GCIS etching, we not only discern the elemental composition, chemical bonding, and electronic states of these materials with exceptional precision but also unravel their depth-dependent characteristics. The incorporation of GCIS etching facilitates controlled removal of surface layers, enabling depth profiling to uncover buried interfaces, defects, and contamination effects that influence spectral results.

The combined approach allows for the characterization of MoS2-graphene heterostructures, providing insights into interfacial interactions and electronic coupling mechanisms. Through systematic analysis, we demonstrate the complementary advantages of XPS and GCIS etching in elucidating the structural and electronic complexities of 2D materials.

The integration of GCIS etching with XPS not only enhances the depth resolution and sensitivity of the analysis but also offers a deeper understanding of the nanoscale landscape of MoS2, graphene, and their heterostructures. This multidimensional approach accelerates the development of tailored devices and applications based on 2D materials, propelling advancements in nanotechnology and beyond.

3:15pm 2D+LS+NS+SS-TuA-5 Monark Quantum Foundry: Advancing 2d Quantum Materials Through Automated Pipelines, *Amirhossein Hasani, Nicholas J. Borys,* Montana State University, USA*; Hugh Churchill,* University of Arkansas

At the MonArk Quantum Foundry, located at Montana State University and the University of Arkansas, we are advancing the field of 2D quantum materials through the development of 2D Quantum Materials Pipelines (2D-QMaPs). These pipelines automate and streamline the critical stages of 2D quantum material sample preparation and device fabrication.

Robotic Exfoliation and Flake Hunting: Our process begins with an automated robotic exfoliator designed to produce up to 50 chips per hour, each measuring 1 cm by 1 cm. This machine carefully peels off thin layers from bulk materials, allowing precise control over factors such as temperature, pressure, and applied force, which is crucial for producing high-quality thin flakes, including single-layered crystals. After exfoliation, an automated optical cataloger identifies and catalogs the thin flakes. This system scans the entire chip, locates these flakes, and stores their information in a database. The cataloger uses advanced machine learning and AI algorithms for quick and accurate detection and features a motorized stage with photoluminescence and Raman spectroscopy capabilities, completing a full scan at 20x magnification in approximately 5 minutes.

Device Fabrication and Packaging: The identified flakes are then transferred to a specialized environment for device fabrication and packaging. This stage employs high-resolution thermal scanning probe lithography, laser writing systems, and electron beam evaporators to create devices. The entire process is conducted in an inert atmosphere (glove box), preserving the material's integrity by preventing exposure to air and moisture.

Characterization: The final stage integrates quantum device characterization tools, including photoluminescence (PL), Raman spectroscopy, magneto-optical probes, nano-optical spectroscopy, bulk and nanoscale cryogenic magnetometry, and magneto-transport measurements. These tools provide a comprehensive analysis of material and device properties, including mobilities, transition temperatures, photon autocorrelations, coherence times, and more.

Through the development of the 2D-QMaPs, the MonArk Quantum Foundry is revolutionizing the study of 2D quantum materials, paving the way for significant advancements in quantum computing, sensing, and other technologies.

4:00pm 2D+LS+NS+SS-TuA-8 Manipulation of Chiral Interface States in a Moiré Quantum Anomalous Hall Insulator, *Tiancong Zhu,* Purdue University **INVITED**

Quantum anomalous Hall (QAH) effect reflects the interplay between magnetism and non-trivial topology characterized by integer Chern numbers, which is expressed by chiral edge states that carry dissipationless current along sample boundaries. The recent discovery of QAH effect in van der Waals moiré heterostructures provides new opportunities in studying this exotic two-dimensional state of matter. Specifically, magnetism in these moiré QAH systems is induced by orbital motion of electrons, which allows full electrical control of the magnetic and the corresponding topological state. In this talk, I will discuss our recent scanning tunneling microscopy and spectroscopy (STM/STS) measurements on twisted monolayer-bilayer graphene (tMBLG), where QAH effect with gate-switchable Chern numbers have been observed previously in transport measurement. First I will discuss local scanning tunneling spectroscopy measurements on the correlated insulating states at v = 2and v = 3electrons per moiré unit cell, where the v = 3state shows a total Chern number of ±2. Under a small magnetic field, the sign of Chern number at the v = 3states can be switched by changing the local carrier concentration with gating, which is a result of competition between bulk and edge orbital magnetization of the QAH state.[1] The observation of a gate-switchable Chern number provides us an opportunity to directly visualize the chiral edge state in a moiré QAH insulator for the first time, which I will show through gate-dependent STS measurement and dI/dV mappings.[2] I will also demonstrate the capability to manipulate the spatial location and chirality of the QAH edge state through controlling the local carrier concentration with the STM tip.

[1] C. Zhang, T. Zhu et al,. Nature Communications, 14, 3595 (2023)

[2] C. Zhang, T. Zhu et al., Nature Physics (2024)

4:30pm 2D+LS+NS+SS-TuA-10 Scanning Tunneling Microscopy and Spectroscopy of Single Layer NiTe$_2$ on Au, *Stephanie Lough,* University of Central Florida*; Masahiro Ishigami,* University of Central Florida

Previous angle-resolved photoemission studies [1, 2] have shown that NiTe$_2$ is a type II Dirac material that possesses a Dirac point very close to the Fermi level. In addition, the material has a topological surface state which can be valley spin-polarized.A recent study [3] has shown that this state can be exploited to develop Josephson diodes with potential applications as memory devices which can be coupled to qubits. There has been a significant interest [3-5] in studying properties of single layer NiTe$_2$ due to its strong interlayer coupling in bulk via Te Pz orbitals.

In this talk, we will discuss the properties of single layer NiTe$_2$ on Au generated by gold-assisted exfoliation measured using low temperature scanning tunneling microscopy and spectroscopy. We find that this interface possesses rectangular lattice with periodicities that are different from bulk NiTe$_2$ or Au (111) by over 30%.Tunneling spectra reveals strong coupling between NiTe$_2$ and Au (111).We compare these results recent theoretical calculations [6] on strained NiTe$_2$ and its impact on topological surface states.

1.Ghosh, S., et al., *Observation of bulk states and spin-polarized topological surface states in transition metal dichalcogenide Dirac semimetal candidate NiTe2.* Physical Review B, 2019. **100**.

2.Mukherjee, S., et al., *Fermi-crossing Type-II Dirac fermions and topological surface states in NiTe.* Scientific Reports, 2020. **10**(1).

3.Pal, B., et al., *Josephson diode effect from Cooper pair momentum in a topological semimetal.* Nature Physics, 2022. **18**(10): p. 1228-+.

4.Zhao, B., et al., *Synthetic Control of Two-Dimensional NiTeSingle Crystals with Highly Uniform Thickness Distributions.* Journal of the American Chemical Society, 2018. **140**(43): p. 14217-14223.

5.Zheng, F.P., et al., *Emergent superconductivity in two-dimensional NiTe crystals.* Physical Review B, 2020. **101**(10).

6.Ferreira, P.P., et al., *Strain engineering the topological type-II Dirac semimetal NiTe.* Physical Review B, 2021. **103**(12).

4:45pm 2D+LS+NS+SS-TuA-11 Nanoscale heterogeneities at Transition Metal Dichalcogenide-Au Interfaces, *Taisuke Ohta*, Alex Boehm, Andrew Kim, Catalin Spataru, Konrad Thuermer, Josh Sugar, Sandia National Laboratories*; Jose Fonseca Vega, Jeremy Robinson,* Naval Research Laboratory

Two-dimensional geometry renders unique screening properties in transition metal dichalcogenides (TMDs). Consequently, the electronic properties of TMDs are susceptible to extrinsic factors (*e.g.*, substrate, strains, and charge transfer), and display spatial nonuniformities. Thus, material combinations (*i.e.*, TMD, dielectrics, and metals) and their nuanced interactions need to be considered when designing TMD-based devices. Of particular importance are the interfaces with metallic contacts. Uncovering the origin of heterogeneities at TMD-metal interfaces and establishing strategies to control TMD-metal interfaces could enable engineering pathways for future applications. We show that the electronic structures of exfoliated WS$_2$-Au interfaces exhibit pronounced heterogeneity arising from the microstructure of the supporting metal. These electronic structure variations indicate spatially nonuniform doping levels and Schottky barrier height across the junction. Through examination using photoelectron emission microscopy, we reveal key differences in the work function and occupied states. With *ab initio* calculation, electron backscatter diffraction, and scanning tunneling microscopy, our measurements show distinct variations in excess of 100meV due to the crystal facets of Au. Additionally, when multilayer WS$_2$ and Au(111) facets are azimuthally aligned, strong interactions induce mechanical slippage of the interfacing WS$_2$ layer, with respect to the rest of the WS$_2$ layers, resulting in local stacking variations with an occupied state energy shift of 20-50meV. Finally, we employed oxygen plasma treatment of Au to fabricate homogenous TMD-Au interfaces while also tuning the electronic properties of the TMDs. Our findings illustrate that the electronic properties of TMDs are greatly impacted by the interface interactions at energy and length scales pertinent to electronics and optoelectronics.

5:00pm 2D+LS+NS+SS-TuA-12 Xenon Trapping in Silica Nanocages Supported on Metal Powder, *Laiba Bilal,* SBU*; Anibal Boscoboinik,* Brookhaven National Laboratory

Trapping of Xenon gas atoms in silica nanocages supported on metal powders (Ru and Co) is investigated by lab-based ambient pressure X-ray photoelectron spectroscopy (AP-XPS).Xenon, being a noble gas, has very low reactivity[1]. This makes it useful for applications where chemical reactions are unwanted. The first use for Xenon was in flash lamps used in photography[2], and it is still used for this purpose today. It has wide applications, from its use in the cells of plasma television as a propellant in spacecraft that use ion propulsion[3] to its various applications in the medical industry[4].

Xenon occurs in slight traces within Earth, 1 part in 10 million by volume of dry air[2]. Like several other noble gases, xenon is present in meteorites and manufactured on a small scale by the fractional distillation of liquid air. However, Xe's concentration in the earth's crust and the atmosphere are much lower than predicted, which is also known as the "missing Xenon paradox"[5].

The Discovery of an effective way to trap and separate Xenon from other gases can have significant advantages. The presence of Xenon in nuclear fuel rods was partially responsible for the Chernobyl accident[6]. Consequently, the nuclear energy industry is also trying to imprint a way to control the release of Xe, produced during the nuclear fission of uranium. Characteristics of chemical interactions between Xe and metal surfaces have been observed and explained, also several low-energy electron diffraction studies at cryogenic temperatures have experimentally demonstrated an on-top site adsorption preference for Xe adatoms on metal surfaces[7].

Prior studies on 2D silicate bilayers grown on metal supports at Brookhaven National Lab showed that these structures could irreversibly trap all noble gases larger than Ne[8] at room temperature. The noble gas atoms were trapped within hexagonal prism-shaped silicate nanocages-like structures and could then be released by heating the materials to different temperatures, i.e., Ar: 348 K, Kr: 498 K, Xe: 673 K, Rn: 775 K[8,9]. Figure 1A illustrates the potential energy diagram for a noble gas atom getting trapped in a silica nanocage. It can be seen that the activated physisorption mechanism that traps noble gas atoms has a high desorption energy barrier (E_{des}).

Figure 1B shows a silicate bilayer structure (side and top views), while Figure 1C shows a hexagonal prism nanocage, the building block of the bilayer structure.[8]. Since synthesizing such silicate bilayers is very expensive and time-consuming[10] for practical purposes, my project focuses on developing and testing scalable silicate nanocage[9] materials to trap noble gases, with especial focus on Xenon.

Atomic Scale Processing Mini-Symposium
Room 116 - Session AP+PS+TF-TuA

Atomic Layer Etching III: Plasma Processes

Moderators: Robert Bruce, IBM Research, T. J. Watson Research Center, **Udyavara Sagar**, Lam Research

2:15pm AP+PS+TF-TuA-1 Atomic Layer Etching with Plasma Processing for Semiconductor Device Fabrication, *Heeyeop Chae,* Sungkyunkwan University (SKKU), Republic of Korea **INVITED**

The critical dimensions of semiconductor devices are continuously shrinking in nanometer and atomic scale with 3D device structure. The demand for dimension control in angstrom level is drastically increasing also in etching processes. Atomic layer etching (ALE) processes are being actively studied and developed for various metals, semiconductor, and dielectric materials. In this talk, plasma processes for atomic layer etching will be discussed for both isotropic and anisotropic patterning of metals and dielectric materials including molybdenum, ruthenium, cobalt, titanium nitride, tantalum nitride, hafnium oxide, zirconium oxides. [1-9] Typical ALE processes consist of surface a modification step and a removal step. For the surface modification, various fluorination, chlorination and oxidation schemes were applied including fluorocarbon deposition, halogenation, oxidation with radicals generated plasmas. For the removal or etching step, various

schemes were applied including ion-bombardment, heating, ligand volatilization, ligand exchange, and halogenation. The surface characteristics such as surface roughness and surface residue after plasma-enhanced ALE processes will be also discussed.

1) K. Koh, Y. Kim, C.-K. Kim, H. Chae, *J. Vac. Sci. Technol. A*, 36(1), 10B106 (2017)

2) Y. Cho, Y. Kim, S. Kim, H. Chae, *J. Vac. Sci. Technol. A*, 38(2), 022604 (2020)

3) Y. Kim, S. Lee, Y. Cho, S. Kim, H. Chae, *J. Vac. Sci. Technol. A*, 38(2), 022606 (2020)

4) D. Shim, J. Kim, Y. Kim, H. Chae, *J. Vac. Sci. Technol. B.*, 40(2) 022208 (2022)

5) Y. Lee, Y. Kim, J. Son, H. Chae, *J. Vac. Sci. Technol. A.*, 40(2) 022602 (2022)

6) J. Kim, D. Shim, Y. Kim, H. Chae, *J. Vac. Sci. Technol. A.*, 40(3) 032603 (2022)

7) Y. Kim, H. Chae, Appl. Surf. Sci., 619, 156751 (2023)

8) Y. Kim, H. Chae, Appl. Surf. Sci., 627, 157309 (2023)

9) Y. Kim, H. Chae, ACS. Sustain. Chem. Eng., 11, 6136 (2023)

2:45pm AP+PS+TF-TuA-3 Atomic Layer Etching in HBr/He/Ar/O_2 Plasmas, *Qinzhen Hao, Mahmoud Elgarhy,* University of Houston*; Pilbum Kim, Sang Ki Nam, Song-Yun Kang,* Samsung Electronics Co., Republic of Korea*; Vincent Donnelly,* University of Houston

Atomic layer etching (ALE) of Si is reported in a radio frequency (RF) pulsed-power inductively-coupled plasma (ICP), with periodic injections of HBr into a continuous He/Ar carrier gas flow, sometimes with trace added O_2. Several pulsing schemes were investigated, with HBr injection simultaneous with or alternating with ICP power. The product removal step was induced by applying RF power to the substrate, in sync with ICP power. Etching and dosing were monitored with optical emission spectroscopy. Little or no chemically-enhanced ion-assisted etching was observed unless there was some overlap between HBr in the chamber and ICP power. This indicates that HBr dissociative chemisorption deposits much less Br on Si, compared with that from Br created by dissociation of HBr in the ICP. Chemically-assisted etching rates nearly saturate at 2.0 nm/cycle as a function of increasing HBr-containing ICP dose at -75 V_{DC} substrate self-bias. The coupled effects of O_2 addition and substrate self-bias DC voltage on etching rate were also explored. Etching slowed or stopped with increasing O_2 addition. As bias power was increased, more O_2 could be added before etching stopped.

3:00pm AP+PS+TF-TuA-4 Comparisons of Atomic Layer Etching of Silicon in Cl_2 and HBr-Containing Plasmas, *Mahmoud Elgarhy, Qinzhen Hao,* University of Houston*; Pilbum Kim, Sang Ki Nam, Song-Yun Kang,* Samsung Electronics Co.*; Vincent Donnelly,* University of Houston

This talk will report an experimental investigation of Cl_2 vs. HBr for plasma atomic layer etching (ALE) of silicon. An inductively coupled plasma (ICP) source with a constant flow of Ar (and sometimes He) carrier gases, and HBr or Cl_2 as a dosing gas was used for etching Si (100) samples. Optical emission spectroscopy was used to follow relative yields of SiCl, SiCl_2, SiBr and SiBr_2, and scanning electron microscopy and profilometry were used to measure etching rates. HBr and Cl_2 residence times in the chamber were determined by measuring time-resolved pressure during gas dosing. It was found that the pressure rise and fall times were much longer for HBr compared to Cl_2, suggesting that HBr hangs up on the chamber wall after gas dosing. The effect of the delay time between gas dosing and the start of ICP power on the etching rate was also investigated. When HBr or Cl_2 were injected into the reactor with the plasma on, etching occurs for both sources, with Cl_2 having a higher etching rate. When HBr or Cl_2 were fed to the reactor with the plasma off, only Cl_2 etches. This indicates that the HBr does not chemisorb on Si, and bromination of the surface requires the plasma to form Br atoms, which do adsorb.

3:15pm AP+PS+TF-TuA-5 Atomic Layer Etching of Crystalline MoS_2 by Plasma Fluorination and Oxygenation, *Sanne Deijkers[1], Christian Palmer, Nick Chittock, Erwin Kessels, Adrie Mackus,* Eindhoven University of Technology, The Netherlands

Molybdenum disulfide (MoS_2) is a two-dimensional (2D) transition metal dichalcogenide (TMD) with applications in catalysis and nanoelectronics.[1–3] To enable integration of 2D materials in nanoelectronics, highly controlled and low-damage etching processes are required. One example of such a

process is the atomic layer etching (ALE) of WSe_{-2}.[4] In this work, we present a plasma ALE process to etch crystalline MoS_2. The process involves plasma fluorination and oxygenation, targeting Mo-O-F as a volatile species. Previous work using the approach of fluorination and oxygenation involved thermal chemistries with an etch-per-cycle (EPC) of 0.5 Å for amorphous films and 0.2 Å for crystalline films.[5] As plasmas are more reactive than their gaseous counterparts, they are expected to allow for etching crystalline materials.

Fluorination was performed by a SF_6-based plasma, and as removal step various oxygen sources were tested. To avoid continuous etching of the MoS_2, the plasma composition of the fluorination step had to be optimized.[6] Addition of H_2 to the plasma mixture reduces F radical concentration by creating HF species *in situ*.[7] With an adequate H_2 content using a ratio of $SF_{-6}:(SF_6+H_2) < 0.3$, continuous etching is suppressed, and only modification of the top surface takes place. As second half-cycle, H_2O, O_2 gas and O_2 plasma exposures were tested. Of these only an O_2 plasma resulted in etching, while dosing H_2O or O_2 gas resulted in no measurable thickness change. Raman measurements showed a strong decrease in the characteristic E^1_{2g} and A_{1g} peaks, indicating etching of crystalline MoS_{-2}. The complete ALE recipe with saturated SF_{-6}-based plasma and O_2 plasma exposures had an EPC of 1.1 ± 0.2 Å at 300 °C table temperature.

1. Cao, Y. *ACS Nano* **15**, 11014–11039 (2021).

2. Mahlouji, R. *et al. Adv. Electron. Mater.* **8,** (2022).

3. Deijkers, J. H. *et al.* Adv. Mater. Interfaces 4–9 (2023).

4. Nipane, A. *et al. ACS Appl. Mater. Interfaces* **13**, 1930–1942 (2021).

5. Soares, J. *et al. Chem. Mater.* **35**, 927–936 (2023).

6. Xiao, S. *et al. Sci. Rep.* **6**, 1–8 (2016).

7. Hossain, A. A. *et al. J. Vac. Sci. Technol. A* **41**, (2023).

4:00pm AP+PS+TF-TuA-8 A Reduced Order Model of Plasma-Surface Interactions in Atomic Layer Etching, *David Graves,* Princeton University*; Joseph Vella,* TEL Technology Center, America, LLC

Any future physics-based, rather than purely data-driven, digital twin of a plasma tool and process will need a reduced order model (ROM) of the effects of the plasma on the surface being processed. In this talk, I present one possible version of a ROM for simulating a plasma atomic layer etching (ALE) process. The ROM is based on a transient version of a surface site balance model that was first applied in the 1980s for plasma etching. Classical molecular dynamics (MD) simulations of ALE of Si using Cl_2/Ar^+ cycles are first validated with experimental measurements and then used to provide values for parameters (e.g., ion energy dependent etch yields) for a transient site balance model of the process. The ROM is computationally much faster than the MD simulations and is shown to reproduce additional, and previously unexplained, experimental results. Future applications of MD to plasma-surface interactions in semiconductor device fabrication will likely use another type of ROM. MD methods require interatomic potentials or force fields for all simulated atomic interactions. The force field parameters can be inferred from higher level methods such as density functional theory (DFT), coupled with neural net data-driven algorithms. I will conclude with preliminary results using one such approach, namely Deep Potential MD (DeePMD), to develop illustrative force fields.

4:15pm AP+PS+TF-TuA-9 Atomic Layer Etching of SiO_2 using Sequential Exposures of $Al(CH_3)_3$ and H_2/SF_6 Plasma, *David Catherall, Azmain Hossain, Austin Minnich,* California Institute of Technology

On-chip photonic devices based on SiO_2 are of interest for applications such as microresonator gyroscopes and microwave sources. Although SiO_2 microdisk resonators have achieved quality factors exceeding one billion, this value remains an order of magnitude less than the intrinsic limit due to surface roughness scattering. Atomic layer etching (ALE) has potential to mitigate this scattering because of its ability to smooth surfaces to sub-nanometer length scales. While isotropic ALE processes for SiO_2 have been reported, they are not generally compatible with commercial reactors, and the effect on surface roughness has not been studied. Here, we report an ALE process for SiO_2 using sequential exposures of $Al(CH_3)_3$ (trimethylaluminum, TMA) and $Ar/H_2/SF_6$ plasma. We find that each process step is self-limiting, and that the overall process exhibits a synergy of 100%. We observe etch rates up to 0.58 Å per cycle for thermally-grown SiO_2 and higher rates for ALD, PECVD, and sputtered SiO_2 up to 2.38 Å per cycle. Furthermore, we observe a decrease in surface roughness by 62% on a roughened film. The residual concentration of Al and F is around 1-2%, which can be further decreased by O_2 plasma treatment. This process could

---

[1] **TFD James Harper Award Finalist**

find applications in smoothing of SiO_2 optical devices and thereby enabling device quality factors to approach limits set by intrinsic dissipation.

4:30pm AP+PS+TF-TuA-10 Atomic Layer Etching of Cu Using Alternating Cycles of Hexafluoroacetylacetone and O_2 Plasma, *Yusuke Nakatani,* Hitachi High-Tech, Japan*; Andrew Kaye,* Colorado School of Mines, USA*; Yasushi Sonoda, Motohiro Tanaka, Kenji Maeda,* Hitachi High-Tech, Japan*; Sumit Agarwal,* Colorado School of Mines, USA

Atomic layer etching (ALE) is a critical technology in semiconductor device fabrication, including for interconnect metals such as Cu and Co. Previously, thermal ALE of Cu has been reported using alternating half-cycles of hexafluoroacetylacetone (hfacH) and O2 or O3 at ~275 °C. It has also been shown that hfacH cannot spontaneously etch Cu, and peroxidation of the Cu surface is required. In this presentation, we will report on ALE of Cu at a much lower temperature of 150 °C using hfacH and O2/Ar plasma half-cycles.

The ALE process was monitored using in situ reflection-absorption infrared spectroscopy (RAIRS). Prior to ALE, the Cu wafers were cleaned using a H2 plasma at a temperature of 300 °C to reduce the native oxide, and to remove the surface carbonates and adsorbed hydrocarbons. Initially, we tested the reactivity of hfacH at 150 °C with a reduced Cu surface, and after re-oxidation with an O2 plasma. In both cases, in the infrared spectra, we observed absorption bands related to CF3 (1240 cm^{-1}), C=C, and C=O (1645 cm^{-1}) vibrations. On a reduced Cu surface, the C=C and C=O bands were much weaker indicating decomposition of hfacH. Since hfacH does not spontaneously etch Cu, this indicates that an oxidized Cu surface is required for the adsorption of hfacH. Our infrared data also show that the ALE window is very narrow, and the etch rate could only be measured at 125 and 150 °C. At temperatures lower than 125 °C, our infrared data shows that hfacH does adsorb onto the CuOx surface, but the temperature is likely too low for the formation of the etch products— Cu(hfac)2 and H2O. The subsequent O2 plasma half-cycle simply removes the hfac ligand and oxidizes the surface further. At 150 °C, a balance is established between surface oxidation and removal of CuOx from the surface as Cu(hfac)2 and H2O. The etch per cycle at 125 and 150 °C were 0.1 and 0.7 Å, respectively. At temperatures higher than 150 °C, atomic force microscopy shows that the Cu surface roughens due to severe oxidation, and the Cu film thickness cannot be measured with ellipsometry.

4:45pm AP+PS+TF-TuA-11 Enabling Anisotropic and Selective Etch Through Surface Modification of Ru, *Owen Watkins,* UCLA*; Harsono Simka,* Samsung Electronics*; Jane Chang,* UCLA

Ruthenium is a potential replacement for copper in metal interconnects below 10 nm, where the grain boundary scattering and the need for a barrier layer increases the effective resistivity of Cu. Unlike Cu, Ru can be directly etched using O_2-plasma-based processes, allowing a subtractive metal patterning to be used. Current Ru etching processes largely rely on O_2/Cl_2-based RIE. While this process is able to anisotropically etch Ru, it requires Cl_2 and damages the hard mask, resulting in ballooning and low selectivity. A cyclic process that is halogen-free, anisotropic, and selective has been proposed. The process consists of a nitrogen plasma passivation step, hydrogen plasma reduction step, and oxygen plasma etching step. The passivating layer of RuN formed by N_2 plasma exposure can be reduced in H_2 plasma. Bias applied to the substrate during the H_2 step results in the selective reduction of RuN on the vertically-exposed surface, leaving a layer of RuN on the sidewalls. During the O_2 plasma step, RuN passivates the sidewall from O radicals that would otherwise etch the sidewall. The two surface modification steps cause the normally isotropic O_2 plasma etch to become anisotropic, while maintaining a high selectivity vs. SiO_2 and SiN used as the hard mask. The sequential process has been experimentally shown to be anisotropic and selective, and results in lower resistivity and surface roughness vs. O_2 plasma alone. To understand the effects of the surface modification steps on the overall process, each step of the sequential process has been examined, including the surface composition and structure of the Ru film after each plasma exposure. RuO2 and RuN thin films were deposited as references, allowing the presence of RuN after nitridation to be confirmed using XPS and XRD. The etch rate of nitrided Ru films was found to be 0.4 nm per minute in O_2 plasma, more than 15 times less than the etch rate of Ru in O_2 plasma at the same conditions. Removal of the N_2 plasma step from the process resulted in isotropic etching, confirming that nitridation is responsible for sidewall passivation. XPS was used to confirm that most, but not all of the RuN surface layer is reduced after exposure to H_2 plasma. H_2 plasma was also found to significantly affect the etching of hard mask SiO2. Reduction of the plasma density by lowering the power and increasing the pressure was necessary

to reduce SiO_2 etching and corner faceting during the H_2 step. The combination of surface modification techniques results in a process that has been demonstrated for features down to 32 nm pitch.

5:00pm AP+PS+TF-TuA-12 Enhanced Control of Plasma Surface Interaction to Etch Alloys Using Transient Assisted Plasma Etching (Tape), *Atefeh Fathzadeh,* KU Leuven/ IMEC, Belgium*; Philippe Bezard,* IMEC Belgium*; Thierry Conard, Frank Holsteyns,* IMEC, Belgium*; Stefan De Gendt,* KU Leuven/Imec, Belgium

A novel plasma process design called transient-assisted plasma process (TAPP) has been recently introduced to tackle multiple patterning challenges brought by the introduction of 3D devices, new ultra-thin films, and compound materials without suffering from the poor throughput of Atomic layer etching. In the realm of dry-etching, it has exhibited promising patterning capabilities at etch rates compatible with high-volume manufacturing. In deposition applications, It also has demonstrated superior control over precursor dosage and fragmentation for in-situ hard-mask deposition compared to conventional methods. Moreover, from a sustainability perspective, Transient-assisted processing (TAP) presents considerable advantages by notably reducing the consumption of problematic gases. TAPE operates in cycles, involving at least two phases: Time-limited injection of the reactant (with or without plasma), and when the injection is stopped, a gas transient happens in the plasma, where the reactant concentration diminishes over time, as shown in Figure 1. The fluence of reactive species is regulated by the gas pulse characteristics (partial pressure, etc.) and its associated plasma transient, while ion fluence is governed by the duration of the plasma phase. This segregation yields significantly enhanced control over plasma-surface interactions compared to conventional plasma etching techniques. This design is compatible with any gas mixture, and energy sources (ions, photons, electrons, fast neutral species/clusters, etc.).

Enhancing control over plasma-surface interactions holds promise in rectifying the uneven etching observed in multicomponent materials like alloys. This imbalance in etching induces a compositional drift, thereby impeding the process and deteriorating material characteristics as shown in Figure 2a. Typically, one component undergoes predominantly chemical etching, while the other experiences primarily physical etching. In TAPE, most chemically-driven etching occurs early during the plasma step when a substantial amount of etchant is present. The modified surface/profile will then be exposed to a reduced etchant quantity and a continued ion bombardment. Each cycle is thus capable of providing the necessary species for a balanced etching of the compound's elements. Figure 2b compares the chemical composition of InGaZnO after conventional etching and TAPE, while Figure 2c compares the etch rate, and profile relative to a previously published ALE process. Meanwhile, TAPE consumes 25 times less CH_4 than the ALE process.

5:15pm AP+PS+TF-TuA-13 Leveraging Plasma Nitridation for Atomic Layer Etching of Ni_3Al, *Taylor G. Smith,* University of California, Los Angeles*; Jean-François de Marneffe,* imec, Belgium*; Jane P. Chang,* University of California, Los Angeles

Extreme ultraviolet (EUV) lithography is entering a new era with high numerical aperture (NA) EUV, increasing the importance of integrating new absorber layer materials like Ni_3Al to mitigate mask 3D effects. However, Ni_3Al adoption has been limited by difficulties in anisotropically etching Ni_3Al with high selectivity to the underlying Ru capping layer. A previously reported ALE based on plasma oxidation was shown effective at etching Ni_3Al but had poor selectivity to Ru, which etches spontaneously in oxygen plasma. An atomic layer etch (ALE) based on plasma nitridation and formic acid (FA) vapor exposure was previously demonstrated to etch Ni[1], and in this work the nitridation-based ALE process is extended to the more complex and industrially relevant Ni_3Al.

X-ray photoelectron spectroscopy (XPS) is used to analyze the surface composition of blanket Ni_3Al films after plasma nitridation, showing the nitrided films have a stoichiometry of $Ni_{2.4}AlN$. The effects of plasma power, from 200 to 700 W, and pressure, from 8 to 50 mTorr, on plasma nitridation are examined, with current results indicating that high power and low pressure lead to the greatest amount of surface nitridation. Langmuir probe measurements are used to correlate these effects with changes in plasma density and electron temperature. For the removal half-cycle, FA vapor was shown to remove the nitride layer as indicated by the disappearance of the characteristic metal nitride peak in the N 1s spectrum at 397.2 eV. XPS also shows depletion of Ni as successive ALE cycles are applied, an effect that can be mitigated using basic etchants due to their selective removal of Al over Ni. Selectivity to Ru is measured by etching blanket Ru films and

measuring the thickness with SEM, with a current selectivity of 2.4. To assess anisotropy, Ni_3Al is first conformally deposited over a patterned Si substrate by physical vapor deposition (PVD), and the samples are subsequently processed by ALE. The ion energy of the nitrogen plasma is varied by changing the voltage applied to an ion extraction grid from -100 to +100 V, with the sidewall Ni_3Al etch compared to the vertical Ni3Al etch using scanning electron microscopy (SEM).

[1] T.G. Smith, A.M. Ali, J.F. de Marneffe, J.P. Chang, J. Vac. Sci. Technol. A 42, 022602 (2024).

Applied Surface Science
Room 117 - Session AS-TuA

Theory, Surface Structure and Processes

Moderators: Paul S. Bagus, University of North Texas, **Jodi Grzeskowiak**, Tokyo Electron America, USA

2:15pm AS-TuA-1 Advances in Understanding Structure and Electron Transfer Dynamics at Iron Oxide/Water Interfaces, *Kevin Rosso,* Pacific Northwest National Laboratory   **INVITED**
Structure and dynamics at iron oxide/water interfaces, which govern rates of adsorption, electron transfer, growth/dissolution, have long been challenging to accurately simulate because of the prominent role of iron cation valence on acidity and ligand exchange behavior, and unique electronic structure considerations in the solid state. Iron oxides are wide band gap semiconductors with a narrow conduction band arising from strongly localized 3d orbitals. Consequently, charge carriers tend to self-trap as polarons whose mobilities are controlled by thermally activated site-to-site hopping. Proper theoretical description of such properties requires thoughtful trade-off's between necessary accuracy versus efficiency.

I will provide a decadal perspective on computational efforts applied to processes at hematite/water interfaces, highlighting the importance of steady methodological improvements. The talk will feature 1) how water organizes and is dynamically stabilized at distinct hematite facets, 2) the structure and hopping kinetics of electron and hole polarons, and 3) the free energies of ferrous iron adsorption and valence interchange electron transfer with the surface. It will be shown that ab initio molecular dynamics is now both a viable and essential tool for accurately determining the H-bonding network of adsorbed water and the acidity constants of surface hydroxo groups, while static density functional theory is still a useful tool for water binding energetics. Gap-optimized hybrid functionals show that while the hole polaron generally localizes onto a single iron site, its mobility is limited by the tetragonal distortion it induces, whereas the electron polaron induces a smaller distortion resulting in delocalization over two neighboring Fe units and a factor of three higher mobility. Finally, for computationally intensive processes such as ferrous iron adsorption, it will be shown that use of neural network potentials such as the Behler-Parrinello type is a promising alternative to classically parameterized molecular dynamics, offering both the precision of first principles calculations and the same order of computational efficiency to that of classical simulations. The collective findings bode well for ultimately enabling a robust basis for interpretation of experimental observables near the atomic-scale including complex multi-step processes such as redox-catalyzed dissolution and growth.

2:45pm AS-TuA-3 Manifestation of Correlated Electronic Structure in a Kagome Metal YbTi₃Bi₄, *Anup Pradhan Sakhya,* University of Central Florida*; Brenden R. Ortiz,* Materials Science and Technology Division, Oak Ridge National Laboratory*; Barun Ghosh,* Northeastern University, US*; Milo Sprague, Mazharul Islam Mondal,* University of Central Florida*; Matthew Matzelle,* Northeastern University, US*; Iftakhar Bin Elius, Nathan Valadez,* University of Central Florida*; David G. Mandrus,* University of Tennessee Knoxville*; Arun Bansil,* Northeastern University, US*; Madhab Neupane,* University of Central Florida
Kagome lattices have emerged as an ideal platform for exploring various exotic quantum phenomena such as correlated topological phases, frustrated lattice geometry, unconventional charge density wave orders, Chern quantum phases, superconductivity, etc. Here, we report the discovery of a new Ti-based kagome metal YbTi₃Bi₄ which is characterized using angle-resolved photoemission spectroscopy (ARPES) and magneto-transport, in combination with density functional theory calculations. Our ARPES results reveal the complex fermiology of this system along with the spectroscopic evidence of four flat bands. Furthermore, our electronic structure measurements show the presence of multiple van Hove singularities originating from Ti 3d orbitals. We have identified that the system exhibits topological nontriviality with surface Dirac cones at the Γ point and a bulk linearly dispersing gapped Dirac-like state at the K point as indicated by our theoretical calculations. These results establish YbTi3Bi4 as a novel platform for exploring the intersection of nontrivial topology, and electron correlation effects in the wider LnTi3Bi4 (Ln= lanthanide) family of materials.

3:00pm AS-TuA-4 Impact of Surface Pretreatment on Al₂O₃/GaN and HfO₂/GaN Band Offsets Measured by X-Ray Photoelectron Spectroscopy, *Melissa Meyerson, Peter Dickens, Joseph Klesko, Brian Rummel, Paul Kotula, Andrew Binder,* Sandia National Laboratories
The need for modern power devices with lower ON-resistances, higher breakdowns, and improved efficiencies is increasing as power demands in electronics continue to rise. Gallium nitride (GaN) has emerged as a promising candidate to satisfy these demands due to its advantageous material properties as a wide bandgap semiconductor (e.g., high breakdown electric field, enhanced mobility, and a high saturation velocity). The use of GaN in power electronics often relies on the interactions between the GaN and a dielectric layer, such as Al₂O₃, which are highly dependent on the properties of the materials at the interface. Variations in the band offset and interface trap state densities can be impacted by a variety of processing factors, including the surface chemistry of the GaN prior to dielectric deposition. Since the surface chemistry of the GaN is affected by the methods used to clean the surface prior to deposition of the dielectric, it is expected that these interfacial properties will also be affected by the cleaning method used. Here, we study the interfacial properties of Al₂O₃/GaN and HfO₂/GaN films using X-ray photoelectron spectroscopy (XPS) to measure the band offsets as a function of GaN cleaning method. Additionally, a GaₓOᵧ interlayer has been identified at this interface by XPS, which is correlated with interface trap state densities measured from capacitance-voltage measurements of subsequently fabricated MOS-capacitors.

Sandia National Laboratories is a multi-mission laboratory managed and operated by National Technology & Engineering Solutions of Sandia, LLC (NTESS), a wholly owned subsidiary of Honeywell International Inc., for the U.S. Department of Energy's National Nuclear Security Administration (DOE/NNSA) under contract DE-NA0003525.

4:00pm AS-TuA-8 Calculation of X-Ray Absorption Spectra of f-Element Compounds from First Principles, *Jochen Autschbach,* University at Buffalo, SUNY   **INVITED**
This talk will be concerned with calculations of X-ray absorption near-edge structure (XANES) spectra for f-element compounds using multi-configurational wavefunction methods (using complete and restricted active space self-consistent field (CAS/RASSCF) methods and variants thereof), along with supporting density functional calculations. A focus of our research has been the connection of the observed spectral features and the underlying covalent bonding in the systems, in particular, the involvement of the valence f-shells of lanthanides and actinides. The talk will cover published studies of actinyl(VI) species, actinide hexa-chlorides, cerocene vs. CeO₂, as well as on-going research on a variety of Ce(IV) materials.

Selected relevant references:

[1] Sergentu, D.-C.; Autschbach, J., 'Covalency in Actinide(IV) Hexachlorides in Relation to Chlorine K-Edge X-ray Absorption Structure', Chem. Sci. 2022, 13, 3194–3207. https://doi.org/10.1039/D1SC06454A

[2] Sergentu, D.-C.; Autschbach, J., 'X-ray absorption spectra of f-element complexes: Insight from relativistic multiconfigurational wavefunction theory', Dalton Trans. 2022, 51, 1754–1764. https://doi.org/10.1039/d1dt04075h

[3] Sergentu, D.-C.; Booth, C. H.; Autschbach, J., 'Probing multiconfigurational states by spectroscopy: The cerium XAS L₃-edge puzzle', Chem. Eur. J. 2021, 27, 7239–7251. https://doi.org/10.1002/chem.202100145

4:30pm AS-TuA-10 The XPS of Ni Compounds – A Comparative Study, *Paul S. Bagus,* University of North Texas*; Connie J. Nelin,* Consultant*; Nabajit Lahiri,* pacific Northwest National Lab*; Eugene S. Ilton,* Pacific Northwest National Lab
The Ni 2p XPS of the ionic compounds NiO, Ni(OH)2, and Ni(CO)3 are analyzed, interpreted, compared with each other and, as well, the

theoretical results are compared with XPS measurements. The main features as well as the satellite, shake, features are considered. The theoretical analysis is based on the properties of ab initio molecular orbital wavefunctions, WFs, for cluster models of the compounds. We distinguish two theoretical approaches. The first is where only the angular momentum coupling of the core 2p open shell and the valence open shell which contains 8 dominantly Ni 3d orbitals is considered to form the ionic wavefunctions, WFs. The second is where excitations from closed shell orbitals into the valence open shell space is added. The second approach properly describes the XPS satellites and puts, for the first time, the concept of "charge transfer" in the core ionic states on a firm theoretical basis. It is important to choose orbitals and WFs which allow the mixing of normal and shake character and novel methods are used to characterize the orbitals and to describe the WF character. The consequences for the XPS of the variation of the Ni-ligand distance are examined. Three key results are: (1) The extended theoretical approach must be used to describe the satellites and it also somewhat modifies the main XPS peaks. (2) The choice of orbitals is critical to properly describe the XPS, especially the satellites, and this can be related to the electronic structure of the excited states. The differences between the XPS of the different compounds are mainly for the satellite features and the reasons for this are explained.

4:45pm AS-TuA-11 The Experimental Asymmetry of the 2*p*, 3*d*, and 4*f*, Photoemission Spectra of the Elements of the 3rd, 4th, and 5th Periods, *Alberto Herrera-Gomez,* Cinvestav, Mexico; *Anthony Dutoi,* University of the Pacific; *Dulce Guzman-Bucio,* CINVESTAV-Queretaro, Mexico; *Dagoberto Cabrera-German,* Universidad de Sonora, Mexico; *Abraham Carmona-Carmona,* Benemerita Universidad Autonoma de Puebla, Mexico; *Orlando Cortazar-Martinez,* CINVESTAV-Unidad Queretaro, Mexico; *B. Vincent Crist,* The XPS Library; *Marisol Mayorga-Garay,* CINVESTAV-Unidad Queretaro, Mexico

We carried out a peak-fitting analysis of the 2*p*, 3*d*, and 4*f*, spectra of the elements of the 3rd, 4th, and 5th periods, respectively. We found that the Double-Lorentzian lineshape (DL) [1] closely reproduces the asymmetry in all cases. Moreover, the DL asymmetry shows clear trends with atomic-number. This contrasts with the Doniach-Sunjic lineshape, which, in most cases, does not reproduce the experimental data; besides, it cannot be used in quantitative studies because it is not integrable.

The asymmetry parameter (a_{DL}) for the $2p_{3/2}$ photoemission line shows a decreasing trend with increasing atomic number, with a pronounced shoulder in the region of the ferromagnetic metals. For the $2p_{1/2}$ photoemission line, the DL asymmetry increases for the ferromagnetic metal. This indicates a relationship between the asymmetry and the electronic structure of the metals.

a_{DL} also shows interesting tendencies for the 3*d* photoemission spectra of the 5th-period elements from Rb to In. There is a significant difference in the DL parameter between the two 3*d* branches for elements with an empty 4*d* bandy (Rb and Sr). a_{DL} is lower for the elements with a half-filled (Mo [Kr]$5s^14d^5$), almost filled (Ru [Kr]$5s^14d^7$ and Rh [Kr]$5s^14d^8$) and filled 4*d* band (Ag [Kr]$5s^14d^{10}$, Cd [Kr]$5s^24d^{10}$, and In [Kr]$5s^15p^1$). These results suggest that the asymmetry is related to the 4*d* valence electrons.

A theoretical approach is proposed.

[1] A. Herrera-Gomez, D.M. Guzman-Bucio, A.J. Carmona-Carmona, O. Cortazar-Martinez, M. Mayorga-Garay, D. Cabrera-German, C.A. Ospina-Ocampo, B.V. Crist, J. Raboño-Borbolla, Double Lorentzian lineshape for asymmetric peaks in photoelectron spectroscopy, Journal of Vacuum Science & Technology A 41 (2023). https://doi.org/10.1116/6.0002602.

5:00pm AS-TuA-12 Computational Exploration of Dimension Limits for Narrow Gap Transport of Reactive Species, *Greg Hartmann, Shyam Sridhar, Peter Ventzek,* Tokyo Electron America, Inc.

State of the art device fabrication is pushing the limits of etch processes in terms of achievable critical dimensions. Passing these limits requires an insight into the fundamentals of dry etch processes, i.e. fluxes of radicals and ions reaching the etch front and how they are transported into the feature. Here we discuss the 'in-feature' transport of radicals for narrow trenches beyond the limits of the conventional perspective of Knudsen diffusion. Advances in computational techniques, particularly density functional theory (DFT), enable theoretical models on the scale of a few molecular diameters to elucidate transport processes on the atomic scale. Van-der-Waals corrected DFT predicts significant intermolecular interactions provide a severely-constricted transport regime where a diffusing species is always interacting with at least one wall; surface diffusion has been identified as significant within typical process dimensions but may be the dominant mode of transport under this condition. Cessation of transport is predicted at the transition to solid-state diffusion. Multiphysics models utilizing kinetic data predicted via DFT predict a critical depth under which radical or by-product transmission is limited; the radical-starved limit is predicted to occur on the order of hundreds of nanometers. Consequently, a range of critical dimensions are predicted to create an inherently radical-starved condition. Scaling relationships provide insight into critical dimension limits across varied material selection.

5:15pm AS-TuA-13 High-Temperature Diffraction and Surface Electron-Phonon Coupling of the Unreconstructed Metallic and (3x1)-O Reconstructed Nb(100) Surfaces by Helium Atom Scattering, *Michael Van Duinen, Caleb Thompson,* University of Chicago; *Michelle Kelley, Cristobal Mendez,* Cornell University; *Sarah Willson, Van Do,* University of Chicago; *Tomas Arias,* Cornell University; *Steven Sibener,* University of Chicago

Superconducting radio frequency (SRF) cavities are the fundamental accelerating components of linear particle accelerators. Niobium is the material of choice for SRF cavities due to its high malleability, thermal conductivity, and superconducting critical temperature (T_C). Despite Nb having a T_C of ~9 K, the practical operating temperature of a Nb SRF cavity is ~2 K, below the boiling point of He and consequently quite expensive to operate. The improvement of Nb SRF cavities and the lowering of operating costs has been focused primarily on the development of new materials on the Nb surface. Due to the ~100 nm superconducting penetration depth of Nb, only ~1 micron of material need be deposited onto the Nb surface to completely change its superconducting properties. One of the primary limitations to both Nb SRF cavities and the new materials under study is the presence of a thermally stable and robust oxide. Understanding the formation, stability, and dynamics of the oxide and its effects on the operation of Nb SRF cavities requires study both of material superconducting properties and atomic-scale surface material chemistry. Helium atom scattering (HAS) is a surface diffraction technique that has the ability to probe surface structure, bonding, and dynamics. The chemically inert He and an ultra-high vacuum (UHV) environment make HAS an ideal probe for the chemically reactive and sensitive Nb surface. Furthermore, experts in the field have developed theory involving the He-electron interaction and the surface electron-phonon interaction to formulate an equation by which HAS data can be used to determine an electron-phonon coupling (EPC) constant (λ) for the surface (λ_S). These data can then be used to find surface analogues for T_C along with other superconducting properties relevant to SRF cavity operation. We study the Nb(100) surface for its recognizable and stable (3x1)-O NbO oxide reconstruction. We find a λ_S of 0.50 ± 0.08 for the metallic Nb(100) versus a bulk λ of ~1, demonstrating that the superconducting state is significantly modified at the surface. We also find a λ_S of 0.20 ± 0.06 for the (3x1)-O reconstruction. Lower λ_S corresponds to lower T_C and overall poorer superconducting performance. Therefore, our studies strongly corroborate a strong body of previous literature that has hypothesized that the oxide diminishes superconducting performance for both bare Nb and new materials built atop it. From this fundamental starting point, we can further demonstrate the effect that doping, alloying, and thin-film material growth on the Nb surface have on its superconducting performance.

5:30pm AS-TuA-14 The Type of Ru Oxide on Ru(0001) Determines the Activity for the Decomposition of Silane, *Ester Perez Penco, Roland Bliem,* ARCNL

Hydrogen plasma is commonly applied for the cleaning of functional surfaces, because it effectively removes most surface oxides and carbon-based deposits by reacting to form volatile species. However, this etching by hydrogen plasma also occurs for other elements, such as Si, which is widely abundant and forms silane gas (SiH_4) when exposed to hydrogen radicals and ions. The resulting silane molecules can serve as a means to transport Si through the plasma setup and lead to Si redeposition. Typically, Si growth from silane only occurs at specific conditions, often involving high surface temperatures. However, in the presence of catalytically active materials such as Ru and Ru oxide, decomposition of silane occurs already at significantly milder conditions. The interaction mechanisms of silane with the surfaces of Ru and its oxides and the criteria for the deposition of Si,

however, are unclear.

Here, we present an in situ study of the mechanism that leads to plasma-assisted deposition of Si on Ru surfaces. We isolate the interaction of the transport agent, silane gas, with Ru(0001) single-crystal surfaces using near-ambient pressure X-ray photoelectron spectroscopy (XPS). A comparison of Ru metal to a thin, defective type of Ru oxide and bulk-like RuO_2 demonstrates a decisive impact of surface oxidation on the reaction with SiH_4 and the nature of the deposited Si. On Ru metal, silane decomposition is barrierless and results in the formation of Ru silicide. The initial layers of a (metastable) Ru oxide structure readily catalyze the deposition of Si, forming a Ru-Si-O compound that consumes the Ru oxide phase. Already a few nanometers of the bulk-like RuO_2 phase, on the other hand, are observed to be fully inert towards the decomposition of silane at room temperature. This striking difference between two similar oxides is attributed to their different density surface vacancies, which aid the dissociation of SiH_4.

Our in situ XPS results demonstrate that the type of Ru oxide and its structural integrity is decisive for surface chemistry of Ru under oxidizing conditions. The contrast of facile silane decomposition for a thin defective oxide and its full inhibition for bulk-like RuO_2 serves as an illustration of the influence of seemingly subtle changes to the surfaces of materials with a wide application potential.

Biomaterial Interfaces
Room West Hall - Session BI-TuA

Future of Biointerface Science Collection (ALL-INVITED SESSION)

Moderators: Kenan Fears, U.S. Naval Research Laboratory, **Tobias Weidner**, Aarhus University, Denmark

3:15pm **BI-TuA-5 Exploring the Dynamics of Proteins, Nucleic Acids, and Their Interplay by Coherent Anti-Stokes Raman Spectroscopy**, *Pablo G. Argudo, Mateusz Brzezinski,* Max Planck Institute for Polymer Research, Germany*; Weixiang Chen, Brigitta Dúzs, Avik Samanta, Andreas Walther,* Johannes Gutenberg University, Germany*; Sapun H. Parekh,* The University of Texas at Austin **INVITED**

The comprehension of proteins and nucleic acid chains, along with their interactions, is vital in contemporary biochemistry and molecular biology. These molecules can induce biological phase separation, resulting in the formation of membraneless organelles (MLOs) within cells. Consequently, understanding their structure is key, as it directly influence their ultimate behaviour. Moreover, external factors or interactions can directly impact their characteristics and final function, as evidenced in degenerative diseases like amyotrophic lateral sclerosis (ALS) or frontotemporal dementia (FTD).

In this context, we present the employment of Coherent Anti-Stokes Raman spectroscopy (CARS) as an appropriate method to characterize the changes happening over time in condensates. By examining the fingerprint region of nucleic acids, we can determine the biological interactions taking place. In designed DNA condensate model systems, ssDNA to dsDNA hybridization or salt effects can be monitored in the final assembled conformation. For proteins, their secondary structure can be elucidated, ranging from an ordered α-helix or β-sheet to a disordered random coil. Finally, protein-RNA interactions can be also characterized, as for TDP-43 low complexity domain (TDP43-LCD) and RNA. While introducing further complexity, the Raman shifts observed in specific regions of the formed condensates can indicate the RNA's effect on the protein, including secondary structure control.

Electronic Materials and Photonics
Room 114 - Session EM+2D+BI+QS+TF-TuA

Advances in Photonic Materials and Devices

Moderators: Leland Nordin, University of Central Florida, **Philip Lee**, University of Kentucky

2:15pm **EM+2D+BI+QS+TF-TuA-1 New Materials for Metamaterials: Electrochemical Materials and Switchable Chiral Nanostructures**, *Vivian Ferry,* University of Minnesota **INVITED**

Alternative materials for metasurfaces enable new properties and lay the foundation for advantage applications. This talk will discuss two strategies for new, tunable metasurfaces. The first part of the talk will discuss the use of electrolyte gating to control the optical properties of materials, focusing on $La_{1-x}Sr_xCoO_{3-d}$ (LSCO) as an exemplary case. We fabricate electric double layer transistors using LSCO and an ion gel, and under application of positive gate voltage gating facilitates the formation and migration of oxygen vacancies, and a transition from a perovskite phase to an oxygen-vacancy-ordered brownmillerite phase. This is accompanied by substantial change in optical properties, as measured with spectroscopic ellipsometry. The talk will discuss how LSCO can be incorporated with metasurfaces to produce tunable optical response. The second part of the talk will discuss chiral metamaterials, and particularly novel materials comprised of nanopatterned, light emitting nanocrystals with simultaneous control over both directionality and polarization state.

2:45pm **EM+2D+BI+QS+TF-TuA-3 Optoelectronic Nanowire Neuron**, *Thomas Kjellberg Jensen,* Lund University, Sweden*; Joachim E. Sestoft,* Niels Bohr Institute, Denmark*; David Alcer, Nathanael Löfström, Vidar Flodgren, Abhijit Das,* Lund University, Sweden*; Rasmus D. Schlosser, Thomas Kanne Nordqvist,* Niels Bohr Institute, Denmark*; Magnus Borgström,* Lund University, Sweden*; Jesper Nygård,* Niels Bohr Institute, Denmark*; Anders Mikkelsen,* Lund University, Sweden

Three different semiconductor nanowires are combined into a single optoelectronic artificial neuron. In general, artificial neurons sum and weight input signals, and output a signal according to a non-linear function which may be sigmoid-shaped (a generalized artificial neuron is shown in Fig. 1a). Figure 1b schematically shows the artificial neuron realized using nanowires. Here, neural excitation/inhibition is achieved by balancing inputted light across two pin-diode nanowires outputting a summed voltage measured by a nanowire-based field-effect transistor (FET).

The false-colored electron microscope image shown in Figure 1c depicts the fabricated nanowire neuron. In Figure 1d we show the current measured across the FET nanowire as a function of laser beam position, demonstrating the excitatory and inhibitory behavior. Selectively illuminating the excitatory nanowire diode, the change in conductance follows a sigmoidal curve as a function of linearly increasing light intensity (Figure 1e) – the necessary non-linear part of a neural network. Taken together, these properties provide the device with the basic functionalities needed for a neuromorphic computing node [1,2]. Future measurements will explore the time-domain effects.

Our artificial neuron provides a promising future platform for combining diverse materials with low power consumption and significantly reduced circuit footprint, this way addressing critical limitations for future-proofing photonics-based applications in neuromorphic computing.

REFERENCES:

[1] D. O. Winge, S. Limpert, H. Linke, M. T. Borgström, B. Webb, S. Heinze, and A. Mikkelsen, "Implementing an insect brain computational circuit using III-V nanowire components in a single shared waveguide optical network", *ACS Photonics*, vol. 10, pp. 2787-2798, 2020.

[2] D. Winge, M. Borgström, E. Lind, and A. Mikkelsen, "Artificial nanophotonic neuron with internal memory for biologically inspired and reservoir network computing", *Neuromorph. Comput. Eng.*, vol. 3, no. 034011, 2023.

3:00pm EM+2D+BI+QS+TF-TuA-4 Modulation of Optical and Plasmonic Properties of Epitaxial and Precision Titanium Nitride Thin Films, *Ikenna Chris-Okoro,* North Carolina A&T State University; *Sheilah Cherono,* North Carolina A & T State Uni; *Catalin Martin,* Ramapo College of New Jersey; *Valentin Craciun,* National Institute for Laser, Plasma, and Radiation Physics, Romania; *Soyoung Kim, Johannes Mahl, Junko Yano,* Lawrence Berkeley National Laboratory; *Ethan Crumlin,* Lawrence Berkeley Lab; *Dhananjay Kumar,* North Carolina A & T State Uni; **Wisdom Akande,** North Carolina A&T State University

The present study arises from the need for developing negative-permittivity materials beyond commonly employed plasmonic metals (e.g., Au, Ag), which are often incompatible (i.e., low melting point, mechanically soft, chemically unstable) with real operating environments. This work reports a pulsed laser-assisted synthesis, detailed structural characterization using x-ray diffraction (XRD), x-ray photoelectron spectroscopy (XPS), x-ray absorption spectroscopy (XAS), Rutherford Backscattering spectroscopy (RBS), and plasmonic properties of three sets of TiN/TiON thin films. The first two sets of TiN films were grown at 600 and 700 °C under a high vacuum condition (≤2 ×10^{-7} Torr). The third set of TiN film was grown in the presence of 5 mTorr of molecular oxygen at 700 °C. The purpose of making these three sets of TiN/TiON films was to understand the role of film crystallinity and the role of the oxygen content of TiN films on their optical and plasmonic properties. The results have shown that TiN films deposited in a high vacuum are metallic, have large reflectance, and high optical conductivity. The TiN films, grown in 5 mTorr, were found to be partially oxidized with room temperature resistivity nearly three times larger than those of the TiN films grown under high vacuum conditions.

The optical conductivity of these films was analyzed using a Kramers-Kronig transformation of reflectance and a Lorentz-Drude model; the optical conductivity determined by two different methods agrees very well. The good agreement between the two methods is indicative of a reliable estimate of the absolute value of reflectance in the first place. The existence of significant spectral weight below the interband absorptions is shared between two Lorentzians, one around 250 cm^{-1} and one around 2,500 cm^{-1}. We discuss here the dependence of the two bands on the deposition conditions and their effect on the plasmonic performances of TiN/TiON thin films, in particular on the surface plasmon polariton (SPP) and localized surface plasmon resonance (LSPR) quality factors.

3:15pm EM+2D+BI+QS+TF-TuA-5 Nano-Focusing and Characterization of the OAM Beam Through an Optical Fiber Using Plasmonic Nanostructure, **Rohil Kayastha,** *Wei Zhang, Blake Birmingham,* Baylor University; *Zhi Gao,* Texas A&M University; *Jonathan Hu,* Baylor University; *Rafael Quintero-Torres,* UNAM, Mexico; *Alexei V. Sokolov,* Texas A&M University; *Zhenrong Zhang,* Baylor University

Optical vortex beam has been used in many applications such as nanoscale imaging, telecommunication, sensing, and so on due to its unique azimuthal phase distribution. Many of these applications utilize optical fibers as a sensor or to propagate the beam to transmit data and information. The vortex beam carrying an orbital angular momentum (OAM) has a phase singularity giving the beam a doughnut intensity profile. Due to its helical wavefront nature, the vortex beam carrying OAM has also been used to distinguish the enantiomers of the chiral molecule. However, coupling efficiency remains a problem due to the size mismatch of the beam and the molecule. Our work uses vortex fibers with plasmonic nanostructures to nano-focus the vortex beam to enhance the coupling between light and chiral matter. To achieve this goal, characterization of vortex beam in free space and through vortex fiber (a polarization-maintaining ring core optical fiber), and fabrication of nanostructure on fiber facet were performed.

Generation and propagation of OAM beams were characterized in free space and through a vortex fiber. The free-space OAM beam was coupled and transmitted successfully through the vortex fiber with a pure and stable output beam. The helicity characterization and polarization analysis of the free-space and fiber-coupled output vortex beams showed consistent polarization and OAM. The direction of the phase front was maintained after propagation of the OAM through the vortex fiber, as observed from the spiral interference pattern. Nano-focusing of the OAM beam using nanostructure on the fiber facet was observed from the simulation. The circular array of plasmonic nanobars was fabricated on the fiber facet core,

and the far-field image of the output OAM beam was observed after transmission through the fiber with the nanostructure. The near-field image of the nano-focused OAM beam on the fiber will be investigated using a near-field scanning optical microscope (NSOM). The focusing of the OAM beam on a fiber facet with the nanostructure could enhance the coupling efficiency of the beam with chiral molecules. The nano-focused OAM on the fiber could be used as a scanning and sensing probe for single-molecule chirality detection.

4:00pm EM+2D+BI+QS+TF-TuA-8 Templated Block Copolymer Network Thin Films as 3D Chiral Optical Metamaterials: Connecting Finite-Difference Time-Domain and Self-Consistent Field Theory Simulations, *Emily McGuinness, Benjamin Magruder, Pengyu Chen, Kevin Dorfman, Christopher Ellison,* **Vivian Ferry,** University of Minnesota

Optical metamaterials, whose properties depend not only on material selection but also the spatial arrangement of the material, provide access to interactions with light that are not present in bulk materials alone. Block copolymer self-assembly is a scalable method for creating 3D spatially periodic nanoscale structures to act as metamaterial templates. The gyroid morphology, whose curved, percolating structure is composed of triply connected struts, possesses chiral elements such as helices in bulk and chiral structures at certain surface terminations. As a result of their chirality, when templated with a plasmonic material, gyroids exhibit circular dichroism (CD) with applications in anti-counterfeit as well as molecular and protein sensing. While many optical simulations of gyroids assume a perfect cubic structure, most applications utilize thin films whose processing results in distortions such as compression normal to the substrate or surface rearrangements due to interactions with interfaces. Distorted gyroids, as well as the growing library of additional network structures possible from block copolymer self-assembly, are increasingly challenging to model from a purely mathematical basis and require better basis in physical reality. Combining the output of polymer self-consistent field theory (SCFT) with finite-difference time-domain (FDTD) optical simulations enables the exploration of thermodynamically equilibrated structures for both distorted gyroids and expanded network geometries. This presentation will investigate the CD response of compressed double gyroid thin films as well as that of newly hypothesized network structures such as H^{181}. In the first example, compression of (110) oriented silver double gyroid thin films yields a switching phenomenon from left to right circularly polarized light preferential absorption, offering the potential for dynamic systems (**Figure 1a**). Mechanistically, this behavior depends both on the surface and sub-surface structures of the compressed double gyroids. In the second example, (001) oriented silver templated thin films of the newly computationally uncovered H^{181} structure are shown to support a broadband visible light CD response (spanning 200 nm) with a g-factor (CD normalized to average absorption) of at least 0.14 across that entire wavelength range (**Figure 1b**). Overall, this work moves the optical simulations of metamaterials from block copolymers closer those physically realized, introducing additional opportunities for engineering their optical response.

4:15pm EM+2D+BI+QS+TF-TuA-9 Solution Processing of Optical Phase Change Materials, **Brian Mills,** Massachusetts Institute of Technology; *Rashi Sharma, Daniel Wiedeman,* University of Central Florida; *Casey Schwarz,* Ursinus College; *Nichole Li,* Massachusetts Institute of Technology; *Eric Bissell,* University of Central Florida; *Cosmin Constantin Popescu,* massachusetts Institute of Technology; *Dennis Callahan,* Charles Stark Draper Laboratory, Inc.; *Parag Banerjee, Kathleen Richardson,* University of Central Florida; *Juejun Hu,* Massachusetts Institute of Technology

Chalcogenide optical phase change materials (O-PCM) serve as the functional material in a variety of non-volatile photonic devices, from reconfigurable metasurface lenses to tunable integrated photonic resonators. Although a handful of high figure of merit O-PCMs have been identified and implemented in prototype devices, the space of O-PCM composition remains relatively unexplored, precluding the possibility of application specific choices in material composition that optimize device performance. This is due, in large part, to the lack of time and cost efficient methods for O-PCM thin film deposition and characterization, for which vacuum chamber deposition is the most common method. In this work, we present the first implementation of a solution processing approach for O-PCM film synthesis and deposition, providing evidence of the method's viability in creating high quality, functioning O-PCM films with close adherence to target stoichiometry. This method serves as a robust platform for materials exploration of O-PCM composition and allows for the identification of candidate O-PCM, as well as an understanding of the effect

of compositional changes in O-PCM optical and cycling properties.

4:30pm **EM+2D+BI+QS+TF-TuA-10 Effects of Ce Concentration on the Microstructural, Optical, and Luminescence Properties in Ce:GAGG Ceramic Phosphors**, *William Bowman, Steven Lass,* University of Central Florida; *Federico Moretti, Weronika Wolszczak,* Lawrence Berkeley National Laboratory; *Romain Gaume,* University of Central Florida

Efficient luminescence and optical quality are necessary phosphor attributes for applications such as down-conversion layers in photovoltaics and computed tomography. Cerium-doped gadolinium aluminum gallium garnet (Ce:GAGG) is highly applicable for these purposes. It has been shown in other garnet hosts such as Ce:YAG and Ce:LuAG that Ce concentration alters both the luminescence and optical properties of the materials. In the case of Ce:GAGG single crystals and Ce concentrations lower than 1 at%, radioluminescence decay constants decrease by increasing the Ce concentration while light yield reaches a maximum at 0.3 at%. For Ce:GAGG ceramics, the effect of Ce concentration on these properties has not been systematically investigated. There is at current no work on determining the solid solubility limit of Ce in GAGG, which is critical in controlling the development of secondary phases and subsequent optical quality.

This study aims to investigate the effects of Ce concentration on the microstructural, optical, and luminescence properties of GAGG optical ceramics with dopant concentrations in the 0.1at% to 10at% range. Transmission of the material increases with increasing Ce concentration up to 5.0at%. At the same time, the optical and luminescence properties of these samples show a complex evolution upon Ce concentration, highlighting the complex interplay among optical characteristics of the samples, concentration-related luminescence quenching phenomena, and charge carrier trapping defects.

This material is based upon work supported by the U.S. Department of Homeland Security under Grant Award Number 20CWDARI00038-01-00. The views and conclusions contained in this document are those of the authors and should not be interpreted as necessarily representing the official policies, either expressed or implied, of the U.S. Department of Homeland Security.

4:45pm **EM+2D+BI+QS+TF-TuA-11 Solution Based Processing of $Ge_2Sb_2Se_4Te_1$ Phase Change Material for Optical Applications**, *Daniel Wiedeman, Rashi Sharma, Eric Bissel, Parag Banerjee,* University of Central Florida; *Brian Mills, Juejun Hu,* Massachusetts Institute of Technology; *Marie Sykes, Jasper Stackawitz, Jake Lucinec, Casey Schwarz,* Ursinus College; *Kathleen Richardson,* University of Central Florida

Chalcogenide based phase change materials are important for creating novel optical and photonic devices, improving on current devices for future applications. Solution processing, via dip coating, spin coating, or drop-casting, is a low-cost, high-throughput alternative method of depositing thin films, which allows for greater composition diversity. In this work, we performed a detailed systematic study of the solution derived drop-casted film of Ge2Sb2Se4Te1 alloy in an ethylenediamine and ethanedithiol mixture. The composition, morphology and structural properties of the films were analyzed by employing scanning electron microscopy, energy dispersive X-ray spectroscopy, Raman spectroscopy, and X-ray diffraction. Our findings provide insight into a potential route for scalable $Ge_2Sb_2Se_4Te_1$ films.

5:00pm **EM+2D+BI+QS+TF-TuA-12 Multi-Dimensional p-WSe$_2$/n-Ga$_2$O$_3$ Enhancement-Mode Phototransistors for Stand-Alone Deep-Ultraviolet Sensing**, *Jihyun Kim, Soobeen Lee,* Seoul National University, South Korea

β-Ga$_2$O$_3$ is an ultra-wide bandgap (UWBG) semiconductor with a bandgap of 4.9 eV, resulting in a high breakdown field of approximately 8 MV/cm and a high Baliga's figure-of-merit. β-Ga$_2$O$_3$ is a promising material for deep-ultraviolet (DUV) photodetector (PD) applications due to its direct bandgap of 4.9 eV, excellent thermal stability, and high absorption coefficient. Self-powered β-Ga$_2$O$_3$ PDs can be realized through p-n heterojunction (HJ) field-effect transistor architectures, exhibiting normally-off operation owing to the depletion region in the β-Ga$_2$O$_3$ channel. With intrinsic n-type conductivity caused by unintentional doping and challenges in p-type doping, fabricating self-powered β-Ga$_2$O$_3$ PDs necessitates combining β-Ga$_2$O$_3$ with p-type semiconductors such as transition-metal dichalcogenides (TMDs), nickel oxide, or silicon carbide. Tungsten diselenide (WSe$_2$), one of the TMDs, stands out as a promising material with a high monolayer mobility of approximately 180 $cm^2V^{-1}s^{-1}$. Their dangling-bond-free surfaces provide an advantage in forming sharp interfaces with other materials in HJs. Moreover, efficient p-type doping of WSe$_2$ is achieved via charge transfer by utilizing the high electron affinity of its self-limiting oxide, sub-stoichiometric tungsten oxide (WO$_{3-x}$), which is used as a dopant.

In this work, we introduce normally-off p-WSe$_2$/n-β-Ga$_2$O$_3$ phototransistors and demonstrate their self-powered operation under 254 nm light. p-Type WSe$_2$ was realized through charge transfer doping of WO$_{3-x}$ formed by O$_3$ treatment, and the p-type doping effect of this oxide was confirmed through electrical characteristics. The cross-sectional structure of the fabricated p-WSe$_2$/n-β-Ga$_2$O$_3$ phototransistors was analyzed, and the electrical and optical properties were evaluated before and after WSe$_2$ oxidation. The device demonstrated a responsivity of 2 A/W under 254 nm light without an external bias, surpassing the performance of previously reported p-n HJ-based β-Ga$_2$O$_3$ PDs. Furthermore, we investigate the enhanced optoelectronic performance of multi-dimensional β-Ga$_2$O$_3$ phototransistors with plasmonic metal nanoparticles. In this presentation, we will discuss the potential of the self-powered multi-dimensional DUV β-Ga$_2$O$_3$ PDs with improved performance and their prospects in practical applications.

This work was supported by Korea Institute for Advancement of Technology (KIAT) grant funded by the Korea Government (P0012451, The Competency Development Program for Industry Specialist) and the Korea Research Institute for defense Technology planning and advancement (KRIT) grant funded by Defense Acquisition Program Administration (DAPA) (KRIT-CT-21-034, and KRIT-CT-22-046).

MEMS and NEMS
Room 125 - Session MN1-TuA

Bio and Environmental MEMS

Moderators: Matthew Jordan, Sandia National Laboratories, **Yanan Wang**, University of Nebraska-Lincoln

2:15pm **MN1-TuA-1 Gaede-Langmuir Award Talk: Ingestible Technologies for Disease Assessment and Treatment in the Gastrointestinal Tract**, *Reza Ghodssi[1]*, University of Maryland, College Park **INVITED**

MEMS and Microsystems have shown the potential to improve healthcare through advanced monitoring and treatment approaches among other applications. Microsystems, like wearable electronics, that interface with the body have been thoroughly explored in academic research and commercially. A rising field of research is the development of ingestible technologies to address gastrointestinal (GI) and related diseases. The GI tract is the only internal organ that can be non-invasively accessed, so it provides a gateway to analyze bodily processes and reach specific organ systems for treatment. Moreover, digestive diseases affect more than 40 million people in the US alone. My group's research focuses on the development of ingestible tools for diagnostics and treatment of gastrointestinal and systemic diseases. Embedded electronics and sensors enable analysis of critical biomarkers, like hydrogen sulfide (H$_2$S) and tissue impedance, while actuators allow sampling and drug delivery at precise locations in tissue for diagnostics and highly effective on-command treatment. In this talk, I will discuss current progress toward integrated capsule systems capable of biomarker sensing, localized actuated drug injection and intestinal sampling for further analysis.

2:45pm **MN1-TuA-3 Packaging Development with an Integrated Wireless System for an Electrochemical Cardiac Biosensor**, *Jorge Manrique Castro,* The University of Texas at El Paso; *Blake Walker, Faisal Kashem, Swaminathan Rajaraman,* University of Central Florida

Cardiovascular disease is one of the main causes of mortalities globally. It is of high importance to identify early conditions given by the analysis of biomarkers in blood such as troponin, D-Dimers and brain natriuretic peptide **[1]**. In order to capture information emanating from these biomarkers, BioMEMS technologies have emerged as solution for the development, and packaging of biosensors aimed for accurate diagnosis and prognosis of cardiac diseases **[2]**. Among them, wearable cardiac biosensors **[3]**, and point-of-care platforms **[4]** have been proposed.

Data collection, processing, and telemetry is a challenge due to limitations in power source, consumption, and range of operation accompanied by issues in biocompatibility, size, and hermeticity. There is also a lack of exploration in processing techniques for biocompatible materials to minimize wound infection; point-of-care immunosensors optimization to

---

[1] **Gaede-Langmuir Award Winner**

improve patient compliance; and continuous monitoring for making informed decisions in real-time to overcome any life threatening situation in the short and long term.

Here, we present the development of a cardiac microsystem for electrochemical sensing with wireless data extraction. Two workflows are presented: Packaging and system integration. Material processing for packaging was performed with multimodal and CO_2 lasers on fused silica. This material was selected due to its great biocompatibility, chemical and mechanical robustness, and its transparency to optical and RF signals [5]. **Fig. 1** details results from the laser micromachining process with different parametrization. After engraving a microcavity on fused silica quartz, laser confocal characterization was carried out to measure the 3D profile and surface roughness (**Fig. 2**). On the other hand, system integration started at the macrolevel with Arduino-based board (Elegoo Uno R3), bluetooth module (HC-05), and impedance converter board (EVAL-AD5933EBZ) as presented in **Fig. 3**. Miniaturization of the impedance board was implemented by extracting the AD5933 chip from the board (**Fig. 4**). It was connected and programmed using I^2C communication protocol and customized script [6]. To test impedance measurements, 1 kΩ resistor was used as device under test. Real, imaginary and magnitude impedance were collected and sent wirelessly to a remote laptop (**Fig. 5**).

Ongoing work exploring different techniques for etching glass are being studied. Miniaturization of the Arduino board and bluetooth module into a single microcontroller unit is in progress to reduce footprint. A flex circuit with an interdigitated electrode is conceived to be encapsulated within the fused silica cavity.

3:00pm MN1-TuA-4 Self-Powered, Eco-Friendly, and Edible UV Sensors for Food Packaging Applications, *Pouya Borjian, Mohammadreza Chimerad, Pawan Pathak, Hyoung Jin Cho,* University of Central Florida

We present a novel self-powered ultraviolet (UV) sensor based on non-toxic and edible materials. UV radiation can play an important role in food spoilage. Prolonged exposure to UV can lead to the degradation of different nutrients such as vitamins in the food. Proper control and monitoring UV exposure levels are crucial to minimizing food spoilage and maintaining food quality throughout production and distribution. Although there are some sensors available in the food industry for detecting UV radiation, many of them are fabricated using toxic or harmful materials. Additionally, most of these sensors require external power sources to perform. In this work, a flexible UV sensor was developed based on a non-toxic and edible ethyl cellulose (EC) substrate coated with gold interdigitated electrodes using sputtering. The interdigitated electrodes were incorporated with an algae-based electrolyte and safe-to-eat zinc oxide (ZnO) nanoparticles as a UV-absorbent material. The formation of ZnO nanoparticles was characterized using scanning electron microscopy (SEM). Moreover, the optical response of the EC coated with the ZnO layer showed an absorbance edge around 370 nm compared to a bare EC film. The photocurrent response of the sensor was tested at various bias voltage and zero bias. At zero bias, the fabricated UV sensor displayed repeatable and steady photocurrent responses. In conclusion, a self-powered UV sensor was successfully demonstrated utilizing sustainable materials certified for food-grade applications.

3:15pm MN1-TuA-5 Inkjet Printing of AgNO₃ inks With Solvent-Selective Morphologies on Liquid Crystal Polymer Substrates, *Likith Krishna Lakshmi Narashima Murthy, Christian Zorman, Allison Hess-Dunning,* Case Western Reserve University

Inkjet printing offers unique prototyping and customization advantages for microfabricated biosensors, in particular sensors printed on flexible substrates. Electrochemical biosensors exhibit analyte sensitivities that increase with total exposed sensor area; therefore, rough or porous electrode structures with high specific surface areas are desirable for maximizing analyte sensitivity. In this work, we explored the properties of inkjet printed silver structures from plasma-reduced silver nitrate inks on liquid crystal polymer (LCP) substrates. LCP is an attractive substrate material for biosensing applications due to its biocompatibility, low moisture absorption and mechanical flexibility. Unfortunately, high quality printing of microscale structures on LCP can be challenging. We evaluated the pattern fidelity, conductivity, and surface morphology of silver nitrate in monoethylene glycol (mono-EG) and triethylene glycol (tri-EG) ink solvents in terms of their use in electrochemical sensors for measuring hydrogen peroxide concentration.

Inks were prepared by dissolving silver nitrate in a mono-EG/water or tri-EG/water solution. LCP substrates were prepared by cleaning the substrate surface with appropriate solvents and then exposing the substrates to a low

power oxygen plasma. Structures were printed on the LCP substrates using a Dimatix inkjet printer. The substrates were then exposed to a low-pressure argon plasma to reduce the dissociated silver cations and form elemental silver.

We found that the ink solvent had a strong influence on all measured parameters. While the mono-EG ink demonstrated good print fidelity on LCP, the tri-EG ink displayed either excessively hydrophobic or excessively hydrophilic behavior, leading to poor print fidelity. Silver structures printed from the tri-EG inks displayed a sheet resistivity three order of magnitude higher than structures printed using mono-EG inks. Scanning electron microscope images indicated that silver structures from the mono-EG inks were dense and flat, while those from tri-EG inks had a rough surface morphology. As no single ink could meet the requirements for the hydrogen peroxide sensor, we developed a bilayer approach in which the interconnect and base contact pads were printed from the mono-EG ink and a sensing electrode consisted of a tri-EG/mono-EG bilayer. Compared to the smooth Ag from mono-EG inks alone, the addition of the rough Ag coating from the tri-EG improved the electrochemical sensitivity to hydrogen peroxide by a factor of 3.6. The bilayer approach allowed for leveraging the advantageous characteristics of both ink types for improving sensor characteristics.

MEMS and NEMS
Room 125 - Session MN2-TuA

MEMS Sensing and Computation
Moderators: Matthew Jordan, Sandia National Laboratories, **Yanan Wang**, University of Nebraska-Lincoln

4:15pm MN2-TuA-9 Facile Fabrication of CuO/ZnO Heterojunctions from Sputtered Films UV Sensing, *Pawan Pathak, Mohammadreza Chimehrad, Pouya Borjian, Hyoung Jin Cho,* University of Central Florida

UV sensors are highly demanded for environmental monitoring, healthcare, and manufacturing, where understanding UV radiation's impacts is essential. Despite the prevalence of silicon-based photodetectors, their reliance on external power and broad absorption spectra are significant drawbacks. Addressing these challenges, we present a novel low-cost wet chemical method for constructing CuO/ZnO heterojunctions from sputtered thin films. This technique simplifies the traditional complex fabrication processes by using a one-step oxidation of DC-sputtered zinc and copper films on ITO-coated glass slides, resulting in the formation of p-type CuO nanowires and n-type ZnO nanoparticles that create a self-powered p-n junction. The morphological and chemical properties of the fabricated heterojunctions were meticulously analyzed using Scanning Electron Microscopy (SEM), X-ray Diffraction (XRD), and X-ray Photoelectron Spectroscopy (XPS). These analyses confirmed the successful creation of heterojunctions, which are critical for the desired sensor functionality. The optical properties were evaluated through UV-visible spectroscopy, demonstrating a strong absorption in the UV range, which is essential for UV sensing applications. Photonic responses based on current-voltage (I-V) relationships under a 365 nm laser were examined. The fabricated sensing device exhibited excellent photovoltaic behavior with a significant increase in current under illumination compared to dark conditions, showcasing an ideal p-n junction behavior with impressive responsivity (0.108 A/W) and photosensitivity (114). These characteristics indicate an efficient separation of photo-generated charge carriers at the junction which facilitates a strong and stable photoresponse without the necessity for an external power source. This work not only pioneers a simplified approach to heterojunction fabrication but also positions the resultant UV sensors as a good candidate for sustainable, low-power applications. The development presents significant advancements over traditional multi-step and high-temperature processes, offering a promising avenue for the scalable, low-temperature production of efficient UV sensors out of sputtered films

4:30pm MN2-TuA-10 Design and Development of a Wearable to Monitor UV Exposure, *Sushma Kotru, Sneha Kothapally,* The University of Alabama

With more than 5 million diagnoses per year, skin cancer outpaces the instances of diagnosis for breast, lung, colon and prostate cancer combined. It is estimated that one in five Americans will have skin cancer at some point in their life and 90% of the most widely diagnosed skin cancers are from exposure to the sun. Excessive exposure to sunlight can result in sunburn, which over a period of time, under repeated sun exposures, is responsible for cell and DNA damage, increasing the risk of developing skin cancer. The extent and nature of the damage depends on the type and

dosage of UV exposure and differs for individuals based on many factors including their skin type. Thus, having a way to monitor UV exposure and getting feedback on sun protection using a wearable would be beneficial.

Our group has developed a wearable using a UV sensor based on ferroelectric thin films which responds to UVA and UVB radiations. The sensor is fabricated on Si for scalability and future commercialization. In this talk fabrication and testing of the thin film-based UV sensors, approaches used to enhance the UV response of these sensors, integration of UV sensor with other electronic components to create a wearable for monitoring UV index in real-time, and development of a phone app will be presented.A review of similar wearables currently being researched or commercialized will be presented. Further, results and insights from market analysis and customer discovery from participation in NSF's I-Corps program will be shared.

4:45pm **MN2-TuA-11 Diamagnetically Levitating Graphite Plate Resonators**, *Yunong Wang, S M Enamul Hoque Yousuf,* University of Florida; *Jaesung Lee,* University of Central Florida; *Philip Feng,* University of Florida; *Alexander Gage,* University of Central Florida

Diamagnetically levitated and trapped systems hold great promise for developing high-performance anchor-less resonant devices with excellent stability. This scheme generates sufficiently large levitation force via diamagnetism, effectively counteracting gravity and facilitating levitation at room temperature without external power. Also, they are mechanically isolated from the external environments, enabling outstanding stability and minimal energy dissipation.

In this work, we combine theoretical analysis with experimental investigations to explore the complete levitation and rigid body resonances of diamagnetically levitating millimeter-scale graphite plates. Leveraging the strong diamagnetic susceptibility of graphite, we employ a square graphite plate (length of L=2.5mm, thickness of t=0.5mm, and mass of m=7mg), which exhibits stable levitation above permanent magnets without requiring active control. The resonance motions of the levitating graphite device are excited by electrostatic or dielectric gradient forces and detected by using an ultrasensitive optical interferometry system. We observed two distinct rigid body resonance motions at frequencies of f_1=37.7Hz and f_2=49.1Hz with quality (Q) factors of Q_1=48 and Q_2=37 in atmospheric pressure at room temperature. Notably, we find that the Q factors are primarily compromised by air damping.

Our initial study represents a significant step toward developing stabilized levitating systems at room temperature with a large mass. Furthermore, the findings presented here shall contribute to building high-performance resonant sensors.

Plasma Science and Technology
Room 124 - Session PS-TuA

Plasma Chemistry and Catalysis II

Moderators: Michael Gordon, University of California at Santa Barbara, **Michael Johnson**, Naval Research Laboratory, USA

2:15pm **PS-TuA-1 Nonthermal Plasmas for Advanced Nanomanufacturing**, *Rebecca Anthony,* Michigan State University   **INVITED**

Advanced manufacturing strategies have immense potential to reduce time and production costs for a range of applications.Meanwhile, the multiple functionalities and small size of nanomaterials can influence the versatility and capabilities of many devices including solar cells and solid-state lighting, energy conversion technologies and batteries, wearable electronics, and coatings. Combining advanced manufacturing with nanotechnology opens the door to exciting applications based on thin films and microstructures, with on-demand tunable functionality.

One promising route to achieving advanced nanomanufacturing is to use low-temperature plasmas for synthesis of nanoparticles, together with additive manufacturing methods which are compatible with roll-to-roll or additive printing methods. Here, synthesis of nanocrystals from semiconductor materials such as Gallium Nitride (GaN), Indium Nitride (InN), Silicon, and Carbon using low-temperature flow-through plasma reactors is presented. By tuning frequency, power, pressure, and gas composition, nonthermal plasmas open the door to allowing tuning of physical nanoparticle properties including size and surface defect concentration, as observed via x-ray diffraction (XRD), transmission electron microscopy (TEM), and electron paramagnetic spin resonance (EPR). Additionally, the tunable reactor parameters open the door to controlling

bonding configuration in some materials, such as carbon. This is a promising prospect, as the ratio of sp^2 / sp^3 hybridization represents significant changes in the properties of carbon materials, and in nanoparticles these changes can be paired with size-induced shifts in physical and optoelectronic properties. Nonthermal plasma synthesis can also be merged with an additive manufacturing approach to deposit tunable-property nanoparticle layers and patterns. The low-temperature synthesis of otherwise difficult-to-make semiconductor nanoparticles can thereby be uniquely paired with direct deposition onto arbitrarily chosen substrates – including temperature-sensitive materials such as polymers – for versatile deposition with on-demand property modulation.

2:45pm **PS-TuA-3 Conversion of Liquid Hydrocarbons to H₂ and C₂ Olefins in AC Plasma Discharges**, *Norleakvisoth Lim, Michael Gordon,* UCSB Chemical Engineering

Growing concerns regarding fossil fuel depletion, coupled with efforts to transition towards sustainable and low-carbon energy sources, have prompted innovative solutions for sustainable and efficient utilization of natural resources. This has led to increasing interest in developing technologies to transform light and heavy hydrocarbons to H_2 and more valuable hydrocarbons, such as ethylene and acetylene. Direct plasma-based conversion of liquid hydrocarbons offers a new approach to hydrocarbon reforming. It leverages the high energy density of the liquid phase to achieve fast reaction rates and compact reactor design, and may enable selective production of intermediate products through quenching at the gas-liquid interface. In this work, we explore the use of low current AC discharges in liquid hydrocarbon jets (**Figure 1**) to produce gaseous hydrogen, C_2 olefins, and separable solid carbon.

This talk will examine the influence of discharge frequency, liquid jet velocity and hydrocarbon feedstock on production rates, specific energy requirements and gaseous and liquid product distributions (**Figure 2**). Direct discharges in liquid hexanes predominantly produced H_2 (56.6 mol %), C_2H_2 (23.6 mol%), C_2H_4 (13.1 mol%) and CH_4 (6.7 mol%) under 60 Hz AC frequency. As the AC frequency increased to 17.3 kHz, the energy efficiency improved by a factor of two or more, owing to the change in plasma-generated bubble formation and transport dynamics surrounding the electrode region. A single-shot multi-frame imaging system was developed for consecutive nanosecond shadowgraph acquisitions, which allows us to further investigate the changes in bubble dynamics due to discharge duration and frequency. Decrease in bubble formation/contact time was shown to improve energy efficiency. For a liquid jet flow velocity of ~270 cm/s, the specific energy requirements (SER) for H_2, C_2H_4 and C_2H_2 production were 24 kWh/kg H_2, 3.2 kWh/kg C_2H_4 and 4.9 kWh/kg C_2H_2, respectively. We also examined the reactivities and product distributions of cyclohexane, benzene, toluene and xylene (BTX) feedstocks and ultimately demonstrate the potential of using AC discharges to upgrade less valuable hydrocarbon reformate. Additional characterization of the liquid (GC-MS) and solid (SEM, TEM and Raman) products will be discussed.

3:00pm **PS-TuA-4 Pulsing a Methane Discharge for Temperature Control and Better Energy Efficiency for Hydrogen Production**, *Thomas Fontaine, Linus Nyssen, David Petitjean,* Université libre de Bruxelles, Belgium; *Nathalie De Geyter,* Ghent University, Belgium; *Rony Snyders,* University of Mons, Belgium; *François Reniers,* Université libre de Bruxelles, Belgium

In the quest for CO₂-free energy, new fuels and energy storage media are gaining attention. The hydrogen molecule is of interest, as it presents industrial potential and can serve as an energy carrier. H_2 is mainly obtained from CH_4 steam reforming and water gas shift reactions, emitting CO_2. Cracking of CH_4 is an alternative route for H_2 production, with competitive theoretical energetical cost (standard enthalpy of the reaction at 0°C: 37.5 kJ for 1 mol of hydrogen, i.e. 7.5 times less than H_2O splitting) and no direct CO_2 emission. Various plasma processes can form H_2, but all struggle to enhance energy efficiency.

Tuning the shape of the voltage applied to the system is known to have beneficial impact on the energy efficiency, mostly by allowing a better control of the discharge energy. It is indeed well known that temperature of the discharge is a key factor, as some dehydrogenation steps are favored by higher temperatures, but elevated temperatures also lead to thermal losses. [1]

We investigate pulsing at different time scales (ms (AC pulses, called "burst"), µs, ns) in an atmospheric pressure discharge. A dielectric barrier discharge reactor is used to investigate the energy efficiency. DBD notably allows for operation with different high voltage sources. The reactor is composed of a central copper rod (high voltage electrode), a borosilicate glass tube (dielectric) and a stainless-steel mesh wrapped around the glass

(ground electrode). Conversion is measured over time by mass spectrometry. Interesting conditions were further investigated by optical emission spectroscopy. Rotational temperatures during the pulses are derived from the Swan band. A T_{rot} increase is measured for shorter duty cycle in burst mode. Switching from burst to nanosecond pulses also increases T_{rot}. Impact of the pulse energy on the temperature is studied by tuning the pulse energy (voltage tuning) and the total power (frequency tuning). T_{rot} is linked to the pulse energy, but not to the total power. Conversion for same SEI through different pulse lengths is compared in identical experimental conditions, which is rarely observed in the literature. We conclude that ms and ns pulses lead to similar energy efficiencies and perform better than ms pulses.

[1]M. Scapinello *et al.*, *Chem. Eng. Process. Process Intensif.*, vol. 117, pp. 120–140, Jul. 2017, doi: 10.1016/j.cep.2017.03.024

4:00pm PS-TuA-8 Integrated Reactor Models of Diamond Growth: Advancing Towards Low-Temperature CVD, *Yuri Barsukov, Igor Kaganovich, Mikhail Mokrov,* PPPL; *Alexander Khrabry,* Princeton University

In modern diamond chemical vapor deposition (CVD) techniques, substrates are commonly exposed to temperatures above 1200K. This high-temperature requirement restricts the selection of substrate materials to those that can withstand such extreme conditions. Low-temperature diamond CVD attracts major interest because it enables broader applications, e.g., utilization of diamond materials in the architecture of three-dimensional integrated circuits.

The objective of this study is to identify conditions that would allow to significantly reduce the substrate temperature for diamond CVD growth. To investigate the potential for reducing the substrate temperatures, we developed a comprehensive reaction kinetic model of (100) diamond surface growth from a CH_4/H_2 gases, which are typical feed gases [1]. This model involves 91 surface reactions, which were investigated using quantum chemistry methods. Subsequently, we integrated this reaction kinetic model with a gas-phase chemistry model of typical hot-filament and microwave reactors. The models were validated against previously reported experimental data, accurately predicting the measured diamond growth rates under various operating conditions.

Our results show that the effect of C_2H_2 on diamond growth is minor at temperatures above 1200 K, as previously reported. For temperatures below a critical value predicted by our model, C_2H_2 molecules nucleate the sp^2-phase (soot) instead of diamond, thus hampering diamond growth. At temperatures above the critical, C_2H_2 does not nucleate the sp^2-phase (soot) and its effect on the diamond growth is not important (compared to the main precursor CH_3). However, for a low-temperature CVD regime, C_2H_2 deleteriously affects the diamond growth, and its presence in the CVD mixture is highly undesirable.

Using ab initio quantum chemistry methods coupled with a numerical plasma model, we developed an integrated model that not only reproduces the experimental results but also identifies a critical bottleneck in modern CVD reactors. Our findings suggest that an optimization of low-temperature CVD reactor design implies maximizing the CH_3 radical production and minimizing the generation of C_2H_2 and other sp and sp^2 hydrocarbons.

[1] Y. Barsukov, I. D. Kaganovich, M. Mokrov, and A. Khrabry, *Quantum Chemistry Model of Surface Reactions and Kinetic Model of Diamond Growth: Effects of CH3 Radicals and C2H2 Molecules at Low-Temperatures CVD*, (2024). https://doi.org/10.48550/ARXIV.2405.03050

4:15pm PS-TuA-9 Solid State Generated Microwave Power for Hydrogen Plasma Reduction of Iron Oxide, *Daniel Ellis, Jazline Rebollar,* University of Illinois Urbana-Champaign; *Brian Jurczyk,* Starfire Industries; *Jessica Krogstad, Mohan Sankaran,* University of Illinois Urbana-Champaign

The reduction of iron ore is a key step in steel production. Current approaches lead to substantial carbon dioxide emission and there has been growing interest in low-temperature hydrogen plasmas that would avoid carbon-based feedstocks and lower the heating required by increasing reactivity. Microwave excitation is of particular interest because of the potential to energy efficiently generate reactive plasma species. However, microwave power is typically generated by magnetrons, which utilize rigid and bulky waveguides to couple the microwave radiation to a cavity, and the plasmas that are formed at atmospheric pressure are filamentary, hot, and confined to cavities.

Here, we studied a low-temperature, atmospheric-pressure hydrogen plasma for iron oxide reduction powered by microwave generated from solid state amplifiers. Solid state technology allows the microwave power to be transmitted by standard coaxial cables to an antenna. By configuring the antenna in a coaxial geometry where gas flow is simultaneously coupled, a plasma jet free from any surface is generated which can be used to treat a material surface downstream. To demonstrate the applicability of this unique plasma to iron oxide reduction, films of iron oxide prepared from hematite powder were prepared and treated. The effect of various process parameters, including plasma power, treatment time, distance between the plasma electrode and substrate, and feed composition, on reduction were investigated. The reduction of the iron oxide samples was evaluated ex-situ by mass loss measurements, X-ray diffraction, and scanning electron microscopy. The reduction was found to especially depend on the distance of the plasma and the concentration of molecular hydrogen in a background of argon gas. In support of these experimental results, an advection-diffusion-recombination model was developed to calculate the hydrogen radical concentration in the gas phase. The study clarifies opportunities and challenges for iron oxide reduction by low temperature plasmas.

4:30pm PS-TuA-10 Plasma Synthesis of Hydrogen from Ethanol Solution: A Mechanistic Study, *Dane Lojen, Thomas Fontaine, Linus Nyssen, Nepal Roy,* Université Libre de Bruxelles, Belgium; *Rony Snyders,* Universite de Mons, Belgium; *Nathalie De Geyter,* Ghent University, Belgium; *François Reniers,* Université libre de Bruxelles, Belgium

Routes to produce hydrogen at low energy cost and without emission of carbon dioxide are extensively studied nowadays, going from methane splitting (either thermal or plasma) to water electrolysis. In a previous preliminary study, we showed that production of hydrogen from liquid ethanol could be a possible route of interest, although the energy cost was still too high. In this paper, we present new results of the plasma induced splitting of liquid ethanol, using a nanopulsed generator. The plasma reactor consists of a 6 pin-to-plate electrode geometry, with the plate electrode being submerged in an ethanol-water solution. The gaseous products of reaction were analysed and quantified by atmospheric mass spectrometry (Hiden), after appropriate calibration, and the discharge is characterized using a high speed Photron camera, electrical measurements, and optical emission spectrometry. Ethanol – water solutions of different concentrations and liquid thicknesses have been investigated. In our previous study we focused on the drastic effect of the liquid thickness on the plasma regime (DBD-like for high thicknesses, hot plasma for small thicknesses). Here we focus on the hot plasma regime. We show that, together with hydrogen, valuable gaseous byproducts are formed, namely acetylene, ethylene, and carbon monoxide, most often without any detectable CO_2 release. Compared to methane splitting, the deposition of solid carbon on the electrodes is also strongly reduced. OES characterization of the plasma reveals that the plasma temperature, the electron density and the electron average energy depend on the composition of the solution. The amount of hydrogen produced as a function of the solution composition is also investigated, leading to a proposed mechanism for hydrogen formation in such conditions.

Acknowledgements:

4:45pm PS-TuA-11 Study of Plasma-Catalyst Surface Interactions for Coking Reduction, *Michael Hinshelwood, Gottlieb Oehrlein,* University of Maryland, College Park

Methane reforming is important for the production of both pure hydrogen and syngas (H_2 + CO) which can be used to produce other valuable chemicals. Dry methane reforming (DRM) with CO_2 is a promising technique for converting greenhouse gases into syngas. However, catalyst deactivation by carbon deposition on the catalyst surface (coking) is an issue. Non-thermal plasma may be a useful technique for mitigating coke formation in DRM performed at atmospheric pressure. Reactive species generated by the plasma may react with coke deposits, regenerating the catalyst. To better understand this plasma-surface interaction, we use in-situ IR spectroscopy techniques with a remote plasma-catalysis setup. Diffuse Reflectance Infrared Fourier Transform Spectroscopy (DRIFTS) is used to probe surface adsorbates formed during the reaction, while Fourier Transform Infrared Spectroscopy (FTIR) is used to quantify the product species downstream of the reaction. A nickel catalyst supported by SiO_2/Al_2O_3, commonly used for dry reforming reactions, is used as a test material. By exposing the catalyst to Ar/CH_4 plasma, or just Ar/CH_4 at elevated temperatures, the catalyst's dry-reforming activity is reduced, and a lower product concentration is measured downstream. Surface

characterization under the same conditions reveals a growth of adsorbed C-H species, CH_2 (2930 cm^{-1}) and CH_3 (2960 cm^{-1}, 2860 cm^{-1}), suggesting that they are responsible for this deactivation. Subsequent exposure to Ar/CO_2 plasma results in the removal of the adsorbed CH_n surface species on the timescale of minutes. The experimental setup allows for variation of the catalyst temperature to test the reactivity of the plasma produced flux with surface carbon at different temperatures. CH_n removal is seen to be more effective at high temperatures and plasma powers, suggesting a synergistic effect of temperature and reactive species flux to the surface. At lower plasma powers or catalyst temperatures, both the removal rate and amount removed are less. For surface cleaning experiments using high temperature and high plasma power, the bulk of the CH_n removal takes place during the first minutes of CO_2 plasma exposure. By comparing the effect of CO_2 plasma on surface CH_n to its effect on the subsequent dry reforming performance, the potential of plasma to reduce catalytic deactivation during dry reforming will be demonstrated. Increased understanding of this time-dependent relationship will help inform future development of plasma enhanced DRM systems.

Quantum Science and Technology Mini-Symposium
Room 123 - Session QS-TuA

Advances in Quantum Dots and Dynamic Effects in Josephson Junctions

Moderators: Sisira Kanhirathingal, Rigetti Computing, **Ekta Bhatia**, NY CREATES

2:15pm QS-TuA-1 Toward Robust Spin-Optical Interfaces in Molecular Spin Qubits, *Leah Weiss, Grant T. Smith,* University of Chicago; *Ryan A. Murphy, Bahman Golesorkhi, Jeffrey R. Long,* University of California at Berkeley; *David D. Awschalom,* University of Chicago **INVITED**
Efficient spin-optical interfaces play a key role in quantum technologies ranging from generation of multi-qubit entangled states to remote nanoscale quantum sensing. This interface can be designed from the bottom up in organometallic molecules to enable optical initialization and read out of ground-state molecular spins [1], providing a synthetic analog of solid-state spin qubits. We have shown that by changing the atomic structure of either the molecule or its local environment, the spin and optical properties of this class of qubits can be chemically modified [2,3]. Building on these demonstrations, we report the development of molecular ground-state spin qubits with robust spin-optical coupling. We utilize the observed spin-photon interface to demonstrate all-optical detection of ground-state spin properties in molecular ensembles. These results open avenues for the tailored design of molecular qubits for targeted sensing applications requiring efficient coupling of spins with photons.

[1] S. L. Bayliss, et al., Science. **370**, 6522 (2020).

[2] D. W. Laorenza, et al. JACS. **143**, 50 (2021).

[3] S. L. Bayliss, et al. Phys. Rev. X. **12**, 3 (2022).

2:45pm QS-TuA-3 Characterization of epitaxially grown Al-Ge/SiGe quantum wells for voltage-controlled Josephson junctions, *Joshua Thompson,* Laboratory for Physical Sciences; *Shiva Davari,* University of Arkansas; *Chomani Gaspe, Kasra Sardashti,* Laboratory for Physical Sciences; *Hugh Churchill,* University of Arkansas; *Christopher Richardson,* Laboratory for Physical Sciences
Strained germanium quantum wells host heavy holes with high mobility and low effective mass, which combined with highly transparent epitaxial aluminum creates a promising platform for voltage-controlled superconductor-semiconductor devices that are compatible with standard Si fabrication methods. This talk will discuss the characterization of undoped germanium quantum wells in a SiGe heterostructure grown by molecular beam epitaxy and the fabrication of planar Josephson junctions. By applying an electrostatic gate, the induced two-dimensional hole gas was observed to have a carrier mobility > $2x10^4$ cm^2/Vs with a density < $1x10^{12}$ cm^{-2}. Using an etch process, 50-100 nm Josephson junctions where fabricated on a tall mesa structure and characterized by measuring I_cR_N and the supercurrent dependance on applied gated voltage and magnetic field.

3:00pm QS-TuA-4 Nanoscale Spatial Control of Colloidal Quantum Dots and Rods Using DNA for Next-Generation Quantum Devices, *Xin Luo, Chi Chen, Mark Bathe,* MIT
Advances in photonic quantum technologies require precise control over quantum emitters at sub-10 nanometer scales for quantum computing and sensing applications. Conventional top-down fabrication methods face limitations in resolution and scalability on this front. In contrast, scalable bottom-up approaches utilizing DNA self-assembly offer unprecedented control over colloidal quantum materials at the nanoscale, such as quantum dots (QDs) and rods (QRs). We program and manipulate QDs and QRs using DNA nanostructures as templates, towards their scalable and precise incorporation into quantum photonic devices. DNA nanotechnology has emerged with unparalleled versatility and accuracy in creating complex, programmable architectures at the nano- to micro- scale (1, 2). Using versatile 3D wireframe DNA templates of customized geometry and chimeric single-stranded DNA (ssDNA) wrapping, we developed a general strategy to program ssDNA valences on QD surfaces (3). This valence-geocoding approach enabled the fabrication of QD energy transfer circuits (3). Using a rigid, planar wireframe DNA origami template, we arranged aligned QRs into 2D arrays on surfaces with nanoscale precision (4). We developed an ultrafast dehydration-assisted method to conjugate a dense layer of ssDNA onto QDs/QRs directly from organic solvent to facilitate their precise and stable assembly to 2D DNA template lattices up to a micron in size (4). To integrate DNA templated QDs/QRs into chip-based photonic devices, we further employed electron beam lithography (EBL) to guide the deterministic patterning of precisely positioned and oriented DNA templates on silicon chips, which were then used to template QDs and QRs with nanoscale accuracy. Scalable production of DNA templates using biologically produced DNA molecules (5) and its application in quantum photonics aligns with initiatives promoting biomanufacturing innovation for a sustainable bioeconomy (6). Combining the strengths of top-down lithography methods and bottom-up DNA self-assembly holds the potential of a scalable, parallel and environmentally benign nanofabrication framework that accurately patterns single colloidal quantum emitters over 2D surfaces on the wafer-scale.

1. Bathe, M. and Rothemund, P. (2017). MRS Bulletin, 42: 882.
2. Knappe, G.A., et al. (2023). Nature Reviews Materials, 8: 123.
3. Chen, C., et al., (2022). Nature Communications, 13: 4935.
4. Chen, C., et al., (2023). Science Advances, 32: eadh8508.
5. Shepherd TR, et al., Scientific Reports. 2019;9(1):6121.

4:00pm QS-TuA-8 Developing a Novel Approach to Extract the Current-Phase Relation of Josephson Junctions with On-Wafer Microwave Probing and Calibration Techniques, *Elyse McEntee Wei,* Colorado School of Mines; *Paul Dresselhaus, Anna Fox, Dylan Williams, Christian Long,* National Institute of Standards and Technology, Boulder; *Serena Eley,* University of Washington
We are developing a novel approach to characterize the current-phase relation (CPR) of Josephson junctions using on-wafer microwave probing and calibration techniques. Josephson junctions are the integral component in superconducting quantum circuits and exhibit a supercurrent that is modulated by a function of the phase difference between the order parameters of the superconducting electrodes, known as the CPR. Typically, the CPR is assumed to be sinusoidal. However, skewing has been observed in junctions with various barrier compositions such as normal metals, ferromagnetic materials, InAs nanowires, and graphene. This skewing can significantly affect the output of devices such as timing in single-flux quantum circuits used for digital logic, as well as the harmonic power in pulsed junction arrays used in voltage standards. The CPR is commonly measured using specialized superconducting quantum interference device (SQUID) circuitry. However SQUIDs are very sensitive to flux noise and can easily couple to nearby circuit components, limiting the ability of the SQUID circuit to measure the CPR. Our approach employs a homebuilt cryogenic probe station for measurements of Josephson junction arrays embedded in superconducting coplanar waveguides. It then involves extracting the Josephson inductance from Josephson transmission lines as a function of bias current using scattering-parameters calibrated with an on-wafer multiline Thru-Reflect-Line calibration to reconstruct the CPR. Here, we apply this approach to studying the CPR in niobium-doped amorphous silicon Josephson junction arrays, in which preliminary data shows evidence of skewing and higher order harmonics. Upon validation, this novel approach would offer broadband, low noise measurements of the CPR, providing critical design information for circuits that are based on Josephson junctions.

4:15pm **QS-TuA-9 Aging effects after Alternating Bias Assisted Annealing of Josephson Junctions**, *David P. Pappas, Xiqiao Wang, Joel Howard, Eyob Sete,* Rigetti Computing*; G.M. Stiehl,* rice University*; Stefano Poletto, Xian Wu, Mark Field, Nicholas Sharac, Christopher Eckberg, Hilal Cansizoglu, Josh Mutus, Kameshwar Yadavalli, Andrew Bestwick Bestwick,* Rigetti Computing

New avenues of trimming the resistance of Josephson junctions promise to allow for precise frequency allocation. This can be expected to significantly improve the yield and fidelity of chips and measurements, respectively. In this talk we will discuss the stability of the junction normal resistance over a wide range of time scales.

4:30pm **QS-TuA-10 Evaluating Radiation Impact on Transmon Qubits Using a Fast Decay Protocol in Above and Underground Laboratories**, *Tanay Roy,* Fermi Lab

Superconducting qubits can be sensitive to sudden energy deposits caused by ambient radioactivity and cosmic rays. Previous studies have focused on understanding possible correlated effects over time and distance due to this radiation. In this study, for the first time, we directly compare the response of a transmon qubit measured initially at the SQMS above-ground facility (Fermilab, Illinois, USA) and then at the deep underground Gran Sasso Laboratory (INFN-LNGS, Italy). We observe the same average qubit lifetime of roughly 80 microseconds at both facilities. We then apply a fast decay detection protocol and investigate the time structure and relative rates of triggered events due to radiation versus intrinsic noise, comparing the above and underground performance of several high-coherence qubits. Using gamma sources of variable intensity we calibrate the response of the qubit to different levels of radiation in an environment with minimal background radiation. Results indicate that qubits respond to a strong gamma source, and it is possible to detect particle impacts. However, we do not observe a difference in radiation-induced-like events when comparing the above and underground results for niobium-based transmon qubits with sapphire substrates. We conclude that the majority of these events are not radiation-related and are attributed to other noise sources, which by far dominate single-qubit errors in modern transmon qubits.

[1] Dominicis, Roy et al. arXiv:2405.18355

4:45pm **QS-TuA-11 Quantum Enhanced Josephson Junction Field-Effect Transistors for Logic Applications**, *W. Pan, A.J. Muhowski, W.M. Martinez, C.L.H. Sovinec, J.P. Mendez, D. Mamaluy,* Sandia National Laboratories

Josephson junction field-effect transistors (JJFET, Fig. 1a) have recently emerged as a promising candidate for low-energy, power-efficient microelectronics applications. JJFETs are particularly useful for low power consumption applications as they are operated with, in the superconducting regime, zero voltage drop across its source and drain. For JJFETs to perform logic operations, the gain-factor (a_R) value must be larger than 1. Here a_R = dIc/d(Vg–Vt) x $\pi\Delta$/Ic, Δ is the superconducting gap, Vg the gate bias voltage, Vt the threshold voltage. Ic ~ exp(-L/ξ_c) is the critical supercurrent, where L is the channel length and ξ_c the carrier coherence length. In a conventional JJFET, ξ_c ~ (Vg–Vt)0.5 (Fig. 1b), and thus dIc/d(Vg–Vt) is small (Fig. 1c). This translates to a requirement of superconducting transition temperature of ~ 400K for a_R larger than 1, far exceeding any recorded critical temperatures. As such, it is impossible to use conventional JJFETs for logic operations.

Here, we propose a novel type of JJFET based on quantum phase transition, such as the excitonic insulator (EI) transition in an InAs/GaSb type-II heterostructure, for low-energy, power-efficient logic applications. The nature of the collective phenomenon in the EI quantum phase transition can provide a sharp transition of the supercurrent states (e.g., ξ_c ~ (Vg–Vt)5 and dIc/d(Vg–Vt) very large, as shown in Figs. 1b and 1c, respectively) which will enable a_R larger than 1 with an easy-to-achieve superconducting transition temperature, e.g., ~ 40K.

In this talk, we will present some preliminary results demonstrating that indeed the gain factor in these quantum enhanced JJFETs can be greatly improved, thus making them a promising candidate for logic applications. Fig. 2a shows a JJFET made of a zero-gap InAs/GaSb heterostructure with tantalum (Ta) as the source and drain electrodes. The superconducting critical current in the JJFET is zero when Vg-Vt ≤ 0.23V, but sharply jumps to a finite value at Vg-Vt = 0.24V and then increases slowly as Vg-Vt continues to increase (Fig. 2b). The gain factor is calculated to be ~ 0.06. Though still less than 1, it is already more than 50 times larger than that recently reported in a conventional JJFET made of InAs quantum wells. With further optimization, a sharper excitonic insulator transition can be achieved. Together with a higher superconducting transition temperature, a large gain factor can be expected.

5:00pm **QS-TuA-12 Revealing Signatures of Unconventional Superconductivity in Tunneling Andreev Spectroscopy**, *Petro Maksymovych, Sang Yong Song,* Oak Ridge National Laboratory*; Christopher Lane,* Los Alamos National Laboratory*; Jiaqiang Wang,* Oak Ridge National Laboratory*; Wonhee Ko,* University of Tennessee Knoxville*; Jose Lado,* Aalto University, Finland

Understanding order parameter symmetry in superconductors continues to be a frontier topic in condensed matter, particularly with the recent surge of new superconducting materials and their prospective applications in quantum information processing. Recently we introduced a new technique to detect Andreev reflection across the tunneling gap - dubbed Tunneling Andreev Reflection (TAR) [1] - which essentially measures the probability of injecting Cooper pairs with atomic-scale contacts. When combined with scanning tunneling microscopy (STM), this method can achieve true atomic-scale imaging of the superconducting state and extend the ability of STM to probe pairing symmetry, magnetism, and topological properties by analogy with Andreev measurements in devices and heterostructures. For example, we used TAR to unambiguously confirm the sign-changing order parameter in paradigmatic FeSe, and further revealed suppression of superconductivity along the nematic twin boundaries above 1.2 K [2].

To achieve atomic-scale resolution, TAR makes a necessary trade-off in the loss of momentum resolution. It is one of the main differences between TAR and the more traditional, point contact method to measure Andreev reflection, and one the requires a fundamental rethinking of the origins of specific tunneling Andreev spectra. In this talk, based on detailed tight-binding modeling of model Hamiltonians with support from model experiments, we will reveal the basic mechanisms by which TAR spectra connect to the properties of the superconductor. Remarkably, the key ingredients of these spectra can all be rationalized by considering four contributing phenomena: (1) competition between Andreev and single electron tunneling in any given junction; (2) electronic changes of the conductance spectra as a function of increasing coupling strength; (3) energy-dependence of Andreev tunneling, particularly for sign-changing and nodal order parameters; (4) specific details of the band structure. Therefore, tunneling Andreev spectra will in general reflect both intrinsic properties of the superconductor as well as those of the tunneling transport - providing a wealth of information to characterize complicated materials and dramatically expanding the ability of tunneling spectroscopy to search for exotic quantum materials. Research sponsored by Division of Materials Science and Engineering, Basic Energy Sciences, Office of Science, US DOE. SPM experiments were carried at the Center for Nanophase Materials Sciences, Oak Ridge National Laboratory, a US DOE User Facility.

Surface Science
Room 120 - Session SS+CA+LS-TuA
Electrochemistry and Photocatalysis

Moderators: Jared Bruce, University of Nevada Las Vegas, **Taku Suzuki**, NIMS (National Institute for Materials Science), Japan

2:15pm **SS+CA+LS-TuA-1 Surface Sensitive Studies of the Electrolyte-Electrode Interface**, *Edvin Lundgren,* Lund University, Sweden   **INVITED**

The electrified electrode electrolyte interface is notoriously difficult to study during electrochemical (EC) reactions. Most traditional surface science techniques are disqualified due to the use of electrons, on the other hand, several new in-situ experimental methods have been developed recently. Examples are Electro Chemical X-ray Photoelectron Spectroscopy (ECXPS), Scanning Tunneling Microscopy (STM), Atomic Force Microscopy (AFM), High Energy Surface X-Ray Diffraction (HESXRD) [4] and EC-IRAS [5].

In the first part of the talk, the corrosion of an industrial Ni base Ni-Cr-Mo alloy will be addressed. A comprehensive investigation combining several synchrotron-based techniques are used to study the surface region of a Ni-Cr-Mo alloy in NaCl solutions in situ during electrochemical polarization. X-Ray Reflectivity (XRR) and ECXPS were used to investigate the thickness and chemistry of the passive film. Grazing Incidence X-ray Diffraction (GIXRD) was used to determine the change in the metal lattice underneath the passive film. X-Ray Fluorescence (XRF) was used to quantify the dissolution of alloying elements. X-ray Absorption Near Edge Structure (XANES) was used to determine the chemical state of the dissolved species in the electrolyte. Combining these techniques allowed us to study the corrosion process, detect the passivity breakdown in situ, and correlate it to the onset of the Oxygen Evolution Reaction (OER) [6].

In the second part, an alternative approach to study the development of a model electro catalyst surface is presented. By using a combination of Grazing Incidence X-ray Absorption Spectroscopy (GIXAS) [7], 2D Surface Optical Reflectance (2D-SOR) [8] and Cyclic Voltammetry (CV) and a Au(111) electrode model surface, direct surface information during real-time CV can be obtained.

[1] S. Axnanda et al, Sci. Rep. **5** (2016) 9788.

[2] A. A. Gewirth, B. K. Niece, Chem. Rev. **97** (1997) 1129.

[3] K. Itaya, Prog. Surf. Sci. **58** (1998) 121.

[4] M. Ruge et al, J. Electrochem. Soc. **164** (2017) 608.

[5] T. Iwasita, F. C. Nart, Prog. Surf. Sci. **55** (1997) 271.

[6] A. Larsson et al, Adv. Mat. (2023) 230462.

[7] H. Abe, Y. Niwa, M. A. Kimura, Phys. Chem. Chem. Phys. **22** (2020) 24974.

[8] S. Pfaff et al, ACS Appl. Mater. Interfaces **13** (2021) 19530.

2:45pm SS+CA+LS-TuA-3 Operando Studies of CO2, CO and N2 Catalytic Hydrogenation Reactions investigated with Ambient Pressure XPS, *Peter Amann,* Scienta Omicron, Germany; *Andrew Yost,* Scienta Omicron, USA

Some of the most essential catalytic reactions for our energy society is to reduce CO_2 to hydrocarbons and alcohols to be used as fuels and base chemical for the chemical industry. Furthermore, the catalytic reduction of N_2 to ammonia has been considered as one of the most important discoveries during the 20th century to produce fertilizers for a growing population. Despite an enormous effort in studying these catalytic reactions we are still lacking experimental information about the chemical state of the catalytic surface and the adsorbates existing as the reaction is turning over. X-ray photoelectron spectroscopy (XPS) is a powerful surface sensitive technique that can provide almost all essential chemical information and it has been developed to operate also in a few mbar of pressure with great success for probing oxidation catalytic reactions. Unfortunately, this pressure regime is too low for the hydrogenation reactions to turn over. Here we will present how Fischer-Tropsch, methanol and ammonia synthesis reactions on single crystal metal surfaces have been probed during operando conditions in the pressure range 100 mbar-1 bar using a specially engineered XPS system built at Stockholm University (1) and permanently located at the PETRA III synchrotron in Hamburg. The instrument is commercially available at Scienta Omicron (BAR XPS) and can vary the incidence angle of the X-rays allowing it to be either surface or bulk sensitive. Examples will be presented about the chemical state of Zn in Cu-Zn methanol (2) and of Fe in Fischer-Tropsch (3,4) and ammonia synthesis reactions (5) as well as the various adsorbates at different pressures and temperatures.

(1) P. Amann et al. Rev. Sci. Instrum. **90**, 103102 (2019)

(2) P. Amann et al. Science 376, 603-608 (2022)

(3) D. Degerman et al. J. Phys. Chem. C 128, 13, 5542–5552 (2024)

(4) M. Shipilin et al. ACS Catalysis 12, 7609-7621 (2022)

(5) C.M. Goodwin et al. Nature, 625, 282-286 (2024)

3:00pm SS+CA+LS-TuA-4 Understanding the Intrinsic Activity and Selectivity of Cu for Ammonia Electrosynthesis from Nitrate, *Zhuanghe Ren, Kaige Shi, Zhen Meng, Xiaofeng Feng,* University of Central Florida

Electrocatalysis play a central role in the development of renewable energy technologies towards a sustainable future, such as the recycling of nitrate from wastewater sources. The concentration of nitrate (NO_3^-) in ground water, rivers, and lakes has been increasing due to the excessive use of agricultural fertilizers and the discharge of industrial wastewater, which has caused severe environmental problems such as eutrophication. Electrochemical reduction of nitrate to ammonia has emerged as a promising route for the recycling of nitrate from wastewater and sustainable ammonia production when powered by renewable electricity. Here I present our recent study of Cu catalyst for nitrate electroreduction, with a focus on its intrinsic activity and selectivity. Using polycrystalline Cu foils for benchmarking, we elucidated the impact of often overlooked factors on nitrate reduction, including Cu facet exposure, nitrate concentration, and electrode surface area. We find that an electropolished Cu foil exhibits a higher activity and selectivity for nitrate reduction to ammonia than a wet-etched Cu foil, benefiting from a greater exposure of Cu(100) facets that are more favorable for the reaction. While the NH_3 selectivity shows no apparent dependence on the nitrate concentration, it increases with Cu electrode area, which is attributed to a promoted conversion of intermediately produced NO_2^- to NH_3 on a larger electrode.

Based on the understandings, we developed a modified Cu foil electrode with increased Cu(100) facets and surface area, which enhanced the NO_3RR activity by ~50% with a NH_3 Faradaic efficiency of 91% at −0.2 V vs RHE.

This work is supported by the National Science Foundation (NSF) Chemical Catalysis Program under Grant No. 1943732.

References:

(1) Ren, Z.; Shi, K.; Feng, X. Elucidating the intrinsic activity and selectivity of Cu for nitrate electroreduction. *ACS Energy Lett.* **2023**, *8*, 3658−3665.

3:15pm SS+CA+LS-TuA-5 Insights Into Photocatalytic Reduction Activities of Different Well-Defined Single Bulk Crystal TiO₂ Surfaces in Liquid, *Olawale Ayoade, Weigang Lu, Hao Zhu, Zhenrong Zhang,* Baylor University

Understanding the activity of TiO_2 photocatalysts is crucial for designing and optimizing efficient photocatalysts, requiring a fundamental understanding of the photooxidation and photoreduction activities of different TiO_2 crystal facets. Although photoreduction activities on several TiO_2 crystal facets have been extensively studied in reactor or ultra-high vacuum environments, studies of well-defined TiO_2 crystal facets in a liquid environment are still lacking.In this study, the photocatalytic reduction activities of resazurin (RZ) were investigated using well-defined bulk single-crystal anatase (001), anatase (101), rutile (001), and rutile (110) facets. The experiment used a liquid cell containing RZ solution and TiO_2 crystal. A lab-built Raman microscope monitored the photoluminescence (PL) spectra of RZ under UV irradiation. We observed an increase in peak intensity at 583 nm and a decrease at 630 nm in the PL spectra of the solution on the TiO_2 crystal facets upon UV illumination, suggesting a conversion from RZ to its product, resorufin (RS). Given that both RZ and RS have distinctive peaks, we used their ratios to estimate their concentrations. This enabled us to assess the conversion rate and reaction rate of the crystals.Our results show that rutile had significantly higher conversion rates and faster reaction rates than anatase for RZ reduction. Rutile (110) had conversion rates about four times greater, and rutile (001) about three times greater than anatase. Rutile (110) reaction rates were about 1.5 times faster than rutile (001) and significantly faster than anatase (101) & (001). Further evaluation of the photoreactivity was conducted using pseudo-order kinetics to determine the rate constant. The significant difference observed in rates between the rutile and anatase phases highlights the successful migration of electrons to the surface of the rutile crystal compared to the anatase surface, emphasizing the importance of crystal structure. The difference observed between rutile (001) and rutile (110) (as well as anatase facets 001 and 101) shows the effect of surface structure on photocatalytic activity. To advance the development of effective TiO_2-based photoreduction materials, we explored plasmon-assisted photoreactions. We have studied the impact of Au nanoparticles on the reactivity of the aforementioned TiO_2 facets. This study will involve modulating hot electron generation and increasing electric fields to better understand their effects on photoreactivity.

4:00pm SS+CA+LS-TuA-8 Selectivity Control by Ionic Liquid Layers: From Surface Science to the Electrified Interface, *Joerg Libuda,* Friedrich-Alexander-Universitaet Erlangen-Nuernberg, Germany   **INVITED**

Recently, the concept of "Supported Catalysts with Ionic Liquid Layer" (SCILL) has attracted much attention in heterogeneous catalysis and electrocatalysis. In the SCILL concept, a heterogeneous catalyst is impregnated with a thin layer of ionic liquid (IL) that serves as a catalytic modifier. In this presentation, we will give an overview of selected surface science and electrochemical surface studies on the origin of this selectivity control.

In the surface science studies, we investigated the growth, wetting behavior, structure formation and thermal behavior of various ILs on a wide range of model catalysts (Pt, Pd and Au single crystal surfaces and supported nanoparticles) using scanning tunneling microscopy (STM), atomic force microscopy (AFM) and infrared reflection absorption spectroscopy (IRAS). We were able to show that most ILs form a strongly interacting wetting layer with a high degree of intrinsic structural flexibility. Depending on the conditions, 2D glassy or different crystalline wetting layers are formed, in which the molecular orientation is dynamic and allows the embedding of reactants and thus the modification of the reaction environment.

In our electrochemical surface science studies, we investigated the interaction of selected imidazolium-based ILs with reactive and non-reactive single-crystal electrodes (Au, Pt). Using electrochemical IRAS (EC-IRRAS), we monitored the potential-dependent adsorption of IL ions on the electrode and used electrochemical STM (EC-STM) to investigate the effects

of the ILs on the electrode structure. We used the selective oxidation and reduction of hydrocarbon oxygenates as test reactions. For the selective electrooxidation of 2,3-butanediol (a very structure-sensitive reaction at Pt electrodes), we were able to show that small additions of specific ILs (e.g. [C_1C_2Im][OTf]) have a large effect on selectivity (e.g. on C-C bond cleavage and selectivity towards the two partial oxidation products acetoin and diacetyl). We attribute these effects to the possible adsorption of the IL anions on the Pt surfaces.

Our results rationalize the origin of selectivity control by IL coatings in heterogeneous catalysis and demonstrate the potential of ILs for selectivity control in electrocatalysis.

[1] R. Eschenbacher et al.,. J. Chem. Phys. Lett. 12, 10079 (2021)
[2] T. Yang et al., Angew. Chem. Int. Ed. 61, e202202957 (2022)
[3] M. Kastenmeier et al., J. Phys. Chem. C 127, 22975 (2023)
[4] H. Bühlmeyer et al., Chem. Eur. J., in press (2024), DOI10.1002/chem.202301328
[5] Y. Yang at al., J. Phys. Chem. C, accepted for publication (2024)

4:30pm SS+CA+LS-TuA-10 Area Selective Atomic Layer Deposition for Spatial Control of Reaction Selectivity on Model Photocatalysts, *Wilson McNeary,* National Renewable Energy Laboratory*; William Stinson,* Columbia University*; Wenjie Zang, Moaz Waqar, Xiaoqing Pan,* University of California Irvine*; Daniel Esposito,* Columbia University*; Katherine Hurst,* National Renewable Energy Laboratory

Photocatalytic water splitting holds great potential in the pursuit of the U.S. Department of Energy's Hydrogen Shot initiative to bring the cost of H_2 to $1/kg by 2031. A key challenge in the development of photocatalysts is increasing their overall solar-to-hydrogen efficiency by enhancing charge separation yields and redox selectivity. In this work, we use area selective ALD of oxide films (e.g., TiO_2 and SiO_2) to develop tunable interphase layers for selective oxidation and reduction reactions on a single substrate. This presentation details initial synthesis and characterization of monometallic Pt- and Au-based planar thin film electrodes in which Au regions were deactivated towards ALD growth through self-assembled thiol monolayers. The efficacy of thiols in suppressing ALD growth was assessed through ellipsometry, X-ray photoelectron spectroscopy (XPS), and cyclic voltammetry. A patterned planar sample comprised of interdigitated arrays of Au and Pt, used as a surrogate for a photocatalyst particle containing two different co-catalysts, was exposed to ALD growth and removal of the inhibitor species. Area selectivity of the ALD coatings on the patterned substrates was evaluated through cross-sectional scanning transmission electron microscopy with energy dispersive X-ray spectroscopy (STEM-EDS). Scanning electrochemical microscopy (SECM) was then used to probe the local activity of different regions of the patterned surface towards the hydrogen evolution reaction (HER) and iron oxidation and correlated with the ionic and e- blocking effects of the area selective ALD coating. We will also detail the application of these findings to the ongoing development of 3D, particle-based photocatalysts

4:45pm SS+CA+LS-TuA-11 Titanium-Based Catalysts for CO_2 Activation: Experimental Modelling of Hybride (Photo-)Catalysts, *Niko Kruse, Justin Klimek, Celina Groothuis,* **Lars Mohrhusen**, University of Oldenburg, Germany

Conversion of greenhouse gases and especially CO_2 into useful hydrocarbons via a low-cost route is among the major challenges of the current energy transition. For this purpose, photocatalysis may be a relevant technology, as sunlight is a free and unlimited energy source, and photoreactions usually do not require high temperatures. Oxide-based photocatalysts usually consist of a semiconducting oxide support with nanostructured (noble) metal particles.[1] Unfortunately, these metals are often expensive and have limited lifetimes due to for example sintering, coking or poisoning with carbon monoxide. Thus, for several reasons, it is attractive to develop strategies to replace noble metal in such systems.[2]

Titanium is one of the few elements, that are attractive in terms of its natural availability and considering various economic and ecological aspects. Titanium dioxide (TiO_2) for example offers a broad platform, as e.g. defects such as Ti^{3+} interstitials can boost the photocatalytic activity towards oxygen containing molecules.[3,4] TiO_2 also readily forms hybrid systems with other oxides (e.g. WO_3 clusters)[4] or sulfides such as MoS_2.[5] Thus, we investigate titanium-based hybrid photocatalytic systems using well-defined model catalysts under ultrahigh-vacuum conditions.

Herein, we present selected results from well-defined model catalysts en route to the desired Ti-based hybrid materials, for example, nanostructured combinations of TiS_2 and TiO_2. TiS_2 has a broad light absorbance throughout the visible range, is easily reduceable and widely inert to CO poisoning,

rendering it an attractive material. Our multi-method approach involves combinations of spectroscopy (esp. photoelectron spectroscopy (XPS)), microscopy (scanning tunneling microscopy (STM)) and reactivity studies (temperature-programmed desorption (TPD)). As one example, nanoparticles of TiS_2 as a classic 2D TMDC can be fabricated and studied on various substrates to derive an atomic-level understanding of structure-reactivity relationships.

<u>References</u>

[1] Linsebigler, Lu, Yates: Chem. Rev. **95**, 735-758 (1995).

[2] Shen et al. Solar RRL **4**, 1900546 (2020).

[3] Mohrhusen, Al-Shamery Catal. Lett. **153**, 321-337 (2023).

[4] Mohrhusen, Kräuter, Al-Shamery PCCP **21**, 12148-12157 (2021).

[5] Kibsgaard et al., J. Catal. **263** 98-103 (2009).

5:00pm SS+CA+LS-TuA-12 Tracking the Ultrafast Dynamics of a Photoinduced Reaction at the Surface of a Reactive Semiconductor: CH_3I Photoinduced Reaction on TiO_2 (110) Surface, *Aakash Gupta,* University of Central Florida*; Tian Wang,* University of Washington*; Keith Blackman, Corine M. Smith,* University of Central Florida*; Xiaosong Li,* University of Washington*; **Mihai E. Vaida**,* University of Central Florida

The detection of intermediate species during surface photoinduced reactions and the correlation of their dynamics with the properties of the surface is crucial to fully understand and control heterogeneous reactions. In this study, a technique that combines time-of-flight mass spectrometry with laser spectroscopy and fast surface preparation with molecules is employed to investigate the mechanism of photoinduced CH_3I reactions on a $TiO_2(110)$ surface through the direct detection of intermediate species and final products. On a freshly prepared $TiO_2(110)$ surface, the photoinduced reaction dynamics of CH_3I follows similar trends observed on other metal oxide surfaces.[1, 2] Specifically, the pump laser pulse at 266 nm excites the CH_3I molecule into the dissociative A-band, which leads to the formation of CH_3 and I intermediates that can further react to form I_2 and reform the CH_3I molecule. Subsequently, the probe laser pulse ionizes the intermediate and final products, which are detected by a mass spectrometer as a function of the pump-probe time delay. The minimum dissociation time of CH_3I obtained by monitoring the CH_3^+ fragment, which is 110 fs, and the fast rise of the CH_3^+ signal, indicates that CH_3I is adsorbed on pristine $TiO_2(110)$ with I atom facing the surface. A fraction of the I atoms produced on a freshly prepared $TiO_2(110)$ are trapped on the surface. On this $TiO_2(110)$ surface decorated with I atoms, the CH_3 fragment can react with CH_3I to form CH_3ICH_3, which leads to a completely different dynamics at the surface due to a change into the pump-probe schema. The evolution dynamics of CH_3^+ and CH_3I^+ after the CH_3ICH_3 photoexcitation will be discussed and compared with results obtained for CH_3I dosed on a freshly prepared $TiO_2(110)$ surface.

1. M. A. K. Pathan, A. Gupta and M. E. Vaida, *J. Phys. Chem. Lett.*, 2022, **13**, 9759-9765.

2. M. E. Vaida and T. M. Bernhardt, in *Ultrafast Phenomena in Molecular Sciences: Femtosecond Physics and Chemistry*, eds. R. de Nalda and L. Bañares, Springer International Publishing, Cham2014, pp. 231-261.

5:15pm SS+CA+LS-TuA-13 Kinetic Theory of Mixed-Potential-Driven Catalysis and the Experimental Proof, *Mo Yan, Nuning Namari, Rafiq Arsyad, Hiroaki Suzuki,* University of Tsukuba, Japan*; Junji Nakamura,* Kyushu University, Japan*; **Kotaro Takeyasu**,* Hokkaido University, Japan

It has recently been suggested that thermal heterogeneous catalysis can also involve electrochemical processes, resulting in selectivity that is markedly different from that of conventional thermal catalysis. If the catalyst is conductive and a suitable electrolyte is present nearby, anodic and cathodic half-reactions may occur simultaneously on a single catalyst surface, forming a mixed potential. This reaction is characterized by the anode and cathode being exposed to the same reactant, unlike conventional fuel cells where different reactants are supplied to each electrode. Interestingly, mixed potentials have been reported to be involved in reactions with gas molecules, such as the formation of H_2O_2 and the oxidation of alcohol. These reports suggest that electrochemical processes play a role in controlling catalytic activity and selectivity without external energy. Catalysts based on mixed potentials are a promising new category of catalysts for both basic research and industrial applications, but the principles that determine their activity and selectivity are not yet fully understood.

We first report the theoretical framework of mixed-potential-driven catalysis, including exchange currents, as a parameter of catalytic activity. The mixed potential and partitioning of the overpotential were determined from the exchange current by applying the Butler–Volmer equation at a steady state far from equilibrium [1].

To prove the theoretical framework, we measured the short-circuit current in a model reaction system without applying an external potential to demonstrate electron transfer for enzyme-like glucose oxidation. Specifically, glucose oxidation includes paired electrochemical anodic glucose oxidation and cathodic oxygen reduction, as evidenced by the consistency between the predicted and measured mixed potentials in identical reaction environments. Therefore, it can be categorized as a mixed-potential-driven catalysis. We further demonstrated that the Gibbs free energy drop, as the total driving force, was partitioned into overpotentials to promote each half-reaction in the mixed-potential-driven catalysis. This driving force partitioning, which is controlled by catalytic activity, is a powerful tool for guiding the design of mixed-potential-driven catalytic systems [2].

[1] M. Yan, N. A. P. Namari, J. Nakamura, K. Takeyasu, Commun. Chem. 7, 69 (2024).

[2] M. Yan, R. Arsyad, N. A. P. Namari, H. Suzuki, K. Takeyasu, ChemCatChem, accepted (2024).

Thin Films
Room 115 - Session TF1-TuA

Thin Films for Energy Applications II: Batteries
Moderator: Mark Losego, Georgia Institute of Technology

2:30pm **TF1-TuA-2 Surface Chemistry of Plasma Exposure on Sulfide Solid Electrolytes**, *Alexander Kozen,* University of Vermont; *Yang Wang, Daniela Fontecha, Gary Rubloff, Sang Bok Lee,* University of Maryland, College Park
Sulfide solid state electrolytes (SSEs) are considered one of the most promising materials to replace liquid electrolytes in next-generation batteries due SSEs astonishing ionic conductivities. However, the high reactivity of sulfide SSE materials precludes direct contact with Li metal anodes. One approach to stabilize the sulfide SSEs is passivating the sulfide interface with thin films of stable chemical species, forming an artificial solid electrolyte interphase (ASEI) layer. Ideal passivation materials for the anode/SSE interface are generally comprised of Li_3N or LiF species, which are stable at Li metal potentials. Here, we investigate the impact of plasma treatment on sulfide SSEs, as well as deposition of plasma-based ASEI materials using atomic layer deposition (ALD).

I will discuss the implications of Ar, N_2, and NH_3 plasma exposures on sulfide solid electrolytes (LGPS, LPSCl) and the resulting surface chemical changes as determined by in-vacuo x-ray photoelectron spectroscopy (XPS) measurements. N_2 and NH_3 plasma exposure can cleave Li_2S surface bonds and replace them with Li_3N surface species, however due to a lack of Li available at the surface this coverage is limited to ~30% and cannot form complete ASEI layers. Additionally, I will report the changes in electrochemical behavior of these pellets in Li/SSE/Li symmetric cells. Due to the incomplete surface coverage of Li_3N species, the surface nitride passivation is reduced and still allows deleterious reactions to occur after contact with Li metal. These results indicate that for complete Li_3N surface coverage, additional Li species must be available on the sulfide SSE surface before plasma treatment. I will also discuss the initial stages of ALD ASEI layer deposition on the sulfide SSE materials and evaluate their protection efficacy.

2:45pm **TF1-TuA-3 Tuning the Composition and Structure of High Mobility Nasicon-Type Thin Films Through Atomic Layer Deposition**, *Daniela R. Fontecha*[1], University of Maryland College Park; *Alexander C. Kozen,* University of Vermont; *David M. Stewart, Gary W. Rubloff, Keith E. Gregorczyk,* University of Maryland College Park
Fast Li^+ ion conducting thin film solid state electrolytes (SSEs) by atomic layer deposition (ALD) enable high power density, fast time constants, and high operating frequency regimes in solid state ionic devices. However, the ionic conductivity of thin film SSEs fabricated by ALD has been limited by material development challenges, phase purity concerns when dealing with tertiary and quaternary systems, and challenges related to crystallinity. These complexities require careful consideration of the material system,

precursor selection, process parameters, and post-annealing conditions to realize ideal ALD thin-film SSE materials with ionic conductivities $>10^{-6}$ S/cm. Bulk oxide SSEs, such as $Li_{1+x}Al_xTi_{2-x}(PO_4)_3$ (LATP) have a NASICON-type crystal structure, show high ionic conductivity when crystalline (10^{-3} S/cm), demonstrate air & water stability, and a high voltage stability window. ALD synthesis of LATP can be broken down into well-known constituent processes (e.g., Li_3PO_4, Al_2O_3, TiP_2O_7) which can be combined with respect to stoichiometric ratios.

LATP can be considered Al-doped $LiTi_2(PO_4)_3$ (LTP), in which Al^{+3} ions partially replace Ti^{+4} ions in the NASICON-type structure. This facilitates fast Li^+ ion conduction through the 3D network. With that in mind, an ALD process for LTP was first developed by alternating between Li_2O and TiP_2O_7 sub-processes. The Li_2O sub-process uses lithium *tert*-butoxide (LiO^{t}Bu) as the lithium source and water to complete the surface reaction. The TiP_2O_7 sub-process uses titanium (IV) isopropoxide (TTIP) as the titanium source, trimethyl phosphate (TMP) as the phosphorous source, and water. The growth rate of LTP was measured to be 0.4 Å/cycle at 300 °C. By adjusting the ratio between Li_2O and TiP_2O_7 cycles, the Li concentration in LTP can be tuned between 8.4-34.3 at % Li.

A NASICON-type crystalline structure is achieved by post-annealing the LTP films between 650 °C – 850 °C. The ideal annealing temperature was found to be a function of Li-ion concentration. The resulting measured ionic conductivity of partially crystalline LTP thin films is 3.6×10^{-5} S/cm at 80 °C. In this talk, we will discuss the complex issues related to process parameters, stochiometric tunability, and the resulting ionic conductivity when exploring ternary and quaternary LTP/LATP metal phosphates phase space.

3:00pm **TF1-TuA-4 Unlocking Novel Chemistry in Atomic Layer Deposition: Transformative Insights from Trimethylaluminum Interactions with Battery Materials**, *Donghyeon Kang, Anil Mane, Jeffrey Elam,* Argonne National Laboratory
Trimethylaluminum (TMA) stands as a keystone in atomic layer deposition (ALD), widely esteemed for its role in crafting aluminum-based coatings across diverse applications. Notably, TMA is used to produce Al_2O_3 with H_2O, AlF_3 with HF-pyridine, and Al_2S_3 with H_2S, adhering to well-defined ALD mechanisms. These processes have permeated various substrates, leading to ultra-thin Al-based coating layers, particularly within the realm of energy storage materials such as battery cathodes, anodes, and solid electrolytes.

Our research group has embarked on a profound exploration of TMA's ALD chemistry, unveiling captivating interactions with reactive metal substrates, solid-state electrolytes, and battery cathode materials. Interestingly, when subjected to Li-metal anodes, TMA deviates from conventional ALD pathways, engendering a carbon composite layer atop the Li metal. This unconventional behavior arises from the inherent reactivity of both TMA and Li metal, diverging from established ALD paradigms. Moreover, our investigations reveal TMA's propensity to engage with Li-based impurities on solid electrolyte and cathode surfaces, yielding protective layers with beneficial attributes. Astonishingly, despite TMA's extensive utilization, this phenomenon has eluded prior scrutiny.

In this presentation, we unveil our findings on the intricate chemistry between TMA and battery materials (Li-metal, cathode, solid electrolytes) elucidated through in-situ quartz crystal microbalance (QCM), high-resolution X-ray photoelectron spectroscopy (XPS), scanning electron microscopy (SEM), and Raman spectroscopy studies. Furthermore, we demonstrate the transformative potential of these discoveries in the realm of battery materials surface treatment, offering tantalizing prospects for streamlined industrial applications.

3:15pm **TF1-TuA-5 Mapping Lithium Diffusion in Thin-Film V_2O_5 using Raman Spectroscopy**, *Daniel MacAyeal,* University of Vermont; *Leopoldo Tapia-Aracayo, Spencer Caverly, David Stewart, Gary Rubloff,* University of Maryland; *Alexander Kozen,* University of Vermont
Understanding lateral diffusion of lithium in thin-film solid-state battery (SSB) materials is critical to improving SSB performance, stability, lifespan, and architecture. Using model test structures of sputtered V_2O_5/W/LiPON, we use Raman spectroscopy peak shifts to map Lithium concentration in V_2O_5. We evaluate the diffusion of lithium from LiPON layers into thin-film V_2O_5, measure the impact of different sputter deposition process conditions on lateral lithium diffusion, and investigate the effects of post-annealing the fabricated test structures. We will discuss the benefits of front versus back-side Raman spectroscopy for analyzing masked devices and correlate Raman spectroscopy mapping to XPS data to confirm compositional accuracy. Additionally, we will discuss the impact of electrochemical cycling at C/10 on lateral Lithium diffusion for symmetric V_2O_5/LiPON/V_2O_5 devices. Lastly, we will discuss the important implications of the lateral spacing

---

[1] **TFD James Harper Award Finalist**

limitations of clustered SSB devices due to lateral diffusion and propose architectural design rules based on this diffusion behavior for optimized device performance.

Thin Films
Room 115 - Session TF2-TuA

Vapor Synthesis of Hybrid, Organic, and Polymeric Materials (VSHOP I)
Moderator: Mark Losego, Georgia Institute of Technology

4:00pm TF2-TuA-8 Roll-to-Roll Photoinitiated Chemical Vapor Deposition of Polymer Films for Liquid-Repellent Textiles, *Trisha Andrew,* University of Massachusetts - Amherst*; Wesley Viola, Elie Chalouhi,* Soliyarn **INVITED**
Textile manufacturers currently use fluorocarbon based coatings/finishes to produce the liquid repellency that is now expected of fabrics in many contexts, including sporting apparel, upholstery, wall/floor covering, and personal protective equipment. However, it is increasingly apparent that these fluorocarbon chemicals spread throughout the global environment and bioaccumulate in groundwater and aquatic ecosystems because they cannot be chemically degraded by either naturally occurring microorganisms or prevalent atmospheric/oceanic/aquatic reactions. Selected vacuum-based coating processes, such as sputter coating and plasma-enhanced chemical vapor deposition, have been periodically explored over the past three decades to produce fluorine-free liquid repellent textile finishes. To date, the capital equipment and maintenance costs of continuous-process sputter coaters and similar plasma-based coaters, which require ultrahigh vacuum levels (<10^{-6} Torr) to function, is too prohibitive for the textile industry to feasibly adopt. Further, historic experience has revealed that ultrahigh vacuum dependent processes have limited applicability in high-throughput textile finishing due to the microfibers and lint generated by most commodity textiles as they travel through a continuous process coater, which contaminate the process chamber and prevent pump down.

Recently, research spun-out from the University of Massachusetts Amherst and matured by Soliyarn Inc. has validated the concept and manufacturing readiness of photoinitiated chemical vapor deposition (piCVD) as a sustainable process for textile finishing. piCVD is a low-vacuum process during which a photoinitiated chain growth polymerization reaction is enacted within a custom-designed reactor to produce surface-grafted, functional polymer coatings on a diverse selection of substrates, including synthetic and naturally-derived woven or knit fabrics. Informed monomer choice has lead to the development of fluorine-free polymer coatings that match or outcompete commercial water-repellent finishes. With informed selection of high quantum yield molecular photoinitiators and coupled mechanical engineering design to optimize vapor delivery to the fabric surface(s), piCVD can be executed over large areas in a continuous, roll-to-roll format under mild vacuum (<1 torr). During this talk, we will survey the major design features of our roll-to-roll piCVD coater, detail the learning milestones that lead to the conception, improvement and optimization of this system and highlight the properties of the liquid-repellent finishes created via piCVD.

4:30pm TF2-TuA-10 Battery Separators with Ultrathin iCVD-Polymer Coatings Mitigate Polysulfide Crossover in Lithium-Sulfur Batteries, *Ramsay Nuwayhid,* Hunter Ford, Junghoon Yeom, Corey Love, Jeffrey Long, Rachel Carter, U.S. Naval Research Laboratory
Lithium-ion batteries are approaching theoretical energy limits, necessitating development of advanced battery chemistries for critical applications. Lithium-sulfur (Li-S) batteries are an attractive alternative, due to the high abundance of sulfur in the earth's crust and high capacity of sulfur cathodes based on the conversion reaction of sulfur (S_8) to Li_2S. A major challenge in the practical implementation of Li-S batteries is the dissolution of intermediate lithium polysulfides formed during the conversion reaction, which react with the Li anode and sulfur cathode to form impeding interphases leading to loss of active material and poor cycle life. To overcome this technical challenge, we employ initiated chemical vapor deposition (iCVD) to conformally coat porous polyethylene separators used in Li-S cells to shield polysulfide crossover from the sulfur cathode to Li anode and enhance cycling performance. A novel copolymer, poly(divinylbenzene-co-(dimethylaminomethyl)styrene) (pDVB-co-DMAMS), is synthesized by iCVD and optimized to maintain cross-linking ability through DVB while the DMAMS functions to mitigate adverse polysulfide dissolution via specific adsorption at amine moieties. We first evaluate the electrochemical properties of pDVB-co-DMAMS in Li/Li symmetric cells through electrochemical impedance spectroscopy (EIS), demonstrating that iCVD-coated separators significantly reduce cell resistivity compared to cells with bare separators. Conformal coatings from 40-400 nm are evaluated in Li-S cells, in which thicker coatings show superior shielding of polysulfide cross-over through electrochemical self-discharge tests and UV-VIS spectroscopy. Furthermore, XPS and SEM analysis of the Li metal anode post-cycling reveals less crossover of polysulfide species and a smoother surface morphology for cells with iCVD-coated separators. Ultimately, 40 nm coatings are demonstrated to be the optimal thickness, maintaining high porosity of the separator and enabling high capacity retention at high gravimetric rates based on sulfur loading. Overall, this work demonstrates iCVD as a promising technique to stabilize reactive interfaces in beyond Li-ion battery systems.

4:45pm TF2-TuA-11 Synthesis and Characterization of Ion Beam Nano-Engineered Metal-Polymer Nanocomposite Thin Films for SERS Application, *Jai Prakash,* National Institute of Technology Hamirpur, India*; Hendrik Swart,* University of the Free State, South Africa
Ion beam induced nano-engineering of thin film surfaces provides a unique way to tailor the surface properties for various functional applications. Ion beam induced sputtering and bi-layer interface mixing lead to nanopatterning of the surfaces with unique morphologies that are useful for a variety of applications. The present work deals with nanopatterning of thin noble metal films (deposited by e-beam evaporation) on polymer surfaces, deposited with different techniques, such as chemical vapour deposition or spin coating. Ion beam induced nano-engineering creates noble metal nanoparticles on surfaces or embedded nanoparticles within the polymer films. Such noble metal nanoparticles exhibit unique optical properties due to their localized surface plasmon resonance properties. Synthesis and characterizations (RBS, SIMS etc.) of such ion beam nano-engineered surfaces with unique optical properties for SERS applications will be discussed, with an emphasis on the role of ion beam synthesis and tailoring of surfaces.

5:00pm TF2-TuA-12 In situ Analysis of Temperature Dependence During Molecular Layer Deposition of Polyurea, *Wallis Scholl,* Colorado School of Mines*; Thorsten Lill, Harmeet Singh, Mingmei Wang,* Lam Research Corporation*; Sumit Agarwal,* Colorado School of Mines
The use of molecular layer deposition (MLD) in practical applications is hindered by the lack of a well-defined temperature window and low growth per cycle (GPC), which is often much less than one repeat unit of the polymer chain. Multiple studies report a lower GPC at higher deposition temperatures, and as a result MLD is typically conducted at room temperature.The mechanism behind this temperature dependence is not well understood; different sources attribute lower GPC at higher temperatures either to an increased rate of double reactions, where both functional groups in a bifunctional molecule react with the surface, or to a lower degree of physisorption of the growth precursors onto the film's surface.

In this study, we used *in situ* attenuated total reflection Fourier transform infrared (ATR-FTIR) spectroscopy as well as *in situ* ellipsometry to monitor the film composition and thickness throughout MLD of polyurea film using toluene diisocyanate (TDIC) and ethylene diamine (ED) as precursors. The polyurea films were deposited at 0, 22, and 45 C. In agreement with previous literature (see Figure 1), over 25 MLD cycles, we observed a lower GPC at higher temperatures. The infrared spectra recorded during MLD reveal the temperature dependence of the chemical reactions and precursor physisorption. The amide I/II bands observed in the infrared spectra are related to the polyurea linkage, and indicate film growth. We find that the integrated absorbance for the amide I/II bands decreased with increasing temperature during both half cycles (see Figure 2). Further, we show evidence that precursor physisorption is the main cause for the temperature dependence of MLD. The two MLD precursors have different probability of double reaction and physisorption, and we typically observe a larger increase in integrated absorbance for the amide I/II modes during the TDIC half-cycles compared to the ED half-cycles. This discrepancy suggests that ED is more likely to physisorb than TDIC into the film and not form the polyurea linkages by reaction with the isocyanate groups. Additionally, the degree of physisorption of ED increases as the temperature is lowered. During the TDIC half-cycle, polyurea linkages are created due to chemical reaction between the physisorbed ED molecules. This also implies that to maintain a linear growth rate, as the temperature is lowered, site balance is achieved by a higher degree of double-reactions of

TDIC.

Vacuum Technology
Room 121 - Session VT1-TuA

Aerospace Research and Applications

Moderators: Giulia Lanza, SLAC National Accelerator Laboratory, **Julia Scherschligt**, National Institute of Standards and Technology

2:15pm **VT1-TuA-1 Gas Analysis and Vacuum Characterization for Space and Lunar Exploration**, *Andres Diaz*, INFICON   **INVITED**
Mankind is always curious and looking for the next frontier. In recent years there has been a sharp increase in all sorts of space activities, from numerous rocket launches to new space vehicles and landers trying to reach orbit, Moon, Mars, and beyond.National government agencies in charge of space activities like NASA, ESA, ISRO, JAXA, DLR, ASI, ROSCOSMOS, CNSA, etc, and commercial entities like Blue Origin, Space X, ULA, Rocket Lab, Sierra Space, Astra Bigelow, CASC, Astrobotics, Intuitive Machines, etc, are speeding efforts to build rockets, spacecraft, probes, space stations, satellites, telescopes, landers, rovers and even drones, to explore space and planets in a rate never seen before.

This new wave is targeting the Moon as a stepping stone for human exploration. Many missions have been launched or are targeted to be launched in the coming years and this brings a need for sensors and instruments that can measure and characterize either the vacuum surrounding the spacecraft while approaching a planet or moon, or the quality of air inside the cabin when transporting humans, or else deployed onboard a lander or a rover to characterize the lunar atmosphere, its surface and subsurface looking for water and volatiles for in situ resource utilization (ISRU) activities.

There have been many unique successful gas analysis instruments that have been flown into space or landed on planets, such as mass spectrometers (MS) and optical emission spectrometers, providing extremely useful gas composition data and vacuum characterization conditions of the exploration target. Nevertheless, in the same way rockets are now being manufactured with orders of magnitude lower cost by commercial rocket companies, this new wave of exploration requires commercial instruments developed by companies, not government agencies, that can provide time and time again, ready-to-use, space-qualified, cost-effective systems to be carried in any space exploration vehicle when vacuum and gas analysis are necessary.

This presentation provides an overview of the different instruments used in gas analysis and vacuum measurements in space exploration over the years, especially targeting planetary and moon exploration.It also includes the most recent developments of commercial-off-the-shelf (COTS) space-ready mass spectrometer planned to be used in different lander missions through the Commercial Lunar Payload Services (CLPS) initiative as part of NASA ARTEMIS going back to the Moon program, as an example of this new approach to do commercial instrumentation for space applications.

Vacuum Technology
Room 121 - Session VT2-TuA

Vacuum Technology for Fusion Energy

Moderators: Giulia Lanza, SLAC National Accelerator Laboratory, **Julia Scherschligt**, National Institute of Standards and Technology

3:00pm **VT2-TuA-4 ITER Service Vacuum System Client Connections**, *Charles Smith III, **Jared Tippens**,* Oak Ridge National Laboratory
The ITER project has the goal to demonstrate the feasibility of fusion and to advance the scientific and engineering understanding of fusion for future commercial reactors. Nearly five thousand volumes, commonly called "clients", throughout the ITER facility require vacuum service during operations. This vacuum is provided by seventy-seven distribution boxes around the complex, where "client connections" in the form of stainless-steel tubing bridge the gap between distribution boxes and individual clients.

There is an estimated total of 42 kilometers of 6 mm outer diameter tubing, 2 kilometers of 12 mm outer diameter tubing, and 1 kilometer of 38 mm outer diameter tubing. The size of the tubing is correlated to the volume of the clients needing vacuum service. Most clients throughout the facility are below 50 liters, often taking the form of interspaces of double-contained pipes, valves, and flanges. Many of these client connections have the possibility of containing tritium, a radioactive isotope of hydrogen. This creates the need for the tubing to be capable of handling combinations of pressure, thermal, and seismic loads and for the analysis to validate this.

In addition to the structural qualification of the client connections and their associated supports, several practical challenges exist. The first challenge is routing space constraints, as the majority of areas where the tubing is routed are congested and often require complicated routings to avoid clashes. The bigger challenge is installation, as the tubes are routed with a high packing density and the installers will have limited space to compress fittings or weld tubes together.

A solution has been proposed by US ITER and design is approaching completion for this client connection system. A packaging solution is being implemented for bundles of tubing, and mitigation strategy for thermal loads is underway. An installation plan for the tubing is in progress that will allow the routing of nearly five thousand tubes in a congested environment.

An overview of the Client Connections System and the associated qualification effort will be given. These design details are applicable to other fusion facilities where tritium will be present, particularly for large power plants where vacuum is required on many supporting systems.

3:15pm **VT2-TuA-5 All-Metal Mechanical Pumping Solution Replacing the ITER Cryogenic Regeneration Roughing Pump System**, *Jonathan Perry,* Oak Ridge National Laboratory*; Shaun Hughes,* ITER Organization, France*; Charles Smith,* Oak Ridge National Laboratory
This paper gives an overview of replacing the ITER[1] Cryogenic regeneration roughing pump system with a newly developed all-metal mechanical pumping solution.

The United States Domestic Agency of ITER is responsible for the final design, procurement, and acceptance testing of the ITER roughing pump system (RPS). The current Torus cryopump (TCP) and Neutral Beam cryopump (NBCP) regeneration roughing pump systems are based around Cryogenic Viscous Compressor (CVC) which requires substantial cryogenic infrastructure to be provided, operated, and maintained within the RPS. However, due to advancements in mechanical all-metal vacuum pumps, opportunities from partnerships with various experts in the fusion and tritium communities, in addition to refinement of ITER operational principles, the use of all-metal mechanical pumps to move tritiated gas, is now a potential design solution.

This paper will present an overview of the current configuration, as well as the design history evolution. The paper will then review the main performance requirements for the Cryogenic regeneration roughing system and present results of analytical modeling of the performance of the system using an all-mechanical pump configuration. The paper will also discuss the advantages in progressing the all-mechanical pump option, while outlining remaining testing for this solution and ultimately replacing the current cryogenic configuration.

[1] Nuclear Facility INB-174

This manuscript has been authored by UT-Battelle, LLC under Contract No. DE-AC05-00OR22725 with the U.S. Department of Energy. The United States Government retains and the publisher, by accepting the article for publication, acknowledges that the United States Government retains a non-exclusive, paid-up, irrevocable, world-wide license to publish or reproduce the published form of this manuscript, or allow others to do so, for United States Government purposes. The Department of Energy will provide public access to these results of federally sponsored research in accordance with DOE Public Access Plan (http://energy.gov/downloads/doe-public-access-plan)

4:00pm **VT2-TuA-8 Exploring Vacuum Technology in Nuclear Fusion: Challenges and Opportunities within STEP Fuel Cycle**, *Sophie Davies,* United Kingdom Atomic Energy Authority, UK*; Antulio Tarazona,* United Kingdom Atomic Energy Authority (UKAEA), UK   **INVITED**
Generating energy through fusion has garnered significant attention from research institutions, government programs, commercial entities, and investors due to its potential to provide virtually unlimited low-carbon and renewable energy supplies. Deuterium and Tritium stand out as the primary fuels for fusion devices, from inertia to magnetic confinement systems, owing to the net fusion energy released in their reaction, despite facing various fundamental and engineering challenges. Vacuum pumping, a critical aspect among these challenges, plays a pivotal role in preventing plasma contamination, minimizing losses through particle collisions with

Tuesday Afternoon, November 5, 2024

residual gas molecules, and ensuring the overall efficiency of the fusion reaction. This paper provides an overview of the most relevant nuclear fusion devices where vacuum technology plays a crucial role, focusing on the vacuum requirements for experimental Tokamaks. Furthermore, it delves into the challenges associated with vacuum pumping, highlighting its significance for successfully operating fusion power plants. As a case study, the discussion extends to the STEP (Spherical Tokamak for Energy Production) program, elucidating its vacuum challenges and some strategies to address them. This work aims to contribute to understanding the intricate interplay between vacuum technology and nuclear fusion, shedding light on advancements and challenges in this ground-breaking field.

4:45pm VT2-TuA-11 Overview of the Vacuum Pumping Systems for the SPARC Tokamak, *Matt Fillion, Adam Kuang, Oliver Mulvany, James Fountas, Peter Winn,* Commonwealth Fusion Systems

Commonwealth Fusion Systems (CFS) is a spin-off from the Massachusetts Institute of Technology aiming to bring fusion energy to the grid. CFS is currently building the SPARC tokamak—a superconducting, high-field, deuterium-tritium fueled tokamak that is designed to reach Q>1. SPARC is a crucial step to develop the technologies and refine the physics necessary for ARC, a commercial fusion power plant capable of delivering net energy to the grid.

The Vacuum Pumping System of SPARC consists of three primary subsystems. The cryostat pumping system generates and maintains vacuum insulation of the cryostat to support the superconducting magnets. The leak detection system provides vacuum guarding for the many tritium secondary interspaces and double seals throughout SPARC. Lastly, the torus pumping system is responsible for four main functions: the containment of tritium, reaching and maintaining the primary vacuum vessel base pressure, the recovery of the inter-pulse pressure, and providing particle control during the plasma discharge by pumping from the divertor regions.

Each of the three vacuum pumping subsystems has an independent set of two dry screw pumps to provide rough vacuum and fore line pumping, mag-lev turbomolecular pumps for achieving ultrahigh vacuum, and a residual gas analyzer for leak detection and analysis of the plasma exhaust composition. In addition, the cryostat and torus pumping systems each contain custom tritium compatible closed loop refrigerator cooled cryogenic pumps to provide temporary enhanced pumping speeds. The cryostat and torus pumping systems also feature piping up to DN540, which calls for the development of a custom CF-style knife-edge flange.

The magnetic field strength and neutronic flux can damage or heat components near the tokamak, including the cryogenic pumps, sensors, turbomolecular pumps, and cables. This provides a narrow design window for equipment, and in some cases requires local shielding to protect sensitive components. Boron carbide (B4C) neutronic shielding will be used to prevent a large flux of neutrons from the plasma through the vacuum ducting. The vacuum conductance was analyzed in the molecular and transitional flow regimes to optimize the size, shape, and position of the B4C.

This talk will provide a general overview of the SPARC vacuum pumping systems and associated challenges, with a focus on the torus pumping system and the design of custom tritium compatible pumps required by this system.

5:00pm VT2-TuA-12 Design and Development of an Optical Gas Sensor for Fusion Applications, *Joe Brindley*, Patrick McCarthy, Gencoa, UK*; Chris Marcus, Christopher Klepper, Brendan Quinlan,* ORNL

Fast and accurate neutral gas measurement systems will be critical for the realisation of future deuterium-tritium (D-T) fusion reactors. This is required for the closed loop fuelling cycle of the reactor, where quantities of exhaust fuel gases, consisting primarily of isotopes of hydrogen (H) and helium (He), are monitored in real time.

Typically, quadrupole mass spectrometry (QMS) is employed to measure gas partial pressures, however the very similar mass-to-charge ratios of fusion gas species makes this measurement using QMS extremely challenging. For example, the masses of D_2 and ^{4}He are separated by 0.02 amu. Techniques such as threshold ionisation mass spectrometry can be utilised to separate closely spaced masses, however this method has difficulty resolving low concentrations with adequate speed.

An alternative route, using remote optical emission spectroscopy (ROES), was demonstrated by Klepper et al[1] and this is seen as a promising method for overcoming the inherent mass measurement problem encountered by QMS. ROES involves the generation of a small, remote plasma which is used to excite gaseous species into emitting light, which can then be measured by an optical spectrometer and the gases identified and quantified by their light emission.

Whilst ROES is an extremely promising technique it is not without its challenges for use in fusion applications. Whilst D and ^{4}He light emissions are separated by > 10 nm, the isotopic emissions of He and H are very closely spaced, requiring high resolution optical spectroscopy. Furthermore, the sensor will be required to operate in reactor fringing fields of more than 0.2T whilst maintaining a stable plasma within the sensor. A further complication is the inherent presence of ionising radiation produced by the fusion reactor.

In this paper we present the development and design of a ROES sensor for fusion applications. The sensor is qualified in its ability to detect small (<0.1%) concentrations of H and He gas isotopes with a speed of response of less than 1 second. This surpasses the requirement for the future fusion reactor, ITER. Optimisation of the sensor's plasma for resolving closely spaced emissions will be presented. Finally, the stability of the sensor's operation in a representative fusion environment is discussed. Experimental results of sensor operation during exposure to magnetic fringing fields and gamma radiation (up to 0.5 T and 500 kGy respectively) will be presented.

1. C. C. Klepper et al., "Developments and Challenges in the Design of the ITER DRGA," in IEEE Transactions on Plasma Science, vol. 50, no. 12, pp. 4970-4979, Dec. 2022

5:15pm VT2-TuA-13 Development of the SPARC Tokamak Exhaust Purification System, *Eric Dombrowski,* Commonwealth Fusion Systems

The SPARC device is a high-field, compact, D-T burning tokomak with the goal of demonstrating net energy gain (Q>2). Burning plasmas on SPARC are anticipated to require less than 1g of tritium fueling. During a fusion pulse, the unspent D-T mixture and helium ash are pumped through the divertor via eight cryosorption pumps which are subsequently regenerated and exhausted through the torus vacuum pumping system. During tritium operations this exhaust gas is directed to the first stage of the tritium fuel cycle, the torus exhaust purification (TEP) system. The impurities are separated from the hydrogenic species and sent to the trace tritium recovery system for further processing. The hydrogen is sent to isotope separation where a new D-T mixture is prepared.

TEP has three main operations. The torus exhaust gas is passed through a high conductance, liquid nitrogen cooled, zeolite based cryosorption pump. All species except for helium and neon are adsorbed onto the zeolite media. The helium is extracted through the back end of the cryosorption pump by an all-metal scroll pump and exhausted to the Trace Tritium Recovery System. The cryosorption pumps' regeneration gasses are passed through a Pd/Ag permeator to generate a pure stream of hydrogenic species for isotope separation. Periodically, a full regeneration of the cryosorption pump to 350 °C is carried out at the end of a day's campaign to liberate chemically bound tritium from the zeolite packing material. This effluent is reacted over a nickel catalyst and passed through a second Pd/Ag permeator onto isotope separation.

A full-scale experimental test loop has been assembled and validated with hydrogen and deuterium isotopes at CFS' SPARC location in Devens, Massachusetts. These components are now in final design for manufacturing in collaboration with Torion Plasma Corporation where they will be integrated into the tritium compatible processing assembly to be completed in Q2 of 2025.

2D Materials
Room 122 - Session 2D+EM+MI+QS-WeM

2D Materials: Heterostructures, Twistronics, and Proximity Effects

Moderators: Aaron Bostwick, Advanced Light Source, Lawrence Berkeley National Laboratory, **Tiancong Zhu**, Purdue University

8:00am 2D+EM+MI+QS-WeM-1 Van der Waals Semiconductors: From Stacking-Controlled Crystals to Unconventional Heterostructures, *Peter Sutter, Eli Sutter,* University of Nebraska - Lincoln **INVITED**

2D materials have attracted broad interest due to novel properties that arise in atomically thin crystals. As interesting scientifically and important technologically, but much less explored are van der Waals (vdW) crystals that, assembled from 2D building blocks, lie between a monolayer and the bulk. In this regime, phenomena such as phase separation, transformations between crystal polymorphs, and competition between different stacking registries provide unprecedented opportunities for controlling morphology, interface formation, and novel degrees of freedom such as interlayer twist. But going beyond a single layer also poses significant challenges, both due to the diversity of the possible few-layer structures and the difficulty of probing functionality such as optoelectronics and ferroics at the relevant length scales.

Here, we discuss our recent research that addresses these challenges focusing on group IVA chalcogenides, an emerging class of anisotropic layered semiconductors promising for energy conversion, optoelectronics, and information processing. Advanced *in-situ* microscopy provides insights into the growth process, interlayer twisting, and emerging functionality such as stacking-controlled ferroelectricity. Nanometer-scale electron excited spectroscopy identifies photonic light-matter hybrid states and reveals anisotropic and valley-selective charge carrier flows across interfaces in heterostructures. Our results highlight the rich sets of materials architectures and functionalities that can be realized in van der Waals crystals and heterostructures beyond the 2D limit.

8:30am 2D+EM+MI+QS-WeM-3 Deterministic Assembly, Transfer, and Flipping of 2D Materials Using Tunable Polymer Films, *Jeffrey J. Schwartz, Son T. Le,* University of Maryland, College Park*; Karen E. Grutter, Aubrey T. Hanbicki, Adam L. Friedman,* Laboratory for Physical Sciences

Assembly of two-dimensional (2D) materials into van der Waals heterostructures is a crucial step in creating precisely engineered nanoscale and quantum devices for use in a wide variety of spintronic, electronic, and other applications. Numerous strategies exist to pick-up, stack, transfer, and even flip over these atomically thin structures. One popular strategy leverages the ability to tune the adhesion between a polymer stamp and 2D sheets to pick-up, stack, and release structures at different temperatures. Although relatively easy to implement, this technique is tedious to perform and has a low throughput. Here, we demonstrate a significant improvement to a deterministic, all-dry, polymer-assisted transfer technique using polyvinyl chloride (PVC) thin films to manipulate 2D materials and to fabricate devices. We construct stamps from pairs of commercially available PVC films that controllably pick-up and release 2D sheets within known, overlapping temperature ranges. These mechanically durable stamps can be produced quickly and without the time-consuming preparation and annealing steps required by most other commonly used polymers. Importantly, these stamps not only facilitate deterministic transfer of 2D materials, but they also enable polymer-to-polymer transfer (e.g., between separate stamps) and flipping of material stacks to create inverted heterostructures that are important for many applications, including scanning tunneling microscopy measurements. We characterize the thermal transition properties of the PVC films employed here as well as assay the cleanliness and performance of devices produced using this technique. These improvements enable rapid production of 2D devices with fewer interactions required by the operator, which is especially significant when working in controlled environments (e.g., glovebox) or in remote or autonomously controlled contexts.

8:45am 2D+EM+MI+QS-WeM-4 Cleaning of Low-Dimensionality Materials: Challenge and Solutions, *Jean-Francois de Marneffe, Pieter-Jan Wyndaele, Marina Timmermans, Carlos Cunha,* IMEC, Belgium*; Barbara Canto, Zhenxing Wang,* AMO GmbH, Aachen, Germany*; Robbe Slaets, Gaohang He, Inge Asselberghs, Cesar J. Lockhart de la Rosa, Gouri Sankar Kar, Clement Merckling, Stefan De Gendt,* IMEC, Belgium

Over the last few years, significant efforts have been made in exploring low-dimensionality materials such as single layer Graphene (SLG), transition metal dichalcogenides (TMDCs) and carbon nanotubes (CNTs), for a wide range of applications covering beyond CMOS logic, EUV pellicles, photonics, and sensing (amongst others). Due to their intrinsic 2D or 1D nature, these materials are highly sensitive to processing damage leading to stoichiometric changes or crystalline defects. Among the many manufacturing steps required for building devices, the cleaning of these systems is an absolute requirement and a bottleneck. Typically, during processing, residual polymers or carbon of ambient origin, do contaminate the surface leading to nanometric deposits that change the intrinsic transport/optical properties of the materials, and cause parasitic dielectric drift or high contact resistance. Wet cleaning, using organic solvents, is a mainstream approach, which proves to be inefficient for irreversibly physically adsorbed polymer residues. In this paper, we explore dry cleaning approaches, based on plasma treatment and UV cure. Plasma-based cleaning proves to be very efficient but leads to material damage, which can be minimized by tuning the average ion energy, the processing temperature, the plasma chemistry or adding a post-cleaning restoration step. For TMDCs, damage consist essentially in the creation of chalcogen vacancies, which lead to metal oxidation upon ambient exposure. For Graphene and CNTs, damage consist in carbon vacancies, causing lattice distortions, oxidation and ultimately a dramatic change of the material's transport properties. Part of this presentation will explore the use of UV cure, which is a known method for cleaning polymers from semiconductor surfaces.

9:30am 2D+EM+MI+QS-WeM-7 Exploring Incommensurate Lattice Modulations in BSCCO van der Waals Heterostructures: Implications for Q-Bit Development, *Patryk Wasik,* Brookhaven National Laboratory*; Shu Yang Frank Zhao,* Harvard University*; Rahul Jangid,* Brookhaven National Laboratory*; Alex Cui,* Harvard University*; John Sinsheimer,* Brookhaven National Laboratory*; Philip Kim,* Harvard University*; Nicola Poccia,* IFW Dresden, Germany*; Claudio Mazzoli,* Brookhaven National Laboratory

Quantum computers (QC) are poised to revolutionise computational capabilities by naturally encoding complex quantum computations, thereby significantly improving computation time compared to silicon-based technologies. Currently, Q-bits, the essential components of QCs, are made from conventional superconductors that operate efficiently only near absolute zero temperatures. To address this limitation, two-dimensional van der Waals (vdW) encapsulated high-temperature superconductor (HTSC) stacks have been proposed as future Q-bit candidates, driven by recent advancements in nanofabrication techniques. However, a detailed understanding of their structural and electronic properties is crucial.

We present low-temperature resonant soft X-ray investigations on ultrathin $Bi_2Sr_2CaCu_2O_{8+y}$ (BSCCO) vdW heterostructures, promising candidates for large-scale Q-bit applications. BSCCO crystals exhibit two incommensurate lattice modulations (ILMs), providing an excellent opportunity to explore the relationship between structure and electronic behaviour in low dimensions. We report ILMs (Cu L_3) and structural peak (off resonance) maps obtained across the superconducting transition temperature ($T_c \approx 60$ K). These signals, under external gating, present significant potential for further exploration offering new insights into the electronic interactions in vdW HTSC systems.

11:00am 2D+EM+MI+QS-WeM-13 Atomic Layer Deposition of Transition Metal Dichalcogenides: Precursors, Processes, and Applications Perspectives, *Thong Ngo, Angelica Azcatl, Nguyen Vu, Ching-Jung Cheng, Michael Miller, Charlene Chen, Ravi Kanjolia, Mansour Moinpour, Mark Clark,* EMD Electronics, USA **INVITED**

Transition metal dichalcogenides (TMD) are three-atom-thick layer materials that possess a wide array of properties, such as insulating, semiconducting, conducting, and superconducting. While there has been a significant amount of research on TMD for various applications including energy storage, photovoltaics, biomedicals, catalysis, hydrogen production processes, and healthcare, the usage of TMD for electronic applications has been researched most in the past two decades.

Each layer of TMD is a 2D sheet with the thickness of ~6-7Å. These layers are bonded by Van der Waals force. The ultra-thin structure enables TMD for semiconductor industry applications, which continuously requires both size-scaling of materials layers and electrical performance improvement of devices. The semiconductor-range band gap and the high electron/hole mobility of several TMD, such as MoS_2, WS_2, WSe_2, and $MoSe_2$ allow their usage for high mobility ultra-thin channel transistor. In addition, the relatively high conductivity of some other TMD, such as TaS_2 and NbS_2 make them promising candidates for interconnect barrier/liner as a replacement of TaN/Ta bilayer.

TMD materials need to pass certain quality requirements to provide desirable property/performance; therefore, method of synthesizing TMD plays an important role for high quality materials. Solution-based deposition, non-vacuum electrodeposition, polymer-assisted deposition, physical vapor deposition (PVD), chemical vapor deposition (CVD), and atomic layer deposition (ALD) have been used to deposit ultra-thin TMD. Among these techniques, CVD is the most popular deposition method, and to date, the highest quality of TMD for semiconductor applications is CVD-TMD. However, the need of lower thermal budget, better layer controllability, uniformity, and conformality requires the semiconductor community to explore ALD methods. In this presentation, we will review multiple ALD processes for TMD including precursors, process requirements for high mobility channel and barrier/liner applications. We will highlight challenges of TMD applications for logic, memory, and interconnects. The presentation will also feature our recent work on ALD MoS_2 for high-mobility channel transistor with >5 decades On/Off ratio and >1 µA/µm Ion. Our achievement of 300mm ALD MoS_2 deposition brings ultra-thin TMD materials closer to a manufacturable fab process for semiconductor industry.

11:30am **2D+EM+MI+QS-WeM-15 Writing and Detecting Topological Spin Textures in Exfoliated Fe$_5$-xGete$_2$**, *Luis Balicas,* Florida State University - National High Magnetic Field Lab - FSU Quantum Initiative

Fe$_{5-x}$GeTe$_2$ is a centrosymmetric, layered van der Waals (vdW) ferromagnet that displays Curie temperatures T_c (270-330 K) that are within the useful range for spintronic applications. Little is known about the interplay between its topological spin textures (e.g., merons, skyrmions) with technologically relevant transport properties such as the topological Hall effect (THE), or topological thermal transport. We found via high-resolution Lorentz transmission electron microscopy that merons and anti-meron pairs coexist with Néel skyrmions in Fe$_{5-x}$GeTe$_2$ over a wide range of temperatures and probe their effects on thermal and electrical transport [1]. It turns out that we detect a THE, even at room T, that senses merons at higher T's as well as their coexistence with skyrmions as T is lowered, indicating an on-demand thermally driven formation of either type of spin texture.Remarkably, we also observe an unconventional THE, i.e., in absence of Lorentz force, and attribute it to the interaction between charge carriers and magnetic field-induced chiral spin textures. We find that both the anomalous Hall effect (AHE) and THE can be amplified considerably by just adjusting the thickness of exfoliated Fe$_{5-x}$GeTe$_2$, with the THE becoming observable even under zero magnetic field due to a field-induced unbalance in topological charges [2]. Using a complementary suite of techniques, including electronic transport, Lorentz transmission electron microscopy, and micromagnetic simulations, we reveal the emergence of substantial coercive fields upon exfoliation, which are absent in the bulk, implying thickness-dependent magnetic interactions that affect the topological spin textures (TSTs). We detected a 'magic' thickness of t ~30 nm where the formation of TSTs is maximized, inducing large magnitudes for the topological charge density, and the concomitant AHE and THE resistivities at T ~ 120 K. Their values are observed to be higher than those found in magnetic topological insulators and, so far, the largest reported for 2D magnets. The hitherto unobserved THE under zero magnetic field could provide a platform for the writing and electrical detection of TSTs aiming at energy-efficient devices based on vdW ferromagnets.

[1] B. W. Casas *et al*., Adv. Mater. **35**, 202212087 (2023).

[2] A. Moon *et al.*, ACS Nano **18**, 4216-4228 (2024).

AI/ML for Scientific Discovery
Room 125 - Session AIML-WeM

AI/ML for Scientific Discovery

Moderators: Alain Diebold, University at Albany-SUNY, **Erica Douglas**, Sandia National Laboratories

8:00am **AIML-WeM-1 "Beyond Fingerprinting": Rapid Process Exploration and Optimization via High-Throughput and Machine Learning**, *Brad Boyce*, Sandia National Laboratories, USA*; Remi Dingreville, Jonathan Coleman, Elliott Fowler, Carianne Martinez,* Sandia National Labs*; David Adams,* Sandia National Laboratories **INVITED**

Material properties are governed by composition and associated microstructure dictated by the thermodynamics and kinetics of manufacturing processes.Often, the connectivity between process conditions and the resulting structure and properties is complex, evading full predictivity via high-fidelity modeling.In this work, we are exploring three manufacturing processes where material properties are difficult to predict directly from process settings: physical vapor deposition, electroplating and additive manufacturing (laser powder bed fusion).Each of the three processes offer unique challenges and opportunities.Across these three exemplars, we are augmenting traditional process-structure-property investigations with an accelerated workflow to detect material structure/composition, prognose associated properties, and adapt the associated process to achieve improved product outcomes.This accelerated detect-prognose-adapt cycle is aided by four key elements: (1) automated combinatorial synthesis to enable rapid parameter sweeps, (2) high-throughput evaluation of both conventional and surrogate indicators of material chemistry, structure, and properties, (3) unsupervised learning algorithms to unravel correlations beyond expert cognition, and (4) Bayesian optimization strategies to efficiently explore and exploit high-dimensional process parameter space.In each of these four domains, we take advantage of previously developed capabilities, or where such capabilities are insufficient, we develop novel techniques.For example, in the domain of electroplating synthesis, we have employed an existing robotic pipetting system for formulation of solution chemistries while developing a custom 12-cell parallel electroplating system that enables hundreds of unique conditions to be explored in about a day.While we consider purely data-driven ML algorithms for some correlation analysis, a more interpretable and robust solution includes physical models based on established governing equations.In this regard, we have developed a physics-informed multimodal autoencoder that fuses data from multiple characterization modalities alongside physical models to provide a deeper fingerprint of material state, enabling cluster disentanglement and cross-modal inference.SNL is managed and operated by NTESS under DOE NNSA contract DE-NA0003525.

8:30am **AIML-WeM-3 Simulations of Epitaxial Inorganic Interfaces Using DFT with Machine-Learned Hubbard U Corrections**, *Noa Marom,* Carnegie Mellon University **INVITED**

Epitaxial inorganic interfaces lie at the heart of semiconductor, spintronic, and quantum devices. At an interface between two dissimilar materials physical properties and functionalities may arise, which do not exist in any of the isolated components in the bulk. To predict the structure of domain-matched epitaxial interfaces, we use a combination of lattice matching and surface matching algorithms implemented in the Ogre Python package [J. Chem. Phys., 155, 034111 (2021); J. Phys. Condensed Matter, 34, 233002 (2022)]. To study the electronic and magnetic properties of interfaces we use density functional theory (DFT). Within DFT, the many-body interactions between electrons are described by approximate exchange-correlation functionals. The accuracy of the results hinges on an appropriate choice of functional. We have developed a method of machine learning the Hubbard U correction added to a DFT functional by Bayesian optimization (BO) [npj Computational Materials 6, 180 (2020)]. The DFT+U(BO) method balances accuracy with computational cost, enabling unprecedented simulations of large models of surfaces and interfaces of interest for applications in quantum computing. Examples include InAs and InSb surfaces [Advanced Quantum Technologies, 5, 2100033 (2022)], which are the substrates of choice for superconductor/semiconductor Majorana devices; the HgTe/CdTe and InAs/GaSb interfaces [Phys. Rev. Mater. 5, 084204 (2021)], in which a 2D topological insulator phase may arise; the EuS/InAs interface [Phys. Rev. Mater. 5, 064606 (2021)], proposed as a candidate for the realization of a ferromagnet-semiconductor-superconductor Majorana devices without an external magnetic field; and CdTe as a tunnel barrier to control the coupling strength at the interface between InSb and α-Sn [ACS Applied Materials & Interfaces 15, 16288 (2023)].

9:00am **AIML-WeM-5 On-The-Fly Analysis of RHEED Images During Deposition Using Artificial Intelligence**, *Tiffany Kaspar, Jenna Pope, Sarah Akers, Henry Sprueill, Arman Ter-Petrosyan, Derek Hopkins, Ethan King, Jan Drgona,* Pacific Northwest National Laboratory

Modern synthesis methods enable the fabrication of an ever-expanding array of novel, non-equilibrium, and/or metastable materials and composites that may possess unique and desirable functionality. Thin film deposition by molecular beam epitaxy (MBE) can produce atomically precise (or nearly so) materials with a wide range of functional electronic, magnetic, ferroelectric/multiferroic, optical, and/or ion-conducting properties.We are working to employ artificial intelligence (AI)-accelerated analysis of in situ and ex situ data streams for on-the-fly feedback control of the MBE deposition process that will enable targeted synthesis of novel

materials with desired structure, chemical stability, and functional properties.Here we present a machine-learning-enabled framework for analysis of reflection high energy electron diffraction (RHEED) pattern images in real time (one image per second).Our approach utilizes pre-trained neural networks for image preprocessing, statistical analysis to identify changepoints in the images over time, and network graph analysis methods to precisely identify and classify changes.We demonstrate this framework using RHEED images collected from the deposition of epitaxial oxide thin films such as anatase TiO_2 on $SrTiO_3$(001).Advantages and disadvantages of our approach will be discussed, as well as its potential use as the basis for on-the-fly feedback control of deposition parameters.

9:15am **AIML-WeM-6 An Unsupervised Machine Learning Approach for the Identification of Adsorbates on a Semiconductor Surface: BCl_3 Adsorption on Si(100)**, *Azadeh Farzaneh,* University of Maryland, College Park*; Chun Yin Tommy Wang, Sergei Kalinin,* University of Tennessee Knoxville*; Robert Butera,* Laboratory for Physical Sciences

A more thorough understanding of the reaction of molecular precursors on crystalline and amorphous surfaces will play a significant role in the optimization of industrially relevant processes, such as chemical vapor deposition and atomic layer deposition. Here, we explore an unsupervised machine learning approach to identify reaction products related to molecular precursor adsorption on a semiconductor surface and provide a general framework for analyzing surface species. In particular, we focus our investigations on the adsorption of BCl_3 on Si(100) using scanning tunneling microscopy (STM). We designed an unsupervised workflow that results in the identification of distinct surface moieties and their relative concentrations following the initial adsorption of BCl_3 and subsequent decomposition reactions on the surface. While previous methods have relied on manual cropping of STM images based on defect coordinates, our workflow isolates surface features from the base lattice to generate a training dataset. Two key components of the Si(100) surface are taken into account for isolating surface features: (1) steps and (2) orientation of Si dimer rows. This unsupervised method eliminates the need for manual labeling an untenable amount of surface features, thereby removing any label bias introduced by the operator. It circumvents the bottleneck of machine learning workflows when experimental conditions change and new labeled data is required. We optimize the performance of the unsupervised neural networks by selecting the proper number of feature classes that minimize the image-to-image identification error of distinct surface features in a given experimental data set. This methodology can be generalized and extended to other material systems to provide insight into reactions on surfaces.

9:30am **AIML-WeM-7 Quantum and Classical Supervised Learning Analysis of Synthesis–Structure Relationships in Epitaxially–Grown Semiconductors**, *Andrew Messecar,* Western Michigan University*; Steven Durbin,* University of Hawaiʻi at Mānoa*; Robert Makin,* Western Michigan University

The design of material synthesis experiments occurs within highly multidimensional processing spaces that are defined by many design parameters. Identifying the optimal values for each synthesis parameter is often performed through an expensive, Edisonian, trial–and–error approach to experiment design. Considerable interest exists in the development of machine learning–based approaches for the rapid and accurate identification of optimal materials designs and synthesis conditions yielding material samples that display target properties of interest. In this work, data detailing hundreds of plasma–assisted molecular beam epitaxy (PAMBE) growth trials each of ZnO and various nitride semiconductors have been organized into separate, composition–specific data sets. For each growth record, the complete set of experiment parameters (substrate temperature, effusion cell temperatures, growth duration, etc.) are associated with binary measures of crystallinity as well as surface morphology as determined by *in–situ* reflection high–energy electron diffraction (RHEED) patterns. A Bragg–Williams measure of lattice disorder (S^2) is included as an additional, continuous figure of merit for investigation. Quantum and conventional machine learning algorithms – including logistic regression, tree–based algorithms, and quantum support vector machines – are trained on the data to investigate which growth parameters are most statistically significant for influencing crystallinity, surface morphology, and S^2. When predicting the occurrence of monocrystalline GaN PAMBE, we show that supervised machine learning algorithms for quantum computers can display significant advantage over their classical machine learning counterparts. The class conditional probabilities of obtaining single crystalline and atomically flat thin film crystals are predicted across processing spaces of the two PAMBE operating parameters determined to be most statistically important. S^2 is also forecasted across the same growth spaces. These predictions are compared to conventional experimental wisdom as well as the results described within published literature regarding the PAMBE growth of these materials. The predictions indicate that different growth conditions are of interest depending on whether a single crystalline sample, a flat surface, or a well–ordered lattice is desired. The superior generalization performance displayed by the quantum machine learning algorithms when predicting GaN crystallinity implies possible advantage gained via quantum algorithms when studying synthesis–structure relationships in other material systems.

9:45am **AIML-WeM-8 'DECIEDD with CARE' - Building an Autonomous Ecosystem for the Discovery and Optimization of Metal Nanoparticle Inks**, *J. Elliott Fowler,* Sandia National Laboratories*; Nat Trask,* University of Pennsylvania*; Matthew Kottwitz, Nelson Bell, Alan Hesu, Alison Roth,* Sandia National Laboratories*; Josiah Hanna,* University of Wisconsin - Madison*; John Foster,* University of Texas at Austin*; Jacob Boissiere,* Sandia National Laboratories

The end-to-end design and manufacturing of printed circuit boards substrates, a ubiquitous and critical technology in energy storage, communication, and defense systems, is poised to undergo a transformation following developments in additive manufacturing within the last decade. These advancements include droplet-on-demand inkjet printing of conductive inks—suspensions of metallic nanoparticles, graphene, carbon nanotubes, etc.—onto dielectric substrates. Despite extensive research, few printed commercial inks possess the conductivity and robustness desired by high-reliability design agencies. A major contributor to the limited availability of viable inks is the enormous parameter space of processing conditions and material structure, property, and performance criteria that must be balanced during development.

For this reason, Sandia National Laboratories, together with university partners, has engaged in the design and implementation of an autonomous materials discovery platform to efficiently (1) synthesize Cu, Ag, and Au nanoparticles, (2) formulate those nanoparticles into inks, and (3) print those inks to form devices. At each step of the process, characterization data of the structure, properties, and performance is provided to a machine learning algorithm utilizing a self-consistent and scalable/tunable data schema and data management application. Initial campaigns have utilized off-the-shelf machine learning methods to autonomously optimize the size and dispersity of silver nanoparticle via manipulating the stoichiometric ratio of mono-, di- and tri- functionalized carboxylic acid ligands, amongst other variables. Concurrently, development of bespoke solutions such as multifidelity reinforcement learning and scientific machine learning continues to address the challenges of relatively sparse data sets, multimodality and fidelity, and the need identify underlying process-structure-property-performance relationships.

11:00am **AIML-WeM-13 Machine Learning for Accelerating Atomic Layer Deposition Process Optimization**, *Minjong Lee, Doo San Kim, Thi Thu Huong Chu, Dan Le, Jin-Hyun Kim, Dushyant Narayan, Jiyoung Kim,* University of Texas at Dallas

In the era of Industry 4.0, artificial intelligence (AI) and machine learning (ML) are revolutionizing manufacturing processes, enhancing flexibility and efficiency while minimizing process errors [1]. ML integration is particularly valuable in semiconductor fabrication, where current techniques often require over 30 steps to deposit a single high-quality film layer. Out of semiconductor fabrication techniques, atomic layer deposition (ALD) stands out as a promising deposition method due to its precision in atomic-scale film engineering and compatibility with advanced 3D architectures. However, ALD involves numerous critical parameters affecting film quality, and comprehensive exploration of all conditions is economically unfeasible, with each experimental run costing over a thousand dollars per wafer, plus additional labor and analysis costs [1]. This limitation constrains inspection ranges of ALD conditions, hindering the development of accurate, atomic-scale process models. The incorporation of AI/ML technologies into ALD processes is thus beneficial in improving cost-efficiency for process optimization by potentially decreasing the volume of data necessary.

This study presents a deep neural network (DNN) framework for ML-driven ALD processes, focusing on optimizing hafnium oxide film deposition. While previous ML applications in ALD processes have primarily focused on monitoring film thickness [2], we investigate the film quality, particularly density, which is crucial property for film performance. We incorporate film density using the wet etch rate (WER) test into our DNN framework,

leveraging the principle that higher density films have more tightly packed atoms (i.e., slow WER). In this presentation, we report that the DNN case studies involve four ALD process parameters (deposition temperatures, precursor temperatures, and sample locations (x, y)) and three film properties (thickness (T_{ox}), refractive index (RI), and WER). The DNN system demonstrates significant advantages in terms of high prediction accuracy, exceeding 90% for all film properties within prediction ranges of ±1.0 nm, ±0.04, and ±0.9 Å/min for T_{ox}, RI, and WER, respectively. We also investigate prediction maps of film properties for further efficiency toward"digital twin" of ALD process.

[1] K. J. Kanarik et al., Nature, 616, 707 (2023).

[2] A. Arunachalam et al., JVST A 40, 012405 (2022).

11:15am AIML-WeM-14 Utilizing a Machine Learning Potential for Investigating Defects in Hexagonal Boron Nitride, *John Janisch, Duy Le, Talat Rahman,* University of Central Florida
Defects in materials can bring rise to many unique properties and behaviors, and engineering these defects to appear in desirable ways is of utmost importance in maximizing these properties and behaviors. We need atomistic simulations with high accuracy to study not only the defect itself, but also the area around the defects that are affected by its presence. This influence can range from small, local areas near single atom defects, such as a vacancy, to much larger, sprawling areas near large defects, such as grain boundaries. It is not feasible to study large systems with typical high-accuracy methods such as Denstiy Functional Theory (DFT) due to prohibitively long calculation times but utilizing Machine Learning we can construct Machine Learning Potentials (MLP) and overcome these issues. Here, we will present the performance of a MLP for Hexagonal Boron Nitride with and without defects, demonstrating the DFT-level accuracy prediction of material properties such as phonon dispersion as well as defect properties such as vacancy structures and the motion of grain boundaries.

11:30am AIML-WeM-15 Accelerating Innovation: Using AI for Process Pathfinding, *Leandro Medina,* SandBox Semiconductor; ***Mokbel Karam, Steve Sirard, Meghali Chopra,*** Sandbox Semiconductor
While AI is becoming more common in high volume manufacturing, it remains underleveraged in R&D and technology development settings. In these research environments, where data sets are often sparse and the process requirements constantly changing, it is challenging to establish robust data pipelines to take advantage of traditional AI/ML approaches. In this work, we show how AI can be used to provide key process and pathfinding insights for even small datasets, using a gate-all-around etch (GAA) as a case study. Using the software platform SandBox Studio™ AI, we demonstrate how physics-enabled AI can be used to (1) improve process metrology, (2) generate predictive models of the process space, (3) quickly rule out insufficient process regimes and target more viable spaces, and (4) evolve with pathfinding development cycles with novel process parameters permutations. We first collect a limited set of metrology data from disparate sources and use it to generate a high accuracy predictive model of the process space for the GAA etch. We specifically target common metrology sources which are non-destructive, and cost-effective, including Optical Critical Dimension (OCD) scatterometry, ellipsometry, and CD-SEM. We then illustrate how an AI-based model can be used to capture the experimental process space accurately and efficiently. Next, we demonstrate a search strategy for identifying an optimal set of process conditions subject to a defined set of constraints. We highlight that entire process regimes can be visualized, searched, and/or ruled out using the predictive model. Lastly, representative of an R&D environment, we illustrate how the model can be updated to predict outcomes for new process parameters.

11:45am AIML-WeM-16 AI-Driven Synthesis of Thin Films with Pulsed Laser Deposition, *Sumner Harris,* Oak Ridge National Laboratory; *Arpan Biswas,* University of Tennessee, Oak Ridge National Laboratory; *Christopher Rouleau, Alexander Puretzky, Seok Joon Yun, Rama Vasudevan, David Geohegan, Kai Xiao,* Oak Ridge National Laboratory
Traditional methods for synthesizing thin films have typically involved slow, sequential processes requiring significant human intervention, with material optimization often relying on a mix of expertise and chance discoveries. Recent technological progress in autonomous synthesis experiments which combine automated synthesis and characterization with artificial intelligence (AI) has enabled rapid exploration of large parameter spaces, promising to greatly accelerate and advance our understanding of synthesis science. In this presentation, I will highlight the development of

two flexible, autonomy-enabled pulsed laser deposition (PLD) platforms: one incorporating real-time, in situ gas-phase and optical diagnostics, and the other featuring in vacuo robotic transfer for subsequent characterization. I will detail how we merged in situ, real-time diagnostics and characterization with high-throughput methodologies and cloud connectivity to execute an autonomous synthesis experiment using PLD. We synthesized ultrathin WSe_2 films via co-ablation of two targets, employing real-time laser reflectivity for precise thickness control, and achieved a tenfold increase in throughput over conventional PLD workflows. Bayesian optimization with Gaussian process regression, utilizing in situ Raman spectroscopy, directed the synthesis process and autonomously identified the optimal growth windows after sampling 0.25% of a 4D parameter space. Furthermore, the Gaussian process surrogate model predicted process-property relationships, revealing two distinct growth regimes and providing a broader understanding of the synthesis space than would be feasible in traditional PLD workflows. Our platforms and methodologies enable the autonomous synthesis of any material that can be grown by PLD, promising to greatly accelerate thin film synthesis with automated, AI-driven workflows.

12:00pm AIML-WeM-17 Active-Learning Based Structure Discovery in STM, *Ganesh Narasimha,* Oak Ridge National Laboratory; *Saban Hus,* Oak Ridge National Lab (ORNL); *Arpan Biswas,* Oak Ridge National Laboratory, USA; *Dejia Kong,* University of Virginia, USA; *Zheng Gai, Rama Vasudevan,* Oak Ridge National Laboratory, USA; *Maxim Ziatdinov,* Pacific Northwest National Laboratory
Scanning tunneling microscopy (STM) is a widely used tool for atomically-resolved imaging of materials and their surface energetics. However, the optimization of the imaging conditions is a time-consuming process due to the extremely sensitive tip-surface interaction. Additionally, conventional experimentation involves sequential imaging procedures, and the material-property correlations are usually deciphered by an operator based on auxiliary spectroscopic information. This limits the experimental throughput. Here we show a Bayesian optimization-based framework to improve imaging conditions in real time [1]. Further, we demonstrate a characterization technique using a probabilistic deep learning framework to automatically correlate structure-property relationships in a Europium-based semimetal, $EuZn_2As_2$ [2]. The data-driven inference is dynamically incorporated to drive STM exploration in regions that optimize a given material property. This framework employs a sparse sampling approach to efficiently construct the property space using minimal measurements, as little as 1 % of the data required in conventional hyperspectral imaging methods. We further demonstrate property-guided sample exploration using a multiscale-process implementation for the autonomous discovery of structural origins of an observed material property. Our findings reveal correlations of the electronic properties unique to local defect density, surface terminations, and point defects [3]. The deep learning framework offers future implications to study and induce dynamic processes such as molecular manipulations to assemble artificial quantum structures.

References:

1. Narasimha, G., Hus, S., Biswas, A., Vasudevan, R., & Ziatdinov, M. (2024). Autonomous convergence of STM control parameters using Bayesian optimization. *APL Machine Learning*, *2*(1).
2. Blawat, J. *et al.* Unusual Electrical and Magnetic Properties in Layered EuZn2As2. *Advanced Quantum Technologies* **5**, 2200012 (2022).
3. Narasimha, G., Kong, D., Regmi, P., Jin, R., Gai, Z., Vasudevan, R., & Ziatdinov, M. (2024). Multiscale structure-property discovery via active learning in scanning tunneling microscopy. *arXiv preprint arXiv:2404.07074.*

Atomic Scale Processing Mini-Symposium
Room 116 - Session AP1+EM+PS+TF-WeM

Energy-Enhanced Atomic Layer Processing
Moderators: Ashley Bielinski, Argonne National Laboratory, USA, **John F. Conley, Jr.**, Oregon State University

8:00am AP1+EM+PS+TF-WeM-1 Low-Temperature Synthesis of Crystalline $In_xGa_{1-x}N$ Films via Plasma-Assisted Atomic Layer Alloying, *Steven Allaby, Fatih Bayansal, Helena Silva, Brian Willis,* **Necmi Biyikli,** University of Connecticut
Based on our first demonstration of crystalline III-nitride film growth via hollow-cathode plasma-assisted atomic layer deposition (HCP-ALD) at substrate temperatures as low as 200 ℃, this technique is attracting

increasing interest for the low-temperature deposition of various semiconductor layers. Despite its success for binary III-nitride films, ternary III-nitrides pose additional challenges including limitation on fine stoichiometry control, potential incompatibility of plasma gas mixtures, and complexity of in-situ ellipsometry analysis of the growing film. In this work, we share our experimental findings on the self-limiting growth of $In_xGa_{1-x}N$ films on SiO_2/Si, quartz, and sapphire substrates using digital alloying technique in an HCP-ALD reactor at 200 °C.

The $In_xGa_{1-x}N$ alloy films were deposited using conventional metal-alkyl precursors (triethylgallium, trimethylindium) and two different nitrogen plasmas (N_2/H_2, N_2/Ar) as metal precursor and nitrogen co-reactant, respectively. GaN and InN unit ALD cycle parameters have been determined using the saturation curves for each binary compound. Digital alloying technique was used by forming ALD supercycles with the following GaN:InN cycle ratios: (9:1), (6:1), (3:1). The targeted indium concentrations ranged within (10% – 50%) range. $In_xGa_{1-x}N$ alloy films with different stoichiometries and thickness values around 50 nm were synthesized to further characterize the structural, chemical, optical, and electrical film properties.

In-situ ellipsometry was employed to monitor the surface ligand-exchange reactions and plasma surface interactions. XRD, XRR, XPS, spectroscopic ellipsometer, UV/Vis spectroscopy, and Hall-effect measurements are carried out to characterize the crystal structure, average crystal grain size, film density, stoichiometry (Ga:In ratio), impurity content, complex refractive index, optical bandgap, film resistivity, carrier concentration and electron mobility, respectively. The experimental results will be discussed along with faced challenges, potential solutions and follow-up studies.

8:15am AP1+EM+PS+TF-WeM-2 Comparison of Low Temperature Methods for Crystallization of Vanadium Oxide Produced by Atomic Layer Deposition, *Peter Litwin,* Naval Research Laboratory, USA*; Marc Currie, Neeraj Nepal, Maria Sales, David Boris, Scott Walton, Virginia Wheeler,* US Naval Research Laboratory

Crystalline VO_2 (c-VO_2) undergoes a phase transformation between two crystalline states near room temperature ($\approx$ 68 °C), which is accompanied by a metal-to-insulator transition (MIT). This favorable MIT in stoichiometric c-VO_2 is of interest for numerous applications such as passive thermal regulation (e.g. energy efficient windows), thermal sensors, and passive radio frequency components. Current VO_2 films deposited by thermal atomic layer deposition (ALD) processes are amorphous and require a high temperature post-deposition annealing step ($\geq$ 400 °C) to crystallize, which often limits the application space of ALD VO_2 due to thermal budget constraints. Thus, the development of processes to produce ALD c-VO_2 without the need of a high-temperature annealing step are desired.

Two possible routes to c-VO_2 are plasma-enhanced ALD (PEALD) and femtosecond laser processing (fsLP). PEALD offers increased kinetics through the simultaneous delivery of a flux of both energetic and reactive plasma species to the growth surface, allowing for deposition and crystallization at lower processing temperatures. However, the enhanced reactivity of oxidizing-plasma sources poses challenges not present in thermal ALD processes of VO_2. For example, the oxidation state of the V in the metal-organic precursor is less of a driver for stoichiometric control often resulting in the more stable V_2O_5 with plasma processes. In fsLP, crystallization is initiated as a result of non-equilibrium excited-state dynamics in the film occurring on sub-ps timescales. This produces a combination of athermal and thermal annealing expected to promote the formation of c-VO_2, even under ambient conditions. Both methodologies maintain sub-200 °C temperature windows which facilitate the use of c-VO_2 in a wider range of applications. For example, high-temperature annealing of VO_2 on metal substrates often results in the dewetting of VO_2 films; both PEALD and fsLP are potential solutions.

Here we report on investigations into the efficacy of PEALD and fsLP to produce c-VO_2. A focal point of the PEALD studies is correlating plasma properties, including plasma power, Ar/O_2 ratio, system pressure, and total gas flow during the plasma step, with the control of the VO_x stoichiometry and crystallinity. We demonstrate control of the amorphous to crystalline transition as a function of PEALD parameters and comment on control of the V^{4+}/V^{5+} ratio. fsLP is shown effective at producing c-VO_2 from amorphous ALD films under ambient conditions. We also discuss the ability of the technique to produce c-VO_2 on polymer and metal substrates, an application space often incompatible with high-temperature annealing.

8:30am AP1+EM+PS+TF-WeM-3 Temperature-Dependent Dielectric Function of Plasma-Enhanced ZnO Atomic Layer Deposition using in-Situ Spectroscopic Ellipsometry, *Yousra Traouli, Ufuk Kilic,* University of Nebraska-Lincoln, USA*; Mathias Schubert,* University of Nebraska - Lincoln*; Eva Schubert,* University of Nebraska-Lincoln, USA

In this study, *in-situ* spectroscopic is employed to real-time monitor the growth of ZnO thin films fabricated by plasma-enhanced atomic layer deposition for different temperatures. The process involves dimethylzinc, $Zn(CH_3)_2$, organometallic precursor and oxygen plasma as the primary reactant and co-reactant, respectively. We investigate the cyclic surface modifications and growth mechanisms of ZnO for different substrate temperatures. Subsequently, the deposition chamber is then used as an thermal annealing chamber to investigate the evolution of dielectric function of ZnO ultra-thin films for different temperature values (22°C ≤ T ≤ 300°C).

Hence, the temperature-dependent complex dielectric function spectra of ZnO ultra-thin film is obtained. Complementary x-ray photoelectron spectroscopy, x-ray diffraction, and atomic force microscopy are also used to provide the compositional, structural, and morphological characteristics of the ZnO films, respectively. These findings highlight the critical role of precise thermal management in ALD processes for tailoring the dielectric properties of ZnO thin films. The insights gained from this study are crucial for the development and optimization of ZnO PE-ALD recipe but also for optoelectronic devices, ensuring enhanced performance and reliability.

8:45am AP1+EM+PS+TF-WeM-4 Optical Properties and Carrier Transport Characteristics of NiO Films Grown via Low-Temperature Hollow-cathode Plasma-assisted Atomic Layer Deposition, *Fatih Bayansal, Steven Allaby, Habeeb Mousa, Helena Silva, Brian Willis, Necmi Biyikli,* University of Connecticut

While there is an abundance of as-grown unintentionally doped n-type semiconductor materials, only a few alternative materials exhibit p-type conduction without requiring additional high-temperature doping processes. NiO is of particular interest mainly due to its relative stability and promising performance as hole-transport layers in emerging solar cell device structures. However, the stability of film properties including carrier concentration and mobility of NiO needs to be substantially improved for its use as reliable transistor channel layers. While low-temperature thermal, plasma, and ozone-assisted ALD efforts have resulted in NiO films with p-type behavior, degrading film properties over time and at higher temperatures, and low hole mobility values prevent the usage of these layers for devices.

To enhance film properties in low-temperature as-grown NiO layers, our study conducts a comprehensive investigation on plasma-enhanced ALD (PEALD) of NiO films on Si, SiO_2/Si, glass, sapphire, and quartz substrates. This process utilizes nickelocene ($NiCp_2$) and O_2 plasmas within a plasma-ALD reactor featuring a stainless steel-based hollow-cathode plasma (HCP) source, equipped with an in-situ ellipsometer. 800-cycle deposition runs at 100 – 250 °C substrate temperatures were carried out to achieve at least 30 nm thick films for further characterization.

The resulting as-grown crystalline (c-NiO) films are characterized for their optical and electrical properties. Films grown at 200 °C exhibited higher refractive index values reaching 2.3, which is in good agreement with reported values for the best polycrystalline NiO films in the literature. NiO films deposited on sapphire and quartz substrates showed strong absorption in the UV region (l=190-380 nm) yet demonstrated minimal absorption in the visible and near-IR regions. As a result of the analysis using the Tauc relation, it was found that the band gaps of all films were close to the bulk value of 3.6 eV. Furthermore, we will also present the results of Hall-effect measurements conducted at room temperature to determine the film resistivity, type of conduction mechanism, Hall mobility, and carrier concentration. The long-term stability of the NiO films will be investigated at ambient and higher temperature annealing conditions.

9:00am AP1+EM+PS+TF-WeM-5 Characterizing Inductively Coupled Plasmas in Ar/SF_6 Mixtures for Atomic Layer Deposition, *David Boris, Virginia Wheeler,* U.S. Naval Research Laboratory*; Maria Sales,* NRC Research Associateship Program*; Luis Rodriguez de Marcos, Javier Del Hoyo,* NASA Goddard Space Flight Center*; Andrew Lang,* U.S. Naval Research Laboratory*; Edward Wollack, Manuel Quijada,* NASA Goddard Space Flight Center*; Mackenzie Meyer,* NRC Research Associateship Program*; Scott Walton,* U.S. Naval Research Laboratory

Low temperature plasmas containing sulphur hexafluoride (SF_6) are particularly rich plasmas from the perspective of gas phase chemistry and plasma physics.They possess a wide range of positive and negative ion (SF_x^+,

SF_y^-, F^-, F_2^+, etc.) and reactive neutral species (SF_x, F, F_2, etc.) that play important roles in materials processing applications ranging from semiconductor etching [1] to the formation of fluoride based optical thin films[2]. Understanding the physical mechanisms at play in these plasmas is often challenging and requires a comprehensive approach employing multiple diagnostic tools.

In this work, we use a combination of Langmuir probes and optical emission spectroscopy to examine the effects of varying process parameters on the physical characteristics of Ar/SF_6 plasmas generated in a remote, inductively coupled plasma (ICP) geometry.In particular, a range of applied RF powers,gas flows, and pressures are explored with a focus on the resulting changes in atomic F density, plasma density, plasma potential, and the ratio of positive to negative ions in the plasma.These changes in plasma properties are then tied to changes in the material characteristics of aluminum tri-fluoride (AlF_3) thin films grown via plasma-enhanced ALD using a remote ICP employing Ar/SF_6 gas mixtures. This work is supported by NASA Astrophysical Research and Analysis (APRA) grant 20-APRA20-0093/ N0017322GTC0044. This work was also partially supported by the NRL Base program through the Office of Naval Research.

[1] D.C. Messina et al, J. Vac. Sci. Technol. A 41, 022603 (2023)

[2] L. V. Rodgriguez de Marcos et al, Optical Materials Express 13 (11), 3121-3136 (2023)

9:15am AP1+EM+PS+TF-WeM-6 Dynamic Global Model of Cl₂/Ar Plasmas: In-Depth Investigations on Plasma Kinetics*, Tojo Rasoanarivo, Cédric Mannequin,* Institut des Matériaux de Nantes Jean ROUXEL - Nantes Université, France*; Fabrice Roqueta, Mohamed Boufnichel,* ST Microelectronics, France*; Ahmed Rhallabi,* Institut des Matériaux de Nantes Jean ROUXEL - Nantes Université, France

Plasma processes such as Atomic Layer Etching (ALE) using Cl_2/Ar gas mixture are often reported in the literature as chlorine chemistry is suitable for a wide variety of materials [1]. ALE is a cyclic process and Cl_2 and Ar plasmas are implemented for the adsorption and activation steps, respectively, through alternating feedgas overtime or overspace. However, these studies mostly focus on experimental approaches and modeling investigations are scarce. Some others ALE recipes rely on plasma kinetics through specific recipes [2] and to better understand plasma/surface interactions at atomic scale, we must first precisely investigate plasma behavior especially during the switching durations.

In most cases, global models have been well implemented to determine the plasma composition at specific plasma reactor parameters, with good computational time effectiveness [3] in steady-states conditions [4]. We have implemented the dynamic mode to investigate the plasma kinetics during the transitions between the modifying Cl_2 plasma and the Ar activation plasma.

We closely investigate the influence of the switch duration between the Cl_2 to/from Ar feedgas, for different RF powers. We found that under a critical switch duration there is a competition between the plasmas kinetics mainly governed by electrons collisions with the neutrals and the physical residence time depending of the working pressure. For short switch duration from Cl_2 rich plasma toward Ar plasma, we observed discrepancies compared to equivalent steady-state composition on chlorine species. These differences are associated with longer characteristics time reactions than the switch duration. In the case of RF power source switch, we observed for switch duration lower than 100 ms, overshoots of the electron temperature (T_e). These stiff T_e variations observed are assumed to originate from quasi-instantaneous electrons acceleration before first collisions with neutrals.

These results may be used to predict plasma behavior during ALE transitions steps or for fast-paced plasma etching processes.

References

[1] K. J. Kanarik, T. Lill, E. A. Hudson et al., J. Vac. Sci. Technol A: 33, 020 802 (2015).

[2] A. Fathzadeh,P. Bezard, M. Darnon, I. Manders, T. Conard, I. Hoflijk, F. Lazzarino, S. de Gendt, J. Vac. Sci. Technol. A 42, 033006 (2024).

[3] A. Hurlbatt, A. R. Gibson, S. Schröter, J. Bredin, A. P. S. Foote, P. Grondein, D. O'Connell, T. Gans, Plasma Process Polym, 14: 1600138 (2017).

[4] R. Chanson, A. Rhallabi, M. C. Fernandez, C. Cardinaud, J. P. Landesman, J. Vac. Sci. Technol A, *A 31, 011301* (2013).

9:30am AP1+EM+PS+TF-WeM-7 Precise Growth and Removal of Carbon Films by Electron-Enhanced Chemical Vapor Deposition (EE-CVD) and Chemical Vapor Etching (EE-CVE)*, Zachary Sobell, **Steven George**,* University of Colorado at Boulder

Electron-enhanced chemical vapor deposition (EE-CVD) was used to grow carbon films at T < 70 °C. EE-CVD employs a continuous flux of low energy (~100 eV) electrons that are incident on the sample through a methane (CH_4) reactive background gas (RBG). Electron-enhanced chemical vapor etching (EE-CVE) was also used to etch carbon films at < 70 °C. EE-CVE employs a continuous flux of low energy electrons that are incident on the sample through an oxygen (O_2), ammonia (NH_3), or hydrogen (H_2) RBG. Both EE-CVD and EE-CVE were accomplished with precise rate control.

The EE-CVD and EE-CVE used an electron beam from a hollow cathode plasma electron source with currents on the sample of ~30 mA over ~10 cm^2. The electron beam can desorb surface species by electron stimulated desorption. The electron beam also travels through the RBG in the reactor at pressures of ~1-3 mTorr. Electron induced dissociation can form radicals and ions that facilitate the growth or removal of the carbon film. In addition, a negative voltage (-30 V) on the substrate (sample bias) was observed to greatly enhance both the deposition and etching of carbon films. The negative voltage is believed to pull positive ions to the substrate to enhance the growth or removal.

With no applied sample bias, carbon deposition proceeded at ~22 Å/min for a CH_4 flowrate of 10 SCCM (Fig. 1). The introduction of a sample bias of -30 V increased the deposition rate by >20 times to ~480 Å/min. In contrast, carbon deposition with a +30 V sample bias proceeded at a similar rate to carbon deposition with no sample bias. For etching of carbon films with a -30 V sample bias and RBG flow rates of 4 SCCM, O_2 produced the highest carbon etch rate at ~225 Å/min (Fig. 2). In contrast, NH_3 displayed a slower carbon etch rate of ~48 Å/min and H_2 had an even slower carbon etch rate of ~18 Å/min.

Raman spectroscopy was used to characterize the carbon films grown at different sample biases. At negative substrate voltage, the carbon films displayed faster growth, were more disordered (D:G peak ratio=2.29), and exhibited faster etching. At zero substrate voltage, the carbon films displayed slower growth, were more ordered (D:G peak ratio=1.18), and exhibited slower etching.

Many applications are possible for the EE-CVD and EE-CVE of carbon films. More ordered carbon films may find use as hard masks or diffusion barriers. Amorphous carbon films may be employed as channel materials. Carbon hard masks are currently removed with an O_2 plasma which also oxidizes the surrounding and underlying material. Using H_2 and electrons may allow for a single-step oxygen-less hard mask removal.

9:45am AP1+EM+PS+TF-WeM-8 Microwave Enhanced ALD of Al₂O₃*, **Benjamin Kupp**, Jessica Haglund, Shane Witsell, John Conley,* Oregon State University

The low deposition temperatures typical of ALD are advantageous for many applications. However, low deposition temperatures can allow incorporation of -OH groups or residual impurities from unreacted ligands which can lead to non-ideal stoichiometry and sub-optimal physical, optical, and electrical properties. Although increasing the deposition temperature and post deposition annealing can both help drive off impurities and improve film properties, the temperatures required may (i) move a process out of the ALD regime or (ii) exceed the thermal budget, respectively. To maintain a low ALD temperature while maximizing film properties, adding energy in-situ *during* each ALD cycle or supercycle can help drive/speed reactions and reduce impurity incorporation. For example, including rapid thermal annealing as part of the ALD cycle have been shown to improve density, stoichiometry, electrical, and optical properties that cannot be achieved by post deposition annealing alone [1-4]. Other reported in-situ energy enhanced EE-ALD methods include flash lamp annealing, plasma, UV, and laser exposure, electric fields, and electron-beams [5-15]. Here, we introduce microwave enhanced MWE-ALD.

Al_2O_3 films were deposited at 300 °C using TMA and H_2O in a Picosun R200 PE-ALD chamber integrated with a custom microwave antenna and an MKS SG 1024 solid state microwave (MW) generator. Film thickness and refractive index, *n*, were modeled using a Film Sense FS-1 mapping ellipsometer. A 30 s in-situ 400 W MW exposure (*without* plasma generation) during either the TMA or H_2O purge part of each ALD cycle reduced film thickness by ~7% and ~ 25%, and increased *n* by ~2% and ~6%, respectively, across a 150 mm Si wafer as compared to a control without MWs (Fig. 1). Preliminary electrical measurements on MOS devices indicate an associated reduction in low field leakage. Additional electrical and

analytical data will be presented, including MWE-ALD deposition temperatures.

1. Conley, Jr. *et al.*, Appl. Phys. Lett. 84, 1913 (2004).
2. Conley, Jr. *et al.*, MRS Proc. Vol. 811, 5 (2004).
3. Conley, Jr., *et al.*, in *Physics and Technology of High-k Gate Dielectrics II*, ECS Proc. vol. 2003-22.
4. Clark *et al.*, ECS Trans. 41(2), 79 (2011).
5. Henke *et al.*, ECS J. Sol. Sta. Sci. Tech. 4(7), 277 (2015)
6. Miikkulainen *et al.*, ECS Trans. 80(3), 49 (2017).
7. Chalker *et al.*, ECS Trans. 69, 139 (2015).
8. Holden *et al.* J. Vac. Sci. Technol. A. **40,** 040401 (2022).
9. No *et al.*, J. ECS 153, F87 (2006).
10. Österlund *et al.* J. Vac. Sci. Tech. A 39, 032403 (2021).
11. Ueda *et al.*, Appl. Surf. Sci. 554, 149656 (2021).
12. Liu and Chang. J. Chem. Phys. 116, (2002).
13. Becher *et al.*, Adv. Eng. Mater. 2300677 (2023).

Atomic Scale Processing Mini-Symposium
Room 116 - Session AP2+EM+PS+TF-WeM

New Advances in Atomic Layer Deposition

Moderators: Ashley Bielinski, Argonne National Laboratory, USA, **John F. Conley, Jr.**, Oregon State University

11:30am AP2+EM+PS+TF-WeM-15 Electrical and Optical Properties of Macroscopic Nanocomposites Fabricated by ALD Infiltration and Pressure-Assisted Sintering of Nanoparticle Compacts, *Benjamin Greenberg, Kevin Anderson, Alan Jacobs,* U.S. Naval Research Laboratory; *Austin Cendejas,* American Society for Engineering Education; *Eric Patterson, Jaime Freitas, James Wollmershauser, Boris Feigelson,* U.S. Naval Research Laboratory

Over the past 20+ years, a wide variety of nanocomposite thin films with unique property combinations have been produced by atomic layer deposition (ALD) infiltration of nanoparticle (NP) films. Examples include electrochromic WO_{3-x} NP films with photochemical stability enhanced by Ta_2O_5 ALD[1] and superhydrophilic and antireflective TiO_2/SiO_2 NP films with elastic modulus and hardness enhanced by Al_2O_3 ALD.[2] Applications of such nanocomposite films, however, are limited by their small thickness (typically a few μm or thinner), reliance on substrates, and/or residual porosity that can remain after ALD infiltration.

In this work, we explore fabrication of macroscopic, freestanding, dense nanocomposites—pucks with ~1 mm thickness, ~10 mm diameter, and solid volume fraction that can exceed 99%—via ALD infiltration of NP compacts followed by pressure-assisted sintering. For a prototype, we use monodisperse 100 nm SiO_2 NPs and an ALD coating of Al-doped ZnO to form electrically conductive ceramic nanocomposites with electrical and optical properties dependent on the coating thickness. Infiltration of the ultra-high-aspect-ratio (>10,000) SiO_2 NP compacts with ZnO:Al is accomplished via a recently developed cyclical-temperature ALD process.[3] The ZnO:Al-coated SiO_2 compacts are then densified via environmentally controlled pressure-assisted sintering (EC-PAS), wherein NPs are cleaned and kept in an inert atmosphere to maintain high surface energy, which enables low-temperature densification with minimal grain growth.[4] An EC-PAS process with a maximum pressure of ~2 GPa and a maximum temperature of 450 °C yields dense SiO_2/ZnO:Al nanocomposites that contain nanocrystalline ZnO:Al networks and exhibit low electrical resistivity, ρ. At nominal ZnO:Al coating thicknesses, t, of ~3 nm and ~6 nm, ρ is on the order of 1 and 0.1 Ω-cm, respectively, at 300 K. Moreover, at $t \approx$ 6 nm, the Hall mobility approaches 1 $cm^2V^{-1}s^{-1}$ at 300 K, and ρ increases by less than a factor of 3 upon cooling to 10 K, suggesting proximity to the metallic/band-like charge transport regime. Interestingly, the nanocomposites are blue in color with transparency and hue apparently dependent on t. Characterization techniques employed in our investigation into these electrical and optical properties include X-ray diffractometry, scanning electron microscopy, Hall and Seebeck effect measurements, absorption/transmission/reflection spectroscopy, and photoluminescence spectroscopy and imaging.

1. Y. Wang *et al.*, *Chem. Mater.* **28**, 7198 (2016)
2. M. I. Dafinone *et al.*, *ACS Nano* **5**, 5078 (2011)
3. B. L. Greenberg *et al.*, *J. Vac. Sci. Technol. A* **42**, 012402 (2024)
4. H. Ryou *et al.*, *ACS Nano* **12**, 3083 (2018)

11:45am AP2+EM+PS+TF-WeM-16 Tunable Growth of Layered Double Hydroxide Nanosheets through Hydrothermal Conversion of ALD Seed Layers, *Daniel Delgado Cornejo, Alondra Ortiz-Ortiz, Kalyn Fuelling,* University of Michigan, Ann Arbor; *Ashley Bielinski,* Argonne National Laboratory, USA; *Tao Ma, Neil Dasgupta,* University of Michigan, Ann Arbor

Nano-architected materials have seen a rise in recent years and have produced advancements in a variety of fields including biomedicine, energy storage, and catalysis. As such, there is great motivation to develop novel synthesis and processing methods designed to improve the degree of fine control over the material's geometric parameters. In this study, we explore a method known as surface-directed assembly which makes use of the synergy between atomic layer deposition (ALD) and hydrothermal synthesis to grow layered-double hydroxide (LDH) nanosheets. The formation of the LDH product stems from the interaction between the deposited ALD Al_2O_3 film and an aqueous zinc solution. Unlike other reported seeded hydrothermal syntheses, which rely on epitaxial growth from a seed layer, this interaction results in the consumption and conversion of the initial ALD film into the LDH product, where aluminum from the ALD film serves as a limiting reagent in the kinetic processes of nucleation and growth. Geometric parameters such as the nanosheet inter-spacing and length can be tuned by varying the thickness of the ALD film with sub-nanometer precision. A non-linear trend in nanosheet length is observed and characterized within three regimes: (I) depletion limited, (II) length independent, and (III) steric hindrance. In addition, we observe an inverse relationship between the nanosheet inter-spacing and the ALD film thickness. Finally, this process enables the formation of hierarchical nanostructured surfaces onto three-dimensional substrates including microposts, paper fibers, and porous ceramic supports. By leveraging the tunability and conformality of the ALD process, this work enables the programmable control of nano-architected material geometries for a variety of applications, including for energy and medical devices.

12:00pm AP2+EM+PS+TF-WeM-17 Passivation Strategies for Far-Ultraviolet Al Mirrors Using Plasma-Based AlF_3 Processing, *Maria Gabriela Sales, David Boris,* U.S. Naval Research Laboratory; *Luis Rodriguez de Marcos,* NASA Goddard Space Flight Center; *James Hart, Andrew Lang, Benjamin Albright, T. Jude Kessler,* U.S. Naval Research Laboratory; *Edward Wollack, Manuel Quijada,* NASA Goddard Space Flight Center; *Scott Walton, Virginia Wheeler,* U.S. Naval Research Laboratory

Far-ultraviolet (FUV) astronomy (λ = 100-200 nm) relies on efficient Al mirrors because Al has a very high theoretical reflectance in this region. However, since Al readily oxidizes in air, the strongly absorbing native oxide layer appreciably degrades its FUV performance. A novel surface passivation technique for Al mirrors was previously demonstrated using an electron beam (e-beam) generated SF_6/Ar plasma, which proceeds via a combined etching of the native oxide and simultaneous fluorination of the Al surface [1].

In our present work, this novel e-beam plasma technique is integrated into a plasma-enhanced atomic layer deposition (PEALD) system. We use a Veeco Fiji G2 reactor, equipped with substrate biasing, that has been uniquely modified to include an on-axis e-beam generated plasma source. Trimethylaluminum (TMA) and SF_6/Ar plasma, produced with an inductively coupled plasma (ICP) source, were used as our precursor and reactant for the ALD AlF_3 process. Optimization of the ALD parameters was performed, and our best ALD AlF_3 films (F/Al $\approx$ 3, ~1% oxygen content, and roughness < 1 nm) were attained using 100 W ICP power and total plasma gas flows > 30 sccm. Our ALD AlF_3 films provide improved FUV reflectivity compared to oxidized bare Al, however, these optical properties are still limited by Al oxide at the AlF_3/Al interface. To overcome this, we utilize our in-situ e-beam plasma, produced in a gas mixture of SF_6/Ar, to minimize the native oxide layer prior to ALD.

In this talk, we discuss the processing parameters of the in-situ e-beam plasma (SF_6/Ar ratio and flow, sample bias) and how they affect the AlF_3 growth rate, film/interface chemistry, and surface roughness. These material properties are related to optical performance, which compares favorably to state-of-the-art coatings (≈90% at 121 nm). We then discuss hybrid AlF_3 films, in which the growth is initiated by e-beam plasma, and then continued using an optimized ALD AlF_3 recipe. For the initial step, pre-treatments using the in-situ e-beam plasma and the previously developed ex-situ e-beam plasma [1] are compared. We show that both in-situ and ex-situ hybrid techniques significantly reduce the interfacial oxygen compared to ALD AlF_3 alone (no pre-treatment), which enhances the FUV reflectivity. This work highlights the importance of the interface quality of passivated Al mirrors on their optical performance in the FUV range.

Applied Surface Science
Room 117 - Session AS-WeM

Quantitative Surface Analysis

Moderators: David Morgan, Cardiff University, **Samantha Rosenberg**, Lockheed Martin

8:00am AS-WeM-1 Analyzing the Extrinsic Inelastic Background of HAXPES Spectra Accounting for X-Ray Extinction in an Iron Oxide Finite Thickness Film, *Dulce-Maria Guzman-Bucio, Orlando Cortazar-Martinez,* CINVESTAV-Unidad Queretaro, Mexico*; Dagoberto Cabrera-German,* Universidad de Sonora, Mexico*; Jorge-Alejandro Torres-Ochoa,* Universidad Politecnica de Juventino Rosas, Mexico*; Abraham-Jorge Carmona-Carmona,* CINVESTAV-Unidad Queretaro, Mexico*; Oscar Ceballos-Sanchez,* Universidad de Guadalajara, Mexico*; Will Limestall, Zhengrong Lee, Jeff Terry, Mark Warren,* Illinois Institute of Technology*; Alberto Herrera-Gomez,* CINVESTAV-Unidad Queretaro, Mexico

The extrinsic inelastic part of the background is part of all photoemission spectra. Its identification and modeling, as well as other background contributions, play a crucial role in assessing the peak signal used in the quantification of chemical composition. However, existing methods cannot directly apply to finite-thickness films because they only apply to semi-infinite-homogeneous samples [1]. Moreover, they are not appropriate for spectra obtained with Hard X-ray Photoemission Spectroscopy (HAXPES), where the mean free path of the photoelectrons may be comparable to the absorption length of the photons at certain incident angles.In this study, we model the extrinsic inelastic background for photoemission spectra for a finite-thickness Fe_2O_3 film for which a grazing X-ray incident angle was employed. We analyzed Fe $2s$, $2p$, $3s$, and $3p$ photoemission spectra acquired with synchrotron light at eight photon energies around the Fe $1s$ threshold at Beamline 10-ID-B at the Argonne National Laboratory. Our calculations assume a straight-line inelastic scattering path and account for the decay of the X-rays as they travel through the sample [2]. It was assumed that the inelastic electron cross section (λK) for iron oxide does not change drastically for electron primary energies higher than 2 keV, and one acquired at this primary electron energy was employed [3]. The comparison with the experimental data and information about sample processing shows great agreement.

This presentation summarizes the requirements and challenges involved in correctly analyzing the extrinsic inelastic background of HAXPES data. This includes using appropriate inelastic mean-free paths and effective attenuation lengths. Obtaining REELS data along with photoemission data, and calculating inelastic electron cross sections for primary excitation energies in the hard X-ray regime is essential.

[1] S. Tougaard, P. Sigmund, Influence of elastic and inelastic scattering on energy spectra of electrons emitted from solids, Phys Rev B 25 (1982) 4452–4466. https://doi.org/10.1103/PhysRevB.25.4452.

[2] A. Herrera-Gomez, The photoemission background signal due to inelastic scattering in conformal thin layers -Internal Report, 2019.

[3] N. Pauly, F. Yubero, J.P. Espinós, S. Tougaard, Optical properties and electronic transitions of zinc oxide, ferric oxide, cerium oxide, and samarium oxide in the ultraviolet and extreme ultraviolet, Appl. Opt. 56 (2017) 6611–6621. https://doi.org/10.1364/AO.56.006611.

8:15am AS-WeM-2 Non-Destructive Characterization of Multi-Layered Thin Films Using XPS, HAXPES and Structure Modeling in StrataPHI, *Norbert Biderman, David Watson, Kateryna Artyushkova,* Physical Electronics USA

X-ray photoelectron spectroscopy (XPS) is a well-established technique for non-destructive analysis of the chemical composition of thin layers and interfaces. Angle-resolved XPS (AR-XPS) has been used to determine the composition of depth profiles and layer thicknesses, traditionally with Al Kα (1486.6 eV) X-ray beams for depths up to 5-10 nm below the surface. In recent years, new ARXPS capabilities have been added to Physical Electronics XPS scanning microprobe instruments including Cr Kα (5414.8 eV) hard X-ray photoelectron spectroscopy (HAXPES) that can probe buried interfaces up to 15-30 nm below the surface. Coinciding with the HAXPES development, the *Strata*PHI analysis software was developed to reconstruct quantitative, non-destructive XPS/HAXPES depth profiles from angle-dependent and single-angle photoelectron spectra.

In this talk, we will show that the *Strata*PHI software has been further developed to combine Al Kα and Cr Kα XPS and HAXPES data within a single depth profile to enhance extracted analytical information from various depths below the surface. We will explore the method of the combined technique as well as its application to multilayered thin film samples. Such added *Strata*PHI capabilities allow for scientists and engineers in metrology and research & development to analyze multi-layered thin films and ultra-thin films rapidly and non-destructively without potentially damaging ion beam sputtering that might otherwise be required to depth-profile or sputter-clean adventitious contamination off the surface.

8:30am AS-WeM-3 The Challenge of Quantifying Photoemission Spectra Using Multiple Photon Energies, *Thierry Conard, Anja Vanleenhove,* IMEC, Belgium*; Ilse Hoflijk, Inge Vaesen,* IMEC Belgium **INVITED**

The development of Photoemission spectroscopy in laboratories during the last decades has been focused on the use of AlKa radiation. Extensive work has been performed to tackle the issue of quantification of acquired spectra. These include aspects such as the determination of sensitivity factor, understanding spectral background, determining transmission function of spectrometers, and understanding electron transport inside materials (inelastic mean free path, ...).

The use of higher energy photons (HAXPES) has the potential to significantly increase the application field of PES due to its larger depth information making it more suitable for multilayers systems. One of the major limitations of HAXPES is the strong decrease of the photoemission cross-section at higher photon energy which, until a few years ago limited the use of HAXPES to synchrotron, where higher photon flux are achieved than in laboratory instruments. As such, the challenges to quantify HAXPES spectra do not differ significantly from lower photon energy experiment, but this was not the prime focus of synchrotron-based experiment. With the introduction of performant laboratory-HAXPES systems a few years ago, the need of better quantification for HAXPES has strongly been increasing.

In this presentation, we will start by presenting examples of the efforts made regarding the development of reliable quantification protocols, based, as for AlKa-based PES data, on the determination/analysis of sensitivity factors, background, transmission function, ...

Next to the "classical" challenges, some additional aspects need (more often) to be considered. First, energy referencing is critical for chemical state quantification. It is however more complex than with lower energy PES as it is very impractical to use contamination peak for referencing and the likelihood of vertical potential variations increases. Second, thanks to the larger photon energy, for many elements, additional photoemission peaks are available for analysis and peak-independent quantification would be interesting. For both aspects, we will present examples of applications and improvement.

Unfortunately, even if all the above-mentioned challenges would be solved, depending on the scientific question to be answered a single experiment may require the use of multiple photon energies, for instance for varying the analysed depth or improving on the chemical identification. We will discuss strategies to combine analysis with multiple photon energies to achieve the best possible understanding of the studied system. This will include consideration about results presentation for a better understanding by non-specialist.

9:00am AS-WeM-5 Angle-Resolved XPS Depth Profiling for Extreme Ultraviolet (EUV) Lithography Optics Research – Monoatomic vs Cluster Ion Source, *Veronique de Rooij-Lohmann, Shriparna Mukherjee,* TNO Science and Industry, the Netherlands*; Jonathan Counsell,* Kratos Analytical Limited, UK

In the Semicon Equipment Life-time department of TNO, X-ray photoelectron spectroscopy (XPS) analysis is utilized for characterization of optical surfaces, particularly mirrors and reticles for extreme ultraviolet (EUV) lithography. This study focuses on assessing the sensitivity of XPS depth profiling to multilayer mirrors which are similar to the EUV mirrors.

A commercial Ru-capped Mo/Si multilayer mirror was annealed in vacuum at 330 °C for 48 hours, to induce thermal degradation, i.e. intermixing and oxidation. Pre and post-annealing, traditional XPS depth profiling was conducted using a monatomic Ar ion-gun.

However, monatomic Ar+ depth profiling results in artefacts because preferential sputtering of light elements alters the stoichiometry, while ion-induced intermixing compromises layer contrast. Development of sputtering methods that reduce those artefacts is therefore of importance.

To address these challenges, we explore the potential of a Gas Cluster Ion Source (GCIS), known for minimizing the said artefacts. While GCIS is gaining traction in XPS, its applicability to EUV mirror analysis requires validation because the ion-solid interaction is material-dependent.

Moreover, given the limited thickness of the layers in an EUV-mirror compared to the XPS information depth, we also investigated the combination of sputter depth profiling with angle-resolved (AR-)XPS to enhance the surface sensitivity. The results are shown in Figure (a) and (b). This comparative study between traditional XPS depth profiling and GCIS, along with the exploration of AR-XPS, provides insights into optimizing analysis techniques for EUV mirrors and reticles. These findings inform further development towards metrology and understanding of EUV optics degradation.

9:15am AS-WeM-6 Beyond the Surface: A Simple Algorithm for Obtaining Surface-Free Depth Distribution Information from Combined XPS and HAXPES Spectra, *Benjamen Reed,* National Physical Laboratory, UK*; Jonathan Counsell,* Kratos Analytical Limited, UK*; Alexander Shard,* National Physical Laboratory, UK

There is a recurrent demand from the semiconductor, energy, and coatings industries to measure the chemical state of elements in subsurface layers. X-ray photoelectron spectroscopy (XPS) has unparalleled capabilities for chemical state measurements, but it has a limited information depth, typically around 10 nm for instruments using an Al Kα X-ray source. The traditional method for measuring subsurface chemistry is to perform a depth profile, alternating ion beam sputtering to remove surface layers and XPS measurements. Gas cluster ion beam technology has enabled damage-free sputtering of organic materials, but low sputtering rates for inorganic materials gives impractical experiment durations. Increasing the energy per atom in clusters will typically improve sputtering rates but also generates a thin altered, or damaged, layer either through chemical changes or preferential removal of elements. Some materials are particularly sensitive to ion sputtering, and so will exhibit sputtering damage regardless of parameters used during depth profiling.

To aid in the analysis of these sputter sensitive materials, we present a data processing algorithm which attempts to isolate the spectroscopic information of the undamaged subsurface material from the damaged surface material during a depth profile. The algorithm utilises the different intensity depth distributions that arise from Al Ka and Ag La X-ray generated spectra. An empirically determined scaling parameter is used to equate the surface intensity contribution from Al Ka and Ag La X-ray generated spectra, allowing a difference spectrum to be obtained that has a surface-free depth distribution, and therefore reduces (or completely removes) the intensity contribution from the sputter damaged layer. This method also works for very thin overlayers on homogenous materials, such as native oxides or adventitious carbon contamination.

9:30am AS-WeM-7 Depth Differentiated Surface Analysis by a Combination of XPS, HAXPES and Ion Scattering Spectroscopy, *Paul Mack,* Thermo Fisher Scientific, UK

Complementary multi-technique surface analysis has been available on XPS systems for many years.It is only recently, however, with the advent of more user-friendly software interfaces that these complex experiments have become routinely accessible by all users.XPS systems with easily switchable monochromated X-ray sources are now commonplace, allowing the analyst to switch between Al-Ka X-rays and some other higher energy photon source (Ag-La, for example).The use of two different X-ray energies enables some level of effective depth profiling without having to physically sputter the sample with an ion source.

XPS is known as a surface sensitive analytical technique, with Al-Ka X-rays typically enabling analysis from the top 10-15nm of the surface, depending on the material.With a Ag-La monochromated source, the sampling depth may be similar for the photoelectron signals in the higher binding energy portion of the spectrum but up to double the sampling depth for the higher kinetic energy XPS peaks.If the analyst wants to probe the very top surface, including the top monolayer, then a different analytical technique is required.Ion Scattering Spectroscopy (ISS) is even more surface sensitive than XPS and when combined with XPS and its higher energy counterpart, HAXPES, a far more comprehensive picture of the surface composition and profile can be developed.

In this work, XPS, HAXPES and ISS have been combined on a XPS system enabling non-destructive depth differentiated analysis of a variety of samples.By bringing all three techniques together the depth distributions of elements and chemical states, from the top monolayer to beyond 20nm into the surface can be investigated.

9:45am AS-WeM-8 Investigating the Chemical and Physical Changes of the Boehmite Layer as a Result of AA6061 Surface Etching and Film Growth Time, *Lyndi Strange, Sridhar Niverty, Mark Bowden, Shalini Tripathi, Rick Shimskey, Jonathan Wierscheke, Mayur Pole, Vineet Joshi,* PNNL

Low-enriched uranium alloyed with 10% Mo (U-10Mo) is currently being considered to replace high-enriched uranium in research reactors. The configuration consists of a U-10 Mo plate fuel with a 25 µm Zr interlayer barrier with an AA6061 alloy. The AA6061 alloy can be coated with boehmite (an aluminum oxyhydroxide) to prevent corrosion due to its high pH passivation range. Boehmite coatings are usually formed on AA6061 substrates via autoclave processing in alkaline media. Before boehmiting, the AA6061 can be cleaned via dry polishing or wet etching, which can cause changes in the surface likely affecting boehmite nucleation sites and subsequent adhesion to the AA6061 substrate. In this work, we seek to understand how the AA6061 pre-treatment methods as well as the boehmite layer thickness affect the chemical composition of the layer, corrosion resistivity, and adhesion to the AA6061 substrate. X-ray photoelectron spectroscopy (XPS) was used to determine the surface chemistry of boehmited samples as well as etched AA6061 samples. Grazing incidence X-ray diffraction (GI-XRD) was used to investigate aluminum oxide derivatives throughout the boehmite layer. For a more in depth investigation of aluminum oxide derivatives, transmission electron microscopy (TEM) was used to examine the differences at the interface of the AA6061 and boehmite. Tribology analysis was used to gain insight to boehmite adhesion onto the AA6061 substrate and changes as a result of pre-treatment. Lastly, the corrosion resistivity was examined using electrochemical techniques such as potentiodyanamic polarization (PD), electrochemical impedance spectroscopy (EIS), and long-term corrosion experiments which gave insight to the oxidation dynamics of the coating and oxide layer resistiveness. techniques allow a clear delineation of how the different etching techniques and layer thickness affect the overall physical properties of the formed boehmite layer as well as explain variation in the interfacial properties of the AA6061/boehmite. These results provide insight to the most efficient and highest quality method to grow boehmite on the surface of AA6061 for use in research reactors.

11:00am AS-WeM-13 Femtosecond Laser Ablation (fs-LA) – A New Approach to XPS Depth Profiling, *Simon Bacon,* Thermo Fisher Scientific, UK*; Stephen Sweeney,* University of Glasgow, UK*; Steven Hinder,* University of Surrey, UK*; Adam Bushell, Tim Nunney, Richard White,* Thermo Fisher Scientific, UK*; Mark Baker,* University of Surrey, UK

XPS depth profiling is a widely employed analytical technique to determine the chemical composition of thin films, coatings and multi-layered structures, due to its ease of quantification, good sensitivity and chemical state information. Since the introduction of XPS as a surface analytical technique more than 50 years ago, depth profiles have been performed using ion beam sputtering. However, many organic and inorganic materials suffer from ion beam damage, resulting in incorrect chemical compositions to be recorded during the depth profile. This problem has been resolved for most polymers by using argon gas cluster ion beams (GCIBs), but the use of GCIBs does not solve the issue for inorganics. A prototype XPS depth profiling instrument has been constructed that employs a femtosecond laser rather than an ion beam for XPS depth profiling purposes. This novel technique has shown the capability of eradicating chemical damage during XPS depth profiling for all initial inorganic, compound semiconductor and organic materials examined. The technique is also capable of profiling to much greater depths (several 10s microns) and is much faster than traditional ion beam sputter depth profiling. fs-LA XPS depth profile results will be shown for selected thin films, coatings, multilayers and oxidised surfaces and the outlook for this new technique discussed.

11:15am AS-WeM-14 Top Atomic Layer Analysis of Bimetallic Nanoparticles by Low-Energy Ion Scattering (LEIS), *Philipp Brüner,* IONTOF GmbH, Germany*; David Niedbalka, Paula M. Abdala, Christoph R. Müller,* ETH Zürich, Laboratory of Energy Science and Engineering, Switzerland*; Thomas Grehl,* IONTOF GmbH, Germany

The composition of the outer atomic layer often differs significantly from subsequent layers. Since the performance of a heterogeneous catalyst heavily depends on its outer atomic layer, high surface sensitivity analytical techniques are required. Most available surface analytical techniques probe to a depth of at least a few nm. Any result will thus be an average over the first few (or many) monolayers, such that unique properties of the outer monolayer may be missed due to the diluted effect on the analysis result.

Low energy ion scattering (LEIS) is the only technique available that selectively probes the elemental composition of the outer atomic layer [1].

This is achieved by bombarding the sample surface with noble gas ions at an energy of some keV. These primary ions may scatter from surface atoms, and their characteristic energy loss is a measure for the mass of the scattering partners. Evaluating the energy spectra of the backscattered primary ions results in the quantitative elemental composition of the outer monolayer, since neutralization effectively suppresses the signal from scattering events below the outer surface.

Since LEIS is not sensitive to surface charging and topography, it is routinely applied to study (even supported and dispersed) nanoparticles and their terminating atomic layer. This contribution will introduce this application including results from several sample systems. The core results are from monometallic Co and Pt as well as bimetallic CoPt nanoparticles with varying Co/Pt ratios prepared on an SiO_2 support with a total metal loading of 1.5 – 4 wt. %. The catalysts were activated in a 10 % H_2/N_2 mixture at 800 °C for 1 h, resulting in average particle sizes ranging from 1.7 – 3 nm.

LEIS analyses were conducted using a Qtac 100 (IONTOF GmbH) with a double toroidal electrostatic analyzer optimized for high sensitivity and mass resolution, allowing for top atomic layer analysis without significant surface damage by the probing ion beam.

3 keV He[+] ions were used for overview scans, as all elements C and heavier can be detected by He^{+} analysis. Subsequent analysis with 5 keV Ne[+] ions offers improved mass resolution and sensitivity for heavy elements. For some of these samples, sample pretreatment is more challenging than usual, due to the H physisorption on Pt which must be reproducibly reduced to yield robust results.

The LEIS results relate the bulk composition of the CoPt nanoparticles to their surface composition, catalytic activity and stability. Reference samples were used to determine the precise surface coverage of Co and Pt.

[1] Cushman, C. V. et al., *Analytical Methods* **2016**, 8, 3419

11:30am AS-WeM-15 Multilayer Adhesives-Ideal Samples for Showcasing GCIB Profiling Capabilities, *Michaeleen Pacholski, Bryan Caruso,* Dow Chemical Company; *Isabelle Uhl,* Dow Chemical Company, France; *Asghar Peera,* dow; *David Keely, Ethan Glor,* Dow Chemical Company

There are many manufacturing methods that can produce multilayer coatings, but for pressure sensitive adhesives there has been growing use of curtain coaters that can create a multilayer coating in a single step.This allows manufacturers to balance the performance and cost of each layer of the coating to the application.Most of these adhesives are around 25 μm thick, meaning accessing buried layers, which cannot be delaminated, has involved laborious sample preparation prior to the application of GCIB profiling.With the application of this multilayer coating technology new questions are being asked of the analytical group that include:Do the adhesive layers mix?Do surfactants and tackifiers migrate between the layers?If the adhesive fails cohesively, in which layer does it fail?In this presentation the curtain coating method and measurements of importance in the liquid state will be discussed, as well as GCIB approaches to answer the questions above.

11:45am AS-WeM-16 Similarities between Silicon and Aluminum with Suboxides Formation Using XPS Spectra, *Orlando Cortazar-Martinez, Dulce Maria Guzman Bucio, Jorge Alejandro Torres Ochoa, Celia Lizeth Gómez Muñoz, Joaquin Raboño Borbolla, Alberto Herrera-Gomez,* CINVESTAV-Unidad Queretaro, Mexico

Aluminum, recognized as a reactive metal, rapidly reacts with oxygen to form a dense protective layer of aluminum oxide. Its valence band contains three electrons, which can be shared to form Al^{1+}, and Al^{2+}, and Al^{+3} oxidation states; the stable form is the latter, there have been reports of the presence of the first two.

Initial oxidation stages of aluminum were achieved by exposing the surface to a precisely controlled ultra-pure oxygen atmosphere with varying gas dosages. The metallic and oxidized film was characterized with angle-resolved X–ray photoelectron spectroscopy; the data was analyzed with state-of-the-art techniques.Two surprising results were found: 1) the appearance of two extra peaks in the Al 2p spectra, corresponding to Al^{1+}, and Al^{2+} at the interface; and 2) a protrusion-mode growth of Al_2O_3.The first shows many similarities with silicon, which is the next element in the periodic table.The second is also surprising because, contrary to current perception, the oxide does not grow conformally in the initial oxidation stages; this contrasts with silicon because it does grow conformally from the very initial oxidation.

This work was partially financed by Proyecto Fronteras 58518, Conahcyt, Mexico.

[1] A. Herrera-Gomez, F. Servando Aguirre-Tostado, and P. Pianetta, Formation of Si1+ in the early stages of the oxidation of the Si[001] 2 × 1 surface, Journal of Vacuum Science & Technology A 34, 020601 (2016).

[2] A. Herrera-Gomez, M. Bravo-Sanchez, F.-S. Aguirre-Tostado, M.-O. Vazquez-Lepe, The slope-background for the near-peak regimen of photoemission spectra, J. Electron Spectros. Relat. Phenomena. 189 (2013) 76–80.

Electronic Materials and Photonics
Room 114 - Session EM+AIML+AP+QS+TF-WeM

Ferroelectrics and Memory Devices

Moderators: Samantha Jaszewski, Sandia National Labs, **Erin Cleveland**, Laboratory of Physical Sciences

8:00am **EM+AIML+AP+QS+TF-WeM-1 A Scalable Ferroelectric Non-Volatile Memory Operating at High Temperature**, *Dhiren Pradhan,* Department of Electrical and Systems Engineering, University of Pennsylvania; *David Moore,* 2Materials and Manufacturing Directorate, Air Force Research Laboratory, Wright-Patterson AFB; *Gwangwoo Kim,* Department of Engineering Chemistry, Chungbuk National University, Cheongju, Republic of Korea; *Yunfei He,* Department of Electrical and Systems Engineering, University of Pennsylvania; *Pariasadat Musavigharavi,* Department of Materials Science and Engineering, University of Central Florida; *Kwan-Ho Kim, Nishant Sharma, Zirun Han, Xingyu Du,* Department of Electrical and Systems Engineering, University of Pennsylvania; *Venkata Puli,* Materials and Manufacturing Directorate, Air Force Research Laboratory, Wright-Patterson AFB; *Eric Stach,* Department of Materials Science and Engineering, University of Pennsylvania; *W. Joshua Kennedy, Nicholas Glavin,* Materials and Manufacturing Directorate, Air Force Research Laboratory, Wright-Patterson AFB; *Roy H. Olsson III, Deep Jariwala,* Department of Electrical and Systems Engineering, University of Pennsylvania

Non-volatile memory (NVM) devices that reliably operate at temperatures above 300 °C are currently non-existent and remain a critically unmet challenge in the development of high- temperature (T) resilient electronics. There are numerous emerging harsh environment applications including aerospace, space exploration, oil and gas exploration, nuclear plants, mining and others that require complex, in-situ computing and sensing capabilities, for which high temperature NVM is critical. Current Silicon (Si)-based micro(nano)electronics, utilizing complementary metal oxide semiconductor (CMOS) technology, encounter reliability challenges above 200 °C and cannot retain their functional properties at high temperatures. Ferroelectric $Al_xSc_{1-x}N$ exhibits strong potential for utilization in NVM devices operating at very high temperatures (> 500 °C) given its stable and high remnant polarization (P_R) above $100\mu C/cm^2$ with demonstrated ferroelectric transition temperature (T_C) > 1000 °C. Here, we demonstrate an $Al_{0.68}Sc_{0.32}N$ ferroelectric diode based NVM device that can reliably operate with clear ferroelectric switching up to 600 °C with distinguishable On and Off states. The coercive field (E_C) from the Triangle Wave I-V measurements is found to be -5.84 (E_{C-}) and +5.98 (E_{C+}) (+/- 0.1) MV/cm at room temperature (RT) and found to decrease with increasing temperature up to 600 °C. The devices exhibit high remnant polarizations (> 100 $\mu C/cm^2$) which are stable at high temperatures. At 600 °C, our devices show 1 million read cycles with On-Off ratio above 1 for > 60 hours. Finally, the operating voltages of our AlScN ferrodiodes are < 15 V at 600 °C which is compatible with Silicon Carbide (SiC) based high temperature logic technology, thereby making our demonstration a major step towards commercialization of NVM integrated high-T computers. NVM characteristics of engineered ferrodiodes with higher On-Off ratios at > 600 °C will also be presented in the meeting.

[a] Dhiren K. Pradhan and David C. Moore contributed equally to this work.

[*]Authors to whom correspondence should be addressed: dmj@seas.upenn.edu.

8:15am **EM+AIML+AP+QS+TF-WeM-2 Oxygen Diffusion Coefficients in Ferroelectric Hafnium Zirconium Oxide Thin Films**, *Jon Ihlefeld, Liron Shvilberg,* University of Virginia; *Chuanzhen Zhou,* North Carolina State University

Just over a decade ago, ferroelectricity – the presence of a permanent reorientable dipole – was reported in doped hafnium oxide thin films. This

report generated a great deal of excitement as the inherent silicon compatibility of HfO$_2$, coupled with the extreme thinness of the films that exhibited the ferroelectric response promised to overcome a number of technological hurdles limiting utilization of ferroelectrics in microelectronics. While the material is moving toward mass production, there are lingering issues of insufficient endurance and limited retention. These issues are commonly attributed to oxygen point defects, including the drift of these defects in poled devices. As such, knowledge of oxygen transport in the ferroelectric phase is vital toward overcoming the current shortcomings. In this presentation, we will show the results of experiments using ^{18}O tracers to evaluate the diffusion coefficient of oxygen in the ferroelectric phase. Hafnium zirconium oxide films containing ^{16}O were prepared via plasma-enhanced atomic layer deposition followed by post-metallization annealing to form the ferroelectric phase. Following removal of the metal layer, an ^{18}O-containing hafnium zirconium oxide film was deposited via thermal atomic layer deposition with ^{18}O provided from a H$_2^{18}$O source. Tracer anneals were then performed and the ^{18}O position evaluated with secondary ion mass spectrometry. The results will show that the oxygen diffusion coefficients in the ferroelectric phase are extremely low, with extrapolated room temperature values of only 10^{-26} cm^2/sec derived. The activation energy for oxygen diffusion was calculated to be 1 eV, which is intermediate the values calculated for the equilibrium monoclinic phase and amorphous films. These results indicate that oxygen vacancies may be relatively immobile in ferroelectric hafnia devices and that other charged defects may be the primary source of degradation.

9:00am EM+AIML+AP+QS+TF-WeM-5 Iridium Etching: Exploring Reactive Ion Etching Parameters for Efficient Electrode Fabrication in Ferroelectric Memory, *Yanan Li, Philippe Bezard, Shreya Kundu, Frederic Lazzarino, Xiaoyu Piao, Yann Canvel,* IMEC Belgium

Non-volatile Ferroelectric lead zirconium titanate (PZT) are interesting candidates for future memory applications but the fatigue resistance of the electrode material from the capacitors is a challenge. Iridium (Ir) is being investigated as electrode material for its superior characteristic. Thus, a patterning process must be developed. Due to the low volatility of the etch products, etching Ir is typically performed by ion beam etching (IBE). The low-throughput, relative scarcity of IBE chambers in the industry, as well as the limited tunability of the sputtering process are motivations for the development of a plasma-based etching approach.

In this work, we conducted experiments with TiN as a hard mask, following the process flow shown in Figure 1. Preliminary data indicates that Ir can be etched using both fluorine-based and chlorine-based gases. We identify and highlight the primary parameters affecting the Ir etch rate in the RIE process, focusing on gas flow rates, power settings, pressure, and substrate temperature. We also compare the relative contributions of physical and chemical reactions to the etch rate of Ir.

XSEM pictures for those experiments are shown in figures 2 and 3. It is observed that selectivity with a TiN hard-mask is a challenge when using these chemistries. Sidewall residues have also been observed in conditions where ion sputtering is dominant. Therefore, optimization of the etch processes based upon an understanding of the etch mechanisms in place is necessary.

9:15am EM+AIML+AP+QS+TF-WeM-6 Investigations in Current Transport Mechanisms of Multi-Resistance State Hafnia Zirconia Ferroelectric Tunnel Junctions, *Troy Tharpe,* Sandia National Laboratories*; Megan Lenox,* University of Virginia*; Samantha Jaszewski, Giovanni Esteves,* Sandia National Laboratories*; Jon Ihlefeld,* University of Virginia*; M. David Henry,* Sandia National Laboratories

Since the discovery of ferroelectricity in doped hafnia (HfO$_2$) and alloyed hafnia zirconia thin films (Hf,Zr)O$_2$ over a decade ago, fluorite-structure binary oxides have garnered great interest for use within ferroelectric memory devices to realize compute-in-memory (CiM) and neuromorphic applications. With conformal atomic layer deposition (ALD) techniques, process temperatures below 400 °C, coercive fields close to 1 MV/cm, and ferroelectricity down to ~ 1nm, hafnia thin films are ideal candidates for back-end-of-line (BEOL) integration with complementary metal oxide semiconductor (CMOS) circuits. Leveraging these qualities, recent research has extensively focused on charge-based hafnia devices, such as ferroelectric random access memory (FeRAM) and ferroelectric tunnel junctions (FTJs). FTJs are realized by sandwiching a 4-7nm ferroelectric between electrodes to form a metal-ferroelectric-metal (MFM) structure with a voltage-controlled resistance modulated by polarization. Thinner than FeRAM and able to generate multistate resistances, FTJs are poised to

enable energy efficient CiM devices and artificial intelligence (AI) hardware accelerators with improved performance and small form factor.

In this work, we study FTJs with 7 nm thick Hf$_{0.5}$Zr$_{0.5}$O$_2$ deposited by plasma enhanced ALD, and asymmetric 20 nm niobium (Nb) / 115 nm niobium nitride (NbN) electrodes deposited by magnetron and reactive sputter, respectively. Film ferroelectricity is stabilized by subsequent anneal at 565 °C for 90s in argon ambient. Fig. 1 (a) depicts an optical image of fabricated HZO FTJs while Fig. 1 (b) illustrates a cross section of device layers. Current density vs voltage (J-V) sweeps are taken at 294, 323, 348, 373, and 398 K for HZO FTJs with diameters varying from 74 μm to 117 μm. Fig. 2 (a) shows these J-V sweeps for a 100 μm diameter device, after application of 10 wakeup cycles. Fig. 2 (b) shows high resistance state (HRS) and low resistance state (LRS) trends across temperature for this same device at 0.2V and 0.3V. Fig. 3 (a, b) shows average and outlier resistance ratio (RR) temperature dependence for 4 devices at 0.2 V and 0.3V, respectively. Fig. 3 (c) depicts pulsed hysteresis curves for a 99 μm diameter device at 294 K and 398 K. Device resistance is read at 0.2V and a pulse width of 100ms, following a write pulse progressing from 1.5V to 1.3V and back with 100mV step and 100ms pulse width. The nonlinear HRS, LRS and RR temperature trends indicate a complex conduction system within HZO FTJs, highlighting the need for continued investigation of current transport mechanics for the realization of ferroelectric CiM devices and multistate AI accelerators.

9:30am EM+AIML+AP+QS+TF-WeM-7 Correlation between Elastic Modulus and Biaxial Stress in Hafnium Zirconium Oxide (HZO) Thin Films, *Megan Lenox,* University of Virginia*; Samantha Jaszewski,* Sandia National Laboratories*; Shelby Fields,* Naval Research Laboratory*; Alejandro Salanova, Md. Rafiqul Islam, Md. Shafkat Bin Hoque,* University of Virginia*; Jon-Paul Maria,* Penn State University*; Patrick Hopkins, Jon Ihlefeld,* University of Virginia

The discovery of ferroelectricity in hafnium oxide based thin films has catalyzed significant research focused on understanding the ferroelectric property origins when fabricated in conventional metal-ferroelectric-metal geometries. Studies have revealed that electrode material selection impacts oxygen vacancies, interfacial layers, and biaxial stress, all noted responsible ferroelectric mechanisms. The coefficient of thermal expansion (CTE) incongruency between the hafnia and the electrode material induces an in-plane tensile stress following post-metallization annealing. However, recent work has shown that while the electrode material CTE does have an effect, the overall strain resulting from the device is primarily from the CTE of the silicon substrate and densification of the hafnia film during crystallization. This notwithstanding, comparisons between electrode materials have shown significant differences in ferroelectric remenant polarization (P_r) behavior. This work describes these polarization differences through the lens of the elastic modulus of the electrode material. TaN/HZO/TaN/M devices, where M is platinum, TaN, iridium, tungsten, and ruthenium, were fabricated using plasma enhanced atomic layer deposition and sputtering for the hafnia and metal layers, respectively. Wafer flexure measurements done using stylus profilometry revealed each metal electrode material was compressive as deposited. Two-dimensional X-ray diffraction, utilized to derive the sin^2(ψ) in-plane biaxial stress in the HZO, revealed a strong correlation between stress and electrode elastic modulus (E). Further, Polarization-electric field ($P(E)$) measurements at 2.5 MV cm^{-1} field also showed dependence of P_{-r} on measured E. Conversely, no correlation exists between the electrode CTE and P_r or biaxial stress, respectively. Increasing modulus results in a greater resistance to deformation of the electrode, which when deposited prior to annealing the HZO to crystallize from the amorphous state, restricts the out-of-plane expansion of the HZO, promoting the stabilization of the ferroelectric orthorhombic phase, in a phenomenon known as the "capping effect". This work further promotes the acceleration integration of HZO into MFM devices, such a non-volatile memory devices.

9:45am EM+AIML+AP+QS+TF-WeM-8 Ferroelectric Behavior of ε−Wo3, *Mohammad Mahafuzur Rahaman, Anthony Annerino, Jacob Shell, Pelagia-Irene Gouma,* The Ohio State University

Designing novel ferroelectric polymorphs having fast and low energy dipole switching responses is crucial for developing next generation's neuromorphic devices. Reported here a unique binary ferroelectric polymorph called ε−WO$_3$ and it's dipole response to electro-optical stimuli, contributed from the stabilization of ε−phase nanoparticles of ~20 nm grains at RT, previously was at −43°C in bulk, by our group using FSP. The epsilon phase of the material is confirmed from XRD and Raman analysis. The nano-domains of ferroelectric ε−WO$_3$ shows switching behavior within few KV/cm electric field. The ferroelectric nanodomains interact with light

and shows blue coloration under electro-optical stimuli. The response of these nanodomains with visible light and it's switching behavior with electric field is studied via C vs V measurement. Furthermore, the origin of the observed "ferro-chromic effect", the unique, rapid and reversible coloration of the e-WO3 thin films upon application of a voltage in the absence of an electrolyte has been deduced from X-ray Photoelectron Spectroscopy. An important finding for all solid-state single layer ubiquitous displays, energy-saving windows and next generation's non-volatile memory device for neuromorphic computation.

11:00am EM+AIML+AP+QS+TF-WeM-13 Innovations in DARPA's Optimum Processing Technology Inside Memory Arrays (OPTIMA) Program, *Todd Bauer,* DARPA **INVITED**
Fast,compact, and power-efficient compute-in-memory (CIM) accelerators can move machine learning from data centers to edge compute devices, enabling training and inference to be done where the training data is collected. However, conventional accelerators that use vonNeumannarchitectureshave poor area and computationalpowerefficiency and longexecutionlatency.CIMarchitectureswithMultiplyAccumulateMacros(MA Ms)canaddressthe power and performancelimitationsof approaches that use von Neumann hardware architectures. To date these MAM implementationshavebeenhinderedbythelargephysicalsizeofmemoryeleme ntsandthehigh-powerconsumptionofsupportingcircuitry.The Defense Advanced Research Program Agency's OptimumProcessingTechnologyInsideMemoryArrays(OPTIMA)programseek stodeveloparea-andpower-efficienthigh-performanceMAMswithinnovativesignalprocessingcircuits. The key technical challenges that performers are addressing include 1) developing area-efficient, multi-bit memory elements (i.e. 8 bits of storage in a 1T-1C structure) that can be incorporated into compact multiply compute elements (MCEs) and 2) achieving compact, scalable, and power-efficient MAM circuits. This presentation will provide an overview of the OPTIMA program goals and approaches to achieving those goals.

Distribution Statement A - Approved for Public Release, Distribution Unlimited

11:30am EM+AIML+AP+QS+TF-WeM-15 A Transition Toward Solid-State in TiO₂ Protonic ECRAM, *John Hoerauf,* University of Maryland, College Park*; Marshall Schroeder,* Army Research Laboratory*; David Stewart, Gary Rubloff,* University of Maryland, College Park
AI and inference learning energy demands are on pace to surpass global energy production[1], but analog in-memory computing hardware can reduce the energy required by up to six orders of magnitude[2]. Electrochemical RAM (ECRAM) is a new and promising transistor technology to realize physical neuromorphic analog in-memory computing circuits, achieved on the device level by modifying a thin-film battery stack to measure the impedance of a selected electrode. The impedance is controlled by changing the state of charge of the battery, electrochemically doping the selected electrode with the electrochemically active species. ECRAM that utilizes protons as the electrochemically active species is compatible with existing CMOS devices, has faster programming speed and increased device durability compared to more established Lithium ion ECRAM. As a less well studied system, it is helpful to understand the insertion of protons in and out of the electrode of interest using a more traditional liquid cell before advancing to a solid-state system. In this presentation, the liquid cell electrochemical characteristics and degradation mechanisms in anatase TiO₂ are discussed with and without a capping Nafion film. It is observed that the anatase TiO₂ electrode's typically quick degradation is suppressed by adding a spin-cast Nafion film, increasing cyclability in an aqueous acetate buffer solution by >10x cycles and altering the H+ insertion kinetics. Subsequently, TiO₂ is used in an all-solid-state three electrode transistor by splitting the bottom current collector into a source-drain configuration and using PdH$_x$ as the counter electrode and H+ reservoir. Results toward novel solid state anatase TiO₂ based protonic ECRAM are discussed with a focus on device state modulation by electrochemical doping.

[1] B. Bailey, "AI Power Consumption Exploding," Semiconductor Engineering. Accessed: May 09, 2024. [Online]. Available: https://semiengineering.com/ai-power-consumption-exploding/

[2] E. J. Fuller et al., "Li-Ion Synaptic Transistor for Low Power Analog Computing,"Advanced Materials, vol. 29, no. 4, p. 1604310, 2017

11:45am EM+AIML+AP+QS+TF-WeM-16 Effects of Gamma Radiation on the Structural and Ferroelectric Properties of Hafnium Zirconium Oxide Capacitors, *Samantha Jaszewski,* Sandia National Laboratories*; Megan Lenox, Jon Ihlefeld,* University of Virginia*; M. David Henry,* Sandia National Laboratories
Ferroelectric hafnium oxide (HfO₂) presents opportunities for technological developments in microelectronics, such as scaling of ferroelectric random-access memory (FeRAM) and new devices such as ferroelectric field-effect transistors (FeFETS) and ferroelectric tunnel junctions (FTJs), that were not previously possible with conventional ferroelectrics. This is due to its compatibility with silicon and ability to exhibit a ferroelectric response in films as thin as 1 nm. Understanding the interaction between radiation and HfO₂-based ferroelectrics is necessary before this material can be utilized in devices facing radiation-hostile environments. In this work, the effects of varying doses of gamma radiation (1 to 8 Mrad) on the structural and electrical properties of metal-ferroelectric-metal capacitors fabricated with 17 nm thick hafnium zirconium oxide (HZO) layers is investigated. Additionally different electrode materials, titanium nitride and tungsten, will be compared. Polarization-electric field, capacitance-voltage, and leakage current measurements were made after electric field cycling with voltages ranging from 2.6 to 4 V. It will be shown that the devices experience decreased endurance and a shift in the coercive voltage that scales with the applied gamma dose and depends on the electrode material. Synchrotron nano-Fourier transform infrared spectroscopy measurements demonstrated that no significant phase changes occur after radiation in these films. This work advances the understanding of the interaction between radiation and HfO₂-based ferroelectrics in order to probe the fundamental limits of radiation tolerance in this material.

12:00pm EM+AIML+AP+QS+TF-WeM-17 Reconfigurable Ferroelectric Field-Effect Transistor Arrays from SWCNTs, *Dongjoon Rhee, Kwan-Ho Kim, Seunguk Song,* University of Pennsylvania*; Lian-Mao Peng,* Peking University, China*; Joohoon Kang,* Sungkyunkwan University (SKKU), Republic of Korea*; Roy Olsson III, Deep Jariwala,* University of Pennsylvania
Ferroelectric field-effect transistor (FeFET) is a promising nonvolatile memory device due to its simple and compact device structure for high-density integration, fast switching peed, and non-destructive readout. Recent progress in FeFETs based on two-dimensional (2D) semiconductor channels and ferroelectric Al$_{0.68}$Sc$_{0.32}$N (AlScN) has enabled high-performance nonvolatile memory devices with remarkably high ON-state currents, large current ON/OFF ratio, and large memory windows. However, the wafer-scale synthesis of these 2D semiconductors typically demands growth temperatures exceeding 500 °C, rendering the synthesis process incompatible with back-end-of-line (BEOL) processing and necessitating a subsequent transfer step. Solution-based assembly of semiconducting single-walled carbon nanotube (SWCNT) has shown promise as a strategy to fabricate high-quality semiconducting channels at room temperature, but their integration with AlScN for FeFETs has not yet been achieved. In this work, we present a large array of FeFETs utilizing a dense monolayer film of highly aligned semiconducting SWCNTs and ferroelectric AlScN. Our SWCNT FeFETs can be engineered from *p*-type to ambipolar by changing the contact metals at the metal-semiconducting interface. The ambipolar FeFETs showed high electron and hole current densities, both exceeding 300 µA um^{-1}, along with stable memory retention over 10^4 s and endurance greater than 10^4 cycles. Our devices can also function as reconfigurable *p*- and *n*-FETs by switching the polarization direction of AlScN, potentially enabling multifunctional logic and memory applications at the circuit level.

Magnetic Interfaces and Nanostructures
Room 121 - Session MI+2D+AC+TF-WeM

Altermagnetism and Spin-Dependent Systems
Moderators: Markus Donath, Muenster University, Germany, **Valeria Lauter**, Oak Ridge National Laboratory

8:00am MI+2D+AC+TF-WeM-1 Twisted Electrons in Momentum Space: A Photoemission Perspective on Spin and Orbital Angular Momentum in Quantum Materials, *Maximilian Ünzelmann,* University of Würzburg, Germany*; Begmuhammet Geldiyev,* Univsersity of Würzburg, Germany*; Tim Figgemeier,* University of Würzburg, Germany*; Hendrik Bentmann,* NTNU Trondheim, Norway*; Friedrich Reinert,* Univsersity of Würzburg, Germany **INVITED**
Beyond the spin, electronic states in crystalline solids can exhibit finite expectation values of orbital angular momentum (OAM). This phenomenon has attracted considerable attention in recent years and can particularly be

traced back to the following key applications: (i) Since OAM is formed solely by inversion symmetry breaking (ISB) – and thus can also be present without magnetism or strong spin-orbit coupling (SOC) – it appears as an interesting quantum degree of freedom raising the potential of orbital analogs to spintronic phenomena, i.e. the field of *orbitronics*. (ii) OAM has been proposed to be a useful observable to assess nontrivial topology in the band structure of topological quantum matter. Lastly, if the atomic SOC strength is sizable, OAM is coupled to the electron spin giving rise to rich spin and orbital momentum space textures.

In this talk, I will shed light on those textures from the perspective of angle-resolved photoemission spectroscopy (ARPES). Combining ARPES with light-polarization-dependent and spin-resolved measurements allows us to address the momentum-dependent properties of the spatial and spin part of the wave functions, respectively. I will present experimental results on model-like monolayer systems and topological quantum materials and show that – as well as how – the complex interplay of ISB and SOC forms striking spin-orbital textures. Based on these findings, I will discuss the potential of utilizing OAM (i) towards orbitronic transport and (ii) to detect unexpected topological features.

8:30am MI+2D+AC+TF-WeM-3 Falicov Student Award Finalist Talk: Gap Tuning by Hole Doping in EuZn2As2 Semimetal, *Dejia Kong*[1], University of Virginia; *Siavash Karbasizadeh,* University of South Carolina; *Ganesh Narasimha,* Oak Ridge National Laboratory; *Paras Regmi,* University of South Carolina; *Chenggang Tao,* Oak Ridge National Laboratory; *Sai Mu,* University of South Carolina; *Rama Vasudevan,* Oak Ridge National Laboratory; *Ian Harrison,* University of Virginia; *Rongying Jin,* University of South Carolina; *Zheng Gai,* Oak Ridge National Laboratory

$EuZn_2As_2$ is an ideal candidate for topological magnetism study in comparison to other europium-based semimetals that exhibit a similar type of magnetic transition from the antiferromagnetic phase to the ferromagnetic phase at a low temperature. [1] Theoretical calculations predict gapped and flatter bands in $EuZn_2As_2$ but a gapless Γ point in $EuCd_2As_2$. [2] In this work, a low-temperature cleaved $EuZn_2As_2$ crystal is studied using scanning tunneling microscopy/spectroscopy (STM/S) and density functional theory (DFT). A group of triangular-shaped defects in combining with the DFT calculations are used to identify the existence of the europium-terminated and arsenic-terminated surfaces at the cleavage. Large bandgaps are observed on the two pristine terminations. However, the bandgap width is found to be very sensitive to local heterogenous, like defects and step edges. Two defect groups that create local electron deficiency, i.e. substitutional defect of As replacing Zn, and Zn vacancy, can drastically lower the bandgap. Furthermore, the modification of the bandgap width shows a discrepancy on the two terminations, bigger on Eu termination but much smaller on As-Zn termination. So, we predict that purposely hole doping the system during the crystal growth stage may create a new topological semimetal material with a gapless europium layer sandwiched by a gapped As-Zn lattice.

Reference:

1 Blawat, J. *et al.* Unusual Electrical and Magnetic Properties in Layered EuZn2As2. *Adv Quantum Technol* **5** (2022).

2 Wang, Z. C. *et al.* Anisotropy of the magnetic and transport properties of EuZn2As2. *Phys Rev B* **105** (2022).

8:45am MI+2D+AC+TF-WeM-4 Characterization of LaMnO₃/SrTiO₃ Thin Films and Its Mn Valance State Correlated with Ferromagnetism, *Ghadendra Bhandari*, Pedram Tavazohi, Vikum Dewasurendra, Matthew Johnson, Mikel Holcomb, West Virginia University

Thin films of $LaMnO_3$ (LMO) / $SrTiO_3$ (STO) perovskite have gained interest for their abilities to be an essential component of some heterostructures while still exhibiting an interesting magnetic phase diagram. We have grown $LaMnO_3$ thin films on $SrTiO_3$ using pulsed laser deposition and deposition has been monitored by reflection high energy electron diffraction (RHEED) to verify layer-by-layer growth. Structure and magnetic properties have been characterized by X-ray diffractometry (XRD), and vibration sample magnetometry (VSM). LaMnO3 thin films exhibit ferromagnetic FM phases whereas bulk LaMnO3 is antiferromagnetic A-type. All thin films are coherently strained, forcing them to have the in-plane lattice parameter of the STO substrate (3.905 Å), but the out-of-plane parameter varies (3.89-3.93 Å). The variation in the c-lattice is developed from O_2 growth pressure

and consequently the Mn cation is in mixed valence state $Mn^{3+/4+}$. The valence state of the Mn cation is realized from XPS and XAS study. The ferromagnetic magnetization is originated by the double exchange of Mn^{3+}-O-Mn^{4+}. The thickness averaged magnetizations from PNR measurements are comparable with magnetization obtained from VSM. The strength of magnetization correlates with content of Mn^{4+}.

9:30am MI+2D+AC+TF-WeM-7 Growth Study of Kagome-structured Mn₃Sn on Gallium Nitride (000_1) Using Molecular Beam Epitaxy, *Hannah Hall, Sneha Upadhyay, Tyler Erickson, Ashok Shrestha, Ali Abbas,* **Arthur Smith**, Ohio University

Over the past few years, there has been a large amount of interest in Kagome-structured magnetic materials with non-collinear antiferromagnetic ordering [1]. Such materials show interesting magnetic properties including anomalous Hall effect and topological Hall effect [2]. In recent work, we have reported growth of Mn_3Sn on sapphire (0001) which resulted in either *a*-plane or *c*-plane film orientations [3,4]. The substrate however was not ideal, and frequently we observed the disappearance of the diffraction pattern upon opening the Mn and Sn shutters with the pattern reappearing after some amount of resting time. In the case of the *c*-plane orientation, theory suggested this could be due to interfacial disordering of the lattice. This might be due to the ~19% lattice mismatch which also is one reason for the preferred growth of *a*-plane oriented Mn_3Sn on sapphire (0001) due to the much smaller lattice mismatch (<5%) along that direction. Nonetheless, high quality films prove difficult to obtain on sapphire (0001), and a better substrate is desirable. As such, we have investigated the growth of Mn_3Sn films on freshly grown gallium nitride surfaces. The Mn_3Sn growth follows immediately after the growth of N-polar GaN (0001), thus giving a perfectly clean and well-ordered substrate surface with only ~2.66% lattice mismatch along the 30° line to the high symmetry axis of GaN. We have investigated this as a function of substrate temperature and find an optimal temperature range in which streaky and clear RHEED patterns are obtained from the beginning of the growth. Next plans include studying of this surface with high-resolution STM and spin-polarized STM. This research has been supported by the U.S. Department of Energy, Office of Basic Energy Sciences, Division of Materials Sciences and Engineering under Award No. DE-FG02-06ER46317.

[1] H. Yang *et al.,* New J. of Physics **19**, 015008 (2017).

[2] S. Nakatsuji, N. Kiyohara, and T. Higo, Nature **527**, 212 (2015).

[3] S. Upadhyay *et al.*, J. Vac. Sci. & Technol. A **41**, 042710 (2023).

[4] S. Upadhyay *et al.,* Surfaces and Interfaces **42**, 103379 (2023).

9:45am MI+2D+AC+TF-WeM-8 Exchange Bias Effect in Single-Layer Antiferromagnetic Mn3GaN Films, *Ali Abbas, Ashok Shrestha,* Ohio University; *Daniel Russell, Fengyuan Yang,* The Ohio State University; *Arthur R. Smith,* Ohio University

Strain-induced spin structures in non-collinear antiferromagnetic materials like Mn_3GaN can be controlled by an external magnetic field[1][2]. In this work, we report the intrinsic exchange bias in the "single" antiferromagnetic Mn_3GaN films fabricated by epitaxial growth of Mn_3GaN on MgO (001) substrate using molecular beam epitaxy under *in–plane* tensile and *out–of–plane* compressive strain. Scanning transmission electron microscopy confirms significant strain at the Mn_3GaN/MgO interface due to substrate induced tetragonal distortion. Superconducting quantum interference device measurements reveal an exchange bias field (Heb=1225 Oe) and a vertical magnetization shift below 300 K. Furthermore, magnetization M vs. the applied field H measurements from 300K down to 50K reveal the consistent horizontal and vertical shift of the hysteresis loop, which are usually observed only in ferro–/antiferromagnetic bilayers. Here, the exchange bias effect may be attributed to strain, leading to canted and uncompensated Mn spins coupled with an upper antiferromagnetic region, as reported in another system [2][3]. The findings of strain–induced exchange bias in antiferromagnetic Mn_3GaN films may open a new route/ novel system for spintronic properties by design. This research has been supported by the U.S. Department of Energy, Office of Basic Energy Sciences, Division of Materials Sciences and Engineering under Award No. DE–FG02–06ER46317 (work done at Ohio University, not including XRD) and under award No. DE–SC0001304 (XRD and SQUID measurements done at The Ohio State University).

References:

[1] X.F. Zhouet al., "Exchange Bias in Antiferromagnetic Mn3Sn Monolayer Films," Physical Review Applied, 14(5), 054037 (2020).

[2] B. Cuiet al., "Strain engineering induced interfacial self-assembly and intrinsic exchange bias in a manganite perovskite film". Scientific reports, 3(1), 2542, (2013).

[3] L. Wanget al., "Exchange bias and vertical shift of the magnetic hysteresis loop in Co/BiFeO3 bilayers. Ferroelectrics Letters Section, 48(4–6), 65–71, (2021).

11:00am MI+2D+AC+TF-WeM-13 L-Gap Surface Resonance at Pt(111): Influence of Atomic Structure, d Bands, and Spin-Orbit Interaction, *Markus Donath, Fabian Schöttke, Peter Krüger,* University of Münster, Germany; *Lutz Hammer, Tilman Kißlinger, M. Alexander Schneider,* University of Erlangen-Nürnberg, Germany

Pt(111) hosts a surface resonance with peculiar properties concerning energy vs momentum dispersion and spin texture. At variance with the free-electronlike behavior of the L-gap Shockley-type surface states on the fcc(111) surfaces of Au, Ag, and Cu, it splits into several branches with distinct spin polarization around the center of the surface Brillouin zone. Theoretical predictions based on density-functional theory vary depending on the particular functionals used. To clarify this issue, we investigate the atomic structure of Pt(111) by low-energy electron diffraction and the unoccupied electronic structure by spin- and angle-resolved inverse photoemission. The experimental results are backed by theoretical studies using different functionals which show that the characteristics of the surface band depend critically on the lattice constant. We identified a delicate interplay of several contributions: Lattice constant, hybridization with d bands, and the influence of spin-orbit interaction are critical ingredients for understanding the peculiar energy dispersion and spin character of the unoccupied surface resonance.

11:15am MI+2D+AC+TF-WeM-14 Substrate-Induced Strain Effects on SrFeO₃ Thin Films, *Lucas Barreto,* University of Pennsylvania; *Paul Rogge, Jiayi Wang, Benjamin Lefler,* Drexel University; *Danilo Puggioni, James Rondinelli,* Northwestern University; *Skylar Koroluk, Robert Green,* University of Saskatchewan, Canada; *Steven May,* Drexel University

Materials with non-trivial magnetic ordering give rise to exotic topological phenomena that can enhance spin-based devices' performance. In this scenario, the cubic perovskite $SrFeO_3$ exhibits a rich magnetic ordering, described by a multi-**q** magnetic arrangement. In this work, we evaluate how in-plane lattice stress influences the structural, magnetic, and electronic of $SrFeO_3$ films. We grow epitaxial $SrFeO_3$ films on different substrates to induce compressive and tensile strains, characterize them using X-ray diffraction, and probe the electronic transport as a function of temperature. The experimental data are supported by density functional theory calculations, from which we obtain the structural and electronic properties of the strained $SrFeO_3$ structure. We map the magnetic ordering via resonant x-ray magnetic diffraction and observe shifts in the projection of the magnetic wavevector **q** along the [111] direction. Our results indicate that the lattice strain can tune the magnetic propagation vector on the films while maintaining the $SrFeO_3$ metallic behavior.

11:30am MI+2D+AC+TF-WeM-15 Tunable Localized Currents at Crystallographic Domain Boundaries in Altermagnet RuO2, *Gina Pantano, Eklavya Thareja,* University of South Florida; *Libor Šmejkal,* the Czech Academy of Sciences and Johannes Gutenberg Universität Mainz, Germany; *Jairo Sinova,* Johannes Gutenberg Universität Mainz, Germany; *Jacob Gayles,* University of South Florida

Research on interfacial phenomena in condensed matter physics has garnered significant interest over the last few decades due to the discovery of new properties and phases distinct from the bulk, enabling the manipulation of materials for technological applications. In this work, we investigate the novel effects that arise from the presence of a locally chiral crystallographic domain boundary in the altermagnet ruthenium dioxide (RuO2). Altermagnets are characterized by having a substantial non-relativistic spin splitting comparable to ferromagnetic materials but with compensated magnetic ordering. The spin splitting originates from the Heisenberg exchange interaction combined with the anisotropic octahedral crystal field from the surrounding nonmagnetic O atoms, which reduces the symmetry relating the two opposite spin sublattices to an antiunitary rotation or mirror symmetry. This introduces a new mechanism for controlling spin-dependent transport phenomena by altering the crystal configuration, specifically through its local chirality, such as the crystal Hall effect. Thus, looking at an interface where the local chirality reverses allowed for a more detailed analysis of how the change of symmetry affects electronic transport. RuO2 was chosen for this study due to its high Néel temperature, metallic nature, and exhibiting one of the largest spin splittings in this new material class. We use first-principle calculations to

characterize the interfacial states and their contribution to electronic transport. We observe an induced magnetization at the domain boundary and enhanced anomalous transport along the interface when spin-orbit coupling is considered, due to the change of symmetry. We theorize the localized currents are tunable by the direction of the magnetization at the interface. Our findings will contribute to the understanding of how altermagnetic properties evolve toward interfaces with the reduction in dimensionality and symmetry and contribute to advancements toward the design of sustainable, energy-efficient devices.

Plasma Science and Technology
Room 124 - Session PS-WeM

Plasma Modelling

Moderators: Pingshan Luan, TEL Technology Center America, **Mackenzie Meyer**, US Naval Research Laboratory

8:00am PS-WeM-1 Challenges and Opportunities of a Holistic Approach toward Simulation-Assisted Plasma Etch Technology Development, *Du Zhang, Yu-Hao Tsai,* TEL Technology Center, America, LLC; *Tetsuya Nishizuka,* Tokyo Electron Miyagi Limited, Japan; *Akiteru Ko, Peter Biolsi,* TEL Technology Center, America, LLC

Technological advancements in plasma etching crucially rely on the synergy of various areas of expertise due to its highly interdisciplinary nature, requiring subject matter knowledge ranging from plasma physics and surface chemistry, to transport, metrology, etc. Many simulation techniques exist, each targeting a different scope, and each with its own limitations and advantages; therefore, none should be considered the silver bullet. Nevertheless, from a pragmatic point of view, if the ultimate goal is to accelerate process and product development, the foremost priority is to identify the key issues and variables, then use suitable simulation tools to test out hypotheses and determine next action plans in an organized workflow. In this paper, focusing on the very thought process, we examine several examples of process and product development in which computational simulations provide insights to complement experimental techniques. We also discuss requirements for further simulation technology development in accordance with such industry needs.

8:15am PS-WeM-2 Some Lessons from Particle-in-Cell Modeling of Intermediate Pressure Capacitively Coupled Plasmas, *Shahid Rauf, Abhishek Verma, Rupali Sahu, Nakul Nuwal, Kallol Bera,* Applied Materials, Inc.

Capacitively coupled plasmas (CCPs) are widely used for thin film etching and deposition in the semiconductor industry. The pressure in these plasmas varies over a broad range, from a few mTorr to tens of Torr. At low pressure, non-local phenomena are important in both plasma production and charged species transport, necessitating the use of kinetic or hybrid kinetic-fluid models for accurately capturing the CCP physics. Fluid plasma models are typically used at intermediate pressures (> 100s of mTorr). It is important to understand how well fluid plasma models capture the behavior of intermediate-pressure CCPs and what improvements in the fluid models would render them more accurate. 1-dimensional particle-in-cell (PIC) simulations are done for 13.56 MHz N_2 and Ar CCPs between 100 mTorr – 1.5 Torr. Once the time-dependent simulation reaches steady state, the particle data is analyzed to obtain all the terms in the continuity, momentum conservation, and energy balance equations for the charged species. The potential and current in the plasma are also processed to determine the spatially resolved impedance in the plasma and sheaths. Comparison of PIC results to fluid plasma model under the same conditions and using the same plasma chemistry shows significant differences. This disparity between the two models can be linked to the assumptions about the electron energy distribution function (EEDF) and the electron transport coefficients in the fluid plasma model. In addition, the PIC simulations indicate that the EEDF is not spatially uniform. The drift-diffusion approximation appears reasonable for electron transport. However, it is necessary to solve the ion momentum equation as ion inertia effects are important. Analysis of the electron energy equation highlights that energy transport mechanisms such as the Dufour effect should be included in fluid plasma models.

8:30am PS-WeM-3 Modeling to Inform Optimization of Radiofrequency Plasma Sources, *Amanda Lietz, Cameron Wagoner, Syed Zulqarnain, Sk Azmaeen Bin Amir, Mohammad Sazzad Hossain,* North Carolina State University **INVITED**

Radiofrequency (RF) plasmas are essential for the processing of semiconductors, but also are also used in other applications, including medical treatments and auxiliary heating devices for fusion. In this work, we will discuss the role of computational modeling in informing the design and operation of RF plasmas sources, including examples of hydrogen inductively coupled and argon capacitively coupled plasmas. These plasma sources often operate in a regime where the commonly used fluid approximations (e.g. the local mean energy approximation) fail. Because there are insufficient collisions compared to the rate of acceleration by the electric field, the electron energy distributions are no longer a function of only local quantities like the electric field and the electron energy. First the failures of the fluid approach will be discussed with an example of particle-in-cell simulations investigating tailored voltage waveforms applied to argon capacitively coupled plasmas at the low pressures relevant for plasma etching (<20 mTorr). The fully kinetic approach is used for a detailed mechanistic understanding of the plasma dynamics in this system, though the timescales and chemistry are limited. The kinetic approach and results will be contrasted with fluid and hybrid modeling of hydrogen inductively coupled plasma sources for fusion. In this example, some fluid approximations are necessary to address neutral dissociation dynamics and flow timescales. These approximations also facilitate the rapid turnaround required in a design cycle. Finally, a new approach to use machine learning to incorporate non-local information into a fluid closure will be discussed and applied to a capacitively coupled plasma. As pressure decreases, an increasing amount of non-local information is required to obtain accurate fluid fluxes. The potential advantages and challenges of this approach will be discussed for a 1-dimensional, single frequency, capacitively coupled plasma.

9:00am PS-WeM-5 Stability Model for Capacitively Coupled Radiofrequency Argon Plasma at Moderate Pressures*, *Omar Alsaeed,* NCSU - Nuclear Engineering Department*; Amanda Lietz,* North Carolina State University*; Benjamin Yee, Brett Scheiner, Meenakshi Mamunuru, Chenhui Qu,* Lam Research Corporation

Wafer-scale uniformity is essential in semiconductor manufacturing but can be disrupted by plasma instabilities due to energy transport phenomena that are not well understood. This work reports on the operational conditions that can lead to plasma instabilities and thus self-organization in plane-parallel radiofrequency capacitively coupled argon plasmas at moderate pressures (0.1-10 Torr). Plasma processing equipment often employs this simple configuration and striations in the direction transverse to the electric field have not been theoretically analyzed using a linear stability analysis. We use a fluid description that relies on the drift-diffusion approximation and includes the thermoelectric electron energy which proves essential in describing the pattern formation mechanism[1] and is critical for plasmoid formation in capacitively coupled plasmas[2]. The equilibrium electron density and temperature solutions are derived using the inhomogeneous model for a capacitive discharge[3]. The ionization rates and electron transport coefficients are computed using a multi-term Boltzmann equation solver, MultiBolt[4]. A stability criterion dictating the allowed values of the thermoelectric electron energy transport coefficient as a function of discharge parameters is analyzed. Stable plasma processing windows are theoretically established as a function of background gas pressure, gas composition (He), and inter-electrode gap size.

1. Désangles, V., Jean-Luc R., Alexandre P., Pascal C., and Nicolas P., Phys. Rev. Lett. 123, 265001 (2019).

2. Bera, Kallol, Shahid Rauf, John Forster, and Ken Collins. J. of Appl. Phys. 129, 053304 (2021).

3. M. A. Lieberman and A. J. Lichtenberg, Principles of Plasma Discharges and Materials Processing: Lieberman/Plasma 2e. Hoboken, NJ, USA: John Wiley & Sons, Inc., (2005).

4. Flynn, M., Neuber, A., & Stephens, J., *Journal of Physics D: Applied Physics*, 55(1), 015201 (2021).

_____

9:15am PS-WeM-6 Plasma Modeling Guided Process Development and Optimization forHigh Density Plasma Sources, *Qiang Wang, Gregory Hartmann, Patrick Conlin, Roberto Longo, Shyam Sirdhar, Peter Ventzek,* Tokyo Electron America, Inc.

High density plasmas have been demonstrated to be robust tools for advanced node logic/memory device fabrication. With a plethora of plasma operating parameters, optimizing an etch process is quite complex, requiring a significant investment of time and resources. Plasma modeling guided process development is aiming to provide clear and prompt guidelines in the development of etch recipes. We present our approach on pairing first principle-based multi-scale plasma modeling with advanced surrogate optimization techniques in selecting optimized pulsing recipes for conductor etch applications. The modeling framework integrates a zero-dimensional global model, a circuit/sheath dynamic model and a surface/etch model, allowing rapid calculations of in-chamber (e.g., ions and radicals densities and fluxes), on-wafer (e.g., Ion Energy and Angular Distribution) and in-feature (e.g., surface site coverage) during etching. An advanced methodology of surrogate modeling with a machine learning (ML) technique is applied to reduce computation time of simulation-based optimization and enhance prediction reliability. Using this integrated modeling approach, the pulsing sequence was optimized for a single objective (e.g., minimizing aspect ratio dependent etch, minimizing bow CD etc.), or to optimize trade-offs among multiple objectives. We will further demonstrate examples of applying the developed modeling framework in handling increasingly challenging problems in conductor etch applications and its validation with process experiments.

9:30am PS-WeM-7 Investigating Instabilities in Magnetized Low-Pressure Asymmetric Capacitively Coupled Plasma Sources, *Sathya Ganta, Kallol Bera, Shahid Rauf,* Applied Materials, Inc.*; Igor Kaganovich, Alexander Khrabrov, Andrew Powis,* Princeton University Plasma Physics Lab*; Dmytro Sydorenko,* University of Alberta, Canada*; Liang Xu,* Soochow University (SUDA), Suzhou, Jiangsu, China

Asymmetric capacitively coupled plasma (CCP) chambers at low pressures (< 100 mTorr) are used in the semiconductor industry for thin film deposition and etch applications. Low pressure ensures low collisionality in the sheaths resulting in high energy ions. Low pressure plasma with relatively lower collisions diffuses towards the chamber center creating a center high non-uniformity in the deposition thickness or etch profile on the wafer. An external magnetic field can be used to make the plasma more uniform and mitigate the center high non-uniformity on the wafer. We performed an investigation previously of magnetized low pressure RF plasma in asymmetric CCP chambers using Particle in Cell (PIC) plasma model which indicated the possibility of instabilities at high magnetic field strengths (≥75 Gauss for 10 mTorr). These instabilities could adversely affect process uniformity on the wafer. This investigation was done at 40 MHz radio frequency (RF) with a vacuum gap between ground and RF powered electrodes. The effects of changing magnetic field strength, pressure, ground to RF powered electrode area ratio and an external capacitor were examined. The investigation provided guidelines for the upper limit of magnetic field strength to have an instability-free operation within the range of design and operating parameters studied. It was found that only pressure affected such upper limit of magnetic field strength as the increasing collisions dampened instabilities at higher pressure. In this paper, we continue the investigation in low pressure magnetized CCPs to observe the effect of changing frequency; dielectric boundary between electrodes instead of a vacuum boundary; and the chamber geometry on instabilities at high magnetic field strengths. The previous investigation showed waves of instabilities that had a continuous spectrum with peak frequency at around 1.9 MHz. We investigate if there is an enhancement in instabilities if the RF source frequency is around this peak frequency.

9:45am PS-WeM-8 Fast Kinetic Modeling of Magnetron Sputtering, *Daniel Main, Thomas Jenkins,* Tech-X Corporation*; Joseph Theiss, Gregory Werner,* University of Colorado Boulder*; Scott Kruger, John Cary,* Tech-X Corporation

Magnetron sputtering devices have a wide range of uses in the coatings industry, where they are used for optical coatings, metallization in integrated circuits, and coatings for wear resistance.Numerical simulations can aid in the design of such systems, as computation can allow one to predict the figures of merit, eliminating the need to test each conceived configuration on the path to the final design. Such figures of merit include the uniformity and extent of the distribution of sputtered material, the power consumption of the system, and the erosion of the cathode. Such computations must be self-consistent and kinetic, i.e., they must follow particle trajectories, since fluid approximations make simplifying assumptions that may not be valid (especially at low pressure) and only a

kinetic approach can properly account for the critical physics, including the energy-angle distribution of the impacting sputterers and the resulting distribution. The Particle-In-Cell, Monte Carlo Collision (PIC-MCC method) is ideal for this, as it can properly account for the above physics as well as the physics involved in plasma creation, electron trapping by the magnetic field, and even dynamics that occurs in High Power Impulse Magnetron Sputtering (HIPIMS). Unfortunately, these calculations can take significant computing time, as the time scales for relaxation to steady-state are long compared with plasma processes. This talk presents computations using multiple techniques to speed up these calculations. The methods include using a circuit model that allows one to rapidly reach the final state, steady-state relaunch (where the results of one simulation that has reached steady-state are used to initialize another), and physics minimization, where initial analysis using a global model minimizes the number of included collisional processes. We also present a method that reduces the calculation of the deposition rate onto the substrate. Using our approach, we first use VSim to evolve the plasma and sheath dynamics over electron time scales. Then after reaching steady state, we then maintain the discharge and sheath while computing the spatially dependent deposition rate onto the substrate over longer time scales. Results are compared with those available in the literature.

11:00am PS-WeM-13 Advancements in Multiscale Simulation of Silicon Etching: Broader Implications for Plasma Processing, *Rim Ettouri, Ahmed Rhallabi,* Nantes Université, CNRS, Institut des Matériaux de Nantes Jean Rouxel, France

The Bosch process [1] is fundamental in semiconductor manufacturing, enabling precise etching of deep, high-aspect-ratio silicon structures through alternating etching and passivation cycles. It uses sulfur hexafluoride (SF_6) for etching and octafluorocyclobutane (C_4F_8) for sidewall polymer films, maintaining etch precision and integrity.

Recent studies [2], [3], experimentally explore variations in C_4F_8 plasma parameters and their effects on passivation films, our research approaches these phenomena through advanced simulation [4]. Our research employs a sophisticated Bosch simulator using a multiscale approach, composed of three modules: **global plasma kinetics** for SF_6 and C_4F_8, a **sheet module**, and a **surface module**. This simulation framework allows us to dissect the plasma-assisted etching dynamics [5], examining how operating conditions affect etch profiles and rates.

Building on analyses of oxygen's impact on C_4F_8 plasma [4], we use updated tools to study broader plasma compositions' influences on etching behavior. These studies reveal subtle yet critical shifts in plasma behavior from variations in component ratios, emphasizing the importance of atomic and molecular interactions. Our Monte Carlo cellular approach investigates how changes in machine parameters such as pressure, gas flow, and duty cycle affect scalloping—irregularities in the sidewalls of etched structures—enabling detailed predictions on optimizing etching cycles to minimize these defects. Our findings enhance the understanding of the Bosch process, providing theoretical insights that can inform practical adjustments to improve etch precision and efficiency in semiconductor manufacturing. The implications of this work suggest new avenues for research and application, potentially setting new industry standards.

References
[1] F. Laermer and A. Schilp, "*Method of anisotropically etching silicon*," US5501893A, 1996.
[2] T. Nonaka, K. Takahashi, A. Uchida, S. Lundgaard, and O. Tsuji, "*Effects of C_4F_8 plasma polymerization film on etching profiles in the Bosch process*", J. Vac. Sci. Technol. A, vol. 41, no. 6, 2023.
[3] D. Levko, C. Shukla, K. Suzuki, and L. L. Raja, "*Plasma kinetics of c-C_4F_8 inductively coupled plasma revisited*," J. Vac. Sci. Technol. B, vol. 40, no. 2, p. 022203, 2022.
[4] G. Le Dain, A. Rhallabi, M. C. Fernandez, M. Boufnichel, and F. Roqueta, "*Multiscale approach for simulation of silicon etching using SF_6/C_4F_8 Bosch process*," J. Vac. Sci. Technol. A, vol. 35, no. 3, 2017.
[5] G. Le Dain et al., "*Modeling of silicon etching using Bosch process: Effects of oxygen addition on the plasma and surface properties*," J. Vac. Sci. Technol. A, vol. 36, no. 3, 2018.

11:15am PS-WeM-14 Modeling of Modern Plasma Processing Reactors Using Particle-in-Cell Codes, *Igor Kaganovich,* Princeton Plasma Physics Laboratory, Princeton University; *Dmytro Sydorenko,* University of Alberta, Canada; *Alexander Khrabrov,* Princeton Plasma Physics Laboratory, Princeton University; *Sarveshwar Sharma,* Institute for Plasma Research, India; *Sierra Jubin, Andrew Tasman Powis, Willca Villafana, Stephane Ethier,* Princeton Plasma Physics Laboratory, Princeton University

For plasma processing, there is a need to simulate large plasma devices via kinetic means, because the Electron Velocity Distribution Function in these devices is non-Maxwellian and therefore a fluid treatment is insufficient to accurately capture the physics. The method of choice for many fully kinetic simulations has been the particle-in-cell (PIC) technique due to relatively ease of implementation of the method and that it can be parallelized effectively over many processors and accelerated on GPUs. However, PIC codes that use standard explicit schemes are constrained by the requirement to resolve the short length and time scales associated with the plasma Debye radius and plasma frequency respectively [1]. This makes it extremely challenging to perform long time 2D PIC simulations for large plasma devices. For this reason, many 2D kinetic simulations of plasmas have been limited to small or artificially scaled systems. Energy conserving [2] or implicit methods [3] must be used to remove these limitations. Effects of numerical noise in simulations using PIC code need to be analyzed and taken into account [1]. The PIC codes have been applied to study plasma processing applications, such as capacitively coupled plasmas, electron beam produced plasmas, inductively coupled, hollow cathodes [4-9]. The Darwin scheme was implemented for simulations of inductive discharges.

[1] S. Jubin et al, Phys. Plasmas **31**, 023902 (2024).
[2] A.T. Powis, et al, Phys. Plasmas **31**, 023901 (2024).
[3] H. Sun, et al, Phys. Plasmas **30**, 103509 (2023).
[4] S. H. Son, et al, Appl. Phys. Lett. **123**, 232108 (2023).
[5] L. Xu, et al, Plasma Scie. and Technol. **32**, 105012 (2023).
[6] S. Rauf, et al, Plasma Scie. and Technol. **32**,055009 (2023).
[7] S. Simha, Phys. Plasmas **30**, 083509 (2023).
[8] S. Sharma, Phys. Plasmas **29**, 063501 (2022).
[9] A. Verma, et al, "Study of synchronous RF pulsing in dual frequency capacitively coupled plasma" Plasma Scie. and Technol., to be published (2024).

11:30am PS-WeM-15 Intermediate Pressure Capacitively Coupled Ar/N₂ Plasmas – Experimental Diagnostics and Modeling, *Abhishek Verma, Kallol Bera, Shahid Rauf,* Applied Materials Inc.; *Shadhin Hussain, Matthew Goeckner,* University of Texas at Dallas

Intermediate pressure (1-10 Torr) capacitively coupled plasmas are used for numerous deposition and etch applications in the semiconductor industry. In this work, we describe experiments in a modified Gaseous Electronics Conference (mGEC) reference cell. These measurements are used to validate an in-house hybrid fluid plasma modeling framework for Ar/N₂ capacitively coupled plasmas (CCP) operating at intermediate pressures. The model validation is critical for providing confidence in the model as a predictive tool for development of semiconductor applications as well as elucidate the underlying physics behind the complex mechanisms associated with the plasma processes. For this study, we focused model validation for Ar/N₂ CCP processes in an asymmetric electrode chamber configuration with complex electrical connections. As part of model validation process, the experimental measurements are performed over a range of pressures and powers. The model includes fluid plasma equations for charged and neutral species and a Monte Carlo model for secondary electrons, coupled with Poisson's equation for self-consistent electrostatic plasma description. The model validation study accompanies sensitivity analysis of critical model input parameters for overall uncertainty of model output as well as discussion on experimental uncertainties. Our findings include the model performance over a range of parameters and plasma characterization of Ar/N₂ CCP.

11:45am PS-WeM-16 Controlling the Etch Process by Changing the Plasma Chemistry Through Pulsing, *Evrim Solmaz, Du Zhang,* TEL Technology Center America; *Barton Lane,* Tokyo Electron America; *Yasuaki Sakakibara, Shuichiro Uda, Masahiro Yamazaki, Cedric Thomas, Takehisa Saito,* Tokyo Electron, Japan; *Yu-Hao Tsai,* TEL Technology Center America; *Toru Hisamatsu, Yohei Yamazawa,* Tokyo Electron, Japan

Plasma etching has been a key part of modern integrated circuit fabrication technology. The plasma etch process can be both material-selective and

directional, enabling significant control of etch profiles. Among various plasma tuning features, the pulsed power operation has emerged as an effective option to provide additional controls to plasma properties for improving the etch results. A challenge of optimizing the pulse setting for each target, no different from other conditions, is the tremendous number of possible combinations which makes the purely empirical process development costly. As a remedy, we show that the pulsed plasma modeling can guide not only the process development but also real time control. Pulsing changes the plasma chemistry through the differences in the timescales of important phenomena. We identify and exploit these timescales to enhance the process control and address challenges associated with high aspect ratios and small CDs (critical dimensions). We show how the pulse repetition frequency (PRF) affects individual radical neutral fluxes, hence the F/C ratio in fluorocarbon plasmas. The result implies a possible etch/deposition flavor change as the differences in the generation and decay times of F and C radicals (C, CF, CF_2, CF_3) are the culprits for the lean and polymerizing regimes. Pulsing also affects electronegativity by separating the electron and ion decay timescales. In addition to the radical ratio, we show simulation results of an ion-ion chlorine plasma where the electrons are depleted quickly in the afterglow of the pulsed discharge. The formation of an ion-ion plasma explains the mechanism by which etching continues into the afterglow, as evidenced by recent experimental data. With an offset bias pulse, we observe a continued albeit slower directional etch process. Electrons are long gone in the source afterglow, but vertical etching still carries on, which shows that there are still ions present. This finding suggests that it is possible to control the electronegativity and the vertical etch rate by selecting when to employ the offset bias pulse.

Quantum Science and Technology Mini-Symposium
Room 123 - Session QS-WeM

Quantum Technologies: From Networks and Education to Sensors and User Facilities

Moderators: Vijaya Begum-Hudde, University of Illinois at Urbana-Champaign, **Sean Jones**, Argonne National Laboratory

8:00am QS-WeM-1 The New York Quantum Network: An Advanced Platform for Experiments in Real-Life Conditions, *Gabriella Carini,* Brookhaven National Laboratory **INVITED**
The BNL – SBU (Brookhaven National Laboratory – Stony Brook University) team has built one of the longest and most advanced quantum networks now covering more than 161 miles with five distinct nodes on Long Island. The network uses commercial optical fibers and operates at standard telecommunication wavelengths. It includes quantum memories and remote-control capabilities. Research to expand the use of different quantum platforms and network links including free space link for a truly heterogeneous quantum network is ongoing. The team is focused on developing quantum network key technologies as well as novel applications of entanglement distribution network. An overview of the activities will be presented at the conference.

8:45am QS-WeM-4 The UCSB NSF Quantum Foundry, *John Harter,* UC Santa Barbara **INVITED**
Founded through the NSF's Q-AMASE-i initiative, the Quantum Foundry at UC Santa Barbara is a next generation materials foundry that develops materials and interfaces hosting the coherent quantum states needed to power the coming age of quantum-based electronics. The mission of the Foundry is to develop materials hosting unprecedented quantum coherence, train the next generation quantum workforce, and to partner with industry to accelerate the development of quantum technologies. In this talk, I will present a broad overview of the activities and services of the UCSB NSF Quantum Foundry over the last several years.

9:15am QS-WeM-6 Recent Progress in Quantum Applications via the Q-One Single Ion Implantation System, *Gianfranco Aresta, Kristian Stockbrodge,* Unit B6, UK*; Kate McHardy, Paul Blenkinsopp,* Ionoptika Ltd., UK
Quantum computing has the potential to revolutionize many aspects of modern technology, including digital communications, "quantum-safe" cryptography, and incredibly accurate time measurements. The development of this technology represents the next great frontier of science and engineering.

Devices based on single impurity atoms in semiconductors are receiving attention as potential quantum technologies and shown to be promising proof-of-concept.

However, such devices are incredibly challenging to manufacture, as single atoms must be placed within nanometric precision in isotopically pure host matrix such as ^{28}Si.

All working devices thus far have been fabricated using hydrogen lithography with an STM followed by atomic layer deposition. This is labor-intensive and requires several days of meticulous preparation to create just a single quantum bit (qubit).

Real-world devices will require arrays of hundreds or thousands of impurity atoms, highlighting the requirement for a scalable method of positioning single atoms with nanometer precision.

In 2019, Ionoptika launched a new commercial focused ion beam (FIB) instrument specifically made for the fabrication of quantum materials and devices via single ion implantation, the Q-One.

With a continuously expanding range of available ion species, a high-resolution mass-filter system, high-precision stage and proven capability of single ion deterministic implantation with isotopic resolution, Q-One is, nowadays, the instrument of choice for Universities and Research Institutes.

During last year's AVS Conference we reported on the overall Q-One performances and Liquid Metal Alloy Ion source development carried out at Ionoptika, since the instrument launch.

This year we will report on the results achieved with the Q-One instrument by different research groups. Due to the fact that the ion dose delivered to the sample can be adjusted across a wide range, providing many nanoscale material engineering capabilities in a single tool, examples of the Q-One use as a photolithographic tool, to achieve a ^{28}Si matrix, and single ion implantation will be reported and discussed.

9:30am QS-WeM-7 Laying the Foundation for a Global Quantum EconomyThrough Sensors and Standards, *Barbara Goldstein,* NIST **INVITED**
Bringing quantum technologies out of the lab and into the market requires a new foundation of metrology and standards. Quantum 2.0, which exploits properties like superposition and entanglement, presents a new suite of parameters to measure, requires the characterization of components in new environments such as at cyrogenic temperatures, and challenges us to come up with benchmarks that work across multiple and rapidly changing hardware platforms, such as for quantum computing and networking. This talk will explore the role of standards in critical and emerging technologies, how the broader quantum community is working together to develop pre-standards (NMI-Q) and standards (IEC/ISO JTC-3), and will provide an overview of the NIST on a Chip program which is developing a suite of intrinsically accurate, fit-for-function quantum-based sensors and standards.

11:00am QS-WeM-13 PARADIM: An NSF-Supported National User Facility that can help YOU Discover and Perfect Quantum Materials, *Darrell Schlom,* Cornell University **INVITED**
Creating quantum materials with unprecedented properties, by design rather than by serendipity, is accomplished in PARADIM through a synergistic set of user facilities dedicated to theory, synthesis, and characterization. Each of these world-class user facilities is equipped with the latest tools, techniques, and expertise to help users like you realize this materials-by-design dream. Users from throughout the nation are using PARADIM to discover and create quantum materials.*

PARADIM's vision is to democratize materials discovery in the U.S.A. and to enable a more effective way of pursuing materials research, one that accelerates materials discovery by establishing a materials discovery ecosystem—a national community of practitioners—and equipping them with theoretical and experimental methods that enable them to reduce to practice the inorganic materials of which they dream. Among the tools that PARADIM provides it users are:

• A fully automated MBE system in which users can select among 62 elements of the periodic table and grow at substrate temperatures as high as 2000 °C—the most elements and the hottest growth temperatures of any MBE system in the world—to make the inorganic materials desired. Any 11 of these elements may be loaded into the MBE system at one time.

• An *in situ* UHV connection between PARADIM's 62-element MBE system and a spin-resolved ARPES system enabling users to determine the electronic structure of the new materials and interfaces they create.

• A scanning transmission electron microscope that has achieved the highest resolution ever reported (0.16 Å). This is made possible by a new electron microscope pixel array detector (EMPAD), developed at Cornell, and made available first in PARADIM's electron microscopy user facility.

Use of PARADIM facilities and associated user facilities at Cornell and Johns Hopkins is free to users from academia and national labs from the U.S.A. provided their 2-page proposal is highly ranked by PARADIM's User Proposal Review Committee. All data from PARADIM facilities is recorded and stored for future use. After a period of inactivity or completion of scientific publications by the primary users, all data associated with user projects is made publicly available. PARADIM is also open to users from industry, who pay for access to PARADIM user facilities, but whose data are never made public.

*The capabilities and success stories described in this talk made use of the facilities of the *Platform for the Accelerated Realization, Analysis, and Discovery of Interface Materials* (PARADIM), which are supported by the National Science Foundation under Cooperative Agreement No. DMR-2039380.

Surface Science
Room 120 - Session SS+2D+AMS-WeM

On-Surface Synthesis: Atomic and Molecular Ensambling on Surfaces

Moderators: Irene Groot, Leiden University, The Netherlands, **Nan Jiang**, University of Illinois - Chicago

8:30am **SS+2D+AMS-WeM-3 Tailoring Pt-Based Organometallic Nanomesh on Ag(111): A Model System for "Host-Guest" Chemistry**, *Vanessa Carreño-Diaz, Alisson Ceccatto, Eidsa Brenda da Costa Ferreira, **Abner de Siervo**, University of Campinas (UNICAMP), Brazil*
On-surface synthesis has been extensively used to produce complex functional nanostructures, such as Metal-Organic Frameworks (MOFs). MOFs are composed of highly ordered molecular structures, where metal adatoms act as connecting nodes, generating porous structures that exhibit a long-range order, offering a favorable environment for the adsorption and reaction of molecules in confined spaces, the so-called "host-guest" chemistry [2]. In the present work, we have studied the formation of bidimensional porous networks with hexagonal geometry (nanomesh) resulting from the combination of two molecular precursors: 1,3,5-tris[4-(pyridin-4-yl)-[1.1'-biphenyl])benzene (TPyPPB) and dichloro-(1,10-phenanthroline) -platinum(II) (Cl$_2$PhPt), deposited on the surface of Ag(111). Our results reveal that when the TPyPPB molecules are deposited on the Ag(111) surface, they adopt a porous arrangement with triangular packing mediated by hydrogen bonds [3]. On the other hand, in the presence of the Cl$_2$PhPt molecule, the chemical interactions between both molecules change upon annealing at 400K, which leads to various ordering patterns before stabilizing in a network with hexagonal geometry. After dehalogenation, the Cl$_2$PhPt molecule is transformed into a new complex, PhPt, maintaining the Pt atom in its structure. The Cl atoms dissociated from the Cl$_2$PhPt precursor decorate the periphery of TPyPPB molecules. PhPt molecules can interconnect TPyPPB molecules through metallic coordination between the Pt atom and the N from the pyridyl group (N–Pt–N). The present investigation is based on room temperature scanning-tunneling microscopy (STM) measurements. This experimental approach allows us to explore the properties and structure of these materials at the atomic and molecular levels, opening new perspectives on the design and properties of MOFs.

Acknowledgments:

This work was financially supported by FAPESP (2022/12929-3), CNPq, and CAPES from Brazil.

1.Barth, J., Costantini, G. & Kern, K. Engineering atomic and molecular nanostructures at surfaces. Nature 437, 671–679 (2005).

2.Marta Viciano-Chumillas, et al. "Metal-Organic Frameworks as Chemical Nanoreactors: Synthesis and Stabilization of Catalytically Active Metal Species in Confined Spaces". Accounts of Chemical Research 53 (2020) 520–531.

3.Alisson C. dos Santos, Vanessa Carreño-Diaz, et al. "On-Surface Design of Two-Dimensional Networks through Nonmetal Atoms" (under preparation).

8:45am **SS+2D+AMS-WeM-4 Modulating the Reactivity of "Single-Atom Catalyst" Sites Within 2D Metal-Organic Frameworks by Small Structural Distortions**, ***Zdenek Jakub***, CEITEC - Central European Institute of Technology, Czechia*; Jakub Planer, Dominik Hruza, Azin Shahsavar, Pavel Prochazka, Jan Cechal, CEITEC, Czechia*
Detailed atomic-scale understanding is a crucial prerequisite for rational design of next-generation single-atom catalysts (SACs). However, the sub-angström precision needed for systematic studies is difficult to achieve on working SACs. We present a 2D metal-organic system featuring Fe-N$_4$ single-atom sites,[1,2] in which the height of the atomically-defined structure is modulated by the 0.4 Å corrugation of the inert graphene/Ir(111) support. We show that the support corrugation significantly affects the system reactivity, as the sites above the support "valleys" bind TCNQ (tetracyanoquinodimethane) much stronger than the sites above the "hills".[3] The experimental temperature stability of TCNQ varies by more than 60 °C on these seemingly identical sites. We expect that similarly strong effects of sub-angström structural distortions will likely take place whenever large molecules interact with neighboring "single-atom catalyst" sites or when multiple reactants co-adsorb on such sites.

References

[1] Z. Jakub, A. Shahsavar, et al., *JACS*, **146**, 3471–3482 (2024)

[2] Z. Jakub, A. Kurowská, et al., *Nanoscale*, **14**, 9507-9515 (2022)

[3] Z. Jakub, J. Planer, et al., in preparation

9:00am **SS+2D+AMS-WeM-5 On-Surface Synthesis of Polycyclic Heteroatom-Substituted Nanocarbon Materials**, *Willi Auwärter,* Technical University of Munich, Germany **INVITED**
On-surface synthesis protocols provide elegant routes to individual molecular complexes, oligomers, and other nanocarbon materials on metal supports [1]. The resulting structural, physical, and chemical properties can be controlled by heteroatom-substitution.

In this talk, I will present an overview of our activities employing temperature-induced reactions on coinage metal supports in an ultrahigh vacuum environment, affording specific porphyrinoids and BN-substituted nanocarbon materials. On the one hand, routes to unsubstituted, square-type porphyrin tetramers [2] and peripherally O-doped porphyrins are addressed. On the other hand, dehydrogenation processes of borazine [3] and BN-functionalized carbon scaffolds will be discussed, in view of the synthesis and potential transfer of two-dimensional BNC materials.

[1] Grill, L.; Hecht S. Nat. Chem.**2020***, 12*, 115.

[2] Corral Rascon, E. *et al.* J. Am. Chem. Soc. **2023,** *145*, 967.

[3] Weiss, T. *et al.*, Adv. Mat. Interfaces **2024**, 11, 2300774

9:30am **SS+2D+AMS-WeM-7 Atomic-Scale Investigation of the Highly Enantiospecific Decomposition of Tartaric Acid on Chiral Cu Surfaces**, *Avery Daniels, Charles Sykes,* Tufts University*
Enantioselectivity is the quintessential form of structure-sensitive surface chemistry, as differences in reactivity arise solely from the lack of mirror symmetry of the surface. Studying enantioselectivity on chiral surfaces provides insight into the design of enantioselective heterogeneous catalysts, which areimportant in pharmaceutical, agrochemical, and other industries. To determine the optimumsurface facet for a given chemical reaction, it is essential to study the reaction on a wide variety of surface facets. Given the serial nature of surface science experiments on single crystals, high-throughput methods to study multiplefacets at the same time would circumvent this issue. We have designed surface structure spread single crystals (S4Cs) that expose a vast variety of different surface facets ona single sample. Interestingly, a large portion of these facets are also chiral and therefore the use of S4Cs is ideal for studying for enantioselective surface chemistry. Tartaric acid decomposition on chiral Cu surfaces is known to be highly enantiospecific. With spatially resolved X-ray photoelectron spectroscopy (XPS), we have previously investigated the decomposition of tartaric acid on a Cu(110) ± 14o S4Cwhere surfaces vicinal to Cu(14,17,2)R&Swere found to be the most enantiospecific. We have now combined these XPS results with scanning tunneling microscopy (STM) imaging to unveil the atomic-scale origins of the highly enantiospecific decomposition of tartaric acid on chiral Cu surfaces. We found extensiveenantiospecific surface restructuring of surfaces vicinal to Cu(110) leading to the formation of facets vicinal to Cu(14,17,2). This reconstruction of the surface depends on both the TA enantiomer and the chirality of the surface itself, and is therefore enantiospecific. These results provide valuable insight into the origins of structure sensitivity for enantioselective

reactions and demonstrate the efficacy of S4Cs in performing high-throughput surface science investigations.

9:45am SS+2D+AMS-WeM-8 Competition between Hydrogen Bonding and van der Waals Interactions During Binary Self-Assembled Monolayer Formation, *Rachael Farber, Lindsey Penland, H. H. Hirushan, N. Dissanayake,* University of Kansas

Binary self-assembled monolayers (SAMs) comprised of polar and nonpolar molecules, such as 3-Mercaptopropioninc Acid (MPA) and 1-Decanethiol (DT), offer the ability to carefully tune the interfacial properties of Au surfaces. The formation of molecularly precise binary SAMs through the displacement of one molecule with another *via* solution phase processing requires fine control over the structure and composition of the initial SAM. While DT has been extensively characterized using ultra-high vacuum (UHV) surface science techniques, the structural properties of MPA SAMs are less well understood. The relationship between solution phase processing procedures of MPA and island vacancy density, domain size, film uniformity, and the subsequent displacement behavior when exposed to DT, has not been established.

In this work, the effects of solution phase incubation temperature and time on MPA SAM formation and subsequent DT displacement behavior were determined using UHV scanning tunneling microscopy. Three MPA incubation procedures were studied: 3 hr MPA incubation at 35 °C (**MPA-1**), 3 hr MPA incubation at 25 °C (**MPA-2**), and 24 hr MPA incubation at 25 °C (**MPA-3**). While **MPA-1** and **MPA-2** both showed the characteristic MPA lattice, **MPA-1** had fewer domain boundaries and vacancy islands compared to **MPA-2**. **MPA-3**, which had the fewest domain boundaries and vacancy islands, showed regions of an MPA bilayer species across the surface. To determine the consequences of defect density and the presence of an MPA bilayer on DT displacement, **MPA-1**, **MPA-2**, and **MPA-3** were subsequently placed in a 2 μM DT solution for 20 min, 60, min, 3 hr, and 24 hr. **MPA-1** and **MPA-2** had comparable rates of DT displacement, with the formation of a high-density DT film across the surface within 3 hr.**MPA-3** had markedly slower DT displacement. Following a 24 hr incubation of **MPA-3** in the DT solution, small regions of the low-coverage, lying down phase (β) and 2-D gas phase (α) of DT were found across the surface. Only after a 48 hr incubation of **MPA-3** in DT did the high-density DT phase form. These results highlight the significance of the bonding interactions of the initial SAM on displacement kinetics during the formation of binary SAMs.

11:00am SS+2D+AMS-WeM-13 Paul Holloway Awardee Talk: Learning More with Less: High-Throughput Screening of Molecular Layer Deposition Processes, *David Bergsman*[1], University of Washington **INVITED**
Because of its ability to deposit organic, inorganic, and hybrid ultrathin films with sub-nanometer thickness and compositional control, molecular layer deposition (MLD) has seen growing interest for use in technologies where precise interfacial control is essential, such as in semiconductor processing, membrane separations, and catalysis. However, development of these technologies is inhibited by the relatively slow process times for MLD vs atomic layer deposition and the large number of combinations of inorganic & organic reactants available to MLD.

This presentation will highlight the intrinsic advantages of accelerating MLD process development, both for technology development and for fundamental research. First, previous work in MLD process development will be highlighted, focusing on areas where comparisons between processes yielded fundamental insight into film growth phenomena. Then, an approach for rapidly screening new materials deposited by MLD using a custom-built, high-throughput, multiplexing MLD-style reactor will be discussed. In such a system, multiple reaction chambers are connected to shared reactants and pumping lines, allowing for the elimination of redundant reactor components and reducing capital costs compared to an equivalent number of independent systems. Finally, an example of how this approach can be applied to future technologies, such as EUV photolithography, will be given, demonstrating how materials made using these parallel systems can be screened for their properties of interest and be used to obtain process-structure-property relationships.

11:30am SS+2D+AMS-WeM-15 Organic Molecular Architectures Synthesized on Si(001) by Means of Selective Click Reactions, *Timo Glaser, Jannick Peters,* Justus Liebig University Giessen, Germany*; Dominik Scharf, Ulrich Koert,* Philipps University Marburg, Germany*; **Michael Dürr,** Justus Liebig University Giessen, Germany

The concept of molecular layer deposition on solid surfaces is promising for the synthesis of layers with well-controlled physical and physicochemical properties. Molecules with two functional groups are suitable building blocks for covalent layer-by-layer synthesis. However, with symmetric bifunctional organic molecules, i.e., with two identical functional groups at one molecule, side reactions which hinder the well-controlled layer-by-layer growth, e.g., by chain termination, may occur.

Here we solve this problem using a combination of two selective and orthogonal click reactions for controlled covalent layer-by-layer growth on Si(001). In order to do so, we combine ultrahigh-vacuum- (UHV)-based functionalization of the Si(001) surface with solution-based click chemistry for the attachment of the further layers. The starting point is the Si(001) substrate which is functionalized via selective adsorption of the bifunctional ethynylcyclopropylcyclooctyne (ECCO) molecule under UHV conditions [1]. This first-layer sample is then transferred into solution [2] in order to perform the subsequent layer-by-layer synthesis using the two orthogonal click chemistry reaction steps in an alternating fashion: First, a diazide is coupled in acetonitrile via a copper-catalyzed azide-alkyne click reaction; second, a layer of ECCO molecules is coupled via a catalyst-free, strain-promoted azide-alkyne click reaction. Without contact to ambient conditions, the samples are analyzed by means of X-ray photoelectron spectroscopy in UHV after each reaction step in solution; the N 1s spectra clearly indicated in the first step the selective click reaction of the primary azido group of the diazide molecule, whereas the tertiary azido group stayed intact. In the second step, this tertiary azido group was reacted selectively with the strained triple bond of the ECCO molecule in solution, forming a third layer of organic molecules on Si(001) with the terminal triple bond of ECCO available for further reactions according to this cyclic reaction scheme. Alternating application of the two orthogonal reaction steps then led to a well-controlled layer-by-layer growth up to 11 layers [3]; it opens the possibility for the controlled synthesis of layers with physical or physicochemical properties that alternate on the molecular scale.

[1] C. Länger, J. Heep, P. Nikodemiak, T. Bohamud, P. Kirsten, U. Höfer, U. Koert, and M. Dürr, J. Phys.: Condens. Matter 31, 34001 (2019).

[2] T. Glaser, J. Meinecke, C. Länger, J. Heep, U. Koert, and M. Dürr, J. Phys. Chem. C 125, 4021 (2021).

[3] T. Glaser, J. A. Peters, D. Scharf, U. Koert, and M. Dürr, Chem. Mater. 36, 561 (2024).

11:45am SS+2D+AMS-WeM-16 Confinement Effects at Surfaces, *J. Anibal Boscoboinik,* **Dario Stacchiola,** Brookhaven National Laboratory
Nanosized spaces at surfaces offer an interesting playground to understand the effect of confinement in chemistry and physics. Two examples will be described in this talk. In the first one, the water formation from hydrogen and oxygen is studied on a metal surface both in its bare state and also covered with a two-dimensional porous silicate. A change in reaction pathway is observed due to confinement effects. In the second example, nanosized silicate cages supported on a metal are shown to trap single atoms of noble gases through a new ionization-facilitated trapping mechanism. In this case, the gas phase species are first ionized. These ions can then enter the nanocages, at which point they get neutralized by an electron donated by the adjacent metal, resulting a neutral species that are kinetically trapped inside the confined space.

12:00pm SS+2D+AMS-WeM-17 Facilitating CO_2 Capture Enabled by Weak Intermolecular Interactions Among CO_2, Water and PEEK-Ionenes Membrane, *Jennifer Yao, Lyndi Strange, Jeffrey Dhas,* PNNL*; Sudhir Ravula, Jason Bara,* University of Alabama*; David Heldebrant, Zihua Zhu,* PNNL
Poly (ether ether ketone) (PEEK)-ionene membranes have shown significant potential for direct CO_2 capture due to their high selectivity, durability, and efficiency.[1] Despite their promise, the mechanisms of CO_2 transport through these membranes and the impact of water vapor on its CO_2 capture and diffusion remain poorly understood. Time-of-flight secondary ion mass spectrometry (ToF-SIMS) can detect and distinguish the characteristic molecular ions,[2, 3] making it an ideal tool for studying complex intermolecular interactions of the CO_2, water and the membrane. In this study, a combination of isotopic labeling and SIMS provides a unique method to track small molecules in organic matrixes at nanoscale. We investigated the interactions of PEEK-ionene membranes with $^{13}CO_2$ and

---

D_2O using cryo ToF-SIMS. ToF-SIMS 3D imaging provided chemical mapping of the distribution of these species from the surface down to several micrometers into the membrane. The cryo ToF-SIMS data did not show any significant enhancement of the $^{13}C^-/^{12}C^-$ ratio, implying weak CO_2-membrane interactions and CO_2 vaporization even at -130 °C in vacuum condition. In contrast, cryo ToF-SIMS revealed a relatively uniform distribution of D_2O within the heavy water-loaded membrane. This suggests that water-membrane interactions are stronger than CO_2-membrane interactions. Additionally, the presence of D_2O in the membrane did not enhance $^{13}CO_2$ retention, indicating weak CO_2-D_2O interactions and minimal impact of water vapor on CO_2 diffusion within membrane. For comparison, ToF-SIMS data demonstrated that $^{13}CO_2$ readily reacts with a basic Na_2CO_3 solution to form $NaH^{13}CO_3$, highlighting the potential for modifying CO_2-membrane interactions via functional group modifications. Specifically, introducing basic functional groups may enhance CO_2-membrane interactions, whereas acidic modifications may reduce them.

References:

1. K. O'Harra, I. Kammakakam, P. Shinde, C. Giri, Y. Tuan, E. M. Jackson and J. E. Bara, ACS Applied Polymer Materials, 2022, 4, 8365-8376.

2. L. E. Strange, S. Ravula, Z. Zhu, J. E. Bara, P. Chen, D. J. Heldebrant and J. Yao, Surface Science Spectra, 2024, 31.

3. L. E. Strange, D. J. Heldebrant, S. Ravula, P. Chen, Z. Zhu, J. E. Bara and J. Yao, Surface Science Spectra, 2024, 31.

Thin Films
Room 115 - Session TF-WeM

Vapor Synthesis of Hybrid, Organic, and Polymeric Materials (VSHOP II)

Moderators: Trisha Andrew, University of Massachusetts - Amherst, **Siamak Nejati**, University of Nebraska-Lincoln

8:00am TF-WeM-1 Chemical Vapor Deposition of Metalloporphyrins: Engineering and Integration of Advanced Conjugated Polymers for Catalysis and Sensing, *Nicolas Boscher,* Luxembourg Institute of Science and Technology (LIST), Luxembourg   **INVITED**

Porphyrins have been intensively investigated as catalysts and sensing materials. The properties of porphyrin-based catalysts and sensors can be tailored from the careful selection of the central metal ion chelated at the centre of the macrocycleand its peripheral substituents. Beyond, several studies have highlighted the cooperative effect promoted by conjugated covalent links between porphyrins on both their catalytic and sensing properties. However, in spite of the many synthetic approaches developed towards the synthesis of porphyrin-based conjugated assemblies, the engineering and integration of porphyrin-based conjugated assemblies has been limited by their weak solubility.

Oxidative chemical vapor deposition (oCVD) was recently demonstrated as a convenient method for the simultaneous synthesis and deposition of porphyrin-based conjugated polymers.[1] Porphyrins possessing free *meso*-positions[1-4] and/or free *beta*-positions[5] and porphyrins bearing thienyl or aminophenyl substituents[6] have both been successfully polymerised using oCVD to yield the formation of formation fused porphyrin tapes and bridged porphyrins covalent organic frameworks, respectively. Importantly in the perspective of practical application, including heterogeneous electrocatalysis and gas sensing, the porphyrin-based conjugated polymers are readily deposited on virtualy any substrate in the form of smooth and thickness-controlled thin films.

Up-to-date, porphyrin-based conjugated polymer thin films prepared by oCVD have been successfully investigated for the electrochemical hydrogen evolution reaction,[2] nitrate reduction reaction,[6] oxygen reduction reaction,[6] oxygen evolution reactions.[3] In addition, porphyrin-based conjugated polymer thin films prepared by oCVD have also been successfully investigated as chemiresistive sensors for ammonia detection.[4] Experimental and theoretical data demonstrate the impact of both the central metal cations and substituents on the catalytic activitiesand sensing properties of the porphyrin conjugated polymer thin films.[2-6] The approach reported in this work circumvents many limitations of solution-based approaches and pave the way to the facile engineering and integration of efficient electrocatalysts and selective sensing materials from porphyrins.

[1] Bengasi *et al.*, *Angew. Chem., Int. Ed.* **2019**. [2] Huerta-Flores *et al.*, *ACS Appl. Energy Mater.* **2020**. [3] Bansal *et al.*, *J. Mater. Chem. A* **2023**. [4] Bengasi *et al.*, *Adv. Elect. Mat.* **2020**. [5] Bansal *et al.*, *Chem. Eur. J.* **2024**. [6] Mohamed *et al.*, *Adv. Mater.* **2024**.

8:30am TF-WeM-3 Introducing Non-Covalent Interactions during initiated Chemical Vapor Deposition (iCVD), *Rong Yang, Pengyu Chen,* Cornell University

Initiated Chemical Vapor Deposition (iCVD) has been increasingly studied in the solvent-free synthesis and manufacturing of polymeric thin films. It eliminates bulk solvents, thus improving the environmental sustainability of polymer synthesis. Its scalability points to a new pathway for accelerating the development and environmentally friendly manufacturing of polymeric nanomaterials. While prior research has predominantly leveraged the all-dry and low-pressure reaction environment to achieve ideal gas behavior and thereby controlled synthesis conditions, recent advances in iCVD synthesis have unlocked an opportunity to depart from the ideal gas regime. In this talk, I will discuss our results on introducing non-covalent interactions to preorganize molecules and access new chemical synthesis pathways to broaden the palette of attainable polymer chemistry and morphologies. Leveraging hydrogen bonding, we demonstrated that complexing 4-vinylpyridine with hexafluoroisopropanol could increase the polymer molar mass by 700%, which in turn led to unprecedented material hardness and surface morphologies. Building from this demonstration, we tackled the challenge of undesirable chain transfer (e.g., to the imidazole group during the polymerization of 1-vinylimidazole), which has limited the synthesis of an important class of amine/imidazole-containing polymers using iCVD polymerization. Using 1-vinylimidazole as an example, we protonated the transfer-to location via a vapor complexation with acetic acid, rendering the chain transfer energetically unfavorable and enabling synthesis of poly(1-vinylimidazole) films with unprecedented purity, molar mass, and highly controllable polymerization kinetics. This new synthetic capability, in turn, led to the discovery of a novel bioactive material.

8:45am TF-WeM-4 oCVD PEDOT Thin Film as the Hole Transport Layer in Perovskite Solar Cellto Enhance Device Stability and Performance, *Meysam Heydari Gharahcheshmeh,* San Diego State University/ Department of Mechanical Engineering

Stability concerns have hindered the practical use of perovskite solar cell (PSC) devices. One significant factor contributing to this issue is the inherent acidity of the commonly used hole transport layer, poly(3,4-ethylene dioxythiophene):polystyrene sulfonate (PEDOT:PSS), potentially jeopardizing the stability of PSC devices. To address this challenge, this study explores employing oxidative chemical vapor deposition (oCVD) with antimony pentachloride (SbCl5) as a liquid oxidant for fabricating PEDOT-Cl thin film. This technique is utilized to create stable and ultrathin PEDOT films with high conformity, presenting a promising alternative as a hole transport layer in PSCs. The resulting oCVD-grown PEDOT-Cl thin films, showcase exceptional optoelectronic properties, precise nanostructure control, stability, and integration capabilities. These attributes establish them as a robust and effective choice to be used as the hole transport layer in PSC device. Integration of oCVD PEDOT-Cl thin films as the hole transport layer in PSCs yields a remarkable power conversion efficiency (PCE) of 20.74%, surpassing the 16.53% PCE achieved by spin-coated PEDOT:PSS thin films treated with dimethyl sulfoxide (DMSO) as a polar solvent. Additionally, PSCs incorporating oCVD PEDOT-Cl thin films exhibit a noteworthy 2.5× improvement in stability compared to their PEDOT:PSS-DMSO counterparts.

Keywords: Oxidative Chemical Vapor Deposition, PEDOT, $SbCl_5$ Oxidant, Perovskite Solar Cells

9:00am TF-WeM-5 Networking Density Effects on the Patterning Performance of Metal-Organic Resists Deposited via Hybrid Molecular Layer Deposition, *Long Viet Than, Giulio D'Acunto, Stacey F Bent,* Stanford University

The implementation of extreme ultraviolet (EUV) lithography in semiconductor manufacturing promises to extend Moore's Law by enabling the patterning of sub-20 nm feature sizes. However, further device scaling is dependent on the implementation of EUV-tailored photoresists that meet requirements in sensitivity, resolution, and line edge roughness. With feature sizes approaching the nanometer scale, stochastic variation in the photoresist molecular structure also affects pattern quality, resulting in the need for new resist chemistries with uniform chemical distribution.

Metal-organic thin films deposited via hybrid molecular layer deposition (MLD) are a promising class of materials to address the challenges of

designing new EUV-compatible resist chemistries, by incorporating EUV-absorbing metal centers into the polymer network while exhibiting Å-level thickness control and atomic-scale homogeneity. In this work, we investigated a series of hybrid MLD-derived aluminum alkoxide (alucone) resists, deposited via trimethylaluminum (TMA) and a series of alcohol counter-reactants (glycerol, ethylene glycol, and sequential dosing of methanol/ethylene glycol). This process yielded thin films that are chemically akin, as demonstrated by x-ray photoelectron spectroscopy (XPS), but exhibit notable differences in networking/crosslinking density. The resist performance was evaluated via electron beam lithography, a well-established proxy for EUV. The alucone resists exhibited negative-tone patterning, attributed to the loss of organic ligands and alumina formation resulting from electron-induced reactions. Decreasing the crosslinking density enhanced the resist contrast, thus improving the resolution. On the other hand, increasing the crosslinking density resulted in drastically reduced developer solubility. The variation observed between these hybrid materials underscores the importance of structure-property relationships for the rational design of metal-organic EUV resists.

9:15am TF-WeM-6 Synthesis of Disulfide Polymer by Oxidative Molecular Layer Deposition (oMLD), *Amit K. Datta,* University of Missouri, Columbia*; Nikhila C. Paranamana, Patrick J. Kinlen, Matthias J. Young,* University of Missouri-Columbia

Poly-2,5-dimercapto-1,3,4-thiadiazole (pDMCT) is a redox-active polymer consisting of heterocyclic monomer units connected by disulfide bonds. pDMCT has been used as a battery material, biocide, and corrosion inhibitor. Upon electrochemical reduction, the disulfide bonds in pDMCT break to form thiolate anions that readily coordinate with cations, providing lithium ion conductivity for battery applications and allowing for capture of heavy metal cations. In this work, our goal is to study the vapor-phase formation of thin films of pDMCT using oxidative molecular layer deposition (oMLD) for use as a protective coating in solid state lithium-ion batteries. We employ alternating vapor exposures of the 2,5-dimercapto-1,3,4-thiadiazole (DMCT) monomer and a molybdenum pentachloride ($MoCl_5$) chemical oxidant to perform oMLD growth in a custom viscous-flow reactor at 150 °C and ~1 Torr. We employ *in situ* quartz crystal microbalance (QCM) studies during growth to understand the film growth chemistry, as well as *ex situ* spectroscopic and electrochemical characterization to confirm formation of pDMCT. QCM studies and *ex situ* thickness measurements indicate controlled linear growth. We examine the effect of precursor dose times on polymer chain length, and the effect of polymer chain length and film thickness on electrochemical properties. The controlled growth of ultrathin films of pDMCT shows promise for the application of this chemistry as a protective coating for lithium-ion battery applications and for passive uptake of heavy metal ions. More broadly, these studies establish that oMLD can be used to create polymers connected by disulfide linkages, opening a new class of polymers accessible by oMLD synthesis.

9:30am TF-WeM-7 High-Throughput MLD for Advanced EUV Photoresists: Stability and Performance of Organic-Inorganic Hybrid Films, *Duncan Reece,* University of Washington, UK*; Emily Crum, Amy Dao, Jane Keth, David Bergsman,* University of Washington

The development of sub-5nm semiconductor architectures requires photoresists that efficiently absorb Extreme Ultraviolet (EUV) light, maintain structural integrity under high-energy exposure, and are sufficiently thin for precise patterning while being robust enough to withstand the processing environment. Molecular Layer Deposition (MLD) is exceptionally well-suited for this purpose due to its precise control over film composition and thickness, which is crucial for tailoring photoresist properties to meet the stringent specifications of next-generation lithography.Using our previously published high-throughput multi-chamber MLD system, we investigated the stability and mechanical properties of organic-inorganic hybrid thin films designed for EUV lithography applications. MLD's capability to layer angstrom-thick films precisely enables the creation of photoresists that are both thin enough for advanced lithographic detail and durable against developers and etchants.We synthesized 18 different film chemistries using combinations of three organometallic precursors—diethyl zinc, trimethylaluminum, and tin(IV) t-butoxide—and six organic precursors: ethylene glycol, 1,2,4-trihydroxybenzene, 1,5-hexadiene-3,4-diol, 2-butyne-1,4-diol, cis-2-butene-1,4-diol, and 2-methylenepropane-1,3-diol. These films were evaluated for stability in air, developer compatibility, and etchant resistance, both before and after UV exposure. Candidates exhibiting enhanced properties post-exposure were further assessed for mechanical robustness using Atomic Force Microscopy and nanoindentation.Further characterization involved Fourier Transform Infrared Spectroscopy and X-ray Photoelectron Spectroscopy to elucidate degradation pathways and confirm structural integrity. Understanding these pathways is essential for assessing film stability and performance. Selected materials demonstrating optimal performance profiles underwent patterning tests using an electron beam source, with results visualized via Scanning Electron Microscopy.Our findings reveal that specific combinations of organic and inorganic components yield films with significantly improved mechanical properties and stability in air and potential developers. This research primarily aims to understand why certain combinations result in superior film properties, providing valuable insights into the development of advanced EUV photoresists. By emphasizing the fundamental aspects of material behavior, we highlight the efficacy of high-throughput MLD in the rapid screening and optimization of photoresist materials, advancing semiconductor technology.

9:45am TF-WeM-8 Development of a 300mm Wafer Scale Molecular Layer Deposition Process, *Christophe Vallee, **Van Long Nguyen,*** University at Albany-SUNY*; Ornella Sathoud, Danny Newman, Jean Felix Sathoud, James McAdams, Cory Wajda, Kandabara Tapily, Gert Leusink,* TEL Technology Center America

Molecular layer deposition (MLD) is an advanced technique for depositing polymeric thin film at the molecular level control. In comparison to the well-known sister method for depositing inorganic thin film, the atomic layer deposition (ALD), research on MLD is still relatively limited in applications, especially in the semiconductor industry, due to the difficulty in finding suitable precursors. Organic precursors for MLD processes are typically low volatility, stability, and reactivity, which is a critical bottleneck limiting its utilization in high-volume semiconductor manufacturing that is based on 300mm wafer process platforms. In this paper, we report the development of a MLD process using a 300mm wafer process tool. MLD of polyamide, nylon 2,6, was first developed at 85ºC using two precursors which are ethylene diamine (ED) and adipoyl chloride (AC). While ED has high vapor pressure providing growth saturation easily, low volatility AC precursor requires longer dosing times to reach the growth saturation and is the critical one for optimizing the growth per cycle (GPC) of our MLD process on the 300mm wafer tool (**Figure 1a**). Furthermore, the bubbling dosing mode is more effective in delivering AC to the chamber in comparison to the vapor-draw dosing mode. Our optimized MLD process shows linear growth of 0.12 nm/cycle with 15 cycles of nucleation delays on the Si wafer (**Figure 1b**). The uniformity of the deposition until 120 cycles was less than 4.8% across a 300mm Si wafer. The process is undergoing further optimization to improve GPC, uniformity, and processing time. Ellipsometry, AFM, ATR-FTIR, and XPS are key techniques for the characterization of the film growth for our MLD process.

11:00am TF-WeM-13 Area Selective Deposition of Ferrocene-Functionalized Thin Films, *Justin Lomax,* The University of Western Ontario, Canada*; Eden Goodwin,* Carleton University, Canada*; Jordan Bentley,* The University of Western Ontario, Canada*; Mark Aloisio, Cathleen Crudden,* Queen's University, Canada*; Seán Barry,* Carleton University, Canada*; **Paul Ragogna,*** The University of Western Ontario, Canada **INVITED**

Ferrocene is a stable molecule with well understood redox activity, and has been utilized extensively in areas such as bio-sensing, organometallic chemistry, and materials science.[1–3] This work leverages the utility of ferrocene precursors for solution and vapour phase depositions that prepare ferrocene-based thin films. There was an affinity for the deposition to occur selectively on metallic substrates, and therefore the area-selective deposition of ferrocene-containing precursors was demonstrated, which has potential applications for onwards application in nanoscale device fabrication.[4] Preparation of the small molecule precursors will be discussed as well as the analysis of the fabricated thin film/monolayers via X-ray photoelectron spectroscopy (XPS), Time-of-Flight Secondary Ion Mass Spectrometry (ToF-SIMS), Atomic Force Microscopy (AFM), surface Raman spectroscopy, and X-ray Reflectivity (XRR)

(1) Ferrocene—Beauty and Function. *Organometallics* **2013**, *32* (20), 5623–5625. https://doi.org/10.1021/om400962w.

(2) van Staveren, D. R.; Metzler-Nolte, N. Bioorganometallic Chemistry of Ferrocene. *Chem. Rev.* **2004**, *104* (12), 5931–5986. https://doi.org/10.1021/cr0101510.

(3) Hauquier, F.; Ghilane, J.; Fabre, B.; Hapiot, P. Conducting Ferrocene Monolayers on Nonconducting Surfaces. *J. Am. Chem. Soc.* **2008**, *130* (9), 2748–2749. https://doi.org/10.1021/ja711147f.

(4) Parsons, G. N.; Clark, R. D. Area-Selective Deposition: Fundamentals, Applications, and Future Outlook. *Chem. Mater.* **2020**. https://doi.org/10.1021/acs.chemmater.0c00722.

11:30am TF-WeM-15 Infiltration of Methanol Vapor Induces Lattice Flexibility in Microporous Ni$_2$(BDC)$_2$DABCO Thin Films, *Greg Szulczewski*, The University of Alabama

Thin films of Ni$_2$(BDC)$_2$DABCO, where BDC is benzendicarboxylic acid and DABCO is 1,4-diazabicyclo[2.2.2]octane, were made by a hot vapor-assisted conversion technique. The thin films were characterized by x-ray diffraction, vibrational spectroscopy and scanning electron microscopy. The polycrystalline films were determined to be phase pure by powder x-ray diffraction. Infrared and Raman spectroscopy reveals the carboxylic acid ligands were converted into carboxylates. The films were activated by heating under high vacuum and adsorption/desorption isotherms were measured for several volatile organic compounds, including alcohols, nitrobenzene, toluene, and methyl iodide vapors at room temperature. The isotherms revealed a Type I behavior for ethanol, isopropanol, toluene nitrobenzene, and methyl iodide vapors. In contrast, the isotherm for methanol has a characteristic S-shape, which is characteristic of a flexible lattice. The adsorption isotherm for methanol has distinct steps, which is attributed to lattice expansion. Upon removal of methanol from the thin film, the lattice relaxes back to the original structure. The results are compared to other pillared microporous coordination compounds.

11:45am TF-WeM-16 Nanomolecularly-Induced Kinetic, Chemical, and Morphological Effects During Thin Film Synthesis of Hybrid Inorganic/Organic Nanolaminate Multilayers, *Collin Rowe, Geetu Sharma,* Materials Science and Engineering Department, Rensselaer Polytechnic Institute*; Arnaud Devos,* Institute of Electronics, Microelectronics and Nanotechnology, CNRS UMR 8250, France*; Henrik Pedersen,* Department of Physics, Chemistry, and Biology, Linköping University, Sweden*; Ganpati Ramanath,* Materials Science and Engineering Department, Rensselaer Polytechnic Institute

Molecular nanolayers (MNLs) at inorganic thin film interfaces are known to improve chemical stability, and stimulate completely unexpected mechanical responses and electrical and thermal transport behaviors[1]. Stacking inorganic/organic thin film interfaces with nanoscale proximity, e.g., in high-interface-fraction multilayers, offers promise to access emergent properties via superposition of nanomolecular effects. Synthesizing such structures requires low-temperature depositions of high-quality ultrathin inorganic nanolayers to preserve the integrity of the MNLs. Here, we will demonstrate the synthesis of titania/organo-diphosphonate[2] and AlO$_x$N$_y$/hydroquinone multilayers with sharp interfaces by sequential atomic- and molecular-layer deposition (ALD/MLD) cycles. Our results from electron microscopy, X-ray diffraction, and ion beam and photoelectron spectroscopy measurements show that MNLs can significantly alter the inorganic nanolayer growth rate, composition, surface roughness, and phase stability. Examples include up to ~50% decrease in titania growth rates by diphosphonate MNLs, and near complete aluminum nitride to oxide conversion by hydroquinone MNLs. Atomistic mechanisms underpinning these changes will be discussed in terms of the impact of the MNL backbone structure and terminal chemistry on the surface reaction pathways. Acoustic pump-probe spectroscopy measurements on our hybrid multilayers reveal unusual acoustic damping responses which will be described in terms of the MNL interface chemistry and nanolayer periodicity. Further understanding and harnessing such MNL-induced effects and their correlations with emergent properties is crucial for designing high-interface-fraction hybrid nanolaminates for applications.

[1] *Engineering inorganic interfaces using molecular nanolayers*, G. Ramanath, C. Rowe, G. Sharma, V. Venkataramani, J. G. Alauzun, R. Sundararaman, P. Keblinski, D. G. Sangiovanni, P. Eklund, H. Pedersen, **Appl. Phys. Lett.** 122, 260502 (2023).

[2] *Nanomolecularly-induced effects at titania/organo-diphosphonate interfaces for stable hybrid multilayers with emergent properties*, C. Rowe, A. Kashyap, G. Sharma, N. Goyal, J. G. Alauzun, S. T. Barry, N. Ravishankar, A. Soni, P. Eklund, H. Pedersen, G. Ramanath, **ACS Appl. Nano Mater.** (2024).

12:00pm TF-WeM-17 The Impact of Copolymer Molecular Sequence on Electronic Transport, *Mahya Mehregan,* University of Missouri-Columbia*; Jack Schultz, Matthew R. Maschman, Matthias J. Young,* University of Missouri, Columbia

Conjugated polymers (CPs) have garnered significant attention for application in electronics and electrochemical devices, including supercapacitors, solar cells, electrochromics, batteries, microelectronics, and sensors. Blending different conjugated monomers together into copolymers provides a powerful platform for controlling CP properties. However, to rationally improve the performance of conjugated copolymers in these electronic and electrochemical applications, a fundamental understanding of how copolymer structure influences electronic transport is necessary. Conventional synthesis methods for CPs provide poor control over the short-range molecular structure, or sequence, of copolymers, making it difficult to understand the role of short-range molecular structure on electronic transport. Here, we employ vapor-phase oxidative molecular layer deposition (oMLD) at 150°C and ~1 Torr to deposit thin films of conjugated copolymers one monomer at a time, providing control over the copolymer molecular sequence. Because oMLD is a vapor deposition technique, these polymers are also chemically pure with no side-chains or additives. In this study, we specifically control the molecular sequence of copolymers of 3,4-ethylenedioxythiophene (EDOT) and pyrrole (Py) by adjusting the dosing scheme of EDOT and Py monomers during oMLD growth. Using this synthesis approach, we establish new insights into how short-range molecular structure influences electronic transport through these copolymers. Specifically, we find:(1) a departure from the rule of mixtures, where the block length of each homopolymer within the copolymer influences the overall electronic conductivity even at a constant overall composition; and (2) evidence for a critical hopping distance (or quasi-Debye length) between conductive domains, where electronic conductivity decreases by multiple orders of magnitude when the spacing between conductive domains is greater than this critical distance. The fundamental insights into the electronic conductivity through conjugated copolymers we describe will inform the design of conjugated copolymers for electronic and electrochemical devices. More broadly, this study demonstrates that oMLD can be used as a platform for polymer materials discovery by synthesizing copolymers with precise control of molecular sequence.

2D Materials
Room 122 - Session 2D-WeA

2D Materials: Sensors and Devices
Moderator: Andrey Turchanin, University of Jena

2:15pm 2D-WeA-1 Electric-Field-Sensitive Polymer Electrolytes for Non-Volatile Doping of Two-Dimensional Field-Effect Transistors, *Susan Fullerton Shirey, Dnyanesh Sarawate, Priscilla Prem,* University of Pittsburgh; *Ke Xu,* Rochester Institute of Technology; *Eric Beckman,* University of Pittsburgh **INVITED**

Solid polymer electrolyte gating provides access to regimes of transport in two-dimensional (2D) materials that would otherwise be inaccessible using conventional gate dielectrics. The enabling mechanism is the formation of an electric double layer (EDL) at the electrolyte/2D material interface that creates large fields (~V/nm) and therefore induces large p- and n-type carrier densities in 2D materials (~10^{13}-10^{14} cm^{-2}). In this work, we demonstrate a new type of solid polymer electrolyte wherein the electric field created by the ions serves a dual purpose: driving ions to the channel surface to induce heavy doping, and driving chemical reactions that "lock down" the ions at the interface, thereby providing channel doping that persists even after the gate bias is removed (i.e., non-volatile doping). Specifically, the polyethylene oxide (PEO)-based co-polymer is designed with field-sensitive reactive groups to crosslink the polymer and therefore arrest ion mobility, disallowing the ions from diffusing away from the channel surface once the gate is grounded. We demonstrate the non-volatile doping of graphene FETs by applying positive programing gate voltages ($V_G \geq$ +2 V), and then monitoring the Dirac point shift and change in ON/OFF current. The non-volatile doping density is ~4 x 10^{12} cm^{-2}, estimated by shifts in the Dirac point, which is more than ten times greater than the intrinsic carrier density. Sheet carrier densities measured by Hall effect and chemical/physical characterization of the polymer electrolyte will be presented. The work is supported by the National Science Foundation (NSF, U.S.) under Grant No. ECCS-EPMD-2132006

2:45pm 2D-WeA-3 Systematic Identification of the Optical Characterization of Hexagonal Boron Nitride Thickness on 300-nm Oxide Substrate, *Emily Frederick, Kirsten Lina,* University of Central Florida; *Michael Lodge,* Truventic LLC; *Masahiro Ishigami,* University of Central Florida

This work presents a systematic process to identify the thickness of a hexagonal boron nitride (hBN) flake on 300-nm silicon oxide substrate through optical microscopy data. HBN exhibits periodic optical variations for thickness levels making it difficult for precise thickness determination, necessitating use of other means to accurately determine thickness. Determining the thickness of hBN under optical microscopy integrated with machine learning could significantly reduce the time intensive task of locating and identifying useful flakes alongside reducing potential misidentification of ideal or nonideal flakes. We assigned specific standard red, green, blue color values to theoretical thickness values and incorporated the shadow of the flakes to further distinguish the flake's thickness. By creating a systematic annotation technique, we aim to have a more efficient method for determining flake thickness for all 2D materials to better incorporate machine learning processes.

3:00pm 2D-WeA-4 Selective Etching of Hexagonal Boron Nitride Under Graphene Stack Using Sulfur Hexafluoride Gas in Different Pressure to Create Two-Dimentional Material Devices, *Swastik Ballav, Ryuichi Tsuchikawa, Rachid Ben Khallouq, David Castro,* University of Central Florida; *Michael Lodge,* Truventic; *Masahiro Ishigami,* University of Central Florida

Abstract : Recently, twisted bilayer materials fabricated from two-dimensional (2D) materials have been shown to possess unique electronic and optoelectronic properties.Among these, magic angle graphene sandwiched between hexagonal boron nitride (h-BN) has seen significant interests due to its exotic superconducting properties. Sulfur hexafluoride (SF$_6$) gas commonly utilized for its selective h-BN etching, while it stops at graphene to form electronic contact to these devices.

We will discuss the sensitivity of etching parameters for selective etching of h-BN.Specifically, we measured selective etching of h-BN using SF$_6$as a function of varying pressure from 10 to 80 mTorr in helium environment at 30ºC temperature. At higher pressures, graphene acts as an etch stop and leaves underlying h-BN unetched, which can be exploited to make a via for contacts through insulating h-BN. Such pressure-tunable etch selectivity can create unique device structures such as a suspended bridge structure of graphene by etching the underlying h-BN. The selective etching at higher pressures demonstrates the potential of SF$_6$ for fabricating graphene based superconducting devices stacks which can be used to create highly sensitive bolometric device. These findings can contribute towards fabrication of electronic and optoelectronic devices from other 2D materials.

3:15pm 2D-WeA-5 Printed Contacts to Layered Materials, *Sharadh Jois, Erica Lee, Jason Fleischer, Philip Li, Tsegereda Esatu, Edwin Quinn, Aubrey Hanbicki, Adam Friedman,* Laboratory for Physical Sciences

Over the last decade, there has been an outburst in novel layered materials and devices for advanced computing. The common techniques to create electrical contacts to layered materials rely on electron-beam lithography and photolithography that require polymeric resists that leave behind residues that can be impossible to clean. Several advances in lithography-based contact engineering to improve the quality of electrical contacts to layered materials have been pivotal in enabling basic research. The primary approach taken in these methods was to eliminate polymers from coming in direct contact with the active channel material and reduce defects induced by the deposition of metal films. The encapsulation of the active material with hexagonal boron nitride (h-BN) and creating edge contacts, nano-via contacts, or van der Waals contacts, have given the desirable two-fold benefit. However, these methods require many additional steps that consume several days of fabrication involving dry stamping to make the stack and several steps of lithography to etch undesired areas, deposit metal contacts, and lift-off. Each additional step adds failure modes and reduces device yield, thwarting the rapid prototyping of new devices with layered materials. Direct-write printing is capable of creating microscale metallic contacts in a single step. We demonstrate that printed contacts are an alternate method to achieve high-quality electrical contacts to different layered materials while evading the problems with lithography. We benchmark the printed devices using appropriate measurements, such as gating, resistance vs. temperature, or Hall. Our results show that direct-write printing can be used as an alternative to lithography to fabricate devices of layered materials for rapid testing. Furthermore, our work paves the way for creating printed circuits of layered materials for new applications.

3:30pm 2D-WeA-6 Electrical Transport of High-Quality CVD-Grown MoSe$_2$ Nanoribbons, *Y.-J. Leo Sun,* University of Maryland, College Park; *Ona Ambrozaite, Thomas J. Kempa,* Johns Hopkins University; *Thomas E. Murphy,* University of Maryland, College Park; *Adam L. Friedman, Aubrey T. Hanbicki,* Laboratory for Physical Sciences

Two-dimensional (2D) materials such as transition metal dichalcogenides are excellent candidates for creating novel nano-electronic and photonic devices. Previous research indicates that the edge states of MoS$_2$ could strongly influence its conductivity, and the 2D honeycomb structure enables different electronic performance along the zigzag and armchair edges. Understanding and controlling the conductivity is essential in devices like field effect transistors that use MoS$_2$ as the channel. To date, transport along edge states of MoSe$_2$ nanoribbons, which have substantially reduced dimensionality relative to 2D crystals, has not been explored. In this project, we used chemical vapor deposition (CVD) to synthesize MoSe$_2$ nanoribbons through directed growth on phosphine (PH$_3$)-treated Si substrates. This approach yields directed growth of monolayer MoSe$_2$ to form narrow (< 1μm) nanoribbons. Tip-enhanced photoluminescence (TEPL) maps reveal a significant difference between the emission intensity at the edges and center of the nanoribbon. To perform electronic transport measurements, we used e-beam lithography to pattern contacts on the nanoribbons in a Hall bar configuration with the side contacts at the edges and tips of the nanoribbons. The nanoribbon was encapsulated by hBN flakes, and select regions were etched to facilitate the fabrication of edge contacts to reduce contact resistance. The influence of edge states on the electrical performance of MoSe$_2$ nanoribbons was investigated by conductivity and Hall transport measurements. Current flow in the transverse and longitudinal directions of the nanoribbon was compared to analyze the importance of edge states on MoSe$_2$ nanoribbon conductivity.

4:15pm 2D-WeA-9 Ultra-Low Energy Consumption Memory Study Using 2D Materials Heterostructures, *Young-Jun Yu,* Chungnam National University, Republic of Korea **INVITED**

Van der Waals (vdW) heterostructures using two dimensional (2D) atomic crystals have been attracted intensely for high performance as well as low-power memory applications. Furthermore, floating-gate (FG) memory devices based on 2D heterostructures exhibit stability with dielectric

barriers such as hexagonal boron nitride (hBN) between semiconductors and various charge storage layers. However, the reported operation voltage and energy consumption for hBN barriers cannot be reduced below several tens of volts. In this presentation, I will introduce ultrahigh energy efficiency of 2D material heterostructure-based memory devices for approaching to the biological synaptic energy level with employing ultrathin charge-trap layer underneath 2D semiconductor channel.

4:45pm 2D-WeA-11 2D Metal-Dielectric Hybrid Nanostructures via Electrochemical Deposition, *Chao Dun Tan*, *Manfred Buck*, University of St Andrews, UK

Often described as "surfaces without bulk", carbon nanomembranes (CNMs) are an emerging class of dielectric 2D materials 1-2 nanometers thick. These membranes are derived from aromatic self-assembled monolayers (SAMs) which consist of highly ordered, upright-standing molecules that are formed by spontaneous adsorption at the substrate-liquid interface. By exposing these aromatic SAMs to low energy-electron irradiation, intramolecular bonds are cleaved, resulting in a two-dimensional network by crosslinking of the aromatic molecules. These nanomembranes are sufficiently robust to allow release from the substrate, transfer to other supports, and stacking to multiple layers, thus allowing the tuning from electron tunneling through single CNMs to insulating multilayers. Furthermore, their amorphous structure does not impose limitations with regard to scaling.

It is the electron transfer across monolayers that makes CNMs also an attractive platform for electrodeposition and the design of hybrid structures. The approach taken here contrasts established electrochemical applications of CNMs where they have been employed in area-selective electrodeposition to define passivating regions by exploiting the difference in charge transfer across CNMs and native SAMs. Investigating metal electrodeposition onto CNMs, deposition parameters (e.g. potential and time) allow control of nucleation and growth, thus enabling the morphologies of the deposits to range from individual metal nanoparticles to continuous layers. Moreover, exploiting the transferability of CNMs, the scheme offers the prospect to produce hybrid nanostructures defined by electrode structures which serve as reusable master patterns. Since CNMs are chemically inert, they have a large potential window and, thus, provide flexibility as regards electrolytes used and materials deposited. The possibility of generating templated metal/dielectric nanostructures may open pathways for the implementation of CNMs as nanocircuit boards in combination with other 2D materials, metamaterials, or nano-electromechanical systems (NEMS).

5:00pm 2D-WeA-12 Disentangling Anisotropic Resistivities of the Topological Insulator Bi$_4$Br$_4$, *Bert Voigtländer*, *Jonathan Hofmann*, *Serhii Kovalchuk*, *Vasily Cherepanov*, *Timofey Balashov*, *Felix Lüpke*, Forschungszentrum Juelich GmbH, Germany; *Zhiwei Wang*, *Yugui Yao*, Beijing Institute of Technology, China; *Stefan Tautz*, Forschungszentrum Juelich GmbH, Germany

Bi$_4$Br$_4$ is a promising higher-order topological insulator with a highly anisotropic crystal structure. In this material, topological edge states have been observed at room temperature. As a step towards nanoscale electric transport measurements through possible ballistic edge channels at step edges, we disentangle the resistivities of this material in all directions. We combine four-point resistance measurements in the square geometry on a bulk sample of Bi$_4$Br$_4$ with four-point resistance measurements on thin 2D flakes of this material in the linear configuration. These measurements give sufficient information to disentangle the two lateral resistivities along and perpendicular to the quasi-one-dimensional crystal structure, the latter being seven times lower than the conductivity along the atomic rows. Moreover, we can as well disentangle the vertical resistivity, which is much larger (~ 500 times) than the in-plane components. Due to degradation of this material under ambient conditions, we performed the electrical measurements under UHV conditions. Further, due to the micrometer sizes of the thin flakes of this material, a multi-tip scanning tunneling microscope was used to perform the four-point measurements on the micrometer scale.

5:15pm 2D-WeA-13 Electrical Breakdown of 2D Ruddlesden-Popper Metal Halide Perovskites, *Mengru Jin*, Texas A&M University; *Eugenia Vasileiadou*, Northwestern University; *Ioannis Spanopoulos*, University of South Florida; *Kyeong Yeon Lee*, Texas A&M University; *Mercouri Kanatzidis*, Northwestern University; *Qing Tu*, Texas A&M University
Abstract

2D Ruddlesden-Popper (RP) metal halide perovskites (MHPs) have emerged as promising low-cost, high-performance direct bandgap semiconductor materials in a plethora of energy and electronic applications, offering enhanced environmental stability compared to their conventional 3D analogues. Electrical breakdown (BD) in such devices signifies the cumulative degradation of the internal structure of the 2D MHPs, leading to loss of device functionality. Understanding the BD process, its mechanisms and inducements are critical for the commercialization of the semiconductor devices based on 2D MHPs. Here, we investigate the electrical BD behavior of a prototypical family of 2D RP MHPs, (BA)$_2$MA$_{n-1}$Pb$_n$I$_{3n+1}$ (BA = butylammonium, MA = methylammonium cation, and n indicates the number of PbI$_6^{4-}$ octahedra in one repeating unit), using conductive atomic force microscopy (C-AFM).Thin 2D MHP flakes were mechanically exfoliated onto conductive substrate directly from solution-grown single crystals using the scotch-tape method. I-V curves were obtained from flakes to quantify the breakdown strengths as a function of n, thickness and the ramping rate in a dry environment. When the applied bias surpasses a threshold voltage (defined as V$_{BD}$), the current will increase rapidly, which indicates the electrical BD and a hole will be burnt into the flake. Analysis of the hole depth revealed a layer-by-layer breakdown process very similar to that found in boron nitride (BN). The V$_{BD}$ decreases with reductions in either the thickness or the sweep rate. Conversely, the BD strength exhibits an opposing trend, escalating as the thickness decreases. Furthermore, the BD strength increases with n, which reaches ~ 5.45 × 10^8 V/m for a monolayer 2D MHP with n = 5 at a ramping rate of 1 V/s. The BD strength is comparable to those of BN and self-assembled monolayer, implying good intrinsic reliability of 2D MHPs under electrical field. Our work provides the first systematic investigation of the electrical BD of 2D MHPs, which generates indispensable insights into guiding the 2D MHP materials and device design toward long-term durable applications.

Advanced Microscopy and Spectroscopy to Explore Field-Assisted Chemistry
Room 116 - Session AMS1-WeA

Advanced Microscopy and Spectroscopy to Explore Field-Assisted Chemistry I

Moderators: Sten Lambeets, Pacific Northwest National Laboratory, **Daniel E Perea**, Pacific Northwest National Laboratory

2:15pm AMS1-WeA-1 Influence of External Electric Fields on Catalytic Reactions: An Insight through Atom Probe Microscopy and Field Ion Microscopy, *Thierry Visart de Bocarmé*, Université libre de Bruxelles, Belgium **INVITED**

The study of catalytic reactions under the influence of external electric fields has emerged as a significant area of research in the field of chemistry. This research is driven by the potential to manipulate reaction pathways and enhance catalytic efficiency. This presentation will delve deeper into the role of Atom Probe Microscopy (APM) and Field Ion Microscopy (FIM) in elucidating these effects.

Commercial APM models, with their unique abilities to provide 3D atomic-scale compositional information, enable to probe the catalyst's structure and composition before or after reaction but hardly *during* reaction. Using an isolated counter electrode with a tunable static potential, the static field on the catalyst can be adjusted to the desired value by convenient choices of the respective voltages on the sample and the counter electrode. Short voltage pulses are then superimposed on the static voltage of the counter electrode to raise the electric field at the sample surface to trigger field desorption or field evaporation. This methodology aids in measuring how electric fields modify the catalyst's surface composition during the ongoing reaction, and provides insights on the reaction pathways.

On the other hand, FIM, with its capacity for direct imaging of individual atoms and even surface reactions in real-time, provides an unparalleled view of the instant state of the catalyst surface, i.e. the extremity of a sharp tip the size and shape of which approximate those of one single catalytic grain. This enables to directly visualize how electric fields of some 10 V.nm^{-1} affect the behavior of reactants and products on the catalyst surface, thereby influencing the catalytic reactions.

The presentation will highlight several case studies where APM and FIM have been used in providing insights into the influence of electric fields on catalytic reactions. The hydrogen-oxygen reaction on rhodium surfaces has been monitored by video FIM and probed using voltage pulses. The results show that, on one single catalytic grain, the reaction can proceed

Wednesday Afternoon, November 6, 2024

simultaneously through Langmuir Hinshelwood and Mars Van Krevelen-type mechanisms.The water-gas shift reaction on gold surfaces at room temperature has been investigated by FIM and APM and shows that the reaction proceeds through the formation of an hydroxyl-type surface intermediate that is reacted off by the presence of CO gas. Eventually, the nitrogen oxide adsorption on platinum surfaces and its field-dependance will be discussed.

2:45pm AMS1-WeA-3 Ab-Initio Simulation of Field Evaporation in Atom Probe Tomography, *Wolfgang Windl,* The Ohio State University; *Jiayuwen Qi,* Ohio State University; *Emmanuelle Marquis,* University of Michigan
INVITED
Atom probe tomography (APT) is a three-dimensional characterization technique that ideally can resolve both positions and chemical identities of the atoms in a material. Unlike "focused-beam" microscopy techniques which rely on X-rays or electron beams for imaging, in APT, atoms in the sample are imaged by themselves. Individual atoms or molecules are field-evaporated from the surface of a needle-shape specimen under an intense electric field and fly towards a two-dimensional detector where their impact positions and sequence are recorded. From that, along with the chemical identities revealed by a mass spectrometer, a three-dimensional distribution of the atoms in the specimen can be reconstructed. However, since field evaporation is a destructive process, it is impossible to verify reconstruction results and quantify uncertainties in experiments. In this case, atomic-scale forward modeling becomes the only viable way to produce verifiable virtual data to test reconstruction where each single atom is traceable. A number of atomic modeling approaches have been developed during the past 25 years, however, all of them are implicitly based on harmonic transition state theory which can only predict the rate of transition from one state to another but not describe any dynamics between the two states. As an alternative, we propose to simulate field evaporation with full dynamics using molecular dynamics (MD) simulations. For that, we have integrated field evaporation events as part of the MD simulation by combining the electrostatics from the finite element field evaporation code TAPSim with the MD simulator LAMMPS. With full dynamics, atoms in the specimen are evaporated in an "ab-initio" way as a result of the competition between the interatomic forces and the electrostatic forces. To demonstrate our full-dynamics approach, we will show results that explain for the first time the enhanced zone lines in field evaporation maps, "ab-initio" prediction of the evaporation sequence in [001]-oriented γ-TiAl intermetallic compounds explaining the observed artifact of mixed layers, and simulations of GP-zones in Al-Cu alloys that demonstrate the inherent inaccuracies in resolving atomic positions. The overarching goal of this work is to guide APT reconstruction using our "ab-initio" simulation data, gain better interpretations of fundamental processes, and take the quantification capability of the APT technique to the next level.

Advanced Microscopy and Spectroscopy to Explore Field-Assisted Chemistry
Room 116 - Session AMS2-WeA

Advanced Microscopy and Spectroscopy to Explore Field-Assisted Chemistry II
Moderators: Sten Lambeets, Pacific Northwest National Laboratory, **Daniel E Perea**, Pacific Northwest National Laboratory

4:15pm AMS2-WeA-9 Lanthanide Adsorption in Micas: The Implications for Rare Earth Elements Separations, *Yu Wen,* US DOE Ames National Laboratory; *Krishna K. Verma,* Ames National Laboratory; *Dapeng Jing,* Iowa State University; *Michael D. Lacount, Shawn M. Kathmann,* Pacific Northwest National Laboratory; *Tanya Prozorov,* US DOE Ames Laboratory
INVITED
Rare earth elements (REEs) are critical to the economic growth and national security of the United States, but their supply chain is vulnerable to disruptions. To harness underutilized sources of REEs, it is important to understand the localized environments in which these elements occur. Regolith-hosted ion-adsorption clays selectively absorb heavy REEs (HREEs) released through the weathering and dissolution of granites and other igneous rocks by rainwater. This REE adsorption trend is recognized, yet the adsorption mechanisms remain poorly understood.

Our results show that micas, which are structurally and chemically similar phyllosilicates, exhibit a different pattern of REE adsorption. Notably, micas adsorb Nd (a light REE) more readily than Yb (a heavy REE), deviating from

the HREE adsorption trend in regolith-hosted clays. Our findings further revealed the colocalization of lanthanides with impurity ions within the mica structures, underscoring the significant role of internal electric potentials in influencing REE adsorption. This unusual adsorption behavior in micas due to the electric potentials within their structure provides crucial experimental evidence that impurities can be used to tune REE adsorption and separation in layered materials.

We employ scanning transmission electron microscopy in combination with analytical spectroscopy and electron holography experiments for detailed spatio-chemical analysis of micas exposed to aqueous solutions containing Nd and Yb. We monitor the d-spacing of minerals, using it as a single electron beam-damage indicator throughout our imaging and spectral analysis processes. Atom Probe Tomography (ATP), X-ray Photoelectron Spectroscopy (XPS) and computational modeling in combination to deepen our understanding of the fundamental factors that govern REE adsorption in micas. These insights are instrumental in guiding the development of novel geo-inspired materials for the effective separation of rare earth elements from diverse feedstocks.

4:45pm AMS2-WeA-11 Single-Molecule Spectroscopic Probing of N-Heterocyclic Carbenes on a Two-Dimensional Metal, *Nan Jiang,* University of Illinois Chicago
N-heterocyclic carbenes (NHCs) have recently proven to be powerful ligands for planar surface modification due to their remarkable structural diversity, property tunability, and high affinity to a diverse array of elements.However, the utilization of NHCs for planar surface modification has almost exclusivelybeen limited to bulk substrates; the exploration of NHC modification of two-dimensional (2D) materials remains largely uncharted despite its promise for wide energy and electronic applications. Here we investigate the adsorption of NHCs on a 2D metal, specifically monolayer boron (i.e., borophene), at the single-molecule level using tip-enhanced Raman spectroscopy, scanning tunneling microscopy/spectroscopy (STM/S), and density functional theory calculations. Single-molecule optical spectroscopy reveals the distinct interfacial interactions between individual NHCs and borophene, in covalent (boron–carbon bonding) and van der Waals-type manners,highlighting the role of steric effects in determining the binding mode. Furthermore, the impact of NHC adsorption on borophene's electronic properties is demonstrated by local work function reductions, as measured quantitatively by single-molecule STS. In addition to providing novel insight into NHC–substrate interactions in the 2D regime, this study opens up an avenue for single-molecule studies of NHC chemistry, promising to promote advances in understanding and inform ongoing efforts to devise and realize new NHC-related applications.

5:00pm AMS2-WeA-12 Electric Fields and Co2 Coverage Effects on the Surface Chemistry of La-Based Perovskites, *Ariel Whitten,* Jean-Sabin McEwen, Washington State University; *Eranda Nikolla,* University of Michigan, Ann Arbor; *Reinhard Denecke,* Leipzig University, Germany
Perovskite-based materials are more stable than metal anode catalysts in electrochemical CO_2 reduction processes, but perovskites have reduced activity as compared to metal catalysts such as Ni. For perovskites to be an alternative catalyst for this process, the perovskite surface needs additional augmentations to increase the activity such as the introduction of active sites like oxygen vacancies or external influences like electric fields. We propose using La-based perovskites ($LaNiO_3$, $LaCoO_3$ and $LaFeO_3$) which are known to be highly active in CO_2 reduction and investigate these surfaces using both experimental and first principles-based calculations. In a previous project, we deconvoluted XPS spectra of $LaNiO_3$ and $LaCoO_3$ finding that the higher energy peak in the O 1-s spectra occurred in large part to the adsorption of water but other adspecies (H, O, OH and CO_2) gave smaller contributions to the peak. Although understanding the surface science of co-electrolysis with H_2O and CO_2 is the ultimate goal of the project, the adsorption and conversion of CO_2 are a widely acknowledged barrier to CO_2 reduction. Therefore, studying the nature of CO_2 interactions with the surface is imperative to building on the critical knowledge needed to improve this process. From our initial results studying CO_2 adsorption at differing coverages (Figure 1), we find that interactions calculated using the lattice gas method between adspecies travel mainly through the surface (Figure 2) and cause a surface rearrangement depending on adsorbate configuration, adsorption strength and B-site material. This indicates the limiting factor of CO_2 adsorption is the concentration of charge in the surface that is necessary to stabilize the adspecies. The stabilization of adsorbates can therefore be improved by adding charge via external electric fields. Our studies of electric fields on clean surfaces indicate that

increased electric fields lead to a drastic fluctuation in the plane averaged local potential, which can decrease the stability of the surface. Thus, the strength of the electric field needs to be calibrated so that it adds charge to the surface without causing its decomposition. Moreover, the formation of surface oxygen vacancies is spontaneous under negative electric fields on $LaFeO_3$. Thus, the perovskite anode of an electrochemical cell will form active sites that spontaneously increase its activity. In further studies, we aim to understand the effects of coverage on the adsorption of CO_2 using nudged elastic band calculations and an effect of electric fields has on the adsorption and activation of CO_2.

5:15pm **AMS2-WeA-13 Interfacial Quantum Electric Fields**, *Shawn Kathmann,* Pacific Northwest National Laboratory

Electric fields and voltages within and at the interfaces of matter are relevant to catalysis, crystallization, materials science, biology, and aqueous chemistry. Accurate measurements of fields and voltages of matter has been achieved using electron holography/tomography (EHT) and can be directly compared with quantum mechanical calculations. From these findings all interfaces have large intrinsic local electric fields (~10 GV/m = 1 V/Å) and voltages even if these materials are macroscopically electrically neutral. The use of very weak applied fields (<10^{-3} V/Å) causes materials to respond, changing both the magnitude and spatial distribution of the intrinsic electric fields. The resulting interfacial response fields, i.e., $E_{resp}(r) = E_{intr}(r) + E_{appl}(r)$, have been measured using EHT and are similarly large as the intrinsic fields even though the applied field is very weak. These large fields can and do alter adsorbed species electronic states (e.g., bonding/antibonding orbitals, luminescence, chemical reaction barriers, electron transfer, etc.) as well as rotational and vibrational states. When characterizing fields and voltages in matter, it is essential to specify exactly where they are being evaluated and over what spatial regions of the quantum charge density do different measurements probe (e.g., electron holography tomography vs. vibrational Stark spectroscopies). Here we outline the chemical physics, quantum, and statistical mechanics relevant to these findings and their consequences on how we understand, control, and exploit interfacial fields.

This work is sponsored by the U.S. Department of Energy, Office of Basic Energy Sciences, Division of Chemical Science, Geosciences, and Biosciences Condensed Phase and Interfacial Molecular Sciences Program. Pacific Northwest National Laboratory (PNNL) is a multiprogram national laboratory operated for DOE by Battelle.

Applied Surface Science
Room 117 - Session AS-WeA

Advanced Materials and Methods

Moderators: Tanguy Terlier, Rice University, **Julia Zakel**, IONTOF GmbH, Germany

2:15pm **AS-WeA-1 Ion Migration and Chemical Phenomena in Functional Materials: Correlative Studies via Combined AFM/Tof-SIMS Approach**, *Anton Ievlev,* Oak Ridge National Laboratory   **INVITED**
The performance of various electronic devices is defined by the delicate interplay of electrical response and charge carrier migration at the nanoscale. Although physical behavior and macroscopic functional response of these materials is well established, intrinsic chemical phenomena associated with ionic motion or localized electrochemical reactions can dramatically alter their behavior and thus restrict area of utilization. Over the last decade, advancements in development of novel nanoscale characterization tools such as atomic force microscopy (AFM) have revolutionized our understanding of the electrical and mechanical response of materials; however, *dynamic* electrochemical behavior and ion migration remain poorly understood. Recently time-of-flight secondary ion mass spectrometry (ToF-SIMS) has proven to be effective tool for characterization of static chemical states in energy materials. However, its application to study of dynamic electrochemical processes still requires development.

Here we introduce approach based on combined AFM/ToF-SIMS approach for correlated studies of the dynamic chemical phenomena on the nanoscale in operando conditions. Being used for characterization of the range of electronic materials, including ferroelectrics, photovoltaics and memristors it allowed direct observation of the ionic migration within the device in externally applied electric fields, which is important for fundamental understanding of the material functionality. Altogether, developed approaches enable direct characterization of interplay between

chemical and functional response in variety of materials, which aids in the development and optimization of novel devices and applications.

This research was conducted at the Center for Nanophase Materials Sciences, which is a DOE Office of Science User Facility and using instrumentation within ORNL's Materials Characterization Core provided by UT-Battelle, LLC under Contract No. DE-AC05-00OR22725 with the U.S. Department of Energy.

2:45pm **AS-WeA-3 Elemental and Chemical Quantification of Porous Transport Electrodes with X-Ray Photoelectron Spectroscopy Analysis and Scanning Electron Microscopy – Energy Dispersive X-Ray Spectroscopy**, *Lonneke van Eijk,* Colorado School of Mines; *Jayson Foster,* Colorado School of Mines, USA; *Sunilkumar Khandavalli,* National Renewable Energy Laboratory; *Lei Ding,* University of Tennessee, Knoxville; *Genevieve Stelmacovich,* Colorado School of Mines, USA; *Scott Mauger,* National Renewable Energy Laboratory; *Feng Zhang,* University of Tennessee, Knoxville; *Adam Paxson,* Plug Power; *Svitlana Pylypenko,* Colorado School of Mines, USA

Optimization of proton exchange membrane water electrolyzers (PEMWEs) is essential to ensure reliable hydrogen generation and societal transition towards greater hydrogen energy use. Further improvements are crucial for facilitating the widespread adoption of hydrogen as a sustainable energy source. Various avenues are under exploration to advance PEMWEs further, aiming for increased activity and stability of catalysts, alongside the optimization of catalyst layer (CL) structure. This work focuses on the development of porous transport electrodes (PTEs), consisting of an iridium oxide-based catalyst layer and a titanium-based porous transport layer coated with a platinum protective layer. This project explored several CL deposition methods, including airbrush, rod coating, ultrasonic spray coating, and electrodeposition, to achieve homogeneous CL coatings and control of catalyst loadings. Additionally, post-treatments of PTEs were explored to elucidate the interplay between activity and stability of CLs and further optimize the performance.

The main goal of this study was the development of quantitative metrics that can be used for comparative studies of the quality of CL coatings and their performance. The first part of my talk will discuss scanning electron microscopy – energy dispersive X-ray spectroscopy (SEM-EDS) analysis of a series of PTEs produced with various routes. SEM-EDS was used to assess the elemental composition and the distribution of elements of interest. In addition to qualitative assessment of SEM-EDS images, this study also implemented quantitative metrics based on Pt:Ir ratios. The implementation of proper characterization of these PTEs can help aid future decisions on which fabrication and processing parameters should be used to achieve coatings with desired quality and loadings. This approach can also be used for quality control, enabling quick screening of commercially produced samples. The second part of my talk will discuss the X-ray Photoelectron Spectroscopy (XPS) data analysis for chemical analysis of PTEs annealed under various environmental conditions and temperatures, with the goal of elucidating the impact of these parameters on material properties and electrochemical performance. This talk will discuss results and challenges associated with the analysis of Ir-based materials and will highlight trends between several quantitative metrics derived from XPS data and their correlations with electrochemical parameters. The findings not only contribute to advancements in PEMWE technology but also underscore the importance of the identification of simple metrics that can be used for trend identification in complex datasets.

3:00pm **AS-WeA-4 Comprehensive Characterization of Porous Transport Layers and Porous Transport Electrodes with Time-of-Flight Secondary Ion Mass Spectrometry**, *Genevieve Stelmacovich, Lonneke van Eijk, Jayson Foster,* Colorado School of Mines; *Lei Ding,* University of Tennessee, Knoxville; *Samantha Ware, James Young,* National Renewable Energy Laboratory; *Feng Yuan Zhang,* University of Tennessee, Knoxville; *Adam Paxson,* Plug Power Inc.; *Guido Bender,* National Renewable Energy Laboratory; *David Cullen,* Oak Ridge National Laboratory; *Svitlana Pylypenko,* Colorado School of Mines

Proton Exchange Membrane Water Electrolysis (PEMWE) is a promising technology towards the realization of the hydrogen economy. PEMWE components include the porous transport layer (PTL), a sintered or felt titanium material, and the adjacent catalyst layer (CL) which is typically made with IrO_x or $IrRuO_x$ catalyst. Recent advancements in manufacturing have pushed towards the fabrication of porous transport electrodes (PTEs), where the anode CL is directly coated onto the PTL. To mitigate degradation of the PTL and improve the interface between CL and PTL, PTLs are typically

coated with a thin protective coating, usually Pt. This leads to a complex layered PTE structure that consists of catalyst layer, protective coating, and porous transport layer ($IrO_x/Pt/Ti$ or $IrRuO_x/Pt/Ti$) and is difficult to characterize.

Previously, we have demonstrated Time of Flight Secondary Ion Mass Spectrometry (TOF SIMS) as a powerful characterization technique for the qualitative and comparative characterization of PTLs, enabling the assessment of the interface between protective coating and PTL. Further, we focused on analysis of protective coatings with a focus on their thickness. We correlated TOF SIMS data and Scanning Transmission Electron Microscopy (STEM) measurements to demonstrate that TOF SIMS can be used to reliably compare coatings with different thicknesses despite the complex morphology of the substrate. More recently we used TOF SIMS to characterize a series of PTEs made with electroplated $IrRuO_x$ catalyst that underwent various post-treatments. A combination of spectroscopy, imaging, and depth profiling analysis was utilized to identify chemical and spatial differences. This data was combined with Scanning Electron Microscopy Energy Dispersive X-Ray Spectroscopy (SEM-EDS), STEM, and X-Ray Photoelectron Spectroscopy (XPS) analysis to highlight the complementary nature of TOF SIMS analysis and demonstrate the need for comprehensive characterization with multiple techniques.

3:15pm AS-WeA-5 Characterization of the Nanostructure and Composition of Mollusc Shells Using Advanced Spectroscopic and Imaging Techniques, *David Morgan*, Cardiff University, UK

Biomineralization is an important field, informing researchers across many disciplines, on materials design, understanding of evolution and the development of tissue-engineering. Molluscs biomineralize to form shells as a means of protecting their internal soft tissues and these strong shells have led to molluscs becoming the second largest invertebrate phylum with over 70,000 species.

These shells are organo-mineral composite structures consisting of two key components - aninorganic carbonate mineral and organic macromolecules (e.g. proteins, polysaccharides). This complex structure imbues them with enhanced mechanical properties, such as high strength and fracture toughness. In recent years, much attention has been focused on the nacreous shell structureto replicate materials with similar strengths and toughness. To date, most research papers have focused on the microstructures of these shells, little work has been done on their nanostructure which representsa key gap in our knowledge of biomineralization since amorphous calcium carbonate nanostructures form the first building blocks of these hierarchical structures.

The presented work focuses on the intricate nanostructure and composition of the Fluted Giant Calm (*Tridacna squamosa*) by means of Photo-induced Force Microscopy (PiFM) and X-ray Photoelectron Spectroscopy (XPS).We show that XPS unequivocally confirms the presence of calcium (Ca) and magnesium (Mg) within the z-axis of the shell matrix, whilst, PiFM unveils a multifaceted composition, indicating that the shell comprises a mixed-phase carbonate structure, intricately woven from both structured and amorphous aragonite and magnesite. Notably, PiFM analysis reveals a structural distinction between the Inner and Outer Shell layers, with the outer layers displaying distinct "zebra stripe" patterns, denoting magnesite and dolomite-like bonding that traverses the aragonite structure. This study significantly contributes to advancing our comprehension of mollusc shell structure and composition.

3:30pm AS-WeA-6 Development of Best Practices for Cryo-XPS – Opening the Possibility to New Sample Analysis and Paving a Route to Standardization, *Khadisha Zahra, **Liam Soomary**, Kratos Analytical Limited, UK; Christopher Moffitt, David Surman, Kratos Analytical Inc.; Jonathan Counsell,* Kratos Analytical Limited, UK

Conventional x-ray photoelectron spectroscopy (XPS) has typically limited samples to solids, powders, and thin films due to the ultra-high vacuum (UHV) requirements of analysis. This has constrained the utilization of XPS in various industries (e.g. biological/ medical and battery manufacturing), due to the preparation requirements to create vacuum compatible samples often resulting in analysis in non-native environments. Developments in near-ambient pressure (NAP-XPS) and frozen hydrated sample (cryo-XPS) analysis is beginning to bridge these gaps. NAP-XPS systems are widely available at synchrotron facilities, with commercial instruments also on the market. However, beamtime is highly competitive and commercial instruments are currently expensive.

Previous comparisons in the literature between the two methods have shown both give comparable data [1]. Still the ability to maintain UHV conditions using cryo-XPS minimises surface contamination and provides higher signal intensity, therefore enabling shorter acquisition times. Cryo-XPS is also an accessory added to conventional XPS making it a cost-effective option.

Rate of cooling is a major consideration in cryo-XPS. Slow rates of freezing result in fewer nucleation sites, thus larger crystals, which cause cellular damage. Flash-freezing is essential to produce vitreous (amorphous, glass-like) ice, preventing crystal formation. In biological and medical research this preserves cellular structures and maintains a near-native state. It also preserves compounds, avoids surface restructuring, and minimises surface degradation. After vitrification, sample temperatures need to remain below -137 °C to prevent devitrification [2]. Thus, sample transfer between the load-lock and analysis chamber must be fast and dependable.

In this talk we hope to provide industry relevant guidelines for sample preparation with a focus on reproducibility using cryo-XPS. We will also demonstrate how layered analysis is achieved when cryo-XPS is coupled with Gas Cluster Ion Source (GCIS) etching to delve deeper into the surface. Finally, we will comment on directions for future improvements in the technique.

[1] M. Kjaervik et al., Comparative Study of NAP-XPS and Cryo-XPS for the Investigation of Surface Chemistry of the Bacterial Cell-Envelope, Front. Chem., (2021) 9:666161.
DOI: 10.3389/fchem.2021.666161

[2] G. Weiseenberger et al., Understanding the invisible hands of sample preparation for cryo-EM, Nat. Methods, (2021) 18:5.
DOI: 10.1038/s41592-021-01130-6

4:15pm AS-WeA-9 ASSD Student Award Finalist Talk: 3D ToF-SIMS Imaging of Polyethylene Oxide-Lithium Nitrate Electrolytes in Lithium Ion Batteries, *Reyhane Shavandi*[1], University of Illinois Chicago

Time-of-flight secondary ion mass spectrometry (ToF-SIMS) is increasingly used to reveal three dimensional atomic and molecular distributions in the solid-electrolyte interface (SEI) of lithium ion batteries [1,2]. Solid electrolytes were previously sandwiched between lithium foil and copper electrodes, subjected to charge-discharge cycling until electrical failure, then lithium dendrites responsible for failure were detected by post-mortem ToF-SIMS analysis [3]. However, the requisite mechanical removal of the lithium foil prior to ToF-SIMS analysis can inadvertently remove some of the SEI. An alternate strategy was pursued here in which the lithium foil was replaced with thin layers of lithium evaporated *in vacuo* [4], allowing ToF-SIMS to follow the reaction of metallic lithium with the electrolyte. A micrometer-thick solid electrolyte composed of polyethylene oxide (~600 kDa) and lithium nitrate was slot dye coated onto a copper substrate and compared by ToF-SIMS with the same samples on which 10 or 100 nm thick layers of lithium were evaporated. 30 keV Bi_3^+ primary ions from a liquid metal ion gun were used to collect positive ion spectra during simultaneous sputtering with a 10 keV argon gas cluster ion beam (IONTOF M6, Münster, Germany). The depth profiles for NO_2^+representing the lithium nitrate salt, $C_2H_5O^+$ representing polyethylene oxide and Cu_3^+ representing the copper electrode indicated that the addition of lithium increased the total fluence of argon cluster ions through the solid electrolyte. A limited number of negative ion spectra were recorded that showed NO_2^- and Cu_3^- following similar trends as in their positive ion counterpart spectra. However, high $NO_2^{+/-}$ signals persisted after the $Cu_3^{+/-}$ signals leveled off and changes were observed in copper cluster secondary ions with lithium addition. These effects are discussed in terms of cluster ion-induced mixing or substrate roughening, and the higher sputtering efficiency expected for the polyethylene oxide and lithium nitrate compared to the copper substrate.

1. T. Lombardo, M. Rohnke, *et al.*, *J. Vac. Sci. Technol. A* **41** (2023) 053207. https://doi.org/10.1116/6.0002850

2. Q. Ai, J. Lou, *et al.*, *ACS Energy Lett.* **8** (2023) 1107. https://doi.org/10.1021/acsenergylett.2c02430

3. M.J. Counihan, S. Tepavcevic, *et al.*, ACS Appl. Mater. Interf. **15** (2023) 26047. https://doi.org/10.1021/acsami.3c04262

4. M. Counihan, S. Tepavcevic, *et al.*, *ACS Appl. Mater. Interf.* **15** (2023) 26047. https://doi.org/10.1021/acsami.3c04262

---

[1] **ASSD Student Award Finalist**

Wednesday Afternoon, November 6, 2024

4:30pm AS-WeA-10 Understanding the Impacts of Battery Electrode Manufacturing Processes through Surface Characterization Techniques, *Mikhail Trought*, *Tatyana Kravchuk, Sabrina Peczonczyk, Ann Straccia, Mark Nichols,* Ford Motor Company

The automotive industry has collectively adopted the shift towards manufacturing lithium (Li)-ion battery powered electric vehicles (EVs) to mitigate the environmental impacts of internal combustion engine vehicles, and to meet the evolving government regulations. Manufacturing of Li-ion batteries, and in particular their electrodes, is multifaceted and consists of multiple process steps that can affect the chemical and physical properties of the battery materials, which directly influences the battery's performance. In this study, we have characterized model solvent-based Li-ion battery electrodes: NMC-based cathodes with polyvinylidene fluoride (PVDF) binder and graphite-based anodes with carboxymethyl cellulose (CMC) and styrene butadiene rubber (SBR) binders. The effects of the drying and calendaring manufacturing processes on the chemical properties and morphology were studied. X-ray photoelectron spectroscopy (XPS) and time of flight secondary ion mass spectroscopy (ToF-SIMS) were used to assess the chemical composition of these battery materials after drying. In parallel, atomic force microscopy (AFM) was used to assess the battery electrode's morphology after drying and after exposure to mechanical stimuli similar to that of the calendaring process. The quality of the battery electrode is highly dependent on manufacturing processes; characterization techniques need to be implemented to understand how these processes affect the electrode and how that ultimately affects the battery's performance.

4:45pm AS-WeA-11 Characterization of Sodium Ion Batteries - from *Postmortem* **to** *Operando, Marcus Rohnke, Till Ortmann, David Schäfer, Jürgen Janek,* Justus Liebig University Giessen, Germany   **INVITED**

Lithium-ion batteries (LIBs) have been at the forefront of energy storage technology since the early 1990s due to their relatively high energy density (260 Whkg^{-1}), reasonable cost ($153/kWh), and long lifespan.[1] However, the high demand, lack of raw material availability, poor ecological, political and working conditions in the mining countries require new battery concepts. Despite their lower energy density (~150 Whkg^{-1}) compared to LIBs, sodium ion batteries (SIBs) appear to be an interesting alternative, especially for non-portable applications where weight is secondary. SIBs could be used for stationary storage of excess energy from renewable sources such as wind or solar power. Moreover sodium is the 6th most abundant element on earth and is more evenly distributed throughout the globe than lithium.

Researchers around the world are working on concepts for SIBs with liquid and solid electrolytes, so-called solid-state sodium ion batteries.[2] In most cases, the interface properties between the materials used determine the battery kinetics and long-term cycling behavior. Here surface analytical methods such as time-of-flight secondary ion mass spectrometry (ToF-SIMS) or X-ray photoelectron spectroscopy (XPS) play a key role, in combination with 3D analysis and cross-section preparation.[3] They offer the opportunity to learn more about interfacial processes taking place. This knowledge is essential for continuously improving the performance of batteries.

Within this talk we will give insights in our ongoing work on SIBs with liquid as well as solid electrolytes. We will highlight how SIMS, XPS, SEM and TEM can be used in combination with classical electrochemical methods to learn more about electrode and decomposition reactions in SIBs. The first example focuses on the interfacial kinetics in solid state Na batteries with the solid electrolyte NASICON (Na$_{3.4}$Zr$_2$Si$_{2.4}$P$_{0.6}$O$_{12}$). In the second example classical hard carbon electrodes from electrochemical cells with liquid electrolytes are characterized in 3D with a special focus on the so called solid electrolyte interface (SEI). Here a decomposition layer is formed, which has a significant impact to the cellular kinetics.

Funding was received through POLiS Cluster of Excellence – Post Lithium Storage.

[1]R. Zhao, S. Zhang, J. Liu, J. Gu, *J. Power Sources***2015**, *299*, 557–577

[2] D. Schäfer, K. Hankins, M. Allion et. al., *Adv. Energy Mater.***2024**, 2302830

[3] T. Lombardo, F. Walther, C. Kern et al., *J. Vac. Sci. Technol. A* 41 **2023** 053207

5:15pm AS-WeA-13 Surface Analysis of Engineered Particles for Improved Battery Performance and Stability, *Jennifer Mann, Sarah Zaccarine,* Physical Electronics*; Isaiah Oladeji,* ULVAC Technologies, Inc.*; Koukou Suu,* Ulvac Technologies, Inc., Germany*; Kateryna Artyushkova,* Physical Electronics

We require next-generation battery materials to achieve optimal energy density, rapid charging capabilities, and extended device longevity, all while maintaining affordability and reliability. Lithium metal batteries present a promising alternative to lithium-ion batteries; however, they encounter stability issues such as unstable solid-electrolyte interphase (SEI) growth and the formation of lithium dendrites. Similarly, cathode materials with high energy density, such as nickel manganese cobalt (NMC), demonstrate stable performance at high potentials but are vulnerable to dissolution within the electrolyte and unstable SEIs. Engineered particles (Ep) offer a solution by stabilizing electrode interactions, thus enhancing battery safety, SEI formation, and overall performance. Nonetheless, batteries are multi-layered, complex systems with numerous components and interfaces, posing challenges to characterization. A comprehensive understanding of the chemical composition, distribution, and morphology of Ep-treated anodes/cathodes is essential for fabricating uniform, well-dispersed electrodes with high capacity, thereby optimizing battery performance.

Advancements in X-ray photoelectron spectrometers have broadened their capabilities to effectively tackle these hurdles. X-ray photoelectron spectroscopy (XPS) emerges as an ideal method for scrutinizing the thin layers and interfaces of battery materials, due to its surface sensitivity (approximately 10nm) and ability to discern chemical states. Multi-technique XPS instruments offer an array of operational modes and analytical choices, facilitating comprehensive characterization of battery materials. This presentation showcases the utilization of a fully automated, multi-technique scanning XPS/HAXPES microprobe to address various challenges in battery material analysis. It incorporates an inert environment transfer vessel for air-free handling, a microprobe X-ray source with sub-5µm spatial resolution for precise area selection in small-area spectroscopic analysis and chemical mapping, and the utilization of hard X-ray and cluster ion gun sources for examining buried interfaces without compromising the underlying chemistry. The combination of these powerful capabilities allows for thorough analysis of battery materials at both macroscopic and microscopic levels, establishing a clear link between the chemistry and performance of electrodes treated with Engineered particles (Ep).

5:30pm AS-WeA-14 X-ray Photoelectron Spectroscopy for Battery Research Applications, *Tatyana Bendikov, Ayan Maity, Nadav Yahalom, Yuval Steinberg, Haim Weissman, Boris Rybtchinski, Michal Leskes,* Weizmann Institute of Science, Israel

X-ray Photoelectron Spectroscopy (XPS), as a surface sensitive technique with the sensitivity down to single atomic layer, provides unique information about elemental composition and chemical and electronic states of elements in the material. It is not surprising that XPS is considered as one of the prominent tools in battery research, which enables determination of the electrodes/electrolyte composition during battery cycling, detection of the interfacial phases and follow their structural and compositional variations through depth profiling using ion sputtering. We show two examples where XPS was successfully used for the study of: 1) Sulfur-based composite carbon nanotube cathodes;[1] and 2) solid electrolyte interphase (SEI) on Na-Ion anodes.[2]

In spite of high reliability of the XPS technique and its assorted capabilities it should be taken into consideration that experimental conditions (high vacuum requirements) and X-ray radiation damage might alter the composition of the studied sample and can be mistakenly interpreted as nonexistent battery reaction products. We present here systematic study of the LiTFSI, a widely used component of the nonaqueous battery electrolytes. We show how pumping conditions and/or prolonged X-ray exposure result in continuous deterioration of the LiTFSI. We also suggest partial solutions for deceleration of the decomposition processes during XPS measurements.

Literature:

1. N. Yahalom et. al, *ACS Appl. Energy Mater.* **2023**, 6, 4511−4519.
2. Y. Steinberg et. al, *manuscript in preparation.*

Wednesday Afternoon, November 6, 2024

5:45pm AS-WeA-15 AVS Nellie Yeoh Whetten Awardee Talk: Investigating the Substrate Mediated Growth Pathways and High-Field Superconducting Behavior of Nb3Sn Films for Particle Accelerator Cavities, *Sarah Willson[1],* University of Chicago; *Aiden Harbick,* Brigham Young University; *Rachael Farber,* University of Kansas; *Helena Lew-Kiedrowska, Van Do,* University of Chicago; *Mark Transtrum,* Brigham Young University; *Steven Sibener,* University of Chicago

Niobium is the highest temperature elemental superconductor, making it the standard material for superconducting radiofrequency (SRF) cavities in next-generation linear accelerators. These facilities require cryogenic operating temperatures (< 4 K) to limit the formation of superconductivity-quenching hot spots in the near-surface region of the cavity. Widespread efforts are underway both to increase the accelerating fields and reduce the cryogenic burden by improving SRF surfaces. A promising solution is to coat the Nb SRF surface with a Nb₃Sn thin film *via* Sn vapor deposition. The higher critical temperature and critical field makes Nb₃Sn an ideal candidate for capping Nb surfaces. However, persistent Nb₃Sn material defects at the film surface, such as stoichiometric inhomogeneities and surface roughness, preferentially nucleate vortices under high fields that limit the accelerating performance of Nb₃Sn surfaces.

As part of a widespread interdisciplinary effort to optimize SRF accelerating capabilities, this work aims to develop a comprehensive growth model for pristine Nb₃Sn films. The complex interplay between the underlying Nb oxide morphology, Sn coverage, and Nb deposition temperature are examined by depositing Sn vapor on model Nb surfaces in an ultrahigh vacuum (UHV) environment with *in situ* surface characterization capabilities. Fundamental studies were scaled up to visualize how nanoscale features on the Nb oxide surface influence Sn and Nb₃Sn nucleation on unpolished polycrystalline Nb surfaces. These film growth studies collectively demonstrate that the Nb substrate defect sites are critical for stabilizing Sn adlayers.

Furthermore, the morphologies of stoichiometric defects on fully grown Nb₃Sn surfaces were investigated with computational support to simulate how the structures and sizes of Sn-poor and Sn-rich features influence the nucleation of vortices during SRF operation. Nb₃Sn films were prepared under varying conditions to demonstrate how the final cooldown steps of the vapor deposition process influence the stoichiometric homogeneity of the within the first 100 nanometers of the Nb₃Sn surface. Results indicate that the diameter and embedment of elemental Sn islands significantly alter the expected vortex nucleation field for a given global Sn composition. Understanding the effect of Nb₃Sn stoichiometric defect morphology on the high-field vortex nucleation is essential to systematically assess how different surface defects attenuate the achievable accelerating performance of Nb₃Sn coated cavities.

6:00pm AS-WeA-16 Silicon Wafer Doping with Mineral Films Prepared via Tethering by Aggregation and Growth, *Peter Thissen,* KIT, Germany

We investigate a new doping process of silicon wafers without making use of any highly toxic or corrosive chemical substances. Ultra-thin films of minerals, like hydroxyapatite ($Ca_5(PO_4)_3OH$), are prepared via tethering by aggregation and growth (T-BAG) and processed by rapid thermal annealing [1]. A variety of minerals can be used to effectively form metal silicates in contact with silicon oxide. This process is mainly thermodynamically driven and has already been well-studied using calcium silicate as an example [2]. One of the most thermodynamically stable calcium silicate phases is wollastonite ($CaSiO_3$). The main advantage of such formed phases is that they do not need to be etched with HF in the final step of the semiconductor processing; the direct use of mineral acids such as HCl or H_2S is sufficient to remove unwanted reaction byproducts. The doping method used, which uses the T-BAG technique for sample preparation, is not without inherent limitations. Although this method is widely used due to its simplicity and effectiveness, it is important to recognize its disadvantages, in particular the tendency towards an uneven distribution of the dopants across the semiconductor material. This phenomenon leads to an inhomogeneity across the sample, thus setting clear limits to the accuracy and reliability of the doping process. Consequently, although the T-BAG method is simple in sample preparation, its tendency towards non-uniform doping distribution highlights the need for careful consideration and possible refinement of future doping strategies. Using IR spectroscopy, we have already observed that the mineral decomposes at low temperatures (~ 500 K). The transport of 'P' through the native silicon oxide is driven by a phase transformation into a more stable thermal oxide [3]. At around 1000 K, diffusion of phosphorus into the region below the surface

of the oxide-free silicon is observed. Finally, from our in-situ IR measurements in combination with electrical impedance spectroscopy, we conclude that phosphorus (a) is transported through the silicon oxide, (b) diffuses into the oxide-free silicon, and (c) finally changes the electrical activity of the silicon wafer.

[1] Vega, A.; Thissen, P.; Chabal, Y. J., Environment-Controlled Tethering by Aggregation and Growth of Phosphonic Acid Monolayers on Silicon Oxide. Langmuir 2012, 28, 8046-8051.

[2] Thissen, P., Exchange Reactions at Mineral Interfaces, Langmuir 2020 36 (35), 10293-10306.

[3] Longo, R. C.; Cho, K.; Hohmann, S.; Thissen, P., Mechanism of Phosphorus Transport through Silicon Oxide During Phosphonic Acid Monolayer Doping. The Journal of Physical Chemistry C 2018, 122, 10088-10095.

Electronic Materials and Photonics
Room 114 - Session EM+AP+TF-WeA

CMOS and BEOL - Advances in Materials Integration and Devices

Moderators: Erica Douglas, Sandia National Laboratories, **Cheng Gong**, University of Maryland College Park

2:15pm EM+AP+TF-WeA-1 All-Acoustic and Single-Chip Radio Frequency Signal Processing via Heterogeneous Integration of Semiconductors and Piezoelectric Materials, *Matt Eichenfeld,* University of Arizona **INVITED**

Radio frequency front-end signal processors are the workhorses of modern communications and sensing, providing the signal processing link between data and the radio waves that carry that data between transmitters and receivers. These front-end processors typically use a mix of piezoelectric acoustic microchips and semiconductor transistor microchips to achieve the many different functions they need to encode and decode information. Because of the very disparate materials used, these different chips are assembled at the system level into so-called multi-chip modules, and this system-level integration greatly increases the size of RF systems and degrades their performance. In this talk, I will describe how we have used heterogeneous integration of semiconductor materials with piezoelectric materials such as lithium niobate to create the first-ever comprehensive platform for radio-frequency signal processing with gigahertz frequency acoustic waves. This all-acoustic approach means that the entire front-end processor can be made on a single chip, paving the way towards wireless technologies with more than a 100x reduction in form-factor, as well as increased performance and lower power consumption. It is also a sandbox for studying and engineering the complex interactions between electrons and phonons in solid state materials that may lead to new discoveries and innovations in electronics, phononics, and thermal transport.

2:45pm EM+AP+TF-WeA-3 Breaking the Quantum Conductance Barrier in CMOS Interconnect Design, *William Kaden,* University of Central Florida

Moore's law miniaturization has greatly amplified the importance of interconnect resistance as the limiting factor controlling computational power consumption and clock-speed limitations. The most recent inflection point occurred when cross-sectional wire dimensions miniaturized below the electron mean free path for charge transport within the wire. This has led to deleterious deviations from bulk resistivity scaling trends as uncontrolled surface scattering contributions have become increasingly non-negligible. Searches for suitable replacements to copper for bottom level interconnects have emerged as a direct consequence, with a figure of merit consisting of $\lambda*\rho_0$ emerging as a primary screening criteria used to find materials best balancing bulk and surface contributions to wire resistivity within this size regime. With decreasing wire cross-sections has also come decreasing grain size, such that grain-boundary scattering also accounts for a significant fraction of the resistivity size effect trends observed in nanowire test-structures. Despite these challenges introduced by miniaturization, further miniaturization of bottom layer interconnect lengths now has the potential to beneficially reduce wire resistance via a fundamental change in charge-transport enabling ballistic conduction to emerge as wire lengths also begin to decrease below electron mean free paths. For reference, bottom layer interconnects are now comparable in length to the room temperature mean free path of bulk copper (~40 nm). Nonetheless, current interconnects do not support quantum conduction due to several non-phononic scattering contributions associated with interactions with grain boundaries, wire surfaces, and defects, such that the effective electron mean free path observed in industrially fabricated

nanowires is far less than that of the bulk metals from which they are composed. To successfully leverage the potential for quantum conductance at current interconnect dimensions, non-phononic contributions to resistivity must first be mitigated. Our group has aimed to achieve this through the creation of high-quality single-crystalline nanowire test-structures, for which we have established process-mediated phenomenological control over surface scattering specularity. To achieve this, our group has developed and characterized heteroepitaxial Ru(0001) thin-films deposited on Al_2O_3(0001) wafers, leveraged electron-beam lithography to subtractively pattern nanowire devices, and compared wire resistance observations at varied temperatures to establish ballistic contributions to conductance as a function of wire length and temperature.

3:00pm EM+AP+TF-WeA-4 "Suboxide MBE" — A Route to p-Type and n-Type Semiconducting Oxides at BEOL Conditions, *Darrell Schlom,* Cornell University

In this talk* I will describe a variant of molecular-beam epitaxy (MBE)—"suboxide MBE"—that makes it possible to deposit *p*-type and *n*-type semiconducting oxides with excellent structural perfection epitaxially at back end of line temperatures. In suboxide MBE the molecular beams consist of pre-oxidized elements (suboxides) that help navigate kinetic pathways. For example, supplying a molecular beam of indium suboxide (In_2O) eliminates the rate limiting step of conventional MBE to the growth of In_2O_3—the oxidation of indium to its suboxide—and by skipping this step growth with excellent crystallinity, surface smoothness, and at a low growth temperature are achieved. Similarly, Sn^{2+}-based *p*-type oxides that are challenging to deposit due to this delicate oxidation state may be deposited at BEOL conditions by utilizing suboxide MBE. In addition to extensive structural characterization, electrical characterization and working transistors will also be shown.

*This work was performed in collaboration with coauthors from the groups of: S. Chae, K. Cho, S. Datta, F. Giustino, C. Guguschev, G. Hautier, F.V.E. Hensling, D. Jena, I.M. Kankanamge, Z.K. Liu, D.A. Muller, H. Paik, X.Q. Pan, N.J. Podraza, Y.E. Suyolcu, P.A. van Aken, P. Vogt, M.D. Williams, H.G. Xing, and P.D. Ye

3:15pm EM+AP+TF-WeA-5 Epitaxial Metastable Cubic CO(001)/MgO(001): Potential Interconnect Conductor, *Anshuman Thakral, Daniel Gall,* RPI

The phase composition of Co layers deposited by magnetron sputtering is studied as a function of processing gas (Ar or N_2), temperature T_s = 100-600 °C, and substrate [Al_2O_3(0001), MgO(001) and SiO_2/Si] in order to determine the energetics for thin film synthesis of metastable fcc cobalt which has been theoretically predicted to be the most conductive metal in the limit of narrow interconnect lines. Nitrogen gas facilitates the growth of the metastable cubic phase particularly at T_s > 200 °C. Cubic MgO(001) substrates suppress nucleation of hcp Co grains, resulting in fcc Co even in an Ar atmosphere. The highest crystalline quality epitaxial fcc Co(001) layers are obtained with deposition on MgO(001) in 5.0 mTorr N_2 using T_s = 400 °C during deposition, followed by vacuum annealing at 500 °C. The resistivity size effect in FCC Co is quantified with transport measurements at 295 and 77 K. Data fitting with the Fuchs-Sondheimer model of the measured resistivity ρ vs thickness d = 5 – 1000 nm for single-crystal Co(001)/MgO(001) layers indicates an effective electron mean free path λ_{eff} = 27± 2 nm at 295 K and a room-temperature bulk resistivity ρ_o = 6.4 ± 0.3 µΩ-cm. At 77 K, the reduced electron-phonon scattering yields a smaller ρ_o = 1.3 ± 0.1 µΩ-cm and a larger λ_{eff} = 79 ± 6 nm. The resulting benchmark quantity $\rho_o\lambda_{eff}$ = 17.4×10^{16} and 10.2×10^{16} Ω-m^2 at 293 and 77 K, respectively, is 4-6 times larger than the first-principles predictions. The measured ρ_o for fcc Co is identical to that of the stable hcp Co phase. However due to the high effective mean free path and resulting high $\rho_o\lambda_{eff}$ values, cubic Co does not outperform hcp Co for interconnect applications. The developed method for growth of epitaxial fcc Co(001) layers provides opportunities to study this metastable material for potential spintronic applications.

3:30pm EM+AP+TF-WeA-6 Characteristics of Reconfigurable FETs Implemented on Bulk Silicon Using Reduced Pressure CVD, *Seong Hyun Lee, Sang Hoon Kim, Jeong Woo Park, Wangjoo Lee,* **Dongwoo Suh,** Electronics and Telecommunications Research Institute, Republic of Korea

As semiconductor process technology advances, tremendous efforts have been made in device engineering to mitigate the issue of integration density. One of the representative and prospective solutions is the novel device of reconfigurable FET, single FET working either as n- or p-MOSFET according to the polarity of gate bias. Because reconfigurable FET stands in need of intrinsic source/drain and channel, it has been fabricated on expensive and size-limited SOI wafers. Furthermore, its application is

restricted to special devices leaving contemporary CMOS technology irrelevant. In the present study we fabricated reconfigurable FETs on bulk silicon wafers using a lateral epitaxial growth technique unleashing its application potential.

Starting with 6-inch p-type (100) wafers covered with the oxide layer of 0.1 µm, we etched out the oxide layer to form a small seed zone following the epitaxial growth of intrinsic silicon from it using reduced pressure CVD. Having scrutinized the grown epilayer with high resolution transmission electron microscopy, we ensured that its crystal quality was very good in spite of local stacking faults. After planarization of the grown epilayer with CMP, we made Schottky contacts of titanium silicide both on the surface footprint of source and drain to form reconfigurable FET. Our device consists of single control gate in the center of the channel and two polarity gates placed symmetrically around it.

Current-voltage properties are investigated at the drain voltage of 1 Volt for various polarity gate potential. We obtained clear reconfigurable characteristics of n-MOS under positive gate bias and p-MOS vice versa reaching at the maximum current of 0.1 µA/µm for nMOS and 0.8 µA/µm for p-MOS operation. Transfer characteristics show higher current in p-MOS operation on the contrary to conventional FET. This result is caused by the difference of Schottky barrier height of titanium silicide for n-type (0.61 Volts) and P-type (0.49 Volts). Current levels are small overall because spatial gaps between two adjacent polarity and control gates are inevitably formed during the fabrication process. Notwithstanding the gap issue, our device can reduce the load of device integration. In addition, the present device can be a strong candidate for the mitigation of power issue in IC chips when cutting-edge CMOS technology is applied appropriately.

4:15pm EM+AP+TF-WeA-9 Forward Bias Annealing of Proton Radiation Damage in NiO/Ga_2O_3 Rectifiers, *Jian-Sian Li, Chao-Ching Chiang, Hsiao-Hsuan Wan,* University of Florida, Gainesville; *Md Abu Jafar Rasel, Aman Haque,* Pennsylvania State University; *Jihyun Kim,* Seoul National University, Republic of Korea; *Fan Ren,* University of Florida; *Leonid Chernyak,* University of Central Florida; *Stephen Pearton,* University of Florida

17 MeV proton irradiation at fluences from 3-7 x10^{13} cm^{-2} of vertical geometry NiO/β-Ga_2O_3 heterojunction rectifiers produced carrier removal rates in the range 120-150 cm $^{-1}$ in the drift region. The forward current density decreased by up to 2 orders of magnitude for the highest fluence, while the reverse leakage current increased by a factor of ~20. Low-temperature annealing methods are of interest for mitigating radiation damage in such devices where thermal annealing is not feasible at the temperatures needed to remove defects. While thermal annealing has previously been shown to produce a limited recovery of the damage under these conditions, athermal annealing by minority carrier injection from NiO into the Ga_2O_3 has not previously been attempted. Forward bias annealing produced an increase in forward current and a partial recovery of the proton-induced damage. Since the minority carrier diffusion length is 150-200 nm in proton irradiated Ga_2O_3, recombination-enhanced annealing of point defects cannot be the mechanism for this recovery, and we suggest that electron wind force annealing occurs.

4:30pm EM+AP+TF-WeA-10 Studies of the Effects of Doping and Nanolamination on the Temperature Coefficient of Resistivity of Ru-TiO_2 Thin Films, *S. Novia Berriel,* **Gouri Syamala Rao Mullapudi,** University of Central Florida; *Nicholas Rudawski,* University of Florida; *Parag Banerjee,* University of Central Florida

High precision electronics require the use of materials with constant resistivity across a wide range of temperatures. The metric of change of resistivity with temperature is known as temperature coefficient of resistivity (TCR). Low TCR is highly desirable for applications such as wearable strain sensors, automobile electronics, and microelectronics. Materials of low TCR can be difficult to come by. However, metals exhibit positive TCR, and semiconductors and insulators exhibit negative TCR. Thus, a combination of metallic and semiconducting materials could be used to create a net low TCR.

Atomic layer deposition (ALD) is a method well-suited to the task of tuning thin film composition between metal and insulator. To this end, we have studied the effect of nanolaminate-structured vs doped films on TCR for a temperature range spanning from 80 K to 420 K. The compositions of the thin films have been finely controlled by combining Ru - a metal, and TiO_x - an insulator, using a Veeco Fiji G2 ALD chamber. Two types of films were

made: First, a series of nanolaminates of 30 nm total thickness were synthesized with 50/50 composition Ru/TiO$_x$ while varying thickness of individual layers. Second, a set of films were made by dosing small amounts of TiO$_x$ into a predominantly Ru film totaling 30 nm thickness. The thickness of the total film and individual layers were monitored using *in situ* spectroscopic ellipsometry. The films have been further investigated via temperature-dependent van der Pauw, XRD, and TEM measurements to determine a cross-over from metallic to insulating behavior thus, precisely targeting a composition that produces low TCR behavior.

4:45pm EM+AP+TF-WeA-11 Dorothy M. and Earl S. Hoffman Scholarship Awardee Talk: Determination of Band Offsets at the Interfaces of NiO, SiO$_2$, Al$_2$O$_3$ and ITO with AlN, *Hsiao-Hsuan Wan*[1], *Jian-Sian Li, Chao-Ching Chiang, Xinyi Xia, David Hays,* University of Florida; *Nahid Sultan Al-Mamun, Aman Haque,* Pennsylvania State University; *Fan Ren, Stephen Pearton,* University of Florida

The valence and conduction band offsets at the interfaces between NiO/AlN, SiO$_2$/AlN, Al$_2$O$_3$/AlN and ITO/AlN heterointerfaces were determined via x-ray photoelectron spectroscopy using the standard Kraut technique. These represent systems which potentially would be used for p-n junctions, gate dielectrics and improved Ohmic contacts to AlN, respectively. The band alignments at NiO/AlN interfaces are nested, type I heterojunctions with conduction band offset of -0.38 eV and valence band offset of -1.89 eV. The SiO$_2$/AlN interfaces are also nested gap, type I alignment with conduction and offset of 1.50 eV and valence band offset of 0.63 eV. The Al$_2$O$_3$/AlN interfaces are type-II (staggered) heterojunctions with conduction band offset -0.47 eV and valence band offset 0.6 eV. Finally, the ITO/AlN interfaces are type-II (staggered) heterojunctions with conduction band offsets of -2.73 eV and valence band offsets of 0.06 eV. The use of a thin layer of ITO between a metal and the AlN is a potential approach for reducing contact resistance on power electronic devices, while SiO$_2$ is an attractive candidate for surface passivation or gate dielectric formation on AlN. Given the band alignment of the Al$_2$O$_3$, it would only be useful as a passivation layer. Similarly, the use of NiO as a p-type layer to AlN does not have a favorable band alignment for efficient injection of holes into the AlN.

5:00pm EM+AP+TF-WeA-12 Ferroelectric Al0.2Sc0.8N Diodes on NbN Electrodes Deposited on Sapphire Substrates, *Giovanni Esteves, Troy Tharpe, Travis Young, David Henry,* Sandia National Laboratories

The emergence of wurtzite ferroelectrics and their scaling below 50 nm has significantly broadened their applications in microelectronics, extending their utility into harsh environments. Ferroelectric aluminum scandium nitride (Al$_{1-x}$Sc$_x$N) exhibits a unique diode behavior due to its internal switchable polarization. Although AlScN is often accompanied by high coercive fields (E_c) exceeding 3 MV/cm, in contrast to its fluorite ferroelectric counterparts which have E_c values below 1 MV/cm, this high E_c is advantageous for high-temperature microelectronic applications where E_c decreases with temperature. When scaling the thickness below 50 nm, challenges related to achieving high crystallographic texture and accurate device measurements become significant. To address these challenges, this study explores the use of NbN films deposited on sapphire substrates to template the AlScN. X-ray diffraction results reveal that a 24 nm AlScN film inherits its in-plane texture from the underlying NbN film deposited on sapphire. Ferroelectric capacitors were fabricated using 100 nm NbN films as both top and bottom electrodes, and current-voltage (IV) measurements were conducted across multiple capacitors. The ratio of the high resistance state (HRS) to the low resistance state (LRS) was studied as a function of drive voltage, demonstrating changes ranging from 2x to 500x, with some capacitors exhibiting changes well above 1000x. The response between the HRS and LRS is controlled via the partial switching of domains—regions of uniform polarization—within the AlScN film. The promising results of this study pave the way for future applications of AlScN in non-volatile memory devices capable of operating at high temperatures, as well as in analog computing systems. Additionally, continued research into the effects of extreme environments on the ferroelectric response of AlScN will further enhance its potential for robust and reliable performance in demanding conditions. These advancements could significantly impact the development of next-generation microelectronic devices, offering improved functionality.

5:15pm EM+AP+TF-WeA-13 Optimizing Sputtering Parameters for Tantalum Oxide-Based Resistive Memory: A Design of Experiments Approach, *Alireza Moazzeni,* Wayne State University; *Sakir Karakaya, Ahmedul Khan, Gozde Tutuncuoglu,* Wayne state university

AbstractThis study optimizes sputtering parameters for Tantalum Oxide-based Resistive Random-Access Memory (TaO$_x$ RRAM, 1<x<2.5) using the Design of Experiments (DOE). By varying oxygen partial pressure (20% and 35%) and DC power (75 W and 250 W), we aim to control device performance metrics like forming voltage and power consumption. Response Surface Methodology (RSM) and Central Composite Design (CCD) were used, with 12 experimental settings and four center points, to explore parameter interactions. The goal is to improve the uniformity and reliability of TaO$_x$ RRAM fabrication for future high-performance memory systems.

IntroductionTantalum Oxide-based RRAM is a promising non-volatile memory technology for neuromorphic computing, integrating memory and processing to reduce data transfer bottlenecks [1]. TaO$_x$ RRAM's endurance, thermal stability, and scalability make it suitable for various applications [2]. The material's properties can be tuned via thin-film synthesis, particularly by adjusting DC sputtering parameters, allowing control over oxygen vacancies [3, 4]. TaO$_x$ RRAM has achieved fast switching, low power consumption, and high endurance, positioning it as a key technology for future computing systems [5].Despite these advantages, variability, particularly forming voltage, remains a challenge [6]. This is influenced by oxygen vacancy concentration, film thickness, and sputtering conditions [7, 8]. Controlling these factors can reduce device variability [9]. While previous studies looked at oxygen pressure and power independently, this study explores their combined effects on performance.Design of Experiments (DOE), specifically RSM and CCD, was used to optimize the sputtering process within limited operational ranges. CCD allowed efficient exploration of factor values, while RSM provided a framework for modeling multiple variables. The objective is to optimize sputtering parameters, develop a predictive model, and enhance performance metrics like forming voltage and power consumption. Oxygen pressure levels (20% and 35%) and power levels (75 W and 250 W) were chosen with significant separation to identify key trends. Interactions between parameters were also examined, with four center points included for validation, resulting in 12 experimental settings. Figure 1 and Table 1 illustrate the setup and design points.

By optimizing sputtering parameters and investigating their interactions, this study aims to reduce variability in TaO$_x$ RRAM devices and improve performance metrics, contributing to the scalable integration of this technology in next-generation computing systems.

Magnetic Interfaces and Nanostructures
Room 121 - Session MI+2D+AC+TF-WeA

2D Magnetism and Magnetic Nanostructures
Moderators: Mikel Holcomb, West Virginia University, **Tiffany Kaspar**, Pacific Northwest National Laboratory

2:15pm MI+2D+AC+TF-WeA-1 Interface Tunable Magnetism in Transition Metal Telluride Thin Films and Heterostructures, *Hang Chi,* University of Ottawa, Canada **INVITED**

Novel quasi-2D magnets are attracting much attention recently. In situ prepared sharp interfaces are desirable for strain engineering and/or hybridizing with other quantum systems, enabling fundamentally new phenomena and opportunities for spintronics [1]. Ferromagnetic Cr$_2$Te$_3$ ultrathin films, optimally grown on Al$_2$O$_3$(0001) and SrTiO$_3$(111) using molecular beam epitaxy, manifest an extraordinary sign reversal in the anomalous Hall conductivity as temperature and/or strain are modulated. The nontrivial Berry curvature in the electronic-structure momentum space is believed to be responsible for this behavior [2]. Furthermore, when proximitized with (Bi,Sb)$_2$Te$_3$-type topological insulator, via the Bloembergen-Rowland interaction, magnetic ordering in monolayer Cr$_2$Te$_3$ is favorably enhanced, displaying an increased Curie temperature [3]. Combining ab initio simulation, advanced scanning tunneling microscopy, magnetic force microscopy, transmission electron microscopy, magneto transport and particularly depth-sensitive polarized neutron reflectometry, Cr$_2$Te$_3$ has been established as a far-reaching platform for further investigating the marriage of magnetism and topology. These findings provide new perspectives to the magnetic topological materials in general, that are topical for the future development of topological spintronics.

References

[1] H. Chi and J. S. Moodera, "Progress and prospects in the quantum anomalous Hall effect", APL Mater. 10, 090903 (2022). https://doi.org/10.1063/5.0100989

[2] H. Chi, Y. Ou, T. B. Eldred, W. Gao, S. Kwon, J. Murray, M. Dreyer, R. E. Butera, . . . J. S. Moodera, "Strain-tunable Berry curvature in quasi-two-dimensional chromium telluride", Nat. Commun. 14, 3222 (2023). https://doi.org/10.1038/s41467-023-38995-4

[3] Y. Ou, M. Mirzhalilov, N. M. Nemes, J. L. Martinez, M. Rocci, A. Akey, W. Ge, D. Suri, . . . H. Chi, "Enhanced Ferromagnetism in Monolayer Cr_2Te_3 via Topological Insulator Coupling", arXiv:2312.15028 (2024). https://doi.org/10.48550/arXiv.2312.15028

2:45pm MI+2D+AC+TF-WeA-3 AVS National Student Awardee Talk/Falicov Student Award Finalist Talk: Probing Intrinsic Magnetization Dynamics of the $Y_3Fe_5O_{12}/Bi_2Te_3$ Interface at Low Temperature, *Alexandria Willcole,* Sandia National Laboratories, USA*; Valeria Lauter,* Oak Ridge National Laboratory, USA*; Alexander Grutter,* National Institute of Standards and Technology (NIST)*; Carsten Dubs,* INNOVENT e.V. Technologieentwicklung, Germany*; David Lidsky,* Sandia National Laboratories, USA*; Bin Luo[1][2],* Northeastern University, US*; Morris Lindner, Timmy Reimann,* INNOVENT e.V. Technologieentwicklung, Germany*; Nirjhar Bhattacharjee,* Northeastern University, US*; Tzu-Ming Lu, Peter Sharma, Nichole R. Valdez, Charles J. Pearce, Todd C. Monson,* Sandia National Laboratories, USA*; Matthew Matzelle, Arun Bansil, Don Heiman, Nian Xiang Sun,* Northeastern University, US

Topological insulator-magnetic insulator (TI-MI) heterostructures are essential in spintronics, enabling magnetization control via topological surface state-induced spin orbit torque. However, many TI-MI interfaces often face issues like contamination in the magnetic insulator and a low-density transitional region in the topological insulator, which obscure the system's intrinsic properties. In this study, we addressed these challenges by depositing sputtered Bi_2Te_3(BT) on liquid phase epitaxy grown $Y_3Fe_5O_{12}$ (YIG)/$Gd_3Ga_5O_{12}$. The liquid phase epitaxy grown YIG exhibits exceptional interface quality, without an extended transient layer derived from interdiffusion processes of the substrate or impurity ions, thereby eliminating rare-earth impurity-related losses in the MI at low temperatures. At the TI-MI interface, high resolution depth-sensitive polarized neutron reflectometry confirmed the absence of a low-density transitional growth region of the TI. The demonstrated BT/YIG system is uniquely suited to elucidate the intrinsic TI-magnetic insulator magnetization dynamics due to the lack of an extended transient layer in the magnetic insulator at the magnetic insulator-substrate interface and lack of a low density, intergrowth region of the TI at the TI-magnetic insulator interface.

By overcoming these undesirable interfacial effects, we isolate and probe the intrinsic low-temperature magnetization dynamics and transport properties of the TI-MI interface. Using temperature dependent ferromagnetic resonance (FMR) we found a strong damping enhancement at low temperature due to the topologically protected Dirac surface states (TSS) in the Bi_2Te_3 film – a signature of significant spin pumping. Accompanying the damping enhancement, we also observed a large induced in-plane magnetic anisotropy for the BT/YIG heterostructure. We explain this by spin-pumping and spin-momentum locking, due to which the precessing spins of the YIG are forced to align with the spins pumped into the TSS and therefore remain locked in the plane of the BT/YIG interface. The temperature dependence of the magnetotransport which supports the suppression of bulk conduction, and the emergence of weak-antilocalization is consistent with the low temperature enhanced spin pumping in the BT/YIG that we observed, highlighting the interplay between the transport and spin pumping behavior in the TI-MI system. Further study of TI-magnetic insulator interfaces, specifically magnetic insulators with perpendicular magnetic anisotropy, are pertinent to potentially unlock high temperature quantum anomalous hall effect (QAHE) heterostructures, and the next generation of low power spintronics.

3:00pm MI+2D+AC+TF-WeA-4 Falicov Student Award Finalist Talk: Surface Investigation of ε-phase Mn3Ga on GaN (0001) Substrate using Scanning Tunneling Microscopy, *Ashok Shrestha[3], Ali Abbas, David C. Ingram, Arthur R. Smith,* Ohio University

Antiferromagnetic materials have garnered significant attention due to their exotic properties and possible applications in next generation spintronic memory and computing devices [1]. In recent years, research on non-collinear antiferromagnetic materials such as Mn_3X (X: Ir, Ge, Sn, Ga) has heightened due to non-trivial, topological properties of these materials with unique spin textures [2]. Among these Mn-based antiferromagnets, Mn_3Ir has been commonly employed for applications [3]. As Ir is an expensive metal, efforts have been made to explore Ir-free antiferromagnets. Particularly, Mn_3Ga emerges as a promising candidate due to its versatile texture, magnetic ordering, and properties akin to Mn_3Ir [4]. Among the three distinct phases of Mn_3Ga, one of the most intriguing yet less explored is the ε-phase ($D0_{19}$-Mn_3Ga), which exhibits anomalous Hall effect and topological Hall effect in distinct temperature ranges [3]. In this presentation, we will delve into the growth and surface studies of a thin film of $D0_{19}$-Mn_3Ga on a Ga polar- GaN (0001) substrate.

We have successfully grown an epitaxial ε-phase Mn_3Ga layer using molecular beam epitaxy. The sample quality, lattice constants and crystal structure of the grown film were determined by *in-situ* reflection high energy electron diffraction and *ex-situ* X-ray diffraction. Upon examination with scanning tunneling microscopy, the surface revealed multiple terraces and row-like structures. Notably, the edges of the terraces form 120° angles with each other, consistent with the hexagonal crystal structure of the ε-phase Mn_3Ga. Additionally, we observed several stackings of just a monolayer, with their heights matching the c/2 value of Mn_3Ga. These measurements are further confirmed by X-ray diffraction. At atomic resolution, hexagonally arranged atoms with a 1 × 1 crystal structure were observed. The measured average *in-plane* atomic spacing was 5.37 ± 0.05 Å, deviating only -0.56% from theoretical predictions (5.40 Å). However, atomic spacing exhibited local variations. Other interesting structures were also observed in the scanning tunneling microscopy images, which will be discussed in the presentation. Chemical analysis via Rutherford backscattering confirmed the sample's Mn:Ga ratio as 3.2:1.0, which depends on the growth temperature. Further research will involve exploring non-collinear antiferromagnetism using spin-polarized scanning tunneling microscopy, with results to be presented at the conference.

References:

Chen et al., APL Mater.**11**, 111026 (2023).

Qin et al., Nature **613**(7944), 48 (2023).

Hernandez et al., Surf. and Interface **41**, 103167 (2023).

1. Liu et al., Sci. Rep. **7**(1), 515 (2017).

3:15pm MI+2D+AC+TF-WeA-5 Thermally Generated Spin Transport Across Magnetic Interfaces, *Hari Srikanth,* USF Tampa   **INVITED**

Spin-heat coupling and thermo-spin transport are topical areas of interest for the spintronics community. The origin of longitudinal Spin Seebeck effect (LSSE) and its relationship with magnetic anisotropy as well as magnon propagation across magnetic insulator/heavy metal interfaces have remained challenging issues. LSSE induces incoherent magnon excitations with the application of a temperature gradient across the thickness of a magnetic material. Although the ferrimagnetic insulator $Y_3Fe_5O_{12}$ (YIG) is known as the benchmark system for LSSE, other members of the insulating rare earth iron garnet family, *e.g.* the compensated ferrimagnet Gd_3Fe5O_{12} (GdIG), ferrimagnet insulator $Tm_3Fe_5O_{12}$ (TmIG) etc., are of interest and have received less attention from the point of view of spin-caloritronics. We have pioneered the technique of RF transverse susceptibility to probe the effective magnetic anisotropy in magnetic materials and heterostructures. Combining the RF transverse susceptibility with LSSE measurements, we have shown correlation between bulk and surface anisotropy with the field and temperature dependence of LSSE in YIG/Pt heterostructures and other compensated ferrimagnets like GdIG. Our recent work on TmIG/Pt heterostructures with varying film thickness reveals the clear role of anisotropy and Gilbert damping on the LSSE. From RF susceptibility, LSSE and broadband FMR experiments, quantitative analysis of the magnon propagation length and its correlation with magnetic anisotropy and Gilbert damping has been done. Overall, this talk would present new results in the thermal spin transport of garnet heterostructures which are of fundamental importance in spin transport across magnetic interfaces.

---

[1] **AVS National Student Awardee**
[2] **Falicov Student Award Finalist**

[3] **Falicov Student Award Finalist**

4:15pm MI+2D+AC+TF-WeA-9 Spin Switchable 2D-Superlattice Metal-Halide Perovskite Film via Multiferroic Interface Coupling, *Bogdan Dryzhakov,* Oak Ridge National Laboratory; *Bin Hu,* University of Tennessee Knoxville; *Valeria Lauter,* Oak Ridge National Laboratory

Solution-processible 2D-phase metal-halide perovskites have emerged as a remarkable class of semiconducting, exhibiting a wide-range of optoelectronic properties and multi-functionalities. In this work, interfacing ferromagnetic spins with this semiconductor's Rashba band yields magnetic field control over the excited state spin degrees of freedom, as demonstrated through optical analogues that resolve the spin polarization in steady-state and dynamics, and in-situ neutron scattering methods, where a photo-ferromagnetic profile is depth-resolved. The 2D-superlattice perovskite films are prepared using an optimized, low-cost spin-cast method, resulting in highly crystalline and smooth thin films with a well-defined alternating layered structure of self-assembled organic cations and lead-iodide octahedra. Within the anisotropic 2D-planes of MHPs, fluorinated A-site ligands distort the lattice, yielding robust ferroelectricity and Rashba bands arising from broken inversion symmetry and strong spin-orbit coupling. Spin-switchable circularly polarized photoluminescence (CPL) between σ+ and σ- polarizations is achieved at the multiferroic perovskite/Co interface by manipulating the ferromagnetic spins on the Co surface between positive and negative magnetic field directions. This switching behavior arises from selective interactions between the ferromagnetic spins on the Co surface and the circularly polarized σ+ and σ- orbitals within the perovskite's Rashba band structures. Polarized neutron reflectometry measurements reveal long-range interactions of the Co magnetism to the perovskite's spin-polarized excitons, with chemical (NSLD) and magnetization (MSLD) depth profiles indicating optically induced magnetization through the perovskite's thickness. This work presents a fundamental platform for exploring spin selectivity effects within Rashba band structures using CPL studies in multiferroic perovskite/ferromagnetic interfaces.

4:30pm MI+2D+AC+TF-WeA-10 Engineering the Hybrid Nanocolumnar Metamaterial Platforms for Advanced Optical and Magnetic Applications, *Ufuk Kilic, Chad Briley,* University of Nebraska-Lincoln; *Rene Feder,* Fraunhofer Institute for Microstructure of Materials and Systems, Germany; *Derek Sekora,* University of Nebraska-Lincoln; *Ahsan Ullah,* University of Nebraska - Lincoln; *Alyssa Mock,* Weber State University; *Christian Binek,* University of Nebraska - Lincoln; *Heidemarie Schmidt,* Friedrich Schiller University, Germany; *Christos Argyropoulos,* The Pennsylvania State University; *Eva Schubert, Mathias Schubert,* University of Nebraska - Lincoln

The hybrid metamaterial platforms have garnered remarkable attention in various subdiciplines of physics, chemisty, and biology due to their wide range of advanced functionalities including strong tunable optical and magnetic anisotropies, the ability to confine, modulate, and control of light, to engineer new permanent nanomagnets, for example. In this study, we employed a custom-built ultra-high vacuum electron-beam glancing angle deposition technique [1] to fabricate spatially-coherent, super lattice type nanocolumnar heterostructure metamaterial platforms from both hard (cobalt) and soft (permalloy) magnetic materials. Furthermore, by using atomic layer deposition technique, we incorporate ultrathin interface layer (~1.4 nm) of Al_2O_3 between the magnetic nano-columnar subsegments. This interface engineering at nanoscale provides another angle of freedom to tune both the magnetic and optical properties of hybrid nanocolumnar metamaterial platforms.

By taking the advantage of the generalized spectroscopic ellipsometry technique, we reached out the complex anisotropic dielectric properties of the fabricated structures. Our analysis involves widely used anisotropic Bruggeman effective medium model approach which provides to extract optical and structural properties, accordingly [2]. Moreover, to perform magnetic characterization of our fabricated metamaterial design, we employed both generalized vector magneto-optic ellipsometry and vibrating sample magnetometer measurements [3]. In order to delve into the fundamental driving mechanisms behind the anisotropic tunable magneto-optic responses from the proposed metamaterial platforms, we conducted a series of systematic micromagnetic and finite element modeling simulations, as well. We believe that these new structural metamaterial designs can result in the development of next-generation sensing devices, permenant nanomagnets, magnetic recording technologies, on-chip nanophotonic and opto-magnetic device applications.

References:

[1] Kilic, U., et al. Sci Rep 9, 71 (2019).

[2] Schmidt, D., and Schubert, M., J. Appl. Phys. 114.8 (2013).

[3] Briley, Chad, et al. Appl. Phys. Lett. 106.13 (2015).

4:45pm MI+2D+AC+TF-WeA-11 Magnetic Field Affects Oxygen Evolution Reaction Only in Metal Oxy-Hydroxides, *Filippo Longo,* Chemical Energy Carriers and Vehicle Systems Laboratory, Empa, Swiss Federal Laboratories for Materials Science and Technology, Switzerland; *Reshma Peremadathil Pradeep, Emily Darwin, Hans Josef Hug,* Magnetic and Functional Thin Films Laboratory, Empa, Swiss Federal Laboratories for Materials Science and Technology, Switzerland; *Andreas Borgschulte,* Chemical Energy Carriers and Vehicle Systems Laboratory, Empa, Swiss Federal Laboratories for Materials Science and Technology, Switzerland

Ni-based electrodes have been largely employed in alkaline electrolyzers for the production of H_2 and O_2 [1]. Due to the sluggish kinetics of the oxygen evolution reaction (OER), many experimental approaches have been employed to boost the catalytic performance of such electrodes [2]. The application of an external magnetic field during OER has shown outstanding catalytic improvement [3]. Despite considerable research effort, the understanding of its origin is still object of debate [4,5]. In this work we show how the Ni-based electrodes improve their catalytic activity towards OER during the application of an external magnetic field. We investigate in detail the catalytically active surface, the microscopic, electronic, and magnetic structures by soft- and hard X-ray photoelectron spectroscopy combined with impedance spectroscopy and magneto-optical measurements. It is relevant in this context that the oxy-hydroxide formed during OER is the catalytically active compound, and is thus likely also the origin of the magnetic effect. To underline the importance of the oxy-hydroxide formation, we employ a multilayered system made of Co-Pt-Ru multi-lattices, exhibiting much more favorable magnetic properties (such as strong perpendicular magnetic anisotropy) than nickel. Interestingly, hardly any improvement of OER is found. The various findings corroborate the picture of spin-exchange interaction of metal-oxide bonds as the underlying mechanism of the magneto-chemical effect.

[1] S. W. Sharshir et al., International Journal of Hydrogen Energy (2023).[2] J. S. Kim et al., Adv. Energy Mater. (2018), 8, 1702774.[3] F.A. Garcés-Pineda et al., Nat Energy 4, 519–525 (2019).[4] T. Wu et al., Nat Commun 12, 3634 (2021).[5] X. Ren et al., Nat Commun 14, 2482 (2023).

Plasma Science and Technology
Room 124 - Session PS1-WeA

Plasma Modelling AI/ML

Moderators: Harutyun Melikyan, Micron Technology, **Mingmei Wang**, Lam Research Corporation

2:15pm PS1-WeA-1 Sequential Plasma Process Design by Genetic Algorithm, *Patrick Conlin, Gregory Hartmann, Qiang Wang, Roberto Longo, Shyam Sridhar, Peter Ventzek,* Tokyo Electron America, Inc.

The complexity of modern semiconductor device fabrication has caused the parameter space of plasma process design to balloon to levels which are untenable to navigate without algorithmic guidance. The degrees of freedom provided by so-called process knobs alone present a substantial optimization challenge. "Time" is by far the most flexible process knob and the sequencing of plasma processes is the largest source of complexity, next to the choice of process chemistry. Understanding the interval scheduling problem in the context of plasma-surface interactions is hindered by a sparse fundamental knowledge of species-surface site interactions, and the computational and experimental effort required to elucidate these relationships. An alternative approach to the scheduling problem is to employ phenomenological models to establish guiding principles for how a process is sequenced, i.e. the problem may be split into more tractable parts. For example, how flux and energy interact on a surface can be used to order sequences of fluxes. From sequences of flux and energy, one can work backwards to understand plasma conditions that can be used practically. Many different optimization approaches are available for the scheduling problem. Here we describe the use of a genetic algorithm (GA) to study the impact of time series of plasma-generated species and energy flux on basic surface evolution parameters like etch depth, selectivity, and profile. GAs are well-established in the study of optimization and are considered especially well-suited for solving interval scheduling problems. We encode Langmuir-Hinshelwood plasma-surface interaction kinetics, which form the fundamental basis for plasma processes, into our GA. We recover the intuitive limits where continuous and atomic layer etch equivalents of radical pre-loading are optimal sequences. Models of increasing complexity are demonstrated with

Wednesday Afternoon, November 6, 2024

different objective functions. The limitations of GAs, generally and in this specific context, are discussed.

2:30pm PS1-WeA-2 Machine-Learning-Based Force Fields for Molecular Dynamics Simulation of Silicon and Silicon Dioxide Ion Beam Etching, *Shunya Tanaka, Satoshi Hamaguchi,* Division of Materials and Manufacturing Science, Graduate School of Engineering, Osaka University, Japan; *Hiori Kino,* National Institute for Materials Science (NIMS), Japan

Recently machine-learning (ML) techniques have been developed to create interatomic force fields and potentials for classical molecular dynamics (MD) simulations in the field of materials science. The ML-based force fields are the surrogate model of the realistic interatomic force fields, where the surrogate model can offer the force fields far more quickly than the corresponding density-functional-theory (DFT)-based quantum mechanical calculation by interpolating a large amount of force-filed data with a large number of possible atomic configurations evaluated in advance by the DFT-based calculations. The ML-based force fields are expected to be far more accurate than the widely used classical interatomic force-field models and can be as accurate as those obtained from the DFT-based calculations. However, unlike typical MD simulations in thermodynamical equilibrium widely used in materials science, sputtering/etching simulations require special attention in the development of such force fields; in typical sputtering simulations with high-ion-energy impacts, some interatomic distances can become extremely small and the standard DFT-based force-field data do not cover such cases. Therefore, in our study, the Ziegler-Biersack-Littmark (ZBL) potential functions were used to represent the short-rang repulsive interaction whereas the ML-based force fields were employed otherwise. The ML-based force fields were developed with the Behler-Parinnello Neural Network (BPNN) and the Graph Neural Network (GNN) with active learning based on query by committee sampling. MD simulations with the newly obtained MD-based force fields were performed for ion beam sputtering/etching of Si and SiO_2 and the results were compared with the beam experimental data as well as the existing classical MD simulation results.

2:45pm PS1-WeA-3 Machine Learning Interatomic Potentials for Plasma-Surface Interaction Simulations, *Jack Draney, Athanassios Panagiotopoulos, David Graves,* Princeton University

Results of molecular dynamics (MD) simulations of nonequilibrium plasma-surface interactions are highly sensitive to the accuracy of the underlying interatomic potential. Increasingly complex interatomic potentials, such as ReaxFF [1], have been developed to capture more and more of the underlying physics of atomic forces. The most flexible and accurate potentials are often the slowest, requiring significant computing power to reach the long timescales typical in simulations of plasma-surface interactions. Machine learning potentials (MLP) such as DeePMD [2], originally developed to fit quantum density functional theory (DFT) data, represent maximally flexible models and run quickly on GPUs. In this work, we show how MLPs can not only be derived from DFT, but also from classical potentials like ReaxFF. We demonstrate the quality of the derived MLPs by comparing them to their classical counterparts in simulations of oxygen, hydrogen, and argon plasma interactions with diamond and amorphous carbon surfaces. We use what we've learned from this process to fit MLPs to DFT data for the same system and compare the results to those from classical potentials. Finally, we outline some of the possible pitfalls associated with the successful production and use of MLPs for plasma-surface interactions.

[1] van Duin, A. C. T. et al. ReaxFF: A Reactive Force Field for Hydrocarbons. *J. Phys. Chem. A* **2001**, *105* (41), 9396–9409. https://doi.org/10.1021/jp004368u.

[2] Zeng, J. et al. DeePMD-Kit v2: A Software Package for Deep Potential Models. *J. Chem. Phys.* **2023**, *159* (5). https://doi.org/10.1063/5.0155600.

3:00pm PS1-WeA-4 Dry Etching Process with NLD Plasma Distribution Determined by Machine Learning, *Keiichiro Asakawa, Kenta Doi, Yasuhiro Morikawa,* ULVAC, Inc., Japan

A magnetic neutral line discharge (NLD) is an inductively coupled plasma generated along a magnetic neutral loop (NL). NLD can generate high-density plasma with low electron temperature at low gas pressure, and is used for dry etching of various device structures such as optical devices and MEMS (Micro Electro Mechanical System). Typically, a magnetic field is induced by three electromagnetic coils placed around the chamber, and the NL region is formed in a ring shape where the magnetic fields cancel each other out and become zero. The radius of NL depends on the current value of each electromagnetic coil. Therefore, by adjusting the current values of

the electromagnetic coils, the size of the NL radius can be modified and the spatial distribution of plasma can be optimized for the required etching distribution across a wafer. Conventionally, it was time-consuming to optimize the current values of each electromagnetic coils so that the resultant magnetic field for a given NL radius would be zero. Therefore, we developed a new application that applies machine learning (gradient descent method), and made it possible to instantly output the coil current values for each input NL radius and Z-axis position. This has become an effective means of spatial and temporal control of the NLD plasma distribution, potentially realizing uniform etching condition, i.e., radicals and ions contributions, across a wafer.

3:15pm PS1-WeA-5 Accelerating Plasma-based Process Development and Chamber Productivity with Artificial Intelligence, *Meghali Chopra, Steve Sirard,* SandBox Semiconductor Incorporated

Developing advanced semiconductor chips is becoming more expensive and time consuming due to the growing sophistication of processing tools, recipes, and chip architectures.Traditional brute force trial-and-error approaches for optimizing recipes are becoming unsustainable as it is impractical for human process engineers to experimentally explore the trillions of possible recipe combinations on advanced fabrication tools.Furthermore, many of the recipe parameters for plasma etch and deposition processes display complex, non-linear interactions.Here we showcase a software platform, SandBox Studio™ AI, that efficiently generates optimal recipes for plasma etch and deposition processes in less than 75% of the time of statistical experimental design approaches.Superior performance is achieved by using a hybrid physics-based model coupled with artificial intelligence (AI), thus requiring far fewer experiments to calibrate.The platform is tool agnostic and automatically maps the multi-dimensional process space and provides recipe recommendations to achieve desired feature profile and uniformity targets.The AI-driven approach has been applied across a wide variety of applications and development phases.Successful examples of plasma etch and deposition recipe predictions that optimize both feature profiles and wafer uniformity for logic and memory applications will be discussed.Additionally, we demonstrate how co-optimized multi-step etch and deposition recipes capture step interactions, leading to a larger process window compared to sequentially optimizing each step separately.Beyond process engineering, SandBox Studio™ AI can be used to improve fab tool productivity. The AI toolset has been used to identify the root causes of process drift by correlating tool sensor data to on-wafer results. The software has addressed other common tool issues such as chamber-to-chamber matching and can predict optimal recipe conditions to maximize yield across multiple chambers.An optimized model may be used to make new recipe predictions when minor fluctuations or adjustments are made to the incoming chip stack dimensions.In summary, our approach enables engineers to streamline plasma-based recipe development, cut costs, and enhance manufacturing productivity.

3:30pm PS1-WeA-6 A Unified Global Model Accompanied with a Voltage and Current Sensor for Low-Pressure Capacitively Coupled Rf Discharge, *Inho Seong, Sijun Kim,* Chungnam national university, Republic of Korea; *Woobeen Lee,* Chungnam nation univerisity, Republic of Korea; *Young Lee, Chulhee Cho, Wonnyoung Jeong,* Chungnam national university, Republic of Korea; *Minsu Choi,* Chungnam national univerisity, Republic of Korea; *Byeongyeop Choi,* Chungnam nation univerisity, Republic of Korea; *Huichan Seo, Sangheon Song,* SK Hynix, Korea; *Shinjae You,* Chungnam national univerisity, Republic of Korea

Conventional Global Model (GM) assumes that the ion energy at the electrode is equivalent to the time-averaged sheath voltage. However, our investigations using particle-in-cell simulations reveal a significant difference between the ion energy and the sheath voltage. To address this discrepancy, we introduce a Unified Global Model (UGM) that incorporates real-time voltage and current measurements and integrates plasma circuit and sheath model to accurately calculate both ion energy and collisional energy losses. Comparative analysis with experimental data demonstrates that the UGM provides a closer match to observed results than the conventional GM, with a strong linear correlation indicating its reliability for plasma monitoring applications.

Plasma Science and Technology
Room 124 - Session PS2-WeA

Plasma Processes for Emerging Device Technologies

Moderators: Phillipe Bezard, IMEC Belgium, **Catherine Labelle**, Intel Corporation

4:15pm PS2-WeA-9 Low Damaged GaN Surface Through Passivating Plasma Etching and Post-Etch Treatments for Improved GaN-MOS Capacitor Performance, *David Cascales,* CEA-LETI & LTM, France; *Patricia Pimenta-Barros, Eugénie Martinez,* CEA-LETI, France; *Bassem Salem,* LTM - MINATEC - CEA/LETI, France

The power electronics industry is facing new challenges to meet the increasing needs of electrical power in modern devices[1]. These needs require an efficiency rise of power converters, also accompanied by higher operating voltages, currents and frequencies. Wide bandgap materials such as GaN are then investigated and preferred to Si-IGBT converters due to silicon limits being reached[2]. Lateral and vertical GaN-based power devices have emerged such as the vertical MOSFET or the lateral MOS-channel High Electron Mobility Transistor (MOSc-HEMT). With both technologies, normally OFF properties are needed and can be achieved with a gate recess, while a MOS gate controls the channel operation.

Plasma processing is crucial for channel and gate performance[3]. For instance, the recess shape can directly affect channel conducting properties and gate leakage, while the damaged GaN layer can influence the gate's behavior by deteriorating the flat band voltage. Indeed, flat band voltage is driven by charge generation that is caused by lattice amorphization, nitrogen depletion, element implantation or etching by-products deposition[4].

This study aims to investigate negative charge generation at the GaN/dielectric interface in order to shift threshold voltages towards greater values. Plasma etchings and post etch treatments (PET) were performed in an ICP chamber, together with pre-deposition treatments in the ALD chamber prior to dielectric deposition to limit nitrogen depletion and lattice amorphization.

First, thanks to X-ray Photoelectron Spectroscopy measurements, we will discuss the chemical modifications induced by silicon introduction ($SiCl_4$) in a Cl_2 plasma etching chemistry. A Si-based layer protecting GaN from ion bombardment is present at the Al_2O_3/GaN interface. The Si-layer and GaN evolution through the MOS capacitor fabrication steps will then be analyzed, including the O_2 PET, and the Al_2O_3 ALD preceded by an HCl gallium oxide removal. $SiCl_4$ addition shows a significant flat band voltage improvement with C-V measurements. As well, HCl replacement by a dry *in situ* N_2/H_2 pre-deposition treatment for high $SiCl_4$ etching ratios will also be examined.

Finally, we will explore the impact of PET chemistry variations after $SiCl_4/Cl_2$ etching with addition of N_2 to the O_2 chemistry, giving a better understanding of the plasma interactions with GaN, the SiN holder and chamber walls. The goal is to restore the N/Ga ratio with nitrogen supply.

[1]International Energy Agency (IEA), World Energy Outlook (2022)
[2]E. A. Jones et al., *IEEE WiPDA* (2014)
[3]S. Ruel *et al.*, *J. Vac. Sci. Technol. A*, 39(2), p. 022601
[4]P. Fernandes Paes Pinto Rocha, *Energies*, 16(7), p. 2978

4:30pm PS2-WeA-10 Anisotropic and Sub-Micrometric InGaP Plasma Etching for High Efficiency Photovoltaics, *Alison Clarke, Mathieu de Lafontaine,* University of Ottawa, Canada; *Richard R. King, Christiana B. Honsberg,* Arizona State University; *Karin Hinzer,* University of Ottawa, Canada

Nanoscale III-V semiconductor etching enhances light trapping, enabling low cost and efficient photovoltaic devices [1]. Mitigating sidewall erosion and chlorine-based defects is crucial for increased device performance. However, anisotropic III-V patterning with sub-micrometric definition has many challenges, such as sidewall erosion and surface damage [2]. Room-temperature InGaP plasma etching is challenging due to non-volatile $InCl_x$ subproducts. Chlorine-based plasmas lead to defects which can be passivated by introducing hydrogen-based plasma chemistries [3].

InGaP nanotextures with vertical sidewalls were patterned using electron-beam lithography and inductively coupled plasma etching. Circular nanotextures with 850 nm diameter and 150 nm minimum spacing were patterned in a hexagonal array. The etch was performed at room temperature to limit sidewall erosion [3], using the resist as a mask. To assess the impact of chlorine and hydrogen, four plasma chemistries were investigated: Cl_2/Ar, Cl_2/H_2, $Cl_2/Ar/H_2$, and Ar/H_2. The etched InGaP was

investigated with atomic force microscopy. The Cl_2/H_2 plasma produced the fastest average etch rate (150 nm/min), with aspect ratio of 0.66. The Ar/H_2 plasma had the slowest average etch rate (75nm/min) due to the absence of Cl-based chemical etching. All etch rates were low due to the high (~25%) In content in the InGaP which creates poor volatility byproducts. Hydrogen improved the etching process, suppressing chlorine-based defects and decreasing the line edge roughness by up to 48% compared to the plasma without hydrogen.

These results show that hydrogen-based plasma chemistries improve pattern transfer for photovoltaics applications, where precise control of critical dimensions is required to improve conversion efficiencies. Ongoing work on top view and cross-sectional scanning electron microscopy will also be presented along with device performance measurements to confirm light-trapping properties. Complimentary characterizations such as energy-dispersive X-ray spectroscopy will be performed to benchmark the passivation properties of hydrogen plasmas.

[1] N.P. Irvin et al., "Monochromatic Light Trapping in Photonic Power Converters," *49th IEEE Photovoltaics Specialists Conference,* 0143 (2022).

[2] M. Bizouerne et al., "Low damage patterning of In0.53Ga0.47As film for its integration as n-channel in a fin metal oxide semiconductor field effect transistor architecture," *J. Vac. Sci. Technol.*, 36(6):061305 (2018).

[3] M. de Lafontaine et al., "Anisotropic and low damage III-V/Ge heterostructure etching for multijunction solar cell fabrication with passivated sidewalls." *Micro Nano Eng.*, 11:100083 (2021).

4:45pm PS2-WeA-11 On the Plasma Etching Mechanisms of Patterned Aluminum Nitride Nanowires with High Aspect Ratio, *Saron Sales de Mello,* **Lucas Jaloustre,** University Grenoble Alpes, CNRS, LTM, France; *Sebastien Labau, Camille Petit-Etienne,* University Grenoble Alpes, CNRS,LTM, France; *Gwénolé Jacopin,* University Grenoble Alpes, CNRS, Institut Néel, France; *Erwine Pargon,* University Grenoble Alpes, CNRS, LTM, France

III-nitride (III-N) semiconductor light-emitting diodes (LEDs) are a particularly promising alternative to mercury vapor lamps as ultra violet (UV) sources [1]. However, the external quantum efficiency (EQE) of current planar Al_xGa_yN well-based UV LEDs is extremely low (<1% for wavelengths below 250 nm)[2]. Three-dimensional (3D) core−shell architecture offers some promising solutions to increase UV LED efficiency up to 50%.This approach consists in radially growing emissive quantum wells on predefined aluminum nitride (AlN) nanowires (Fig.1) [3]. The top-down combining lithography and plasma etching transfer is the only viable approach to fabricate the well-organized arrays of high Aspect Ratio (AR) AlN nanowires required.

This study aims to develop a chlorine (Cl_2) plasma etching process in a Inductively Coupled Plasma (ICP) reactor dedicated to high AR AlN nanowires (AR>10, i.e. sub-500nm diameters, 4μm-high) fabrication, based on a fundamental understanding of the etching mechanisms involved. The samples are AlN (4μm) grown on sapphire substrate with a silicon oxide (SiO_2) 1.4μm thick hard mask on top. Electron beam lithography is used to design dots with several diameters, densities and shape. We investigate the impact of the plasma parameters (source, bias and pressure) on the AlN etch rates, AlN/SiO_2 etch selectivity, pattern profiles and sidewalls roughness. We observe that the carrier wafer (CW) chemical nature (Si or Si_3N_4) affects the nanowire profile. Under the same plasma conditions, the use of Si_3N_4 CW always leads to passivation layer formation on the AlN sidewalls, which creates more tapered AlN pillars than using Si CW (Fig. 2). In both cases $SiCl_x$ etch by products coming from the CW are present in the plasma and are likely to redeposit on AlN sidewalls [4]. However, with Si_3N_4 CW, the presence of N helps to fix the $SiCl_x$ and to form a SiNCl passivation layer.

Ion flux, ion angular distribution and ion energy measurements show that, the plasma conditions that favor high ion flux over radical flux (higher source power, lower pressure, higher bias) enhance the AlN etching, suggesting an ion-enhanced chemical etching mechanism. In addition, conditions for which the physical component of the plasma dominates lead to tapered profiles, while anisotropic ones can be obtained when the chemical component dominates. Fig. 3 shows the source power impact on the profiles. Charging and ion angular distribution effects also affect the pattern profiles. Finally, we also observe a crystal orientation preferential etching phenomenon. Cl_2 plasma etching tends to reveal nonpolar a-planes, suggesting that they are the most stable in this process.

Wednesday Afternoon, November 6, 2024

5:00pm PS2-WeA-12 Development of a New Underlayer to Improve the Adhesion of Photoresist for EUV, *Wafae Halim,* KU Leuven and Imec, Belgium; *Philippe Bezard,* Imec, Belgium; *Stefan De Gendt,* KU Leuven and Imec, Belgium

Metal Oxide Resist (MOR) is a promising resist candidate for Extreme ultraviolet lithographyexhibiting a sufficient etch contrast with carbon-based hard masks to no longer impose a particular etch resistance to the EUV underlayer. The main objective of this study is removing spin on glass from the conventional stack to avoid using the high Global Warming Potential gases used for its patterning (Fig.1). Thus, MOR should be coated on the top of a carbon hard-mask.One of the ways to achieve this objective is by treating the surface of amorphous carbon (aC) to promote adhesion between MOR and aC.

In this work, PECVD processes have been developed and their impact on the surface energy of amorphous carbon has been investigated. The MOR spin-coated on the differently treated carbon hard-masks has then been exposed to EUV light, and developed, so that the impact of the surface treatment on pattern collapse could be studied.

Figure 1 An approach to remove the SOG from the standard flow in order to have a good adhesion between MOR and aC

Surface Science
Room 120 - Session SS+2D+AMS-WeA

Defects Nanoarchitecture and Complex Systems
Moderator: Dario Stacchiola, Brookhaven National Laboratory

2:30pm SS+2D+AMS-WeA-2 Molecular Sensing ZnO Surfaces Studied by Operando Low-Energy Ion Beam Analysis, *Taku Suzuki, Yutaka Adachi, Takeshi Ogaki, Isao Sakaguchi,* National Institute for Materials Science, Japan

1. Introduction

The basic mechanism of the resistive gas sensing has been established; it is essentially a redox reaction of the surface mediated by the negatively charged oxygen adsorbate. For example, the sensing of ethanol (EtOH) with the ionosorbed oxygen of O^{2-} is written as,

$$EtOH(ads)+O^{2-}(ads) \rightarrow CH_3CHO+H_2O+2e-,(1)$$
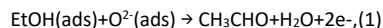
where (ads) denotes an adsorbate. It is reasonable to assume that the gas sensing properties differ between crystallographic atomic planes. Indeed, the crystal plane dependent gas sensing response has been studied by many research groups in the last decade for EtOH sensing by ZnO, which is one of the most intensively studied target gas – sensing material combinations. The specific knowledge of the crystal plane dependence of gas sensing is useful for the development of sensing materials.

The ZnO crystal plane dependence of the gas sensing properties has typically been studied using a nanocrystal. However, the effect resulting from the contact between the particles has hindered straightforward interpretation. To overcome this problem, the ZnO crystal plane dependence of the EtOH sensing was investigated using an analytical approach in the present study, namely low-energy ion scattering spectroscopy (LEIS) combined with the pulsed jet technique.

2. Method: LEIS combined with pulsed jet

We applied a newly developed He+ LEIS combined with the pulsed jet technique to analyze the surface structure of ZnO during the EtOH sensing. In this novel technique, the free gas jet is periodically blown onto the sample surface to simulate the gas sensing surface in a vacuum as one under the realistic working condition, while the background pressure is kept low enough for the operation of He+ LEIS.

The sample was ZnO single crystals with an atomically flat mirror-polished surface. Four dominant low-index surfaces, which are Zn-terminated (0001) (*c*(+)), O-terminated (0001) (*c*(-)), (10-10) (*m*), and (11-20) (*a*), were used to evaluate the crystal orientation dependent gas sensing properties.

References

[1] N. Saito et al., Chemical Sensors 39(2023)108. (Japanese)

[2] T. Suzuki et al., Surfaces and Interfaces 35(2022)102371.

[3] T. Suzuki et al., Appl.Surf.Sci.538(2021)148102.

2:45pm SS+2D+AMS-WeA-3 Finding Surface Defects in Electronic Materials, *Sujitra Pookpanratana,* National Institute of Standards and Technology **INVITED**

All electronic materials contain a wide range of defects ranging in length scales from point defects to micrometer (or sub-millimeter) scale features. Some defects can be beneficial, benign, or detrimental to the functionality of the material. It's critical to identify and locate defects, and determine their impact in the host material. Here, I will highlight the identification of defects and their impact in 2D graphene based systems and wide bandgap semiconductors using photoemission electron microscopy (PEEM). PEEM is a nanoscale, surface-sensitive, full-field imaging technique based on the photoelectric effect. PEEM provides real space imaging of surfaces with enhanced contrast mechanism based on topographic and electronic properties, and measurement of electronic properties. In the first example, we image epitaxial graphene (EG) topography in real space and measure the electronic structure of monolayer EG regions with micrometer-scale angle resolved photoemission (μ-ARPES). We detect characteristic electronic features of graphene such as the Dirac points and the π-band, and the electronic flat band at region with different contrast [1]. Through Raman spectroscopy on the same regions that were analyzed by PEEM, and we estimated a significant amount of compressive strain (~1.2%) coinciding with the flat band region [1]. In the second example, we highlight the full-field PEEM capability by following the de and re-intercalation of 2D Ag within EG under heating conditions. For the 2D Ag system, we find Ag clusters initially diffuse to the top EG surface and finally re-intercalate through defects with the Ag intercalation front to be 0.5 nm s-1 ± 0.2 nm s-1 [2]. The EG defects serve as intercalation "doors." Lastly, we will show extended surface defects propagating through epitaxy GaN and β-Ga2O3 which also induce the presence of bandgap states.

[1] F. Niefind, H. G. Bell, T. Mai, A. W. Hight Walker, R. E. Elmquist, S. Pookpanratana, J. Appl. Phys. 131, 015303 (2022).

[2] F. Niefind, Q. Mao, N. Nayir, M. Kowalik, J. J. Ahn, A. Winchester, C. Dong, R. A. Maniyara, J. Robinson, A. van Duin, and S. Pookpanratana, Small 20, 2306554 (2024).

3:15pm SS+2D+AMS-WeA-5 SSD Morton S. Traum Award Finalist Talk: Silver Iodide – Surface Structure and Ice Nucleation Investigated by Noncontact AFM, *Johanna Hütner*[1], *David Kugler,* Vienna University of Technology, Austria; *Franziska Sabath,* Bielefeld University, Germany; *Michael Schmid,* Vienna University of Technology, Austria; *Angelika Kühnle,* Bielefeld University, Germany; *Ulrike Diebold, Jan Balajka,* Vienna University of Technology, Austria

Silver iodide (AgI) is used as a cloud seeding material due to its ability to nucleate ice efficiently, which is explained by the good lattice match between AgI and hexagonal ice. The basal (0001) cleavage plane of AgI deviates from the lattice of hexagonal ice by as little as 2.5%. However, AgI consists of stacked planes of positively charged Ag+ alternating with negatively charged I-. Cleaving a AgI crystal along the (0001) plane thus exposes Ag+ and I- terminated surfaces. Both terminations are polar and inherently unstable.

We present atomically resolved noncontact atomic force microscopy (NC-AFM) images that show how AgI(0001) surfaces compensate for this non-zero electric dipole perpendicular to the surface. Both Ag and I terminated surfaces form reconstructions, whose structure affects their ice nucleating abilities. NC-AFM images of UHV cleaved surfaces exposed to water vapor reveal that ice forms an epitaxial layer only on the Ag terminated surface, whereas on the I termination ice forms three-dimensional clusters.

These atomic-level observations could enhance our understanding of ice formation processes in the atmosphere.

3:30pm SS+2D+AMS-WeA-6 SSD Morton S. Traum Award Finalist Talk: Reversible Non-Metal to Metal Transition and Effective Debye Temperatures of Highly Crystalline NiFe₂O₄ Thin Films, *Arjun Subedi*[2], *Detian Yang, Xiaoshan Xu, Peter Dowben,* University of Nebraska-Lincoln, USA

The surface of $NiFe_2O_4$ thin film undergoes a conductivity change with temperature. X-ray photoelectron spectroscopy (XPS) of $NiFe_2O_4$ thin film at room temperature showed large binding energy shifts in Ni $2p_{3/2}$, Fe $2p_{3/2}$, and O 1s core levels, due to photovoltaic surface charging indicating that prepared $NiFe_2O_4$ thin film was dielectric or non-metallic at room temperature. The core level binding energy shifts, due to photovoltaic

---

surface charging, were found to be around 5 eV for each of the core levels at room temperature. The core level binding energy shifts decreased when the thin film was annealed in vacuum. The XPS core level binding energy shifts from the expected values became negligible at an elevated temperature of 410 K and beyond. This suggests that $NiFe_2O_4$ thin film became metallic at the temperature of 410 K and beyond. When the sample cooled down to room temperature, the sample reversibly became more dielectric, showing again the same core level binding energy shifts of 5 eV. Such reversible phase change of the thin film was further supported by the reversible Fermi edge shift with temperature. Low energy electron diffraction (LEED) images, taken for the $NiFe_2O_4$ thin film surface, showed that the surface was highly crystalline throughout the reversible temperature controlled non-metal to metal transition. The XPS spectra of Ni $2p_{3/2}$, Fe $2p_{3/2}$, and O 1s core levels taken at different temperatures showed that the changes in core level binding energies followed a proposed Arrhenius-type model with temperature. The effective bulk Debye temperatures of 629.10 ± 58.22 K and 787.03 ± 52.81 K were estimated using temperature dependent intensities of Fe $2p_{3/2}$ and Ni $2p_{3/2}$ XPS spectra respectively indicative of different sites for Fe and Ni. The effective surface Debye temperature of 249.7 ± 11.1 K was estimated using temperature dependent intensities of LEED. Lower effective Debye temperature was observed for surface, as expected. The phase transition, the estimates of the effective Debye temperatures, and the model applied to the core level binding changes with temperature altogether shed light on the fundamental properties of the material with temperature.

4:15pm **SS+2D+AMS-WeA-9 In situ Structure Study of a MnOX-Na2WO4/SiO2 Catalyst for OCM under Na₂WO₄ Melting Conditions**, *Yong Yang*, ShanhaiTech University, China; *Danyu Wang, Evgeny Vovk*, Shanghaitech.edu.cn, China; *Yang Liu, Junyu Lang*, ShanghaiTech University, China

MnO_x-Na_2WO_4/SiO_2 catalyst exhibited notable C_2 selectivity/yield in the oxidative coupling of methane (OCM), a promised green chemistry reaction[1, 2]. Nevertheless, the reaction mechanism of this catalyst remains a subject of contention, particularly regarding the role of Na_2WO_4 in the activation[3, 4]. In this study, *in situ* characterizations of a TiO_2-modified MnO_x-Na_2WO_4/SiO_2 catalyst, are conducted by XRD and XPS correlating to the OCM reaction condition, focusing on the simultaneous phase transition of catalyst components within its activation temperature zone. The online MS along with XPS/XRD coupled activity study confirm that transition from Mn^{3+} to Mn^{2+} stands as a pivotal factor influencing the reactivity. *In situ* XRD further revealed that in this narrow temperature window there is a particular three-step Na_2WO_4 phase change, ending as molten salt, right before the substantial Mn^{3+} to Mn^{2+} transfer initiated. In addition, the rarely observed Na_2WO_4 behavior as molten salt is obtained by *in situ* XPS with rapid spectra collected during an on-stage heating process. A sensitive self-reduction of the tungsten upon heating to melting point is found. These comprehensive *in situ* catalyst characterizations, covering the extensive structure-activity relationship from solid state to partial molten salt condition, providing a interlocking pathway for the reactive oxygen species transfering at high temperature. The results provides new important insight into the complex MnO_x-Na_2WO_4/SiO_2 catalyst as a key to understand the activation mechanism of NaWMnSi catalyst in OCM.

[1] Lunsford JH, Catalytic conversion of methane to more useful chemicals and fuels: a challenge for the 21st century. Catalysis today 63 (2000) 165-174;

[2] Lunsford JH The Catalytic Oxidative Coupling of Methane. Angewandte Chemie International Edition in English 34 (1995) 970-980;

[3] Si J, Zhao G, Sun W, Liu J, Guan C, Yang Y, Shi XR, Lu Y Oxidative Coupling of Methane: Examining the Inactivity of the MnOx-Na2WO4/SiO2 Catalyst at Low Temperature. Angewandte Chemie International Edition 61 (2022) e202117201

[4] Fang X, Li S, Gu J, Yang D Preparation and characterization of W-Mn catalyst for oxidative coupling of methane. J Mol Catal 6 (1992) 255-261

4:30pm **SS+2D+AMS-WeA-10 Characterization of Nanoplastics Samples**, *Tycho Roorda, Maxime Brohet, Sergi Campos Jara, **Irene Groot**,* Leiden University, Netherlands

Plastic particles in the ocean have become a contaminant of emerging concern due to their damage to humans and marine animals. Of all plastic production, which is increasing still, it has been shown that more than 99% of plastic waste which ends up in the oceans cannot be accounted for. The belief is that all of this plastic degrades to a nano-sized scale which is extremely hard to detect. In order to understand the fate of nanoplastics in aquatic environments, we must have a better understanding of the

degradation mechanisms at an atomic and chemical level. In this project, we have developed procedures to evaporate powdered materials and deposit them onto a prepared surface. The deposition of nanoplastics is confirmed by mass spectrometry, Auger electron spectroscopy, and X-ray photoelectron spectroscopy. Using atomic force microscopy combined with scanning tunneling microscopy, the deposited plastics are investigated.

We also investigate plastics samples after several degradation mechanisms, such as oxygenation, hydrogenation, UV exposure, and thermal annealing. After degradation, the plastics samples are studied in ultra-high vacuum with atomic force microscopy combined with scanning tunneling microscopy and with X-ray photoelectron spectroscopy.

4:45pm **SS+2D+AMS-WeA-11 Oxidation of NiCr and NiCrMo- Unraveling the Role of Mo with XPEEM Studies**, *Keithen Orson, Devin Jessup*, University of Virginia; *Will Blades*, Juniata College; *Jurek Sadowski*, Brookhaven National Laboratory; *Yuran Niu, Alexei Zakharov*, Lund University, Sweden; *Petra Reinke*, University of Virginia

Nickel-chromium based superalloys combine good mechanical strength with excellent resistance to corrosion over a wide range of conditions. Passivity stems primarily from a thin layer of chromium oxides and hydroxides and increasing Cr content above a threshold of 11-15wt% results in a protective passive layer. Adding minor alloying elements like Mo has an outsized impact on corrosion resistance, but there is debate in literature over the mechanism of this action. To investigate the interplay of Cr concentration and Mo alloying, the early-stage oxidation (0-65 Langmuir of O_2) of Ni22Cr, Ni5Cr, and Ni22Cr6Mo were studied on a clean metal surface and moderate temperatures (450-500˚C). The oxidization was studied in-situ using x-ray photoelectron microscopy (XPEEM), which yields x-ray absorption hyperspectral images at 0, 5, 20, and 65 L of exposure, and a timeseries observing the oxide evolution from 0 to 65L at a single photon energy representative of Cr_2O_3. XPEEM valence band spectra, and conventional XPS study of the same samples complement the experiment. To analyze the $\sim 10^7$ spectra produced by hyperspectral imaging, several data dimensionality reduction techniques including principal component analysis and non-negative matrix analysis were used to gain insight into the oxide evolution, the species present, and their spatial distribution. The amounts of each species present in the hyperspectral images were quantified using cosine similarity. Oxidation of Ni22Cr produces islands of Cr_2O_3 along with a surface oxide, while on Ni5Cr larger, sparser islands are observed. For both binary alloys the oxide grows in a layer-plus-island morphology. The oxide island chemistry of Ni5Cr appears to include some NiO as well as Cr_2O_3. Ni22Cr6Mo, on the other hand, does not nucleate oxide islands visible with XPEEM but instead forms a continuous oxide layer whose thickness increases over time. This is commensurate with a layer-by-layer growth mode which is a significant advantage for protective function. This observation has implications for Mo's protective mechanism in the passive film, suggesting that Mo may be protecting from localized breakdown by altering the morphology of the oxide to produce a more uniformly protective oxide layer.

5:00pm **SS+2D+AMS-WeA-12 An Investigation of Local Distortions on High Entropy Alloy Surfaces**, *Lauren Kim*, University of Wyoming; *Prince Sharma*, Lehigh University; *Ganesh Balasubramanian*, lehigh University; *TeYu Chien*, University of Wyoming

High entropy alloys (HEAs) are a widely studied family of materials that typically contain five or more elements. There are many combinations of elements that can create HEAs, and material properties can be tuned simply by changing elemental compositions. These properties of HEAs result in numerous applications, such as catalysis, energy storage, and aerospace engineering refractory materials. Severe-lattice-distortion is identified as one of the four core effects impacting the physical properties in HEAs. In this work, we demonstrate atomic resolution images of the surface of a CrMnFeCoNi HEA (Cantor alloy) using scanning tunneling microscopy (STM). This data allows us to determine lattice local distortions unambiguously. Additionally, we report our findings on the types of local defects on the surface, such as grain boundaries, phase changes, and amorphization, and how these defects can impact local distortions of the crystals nearby.

5:30pm **SS+2D+AMS-WeA-14 Charge Ordering Phase Transition in Bilayer Sn on Si(111)**, *Nathan Guisinger, Maria Chan*, Argonne National Laboratory; *Carmen Lilley*, University of Illinois - Chicago

The atomic-scale investigation of the "bilayer" reconstruction of Sn on heavily doped n-type Si(111) was performed with scanning tunneling microscopy. When cooled to 55K, the bilayer reconstruction undergoes both a structural and electronic transition. Structurally, the dimer units of

the bilayer shift to form a herringbone pattern with a rhombohedral ordering. The electronic structure transitions into a very uniform square lattice with similar dimensions to the structural dimers. There are distinct differences between the structural and electronic spacing that resolves itself when counting multiple periods. This ordering is like behavior observed in materials that exhibit charge density waves. Furthermore, STS point spectra show a transition from a small gap to a large insulating gap at low temperature that is consistent with a transition to a Mott insulating ground state. The charge ordering coupled with the relaxation to a Mott insulating phase upon cooling the Sn bilayer presents unique physics when the dimensionality is reduced from the bulk.

5:45pm SS+2D+AMS-WeA-15 SSD Morton S. Traum Award Finalist Talk: On-Surface Design of Highly-Ordered Two-Dimensional Networks Stabilized by Nonmetal Atoms, *Alisson Ceccatto*[1], University of Campinas (UNICAMP), Brazil*; Gustavo Campi,* Yachay Tech University, Ecuador*; Vanessa Carreño, Eidsa Ferreira,* University of Campinas (UNICAMP), Brazil*; Natalie J. Waleska-Wellnhofer, Eva Marie Freiberger, Simon Jaekel,* Friedrich-Alexander-University Erlangen-Nürnberg (FAU), Germany*; Christian Papp,* Freie Universität Berlin, Germany*; Hans-Peter Steinrück,* Friedrich-Alexander-University Erlangen-Nürnberg (FAU), Germany*; Duncan John Mowbray,* Yachay Tech University, Ecuador*; Abner de Siervo,* University of Campinas (UNICAMP), Brazil

Supramolecular nanoarchitectures have been widely explored to precisely design low-dimensional materials at atomic and molecular levels [1]. Such control is mainly based on bottom-up fabrication methods, e.g. on-surface synthesis, by combining molecular building blocks and atoms to engineer novel nanomaterials [2]. Particularly, the self-assembled monolayers (SAMs) of organic molecules present the potential for applications in nanoelectronics due to their reversible non-covalent interactions [3]. Such intermolecular interactions allow the fabrication of almost defect-free supramolecular nanostructures. Typically, the geometry of these nanoarchitectures can be controlled by the insertion of metal and non-metal atoms in the reaction process. To date, the adatom-mediated SAM fabrication concentrates on the use of metal adatoms, especially d metals (Cu, Co, Au, and Fe) [4]. Herein, by combining scanning tunneling microscopy (STM) measurements and density functional theory (DFT) calculations, we report the 2D self-assembled of 1,3,5-tris[4-(pyridin-4-yl)-[1,1'-biphenyl])benzene (TPyPPB) molecules on Ag(111) in the presence of Cl adatoms. The adsorption of the TPyPPB molecules on the clean Ag(111) surface forms an almost defect-free porous SAM stabilized by hydrogen bonds, so-called triangular packing. Such packing can be explored as a host-guest material for atom/molecular confinement. However, in the presence of Cl adatoms, the molecular arrangement changes dramatically. The molecular assembly changes its geometry, forming a non-porous SAM stabilized by H···Cl···H bonds. Such halogen-mediated SAM presents the advantage that the adatom used to stabilize the nanostructure has less influence on the electronic density compared to the typical metal adatoms.

Keywords: On-surface synthesis, STM, Self-assembly monolayer, Nanoporous networks.

References

1. Fan, Q. et al. Accounts of Chemical Research 48, 2484–2494 (2015).

2. Pawlak, R. et al. Journal of the American Chemical Society 142, 12568–12573 (2020)

3. Casalini, S. et al. Chemical Society Reviews 46, 40–71 (2017)

4. Shi, Z. et al. Journal of the American Chemical Society 133, 6150–6153 (2011)

Thin Films
Room 115 - Session TF-WeA

Vapor Synthesis of Hybrid, Organic, and Polymeric Materials (VSHOP III)

Moderators: David Bergsman, University of Washington, **Rong Yang**, Cornell University

2:15pm TF-WeA-1 Chemical Vapor Deposition of Polymers for Lithium Ion Batteries, *Kenneth Lau,* Rowan University   **INVITED**
The lithium ion battery (LIB) technology is rapidly dominating the energy storage market due to its competitive cost and energy capacity. However, due to growing market demands, there is a continued push to enhance LIB energy and power density. As such, there is significant research into high capacity, high voltage cathode materials based on transition metal oxides that provide more lithium ion intercalation. However, at high voltages and high reactivity, the intercalation process becomes unstable and the transition metals tend to leach out into the electrolyte, leading to degrading battery performance with repeated charge-discharge cycling. Our work aims to protect and stabilize LIB cathode materials by conformally coating individual cathode particles with conducting polymers by oxidative chemical vapor deposition (oCVD). The hypothesis is that the protective conducting polymer helps to stabilize the cathode-electrolyte interface against degradation processes. In a second approach towards increasing LIB energy and power density, there is increasing research in moving away from 2D planar sandwich cells to pursuing 3D LIB architectures in which the electrodes are intentionally constructed into microstructured geometries (e.g. micropillars) to provide higher surface area and shorter lithium ion diffusion pathways. Our work aims to create 3D LIB anode microstructures through the carbonization of aromatic polymers grown by initiated chemical vapor deposition (iCVD). The hypothesis is that the simplified iCVD process scheme allows facile microstructural formation of polymer geometries that lead to viable microstructured carbon anodes. In this talk, we will highlight our recent work in using oCVD and iCVD to create polymers relevant for enhancing the performance of LIBs, particularly in improving capacity retention. We will present experimental correlations of how oCVD and iCVD processing chemistries and conditions impact material structure and device behavior, knowledge that has helped to understand the role of different dynamic processes, including adsorption, nucleation and growth kinetics.

2:45pm TF-WeA-3 Exploring the Influence of Reduced Vacuum Conditions on Structural and Chemical Variations in Hybrid Perovskite Films Deposited by Resonant Infrared Matrix-Assisted Pulsed Laser Evaporation, *Joshua Ayeni, Adrienne Stiff-Roberts,* Duke University
This study examines how gas kinetics impact the structural properties and chemical environment of phenylethylammonium lead iodide ($(PEA)_2PbI_4$) films deposited by resonant infrared matrix-assisted pulsed laser evaporation (RIR-MAPLE) under various background pressures (BGPs) of inert gas. $(PEA)_2PbI_4$ is a promising hybrid perovskite material for optoelectronic applications such as LEDs [1-2], yet less extensive research exists on vacuum deposition compared to solution deposition. RIR-MAPLE uses a low-energy Er:YAG laser at 2.94μm to reduce material degradation by resonant absorption of a host matrix [3]. Hybrid perovskite materials are typically grown under an active vacuum in RIR-MAPLE. Thus, understanding film deposition in a reduced vacuum with a BGP of inert gas is critical to determining industrial scalability.

Films were deposited from active vacuum (10^{-5} Torr) to 500 mTorr in a nitrogen atmosphere. Standard film characterization such as AFM, SEM, XRD, PL, and UV-Vis absorbance do not reveal significant changes in film properties with increasing BGP. X-ray photoelectron spectroscopy (XPS) was used to characterize the chemical composition of film surfaces. Pristine films show two characteristic Pb peaks from the spin-orbit splitting at ~138.0 eV for $4f_{7/2}$ and ~143 eV for $4f_{5/2}$, corresponding to a fully coordinated Pb^{2+} in the perovskite system. Variations in the binding energies (BEs) and elemental ratio are observed for different BGPs, implying different chemical environments for the Pb element. At high BGPs, peak splitting is observed for Pb 4f, I 3d, and C 1s. Also, the I/Pb ratio determined from XPS exhibits marked differences with BGP. For BGP below 250 mTorr, the decrease in the I/Pb ratio relative to the stoichiometric ratio suggests iodine vacancies [4]. Conversely, at higher BGPs, high iodine content indicates an iodine-rich phase is present in the films.

Therefore, this study will explore how BGP affects gas diffusion, adsorption kinetics, and nucleation processes to provide better insight into gas-phase kinetics and film growth mechanisms. By combining experimental results

with theory to understand the role of BGP in compositional changes, better control of stoichiometry, purity, bonding, or doping by RIR-MAPLE could be enabled.

References

[1] G. Tanbo et al,. J All & Comp 940, 168894 (2023)

[2] W. Dou et al,. Nanomaterials, 12, 2556 (2022)

[3] A. D. Stiff-Roberts & W. Ge. *Appl. Phys. Rev.* **4** 041303 (2017)

[4] H. T. Chen *et al* Adv. Optical Mater., **8**, 1901390 (2020)

3:00pm **TF-WeA-4 Low Surface Energy for Tuning the Surface Repellency through Initiated Chemical Vapor Deposition**, *Syed Ibrahim Gnani Peer Mohamed*, *Graham Kaufman, Daniel Egbebunmi, Mona Bavarian, Jeffrey Shield, Craig Zuhlke, Siamak Nejati,* University of Nebraska Lincoln

Surface-wetting properties are crucial in various applications, such as microfluidics, water treatment, drag reduction, immersion cooling, degassing, and self-cleaning surfaces. For instance, traditional additive manufacturing techniques have been used to fabricate omniphobic surfaces, but concerns about durability and scalability remain. This study presents a novel approach to ultra-low surface tension repellency through a two-stage fabrication method, which integrates scalable techniques to restructure the surface and initiated chemical vapor deposition (iCVD). By applying this method to bulk aluminum, we achieved robust, hierarchal roughened surfaces that repel ultra-low surface tension liquids, including n-hexane (ɣ = 18.2 mN/m). This approach offers flexibility in substrate material and shows promising results for scalability and durability. Surface and subsurface chemical analysis revealed the preservation of perfluoroalkyl side groups crucial for imparting superhydrophobic functionality. Wetting characteristic assessments highlighted the impact of hierarchal roughness on repellency, with the PTFE-co-PPFDA coating outperforming PPFDA for lower surface tension liquids. We present data on the coating at a high value of surface availability and note the transition in properties of the coated materials as a function of surface availability. Importantly, this study's findings have practical implications, providing insights into the design and fabrication of hierarchal roughened surfaces for ultra-low surface tension repellency, three different applications of these surfaces will be discussed for the very-low surface energy samples that show surface energy in the range of 12 mN/m.

3:15pm **TF-WeA-5 From iCVD Thin Films to 3D Aeropolymers for Biomedical Applications**, *Torge Hartig* [1] , *Joschka Paulsen, Wiebke Reichstein, Margarethe Hauck, Julia Piehl,* Kiel University, Germany*; Mohammadreza Taale,* Universität Heidelberg, Germany*; Thomas Strunskus,* Kiel University, Germany*; Christine Selhuber-Unkel,* Universität Heidelberg, Germany*; Georg Schnell,* University of Rostock, Germany*; Amal Amin,* National Research Center, Giza, Egypt*; Rainer Adelung,* Kiel University, Germany*; Benjamin Freedman,* Harvard University*; Fabian Schütt, Franz Faupel, Stefan Schröder,* Kiel University, Germany

With rising requirements for functional polymer surfaces, wet chemical approaches meet their limits. Representing an all-dry technology initiated Chemical Vapor Deposition (iCVD) thin films are highlighted regarding conformal coating of nanoscale features, tailoring of chemical functional groups, as well as crosslinking via copolymerization. The conformal nature of the iCVD process is used in PFAS-free superhydrophobic coatings based on femtosecond-laser processed substrates.

To understand the impact of certain functional groups on the bio-interface-performance, tailored surface chemistry coatings as well as nanocomposite coatings are compared regarding applications for human fibroblasts and respiratory viruses.

Furthermore, the conformal nature of iCVD coatings is used to fabricate freestanding 3D thin film scaffolds. For this, sacrificial porous tetrapodal ZnO is coated and etched wet-chemically resulting in so-called aero-polymers of more than 99% empty space. The used aero-hydrogels have striking compressive properties that can be tailored by crosslinking ratios. The scaffolds mimic the extracellular matrix shape allowing the use in 3D cell culture for muscle cell applications. To include electrical conductivity in the aero-hydrogels multilayers of graphene and iCVD hydrogels are fabricated resulting in optimized cell interaction.

3:30pm **TF-WeA-6 Investigating PEDTT Thin Films: Comparing Synthesis Methods and Properties for Electronic Applications**, *Siamak Nejati, Syed Ibrahim Gnani Peer Mohamed, Lawson Okpaire, Vojislav Medic, Mona Bavarian,* University of Nebraska-Lincoln, USA

This study explores the properties and characteristics of poly(3,4-ethylenedithiathiophene) (PEDTT) thin films synthesized using oxidative molecular layer deposition (oMLD) and oxidative chemical vapor deposition (oCVD). The investigation focuses on conductivity, defect-free film formation, and the influence of structural variations on the overall properties of these films. PEDTT, notable for its solvent-free synthesis, is examined for its potential applications in electronic devices, drawing comparisons with poly(3,4-ethylenedioxythiophene) (PEDOT). A comparative analysis of the oMLD and oCVD techniques highlights their efficiency, scalability, and resultant film properties. oMLD offers precise, controlled layer-by-layer deposition, while oCVD provides versatility with the thermal decomposition of organic precursors. This study aims to elucidate the relationship between synthesis methods and thin film properties through detailed experimentation. A key aspect of this research is understanding the mechanisms governing PEDTT's electrical conductivity, examining molecular structure, doping levels, and processing parameters. The study also evaluates PEDTT's ability to form defect-free films, emphasizing factors influencing film uniformity and integrity. Structural differences between PEDTT and PEDOT, particularly the roles of sulfur and oxygen atoms, are analyzed to reveal their impact on electronic properties and chemical reactivity. Furthermore, the structural features of PEDTT, including steric repulsion and twisted conformations, are shown to affect its porosity and surface area, with implications for surface modifications and interfacial interactions. The research delves into the deposition processes, focusing on the flow dynamics and vapor pressure of the ethylenedithiathiophene (EDTT) precursor, to achieve a comprehensive understanding of thin film fabrication. This investigation provides valuable insights into the interplay between synthesis methods, molecular structure, and thin film properties of PEDTT-based materials. By uncovering the mechanisms behind conductivity, defect-free film formation, and structural characteristics, this research advances the field of electroactive polymers and their applications in emerging technologies.

4:15pm **TF-WeA-9 Exploring New Avenues Resulting from the Rational Process Design of Sequential Infiltration Synthesis**, *Nari Jeon,* Chungnam National University, Republic of Korea **INVITED**

Sequential infiltration synthesis (SIS) has been demonstrated as a novel approach for fabricating inorganic–organic hybrid materials and inorganic porous materials, thereby offering precise control overnano- to microscale morphology. This method relies on the infiltration of vapor-phase precursors into a polymer matrix, followed by the reaction of these precursors with coreactants in the matrix. SIS-derived thin films and nanostructures show promise for applications in lithography, photovoltaics, tribology, and water remediation. Despite the continuous expansion of the material library prepared through SIS, a comprehensive understanding of the growth mechanism of SIS is limited. During SIS, precursor diffusion and reactions occur concurrently in the polymer matrix. SIS-derived thin films exhibit various compositional and structural complexities. This study investigates the complex relationship between the key physical/chemical phenomena governing the SIS process and the structural/compositional distribution of SIS-prepared films using *in situ* and *ex situ* characterization techniques. Moreover, it explores the potential of using organic coreactants in SIS as a new means of controlling the compositional distribution of inorganic–organic hybrid thin films and the pore morphology of inorganic porous thin films. Finally, future research directions are provided to help establish SIS as a mainstream technique in the fields of atomic layer deposition (ALD) and ALD-derived processing.

4:45pm **TF-WeA-11 Vapor Phase Infiltration of ZnO into Photo-Polymerizable Polyacrylates: Patterning and the Importance of Free Volume**, *Mark Losego,* Georgia Tech*; Lisanne Demelius,* Graz University of Technology, Austria*; Anna Maria Coclite,* University of Bari, Italy

Vapor phase infiltration (VPI) exposes polymers to inorganic vapors that sorb into the polymer to transform it into an organic-inorganic hybrid material with properties unique from its parent polymer. This talk will discuss our work investigating VPI of ZnO into photopolymerized polyacrylates. Photopolymerizable polymers are easily micropatterned with standard photolithography or advanced two-photon lithography processes. VPI offers a way to transform these micro-patterned polymeric structures into more functional hybrid materials or even fully inorganic structures upon combustive removal of the polymer. However, this transformation from polymer to hybrid to inorganic requires control and understanding of

---

the inorganic loading during the VPI process. Here, we will show how the addition of "soft" acrylate segments containing ethoxylated chains can increase the free volume of these network polymers and permit greater VPI uptake of inorganic precursors, leading to more inorganic loading. The increased free volume of these polymers is confirmed with thermal expansion measurements. These more "flexible" polymer networks increase both the VPI kinetics and the total inorganic mass loading. In the compositional depth profiles, we can also detect a transition from a diffusion-limited process to a reaction limited process. We will also demonstrate the basic ability to photo-pattern these polyacrylates and then VPI the structures to make micro-patterned hybrid materials.

5:00pm **TF-WeA-12 Effect of Alumina Priming on Structural and Electrical Properties of Zno Nanostructures Synthesized via Vapor-Phase Infiltration Into Self-Assembled Block Copolymer Thin Films**, *Chang-Yong Nam, **Won-Il Lee**, Ashwanth Subramanian,* Stony Brook University/Brookhaven National Laboratory*; Kim Kisslinger,* brookhaven National Laboratory*; Nikhil Tiwale,* Brookhaven National Laboratory

Alumina priming is a technique that can improve the fidelity of the vapor-phase infiltration (VPI) of weakly reactive organometallic precursors into polymer templates, such as self-assembled block copolymer (BCP) thin films. The process begins with the infiltration of trimethylaluminum (TMA), a strong Lewis acid that can diffuse and bind to Lewis-basic groups within polymers. Upon exposure to water vapor, TMA forms molecular alumina terminated with hydroxyl groups. This priming step promotes subsequent infiltration of weakly reactive organometallic precursors of target inorganic materials by activating the polymer matrix. While alumina priming expands the range of inorganics applicable to VPI, the insulating properties of bulk alumina can negatively affect the electrical properties of the final inorganic nanostructures produced by VPI. In this study, we explore the impact of alumina priming on the structural and electrical properties of zinc oxide nanowires derived from the VPI of diethylzinc (DEZ) and water into self-assembled poly(styrene-block-methyl methacrylate) (PS-*b*-PMMA) BCP thin films. We demonstrate the ability to easily adjust the characteristic dimensions, chemical composition, and electrical conductivity of the resulting aluminum-doped ZnO (AZO) nanowires by varying the TMA exposure time during a single-cycle alumina priming. Increasing the TMA exposure duration enhances not only ZnO infiltration fidelity but also ZnO electrical conductivity with the minimized resistivity of 14.3 k$\Omega \cdot$cm with an Al concentration of 6.02 % at a TMA exposure time of 100 s. Simultaneously, the variation of the TMA exposure time provides control over the final AZO nanowire feature sizes with width and height in the ranges of 26 – 33 nm and 23 – 47 nm, respectively. These findings provide a guideline for controlling the composition, dimensions, and electrical properties of alumina-primed metal oxide nanostructures based on VPI in polymer templates.

5:15pm **TF-WeA-13 Spectroscopic Study of the Inorganic Structure in Pim-1/Metal Oxyhydroxide Hybrid Membranes Synthesized via Vapor Phase Infiltration**, *Benjamin Jean, Ian Slagle, Faisal Alamgir, Mark Losego,* Georgia Tech

Polymers of intrinsic microporosity (PIMs) have well-defined microporosity that provide excellent chemical separation ability. However, the chemical stability of these polymers in organic solvents limit their use in organic separations. Vapor phase infiltration (VPI) can be used to transform PIM membranes into organic-inorganic hybrid membranes with superior chemical stability and separation performance. This talk will address our recent efforts to better understand the physicochemical structure of VPI-synthesized hybrid PIM-1 membranes and the importance of the inorganic's network structure within the hybrid to affect the membrane's chemical stability and separation performance. We use a combination of spectroscopic techniques including advanced X-ray absorption spectroscopies (XANES and EXAFS) to study the structure of inorganic clusters in VPI treated PIM-1 hybrid membranes. In PIM-1/ZnO$_x$H$_y$ hybrids, XPS and FTIR show the inorganic structure is primarily a hydroxide structure. EXAFS indicates that these inorganics readily form several metal atom clusters as well. The degree of inorganic clustering can be controlled by processing conditions such as exposure time and number of cycles. The membrane solvent stability appears to be most influenced by the degree of clustering. For PIM-1/AlO$_x$H$_y$ hybrid membranes, XPS and FTIR in conjunction with DFT calculations indicate that the final inorganic species is an oxyhydroxide species. Solid state NMR and XANES provide additional evidence that these aluminum hydroxide clusters network with each other into larger chains or sheets. The degree of inorganic clustering can be controlled by processing conditions such as exposure time and number of cycles. The membrane material properties such as membrane selectivity and solvent stability can be modified significantly based on the degree of clustering. This talk will discuss these finding and provide guidance for how to design these materials to achieve desired properties like solvent stability and membrane selectivity.

5:30pm **TF-WeA-14 Nanoporous TiO₂ Coating Designed by Swelling-Assisted Sequential Infiltration Synthesis (SIS) of Block Copolymer for Self-Cleaning Application**, *Khalil Omotosho, Diana Berman,* University of North Texas

Highly porous photoinduced self-cleaning coatings are pivotal across a broad range of applications like surfaces for optical coatings, solar panels, mirrors, etc. In this work, we described a new technique to design nanoporous photocatalytic self-cleaning TiO₂ coating with very high hydrophilicity. This coating was created by the swelling-assisted sequential infiltration synthesis (SIS) of a block copolymer template (PS75-b-P4VP25), followed by the elimination of the polymer via oxidative thermal annealing in a furnace at 450 oC for 4 h. The optimization of the infiltration process was realized with the quartz crystal microbalance (QCM), by estimating the mass of infiltrated precursor molecules as a function of the number of SIS cycles. SEM image show that the adopted swelling-assisted SIS approach is suitable for designing smooth uniform TiO₂ film with an interconnected network of pores. The films exhibited good crystallinity in the anatase phase. Hydrophilic property of the film was improved upon 1 h Ultraviolet (UV) exposure, leading to unmeasurable contact angle values upon contact with water droplets. The photocatalytic self-cleaning performance of the synthesized porous TiO₂ nanostructures were tested by measuring the photocatalytic degradation of methylene blue (MB). They displayed promising photocatalytic activity, with ~92% of the MB degraded after 180 min of UV irradiation, thus demonstrating comparable level of photoactivity with commercial anatase TiO₂ nanoparticles of the same quantity. This result highlights a new robust approach for designing hydrophilic self-cleaning coatings with controlled porosity and composition.

5:45pm **TF-WeA-15 Permanent Electric Polarization in Vapor Phase Deposited Polymer Thin Films**, *Stefan Schröder, Torge Hartig, Lynn Schwäke, Thomas Strunskus, Franz Faupel,* Kiel University, Germany

Dielectric materials with a permanent electric polarization, i.e. electrets, have been attracting great interest in application fields such as sensors/transducers, catalysis, cell growth and microfluidics. The increasing demand for device miniaturization and new application pathways, e.g. in organic electronics, creates the need for high precision thin films of such materials. However, since polymers exhibit the best electret properties, the production of precise, high-quality polymer electret films with sufficient dielectric breakdown strength on large-area substrates is a challenge for conventional wet chemical approaches. In this work, we present the latest results on electret thin film fabrication via initiated chemical vapor deposition (iCVD). The iCVD process is a single-step, solvent-free polymer thin film fabrication process capable to grow precise films of high dielectric breakdown strength on large-area substrates as well as complex geometries. Due to the CVD-typical growth, the process can be integrated into existing microelectronics process lines and enables e.g. the use of electret films in complex micro-electromechanical systems (MEMS). The electronic structure, trap landscape as well as polarization response of the electret films can be tailored by the deposition parameters and (co-)monomer combinations. First principle calculations assist in the search for suitable monomers which yield effective electret properties. The fabricated films are tested in different transducer and sensor devices, where they can provide new pathways for next-generation devices.

6:00pm **TF-WeA-16 Using ALD to Alter the Biological Response of Cellulose Fabrics**, *Li Zhang, Mark Losego,* Georgia Institute of Technology

Atomic layer deposition (ALD) of metal oxides onto fabrics has previously been shown to alter the biological response various microbes have with a textile. For example, ALD ZnO$_x$ coatings have been shown to both accelerate bacterial growth ("feeds" the bacteria) at low coating thicknesses (< 3 nm) and kill the bacteria at higher thicknesses. In this study, we examine how ALD coatings can alter the enzymatic biodegradation of cotton fabrics. Specifically, we study how AlO$_x$ ALD coatings affect the cellulase enzyme *Trichoderma viride's* abilityto hydrolyze and degrade cotton fabrics. ALD coatings of AlO$_x$ are deposited using trimethyl aluminum (TMA) and H₂O with cycle counts varying from 1 – 750 cycles (~0.12-93 nm). It was found that as little as one ALD cycle of AlO$_x$ could reduce the enzymatic degradation by as much as 5% over a period of 5 days. Deposition of 10 ALD cycles resulted in a further reduction of enzymatic degradation of around 8% over the same time period. However, additional layers of deposition, up to 750 cycles, did not significantly reduce the degradation rate further. To

explain both the initial reduction in degradation and the plateauing in rate, the chemical and physical structures of the coated fabrics were studied with X-ray photoelectron spectroscopy (XPS) and scanning electron microscopy (SEM). XPS indicates that after 3 days of enzymatic degradation the deposited alumina layer is etched away. This dissolution may be due to the alumina layer dissolving in the acetic acid buffer required for the enzyme or because the enzyme is hydrolyzing the surface glucose monomers bound to the alumina. In contrast, the alumina layer on the 10 cycle treated fabric remains intact throughout all 5 days of the enzymatic degradation. This indicates that, on the time-scale studied, ALD deposition of 10 or more cycles results in an alumina coating that is able to survive the enzymatic hydrolysis process resulting in this large disparity between the untreated, 1 cycle and 10 cycle samples. SEM images of the fabrics coated with more cycles indicate crack formation in the as-deposited state and after submerging the fabric in water for 2 days, the amount of cracks present increases significantly. In summary, the large difference in enzymatic degradation for low cycle count fabrics can be explained by the alumina layer surviving and the much smaller difference between higher cycle count treatments can be explained by the primary diffusion mechanism of the enzyme being through the cracks formed in the alumina layer, bypassing any changes in thickness of the alumina.

2D Materials
Room 122 - Session 2D-ThM

2D Materials: Defects, Dopants, Edges, Functionalization, and Intercalation

Moderator: Young Hee Lee, Sungkyunkwan University

8:00am **2D-ThM-1 Electronic and Magnetic Properties of Intrinsic Defects in TiS$_2$**, *Patrick Keeney,* university of North Florida*; Anne Evans, Thomas Pekarek, Jason Haraldsen, **Paula Mariel Coelho,*** University of North Florida
Transition metal dichalcogenides (TMDCs) are materials with unique electronic properties due to their two-dimensional nature. Recently, there is a large and growing interest in synthesizing ferromagnetic TMDCs for applications in electronic devices and spintronics. Apart from intrinsically magnetic examples, modification via either intrinsic defects or external dopants may induce ferromagnetism in non-magnetic TMDCs [1-2]. Our study focuses on intrinsic defects in TiS$_2$, which is a system known for potential applications in energy storage. We use scanning tunneling microscopy (STM) and superconducting quantum interference device (SQUID) magnetometry to characterize the crystal structure and magnetic properties of TiS$_2$ crystals. Atomically resolved STM images suggest the formation of sulfur vacancies and possibly interstitial defects creating brighter triangular shape regions. Preliminary analysis of magnetic data indicates low-spin paramagnetic response, with a saturated magnetization of ~0.16 emu/g and 80% saturation by ~2.5 T. To rule out ferromagnetism, hysteresis loops were analyzed and showed the coercive field to be zero within experimental error. Concurrently, DFT calculations on formation energy and electronic density were also being performed for proper identification of defect formations. Additionally, simulated STM images were generated by calculations that map the electronic density of the surface for the energetically favorable defects. An initial comparison to experimental STM images corroborates with the initial hypothesis of sulfur vacancies and titanium interstitial defects. Further studies include doping of TiS$_2$ with transition metals and further investigation of the electronic and magnetic properties of these doped TMDC systems.

[1] Magnetic doping in transition metal dichalcogenides, PM Coelho, J. Phys.: Condens. Matter 36 203001 (2024).

[2] Room-Temperature Ferromagnetism in MoTe$_2$ by Post-Growth Incorporation of Vanadium Impurities, PM Coelho, HP Komsa, K Lasek, V Kalappattil, J Karthikeyan, MH Phan, AV Krasheninnikov, and M Batzill, Adv. Electron. Mater., 1900044 (2019).

8:15am **2D-ThM-2 DFT-Based Investigation of Formation Energies and Properties of 2D TiS$_2$ with Various Defects**, ***Patrick Keeney**, Paula M. Coelho, Jason T. Haraldsen,* University of North Florida
Titanium disulfide (TiS$_2$) belongs to a family of materials known as transition metal dichalcogenides (TMDs). These materials exhibit relatively weak van der Waals forces between layers, allowing them to be reduced down to thin films and even one monolayer in thickness. While graphene is the most well researched 2D material, it does not possess a bandgap and thus has limited applications with regard to electronic devices. TMDs often have tunable bandgaps, filling a clear need within 2D materials. They also exhibit sandwich-like structures, with one layer of transition metal atoms sandwiched by two layers of chalcogen atoms.

The most researched applications of 2D TiS$_2$ are those regarding ion batteries, photovoltaic devices, and spintronics. This study investigates the effects of intrinsic point defects within a 2D (TiS$_2$) lattice on the electronic and magnetic properties. By comparing post-annealed scanning tunneling microscopy (STM) images with SGGA+U-based density functional theory (DFT) calculations, we examine which defects are more likely to occur by connecting specific geometries that arise from typical intrinsic defects. We also compare a base, benchmarked 2D TiS$_2$ supercell with supercells containing various point defects, allowing us to interpret the total energy differences and identify which are most energetically favorable.

8:30am **2D-ThM-3 Role of Chalcogen Vacancies and Hydrogen in Bulk and Monolayer Transition-Metal Dichalcogenides**, ***Shoaib Khalid**,* Princeton University Plasma Physics Lab*; Anderson Janotti,* University of Delaware*; Bharat Medasani,* Princeton University Plasma Physics Lab
Like in any other semiconductor, point defects in transition-metal dichalcogenides (TMDs) are expected to strongly impact their electronic and optical properties. However, identifying defects in these layered two-dimensional materials has been quite challenging with controversial conclusions despite the extensive literature in the past decade. Using first-principles calculations, we revisit the role of chalcogen vacancies and

hydrogen impurity in bulk TMDs, reporting formation energies and thermodynamic and optical transition levels. We show that the S vacancy can explain recently observed cathodoluminescence spectra of MoS$_2$ flakes and predict similar optical levels in the other bulk TMDs. In the case of the H impurity, we find it more stable sitting on an interstitial site in the Mo plane, acting as a shallow donor, and possibly explaining the often observed n-type conductivity in some bulk TMDs. We also predict the frequencies of the local vibration modes for the H impurity, aiding its identification through Raman or infrared spectroscopy.

Our results show that the chalcogen vacancies are deep acceptors and cannot lead to n-type or p-type conductivity in monolayer TMDs. Both the (0/-1) and (-1/-2) transition levels occur in the gap, leading to paramagnetic charge states S=1/2 and S=1, respectively, in a collinear-spin representation. We discuss trends in terms of the band alignments between the TMDs, which can serve as a guide to future experimental studies of vacancy behavior.

8:45am **2D-ThM-4 Defect-engineered High-gain WS$_2$ Photodetector after 10 MeV Proton Irradiations**, ***Joonyup Bae**, Donggyu Lee, Seungjae Kwak, Jihyun Kim, Wonbo Lee,* Seoul National University, Republic of Korea
As silicon-based electronics approach their physical limitations, two-dimensional (2D) transition-metal dichalcogenides (TMDs) have emerged as potential alternatives due to their unique mechanical and electrical properties. Among TMDs, WS$_2$ exhibits layer-dependent bandgaps and impressive electron and hole mobilities. However, to effectively integrate 2D TMDs into advanced applications, reliable doping strategies must be developed.

Conventional ion implantation doping methods used in silicon and GaAs-based semiconductors are not suitable for 2D TMDs due to lattice damage and high post-annealing temperatures. Alternative techniques, such as substitutional doping and charge transfer doping, have been explored but face limitations related to high-temperature processes and dopant carrier concentration control.

This study investigates the n-type doping effect of high-energy proton beam irradiation on intrinsic n-WS$_2$ using various fluences. Previous studies have focused on post-fabricated devices, making it difficult to isolate the specific interactions between the substrate and TMD materials. By examining the effects of proton irradiation on bulk WS$_2$ crystals, this study aims to understand the intrinsic impacts with different proton fluences on 2D WS$_2$.

Electrical properties, defect state formation, and work function variations were assessed using transmission line measurement, Raman spectroscopy, low-temperature photoluminescence spectroscopy, and Kelvin probe force microscopy. Density Functional Theory (DFT) calculations suggest that sulfur vacancies generated by proton irradiation contribute to the formation of defect states near the conduction band, facilitating an n-type doping effect.

To validate the effects of proton beam irradiation-induced defects, multilayer WS$_2$ photodetectors exposed to varying proton fluences were fabricated. Increasing proton fluence led to a significant improvement in internal photo-gain under 530 nm wavelength illumination, attributable to the creation of mid-gap states. This proton-mediated doping technique offers insights into the direct effects of high-energy protons on WS$_2$, potentially informing the development of advanced ultra-large-scale integration devices with controllable proton irradiations.

This work was supported by the Korea Research Institute for defense Technology planning and advancement (KRIT) grant funded by Defense Acquisition Program Administration (DAPA) (KRIT-CT-21-034).

9:00am **2D-ThM-5 Doping Transition Metal Dichalcogenides by Low Energy Ion Irradiation**, *William Blades,* Juniata College*; Farzad Bastani, Elaina Truhart, Kory Burns, **Petra Reinke,*** University of Virginia
Transition metal dichalcogenides (TMD) MX$_2$ offer unique and versatile functionality for a wide range of electronic, photonic, and quantum devices. It remains a significant challenge to achieve electronic or magnetic doping. In conventional semiconductors such as Si, or III-V materials ion implantation is well-established as a versatile method of doping but TMDs are much more susceptible to damage. We introduce a new concept termed "backdoor doping" which mimics low energy ion irradiation with an energy below 50 eV with the goal of doping of the metal sub-lattice with a wide range of elements while at the same time minimizing damage.

We combine experimental studies of defects in TMDs with computational models describing the ion-matter interactions, and defect signatures using DFT. We will compare defects created by (i) annealing, (ii) ion irradiation, and (iii) plasma exposure in a semiconducting and a metallic TMD (e.g.

MoS_2, TaS_2). We observed defects created by annealing in WSe_2 with scanning tunneling microscopy and spectroscopy (STM, STS) and density functional theory (DFT). Initially chalcogen vacancies dominate but larger, extended defects with multiple damaged bonds develop rapidly. The defects introduce numerous states in the gap and damage the structural and bonding integrity of the TMD layer. A small background pressure of the chalcogen might help to repair broken M-X bonds and offer a path to defect repair. We will systematically compare the different modes of defect formation using experiment and DFT modeling. If time permits, STEM (scanning transmission electron microscopy) will be included for detailed structural and phase information.

The low energy ion irradiation is achieved by using a "sandwich structure" made of a TMD layer which is capped with a thin metal layer made of the desired dopant. For proof of concept we are using Au and Fe metal layers. The sandwich structure is irradiated from the metal layer side and the projectile (a noble gas ion with an energy <5 keV) will initiate a collision cascade. The collision cascade is adjusted to eject metal atoms from the thin layer into the TMD while limiting transmission of the projectile. The defect formation in the metal is modeled with SRIM/TRIM (stopping and range of ions in matter) and SDTrimSP which are Monte Carlo simulations of collision events in matter. These simulations predict the energy of ions leaving the metal layer and entering the TMD. The TMD layer is then studied with STM to assess the defect inventory, XPS to understand compositional variations, and other methods to fully characterize the TMD.

9:15am 2D-ThM-6 Atomic-scale Manipulation of Two-dimensional Materials with Ion Beams: From Aberration-corrected STEM to Monochromated EELS, *Kory Burns, Tinsae Alem, Elaina Truhart,* University of Virginia, USA*; Christopher Smyth,* Sandia National Laboratories, USA*; Stephen McDonnell,* University of Virginia, USA*; Taisuke Ohta,* Sandia National Laboratories, USA*; Jordan Hachtel,* Oak Ridge National Laboratory, USA

Heterogeneities can be selectively engineered in 2D materials from the interaction of charged projectiles at varying velocities, angle of incidences, and stage temperatures. These heterogeneities exist as intrinsic structural defects, impurities in lattice sites, topological disorder, and strain-driven interfaces. So, how can we study these defects in detail to correlate their impact on materials properties? In this talk, aberration-corrected scanning transmission electron microscopy (STEM) is combined with monochromatic electron energy loss spectroscopy (EELS) to combine unprecedented spatial resolution with world-class energy resolution from an electron probe to decouple the nature of bosons arising from subtle heterogeneities. On-axis EELS, where our bright field disc is perfectly aligned with the EELS entrance aperture, leaves our signal being dominated by dipole scattering, so we get a delocalized signal. To get a localized signal from adatoms and vacancies in our material, we must go off-axis to suppress the long-range signals and highlight hyperbolic phonon polaritons. Hereby, off-axis EELS is employed, where a bright-field disc is electrically shifted outside of the EELS entrance aperture by the projector lenses such that a portion of the dark field disc now enters the spectrometer window to give information on the impact scattering in the off-axis regime. We use the selection rules inside an electron microscope to decouple the optical transitions arising from single anomalies in 2D materials. Ultimately, this work not only pushes boundaries in electron microscopy, but provides avenues to the entire scientific landscape on decoupling the defect-property relationship in solids for the better design of next-generation nanoelectronics.

9:30am 2D-ThM-7 MoSSe/MoSeS Janus Crystals: Nanoscale Defects and Composition Misconceptions Revealed Through Cross-Correlated AFM and TERS Imaging, *Andrey Krayev,* HORIBA Scientific*; Tianyi Zhang,* MIT*; Lauren Hoang,* Stanford University*; Nannan Mao,* MIT*; Andrew Mannix, Eric Pop,* Stanford University*; Jing Kong,* MIT

In this talk we'll present the results of an extensive collaborative project aimed at the cross-correlated nanoscale AFM (atomic force microscopy) and TERS (tip enhanced Raman scattering) characterization of various defects appearing in the course of synthesis of Janus transition metal dichalcogenides (TMDs). Optoelectronic and catalytic properties of Janus TMDs differ from normal TMDs, thus Janus materials are of great interest for the research community.

In the course of our study, we characterized MoSSe and MoSeS Janus materials derived from MoS_2 and $MoSe_2$ correspondingly via the cold plasma-assisted replacement of the top chalcogen layer. Preliminary Raman characterization of the as-synthesized crystal performed in a single point with the single excitation wavelength (532nm) showed weak Raman peaks

of the precursors, what was misinterpreted as incomplete conversion to Janus material.

Cross-correlated AFM and TERS imaging revealed that the precursor monolayers, both MoS_2 and $MoSe_2$ featured noticeable number of nanoscale bi-, tri- and higher number of layer islands. These islands have been identified in the Janus crystals transferred to gold or silver via the Kelvin probe imaging and their composition was confirmed by TERS imaging even for the islands of just 20-30 nm in diameter. It was these multi-layer islands which were responsible for the weak Raman bands of the precursor.

The morphology of the Janus crystals derived from MoS_2 and $MoSe_2$ was also fundamentally different. In the course of conversion of $MoSe_2$ to MoSeS pre-existing tensile strain in MoSe2 was complemented by additional tensile strain resulting from the replacement of the selenium atoms with sulfur which led to physical breakage of the crystals. TERS imaging demonstrated that the gaps between the domains in MoSeS monolayers seen in topography and the surface potential images were physical cracks.

Conversely, compressive strain appearing in MoSSe Janus crystals converted from MoS_2 results in the formation of wrinkles that after the transfer to gold or silver looked like cracks in MoSeS, but in reality there was no physical breakage in these crystals. Interestingly, by varying the substrate on which the precursor crystals are grown, nice wrinkle- and crack-free Janus monolayers can be produced.

Finally, we'll briefly discuss the TERS spectral peculiarities with 785 nm and 473 nm excitation.

9:45am 2D-ThM-8 Modulating Epitaxy and Film Domain Morphology of MBE-grown 2D Transition Metal Tellurides ($TMTe_x$) through Engineering the Deposition Sequence and Substrate Selection, *Ossie Douglas, Daniela Zamora Alviarez, Muhammad Shahbaz Rafique, Daiyue Wei, Zhewen Yin,* University of South Florida*; Peter Snapp,* NASA Goddard Space Flight Center*; Michael Cai Wang,* University of South Florida

With increasing interest in transition metal tellurides ($TMTe_x$) for optoelectronic applications, physical vapor deposition (PVD) thin film growth techniques offer unique opportunities to decouple factors influencing material characteristics during growth. $TMTe_x$ thin films are commonly engineered via modulation of their domain morphology and dimensionality through deposition process controls for regulating the crystallinity. Film crystallinity regulation can be achieved using PVD techniques, like molecular beam epitaxy (MBE), through its unique co-deposition process controls. While co-deposition, or simultaneous deposition, of both the transition metal and tellurium (Te) is a common approach, this process obscures the influence of individual precursors due to the complex thermodynamic and kinetic growth conditions. The simultaneous release of precursors directly influences the vapor flux which is correlated to the film roughness and thickness. Thin film growth is further dictated by the interaction between adatoms and the substrate surface. Particularly, lattice mismatch at the film-substrate interface is influenced by the crystalline/amorphous surface nature of Asaro–Tiller–Grinfeld instability, indicating a significant impact on the grown crystalline domain size and morphology. We demonstrated sequential deposition of precursors on substrates with varying crystal structure and chemical composition to decouple the influence of different factors, yielding $TMTe_x$ with distinguishable morphology.

Specifically, we demonstrated control over the film morphology which is dependent on the initial precursor (TM/Te) deposited on either crystalline or amorphous substrates. Initial deposition of either of the precursors on muscovite mica (crystalline) resulted in the formation of fully oriented nanoribbon films with significantly different domain morphology. In contrast, either TM-initiated or Te-initiated deposition on oxidized/nitrided silicon (amorphous) surfaces, led to either disordered films or randomly oriented nanoribbons, respectively. This demonstrates that MBE-grown domain morphology of $TMTe_x$ thin films is highly dependent on precursor sequence and substrate selection, permitting transition between uniform and nanoribbon films for future applications in field-effect transistor or gas sensor device development.

11:15am **2D-ThM-14 Oxidation Stability of SnSe Under Atmospheric Conditions**, *Jonathan Chin, Bonnie Gardner, Marshall Frye,* Georgia Institute of Technology; *Derrick Liu,* Applied Materials; *Sebastian Marini,* Cornell University; *Jeffrey Shallenberger,* The Pennsylvania State University; *Matthew McDowell,* Georgia Institute of Technology; *Maria Hilse, Stephanie Law,* The Pennsylvania State University; *Lauren Garten,* Georgia Institute of Technology

Tin selenide (SnSe) is predicted to exhibit a d_{11} piezoelectric response of 250 pm/V when scaled down to the monolayer limit [1], but as the film thickness is decreased surface interactions can have a greater impact on performance. For example, in 2D transition metal dichalcogenides (TMDs), oxides form not only on the surface but also propagate between layers, degrading the thin film [2]. Oxide layers have been shown to form at the surface of bulk SnSe above 200 °C [3], but the impact of oxygen on the surface and layer stability at room temperature has yet to be fully explored. Therefore, it is critical to understand the stability of the surface and interlayer structure in SnSe under standard operating condition.

This talk describes the chemical and structural stability of SnSe thin films to atmospheric exposure. The structure and composition of thin films of SnSe grown by molecular beam epitaxy is compared immediately upon growth and after a two-year exposure to ambient atmosphere. X-ray diffraction (XRD) taken before and after atmospheric exposure shows no measurable change in the crystallographic phase, orientation, or layer spacing. Similarly, the characteristic Raman vibrational modes of SnSe are unchanged with exposure, and there are no indications of modes corresponding to $SnSe_2$, SnO or SnO_2. These measurements show that the bulk of the SnSe thin film is not degrading over time as incorporating oxygen between layers would have changed the peak spacing in XRD and Raman spectroscopy. The chemical stability of the bulk phase is further supported by x-ray photoelectron spectroscopy (XPS) measurements that show that the film maintains a 1:1 Sn:Se stoichiometry. XPS cross-sections show indications of SnO_2 but only at the surface of the SnSe film. The oxide layer was limited to the surface within approximately 3.5 nm, as confirmed via x-ray reflectivity (XRR) measurements of the layer thicknesses. Resistivity measurements show an electrical response dominated by SnSe, not SnO_2. These XPS, Raman, XRR, and resistivity results suggest that exposure to atmosphere creates a passivated layer of SnO_2 on the surface of SnSe but does not impact the bulk. Overall, SnSe demonstrates long-term chemical stability under atmospheric conditions, rendering it a suitable option for device applications that employ the protective metal oxide layer found in SnSe and possibly other layered chalcogenide structures.

1. R. Fei, W. Li, J. Li, L. Yang, *Appl. Phys. Lett.* **107**, 173104 (2015).
2. Y. Guo, S. Zhou, J. Zhao, *ChemNanoMat* **6**, 838–849 (2020).
3. *Sci.* **21**, 3333–3338 (1986).

11:30am **2D-ThM-15 Nucleation of Ald Grown Gate Dielectrics on WS₂ Using Low Temperature Oxygen Plasma Pretreatment**, *Robert K. Grubbs, Thomas van Pelt, Stefan Nemeth, Daire Cott, Benjamin Groven, Pierre Morin, Cesar de la Rosa, Gouri Kar, Johan Swerts,* IMEC Belgium

Due the ever decreasing device size driven by the electronics industry, the future of channel materials for small transistors is heading toward the use of two dimensional transitional metal dichalcogenide (2d TMD) materials. 2d TMDs are beneficial in the short channel regime because of their potential high on-to-off current ratios and because of their potentially high channel mobilities, or conductance, between the source and the drain.Beyond TMD electrical and structural quality, two large challenges exist for the implementation of TMDs into transistors. First is the electrical contact of source and drain metals to the TMD and second is the deposition of a nanometer thin, high quality, high k, defect free dielectric material on top of the TMD to form the critical transistor gate dielectric. To tackle the second challenge, the surface of WS₂ TMD was functionalized with a low temperature remote oxygen plasma which enabled nucleation sites to form on the surface of multi-layer WS₂ without catastrophic destruction of the long-range order of the WS₂. From these nucleation sites, ALD HfO_2 and Al_2O_3 using TMEAH (tetrakis(methylethylamido)hafnium)/H_2O and TMA (trimethylaluminum)/H_2O at 200C was deposited as the gate dielectric and a 5 nm thin layer with 100% coverage could be achieved at increased oxygen plasma exposures. This WS₂ functionalization / nucleation process was explored by measuring the effects of oxygen exposure and temperature and their resulting effect on the ALD deposited gate dielectric film. The ALD gate dielectric coverage and its effects on the underlying 2D materialwas quantified with AFM, XPS, photoluminescence and Raman spectroscopy. This research has led to a process where multi-layer WS₂ can be functionalized and a high-quality gate dielectric can be successfully deposited on the TMD channel materials.

11:45am **2D-ThM-16 Direct Synthesis of Few Layer Graphene on 3D Printed Metal Alloy Substrates for Medical Applications**, *Irma Kuljanishvili, Yoosuk Kim,* Saint Louis University, Department of Physics; *Wilson King,* Saint Louis University, School of Medicine; *Abigail Roe, Zijun Wang,* Saint Louis University, Department of Physics

Single- and double-layer graphene, as well as few layered graphene films continue to attract significant attention due to their unique properties and wide variety of applications, including many in biomedical fields. Synthesis of high-quality graphene films on various metal substrates has been successfully demonstrated to date. In many applications large areas graphene has been prepared by chemical vapor deposition (CVD) on catalytic metal surfaces and subsequently transferred onto target substrates or devices, which include either flat, rigid or flexible substrates However, an increased interest in the use of graphene in medical applications often requires its direct fabrication on the substrates other than common metal surfaces such as Cu, Ni, Co, etc.

Here we report on CVD synthesis/fabrication of quality two -to- three-layered graphene films with controlled morphologies on 3D printed metal alloy substrates. The number of layers, homogeneity and crystallinity of graphene grown on a large area 3D printed samples was studied with Raman spectroscopy, while microstructure, morphology and chemical make up of the graphene films was investigated by atomic force microscopy (AFM), scanning electron microscopy (SEM), X-ray photoelectron microscopy (XPS), respectively. We demonstrate correlation between growth temperature and hydrophobic properties of as-growth graphene films, with highest surface contact angle approaching superhydrophobic characteristics in the optimized growth conditions. Our results demonstrate a viable and robust process of direct growth of graphene film on non-traditional flat and arbitrary shaped 3D printed metal alloy structures. This approach could potentially be applied to the synthesis of other 2D materials which are becoming increasingly popular and viable in biomedical fields. It also opens new opportunities for other arbitrary designs of 3D printed metal constructs being developed for a variety of medical applications including but not limited to medical implants, mechanical prosthetics, electrical stimulation probes, and other.

Actinides and Rare Earths
Room 123 - Session AC+MI-ThM

Superconductivity, Electron Correlation, Magnetism and Complex Behavior

Moderators: Tomasz Durakiewicz, Idaho National Laboratory, **Ladislav Havela**, Charles University, Czech Republic, **David Shuh**, Lawrence Berkeley National Laboratory, **James G. Tobin**, University of Wisconsin-Oshkosh

8:00am **AC+MI-ThM-1 Electronic Structures of f-Electron Superconductors**, *Shin-ichi Fujimori,* Japan Atomic Energy Agency, Japan **INVITED**

The unconventional superconductors in *f*-based materials attract much attention in recent years. In the present talk the electronic structures of *f*-electron superconductors UTe₂ and CeIr₃ will be presented.

Recently, it was discovered that UTe₂ has relatively high transition temperature (T_C=2.1 K), and it is classified into one of such class of materials [1,2]. The electronic structure of UTe₂ was studied by resonant photoelectron spectroscopy (RPES) and angle-resolved photoelectron spectroscopy (ARPES) with soft X-ray synchrotron radiation [3]. The partial U 5*f* density of states of UTe₂ were imaged by the U 4*d*-5*f* RPES and it was found that the U 5*f* state has an itinerant character, but there exists an incoherent peak due to the strong electron correlation effects. The band structure of UTe₂ was obtained by ARPES and its overall band structure was mostly explained by band structure calculations, except for the incoherent band at E_B~0.5 eV. These results suggest that the U 5*f* states of UTe₂ have itinerant but strongly-correlated nature.

The electronic structure of the *f*-based superconductor CeIr₃ (T_{SC}=3.1 K) was also studied by photoelectron spectroscopy [4]. The energy distribution of the Ce 4*f* states were revealed by the Ce 3*d*-4*f* RPES. The contribution of the Ce 4*f* states to the density of states (DOS) at the Fermi energy was estimated to be nearly half of that of the Ir 5*d* states, implying that the Ce 4*f* states have a considerable contribution to the DOS at the Fermi energy. These results suggest that CeIr₃ is an *s*-wave-type superconductor with a considerable contribution from the Ce 4*f* states.

Work performed in collaboration with Ikuto Kawasaki, Yukiharu Takeda, Hiroshi Yamagami, Norimasa Sasabe, Yoshiki J Sato, Ai Nakamura, Yusei

Shimizu, Arvind Maurya, Yoshiya Homma, Dexin Li, Fuminori Honda, and Dai Aoki.

References

[1] S. Ran *et al.*, Science **365**, 684 (2019).

[2] D. Aoki *et al.*,J. Phys. Soc. **88**, 043702 (2019).

[3] S. Fujimori, *et al.*, J. Phys. Soc. Jpn. **88**, 103701 (2019).

[4] S. Fujimori *et al.*, Electron. Struct. **5**, 045009 (2023).

8:30am AC+MI-ThM-3 RIXS Study of the 5f Configuration in UTe₂: Low-Energy Excitations, Te2 Chains and U Dimers, *Denise S. Christovam, Martin Sundermann, Andrea Marino,* Max Planck Institute for Chemical Physics of Solids, Germany; *Hlynur Gretarsson,* PETRA III, Deutsches Elektronen-Synchrotron DESY, Germany; *Bernhard Keimer,* Max Planck Institute for Solid State Research, Germany; *Andrei Gloskovskii,* PETRA III, Deutsches Elektronen-Synchrotron DESY, Germany; *Maurits W. Haverkort,* Institute for Theoretical Physics, Heidelberg University, Germany; *Ilya Elfimov,* University of British Columbia, Canada; *Eric D. Bauer, Priscila F. S. Rosa,* Los Alamos National Laboratory; *Andrea Severing,* Institute of Physics II, University of Cologne, Germany; ***Liu Hao Tjeng,*** Max Planck Institute for Chemical Physics of Solids, Germany **INVITED**

UTe₂ is a recently discovered odd-parity superconductor, emerging as a promising candidate for topological superconductivity [1-3]. A key challenge in understanding its anisotropic properties and their dependence on tuning parameters is finding the appropriate *Ansatz* for describing such a complex electronic system, situated at the border between localization and itinerancy. It is essential to determine the extent to which local physics persists and to identify the governing electronic f^n configuration. Although the latter has been addressed using various methods, a fierce debate remains about whether the main configuration is f^2 or f^3.

Discrepancies in determining the dominant f^n configuration are common in uranium-based intermetallics. We argue that this apparent contradiction arises from the challenge of accurately analyzing the spectra, given the complexity associated with the underlying many-body problem and uncertainties in the input model parameters.

In our study, we opt for a newly developed spectroscopic method for U materials, namely resonant inelastic x-ray scattering (RIXS) in the tender x-ray range [4]. Applying this method to UTe₂, we can unambiguously detect the presence of atomic-like U 5f-5f low-energy excitations. This establishes the correlated nature of UTe₂ despite the presence of strong covalence and band formation. Moreover, we can also fingerprint the U $5f^2$ as the main configuration without the need to rely on accurate calculations, thus settling the debate about the 5f valence state [5].

The short Te2-Te2 distances, however, seem incompatible with a formal U^{4+} valence. We resolve this puzzle by utilizing band structure calculations and photon energy-dependent photoemission. We found that the charge transfer from the $5p_{y||b}$ band of the Te2 chain is directed not to the U 5f but to the bonding state of the U $6d_{3z2-r2}$ orbitals of the U dimer. Notably, these two band states are non-bonding to each other or to other non-5f states in the material. Yet, both bands hybridize with the U 5f, emphasizing that the description of the physical properties of UTe₂ must include the Te2 $5p_{y||b}$ and U $6d_{3z2-r2}$ bands plus the $5f^2$Ansatz [5] These are all very peculiar findings, making UTe₂ a very special material indeed.

[1] S. Ran *et al.*, Science, **365**(6454), 684–687 (2019).

[2] D. Aoki *et al.*, J. Phys. Soc. Jpn. **88**(4), 043702 (2019)

[3] for recent review: S.K. Lewin *et al.*, Rep. Prog. Phys. **86**(11):114501, 2023.

[4] A. Marino *et al.*, Phys. Rev. B **108**, 045142 (2023)

[5] D. S. Christovam *et al.*,arXiv 2402.03852 [https://arxiv.org/abs/2402.03852] (2024)

9:00am AC+MI-ThM-5 Incommensurate Antiferromagnetism in UTe₂ Under Pressure, *William Knafo*, LNCMI, CNRS, France **INVITED**

The discovery of multiple superconducting phases in UTe₂ boosted research on correlated-electron physics [1,2,3,4]. The proximity to a ferromagnetic quantum phase transition was initially proposed as a driving force to triplet-pairing superconductivity [1], and this heavy-fermion paramagnet was rapidly identified as a reference compound to study the interplay between magnetism and unconventional superconductivity with multiple degrees of freedom.

Here, we present neutron diffraction experiments showing that long-range incommensurate antiferromagnetic order is established in UTe₂ under

pressure [5]. The propagation vector $\mathbf{k_m}$ = (0.07,0.33,1) of the observed antiferromagnetic phase is close to a wavevector where antiferromagnetic fluctuations have previously been observed at ambient pressure [6,7]. Our work shows that superconductivity in UTe₂ develops in the vicinity of a long-range antiferromagnetic phase, which differs from the initial proposition of a nearby ferromagnetic phase. The nearly-antiferromagnetic nature of UTe₂ at ambient pressure and its relationship with superconductivity will be discussed.

This work was done in collaboration with T. Thebault, P. Manuel, D. Khalyavin, F. Orlandi, E. Ressouche, K. Beauvois, G. Lapertot, K. Kaneko, D. Aoki, D. Braithwaite, G. Knebel, and S. Raymond.

[1] Ran et al., Science **365**, 684 (2019).
[2] Knebel et al, J. Phys. Soc. Jpn. **88**, 063707 (2019).
[3] Braithwaite et al., Commun. Phys. **2**, 147 (2019).
[4] Ran et al., Nat. Phys. **15**, 1250–1254 (2019).
[5] Knafo et al., arXiv:2311.05455.
[6] Duan et al., Phys. Rev. Lett. **125**, 237003 (2020).
[7] Knafo et al., Phys. Rev. B **104**, L100409 (2021).

9:30am AC+MI-ThM-7 New Spectroscopic Insights into Correlation Effects and Covalency of U 5f Electrons in Uranium Intermetallic Compounds, *Andrea Marino, Martin Sundermann, Denise S. Christovam,* Max-Planck Institute for Chemical Physics of Solids, Physics of Correlated Matter, Dresden, Germany; *Hlynur Gretarsson,* DESY/PETRA-III, Hamburg, Germany; *Bernhard Keimer,* Max-Planck Institute for Solid State Research, Stuttgart, Germany; *Andrei Gloskovskii,* DESY/PETRA-III, Hamburg, Germany; *Jan Kunes,* Department of Condensed Matter Physics, Masaryk University, Brno, Czechia; *Atsushi Hariki,* Department of Physics and Electronics, Osaka Metropolitan University, Osaka, Japan; *Liu Hao Tjeng,* Max-Planck Institute for Chemical Physics of Solids, Physics of Correlated Matter, Dresden, Germany; ***Andrea Severing,*** Institute of Physics II, University of Cologne, Cologne, Germany **INVITED**

Uranium intermetallic compounds exhibit a wide range of fascinating physical phenomena that arise from the intricate interplay between atomic-like correlations and band formation of the U 5f electrons. Describing their electronic structure is a challenge, particularly as atomic-like states have remained experimentally inaccessible. Ongoing disputes revolve around the existence of atomic-like states and, if present, around determining which configuration—U $5f^3$ or U $5f^2$—provides the Ansatz or starting point for describing the low-energy properties. Furthermore, these correlated compounds exhibit strong intermediate valency, fuelling intense debates about the actual filling of the 5f shell and the degree of covalency.

This presentation introduces two novel and complementary methods: (1) valence band resonant inelastic x-ray scattering (RIXS) using tender x-rays and (2) photon energy-dependent photoelectron spectroscopy (PES & HAXPES) in combination with DFT+DMFT calculations.

(1) Valence Band RIXS: Using high-resolution RIXS at the U M-edges (3.5-3.7 keV), we observe low-energy excitations originating from atomic-like multiplet interactions [1]. The excellent signal-to-background ratio and the multiplet structure serve as a unique fingerprint for the U $5f^n$ configuration involved, offering clear evidence of the presence of local correlation physics. This method unambiguously determines the dominating configuration [1].

(2) Combination of DFT+DMFT calculations with soft and hard x-ray photoemission (PES & HAXPES): The energy dependencies of the photoionization cross-sections allow for the disentanglement of correlated 5f from band-like non-5f spectral contributions, enabling reliable tuning of parameters such as Hund's-J, Hubbard-U_{ff}, and, most importantly, the double counting correction (m_{dc}) to reproduce valence band spectra. We applied this method to UGa₂ and UB₂, two model materials representing the extreme ends of the localization-delocalization range. Despite their vastly different properties, we found the mean 5f shell filling to be almost the same. However, crucially, the distribution of uranium 5f configurations contributing to the ground state differs significantly: narrow in 'localized' UGa₂ and almost statistically broad in 'itinerant' UB₂. This method also reproduces the satellites in the 4f core-level spectra and explains the presence/absence of 5f-5f-multiplet excitations in the RIXS spectra [2].

[1] A. Marino *et al.* Phys. Rev. B, **108** (2023) 045142
[2] A. Marino, A. Hariki *et al.*, to be published

11:00am AC+MI-ThM-13 Isotopic Fingerprinting in Nuclear Forensics: Leveraging Aerogel and LEXAN® SSNTD for Enhanced Analysis, *Rami Babayew, Itzhak Halevy, Noam Elgad, Yaacov Yehuda-Zada,* Ben Gurion Uni., Israel*; Jan Lorincik,* Research Centre Řež, Czech Republic, Israel*; Mark Last, Itzhak Orion, Galit Katarivas-Levy,* Ben Gurion Uni., Israel*; Aryeh M. Weiss,* Faculty of Engineering, Bar Ilan University, Israel

In nuclear forensics, ensuring the reliability and accuracy of the analysis is paramount. Traditional methods rely heavily on the expertise of trained researchers, leading to variations in results. To address this challenge, we present innovative techniques aimed at automating Fission Track Analysis through advanced image processing algorithms applied to microscope images.

Our research introduces a pioneering approach that leverages Monte Carlo simulations, particularly utilizing the GEANT4 software, to generate synthetic models of fission tracks. By simulating various physical parameters such as thermal neutron flux, fission cross-section, particle size, and radiation time, our Trainer2 software accurately calculates fission tracks on our Lexan detector, producing results akin to real-world scenarios.

Moreover, our methodology integrates trajectory data from the fission products trajectory database, derived from GEANT4 simulations, to generate synthetic models closely resembling actual microscope images. This synthetic bank of images serves as a controlled and versatile dataset for the development of robust image analysis tools. These tools aim to automate the identification of fission track clusters, thus eliminating the need for manual intervention and minimizing the likelihood of human errors.

Our preliminary software for image processing demonstrates promising efficacy in detecting fission track clusters, providing a comprehensive record of fission sites for analysis. By identifying the length of tracks and their distribution, we can determine the source isotope and the density of impurities, thus advancing our understanding of nuclear materials.

Additionally, the software calculates the number of tracks, enhancing the efficiency of data interpretation.

Furthermore, we introduce a novel approach utilizing penetrating fluorescent colors for 3D scanning of detectors, enhancing our ability to investigate fission track stars beyond mere projections.

In conclusion, our research underscores the importance of automating FTA for nuclear safeguards, aiming to minimize human intervention while fortifying the precision and efficiency of nuclear investigations. Through the seamless integration of GEANT4 simulations and advanced image processing algorithms, we envision a future where nuclear forensic analysis is more reliable, accurate and streamlined.

Keywords: Nuclear forensics, Fission Track Analysis, Monte Carlo simulations, GEANT4, Image processing algorithms, Automated analysis, nuclear safeguards.

References

[1]Rami Babayew *et al.,* Simulation tools for improvement of the fission track analysis method for nuclear forensics (2024), JRNC, 10.1007/s10967-023-09313-5

11:15am AC+MI-ThM-14 Unusual orders in the heavy-fermion superconductor CeRh₂As₂, *Gertrud Zwicknagl,* TU Braunschweig, Germany
The heavy-fermion compound CeRh$_2$As$_2$ exhibits a complex phase diagram with rather unusual states at low temperatures. A prominent example is multi-phase superconductivity[1] which seems to develop inside a normal state characterized by itinerant multi-polar order. The present talk focusses on the instabilities of the strongly renormalized Fermi liquid state in the heavy-fermion compound CeRh2As2. The central focus is the role played by the non-symmorphic lattice structure and the consequences of the Crystalline Electric Field (CEF) which removes the orbital degeneracy of the Ce 4f states. The narrow quasiparticle bands which arise from the Ce-4f degrees of freedom via the Kondo effect are calculated by means of the Renormalized Band (RB) method. We conjecture that the quasi-quartet CEF ground state in combination with pronounced nesting features of the Fermi surface may give rise to ordered states involving multipolar degrees of freedom [2].

References

1. S. Khim et al., Science 373, 1012 (2021)
2. RevX 12, 011023 (2022)

11:30am AC+MI-ThM-15 Thermoelectric Properties of Strongly Correlated Compounds NpPd₃ and PuPd₃, *Krzysztof Gofryk,* Idaho National Laboratory; *J-C Griveau,* 3DG Joint Research Centre, Directorate G-Nuclear Safety and Security, Germany; *K. A. McEwen,* University College London, UK; *W. J. Nellis,* Harvard University; *J. L. Smith,* Los Alamos National Laboratory

Actinides are characterized by the coexistence of localized and itinerant (delocalized) 5f-states near the Fermi energy. This dual nature of the 5f electrons leads to many exotic phenomena that are observed in these strongly correlated materials, spanning magnetic ordering, heavy-fermion ground state, unconventional superconductivity, and/or a "non-Fermi liquid" state. The unusual transport properties of the strongly correlated electron systems are related to the formation, near the Fermi level, of a narrow band with a large density of states. Therefore, the Seebeck coefficient in these materials, being proportional to the density of states at the Fermi level, often reaches large values and shows the characteristic temperature dependence [Phys. Rev. B 94, 195117 (2016)]. To explore the influence of electronic correlations on the transport properties in the *An*Pd$_3$ system, here we present low-temperature electrical resistivity and Seebeck coefficient measurements of NpPd$_3$ and PuPd$_3$ intermetallics. We show that the electrical resistivity shows characteristic behavior of systems with Kondo interactions. The magnitude and overall temperature dependence of the thermoelectric power of NpPd$_3$ and PuPd$_3$ are characteristic of 4f- and 5f-electron strongly correlated materials. For cubic NpPd$_3$ a sharp transition and change of sign in S(T) at the Néel temperature indicate a first-order nature of the magnetic transition, probably accompanied by a large change in the Fermi surface topology. We have also estimated the power factor (S^2/ρ) of these materials.

Applied Surface Science
Room 117 - Session AS-ThM

Machine Learning and Data Evaluation
Moderators: Steve Consiglio, Tokyo Electron, **Jeffrey Terry**, Illinois Institute of Technology

8:00am AS-ThM-1 Redox XPS: Reliable and Automatic Peak Fitting of XPS Chemical States, *Peter Cumpson,* Sanispectra Ltd, UK; *Dhilan Devadasan,* Thermo Fisher Scientific, UK; *Robert Weatherup,* Oxford University, UK; *Silvia Gazzola,* University of Bath, U.K.; *Tim Nunney,* Thermo Fisher Scientific, UK

At the AVS symposium in 2023 we introduced *Redox XPS*, which removes ambiguities in fitting narrowscan XPS spectra by gas-phase oxidation (or reduction), typically with the assistance of ultraviolet light, within the XPS instrument. Since then we have automated the procedure, so that for a set of samples on a sample block one obtains a montage of spectra, each montage representing a progression of oxidation state. This takes more "wall-clock" time, but no more operator time, than a single spectrum.

Redox XPS is useful to remove some ambiguities, especially around any very small peaks from unexpected elements that are otherwise difficult to identify, but the principal advantage of Redox XPS is the ability to do *automatic* peak-fitting in a reliable and quantitative way. Instead of comparing with spectra obtained using other instruments (for example libraries of spectra acquired on instruments which may have different transmission functions, energy calibrations or energy resolution) one can reach a reliable quantification from *relative* measurements within a set of spectra acquired on one instrument on the same day.

To extract peak shape and intensity corresponding to the plural chemical states originally present in the sample we here apply;

1. A regularization method to avoid over-fitting, by including contraints arising from the physics and chemistry of XPS peak shapes,
2. Non-negativity constraints (valid for all real spectra, where counts and concentrations can never be negative), and
3. A feature of the inelastic background that we identify for the first time, and that has somehow escaped the notice of the community for the 30 years or more that XPS background subtraction has been common.

This algorithm is tested on Redox XPS data from 12 different elements acquired automatically. In most cases (and at the expense of more instrument time) this solves the problem of peak-fitting that otherwise can take up the valuable time and skills of XPS experts. Further, the ability to automatically fit complex peak-shapes means that Auger features that have often been ignored in the past (due to their prohibitively complex line

shapes) will become very useful to analyse quantitatively by this procedure. Most of the data we show are from progressive oxidation using UV and ozone, but we have also demonstrated reduction in some cases.

8:15am **AS-ThM-2 Exploring the Benefits of Automated, Redox Reactions in XPS Analysis**, *Robin Simpson, Tim Nunney, Paul Mack,* Thermo Fisher Scientific, UK

This presentation investigates the benefits of automated, in-situ redox reactions for the purpose of producing well controlled oxide growth on the surface of various sample types. The driving force behind using such a procedure is in the potential for generating a sequence of spectra from a progressively chemically-modified surface to remove ambiguities that can lead to misinterpretation, thus aiding in faster understanding of the unmodified surface. Our study presents XPS results from coupled stepwise oxidation/reduction of surfaces, to aid in resolving such ambiguities across a wide array of materials. We use gas-phase oxidation agents to control the redox states of a specimen, leveraging the logarithmic growth of oxide thickness. This oxidation is implemented using vacuum ultraviolet light (VUV) and the generation of ozone and gas-phase hydroxide free radicals close to the surface of the specimens within the entry-lock of the Thermo Scientific Nexsa surface analysis instrument. This work focusses on the benefits of automating this process to ascertain the potential merits of including it into a standard operating procedure for XPS analysis.

8:30am **AS-ThM-3 Fourier Denoising of X-ray Photoelectron Spectroscopy Data**, *Matthew Linford, Alvaro Lizarbe, Kristopher S. Wright,* Brigham Young University; *Jeff Terry,* Illinois Institute of Technology; *David E. Aspnes,* Brigham Young University

There has long been something of a prohibition on the smoothing/denoising of X-ray photoelectron spectroscopy (XPS) data. In this talk, we reconsider this possibility.

Fourier analysis is powerful for data analysis because it allows one to separate the information in a spectrum in a way that is not possible in direct space. This separation takes place because information in spectra, including XPS spectra, is usually in point-to-point correlations, which ends up in low index Fourier coefficients, while noise is in point-to-point variations, which ends up in high index Fourier coefficients. One of the pillars of Fourier theory is the convolution theorem. It states that convolution in one domain (direct or reciprocal) is equivalent to multiplication in the other.

In this talk, we begin by evaluating the effectiveness of common smooths like the boxcar and Savitzky-Golay smooths. In both cases, these smooths are flawed. They lack the ability to fully remove high frequency noise from data. We then discuss the use of the Gauss-Hermite (GH) filter for removing noise from Fourier transformed XPS spectra. This adjustable filter is unity, or near unity, for lower index Fourier coefficients, but drops off smoothly to zero for the higher index coefficients. We show the use of this filter for a relatively broad Ag 4s XPS peak, a narrow scan (Ag 3d) with sharp, spin-orbit components, and a metal peak that shows a significant step in the baseline. Various positions of the GH filter are considered in each case (this filter function is adjustable). We compare our results to 'true' spectra obtained by significant signal averaging. We make the case that appropriate Fourier filtering of XPS data may have a useful place in XPS data analysis. We also provide cautions for using this capability.

8:45am **AS-ThM-4 Fourier Denoising of X-ray Photoelectron Spectroscopy Data. Applications to the carbon Auger D parameter, HAXPES, and EasyEXAFS**, *Alvaro Lizarbe, Kristopher Wright, Gavin Murray, Garrett Lewis,* Brigham Young University; *Mark Isaacs,* Diamond Light Source, UK; *David Morgan,* Cardiff University, UK; *David Aspnes,* North Carolina State University; *Matthew Linford,* Brigham Young University

We recently argued for the use of Fourier denoising with the Gauss-Hermite filter as a tool for separating the signal and noise in XPS spectra. The Gauss-Hermite filter more effectively removes high frequency noise from spectra than more traditional Savitzky-Golay and boxcar smooths. This type of approach works because noise is contained in point-to-point variations, while signal is in point-to-point correlations. In this talk, we discuss practical ways of implementing this capability. For example, the carbon Auger signal needs to be smoothed before it is differentiated to derive the D-parameter. Otherwise, the numerical differentiation blows up the noise. Denoising with the Gauss-Hermite filter effectively denoises these spectra. Furthermore, differentiation of this signal is then easily performed by differentiating (and summing the derivatives) of the individual harmonics associated with the discrete Fourier transform. HAXPES represents an important direction in modern XPS. However, the

cross sections for photoemission are often considerably lower with the higher energy X-rays used in HAXPES. Accordingly, there are advantages associated with the denoising of these spectra. Finally, EasyEXAFS is an important, laboratory-based way of performing EXAFS. However, again, in a number of cases, the signal-to-noise ratios of the signals are low. Again, the denoising of these signals is advantageous. In addition to demonstrating these new capabilities, we provide guidelines and cautions for using them.

9:00am **AS-ThM-5 ASSD Student Award Finalist Talk: Stitching, Stacking and Multilayering: Practical Evaluation of ToF-SIMS Data with Machine Learning**, *Sarah Bamford[1], Wil Gardner, David Winkler,* La Trobe University, Australia; *Benjamin Muir,* CSIRO Materials Science and Engineering, Australia; *Paul Pigram,* La Trobe University, Australia **INVITED**

Time of flight secondary ion mass spectrometry (ToF-SIMS) is a powerful analytical technique capable of collecting mass spectral information in one, two and three spatial dimensions. ToF-SIMS images and depth profiles are large and complex hyperspectral data sets. Interpretation requires that the complexity of these data sets is reduced. For two-dimensional (2D) data, individual ion peaks are often extracted and overlaid or for three-dimensional (3D) data, a selection of characteristic peaks are plotted in one dimension as a function of depth. These well-established methods are ideal for known or simple samples. However, for complex or unknown samples, these methods struggle to convey the depth of information captured within the data set. Furthermore, the choice of displayed ion peaks has the potential to impart user bias and make a significant difference to the interpretation of results.

Unsupervised machine learning, specifically self-organizing maps with relational perspective mapping (SOM-RPM), allows considered analysis of complex unknown samples. The SOM-RPM approach creates a color-coded similarity map in which changes in color are specifically graded to accord with changes in molecular state, by examining the totality of the data set. By pairing ToF-SIMS and SOM-RPM, the complete hyperspectral data set in 2D or 3D can be intuitively visualized, providing a unique picture of the local and global mass spectral relationships between individual pixels. The SOM-RPM methodology has proven to be a robust technique that offers substantial advantages in this field.

This work will present several case studies across a broad range of sample types including:

- Depth profiling of a multilayer double silver low emissivity glass coating which considers the entire mass spectrum at every voxel and illuminates interfacial mixing.
- Depth profiling of polyaniline films highlighting structural flaws such as pinholes as well as subtle changes in chemistry caused by heat treatment.
- Identification of subtle changes in 200nm extracellular vesicles due to inflammatory response in releasing cells.

9:30am **AS-ThM-7 Applications of Machine Learning in TOF SIMS Data Analysis: Classification and Quantitation**, *Lev Gelb, Amy Walker,* University of Texas at Dallas

We present progress towards analysis of TOF SIMS data using machine learning (ML) methods. We posit that TOF SIMS is not more widely used because the data is too complex to be interpreted without expert knowledge, and investigate how machine learning might help. We primarily train models on simulated "big" data sets constructed by combining and/or resampling experimental spectra, with a focus on neural-network architectures. A particular interest is in uncertainty quantification and evaluation of the reliability of the models.

In the case of classification, models are constructed that can identify the type of material studied from a TOF SIMS spectrum. These are trained on libraries of reference data. Of particular interest in this application is the number of reference data that are required and how that varies with the number of material types to be distinguished.

We also consider determining the composition of a homogeneous sample consisting of two or more components for which reference spectra are available. That is, the sample consists of compounds which appear in some reference library, and the algorithm should identify what compounds are present and in what relative quantities. Factors complicating this kind of analysis include statistical noise, matrix effects, background, calibration error, and the likely case that the reference spectra were not taken under the same conditions (primary ion, ion energy, instrument manufacturer,

---

[1] **ASSD Student Award Finalist**

etc.) as the data to be analyzed. Our approach is to generate a large number of simulated high-resolution TOF SIMS spectra of multicomponent samples, again based on TOF SIMS reference data. Complicating factors are also incorporated to varying degrees, and the resulting data sets are used to train the models. Model performance is then studied and related to spectrum quality, complexity and complicating factors.

9:45am AS-ThM-8 Dorothy M. and Earl S. Hoffman Awardee Talk/ASSD Student Award Finalist Talk: Advancements in Tracer Diffusion Modeling with ToF-SIMS Depth Profiling, *Nicolas Molina[12], Andrei Dolocan, Gregory Rodin, Filippo Mangolini,* The University of Texas at Austin

Time-of-flight secondary ion mass spectrometry (ToF-SIMS) stands as a robust analytical characterization technique for determining the depth distributions of chemical moieties within solids. One of its main advantages is its capability to acquire and differentiate between the characteristic signals of isotopes of the same chemical element during a measurement. As such, stable isotopes have been employed as diffusion sources in tracer diffusion studies in a variety of fields, from energy storage to failure analysis. The standard methodology for these tracer diffusion experiments includes sample preparation, isotope dosing, ToF-SIMS depth profiling, and diffusion modeling. In this presentation, we highlight current shortcomings when modeling ToF-SIMS depth profiles in tracer diffusion experiments and proposed improvements to overcome them, namely: 1) incorporation of the spatio-temporal experimental path of the diffusing isotope, which is crucial when ToF-SIMS acquisition and diffusion timescales are comparable (i.e., the depth profile cannot be considered frozen in time anymore) and allows for correcting the calculated transport constants, i.e., diffusivity (D) and surface exchange coefficient (Γ); 2) refinement of Fick's diffusion equations when the isotopic abundance (i.e., $^2H / (^1H + ^2H)$) is used as a proxy for concentration instead of the isotope intensity (e.g., ^2H), as classical Fick's laws along with their boundary conditions do not hold for the isotopic abundance. These advancements in diffusion modeling open the path for the accurate use of ToF-SIMS for quantifying transport constants in tracer diffusion studies across a broad range of applications, including in those involving the use of ultrathin films.

11:00am AS-ThM-13 ASSD Peter Sherwood Award Talk: Hybrid SIMS: Evolution of a SIMS Instrument Combining Time-of-Flight and Orbital Trapping Mass Spectrometry, *Alexander Pirkl[3],* ION-TOF GmbH, Germany **INVITED**

Secondary ion mass spectrometry (SIMS) offers the possibility to acquire laterally resolved chemical information from submicron regions on inorganic and organic samples. However, SIMS analysers usually lack the required mass resolution, mass accuracy and high resolution MS/MS capabilities required for the thorough investigation of complex biological materials.

To specifically address the imaging requirements in the life science field and following the original idea of Prof Ian Gilmore (NPL), a Hybrid SIMS instrument was developed in a research project by IONTOF and Thermo Fisher Scientific in close cooperation with other partners of the 3D OrbiSIMS project [1]. The instrument combines an Orbitrap-based Q Exactive HF mass analyser with a high-end ToF-SIMS system, providing a mass resolution > 240,000 and a mass accuracy < 1 ppm in conjunction with high lateral resolution cluster SIMS imaging capabilities. In this contribution we will put a spotlight on the different development steps involved in the initial project and later during its still ongoing evolution, always aiming at making this technology available to more applications.

[1] Passarelli, et al. Nature Methods volume 14, pp 1175–1183 (2017)

11:30am AS-ThM-15 Multiplexing Analysis Using Microarray Plate for Fast Analysis by ToF-SIMS, *Tanguy Terlier, Carlos Gramajo,* Rice University

Multiplexing analysis is a type of assay that permits to characterize complex samples in a single run analysis. Here, we used a computer-controlled CO2 laser cutter for machining glass plates to pattern multiples 10-microns depth microwell. Among the most suitable characterization tool for producing multiplexing analysis, time-of-flight secondary ion mass spectrometry is a powerful surface analytical technique for providing detailed elemental and molecular information about the surface, thin layers, interfaces, and full 3D analysis of the samples.

Thanks to integrated large imaging capability by scanning an area of few mm2, ToF-SIMS characterization permits a deeper exploration and a better

knowledge of the organic and biological materials with complex chemical structures. ToF-SIMS produces hyperspectral images where each individual pixel contains a full mass-range spectrum. Spot areas can be selected by generating a region of interest area to treat each individually each sample. Our glass plate permits to create a library of 120 individual samples. After identification of the characteristic fragment ions, multivariate analysis is used to establish the correlation between the molecular ions and to classify the relationship between the samples.

Beyond the combination of the hyperspectral images with MVA techniques, we can elucidate the chemical composition of a large set of specimens to address complex analytical challenges or chemical reactions. The operation consists of performing a rapid single-scan ToF-SIMS analysis of the plate and then classifying the dataset for database-matching or quantification of the composition. In an initial study, a small number of monomers were characterized and then we used the dataset to discriminate the molecular signature as function of the functional groups. The method has been extended to several lipids to establish a library of characteristic fragments for further understanding of lipid deposition profiles from foreign body responses. A second study has consisted of identifying the surface composition of antibody-conjugated gold nanoparticles. Our final example will focus on developing methods for inhibiting asphaltene deposition.

To conclude, we will demonstrate through various case studies how multiplexing analysis using microarray plate for fast analysis by ToF-SIMS can offer a rapid solution for building databases and establishing reference libraries of fragmented ions. In addition, this approach allows the classification and the correlation of chemical profiles from complex compounds, and potentially the quantification of mixture by dosing species ions from ToF-SIMS data.

11:45am AS-ThM-16 Exploring the Power of TOF-SIMS by Coupling Collision-Induced Dissociation with Surface-Induced Dissociation for Structural Analysis, *Jacob Schmidt, Gregory Fisher,* Physical Electronics USA

TOF-SIMS with kilo-electron volt collision-induced dissociation (CID) tandem MS is a powerful tool for compositional identification and structural elucidation of molecules, metabolites, and degradation products due to its ability to isolate ions of interest and provide further insights into its molecular structure and composition. TOF-SIMS tandem MS has been used to unambiguously verify analytes and to generate 2D and 3D maps of a brass corrosion inhibitor[1], to image organelles in single cells[2], and to discern the degradation pathway of OLEDs[3].

In this presentation, we will explore the application of surface-induced dissociation (SID) coupled with CID, to assist in the confirmation of molecular assignments. In contrast to CID, which promotes cleavage at every molecular bond, SID is more subtle in that the bond cleavages result predominantly in the observation of functional group chemistry, as shown in Figure 1. The fragmentation energetics between SID and CID are distinct, even at the same kinetic energy, which leads to pronounced effects on mass calibration. This difference in fragmentation energies can have a significant effect on calibration, which we will address using isotopic abundances to confirm compositional assignments.

1. M. Finšgar, *Corrosion Science*. **182** (2021) 109269.
2. P. Agüi-Gonzalez, et. al, *J. Anal. At. Spectrom*. **34** (2019) 1355-1368
3. K. Sawada, et. al, *SID Symp. Dig. Tec.* **54** (2023) 1291-1293

12:00pm AS-ThM-17 Dealing with Reproducibility and Replication Challenges in Surface Analysis: Sample Provenance Information, Parameter Reporting, and Cultural Issues, *Donald Baer,* Pacific Northwest National Laboratory

It has been increasingly recognized that in many areas of surface and materials science faulty data and analyses, along with sparse reporting of experimental and analysis details, complicate the ability of other researchers to assess and replicate published results. In the past several years, the surface analysis community has initiated multiple efforts to address these issues, mostly providing information and guidance to help researches appropriately collect and analyze data. The status of some of these efforts will be reported during this talk with a focus on topics related to collecting sample provenance information, methods to facilitate parameter collection and reporting, and the importance of addressing cultural issues. The increased use of surface methods by both inexperienced analysts and use of the methods outside the surface analysis community contribute to the problem. Therefore a variety of guides, tutorials and helpful websites have been and are being prepared including two collections of papers on reproducibility challenges and solutions published in the Journal of Vacuum Science and Technology A, a series of

---

[1] **ASSD Student Award Finalist**
[2] **AVS National Student Awardee**
[3] **ASSD Peter Sherwood Award**

Notes and Insight papers in Surface and Interface Analysis, with the objective of providing short focused discussions on important topics, a discussion of common XPS errors and parameter reporting in Applied Surface Science Reports, and the information in the websites XPSlibrary.com and XPSOasis.org. The ISO Committee TC201 on Surface Chemical Analysis is developing a standard on reporting information regarding preparation of samples for surface analysis.This information is important for a sample provenance record that provides a traceable history of samples undergoing analysis. Recent reports on the lack of information about instruments used for data collection and analysis will be partially addressed by new publications in Surface Science Spectra providing referenceable details about widely used commercial instruments along with descriptions of operator selected modes of instrument operation. Finally, these efforts will be effective only to the extent that the members of the community accept, use, and promote the use of these tools and concepts.Specifically, it is important that the culture of the community values and supports efforts to enhance research quality. There are important roles for reviewers, colleagues, educators, editors, professional societies, and granting agencies in identifying and addressing sloppy science.

Chemical Analysis and Imaging of Interfaces
Room 121 - Session CA-ThM

In Situ and Operando Analysis of Energy and Environmental Interfaces I
Moderators: Sefik Suzer, Bilkent University, Turkey, **Xiao-Ying Yu**, Oak Ridge National Laboratory, USA

8:00am **CA-ThM-1 Rationally Engineering Interfaces to Improve Performances of Li Metal Batteries**, *Bin Li,* Oak Ridge National Laboratory, USA **INVITED**
Lithium (Li) metal batteries have attracted world-wide attention due to its low density (0.534 g/cm³), high theoretical capacity (3,860 mAh/g), and low electrochemical potential (-3.04 V vs. SHE), enabling their potential to double the cell-level energy of the state-of-the-art lithium-ion batteries. However, there are still key materials issues that inhibit lithium metal from being commercialized as an anode for rechargeable battery applications. The chemical and morphological (e.g., grain distribution, surface roughness, etc.) non-uniformity, coupled with the high reactivity of lithium drive heterogeneous solid-electrolyte interphase (SEI) formation, poor ionic flux distribution, active material consumption, and rapid dendrite growth. Currently, there are ex-situ and in-situ approaches to address the above issues. For example, one of approaches is to coat artificial SEI layers on Li metal anode surfaces. The component, distribution and structures of SEI layers should be designed and well controlled. The other approach is to exploit advanced electrolyte to in-situ form high-performance SEI layers. In this talk, we will present our recent work from the two aspects: a) novel closed-host bi-layer porous/dense artificial SEI layers were designed[1]; b) the microstructures of localized high-concentration electrolyte were deeply understood and thus new electrolytes with high-performance SEI layers being formed were discovered.[2]

References:

[1] Efaw, Corey M., et al. "A closed-host bi-layer dense/porous solid electrolyte interphase for enhanced lithium-metal anode stability." *Materials Today* 49 (2021): 48-58.

[2] Efaw, Corey M., et al. "Localized High-Concentration Electrolytes Get More Localized Through Micelle-Like Structures." *Nature Materials*, 2023.

8:30am **CA-ThM-3 Dynamic Molecular Investigation of the Solid-Electrolyte Interphase of an Anode-Free Lithium Metal Battery Using in situ Liquid SIMS and Cryo-TEM**, *Zihua Zhu, Yaobin Xu, Peiyuan Gao, Chongmin Wang,* Pacific Northwest National Laboratory
A fundamental factor that governs the performance of a lithium battery is the formation and stability of the solid-electrolyte interphase (SEI) layer on the anode surface. Despite a large body of literature documenting the structural and chemical nature of the SEI layer, essentially three levels of information regarding the SEI layer have never been fully understood: the formation dynamics, the molecular nature, and the spatial configuration. In this work, we use *in situ* liquid secondary ion mass spectroscopy, cryogenic transmission electron microscopy, and density functional theory calculation to delineate the molecular process in the formation of the SEI layer under the dynamic operating conditions. We discover that the onset potential for SEI layer formation and the thickness of the SEI show dependence on the

solvation shell structure. On a Cu film anode, the SEI is noticed to start to form at around 2.0 V (nominal cell voltage) with a final thickness of about 40−50 nm in the 1.0 M LiPF$_6$/EC-DMC electrolyte, while for the case of 1.0 M LiFSI/DME, the SEI starts to form at around 1.5 V with a final thickness of about 20 nm. Our observations clearly indicate the inner and outer SEI layer formation and dissipation upon charging and discharging, implying a continued evolution of electrolyte structure with extended cycling.

8:45am **CA-ThM-4 Understanding the Surface and Bulk Transitions of Functional Inorganic Materials for Energy Applications**, *Ajay Karakoti,* Pacific Northwest National Laboratory; *Kavin Thangaraj,* Washington State University, US; *Tanmayi Bathena,* Oregon State University; *Vaithiyalingam Shutthanandan,* Pacific Northwest National Laboratory; *Shannon Lee, Karthikeyan Ramasamy, Vijayakumar Murugesan,* Pacific Northwest National Lab
The research encompassing the discovery of novel materials has been the cornerstone for multiple major advancements in energy storage, utilization, and conversion. However, the design and selection of materials has become highly challenging owing to the complex requirements of energy applications that requires the desired properties of materials to be maintained under dynamic operational conditions. The independent characterization and property measurement of such materials can shed light on the structure-property correlations of materials in static conditions however, in-situ and operando measurements allow the researchers to understand the evolution of materials properties during the application of external stimuli such as temperature, pressure, voltage, and environment.

This talk will focus on the characterization of materials used in energy storage and catalysis under different stimuli such as high temperature and gaseous environment using multi-modal analytical capabilities. Specifically, we will demonstrate the temperature dependent phase transition of lead dioxide, critical to its application as an active electrode material in lead-acid batteries, using in-situ X-ray photoelectron spectroscopy (XPS) combined with residual gas analysis. We will follow this with the demonstration of high temperature X-ray diffraction (XRD) measurements of copper hydroxy chloride (CHC) along with thermogravimetric analysis for understanding its potential as a material for thermochemical energy storage (TCES) applications. We will demonstrate that CHC could be used for TCES based on its hydration and dehydration characteristics however, the hydration-dehydration reversibility is limited by the decomposition of CHC at higher temperatures. We also show that the decomposition of CHC at higher temperatures proceeds with loss of chlorine accompanied by the formation of copper oxide and that its application as a TCES material hinge on preventing its decomposition reducing the chlorine loss. Finally, we will conclude by demonstrating the use of in-situ XPS for understanding the changes in the oxidation states of bismuth and molybdenum in bismuth molybdate catalyst during its redox cycling. We show that the bismuth molybdate catalyst undergo surface oxidation state and stoichiometry changes during initial 3-5 redox cycles, which are also reflected in the dynamic phase changes observed by the X-ray Diffraction, before stabilizing into an temperature dependent equilibrium composition.

9:00am **CA-ThM-5 In situ Imaging and Spectroscopy of Boehmite Particles in Liquid**, *Xiao-Ying Yu,* Oak Ridge National Laboratory
This work presents in situ imaging of boehmite (γ-AlOOH) particles, suspended in liquid, in a vacuum compatible microfluidic sample holder using a suite of tools including scanning electron microscopy (SEM) and time-of-flight secondary ion mass spectrometry (ToF-SIMS), highlighting the advantage of multiscale analysis in material sciences.Boehmite particles are known to exist in high-level radioactive wastes at the Hanford site.These particles are difficult to dissolve and cause rheological problems for processing in the nuclear waste treatment plant.Therefore, it is important to understand how boehmite particles form aggregates in waste tanks.Of particular interest is the pH effect on the boehmite aggregation and morphological change simulating tank waste relevant conditions. Polydisperse boehmite particles under different pH conditions in deionized (DI) water were studied using in situ SEM and liquid SIMS imaging in high vacuum, enabled via a transferrable and vacuum compatible microfluidic interface, System for Analysis at the Liquid Vacuum Interface (SALVI) [1, 2].In situ liquid SEM provides descriptions of particle size, shape, morphology enhanced with elemental mapping [3].When comparing particle morphology and shape changes under different pH conditions, more aggregates are seen.In situ liquid SIMS is used to study particle molecular structure and composition.In situ SIMS provides detailed submicron molecular mapping of the particle and its surrounding water cluster environments as well as molecular identification of small molecules

in liquid. These new results demonstrate advancements of in situ correlative imaging of liquid surfaces and solid-liquid interfaces using a universal microfluidic interface [4].

References:

[1] L Yang *et al.*, J. Vac. Sci. Technol. A **29** (2011), art. no., 061101. doi: 10.1116/1.3654147.

[2] L Yang *et al.*, Lab Chip **11** (2011), 2481-4. doi: 10.1039/c01c00676a.

[3] X-Y Yu *et al.*, Surface Interface Analysis A **51**(13) (2019), 1325-1331. doi: 10.1002/sia.6700.

[4] X-Y Yu, J. Vac. Sci. Technol. A **38** (2020), art. no., 040804. doi: 10.1116/1.5144499.

9:15am CA-ThM-6 Square Wave Modulated Xps Enables Capturing Dynamics of Local-Electrical Potential Variations of Solid-Liquid Interfaces, *Ezgi Kutbay,* Bilkent University, Ankara, Turkey*; Pinar Aydogan-Gokturk,* Koc University, Istanbul, Turkey*; Said Ergoktas, Coskun Kocabas,* Manchester University, UK*; **Sefik Suzer**,* Bilkent University, Chemsitry Department, 06800 Ankara, Turkey

X-Ray Photoelectron Spectroscopy (XPS) has been utilized to extract local electrical potential profiles by recording core level binding energy shifts upon application of a DC and/or AC [Square Wave (SQW)] bias with different frequencies. In this work, to carry out these measurements on a co-planar capacitor with a polyethylene membrane (PEM) coated with a 1:1 by volume mixture of **I**onic **L**iquids (ILs) N,N-Diethyl-N-methyl-N-(2-methoxyethyl) ammonium bis(trifluoromethanesulfonyl)imide (DEME-TFSI) and N,N-Diethyl-2-methoxy-N-methylethanaminium tetrafluoroborate (DEME-BF$_4$). Analyses were carried out in-operando; such that XPS measurements were carried out simultaneously with current measurements. ILs have complex charging/discharging processes and they induce formation of the Electrical Double Layer (EDL) at the interface of the electrode. Certain properties of this process can be extracted via AC modulation under appropriate time windows. Here, two frequencies, 10 kHz and 0.1 Hz, were selected to investigate the effects of the fast polarization and the slow migratory currents, respectively. Local electrical potential developments were extracted at different locations of the device, from the variations in binding energies before and after adding two equivalent resistors in series to the device. This simple modification of the circuit allows us to quantify the AC currents passing through the device as well as the system's resistance and capacitance under specific conditions. Moreover, we were able detect differences in the time-behavior of the two anionic (BF$_4^-$ and TFSI$^-$) moieties. With this relatively non-invasive methodology, XPS becomes a useful tool for extracting localized electrochemical information and may be of great importance in better understanding of energy harvesting and storage systems.

9:45am CA-ThM-8 Scanning Photoelectron Spectro-Microscopy – Opportunities and Possibilities of Operando Micro-Imaging and Chemical Analysis, *Zygmunt Milosz, Matteo Amati, Luca Gregoratti,* Elettra-Sincrotrone Trieste, Italy

Due to the short escape depth of electrons X-ray Photoelectron Spectroscopy (XPS) is the best surface sensitive analytical techniques for probing surface and interface chemical composition. The Scanning PhotoEmission Microscope (SPEM) uses a direct approach to add the spatial resolution and characterize materials at the submicron scale i.e. the x-ray photon beam is downsized to a submicron spot and the sample surface is mapped by scanning the sample with respect to the focused beam. With the SPEM hosted at the Escamicroscopy beamline (Elettra-Sincrotrone Trieste) the beam can be downsized, by using Zone Plates, to a diameter of up to 150 nm with overall energy resolution better than 200 meV [1].

Investigation of complex systems in electrochemistry and catalysis often requires Near Ambient Pressure (NAP) conditions. Due to samples inhomogeneity in submicron scale conventional XPS systems did not allow to examine them in proper way. We present an alternative way for operando XPS measurements based on a special NAP cell [2] (SI fig. 1) with working pressure up to 2x10^{-1} mbar and temperature range from room temperature (RT) up to 550°C. The NAP cell combined with focused synchrotron beam allows for continuous operando chemical characterization of the systems and imaging the surface within scanning areas of 450 µm^2 [1]. It opens new opportunities for operando measurements on the systems in micro- and nanometric scale.

Fuel cells are electrochemical devices providing efficient and environmentally-friendly production of electricity directly converting the electrons exchanged in a redox reaction (such as a combustion) into electric current. One of the still unresolved issues that impedes their widespread applications is related to the limited durability of crucial components and mass transport events that deteriorate the performance.

Recent achievements in the chemical and electronic characterization of fuel cell components will be presented providing an overview of the capabilities of The NAP cell technique. For example the in situ characterization of novel non-noble metal catalysts for the Oxygen Reduction Reaction (ORR) and the characterization of a Self-Driven Single Chamber SOFC in operando condition will be shown [3].

[1] https://www.elettra.eu/elettra-beamlines/escamicroscopy.html

[2] H. Sezen et al. ChemCatChem, Vol. 7 - 22, pp. 3665-3673 (2015)

[3] B. Bozzini et al. Scientific Report 3, 2848, 2013

11:00am CA-ThM-13 The Dynamics of Encapsulated Clusters Under the Microscope, *Barbara A.J. Lechner,* Technical University of Munich, Germany **INVITED**

Catalysts on reducible oxide supports often change their activity significantly at elevated temperatures due to the strong metal-support interaction (SMSI), which induces the formation of an encapsulation layer around the noble metal particles. However, the impact of oxidizing and reducing treatments on this encapsulation layer remains controversial, partly due to the 'pressure gap' between surface science studies and applied catalysis.

In the present work, we employ near-ambient pressure scanning tunneling microscopy (NAP-STM) and X-ray photoelectron spectroscopy (NAP-XPS) to study the effect of reducing and oxidizing atmospheres on the SMSI-state of well-defined oxide-supported Pt catalysts at pressures from UHV up to 1 mbar. On a TiO$_2$(110) support, different sintering and encapsulation dynamics are observed in O$_2$, H$_2$ and CO$_2$ environments, respectively, and we show that the degree of support reduction plays an important role. We also compare the encapsulation of nanoparticles, which is well established, with that of small clusters, where no satisfying atomistic model exists to date. On Fe$_3$O$_4$(001), encapsulation stabilizes small Pt clusters against sintering [1]. Moreover, the cluster size and the cluster footprint on the support affect its diffusivity and can therefore be used to tune the sintering mechanism. Interestingly, small clusters of up to 10 atoms even still diffuse intact after encapsulation, and we can observe and track this diffusion in real time using our FastSTM [2].

[1] S. Kaiser et al., *ACS Catalysis* 13, 6203-6213 (2023).

[2] C. Dri et al., *Ultramicroscopy* 205, 49-56 (2019).

11:30am CA-ThM-15 Scanning Tunneling Microscopy for High Entropy Materials, *TeYu Chien,* University of Wyoming

High entropy materials, including high entropy alloys (HEAs), high entropy Van der Waals materials, and high entropy oxides, have drawn the attention of scientists and engineers for their various functionalities and properties. While a wide variety of properties are being studied in these materials, microscopic understanding is still challenging. In this talk, I will talk about our recent efforts in using scanning tunneling microscopy (STM) based techniques to study this intriguing material system. Including synchrotron X-ray STM (SX-STM) in which combining the atomic scale spatially resolving STM with the elemental resolving X-ray absorption spectroscopy (XAS) to achieve distinguishing elements at sub-nm scale on the surface of HEA; revealing short-range order and local lattice distortion; and revealing gap features in high entropy alloys and compounds, which might originate from strong correlation physics in the high entropy materials.

11:45am CA-ThM-16 *in-Situ* Observation of Chemical and Morphological Transformations by Multi-Modal X-Ray Characterization, *Slavomir Nemsak,* Lawrence Berkeley National Laboratory

In the last two decades, Ambient Pressure X-ray Photoelectron Spectroscopy (APXPS) in both soft and tender/hard X-ray regime has established itself as a go-to technique to study heterogeneous and complex materials under reaction environments. Multimodal approaches, which correlate information from two or more complementary techniques, are currently one of the forefronts of the APXPS development [1]. In the past three years, the ALS contributed one such setup: a combined Ambient Pressure PhotoEmission and X-ray Scattering (APPEXS) instrument commissioned and operated at beamline 11.0.2 of the Advanced Light Source [2]. The combination of the two in-situ techniques allows correlating structural and chemical information. By using APPEXS, we observed dynamics of the exsolution process of catalyst metallic nanoparticles [3]. To expand the capabilities of APPEXS further, we introduced a new platform

using arrays of patterned nanoparticles to study the evolution of catalytic systems under reaction conditions [4]. Future developments of the technique(s) and the beamline will be also discussed.

References

[1] H. Kersell, L. Falling, A. Shavorskiy, S. Nemsak, *Ambient Pressure Spectroscopy in Complex Chemical Environments*, 333-358 (2021).

[2] H. Kersell, P. Chen, H. Martins, Q. Lu, F. Brausse, B.-H. Liu, M. Blum, S. Roy, B. Rude, A. Kilcoyne, H. Bluhm, S. Nemšák, *Rev. Sci. Instr.* **92**, 044102 (2021).

[3] H. Kersell, M.L. Weber, L. Falling, Q. Lu, C. Baeumer, N. Shirato, V. Rose, C. Lenser, F. Gunkel, S. Nemšák, *Faraday Discussions* **236**, 141-156 (2022).

[4] H. Kersell, S. Dhuey, D. Kumar, S. Nemsak, *Synchr. Rad. News* **35**, 61-66(2022).

12:00pm CA-ThM-17 NO Adsorption on Pd(111): A Relationship between Coverage and Spectral Shift, *Sayantani Sikder,* Stony Brook University*; Esteban Fornero,* Universidad Nacional del Litoral (UNL), Argentina*; Anibal Boscoboinik,* Center for Functional Nanomaterials, BNL

Understanding the adsorption of nitric oxide (NO) on catalytic surfaces like Pd (111) is crucial for environmental and health reasons. Despite previous research, there is a gap in understanding spectral changes across different coverage ranges. Addressing this, we investigate the relationship between spectral shifts, integrated intensity, and coverage of NO on Pd (111) in IRRAS (Infra-red reflection Adsorption Spectroscopy). We conducted experiments at 200 K under ultra-high vacuum conditions to high doses of NO ~ 5L, to ensure precise control over NO exposure and adsorption. A mathematical expression was developed for the relationship of coverage & dose. We observed that as we approach the saturation coverage, the coverage/dose correlation changes from linear (0.3 to 0.6 ML), when NO adsorbs in three-fold and bridge sites, to a more complex correlation above 0.6 ML, when the adsorption is a combination of atop and bridge sites. The IRRAS peak positions are useful in providing insights toward this conclusion. In short, our research provides valuable insights into NO adsorption dynamics on Pd (111), advancing our comprehension of surface adsorption phenomena with implications for catalytic converter design and environmental mitigation strategies.

Electronic Materials and Photonics
Room 114 - Session EM+2D+AP+QS+TF-ThM

Epitaxy: Advances in Materials Integration and Devices
Moderator: Somil Rathi, Arizona State University

8:00am EM+2D+AP+QS+TF-ThM-1 Electronic and Photonic Integrated Devices Enabled by Local III-V on Si Heteroepitaxy, *Markus Scherrer,* IBM Research GmbH, Zurich Research Laboratory, Switzerland*; Kirsten E. Moselund,* Paul Scherrer Institute, Switzerland*; Heinz Schmid,* IBM Research GmbH, Zurich Research Laboratory, Switzerland

Heterogeneous integration of electronic chiplets is one of the key performance drivers in today's HPC and consumer products. Similarly, a performance benefit can be envisioned by heterogeneous integration of preferred materials at the device level. Here we explore this bottom-up path and report on local growth of III-V compound semiconductors on silicon for electronic and photonic applications. For electronic applications the high charge carrier mobility in III-V materials is particularly interesting, while for optical devices, the direct bandgap and in-plane coupling to Si waveguides are key benefits. We will detail the epitaxial growth of III-Vs on Si by template-assisted selective epitaxy using MOCVD and highlight this method´s uses by discussing selected device characteristics for field-effect transistors [1] and pin photodetectors directly integrated to Si waveguides [2]. The dense and precise co-placement of III-V gain material with Si allows for novel device designs, which will be illustrated by recent results on lasers based on hybrid III-V/Si photonic crystal cavity designs [3].

This research is supported by EU Grant 860095, 678567, 735008 and SNF grant 188173.

[1] C. Convertino et al. Nat. Electron. (2021) doi.org/10.1038/s41928-020-00531-3

[2] P. Wen et al. Nat. Comm. (2022) doi.org/10.1038/s41467-022-28502-6.

[3] M. Scherrer et al. ACS Photonics (2024) doi.org/10.1021/acsphotonics.3c01372

8:15am EM+2D+AP+QS+TF-ThM-2 In situ Graphene Barriers for Remote Epitaxy of SiC*, Daniel Pennachio, Jenifer Hajzus, Rachael Myers-Ward,* US Naval Research Laboratory

Remote epitaxy (RE) is a thin film growth technique where epitaxial alignment is directed by interactions with a substrate despite it being covered by a top layer of material.[1] This top layer must be inert and atomically thin for the underlying substrate's potential field to dominate the epitaxial alignment. Since the intermediate layer is inert, the epitaxial thin film is weakly bonded to the substrate and can be removed as a freestanding membrane and the substrate can be reused, without the damage associated with other transfer techniques such as controlled cleaving or ion implantation. Transferred 2D two-dimensional (2D) material, such as graphene, is commonly used for a layer, but the transfer can degrade the film and increase process complexity. To avoid this, we aim to grow in situ graphene in the same chemical vapor deposition (CVD) RE growth as SiC. RE SiC is advantageous since the high cost of SiC makes substrate reuse appealing and isolated SiC membranes are excellent for quantum photonics. Despite these benefits, SiC's high-temperature hydrogen-containing CVD environment can easily damage graphene, making RE difficult.

This study established growth windows for in situ graphene via propane-based hot wall CVD followed by subsequent SiC deposition. Growing at 1620 °C in 20 slm H2 with 20 sccm propane flow produced predominantly monolayer (ML) graphene films on on-axis 6H-SiC(0001) substrates and 2-3 ML films on 4° off-axis 4H-SiC(0001) substrates with minimal defects found in Raman spectral maps. These films exhibited increased uniformity over graphene grown via Si sublimation from the SiC substrate, as determined by atomic force microscopy (AFM) and Raman spectral maps. This optimal graphene growth condition was used for subsequent RE attempts to study the effect of SiC growth temperature, precursor C/Si ratio, and growth rate on epilayer crystallinity and graphene barrier damage. Nomarski microscopy, scanning electron microscopy (SEM), and AFM found SiC grown at 1620°C with a C/Si ratio of 1.55 to have the smoothest surface morphology and fewest polytype inclusions. SiC crystalline quality appeared correlated to growth rate, with lower growth rates producing smoother films with fewer polytype inclusions. Single-crystalline, polytype-pure SiC epilayers was achieved on 4° off-axis CVD graphene/4H-SiC(0001). Cross-sectional transmission electron microscopy (TEM) of some growth interfaces in this study exhibited non-uniform multilayer graphitic carbon, motivating further study of this growth system to improve boundary uniformity and SiC epilayer quality.

[1] Kim, Y., Cruz, S., Lee, K. et al. Nature 544, 340–343 (2017).

8:30am EM+2D+AP+QS+TF-ThM-3 Basal Plane Dislocation Mitigation via Annealing and Growth Interrupts*, Rachael Myers-Ward, Nadeemullah Mahadik, David Scheiman, Jenifer Hajzus, Samuel White, Daniel Pennachio,* Naval Research Laboratory

Basal plane dislocations (BPD) in SiC are high-voltage bipolar device killers that source Shockley-type stacking faults in the presence of an electron-hole plasma [1].Multiple research groups have been successful in mitigating their propagation from the substrate into the epitaxial layer [2-5]. While these are sufficient for typical SiC devices, for high pulsed power current density or high surge current capability applications, the injected carrier concentration is significant enough to expand converted BPDs. Here, we will report results from comparisons of H_2 etching to Ar annealing and the use of H_2 versus Ar during growth interrupts to prevent BPD expansion.

SiC epitaxial layers were grown using a CVD reactor on 4° off-axis substrates toward the [11-20] that are known to have BPDs. A H_2 etch or Ar anneal was performed before the buffer layer (BL) growth while a growth interrupt in H_2 or Ar was conducted prior to the intentionally low doped drift layer. Ultraviolet photoluminescence (UVPL) imaging was used to image the samples before and after UV stressing up to 13 kWcm^{-2}.

The H_2 etch and H_2 growth interrupt prevented BPDs from expanding under UV stress of 13kWcm^{-2} and it is believed that the H_2 treatment specifically inhibited this expansion. To confirm the role of H_2, we performed a growth using the same conditions as the H_2 etch/interrupt, however, an Ar anneal was used instead of a H_2 etch and the growth interrupt was conducted in an Ar atmosphere instead of H_2. The sample was UV stressed up to 1000 Wcm^{-2} and it was found that four BPD expanded from the substrate into the epilayer. For comparison, a sample grown with a double H_2 etch (before the buffer layer growth and drift layer) and a sample grown with a H_2 etch plus H_2 growth interrupt did not produce faulting at the same power density. This indicates that H_2 influences BPD expansion. We will present detailed parametric results of samples grown with various etching/ annealing,

growth interrupts, anneal times, buffer layer thickness, gas flow rates and interrupt temperature, both in H_2 and Ar.

[1]J.P. Bergman, *et. al.*, Mater. Sci. Forum Vol. 353-356, 299 (2001).

[2]N.A. Mahadik *et.al.*, Mater Sci Forum 858, 233 (2016).

[3]R. E. Stahlbush, et al., Appl. Phys. Lett. 94, 041916 (2009).

[4]M. Kato, *et al.*, Sci. Rep., 12, 18790 (2022).

[5]N.A. Mahadik *et. al.*, Appl. Phys. Lett., 100, 042102 (2012).

8:45am EM+2D+AP+QS+TF-ThM-4 Shadow Mask Molecular Beam Epitaxy, *Shagorika Mukherjee, Rahul Sitaram, Xi Wang,* University of Delaware*; Stephanie Law,* Pennsylvania State University

Shadow mask molecular beam epitaxy (SMMBE) is a form of selective area epitaxy (SAE)which uses a mask either directly fabricated on or placed in contact with the substrate. During film deposition, epitaxial layers are grown on the substrate through apertures in the mask. In addition to selective area growth, SMMBE also produces a shadowing effect near the mask edges in which elemental fluxes vary as a function of position. This results in a gradient of film thickness and/or composition near the mask edges. The steepness of the gradient can be controlled by varying the mask thickness and/or the angle of the mask edges. In this paper, we demonstrate the potential of the SMMBE technique to create in-plane gradient permittivity materials (GPMs) by taking advantage of the shadowing effect. A GPM is a material in which the permittivity varies as a function of location. Our aim is to synthesize in-plane GPMs, in which the permittivity varies in the lateral in-plane direction rather than in the vertical growth direction. In an in-plane GPM, different wavelengths of light can be confined at different in-plane locations on the chip. We are interested in creating an infrared GPM, so we chose Si:InAs as our material. To create our GPMs, we use the SMMBE approach: by creating flux gradients of both indium and silicon near the edges of the mask, we can control the doping density and thus the permittivity of Si:InAs in the lateral in-plane direction. We started with reusable Si masks that are 200 um thick and 1 cm x 1 cm in dimension. Each mask has an aperture at its center which has a dimension of 0.5 cm x 0.5 cm at the top and 0.528 cm x 0.528 cm at the bottom. Nano-FTIR spectra obtained via s-SNOM using a mid-IR nano-FTIR module demonstrates that we successfully synthesized infrared GPMs. The GPM grown using a 200 um mask can confine light with wavenumbers 650 cm^{-1} to 900 cm^{-1} over an in-plane distance of 13 um. In this talk, I will discuss the influence of several growth parameters in controlling the in-plane permittivity of the GPMs, including the growth temperature, mask thickness, and As:In ratio. In particular, the 500 um mask provides a larger shadowing effect in comparison to 200 um mask. This leads to a larger gradient in permittivity over a longer in-plane distance in the GPM: light with wavenumbers 650 cm^{-1} to 1400 cm^{-1} can be confined over an in-plane distance of 30 um. This provides a larger surface area for the construction of an ultracompact spectrometer. Tailored mask designs can be employed to synthesize in-plane GPMs with tailored permittivity gradients in the future.

9:00am EM+2D+AP+QS+TF-ThM-5 Impact of Excess Ga on Electronic Properties in Plasma-assisted MBE-grown β-Ga₂O₃, *Thaddeus Asel, Brenton Noesges, Jian Li, Yunjo Kim, Adam Neal, Shin Mou,* Air Force Research Laboratory, Materials and Manufacturing Directorate, USA

β-Ga_2O_3 has been of significant interest due to its high electric breakdown field, commercially available native substrate, and shallow n-type donors. However, β-Ga_2O_3 differs from other Ga-based semiconductors where metal-rich growth conditions are utilized to achieve adsorption-controlled growth by consuming the Ga flux entirely. Instead, β-Ga_2O_3 growth must balance the incorporation of Ga with the desorption of a volatile suboxide species, Ga_2O where this suboxide is a limiting step when growing β-Ga_2O_3 via molecular beam epitaxy (MBE) with a traditional Ga source. Increased Ga_2O desorption causes the growth rate of β-Ga_2O_3 to decrease as the Ga flux is increased beyond the stoichiometric point of the material and can impact the stoichiometry of the grown film. In this work, we explore the impact of O-rich and Ga-rich conditions on electronic properties in films of β-Ga_2O_3 grown via plasma-assisted MBE (PAMBE). Initial results comparing two samples under O-rich and Ga-rich conditions showed a large difference in peak low-temperature mobility. The O-rich sample showed a peak low temperature mobility of 793 cm2 /V·s while Ga-rich sample peaked at only 198 cm2 /V·s. The mobility and volume carrier density versus temperature data was fit using a model to extract out donor and compensating acceptor density. The Ga-rich sample showed an acceptor concentration of 2.0×10^{16} cm^{-3} compared to the O-rich sample that was measured to have an acceptor concentration of 3.0×10^{15}, and order of magnitude lower. This is possibly due to the formation of V_{Ga} during the Ga_2O desorption process during the growth of the films. Another series of films were grown across a wider range of O- to Ga-rich conditions to further establish a trend between growth conditions and compensating acceptor density. Only Ga flux varied between samples and substrate temperature, Si source temperature and RF oxygen plasma conditions were held constant. Si concentration in each film was anti-correlated with the growth rate which is expected. Conversely, compensating acceptor density increased with increasing Ga-rich conditions and does not follow the trend of the growth rate. The best peak low-temperature mobility occurred for the sample grown in the most O-rich conditions (789.6 cm^2/Vs) and mobility decreased with increasing compensating acceptor concentration. Overall, these results indicate the importance of Ga:O ratios in β-Ga_2O_3 films grown via MBE with conventional Ga sources. These results demonstrate how improved electronical performance can be achieved in β-Ga_2O_3 by growing under O-rich conditions and limiting the formation of V_{Ga} due to suboxide desorption.

9:15am EM+2D+AP+QS+TF-ThM-6 Advancing Single-Crystalline Oxide Membrane Growth via Molecular Beam Epitaxy, *Shivasheesh Varshney, Sooho Choo,* University of Minnesota*; Martí Ramis,* Institute of Materials Science of Barcelona (ICMAB-CSIC), Spain*; Liam Thompson, Jay Shah, Zhifei Yang, Jiaxuan Wen, Steven J. Koester, K. Andre Mkhoyan, Alexander S. McLeod,* University of Minnesota*; Mariona Coll,* Institute of Materials Science of Barcelona (ICMAB-CSIC), Spain*; Bharat Jalan,* University of Minnesota

A sacrificial layer method has proven to be an effective route for synthesizing free-standing membranes. In this approach, a crystalline sacrificial layer is selectively dissolved in water, allowing the target film to be transferred onto a host substrate. However, commonly used sacrificial layers (such as $SrCa_2Al_2O_6$) have complex stoichiometry, posing synthesis challenges in molecular beam epitaxy (MBE). In this presentation, we will discuss two distinct but MBE-friendly, fast and facile approaches to synthesize single-crystalline oxide nanomembranes using hybrid MBE [1,2]. In particular, we synthesize epitaxially, single-crystalline $SrTiO_3$ membranes, ranging from a few unit cells to several hundred nanometers in thickness, using an SrO sacrificial layer, and a solution-processed amorphous $SrCa_2Al_2O_6$sacrificial layer. Films grows in a layer-by-layer growth mode on a solution-processed amorphous $SrCa_2Al_2O_6$ whereas in a step-flow growth mode on SrO sacrificial layer. Films grown on SrO layer dissolve rapidly (< 5 minutes) in water, resulting in millimeter-sized membranes. Combining structural characterization using x-ray diffraction (XRD), atomic force microscopy (AFM), piezo force microscopy (PFM), and scanning transmission electron microscopy (STEM), we will present the structure-property relationships in these membranes with particular emphasis on investigating the role of non-stoichiometry on dielectric properties. Using PFM, we demonstrate that Sr-deficient films exhibit robust polarization at room temperature, while stoichiometric films remain consistent with the paraelectric phase. Finally, we will present the growth of single crystalline complex oxide films on a compliant substrate consisting of a few unit-cell $SrTiO_3$ seed layers onto an amorphous SiO_2 wafer.

1. S. Varshney, S. Choo, L. Thompson, Z. Yang, J. Shah, J. Wen, S. J. Koester, K. A. Mkhoyan, A. McLeod, and B. Jalan, **"Hybrid Molecular Beam Epitaxy for Single Crystalline Oxide Membranes with Binary Oxide Sacrificial Layers"** *ACS Nano* 8, *18,* 6348-6358 (2024).
2. S. Varshney, M. Ramis, S. Choo, M. Coll, and B. Jalan, **"Epitaxially Grown Single-Crystalline SrTiO₃ Membranes Using a Solution-Processed, Amorphous SrCa₂Al₂O₆ Sacrificial Layer"** under review (2024) http://arxiv.org/abs/2405.10464

Plasma Science and Technology
Room 124 - Session PS-ThM

Plasma Sources, Diagnostics and Control I

Moderators: John Arnold, IBM Research Division, Albany, NY, **Michael Gordon**, University of California at Santa Barbara

8:00am PS-ThM-1 Radio-frequency Hollow Cathode Discharge: Modeling and Experimental Diagnostics, *Kallol Bera,* Applied Materials, Inc.*; Han Luo,* Applied Materials, Inc., Canada*; Xingyi Shi,* Applied Materials, Inc.*; Ihor Korolov,* Ruhr Universität Bochum, Germany*;* **Abhishek Verma***, Shahid Rauf,* Applied Materials, Inc.*; Jan Guttmann, Julian Schulze,* Ruhr Universität Bochum, Germany

Low to intermediate pressure radio-frequency (RF) hollow cathode discharges (HCDs) have gained significance for advanced plasma processing in the semiconductor industry. HCDs form in the cavities in the cathode that is separated from the anode by a dielectric. In the HCD, RF sheath heating as well as secondary electron acceleration can lead to plasma production. Complementary modeling and experimental studies are performed for slotted hollow cathode discharge to validate plasma model as well as to elucidate discharge physics behavior at various operating conditions in several designs. The design parameters include the slot width (10 - 20 mm), angle (0 - 10º) and shape (linear and curvilinear), while the process parameters are pressure (2.5 – 100 Pa), RF voltage (200 – 500 V) and gas mixture. Electropositive Ar, electronegative O_2, and their mixtures are considered. For the experiments, slot structures are constructed in the cathode, and Phase Resolved Optical Emission Spectroscopy (PROES) is performed for Ar I emission. From the emission spectrum, spatio-temporal distribution of excitation rate is obtained. A hairpin probe is utilized to diagnose plasma density in the transverse direction. For plasma modeling, a 2-dimensional planar computational domain in transverse plane to the slot is considered. At low-pressure (tens of mTorr), where kinetic effects are important, particle-in-cell Monte Carlo collision (PIC-MCC) modeling scheme is used.The PIC-MCC model includes evolution of charge densities from charged particles and electrostatic field and charged particle collisions with each other and with neutral fluid using a Monte Carlo model. At intermediate pressure (several hundreds of mTorr), due to high collisionality, the PIC-MCC modeling becomes computationally prohibitive. Therefore, hybrid-fluid plasma model is used that includes fluid plasma equations for charged and neutral species, and a Monte Carlo model for secondary electrons, coupled with Poisson's equation for self-consistent electrostatic plasma simulation. At low pressure the behavior of excitation rate using PIC-MCC simulation matches reasonably well with experimental data. However, excitation rate distribution at moderate pressure using the hybrid-fluid model has some discrepancies. The plasma density profiles from PIC-MCC and fluid simulations are consistent with the experiments. Based on our analysis, the hybrid-fluid plasma model is being improved to better describe RF hollow cathode characteristics.

8:15am PS-ThM-2 Advancing In situ Transmission Electron Microscopy to Study Plasma-Nanomaterials Interactions, *Jae Hyun Nam,* University of Minnesota, USA*; Daan Hein Alsem,* Hummingbird Scientific*; Peter Bruggeman,* University of Minnesota, USA

Non-thermal plasma (NTP) has been increasingly recognized as a promising alternative to conventional technologies in diverse fields due to its high reactivity and non-equilibrium characteristics. These properties make NTP particularly effective for material interactions, such as materials synthesis, etching, deposition, and chemical redox processes. Although NTP is extensively employed for the synthesis and functionalization of nanomaterials, the direct observation and mechanistic understanding of these interactions have been limited due to the significant technical challenges associated with the development of *in situ* diagnostic capabilities.

Significant advances have been made in *operando* environmental Transmission Electron Microscopy (TEM) enabling the monitoring of nanoparticle growth in solutions in an environmental TEM configuration. Despite these advancements, applications of *in situ* TEM in the NTP field have been sparse, primarily due to the challenges of integrating the necessary vacuum conditions and microscale requirements of TEM with the gaseous environment and high-voltage requirements of NTP. A decade ago, an integration of microplasma within a TEM was performed by demonstrating gold sputtering by argon plasma, albeit with a spatial resolution restricted to approximately 100 nm. Our recent new developments have successfully overcome these limitations, establishing an *in-situ* plasma TEM capability with a spatial resolution of less than 1 nm.

This was achieved through the introduction of micron-sized electrodes in a gas environmental TEM cell enabling atmospheric micro-plasmas directly inside an electron microscope. The new device allows us to sustain atmospheric plasma steadily for several hours.

We demonstrate our *in situ* TEM capability through the real-time observation of morphological changes in iron oxide nanoparticles (magnetite, Fe_3O_4), likely induced by reduction processes, under DC hydrogen microplasma (He/H_2, 0.5 %) exposure with a temporal resolution of 1 s. This novel technique not only deepens our understanding of plasma and material interactions on a small scale, but also significantly expands the potential for *in situ* TEM studies in the NTP field.

Acknowledgement: This material was also based upon work supported by the Army Research Office accomplished under Grants No. W911NF-20-1-0322 and W911NF-20-1-0105.

8:30am PS-ThM-3 Sensing and Control of Radio-Frequency Driven Plasmas, *Timo Gans,* Dublin City University, Ireland **INVITED**

Sensing and control of radio-frequency driven plasmas is crucial for next-generation plasma manufacturing. Surface interactions and negative ions play key roles in the properties of reactive molecular processing plasmas. Radio-frequency driven oxygen and hydrogen plasmas are ideal test-beds for investigations into the role of surface interactions for the chemical kinetics of the plasma and associated negative ion formation. Oxygen containing plasmas can exhibit either mostly electro-negative or mostly electro-positive characters [1, 2]. Oxygen negative ions can be efficiently destroyed by singlet oxygen which in turn is itself strongly influenced by surface reactions and surface properties [3]. Atomic oxygen, as a key reactive species, can also be dependent on surface properties [4]. In hydrogen plasmas, negative ions can be produced through surface processes as well as volume processes [5]. Nitrogen doped diamond surfaces are promising candidates for enhanced surface production of negative hydrogen ions [6,7,8]. Volume processes are determined by dissociative attachment involving vibrationally exited hydrogen molecules. These in turn are also dependent on surface properties [5]. This interplay between surface properties and the plasma chemical kinetics as well as plasma dynamics will be discussed for the examples of single [1, 3, 4, 5, 6, 7, 11] and multi-frequency [2, 9, 10] driven oxygen and hydrogen plasmas.

REFERENCES:

[1] A Greb et al., APL 103 (24), 244101 (2013)

[2] AR Gibson et al., APL 106 (5), 054102 (2015)

[3] A Greb et al., PSST 24 (4), 044003 (2015)

[4] T Tsutsumi et al. JApplPhys 121 (14), 143301 (2017)

[5] J Ellis et al., JPhysD 53 (48), 485202 (2020)

[6] GJ Smith et al., JPhysD 53 (46), 465204 (2020)

[7] GJ Smith et al., JPhysD 54 (43), 435201 (2021)

[8] R Magee et al., PSST 32 (2), 075021 (2023)

[9] A Derzsi et al., PSST 26 (3), 034002 (2017)

[10] B Bruneau et al., PSST 25 (1), 01LT02 (2015)

[11] GJ Smith et al., PSST 33 (2), 025002 (2024)

9:00am PS-ThM-5 Dorothy M. and Earl S. Hoffman Scholarship Awardee Talk: Time Resolved Diagnostics of HiPIMS Discharges With Positive Cathode Reversal, *Zachary Jeckell[1],* University of Illinois at Urbana Champaign*; Tag Choi, Nicholas Connolly,* University of Illinois at Urbana-Champaign*; Satadal Das,* University of Illinois at Urbana Champaign, India*; Md. Amzad Hossain,* University of Illinois Urbana-Champaign, Bangladesh*; David Kapelyan, Nikhil Vishnoi, Ricky Pickering,* University of Illinois at Urbana Champaign*; Dren Qerimi,* University of Illinois Urbana-Champaign*; David Ruzic,* University of Illinois at Urbana-Champaign

This work investigates the temporal evolution of a high-power impulse magnetron sputtering (HiPIMS), with a positive cathode reversal, discharge by using a number of different diagnostics such as gated fast cameras, time resolved Langmuir probes, and time and energy resolved mass spectrums acquired using the plasma sampling mass spectrometer (PSM). Using time resolved Langmuir probes we have studied that the rise time of the plasma potential is 1-2 μs which correlates to the time scale over which the ion energy distribution function (IEDF) is seen to increase. This, paired with PSM data collected where the magnetron and PSM are 90 degrees off axis from each other still showing an increase in the Ag^+ energy suggests that

---

[1] **AVS National Student Awardee**

the plasma potential commuting throughout the volume is one of the primary causes of increased ion energy after the positive cathode reversal. The Langmuir probe setup also allows for the creation of time resolved electron energy distribution functions (EEDF) both near the substrate and near the target which offers valuable insight into the discharge physics. Using the PSM we have shown that at early stages of the positive cathode reversal there is an elevated population of metal ions and that the overall fraction of metal to working gas fraction is at its highest. Time and energy resolved mass spec data was collected on this system for a variety of conditions such as pulse lengths, pressures, and target material with the objective of developing a better understanding for the energetics at play. Additionally, it was discovered that for the reactive sputtering of TiN that the IEDF of the N^+ species has a high energy tail of 40 eV at a pressure of 4 mTorr. This distribution mirrors that of Ti^+ which indicates that the target poisoning is responsible for an increase in the energy of the nitrogen species and that target poisoning could be the source of nitrogen in the film. Gated fast camera measurements taken with the PI-MAX 4 camera have been performed to investigate the formation of hot spots and observed that the formation of hot spots occurs above the critical current density for silver. Fast camera measurements are also taken on and off axis to visualize the 3-D structure of spokes, and to visualize how the discharge changes when the positive cathode reversal occurs. Additionally, it was found that for cases with current four times higher than the critical current threshold that the hot spots seem to disappear, however, coupling PSM measurements with the fast camera we can see linear correlation between discharge current and counts of Ag^{+2} which suggests that the hot spots have disappeared due to rarefaction of the working gas.

9:15am **PS-ThM-6 Understanding Plasma Surface Dynamics Through Time Resolved Ion Energy Analysis for Deposition/Etch Processes**, *Angus McCarter,* Impedans Ltd., Ireland*; Anshu Verma,* Impedans Ltd., India

As semiconductor critical dimensions are decreasing rapidly, reproducible control of etching and deposition processes has become crucial. These processes are heavily dependent on the chemical/physical processes occurring on the wafer surface. Like any other surface in contact with plasma, a sheath usually develops on the wafer which pulls down the ions out of bulk plasma necessary to complete the process on the wafer. Furthermore, external RF/DC/tailored waveform biases are applied to the wafer to modify the ion behaviors as it can affect the chemical composition, microstructure and the associated electrical properties of the thin films during plasma assisted deposition processes as well as the selectivity and anisotropy of high aspect ratio trenches in etching processes. Therefore, the characterization of only bulk plasma is not sufficient in providing insights necessary to understand the plasma surface interactions. A high-speed monitoring of the ion energy distribution function and ion flux can lead to enhanced understanding of the plasma surface interactions and improved process performance.

We will highlight the successful measurements done by the *Semion* RFEA diagnostic under different chamber and bias conditions. Such applications enabling accurate and precise control of etching profiles on different materials and various plasma chemistries. The *Semion* measures the ion energies hitting a surface, the ion flux, negative ions and bias voltage at any position inside a plasma chamber using an array of integrated sensors. On the other hand, the *Semion pDC system* measures these parameters in real time over an energy range up to 2000 eV (process dependent). It can do sub-microsecond time resolved measurements, for studying pulsed ICPs, or pulsed DC biases, as well as floating and grounded substrate conditions. The Semion Pulsed DC system is the key instrument used to measure the temporal evolution of the ion energy and flux at different times through the pulse period of a pulsed DC plasma process.These measurements are essential for establishing the correlation between the plasma inputs and the ion energy/flux which, in-turn, determines the effectiveness of the surface treatment.

References

[1] Impedans Ltd, Dublin, Ireland [www.impedans.com]

[2] S. Sharma et al., Ph.D. Thesis, Dublin City University (2016)

[3] H. B. Profijt et al., J. Vac. Sci. Technol. A 31, 1 (2013)

[4] M. H Heyne et al., 2D Mater. 6, 035030 (2019)

[5] S. Karwal et al., Plasma Chemistry and Plasma Processing 40, 697–712 (2020)

9:30am **PS-ThM-7 The Plasma Dynamics of Dual Frequency Capacitively Coupled Argon Discharge using Tailored Voltage Waveforms**, *Syed M Zulqarnain, Amanda M. Lietz,* North Carolina State University*; James Prager, Timothy Ziemba, Joshua Perry, Paul Melnik,* EHT Semi

Ion energy and flux represent the primary factors of significance for etching and deposition plasmas in the semiconductor industry. The independent control over ion energy and flux to some degree can be achieved by harnessing the dual-frequency capacitively coupled plasmas. Tailoring the voltage waveform shape beyond simple sinusoids has unlocked a regime where ion energy distributions can be controlled. In this work, we simulate a dual-frequency capacitively coupled argon discharge employing a high-frequency (60 MHz) sinusoidal voltage waveform at the upper electrode and low-frequency (400 kHz) tailored triangular-shaped waveform at the lower electrode using a Monte-Carlo collision-based, particle-in-cell simulation (EDIPIC[1]). This exploration entailed a comprehensive assessment of plasma dynamics in response to alterations in the shape (including peak width and slope of the negative and positive regions) of the tailored voltage waveform. The temporal control of ion energies, synchronized with the shape of the tailored voltage waveform, was observed, offering potential benefits for regulating the chemistry during processing. The ion energies exhibited a correlation with the cumulative effects of the two applied waveforms. The low-frequency waveform dominated ion acceleration and temporal variations of ion energies. However, the energetic ions were slightly influenced by the high-frequency component leading to the emergence of two energetic peaks. The most power was delivered to the ions primarily during the negative cycle, especially after the positive pulse ended, while the electrons gained power mostly in the sheath edge with most power delivered during the positive pulse. The rate of rise of the positive portion of the waveform had minimal impact on ion distribution, but it did result in an increase in the number of electrons (of energies between 20-40 eV) reaching the lower electrode. This outcome could potentially aid in addressing charging concerns in the process of semiconductor etching of high aspect ratio features.

Reference:

1.https://pcrf.princeton.edu/capabilities/modeling-tools-and-computer-codes/edipic-code/

9:45am **PS-ThM-8 A Real-Time 2-D Gas Temperature Monitoring Sensor Based on Molecular Emission Spectroscopy**, *Dhruval Patel,* University of Illinois at Urbana-Champaign*; Daniel Jacobson,* Lyten*; Dren Qerimi,* University of Illinois at Urbana-Champaign*; Michael Stowell,* Lyten*; David Ruzic,* University of Illinois at Urbana-Champaign

Recent trends have indicated a growth in the usage of thermal and non-thermal plasmas for material processing applications. In these processes, gas temperature is a critical thermodynamic state variable, but sensors suitable for monitoring its fluctuations in plasmas are few and often not applicable. The most straightforward method is to estimate the gas temperature based on the rotational temperatures obtained from molecular transitions in plasma. Not only does this require access to a spectrometer, but analysis can often be time-consuming. This study aims to address this by designing and testing a stand-alone 2-D optical sensor capable of simultaneous *in-operando* measurements of rotational and vibrational temperatures.

The proposed optical sensor monitors the emission intensity of specific rovibronic transitions of the $\Delta v = 0$ and +1 sequences of C_2 swan system. The light collected from a point source is split into three different color channels using beam-splitters and carefully selected bandpass filters. The net intensity of light from each channel is monitored with photodiodes/CCD sensors. The rotational and vibrational temperatures are inferred by comparing relative intensity of light collected from each channel to those predicted by simulations. The simulations used in this work assume that the rotational and vibrational states follow Boltzmann statistics to minimize the number of channels required in this device. The applicability of this sensor is limited to cases which satisfy this assumption. As a result, it is necessary to test the feasibility of this sensor in various discharge conditions on a case-by-case basis. For the scope of this work, we limit ourselves surface wave microwave discharges, operated at low and high pressures.

The accuracy in temperature measurements is evaluated by comparing them to those obtained using the well-known Boltzmann analysis technique. A high-resolution Czerny-Turner spectrometer is employed to obtain well-resolved ro-vibronic transitions of the Δv= +1 sequence. Boltzmann analysis of these transitions is not only used to estimate the rotational and vibrational temperatures, but also monitor any departure from expected density distributions. In addition, rotational temperatures

are also compared to gas temperature measurements obtained from the doppler broadening of the H_β line. Combined these results will demonstrate the viability of this sensor for its usage as a gas temperature monitoring device.

11:00am PS-ThM-13 Fiber PROES: Phase-Resolved Optical Emission Spectroscopy by Time-Correlated Photon Counting Through Optical Fibers, *Florian Beckfeld, Ihor Korolov,* Ruhr University Bochum, Germany; *Michael Höfner,* SENTECH Instruments GmbH, Germany; *Julian Schulze,* Ruhr University Bochum, Germany

Phase-resolved optical emission spectroscopy (PROES) is a powerful, non-intrusive plasma diagnostic tool that can give useful insight into plasma parameters like the electron density or surface coefficients by visualizing the dynamic of the highly energetic electrons in the plasma. Furthermore, PROES may also be used to calculate the energy distribution function of these highly energetic electrons by applying a rate equation model. Despite these benefits, PROES has not been able to make a transition into the industry, as it requires optical access to wide regions of the discharge, which is not given in industrial plasma chambers. Additionally, the intensified charged-coupled device (ICCD) cameras commonly used for the diagnostic require expensive investments. To address these issues, we propose a technique for PROES based on photon counting. This brings several benefits: photon counting can be realized with a photomultiplier tube (PMT), which has fractions of the cost of an ICCD camera. This PMT can then be connected to the plasma chamber with an optical fiber, making the diagnostic easy to integrate into existing structures. In this work, measurements of the heating mode in a geometrically symmetric capacitively coupled plasma will be shown to demonstrate the capability of the approach to PROES with a PMT compared to measurements with an ICCD camera.

11:15am PS-ThM-14 Atomic Hydrogen Density, Electron Density and Ion Flux Energy Distribution of an Ar/H2 Remote CCP Plasma Source for Atomic Scale Processing, *Marnix van Gurp,* **Thomas van den Biggelaar**, *Jente Wubs, Antoine Salden, Harm Knoops, Erwin Kessels,* Eindhoven University of Technology, Netherlands

A remote CCP source (Oxford Instruments PlasmaPro ASP) has been developed for higher throughputs for atomic layer deposition (ALD) processes, by generating high radical fluxes combined with controlled ion bombardment. In a previous study [1], it has been shown that this plasma source is well suited for Al_2O_3 deposition on GaN when operated with Ar/O_2 plasmas. This work uses a testbed setup containing the remote CCP source. The setup has optical access that allows extensive studies on plasma-surface interaction (PSI), relevant for ALD, atomic layer etching (ALE) and 2D material modification. Ar/H_2 plasmas can generate hydrogen atoms that, combined with ions, could modify materials synergistically. In this study, an Ar/H_2 (95%/5%) plasma is characterized by three diagnostics as a starting point for PSI studies. First, two-photon absorption laser induced fluorescence (TALIF) has been employed to measure the absolute atomic hydrogen density as a function of distance to the substrate surface for different pressures (38-375 mTorr). In this pressure range, a constant dissociation degree of 10% has been found, with $n_H = 10^{12} - 10^{13}$ cm^{-3}. Second, a Langmuir probe has been used to spatially measure the electron density, which is in the order of 10^{10} cm^{-3}. Third, a retarding field energy analyzer (RFEA) probe has been employed to determine the ion flux energy distribution, ion energies and ion fluxes at the substrate table. The measured ion flux energy distribution has been found to be bimodal, with ion energies and fluxes that are dependent on pressure and power. Both the Langmuir probe and the RFEA probe show that the electron density at the substrate table rapidly drops at pressures greater than 263 mTorr. Since the hydrogen dissociation degree remains constant in this region, it is hypothesized that the plasma source becomes remote at pressures above 263 mTorr, i.e. the plasma becomes confined near the electrodes instead of filling the whole reactor. Given the outcomes, PSI for atomic scale processing will be further investigated specifically for hydrogen atoms and ions.

[1] Knoops, H *et al*. (2021). Innovative remote plasma source for atomic layer deposition for GaN devices. *Journal of Vacuum Science & Technology A, 39*(6).

11:30am PS-ThM-15 Spatially Resolved Measurement of Fluorine Radical Density Using Reactive Radical Probes, *Jeremy Mettler,* University of Illinois at Urbana-Champaign; *Takashi Tohara,* Tokyo Electron; *Dren Qerimi, David Ruzic,* University of Illinois at Urbana-Champaign

Plasma etching kinetics and reaction mechanisms often involve complex interactions between radical and charged species. Characterization of these mechanisms requires accurate measurement of reactant concentrations, which is often achieved using spectroscopic techniques. While nonintrusive, these techniques have significant limitations in their spatial resolution and ability to produce absolute measurements. For complex plasma and reactor geometries, spatial distribution of radical species can play a key role in the observed etching characteristics.

In this work we discuss the development of etching based, nonequilibrium radical probes for measuring fluorine radical densities across industry relevant pressures, powers, and radical densities. Tungsten pellets are used as the active probe surface and to preserve probe lifetime a nonequilibrium analysis method was developed. The tungsten etching rate is determined in-situ by measuring the rate of energy deposition to the probe via temperature response. Fluorine radical density is determined from the etching rate, independently of ion exposure, due to the purely chemical nature of tungsten etching at high temperatures. Results from the radical probe are compared against actinometry in spatially uniform and nonuniform plasmas to validate the probe technique and highlight its spatial resolution. Fluorine density profiles are then characterized for SF_6, NF_3, and CF_4 plasmas to demonstrate the generality of the technique to multiple fluorine process gases. Measured fluorine densities ranged from $1.4\times10^{20} \pm .2\times10^{20}$ (#/m^3) to $3.9\times10^{21} \pm .6\times10^{21}$ (#/m^3).

11:45am PS-ThM-16 The Applicability of a Microwave Resonant Probe to the Plasma Processing of Silicon Oxide, *Daryl White, Geoff Hassall,* **James Ellis**, Oxford Instruments Plasma Technology, UK

In-situ diagnostics for industrial scale plasma processing represents a sizeable challenge for multiple semiconductor hardware companies. Simple, robust, and inexpensive sensors are required both to understand process development challenges and for real-time monitoring of the plasma process; the advent of machine learning only enhances the importance of such sensor development. A microwave enhanced resonance probe with a spiral-shaped slot design, also known as a curling probe[1-3], has been used to measure relative electron densities in the edge region of a Plasma Pro 100 Oxford Instruments Plasma Technology reactor. Etch tests were run across a broad range of plasmas processing parameters centred around a CF_4/O_2 plasma chemistry to ascertain the potential impact of the curling probe on the process. It was confirmed through both global and localised etch rate measurements that the curling probe was not observed to have any impact on the wafer outcomes. The sensitivity of the curling probe enabled changes in the plasma conditions to be tracked in real time with failure modes clearly visible from the measured shift in the resonant frequency.

[1] R. L. Stenzel; *Rev. Sci. Instrum., 47,* 603 (1976).

[2] I. Liang, K. Nakamura, and H. Sugai, *Appl. Phys. Express*, **4**, 066101 (2011)

[3] F. Boni *et al., Rev. Sci. Instrum.*, **92**, 033507 (2021)

12:00pm PS-ThM-17 Terahertz Absorption Spectroscopy for Measuring Atomic Oxygen Densities: A Comparison with ps-TALIF and CRDS, *Jente Wubs, Uwe Macherius, Andy Nave,* Leibniz Institute for Plasma Science and Technology (INP), Germany; *Laurent Invernizzi, Kristaq Gazeli, Guillaume Lombardi,* Laboratoire des Sciences des Procédés et des Matériaux (LSPM), CNRS, France; *Xiang Lü, Lutz Schrottke,* Paul-Drude-Institut für Festkörperelektronik Leibniz-Institut im Forschungsverbund Berlin, Germany; *Klaus-Dieter Weltmann, Jean-Pierre van Helden,* Leibniz Institute for Plasma Science and Technology (INP), Germany

Oxygen-containing plasmas are widely used in industry for a variety of applications, including etching, thin-film deposition, and other surface modification processes. Atomic oxygen is a key species in most of these applications. An accurate method for determining atomic oxygen densities is therefore of great importance, not only to gain a fundamental understanding of the plasma chemistry, but also to improve industrial processes. However, existing techniques, such as two-photon laser induced fluorescence (TALIF), vacuum ultraviolet (VUV) absorption spectroscopy, cavity ring-down spectroscopy (CRDS), and optical emission spectroscopy (OES), are all either bulky and expensive, experimentally challenging, or indirect and relying on a multitude of assumptions.

Terahertz (THz) absorption spectroscopy with quantum cascade lasers (QCLs) has recently been developed and implemented as a novel diagnostic technique for determining atomic oxygen densities. It is based on detecting the $^3P_1 \leftarrow {}^3P_2$ fine structure transition of ground-state atomic oxygen at approximately 4.75 THz (i.e. approximately 63 µm). THz absorption spectroscopy allows for direct measurements (i.e. no calibration is required) of absolute ground-state atomic oxygen densities, and its

accuracy depends almost exclusively on the accuracy to which the line strength of the transition is known. Furthermore, the narrow laser linewidth of QCLs makes it possible to determine the temperature from the detected absorption profiles as well. In addition, the experimental setup for THz absorption spectroscopy is relatively compact (especially compared to TALIF setups that typically involve bulky laser systems), vacuum conditions are not essential (as opposed to when working in the VUV), and the requirements for the optical alignment are not as strict as for CRDS. These features make THz absorption spectroscopy an attractive alternative to existing diagnostic techniques.

To confirm the accuracy of THz absorption spectroscopy, we performed picosecond TALIF (ps-TALIF) and CRDS measurements of atomic oxygen densities on the same capacitively coupled radio frequency (CCRF) oxygen discharge, for a variation of the applied power (20 to 100 W) and the gas pressure (0.7 and 1.3 mbar). The obtained atomic oxygen densities (all of the order of 10^{14} cm^{-3}) were found to be in excellent agreement, both qualitatively and quantitatively. This demonstrates that the three different diagnostic techniques all allow for accurate measurements and can be used interchangeably, provided that no spatial resolution is required.

Surface Science
Room 120 - Session SS-ThM

Celebration of Robert J. Madix and his Contributions to Surface Science (INVITED SESSION)

Moderators: Dan Killelea, Loyola University Chicago, **Jason Weaver**, University of Florida, **Liney Árnadóttir**, Oregon State University

8:30am SS-ThM-3 Infrared Spectroscopy Studies of Surface Chemical Reactions on Single Atom Alloys, *Michael Trenary*, University of Illinois - Chicago **INVITED**
Low coverages of catalytically active metals deposited onto the surfaces of less active host metals can form single atom alloys (SAAs), which often display unique catalytic properties. The catalytic properties of SAAs are ultimately determined by their surface structure. We have used reflection absorption infrared spectroscopy (RAIRS) and temperature programmed desorption (TPD) of adsorbed CO to probe the structure of Pd/Cu(111), Pt/Cu(111) and Pd/Ag(111) SAA surfaces. At certain values of the surface temperature and/or CO coverage, CO adsorbs only on Pd or Pt atoms and not on Cu or Ag sites. For low Pd and Pt coverages, only CO adsorbed at atop Pd or Pt sites is detected. At higher Pd or Pt coverages, CO adsorption at bridge sites is observed indicating that metal dimers or other aggregates have formed. Polarization dependent RAIRS was used to study selective hydrogenation reactions of acetylene, propyne, and 1,3-butadiene over a Pd/Cu(111) SAA surface. Reactants and products were monitored in the gas phase with s-polarized spectra, while p-polarized spectra were obtained to identify surface species present during the reaction. In each case, no hydrogenation occurred over the Cu(111) surface, but selective hydrogenation occurred over the Pd/Cu(111) SAA. Full hydrogenation to the saturated alkane did not occur. It is also found that coupling reactions occur to produce a carbonaceous layer on the surface, but that hydrogenation proceeds even in the presence of this layer.

9:00am SS-ThM-5 Vibrationally Hot Precursors as Reactants in the Dissociative Chemisorption of Methane on Ir(111) and Ir(110), *Arthur Utz*, Tufts University **INVITED**
Precursor-mediated reactions can potentially play a key role in the dissociative chemisorption of methane at the high temperatures (> 1000K) typical of steam-reforming reactors. At the average kinetic energies present, reactants can first physically adsorb to the surface as a precursor prior to undergoing subsequent diffusion and reaction (or desorption)[1,2]. High process temperatures also lead to significant populations of vibrationally excited gas-phase reagents and thermally excited lattice motion. This presentation will focus on the unique role that vibrational energy in the incident reactant and surface can play in activating these reactions.[3]

We use beam-surface scattering measurements coupled with infrared laser vibrational-state-selective excitation to prepare methane reactants with well-defined kinetic and vibrational energies. In this work, we study the role of methane's v_3 antisymmetric C-H stretching vibration (E_{vib} = 36 kJ/mol). The prepared molecules impinge on the surface held at a fixed temperature (which dictates the extent of thermal lattice vibration), and we quantify reaction probability as a function of incident kinetic energy, vibrational state, and surface temperature.[2,3] Independent control over these energetic

coordinates allows us to unravel their contribution to reactivity. We chose to study the low-index Ir(111) and Ir(110)(1x2) surfaces because their minimum barrier height for dissociation is similar to, or slightly higher than the vibrational energy content of the laser-prepared molecules.

The experiments, when coupled with quasiclassical trajectory calculations, show that vibrational energy in a physisorbed precursor molecule survives long enough to promote reactivity with the same efficacy as reactivity occurring via a direct reaction mechanism. The calculations also point to the pivotal role of surface excitation in providing energetically accessible reaction paths for the physisorbed molecules.

1. J. F. Weaver, A. F. Carlsson, R. J. Madix, The adsorption and reaction of low molecular weight alkanes on metallic single crystal surfaces. *Surf. Sci. Rep.* **50**, 107-199 (2003).

2. E. Dombrowski, E. Peterson, D. DelSesto, A. Utz, Precursor-Mediated Reactivity of Vibrationally Hot Molecules: Methane Activation on Ir(111). *Catalysis Today* **244**, 10-18 (2015).

3. R. Moiraghi *et al.*, Nonthermalized Precursor-Mediated Dissociative Chemisorption at High Catalysis Temperatures. *J. Phys. Chem. Lett.* **11**, 2211-2218 (2020).

4. P. R. Shirhatti *et al.*, Observation of the adsorption and desorption of vibrationally excited molecules on a metal surface. *Nature Chemistry* **10**, 592-598 (2018).

9:30am SS-ThM-7 Modeling of Reaction Mechanisms and Kinetics on Metal Surfaces and the Connection to Experimental Catalysis, *Líney Árnadóttir*, Oregon State University/PNNL **INVITED**
Chemical reactions on surfaces are of central importance for our understanding of catalytic activity in heterogeneous catalysis. Density functional theory calculations and microkinetic modeling are often used to determine reaction mechanisms and kinetics and to model changes in surface coverage and product distribution and for comparison with experiments. With fast-growing computational resources, theoretical studies for reaction mechanisms and microkinetic models have become more commonplace. Traditionally researchers approximate the vibrational frequencies of an adsorbate from an Hessian matrix calculated using a finite difference approach and then use the harmonic oscillator approximation to calculate all modes of motion in the partition function but some of Bob Madix's early work on preexponential factors[1] motivated me and C.T. Campbell to propose the hindered translator/rotor model for the three modes of motion parallel to the surface, one for each of the two translations in the directions parallel to the surface and one for rotation about the axis perpendicular to the surface. These methods have since been modified and improved by other scientists and applied to microkinetic modeling by myself and others, inspired by Bob Madix work. Here we will discuss the implementation of these methods and recent DFT and microkinetic models for propane hydrogenation on Pt and Al_2O_3-decorated Pt surfaces and as well as complimentary temporal analysis of products (TAP) experiments by our collaborators at INL and ForgeNano, and the many ways Madix influenced our work and effort to bridge the gap between surface science and catalysis.

[1] R.J. Madix, G. Ertl and K. Christmann, Preexponential factors for hydrogen desorption from single crystal metal surfaces, *Chemical Physics Letters*, 62, 1, 1979

11:00am SS-ThM-13 Crossing the Great Divide Again: Bridging Atomic-Scale Mechanistic Insight from Single-Crystals to Functional Catalysts Using Transient Flow and Spectroscopy., *Christopher O'Connor*, Harvard University*; Eric High*, Tufts University*; Taek-Seung Kim*, Korea Institute of Energy Research, Republic of Korea*; **Christian Reece**, Harvard University **INVITED**
A key aspiration in the rationale design of catalysts is predictive performance (activity, selectivity, and stability) and surface properties (composition and structure) under realistic reaction conditions. This requires an atomic-scale understanding of catalyst reaction systems. Surface science studies on model catalytic systems are the "gold standard" for providing kinetic and mechanistic insight into heterogeneous catalysis. However, transferring this fundamental insight often measured on planar single crystals under ultra-high vacuum (UHV) conditions to applied catalytic reactors using technical catalytic materials at elevated temperatures and pressure can be challenging. Herein, we demonstrate our newly developed transient flow reactor to perform step transient experiments in a packed bed reactor at atmospheric pressure. We examine CO oxidation over palladium-based catalysts as a probe catalytic system to recreate the catalytic performance of planar Pd/Al2O3 in coincident

molecular beams experiments under vacuum. We demonstrate that surface science derived kinetics can quantitatively model CO_2 production in our step transient experiments in an atmospheric pressure flow reactor. We establish a continuity of surface species under steady-state reaction conditions and sub-second evolution of surface species for step transient experiments using a custom low-volume Diffuse reflectance infrared Fourier transform spectroscopy (DRIFTS) reactor. This work demonstrates a unique ability to bridge the understanding of the state of the catalyst surface and reaction kinetics from vacuum conditions established using molecular beam experiments to ambient pressure conditions using a transient flow reactor and numerical simulations. Our technique provides a new regime for studying technical catalysts under applied reaction conditions.

11:30am SS-ThM-15 Recent Games in the Surface Chemistry Stadium; Bob helped Build It, and They Came, *Charles Sykes,* Tufts University   **INVITED**
One cannot overstate Robert Madix's influence on the modern field of well-defined surface chemistry. His numerous contributions have brought a deep understanding of important chemical processes at surfaces. Inspired by Bob's works linking molecular scale processes and well-defined active sites with the rates and selectivity of real catalysts I have strived to collaborate broadly in order to achieve this level of understanding and control. Bob performed fundamental studies with the belief that one day they will inform the design of catalysts. In this talk I will argue we have reached that point and I will discuss a new class of heterogeneous catalysts called *Single-Atom Alloys* in which precious, reactive metals are utilized at the ultimate limit of efficiency.[1-6] These catalysts were discovered by combining atomic-scale scanning probes with more traditional approaches to study surface-catalyzed chemical reactions. This research provided links between atomic-scale surface structure and reactivity which are key to understanding and ultimately controlling important catalytic processes. In collaboration with Maria Flytzani-Stephanopoulos these concepts derived from our surface science and theoretical calculations have been used to design *Single-Atom Alloy* nanoparticle catalysts that are shown to perform industrially relevant reactions at realistic reaction conditions. For example, alloying elements like platinum and palladium with cheaper, less reactive host metals like copper enables 1) dramatic cost savings in catalyst manufacture, 2) more selective hydrogenation and dehydrogenation reactions, 3) reduced susceptibility to CO poisoning, and 4) higher resistance to deactivation by coking. I go on to describe very recent theory work by collaborators Stamatakis (Oxford University) and Michaelides (Cambridge University) that predicts reactivity trends for a wide range of *Single-Atom Alloy* combinations for important reaction steps like H-H, C-H, N-H, O-H, and CO_2 activation. Overall, I hope to highlight that this combined surface science, theoretical, and catalyst synthesis and testing approach (that Bob contributed so much to) provides a new and somewhat general method for the a priori design of new heterogeneous catalysts.

References:

[1] Kyriakou et al. Science **335**, 1209 (2012).

[2] Marcinkowski et al. Nature Materials **12**, 523 (2013).

[3] Lucci et al. Nature Communications **6**, 8550 (2015).

[4] Liu et al.JACS **138**, 6396 (2016).

[5] Marcinkowski et al. Nature Chemistry **10**, 325 (2018).

[6] Hannagan et al. Science **372**, 1444 (2021).

Thin Films
Room 115 - Session TF1+AP-ThM

Thin Films: Fundamentals of ALD

Moderators: Matthias Young, University of Missouri, **Sarah Atanasov**, Intel

8:00am TF1+AP-ThM-1 AVS Medard W. Welch Award Talk: The Surface Chemistry of the Atomic Layer Deposition of Metal Thin Films, *Francisco Zaera*[1], University of California - Riverside   **INVITED**
The deposition of thin solid films is central to many industrial applications, and, thanks to the isotropic nature of the adsorption of chemical species (which affords even coverages on surfaces with rough topographies), chemical vapor deposition (CVD) methods are particularly useful for this task.Moreover, by splitting the overall film-depositing reactions into two or more complementary and self-limiting steps, as it is done in atomic layer depositions (ALD), film thicknesses can be controlled down to the sub-

monolayer level.Thanks to the availability of a vast array of inorganic and metalorganic precursors, CVD and ALD are quite versatile and can be engineered to deposit virtually any type of solid material.However, the surface chemistry that takes place in these processes is often complex and can follow undesirable side reactions leading to the incorporation of impurities in the growing films.Appropriate precursors and deposition conditions need to be chosen to minimize these problems, and that requires a proper understanding of the underlying surface chemistry.

In this presentation we discuss the progress made in our laboratory toward that goal.Our focus has been on the deposition of late transition metals.We will comment on the general nature of the metallorganic complexes used as precursors for these depositions, and the uniqueness that solid surfaces and the absence of liquid solvents bring to the ALD chemistry and differentiate it from what is known from metalorganic chemistry in solution.We then delve into the adsorption and thermal chemistry of those precursors, highlighting the complex and stepwise nature of the decomposition of the organic ligands that usually ensued upon their thermal activation.We discuss the criteria relevant for the selection of co-reactants to be used on the second half of the ALD cycle, with emphasis on the redox chemistry often associated with the growth of metallic films starting from complexes with metal cations.Another consideration is the nature of the growing films, which rarely retain the homogeneous 2D structure often aimed for.We end with some general conclusion and with a personal outlook of this field.

8:30am TF1+AP-ThM-3 Effects of ALD Chemistry on Process Windows, Thin Film Composition and Modification of the Underlying Substrate Surface, *Jay Swarup, James Engstrom,* Cornell University
In this work we have examined explicitly how the choice of ALD chemistry (precursor and co-reactant) can affect the process temperature window, composition of the deposited thin film, and possible modification of the underlying substrate.Growth of Al_2O_3 from $Al(CH_3)_3$ (TMA) and H_2O may be the most studied and robust ALD process.Here we consider two perturbations from this benchmark process by considering both a different precursor (a heteroleptic Al complex, void of halogens and Al-C bonds, L'_2AlL''), and a different organic oxidizing compound (RO_x).We have employed a quartz-crystal microbalance (QCM) to monitor ALD *in situ* and in real-time, and the deposited thin films have been characterized using X-ray photoelectron spectroscopy, spectroscopic ellipsometry, and X-ray reflectivity.Growth of thin films of Al_2O_3 using TMA and either RO_x or H_2O as the co-reactant at T = 285 °C produces thin films of similar physical properties (density, stoichiometry, minimal carbon incorporation), and the growth rate per cycle is similar for the two co-reactants at this temperature.At a lower temperature of T = 120 °C, the behavior is starkly different, where growth occurs with H_2O but not with RO_x.At either process temperature, we find no evidence for significant coverages of a long-lived intermediate from the reaction of RO_x. Growth from the heteroleptic Al precursor is similar to that observed with TMA—essentially stoichiometric Al_2O_3 is formed, and growth occurs readily with H_2O at T = 120 and 285 °C, while there are differences in the species formed at the end of the precursor half cycle.Growth with the heteroleptic precursor and the organic oxidizing species exhibits a similar dependence on temperature as observed with TMA—deposition at T = 285 °C, but not at T = 120 °C.Deposition of thin films of Al_2O_3 on metal surfaces of Cu and Co has been examined for evidence of interfacial oxidation.[1] While growth with either co-reactant (H_2O or RO_x) does not lead to the oxidation of the underlying Cu substrate, use of H_2O leads to the oxidation of Co, while use of RO_xas the co-reactant does not. We postulate that the size of the co-reactant in this case plays a role, where the diffusion of species through the deposited Al_2O_3 thin film could result in oxidation at the Al_2O_3|metal interface, a process that is strongly hindered in the case of RO_x due to its size.

[1]*ACS Appl. Mater. Interfaces* **16**, 16983−16995 (2024).

8:45am TF1+AP-ThM-4 Atomic Layer Deposition Chemistry – Trimethylaluminum on SiO_2 and Cu from a Surface Science Perspective, *Leonhard Winter, Francisco Zaera,* University of California, Riverside
Atomic Layer Deposition (ALD) is a chemical method used to grow thin films by sequentially employing complementary, self-limiting half-reactions. ALD offers the possibility to grow high-quality films on geometrically challenging substrates with sub-monolayer thickness control. An important development in ALD research is the ability to perform the growth selectively on specific areas.[1] For example, in the microelectronics industry, an ALD film often needs to be grown only on the dielectric (often SiO_2) or only on the electric contacts (often Cu) while avoiding the other material. Therefore, it is important to understand the surface chemistry of

the ALD precursors on the competing surfaces. There has been some progress towards this goal,[2] but more mechanistic details are needed to tailor the selective ALD chemistry.

To this end, we have set to first study and contrast the surface chemistry of trimethylaluminum (TMA), a precursor commonly used to deposit Al_2O_3 films, on SiO_2 versus Cu surfaces by using X-ray photoelectron spectroscopy (XPS) and temperature-programmed desorption (TPD). On SiO_2, we have observed high chemical reactivity of this precursor at unexpectedly low temperatures and exposures, below the cryogenic temperatures required for multilayer condensation. This low-temperature chemistry appears to be complex, with desorption of Al-containing fragments being accompanied with changes in the relative Al/C atomic ratio on the surface. It was also determined that the initial sticking coefficient at room temperature is approximately 4-5 times smaller than at cryogenic temperatures, and that the TMA uptake is self-limiting. This high TMA reactivity on SiO_2 surfaces will need to be compared with that on Cu substrates, as the differences are expected to have significant implications for the selectivity of the ALD and for strategies to control it.

[1] A. J. M. Mackus, M. J. M. Merkx, W. M. M. Kessels, *Chem. Mater.* **2018**, *31*, 2-12.
[2] S. T. Barry, A. V. Teplyakov, F. Zaera, *Acc. Chem. Res.* **2018**, *51*, 800-809.

9:00am TF1+AP-ThM-5 Spatial Atomic Layer Deposition: Transport-Reaction Modeling and Experimental Validation of Film Geometry, *Daniel Penley*, *Neil P. Dasgupta,* University of Michigan, Ann Arbor

Close-proximity atmospheric-pressure spatial atomic layer deposition (AP-SALD) is a powerful technique to control nanoscale surfaces and interfaces at scales relevant to large-scale manufacturing. To investigate the manufacturing tradeoffs in an AP-SALD system (film quality-throughput-cost-sustainability), many studies utilize computational modeling to gain insight into the difficult to observe process region that contains the isolated precursor zones. However, there is limited investigation into the effects of process parameters on the spatial separation and distribution of the precursor zones and their resulting impact on the deposited film. Additionally, few previous works have paired a computational model with an experimental system that has comparable, closed-loop control over the many system parameters, including gap size, relative alignment, gas flow rates, and substrate velocity.

In this work, we introduce a transport-reaction model to study how variations in process parameters affect the resulting deposited film. A finite element method model uses laminar flow fluid mechanics and transport of dilute species to give insight into the pressure, velocity, and partial pressure gradients within the process region. These outputs are then input into a surface reaction model that simulates the chemical reactions, yielding predicted film thickness maps. The model is validated and parameterized by comparing the simulated film geometries with TiO_2 films deposited using a mechatronic AP-SALD system. By coupling an experimental system with the transport-reaction model, process parameters can be tuned both physically and digitally to provide new insights into AP-SALD process control and optimization for thin film deposition at large scales.

9:15am TF1+AP-ThM-6 Deposition Efficiency Modeling according to Precursor Flow Rate in ALD Process with Fixed Chamber Pressure, *Dongho Shin,* Samsung Electronics, Republic of Korea

Atomic Layer Deposition (ALD) is a key technology for achieving excellent thin film step coverage in a high aspect ratio structure. Therefore, many studies regarding various ALD technologies and ALD mechanism modeling in microstructure have been conducted. However, there are few studies of ALD technologies in terms of cost and environment, related to the efficiency of precursor used during ALD process. Deposition Efficiency (DE) is defined as the ratio of the thickness of deposited film to the volume of the precursor consumed. Research on ALD technologies that reduce precursor consumption by increasing DE of precursor is urgently needed considering cost reduction and ESG management. Therefore, in this paper, a new precursor supply model representing DE is established for ALD system with fixed pressure control. Based on the model, we found that precursor flow rate and DE are inversely proportional. Due to this characteristic, the decrease of the flow rate results in the higher DE. The feasibility of the model has been confirmed through CFD simulation and the model is finally verified through pattern evaluation. This proposed concept presents an additional direction to be pursued in ALD research in the future.

9:30am TF1+AP-ThM-7 Time-Resolved Heat Generation of ALD MgO Surface Reactions, *Ashley Bielinski, Jiayi Xu,* Argonne National Laboratory*; Swan Htun,* Northwestern University*; Stephan Hruszkewycz, Cong Liu, Alex Martinson,* Argonne National Laboratory

Many of the properties that are prized in films deposited with atomic layer deposition (ALD) such as precise control of composition and thickness, as well as conformal coverage on high aspect ratio structures, rely on the self-limiting nature of ALD surface reactions.A deeper understanding of the fundamental thermodynamics, kinetics, and mechanisms of ALD precursor reactions is essential to enable emerging applications such as site-selective ALD and area-selective ALD, which rely on chemical selectivity between precursor molecules, inhibitors, and the substrate surface.Differences in the surface composition and availability of reactive sites, as well as the precursor ligands can have a significant influence on the properties of the deposited film and the formation of interfaces, even within a given material system.

ALD pyroelectric calorimetry measures the in situ, time-resolved heat generated by ALD surface reactions under standard ALD conditions. Previously, we used this technique to measure the heat generation rates of trimethylaluminum (TMA), tetrakis(dimethylamino)zirconium (TDMAZr) and water to form Al_2O_3 and ZrO_2.Here we extend this technique to study the reaction between bis(ethylcyclopentadienyl)magnesium (Mg(CpEt)$_2$) and water to form MgO.To fully extract the heat generated by these ALD surface reactions over longer time scales, the data was fit to a calibrated model to account for cooling and electronic decay.These results were then compared to computational first principles models of various surfaces and reaction steps as well as calculations of the standard reaction enthalpies.Pyroelectric calorimetry provides a unique opportunity to quantitatively benchmark the values provided by computational models.This can help evaluate the accuracy of proposed processes and mechanisms.Heat generation rates provide new insight into ALD processes, helping us to untangle the thermodynamics, kinetics, and mechanisms of these heterogenous surface reactions.

9:45am TF1+AP-ThM-8 In situ Stress Measurements During Tungsten Atomic Layer Deposition, *Ryan B. Vanfleet, Steven M. George,* University of Colorado at Boulder

In situ film and surface stresses were measured during tungsten (W) atomic layer deposition (ALD) using wafer curvature techniques. Tungsten was deposited at temperatures between 130 °C and 300 °C using tungsten hexafluoride (WF$_6$) and disilane (Si$_2$H$_6$) as the reactants on aluminum oxide (Al$_2$O$_3$) ALD surfaces. The stress was initially compressive during nucleation over the first 8-10 W ALD cycles as expected from a Volmer-Weber growth model. The stress was then tensile as the film became continuous.

Large tensile stresses were measured for the W ALD films. The film stress was ~2.0 GPa at a deposition temperature of 200 °C (Figure 1). For comparison, Al$_2$O$_3$ ALD films deposited at low temperatures have much smaller tensile film stresses of ~0.45 GPa. The large tensile stress in W ALD films may be generated at the grain boundaries. Atoms are too far apart at grain boundaries and experience an attractive force that wants to pull them together.

Surface stresses were also measured during the individual WF$_6$ and Si$_2$H$_6$ exposures (Figure 2). The WF$_6$ exposures produce a tensile stress of ~+2 N/m. This tensile stress is correlated with WF$_6$ reacting with SiF$_2$H* sacrificial surface species to deposit WF$_5$* surface species (SiF$_2$H* + WF$_6$(g) -> WF$_5$* + SiF$_3$H(g)). The Si$_2$H$_6$ exposures then partially release the tensile stress with a stress change of ~-1 N/m. The Si$_2$H$_6$ exposures redeposit SiF$_2$H* sacrificial surface species (WF$_5$* + Si$_2$H$_6$(g) -> WSiF$_2$H* + SiF$_3$H(g) + 2H$_2$(g)).

The large tensile stress in the W ALD films can lead to film cracking and delamination. This phenomenon is clearly evidenced by the *in situ* stress measurements (Figure 3). A large reduction in tensile stress is observed during film failure. The film failure was also obvious by visual inspection of the W ALD films when the W films began to peel off the underlying wafer.

Additional in situ measurements have observed that the large tensile film stress in W ALD films may be reduced by occasional exposures to trimethylaluminum (TMA). The addition of Al breaks the crystalline continuity in the W ALD film and forces the W ALD film to re-nucleate. These observations suggest that film stress can be controlled by adding dopants during film growth.

Thin Films
Room 115 - Session TF2+EM-ThM

Thin Films for Microelectronics I: BEOL
Moderators: **Sarah Atanasov**, Intel, **Matthias Young**, University of Missouri

11:00am **TF2+EM-ThM-13 Inherently Selective Thermal Atomic Layer Deposition of Copper Metal Thin Films**, *Charles Winter,* Wayne State University **INVITED**

The continued miniaturization of microelectronics devices has created the need for new high-performance materials and appropriate nanoscale deposition processes. Atomic layer deposition (ALD) is a growth technique that affords Angstrom level control of film thicknesses and can give perfect conformal coverage in high aspect ratio nanoscale features. Copper (Cu) is a central interconnect metal and its growth by ALD remains a topic of significant interest. Many Cu ALD processes have been reported, but most are limited to lower temperatures (<200 °C) because of limited thermal stability of the Cu precursors. Herein, we will describe a new thermal Cu ALD process that employs bis(2,2,6,6-tetramethyl-3,5-heptanedionate)copper(II) ($Cu(thd)_2$) and nitrogen compounds as precursors. Cu metal film growth trials were conducted between 175 and 300 °C using $Cu(thd)_2$ and hydrazine on a variety of substrates, including Ru, Cu, TiN, SiO_2, Si with native oxide, and Si-H. Self-limited growth of Cu films on Ru substrates was demonstrated at 225 °C for both $Cu(thd)_2$ and hydrazine, with a growth rate of about 0.25 Å/cycle. An ALD window was observed for this process between about 225 and 275 °C. The characterization of the Cu films will be overviewed, including compositions, resistivities, and surface morphologies. Inherently selective growth of Cu metal films was observed on metal substrates such as Ru, Cu, and TiN. No growth occurred on insulating substrates such as Si-H and SiO_2. Inherently selective growth of Cu films by ALD on metal substrates offers many new opportunities for metallization.

11:30am **TF2+EM-ThM-15 Effect of Hydrogen Annealing on Grain Growth of Tungsten Films**, *Seunghyun Park,* School of Advanced Materials Science & Engineering, Sungkyunkwan University, Republic of Korea; *Sungjun Kim,* Department of Semiconductor and Display Engineering, Sungkyunkwan University, Republic of Korea; *Changyu Park, Hyoungsub Kim,* School of Advanced Materials Science & Engineering, Sungkyunkwan University, Republic of Korea

Tungsten (W) has been widely used for first level metallization in memory and logic devices due to its low electrical resistivity and high thermal stability. In addition, it can be easily deposited as an ultrathin film with high step coverage through chemical vapor deposition (CVD) or atomic layer deposition, rendering it suitable for complex device structures. However, the dimensional down-scaling of metal lines to less than 10−20 nm is accompanied by a simultaneous decrease in grain size, which results in an inevitable increase in the resistance due to enhanced surface and grain boundary scattering [1]. Therefore, one possible approach to maintain low resistivity of the ultrathin W film at small dimensions could be the introduction of additional thermal annealing that effectively increases the grain size while using a low temperature below 400 °C.

A couple of researchers observed abnormal grain growth of nickel and vanadium by introducing H_2 during the annealing process at high temperatures above 600 °C [2, 3]. Based on these findings, this presentation aims to explore the annealing of ultrathin W films in an H_2 environment at various temperatures (300−500 °C). To evaluate the effectiveness of H2 in increasing grain size, N_2 and high-pressure H_2 annealing were also introduced. The W film of 20 nm thickness was deposited using CVD on a SiO_2/Si substrate coated with a TiN adhesion layer. Grazing incidence X-ray diffraction measurements revealed that H_2 annealing at 1 bar resulted in an increased crystallite size, indicative of grain size, compared to N_2 annealing under all temperature conditions, which was accompanied by a decrease in resistivity. In addition, the increase in the H_2 pressure to 5 bar increased crystallite size further and reduced electrical resistivity accordingly.

[1] D. Gall, J. Appl. Phys. 127, 050901 (2020).

[2] T. Wagner et al., Int. J. Mater. Res. 93, 401−405 (2002).

[3] M. L. Martin et al., Acta Mater. 155, 262−267 (2018).

11:45am **TF2+EM-ThM-16 Textured Growth of Zinc Sulfide on Back-End-of-the-Line (BEOL) Compatible Substrates**, *Claire Wu,* University of Southern California; *Mythili Surendran,* Lawrence Berkeley National Laboratory; *Pei-Jer Tzeng, Cheng-Hsien Wu, Xinyu Bao,* TSMC, Taiwan; *Jayakanth Ravichandran,* University of Southern California

Scaling of transistors has enabled continuous improvement in the performance of logic devices, especially with recent advances in materials engineering for transistors. However, there is a need to surpass the horizontal limitations in chip manufacturing and incorporate the vertical or third dimension. To enable monolithic three-dimensional (M3D) integration of high-performance logic, one needs to solve the fundamental challenge of low temperature (<400 °C) synthesis of high mobility n-type and p-type semiconductor thin films that can be utilized for fabrication of back-end-of-line (BEOL) compatible transistors.1 Transition metal oxides are promising n-type materials; however there is a lack of p-type materials that can meet the stringent synthesis conditions of BEOL manufacturing. Zinc sulfide (ZnS), a transparent wide band-gap semiconductor, has shown room temperature p-type conductivity when doped with copper and crystallizes below 400oC when grown by pulsed laser deposition (PLD).2, 3 Here, we report growth of crystalline thin films of ZnS by PLD on a variety of amorphous and polycrystalline surfaces including silicon nitride, (SixNy) thermal silicon dioxide, (SiO2), hafnium dioxide (HfO2) and titanium nitride (TiN). High-resolution thin film X-ray diffraction shows texturing of ZnS on all three substrates. Crystalline quality was investigated using rocking curve measurements. Surface and interface quality was measured using X-ray reflectivity and atomic force microscopy measurements. Further work in characterizing the film quality through electrical measurements such as conductivity and capacitance shall be discussed. This work showcases the capability of thin film growth of a wide band-gap semiconductor in BEOL compatible conditions with technological applications in transistor manufacturing.

References:

1. IEEE Micro. 2019, 39, 6, 8-15.

2. Adv. Electron. Mater. 2016, 2, 1500396

3. Adv. Mater.2024, 36, 2312620

12:00pm **TF2+EM-ThM-17 Steep-Slope IGZO Transistor with an $Ag/Hf_{1-x}Zr_xO_2$ Atomic Threshold Switch**, *Junmo Park, Deokjoon Eom, Hyunhee Kim, Yong-Hoon Kim, HyoungSub Kim,* Sungkyunkwan University, Republic of Korea

Atomic threshold switch (ATS) exhibits abrupt switching characteristics due to the formation of electrochemical metallization filaments by the diffusion of Ag or Cu atoms towardsthe dielectric [1].Recently, it has been consideredfor integration with a field-effect transistor (FET) to build a steep-slope FET that overcomes the conventional subthreshold swing (SS) limit of 60 mV/dec [2]. Up to now, various FETs implemented with Si, transition-metal dichalcogenide, and oxide channels have been actively adopted for integration with ATS devices [3]. Particularly, the steep-slope FET built with an indium gallium zinc oxide (IGZO) transistor isattracting great attention because its fabrication temperature is low enough to meet thethermal requirements of a back-end-of line (BEOL) process [4]. However, it was demonstrated not through monolithic integration but through electrical wiring after fabrication of individual devices [5].

In this presentation, we suggest a novel BEOL-compatible steep-slope FET where an IGZO transistor is monolithically integrated with an $Ag/Hf_{1-x}Zr_xO_2$ (HZO) ATS at less than 400 °C. The IGZO and HZO films were deposited using sputtering at room temperature and atomic layer deposition at 200 °C, respectively.The Ag/HZO ATS is connected to the drain electrode of the IGZO FET in series. The SS of IGZO transistors was controlled by varying the composition of the HZO film, resulting achievement of SS muchless than 60mV/dec.Furthermore, we found that the HZO film with a Zr content (x) of ~25% led to a lower threshold voltage compared to the same thickness HfO_2 single-layerand did not require a high voltage electroforming process (initialization). The detailed electrical characterization results of individual ATS, FET, and integrated ATS-FET devices will be discussed along with the physical and chemical characterization results of the HZO and IGZO films.

This work was supported by the GRRC Program of Gyeonggi Province (GRRC Sungkyunkwan 2023-B01)

[1] Li et al., Adv. Sci. **7**, 2002251 (2020).

[2] Hua et al., Nat. Commun. **11**,6207 (2020).

[3] Elahi et al., Mater. Today Phys. **30**, 100943 (2023).

[4] A. Choi et al., Chem. Mater. **36**, 2194 (2024)

[5] Cheng et al., Appl. Phys. Express **12**, 091002 (2019)

2D Materials
Room 122 - Session 2D+EM+QS-ThA

2D Materials: Applications

Moderators: Matthias Batzill, University of South Florida, **Fei Yao**, University at Buffalo

2:45pm 2D+EM+QS-ThA-3 New Graphene Oxide-based Nanozymes for Cancer Theranostics, *Alice Foti, Stefania Sciacca, Gabriella Tranchida, Salvatore Petralia, Roberto Fiorenza, Salvatore Scirè, Luisa D'Urso, Carmela Bonaccorso, Aurore Fraix,* University of Catania, Catania, Italy*; Angela De Bonis,* University of Basilicata, Italy*;* **Cristina Satriano**, University of Catania, Catania, Italy

Graphene oxide (GO) and plasmonic nanoparticles (Pd, Au, Ag NP) nanocomposites were scrutinized in this study as combinative multimodal platform with enzyme-like, photocatalytic and photothermal properties. A green one-pot chemical reduction method by using D-glucose as reducing agent and polyvinylpyrrolidone (PVP) as capping agent, was used to fabricate the hybrid 2D platforms (NP@G) and the reference plasmonic nanoparticles alone. Different molar ratios of the metal precursor/reducing agent were tested to get the best results in terms of stability, reproducibility and reaction yield, as monitored by the plasmonic band of the NPs. The physicochemical characterization of the morphological, compositional, structural, and functional properties of NP@G nanozymes was carried out in terms of X-ray photoelectron spectroscopy (XPS), X-ray diffraction (XRD), transmission electron microscopy (TEM), UV-visible, Raman spectroscopy, Fourier Transformed Infrared Spectrocopy (FTIR), thermocamera, atomic force microscopy (AFM), dynamic light scattering (DLS) and zeta potential (ZP). The enzyme-like activity was tested by colorimetric assays in a cell-free environment to confirm the maintenance of the nanozymes capability in the NP@G samples.The photocatalytic properties were tested in the H_2 evolution by water splitting reaction under simulated solar light. Further, the nanoplatforms were tested in prostate cancer cells (PC-3 line) in terms of cytotoxicity, cell migration and reactive oxygen species (ROS) production, to prove the antitumoral action of the developed nanomedicine. Cell imaging by laser scanning confocal microscopy (LSM) demonstrated the theranostic capability of the developed platforms, including dynamic processes at the level of sub-cellular compartments.

Acknowledgements: ADB and CS acknowledge the financial supported by MUR in the framework of PRIN2022-PNRR call under project CoMu4CaT.

3:00pm 2D+EM+QS-ThA-4 Engineering Novel Hybrid Membranes for Battery Separators from Sustainable Sources, *Suvash Ghimire, Priyanka Makkar, Md. Roxy Islam, Kausik Mukhopadhyay,* University of Central Florida

The surge in device use in transportation, biomedical sectors, and other industries is escalating at an alarming rate, coupled with grave concerns about pollution and global warming that underscores the urgency for developing efficient, safe, and environmentally friendly energy storage devices. There is a growing urgency to reduce planet-warming pollution through mining and other activities at the federal level to drop carbon emissions by half this decade and reach close to zero by the middle of the century to prevent some of the most devastating effects of climate change. Research groups worldwide are developing metal-based substitutes that address sustainability by eliminating the use and generation of hazardous substances during the synthesis and developing cheap, recyclable substitutes for electrode materials, electrolytes, membranes, and separators that are the pivotal components of energy storage devices.

Materials and their interfaces play an essential role in energy storage devices by facilitating ion transports and impeding short circuits by separating anode and cathode. Ion exchange membranes have broad applications in water electrolysis, fuel cells, and flow batteries. To date, Nafion® membranes and polyolefin-based separators are considered the industrial standards due to their excellent proton conductivity and high chemical stability. However, high cost, poor strength, shrinkage at high temperatures, and use of fluorinated chemicals hinder their widespread use. Therefore, there is an urgent need to develop membranes that can be alternatives to existing membranes without compromising the cost and environmental impact. Leveraging their porosity, properties, low cost, and thermal and chemical stabilities, clay-based membranes could be a new alternative for new-generation materials for such applications.

Our research presents a novel pathway for developing flexible and durable hybrid clay membranes by modifying them with zwitterions. The ionic conductivity of the membranes, measured using electrochemical impendence spectroscopy in a non-aqueous electrolyte solution, was found to be in the range of 10^{-4} S/cm, which is comparable to the ionic conductivities of related membranes used in electrochemical energy storage devices; this is a significant new development considering clays are insulators. Our study exhibits a new avenue to engineer highly efficient ion-conducting membranes with high thermal stability (300 °C) that can provide an efficient and recycle-free approach to developing a new generation of separators from sustainable sources for energy applications, especially for battery technology.

3:15pm 2D+EM+QS-ThA-5 Unveiling Composition-Structure Relationships for the Discovery of Novel High-Entropy 2D Materials Using the Mixed Enthalpy-Entropy Descriptor, *Dibyendu Dey,* University of Central Florida*; Olugbenga Ogunbiyi,* University of Missouri*; Biswajit Ball,* University of Central Florida*; Liangbo Liang, Michael J Zachman,* Oak Ridge National Laboratory*; Yingchao Yang,* University of Missouri*; Liping Yu,* University of Central Florida

High-entropy two-dimensional materials (HE-2DMs) represent an emerging class of materials that show promise for numerous functional applications. These materials inherit the distinctive features of conventional 2D materials, such as reduced dimensionality, exceptional flexibility, and a large surface-to-volume ratio, while introducing a high configurational entropy of mixing to the system. Despite their immense potential, the experimental realm of HE-2DMs has thus far been limited to a few materials, leaving the complex interplay between their composition, structure, and synthesizability largely unexplored. In this work, by utilizing the Mixed Enthalpy Entropy Descriptor (MEED) [**1**], the material space of high-entropy 2D chalcogenides, including Group IV (Ti, Zr, Hf), Group V (V, Nb, Ta), and Group VI (Cr, Mo, W) metals in their 2H, 1T, and 1T' phases, has been systematically explored. MEED uniquely encapsulates the chemical and structural attributes critical for synthesizing HE-2DMs in their diverse polymorphs, demonstrating capabilities beyond any existing descriptor. Guided by MEED predictions, several top-candidate high-entropy tellurides and selenides, which exhibit extraordinary potential for applications in flexible electronic devices and advanced batteries, have been synthesized.

Reference:

1. Dibyendu Dey, Liangbo Liang, Liping Yu, Journal of the American Chemical Society 146, 5142 (2024).

3:30pm 2D+EM+QS-ThA-6 Antenna-Coupled Magic-Angle-Twist-Graphene Josephson Junction Millimeter Wave Detector, *David Castro,* University of Central Florida

We designed a sensitive detector of THz and mm waves using an antenna-coupled magic-angle-twist-graphene Josephson junctions. Magic angle twisted bilayer graphene superconducts at a transition temperature of ~2K. We can create a lateral Josephson junction by selectively gating different sections of a single sheet of magic angle graphene. The detection mechanism in our design is based on the change in maximum zero-voltage DC current in response to an applied AC signal at the junction. We expect it to be faster than bolometric detection mechanisms while maintaining high sensitivity. We determined that the bowtie antenna would work best for this device by using finite element electrodynamic simulations. We estimated the responsivity, noise-equivalent-power, and the prospects for single-photon detection. This detector device can be used in the future for sensing applications and quantum information systems.

Acknowledgments

Actinides and Rare Earths
Room 123 - Session AC+MI-ThA

Forensics, Disposal and Pu

Moderators: Itzhak Halevy, Ben Gurion Uni. Be'er Sheva, **Alison Pugmire**, LANL, **Paul Roussel**, AWE

2:15pm AC+MI-ThA-1 A New Approach for Nuclear Forensics Investigations of Uranium Dioxide : Application of Laboratory Based Photoelectron Spectroscopy with Hard and Soft X-ray Sources, *Stuart Dunn, Paul Roussel*, AWE, UK; *Aaron Wood, Ben Spencer, Robert Harrison*, University of Manchester, UK; *Philip Kaye, Matthew Higginson*, AWE, UK; *Wendy Flavell*, University of Manchester, UK **INVITED**

Nuclear Forensic investigations rely on the analysis of the chemical and physical properties to determine the provenance of nuclear materials, found out of regulatory control. X-ray photoelectron spectroscopy (XPS) has been shown to be a powerful tool in supporting material assessment by analysis of the top few nanometres of the surface. With the onset of laboratory based hard x-ray photoelectron spectroscopy (HAXPES) instrumentation, this provides the opportunity to probe deeper into the bulk. Furthermore, HAXPES spectra of high Z elements will have multiple core level peaks occurring over a range of different depths and analysis of these can offer a unique non-destructive depth profile. The work presented in this study demonstrates the utility of a combined XPS and HAXPES analysis to isolate forensic signatures on the surface and into the bulk of uranium dioxide. Survey quantification shows the changing stoichiometry, utilising a 9.25 KeV excitation range of HAXPES, from different average depths within the sample matrix. Peak fitting of high-resolution spectra allows identification of oxidation states as well inspection of secondary features, which provide insight into the material characteristics. Combined with XPS analysis, this shows different chemical and elemental states at the surface into the bulk sample, highlighting the usefulness of this approach. QUASES-Tougaard analysis was performed to determine the in-depth distribution of atoms, developing a consistent model to describe the surface overlayer, correlated to the chemical and stoichiometric differences over the excitation range. Finally, the MNN X-ray excited Auger electron spectra are acquired from uranium dioxides for the first time for use in the application of a Wagner or chemical state plot. This study is the first in a series of analysis campaigns on uranium bearing materials.

2:45pm AC+MI-ThA-3 Making Use of X-ray Emission Signatures in the Scanning Electron Microscope to understand f-Element Speciation and Phase, *Mark Croce*, Los Alamos National Laboratory **INVITED**

While X-ray absorption spectroscopy is exquisitely sensitive to signatures of chemical speciation and phase, what if similar information could be obtained from the scanning electron microscope? Scanning electron microscopes have become more than imaging tools – they are accessible microanalysis platforms with nanoscale spatial resolution and are compatible with a wide variety of samples including those not suitable for X-ray absorption spectroscopy. Although the physics relating the chemical and physical state of an atom to X-ray emission is more complex than for X-ray absorption, there are still distinct signatures present in the X-ray emission spectra. The twofold challenge is to measure them and interpret them. Recent development in low-temperature microcalorimeter spectrometers has made it possible to simultaneously achieve the energy resolution and detection efficiency needed to observe this fine structure in X-ray emission resulting from the interaction of the microscope's electron beam with a sample. In parallel, extending molecular and atomic theory to interpret X-ray emission spectra is beginning to allow use of this capability as a research tool to determine chemical speciation and phase for f-elements including cerium, uranium, and plutonium even in non-ideal samples. We present progress towards developing what we call "Hyperspectral X-ray Imaging" using a large-array microcalorimeter X-ray spectrometer with <10 eV FWHM energy resolution at 3 keV coupled to a commercial scanning electron microscope, recent results on lanthanide and actinide samples, and future applications of the method to support f-element science. LA-UR-24-21795

3:15pm AC+MI-ThA-5 Automated Particle Analysis of Actinide-Bearing Nuclear Wastes, *Edgar Buck*, Pacific Northwest National Laboratory

Automated particle analysis (APA) is performed on the Scanning Electron Microscope/X-Ray Energy Dispersive Spectroscopy (SEM-EDS) and enables the characterization of morphology and composition of particles. This method allows hundreds to thousands of particles to be examined and reduces operator bias. We have applied APA methods to radioactive Hanford tank waste materials containing rare earth elements, uranium, and plutonium. The challenge for APA with highly heterogeneous materials is the variability in particle size. An important component of the APA is the preparation of the samples for analysis and the segmentation routines used to locate particles of interest. Biased results can be generated during the deposition of particles with larger particles tending to fall out more quickly than smaller particles, and therefore can become concentrated at the center of the sample stub, where the material is directly pipetted. It is important to be aware of the factors controlling the deposition of the particles and analyze the entire SEM stub to obtain representative data. Image segmentation routines have to be calibrated to prevent missing particles and for obtaining accurate morphological data. In this presentation, we will describe the efforts to characterize and classify the actinide-rich wastes.

3:30pm AC+MI-ThA-6 Development of X-Ray Spectromicroscopy Techniques for Nuclear Safeguards and Nuclear Forensics, *David Shuh, Alexander Ditter, Nic Cicchetti, Olivia Gunther*, LBNL; *Joseph Brackbill*, UC Berkeley/LBNL; *Rachel Lim, Alexander Baker, Scott Donald, Brandon Chung*, LLNL; *Rebecca Coles*, BNL; *Andrew Duffin, Jesse Ward, Micah Miller*, PNNL

The on-going development of improved characterization methods and signatures is crucial to ensure that nuclear safeguards and forensics activities remain effective. For these purposes, the development of X-ray techniques is particularly useful because of their elemental specificity and non-destructive nature that could enable a first-in capability. Tunable synchrotron radiation X-ray approaches provide a means to extend the scope of safeguards and forensics investigations in elemental, chemical, and structural analysis which can be done in imaging modes that in some cases, reaches to the nanoscale. The ability to use tunable, focused X-ray beams makes synchrotron radiation sources a potentially disruptive tool for addition into the array of characterization techniques currently employed, particularly for the investigation of particles or areas of interest in smaller specimens possessing bulk-like characteristics. However, the use of synchrotron radiation methods also presents some unique challenges for the implementation of safeguards and forensic efforts at the synchrotron radiation facility sites (ALS, APS, NSLS-2, and SSRL). Synchrotron radiation-based safeguards and forensics studies over the past several years conducted at nearly all of the U.S. Dept. of Energy synchrotron radiation user facilities throughout the X-ray spectrum have furthered this case, as well as clearly identifying areas that require improvement. At the same time, there have been significant performance improvements in fixed-energy laboratory-based X-ray instrumentation suitable for contemporary, spatially-resolved safeguards and forensics (primarily XRF) studies. Additionally, there have been continued efforts and strides made towards the realization of true laboratory-based X-ray light sources that could provide competitive X-ray flux and tunability, albeit in the future, that might provide the best combination of performance and characteristics necessary for safeguards and forensics characterization activities. A current assessment of the relative strengths and drawbacks of the respective X-ray approaches, as well as a performance comparison will be presented, leading into an overall the future outlook in terms of safeguards and forensics.

3:45pm AC+MI-ThA-7 Site-Specific and Spatially Resolved Morphological and Chemical Analysis of Plutonium and Uranium Materials, *Brandon Chung, Alexander Baker, Scott Donald, Tian Li, Rachel Lim, Uday Mehta, Debra Rosas, Donya Servando-Williams, Nick Cicchetti*, Lawrence Livermore National Laboratory; *Alexander Ditter, Olivia Gunther, David Shuh*, Lawrence Berkeley National Laboratory

Nuclear forensics requires accurate identification of distinguishing material characteristics to delineate the material's origin-to-interdiction information. Morphological and chemical variation in nuclear materials over large scales of observation can provide valuable information that can assist interpretation of the material's varying provenance, process, and pathways. We will describe our efforts to strengthen operational and scientific methodologies to employ the focused ion beam-scanning electron microscopy (FIB-SEM) on uranium (U) and plutonium (Pu) materials for internal morphological analysis including site-specific 3D microscopy and spatially resolved characterizations of material features using transmission electron microscopy (TEM) and X-ray synchrotron spectromicroscopy. Both U and Pu materials show variations in the internal chemical composition and morphology from their production processes and storage environments. This information is of potential use in discriminating material signals to identify the origin and history of interdicted nuclear materials.

4:00pm AC+MI-ThA-8 An Entropic Approach to Estimating Orbital Occupancies in Plutonium, *Miles Beaux,* Los Alamos National Laboratory

Janoschek, et al. described the ground state of plutonium (Pu) as being "governed by valence fluctuations, that is, a quantum mechanical superposition of localized and itinerant electronic configurations." [*Science Advances*, 1, 6 (2015)]. By representing this ground state generally as

$$[Rn]7s^{2+\gamma s, Pu}5f^{6+\gamma f, Pu}6d^{0+\gamma d, Pu}7p^{0+\gamma p, Pu}$$

where $\gamma_{s,Pu}, \gamma_{f,Pu}, \gamma_{d,Pu}$, and $\gamma_{p,Pu}$ represent potentially non-integer deviations from the integer occupancies of their respective orbitals, a combinatorial approach can be applied to the allowable permutations of quantum electronic configurations as a means of describing the electron degrees of freedom. This approach enables a classical statistical mechanics methodology to be applied to the discrete quantum states for conceptualizing and investigating the multiconfigurational ground state of Pu. Specifically, an over-approximation (with Hund's rule relaxed) and an under-approximation (with Hund's rule enforced) of electronic structure entropy has been established for varying ranges of potentially near energy degenerate occupancy configurations for plutonium. This bracketing of electronic structure entropy is compared with the known molar entropy of Pu to narrow down the set of possible localized and itinerant electronic configurations that can reasonably contribute to the quantum mechanical superposition of Pu's multiconfigurational ground state, as well as to estimate the non-integer orbital occupancies of its $7s$-, $5f$-, $6d$- and $7p$-orbitals.

LA-UR-24-22282

4:15pm AC+MI-ThA-9 The Problem with the Second Derivative Method in EELS*, *JG Tobin,* University of Wisconsin-Oshkosh

The second derivative mode of peak analysis in electron energy loss spectroscopy (EELS) in a Transmission Electron Microscope (TEM) has been quantitatively evaluated in terms of the accuracy of the method.*This includes a demonstration of the importance of the second derivative peak width, the second order dependency of the accuracy upon that peak width and effect of high frequency noise in the spectra.It was found that, while EELS does converge to an X-ray Absorption Spectroscopy (XAS)-like limit (electron dipole transition) at high energies, there are significant issues with the 2nd Derivative Model.

1. There is no fixed relationship between non-derivative peak intensities and 2nd derivative peak intensities.Changing peak-shapes changes the ratio.
2. Assuming that peak-shapes remain constant, which may not be justified, there is a second order dependence of the ratio upon the peak width of the 2nd Derivative peak.
3. The second order dependence upon the peak width manifests itself in two very distinct ways: with random errors and systematic errors.
   - The random error from high frequency noise places a limit on the number of significant digits in the BR result.
   - The systematic error has shown up in the BR predictions and 5f population estimates (n) for the localized systems Pu, PO_2 and UO_2.

The 2nd Derivative Mode in EELS should be used with great caution in quantitative BR analyses of 5f populations.

*J. G. Tobin, "A quantitative evaluation of the 2nd derivative mode in electron energy loss spectroscopy," J. Electron Spectroscopy Rel. Phen. 268, 147387 (2023), https://doi.org/10.1016/j.elspec.2023.147387

Applied Surface Science
Room 117 - Session AS-ThA

Complementary Methods and Industrial Challenges

Moderators: Vincent Smentkowski, GE Research Center, **Suntharampillai Thevuthasan**, PNNL

2:15pm AS-ThA-1 ASSD Student Award Finalist Talk: Elucidating the Interaction Forces between Surface Nanobubbles and Nanoparticles, *Daniela Miano[1], Pierluigi Bilotto,* CEST GmbH, Italy*; Markus Valtiner,* TU Wien, Austria

Efficient surface cleaning protocols are imperative across diverse industries to ensure product quality and performance. The new direction of nanoelectronics requires surfaces to be cleaned at the nanoscale. In the last decade, surface nanobubbles have been shown to remove nanoparticles

from silicon wafers. [1] Nevertheless, the specific surface nanobubble-nanoparticle interaction has not been fully understood, calling for a deeper investigation.

We explore the formation and stability of surface nanobubbles by employing atomic force microscopy (AFM). After solvent/water exchange we characterize them in terms of topography and their interaction in different wettability and environment scenarios (i.e., change in solvent, nanoparticle types, gas concentration, and surface functionalization). The presence of NBs can lead to localize changes in wettability, roughness, and chemical reactivity.

Managing the balance between enhanced cleaning and surface potential is crucial. Over time, this alteration may impact the substrate's integrity or alter its performance characteristics.

Interestingly, we observe the formation of nanoholes, which we interpret in terms of short ranges forces (DLVO theory) and chemical equilibrium in confinement. The latter takes inspiration from *pressure solution* as described in geology. It helps identify the physical and chemical interactions occurring when nanoparticle detachment from the substrate. [2]

Our research work aims to describe solid-liquid interface, with particular interest to the phenomena correlate the interactions force between surface nanobubble-nanoparticles and surface and nanoparticles-surface. Research on surface nanobubble and the study of their possible application is necessary because there is not a unified vision in the scientific community. The results can impact both the scientific and industrial categories, by addressing respectively unsolved interactions at the nanoscale and upscaling nano-cleaning processes at the macroscale.

[1]S. Yang, & A. Duisterwinkel, A. (2011). Removal of Nanoparticles from Plain and Patterned Surfaces Using Nanobubbles. Langmuir, 27(18), 11430–11435. doi:10.1021/la2010776;

[2] K. Kristiansen, M. Valtiner, G.W. Greene, J.R. Boles, J.N. Israelachvili (2011). Pressure solution - The importance of the electrochemical surface potentials. doi:10.1016/j.gca.2011.09.019

2:30pm AS-ThA-2 A Correlative Microscopy Platform for In-Situ AFM-SEM-EDS, *Kerim T. Arat, William K. Neils, Stefano Spagna,* Quantum Design Inc.

In-situ correlation of AFM-SEM techniques implemented in a highly integrated tool offers the complementary strengths of two different imaging modalities without the inherent complications of sample transfer. This is not only a significant convenience for researchers but also ensures a high confidence in correlation accuracy and eliminates the risk of sample contamination and alteration during the sample transfer.

Previously, we have developed a correlative microscopy platform based on AFM-SEM [1]. These techniques can map the surface in high resolution and the trunnion, with up to 80° tilt capability, allows monitoring of process quality such as tip measurement or monitoring tip sample interaction. However, none of these can measure the elemental composition of the material.

We have extended the capabilities of the correlative platform with an energy-dispersive X-ray spectrometer (EDS) to extract the elemental information from the sample. The spectrometer is based on a state-of-the-art silicon drift detector [2], which provides high energy resolution (< 133 eV, Mn-Kα).Its unique graphene window offers better transmission, especially at the lower energy range, allowing elemental detection down to carbon. The EDS elemental identification algorithm uses a background subtraction method and compares the resulting spectra to reference datasets based on the NIST database [3]. Both hardware and software integration allow correlation of elemental information with the other imaging modalities that the tool can provide (see the supplementary document) where one can superimpose topography and elemental information.

Integration of the X-ray detector adds a significant analysis capability to AFM-SEM techniques applicable to a diverse range of materials such as metals, alloys, ceramics, and polymers. With this addition of EDS, researchers can obtain in-situ correlation of high-resolution, localized elemental information with high-resolution lateral and vertical topographical information, without the complications of sample transfer.

[1] A. Alipour et al., Microscopy Today 31 (2023), p. 17-22. doi: 10.1093/mictod/qaad083

[2] D. E. Newbury and N. W. M. Ritchie, Journal of Materials Science 50 (2015), p. 493-518. doi: 10.1007/s10853-014-8685-2

---

[1] **ASSD Student Award Finalist**

[3] D. E. Newbury and N. W. M. Ritchie, Scanning Microscopies 9236 (2014), p. 9236OH. doi: 10.1117/12.2065842

2:45pm AS-ThA-3 Multitechnique Analysis of Ultrathin Films for the Photocatalytic Production of Sustainable Aviation Fuels, *Mark Isaacs*, University College London, UK*; Lee Durndell,* University of Plymouth, UK*; Chris Parlett,* University of Manchester, UK*; Charalampos Drivas,* Cardiff University, UK

In the search for technologies by which to reduce the overreliance on traditional fossil fuel based transport, the utilisation of biomass derived feedstocks to produce aviation fuels represents an exciting avenue for minimising the carbon footprint of global travel. Developing new materials, and improving and optimising the performances and activities of these materials requires a fundamental understanding of the physical, chemical and electronic properties down to the nano-domain - particularly when considering some of the more sophisticated synthetic protocols employed in advanced nanomaterials such as surface modifications vie ultra-thin films, galvanostatic interaction depositions, formation of Schottky junctions and more. X-ray photoelectron spectroscopy (XPS), and surface science in general, is ideally suited to extracting directly relevant information about these properties and, when combined in a coincident manner, develop a completely holistic understanding of how nanomaterial synthesis parameters may be controlled to imbue fine control over the resultant properties - and understand how these may impact upon catalytic activities. In this work, we investigate a series of ultra-thin layers of titania deposited onto the surface of a high surface area silica and correlate material properties with the catalytic performance in the acetalisation of furfural into 2,5-Bis(2-furylmethylene) cyclopentanone. Comprehensive chemical, electronic and structural analysis is performed using a combination of correlative XPS, REELS, UPS, Raman and ISS, and mapped with catalytic performance in the presence and absence of stimulating light.

3:00pm AS-ThA-4 Analysis of Cu-Ag and Ni-Pt High Throughput Survey Results, *Kyle Dorman, Nate Bianco, Rishabh Kothari, Matias Kalaswad, Catherine Sobzcak, Saaketh Desai, Joyce Custer, Sadhvikas Addamane, Manish Jain, Alejandro Hinojos, Frank DelRio, Brad Boyce, Remi Dingreville, David Adams,* Sandia National Labs

Nanocrystalline thin films feature the potential for enhanced or altered material properties compared to their bulk single crystal counterparts. Recent studies on Pt-Au binary thin films have emphasized the role of grain boundary character in successful solute stabilization of otherwise thermally unstable nanocrystalline systems (C. M. Barr et al., Nanoscale, 2021), and means of high-throughput combinatorial synthesis (McGinn, ACS Comb. Sci., 2019) have been developed to complement automated characterization and modern simulation capacity. To further develop our understanding and suite of tools, and to step beyond the most noble alloy into more economically practical material systems, compositional surveys of Cu-Ag and Ni-Pt were performed in search of optimized material properties and greater comprehension of nanocrystalline systems. Facilitated by a fixed substrate and photolithography, a simultaneous co-sputtered deposition of each pair of elements with pulsed DC magnetron methods directing single element sources creates a varied atomic composition across 112 samples on a single 150 mm diameter wafer. A series of such depositions, varying the gun-tilt angle and power at each cathode, allows swift examination of nearly the full range of alloy compositions. Wavelength Dispersive Spectroscopy, Atomic Force Microscopy, X-ray Diffraction, X-ray Reflectivity, sheet resistance, optical profilometry and nanoindentation were employed for automated mapping analysis. The binary collision Monte Carlo program SiMTra (D. Depla et al., Thin Solid Films, 2012) assisted with the deposition design to minimize the necessary quantity of sample batches, and enabled analysis of the energetic and compositional properties of the wafer at deposition with respect to the resultant hardness, modulus, film density, crystal texture and resistivity. This permits specification of desirable processing conditions in relation to exemplary and underperforming films. Accompanied by exploration of the strengths and weaknesses of the dataset, and the means to improve further such surveys.

3:15pm AS-ThA-5 Characterization of Functional Surface Modifications in Medical Devices, *Andrew Francis, Ali Rafati, Anna Belu,* Medtronic, Inc.

Surface modifications provide important functionality for medical devices, such as increased lubricity, improved hemocompatibility, and localized drug delivery. Characterization of these modifications is essential to understanding and controlling their interactions with a patient. Here, the development and characterization of new functional surface modifications for medical devices is reported with several examples shown. In particular, the spatial-chemical distribution and functional testing of a new biomimicry surface modification will be highlighted in combination with key clinical results. A range of analytical techniques (SEM/EDS, TOF-SIMS, XPS, and Raman spectroscopy) and biochemical methods and assays (blood loop model, TAT, etc.) will be discussed.

3:30pm AS-ThA-6 XPS Study of ZrN as a Barrier to Silver Migration in TRISO Fuels, *Jeff Terry,* Illinois Institute of Technology

We have measured simulated TRISO Fuel model structures of SiC and ZrN with and without a 2 nm carbon capping layer. We have used both Sputter Depth Profiling with conventional X-ray Photoemission (XPS) and Ambient Pressure X-ray Photoemission Spectroscopy (APXPS) to explore the reactivity of these layers with both Ag and H_2O. One set of the samples that were depth profiled were measured at room temperature. Another set was annexed to 500 °C and then cooled to room temperature before profiling. The samples measured with APXPS were exposed to 1 mbar of H_2O exposure and annealing up to 500 °C. The exposure was done in a near ambient pressure cell within the XPS system. High resolution scans of the Ag 3d, Zr 3d, O 1s, Si 2p, C 1s and N 1s region were collected and the peaks were fit to identify the chemical species as it is being exposed and annealed. The fitting was performed using our Artificial Intelligence analysis package XPS Neo. This study shows that materials used in TRISO fuel (SiC and ZrN) have a strong reaction to water and high temperature and having a barrier layer of carbon to can effectively prevent oxidation of the materials. The Ag is effectively stopped by the ZrN layer. Adding a layer of ZrN may prevent exposure to workers during shutdowns.

3:45pm AS-ThA-7 Surface Properties of Actinide Dioxide and Their Effect on Reactivity, *Enrique Batista, Gaoxue Wang, Ping Yang,* Los Alamos National Laboratory

Actinide compounds, especially actinide oxides, play a critical role in many stages of the nuclear fuel cycle. The behavior of these materials under different conditions dictates aspects from crystal growth to disposal of spent fuels, and much of those properties start at the surface. In that way, catalytic reactions that can lead to unstable storage conditions stemming from surface interactions with environmental species. Similarly, the morphology and structure is dictated environmental conditions and the reactivity of the incipient solid to the species present in solution. We have recently been focusing on surface properties induced by the presence of surface defects and surface interactions with environmental and non-environmental molecules. In this presentation we discuss the effect of surface defects in the reactivity and catalytic properties of the different exposed surfaces. Examples of reactions catalyzed by actinide surfaces to be discussed include water oxidation and nitrogen reduction to ammonia. Since these interactions can be deleterious, approaches to prevent them without affecting the desired properties of the material will also be discussed. We present results of these studies for a series of actinide dioxides (AnO2).

4:00pm AS-ThA-8 High-Efficient Bifacial Ge-incorporated Sb_2Se_3 Photovoltaic Devices Enabled with Cu_2O Back Buffer, *Sanghyun Lee, Kent Price,* University of Kentucky

Antimony Selenide (Sb_2Se_3) thin-film solar cells have gained attention as third-generation photovoltaic devices with promising properties. With a bandgap of 1.1 eV, it has a high absorption coefficient at visible light (>10^5 cm^{-1}), good carrier mobility (<15 cm^2/Vs), long carrier lifetime (<67 ns). Additionally, the simple binary nature of Sb_2Se_3, along with its high vapor pressure and low melting point, makes it suitable for various cost-effective deposition techniques. The versatility of Sb_2Se_3 thin-films has led to extensive research into their composition and the integration of different elements for a range of uses. Specifically, incorporating Germanium into Sb_2Se_3 (Ge-Sb_2Se_3) has shown promise as an effective polycrystalline absorber, especially when the Germanium content is maintained below 15%.

Enhancing the performance of polycrystalline Sb_2Se_3 devices could be achieved by capturing light on both the front and back sides through a bifacial device design. However, the advancement of bifacial devices in thin-film photovoltaic technologies has been limited due to their short carrier lifetimes (<100 nS), especially when compared to polysilicon-based devices. For example, the highest efficiencies recorded for rear-side illumination are 9.2% for CIGS, 8.0% for CdTe, and 9.0% for Kesterite solar cells. Research into optimizing bifacial photovoltaic structures is ongoing and a key is to select a transparent back buffer layer and a transparent conducting back

contact, adjusting the thickness and doping concentration to enhance the bifaciality factor (efficiency ratio of rear-to-front illumination).

In this study, we have investigated the feasibility of developing bifacial Ge-Sb$_2$Se$_3$ devices, beginning with the creation of Ge-Sb$_2$Se$_3$ absorber thin films and proceeding to assessing their optical characteristics. These characteristics were then employed as critical input parameters for the computational modeling and simulation of the bifacial device structure. Utilizing in-house MATLAB modeling suites connected to external Sentaurus TCAD simulators, we introduced innovative bifacial device designs aimed at enhancing device efficiency and further refined these models by adjusting a set of parameters. After carefully selecting a Cu$_2$O back buffer layer, the best efficiency of front-side illumination is 19.7 %, and Voc is 744.4 mV, Jsc is 40.14 mA/cm^2, and FF is (66.1 %). For the rear-side illumination, efficiency is 13.0 %, Voc is 724.5 mV, Jsc is 31.6 mA/cm^2, and FF is 56.7 %. All in one, the bifaciality factor of Ge-Sb$_2$Se$_3$ devices was 66 %.

Chemical Analysis and Imaging of Interfaces
Room 121 - Session CA-ThA

In Situ and Operando Analysis of Energy and Environmental Interfaces II

Moderators: Ashley Head, Brookhaven National Laboratory, **Andrei Kolmakov**, National Institute of Standards and Technology (NIST)

2:15pm **CA-ThA-1 Understanding the Molecular Rearrangement at Interface by Atomic Modeling**, *Difan Zhang, David Heldebrant,* Pacific Northwest National Laboratory; *Vassiliki-Alexandra Glezakou, Roger Rousseau,* Oak Ridge National Laboratory **INVITED**
A fundamental knowledge of the molecular rearrangement at surfaces, gas/liquid, and solid/liquid interfaces is crucial for many applications. The atomic modeling provides an important tool to quantify the structural variation and corresponding property changes at interfaces. In this presentation, I will highlight our recent studies that combined experimental characterization and computational modeling to reveal how molecules rearrange at different interfaces and how such nanostructure changes impact the interfacial properties. For example, the interfacial interactions between the carbon capture solvent and polymer membrane create unique channels that allow for faster diffusion of carbon oxide gas, enhancing the overall performance of the membrane/solvent device. Interestingly, the addition of a small fraction of water molecules further enhances the transport of carbon oxide gas through the membrane/solvent interface. In a different case, atomic modeling also demonstrates the improved selectivity of a graphene-oxide-modified polymer membrane for the separation of organics and water. Overall, these atomic simulations illustrate the effectiveness of modifying interfacial nanostructures to fine-tune interfacial transport and selectivity in complementary to experimental measurements.

3:00pm **CA-ThA-4 Advances in Electron Microscopy for Imaging Surfaces**, *Saumya Mukherjee, Stefan Böttcher,* SPECS Surface Nano Analysis GmbH, Germany; *Kai Kunze,* SPECS Surface Nano Analysis GmbH, Germany, Gibraltar; *Oliver Schaff,* SPECS Surface Nano Analysis GmbH, Germany
Electron beam-based microscopy faced the challenge of limited accessibility to surface sensitive information and damaging samples owing to the high-kinetic-energy-electron dependent working principle. This led to the development of alternative imaging techniques using low-energy and photo-emitted electrons [1,2]. Photoelectron emission microscopy (PEEM) and Low energy electron microscopy (LEEM) provides the ideal tool to probe surfaces without damaging the sample. Recent advancement in collaboration with Rudolf M. Tromp at IBM, this technique is pushed to produce energy filtered images highlighting its ability for Spectro-microscopy. A lateral resolution below few nanometers is achievable and allowed to measure a wide variety of surfaces. By usage of aperture combinations photoelectrons can be selected within element specific energy range. This provides contrast in images and allows to study delicate biological samples such as imaging of neurons in cells as shown by Boergens et. al [3]. In the present talk, I will discuss in further details the development in surface imaging and complement with results to illustrate the strength of LEEM-PEEM and attract attention of broader imaging community to use this tool beyond conventional electron microscopy on wide variety of sample surfaces.

References:

[1] Ernst Brüche. *Free electrons as probes of the construction of molecules.* In: *Ergebnisse der exakten Naturwissenschaften.* 8 (1929), 185–228.

[2] E. Bauer, "Low energy electron microscopy", Rep. Prog. Phys. 57, 895 (1994).

[3] Kevin M. Boergens, Gregg Wildenberg, Ruiyu Li, Lola Lambert, Amin Moradi, Guido Stam, Rudolf Tromp, Sense Jan van der Molen, Sarah B. King, Narayanan Kasthuri. *Photoemission electron microscopy for connectomics* (bioRxiv 2023.09.05.556423).

3:15pm **CA-ThA-5 The NanoMi Open-source Electron Microscope: Electronics Builds and SEM/STEM Image Generation**, *Darren Homeniuk,* National Research Council, Canada; *Mohammad Kamal,* University of Alberta Edmonton, Canada; *Marek Malac, Makoto Schreiber, Mark Salomons,* National Research Council of Canada; *Sam Ruttiman,* National Research Council, Canada; *Xuanhao Wang,* University of Alberta, Canada; *Ka Wing Kwan,* National Research Council of Canada; *Olivier Adkin-Kaya, Jesus Alejandro Marin Calzada,* University of Alberta, Canada; *Patrick Price, Martin Cloutier, Misa Hayashida,* National Research Council of Canada; *Ray Egerton,* University of Alberta, Canada; *Ken Harada,* RIKEN, Japan; *Yoshio Takahashi,* Hitachi, Ltd., Japan
We are developing a public license electron microscopy platform that we refer to as NanoMi [1,2]. Our goal is for others to be able to build their own version of the platform with minimal money and time invested. The NanoMi platform features modularity in its mechanical and electrical design for adaptability. Further information is available at nanomi.org.

The focus here is to present the electronics builds that support the mechanical hardware. Custom printed circuit boards have been designed, built and tested for the deflectors, beam-shaping stigmators, and piezoelectric movers. The designs were made to be modular, flexible, and cost effective. Through the use of a field-programmable gate array, image generation electronics referred to as a STEM scanner was also created. A first prototype of a custom-built STEM scanner is now complete which provides USB communications to a computer, generation of output X/Y scan signals in 16-bit resolution, simultaneous read-in of 8 14-bit resolution detection signals from the microscope, and an on-board RAM that stores image data until it is ready for transmission. Clock speeds for scanning are 25MHz, which allows the system to acquire samples from the microscope every 40 nanoseconds. A python user interface has been created which allows for settings changes and displays resulting images while allowing the user access to image analysis tools.

Figure 1 shows early results of a 200 mesh copper grid from the new STEM scanner and a comparison image from a simple data acquisition unit, while Figure 2 shows the user interface (UI) during acquisition. Figure 3 shows an image of the board while acquiring Figure 1.

References:

[1] nanomi.org and https://github.com/NRC-NANOmi/NanoMi
[2] M. Malac et. al, NanoMi: An open source electron microscope hardware and software platform, *Micron* **163** (2022) 103362.

3:30pm **CA-ThA-6 Advancing Carbon Dioxide Removal Technologies with Microscopic Insights Gained Using in-Situ and Operando Transmission Electron Microscopy**, *Wei-Chang David Yang,* National Institute of Standards and Technology (NIST) **INVITED**
Carbon dioxide removal is crucial for achieving net-zero emissions and mitigating climate change. Still, technological challenges like inconsistent sorbent performance and catalyst degradation hinder the deployment of carbon dioxide capture and conversion to value-added products [1,2]. Transition metals (Ni, Co, Fe), which catalyze CO$_2$ conversion into hydrocarbon fuels, face deactivation (coking) due to carbon deposition on the catalyst surface [3]. Burning off the carbon deposit coarsens the catalyst and deteriorates performance, highlighting the need for a nonthermal regeneration process. Meanwhile, many mesoporous sorbents impregnated with amine-based polymers for direct air capture show inconsistent performance in the literature [4], requiring high-spatial-resolution multimodal characterization for benchmarking from single pores to overall performance.

This talk covers how in-situ and operando methods developed for an environmental transmission electron microscope (ETEM) address the above issues. Firstly, we used an electron beam to excite and characterize localized surface plasmon (LSP) resonance on aluminum nanoparticles in

the presence of CO_2 using in-situ electron energy-loss spectroscopy (EELS). LSP field enhancement in the ultraviolet (UV) spectral range boosted the reverse Boudouard reaction (RBR), consuming carbon deposits and reactivating transition metal catalysts without heating.[5] We also coupled a TEM gas cell holder to gas chromatography-mass spectrometry (GC-MS) for operando detection of CO produced during the reaction, which can be reused for hydrocarbon fuel production. The findings offer a new solution for regenerating catalysts in CDR technology.

The second part of the talk focuses on developing in-situ cryogenic EELS imaging to characterize the adsorption ability of individual mesopores. The energy-loss near-edge structure (ELNES) obtained at cryogenic conditions showed the carbonyl core to $\pi^*_{C=O}$ transition ($\approx$ 289 eV) in ammonium carbamate [6], indicating the formation of chemisorbed species when exposed to dry CO_2. This is the first direct observation of CO_2 chemisorption on amine-impregnated mesoporous silicas at the single pore level. Ongoing studies aim to elucidate the amine chemistry and kinetics exposed to CO_2 within the mesopores.

References:

[1] S. Choi, J. H. Drese, and C. W. Jones, ChemSusChem **2** (2009), p. 785.

[2] R. W. Dorner et al., Energy Environ. Sci. **3** (2010) p. 884.

[3] M. D. Argyle and C. H. Bartholomew, Catalysts **5** (2015), p. 145.

[4] J. Wu et al., Chem. Eng. J. **450** (2022), p. 137958.

[5] C. Wang et al., Nat. Mater. **11** (2019), p. 47037.

[6] W. G. Urquhart and H. Ade, J. Phys. Chem. B **106** (2002), p. 8531.

4:00pm CA-ThA-8 In situ Photoelectron and Infrared Spectroscopic Studies of Materials Under Various Plasmas, *Ashley Head,* Brookhaven National Laboratory; *Tianhao Hu,* Brookhaven National Laboratory and State University of New York at Stony Brook; *Anibal Boscoboinik, Dario Stacchiola,* Brookhaven National Laboratory

Non-thermal plasma has been used to functionalize materials, to enhance the deposition of films, and as a reactant in catalysis. Depending on how plasma is made, there can be a range of gaseous species. Tools are needed for in situ studies in plasmas environments to understand the interactions with materials.[1,2] The application of infrared reflection absorption spectroscopy (IRRAS) and ambient pressure X-ray photoelectron spectroscopy to plasma environments will be discussed. As an example system, the functionalization and reduction of HKUST-1, a Cu-based metal-organic framework, has been studied with these techniques. IRRAS follows the framework stability while APXPS follows the Cu oxidation state changes. This correlative methodology is being baselined for future studies of plasma-enhanced catalysis of MOFs and metal oxides.

1. G. Li, D.N. Zakharov, S. Sikder, Y. Xu, X. tong, P. Dimitrakellis, J.A. Boscoboinik, *Nanomaterials*, **2024**, *14*, 290.

2. J.T. Diulus, A.E. Naclerio, J.A. Boscoboinik, A.R. Head, E. Strelcov, P.R. Kidambi, A. Kolmakov, *J. Chem. Phys. C* **2024,** *128,* 7591.

4:15pm CA-ThA-9 Chemical and Morphological Stability of Diamond Device Interfaces Under Operando Plasma-XPS, *J. Trey Diulus,* NIST-Gaithersburg; *Ashley Head, Jorge Anibal Boscoboinik,* Center for Functional Nanomaterials, BNL; *Andrei Kolmakov,* NIST-Gaithersburg

Device fabrication of field effect transistors (FET)s and other electronics are still largely dependent on Si, which has been the core semiconductor material for over seven decades. Alternatively, diamond is a promising semiconductor material, with its ultra-wide bandgap (5.5 eV), unmatched thermal conductivity, breakdown voltage, and high charge carrier mobility in the range of 1000 cm^2 V^{-1} s^{-1}, while offering improved chemical stability compared to other wide-bandgap alternatives, like SiC and GaN. However, surface hydrogenation via H_2 plasma is necessary to fabricate high-mobility diamond FETs, and the resulting surface is sensitive to ambient adsorbates that deteriorate the stability of surface conductivity with modern manufacturing processes. Alternatively, introducing the hydrogenation step later in the manufacturing process, i.e. after deposition of metal contacts or the gate dielectric, could allow for improved control of the diamond/metal or diamond/metal-oxide interfaces. Recently, high resolution x-ray photoelectron spectroscopy (XPS) collected under plasma conditions has been reported, allowing for *operando* chemical stability measurements. Herein, we prepared un-doped diamond and B-doped diamond samples with the standard contact metal stack (Ti/Pt/Au) deposited on half of the samples for plasma-XPS in H_2 and O_2 plasmas, respectively. Interestingly, a significant shift of ~50 eV to higher binding energy is seen in the XPS spectra of the un-doped diamond when a plasma is ignited at 13 Pa partial pressure of H_2 that is not seen in the spectra for the metalized part in the

same environment. Additionally, the B-doped diamond exposed to the same pressure of an O_2 plasma also does not exhibit a shift of the same magnitude as the un-doped diamond in H_2. The insulating nature of un-doped diamond creates this significant charging effect seen by XPS, which varies with the surface conductivity of diamond, suggesting a potential route to estimate the conductance state of diamond. Furthermore, with *ex situ* scanning electron microscopy, we see significant erosion in the Au coated surface that is exposed to H_2 plasma, likely due to a sputtering effect from ion impingement. Evidence of parasitic reactions from chamber wall exposure is also seen from residual gas analysis. This stresses the importance of designing a plasma that minimizes ions but maximizes neutrals, while also utilizing a well-cleaned chamber with minimal surface area to avoid scrubbing the chamber during plasma exposure. Overall, our efforts aim to better understand the interaction of plasma with diamond to provide researchers with a streamlined route towards diamond device manufacturing.

Spectroscopic Ellipsometry
Room 116 - Session EL1-ThA

Fundamental Ellipsometry Applications
Moderators: Tino Hofmann, University of North Carolina at Charlotte, **Megan Stokey**, Milwaukee School of Engineering

2:15pm **EL1-ThA-1 Mueller Matrix Ellipsometry for Optical Metasurfaces**, *Morten Kildemo,* Department of Physics; NTNU;Norway   **INVITED**
We review our recent works using spectroscopic Mueller Matrix Ellipsometry together with full wave modeling that has allowed on one hand to reveal new physics of optical plasmonic or dielectric metasurfaces [1-4], and on the other hand achieve high control of the manufactured metasurfaces. Furthermore, as metasurfaces are at the brink of a commercial breakthrough, we aim at showing that it is likely that this transition will be facilitated through the appropriate use of spectroscopic ellipsometry.

In part one of this talk, we discuss the physics of the full wave models of plasmonic metasurfaces realized from Mueller Matrix Ellipsometry, and in particular address the MME metrology of arrays of Au patches supporting both Gap Surface Plasmons and Surface Plasmon Polaritons[2,3]. A plane wave expansion of the field in the insulator shows that the fundamental localized resonances are composed of oppositely propagating modes, and we produce evidence that the sharp dispersive resonances observed in p-polarization, excited near the opening of diffracted orders, are grating coupled SPPs.

In part two, we discuss our recent work on design, manufacturing and a complete characterization of a class of optical metasurfaces: polarization beam splitting metasurfaces [4]. We describe our recently developed methodology using diffractive mode Mueller matrix spectroscopic ellipsometry (MMSE). Hence, we study both experimentally (and thereby with more conviction also numerically), how well these metasurfaces work in practice. In particular, we show that through appropriate control of the optical properties using MMSE, and feedback to both the nano-manufacture and design step, that we reach accurate and reproducible meta-surfaces. It is recalled that meta-surfaces are based on well-designed nano-resonators (in our case a-Si:H) that are manufactured on a plane interface.

References.

[1] P. M. Walmsness, T. Brakstad, B. B. Svendsen, J. P. Banon, J. C. Walmsley and M. Kildemo, JOSA B 36 (2019): E78-E87.

[2] P. M. Walmsness, N. Hale and M. Kildemo (2021). JOSA B 38 (2021): 2551-2561.

[3] P. M. Walmsness, N. Hale and M. Kildemo Opt. Lett. (2021) (in press).

[4] V. M. Bjelland, N. Hale, N. Schwarz, D. Vala, J. Høvik, and M. Kildemo, Opt. Express 32, 703-721 (2024).

3:00pm **EL1-ThA-4 In-Situ Optical Investigation of Electrochemically Controlled Surfaces and Thin Films**, *Christoph Cobet,* Luis Rosillo Orozco, Johannes Kepler University, Austria; *Saul Vazquez-Miranda,* ELI Beamlines Facility, Czechia; *Kurt Hingerl,* Johannes Kepler University, Austria
The applied electrical potential between an electrolyte and a solid electrode, whether it is a metal, semiconductor, polymer or a bio-membrane, could initiate versatile surface or film modifications. First of all, the potential simply redistribute charges. But in the new thermodynamic equilibrium adsorbates or even the conformational appearance could

change and thus determine the catalytic efficiency of an electrode material, for example. From an experimental point of view, the interfacial electric potential is, on the other hand, a very precise and powerful tool to manipulate thermodynamic equilibrium conditions. It can be modified over a huge range of several eV. Similar effects are otherwise only possible with extreme e.g. temperatures or pressures. However, the fundamental knowledge about the atomic structure and the related processes is still relatively limited compared to classical surface science in vacuum. The reasons are theoretical challenges in the description but primarily experimental limitations as electron based methods like XPS are not applicable at solid-liquid interfaces. Motivated by the increasing interests in this topic, we have started to use optical polarization methods such as spectroscopic ellipsometry (SE) and reflection anisotropy spectroscopy (RAS) to obtain new and complementary in-situ information. From experiments in vacuum or gas phase environment it is known that these methods could provide an exceptional surface sensitivity. This sensitivity allows us to observe the formation of surface quantum well states at a metal-electrolyte interface or an in-situ determination of the electronic band banding at semiconductor surfaces like the polar ZnO [0001] and [000-1] surface.

3:15pm EL1-ThA-5 Thz Electron Paramagnetic Resonance Generalized Spectroscopic Ellipsometry, Bloch Equations and Superconvergence Rules in the Frequency-Dependent Magnetic Susceptibility, *Mathias Schubert*, University of Nebraska-Lincoln, USA; *Viktor Rindert, Vanya Darakchieva,* Lund University, Sweden

A new optical technique is presented to detect the signatures of electron paramagnetic resonances in materials at terahertz frequencies and high magnetic fields using generalized spectroscopic ellipsometry.[1] Measurements dispense with the need for modulation techniques and resonance cavities.[1] The elements of the normalized Mueller matrix are determined, which contain hitherto undetected information about the polarization, frequency, and field response of unpaired electron spin moments including nuclear magnetic coupling.[1,2] Approaches to model analysis of the frequency dependent magnetic susceptibility tensor are discussed, Bloch equations are revisited, and an analogue to the Lyddane-Sachs-Teller relationship is shown from theory and experiment.[3,4] Examples include quantification of the defect properties of Fe and Cr in Ga_2O_3, N in 4H-SiC, and Fe in GaN.

[1] Terahertz electron paramagnetic resonance generalized spectroscopic ellipsometry: The magnetic response of the nitrogen defect in 4H-SiC, M. Schubert, S. Knight, S. Richter, P. Kuehne, V. Stanishev, A. Ruder, M. Stokey, R. Korlacki, K. Irmscher, P. Neugebauer, and V. Darakchieva, Appl. Phys. Lett. 120, 102101 (2022)

[2] Editors Highlights, High-field/high-frequency electron spin resonances of Fe-doped β-Ga2O3 by terahertz generalized ellipsometry: Monoclinic symmetry effects, Steffen Richter, Sean Knight, Oscar Bulancea-Lindvall, Sai Mu, Philipp Kühne, Megan Stokey, Alexander Ruder, Viktor Rindert, Viktor Ivády, Igor A. Abrikosov, Chris G. Van de Walle, Mathias Schubert, and Vanya Darakchieva, Phys. Rev. B. accepted (2024)

[3] The paramagnetic Lyddane-Sachs-Teller relation, Viktor Rindert, Vanya Darakchieva, Tapati Sarkar, Mathias Schubert, arXiv:2405.15382 [cond-mat.mtrl-sci]

[4] Bloch equations in Terahertz magnetic-resonance ellipsometry, Viktor Rindert, Steffen Richter, Philipp Kühne, Alexander Ruder, Vanya Darakchieva, Mathias Schubert, arXiv:2404.12805 [cond-mat.mtrl-sci]

Spectroscopic Ellipsometry
Room 116 - Session EL2-ThA

Evolving Methodology and Analytical Methods of Ellipsometry

Moderators: Nikolas Podraza, University of Toledo, **Mathias Schubert**, University of Nebraska - Lincoln

3:30pm EL2-ThA-6 Dirty Ellipsometry: Finding Success with Nonideal Samples and Nonideal Data in a Nonideal World, *Maxwell Junda, Avery Green, Xiang Li,* Covalent Metrology   **INVITED**

Ellipsometry has tremendous utility in commercial pursuits of science and engineering across a range of industries. One of the missions of Covalent Metrology is to make ellipsometry available to as broad a range of applications and users as possible. While much of the industrial scale ellipsometry used in production process monitoring involves repeated measurements of similar samples, Covalent's ellipsometry projects typically have an R&D flavor and are often one-time experiments meant to answer a specific question. Consequently, unavoidable constraints can sometimes lead to data or results that are hampered by nonidealities, and the overall project falls short of the clean results showcased in much of published literature (or at least the vision in our minds upon conceiving the experiments). Several common nonidealities can be understood strictly from a technical perspective: samples are not flat or too rough, films are too thin or inhomogeneous, or a multilayer structure has too many unknown layers. However, there are multiple other less obvious or less visible challenges to be navigated in providing primarily industry-focused ellipsometry measurement services. One example is that it's common to have incomplete information about test samples while planning an experiment, either due to intellectual property-related secrecy, or sometimes a simple lack of knowledge. Budget constraints are another typical nonideality where practicality dictates finding ways to obtain the best possible results to challenging, sometimes open-ended questions within a limited amount of time.

Covalent Metrology has worked on numerous projects in recent years wherein spectroscopic ellipsometry has produced useful results, despite "ugly" optical models, largely unknown samples, or rushed timelines. Specific examples will be described including: (1) optical models for highly inhomogeneous films that have quantitatively poor fits to noisy data yet can still provide key results, (2) use of spectroscopic ellipsometry to monitor the mechanical lapping of layered samples to thin the surface layer to submicron thickness and (3) pairing ellipsometry with other metrologies (such as TEM or XPS) to reverse engineer multi-layer optical filter stacks, the details of which were completely unknown at the project start. Lessons in evaluating the feasibility of hypothetical experiments will also be discussed, focusing on key descriptive factors of sample and experiment that gate project success, and on the value of ellipsometric simulations to both test measurement viability and tune experiment parameters prior to sample measurement.

4:00pm EL2-ThA-8 Numerical Ellipsometry: AI for Real-Time, in situ Process Control for Absorbing Films Growing on Unknown Transparent Substrates, *Frank Urban, David Barton,* Florida International University

Ellipsometry is an optical analytical method in which desired reflecting surface parameters are related to measurements by mathematical models. Recent work has shown that using AI methods can result in predicting reflecting surface parameters faster and more easily than by using iterative methods. This prior AI work used artificial neural networks applied to a growing absorbing film on a known substrate. Each different substrate required a set of separately trained networks across the wavelength spectrum thus necessitating training a new set of networks for each new substrate. The work presented here does not require substrate optical property data. Thus one set of spectroscopic networks can serve a large number of different substrates. This becomes possible by increasing the number of measurements per wavelength from two to three. For now we consider transparent substrates for which k2 = 0 or near zero. As before the non-iterative, stable, and fast performance lends itself to real-time, in situ monitoring of thin film growth. Examples for such growth of an absorbing metal film, chromium, will be given using two different substrates as proof of concept. The multilayer perceptron configuration consists of 6 input and 6 output neurons with two hidden layers of 80 neurons each. Solutions are performed at each wavelength independently and do not rely on fitting functions for optical properties.

4:15pm EL2-ThA-9 Gaining Insight Into InAs Plasma Treatments and Passivation via *in situ* Spectroscopic Ellipsometry, *John Murphy, Glenn Jeringan, Jill Nolde,* Naval Research Laboratory

Indium Arsenide (InAs) is a crucial material for infrared photodiode fabrication. However, its performance is severely hindered by the spontaneous formation of a complex native oxide on its surface, which leads to a high surface state density. This density pins the Fermi level within the conduction band, promoting the formation of shunt paths and increasing the surface recombination velocity. Consequently, these effects contribute to increased dark current and degraded detector performance in InAs-based devices.

To improve the performance of InAs-based devices, a suitable passivation of these dangling bonds must be developed. Atomic layer processing techniques, including remote plasma treatments and self-cleaning processes involving metalorganic precursors, have been explored as possible solutions. These methods aim to control and improve the InAs surface by removing the native oxide and subsequently passivating it with

wide-gap oxides using plasma-enhanced or thermal atomic layer deposition (PE-ALD).

When utilized in conjunction with ALD, in situ spectroscopic ellipsometry has proven invaluable to study ALD oxide growth; however, it can also be utilized to assess the quality of the InAs surface during plasma treatments. In this study, we employ *in situ* critical point analysis of pseudo-dielectric functions to evaluate the efficacy of remote plasma treatments in cleaning InAs (100) surfaces. We will correlate changes in the pseudo-dielectric function with alterations in surface morphology, as measured by atomic force microscopy, and surface chemistry, assessed via x-ray photoelectron spectroscopy. An air-free transfer apparatus will be used to prevent re-oxidation of the surface. Finally, we will characterize the surface state density of plasma-treated and Al_2O_3-passivated InAs surfaces using capacitance-voltage measurements.

Plasma Science and Technology
Room 124 - Session PS-ThA

Plasma Sources. Diagnostics and Control II

Moderators: David Boris, U.S. Naval Research Laboratory, **Necip Uner**, Middle East Technical University

2:15pm PS-ThA-1 Si Etch Characteristics in an Ultra-Low Electron Temperature CF₄ Plasma, *Chin-Wook Chung*, **Junyoung Park**, *Nayeon Kim, Jung-Eun Choi, Unjae Jung, Jiwon Jung, Min-Seok Kim,* Hanyang University, Korea

The etching characteristics of Si in an ultra-low electron temperature (ULET, T_e~0.7 eV) CF_4 plasma using a grid are investigated. Si etching is performed in the ULET CF_4 plasma, and the etch profile of Si is obtained by a Field Emission Scanning Electron Microscope (FE-SEM). When the substrate bias power is not applied, the etch profile of Si in an inductively coupled plasma (ICP, T_e~2 V) shows a rounded shape of the trench, while the etch profile of Si in the ULET plasma shows a flat shape. When a DC pulse bias voltage is applied to the ULET plasma, the etch profile shows a flat shape trench. However, when a substrate bias voltage frequency is 12.56 MHz, the electron temperature is increased and then the etch profile at the bottom of the trench shows a rounded shape as the bias voltage increases. These results show that the ULET plasma has a significant impact on the etch profile, which seems to be the reduction in charge accumulation in the trench due to the low electron temperature.

2:30pm PS-ThA-2 Temporal Evolution of Plasma Parameters and Electron Energy Distribution in a Pulsed-Modulated Capacitively Coupled Plasma, **Satadal Das**, University of Illinois at Urbana-Champaign; *David N. Ruzic,* University of Illinois at Urbana Champaign

Electron energy distribution function (EEDF) controls the production of any radical/species in plasma and the ion energy distribution on the substrate. In recent years, the pulsed-modulated capacitively coupled rf (PM-CCRF) plasma has gained much attention in the semiconductor industry due to the variations of electron temperature and plasma density over a wide range with the operating controls, i.e., the pulse repetition frequency, duty cycle and pulse shape. Recently, our group in CPMI, UIUC proposed a novel concept for controlling the time resolved EEDF at the substrate in a high-power impulse magnetron sputtering (HiPIMS) discharge. In our present work, we study the time resolved plasma parameters and EEDF for various rf powers and working gas pressures in the steady-state plasma and the effect of PM-CCRF on time resolved EEDF.

In our experiment, argon plasma is produced between two parallel-plates with 13.56 MHz rf supply. An external function generator is used for pulsing the rf power supply. An in-house developed single cylindrical Langmuir probe and two different measuring circuits are used to collect the I-V characteristics of plasma. We observe that in the steady-state condition both the plasma potential and density increase four times over the rf cycle. For the argon pressure of 5.7 mTorr (~ 0.76 Pa), the plasma potential and density reach at 33±0.65 Volts and (4.2±0.5)x10^{15} / m^3 respectively. We also measure the time resolved EEDF over the complete rf cycle and it does not change with rf times. However, the shapes are broadly like Maxwellian curve. From the EEDF we calculate the effective electron temperatures (T_{eff}) and it remains constant at 12±0.24 eV over the rf cycle. We also observe that both the plasma density and potential increase with increasing the rf power over the complete rf cycle; however, T_{eff}reduces. During the PM-CCRF, we measure the higher T_{eff} than the steady-state, i.e., 14.67±0.36 eV and it also does not change over the rf cycle. It is important that our measured EEDF gives the density of high energetic tail electrons (up to 50

eV) which are present in plasma. The experimental observations will be discussed in detail during the presentation.

2:45pm PS-ThA-3 Probing Microwave-Driven Plasmas: Investigating Ar Metastable Densities in Ar/N₂ Mixtures via LIF Technique, *Nafisa Tabassum, Corey Dechant,* North Carolina State University; *Abdullah Zafar,* Appled Materials; *David Peterson, Timothy Chen,* Applied Materials; *Steven Shannon,* North Carolina State University

The spatial and time-resolved density of metastable Ar species in microwave-driven plasmas operating at 2.45 GHz is systematically investigated by Laser-Induced Fluorescence (LIF). Effects of gas pressure and microwave power are investigated in the range of 70-200 mTorr and 25-150 W. LIF measurements involve the targeted excitation of metastable atoms using a tunable Nd:YAG laser producing nanosecond duration laser pulses at 100 Hz. The laser is tuned at 696.73 nm to pump the metastable $(^2P^0_{3/2})4s\ ^2[3/2]^0$, J=2 level to the $(^2P^0_{1/2})4p\ ^2[1/2]$, J=1 level. The fluorescence is observed from decay to the $(^2P^0_{3/2})4s\ ^2[3/2]^0$, J=1 level at 727.49 nm. The fluorescence is captured using an ICCD camera along with a bandpass filter centered at a wavelength of 730 nm with 10 nm FWHM bandwidth. The LIF intensity correlates with the expected variation in metastable density. A large density gradient is observed that correlates with power and pressure. Furthermore, the study extends to mapping the population density of metastable atoms by introducing nitrogen admixture (ranging from 0 to 20 %) into the argon plasma environment. The natural lifetime of fluorescence for pure argon and the impact of introducing nitrogen is examined. The effects of varying pressure, power levels and the quenching rate, are examined through fluorescence decay. Additionally, the experimental findings are compared with simulations conducted using the Multiphysics Object Oriented Simulation Environment (MOOSE) platform.

3:00pm PS-ThA-4 Diagnostics of Plasma Parameters and Surface Impedance by Measuring AC Probe Current at Harmonic Frequencies, *Junki Morozumi, Koji Eriguchi, Keiichiro Urabe,* Kyoto University, Japan

To understand the physical and chemical interaction between plasma and material, a methodology to diagnose both plasma and surface properties is necessary. From a physical point of view, the system consisting of bulk plasma, ion sheath, surface (modified) layer, and bulk material can be electrically modeled by a series of nonlinear resistance of the ion sheath and RC parallel circuit of the surface [1]. We have demonstrated that the impedance of the surface layer can be characterized during plasma exposure by measuring the amplitude and phase of the current flowing in the material with applying an AC voltage at various frequencies [2]. To obtain the plasma parameters, a method to analyze the nonlinear resistance of the ion sheath by measuring the current at harmonic frequencies of the applied AC voltage has been developed [3]. In recent years, we have studied the influence of the impedance of surface-modified layers on the generation of harmonic currents to develop a method to monitor plasma parameters and surface impedance simultaneously. In this study, we performed simultaneous monitoring of the plasma parameters and the surface resistance using a single metal probe in a reactive plasma generated in low-pressure Ar/O_2 gas. First, we analyze the nonlinear resistance of the ion sheath by applying AC voltage to the probe at a frequency where the surface impedance can be negligible. (>10 kHz in our system) Then, we calculate a relationship between the surface resistance and the amplitudes of harmonic currents at a frequency where the RC parallel circuit of the surface layer can be considered as a resistance. (<100 Hz) From these analyses and measurement data of the harmonic currents at the low frequency, we decide the surface resistance. By applying the AC voltage at the high and low frequencies alternately, we continuously measured the plasma parameters (electron temperature and ion density) and the surface resistance with a temporal resolution of approximately 10 s. The experimental results obtained in various discharge conditions indicate that the developed method can contribute to advanced control of plasma processing by providing data on plasma and surface properties.

[1] R. A. Olson, J. Appl. Phys. **43**, 2785 (1972).

[2] J. Morozumi *et al*., Jpn. J. Appl. Phys. **62**,SI1010 (2023).

[3] M.-H. Lee *et al*., J. Appl. Phys. **101**, 033305 (2007).

3:15pm PS-ThA-5 Plasma Diagnostics with a Transparent(ITO) Probe Based on the Floating Harmonic Method, *Chin-Wook Chung*, **Beom-Jun Seo**, *Hyeon-Ho Nahm, Deok-Whan Kim,* Hanyang University, Korea

The floating harmonic method is commonly employed for plasma diagnostics in semiconductor processing. From the ratio of harmonic currents flowing through a floating probe in the plasma, parameters such as

electron temperature and ion density can be measured. This technique is effective even when the probe is contaminated or coated with a thin dielectric film. In this study, we propose a diagnostic method that uses a floating probe with a tip made of ITO glass. By applying nonlinear circuit analysis and high-frequency voltage, we could have developed this novel approach. The primary advantage of our method is the ability to acquire both electrical and optical measurements simultaneously at the same location on the chamber wall. This dual measurement capability compensates for the inherent limitations of each individual measurement type, thereby significantly improving the accuracy and comprehensiveness of plasma diagnostics. We measured plasma parameters using the floating probe and performed optical emission spectroscopy measurements through the ITO glass.

3:30pm **PS-ThA-6 Time-Resolved Ion and Neutral Energy Distribution Function Study of High-Power Impulse Magnetron Sputtering with Positive Cathode Reversal using a Linear Magnetron**, *Tag Choi, Zachary Jeckell, Sam Pickholtz, John Miles, Dren Qerimi, David Ruzic,* University of Illinois at Urbana-Champaign

High-Power Impulse Magnetron Sputtering (HiPIMS) plasma is one of the physical vapor deposition (PVD) techniques that utilizes very short voltage pulses and a high peak currents. It can produce higher ionization fraction and denser plasma compared to conventional DC or pulsed DC magnetron sputtering, resulting in higher quality thin films such as denser films, smoother film surfaces, and better adhesion. Several years ago, positive cathode reversal technique was introduced to the HiPIMS sources, which reverses the polarity of the cathode to increase the energy of ions. This work aims to investigate the time-resolved ion and neutral energy distribution functions (IEDF/NEDF) of HiPIMS with positive cathode reversal discharge on a large area linear magnetron using Plasma Sampling Mass spectrometer (PSM) from Hiden Analytical Inc. This work includes IV traces of each pulse, which is used to confirm that the plasma produced is in HiPIMS plasma regime. Ultimately, a better understanding of HiPIMS plasma can contribute to improving film quality such as increasing uniformity, reducing stress, enhancing conductivity, and improving crystallinity. In this study, titanium (Ti) and tungsten (W) targets are utilized while parameters such as main pulse length between 10 – 100 us, peak current between 40 – 400 A, positive pulse length between 20 – 200 us, with/without positive voltage of the cathode, etc. are varied to understand how HiPIMS plasma properties vary.

3:45pm **PS-ThA-7 A Plasma Diagnostic Based Approach to Enabling Low Run-In for Sputter Deposited MoS$_2$ Solid Lubricants**, *Steven Larson, Alex Ming, Tomas Babuska, Michael Dugger, Frank DelRio, Mark Rodriguez, Robert Kolasinski, John Curry,* Sandia National Laboratories

Sputter deposited molybdenum disulfide (MoS$_2$) coatings have long been utilized as dry lubricants for aerospace applications because of their ultra-low friction and high performance in vacuum. Historically, sputter deposited MoS$_2$ films have faced challenges such as low density, poor aging resistance, and inconsistent performance across batches due to variability in material properties. To overcome these issues, the industry resorted to doping MoS$_2$ coatings with various metals (Ni, Ti, Al, Pb, Au, WSe) and nonmetals (Sb$_2$O$_3$, PbO, C), which, while improving density and consistency, undesirably increased initial friction, particularly after aging. In this study we present using a modern, plasma diagnostic based approach to develop high performance undoped MoS$_2$ coatings. Using these methods, we tie deposition parameters directly to ion flux and energy, and eventually to the resulting material properties (crystallinity, hardness, modulus, and stoichiometry) and tribological performance (friction, run-in, and wear rate) of the of the deposited films. The resulting undoped MoS$_2$ coatings demonstrate a near bulk density, and maintain an ultra-low initial friction, both before and after aging. Sandia National Laboratories is managed and operated by NTESS under DOE NNSA contract DE-NA0003525. SAND2024-06329A

4:00pm **PS-ThA-8 Investigations of Focus Ring Electrodes in Inductively Coupled Plasma**, *Tugba Piskin,* LAM Research; *Sang Ki Nam, Hyunjae Lee,* Samsung Electronics Co., Inc., Republic of Korea; *Mark J. Kushner,* University of Michigan, Ann Arbor

The microelectronics fabrication tools have progressed significantly to cover the demand and decrease the cost of ownership. The substrate biases are often used in inductively coupled plasma tools to control ion energy and angle distributions. However, applying bias to the electrode under the wafer can further cause sheath bending, resulting in poor ion angle distribution at the wafer edge. The plasma configuration at the wafer edge,

due to sharp electrical, chemical, and thermal gradients, causes non-uniform deposition and etch profiles in microelectronics processing.

The investigations were carried out for the secondary (ring) electrode located in the focus ring, in addition to the electrode under the wafer. The Ar/O$_2$:80/20 ICP operating at 10 mTorr with 450 W of continuous power was modeled with Hybrid Plasma Equipment Model (HPEM). The ion energy and angles at the edge of the wafer were tracked closely to observe changes. The improvement in the ion angles at the wafer edges was observed under various operating conditions. Parametric studies were completed by altering the operating conditions of the ring electrode and materials of the focus ring and chuck. It was found that the voltage of the ring electrode was the main control knob to achieve anisotropic profiles on the wafer edge. The ion energy and angle distributions will be presented with standard and proposed configurations in the parametric studies for bias voltages and materials.

** Work supported by Samsung Electronics and the National Science Foundation.

Surface Science
Room 120 - Session SS-ThA

Celebration of Robert J Madix and his Contributions to Surface Science & Reception

Moderators: Liney Árnadóttir, Oregon State University, **Dan Killelea**, Loyola University Chicago

2:15pm **SS-ThA-1 Thermodynamics and Kinetics of Elementary Reaction Steps on Late Transition Metal Catalysts: A Tribute to R. J. Madix**, *Charles T. Campbell,* University of Washington **INVITED**

I will review experimental and theoretical results from my own group concerning the thermodynamics and kinetics of elementary chemical reactions of importance in catalysis on late transition metal surfaces. I will focus on topics wherein my interest was inspired by work from Madix's group. These include: (1) the first proposed mechanism for methanol synthesis catalyzed by Cu, (2) measurements of pre-exponential factors and their interpretations through transition-state theory (TST), (3) measurements of the entropies of adsorbates and their trends, (4) using these together with elementary-step rate measurements and adsorbate energies to build microkinetic models for multi-step catalytic reactions, (5) a method for analyzing these that quantifies the extent to which the energy of each elementary-step transition state and intermediate controls the net rate, called the degree of rate control (DRC), and (6) interpreting kinetic isotope effects (KIEs) through DRC analysis.Work supported by NSF and DOE-OBES Chemical Sciences Division.

2:45pm **SS-ThA-3 Alkane Activation and Oxidation on Solid Surfaces**, *Jason Weaver,* University of Florida **INVITED**

In this talk, I will discuss pioneering advances made in Bob Madix's group to understand the mechanisms for alkane activation on metal surfaces and how this knowledge has guided my group's studies of alkane chemistry on late transition-metal oxide surfaces. Madix's work was among the first to distinguish direct vs. trapping-mediated mechanisms for alkane activation on surfaces, and clarify dynamic factors that influence these reactions. My talk will provide an overview of Madix's key findings about alkane adsorption and activation determined from supersonic molecular beam studies and molecular dynamics simulations, including mechanisms for alkane adsorption and initial C-H cleavage, energy exchange processes in alkane trapping and dynamic effects in direct alkane dissociative chemisorption. I will lastly discuss how this fundamental knowledge has influenced my research on the surface chemistry of late transition-metal oxides, and enabled new discoveries.

Thin Films
Room 115 - Session TF+EM-ThA

Thin Films for Microelectronics II: Ferroelectrics, Dielectrics, and Semiconductors

Moderators: Elton Graugnard, Boise State University, **Christophe Vallee**, University at Albany

2:45pm **TF+EM-ThA-3 Effect of Annealing Temperature on the Electrical Characteristics of Hf$_{0.5}$Zr$_{0.5}$O$_2$/InGaZnO Ferroelectric Field-Effect Transistor**, **Deokjoon Eom**, Hyunhee Kim, Woohui Lee, Jehoon Lee, Changyu Park, Jinsung Park, Heesoo Lee, Yong-Hoon Kim, Hyoungsub Kim, Sungkyunkwan University (SKKU), Republic of Korea

Recently, amorphous-oxide-semiconductor (AOS) materials, such as InGaZnO (IGZO), InZnO, and InWO, have been widely studied as channel materials for ferroelectric field-effect transistors (FeFETs) with a Hf$_{0.5}$Zr$_{0.5}$O$_2$ (HZO) gate dielectric because of their superior interface properties compared to Si channel-based FeFETs [1]. Typically, the fabrication of bottom-gate FeFETs with an AOS channel requires post-deposition annealing (PDA) after channel formation, which induces the formation of the ferroelectric orthorhombic phase in the HZO film and activates the AOS channel layer [2]. Meanwhile, it was reported that hydrogen atoms incorporated within the high-k film during atomic layer deposition (ALD) diffuse towards the IGZO channel region under thermal annealing, resulting in a notable change in the transfer characteristics of AOS-based FETs [3]. However, there is still a lack of research observing the detailed changes in the chemical and electrical properties of AOS-based FeFETs as a function of the PDA temperature.

In this presentation, we study the effect of PDA temperature on the electrical properties of bottom-gate HZO/IGZO FeFETs, where the PDA temperature was varied from 300 ℃ to 600 ℃ using rapid thermal annealing. The HZO and IGZO films were deposited in series via ALD with a Hf:Zr cycle ratio of 1:1 and sputtering of an IGZO target (In:Ga:Zn=1:1:1), respectively. Microstructural analysis revealed that, despite a significant volume shrinkage, the IGZO film maintained its amorphous structure after PDA at 600 ℃, while the ferroelectric phase emerged in the HZO films after PDA at 400−600 ℃. Distinct changes in hydrogen content within the IGZO/HZO stack were observed at different PDA temperatures. These changes in hydrogen content, along with the evolution of the ferroelectric phase, significantly influenced the transfer characteristics of the fabricated devices, including parameters such as the threshold voltage and hysteresis loop direction.

References

[1] J. Ajayan et al., Mater. Today Commun. **35**, 105591 (2023)

[2] F. Mo et al., IEEE J. Electron Devices Soc. **8**, 717 (2020)

[3] Y. Nam et al., RSC Adv. **8**, 5622 (2018)

3:00pm **TF+EM-ThA-4 Polarization Switching in Metal-Organic MBE-Grown Metal-Ferroelectric-Metal Heterostructures**, **Anusha Kamath Manjeshwar**[1], Zhifei Yang, University of Minnesota; Ankit Rao, Geoffrey Rojas, University of Minnesota, USA; Jiaxuan Wen, University of Minnesota; Chin-Hsiang Liao, Steven Koester, Richard James, Bharat Jalan, University of Minnesota, USA

Metal-ferroelectric-metal heterostructures have diverse applications ranging from ferroelectric non-volatile memories and sensing to neuromorphic computing. Traditionally, lead-based perovskite oxide ferroelectrics such as PZT and PMN-PT have been leading contenders in some of these applications. However, the toxicity of lead has prompted a renewed interest in the latent potential of lead-free ferroelectrics such as BaTiO$_3$ within the perovskite oxide family.

A long-standing challenge to unlock the potential of BaTiO$_3$ is systematically isolating the effect of parameters such as epitaxial strain, stoichiometry, and dimensionality on the ferroelectric properties of BaTiO$_3$ films. Producing reliable thin-film metal-ferroelectric-metal heterostructures for these studies depends on the (1) degree of control in the synthesis of each layer and (2) the atomic sharpness of the metal-ferroelectric interfaces. Despite molecular beam epitaxy (MBE) being the preferred growth method for heterostructures due to the high quality of the constituent layers and abrupt interfaces, the growth of ferroelectric BaTiO$_3$ with SrRuO$_3$ as metallic electrodes has two key challenges. First, elemental Ru is simultaneously difficult to evaporate and oxidize, requiring the use of electron-beam evaporators and potent oxidants which complicate stoichiometry control.

Second, balancing the retention of molecular flow and preserving ideal oxygen stoichiometry and, consequently, ferroelectricity restricts the oxygen background pressures to ~1-3 orders of magnitude lower than in other synthesis methods.

We present the growth of SrRuO$_3$ and BaTiO$_3$- films using metal-organic MBE, overcoming both challenges. Using a solid metal-organic precursor for Ru, we show the presence of an adsorption-controlled growth window within which the films self-regulate their cation stoichiometry for SrRuO$_3$ films on SrTiO$_3$ (001) substrates. We grow phase-pure, epitaxial, single-crystalline BaTiO$_3$ on SrRuO$_3$-buffered SrTiO$_3$ (001) substrates and note polarization switching with piezoresponse force microscopy for an applied bias of ± 6 V for a ~36 nm BaTiO$_3$ film without any post-growth oxygen annealing. We extend this technique to grow SrRuO$_3$/BaTiO$_3$/SrRuO$_3$ heterostructures on Nb-doped SrTiO$_3$ (001) substrates. For a ~40 nm BaTiO$_3$ layer, we observe a room-temperature static dielectric constant of ~400 and ideal capacitor-like behavior up to 1 kHz using impedance spectroscopy. We demonstrate hysteretic P-E curves with P_r ~ 17 μC cm^{-2} and an E_c ~ 221 kV cm^{-1} at f = 1 kHz. We will discuss the effect of stoichiometry, strain, and dimensionality on the structural and dielectric properties of metal-organic MBE-grown BaTiO$_3$.

3:15pm **TF+EM-ThA-5 Integration of Barium Titanate onto high-Al content AlGaN**, **Peter Dickens**, Andrew Allerman, Christian Harris, Brianna Klein, Sandia National Laboratories

Wide-bandgap transistor development for next generation power electronics is promising. This is due to their higher breakdown field and saturated electron velocity over traditional silicon insulated-gate bipolar-transistors, and within this development, a push towards wider bandgaps in the Al$_x$Ga$_{1-x}$N system by increasing the Al-content is desired to further improve breakdown strengths and power densities in devices.However, even with higher breakdown strength, electric field spikes between the gate-drain on high-electron-mobility-transistors can result in device failure far below the inherent breakdown strength of the semiconductor.This has led to the integration of high-permittivity dielectrics on top of the semiconductor to mitigate these spikes; BaTiO$_3$ has received much of the attention owing to its large dielectric constant.Here we will report on the integration of RF sputtered BaTiO$_3$ thin films onto Al$_{0.85}$Ga$_{0.15}$N substrates with a focus on the film morphology under specific deposition conditions.Results will focus on film morphology (x-ray diffraction, scanning electron microscopy, and atomic force microscopy) and stoichiometry (electron microprobe and x-ray fluorescence).

3:30pm **TF+EM-ThA-6 Understanding the Crystallization of BaTiO$_3$ Thin Films Prepared by Atomic Layer Deposition**, **Jiayi Chen**, Georgia Institute of Technology, USA, China; Asif Khan, Mark Losego, Georgia Institute of Technology, USA

This talk will discuss our work to develop a robust atomic layer deposition process (ALD) to create ferroelectric BaTiO$_3$ thin films.Ferroelectric materials are the potential candidates for future low voltage RAM and NAND memory because of their reversible two polarization states under low external electric field. While the CMOS compatible gate dielectric materials HfO$_2$ and Hf$_{0.5}$Zr$_{0.5}$O$_2$ are ferroelectric, they have high coercive fields which makes it difficult to lower switching voltages to below 1V. Therefore, perovskite ferroelectric materials, like BaTiO$_3$ are desirable to use for these applications because their coercive voltages can be an order of magnitude lower, approaching 0.1 V.However, such a ferroelectric needs to be deposited by ALD to match the conformality and small thickness requirements desired for RAM and NAND memory and unfortunately, the deposition of multicomponent, stoichiometric crystalline phases by ALD is extremely challenging.In this talk we will discuss our efforts to achieve ALD of BaTiO$_3$ and discuss its microstructure, chemistry, and electrical properties.Specifically we will discuss variations caused by the use of different titanium precursors and their potential to lead to reduced oxidation states, hydrated phases, or carbon contamination that can prevent crystallization.We will also discuss the influence of these chemistries on stoichiometry and the ability to get pure crystalline phases.

3:45pm TF+EM-ThA-7 Thermal and Plasma ALD BN for Low-k Applications, *Pegah Bagheri, Mahsa Konh, Ronald Pearlstein, Xinjian Lei, Haripin Chandra,* EMD Electronics, USA

Integration of low dielectric constant thin films in transistors and memories is a crucial step in realization of high speed, low-power and high-performance switches with lower parasite capacitance. Dielectric films, such as SiO_2 and Si_3N_4 and amorphous films deposited via Atomic Layer Deposition (ALD), were studied extensively providing a wide range of dielectric constants from 4.0 to 7.0. However, next generation of low-K spacer films targeting low-power high-performance applications requires conformal films on patterned structures with dielectric constant below silicon oxide (< 4.0) with good leakage current as low as <10^{-7} A.cm^2 at 1 MV/cm. Moreover, these thin films are expected to show high stability and high resistance to etching after exposure to HF which are typical integration steps in semiconductor device processing. Boron nitride is a new materials system in which lower dielectric constant than SiO_2 and Si_3N_4 is expected.- Previous study demonstrated PECVD boron nitride films with k as low as 2.0. Deposition of amorphous BN via ALD seems to be a superb candidate for the next generation of low-K spacer materials with dielectric constant below 3.0.

In this work, BN deposition was studied by use of BCl_3 and NH_3 as Boron and Nitrogen sources. NH_3 reacted with BCl_3 via surface-controlled reactions both thermally at 300°C, 400°C and 500°C and through NH_3 plasma generation at 200W and 300°C. ALD-deposited BN films showed uniformity of below 5% and thickness of 200Å measured by ellipsometer. Furthermore, electrical performance of BN films was measured by Capacitance-Voltage and Current-Voltage in Metal-Insulator-Semiconductor (MIS) structure using Mercury probe. To understand the incorporation of B and N and other elements such as C, O and Cl, crystallinity degree of the films and B-N bonding structures, X-ray Photoelectron Spectroscopy (XPS) and Fourier Transform Infrared Spectroscopy (FTIR) were utilized. Finally, the stability and resistance of ALD BN films to HF exposure was measured and monitored with time.

It was shown that amorphization degree increases at lower temperature and use of NH_3 plasma. However, thermally deposited BN at lower temperature showed high oxygen incorporation leading to degraded properties such as instability, low resistance to etching and poor electrical performances. Plasma ALD BN showed the lowest dielectric constant at 3.4 and wet etch rate below 0.03 time of the thermal oxide. Nevertheless, all BN films deposited with BCl_3 and NH_3 resulted in B/N~1.3 indicative of poor network formation. This led to formation of instable films with rough surfaces and degradation of bulk properties overtime.

4:00pm TF+EM-ThA-8 Quantum Chemical Analysis for Effects of Carbon and/or Nitrogen Bond-Types on Dielectric Constant and Leakage Current in Low-K Dielectric SiOCN Film, *Hu Li, Jianping Zhao, Peter Ventzek,* Tokyo Electron America, Inc.

Silicon Oxycarbon nitride (SiOCN) films are promising low dielectric(low-*k*) materials in semiconductor devices. The SiOCN film is fabricated using various fabrication technologies, that is, atomic layer deposition (ALD) and chemical vapor deposition (CVD), for specific applications such as inner spacers, gate spacers, and bottom contact etch stop layers (BCESL) in the deposition processes. Film deposition requires atomically precise control, with an increasing demand for nanoscale multilayer architectures. To further develop the SiOCN film properties and deposition processes, precise control of the bond-types in the fabrication process is required to maintain a low-k film property without increasing the risk of leakage current and/or decreasing the film density, particularly in a plasma enhanced ALD (PEALD) process. Chemically reactive species, such as radicals and energetic ions, generated in the plasma easily affect the film properties during plasma treatment by modifying the bond-types or surface structures. However, neither the effects of the reactive species on the formation of specific bond-types nor the effects of these bond types on the film properties are fully understood. Therefore, in this study, we examined the effects of various -Si-M-Si- bond-types (M=$C_xN_yH_z$) on the dielectric constant and leakage current using quantum chemical simulation. Our simulation modeling is based on experimental observations (XPS and FTIR). We found that when a carbon atom was present in a film with dangling bonds strongly affects the *k* values. The simulation results also showed that the Si-C-Si bond formed a mid-gap state, resulting in leakage current. When a carbon atom exists in the form of Si-CH_2-Si, no mid-gap state was observed, and such bond-type lowers the k value of the film. These results suggest that hydrogen plasma treatment may effectively prevent leakage current and yield low-k film structures. The effects of other bond-types and

their concentrations on the k values and leakage currentare discussed in this presentation.

4:15pm TF+EM-ThA-9 Electrical Measurement of in-situ Boron-Doped Epitaxial $Si_{1-x}Ge_x$ Films with Crystalline Defects, *Hyung Chul Shin, Deok Joon Eom,* Sungkyunkwan University (SKKU), Republic of Korea*; Dong Min Yoon,* Yonsei University, Republic of Korea*; Kang Won Kim, Hyung Keun Yoo,* Samsung Electronics Co., Republic of Korea*; Dae Hong Ko,* Yonsei University, Republic of Korea*; Hyoung Sub Kim,* Sungkyunkwan University (SKKU), Republic of Korea

Since its introduction as a channel-strain inducer in the early 2000s [1], in-situ epitaxial $Si_{1-x}Ge_x$ films doped with boron (B) have been continuously employed as source and drain (S/D) regions in high-performance p-channel transistors, including the most advanced devices with a gate-all-around structure [2]. However, when the B doping concentration exceeds 10^{21} atoms/cm^3 in the $Si_{1-x}Ge_x$ film, the B atoms may partially occupy interstitial sites or form clusters, producing defects that can reduce the electrical activation ratio [3]. Therefore, it is crucial to assess these defects through electrical characterization because they can significantly impact the final device performance [4]. Furthermore, while the effect of defects on the electrical properties of $Si_{1-x}Ge_x$/Si p^+−n diode has been studied in the context of their application to S/D regions [5], there remains a need for a more extensive study, including further investigation of their effect on the contact properties of $Si_{1-x}Ge_x$ to the overlaid metals.

This presentation discusses various electrical properties of in-situ B-doped $Si_{1-x}Ge_x$ films epitaxially grown on n-type Si substrates, where crystalline defects are intentionally induced by varying the thickness and doping concentration. Various electrical parameters, such as reverse leakage current, on/off ratio, ideality factor, and activation energy, were extracted from the current−voltage characteristics of the p^+−n diodes. These parameters' changes were correlated with the presence of defects in the $Si_{1-x}Ge_x$ film. In addition, the contact resistivity values measured by a circular transmission line method also exhibited a similar trend, demonstrating reliable results regarding the effect of these defects.

[1] S. Thompson et al., 2002 IEEE International Electron Devices Meeting (IEDM) 61−64

[2] S. Barraud et al., 2016 IEEE International Electron Devices Meeting (IEDM) 17.6.1−17.6.4

[3] A. Moriya et al., Thin Solid Films 343-344, 541−544 (1999)

[4] T. Bhat et al., IEEE Trans. Semicond. Manuf. 33, 291 (2020)

[5] H. Huang et al., J. Appl. Phys. 89, 5133−5137 (2001)

2D Materials
Room Central Hall - Session 2D-ThP

2D Materials Poster Session

2D-ThP-2 Topotactical Reaction of NiTe$_2$ Films with Excess Ni, *Nirosha Rajapakse*, *Matthias Batzill, Kinga Lasek,* University of South Florida
Compositional control of layered materials has the potential for creating new 2D materials with desirable properties. Certain transition metal dichalcogenides (TMDs) may be modified by incorporating excess metals in between the 2D sheets and covalently linking them. Such an incorporation of metals may be achieved in a topotaxy approach. Topotaxy is a solid-state reaction in which the crystal structure of a starting material is modified by incorporation of elements into the existing crystal structure. Here this is explored for NiTe$_2$ by reacting it with excess Ni. In our study, NiTe$_2$ thin films were synthesized by molecular beam epitaxy. Subsequently, the composition of these films can be modified by two different approaches; (i) by thermal annealing inducing loss of Te and (ii) by reaction with excess Ni. In both cases the change in the Ni:Te ratio is monitored by XPS and a structural transformation of the film is observed by LEED and STM. With an increase in the Ni-content a ($\sqrt{3} \times \sqrt{3}$) R30 superstructure is observed. In STM it can be shown that this new superstructure phase forms separate domains from the pure NiTe$_2$, suggesting that it is compositional line phase in the Ni-Te phase diagram. The superstructure can be explained by Ni insertion in between NiTe$_2$ layers. From XPS measurements, the Ni-concentration in the intercalation layer is close to 2/3 of the Ni concentration of a NiTe2 layer. The structural models for the intercalation are discussed based on DFT calculations. In STM nanoscale stripe like ripple networks are observed, which may indicate stacking faults in the intercalation layer due to lattice expansion. This study demonstrates a controlled approach to modify the composition of 2D NiTe$_2$, which may help to control proposed properties of the layered Ni-telluride system, such as superconducting phases [1] or make it a more efficient electrocatalyst [2]. In general, the approach of modifying NiTe$_2$ by topotaxy may also allow to modify it with other transition metals than Ni and this will be studied in future work.

Reference:

1. Pan, S. *et al.* On-Site Synthesis and Characterizations of Atomically-Thin Nickel Tellurides with Versatile Stoichiometric Phases through Self-Intercalation. *ACS Nano* **16**, 11444–11454 (2022).
2. Nappini, S. *et al.* Transition-Metal Dichalcogenide NiTe2: An Ambient-Stable Material for Catalysis and Nanoelectronics. *Adv. Funct. Mater.* **30**, (2020).

2D-ThP-3 Compositional Phase Control of MoTe$_{2-x}$ via Growth Temperature, Post-Growth Annealing, and Post-Growth Metal Incorporation, *Onyedikachi Alanwoko*, *Matthias Batzill,* University of South Florida
The ability to control and create different phases of two-dimensional(2D) materials like 2D transition metal dichalcogenides (TMDs) is a promising way of realizing new electronic and chemical properties of 2D materials. MoTe$_2$ has a small formation energy difference (~0.04ev) between its two competing 1H and 1T' phases. In MBE growth it has been shown that low growth temperatures favor the 1T' phase while at higher growth temperatures the 1H phase is preferentially obtained. However, the 1H phase is generally tellurium deficient resulting in the formation of Mo-rich mirror twin grain boundaries (MTBs). This tellurium deficiency at higher growth temperatures may be related to the preferential formation of the 1H phase. Here we show through scanning tunneling microscopy (STM) that the Te-deficiency in the monolayer film can be tuned and a new ordered 2D Mo-telluride phase is obtained. With increasing Te-deficiency the structures change from a disordered MTB network to superstructures with 2($\sqrt{7} \times \sqrt{7}$)R19.1 and 2($\sqrt{3} \times \sqrt{3}$)R30 periodicity. Some of these phases can be assigned to periodic MTB networks. However, the different phases require different synthesis procedures, and once formed these phases appear thermally stable in vacuum to 500°C when they all transform into a tubular Mo$_6$Te$_6$ phase. In this study, we systematically investigate the preparation conditions (which include the variation of the growth temperature, Te-desorption by post-growth vacuum annealing, and vapor deposition of Mo) enabling the controlled synthesis of these new phases. Particularly promising is the observation that we can react MoTe$_2$ with vapor-deposited Mo to obtain new ordered Te-deficient phase, this opens the possibility in future studies to react MoTe$_2$ with dissimilar TM to create new doped or alloyed 2D materials with potentially desirable properties.

2D-ThP-4 Influence of Fluorination and Oxygenation Sources on the Thermal Atomic Layer Etching of MoS$_2$, *Jacob Tenorio,* Boise State University
Atomic layer etching (ALE) has emerged as a pivotal technique in the precise fabrication of two-dimensional (2D) materials, particularly molybdenum disulfide (MoS$_2$), which holds promise in the semiconductor industry due to its high mobility in monolayer form. The ability to precisely etch amorphous and crystalline MoS$_2$ films provides a pathway for controlling thickness, which is critical to achieving desired electrical and optical properties. Previous studies used MoF$_6$ and H$_2$O in thermal ALE of MoS$_2$. Here, we report studies of alternate sources of fluorination and oxygenation and evaluate their impact on thermal ALE of MoS$_2$. Oxygen sources include water and ozone and fluorine sources include HF/Pyridine and MoF$_6$. Etch rates, uniformity, and surface chemistry post ALE were characterized using spectroscopic ellipsometry, atomic force microscopy, and X-ray photoelectron spectroscopy. Preliminary results indicate etch per cycle values of 0.5 A/cycle for MoF$_6$+H$_2$O at 200 C, 0.32 A/cycle for HF+H$_2$O at 250 C, and 0.26 A/cycle for HF+O$_3$ at 250 C. Additionally, ALE processes were combined with ALD to demonstrate thickness control for achieving few-layer MoS2.

2D-ThP-5 SCTD Through Ultraviolet Ozone Treatment for 2D Semiconductor Based Field Effect Transistors, *Jinhong Park, Juwon Lee,* Sungkyunkwan University (SKKU), Republic of Korea
The semiconductor industry is increasingly demanding high-performance, highly integrated circuits and the downscaling of conventional cell size has reached its limits. However, using silicon-based technology into downscaled technology has faced diverse challenges in ensuring high cell transistor performance. Therefore, many researchers are exploring the application of next generation semiconductor materials, such as two-dimensional(2D) metal dichalcogenides (TMDs). TMDs have received significant attention as a novel alternative to silicon in the semiconductor industry because of their excellent electrical, mechanical properties.

To achieve the performance of TMD-based devices, it is very important and essential to have good ohmic contact with Schottky barrier (SB) control. The SB is typically controlled by doping such as ion implantation and thermal diffusion. However, these conventional doping methods are impossible to TMDs because they can damage the crystal lattice or cause defects. This is due to the characteristics of TMDs having a thin layer structure.

Several doping schemes have been investigated to reduce contact resistance in TMD-based devices, including edge contact, interlayer depinning, and surface charge transfer doping (SCTD). Among them, SCTD is an effective doping technique for 2D semiconductors due to its non-destructiveness and simplicity.The SCTD mechanism follows an alignment of Fermi level at the semiconductor and dopant material interface. The difference in work function (WF) between semiconductors and metal oxides is the main factor in charge transfer. When the WF of the metal oxide is larger than that of the semiconductor, the electrons in the semiconductor spontaneously move to the metal oxide, the holes accumulate in the semiconductor, and the energy band at the interface bends upward, eventually the semiconductor is doped p-type. In this study, we introduce a method to oxidize WSe$_2$ to WO$_x$ using ultraviolet (UV) ozone treatment. By this method, the surface of WSe$_2$ is changed to WO$_x$, and WOx is a substance having a larger WF than WSe$_2$, and acts as a dopant material to perform p-type doping of WSe$_2$. As a result, we confirmed that the device characteristics of 2D WSe$_2$-based field effect transistor (FET) were improved.

The SB formed at the interface between the 2D semiconductors and the metals obstructs carrier injection and causes contact resistance to increase. Regardless of metals, an unintended high SB exists due to the Fermi level pinning effect. SCTD can selectively dope 2D semiconductors around metal contacts. Contact doping using SCTD is an effective way to lower the SB and improve the contact characteristics of 2D FETs.

2D-ThP-6 Plasma Assisted Etching of MoS$_2$: An Ab-Initio Molecular Dynamics(AIMD) Study, *Shoaib Khalid, Yuri Barsukov, Stephane Ethier, Igor Kaganovich,* Princeton University Plasma Physics Lab
Molybdenum disulfide (MoS$_2$) in its two-dimensional form represents a leading contender for the fabrication of advanced semiconductors. A critical attribute of MoS$_2$ is its adjustable bandgap, which varies with material thickness. This characteristic is vital for the tailored production of nanoelectronics devices, aligning with industry requirements for precision and flexibility.In this study, we employ ab initio molecular dynamics (AIMD) to investigate the etching mechanisms of Molybdenum disulfide (MoS$_2$).

Thursday Evening, November 7, 2024

Our results provide a basic understanding of plasma assisted etching process. By simulating the interaction of plasma with MoS_2 surfaces, we identify the critical factors that can influence the etching rates and patterns. Our calculations indicate that fluorinating the MoS_2 surface before subjecting it to Ar plasma bombardment can enhance etching yield and improve surface roughness. The presence of fluorine (F) at the surface forms a stronger F-S bond compared to the Mo-S bond, facilitating etching of the surface sulfur (S) atoms without significant damage to the underlying layers. This process is crucial for reducing the surface roughness of the unetched layers. Furthermore, the effect of Ar ion energy on etching yield and surface roughness is also addressed.

2D-ThP-10 Investigating the Electronic Structure of Bilayer Graphene/RuCl3 Heterostructure, *Aalok Tiwari, Souvik Sasmal, I-Hsuan Kao,* Carnegie Mellon University, USA*; Chris Jozwiak, Eli Rotenberg,* Advanced Light Source, Lawrence Berkeley National Laboratory*; Aaron Bostwick,* advanced light Source, Lawrence Berkeley National Laboratory*; Simranjeet Singh, Jyoti Katoch,* Carnegie Mellon University, USA

The stacking of two-dimensional materials to form van der Waals (vdW) heterostructures provides an unprecedented ability to tune electronic structure and engineer interfaces. RuCl3 has recently attracted significant attention as it is a Mott insulator, Kitaev material, and interfacing with graphene results in massive charge transfer, modifying their electronic properties. This can be exploited to create low-power devices for novel optoelectronic applications. In this talk, I will present a comparison of the electronic structure of bilayer graphene on interfacing with α-RuCl3 and hBN, using angle-resolved photoemission spectroscopy with nanoscale spatial resolution (nanoARPES). We can directly explore the charge transfer at the interface due to different work function of the bilayer graphene and RuCl3. I will discuss tuning the electronic structure in bilayer graphene/RuCl3 using electron doping via potassium atom deposition.

2D-ThP-11 2D Materials for Energy-Efficient Nanoelectronics, *Fei (Faye) Yao,* **Huamin Li,** University at Buffalo - SUNY

With the rise of graphene (Gr) since 2004, two-dimensional (2D) have been extensively explored for energy-efficient nanoelectronics due to their novel charge transport properties compared to conventional three-dimensional (3D) bulk materials. However, there are still challenges and issues for practical implementation of 2D materials. Here we take 2D semiconducting MoS2 as an example to review our recent research of energy-efficient nanoelectronics, ranging from materials synthesis to structure engineering and device demonstration. First, by functionalizing the growth substrate, we can achieve on-demand selective-growth of 2D MoS2 using chemical vapor deposition (CVD) and the electron mobility can be up to 20 cm2/Vs at room temperature. At the interface between MoS2 and SiO2 substrates, an interfacial tension can be induced due to a mismatch of thermal expansion coefficients, which creates an anisotropy of in-plane charge transport [1, 2] as well as a self-formed nanoscroll structure [3]. Second, at the interface between MoS2 and metal contact, a monolayer h-BN decoration can enable novel manipulation of charge transport through quantum tunneling, in contrast with conventional thermionic emission [3]. The contact resistance can be suppressed by both localized and generalized doping using transition metals [4]. Third, at the interface between MoS2 and other 2D materials, band-to-band Zener tunneling and cold-source charge injection can be enabled, giving rise to a superior transport factor (<60 meV/decade) in field-effect transistor (FET) configurations. These novel charge transport can be utilized to overcome the fundamental limit of "Boltzmann tyranny", and realize tunnel FETs and cold-source FETs with sub-60-mV/decade subthreshold swings [5-7] or novel anti-ambipolar FETs [8]. Fourth, at the interface between MoS2 and ferroelectric or ionic dielectrics, excellent electrostatic gating leads to a superior body factor (<1), and also improves the energy efficiency for transistor operation [9].

Reference

1. H. Li and co-workers, under review by Nature Communication.

2. H. Li and co-workers, DRC, Ann Arbor, MI, p. 133, 2019.

3. H. Li and co-workers, Adv. Mater., vol. 32, no. 2002716, 2020.

4. H. Li and co-workers, Nanoscale, vol. 12, pp. 17253, 2020.

5. H. Li and co-workers, IEEE IEDM, virtual, p.251, 2020.

6. H. Li and co-workers, ACS Nano, vol. 15, pp. 5762, 2021.

7. H. Li and co-workers, ACS Nano, vol. 11, pp. 9143, 2017.

8. H. Li and co-workers, JVST B, vol. 41, no. 053202, 2023.

9. H. Li and co-workers, Nano Express, vol. 4, no. 035002, 2023.

2D-ThP-12 Unique Nanowire and 2D Material Device Fabrication by Nanofrazor Technology, *Nicholas Hendricks, Fei Yang, Eliott Clerc, Jana Chaaban, Emine Çağın,* Heidelberg Instruments Nano AG, Switzerland

Thermal scanning probe lithography (t-SPL), enabled by the NanoFrazor technology, is a nanolithography technique particularly suitable for patterning, contacting, and modifying 2D materials and nanowires [1-6]. t-SPL generates patterns by scanning a heated ultrasharp tip over a sample surface to induce local changes. By using thermal energy as a stimulus, it is possible to perform various modifications to the sample via removal, conversion, or addition of/to the sample surface. Along with an ultrasharp tip, the t-SPL cantilever contains several other important functions such as an integrated thermal height sensor and an integrated heating element both of which are advantageous for generating devices from nanowires and 2D materials.

Nanowires and 2D materials have been the focus of intense academic and industrial research as these materials provide great promise as next generation electronic devices. However, when patterning electrical contacts to nanowires and 2D materials with conventional fabrication techniques (photolithography, electron beam lithography), the fabrication process becomes challenging and time consuming due to overlay requirements. These techniques can also lead to less than desired device performance due to damage from charged particles or ultraviolet irradiation, as well as contamination from residual resist. The issue of time intensive processing comes from the random positioning of nanowires and 2D material flakes on substrates which makes overlay challenging. This point of overlay is addressed with t-SPL by having an integrated thermal height sensor that allows for a non-invasive, in-situ measurement technique to detect buried nanowires or 2D materials prior to patterning. Such capabilities allow for real-time imaging and markerless overlay with high precision.

Within this presentation, the background and workings of t-SPL will be briefly introduced, nanostructuring on nanowires and 2D materials will be discussed along with electrical and optical device performance for nanowire and 2D material-based devices fabricated using t-SPL.

[1] X. Zheng et al., Nat. Commun., 11, 3463 (2020)

[2] X. Liu et al., APL Mater., 9, 011107 (2021)

[3] A. Conde-Rubio et al., ACS Applied Materials & Interfaces, 14, 37 (2022)

[4] S. Ghosh et al., ACS Appl. Mater. Interfaces, 15, 40709-40718 (2023)

[5] H. Ying et al., Device, 1, 100069 (2023)

[6] L. Shani et al., Nanotechnology, 35, 255302 (2024)

2D-ThP-15 Investigating the Interaction between MXene and Silane through High-Resolution X-ray Photoelectron Spectroscopy (XPS), *Mohamed Nejib Hedhili, Muhsin Ali, Sharat Chandra Barman, Dana Alsulaiman, Husam Niman Alshareef,* KAUST, Saudi Arabia

MXene grafted with silane combines the distinctive properties of MXene nanosheets with the functional advantages of silane molecules, thereby enhancing versatility and performance across various applications, from materials science to biomedical engineering. The modification of MXene with silane involves chemically bonding silane molecules onto the surface of MXene nanosheets. Despite this, the bonding mechanism between silane and MXene remains incompletely understood. This study introduces an XPS-based methodology to unequivocally determine the silane-MXene coupling. The approach involves comparing XPS results of pristine MXene with silane-modified MXene and MXene modified with silane-free agents like alcohol. The XPS data reveal the formation of Ti-O-Si bonds exclusively following silanization of MXene, with no such bonds observed in alcohol-modified MXene. Therefore, this analysis underscores the capability of XPS in identifying the bonding nature between silane and MXene.

2D-ThP-17 Study of Electronic and Optical Properties of TMD Heterostructures Grown by CVD, *Elycia Wright,* Clark Atlanta University*; Kedar Johnson,* Morehouse College*; Selena Coye, M.K. Indika Senevirathna, Michael D. Williams,* Clark Atlanta University

Transition metal dichalcogenides (TMDs) have attracted significant attention in the semiconductor field due to their unique properties. These properties, such as having a direct bandgap in the visible-infrared range, rich valley physical properties, and strong spin-orbit coupling, make them promising for various applications in electronics, optoelectronics, spintronics, and valleytronics. Furthermore, the distinct physical properties of 2D TMD heterostructures further enhance their potential, leading to a growing interest in researching heterostructures composed of different TMD materials.

Chemical vapor deposition (CVD) techniques have proven advantageous in producing TMD materials and their heterostructures with controlled thickness due to their low cost, high yield, and industrial compatibility. However, challenges, such as different growth windows among different TMD materials when growing high-quality large-area TMD heterostructures, need to be addressed.

This work will investigate new strategies for producing large-area TMD heterostructures, such as MoSe2/WS2, using various chemical vapor deposition (CVD) techniques. We will analyze the properties of these materials, including their band gap, optical phonon modes, and excitons, using Raman and photoluminescence spectroscopy.

2D-ThP-18 Synthesis, Fabrication and Mechanical Testing of Freestanding Few-Layer Draphene/Boron Nitride/Polymer Heterostacks Investigated Using Local and Non-Local Measurement Techniques, *Yoosuk Kim, Marcus Lespasio,* Saint Louis University, Department of Physics; *Elena Missale,* University of Trento, Department of Civil, Environmental and Mechanical Engineering, Italy; *Bashar Aziz,* Saint Louis University, Department of Physics; *Giorgio Speranza,* University of Trento, Department of Industrial Engineering,, Italy; *Ralu Divan, David J. Gosztola,* Argonne National Laboratory, Center for Nanoscale Materials; *Chi-Hou Lei,* University of Scranton, Department of Physics and Engineering; *Maria F. Pantano,* University of Trento, Department of Civil, Environmental and Mechanical Engineering, Italy; *Irma Kuljanishvili,* Saint Louis University, Department of Physics

Two-dimensional (2D) van der Waals materials and their heterostructures have gained significant interest in the past two decades due to their unique characteristics, including high aspect ratio and specific physical, electrical, and mechanical properties. Heterostructures composed of two or more 2D materials have emerged as key components for applications in metaphotonics, energy storage, transistors, photodiodes, memory, and photovoltaics. Understanding the mechanical properties of multilayered 2D materials is essential for practical applications which often involve advanced synthesis methods, developing new transfer techniques and designing custom platforms and architectures for their reliable evaluation and measurements. Techniques such as buckling or bending metrology, nanoindentation, bulge testing, atomic force microscopy (AFM) deflection tests, and tensile testing are necessary to measure these properties. Expanding the mechanical characterization of heterostructures like graphene and boron nitride, especially when capped with a polymeric layer, is vital for practical applications.

This study presents the synthesis, fabrication and mechanical testing of 2D hybrid heterostacks, consisting of few-layer boron nitride and two-three layered graphene heterostructures synthesized via chemical vapor deposition, capped with polymethyl methacrylate layer and suspended across ~200 μm wide trenches using a combined wet-dry transfer method. The mechanical characterization of the heterostacks was performed using two independent approaches: (a) non-local tensile testing (b) local load-displacement testing employing atomic force microscopy probes, complemented by finite element simulations. Both approaches provided new results, which are in good agreement with each other. Our findings offer new insights into a combined load capacity in complex multi-material two-dimensional hybrid systems, and underscore the potential of 2D hybrid heterostructures for advancing micro- and nano-scale device designs, particularly in applications requiring large-area mechanical stability.

Actinides and Rare Earths
Room Central Hall - Session AC-ThP

Actinides and Rare Earths Poster Session

AC-ThP-2 Nuclear Forensics, Fission Track Analysis , Star Segmentation and Classification Using Deep Learning, *Noam Elgad, Rami Babayew, Yaacov Yehuda-Zada,* Ben Gurion Uni., Israel; *Jan Lorincik,* Research Centre Řež, Czechia; *Mark Last, Itzhak Orion, Galit Katarivas-Levy,* Ben Gurion Uni., Israel; *Aryeh M. Weiss,* Bar Ilan University, Israel; **Itzhak Halevy,** Ben Gurion Uni., Israel

A novel approach for identifying star shapes in microscopic images via deep learning segmentation and classification.

Semi-automated data tagging: Introducing a new method for labeling data.

U-Net FCN model: Designed for segmenting various star-like shapes in single or multi-class scenarios.

Identifying shapes under a microscope involves separating the sampling paper into ~10,000 images, akin to finding a needle in a haystack due to its grueling nature and human eye limitations.

Star identification has evolved from manual eye scans to recent advancements in automatic

image processing tools.

This work employs a deep learning model, specifically the U-Net network, for segmentation and classification, integrating a 5-fold cross-validation analysis.

Work Content:

- A New image star database was created.
- Characterization of star types, model architecture, and optimization.
- Training for single and multi-class datasets.
- Automation of segmentation for batches of images.
- Research on optimizing frequency, epochs, and threshold settings,
- collaborating on simulated star classification.

Model achieved 92.04% accuracy for small single-class stars (<60μm), with 0.84 ROC area.

Segmentation of dual-class stars reached 86.3% validation accuracy.

Identification of simulated stars with varying leaf counts achieved 82.63% accuracy, while a computational model for higher magnitude stars achieved 0.90 ROC area.

AC-ThP-5 Grain Boundary and Heterointerface Structures and Defects in Pu Oxides: Classical Molecular Statics Study to Inform Further Ab Initio Investigation, *Larissa Woryk, Raymond Atta-Fynn, Aaron Kohnert, Sarah Hernandez,* Los Alamos National Laboratory

Plutonium metal forms a passivated oxide layer upon exposure to air, with varying stoichiometry depending on oxygen conditions. At lower temperatures, interfaces in oxides can facilitate corrosion via fast-transport pathways. This can result in further growth of the oxide layers, or of corrosion via other species, such as hydriding from the absorption and transport of hydrogen throughout the material. Any of these forms of corrosion can have implications on the stability and longevity of material in storage. Structural, defect, and transport properties can vary across different grain boundaries and heterointerface orientations. This study presents structures and associated energies of selected Pu_2O_3-PuO_2 interfaces and selected grain boundaries, calculated with molecular statics, along with associated defect structures and formation energies. Comparisons of interfacial energies can suggest which interfaces might be more prevalent in these materials, which could then play a larger role in influencing material properties and behavior. Comparisons of defect energies, both across different interfaces and between interfaces and in bulk, can suggest influence of interfaces in corrosion and in transport phenomena more broadly.

The Cooper-Rushton-Grimes interatomic potential will be utilized for the molecular statics calculations as it has demonstrated comparable values to experimental lattice and elastic constants, and thermal properties [1]. Where applicable, the modification to this potential to include Pu^{3+} is also included, as developed by Takoukam-Takoundjou, *et al* [2].

[1] M W D Cooper *et al* 2014 *J. Phys.: Condens. Matter* **26** 105401.

[2] C Takoukam-Takoundjou *et al* 2020 *J. Phys.: Condens. Matter* **32** 505702.

AC-ThP-6 Exploring the Combined Influence of Alpha Irradiation, Dissolved Hydrogen, and Palladium Addition on UO2 Corrosion Using a Microfluidic Electrochemical Cell, *Jennifer Yao, Jaeyoung Heo, Bruce McNamara, Eugene Ilton, Edgar Buck,* PNNL

Understanding the influence of alpha irradiation and dissolved hydrogen on the corrosion behavior of uranium dioxide (UO_2) is essential for evaluating the long-term impacts on storage environments.[1] Traditional experiments involving bulk SNF are typically costly due to stringent requirements for radiation shielding. To address these challenges, we have developed a novel particle-attached microfluidic electrochemical cell (PAMEC). This innovative microfluidic technique enables the multimodal analysis of UO_2 corrosion under simulated SNF storage conditions using minimal material quantities, significantly reducing both costs and risks of hazardous exposure.[2, 3]

Recently, we have incorporated palladium—a noble metal commonly found in irradiated nuclear fuel—into the UO_2 working electrode. This modification allows us to investigate how noble metals influence UO_2 degradation behavior in the presence of dissolved H_2 and alpha irradiation. In addition to utilizing electrochemical measurements such as open circuit

potential, for qualitative insights into the degradation of the UO_2 matrix, PAMEC's unique design supports in situ chemical imaging of the UO_2 surface. In this study we employ in situ imaging of the PAMEC working electrode using scanning electron microscopy (SEM) combined with energy-dispersive X-ray spectroscopy (EDS). This integration of techniques offers a comprehensive view that enhances our understanding of the UO_2 corrosion mechanism. The potential applications of this technology are extensive, providing a safer and more effective alternative for conducting corrosion studies on materials that pose high exposure risks or are difficult to access due to their rarity.

References:

1. *Long-term storage of spent nuclear fuel.* Nature Materials, 2015. **14**(3): p. 252-257.
2. *A microfluidic electrochemical cell for studying the corrosion of uranium dioxide (UO(2)).* RSC Adv, 2022. **12**(30): p. 19350-19358.
3. *Advancing radioactive material research method: the development of a novel in situ particle-attached microfluidic electrochemical cell.* Frontiers in Nuclear Engineering, 2023. **2**.

2D image transform was applied to emphasize these characteristics, and by adding color changes, it became possible to simultaneously represent three dimensions of data: time, intensity, and wavelength. By utilizing this characteristic and monitoring both the wavelengths where leaks are detected and where leaks are not detected, we were able to collect SPOES data corresponding to leak, offset, and normal conditions, and clearly to identify the distinguishing features of each.

When CNN was applied to multi-wavelength data, higher accurate leak detect was achieved compared to applying machine learning to single-wavelength data. In an environment with 2.5 Torr N2 gas flow and no offset variation, a leak of approximately 0.4 ppm was detected with a maximum validation accuracy of 97.46% when three types of filters and machine learning algorithms were applied to the single-wavelength data. In contrast, when CNN was applied for classification, the leak was detected with a validation accuracy of 99.5%.

AI/ML for Scientific Discovery
Room Central Hall - Session AIML-ThP

AI/ML for Scientific Discovery Poster Session

AIML-ThP-1 High-Throughput Ab Initio Screening of MAB Phases: Phase Stability and Mechanical Property Relationships, *Nikola Koutna,* TU Wien, Austria*; Lars Hultman,* Linköping Univ., IFM, Thin Film Physics Div., Sweden*; Paul Mayrhofer,* TU Wien, Austria*; Davide Sangiovanni,* Linköping Univ., IFM, Thin Film Physics Div., Sweden

MAB phases (MABs)—alternating atomically-thin ceramic and metallic-like layers—offer an interesting combination of mechanical, magnetocaloric, and catalytic properties, high-temperature oxidation resistance as well as damage tolerance, and have conquered a prominent role in the development of 2D materials. Despite their vast chemical and phase space, relatively few MABs have been achieved experimentally. In this poster I will present high-throughput ab initio screening of MABs that combine group 4–7 transition metals (M); Al, Si, Ga, Ge, or In (A); and boron (B). I will aim on revealing and understanding their phase stability trends and mechanical properties derived from elastic-constants-based descriptors. Considering the 1:1:1, 2:1:1, 2:1:2, 3:1:2, 3:1:3, and 3:1:4 M:A:B ratios and 10 competing phase prototypes for each elemental combination, the corresponding formation energy spectra of dynamically stable phases will be used to estimate the synthesisability of a single-phase MAB. Furthermore, the volumetric proximity of energetically-close MABs will allow identifying systems with possible transformation toughening abilities. The analysis of directional Cauchy pressures and Young's moduli will allow to analyze mechanical response parallel and normal to M–B/A layers. The poster will also suggest the most promising MAB candidates, including Nb_3AlB_4, Cr_2SiB_2, Mn_2SiB_2 or the already synthesised MoAlB.

AIML-ThP-2 Leak Detection Algorithm Through 2D Image Transformation of Multi-Wavelength Data from SPOES and Application of CNN, *Youngjun Yuk,* kihyun Kim, HyoYoung Kim, Tech University of Korea, Republic of Korea

In semiconductor processing, vacuum chambers are utilized for contamination prevention, plasma generation and so on. External air can enter through cracks in the chamber, which is referred to as a "leak." Leak can lead to a reduction in semiconductor yield. Therefore, it is essential to detect leaks in real-time. SPOES(Self-Plasma Optical Emission Spectroscopy) can analyze the gas composition inside the chamber in real-time through spectroscopic analysis and detect changes in gas composition instantaneously.

During the process of detecting leaks using SPOES, the DC offset can change due to various chamber conditions or noises such as thermal noise. If the offset changes, it becomes difficult to determine whether the increase in signal is due to a leak or a change in offset when only a single peak is used for leak detection. As a result, this can lead to the misclassification of leaks, thereby reducing the reliability of the system.

In this paper, to improve the misclassification problem, we propose a leak detection system with high reliability by using CNN classification algorithm with using 2D image transformation to monitor multi-wavelengths.

The most significant characteristics of the leak and offset change appear in the wavelengths where the signal changes. A leak signal affects only within specific wavelengths, whereas an offset change affects all wavelengths. A

Atomic Scale Processing Mini-Symposium
Room Central Hall - Session AP-ThP

Atomic Scale Processing Mini-Symposium Poster Session

AP-ThP-1 Surface Bromination as a Way to Prepare an Atomic-Layer Resist: A Path Towards Area-Selective Deposition, *John R. Mason,* Andrew V. Teplyakov, University of Delaware

As the size of components in electronics is shrinking, and their designs continue to get more complex, we need to find new approaches to meet these design needs. Area-selective atomic layer deposition is a rising technology to address the requirement for reaching single-nanometer sized features, while keeping the high uniformity that is desired. Silicon bromination has been demonstrated to produce a surface that can effectively resist metal oxide deposition; however, such a substrate is difficult to prepare outside of ultra-high vacuum conditions. This study aims to provide alternative methods for brominating silicon (100) wafers without the need for expensive ultra-high vacuum equipment, with strong ability to resist deposition of titanium dioxide. The study looks at various bromine-based chemistries in liquid phase to prepare a non-growth surface and compares the resulting selectivity for TiO_2 deposition using titanium tetrachloride or tetrakis(dimethylamido)titanium as a titanium source and water as the oxygen source. The process is compared with that on the traditional non-growth surface of hydrogen-terminated silicon and on the traditional growth surface of oxidized silicon.

Surface morphology is monitored with atomic force microscopy and scanning electron microscopy. Atomic concentrations are followed with X-ray photoelectron spectroscopy to observe surface ability to serve as a resist. In addition, the deposition process, the chemical environment of the inhibitor species, and the thickness of the ultimately deposited oxide layers are observed using TOF-SIMS.

AP-ThP-2 Thermal Atomic Layer Etching Process for 2D van der Waals Material $CrPS_4$, *Marissa Pina,* Matthew Whalen, John Xiao, Andrew Teplyakov, University of Delaware

$CrPS_4$ is a 2D van der Waals ternary transition metal chalcogenide (TTMC). $CrPS_4$ is an A-type antiferromagnetic semiconductor, in which spins within the same layer are aligned in same direction but spins in adjacent layers are aligned in opposite directions. Ferromagnetic and antiferromagnetic orderings are observed within the same layer and between adjacent layers, respectively. Consequently, thin flakes a few layers thick can display net or zero magnetization depending on whether there is an odd or even number of layers.

In order to understand the magnetism down to the monolayer limit and the dynamic excitations in magnons and excitons, and make devices based on 2D magnetic materials viable for industry, 2D materials with well-controlled layer structures have to be produced. The existing methods for controlling $CrPS_4$ thickness, such as mechanical and liquid exfoliation, are either not well controlled or introduce damage to the crystal structure. In this study, we will show that thermal atomic layer etching (ALE) can be used to controllably etch the 2D crystals of this material without contaminating them. Ultimately, using ALE to manipulate the thicknesses of these flakes will allow for controlling their magnetic and dynamic optical properties.

CrPS$_4$ flakes were exfoliated onto a gold film from a single crystal via mechanical exfoliation. Thermal ALE cycles were performed in an ultra-high vacuum chamber. Each cycle was performed at elevated temperature and consisted of a chlorine dose using a solid-state electrochemical chlorine source followed by an acetylacetone dose. Atomic force microscopy was used to determine an average etching rate of 0.10 ± 0.07 nm/cycle. Although the etching rate appeared to depend on the thickness of the flakes, this average removal rate was recorded for 75 different points for flakes ranging from 4 to 90 nm in thickness. ALE also removed the island defects caused by exfoliation from the top of the flakes. XPS and ToF-SIMS were used to follow chemical changes in the material and to interrogate the distribution of etchant components within the flakes. The formation of chemical species containing acetylacetonate ligands was confirmed for all the components (Cr, P, S) of this TTMC, and the chlorination was followed in ToF-SIMS depth-profiling experiments. The ALE process that resulted in controlled material removal did not result in measurable surface contamination. Importantly, the etching of CrPS$_4$ is highly temperature-dependent, as lowering the process temperature by even 30 °C does not result in noticeable etching. Further, faster etching (above ALE regime) can be achieved using higher temperatures and higher pressures.

AP-ThP-3 Conversion of TiO$_2$ ALD Precursor Selectivity via Amination of Chlorinated Silicon with Primary Amines, *Tyler Parke, John Mason, Andrew Teplyakov,* University of Delaware

Area-selective atomic layer deposition (AS-ALD) is a rapidly developing technique which allows for the fabrication of 3D nanoelectronic architectures. AS-ALD schemes may be made more versatile by introducing surface modification steps which 'switch' non-growth surfaces, which are unreactive to ALD precursors, to reactive growth surfaces. While several studies have demonstrated the conversion of chlorine- or hydrogen-terminated silicon to amino-terminated silicon, both in solution and gas-phase reactions, few have focused on the subsequent use of these prepared surfaces as ALD substrates. Chlorinated silicon resists were modified in vacuo with ammonia and methylamine to produce amino surface ligands and TiO2 ALD was performed on each resulting surface to test its reactivity as a growth or non-growth surface in the presence of titanium tetrachloride or tetrakis(dimethylamino)titanium (TDMAT). Deposition was confirmed by XPS and surface species resulting from reaction of titanium precursors on each surface were probed with in situ FTIR and ex situ time-of-flight secondary ion mass spectrometry (ToF-SIMS). The experimental surface species data was paired with density functional theory (DFT) simulations of the local surface structure to propose a reaction pathway.

AP-ThP-4 Atomic Layer Deposition of Ruthenium and Ruthenium Oxide Thin Films for Electrochemical Water Splitting, *Swapnil Nalawade, Dhananjay Kumar, Shyam Aravamudhan,* North Carolina A&T State University

Electrochemical water splitting is a unique and sustainable hydrogen production cycle with water and oxygen as the only by-products. However, at present, the primary hurdle for hydrogen production from water is the lack of materials that can support the reaction with high efficiency. Addressing the hydrogen challenge requires innovations in catalysis for the oxygen evolution reaction (OER) and hydrogen evolution reaction (HER), the two electrochemical reactions in water splitting. Among the many electrocatalysts, thin films of Ruthenium and Ruthenium Oxide for OER and HER are very promising because of their high catalytic activity, broad pH applicability and long-term stability. In this work, we studied as-grown and post-annealed properties of Ruthenium and Ruthenium Oxide thin films deposited by thermal atomic layer deposition (ALD) technique. ALD Ru films were deposited at 300C using Ru(EthylCycloPentaDienyl)2 and oxygen as co-reactants and characterized for morphology, composition, and resistivity. Post-annealing at higher temperatures (400-600C) in oxygen environment resulted in phase transformation of the as-grown Ru to RuO2. These phase changes were confirmed using XRD, XPS, Raman and resistivity measurements. Finally, repetitive redox cycling (electrochemical studies) were conducted to study thin film stability and polarization behavior.

AP-ThP-5 Fabrication of p-n Junction Photodiodes using Low-Temperature ALD grown ZnO and NiO films on Si substrates, *Hanyu Jiang, Thong Cu, Samzid Bin Hafiz, Heba Saleh, Fatih Bayansal, Iram Sifat, Alexander Agrios,* **Necmi BIYIKLI,** University of Connecticut

In this study, we present findings on the photodiodes made of ALD grown ZnO and NiO films. The ZnO deposition process on p-type Si substrate samples involved the use of diethylzinc as the metal precursor and H$_2$O as the co-reactant. The thermal ALD deposition was done at 120 °C with 20 sccm of N$_2$ flow, 500 ms pulse time for 400 cycles. The thickness of ZnO film was measured as ~48 nm. On the other hand, NiO deposition on n-type Si substrate samples required nickelocene (bis(cyclopentadienyl)nickel) as precursor and O$_2$ plasma as co-reactant. The plasma-ALD process was conducted at 200 °C with 100W RF plasma power. The plasma duration was 20 seconds and total deposition run was 800 cycles. The resulting thickness of NiO film was ~34 nm.

The p-n photodiode device layout was similar to the design of a commercial solar cell with interdigitated electrode metal contacts. We designed 1 x 1 cm devices, in which we used 5/5 μm finger-width/spacing to collect generated photocurrent. After metal-oxide deposition, we fabricated the patterned contact metals via photolithography and lift-off process. 20/30 nm Ti/Al metal layers were e-beam evaporated on n-ZnO/p-Si and p-NiO/n-Si samples. The samples were then socked in remover solution where metal lift-off process was completed with ultrasonication.

The I-V curves of ZnO/Si and NiO/Si devices show typical characteristics of back-to-back Schottky-diode and p-n junction photodiode, respectively. ZnO/Si Schottky photodiodes typically display rectifying behavior, showing minimal current flow under reverse bias due to the presence of a Schottky barrier, followed by a steep increase in reverse current beyond the barrier height. Under forward bias, rectifying behavior is observed, with a turn-on voltage indicating the onset of conduction. For NiO/Si p-n junction photodiode, the curve exhibits a clear rectifying behavior with exponentially increasing current at positive bias voltage, signaling unhindered current flow. Conversely, minimal current is observed under negative reverse bias voltages. These initial results indicate promise in achieving high-performance UV photodetector characteristics using both as-grown crystalline n-type ZnO and p-type NiO layers grown via thermal and plasma-assisted ALD, respectively at substrate temperatures less than 200 °C.

AP-ThP-6 Design of Gas Flow Field for a Microchannel Flow ALD Processing Chamber, *Kyung-Hoon Yoo,* Korea Institute of Industrial Technology, Republic of Korea*; Geun-Soo Song,* KUMYOUNG ENG Inc., Republic of Korea*; Chun-Sik Kim,* TNG Co., Republic of Korea*; Jun-Hyung Hwang, Hye-Jin Lee, Sang-Ho Lee, Ju-Young Woo,* Korea Institute of Industrial Technology, Republic of Korea*; Kun-Hyung Lee,* Samasung Display, Republic of Korea

It is necessary to establish a sustainable manufacturing technology for a high-productivity, high-efficiency ALD processing chamber and cluster tool that reduce the intrinsic excessive consumption of energy and materials because semiconductor ALD processes can be a concern for economic and environmental feasibility.[1,2] In the present study, as the part of countermeasure to the excessive consumption, a microchannel flow ALD processing chamber is considered for the optimized design with the process space volume decreased. The changes in the flow field of nitrogen in the process space of the processing chamber with the gap size of 1 mm or 10 mm respectively are observed at 400 °C, utilizing computational fluid CFD numerical analysis. For the present nitrogen flow field with a inlet static pressure of 1 or 10 Torr and a inlet mass flowrate of $4.233 \times 10\text{-}6$, the Knudsen number Kn=0.223 and Reynolds number Re=1.474 are evaluated. The continuity, momentum and energy equations of a steady-state compressible laminar flow field are considered.[3,4]

References

1. C.Y. Yuan and D.A. Dornfeld, *J. of Manufacturing Science and Engineering* **132**, 030918 (2010).

2. E. J. McInerney, *J. Vac. Sci. Technol. A* **35**, 01B138 (2017).

3. M. R. Shaeri, T.-C. Jen, C. Y. Yuan and M. Behnia, *International Journal of Heat and Mass Transfer* **89**, 468 (2015).

4. D. Pan, L. Ma, Y Xie, T.C. Jen and C. Yuan, *J. Vac. Sci. Technol. A* **33**, 021511 (2015).

Applied Surface Science
Room Central Hall - Session AS-ThP

Applied Surface Science Poster Session

AS-ThP-1 Advances in the Chemical Composition Quantification of Surface and Volume Using HAXPES Data, *Dulce-Maria Guzman-Bucio,* CINVESTAV-Unidad Queretaro, Mexico; *Jorge-Adalberto Huerta-Ruelas,* CICATA Queretaro, Mexico; *Orlando Cortazar-Martinez,* CINVESTAV-Unidad Queretaro, Mexico; *Dagoberto Cabrera-German,* Universidad de Sonora, Mexico; *Jorge-Alejandro Torres-Ochoa,* Universidad Politecnica de Juventino Rosas, Mexico; *Abraham-Jorge Carmona-Carmona,* CINVESTAV-Unidad Queretaro, Mexico; *Oscar Ceballos-Sanchez,* Universidad de Guadalajara, Mexico; *Will Limestall, Zhengrong Lee, Mark Warren, Jeff Terry,* Illinois Institute of Technology; *Alberto Herrera-Gomez,* CINVESTAV-Unidad Queretaro, Mexico

In recent decades, HAXPES has gained scientific and technological relevance.This method offers several advantages, including the capability to analyze both the surface and bulk of materials. It allows for the analysis of buried layers without requiring the removal of top surface layers by ion sputtering, thereby eliminating sample damage. Additionally, the interference with Auger signals decreases. However, there are significant challenges for quantitatively interpreting the data.

As with XPS, assessing chemical composition with HAXPES requires differential photoelectric cross-sections. For HAXPES, it is essential to consider the increasing relevance of non-dipole terms.

This study presents a summary of the requirements and challenges associated with employing HAXPES data for chemical composition analysis of iron oxide samples. Additionally, we provide insights into the application of a MultiLayer-Method to analyze multilayered films using photoemission data from a partially oxidized iron film as the X-ray crossed the iron K edge. These experiments were carried out at Beamline 10-ID-B at the Argonne National Laboratory.

AS-ThP-2 Basic Aspects of the Asymmetry of Lineshapes in Photoemission Spectra Caused by a Cascade of Excitations of Fermi-Level Electrons, *Anthony Dutoi,* University of the Pacific; *Alberto Herrera-Gomez,* Cinvestav, Mexico; *Dulce Guzman-Bucio,* CINVESTAV-Unidad Queretaro, Mexico

The effect of cascade excitations of Fermi-level electrons on the lineshape of photoemission spectra was treated by Doniach and Sunjic (DS) in 1970.[1] Their derived lineshape has many issues such as its lack of integrability and failure to closely reproduce experimental data.[2] We analyze this problem using a formalism rooted only in the basic quantum mechanics of resonances with a minimalist diagrammatic veneer to categorize the many-body of processes (Tougaard losses, plasmons/hole-shielding, multiplet structure, and perhaps the Shirley background). The accounting for these processes can be done with varying levels of rigor, from simple consideration of energy scales, oscillator strengths, and couplings, through to *ab initio* calculations of matrix elements. A density-matrix formulation in the many-body space can be applied to remove spurious interferences of states that have ill-defined/incoherent relative phases (differ from shot to shot, due to pulse noise, sample inhomogeneities, temperature, *etc*.). In our work, we will apply the simplest level of semi-quantitative analysis to propose possible alternatives to the problematic DS lineshape. For example, an incoherent superposition of exponential decay in time yields a lineshape that is asymmetric but integrable.

[1] S. Doniach and M. Šunjic, "Many-electron singularity in X-ray photoemission and X-ray line spectra from metals," Journal of Physics C: Solid State Physics **3**, 285–291 (1970).

[2] A. Herrera-Gomez, D.M. Guzman-Bucio, A.J. Carmona-Carmona, O. Cortazar-Martinez, M. Mayorga-Garay, D. Cabrera-German, C.A. Ospina-Ocampo, B.V. Crist, and J. Raboño-Borbolla, "Double Lorentzian lineshape for asymmetric peaks in photoelectron spectroscopy," Journal of Vacuum Science & Technology A **41**(4), (2023).

[3] A. Herrera-Gomez, D. Cabrera-German, A. D. Dutoi, M. Vazquez-Lepe, S. Aguirre-Tostado, P. Pianetta, D. Nordlund, O. Cortazar-Martinez, A. Torres-Ochoa, O. Ceballos-Sanchez, and L. Gomez-Muñoz, "Intensity modulation of the Shirley background of the Cr 3p spectra with photon energies around the Cr 2p edge," Surface and Interface Analysis **50**, 246–252 (2018).

AS-ThP-3 XPS Study of the Initial Oxidation of Iron for Ultrathin and Thick Films, *Orlando Cortazar-Martinez, Jorge Alejandro Torres Ochoa, Jesus Fernando Fabian-Jacobi, Joaquin Raboño Borbolla, Alberto Herrera-Gomez,* CINVESTAV-Unidad Queretaro, Mexico

We studied the initial stages of oxidation of ultrathin and thick iron films on silicon. Clean films were exposed to a controlled ultra-pure oxygen atmosphere with varying gas dosages at room temperature. The characterization was done with angle-resolved XPS [1]; the data was analyzed using robust analysis techniques including the block approach [2] and simultaneous fitting, as well as background modeling with the active approach, Shirley-Vegh-Salvi-Castle (SVSC), and the Two-Parameter Tougaard background [3].

While thick films oxidize in a layer-by-layer fashion, thin films exhibit oxidation by clusters or islands. The multilayer method (MLM) was employed to quantify the ultrathin films' chemical composition and structure. In both cases, Fe_2O_3 is the oxide composition.

This work was partially financed by Proyecto Fronteras 58518, Conahcyt, Mexico.

[1] A. Herrera-Gomez, O. Cortazar-Martínez, J.F. Fabian-Jocobi, A. Carmona-Carmona, J.G. Raboño-Borbolla, M. Bravo-Sanchez, J.A. Huerta-Ruelas, A self-consistent multiple-peak structure of the photoemission spectra of metallic Fe 2p as a function of film thickness, Surface and Interface Analysis 52 (2020) 591–599. https://doi.org/10.1002/sia.6796.

[2] A. Herrera-Gomez, M. Bravo-Sanchez, O. Ceballos-Sanchez, M.O.O. Vazquez-Lepe, Practical methods for background subtraction in photoemission spectra, Surface and Interface Analysis 46 (2014) 897–905. https://doi.org/10.1002/sia.5453.

[3] S. Tougaard, Universality classes of inelastic electron scattering cross sections, Surf. Interface Anal. 25 (1997) 137. https://doi.org/10.1002/(SICI)1096-9918(199703)25:3<137::AID-SIA230>3.0.CO;2-L.

AS-ThP-4 Rapid Assessment of Detector Linearity and Deadtime Correction for XPS Instruments, *Benjamen Reed, Alexander Shard,* National Physical Laboratory, UK

Confidence in the intensity scale of a photoelectron spectrometer is vital for quantitative analysis of photoelectron spectra. This is because the integrated area under a core level peak is proportional to the atomic fraction of that element in the sample. Sample dependent factors aside, the XPS analyst must calibrate for the intensity response (or transmission function) of their analyser, which is largely a result of electrostatic lens column and is unique for each instrument. However, even before a spectrum is acquired, there must be confidence that the measured count rate of the analyser's detection system is correct. For example, at high count rates, the detector may exhibit a non-linear response that significantly effects the measured count rates, and therefore the peak intensities from which atomic fractions are calculated. At even higher count rates, detector saturation may occur. So, although it is tempting to conduct XPS measurements with increased count rates (e.g. by increasing X-ray emission with high throughput electrostatic lens modes and collimation settings) with the intent to improve signal-to-noise and reduce experiment times, this approach is stymied by the limits of the detection system itself.

Recently an interlaboratory study on XPS intensity calibration was organised by the National Physical Laboratory (NPL) under the auspices of the Versailles Project on Advanced Materials and Standards (VAMAS). In the interlaboratory study, a number of datasets on sputter cleaned gold were submitted that exhibited evidence of detector non-linearities. It appears then, that awareness of this limitation of photoelectron detectors may not be universally known throughout the XPS users' community. Therefore, we shall briefly introduce these concepts and then present a straightforward method for rapidly assessing the linearity and deadtime correction for photoelectron spectrometer detectors which is based on the spectrum ratio method from Annex A of ISO 21270 ("Surface chemical analysis — X-ray photoelectron and Auger electron spectrometers — Linearity of intensity scale").

AS-ThP-5 ASSD Student Award Finalist Talk: Dry and Wet Etching of Single-Crystal AlN, *Hsiao-Hsuan Wan*[1], *Chao-Ching Chiang, Jian-Sian Li,* University of Florida; *Nahid Sultan Al-Mamun, Aman Haque,* Penn State University; *Fan Ren, Stephen Pearton,* University of Florida

The dry etching of high crystal quality c-plane AlN grown by Metal Organic Chemical Vapor Deposition was examined as a function of source and chuck power in Inductively Coupled Plasmas of Cl_2/Ar or $Cl_2/Ar/CHF_3$. Maximum etch rates of ~1500 Å•min^{-1} were obtained at high powers, with selectivity over SiO_2 up to 3. The as-etched surfaces in $Cl_2/Ar/CHF_3$ have F-related residues, which can be removed in NH_4OH solutions. The Al-polar basal plane was found to etch slowly in either KOH or H_3PO_4 liquid formulations with extensive formation of hexagonal etch pits related to dislocations. The activation energies for KOH or H_3PO_4 -based wet etching rates within these pits were 124 and 183 kJ/mol, respectively, which are indicative of reaction-limited etching.

AS-ThP-7 Probing the Adhesive / Substrate Interface Using Back Side Sims Profiling Facilitated by Releasable Thin Metal Films, *Paul Vlasak, Stephen Altum, Thomas Fielitz, Jeremy Beebe,* Dow Chemical Company

Depth profiling using secondary ion mass spectrometry (SIMS) or other surface sensitive methods is an attractive strategy for studying cured adhesive or sealant compositions near their interfaces with substrate materials to take advantage of the extraordinary depth resolution of these methods. A classic problem with this approach is that a poor performing sample may exhibit adhesive failure, so that the interface of interest can be easily exposed and ideally presented to the analyzer, while the exemplary sample exhibits cohesive failure, and the interface of interest remains hopelessly buried beneath an irregular layer of adhesive. Here we present one approach to facilitate back side profiling from the substrate side, allowing analysis of the interface of interest without requiring adhesive failure at the interface. In the demonstrated approach, a 20 nm thick layer of aluminum was deposited on a sacrificial polymer film. The adhesive of interest was cured against the aluminum surface under varying environmental cure conditions. The polymer film was then peeled away, leaving the thin aluminum layer intact on the adhesive. SIMS depth profiles through the aluminum into the adhesive allowed a direct comparison of near surface chemical composition, revealing different distributions of formulation components depending on cure conditions.

AS-ThP-8 Probing the Effects of Surface Chemistry on Quality Factor and Coherence Times of Superconducting Radio Frequency Cavities and Qubits, *Adam Clairmont, Jaeyel Lee, Akshay Murthy,* FermiLab

Understanding the chemistry of both surface and bulk properties is important for improving the performance of superconducting radio frequency (SRF) cavities and superconducting qubits. Utilizing state-of-the art material characterization tools, researchers can better understand the impact subtle changes in chemistry have on quality factors and coherence times of such devices. Fermilab's Material Science Laboratory co-operated by the Applied Physics and Superconducting Technology Directorate and Superconducting Quantum Materials and Systems Center houses a custom-built x-ray photoelectron spectroscopy (XPS) instrument that was designed with the characterization of SRF cavities and qubits in mind.

A monochromatic silver anode accompanies the standard monochromatic aluminum anode. This allows the researcher to increase their information depth from 9-10 nm (Al) to 17-20 nm (Ag), access a greater number of core levels, and to shift Auger transitions to avoid possible peak overlaps. Using a small spot lens mode, XPS mapping can be done with <30um achievable spatial resolution. If increased spatial resolution is needed, the electron source can be used for Auger or scanning Auger microscopy with sub-micron spatial resolution. Band gaps can be analyzed with the Helium (I and II) ultraviolet source. An argon gas cluster ion beam with selectable cluster size, monatomic-3000 Ar ions per cluster, allows rapid low-damage sputtering. A high-pressure chamber can reach temperatures approaching 1073 Kelvin (K) while also introducing gasses such as nitrogen, oxygen, hydrogen, carbon dioxide, and various inert gasses up to pressures of 20 bar. As this chamber is directly attached to the system, samples can be transferred into the load lock and into the analysis chamber following heat treatments without exposure to air. Finally, a liquid helium manipulator is coupled with an e-beam heater for *in situ* characterization from less than 15K to 1073K.

This unique tool has enabled a wide variety of scientific studies that have improved our understanding of sources limiting the performance of SRF

cavities as well as superconducting qubits and I will present results from some of these efforts.

AS-ThP-11 Analysis of High-k Metal Stacks by Hard X-Ray Photoelectron Spectroscopy Under Bias, *Anja Vanleenhove, Thierry Conard,* IMEC Belgium; *Derese Desta, Hans-Gerd Boyen,* Hasselt University, Belgium

While the replacement of $SiO2$ by high-k materials started in the early 2000s, the need for a deep knowledge of band-energies in complex high-k stacks is a hot topic in research and development in the advanced CMOS industry.

Although XPS is most commonly used as a technique to study the chemical composition of the top surface and thin layers plus interfaces in the top of the stack, *Kumar et al.* have demonstrated how the technique could be used to examine band-energies in high-k metal stacks with the established XPS using Al Kα radiation. For XPS using Al Kα, the analysis depth is limited to the top 5-10 nm. With the recently developed laboratory based hard X-ray photoelectron spectroscopes (HAXPES) the path is opened to the analysis of thicker stacks and deeper buried interfaces (20-50 nm).

In this work, we will demonstrate the use of HAXPES under bias to examine relevant high-k metal stacks and illustrate that, as is the case for all other analysis techniques, this technique has its own limitations as well.

The examined samples and measurement set-up are modelled to enable an effective biasing across the stack while executing the HAXPES measurement. The samples consist of Si/SiO2 substrates topped with high-k materials Al2O3 and HfO2 which are covered with TiN. The sample matrix is designed to study different stack orders of the high-k materials as well as different high-k layer thicknesses. HAXPES measurements are executed on the *HAXPES Lab* of Scienta Omicron, a tool which combines a high flux monochromated Ga Kα X-ray source of 9252.1 eV with an Al Kα X-ray source of 1486.6 eV.

Reference: P. Kumar *et al.*, "Development of X-ray Photoelectron Spectroscopy under bias and its application to determine band-energies and dipoles in the HKMG stack," *2018 IEEE International Electron Devices Meeting (IEDM)*, San Francisco, CA, USA, 2018, pp. 17.6.1-17.6.4, doi: 10.1109/IEDM.2018.8614554.

AS-ThP-14 ToF-SIMS Characterization of Mechanocatalytically-Formed Carbonaceous Films on Nanocrystalline $Pt_{0.9}Au_{0.1}$ Alloy: Insights into Chemistry, Structure, and Friction Behavior, *Nicolas Molina, Camille Edwards,* The University of Texas at Austin; *Tomas Babuska, John Curry, Frank DelRio,* Sandia National Laboratories; *Jason Killgore,* National Institute of Standards and Technology, Boulder; *Hsu-Ming Lien,* The University of Texas at Austin; *Michael Dugger,* Sandia National Laboratories; *Filippo Mangolini,* The University of Texas at Austin

Nanocrystalline Pt-Au alloys have emerged as a highly promising class of hard and wear-resistant materials with potential application in several fields, including in electrical contacts (EC) and next-generation nanoelectromechanical systems (NEMS). While the mechanocatalytic formation of carbonaceous surface layers at the interface between sliding metallic contacts has been reported in the case of pure Pt (found to decrease adhesion and friction but increase the electrical resistance, resulting in reliability issues when Pt is used in NEMS switches), remarkably little is known about the chemistry, structure, and tunability of these interfacial layers in the case of Pt-Au alloys. In this study, we conducted tribological experiments on a nanocrystalline $Pt_{0.9}Au_{0.1}$ alloy in the presence of ethanol (C_2H_6O) or isopropanol (C_3H_8O) vapor (partial pressure ranging from ultra-high vacuum (UHV) to 3 mbar). To gain insights into the chemical nature and structural properties of the mechanocatalytic, carbon-rich films formed on $Pt_{0.9}Au_{0.1}$ surfaces, ex-situ time-of-flight secondary ion mass spectrometry (ToF-SIMS) depth profiling measurements were carried out. Notably, the development of a robust ToF-SIMS characterization methodology integrating molecular formula prediction (MFP) and multivariate statistical analysis (MVSA) allowed for highlighting subtle differences in elements' bonding configuration and functional moieties in the ultrathin carbon surface layers formed on $Pt_{0.9}Au_{0.1}$ surfaces, including aromaticity of carbon atoms, hydrogenation, and molecular weight distribution. Our findings, demonstrating the intricate interplay between mechanocatalytic film formation, the nature of the organic gas environment, and gas pressure, not only advance our understanding of the tribological processes occurring on Pt-Au alloys, but also provide guidelines for tailoring the mechanocatalytic formation of carbonaceous surface layers and modulating their tribological behavior by rationally varying the organic gas environments and pressure. SNL is managed and operated by NTESS under DOE NNSA contract DE-NA0003525.

---

[1] **ASSD Student Award Finalist**

AS-ThP-15 Quantification of Surface and Subsurface Structures of Complex Thin Films with LEIS, XPS and Sputter Depth Profile Simulations, *Markus Valtiner, **Camil Bocaniciu**, Julian Pichler, Alper Celebi,* TU Wien, Austria

Sputter depth profiling is an established technique to analyze surface and subsurface concentration profiles on various surfaces using different techniques such as XPS or AES. However, during sputtering both preferential sputtering as well as atomic intermixing do interfere with a detailed evaluation of surface and subsurface species. Here we show how a combination of Low Energy Ion Scattering and angle resolved XPS can reveal accurate depth distributions with high vertical profile resolution. Therefore, we also performed Monte Carlo based simulations of the sputtering processes, and fitted these to elemental distributions measured by LEIS and XPS during sputtering. We can show that our approach allows us to reconstruct accurate surface and subsurface distributions in complex materials and thin films including series of stainless steels, high entropy alloys as well as plasma etched silicon wafers with varying oxide thicknesses. Based on our approach a detailed elemental profiling with close to mono layer elemental distribution accuracy is possible. This is interesting for various fields including catalysis, corrosion as well semiconductor processing.

AS-ThP-16 Multimodal Characterization of Copper Hydroxy Chloride for Advanced Thermochemical Energy Storage Applications, *Kavin Chakravarthy Thangaraj, Xiao Zhang,* Washington State University, US; *Venkateshkumar Prabhakaran, Vijaykumar Murugesan, Ajay Karakoti,* Pacific Northwest National Laboratory

Developing efficient energy storage systems is paramount for achieving carbon neutrality and maximizing the use of renewable energy sources. Thermochemical energy storage systems (TCES), a distinct subclass of thermal energy storage systems (TES), have gained significant attention for their ability to store energy from intermittent energy sources like solar and wind. TCES work by storing and releasing thermal energy through processes such as adsorption, absorption, or chemical reactions. Salt hydrates are commonly studied for TCES applications due to their high energy density, cost-effectiveness, and eco-friendly qualities. However, challenges arise from the limited availability of suitable salt hydrates for specific uses and the need for additional materials like thermal conductive additives and phase stabilizers for optimal performance. Additionally, multimodal and in-situ characterization of TCES materials is required to identify the material degradation modes during energy storage and release cycles, which will enable the design of novel, better-performing materials.

To address these challenges, we explored the potential of copper hydroxy chloride (CHC), a double anion salt of copper, for TCES applications. The insolubility of CHC in water reduces deliquescence-associated performance degradation over extended cycling periods compared to other salt hydrate systems. Our study encompassed a multimodal evaluation of CHC for the application in TCES by analyzing its dehydration and hydration cycling behavior. Specifically, we utilized in-situ X-ray diffraction (XRD) and in-situ X-ray photoelectron spectroscopy (XPS) to discover a stagewise decomposition of CHC at different temperatures during its dehydration, resulting in the release of water and chlorine byproducts. By employing methods such as thermogravimetry- differential scanning calorimetry (TG-DSC), and a calorimeter paired with a humidity generator, we evaluated the temperature range suitable for hydration and dehydration of CHC, the associated heat changes (enthalpies) and the temperature range where the reversibility of reactions could be preserved. The multimodal and in-situ methods developed are largely applicable to other TCES materials for identifying the hydration, dehydration, and degradation mechanisms of salt hydrate-based materials and evaluating their promise as thermal energy storage systems, eventually contributing to the broader goal of sustainable and efficient energy storage.

AS-ThP-18 Quantitative Analysis for Chromium Oxidation, *Milton Vazquez-Lepe,* University of Guadalajara, Mexico; *Alberto Herrera-Gomez, Orlando Cortazar,* CINVESTAV-Queretaro, Mexico; *Servando Aguirre,* CIMAV-Monterrey, Mexico; *Conan Weiland,* Brookhaven National Laboratory

The background in X-ray photoelectron spectroscopy, is formed from inelastic scattering. To evaluate oxide states for quantification, Tougaard background and Shirley background intensity must assessed appropriate. The experimental background can be calculated with several methods with different contributions for the total area. For determination of composition, the Cr3s, Cr3p and O2s core levels were analyzed from 400 eV to 900 eV of

emission source. These intensities were modified to evaluate the appropriate chemical quantification. Also, varying the photon energy applied, Shirley intensity is changing and was incorporated using the SVSC method that allows for accounting the differences for the assessment.

AS-ThP-19 Temperature Dependency of Doping Silicon with Phosphorus Using Ultra-Thin Films of P-Containing Minerals, *Roman Konoplev-Esgenburg, Peter Thissen,* KIT, Germany

This work explores a novel approach using ultra-thin films of P-containing minerals which are Hydroxyapatite ($Ca_5(PO_4)_3OH$), Struvite ($MgNH_4PO_4*6H_2O$), and Monetite ($CaHPO_4$) and we expect high-temperature dependency of doping process due to different decomposition profiles. Thin films were prepared via a tethering by aggregation and growth method and subsequently processed by spike annealing. Minerals offer a large variety of materials that can be used in this doping process.

In-situ infrared (IR) spectroscopy reveals the decomposition of a mineral and its intermixing with the native silicon oxide at low temperatures (for Hydroxyapatite at 200°C). This process involves the migration of phosphate through the native oxide layer driven by a phase transformation into a more stable thermal oxide. Ultimately, the diffusion of phosphorus into the underlying oxide-free silicon layer is observed (for Hydroxyapatite at 700°C). By combining in-situ IR with electrical impedance spectroscopy (EIS) and X-ray photoelectron spectroscopy (XPS), the measurements allow us to conclude the following process. Firstly, the transport of phosphorus through the silicon oxide barrier and subsequent diffusion of phosphorus within the oxide-free silicon layer. Finally, the phosphorus concentration profile was confirmed by Time-of-Flight Secondary Ion Mass Spectrometry (ToF-SIMS).

To further explain and investigate experimental doping processes using thin films of P-containing minerals, mineral interfaces were modeled and DFT calculations were performed. The Nudged Elastic Bands (NEB) method provides us with the mechanism of phosphorus transport. Vibrational frequencies were calculated to correlate them with IR spectroscopy. Additionally, the DFT methods helped us optimize each corresponding doping process from the electrical perspective: electronic band structure, and pinned impurity levels that result in charge carrier trapping as each interface necessarily displays different electrical properties.

AS-ThP-20 Coincident XPS, Raman and SEM Analysis of Additive Manufacturing Devices, *Mark Isaacs,* University College London, UK; *David Morgan,* Cardiff University, UK; *Alex Leung, Kwan Kim, Shishira Bhagavath,* University College London, UK

Additive manufacturing processes are a keenly investigated methodology for the preparation of sophisticated devices for a multitude of technologies, including catalysis, electronics and sensors. At the heart of the functionality of these systems often lies the surface and interfacial properties of the resultant materials. In order to develop a holistic understanding of the eventual nature of these devices, and for the complete assessment of favourable printing parameters, oftentimes a multitude of characterisation methods is required. Coincident analysis of surface analysis techniques such as XPS, SEM, REELS and UPS - along with additional complementary techniques such as Raman spectroscopy - permits a wealth of understanding around the physical, chemical and electronic properties of printed tracks and leads to an overall optimisation of system parameters to develop highly specific and tuneable materials. In this work, we study a range of printing parameters for the deposition of MoO_3 tracks onto a copper support - a material with promising applications in the electrocatalytic reduction of CO_2. Using XPS, linked with SEM/EDX via a CISA (Correlative Imaging and Surface Analysis) Workflow and Raman spectroscopy, we investigate a range of printing parameters in order to determine favourable properties for the creation of phase interfaces understood to be active for electrocatalytic applications. Chemical and electronic properties are also investigated through complimentary surface analysis by REELS and UPS.

AS-ThP-21 Investigation into the Blackening of Lead-Glazed Ceramic Objects, *Alexandra DiCarlo, Amy Walker,* University of Texas at Dallas

Lead glaze on earthenware undergoes blackening in anaerobic environments such as those found in cesspits and canals. The blackening effect is attributed to the formation of black lead(II) sulfide within the glaze. However, the degradation process is not well understood; degraded glazes

exhibit not only black colors but also red and orange colors. In this study, five lead-glazed ceramic pieces excavated from the canals of Amsterdam were analyzed using optical microscopy, X-ray photoelectron spectroscopy (XPS), and Raman spectroscopy to investigate the chemical and physical properties of the aged glazes. Each ceramic piece exhibited different levels of degradation from fully black to off-white. Optical images revealed that the most visibly damaged objects have rougher surfaces and crystals growing in cracks of the glaze. Raman spectra and XPS data indicate that the objects share many of the same components, including lead oxides, tin(II) oxide, and silicon dioxide. Surprisingly, other lead compounds that are not known to be ingredients of glaze are also present, including lead(II) carbonate, lead(II) sulfide, and lead(II) sulfate. To determine if a correlation between the chemical compositions and the perceived colors of the objects existed, principal component analysis (PCA) was conducted, but there does not appear to be any strong correlations. This is likely due to the limited number of samples investigated.

AS-ThP-22 A Computational Approach to Model Radical Formation in Low Temperature Plasma Generated from Pentane and Acrylic Acid as Precursors, *Mackenzie Jackson, Kristina Closser, Morgan Hawker,* California State University, Fresno

Plasma enhanced chemical vapor deposition (PECVD) is an ideal method to change the chemical properties of surfaces without affecting bulk properties. In the literature, PECVD in conjunction with computational studies primarily focus on coating semiconductors with organometallic and semimetal-based films. Many PECVD systems utilize organic precursors, especially to modify surfaces to interface with biological environments. This research seeks to fill the gap by studying thin films deposited using organic plasma precursors, specifically acrylic acid and pentane. Computational modeling of these organic precursors will help in understanding key characteristics of the deposition of the thin film via the thickness of the film, deposition rate, and the chemical composition of the film.

This study models the precursors– acrylic acid and pentane– using computational chemistry. Classical density functional theorem (DFT) functions were used to examine geometries, frequencies, and energies of neutral radicals and cations formed during precursor ionization. Data were obtained using the quantum chemistry program Q-Chem with the methods B3LYP and CCSD(T) along with the 6-311(2d,2p) basis set. Data were then analyzed to determine the most stable fragments, which were subsequently used to predict species most likely formed plasma-polymerized films. Preliminary data shows the most energetically favorable way to break both precursor molecules was between the C2 and C3 bond. The least energetically favorable spot for the split on pentane occurred between the H and C3 bond while acrylic acid required the most energy to separate the O from the C3 carbonyl. Currently, data obtained is limited to the energetics of the split and recombination of pentane and acrylic acid separately. In future work, the fragments from pentane and acrylic acid will be combined to determine the lowest energy co-polymers between the two, in conjunction with experimental surface measurements, and will be used to develop a machine learning model to predict the properties of the co-polymers these compounds form.

AS-ThP-23 Improving Field Emission Device Performance by Optimizing the Emitter Shape, Dimension, and Space Distribution Based on Finite Element Analysis, *Jaden Lu, Olivia Lu,* Hamilton High School

Cold cathode field emission devices have attracted much attention due to its unique properties such as high current density and low working temperature. To gain strong field enhancement factors, the field emitters with high aspect ratio are widely used. However, these sharp tips have a great disadvantage. The strong emission current passing the sharp tips will generate very high temperatures. The tips will melt or crack under such high temperatures, and its morphology will change dramatically. This will result in unstable emission current and cause device failure.

In this research, Finite Element Analysis software COMSOL was used to simulate the field emission device. Various emitter shapes and dimensions were simulated to compare the emission current and resultant temperature increase of the emitter. The field emission failure mechanism will be investigated based on the simulated data. An existing failure model proposed by other researchers is the melting of materials under local high temperatures. However, the high temperature will also cause extra strain due to thermal expansion. The material will crack if the thermal strain is over a certain limit. COMSOL simulation will validate these models. On the other hand, since the practical field emission device is composed of arrays of many emitters, this work also studies the impact of space distribution on the field emission device performance. Different emitter array structures were simulated to understand the electric field distribution.

To mitigate the impact of high temperature generated by emission current, several solutions were proposed and evaluated by COMSOL simulation. The first solution is to dope the materials to reduce its electrical resistivity. This will control the Joule heat from high emission current. Doping impact and surface modification are simulated to study the bandgap change, quantum tunnel efficiency, and current density. The second solution is to optimize the emitter cross section area to reduce the Joule heat. It is known that a higher cross section area will result in lower electric resistance and thus decrease the Joule heat. This solution will require the balance of electric resistance and aspect ratio of the emitter to achieve sufficient emission current under relatively low bias voltage. The third solution is to find different emitter shapes to achieve high thermal conductivity. The generated heat can be quickly transported to the surrounding environment and therefore the damage to the field emitters can be reduced. Based on this research, a stable field emission device structure was proposed with optimal emitter shape, dimension, and space distribution.

AS-ThP-24 Metallic 3D-Printing Materials Analysed by Secondary Ion Mass Spectrometry, *Asel Akhmetova, Daniel Breitenstein,* Tascon GmbH, Germany; *Markus Glauche,* implantcast GmbH, Germany; *Maximilian Kluge,* Fraunhofer Research Institution for Additive Manufacturing (IAPT), Germany; *Elke Tallarek,* **Reinhard Kersting**, *Birgit Hagenhoff,* Tascon GmbH, Germany

In contrast to traditional manufacturing processes, 3D printing offers advantages in terms of the achievable complexity of the printed parts and their individuality. Typically, 3D printing is said to be more efficient in terms of materials, which can go hand in hand with cost savings.

3D printing is now used not only for polymers, but also for metals. Spherical metal powders are melted in a targeted manner using either an electron or a laser beam. The remaining powder can be separated and fed back into the printing process.

However, reusing the powder in metal 3D printing is not yet possible indefinitely: the powders typically show signs of ageing after several printing cycles, meaning that the quality of the 3D print suffers. In practice, the powders therefore have to be disposed of after several printing cycles.

There are indications that these ageing processes correlate with changes in the surface properties of the metal powders used. For a better understanding of powder aging and related printing processes, it is therefore important to study defects in 3D-printed samples as well as raw metal powders with suited analytical methods. In the present study this is performed by means of Secondary Ion Mass Spectrometry (SIMS).

AS-ThP-25 Advanced Automated Workflows and Elemental Identification for Non-Expert XPS Analysis, *Jonathan Counsell, Liam Soomary,* Kratos Analytical Limited, UK; *Chris Moffitt,* Kratos Analytical Inc., UK; *Karol Macak,* Kratos Analytical Limited, UK, Slovakia; *Kevin Good,* Kratos Analytical Limited, UK

A novel peak identification (peak-ID) algorithm has been developed to significantly improve data-dependent acquisition (DDA) in X-ray photoelectron spectroscopy (XPS). Traditional XPS analysis relies heavily on manual peak assignment, which can introduce errors and inconsistencies, particularly in complex or noisy spectra. The new peak-ID algorithm addresses these challenges by automating the detection and classification of spectral peaks, offering a more precise and consistent approach to XPS analysis.

This algorithm enhances the limit of detection by accurately identifying low-intensity peaks that may be overlooked by conventional methods, enabling the detection of trace elements and subtle chemical states with higher confidence. By automating the peak identification process, the algorithm minimizes human error in peak assignment, ensuring more reliable data interpretation. The integration of this peak-ID system into DDA workflows allows for real-time optimization of data acquisition parameters, focusing on regions of interest in the spectrum and thereby improving the overall efficiency and effectiveness of the analysis.

Additionally, this approach reduces the risk of missing critical information by dynamically adjusting the acquisition strategy based on the detected peaks. The algorithm's ability to handle complex spectra with overlapping peaks further enhances its utility in diverse applications, from materials science to surface chemistry. Overall, the new peak-ID algorithm represents a significant advancement in XPS technology, offering improved sensitivity, accuracy, and efficiency in automated surface analysis.

AS-ThP-26 Online Accurate Intensity Calibration for X-ray Photoelectron Spectroscopy Instruments, *Alexander Shard*, *Benjamen Reed, Steve Spencer, Deepthi Sundaram, Tom Fielder, Casey Lambie, David Melling,* National Physical Laboratory, UK

Calibration of the intensity scale in X-ray Photoelectron Spectroscopy (XPS) is important to ensure that quantitative data are reliable, reproducible, and replicable. In the 1980's the National Physical Laboratory established a system for the accurate intensity calibration of electron spectrometers.[1] The method employs accurate reference spectra from clean copper, silver and gold foils suitable for any instrument geometry. The approach underpins, and is more accurate than, the calibration procedure using a secondary reference material, low density polyethylene[2,3] which has now been adopted as international standard ISO 5861. The software originally developed in the late 1990's to disseminate the calibration procedure no longer works on modern computers and had rather stringent data input requirements as well as a slow operation. NPL have updated the method and have implemented it on a web-based portal. The new procedure is approximately 100 times faster than the previous software and can handle up to 21 files input simultaneously, enabling seven instrument modes to be calibrated in a single five-minute session. There are no longer any requirements for files to be entered sequentially in single block VAMAS format, nor for there to be a specified energy step size. The calibration results and associated uncertainties are checked, certified, and digitally delivered to enable analysts to have evidence of calibration as part of their quality system.

1. M. P. Seah, J. Electron Spectr. Rel. Phenom. **71** (3), 191-204 (1995).
2. B. P. Reed et al, J. Vac. Sci. Tech. A **38** (6) (2020).
3. A. G. Shard and B. P. Reed, J. Vac. Sci. Tech. A **38** (6) (2020).

AS-ThP-27 Sublime cryo-XPS, *David Surman,* Kratos Analytical Inc; *Jonathan Counsell,* Kratos Analytical Limited, UK

Cryogenic X-ray photoelectron spectroscopy (cryo-XPS) is an advanced analytical technique that offers unparalleled insights into the surface chemistry of materials at cryogenic temperatures. This method is particularly advantageous for analyzing delicate and volatile samples that might otherwise degrade or alter under standard conditions. One of the significant challenges in cryo-XPS is the formation of frost on the sample surface, which can obscure the true surface chemistry and lead to erroneous interpretations. In this study, we present a novel method for mitigating this issue by employing gentle warming to selectively remove the frosting while preserving the integrity of the underlying frozen surface.

The process begins by cooling the sample to cryogenic temperatures, typically below 120 K, where frost naturally forms due to the condensation of ambient moisture. Rather than allowing this frost to interfere with XPS measurements, we implement a controlled warming protocol. This careful warming is monitored using precise thermocouples and controlled heating elements, ensuring that the sample remains in a stable cryogenic state during the entire procedure.

Our method was tested on various salt solutions known for their sensitivity to temperature and environmental conditions. The results demonstrated a significant improvement in the quality and accuracy of the XPS spectra obtained post-frost removal. The true chemical states and compositions of the samples were revealed, providing deeper insights into their surface properties.

AS-ThP-28 Update on Using Different Instruments on the Same Sample and Getting Similar Results, *Lyndi Strange*, *Donald R. Baer, Mark H. Engelhard, Vaithiyalingam Shutthanandan,* Pacific Northwest National Lab; *Alex Shard,* National Physical Laboratory, U.K.

Literature analyses indicate growing use of XPS in multiple disciplines and increasing observations of faulty analysis. To ensure reliable results, detailed attention is required to acquisition and analysis. Our laboratory has instruments from three vendors, and it may be necessary to collect data from the available instrument. Users often export data for analysis using alternative software. It is useful to know the consistency of data collected on "identical" samples on different systems and analyzed using "native" (or blind) data export to other software packages. This paper describes what we thought was a "simple" test of data collection on three different systems and analysis using the native software for each system and analysis when naively exported to a non-native software package. Copper foil was the test specimen from which survey and high-resolution spectra were collected using Kratos Axis DLD Ultra, Thermo-Fischer NEXSA, and Phi Quantera spectrometers. Using both survey and narrow window data, the analyses included: i) comparison of Cu 3p and Cu 2p peak ratios, ii) Cu 3p and Cu 2p atom ratios using native software and iii) when exported to

CasaXPS. We also compared the wide scan spectra shapes to the ideal Cu spectra provided by the National Physical Laboratory to obtain an approximate instrument response function. Although simple in concept, these comparisons were found to be less than straightforward. High count rate survey spectra ratioed to the ideal spectra produced unexpected variations in the instrument response functions. These ratios made more sense when count rates were reduced by lowering the X-ray intensity or decreasing the pass energy. Cu 3p and Cu 2p peak ratios were determined using peak intensities after removal of an iterated Shirley background between 58.0 eV and 91.0 eV for Cu 3p and 920.0 eV to 970.0 eV for Cu 2p. Because of variations in the instrument geometry and transmission functions, raw peak ratios among the three spectrometers differed by > 2. However, native software analysis on each instrument produced similar amounts of Cu to roughly ± 5%. Note that sensitivity factors are more established for Cu 2p peaks than for Cu 3p peaks which may account for some variation. Naive transfer of data for analysis by non-native software was found to produce results significantly different than expected in some cases. This can be due to sensitivity factors or complications related to the instrument response function. These issues can be corrected but require care and verification or incorrect results will result.

Biomaterial Interfaces
Room Central Hall - Session BI-ThP

Biomaterial Interfaces Poster Session

BI-ThP-1 Optimizing Regenerative Cell Infiltration in Vascular Grafts: Enhanced Strategies to Engineer Pore Microstructures During Fabrication, *Aurora Battistella,* University of Colorado at Boulder

Introduction: In tissue engineering, the goal is to create scaffolds that seamlessly integrate into the human body, guiding native tissue regeneration while slowly degrading. A crucial aspect of this process is achieving scaffold infiltration of functional cells. The initial phase centered on the material aspect, particularly different polymer behaviors, including degradation rates. Production methods represent another modifiable parameter to fine-tune the device structure, especially its porosity. Additionally, post-fabrication techniques can refine the microstructure and enhance interaction with the human body. The investigation originated with a control group, PCL+PEG-NB coaxially electrospun and air-dried. Ultimately, four groups were created by systematically altering one or more parameters and examined to assess their impact.

Methods: Coaxial electrospinning was used to achieve a strong core (PCL/PLCL) surrounded by a functionalized sheath (PEG-NB). The mixed condition was fabricated by directly blending sheath and core solutions for electrospinning. Samples were air-dried or freeze-dried. Surface topography, including fiber structure and porosity, was investigated by SEM. Uniaxial tensile testing was adopted to determine the impacts of different parameters on the mechanical properties of the graft. The groups were implanted subcutaneously and explanted at various time points (1, 4, and 16 weeks). Histological and fluorescent analyses were performed to visualize tissue morphology and cellular penetration.

Results: Freeze-dried samples demonstrate higher Young's Modulus and higher porosity, and, consequently, increased cell infiltration than their air-dried counterparts. PLCL shows faster degradation and higher cell infiltration than PCL. However, PLCL was mechanically weaker and had a less rigid structure than PCL. Mixed fibers also displayed increased degradation compared to the control and were shown to be slightly weaker in tensile tests.

Conclusions: Through systematic experimentation, we have uncovered the benefits of freeze-drying in enhancing scaffold porosity and cell infiltration, while also highlighting the importance of selecting polymers with suitable degradation rates. Work is still ongoing to determine optimal fabrication parameters. Moving forward, these insights may help to guide the development of advanced vascular grafts with improved regenerative capabilities, paving the way for more effective clinical applications in tissue engineering.

BI-ThP-2 Mass-Manufactured Surface Textures Enable Low-Cost Large-Volume Water Analyte Detection and Location Tracking, *Liza White, Caitlin Howell,* University of Maine

Timely detection of aqueous analytes is critical for agriculture, aquaculture, industry, and municipalities. Currently, testing methods are limited to small volumes and discrete, one-location samples. In this work, we show that an industrially manufactured nanotextured diffraction surface can provide

aqueous analyte information across multiple locations over time. Specifically, the aqueous solution can be scanned by changing the location or angle of the light source and detector. By positioning the diffraction surface behind or below an aqueous matrix, the analyte's 3D spatial information and approximate size are determined. The identification and quantification of the analyte can also be determined based on the measurement of light absorbance and transmittance unique to the chemical or biological components of the analyte. The novel development of a sensor capable of large-volume scanning and analyte location detection is beneficial in numerous aqueous sensing capabilities, potentially transforming aqueous analyte monitoring methods.

BI-ThP-3 Low Fouling Amphiphilic Zwitterionic Carboxybetaine/Perfluoropolyether Methacrylate Polymer Coatings, *Onur Özcan, Florian Koschitzki, Robin Wanka, Marc Krisam, Axel Rosenhahn,* Ruhr University Bochum, Germany

Amphiphilic polymer systems have proven to be an effective and non-toxic approach to combat the challenges of biofouling.[1,2] We manufactured a variety of amphiphilic polymers consisting of carboxybetaine methacrylate (CBMA) and perfluoropolyether (PFPE) urethane methacrylate. These polymers were anchored to chemically functionalized substrates by photoinduced grafting-through polymerization.[1] Highly hydrated hydrogels may create a diffuse interphase and thus promote silt incorporation.[3] We were able to show that low amounts of PFPE already reduce silt uptake substantially. Captive bubble contact angle (CBCA) goniometry revealed that the polymer networks possess enough orientational freedom to quickly rearrange upon immersion in water. Dynamic diatom and bacteria accumulation assays revealed enhanced antifouling performances in most of the amphiphilic mixtures compared to the solely hydrophobic compound PFPE. We were further able to identify individual CBMA/PFPE compositions where the synergistic effect of hydrophilic and hydrophobic contents had the strongest impact on their marine anti-fouling and fouling-release properties.

[1] F. Koschitzki, R. Wanka, L. Sobota, J. Koc, H. Gardner, K. Z. Hunsucker, G. W. Swain, A. Rosenhahn ACS Appl. Mater, Interfaces 2020, 12, 34148-34160. [2] A. J. Ruiz-Sanches, A. J. Guerin, O. El-zubir, G. Dura, C. Ventura, L. I. Dixon, A. Houlton, B. R. Horrocks, N. S. Jakubovics, P. Guarda, G. Simeone, A. S. Clare, D. A. Fulton Prog. Org. Coat. 2020, 140, 105524 – 105533. [3] J. Koc, T. Simovich, R. Schoenemann, A. Chilkoti, H. Gardener, G. W. Swain, K. Hunsucker, A. Laschewsky, A. Rosenhahn Biofouling 2019, 35, 454-462

BI-ThP-4 Pore Size Impact on Oil-Release and Fouling Resistance of Macroporous Oil-Infused PDMS Systems, *Regina Kopecz, Sabrina A. Böer, Zeynep Tiris, Axel Rosenhahn,* Ruhr University Bochum, Germany

Since their invention, SLIPS have been known for their self-repairing properties, pressure stability, repellency of water and complex fluids, and low-fouling properties. We created a series of environmentally benign, non-fluorinated liquid paraffin-infused PDMS sponge systems with varying porosities including a thin interfacial PDMS membrane for controlled oil-release kinetics. Different pore volumes and varying interfacial roughness were fabricated by sugar and salt templating. The obtained porous polysiloxane networks were investigated using water contact angle goniometry, scanning electron microscopy, and light microscopy. The macroporous sponge systems revealed excellent oil-uptake and an oil-release between 3% and 14% of initial oil-loading during incubation in MilliQ water for seven days depending on the pore size. The resistance against bacterial fouling by dynamic attachment assays with the freshwater model organisms *Pseudomonas fluorescens*, *Escherichia coli*, and *Bacillus subtilis* was investigated. We found a correlation between bacterial adhesion and the porosity of the interface for the individual bacterial strains. As the porous polymer networks can be fabricated in any shape, they are promising low-fouling bulk materials for a wide range of applications in medicine.

BI-ThP-5 Advancing Catheter Care: Liquid-Infused Catheters as a Novel Approach to Combat CAUTIs, *Zachary Applebee, Caitlin Howell,* University of Maine

Catheter-associated urinary tract infections (CAUTIs) pose a significant challenge in healthcare settings, leading to reduced patient outcomes, extended hospital stays, and increased healthcare costs. Although the current standard of care is to use systemic antimicrobials, there is growing concern that such treatment is contributing to the rise of antimicrobial resistance. Recently, liquid-infused catheters, in which a thin layer of biocompatible oil is used on the catheter surface, have emerged as a promising solution to reduce CAUTIs without the use of antimicrobials. In this work, we explore aspects of the use of liquid-infused catheters,

including the potential for the liquid coating to be lost to the host as well as the integration of bioactive anti-inflammatory compounds into the coating. Our goal is to develop this novel technology further so that it can be translated into the clinic, helping to reduce CAUTIs without the need for antimicrobial treatment.

BI-ThP-6 Developing an Effective Coating Process for Nanoscale Cellulose Fibrils on Biodegradable Substrates, *Sandro Zier, Doug Bousfield, Caitlin Howell,* University of Maine

Bio-derived materials show the potential to replace plastic packaging with similar functionality while also having the advantage of biodegradability and recyclability. Cellulose, the most abundant polymer in the world, can be mechanically ground to have nanoscale dimension which provide good oil/grease and gas barrier properties. However, coating cellulose nanofibrils (CNF) as a thin film onto biodegradable substrates such as paper in a single step comes with significant challenges due to the unique way in which the CNF fibers interact with water. To overcome this challenge, we first simulated CNF coating onto paper to further understand the physics behind the process. We then developed a novel technique that uses a vacuum system to reduce the amount of water associated with the CNF as it is being coated. We found that unlike previous attempts to coat CNF in a single step, which resulted in non-uniform layers, use of our method resulted in a smooth, continuous coating with anywhere between 12 and 28 g/m^2. Tests on gas permeability revealed the CNF coatings could decrease the amount of air that could pass through by ~500x, a critical result for plastic replacement products that serve to keep oxygen and other gasses away from the contents of the package. Finally, analysis of the ability of the CNF coatings to resist oil and grease showed an increase of ~10 times compared to uncoated controls. Our results show that by using our method, nanoscale cellulose fibrils can be effectively coated as a one-step process, preserving their unique properties and laying the foundation for their adoption as plastic replacements.

BI-ThP-7 The Surface Enhancement of Electro-Spun Polycaprolactone (PCL) Using Room Temperature Atomic Layer Deposition of Magnesium Oxide for Use as a Novel Resorbable Membrane for Dental and Corneal Surgery, *Harshdeep Bhatia,* University of Illinois - Chicago*; Farid Esmaeilabadi,* Northern Illinois University*; Cortino Sukotjo, Christos Takoudis,* University of Illinois - Chicago*; Sahar Vahabzadeh,* Northern Illinois University

Polycaprolactone is a popular biomaterial used for dental and corneal surgery. Recently MgO ALD at room temperature has been used to enhance the surface of resorbable membranes. In this study, electro-spun polycaprolactone was coated with different film thickness of magnesium oxide and tested for surface properties and cell proliferation. The ALD was performed at room temperature using a commercial ALD reactor, ALD150 LE. The source of Mg was bis(ethylcyclopentadienyl) Mg(eCp)$_2$ while ozone was used as the oxidizing agent. The composition and thickness of the as-deposited film were characterized by X-ray photoelectron spectroscopy and spectroscopic ellipsometry, respectively. The surface was also viewed using a scanning electron microscope. The water contact angle was measured right after deposition and 24-hour after deposition. A cell proliferation study was also performed to determine if the film had any toxic effects on cells.

BI-ThP-8 Label-Free High-Resolution Molecular Imaging of Sex Steroid Hormones in Zebrafish by Water Cluster Secondary Ion Mass Spectrometry (Cluster SIMS), *Naoko Sano,* Unit B6, Millbrook Cl Chandler's Ford, UK*; Elkan Lau, Johanna von Gerichten,* University of Surrey, UK*; **Kate McHardy**, Paul Blenkinsopp,* Ionoptika, Ltd., UK*; Maya Al Sid Cheikh, Melanie Bailey,* University of Surrey, UK

Sex steroid hormones are essential biomolecules for vertebrates and are involved in the maintenance of pregnancy, development of secondary sexual characteristics and diseases such as osteoporosis and breast cancer. Visualising the distribution of steroids contributes to further understanding of disease. However, analysis of steroids is difficult; their low polarity leads to poor ionisation efficiency, meaning they need to be derivatised for conventional analyses. Furthermore, the steroid signals overlap with a MALDI matrix background.

Water Cluster SIMS is a high-sensitivity mass spectrometry technique for imaging complex-mixture materials without derivatisation or the use of matrix. We demonstrate imaging of sex steroid hormones in zebrafish (an ideal vertebrate model organism) with a Water Cluster SIMS instrument.

An adult female zebrafish was prepared for this work. It was embedded while fresh in 0.75% HPMC and 0.25% PVP embedding media to facilitate

sectioning. The whole block was flash-frozen in a dry-ice and isopropanol bath. The sample was sectioned to 20 µm at -25 °C and thaw-mounted onto a conductive indium-tin-oxide (ITO) coated glass. The section was dried while frozen in a vacuum desiccator, and then directly analysed without any matrix application for the analysis. The Cluster SIMS analyses were then performed with the J105 SIMS Cluster SIMS (Ionoptika Ltd), using a 70 keV $(H_2O)n$ beam, where n is in the range of 15,000-35,000, and also separately with a 40 keV C_{60} beam. High-resolution images were acquired with a pixel size of < 1 micron.

Water Cluster SIMS uses a high-energy beam of ionised clusters of water to sputter and ionise molecules from a surface. It is far less damaging and generates far fewer fragment ions than traditional ToF SIMS, but retains many of the benefits of that technology such as high-spatial-resolution imaging. As a result, detailed images of the distribution of sex steroid hormone molecules in the zebrafish are visible. Preliminary data shows that it is possible to map the chemical distribution of steroids in the ovary area. In addition, we also detected lipid ions related to the embryo or oocyte around the ovary area as unique distributions.

BI-ThP-9 Fouling Inhibition by Replenishable Plastrons on Microstructured, Superhydrophobic Carbon-Silicone Composite Coatings, *Louisa Vogler, Emily Manderfeld, Axel Rosenhahn,* Ruhr University Bochum, Germany

Superhydrophobic surfaces (SHS) exhibit the outstanding ability to retain stable air layers underwater (the so-called plastron), making them resistant to the adhesion of marine organisms and therefore counteracting the detrimental impact of marine biofouling without the use of toxic substances.[1] Since the longevity of such plastrons is limited, we recently established an approach to replenish plastrons on submerged surfaces by Joule heating by only 1-2 °C.[2] In this work mechanically stable, conductive carbon-silicone composite coatings with replenishable plastrons were fabricated by 3D printing. For the fabrication, a striped, an intersected striped, and a hierarchically-shaped mold were used.[3] Characterization of the differently structured coatings was carried out by scanning electron microscopy, water contact angle goniometry as well as dynamic attachment assays against the marine diatom *Navicula perminuta*. We demonstrated that the resulting microstructured, superhydrophobic coatings revealed a plastron formation when being submerged in water, which greatly reduced the adhesion of diatoms on such surfaces by up to 84 %. Furthermore, plastron replenishment and growth of the conductive coatings were accomplished by Joule heating.[3]

[1] G. B. Hwang, K. Page, A. Patir, S. P. Nair, E. Allan, I. P. Parkin, *ACS Nano* **2018**, *12*, 6050., [2] T. Simovich, A. Rosenhahn, R. N. Lamb, *Adv. Eng. Mater.* **2020**, *22*, 1900806., [3] E. Manderfeld, L. Vogler, A. Rosenhahn, *Adv. Mater. Interfaces* **2024**, *2300964*, 1.

BI-ThP-10 iCVD Polymer Thin Film Bio-Interface-Performance Based on Functional Groups and Aerohydrogels, *Torge Hartig, Joschka Paulsen, Wiebke Reichstein, Margarethe Hauck,* Kiel University, Germany; *Mohammadreza Taale,* Universität Heidelberg, Germany; *Thomas Strunskus,* Kiel University, Germany; *Christine Selhuber-Unkel,* Universität Heidelberg, Germany; *Amal Amin,* National Research Centre, Giza, Egypt; *Rainer Adelung,* Kiel University, Germany; *Benjamin Freedman,* Harvard University; *Fabian Schütt, Franz Faupel, Stefan Schröder,* Kiel University, Germany

Interactions of biological species with polymer surfaces are dependent on various factors such as roughness, surface functional groups, wetting, residual liquids and defects. In conventional wet chemical polymers these different influences on the bio-interface cannot be examined independently. Initiated Chemical Vapor Deposition (iCVD) is an all-dry technique used to deposit ultrathin polymer films, which are defect-free and surface-conformal. Via iCVD polymer surfaces can be tailored precisely in monomer-composition, enabling the isolated examination on the bio-interface performance based on functional groups. The influence of the functional groups was examined regarding human fibroblasts, cancer cells and respiratory viruses, including in silico analysis of the interaction of key protein structures with the defined surfaces.

Furthermore, the iCVD conformal coatings are used to fabricate freestanding aerohydrogels. For this tetrapodal ZnO is coated dry-chemically and etched wet-chemically to create a freestanding polymer thin film scaffold with >99% empty space. The compressive properties of the well-defined aerohydrogels can be tailored by the gas phase composition and resulting crosslinking during the iCVD process. The aerohydrogels are used in 3D cell culture application for muscle cells.

BI-ThP-11 Bacterial Co-Culture Methods to Enhance Growth Rates in Mycelial Biomaterials, *Lindsay Pierce, Mehdi Tajvidi, Caitlin Howell,* University of Maine

Mycelia, the hair-like projections that make up the majority of fungal tissue, are gaining attention as a non-toxic, low-cost replacement for chemical adhesives and binders in bio-composite materials. However, the growth of fungal mycelia is a slow process which can take up to several weeks to complete. In this work, we explore the use of bacterial co-culture as a natural method to increase the growth rate of fungal mycelia in bio-composites made of wood particulates. In nature, fungi co-exist and compete with bacteria for space and resources, and previous work has demonstrated that the presence of some species of bacteria can enhance the rate of mycelial spread in response to competition pressure. We adapt these observations to mycelial bio-composites, examining the effect of the extract of a range of species in 3D constructs. Our results show how the use of bacterial co-culture methods can help to enhance the growth rate of mycelial biomaterials, potentially reducing the manufacturing time of these all-natural materials.

BI-ThP-12 Vascularization to Enhance Growth Rates in Mycelial Biomaterials, *Anna Folley, Mehdi Tajv, Caitlin Howell,* University of Maine

Wood bio-composites are of increasing interest as sustainable building materials; however, they are frequently manufactured using hazardous chemicals as particle binders, which reduces their value as eco-friendly products. Fungal mycelia, the fine threads that make up most fungal biomass are a natural alternative to chemical binders, yet their slow growth is one of the major limiting factors in their widespread adoption. In Nature, living organisms use vascular systems to enhance growth rates by delivering nutrients and other essential materials to tissue. Here, we work to develop an internal vascular network for wood bio-composites in an effort to increase the delivery of oxygen and moisture to the fungal mycelial, enhancing the rate of growth. We use modeling to determine the optimal arrangement of vascular channels which maximizes delivery throughout the composite structures while minimizing the impact on strength. We then use 3D printing of specialized molds to create the vascularized bio-composites, testing the rate of growth both with and without active moisturized airflow through the channel network. Our results show how the use of an internal vascular system in wood composite biomaterials can be used to enhance the growth rate of fungal mycelial as a binder, lowering the barriers to wider adoption of this approach for eco-friendly building materials.

BI-ThP-13 Self-Assembled Multifunctional Thin Films with Cerium Dioxide Nanoparticles, *Daniela Topasna, Aiden Psczulkoski, Matthew Albertson, Solomon Harris,* Virginia Military Institute

This study investigated multifunctional ionic self-assembled monolayers thin films composed of cerium dioxide nanoparticles and polymer. Samples of films werefabricated using different molarities, substrates, and layer compositions. Various characterization techniques and tests, such as optical spectroscopy, SEM, EDS, and temperature tests, reveal useful optical and antibacterial properties of these films, with potential applications in biomedicine, remote sensing, or consumer industry.

BI-ThP-14 Electroanalytical Investigation of Preferred Crystal Growth of Piezoelectric Gamma Glycine Biocrystals from Solution-Organic Film Interfaces, *Bijay Dhungana, Craig Neal,* University of Central Florida; *Xudong Wang,* University of Wisconsin-Madison; *Sudipta Seal,* University of Central Florida

Materials with piezoelectric properties, capable of inter-converting mechanical and electrical energy, hold promise as actuators, transducers, sensors, and energy harvesters in modern devices. Due to economic and application-specific constraints for traditional piezoelectric materials, biomaterials with advantages such as biocompatibility, biodegradability, renewable sourcing, and low cost are being studied for wearable and implantable energy-harvesting devices and tissue engineering frameworks. Developing corresponding manufacturing methods is crucial for effective, reliable future production. The presented study utilizes a combination of electroanalytical methods to characterize the nucleation and preferred growth of piezoelectric γ-phase glycine biocrystals at a molecular film interface. Herein, a self-assembled monolayer (SAM)-modified gold electrode surface was utilized to induce the preferred growth of γ-phase over non-piezoelectric polymorphic structures (α,β) through formation of an initial SAM-aqueous glycine coordination structure. We first assess interaction between SAM films and glycine in aqueous solutions electrochemically by focusing on adsorption behavior determined as transient, charging currents and changes in open circuit potential. Continuous measurements of potential change were complemented by

linear sweep voltammetry measurements, to characterize SAM-glycine interface character/strength, and electrochemical impedance spectroscopy (EIS), to reflect changes in the growing crystal layer character. Results from these studies were fit to relevant models (adsorption isotherms and equivalent circuit diagrams, respectively) which were then interpreted in relation to physicochemical processes mediating crystal formation behaviors. Conclusions drawn from these studies provide necessary insights into the biocrystallization process for future manufacturing processes of environmentally friendly piezoelectric materials.

BI-ThP-15 Towards a Biomimetic Approach to Transition Metal Sensing in Water, *William Maza*, *Kenan Fears,* US Naval Research Laboratory

Nature has evolved to express biological molecules displaying extremely high affinities for transition metals. For example, siderophores are known to bind Fe^{3+} with binding affinities exceeding 10^{20} M^{-1}. The core structure of a number in this class of biomolecules is comprised of a cyclic peptide ring. However, the cost of expressing and isolating these molecules makes their commercialization prohibitively expensive and impractical. Here we demonstrate that cyclic peptides that demonstrate reasonable affinities for transition metals can be synthesized at an appreciable scale. Moreover, we further demonstrate that by including the intrinsic naturally fluorescent amino acid tryptophan in the structure of the cyclic peptide we can use fluorescence spectroscopy to determine the presence of transition metals in water. The α- and β-K_3W_3 cyclic peptides discussed here display different affinities for both Ni^{2+} and Zn^{2+}. In both cases, the α-K_3W_3 bind more tightly to the transition metals compared to the β-K_3W_3 by a factor of nearly two in the case of Ni^{2+} and a factor of four for Zn^{2+}.

BI-ThP-16 Optical Tweezers for Electrochemically Manipulated Force Measurements, *Julia Appenroth, Iago Peters, Markus Valtiner,* **Laura Mears,** Vienna University of Technology, Austria

Force measurements can vary in magnitude dramatically depending on the number of individual bonds or interactions that take place. Optical tweezers offer a highly sensitive measurement of forces during binding events of either just a few or even single molecules. In order to bring two molecules together optical tweezers commonly use two beads decorated with the relevant molecules. These beads are either in the optical trap or immobilized by suction to a micropipette or other such mechanism. However this change in geometry compared to techniques such as atomic force microscopy (AFM), may impact the comparability of results with AFM. While AFM is an incredibly flexible technique with many different in situ environmental changes, the force sensitivity is approx. an order of magnitude less than optical tweezers. We have taken inspiration from scanning probe microscopy to overcome some of the environmental limitations of the optical tweezers to include a gold STM tip. This tip can be modified in a similar way to AFM tips and can also form part of a three-electrode electrochemical cell. Here, we present some of our first results with the system on biorelevant molecules. The electrochemical manipulation allows the probability of a binding event to occur to be increased by changing the surface potential of the tip or the oxidation state of any molecules bound to it. This is particularly useful in the context of using force measurements to determine the free energy of a bond using Jarzynski's equality. In that calculation unbinding events with small values in the Gaussian distribution of forces carry more weight than the larger values. Therefore, we hope our changes to the optical tweezer set up can further our understanding of single molecule interactions and the application of Jarzynski's equality.

Chemical Analysis and Imaging of Interfaces
Room Central Hall - Session CA-ThP

Chemical Analysis and Imaging of Interfaces Poster Session

CA-ThP-2 Off-axis EELS Bandgap Measurements at Complex Oxide Interfaces, *Kory Burns,* University of Virginia, USA; *Jordan Hachtel, Jonathan Poplawsky,* Oak Ridge National Laboratory, USA

Complex oxide interfaces have captivated the research community in the last 15 years due to the potential emergent nanoscale phenomena, owing to the strong interaction among charge, spin, orbital, and structural degrees of freedom.Studying these interfaces across a few unit cells is challenging with conventional methods, as optical probes tend to be around 1 µm in diameter. This makes it's impossible to study an individual interface of a vertically stacked transition metal oxide from a cross-sectional sample as the optical probe collects an averaged signal from each layer. In this talk, electron probes are used to overcome the diffraction-limit set by optical

probes. This is done by converging electrons to a focused beam to collect spectroscopic signal from an oxide-interface with electron energy loss spectroscopy (EELS). A monochromated aberration corrected scanning transmission electron microscopy (MAC-STEM) is used to couple unprecedented energy resolution and spatial resolution to do vibrational spectroscopy at atomic resolution. When the EELS aperture is in conventional settings, where the bright field disc is perfectly aligned with the entrance aperture, the EELS signal is delocalized and dominated by optical selection rules. Accordingly, the bright field disc is electrostatically shifted by the projector lens so that the dark field disc is highlighted, which describes a technique known as off-axis EELS. We use this to create a localized signal dominated by impact scattering so that the long-range contributions are suppressed, and band edges can be resolved without plasmon interference. Ultimately, we aim to introduce a novel technique to determine the structure-property relationship of complex oxides to bring oxide-electronics to new heights.

CA-ThP-3 ToF-SIMS Analysis of Biofilms after Overlayer Removal by fs-Laser Ablation, *Gabriel Parker, Anna Karaginnakis, Reyhane Shavandi,* University of Illinois - Chicago; *Xiao-Ying Yu,* ORNL; *Luke Hanley,* University of Illinois - Chicago

The biological secretions from bacterial biofilms contain fatty acids, metabolites, and other components of the extracellular polymeric substances (EPS). These secretions can result in corrosion of hard surfaces. Fatty acids produced by *Paenibacillus sp.* 300A, *Acidovorax* JHL-9, and *Shewanella ondenesis* MR-1 are thought to degrade glasses, polymers, and other materials. Observation of these fatty acids and other metabolites like quinolones, flavonoids, and quorum sensing molecules help reveal the metabolic process that can contribute to material degradation. The depth profiling capabilities of ToF-SIMS are particularly useful for distinguishing processes at the air-biofilm interface from those at the biofilm-material interface. However, ToF-SIMS depth profiling by gaseous cluster ion beams is only reliable for elucidating biofilm composition and structures down to a depth of a few micrometers and biofilms can grow to thicknesses surpassing a millimeter [1]. Ablation with 800 nm, ~75 fs laser pulses (fs-LA) has used for layer removal and depth profiling at much greater depths and without damage to the underlying biofilm [2, 3]. Femtosecond-LA combined with X-ray photoelectron spectroscopy has also been demonstrated for depth profiling in polymers [1]. Stand-alone fs-LA is used here to expose buried regions of biofilms of *Paenibacillus* sp. 300A biofilms cultured on Si wafers and other substrates for analysis using ToF-SIMS. Comparison of the mass spectra of ablated vs. non-ablated regions shows an absence of laser-induced changes in their respective chemical compositions, demonstrating the feasibility of fs-LA for probing buried regions of biofilms that are not readily accessible to gaseous cluster ion beams.

[1]M.A. Baker... R.G. White, Appl. Surf. Sci. 654 (2024) 159405.

[2]S. Milasinovic,... L. Hanley, J. Vac. Sci. Technol. A 28 (2010) 647.

[3]Y. Cui,... L. Hanley, ACS Appl. Mater. Interf. 5 (2013) 9269.

CA-ThP-5 Oxide Layer Characterization of Superconducting Two-layer Tin Films: Al/Nb and Al/Nb-Ti-N on Silicon, *Ghadendra Bhandari, Vikum Dewasurendra, Femi Akinrinola, John Metzger, Aidan Sheppard,* West Virginia University, USA; *Thomas Stevenson, Emily Barrentine, Larry Hess,* NASA Goddard Space Flight Center; *Matthew Johnson,* **Micky Holcomb,** West Virginia University, USA

Superconducting devices are important for the detection of microwave to x-ray radiation. Identifying the factors affecting oxide thickness, uniformity, and chemical composition will lead to the development of more reliable and lower noise detectors. We compare x-ray absorption spectroscopy (XAS) measurements and depth-dependent x-ray photoemission spectroscopy (XPS). We have studied two types of superconducting thin films: Al/Nb and Al /Nb-Ti-N. Depth-dependent niobium oxide (Nb_2O_5, NbO_2 and NbO) formation has been evaluated. We explore the impact of different etching and oxide cleaning treatments to the presence of these oxides. This research is supported by NASA EPSCoR Award# 80NSSC22M0173. We acknowledge the use of the research facilities at the Lawrence Berkeley National Laboratory and West Virginia University Shared Research Facilities.

CA-ThP-6 Deep Probing of Buried Layers with HAXPES - Chemical Analysis with Bias Applied Operando Setup for Electronic Devices, *Marcus Lundwall, Tamara Sloboda,* Scienta Omicron, Sweden; *Daniel Beaton,* Scienta Omicron; *Masatake Machida,* Scienta Omicron, Japan

Introduction

Buried interfaces in electronic devices such as batteries, solar cells, transistors etc. are highly chemically sensitive and reliable instrumentation is necessary for material development. While X-ray photoelectron spectroscopy (XPS) is a powerful method to investigate the chemical nature of surfaces, buried interfaces in device electronics are more difficult to investigate due to scattering. Hard X-rays giving increased information depth, have therefore been increasingly used in the photoelectron spectroscopy field.

HAXPES and XPS applications

Having access to XPS and HAXPES X-ray sources enables measurements of core levels with different resulting kinetic energy of the photoelectrons. With a soft X-ray XPS source, the kinetic energy is low and thus the obtained information is very surface sensitive. With Hard X-rays it is possible to be both surface and bulk sensitive, as electrons stemming from deep core levels will have lower kinetic energy and contain more surface sensitive information. Similarly, electrons stemming from shallow "XPS" core levels will have higher kinetic energy and contain more bulk sensitive information. This is especially valuable when detecting artefacts formed by sample exposure to different environments (e.g. air, moisture, heat, cold etc.) or by preparation steps known to induce chemical changes on the surface (e.g. sputtering). Scienta Omicron's HAXPES Lab uses both an XPS Al Kα source and a monochromatic Ga Kα MetalJet HAXPES source with excitation energy of 9.25 keV, therefore enabling artefact-free investigations with superior information depth, which clearly extends beyond limits of conventional XPS surface analysis. This unlocks a comprehensive and effective characterisation of layered materials. Combined with a hemispherical electron analyzer with a ±30 degree acceptance angle, investigation of buried interfaces, operando devices and real-world samples becomes achievable. (Fig.1). Over the years it has proven invaluable in research of semiconductor materials in thin film electronic devices including the operando characterization of bias induced changes in chemical composition of material interfaces. Other applications include polymer materials, metal surfaces and coatings. This presentation will give an overview of HAXPES applications with focus on buried interfaces in electronic devices such as passivation of luminescent quantum dots studied through a 35 nm overlayer, and semiconductor device band alignment by operando measurement with the Si substrate signal as reference detected through 20 nm TiN + 4 nm ZrO stack without sputtering and risk of artifacts.

CA-ThP-7 Stability and Dielectric Strength of Model Metal/Al$_2$O$_3$/Diamond Interfaces Under Harsh Environments, *J. Trey Diulus, Adam Biacchi, Emily Bittle, Andrei Kolmakov,* NIST-Gaithersburg

Recent progress towards innovation in power electronics has largely been through implementation of new wide-bandgap (WBG) semiconductor materials, like SiC or GaN. Alternatively, diamond is another WBG material with a high theoretical hole mobility (1300 cm^2*V^{-1}*s^{-1}), thermal conductivity, and breakdown voltage that rivals SiC and GaN, while also offering improved chemical and thermal stability over its WBG counterparts. Recently, diamond electronic devices have been fabricated displaying impressive electrical performance and thermal management, however little has been investigated for these model devices at high temperatures in combination with heavily oxidizing or reducing ("harsh") environments. In this work, we fabricated model diamond devices that possess metal/Al$_2$O$_3$/metal/diamond, and metal/Al$_2$O$_3$/diamond interfaces by depositing the standard metal contact stack (Ti/Pt/Au) or pure Pt on un-doped and non–hydrogenated diamond followed by growth of a 40-50 nm Al$_2$O$_3$ film via ALD as a gate dielectric. We then investigated the dielectric properties of this un-gated device by conducting I-V and capacitance measurements prior to any exposure. Next, the sample surface chemistry and morphology are investigated with x-ray photoelectron spectroscopy (XPS) and scanning electron microscopy (SEM), respectively. The device is then annealed to 600 °C, followed by exposures to H$_2$ and O$_2$ partial pressures of up to 10 kPa also at elevated temperature, where XPS, SEM, and 2-point I-V are all collected at each intermediate step *in situ* without breaking vacuum. Overall, we defined the stability range of a model diamond interfaces at high temperature and reactive environments.

CA-ThP-9 Differential Ion Movement is Captured by XPS under Voltage-Bias through a Multi-Layered-Graphene Electrode in contact with a Mixed Ionic Liquid Medium, *Ezgi Kutbay,* Bilkent University, Chemistry Department, 06800 Ankara, Turkey; *Fabien Krebs, Oliver Hoefft, Frank Endres,* Clausthal University of Technology, Germany; **Sefik Suzer,** Bilkent University, Chemistry Department, 06800 Ankara, Turkey

Under application of a voltage bias, asymmetric ion-movement of a mixed ionic liquid (IL), having the same anion [bis(trifluoromethylsulfonyl)imide / TFSI$^-$] but two different cations [1-butyl-1-methylpyrrolidinium / BMP$^+$ and Rb$^+$/ through a multi-layered graphene (MLG) electrode, has been detected by x-ray photoelectron spectroscopy (XPS), via recording the intensities of the C1s, N1s, F1s and Rb3d core level peaks. Accordingly, upon increasing the bias gradually from 1 to 3.5 V, we have observed up to 3-fold increase in the Rb3d peaks signal, accompanied with parallel F1s and N1s peak intensity changes, albeit to a lesser degree. The C1s peak of the graphene layer was observed to decrease, clearly indicating the increase in the surface composition of the IL. Moreover, a discernable differential change in the N1s peaks of the anion (N$^-$) and the cation (N$^+$) was also observed.Additionally, bias dependent binding energy shifts, extracted through the changes in the positions of F1s, N1s and C1s and Rb3d peaks of the IL mixture and the C1s of the graphene electrode indicate that multi-faceted and distinct solid-liquid interfaces develop throughout the entire intercalation process with an additional and pertinent evidence for finite potential drops. Details of the experimental set-up, and dynamics of bias-induced ion movement will be presented and discussed.

CA-ThP-10 ToF-SIMS Analysis of Two-Dimensional Metal Carbide Catalysts, *Tobias Misicko,* Oak Ridge National Laboratory, Louisiana Tech University; *Gabe Parker,* Oak Ridge National Laboratory; *Yang Xiao,* Louisiana Tech University; *Xiao-Ying Yu,* Oak Ridge National Laboratory, USA

MXene is a class of two-dimensional metal carbides with an empirical formula of M$_{n+1}$X$_n$T$_x$, where M is an early transition metal, X is a carbon or nitrogen, and T is a surface functional group (such as F$^-$ or OH$^-$). In our recent studies[1,2], incipient wetness impregnation was used to load platinum (Pt) onto Mo$_2$TiC$_2$ MXene to synthesize a 0.5% (wt.) Pt/Mo$_2$TiC$_2$ MXene catalyst. The catalyst containing Pt nanolayers exhibited excellent catalytic activity in alkane dehydrogenation with turnover frequencies (TOFs, converted molecules per surface Pt atom) of 0.4~1.2 s^{-1} for converting methane[1] and ethane[2], respectively. Time-of-flight secondary ion mass spectrometry (ToF-SIMS) measurements, including surface spectra, mass spectral imaging, secondary electron imaging, and depth profiling, were used to investigate the surface and subsequent monolayer structures of both unsupported Mo$_2$TiC$_2$ MXene and 0.5% Pt/Mo$_2$TiC$_2$ MXene catalysts. These analyses were used to derive the structure-activity relationship between Pt/Mo$_2$TiC$_2$ catalysts and their catalytic dehydrogenation performance in this work.

[1]Li Z.,*et al.*, *Nano Research,* 17 (**2024**) 1251–1258.

[2]Li Z,*et al.*, *Nature Catalysis,*10 (**2021**) 882–891.

Keywords: ToF-SIMS, MXene, Catalyst, Alkane Dehydrogenation, Methane Activation

CA-ThP-11 Surface Chemistry and Film Growth at Complex Air/Solution/Iron Interfaces, *Kathryn Perrine,* Michigan Technological University

Complex interfaces are prevalent in the natural and industrial environments, including water pipelines, batteries, geochemical transformations, and environmental processes. Surface chemistry occurs through adsorption, reduction-oxidation, and catalysis at the air/liquid or liquid/solid interface. Uncovering these reactions are essential for addressing environmental challenges, such as rising CO$_2$ levels. Mitigating CO$_2$ levels are addressed by geological sequestration, through capture and

conversion to carbonates. Iron is an earth abundant catalyst that is found in soils and dust as iron oxides. In the environment, iron interfaces interact with ions, particularly chloride, thus initiating corrosion, altering the physical structure. Here we show how surface corrosion, spontaneous reduction-oxidation, and deposition lead to film formation on iron interfaces for CO_2 capture mechanisms.

This poster will summarize our group's research on our advanced method to measure surface vibrational signatures of CO_2 adsorption and conversion to carbonate films. Polarized modulated – infrared reflection absorption spectroscopy (PM-IRRAS) was used to probe through an ultra-thin liquid layer to observe *in situ* reactions at the air/solution/iron interface. We observe iron surface oxidation and mineral formation, using the vibrational modes to track air adsorption and mineral film growth. The results are corroborated with XPS and ATR-FTIR spectroscopy to show the films produce signatures of different natural carbonates. *In situ* liquid AFM was used to verify the corrosion rate and resulting morphologies after air oxidation.

The electrolyte (from alkali and alkaline chlorides) is found to influence the type and rate of film grown at the air/electrolyte/iron interface. The divalent cations (from $MgCl_2$, $CaCl_2$, $FeCl_2$) are compared with the monovalent cations (from KCl, NaCl) as well as electrolytes of various pH's (HCl, NaOH). The Cl ions are found to initiate the corrosion, pitting through the native oxide layer, thus producing nucleation sites for film growth. The adsorption of atmospheric CO_2, and O_2, results in carbonate film growth, resulting in a specific-cation effect. The Fe^{2+} that dissolves during corrosion competes for adsorption with the other cations suggesting other surface-solution mediated mechanisms exist. These findings are relevant for understanding surface chemistry impacting mechanisms of CO_2 capture, geochemical formations, and other processes at complex air/liquid/solid interfaces.

CHIPS Act Mini-Symposium
Room Central Hall - Session CPS-ThP

CHIPS Act Mini-Symposium Poster Session

CPS-ThP-1 Expanding the AVS Science Educators Workshop to Historically Underserved Communities to Support Needs of the CHIPS in Science Act, *Timothy Gessert,* Chair - AVS Education Committee
For ~30 years the AVS has trained groups of high-school teachers in vacuum technology through the Science Educators Workshop (SEW). This training also provides teachers with a small vacuum system designed for classroom demonstrations. The SEW training occurs at the annual International Symposium of the AVS, with travel and lodging paid for by a combination of funds from National AVS Education Committee and Regional AVS Chapters. It is estimated that between 500-1000 kits have been distributed to high-schools across the US during the past ~30 years. Although the SEW is viewed as an important AVS educational outreach activity to secondary-school educators, discussions with SEW teachers has suggested that the majority of teachers come from relatively well-funded school districts. Discussions with SEW Committee and AVS regional chapter members has further suggested, while many school districts strongly support continuing education for their teachers (such as the SEW), others are much less able to do this because of financial constraints. These realizations prompted the AVS to consider how future SEW-like activities might be designed to better align with the needs and resources of "Historically Underserved Communities" (HUCs). To pursue this goal, the AVS submitted a multi-year Venture Fund proposal to the American Institute of Physics, and this proposal was funded starting in 2021. Project goals include: (1) Understand the locations and needs HUCs better; (2) Determine how the AVS SEW might reach out to HUCs more effectively; and (3) Understand how the AVS SEW might modify its content and delivery methods to better align with HUC needs. Although these goals were designed in 2021 to improve the AVS SEW, it has recently been noticed that these goals reflect Workforce Development Guidance associated with Chips in Science Act (passed in 2022, with implementation starting in 2023). This presentation will describe ongoing progress in the AVS/AIP Project, focusing on lessons learned that may assist similar efforts in AVS Workforces Development activities related to the Chips in Science Act.

Spectroscopic Ellipsometry
Room Central Hall - Session EL-ThP

Spectroscopic Ellipsometry Poster Session

EL-ThP-1 Training Neural Networks with Simulated Spectroscopic Ellipsometry Data for Cadmium Telluride Photovoltaic Applications, *Alexander Bordovalos, Balaji Ramanujam, Ambalanath Shan, Nikolas Podraza,* University of Toledo
Ellipsometric spectra can be simulated if the thicknesses and complex index of refraction ($N = n + ik$) spectra are known for the substrate and each layer of the film stack, such as, for example cadmium telluride (CdTe) based thin film solar cells. The ability to generate large data sets of simulated ellipsometric spectra enables the application of machine learning algorithms to spectroscopic ellipsometry data analysis tasks. Based on information learned from the analysis of ellipsometric spectra collected from real CdTe thin films and solar cells, ellipsometric spectra are simulated to assess characterization challenges that could be notably enhanced by machine learning. A promising machine learning task is compositional mapping. A bilayer structure of soda-lime glass / cadmium selenide telluride (CdSe(1-x)Te(x)) where x is one of nine values between 0.037 – 0.81 / cadmium telluride (CdTe) is selected as a proof of concept structure to simulate ellipsometric spectra for training a neural network. Large numbers of data sets are generated for each alloy composition and the thicknesses of the CdSe(1-x)Te(x) and CdTe layers are randomly selected from a common range for photovoltaic applications. A neural network is trained with these data sets to determine which of the nine possible CdSe(1-x)Te(x) compositions was used to simulate the ellipsometry data as well as predict the thickness for the CdSe(1-x)Te(x) and CdTe in the bilayer stack. The neural network determined the correct CdSe(1-x)Te(x) composition 99% of the time on the test set, and 95% of the layer thickness predictions for the CdSe(1-x)Te(x) are within 10% of the ground truth values while 95% of the layer thickness predictions for the CdTe are within 1.2% of the ground truth values. The development of rapid compositional mapping from spectroscopic ellipsometry data could be highly impactful for determining compositional uniformity for thin-film technologies. This approach can be developed further to examine compositional gradient profiles within the film stacks.

EL-ThP-2 Numerical Ellipsometry: Artificial Intelligence for rapid analysis of Indium Tin Oxide films on Silicon, *Frank Urban, David Barton,* Florida International University
Ellipsometry is a well-known material analytical method widely used to measure thickness and optical properties of thin films and surfaces across a wide range of industrial and research applications including critical dimensions in chipmaking.The method employs the fact that light undergoes a change in polarization state upon reflection from or transmission through a material. The desired properties of the surface structure are related to measurements by the electromagnetic models expressed by Maxwells equations as well as models of material properties. The work here demonstrates the use of Artificial Intelligence (AI) in the form of a multilayer perceptron artificial neural network to apply the electromagnetic model. The reflecting surface examined here is composed of indium tin oxide films (ITO) approximately 400 nm in thickness deposited on silicon substrates. Solutions are provided by 299 artificial neural networks, one per wavelength from 210 nm to 1700 nm across which ITO exhibits transparent as well as absorbing characteristics. Thus, it serves as a proxy for a wide range of other materials. To train the network, simulated measurements are computed at two thicknesses which differ randomly by 1 to 6 nm and at three different incidence angles, 55°, 65°, and 75°. Following training, results are obtained in less than one second on a conventional desktop computer.

EL-ThP-3 Accurate Determination of Critical-Point Parameters in Spectra, *Long Le,* Vietnam Academy of Science and Technology, Viet Nam*; Young Kim,* Kyung Hee University, Republic of Korea*; **David Aspnes**,* North Carolina State University
The determination of the locations of critical points of overlapping features in spectra, optical and otherwise, continues to be a challenge even in the absence of complications due to baseline effects and noise.Recent progress in the use of nonlinear (maximum-entropy) methods to eliminate the noise and apodization artifacts characteristic of linear filters, and to detect weak singularities that otherwise would be overlooked, has highlighted the importance of working directly with low-order Fourier coefficients, where information is separated from baseline effects and noise.Here, we report the results of a systematic investigation of critical-point determination in

both direct and reciprocal space, with emphasis not only on accuracy but also on uncertainty, using multiple averages of spectra with added noise.Reciprocal-space analysis can be viewed as the logical limit of classic derivative methods of extracting these parameters, which draw conclusions from a relatively narrow range of information-containing coefficients.

EL-ThP-4 Optical Analysis of Ferroelectric PLZT Films Using Spectroscopic Ellipsometry, *Sushma Kotru, Sneha Kothapally,* The University of Alabama; *James Hilfiker,* J. A. Woollam Co., Inc.

Spectroscopic ellipsometry was utilized to study the optical properties of ferroelectric lead lanthanum zirconate titanate (PLZT) films. These films were deposited on platinized silicon [Si(100)/ SiO₂/TiO₂/Pt(111)] substrates using the chemical solution deposition method. Films were annealed at two different temperatures (650 and 750 °C) using rapid thermal annealing. Shimadzu UV-1800 UV-VIS spectrophotometer with a resolution of 1 nm was used to measure the reflectance data in the spectral range of 300–1000 nm with a step size of 1 nm. The bandgap values were determined from the reflectance spectra using appropriate equations. A J.A. Woollam RC2 small spot spectroscopic ellipsometer was used to obtain the change in amplitude (Ψ) and phase (Δ) of polarized light upon reflection from the film surface. The spectra were recorded in the wavelength range of 210–1500 nm at an incident angle of 65°. Refractive index (n) and extinction coefficient (k) were obtained by fitting the spectra (Ψ, Δ) with the appropriate models. No significant changes were observed in the optical constants of PLZT films annealed at 650 and 750 °C. The optical transparency and the strong absorption in the ultraviolet (UV) region of PLZT films make them an attractive material for optoelectronic and UV sensing applications.

EL-ThP-6 Spectrally Resolved Absorption Based Kuhn's Dissymmetry Factor from Mueller Matrix Polarimetry, *Ufuk Kilic,* University of Nebraska-Lincoln; *Alexander Ruder, Matthew Hilfiker,* Onto Innovation; *Shawn Wimer,* University of Nebraska Lincoln; *Eva Schubert, Mathias Schubert,* University of Nebraska-Lincoln

Chirality or handedness is one of the most intriguing material properties of an object which cannot be made superimposable on its mirror image [1]. Within the last few decades, this symmetry breaking phenomenon has attracted great attention due to its application in various subdisciplines of physics, chemistry and biology [2-4]. The optical manifestation of chirality known as circular dichroism (CD) which is the difference between the absorbance (A) of left circularly of polarized (LCP) light from the right circularly polarized (RCP) light. Recently, Kuhn's dissymmetry factor, so-called g-factor (given as g-factor=2CD/(A_{LCP}+A_{RCP})) is employed as a metric to quantify and compare the chiroptical ability of various systems: nanostructures, molecules, and thin films independent from their fabrication and characterization methods [5]. In this study, we provide a route to reach out the Kuhn's dissymmetry factor in terms of Mueller matrix elements for accurate evaluation and investigation of the chiroptical response of nanostructured thin film samples fabricated via glancing angle deposition technique [6-7]. Therefore, due to the semi-transparent nature of such fabricated structures, it is necessary to reach out both reflectivity and transmissivity properties. Hence, in this study, we present and discuss full road map of obtaining the spectral evolution of Kuhn's dissymmetry factor that utilizes a combinatorial reflection and transmission mode generalized spectroscopic ellipsometry in Mueller matrix configuration. Our method offers the differentiation of circular dichroism information from the other optical anisotropy types which paves the way through a universal and robust method for direct extraction of chirality.

References

1. S. Han, Q. Yun, S. Tu, L. Zhu, W. Cao, and Q. Lu, Journal of Materials Chemistry A 7, 24691 (2019).

2. M. W. Glasscott, A. D. Pendergast, S. Goines, A. R. Bishop, A. T. Hoang, C. Renault, and J. E. Dick, Nature communications 10, 1 (2019). 8

3. J. P. Mazaleyrat and D. J. Cram, Journal of the American Chemical Society 103, 4585 (1981).

4. X. Wang and Z. Tang, Small 13, 1601115 (2017).

5. W. Kuhn, Ann. Rev. Phys. Chem. 1958, 9, 417

6. Kilic, U., Hilfiker, M., Wimer, S., Ruder, A., Schubert, E., Schubert, M., & Argyropoulos, C., *Nature communications*, 15(1), 3757 (2024).

7. Kilic, U., Hilfiker, M., Ruder, A., Feder, R., Schubert, E., Schubert, M., & Argyropoulos, C., Advanced Functional Materials, 31(20), 2010329 (2021).

EL-ThP-7 The Optical Constants of Calcium Fluoride from 0.03 – 9 eV, *Jaden R. Love, Carlos A. Armenta,* New Mexico State University; *Megan Stokey, Mathias Schubert,* University of Nebraska - Lincoln; *Stefan Zollner,* New Mexico State University

In this presentation we describe the optical properties of calcium fluoride (CaF₂), an insulating material for which most optical studies were conducted in the 1960's and are discussed in [1]. Our goal is to reexamine the optical constants of CaF₂ (111) and (100) MTI manufactured substrates in the range 0 – 9 eV using modern ellipsometry equipment and analysis techniques. From these early studies CaF₂ is known to have an ultrawide bandgap of 12 eV, a large exciton binding energy of 1 eV, and a wide transparency range from 125 meV – 10 eV. The large range of transparency makes CaF₂ a suitable material for use in optical components such as those found in infrared detectors and telescopes.

CaF₂ crystalizes in the FCC fluorite structure within the space group Fm-3m and has a lattice constant of 5.4626 Å. Ca 2^+ atoms are in the Wyckoff (4a) position at the origin. F $^-$ atoms are at the (8c) positions (¼, ¼, ¼) and (¼, ¼, ¾). CaF₂ has a three-fold degenerate Raman-active T_{2g} mode and a three-fold degenerate infrared active T_{2u} mode. The T_{2u} mode splits into a transverse optical (TO) doublet and a longitudinal optical (LO) singlet that were observed using infrared ellipsometry and modeled with a Lorentzian. The TO and LO energies are 261 and 477 cm^{-1} , respectively, with an amplitude A = 4.1, a broadening of 4 cm^{-1} , and a high-frequency dielectric constant of 1.98(1). There is a dip in the reststrahlen band formed by two phonon absorption that was modeled using an anharmonically broadened Lorentzian.

Data for the visible and near ultraviolet was obtained using an RC2 ellipsometer and VUV-SE at the University of Nebraska - Lincoln. The data sets were merged to form a continuous spectrum over the range from 0 – 9 eV. In this region the data shows normal dispersion that is modeled using a Tauc-Lorentz oscillator at 7.24 eV and a pole at 9.24 eV. The pseudo-dielectric function <ε_2> is negative above 3 eV indicating the presence of a surface layer with larger refractive index than that of CaF₂. In the region between 7 – 9 eV there is a small peak in <ε_2> modeled by a Gaussian at 7.6 eV with an amplitude A = 0.05. A Cauchy layer was added above the bulk CaF₂ substrate to improve the fit. We determined that the surface layer present on the samples has a thickness of 15 Å.

[1] D. F. Bezuidenhout in Handbook of Optical Constants of Solids II, edited by E. D. Palik (Academic, San Diego, 1998).

EL-ThP-8 Metrology of Ultrathin Iron Catalyst Films by Spectroscopic Ellipsometry, *Nicholas Allen, Richard Vanfleet, Matthew Linford, David Allred, Robert Davis,* Brigham Young University

Vertically aligned carbon nanotube (VACNT) forest growth is a chemical vapor deposition process that uses a thin-film iron catalyst on an alumina support. Iron catalyst thickness for VACNT growth is typically from ~1-10 nm and thickness strongly affects forest morphology. Consequently, characterization of iron thin films could improve process control of VACNT growth. In this study, we explored the use of spectroscopic ellipsometry (SE) to measure these iron thin films because the technique is rapid, highly sensitive, and non-destructive. SE does have challenges, however, as it is difficult to break the correlation in the analysis between the optical constants and thickness of ultra-thin films. The partial oxidization and the absorptive nature of the iron/iron oxide films adds further difficulty. We performed a multi-sample analysis of thermally evaporated iron films with target thicknesses of 1, 2, 4, 7, and 14 nm. To improve sensitivity, we used contrast enhancement by incorporating a 350 nm silicon oxide layer under the iron film and alumina support. We used a consecutive layers approach, collecting SE data and fitting the model for each film before depositing the next. We found high sensitivity to iron thickness with SE, with reproducible thickness results. We modeled the iron/iron oxide film as a composite with an effective medium approximation layer. Our SE model fits the data well with a relatively low mean squared error. We explored the sensitivity of iron/iron oxide thickness results to errors in the alumina thickness while using the consecutive layers approach, which explained most of the variance we found in measured iron thickness.

EL-ThP-9 IR Ellipsometry on Thermally Oxidized Germanium (100), *Danissa Ortega, Danissa Ortega, Atlantis Moses, Carlos Armenta, Jaden Love, Sonam Yadav, Stefan Zollner,* New Mexico State University

The use of germanium as a semiconductor has been heavily studied but further details about its thermal oxidation, more specifically: its growth methods and process parameters, can show its promise for widespread optoelectronic applications. By performing a Deal-Grove thermal oxidation on bulk Ge, its infrared (combined with ultra-violet) dielectric function can

be determined by utilizing J.A. Woollam Vertical Angle Spectroscopic Ellipsometers (VASE) through ellipsometric angles ψ and Δ.

The cleaved 5x10 mm samples were first ultrasonically cleaned in deionized water at room temperature and dried with nitrogen to achieve a native oxide layer of ~1 nm. The samples were then rapidly thermally annealed in ultrapure oxygen at temperatures ranging from 525-575°C in 40 psi pressure for up to 2 hours, reaching thermal oxide layers as high as 35 nm. Spectroscopic ellipsometry measurements were taken using the IR-VASE and UV-VASE to achieve its dielectric function of ψ and Δ in the photon energy range of 0.05-6 eV at room temperature. IR-VASE and UV-VASE measurements were taken at incidence angles from 50-80° which revealed excitations at photon energies ranging 0.09-0.14 eV. The dielectric function was characterized using a two-layer model: the Ge substrate, then the GeO$_2$ oxide. In the UV range, a Tauc-Lorentz model was utilized, which characterized the fit parameters in the IR range. In the IR range, a Gaussian model fit with peak energy at 0.015 presented a lower MSE than if it were fit with a Tauc-Lorentz or two Gaussians. The modelling will continue to be improved with further growth of the thermal oxide layer at longer annealing times.

Electronic Materials and Photonics
Room Central Hall - Session EM-ThP

Electronic Materials and Photonics Poster Session

EM-ThP-2 Improvement of Al Undercut Defect in sub 20 Nm DRAM, *DONG-SIK PARK, byongdeog Choi,* Sungkyunkwan University (SKKU), Republic of Korea

In the era of the Fourth Industrial Revolution, the utilization of high-performance and high-speed DRAM is increasingly expanding. In response to this trend, the integration density of DRAM is also improving. Since transitioning to the 10 nm design rule, scaling is continuously demanded not only for the DRAM cell size but also for the wiring. The wiring, responsible for supplying electrical signals and power to the DRAM, consists of 4 to 5 layers, with the final wiring utilizing Al lines. Low resistance is necessary to accommodate the delivery of high power for the Al layers.

The composition of Al wiring is as follows: Ti is applied as a barrier metal to connect with the Via tungsten, followed by the formation of Al wiring with a thickness of over 500 nm using the PVD method. On top of this, TiN is applied as an anti-reflecting layer. The Al wiring is patterned using lithography and dry etching techniques. With the scaling of Al wiring, the spacing between metal lines has decreased to 50 nm or less. This means that the space for dry etching the 500 nm-thick Al has become 50 nm, resulting in an aspect ratio of 10:1, posing extreme difficulty. This has led to various serious defects, with the most common being Al undercut defects.

The defect occurs when etching extends from the bottom of the Al layer to the sidewalls, causing it to disconnect. The cause of this issue is that as the aspect ratio increases, the polymer, which serves to protect the Al sidewalls during dry etching, cannot effectively reach the bottommost part, resulting in etching. To overcome this, if the shape of the Al line is formed with a positive slope, it becomes highly susceptible to Al bridge defects.

Two methods were devised to overcome this, implemented in Samsung's 20 nm DRAM technology to confirm their effectiveness. Firstly, it was observed that Al undercut defects primarily concentrated at the edges of wafer. This is influenced by the temperature of the high chuck during dry etching, and it was found that precise temperature control was difficult with the current structure. Therefore, the chuck structure was modified from 2 zones to 4 zones to enable fine temperature adjustment, and the edge area was dry etched at a lower temperature to facilitate the transmission of more polymer.Secondly, the layout structure of the Al layer was reinforced. It was found that having discontinuous vulnerable patterns was more advantageous than continuously existing patterns. Therefore, irregular step patterns were created compared to patterns resembling hammers, and their effectiveness was confirmed.These two improvements were validated through test results of real 8G DDR4 products.

EM-ThP-3 Enhancing Electro-Physical Properties of DRAM Through Control of Silicon Diffusion in Titanium Nitride Based Barrier Layer, *Jina Kim, Yunseok Kim,* Sungkyunkwan University, Korea

As DRAM cell sizes substantially scale down, silicon voids in CMOS gate electrode and memory cell bit-line connection nodes cause serious issues in DRAM performance. These voids are formed at the silicon-metal interface as a result of the each material's difference in diffusivity, where silicon atoms are sucked into the metal layer by the Kirkendall effect, and they are accelerated by heat. Due to the increase in the heat budget of subsequent processes to over 1000 degrees, innovative process for barrier metals preventing silicon diffusion becomes critically essential. In this study, we demonstrate the impact of silicon void defects through variations in thickness, composition, and other parameters of the Titanium silicon nitride (TSN) based barrier metal. To meet the higher barrier properties, TSN has been developed as multi-layer film structure of TiN/SiN, providing low resistance even at low thickness and with the ability to control the composition of Ti, Si and N to maximize barrier properties. Increasing the thickness of TSN can increase the diffusion path of Si, thereby reducing the frequency of Si void occurrence. Furthermore, by increasing the concentration of Si within TSN, it is possible to suppress TiN grain growth while promoting amorphization or the formation of fine grains, thereby inhibiting diffusion through grain boundary. We investigated the frequency of Silicon void occurrence before and after heat treatment using SEM/TEM, and confirmed the extent of improvements for each conditions. Finally, we have confirmed improvements in DRAM data write performance as resistance and short circuit decreased due to silicon void defects. Hereby we have provided a significant opportunity for the development of 10-nano-class DRAM.

EM-ThP-4 Integrating Molecular Photoswitch Memory with Nanoscale Optoelectronics, *Nelia Zaiats, Thomas Kjellberg Jensen,* Lund University, Sweden

Using light for interconnectivity in artificial neural networks can be highly energy efficient and allow multiplexing. Important is the introduction of dynamic memory weights in these connections that can be integrated on-chip with nanophotonic components. We show that photochromic dyes, that reversibly switch their absorption of light, can be used as optical memories combined with highly efficient III-V nano-optoelectronics. We find that the dyes can be used for both short- and long-term memory by varying chemical and physical parameters of the sample, allowing to access a wide range of timescales. We demonstrate the effect both on individual nanostructures and arrays. We demonstrate the robustness over many switching cycles. Using the dye performance parameters, we find that it can function as the memory component in an anatomically verified model of the insect brain navigation complex. The work opens for artificial neural networks with energy-efficient light communication and on-chip molecular memory elements.

EM-ThP-5 Charge Trapping in a-Si$_3$N$_4$: Hydrogen as Savior and Saboteur, *Lukas Hückmann, Jonathon Cottom, Jörg Meyer,* Leiden University, The Netherlands

Amorphous silicon nitride (a-Si$_3$N$_4$) is an essential material for nanoelectronics due to its ability to trap charges, particularly in flash memory devices. EPR experiments combined with electronic structure calculations suggest that undercoordinated Si atoms (K-centers) are responsible for this phenomenon [1]. The propensity of such defects towards hydrogen passivation, however, raises the question of the completeness of this picture.

In this work, we combine simulations at force field (FF) up to hybrid density functional theory (DFT) level. Employing the MG2 force field [2], a comprehensive statistical ensemble of structural models for a-Si$_3$N$_4$ was generated through the melt-quench procedure, ensuring robust statistical significance in our analysis [3]. Adding charges to those models, we perform structural optimization using the HSE06 hybrid DFT-functional to ensure the localization of the band edges and defect trapping energies are well described. We identify a hitherto unknown mode of intrinsic polaronic trapping of electrons in a-Si$_3$N$_4$: Charging can generate either a K-center or Si-Si-type defect. At the same time, discharging recovers the amorphous network's original structure [3]. Crucially, this study bridges the previously fragmented understanding of charge trapping and hydrogen incorporation. We demonstrate that hydrogen plays a dual role: It can repair coordination defects, healing the network, yet also promotes Si-N bond breaking in strained areas, thus compromising the network integrity [4]. Our findings offer a unified perspective on the interplay between defect formation, hydrogen behavior, and charge trapping, providing insights critical for optimizing a-Si$_3$N$_4$'s electronic properties in nanoelectronic applications.

[1] Warren, W. L. et al.J. Appl. Phys.**1993**,*74*, 4034–4046.
[2] Marian, C. M.; Gastreich, M.; Gale, J. D.*Phys. Rev. B***2000**,*62*, 3117–3124.
[3] **Hückmann, L.**; Cottom, J.; Meyer, J.*Adv. Phys. Res.***2024**,*3*, 2300109.
[4] Cottom, J.; **Hückmann, L.**; Olsson, E.; Meyer, J.*J. Phys. Chem. Lett.***2024**,*15*, 840–848,*Selected for cover*.

EM-ThP-6 Graded CdSexTe1-X /CdTe Thin-Film Solar Cells: In-Situ Dopant Profiling During Light Soaking, *Sanghyun Lee,* University of Kentucky*; Kent Price,* Morehead State University

Cadmium Telluride (CdTe) thin-film solar cells have made significant progress in efficiency, with laboratory-scale tests surpassing 22.1%, edging closer to the theoretical Shockley-Queisser limit of around 32%. Recent research has been focused to integrate selenium (Se) into CdTe absorbers, creating band grading without CdS window layers. $CdSe_xTe_{1-x}$ is a prominent candidate to enhance the short-circuit-current (Jsc) by bandgap lowering below 1.45 eV. While CdS window layer intermixing mitigates the lattice mismatch, it concurrently limits absorbing light in the critical 300 - 525 nm range, resulting in efficiency loss. Thus, strategies to overcome this drawback have been focused on introducing Se to create band grading. $CdSe_xTe_{1-x}$ is promising, with bandgap lowering below 1.45 eV, pushing Jsc to their theoretical limit.

In this contribution, $CdSe_xTe_{1-x}$/CdTe devices were fabricated by vapor transport technology, and the mechanism of efficiency improvement was studied through in-situ Cu dopant profiling during light soaking. Moreover, devices were stressed at elevated temperatures simultaneously under various bias conditions, both with illumination and in the dark. The morphological and cross-sectional structure of the graded absorber were confirmed by Scanning Electron Microscopy and Electron Dispersive Spectroscopy. During light soaking, different intensities of light and temperatures were tested to characterize devices. Concurrently, we modeled the electronic structure of characterized devices using our in-house MATLAB modeling suites, connected to the external TCAD simulators, to explain the result with material and device input parameters. The results indicate that $CdSe_xTe_{1-x}$/CdTe devices have shallow donor and acceptor energy states near the main front junction interface. The concentration of Cu dopant is approximately 4 x 10^{14} cm^3 in the wake-up condition. The Cu dopant progresses toward the front $CdSe_xTe_{1-x}$ /CdTe junction during in-situ measurements.Interestingly, the stability of $CdSe_xTe_{1-x}$ solar cells was found to be bias-dependent and device-specific during light and dark soaking. $CdSe_xTe_{1-x}$ /CdTe devices without Cu dopant demonstrated depletion reduction width under light and dark-biased conditions. The depletion width of $CdSe_xTe_{1-x}$ devices without Cu is reduced to approximately 47 % under applied soaking conditions. Simultaneously, efficiency, Voc, and FF decreased, whereas Jsc show no clear dependency. Under light soaking conditions at 95 C, the increases in Voc, FF, and efficiency depend on light soaking conditions. The peak efficiency after 9 hr light soaking at 95 C is 12.90 %.

EM-ThP-7 Optimization of NiO Doping, Thickness, and Extension in Kv-Class NiO/Ga2O3 Vertical Rectifiers, *Chao-Ching Chiang, Jian-Sian Li, Hsiao-Hsuan Wan, Fan Ren, Stephen Pearton,* University of Florida

We conducted a thorough analysis of vertical geometry NiO/Ga_2O_3 rectifiers using the Silvaco TCAD simulator to establish optimized breakdown voltages ranging from 1 to 7 kV. By manipulating key NiO parameters such as doping concentration (ranging from 10^{17} to 10^{19} cm^{-3}), thickness (ranging from 10 to 70 nm), and junction extension beyond the anode to form a guard ring (ranging from 0 to 30 μm), we determined the electric field distribution within each design. The factors of doping concentration, thickness, and junction extension were found to significantly influence the site of device breakdown, which could occur anywhere from the edge of the NiO extension to the edge of the top contact, consistent with experimental results. Further investigations also revealed varying breakdown voltages based on theoretical critical electric fields for different NiO bilayer thicknesses and doping concentrations.

EM-ThP-10 SOH Bake Time Optimization for SOH Void Reduction in Semiconductor Manufacturing, *Jaehyeon Jeon, Byoungduk Choi,* Sungkyunkwan University (SKKU), Republic of Korea

Spin-On Hardmask (SOH) materials are pivotal in semiconductor manufacturing for their superior masking quality, alignment accuracy, process control, and cost-effectiveness, crucial in patterning formation. However, insufficient chemical bonding between SOH and other layers, improper spin speed, or thickness can lead to void formation. In 10nm-scale DRAM products, where pattern sizes are extremely small, SOH voids can cause defects such as bridging and discontinuity in cell transistor gates. This paper demonstrates methods to minimize SOH void formation during the manufacturing process, focusing on the bake time. During SOH baking, condensation reactions and thermal degradation occur, leading to outgassing. In the early stages of baking, polymer condensation is prominent, and once cross-linking is complete, outgassing due to condensation diminishes. However, as bake time increases, outgassing due

to thermal degradation becomes more significant. Thus, minimizing void formation by reducing outgassing at the completion of condensation reactions can be observed, leading to improvements in defects such as bridging and discontinuity caused by SOH voids in final patterns.

EM-ThP-12 Thin Film Electrets Fabricated by Initiated Chemical Vapor Deposition (iCVD), *Stefan Schröder, Torge Hartig, Lynn Schwäke, Thomas Strunskus, Franz Faupel,* Kiel University, Germany

Electrets are the electrostatic counterpart to permanent magnets, as they provide a (quasi-)permanent electric field. They have attracted great interest in the field of electronic applications ranging from sensors to energy harvesting. Polymers are usually selected as the starting material for the fabrication of stable electrets. New application pathways, e.g. in organic electronics, are increasing the demand for such materials in the form of thin films. Current wet-chemical polymer thin film fabrication is limited in the production of precise electret film thickness and dielectric breakdown strength. The reason for this are surface tension and dewetting effects in solution-based approaches as well as residual solvent molecules. This work highlights the fabrication of ultra-stable electret films by vapor phase deposition. Solvent-free, single-step initiated chemical vapor deposition (iCVD) is applied to fabricate precise polymer thin films of high dielectric breakdown strength on large-area substrates as well as complex geometries. Suitable material compositions are identified with the help of first principle calculations, based on electronic structure calculations. Furthermore, polarization effects are investigated, which result in long-term stability and precise tailoring of the iCVD electret surface potential. The fabricated films are tested in different electret transducers and show great potential for the application in next-generation devices.

EM-ThP-15 Revisiting Materials from the B-C-N Family for Interconnect Dielectric Applications, *Michelle Paquette, Raja Bale, Feyza Berber Halmen, Gyanendra Bhattarai, Shahla Daneshmehr, Shailesh Dhungana, Michael Stoll,* University of Missouri-Kansas City

Fundamentally, the back-end interconnect system is made up of two material types: a metallic conductor, and an insulating dielectric. With the ongoing push for high-performance computing, the higher device and power density as well as speed requirements for integrated circuits place new and more challenging demands on these materials. As the semiconductor industry perseveres toward a replacement for the copper conductor, multiple different challenges face dielectrics, including more stringent deposition control, patterning flexibility, and property specifications (electrical, mechanical, thermal, etc). Boron-based solids have been considered as an alternative to silicon-based dielectrics due to their combination of potentially ultra-low dielectric constant with robust mechanical, electrical, and chemical properties. This contribution will cover recent advances and future potential for boron-based dielectrics from our group and others.

EM-ThP-16 Photoluminescence Measurements of Te-Doped Gasb from 10 K to 300 K Using FTIR Spectroscopy, *Sonam Yadav, Sonam Yadav, Carlos A. Armenta, Jaden R. Love,* New Mexico State University*; Perry C. Grant,* University of Arkansas*; Stefan Zollner,* New Mexico State University

Gallium antimonide (GaSb) is a vital semiconductor for fabricating infrared optoelectronic devices, making it significant for next-generation infrared imaging systems. In this study, we investigated the photoluminescence (PL) properties of Te-doped GaSb with a doping level of 2 – 5 x 10^{17} cm^{-3}, across a temperature range from 10 K to 300 K using 400 mW laser power by using Fourier Transform Infrared Spectroscopy (FTIR) in the near IR spectral range. Our experimental results revealed that at room temperature, GaSb exhibits weak PL, which significantly increases as the temperature drops below 170 K. At 10 K, the PL intensity peaks sharply, corresponding to the direct band gap of 0.726 eV. As the temperature increases to 170 K, an additional peak emerges around 0.75 eV, which we attribute to the indirect recombination of L-valley electrons. We quantified the total number of electrons in both the L and Γ valleys, and the ratio of those enabling us to calculate the carrier concentration in each valley as a function of temperature. Our interest in GaSb PL stems from its analogous behavior to GeSn alloys with 10% Sn, making it a potential candidate for use in photodetectors. This work provides valuable insights into the temperature-dependent electronic properties of GaSb, highlighting its relevance in advanced optoelectronic applications.

Light Sources Enabled Science Mini-Symposium
Room Central Hall - Session LS-ThP

Light Sources Enabled Science Mini-Symposium Poster Session

LS-ThP-1 Near-Ambient Pressure XPS/Nexafs at Diamond Light Source, *Georg Held,* Harwell Science Campus, UK

The near-ambient-pressure beamline B07 (Versatile Soft X-ray beamline) at Diamond Light Source opened for users in July 2017. It features a design, where beamline and electron analyser meet in the same flange, such that experimental chambers and reaction cells can be exchanged relatively easily. The energy range 250 – 2800 eV allows accessing a wide range of core levels and is optimised for the electron kinetic energy range necessary to penetrate gas environments in the 10 mbar range. The differentially pumped beamline entrance and analyser enable measurements routinely up to 30 mbar. We will present the beamline design and performance and present results of experiments studying industrial and model catalysts in ambient-pressure conditions, demonstrating the research possibilities it offers.

Magnetic Interfaces and Nanostructures
Room Central Hall - Session MI-ThP

Magnetic Interfaces and Nanostructures Poster Session

MI-ThP-1 Molecular Beam Epitaxy of Antiferromagnetic Kagome Alloy CrSn on LaAlO3 (111), *Tyler Erickson,* Ohio University*; Sneha Upadhyay,* Oak Ridge National Laboratory, USA*; Hannah Hall, Ashok Shrestha, Ali Abbas,* Ohio University*; Senthur Pandi Rajasabai,* Vellore Institute of Technology, India*; David Ingram, Savas Kaya,* Ohio University*; Uma Mahendra Kumar,* Vellore Institute of Technology, India*; Arthur Smith,* Ohio University*; Daniel Russell, Fengyuan Yang,* Ohio State University

Antiferromagnetic Kagome materials with topologically non-trivial electronic structure provide hosts for exotic magnetic phenomena that is useful for spintronic devices [1-3]. The localization of spin states within the Kagome layers provides opportunities for creating quantum spin-liquid ground states [1], and the capability of tuning the Berry curvature near the Weyl points, thereby engineering moment orientations which could lead to large anomalous Hall effects [2], give these materials a bright future in spintronic devices.At present, we are exploring the possibility of CrSn as a future candidate. Rajasabaiet al.recently published introductory work suggesting an antiferromagnetic Kagome crystal structure for CrSn with spin orientations aligned coplanar and anti-aligned between planes [3]. We have attempted to grow this CrSn alloy using molecular beam epitaxy and to compare it to the expected structure predicted by theory. We have grown multiple CrSn samples and investigated their crystallographic structures and magnetic properties through reflection high-energy electron diffraction, x-ray diffraction, atomic force microscopy,and superconducting quantum interference devicemeasurements. Our RHEED measurements give an in-planelattice parameter of 5.33 ± 0.17 Å while XRD measurements give an out-of-plane dspacing of 2.19 ± 0.02 Å and thereforean out-of-planelattice parameter of 4.38 ± 0.02 Å. These lattice parameters are in good agreement with the predicted lattice parameters. Furthermore, SQUID measurements confirm the lack of ferromagnetism and suggest possible antiferromagnetism.

This research has been supported by the U.S. Department of Energy, Office of Basic Energy Sciences, Division of Materials Sciences and Engineering under Award No. DE-FG02-06ER46317.

[1]S. Li,Y. Cui, Z. Zeng,et al.,Phys. Rev. B109, 104403 (2024).

[2]L. Song et al.,Advanced Functional Materials 2316588 (2024).

[3]S. Rajasabai and U. Koppolu,Journalof Superconductivity and Novel Magnetism 35, 839 (2022).

MI-ThP-3 Interactions of Extended Magnetic Defects in Semimetallic Systems, *Samuel Tkacik, Eklavya Thareja, Jacob Gayles,* University of South Florida

Topological semimetals offer a unique opportunity to produce controllable magnetic states and intrinsic spin currents that are robust against backscattering from most types of disorder or defects. This is due to nominal protection offered by the topology of their electronic structure. In this work we study extended magnetic defects in models of semi-metallic structures and examine interactions that arise from the magnetic and electrostatic potentials that characterize these defects. We use scattering theory with a conserved current to study the interactions between extended defects and the bulk with parameters motivated from first-principle calculations of Dirac semimetals. We show that two different regimes exist for a finite and discrete model depending on whether the lattice width is odd or even. We study similarities and differences between bound states in both regimes. Our modelled system is expansive in that it uses parameters derived by first-principle calculations and therefore directly motivates experimental studies in such topological systems. Furthermore, our modelled system serves as a fundamental framework for novel devices with magnetic defects.

MI-ThP-4 Growth and Spectroscopy of Altermagnetic MnTe, *Marco Dittmar, Hannes Haberkamm, Philipp Kagerer, Maximilian Ünzelmann, Friedrich Reinert,* University of Würzburg, Germany

As a new type of fundamental magnetic order next to ferromagnetism and antiferromagnetism, altermagnetism has recently attracted great attention. It is characterized by antiferromagnetic spin alignment combined with rotational lattice symmetry, which is reflected in a spin-split band structure with spin polarized electronic states.

One of the "workhorse" materials potentially exhibiting this type of magnetic order is MnTe in its hexagonal NiAs-type crystal structure. Here, we investigate MnTe thin films grown on different substrates by molecular beam epitaxy. Using structural characterization methods, we discuss the influence of the growth parameters on the observed films. The electronic structure is assessed by soft X-ray angle-resolved photoemission spectroscopy and shows good agreement with band structure calculations.
[1] L. Šmejkal et al., Phys. Rev. X 12, 031042 (2022)

MEMS and NEMS
Room Central Hall - Session MN-ThP

MEMS and NEMS Poster Session

MN-ThP-1 Fundamental-mode Surface Acoustic Wave Magnetoacoustic Nonreciprocal Low-loss RF Isolator for Efficient Control of NV− Centers, *Bin Luo,* Northeastern University, US*; ANDREAS WINKLER, HAGEN SCHMIDT,* SAWLab Saxony, Germany*; BEN DAVAJI, Nian Xiang Sun,* Northeastern University, US

Owing to long coherence time, high fidelity and easy optical initiation and readout of quantum states tuned by magnetic excitations over a broad temperature range, NV− centers are intriguing solid-state platforms for quantum computing, communication, information processing and sensitive non-invasive nanoscale magnetic sensors [1-5]. Traditional control of NV− centers were realized by microwave striplines or antennas, which consume high power on the order of 1~10 W but yields low magnetic field even at a short distance of 1 mm [6-8]. The surface acoustic wave (SAW) delay line driven spin wave enabled by magnon-phonon interactions exhibits superior properties of high-power efficiency, low noise and small footprint, leading to efficient voltage control of NV− center. Recent demonstration of NV− center excited states control by 5th-order-SAW-driven spin wave in a 20 nm Ni film shows comparable Rabi frequencies with 1300 times less power than microwave excitation [9]. However, the low magnitude of high-order SAW and the high damping of Ni film degrades the efficiency and coherence time of NV− center control and hinders the realization of efficient control of NV− center ground states exhibiting longer lifetime.

Recently, magnetoacoustic non-reciprocal RF devices exhibit substantial nonreciprocity with remarkable power efficiency and CMOS compatibility, making them ideally suited for low-power and one-directional quantum transducer. Non-reciprocal magnetoacoustic devices consist of a magnetic stack situated between two interdigital transducers (IDTs) on a piezoelectric substrate. By applying RF voltage on IDTs, the induced SAW propagates and interacts with SW in the magnetic stack. The strong magnon-phonon coupling leads to hybrid magnetoacoustic waves that exhibit a much higher backward loss rate than the forward one or vice versa. Ongoing research strives to enhance non-reciprocity strength and bandwidth while maintaining high transmission between device ports [10]. Despite successful demonstrations of magnitude or phase non-reciprocity in various magnetic stacks such as antiferromagnetically coupled FeGaB/Al$_2$O$_3$/FeGaB stack [11-12], the insertion loss is still high (>50 dB) owing to the low transmission of SAW high-order mode. Here we demonstrated a low-loss magnetoacoustic non-reciprocal device driven by SAW fundamental mode at 2.87 GHz. The 10-dB low insertion loss and strong non-reciprocity of 23.5 dB/mm make the device potential for coherent and efficient control of NV−

center ground states and the realization of non-reciprocal quantum transducer for one-directional quantum information transfer.

MN-ThP-2 3D Carbon Nanotube Collimators Grown on a Transparent Substrate for Diffuse Spectroscopy, *Bridget Kemper, Woodson Parker,* Brigham Young University*; Tyler Westover,* Tula Health*; Richard Vanfleet, Robert Davis,* Brigham Young University

Miniaturized spectrometers could enable the application of spectroscopy in wearable devices such as fitness/health monitors. In prior work, miniaturized spectrometers with carbon nanotube parallel-hole collimators were fabricated for use in diffuse light spectroscopy. The miniaturized collimators were formed using carbon nanotube templated microfabrication (CNT-M). CNT-M collimators were grown on an opaque silicon substrate and removed for use. For the CNT-M structure to be robust enough for transfer, it requires significant carbon infiltration. However, this infiltration step results in increased sidewall reflection, impairing the collimation of light. Here we present the use of a transparent fused silica growth substrate. This allows the collimators to remain on the transparent substrate in spectroscopy applications, circumventing the need for infiltration and substrate removal steps. Omitting the carbon infiltration reduced sidewall reflection and improved collimation performance.

MN-ThP-3 Pressure Controlled Brazing to Form Microscale Metal Fluidic Interfaces, *David Hayes, Jordan Grow, Henry Davis, Brian Jensen, Nathan Crane, Richard Vanfleet, Robert Davis,* Brigham Young University

2D and 3D metal microchannels have been fabricated using diffusion bonding and metal additive manufacturing for applications including micro heat exchangers and microcolumns for gas chromatography. However, creating precise and robust fluidic interfaces remains challenging for these microchannel applications. Brazing is a potential method for forming microscale fluidic interfaces but introduces the risk of clogging the fluidic channel with the molten filler metal. Here, we present brazing methods for interfacing stainless steel capillary to microfluidic parts. We used a powder-based method of pressure control which allowed the filler metal to form a precise hermetic seal at the fluidic interface without clogging the channel. We demonstrate this method by hermetically interfacing two 100 μm inner diameter stainless steel capillaries without clogging. Along with pressure and flow testing results, scanning electron cross-sections (see example in the supplemental figure) show the morphology of the brazed interface.

MN-ThP-4 Concurrent Mitigation of Packaging Stress and Support Loss in Microacoustic Resonators, *Maliha Sultana, Tanvir Hasan, Jennyfer Vivas Gomez, Kevin Chan, Hakhamanesh Mansoorzare, Reza Abdolvand,* University of Central Florida

In this work, the effectiveness of compact isolation frames in mitigating the stress-induced frequency shifts and concurrently boosting the quality factor (Q) of piezoelectric MEMS resonators is studied. Piezoelectric MEMS resonators are a promising candidate for replacing quartz and capacitive resonators. However, having multiple anchor points makes them susceptible to failure due to packaging induced stress. Here, by introducing tailored trenches around said resonators and experimentally comparing their performance with baseline devices, it is shown that the stress-induced frequency shifts are reduced by up to ~94%. Moreover, compared to baseline, the isolation frame boosts the Q of the devices by up to 2.9x, while minimally impacting the device footprint.

Commercially available capacitive MEMS resonators have weak electromechanical coupling which results in higher loss and limits their application in low power scenarios. To overcome this issue, a viable solution is piezoelectrically exciting/detecting the vibration of a single crystal MEMS resonator, as shown in thin-film piezoelectric-on-silicon platform with promising results. However, commercializing this platform is challenging due to packaging and unwanted stresses (e.g., from die attachment material) that translate into the resonant body, causing frequency drifts. This is exacerbated by having two or more anchoring points to substrate that suspend the resonant body. To mitigate this impact, auxiliary trenches with specific geometry are designed (using COMSOL) adjacent to the resonant body to ensure compact footprint. Thickness-lamé mode resonators with low thermoelastic damping are designed and fabricated using a stack of 1um AlN on 21um Si with a frequency around 145MHz.

To evaluate, the resonator die is affixed to a PCB using an epoxy die attachment suspended over another PCB and supported with screws. Stress is applied by tightening screws to bend upper PCB while frequency response of the resonator is recorded by micro-probes connected to network analyzer. Experimental results show, the bending can cause a maximum frequency shift of 18KHz in baseline, which is reduced to around 1KHz (18x reduction) in a device with isolation frame. The curvature of the devices measured using Keyence 3-D Optical Profiler follows the same trend; devices with isolation frame show less bending which implies less impact from stress. Finally, the effectiveness of the isolation frame in reducing the anchor loss is evident by the higher measured Qs compared to baseline. Detailed experimental setup and results demonstrating the effectiveness of isolation frame is available in the provided supplementary document.

Manufacturing Science and Technology
Room Central Hall - Session MS-ThP

Manufacturing Science and Technology Poster Session

MS-ThP-1 Novel Inspection Technology for Detecting Via Open Using Parallel E-beam Scanning and Graphic Design System, *Chihoon Lee,* SSIT (Samsung Institute of Technology), Republic of Korea

As dual-damascene Cu interconnect technique is currently being employed for on-chip interconnect fabrication, and will continue to be used for next technology generations due to significant cost advantage [1]. In this process, however, it has been challenging to detect via open defects occurring in the underlying layer after the completion of the Cu metal line. A viable in-line monitoring to detect via open defects in the back-end of line (BEOL) has been challenging due to the complex multiple via structures connected to the metal line. Today's conventional inspection method do not meet the requirements of a true in-line monitoring strategy [2]. Despite detecting the dark voltage contrast (DVC) signal as a via open defect in the conventional electron beam (E-beam) inspection system, it was not genuine defects in most cases by the transmission electron microscopy (TEM) analysis for detected via open defects. We guess that it is attributed to the complexity of the vertically designed BEOL metal/via structures, which makes it difficult to separate exact via open location in the upper and lower layers. Figure 1 shows exactly detected via open defect image and related metal/via layout with E-beam inspection system.Early in-line detection of these via open defects prior to the electrical die test is crucial for yield improvement. In this talk we demonstrate a novel inspection technology to detect the critical BEOL via open defects using parallel E-beam scanning and graphic design system (GDS). Parallel E-beam scanning is an inspection technique that can detect more electrons by adjusting the stay time of electrons according to the shape of the metal line pattern. It was controlled by the landing energy (LE), scan direction in the E-beam inspection system. In addition, the detecting locations of via open were restricted near single via layout using die to database (D2DB) inspection system to improve the detectability. It can effectively capture the signals of via open defects compared to the conventional E-beam inspection in the complex high dense metal/via structures.

[1] A. V. Vairagar et al., Appl. Phys. Lett. 87, 2005

[2] M. Daino et al., *28th Annual SEMI Advan. Semiconductor Manuf. Conference (ASMC)*, 2017

MS-ThP-2 EES2: Advancing Microelectronics and Computing Energy Efficiency Through a Co-Design Approach, *I-Hsi Daniel Lu,* Energetics

The U.S. Department of Energy's (DOE) Energy Efficiency Scaling for Two Decades (EES2) initiative is a pioneering effort aimed at achieving a 1000x improvement in energy efficiency in all aspects of computing over the next two decades. This ambitious goal is based on the concept of doubling energy efficiency every two years—a new type of scaling—leading to a 1000x over two decades. EES2 focuses on operational efficiency in computing, —from hardware components to software elements.The roadmap leverages an integrated, interdisciplinary co-design approach to optimize energy use across the entire compute stack. Recognizing that the natural slowing of efficiency gains due to factors like the end of Dennard scaling challenge the industry, EES2 emphasizes the importance of co-design, where adjacent layers of hardware and software are developed in tandem to achieve energy efficiency by orders of magnitude without trading off performance.

The roadmap challenges the industry to achieve these ambitious efficiency goals, stimulating innovation and discussion by identifying key technologies that can serve as benchmarks. Through a series of near-, mid-, and long-term strategies, EES2 prioritizes energy efficiency in every aspect of design and development in Microelectronics. Central to this version 1.0 of the EES2 effort are eight working groups: Materials and Devices, Circuits and Architectures, Advanced Packaging and Heterogeneous Integration,

Algorithms and Software, Power and Control Electronics, Metrology and Benchmarking, and Education and Workforce Development. These groups work collaboratively to ensure that the layers of the compute stack enhance energy efficiency, by using co-design as one of the approaches.

As EES2 expands its focus to include emerging technologies such as quantum computing and photonics, the initiative aims to return to or exceed the historical pace of energy efficiency enabled by Dennard scaling by innovations and set new benchmarks for the industry. This poster will explore the collaborative efforts among industry, academia, and national laboratories that underpin this initiative, emphasizing the transformative potential of the co-design approach in driving energy efficiency advancements in microelectronics.

Nanoscale Science and Technology
Room Central Hall - Session NS-ThP

Nanoscale Science and Technology Poster Session

NS-ThP-1 Characterization of MOS Capacitors on 4H Silicon Carbide Substrate Submitted to Beta Ionizing Radiation, *Eloi Magalhaes,* Center for Semiconductor Components and Nanotechnology - CCNano, Brazil*; Rodrigo Reigota Cesar,* **José Alexandre Diniz,** Center for Semiconductor Components and Nanotechnology - CCSNano, Brazil

This work presents a study of the characterization of the MOS capacitors when subjected to ionizing radiation. Such experiments support analyzing the robustness of silicon carbide semiconductor devices, which has attracted increasing attention due to its robustness properties and tolerance to ionizing radiation. For these studies, beta radiation was applied as a source of ionizing radiation, and the Capacitance - Voltage and Current-Voltage characteristics were obtained for devices as-fabricated and post-irradiation. The extracted Flat-band Voltage (VFB) and Leakage Current (LC) parameters were compared to evaluate the irradiation robustness.

In our experiments, MOS capacitors were fabricated with 300 nm thick aluminum upper and down electrodes and 50 nm thick silicon oxide deposited on the N-type 4H-SiC wafers with a 30 μm thick epitaxial layer ($3x10^{15}$ cm-3), and a 350 μm thick substrate ($3x10^{18}$ cm-3). We carried out the beta irradiation experiment on one sample (post-irradiation). Another control sample (as-fabricated) without irradiation was used to compare the electrical values. To irradiate the sample, a Strontium 90 was a beta source with an energy of 1955.7 KeV, a dose rate of 566 Rad/hand, and an exposure time of 72 hours.

Table 1 presents the average values of VFB and hysteresis, which were extracted from C-V curves, and leakage current for accumulation region, extracted from I-V curves. From Table 1, the average values of VFB of -2.01 and -2.33 for as-fabricated and post-irradiation devices were obtained, respectively. If these values are more negative, an increase in effective charge densities at SiO2/SiC structures can be expected after beta irradiation. The difference between them of 0.32 V indicates a 16% charge density increase. The hysteresis values also increased to 0.05 V for 0.36 V, seven times higher. This agrees with the VFB results. Therefore, MOS capacitors are damaged after beta irradiation. However, it can be expected that this damage was not high due to the extracted average values of leakage currents of 297 μA and 201 μA for as-fabricated and post-irradiation devices were obtained, respectively. These values are the same level of magnitude order with a reduction of 32% in the comparison. Thus, our results indicate that the irradiation damage at MOS capacitors on the SiC substrate was not severe. So, SiC devices can be used for applications with irradiation exposure, such as in space aircraft.

NS-ThP-2 Multidimensional Contact Potential Difference Measurements at the Nanoscale in Inorganic Oxides, *Bugrahan Guner,* **Omur E. Dagdeviren,** École de technologie supérieure, University of Quebec, Canada

Inorganic oxide-based sample systems are popular for applications in catalysis, sensing, renewable energy, and fuel cells in which electronic properties play important roles. Environmental conditions, e.g., temperature, can greatly impact the electronic properties and thereby the performance. The lack of basic knowledge of the local variation of electronic properties as a function of temperature limits the fundamental understanding of systems and hampers their robustness. Here, we demonstrate the multidimensionality of contact potential difference (CPD, i.e., the difference in the work functions of the gold-coated probe and the sample when they are in proximity and under thermodynamic equilibrium, a.k.a., volta potential) at the nanoscale in inorganic perovskites and metal-oxides with scanning probe microscopy (SPM) measurements [1, 2]. We concentrated on single-crystal, inorganic perovskites (*e.g.,* strontium titanate, $SrTiO_3$) and metal-oxides (*e.g.,* titanium dioxide, TiO_2) to have the least amount of uncertainty of sample properties. We employed an undoped $SrTiO_3$ and TiO_2, as they are vastly utilized due to their ideal lattice match for similar systems, cost efficiency, stability, and technological and scientific importance. Our experiments reveal three important results: (I) the CPD of both $SrTiO_3$ and TiO_2 evolve with temperature, (II) the measured CPD is dominated by the local surface state at small tip-sample separations (*i.e.,* tip-sample distance < 10 nm), and (III) the thermodynamically driven intrinsic doping of the material is the governing mechanism of the variation of the CPD for these sample systems. These results clearly show that care must be given to identify the temperature-dependent change of electronic properties to attain and preserve the desired performance of inorganic oxide-based sample systems.

[1] Bugrahan Guner and Omur E. Dagdeviren, ACS Applied Electronic Materials **4** (8), 4085 (2022).

[2] Bugrahan Guner, Simon Laflamme, and Omur E. Dagdeviren, Review of Scientific Instruments **94** (6) (2023).

NS-ThP-3 Distributed Injection into a 1D Ballistic Channel, *Bert Voigtländer, Kristof Moors,* Forschungszentrum Juelich GmbH, Germany*; Christian Wagner,* Forschungszentrum Jülich GmbH, Germany*; Helmut Soltner, Felix Lüpke, Stefan Tautz,* Forschungszentrum Juelich GmbH, Germany

The injection of charge carriers into a 1D ballistic channel is usually considered as local injection at opposite ends of the channel. However, in important cases like edge channels of 2D materials, the injection can happen in a distributed manner along the 1D channel. We calculate the potential in the 2D half-plane, terminated by a 1D ballistic channel using proper boundary conditions for the injection of charge carriers into a ballistic channel. We identify hallmark potential-signatures for an 1D ballistic channel and compare them to the behavior of an ohmic conductive channel.

NS-ThP-4 Atomic Force Microscope Customization for Multidimensional Measurements, *Bugrahan Guner, Omur E. Dagdeviren,* École de technologie supérieure, University of Quebec, Canada

Atomic force microscopy (AFM) is an analytical surface characterization tool that reveals the surface topography at a nanometer-length scale while probing local sample properties. Advanced imaging techniques, such as frequency modulation, to achieve high resolution and quantitative surface properties are not implemented in many commercial systems. In this presentation, we illustrate the step-by-step customization of a commercial atomic force microscope [1]. The original instrument was capable of surface topography and basic force spectroscopy measurements while employing environmental control, such as temperature variation of the sample/tip, etc. We demonstrate the capabilities of the customized system with (automated) frequency modulation-based experiments, *e.g.,* voltage and/or distance spectroscopy [2], time-resolved AFM, and two-dimensional force spectroscopy measurements under ambient conditions. We also illustrate the enhanced stability of the setup with active topography and frequency drift corrections. We think that our methodology can be useful for the customization and automation of other scanning probe systems.

[1] Bugrahan Guner, Simon Laflamme, and Omur E. Dagdeviren, Review of Scientific Instruments **94** (6) (2023).

[2] Bugrahan Guner and Omur E. Dagdeviren, ACS Applied Electronic Materials **4** (8), 4085 (2022).

NS-ThP-5 Improving Leakage Current from a Super Clean STI Technology of DRAM, *Hyojin Park, Byoungdeog Choi,* Sungkyunkwan University, Korea

With the arrival of the fourth industrial era represented by AI, the Internet on things (IoT), demands for diverse products and characteristics are increasing in the semiconductor market, and the difficulty of developing

semiconductor processes to satisfy these demands is rapidly increasing. Especially, under the extreme scaling, even small parameters can easily change the characteristics or structures unlike before, and new failure situations that did not exist in the past are continuously occurring. For example, in the case of DRAM, making a right size of active layer was also hard with a previous way, but it is successful making the structure as we designed with silicone liner process called thin poly. With this result, we thought there will be no difficulties with the Si liner, but unfortunately extreme size shrinkage revealed a problem of Si liner scheme. It is the increasing of interfacial leakage current in STI because of the defects in Si liner itself. Fortunately, we were able to develop the new Si liner process that can form liner like epitaxial Si, and with this super clean STI technology we were able to improve the defects of Si liner. The reduction in defects led to an enhancement in interfacial leakage current, and through this, the problems encountered with STI appeared to be resolved. However, the introduction of this super clean STI technology has also caused new problems that we don't expect before.Due to abnormal growth in some STI top regions, a bridge failure occurred between adjacent STI, making it impossible to properly isolate the STI and causing interference between adjacent cell transistors. We conducted various evaluations to solve this problem, and as a result, we were able to provide a truly novel STI technology that improved bridge defects through Si liner thickness control. In the future, scaling will continue, and new and unprecedented problems will continue to arise. However, this super-clean STI technology has become a reassuring cornerstone that supports the STI development even in the middle of difficult hardships and will become a major force in DRAM development beyond D1a node.

NS-ThP-6 Surface Assembly of Tetraphenylporphyrin Mediated by Reaction with Tin Tetrachloride Pentahydrate Investigated with Atomic Force Microscopy, *Quynh Do, Jayne Garno,* Louisiana State University
Free-base tetraphenylporphyrin (H_2TPP) was linked to a Si(111) substrate by reaction with tin tetrachloride pentahydrate ($SnCl_4 \cdot 5H_2O$). Introduction of $SnCl_4 \cdot 5H_2O$ into a solution containing free-base porphyrin resulted in the coordination of a tin atom at the center of the H_2TPP macrocycle. The resulting metalated molecules (Sn-TPP) are skewered together to produce a cofacial arrangement. The metal Sn atom is coordinated to the center nitrogen atoms of the porphyrin macrocycle with O-Sn-O bonding to adjacent molecules. Nanopatterns were prepared by colloidal lithography for subsequent characterizations with atomic force microscopy (AFM). Unsubstituted porphyrin molecules typically attach randomly to surfaces through physisorption. However for Sn-TPP, covalent bonds to the surface and linked individual Sn-TPP molecules was facilitated by O-Sn-O bonds.

The coordination of Sn atoms within the macrocycles of H_2TPP was tracked with UV-Vis spectral analysis, exhibiting a red shift in the Soret band and changes in the relative intensities of the four Q-bands of the porphyrin. The red shift in the Soret band is attributable to the expansion of the porphyrin macrocycle to accommodate the larger Sn atom. Nanostructures were produced using colloidal lithography to facilitate AFM characterizations and to evaluate the influence of experimental parameters of concentration and reaction time for producing stacked Sn-TPP assemblies. A surface mask of silica mesospheres was used to guide the adsorption of Sn-TPP molecules to form defined geometries. After removal of the silica particle mask by steps of rinsing and sonication, nanorings of Sn-TPP were observed. Periodic arrangements of nanorings over broad areas of Si(111) were evident for topography images captured with tapping-mode AFM. Precise control of material properties can be gained by directing the assembly of porphyrins to form nanostructures, and colloidal lithography enables high-throughput at the nanoscale. The conjugated electronic structure of porphyrins leads to thermal stability and distinct electronic and optical properties which are tunable by the choice of functional substituents. Nanomaterials of porphyrins have promising applications in molecular electronics, solar cells, and sensors.

NS-ThP-7 Probing Isotopic Effects on Hyperbolic Phonon Polaritons in MoO₃ with Nanoscale IR Imaging, *Jeremy Schultz, Sergiy Krylyuk,* National Institute of Standards and Technology (NIST); *Jeffrey Schwartz,* University of Maryland, College Park; *Albert Davydov, Andrea Centrone,* National Institute of Standards and Technology (NIST)
Hyperbolic phonon polaritons (HPhPs), hybrids of light and lattice vibrations in polar dielectric crystals, enable nanophotonic applications by providing a method to confine and manipulate light at the nanoscale. Molybdenum trioxide (α-MoO_3) is a naturally hyperbolic material, meaning that anisotropy in its dielectric function determines the directional propagation of in-plane HPhPs within its reststrahlen bands. A range of strategies are being developed to alter the intrinsic dielectric functions of natural hyperbolic materials and control the confinement and propagation of HPhPs. Since isotopic disorder can limit phonon-based processes such as HPhPs, here we synthesize isotopically enriched $^{92}MoO_3$ (^{92}Mo: 99.93 %) and ^{100}MoO3 (^{100}Mo: 99.01%) crystals to tune the properties and dispersion of HPhPs with respect to natural α-MoO_3, which is composed of seven stable Mo isotopes. Real-space, near-field maps measured with the photothermal induced resonance (PTIR) technique were used to compare in-plane HPhPs in α-MoO_3 and isotopically enriched analogues within a reststrahlen band (≈ 820 cm^{-1} to ≈ 972 cm^{-1}). We found that isotopic enrichment (e.g., $^{92}MoO_3$ and $^{100}MoO_3$) alters the dielectric function and shifts the HPhP dispersion (HPhP angular wavenumber × thickness vs IR frequency) by $\approx$ -7 % and $\approx$ +9 %, respectively, and changes the HPhP group velocities by $\approx$ ±12 %, while the lifetimes ($\approx$ 3 ps) in $^{92}MoO_3$ were found to be slightly improved, by $\approx$ 20 %. The latter improvement was attributed to a decrease in isotopic disorder. Altogether, isotopic enrichment was found to offer fine control over the properties that determine the anisotropic in-plane propagation of HPhPs in α-MoO_3, which is essential to its implementation in nanophotonic applications.

NS-ThP-9 Effect of Thermal Annealing on Electrical Property of Platinum Nanowires Deposited by Focused Electron Beam Induced Deposition, *Rajendra Rai, Ujjwal Dhakal, Binod D.C., Yoichi Miyahara,* Texas State University
Focused Electron-Beam Induced deposition (FEBID) is a direct writing technique which can be used for fabrication of nanoelectronic devices such as single-electron transistor. However, FEBID-deposited nanoelectrodes exhibit high resistance because the as-deposited structures contain unwanted precursor elements like carbon due to its precursor Me3CpMePt (IV), (Me: methyl, Cp: cyclopentadienyl). We report the electrical properties of Pt nanowires with thickness ranging from 2 nm to 200 nm deposited by FEBID technique. We investigated the post-deposition processing techniques to turn the deposited nanowires into electrically conducting as pure Pt metals. We found that the thermal annealing of the as-deposited Pt nanowires can increase in electrical conductance by five orders of magnitude. The resulting annealed wire shows metallic electrical conduction down to 100 mK. We will present the length and width dependence of the electrical conductance and their correlation with the structure of the nanowires which are measured by atomic force microscopy and Kelvin probe force microscopy.

NS-ThP-10 Enhancing Ferroelectricity and Controlling Defects in Aluminum Nitride Thin Films through Ion Bombardment, *Bogdan Dryzhakov,* Oak Ridge National Laboratory; *Kyle Kelley,* Oak Ridge Natinal Laboratory
The wurtzite ferroelectric aluminum nitride (AlN) is a promising multifunctional semiconductor in memory applications. However, its inherent structural factors raise coercive often even above breakdown voltage fields, making reducing the domain switching energy barrier is a key focus. Defects, such as Al and N vacancies and their complexes with native impurities like oxygen and carbon, play a crucial role in determining the dynamics of ferroelectric switching through the interaction with the lattice leading to domain nucleation, pinning, lattice softening, and polarization screening. In this study, we leverage the optical signatures of defect chemistries, probed by cathodoluminescence (CL), to correlate with the ferroelectric behavior of AlN. CL overcomes the wide bandgap of AlN (>6 eV) to excite color centers through ionization processes that exhibit nanoscale heterogeneity and small optical interaction cross-sections. With this understanding in hand, we employ helium ion irradiation to induce local structure changes and tune defect density and type by modulating the dose. CL spectra demonstrate irradiation-dose-dependent altered defect chemistry, suggesting the irradiation dose gradually evolves existing defects to favor the formation of nitrogen vacancies and diminishing oxide complexes. From functional atomic force microscopy measurements, the relative increase in dose correlates to a steep drop off in ferroelectric coercive field, which is accompanied by a significant enhancement of piezoelectric coefficient. By leveraging the method of He-ion irradiation to enhance potential nucleation sites, we reduce the barrier to switching by >40% and postulate the type and functionality of defect states crucial for engineering ferroelectric properties in AlN thin films.

NS-ThP-11 Delamination of Epitaxially-Grown Single-Crystalline GeTe Films for Flexible Phase Change Memory, *Seohui Lee, Chang-Hyeon Yoo,* University of Central Florida; *Hankyun Shin,* University of Central Florida, Dong-A University, Republic of Korea; *Sang Sub Han, YeonWoong Jung,* University of Central Florida

Integrating phase change materials with flexible substrates is crucial for advancing technologies like phase change memory (PCM). This study focuses on GeTe as a fundamental PCM, synthesized over large areas using Chemical Vapor Deposition (CVD). Our objective is to develop thin, flexible GeTe-based materials for PCM applications.

To achieve this, we employ a Ni-electroplating-assisted spalling technique to separate GeTe films from Ge wafers. We confirm the successful delamination of GeTe through Raman spectroscopy and X-Ray Diffraction (XRD).

This work focuses on the development of thin, flexible GeTe-based materials to enhance phase change memory applications by integrating them with flexible substrates. By exploring it, we aim to explore new possibilities for future technologies.

NS-ThP-12 The Incorporation of Nanohelical Metamaterial Into 1D Photonic Topological Insulator System: A Route to the Generation of Strong Chiral Response, *Sema Guvenc Kilic,* University of Nebraska-Lincoln; *Ufuk Kilic,* University of Nebraska - Lincoln; *Mathias Schubert, Eva Schubert,* University of Nebraska-Lincoln; *Christos Argyropoulos,* Penn State University

During the last two decades, 1D and 2D photonic topological insulators (PTI) have gained great interest due to their potential applications in quantum information technologies, waveguide systems, and next-generation photonic integrated circuits [1-4]. In this study, we propose to combine a 1D photonic crystal system with a 3D nanohelical metamaterial platform that can potentially achieve large chiral response. The optical manifestation of chirality known as circular dichroism (CD) is the differential absorption (A) of left circularly polarized (LCP) light from that of right circularly polarized (RCP) light case ($CD=A_{LCP}-A_{RCP}$). In the proposed system, we employ one-turn nanohelical structures comprising gold (Au) and silicon (Si) helical subsegments. This helical structure is integrated into a 1D photonic topological structure consisting of alternating TiO_2 and SiO_2 flat thin film layers. Based on our systematic finite element modeling studies, we observe a strong leak mode that emerges in the photonic gap region with perfect transmissivity and strong electric field confinement at the central two layers of 1D-PTI. The spectral location of the leak mode is in excellent agreement with the topological edge mode frequency in the superlattice energy dispersion diagram of the proposed PTI system. As a last step of this study, Si-Au plasmonic nanohelical structure with the highest chiroptical response was placed at the center of the topological interface where the electric field coupling is maximum. By engineering the thickness of individual layers in 1D photonic crystal system, we successfully spectrally matched the chirality of the nanohelical structure with the topological leak mode. We observed that the integration of nanohelical structure into the PTI system provided a solid route to generate a strong chirality response.

NS-ThP-14 Ge(CH₂I)₄ on Si(100): Matching the Molecule to the Surface and the Science, *Brandon Blue, Rafik Addou, Damian Allis, Jeremy Barton, Nina Culum, Michael Drew, Tyler Enright, Aru Hill, Taleana Huff, Oliver MacLean, Terry McCallum, Mathieu Morin, Matthew Moses, Ryan Plumadore, Marco Taucer, Denis Alexander Therien, Dusan Vobornik,* CBN Nano Technologies Inc., Canada

As we approach smaller silicon device sizes and search for new functionalities, a promising avenue of research is the combination of silicon with organic molecules. Despite 50 years of research into this field, a concerted multi-factor effort for targeted molecule reactivity has yet to be applied. Herein, we present one such effort with the on-surface, multi-technique analysis of a newly synthesized, highly symmetrical molecule, **t**etrakis(**i**odo**me**thyl)**ge**rmane (Ge(CH₂I)₄; TIMe-Ge), consisting of four iodomethyl (CH₂I) "legs" bound to a germanium atom "core" in a tetrahedral geometry. TIMe-Ge was selected for this study based on its expected reactivity and surface behavior with Si(100) 2x1, which was supported by simulations and literature precedent. TIMe-Ge's properties enable three of its legs to covalently bond with Si(100) 2x1 in a limited number of configurations via C-I dissociative addition, with the fourth CH_2I pointing near-normal to the surface. The unbound CH_2I group was expected to exhibit a distinctive scanning tunneling microscopy (STM) signature due to its low, but non-zero, rotational barrier. Additionally, the iodine atoms on all legs provide an x-ray photoelectron spectroscopy (XPS) signal that is both straightforward to fit, and predictably high in signal intensity: a crucial factor for quantitative analysis in sub-monolayer depositions. Leveraging these characterization features, we examined the impact of sample temperature on TIMe-Ge surface binding configurations, demonstrating a temperature dependence that changed the number of bound legs. For three-leg-bound TIMe-Ge, ultraviolet irradiation and STM tip-mediated bias-pulse dehalogenation were performed on the remaining CH₂I at 77 K, alongside STM tip-mediated rotation of the remaining CH₂I at 4 K. The dehalogenation processes produced carbon-centered radicals potentially suitable for on-surface synthesis, donation of functional groups, and/or the attachment of new functional groups.

NS-ThP-15 Percolation Electronic Transport in 2D Nanowire Networks Containing Void Type Defects, *Andrew Qiu, Devendra Kumar Gorle, Sara Alzahrani, Ant Ural,* University of Florida

Two-dimensional (2D) networks consisting of one-dimensional (1D) wires, such as carbon nanotubes, metal nanowires, and graphene nanoribbons, are promising candidates for next-generation flexible transparent conducting electrodes in devices such as organic light-emitting diodes (OLEDs), solar cells, touch screens, smart windows, transparent heaters, and liquid crystal displays. 2D nanowire networks also have functionality in device applications such as flexible electronics, thin film transistors, wearables, electronic skin, biosensors, and neuromorphic computation. Electronic transport in 2D nanowire networks is governed by percolation, which deals with the formation of long-range connectivity in random networks. Understanding the impact of void type defects, which could be present due to lack of control in the deposition/fabrication process or introduced intentionally, on percolation electronic transport in nanowire networks is critical for many applications.

In this work, we study the effect of voids on electronic transport in 2D nanowire networks using Monte Carlo simulations. We define the relative void size as the ratio of the length of the side of the void to the length of the side of the nanowire network. We first study the impact of voids on networks consisting of randomly oriented and straight nanowires. We compute the percolation probability in these networks as a function of nanowire density for different relative void sizes. We find that both the mean and standard deviation of the percolation probability density function increase with increasing relative void size. We then compute the relative conductivity change as a function of nanowire density for different relative void sizes and find that it increases approximately linearly with relative void size.The conductivity of 2D nanowire networks exhibits a power-law dependence on nanowire density as predicted by percolation theory. In order to study the effect of voids on this dependence, we extract the local power-law critical exponent as a function of nanowire density for different relative void sizes. We find that the critical exponent approaches 2 at high density for all relative void sizes, in agreement with networks without voids. Using the same procedure as randomly oriented and straight nanowires, we then investigate the impact of voids on the nanoscale charge transport through networks consisting of curvy and aligned nanowires. These results show that Monte Carlo simulations are an essential predictive tool for providing insights into the percolation electronic transport in 2D nanowire networks, which are promising candidates for a wide range of functional applications.

NS-ThP-16 Frequency Shift and Damping Noises of Mechanical Resonator with Quality Factor Modified by Optomechanical Force, *Md Mahamudul Hasan, N. Austin Bingamon, Binod D.C., Yoichi Miyahara,* Texas State University

In Frequency Modulation Atomic Force Microscopy (FM-AFM), several noise sources can affect the accuracy and resolution of measurements. Deflection sensing noise in an FM-AFM cantilever, combined with thermal noise, contributes to noise in the frequency shift (Δf) and damping (γ_{dis})[1]. Therefore, quantifying noise is essential for understanding tip-sample physics and achieving high-resolution imaging in FM-AFM. The optical excitation using laser sources to excite the cantilever not only removes the spurious mechanical crosstalk[2,3] but also allows us to modify the Q for the optimized Δf and γ_{dis} measurements[4]. In our present setup, we developed a low-temperature FM-AFM integrated with a cryogen-free dilution refrigerator (LD250, Bluefors). Here, two lasers with different wavelengths i.e. 1310 nm for excitation and 1550 nm for interferometric detection were deployed. The intensity of 1310 nm was modulated to drive the cantilever at its resonance frequency (f_0) to get a cantilever resonance free from spurious mechanical resonances while the 1550 nm laser was used for deflection sensing. Besides, we also regulated the quality (Q) factor of the cantilever by adjusting the average intensity of the 1310 nm laser without changing the Fabry-Perot cavity length. We carefully observed the Δf and

γ_{dis} noise for varying Q and our results showed these noises are independent of the modified Q. We will present the effect of modified Q on the bandwidth and noises of Δf and γ_{dis} measurements.

References

1) K. Kobayashi, H. Yamada and K. Matsushige, Rev. Sci. Instrum.**80**, 043708 (2009).

2) A. Labuda, Y. Miyahara, L. Cockins and P. H. Grütter, Phys. Rev. B **84**, 125433 (2011).

3) Y. Miyahara, H. Griffin, A. Roy-Gobeil, R. Belyansky, H. Bergeron, J. Bustamante and P. Grutter, EPJ Techn Instrum **7**, 2 (2020).

4) N. Austin-Bingamon, D. C. and Y. Miyahara, Jpn. J. Appl. Phys. **63**, 04SP84 (2024).

NS-ThP-17 Chemical Synthesis of Metal Nitride Nanoparticles for Electrocatalysis, *Rihana Burciaga,* Clark Atlanta University

Copper nitride (Cu_3N) is an intruiging material known for its diverse applications and unique properties. Cu_3N exhibits a range of physical characteristics including high thermal and chemical stability. The material has garnered interest for its potential in semiconductor devices, solar cells, and as a catalyst in various chemical reactions. Studies have demonstrated that Cu_3N can be synthesized through various methods, including reactive sputtering and chemical vapor deposition, and its properties can be tailored for specific applications. However, conventional methods lack of precise control on the size and morphologies of the nitride nanomaterials. Herein, we explore the chemical synthesis of metal nitride nanoparticles by leveraging colloidal chemistry to harness the synthetic control. Uniform size and morphology of pure phases of metal nitride nanoparticles have been successfully obtained. We further explore its electrocatalytic applications in key reactions for sustainable energy applications. Metal nitride nanoparticles demonstrated superior performance in electrocatalysis.

Plasma Science and Technology
Room Central Hall - Session PS-ThP

Plasma Science and Technology Poster Session

PS-ThP-2 Effect of In-Situ Heat Treatments on PVDF Film Characteristics Deposited by Using Atmospheric Pressure Plasma Synthesis, *Heung-Sik Tae,* School of Electronic and Electrical Engineering, College of IT Engineering, Kyungpook National University, Republic of Korea; *Eun Young Jung,* The Institute of Electronic Technology, College of IT Engineering, Kyungpook National University, Republic of Korea; *Habeeb Olaitan Suleiman,* School of Electronic and Electrical Engineering,College of IT Engineering, Kyungpook National University, Republic of Korea; *Choon-Sang Park,* Electrical Engineering, Milligan University, USA

In recent, the development trends of energy storage devices, will be stretchable, bendable, and portable device with light weight in the field of flexible devices, including nanogenerator and sensors. Thus, piezoelectric polymers have received attractive attention for their application [1]. Among of these piezoelectric polymers, polyvinylidene fluoride (PVDF) and its copolymers have been mostly studied due to specific properties. The PVDF thin film is usually used by solution-based synthesis, such as a electrospinning and spin casting [2]. However, these methods are unsuitable for applying the field of flexible devices due to their problems, such as complex, dangerous, and heating procedures according to the chemicals. To solve these problems, it is necessary to develop new processes based on low-pressure and atmospheric pressure plasma (APP) processes. Among these plasma processes, the low-pressure plasma have the biggest disadvantages in industrial applications, including the large equipment, high cost, and difficulty in transmitting heat on film owing to the use of a vacuum system. Thus, the APP process appears to be a promising method to deposit the polymer film on the point of view a simple, low cost, and heating-free process. For this reason, many studies has been currently investigated on the APP process for polymer film deposition [3,4]. Accordingly, to enhance the structural phase of PVDF thin film, this study investigated the effects of in-situ heat treatment on PVDF thin film characteristics during the APP process in terms of different heating temperatures (room temperature, 100, 150, and 200°C) using scanning electron spectroscopy (SEM), Fourier transforms-infrared spectroscopy (FT-IR), X-ray diffraction, and impedance analyzers. The PVDF thin film was deposited by APP process during 1 h using a mixed polymer solution composing of PVDF polymer nano powder and dimethylformamide (DMF) liquid solution. In addition, the in-situ heat treatment was performed through substrate heating on a hot plate while depositing the PVDF thin film by the plasma. Based on the FT-IR and SEM results, after PVDF thin film deposition at 150°Cduring 1 h, PVDF thin film was smoothly formed with PVDF nanoparticles and the DMF component in the form of bubbles was largely reduced. Moreover, in FT-IR spectra, two phases (α and β phases) were observed in in-situ heated PVDF film, which the peaks at 975 and 1402 cm^{-1}represent α-phase and the peak at 1072 cm^{-1} indicates β-phase. The detailed experimental results of PVDF thin films produced by in-situ heat treatment are currently being studied and will be described in detail.

PS-ThP-3 Uniformity Monitoring of Photoresist Etching using Multi-Channel Endpoint Detection in Inductively Coupled Plasma, *Sanghee Han,* Sungkyunkwan University (SKKU), Republic of Korea; *Jaehyun Kim,* Sungkyunkwan University, Republic of Korea; *Heeyeop Chae,* Sungkyunkwan University (SKKU), Republic of Korea

In this work, the uniformity of photoresist (PR) etch rates was monitored with multi-channel optical emission spectroscopy (OES). Etch rate uniformities were controlled from center-high etch rate to edge-high etch rate by varying gas flow rates, source power, bias power, and CF4/O2/Ar plasma pressure in a 300mm cup-type inductively coupled plasma (ICP) descum chamber. Eight fiber optics in an 8-way jig were mounted on a rectangular viewport of the chamber and the eight optical fibers were connected to a switching module that transfers signals to a single spectrometer. We can exclude variations of signals originating from different spectrometers with this configuration. The spatially resolved endpoints were determined with CO (428-431nm) band in all PR etch processes, while other relatively strong peaks such as O (777nm), F (703nm), and CO (481-483nm) show no difference in spatial variation in PR etch rates. The CO (428-431nm) band corresponds to the de-excitation of CO from the state d$^3\Delta$ with a vibrational number of 14 or 16 to the metastable state a$^3\pi$. The results indicate that to monitor etch uniformity effectively, it is necessary to observe emissions from select excited states of etch products, which only transition to a metastable state of those products. The etch profiles across the wafer were determined based on the etch endpoints from 8-channel optical emission spectroscopy (OES) under various conditions, and these results aligned with the trends observed in thickness measurements conducted using a reflectometer.

PS-ThP-4 Effect of Mask Pattern on the Tribological Properties of Pattern Plasma Nitrided AISI H13 Tool Steel, *Junji Miyamoto, Ryo Tsuboi,* Daido University, Japan

Plasma nitriding is widely used for mechanical parts, dies and tools as one of the surface modification processes. Plasma nitrided material is improved the surface hardness, wear resistance and fatigue strength etc. while maintaining the core properties. An advantage of plasma nitriding over conventional nitriding is that the former is a clean, nontoxic process that involves a shorter nitriding time than gas nitriding. However, plasma nitrided sample have not be attained low friction coefficient same as samples nitrided by another nitriding method. A mechanical part that contacts two surface requires a reduction in the friction coefficient. Friction accounts for about 23% of all energy consumption worldwide, among which 20% is needed to reduce friction and 3% is required to remanufacture replacements for worn-out parts and equipment. Consequently, studying the characteristics of contact surfaces that reduce friction not only results in energy savings, but also extends the lifetime and dependability of the component. Surface texture technology is crucial for reducing the friction coefficient of contact surface and enhancing friction performance.

There is technology of surface texturing that create a series of regular microstructures on the surface of a sample using process techniques. The textures with suitable size can act as micro-bearing to increase the dynamic pressure between friction pairs, store lubricants, and capture debris produced during the friction process.

In this study, plasma nitriding was performed partially by Electron-Beam Excited Plasma using mask with hole to create surface texturing on the surface of tool steel. The effects of partially plasma nitriding were investigated, and the tribological properties of surface on the formed partially nitrided layer were clarified.

The results of our experiments show that the hardness of the sample was increased only in the open areas that were not masked. The measured hardness of the nitrided layer of all tool steel work pieces were increased by more than two times that of the core material. Regular micro asperities were formed on the nitrided sample surface.

PS-ThP-6 High-Voltage Custom Waveform Bias for Ion Energy Distribution Control, *James Prager, Timothy Ziemba, Paul Melnik, Josh Perry, Chris Bowman,* EHT Semi

As the market demands solid-state non-volatile memory storage, plasma etching high-aspect-ratio (HAR) features is becoming increasingly important. To minimize feature defects like bowing and twisting defects, precision control of the ion energy distribution (IED) is required. Eagle Harbor Technologies (EHT), Inc. has developed a unipolar wafer bias power system that can operate up to 15 kV at 400 kHz. In this work, EHT is using a retarding field energy analyzer (RFEA) to investigate IEDs with these high-voltage custom waveforms. A 60 MHz capacitively coupled plasma source with a pedestal that can be biased is being used to experimentally test IED control using these high voltage custom waveforms. EHT will present RFEA measurements of the IED with energies above 2.5 kV. Future plans will also be discussed.

PS-ThP-7 High-Voltage Bipolar Tailored Waveforms with Droop Compensation for Ion Energy Control, *Timothy Ziemba, James Prager, Paul Melnik, Josh Perry, Chris Bowman,* EHT Semi

In plasma processing applications, like etching, the ion energy and flux can be independently controlled with the use of multiple power systems. Typically, a high-frequency RF generator is used for plasma production, and a low-frequency RF generator is used to bias the wafer. Using RF for the wafer bias power system produces a very broad ion energy distribution (IED) at the wafer surface. Eagle Harbor Technologies (EHT), Inc. has developed a high-voltage bipolar waveform generator that can be used to provide precision control of the ion energy distribution at the wafer surface. This power system is being tested in an experimental plasma chamber with a 60 MHz capacitively coupled plasma source and a pedestal that can be biased. EHT will present IED measurements collected using a retarding field energy analyzer (RFEA) with energies up to 2.5 kV. Additionally, we will show IED calculations from bias waveforms for ions over 5 kV when the voltage exceeds the limits of the RFEA.

PS-ThP-8 Electron-Assisted Etching of Poly-Si and SiO_2 in Ans Inductively Coupled CF_4 Plasma, *Jiwon Jung, Chin-Wook Chung,* hanyang university, Republic of Korea

Low-energy electron beam is generated to assist the Poly-Si and SiO_2 etching via grid system in an inductively coupled CF_4 plasma. The etch rate of Poly-Si and SiO_2 increases with electron beam energy, which is regarded that the electron assist the surface etching process. To verify this, Poly-Si and SiO_2 etching is performed in several plasma conditions, which leads different etch rate depending on the presence or absence of radicals and electron beams. Poly-Si and SiO_2 are not etched without radicals of CF_4 plasma, while they are etched with radicals. When the electron beam and radicals of CF_4 plasma exist simultaneously, etch rate increases dramatically than the case of CF_4 plasma without electron beam. This is because electrons assist the etching process. Furthermore, F radical density variation as increasing electron beam energy is measured by OES measurement to demonstrate that the reason of etch rate increase is not F radical density variation. The surface roughness is measured after low-energy electron beam etching and compared with that after the ion-assisted etching.

PS-ThP-9 Laser-Induced Fluorescence Transitions Relevant for the Microelectronics Industry, *V S Santosh K Kondeti, Shurik Yatom, Ivan Romadanov, Yevgeny Raitses,* Princeton Plasma Physics Laboratory*; Leonid Dorf, Andrei Khomenko,* Applied Materials Inc.

A diverse combination of feed gases is utilized in creating low-temperature plasmas for applications in the microelectronics industry. These plasmas generate a wide combination of reactive and non-reactive species, with a spatial and temporal fluctuation in the density, the temperature, and the energy. Precise understanding of these parameters and their variations is crucial the advancement of microelectronics through validated modeling and designing relevant devices. Laser-induced fluorescence (LIF) offers spatially and temporally resolved information of the plasma-produced radicals, ions, and metastables. However, implementing this diagnostic tool requires the knowledge of the optical transitions, including the excitation and the fluorescence wavelengths. This information is often scattered across extensive literature from widely different fields. This study analyzes and compiles the available transitions for laser-induced fluorescence of more than 160 chemical species pertinent to the microelectronics industry. The plasma generated by the feed gas mixture and its interaction with the chamber walls and materials generates a complex combination of reactive species. Our analysis will show the overlapping LIF transitions that need to be considered when selecting and implementing LIF in plasmas with a complex combination of feed gases, such as those employed in the processing of microelectronics.

PS-ThP-10 A Dry Process of Iodine Chemistry for Euv Sensitizer/Underlayer, *Phong Nguyen, Nathan Stafford,* Air Liquide

As extreme ultraviolet lithography progresses towards achieving finer details, challenges like stochastics and sensitivity emerge for polymeric photoresists. To meet the demands of high-volume manufacturing and overcome the limitations of EUV source power, enhancing resist sensitivity is crucial for achieving high-resolution patterning while ensuring pattern fidelity and uniformity. One promising approach involves incorporating atoms with high photoemission cross-sections, such as iodine, into the resist composition to significantly enhance material absorbance. Exploring the incorporation of iodine into carbon-containing layers presents an intriguing avenue for advancement.

In recent years, Air Liquide has spearheaded the development of a series of low global warming potential chemistries, facilitating the formation of atomically smooth iodine-containing layers with adjustable thickness and iodine concentration through a low-pressure plasma process. These film properties are studied using scanning electron microscopy (SEM), atomic force microscopy (AFM), and X-ray photoelectron spectroscopy (XPS).

PS-ThP-11 2D Particle-in-Cell Modeling of an Inductively Coupled Plasma for the Semiconductor Industry, *Willca Villafana,* Princeton University Plasma Physics Lab*; Dmytro Sydorenko,* University of Alberta Edmonton, Canada*; Igor Kaganovich,* Princeton University Plasma Physics Lab

The state-of-the-art EDIPIC-2D code [1] now includes self-induced electromagnetic effects using the Darwin Direct Implicit algorithm [2]. The cell size can be greater than the Debye length and the time step may exceed the period of Langmuir oscillations, which are acute constraints to the standard explicit Particle-In-Cell code [3]. Therefore, the code can now model Inductively Coupled Plasma (ICP) Reactors of a realistic size using a modest amount of computational resources. In this work, we showcase the example of an ICP reactor operating in the sub-mTorr range, that could be typically used for etching in the semiconductor industry. We emphasize our analysis of key parameters essential for atomic precision processing such as the ion energy flux and the ion angle distribution function as measured at the wafer.

[1] Sydorenko D., "Particle-in-cell simulations of electron dynamics in low pressure discharges with magnetic fields," Ph.D. dissertation, University of Saskatchewan, Canada, 2006.

[2] Gibbons M. R. and D. W. Hewett, "The Darwin Direct Implicit Particle-in-Cell (DADIPIC) Method for Simulation of Low Frequency Plasma Phenomena", J. Comput. Phys. 120, 231 (1995).

[3] C.K. Birdsall, "Particle-in-cell charged-particle simulations, plus Monte Carlo collisions with neutral atoms, PIC-MCC," IEEE Trans. Plasma Sci. **19**(2), 65–85 (1991).

PS-ThP-12 On the Compensation Method of the Attenuation of the Light Intensities in Fluorocarbon Plasmas, *Chinwook Chung,* hanyang University, Republic of Korea*; Hyeon ho Nahm,* Hanyang University, Republic of Korea*; Jeonghyun Lee,* hanyang University, Republic of Korea

We investigated the attenuation of light intensity due to fluorocarbon film on the view port (quartz window) in a C_4F_8 plasma reactor. For the compensation of the light intensity, fluorocarbon film thickness is measured by using an electrical method. The electrical method is based on the difference of the film impedance when triple AC voltages are applied to the film. Transmittivity of the fluorocarbon film at various conditions are measured. The transmittivity varies depending on wavelengths and the thickness of the film. For accurate plasma parameter measurement by the line ratio technique, it is crucial to account for the attenuation in light intensity caused by the films during plasma processes. Based on the transmittivity data and the real time thickness of the film on the view port, we successfully compensate the attenuation of light intensity. As a results, plasma parameters from the compensated line ratios are consistent with other measurement those from Langmuir probes.

PS-ThP-13 GaN and NiO Metal-Semiconductor-Metal Photodetectors Fabricated via Hollow-Cathode Plasma-Assisted Atomic Layer Deposition, *Steven Allaby, Habeeb Mousa, Matthew Silverman, Heba Saleh, Su-Hyeon Choe, Louis V. Antoine, Jacques Goosen,* **Fatih Bayansal**, *Iram Sifat, Alexander Agrios, Necmi Biyikli,* University of Connecticut

Metal-semiconductor-metal (MSM) photodetectors (PDs) have gained significant interest in optoelectronic applications in industrial, environmental, and even biological fields. MSM PDs benefit from simplicity in design, large active area, fast response, and low dark current. PDs fabricated from materials such as GaN, NiO, AlGaN, ZnO, Nb_2O_5, and TiO_2 have attracted attention from researchers owing to their wide energy band gaps. Among these materials, both GaN and NiO semiconductors stand out as promising candidates for ultraviolet/visible photonic devices due to their wide bandgap energies.

Herein, we report on MSM PDs based on GaN and NiO films which were deposited on sapphire and glass substrates respectively, using hollow-cathode plasma-assisted atomic layer deposition (HCP-ALD). GaN was deposited at 200℃ using triethylgallium (TEG) as the metalorganic precursor and N_2/H_2 plasma as the co-reactant. NiO was deposited at 100℃ using nickelocene ($NiCp_2$) as the metalorganic precursor and O_2 plasma as the co-reactant. The rf-plasma power was maintained at 100W for both films. Aluminum interdigitated electrodes, with widths and spacing of 500 microns, were deposited onto the films using e-beam evaporation.

The deposited films were characterized for their optical and structural properties. Both films deposited showed strong absorption in the UV region (l=190-380 nm) yet demonstrated lower absorption in the visible and near-IR regions. As a result of the analysis using the Tauc relation, the band gaps of GaN and NiO films were found to be 3.32 and 2.95 eV, respectively. XRD analysis revealed a preferred orientation along (002) direction for both films. I-V characteristics of the fabricated MSM PDs were conducted under dark and light conditions. An incandescent light source at a distance of ~10 cm from the sample was applied to generate the photocurrent. Bias-dependent photocurrent signals were observed for both GaN and NiO MSM PD samples. On the other hand, NiO photoresponse showed a significantly slower temporal response indicating a notable persistent photoconductivity.

PS-ThP-14 Dual Capability PEALD/PAALE Reactor Design, *Birol Kuyel,* **Alex Alphonse**, *Joe Alex,* NANO-MASTER, Inc.

Nano-Master has developed a hybrid PECVD/PEALD tool capable of depositing ALD and PECVD layers on silicon wafers within the same chamber with no hardware modifications. In this paper, we will propose a novel reactor design capable of performing PEALD and PAALE in the same chamber without breaking the vacuum. Removing native oxides from a Si wafer using other means, such as reactive ion etching or wet etching, results in substrate damage and defects to the wafer. Here, we will discuss the means of removing the native oxide from the Si wafer surface using plasma-assisted atomic layer etching (PAALE) before depositing AlN in the same chamber and without or low substrate damage. The PEALE of native oxide on the silicon wafer will occur in the same PEALD chamber, which prevents re-oxidation between the steps. The objective of the study is to develop a tool that can perform precise atomic layer etching and damage-free atomic layer deposition of high quality AlN in the same chamber.

PS-ThP-16 SF_6- and CF-based Plasmas Interaction with Si and SiO_2 at Room and Cryogenic Temperature: Insights from Molecular Dynamics Simulation, *Jonathan ROMERO CEDILLO, Gilles CUNGE,* **Emilie DESPIAU-PUJO**, *LTM, CNRS/Universite Grenoble Alpes, France*

Introduced in the early 90s to perform deep etching of silicon, plasma cryoetching involves using highly reactive plasmas, such as SF_6- or CF- based plasmas, to etch materials cooled down to temperatures below -100°C with high anisotropy. During cryoetching of silicon in SF6 plasmas, the addition of small amounts of oxygen allows to form a temperature sensitive SiO_xF_y passivation layer on the sidewalls of the trench, which prevents spontaneous lateral etching and desorbs completely when the substrate is returned to room temperature. Cryogenic processes have the advantage of being polymer-free and clean, which prevents process drift and makes them suitable for new applications where smooth sidewalls or reduced plasma-induced damage are required. These features are attractive for etching porous low-K materials in the back-end-of-line of advanced CMOS technology; applications to atomic layer etching of conventional materials (Si, Ge, GaN, InP) or emerging 2D materials (graphene, MoS_2) are also envisaged. Although the understanding and control of plasma cryoetching has improved over the years, the fundamental mechanisms of the

formation and desorption of passivation layers are not well understood. And differences between elementary plasma-surface interactions at cryogenic and room temperature remain unclear. In this paper, Molecular Dynamics (MD) simulations are performed to study the interaction between F- and CF- based plasmas with Si and SiO2 materials. The objective is to understand the impact of ion and radical plasma species (nature, dose, energy, etc.) on the structural and chemical modification of exposed materials, both at room and cryogenic temperatures. Quantitative information on surface reaction probabilities (sticking, thermal desorption, surface diffusion, sputtering yields) will be compared and discussed, to better understand the key mechanisms behind cryoetching and cryo-ALE processes.

This work was supported by ANR, under the project name PSICRYO (No. ANR-20-CE24-0014).

PS-ThP-17 Ion Energy Distributions in a Kaufman-type Ion Beam Source Operated with Ar and O_2, *Raymond Smith,* Department of Electrical and Computer Engineering, University of Nebraska-Lincoln; *Erik Rohkamm, Peter Birtel, Dmitry Kalanov, Frank Frost,* Leibniz Institute of Surface Engineering (IOM), Germany; *Ufuk Kilic, Eva Schubert,* Department of Electrical and Computer Engineering, University of Nebraska-Lincoln

An energy-selective mass spectrometer has been used to measure ion energy distributions (IEDs) from a broad beam double-grid Kaufman ion source as a function of the grid 1 voltage. Two cases, Ar and mixed Ar/O_2 process gases were studied, and IEDs were measured with and without the presence of a neutralizer current for both cases. A linear, one-to-one relationship between grid one voltage and the energy of single charged and double charged ions produced inside the ion source was observed. For Ar/O_2, a broad triangular peak is observed for atomic oxygen due to the dissociation of O_2. Additional ionization processes were detected for collision events which occurred in the ion beam outside of the source, and charge transitions caused the formation of fast single charged ions and slow double charged ions. The relationship between the presence of a neutralizer current and the ion energy peak positions are discussed for ionization processes inside and outside of the ion source. Knowledge of ion beam energy distributions will guide ion beam-assisted techniques for applications which require precision such as nanofabrication, sputtering, and ion-beam etching.

PS-ThP-19 Spatiotemporal Analysis of Electron Heating in Single Frequency and Pulsed-Rf Capacitively Coupled Plasma Using a Parallelized Particle-in-Cell Simulation, *Hae June Lee, Sun Jeong Hwang,* **Junhee Mun**, *Pusan National University, Republic of Korea*

In recent semiconductor etching processes, pulse-driven capacitively coupled plasma (CCP) is widely used to achieve high etching selectivity. As technology advances, the equipment structures used in these processes become increasingly complex, requiring various conditions. Consequently, diverse issues are emerging within the CCP equipment, and understanding the various plasma phenomena occurring inside the process equipment is essential for solving these problems. To investigate the nonlinear and transient particle dynamics of CCPs, particle-in-cell (PIC) simulations are required [1,2]. This study uses a parallelized PIC simulation called K-PIC to investigate the onset of arcs in the gap between the wafer edge and the focus ring, which occurs in actual CCP equipment. We report the electron heating concentrated in the gap [3] through spatiotemporal data analysis, examining the effects of driving waveforms and the gap length [4] between the wafer edge and the focus ring.

References

[1] J.S. Kim, M.Y. Hur, C.H. Kim, H.J. Kim, and H.J. Lee,*J.Phys. D: Appl. Phys*. **51**, 104004 (2018).

[2] M.Y. Hur, J.S. Kim, I.C. Song, J.P. Verboncoeur, and H.J.Lee, *Plasma Res. Express* **1**, 015016 (2019).

[3] T. Lafleur, P. Chabert, J. P. Booth, *Plasma Sources Sci. Technol,* **23**, 035010 (2014).

[4] J.S. Kim, M.Y. Hur, H.J. Kim and H.J. Lee, *J.Appl.Phys*. **126**, 233301 (2019).

PS-ThP-20 Understanding Olefin Selectivity in Light Hydrocarbon DBD Plasmas, *Ibukunoluwa Akintola,* **Jinyu Yang, Jason C. Hicks, David B. Go**, University of Notre Dame

The conversion of light hydrocarbons into higher-order species, such as olefins and aromatics, offers the potential to upgrade natural gas into other chemicals that are essential to a wide variety of consumer products. This can be achieved using thermal catalysis but there is a need for alternative

carbon-efficient, environmentally friendly, sustainable processes. Low-temperature, atmospheric plasmas (LTPs) produce highly reactive chemical environments and present the potential for an electrical approach to light hydrocarbon conversion into valuable products as a part of the electrification of the chemicals industry. Preliminary findings show plasma activation of methane directly forms C2+ olefins and alkynes with high selectivities at relatively low temperatures and atmospheric pressure, which when combined with certain catalysts can create aromatics or higher molecular weight products. In this work, we use a dielectric barrier discharge (DBD) to systematically study the selectivity of olefins to alkanes for various light hydrocarbon plasmas, including methane (CH_4), ethane (C_2H_6), and propane (C_3H_8). We explore changing operating conditions (temperature, plasma power, and gas composition) and their effect on the plasma and reaction pathways.We utilize optical emission spectroscopy (OES) and electrical characterization to investigate changes to specific gas phase species densities (C_2 and CH) and analyze both gas and liquid phase products to elucidate the mechanisms directing olefin selectivity and identify key parameters affecting product distribution.Complementary plasma simulations also provide a better interpretation of reaction mechanisms that influence observed product formation.

PS-ThP-21 Role of CO in Ar/C4F6/O2 Plasma for Selective Etching of Silicon Oxide over Silicon Nitride, *Hakseung Lee,* Sungkyunkwan University (SKKU), Republic of Korea*; Chanmi Lee, Jaewha Park, Kwangjin Moon,* Samsung Electronics Co., Republic of Korea*; Heeyeop Chae,* Sungkyunkwan University (SKKU), Republic of Korea

This study examines the role of carbon monoxide (CO) as an additive gas in the etching of silicon oxide (SiO) and silicon nitride (SiN_x) using Ar, C_4F_6, and O_2 plasmas. SiO and SiN_x are commonly used in the semiconductor industry, as device designs shift from 2D to 3D structures. The etching gases like CF_4, C_4F_8, and C_4F_6, are commonly used for dielectric etch and additive gas like hydrogen (H_2) is used to control the SiO and SiN_x etch rates and selectivity. However, H_2 is typically used without O_2 condition, whereas CO can be used with O2. This research investigates CO's impact on SiO and SiN_x etch rates and selectivity under different O_2 included process conditions. The SiO and SiN_x surfaces are analyzed using X-ray photoelectron spectroscopy (XPS).

Initial experiments kept the total flow rates of C_4F_6, O_2, and CO constant while increasing the CO ratio. As the CO ratio increased up to 60%, the SiO etch rate rose from 390 Å/min to 1426 Å/min but dropped sharply beyond 80% CO raio. Conversely, the SiN_x etch rate increased steadily from 82 Å/min at 0% CO to 289 Å/min at 100% CO. The selectivity of SiO over SiN_x etching improved from 4.8 to 11.9 with up to 40% CO ratio but declined to 1.4 beyond 60% CO. The XPS analysis showed that the C1s ratio on SiO surfaces decreased until 40% CO, disappearing entirely after 60% CO, correlating with the sharp decline in SiO etch rate. For SiN_x, higher CO ratios reduced the deposition of the FC layer, gradually increasing the etch rate. These findings suggest that increasing CO decreases the partial pressure of C_4F_6, which provides CF_x radicals, thereby reducing FC polymer thickness and affecting etch rates and selectivity.

In another experiment, CO was compared with O_2 as an oxygen source. The SiO etch rate increased from 987 Å/min to 1776 Å/min up to 60% CO, then dropped sharply to 172 Å/min beyond 80%, with deposition occurring at 100% CO. The SiN_x etch rates decreased gradually from 1219 to 0 Å/min as CO increased. The SiO over SiN_x selectivity rose from 0.81 to 3.7 up to 60% CO. XPS analysis indicated that up to 60% CO, SiO was primarily etched, but beyond 80% CO, FC polymer layers formed, inhibiting etching. For SiN_x, the increasing CO ratio reduced Si2p and N1s peaks, suggesting SiN was almost entirely covered by an FC polymer layer, consistent with the gradual decrease in the etch rate. These experiments suggest that the CO serves as more carbon source rather than O radical Source.

PS-ThP-22 Photoresist Ashing at Room Temperature using a Large Area Atmospheric Pressure Plasma, *Branden Bodner,* University of Illinois at Urbana-Champaign

Photoresist ashing is a critical and increasingly common step in semiconductor manufacturing. Conventional methods for ashing are either wasteful, cause undesired damage, or lack the high throughput desired by industry. In this study, a large-area, atmospheric-pressure plasma is studied for ashing. The plasma is powered by radio frequency power (13.56 MHz) and interacts with the substrate through the afterglow which limits bombardment by energetic species. Etch rates of 205 nm/min are achieved, with little damage to the underlying substrate. The process is demonstrated up to 4-inch wafers and on patterned structures.

PS-ThP-23 Fault Detection of Plasma Processes using Optical Emission Spectroscopy Signals and Recurrent Neural Network with Autoencoder, *Jaehyeon Kim, Eunchong Park, Heeyeop Chae,* Sungkyunkwan University (SKKU), Republic of Korea

Plasma processes are extensively used in semiconductor device fabrication, but as devices become more highly integrated and critical dimensions shrink to the nanometer and atomic scale, maintaining high accuracy and stability becomes increasingly challenging. In this work, fault detection model was developed for plasma processing using non-invasive optical emission spectroscopy (OES) and recurrent neural network (RNN) with autoencoder. 13.56 MHz RF source power and 12.56 MHz bias power was applied to an inductively coupled plasma (ICP) with CF_4, Ar, and O_2 gases. To train the model, experimental data were gathered by varying process conditions, including RF source power and CF_4, Ar, O_2 flow rates, as well as pressure, from -50% to +50% of the normal process values. OES signals from the ICP reactor were collected with 3648 channels, and collected optical signals were trained by autoencoder consisted with linear unit, batch normalization and hyperbolic tangent function. Then, 16 hidden features were extracted from 3648 intensities in each time step. For the predicting the hidden features in next time step, the 16 hidden features at the current step and 16 values from process variables to train the RNN: RF powers (4), RF matching variables (4), gas flowrates (3), pressures (3), valve position (1), and temperature (1). Faults were determined when the means squared error between hidden features predicted in post time step and the hidden features extracted in present time step. The model was tested under scenarios involving incorrect input of process conditions. An accuracy of 78.2% was demonstrated for RF power errors, 76.3% for bias power errors, and 63.4% for pressure errors.

Quantum Science and Technology Mini-Symposium
Room Central Hall - Session QS-ThP

Quantum Science and Technology Mini-Symposium Poster Session

QS-ThP-1 Characterization of Planar Ta Damascene Resonators for Quantum Information Science Applications, *Drew Rebar, Francisco Ponce, Brent VanDevender, Marvin Warner, Juan Macy,* PNNL*; Tharanga Nanayakkara, Chenyu Zhou, Mingzhao Liu,* Brookhaven National Laboratory*; Satyavolu Papa Rao,* NY CREATES*; Ekta Bhatia,* SUNY POLY, Albany

Transmon qubits are one of the leading technologies for quantum information science (QIS) with fabrication and characterization techniques accessible by numerous laboratories around the world.In recent years, efforts at coherence time optimization have shifted focus to the performance of the underlying superconducting material and accompanying surface oxides.While earlier devices were fabricated from Al and Nb, the current state-of-the-art transmons are fabricated from Ta with coherence times up to 0.5 milliseconds.Our research focuses on Ta coplanar waveguide (CPW) resonators fabricated by a damascene technique which yields pristine metal structures entrenched in silicon substrates.While the participation ratio of the dielectric substrate is increased, the device edges remain oxide free from the entrenchment and a nitride capping layer.Our recent studies revealed a current best Q value on the order of 105 at low power.This work, performed in collaboration with NY CREATES/SUNY Poly and BNL, will be discussed along with the prospect of further improvements.

QS-ThP-2 DNA-Enabled Precise Arrangement of Colloidal Quantum Dots and Rods on Device Substrates, *Xin Luo, Chi Chen, Mark Bathe,* MIT

Colloidal quantum dots (QDs) and rods (QRs) are promising quantum materials with unique electronic and optical properties for quantum science applications such as quantum computation, sensing, simulation, and communication. While colloidal QDs and QRs can be dispersed in solvents and readily integrated on surfaces and in devices using solution-based assembly techniques, scalable and deterministic arrangement of single and arrayed QDs/QRs on devices with sub-10 nm resolution remains a challenge. We employ robust DNA origami templates to guide the incorporation of colloidal QDs and QRs on device substrates with nanoscale precision.

DNA origami is a powerful platform for the precise assembly and organization of functional nanomaterials, enabling the creation of complex, tailor-made structures with unprecedented accuracy and programmability. While DNA-modified molecules and colloidal metallic nanoparticles are

routinely assembled onto DNA origami, QDs and QRs have been challenging to incorporate due to low DNA conjugation efficiency. We have developed an ultrafast dehydration-assisted method to conjugate a dense layer of ssDNA onto QDs/QRs directly from organic solvent to facilitate their precise and stable assembly on DNA origami templates [1]. To arrange QR arrays on the surface, we developed a Surface-Assisted Large-Scale Assembly (SALSA) strategy to fabricate 2D DNA origami lattices tethered by unique crossover interactions directly on a solid substrate [1]. Alignment of the QRs in the 2D lattice was achieved through predefined binding strands linearly arranged on the origamis to unlock polarized light emission along the long axis of the arrayed QRs. To integrate DNA-templated QDs/QRs into chip-based photonic devices, we further employed lithography to guide the deterministic patterning of precisely positioned and oriented individual DNA origami templates on silicon chips. Landing pads of matching size and shape of the DNA origami were first fabricated using electron beam lithography, followed by origami placement through electrostatic interaction-guided self-assembly. QDs and QRs were then assembled onto the origami templates with predefined position and orientation. Our methods offer significant potential for the precise integration of high-quality colloidal QDs and QRs as quantum emitters for integrated quantum photonics.

1. Chen, C., Luo, X., Kaplan, A. E. K., Bawendi, M. G., Macfarlane, R. J., & Bathe, M. (2023). **Science Advances**, 9(32), eadh8508.

QS-ThP-4 Correlating the Electronic Structure with the Emergence of Magnetism in PdcCo₂, *Jessica McChesney,* Argonne National Laboratory

Long-range ferromagnetism is induced in the nonmagnetic layered oxide $PdCoO_2$ with the implantation of He. This onset of magnetism was found to be reversible with annealing and tied directly with local lattice distortions. In order to correlate the changes in the electronic structure with the onset of magnetic order, we mapped the Fermi surface and performed resonant photoemission to determine the character of the bands as a function of doping.

QS-ThP-5 How Can Quantum-Based Sensors Be Used for "Nist on a Chip" Sustainability Solutions?, *Jay Hendricks,* NIST-Gaithersburg; *Barbara Goldstein,* NIST

This poster covers a bit of metrology history of how we got to where we are today and gives a forward-looking vision for the future of measurement science and its important role in our daily lives. The role of NIST as a National Metrology institute (NMI) is briefly described considering the world-wide redefinition of units that occurred on May 20th, 2019. The re-definition of units is now aligned with physical constants of nature and fundamental physics which opens new realization routes with quantum-based sensors and standards. The NIST on a Chip program (NOAC) is briefly introduced in this context.

The technical core is a deeper dive into research on measurement methods for pressure, the Fixed Length Optical Cavity (FLOC) and for vacuum the Cold Atom Vacuum Standard (CAVS). What is exciting about many of these new measurement approaches is that they are both primary (relying on fundamental physics), are quantum-based and use photons for the measurement readout which is key for taking advantage of the fast-growing field of photonics. The FLOC will enable the elimination of mercury barometers pressure standards worldwide and the CAVS will be first primary standard for making vacuum measurements below 1.3×10^{-5} Pa. A Sensitive Photonic Thermometer (SPOT) will be introduced, along with other sensing technologies that the NOAC program is currently investigating such as flux, magnetic field, and mass and torque.

Quantum-based metrology systems, however exciting, do raise new challenges and several important questions: Can these new realizations enable the size and scale of the realization to be miniaturized to the point where it can be imbedded into everyday devices? What will be the role of metrology institutes in the is new ecosystem of metrology and measurement? What will be the NMI role for solutions aimed at sustainability and environment? This posterwill begin to explore these important philosophical questions.

QS-ThP-6 Advancing Quantum Materials Growth and Characterization with Cluster Systems, *Yashwanth Balaji,* Mythili Surendran, Arian Gashi, Aidar Kemelbay, Shaul Aloni, Adam Schwartzberg, Lawrence Berkeley National Laboratory

Superconducting quantum materials research is increasingly focused towards the fabrication of robust quantum processors to enable practical quantum computation. As these processors scale in size and complexity, they become more susceptible to various loss mechanisms, with material-related losses being a major source of decoherence. Traditional fabrication methods, such as evaporation and sputtering, have shown to introduce defects in thin metallic films, as well as lossy and noisy dielectrics. Advances in fabrication techniques and the exploration of new materials are necessary to develop qubits that are more robust to decoherence. Achieving this requires exploring various material growth techniques in a controlled manner, guided by real-time feedback from in situ characterization. Additionally, employing novel fabrication techniques that allow simultaneous application of multiple growth techniques without breaking vacuum are crucial.

In this context, we present the use of a cluster deposition and characterization system at Berkeley Lab's Molecular Foundry user facility to advance the exploration and optimization of quantum materials. The integrated system combines multiple deposition tools — including e-beam evaporation (deposition, oxidation and ion milling), reactive sputtering and nitride and oxide ALD chambers—with a suite of characterization systems including XPS, ellipsometry, optical emission spectroscopy and Auger spectroscopy. The system also includes a glove box for inert sample loading and unloading, and automated wafer transfer integrated in a unified vacuum system. By facilitating multi-deposition processes, this setup opens up new possibilities for creating novel materials that were previously unattainable. The in situ characterization capability during growth provides a deeper understanding of growth mechanisms and defect control, facilitating rapid feedback and maintaining pristine interfaces between device layers.

We demonstrate the capabilities of this system through the optimization and integration of Josephson junctions incorporating different material stacks and superconducting nitrides (NbN, TiN, and NbTiN) backed up by electrical and material characterization techniques. We will discuss the ongoing and future directions for device development, highlighting how this cluster tool system, along with the characterization suite at the Molecular Foundry, provides an in-depth platform for materials growth and exploration.

QS-ThP-7 Superconducting Nitrides for Next-Generation Quantum Information Processing, *Mythili Surendran,* Yashwanth Balaji, Aidar Kemelbay, Arian Gashi, Adam Schwartzberg, Shaul Aloni, Lawrence Berkeley National Laboratory

Superconducting nitrides such as niobium nitride (NbN) and titanium nitride (TiN) and their alloys are extensively studied for next-generation quantum information processing due to their favorable superconducting properties, including high critical temperature, high critical field and low resistivity. Additionally, their compatibility with standard semiconductor fabrication processes facilitates the integration of superconducting qubits and circuits with other electronics. These materials exhibit low microwave losses, leading to high Q-factors in resonators, thereby enhancing coherence times and qubit performance. The ability to achieve these properties depends on precise control over thin film growth, ensuring accurate structure, stoichiometry, and defect concentration. However, understanding the influence of process parameters, crystalline and interfacial quality and chemical composition is still limited in the literature due to challenges such as lack of controlled experimental setups and characterization techniques. Thus, a systematic investigation into the fundamental properties of these superconductors and their impact on quantum computing device performance is essential.

In this study, we present a comprehensive analysis of NbN, TiN and NbTiN thin films deposited using DC reactive sputtering in a cluster tool system. Extensive structural, chemical and electrical characterization of nitride thin films sheds light on how crystallinity and chemical composition influence the critical temperature. Improved vacuum conditions in the cluster tool reduce oxygen contamination within the films. We also explore the effects of process parameters such as substrate selection, deposition temperature, and nitrogen partial pressure on achieving epitaxial nitride thin films. Additionally, we report on key superconducting properties such as critical temperature, upper critical field, superconducting gap, coherence length, and their relationship to structure and stoichiometry. This work provides a coherent approach to synthesizing high-quality superconducting nitrides with precise and reproducible properties, which is crucial for quantum computing applications.

Advanced Surface Engineering
Room Central Hall - Session SE-ThP

Advanced Surface Engineering Poster Session

SE-ThP-1 High-Temperature Oxidation Resistance of Sputtered (Al,Cr,Nb,Ta,Ti,Si)N Coatings, *Andreas Kretschmer*, TU Wien, Austria; *Paul Mayrhofer,* TU Wien, Institute of Materials Science and Technology, Austria
High-entropy metal-sublattice (Al,Cr,Nb,Ta,Ti)N coatings, with up to 15.0 at.% additional Si content were developed and investigated for their oxidation resistance by exposing them for 3, 30, and 100 h to ambient air at 900, 950, and 1000 °C, which represents the harshest oxidation experiment for crystalline nitrides reported so far. The Si-free coating is rapidly oxidized, but all of the Si-alloyed coatings survive even the harshest oxidation test. The oxides crystallize mostly in the rutile structure with some Ta2O5-type phase fractions at higher Si contents. Detailed TEM investigations reveal a varied microstructure across the oxide scales with a succession of Cr-, Al, and Ti-rich top oxide layers, which agrees with a reported thermodynamical calculation of oxide stabilities.

SE-ThP-2 ASED Rising Star Talk: The Influence of Deposition Parameters on the Structure and Properties of TiZrNbTaMo High Entropy Alloy Films Fabricated by High Power Impulse Magnetron Sputtering, *Chia-Lin Li[1]*, Center for Plasma and Thin Film Technologies, Ming Chi University of Technology; *Sen-You Hou,* Department of Materials Science and Engineering, National Tsing Hua University; *Bih-Show Lou,* Chemistry Division, Center for General Education, Chang Gung University; *Jyh-Wei Lee,* Department of Materials Engineering, Ming Chi University of Technology; *Po-Yu Chen,* Department of Materials Science and Engineering, National Tsing Hua University, Taiwan
TiZrNbTaMo high-entropy alloys (HEAs) with a body-centered cubic (BCC) structure are known for their excellent compressive yield strength and significant compressive plasticity. These advantageous properties are retained even in their thin film forms, making them highly promising for a variety of applications. In this study, we prepared TiZrNbTaMo high entropy alloy films (HEAFs) grown by high power impulse magnetron sputtering and investigated the influence of deposition parameters on their structure and properties. It is well known that several deposition parameters affect the density and microstructure of thin films, influencing the hardness, wear resistance, toughness, and corrosion resistance. The cross-sectional morphology and crystal structure of TiZrNbTaMo HEAFs were characterized using field emission scanning electron microscope (FE-SEM) and X-ray diffractometry (XRD), respectively. Mechanical properties of the HEAFs, including hardness, elastic modulus, adhesion, and wear resistance, were evaluated by nanoindentation, scratch tester, and pin-on-disk wear tester. This study systematically investigated the effects of critical processing parameters, including pulse frequency, duty cycle, substrate bias, and working pressure for TiZrNbTaMo HEAFs for achieving outstanding properties.

SE-ThP-5 Magnetron Sputtering Deposition of Metallic-Based Nanostructured Coatings for Nuclear Energy Applications, *Maria Sole Galli De Magistris*, Davide Vavassori, Valeria Russo, David Dellasega, Politecnico di Milano, Italy; *Marialuisa Gentile, Francisco Garcia Ferré,* newcleo Srl, Italy; *Matteo Passoni,* Politecnico di Milano, Italy
Lead-cooled Fast Reactors (LFRs) are considered among the most promising Generation IV nuclear reactors owing to their inherent safety and high power density [1]. Nevertheless, conventional structural and cladding materials suffer from severe corrosion issues when in contact with liquid lead [2]. Surface coating technology is a valuable technique to improve materials performance in harsh environments without modifying the properties of the bulk [3]. Nonetheless, coatings must also withstand the high temperature and radiation fields characterizing LFRs. Therefore, realizing coatings with improved adhesion and precisely controlled properties is of fundamental importance. In this respect, in recent years, metallic coatings have gained increasing interest thanks to their enhanced compatibility with steel substrates and the possibility of triggering a self-passivation mechanism when strong oxide formers, such as Al and Cr, are present in the optimal amount. Physical Vapor Deposition techniques, particularly Magnetron Sputtering (MS) [4], have proven their effectiveness in realizing films with controlled and tunable properties. Magnetron Sputtering includes different deposition regimes: Direct Current (DCMS), Radio-Frequency (RFMS), and High Power Impulse Magnetron Sputtering (HiPIMS). Compared to DCMS and RFMS, the HiPIMS process generates a

higher fraction of ionized species, with energies further adjustable through substrate biasing or Bipolar HiPIMS. Additionally, according to the working regime, a plethora of process parameters can be adjusted, including sputtering power, duty cycle, pulse width, and bias voltage amplitude, enabling film optimization for the specific application.

This contribution reports the development and characterization of advanced nanostructured mono and multi-elemental metallic coatings produced via magnetron sputtering. In particular, the attention is focused on two types of coatings. The first set consists in steel films, enriched in other elements such as aluminum and tungsten to improve the oxidation and the high-temperature behavior. The other set consists of chromium films; widely investigated for claddings in light water reactors, they might be of interest for LFRs owing to their excellent oxidation behavior. Different deposition conditions were exploited and relevant working parameters were adjusted to tune coatings properties. Morphological and crystallographic studies were performed, together with preliminary tests in LFR relevant conditions. The obtained results provide an insight into the interconnection between process parameters and coatings properties and behavior.

SE-ThP-6 UV-Vis-NIR Optical Analysis to Understand the Electrical Properties of Nitrogen-Incorporated Tetrahedral Amorphous Carbon Thin Films, *Nina Baule*, Fraunhofer USA Center Midwest; *David V. Tsu,* The Mackinac Technology Company; *Lars Haubold,* Fraunhofer USA Center Midwest; *Thomas Schuelke,* Fraunhofer USA
Tetrahedral amorphous carbon (ta-C) thin films have received significant attention due to their diamond-like mechanical properties, achieved via low-temperature synthesis. More recently, the electrochemical behavior of nitrogen-incorporated ta-C:N has attracted interest, as it exhibits electrical conductivity as well as chemical inertness. The modified electrical properties of ta-C:N have been mainly attributed to the conjugation of sp^2 carbon-carbon and/or carbon-nitrogen bonds. Commonly, with an increase in nitrogen incorporation into the growing film, the electrical resistivity decreases proportionally. Here, however, we find that the electrical properties plateau at higher nitrogen content for ta-C:N thin films (100 nm) deposited by laser controlled pulsed cathodic vacuum arc (Laser-Arc), despite the fact that mechanical and structural properties indicate an increase in sp^2 fraction. Hence, to gain a better understanding of the electronic properties, the dielectric constants $[\varepsilon_1]$ and $[\varepsilon_{2-}]$ were obtained from the optical constants, the refractive index $[n]$ and extinction coefficient $[k]$, which were numerically determined from reflectance $[R]$ and transmittance $[T]$ measurements in the wavelength range from 190 to 2500 nm (0.5 to 6.5 eV). The dielectric constant $[\varepsilon_1]$ was used to calculate the dielectric volume of the atom, which is interpreted as a measure of the conjugated electron system. Furthermore, modeling of the dielectric constants yielded the number of conjugated electrons per atom. The ta-C:N samples with the highest values of electrical conductivity, were either characterized by the largest occupied volume or the highest number of conjugated electrons. Through the dielectric volume and number of conjugated electrons, it was discovered that the electrical conductivity does not only depend on the sp^2 content and cluster size, but on how many electrons are conjugated and how much space these electrons occupy.

SE-ThP-7 A Critical Issue in Coatings Nanoindentation: Validity of the 10% Bückle's Rule of Thumb, *Esteban Broitman,* SKF Research and Technology Development, Netherlands
When an indenter penetrates the surface of a film deposited onto a substrate, the mechanical response of the coating will be influenced by the mechanical properties of the substrate, according to its penetration depth h and the film thickness t. As the depth of penetration h increases, more of the mechanical contribution will come from the substrate.

The first who tried to separate the contribution of the substrate from the total measured hardness at the microscale was Bückle, who suggested a 10% rule of thumb: to indent no more than 1/10 of the film thickness to avoid the influence from the substrate. The rule has been adopted later by many researchers for nanoindentation experiments and extended also as valid for the elastic modulus. However, there are many experimental studies and numerical simulations showing that this rule is too strict for a hard coating on a very soft substrate and too loose for a soft coating on a hard substrate [1].

In this presentation, we will review the issue, and will discuss all factors that affect the maximum penetration depth for independent coating measurements. We will also present a simple experimental methodology that, in most of cases, gives the correct values for hardness and elastic modulus, independently of the coating/substrate system.

---

[1] E. Broitman, Indentation Hardness Measurements at Macro-, Micro-, and Nanoscale: A Critical Overview. Tribol Lett **65**, 23 (2017)

SE-ThP-8 Optimizing Laser Surface Melting Parameters to Enhance Corrosion Resistance of AA5083 Aluminum Alloy, *Md Sojib Hossain,* University of Virginia, USA, Bangladesh*; William P. Moffat,* University of Virginia, USA*; Jonathan Skelton,* University of Virginia, USA, United States Virgin Islands*; James Fitz-Gerald,* University of Virginia, USA

AA5083 is a solution-strengthened Al-Mg alloy widely used in marine environments and other harsh, corrosive settings due to its excellent corrosion resistance. However, this alloy is susceptible to a deleterious process known as sensitization, where Mg-rich intermetallic particles, primarily the β-phase, precipitate at grain boundaries under prolonged exposure to moderately elevated temperatures. This anodic β-phase forms a galvanic couple with the cathodic aluminum matrix, leading to intergranular corrosion (IGC). Although several heat treatment processes have been developed to dissolve the β-phase within the matrix, these methods are not feasible for service components, and processed samples can easily be re-sensitized. Laser surface melting (LSM) offers a promising solution to this issue. In this study, a nano-second pulsed laser with varying power was used to investigate LSM's effects on minimizing intergranular corrosion. A low-power excimer laser with 50% overlap was applied to a 1200-grit polished surface, while a high-power ADAPT laser was used on as-received samples with different overlaps. Electrochemical polarization scans of the base and LSM samples in a 0.6 ml NaCl solution showed notable improvements in corrosion properties for all laser-processed samples, as evidenced by low open circuit potential and nearly a two-order-of-magnitude decrease in exchange current density. Backscattered scanning electron micrographs and energy dispersive spectroscopy (EDS) scans confirmed that the improved corrosion resistance was due to a homogenized LSM surface, ranging from only 3 to 7 μm in depth. Electron backscattered diffraction (EBSD) analysis of the excimer LSM samples' cross-sections identified very small sub-grains with different grain boundary characteristics compared to the sensitized base metal. These sub-grains are highly inert to re-sensitization, and create significant interruptions to intergranular corrosion, thereby enhancing IGC resistance.

Surface Science
Room Central Hall - Session SS-ThP

Surface Science Poster Session

SS-ThP-2 Near Ambient Pressure XPS Indicates that the Relevant State of Silver under Ethylene Epoxidation Conditions is Mostly Metallic, *Elizabeth E. Happel,* Tufts University*; Phillip Christopher,* University of California at Santa Barbara*; Matthew M. Montemore,* Tulane University*; E. Charles H. Sykes,* Tufts University

Epoxidation reactions are some of the highest value processes in the chemical industry; however, despite decades of research, the mechanism of ethylene epoxidation is still under debate. A central question in the field is the state of the industrial Ag catalyst under reaction conditions. Controversy remains about whether the active site for selective oxidation is metallic or oxidized and several in situ studies have reported the presence of both phases. We utilize near ambient pressure XPS under both purely oxidizing conditions and ethylene: oxygen ratios at a temperature that yields the same reactant chemical potentials as a typical flow reactor. Our XPS results reveal that electrophilic and nucleophilic oxygen formed on Ag(111) after exposure to pure oxygen at 433 K, with a O : surface Ag ratio of 0.11. However, when ethylene is introduced to the oxygen atmosphere at an industrially relevant 5:2 ratio, the nucleophilic oxygen is reacted away immediately, and the electrophilic oxygen coverage slightly increases which we attribute to the formation of carbonate which has the same binding energy as electrophilic oxygen. Most significantly, the O : surface Ag ratio decreases to 0.05, almost half of which is carbonate. These results indicate that the Ag(111) surface is mostly metallic under simulated reactor conditions meaning that Ag/oxide interfaces, at which the proposed oxametallacycle (OMC) intermediate is formed, must be considered in mechanistic epoxidation models.

SS-ThP-3 Surface Chemistry of Zirconium Borohydride on Zirconium Diboride (0001), *Michael Trenary, Ayoyele Ologun,* University of Illinois - Chicago

Transition metal diborides are known to either have a metal-terminated or boron-terminated surface. While group-V MB_2 has boron-terminated surfaces, group-IV MB_2 has metal-terminated surfaces. ZrB_2, a group-IV metal-terminated diboride, is an extremely hard material with a high melting point of 3246 °C and can be grown conformally via chemical vapor deposition (CVD) using zirconium borohydride $Zr\text{-}(BH_4)_4$ as a precursor. Using reflection absorption infrared spectroscopy (RAIRS), we investigated the surface chemistry of ZrB_2 growth from $Zr\text{-}(BH_4)_4$ on a $ZrB_2(0001)$ surface. Using low-energy electron diffraction and X-ray photoelectron spectroscopy (XPS), we demonstrate that ZrB_2 can have a boron-terminated surface in boron-rich conditions. The RAIR spectrum obtained after exposing the surface at 90 K to $Zr\text{-}(BH_4)_4(g)$ matched that of the pure compound, indicating adsorption without decomposition. However, new surface intermediates were formed upon heating to 280 K, as shown by the presence of vB-Ht stretch (2569 cm^{-1}) and δH-B-H (1228 & 1057 cm^{-1}) peaks in the RAIR spectra. Decomposition of $Zr(BH_4)_4$ on $ZrB_2(0001)$ surface at 1173 K revealed a $\sqrt{3}\times\sqrt{3}$ boron terminated surface, with a stoichiometry of $ZrB_{2.60}$. In contrast to the zirconium-terminated surface, the boron-terminated surface is resistant to oxidation.

SS-ThP-4 Selective Hydrogenation of 1,3-butadiene on a Pd/Cu (111) Single-Atom-Alloy, *Mohammad Rahat Hossain, Michael Trenary,* University of Illinois at Chicago

Selective hydrogenation of 1,3-butadiene (BD) to 1-butene (1-B) is critical in refining alkene streams for high-quality polymer production. Typically, Pd and Pt are employed in hydrogenation reactions due to their nearly negligible barrier for H_2 activation. However, these catalysts are prone to coking and their high activity often reduces selectivity. Single-atom alloy (SAAs) catalysts are being developed to achieve high selectivity while retaining high activity. In an SAA, small amounts of an active metal, such as Pd or Pt, are doped into a less active host metal such as Cu. Previous work has shown that a Pd(111) surface exhibits superior selectivity for BD hydrogenation to 1-B compared to Pt(111),[1-4] suggesting that Pd/Cu(111) could be a suitable SAA model catalyst for this reaction. In this study, we investigated the adsorption and hydrogenation of 1,3-butadiene (BD) to 1-butene (1-B) over a Pd/Cu (111) SAA under ultrahigh vacuum (UHV) and ambient pressure conditions using reflection absorption infrared spectroscopy (RAIRS). Temperature programmed reaction spectroscopy (TPRS) in UHV showed that monolayer BD desorbs at 217 K, while 2nd-layer and multilayer BD desorb between 112 to 180 K. RAIRS detected gas-phase 1-B formation and BD consumption. In ambient pressure conditions, this reaction was found to be first-order (1.12±0.03) in H_2 and zero-order (-0.12±0.01) in BD, correlating to a turnover frequency of 36 s^{-1} at 380 K. The activation energy was calculated to be 63.2 ± 2.8 kJ/mol from an Arrhenius plot of the temperature dependence of the rate constant. Complete conversion of BD was found with 84% selectivity towards 1-B, without butane production. No surface species were detected during the reaction. Post-reaction analysis using Auger electron spectroscopy (AES) revealed carbon deposition, indicating some dissociation during hydrogenation.

References:1.C.-M. Pradier, E. Margot, Y. Berthier and J. Oudar, Appl. Catal. 43 (1), 177-192 (1988).2.G. Tourillon, A. Cassuto, Y. Jugnet, J. Massardier and J. Bertolini, J. Chem. Soc., Faraday Trans. 92 (23), 4835-4841 (1996).3.T. Ouchaib, J. Catal. 119 (2) (1989).4.J. Massardier, J. Bertolini, P. Ruiz and P. Delichere, J. Catal. 112 (1), 21-33 (1988).

SS-ThP-5 The Influence of Substrate Roughness and Long-Range Molecular Order on 3-Mercaptopropionic Acid Displacement by 1-Decanethiol, *Lindsey Penland, Hirushan Hetti Arachchige, Nadith Dissanayake, Rachael Farber,* University of Kansas

Thiolate self-assembled monolayers (SAMs) are widely used for their ability to tune the interfacial properties of Au surfaces for applications such as nano-fabrication and bio-functionalization. This molecular control over interfacial properties can be further enhanced by introducing a second molecular species, resulting in a binary SAM. Binary SAMs offer an appealing route to control the molecular scale density of specific functional groups. One approach to forming binary SAMs is through the displacement of one molecule with another through solution phase deposition. The fabrication of molecularly precise binary SAMs requires precise control of the molecular interactions and substrate properties, such as surface roughness.

In this work, using ultra-high vacuum scanning tunneling microscopy (UHV-STM) and solution-phase preparation methods, the relationship between chain length, functional group, and substrate roughness on the displacement of 3-Mercaptoprorionic Acid (MPA) by 1-Decanethiol (DT) was investigated. First, three categories of MPA substrates were prepared: **MPA-1)** well-ordered smooth surface formed during a 3 hr MPA incubation at 35 °C, **MPA-2)** disordered smooth surface formed during a 3 hr MPA incubation at 25 °C, and **MPA-3)** well-ordered rough surface formed during

a 24 hr MPA incubation at 25 °C. Then, following the formation of **MPA-1, -2**, and **-3**, the substrates were sequentially placed in a 2 µM DT solution for 20 min, 60, min, 3 hr, and 24 hr. UHV-STM analysis of the MPA substrates showed that **MPA-1** and **MPA-2** had faster rates of displacement than **MPA-3** and resulted in a uniform high-density DT film across the surface. **MPA-3**, which started with a uniform MPA SAM and nanoscale roughness due to the formation of Au nano-islands across the substrate related to the longer MPA incubation time, had the slowest rate of displacement. Interestingly, the DT SAM that formed following displacement of the **MPA-3** sample was comprised of the low-coverage, lying down phase (β) and 2-D gas phase (α) of DT. Ongoing work is focused on understanding the relationship between substrate roughness and MPA ordering on the slower displacement rate and low-density DT phases observed for **MPA-3**.

SS-ThP-6 Visualizing on-surface Intramolecular C-C Coupling Reaction Using Scanning Tunneling Microscopy and Tip-Enhanced Raman Spectroscopy, *Soumyajit Rajak, Nan Jiang,* University of Illinois, Chicago

Metal surface-supported physicochemical transformations provide additional degrees of freedom to tune the structural and electronic properties of molecular functional materials. To obtain a higher degree of control over the reaction outcome, submolecular scale characterization of the chemical intermediates and their local environment is required. Determining the real-space surface adsorbed configurations of molecules is challenging using ensemble-averaged surface science techniques. Again, probing the effect of the local environment of chemical species is challenging because the spatial resolution of conventional optical spectroscopic techniques is limited by the diffraction limit of light. Coupling light with plasmonic nano-objects creates highly localized surface plasmons (LSPs), which allows us to break the diffraction limit. Herein we present a combined topographical and chemical analysis of different surface-adsorbed configurations and surface-sensitive arrangements of a tetrabenzoporphyrin molecule and their chemical reactivity on a metal surface using angstrom-scale resolution scanning tunneling microscopy (STM) and ultra-high vacuum tip-enhanced Raman spectroscopy (UHV-TERS). Low temperature (77K) scanning tunneling microscopic images and localized surface plasmon resonance enhanced Raman signals reveal different adsorbate configurations of single molecule entities and their thermal reaction products with a fundamental view of adsorbate-substrate binding interactions. TERS uses the apex of the STM tip made of a plasmonic metal as a nano object to couple light to the near field. The Raman modes of the nanostructure underneath this tip are enhanced by the nano-confined surface plasmons which allows us to obtain chemical information with Angstrom scale spatial resolution. The atomic scale insights obtained into the local environment enable precise control over the fabrication of molecules with tailored optoelectronic properties.

SS-ThP-7 Click Chemistry on Functionalized Silicon Surfaces: UHV- and Solution-Based Strategies, *Timo Glaser,* Justus Liebig University Giessen, Germany*; Jannick Meinecke,* Philipps University Marburg, Germany*; Christian Länger, Lukas Freund,* Justus Liebig University Giessen, Germany*; Ulrich Koert,* Philipps University Marburg, Germany*; **Michael Dürr,*** Justus Liebig University Giessen, Germany

Click chemistry is a well-known and established reaction scheme in organic chemistry for the synthesis of well-defined organic molecular structures. The direct application of click chemistry reactions to selectively functionalized silicon surfaces could thus open the route to synthesizing new organic molecular architectures on these substrates, e.g., with tailored optical or physicochemical properties ("more than Moore"). However, click reactions such as the most prominent alkyne-azide coupling are performed in the presence of a catalyst dissolved in an adequate solvent. On the other hand, highly reactive surfaces such as the technologically most important Si(001) surface, are typically prepared and stored under UHV conditions in order to guarantee a high level of cleanliness and structural perfection. The direct application of solution-based click chemistry schemes to such vacuum processed surfaces thus seems as an experimental contradiction.

Here we show two different approaches to solve this problem: First, we demonstrate how to combine surface functionalization performed under UHV conditions with a solution-based alkyne-azide click reaction in order to build organic molecular architectures on functionalized semiconductor surfaces. The UHV-based functionalization of the Si(001) surface was realized via chemoselective adsorption of ethinyl cyclopropyl cyclooctyne (ECCO) from the gas phase [1]. The samples were directly transferred from UHV into the azide solution without contact to ambient conditions. The second organic layer was then coupled in acetonitrile solution via the copper-catalyzed alkyne-azide click reaction. Each reaction step was monitored by means of X-ray photoelectron spectroscopy in UHV; the N 1s spectra clearly indicated the click reaction of the azide group of the two test molecules employed, i.e., methyl-substituted benzylazide and azide substituted pyrene. Using optimized copper (I) catalysts, effective reaction yields of up to 75 % were obtained [2].

Second, a carefully tuned enolether/tetrazine cycloaddition was shown to be applicable even under UHV conditions and without catalyst [3]. We employed this reaction for coupling a tetrazine molecule to an enol ether group which was covalently attached on a Si(001) surface via cyclooctyne as a linker.

[1] C. Länger, J. Heep, P. Nikodemiak, T. Bohamud, P. Kirsten, U. Höfer, U. Koert, and M. Dürr, J. Phys.: Condens. Matter 31, 34001 (2019).

[2] T. Glaser, J. Meinecke, C. Länger, J. Heep, U. Koert, and M. Dürr, J. Phys. Chem. C 125, 4021 (2021).

[3] T. Glaser, J. Meinecke, L. Freund, C. Länger, J.-N. Luy, R. Tonner, U. Koert, and M. Dürr, Chem. Eur. J. 27, 8082 (2021).

SS-ThP-8 Adsorption of Fluorinated β-Diketones on a Surface of Zno Nanopowder: Dependence of Adsorbates on the Chemical Structure, *Sanuthmi Dunuwila, Andrew V. Teplyakov,* University of Delaware

This study investigates the surface modification of ZnO nanopowder using gas-phase fluorinated β-diketones, namely hexafluoro acetylacetone (hfacH) and trifluoro acetylacetone (tfacH), to elucidate their attachment chemistry.

Surface modification was investigated through i*n-situ* infrared spectroscopy, X-ray photoelectron spectroscopy (XPS), and solid-state NMR analysis (ssNMR) to determine the dominant adsorbate on nanopowder surfaces. To supplement the experimental findings, density functional theory was employed to identify stable surface species of ZnO nanopowder.

This study examines how the binding behavior of β-diketones on the ZnO surface varies depending on the specific nature of the β-diketone molecule. The gas phase for both diketones investigated consisted of the mixture of enol and ketone forms, with enol being most dominant for hfacH. Despite this observation, surface adsorption is dominated by the tetra-σ-bonded diketonate, which is very different from the commonly accepted adsorption model for β-diketones on oxide surfaces. In the case of tfacH, the adsorption is indeed dominated by the dissociated enolate form. These differences are apparently governed by the amphoteric nature of ZnO. When a more basic oxide material, MgO, is used, hfacH does form enolate as a dominant adsorbate, as confirmed by ssNMR.

This work expands our understanding of the β-diketone adsorption on oxide materials that is used in a variety of applications, from surface sensitization to heterogeneous catalysis, and from material growth to etching.

SS-ThP-9 In-situ X-Ray Absorption Spectroscopy (XAS) study of CeO2-based Catalysts for CO₂ Hydrogenation, *Irene Barba-Nieto,* Brookhaven National Laboratory, Spain*; Jose Rodriguez,* Brookhaven National Laboratory

Carbon dioxide (CO₂) is the main gas responsible for the greenhouse effect in Earth's atmosphere, leading to higher global temperatures and climate change. To limit global warming to 1.5ºC and reach net zero carbon dioxide emissions by 2050, it is necessary to advance in industrial processes that facilitate the generation of clean fuels from CO₂. One of the most promising strategies in this regard is the utilization of CO₂ and its transformation into valuable chemicals.

This study examines the effectiveness of two catalyst types, RuCeO₂ and RuCeO₂-TiO₂ systems, for converting CO₂ into methane. Results demonstrate that despite lower Ru content, TiO₂-containing systems exhibit significantly enhanced catalytic activity for CO₂ conversion to methane. To understand this fact, in situ X-ray absorption measurements have been carried out on the Ru K-edge and Ce L₃-edge analyzing their behavior under H₂, CO₂ and H₂+CO₂ between 30ºC to 250ºC. The Ru K-edge results indicate that the RuCeO₂ systems display a remarkable oxidation-reduction capacity, as evidenced by the reduction of the metal center in the presence of both H₂ and CO₂/H₂, along with its oxidation in CO₂ atmosphere. However, this behavior undergoes a drastic change in the TiO₂-containing catalyst, as a consequence of strong CeO₂-TiO₂ interactions, where the presence of hydrogen at 250ºC leads to irreversible reduction of Ru.

The analysis of the Ce L₃-edge revealed that the RuCeO₂ systems predominantly exhibit Ce⁴⁺, which was observed to undergo partial reduction under both H₂ and H₂/CO₂ atmospheres, followed by its re-

oxidation under CO_2. However, the $RuCeO_2$-TiO_2 catalysts demonstrate a substantially higher concentration of Ce^{3+} compared to the $RuCeO_2$ sample under all conditions (H_2, CO_2, H_2/CO_2), with the amount of Ce^{3+} further increasing under atmospheres with H_2 and H_2/CO_2.

Therefore, the XAS findings indicate that the presence of TiO_2 in the catalysts stabilizes the metallic state of Ru, which remains in this state during the methanation reaction. Moreover, TiO_2 promotes the formation of Ce^{3+}, enhancing the catalysts' reactivity. This effect is attributed to TiO_2 facilitating an electronic transfer at the interface and perturbing the regular fluorite geometry of ceria, thus promoting the presence of Ce^{3+}. A trend that is in agreement with previous studies for $CeO_2/TiO_2(110)$ model systems. The presence of Ce^{3+} significantly impacts the catalytic properties of the sample, aiding in the oxidation-reduction of Ce and stabilizing Ru. Consequently, the presence of reduced cerium plays a crucial role in determining the surface chemistry of the catalyst, crucial for efficiently converting CO_2 into methane.

SS-ThP-10 Insights from the Atomic Scale: Cobalt Sulfide Sheets on Au(111) and Initial Oxidation of Pt(111), *Dajo Boden, Mahesh Prabhu, Marcel Rost, Irene Groot, Jörg Meyer,* Leiden University, Netherlands
This poster highlights two recently published articles from a successful experiment-theory collaboration within the Leiden Institute of Chemistry:

1. Cobalt Sulfide Sheets on Au(111) [1]
   Transition metal dichalcogenides (TMDCs) are a type of two-dimensional (2D) material that has been widely investigated by both experimentalists and theoreticians because of their unique properties. In the case of cobalt sulfide, density functional theory (DFT) calculations on free-standing S−Co−S sheets suggest there are no stable 2D cobalt sulfide polymorphs, whereas experimental observations clearly show TMDC-like structures on Au(111). In this study, we resolve this disagreement by using a combination of experimental techniques and DFT calculations, considering the substrate explicitly. We find a 2D CoS(0001)-like sheet on Au(111) that delivers excellent agreement between theory and experiment. Uniquely this sheet exhibits a metallic character, contrary to most TMDCs, and exists due to the stabilizing interactions with the Au(111) substrate.
2. Initial Oxidation of Pt(111) [2]
   In situ scanning tunneling microscopy experiments on the initial oxidation of Pt(111) found complex intermediary platinum surface oxides, consisting of spoke wheel and stripe structures [3]. The structure of the spoke wheels is poorly understood because of their size and complexity. Here we employ atomistic thermodynamics based on an established reactive force field to investigate the structure and stability of spoke wheels at the elevated temperature (>530 K) and pressure (1−4 bar) conditions of the in situ experiments. At those conditions, the thermodynamic stability of the structural model for the spoke wheel is similar to that of the stripes, while the degree of surface oxidation is much lower. The spoke wheel is found to be much more stable than partially formed stripes with a similar degree of oxidation. These results are consistent with experimental findings, where the spoke wheel is observed first, at slightly lower oxygen pressures. They thus provide a better understanding of the oxidation pathway for Pt(111)-based catalysts in the context of oxidative catalysis.

1. M. K. Prabhu, D. Boden, M. J. Rost, J. Meyer, and I. M. N. Groot, *J. Phys. Chem. Lett.* **11**, 9038 (2020).
2. D. Boden, I. M. N. Groot, and J. Meyer, *J. Phys. Chem. C* **126**, 20020 (2022).
3. M. A. van Spronsen, J. W. M. Frenken, and I. M. N. Groot, *Nat. Commun.* **8**, 1 (2017).

SS-ThP-11 Hard X-Ray Photoelectron Spectroscopy Reveals Fe Segregation in NiFe Electrodes During Oxygen Evolution Reaction, *Filippo Longo,* Chemical Energy Carriers and Vehicle Systems Laboratory, Empa, Swiss Federal Laboratories for Materials Science and Technology, Switzerland*; Pedro Javier Lloreda Jurado, Jorge Gil-Rostra, Agustín R. González-Elipe, Francisco Yubero,* Nanotechnology on Surfaces and Plasma, Institute of Materials Science of Seville (CSIC-US), Seville, Spain*; Andreas Borgschulte,* Chemical Energy Carriers and Vehicle Systems Laboratory, Empa, Swiss Federal Laboratories for Materials Science and Technology, Switzerland
Alkaline water electrolysis represents one of the simplest methods employed to perform water splitting reaction [1]. This process is one of the most efficient ways of producing H_2 and O_2 at low cost and high purity [2]. The bottleneck of this reaction stems from the sluggish kinetics of the anodic reaction, i.e., the oxygen evolution reaction (OER), which consists of a four-electron transfer process [3]. The extraordinary performance of NiFe as electrocatalysts for the OER [4] is still a subject of debate. The changes that occur on the electrode surface during electrochemical reactions add another dimension of complexity, which hinders the rational design of electrodes for water splitting. Particularly for binary alloy electrodes, there are various phenomena ranging from the formation of oxides, (oxy)hydroxides and the associated segregation of metal atoms. In this work, we study various NiFe electrodes as model systems for the OER. We have developed the procedure for the quantification of chemical depth-profiling by XPS/HAXPES measurement, showing a marked Fe segregation and dissolution. The results explain the electrochemical performance of NiFe electrodes for OER. All the electrodes studied suffer from segregation of iron and subsequent formation of FeO_x on the surface, with only minor influence from morphology, porosity and total Fe content.

[1] S. W. Sharshir et al., International Journal of Hydrogen Energy (2023).[2] Z.-Y. Yu et al., Advanced Materials 33, 2007100 (2021).[3] A. Wang et al., Mater. Chem. Front. 7, 5187 (2023).[4] F. Dionigi and P. Strasser, Advanced Energy Materials 6, 1600621 (2016).

SS-ThP-12 Surface Modification of Titanium Dioxide Nanomaterials via Functionalization with Triol Compounds, *Asishana Onivefu,* *Andrew Teplyakov,* University of Delaware
Surface modification of titanium dioxide (TiO2) nanoparticles with trimethylolpropane (TMP) and dimethylolpropionic acid (DMPA) holds significant promise for advancing various technological applications. This research explores the functionalization of TiO2 nanomaterials and compares with pigmentary TiO2 surface coatings technologies used at industrial scale. Through a combination of experimental techniques including FTIR spectroscopy, X-ray photoelectron spectroscopy (XPS) and density functional theory (DFT) calculations, the interactions between surface modifiers and TiO2 are elucidated, revealing the formation of specific surface adsorbates. The results obtained from these studies demonstrated the displacement of surface impurities by adsorption of functionalized small molecules and evaluated the displacement processes among these surface modifiers. Hexafluoroacetylacetone (Hfac) was used as a test compound in displacement investigations utilizing fluorine as a spectroscopic label to precisely trace the displacement chemistry with XPS. This work provides fundamental understanding and offers novel strategies and valuable insights for enhancing the performance of TiO2-based materials.

SS-ThP-13 Model Studies of Single-Atom Alloy (SAA) Catalysts, *Francisco Zaera, Ravi Ranjan,* University of California - Riverside
Single-atom alloy (SAA) catalysts have become a prominent way to enhance selectivity in a number of catalytic processes.The mechanism by which these alloys attain their improved performance is still being debated, however, especially when considering the effect of the reaction environment on their structure and chemical composition.We have embarked on a project to emulate those catalysts using model systems where the metals are dispersed as nanoparticles (NPs) onto a flat oxide surface under controlled ultra-high vacuum (UHV) conditions, characterized using a combination of surface-sensitive techniques, and tested for their catalytic behavior using a so-called high-pressure cell. This work focuses on the characterization of the nature of surfaces of SAA catalysts made out of Pt (minority) and Cu (majority) metals and their performance for the promotion of the hydrogenation of unsaturated aldehydes. $Cu/Ta_xO_y/Ta$ surfaces have been prepared via the oxidation of a Ta crystal followed by the vapor deposition of controlled amounts of Cu and characterized using reflection-absorption infrared spectroscopy (RAIRS) and temperature-programmed desorption (TPD) together with carbon monoxide (CO) as a probe molecule. A series of changes in the RAIRS data has been observed as a function of the Cu deposition time, an indication of the development of the Cu NPs from small clusters of atoms with multiple low-coordination sites to larger NPs with more basal planes exposed. These Cu NPs were found to form stable in the temperature range from 300 K to 600 K, but to change beyond 600 K. Like Cu, Pt and Cu-Pt NPs can be grown and characterized via CO titrations using RAIRS and TPD, following a similar approach. Kinetic measurements under catalytic conditions can then be performed to test the efficacy of the Cu, Pt, or Cu-Pt NPs catalysts supported on the tantalum oxide surface and to identify the appropriate structure-reactivity correlations.

SS-ThP-14 Enhancing Gas-Evolving Electrocatalysis by Tuning the Wetting Properties of Catalyst Microenvironment, *Kaige Shi, Xiaofeng Feng,* University of Central Florida

Electrocatalysis plays a critical role in the conversion between electricity and chemical fuels. In addition to the development of electrocatalysts, efforts are made to understand and control their local environment during operations, which may influence the mass transport and kinetics of the reactions. Particularly, when gas-phase reactants or products are involved, the wetting properties of the microenvironment around catalytic sites can determine the distribution and diffusion of gas and liquid near the catalyst, and thus impact the catalytic performance. Here we present a study of catalyst microenvironment by controlling the wetting properties of carbon black, which is widely used as a catalyst support in electrocatalysis. We chose the electro-oxidation of hydrazine (N_2H_4) on carbon-supported Pt nanocatalyst and tuned the wetting properties of carbon support by doping of fluorine (F) or oxygen (O). Interestingly, the electrode with F-doped carbon (more hydrophobic) exhibited a higher activity than that with pristine carbon black. This is attributed to the accelerated removal of N2 gas generated from the catalyst, which would otherwise block the catalyst surface from liquid reactant. Furthermore, the electrode with O-doped carbon (more hydrophilic) showed an even higher activity, benefiting from the increased exposure of catalytic sites to liquid reactant. Our work demonstrates that controlling the catalyst microenvironment by doping of carbon black as catalyst support can be a powerful approach to enhance gas-evolving electrocatalysis.This work is supported by the National Science Foundation (NSF) Chemical Catalysis Program under Grant No. 1943732.

SS-ThP-15 Advanced Evaluation of Sub-nm Surface Roughness using Electron Diffraction, *Rivaldo Marsel Tumbelaka, Ken Hattori,* Nara Institute of Science and Technology, Japan

Achieving precise control over surface roughness at the sub-nanometer scale is paramount for enhancing the physical properties of semiconductor materials, particularly their electrical transport characteristics. Current methodologies, predominantly scanning probe microscopy, facilitate quantitative roughness assessment but face challenges when applied to surfaces with intricate structures such as vertical and facet faces of three-dimensional (3D) structures, owing to steric hindrance. Our prior research effectively utilized reflection high-energy electron diffraction (RHEED) to observe atomic ordering on various structure surfaces in different directions, overcoming the challenge of steric hindrance [1-3]. In this study, we explore the potential of RHEED as an alternative avenue for evaluating surface roughness. Kinematic diffraction theory introducing diffraction spots from atomic positions, we explore the correlation between RHEED spot profile and surface roughness. Our approach involves systematically analyzing RHEED intensity profiles alongside surface roughness measurements of Highly Ordered Pyrolytic Graphite (HOPG), serving as a prototype sample.

HOPG samples with varying degrees of surface roughness were prepared via Ar sputtering, and their roughness was assessed using atomic force microscopy (AFM). Figure 1(a) shows a typical RHEED pattern for the HOPG whose roughness was 0.163 nm. Through the analysis of RHEED spot profiles, we discerned distinct intensity components, and , corresponding to sharpened and broadened spot intensities, respectively (Fig 1(b)). Our findings reveal an excellent correlation between increased surface roughness and the ratio of broadened spot intensity to total intensity (Fig 1(c)), indicating RHEED's adaptability for quantitative evaluation of surface roughness. This study not only shows how effective RHEED can be in measuring surface roughness but also demonstrates its usefulness in analyzing complex 3D surfaces in small-scale research and making semiconductor devices. The details will be discussed in the presentation.

References:

[1] A. N. Hattori, K. Hattori, *et al.,* Surf. Sci. 644 (2016) 86.

[2] A. N. Hattori, K. Hattori, *et al.,* Appl. Phys. Exp. 9 (2016) 085501.

[3] K. Hattori, *et al.,* Jap. J. Appl. Phys. 51 (2012) 055801.

SS-ThP-16 Post-Synthesis Characterization of PtNi Nanowires for Enhanced Durability and Efficiency, *Cesar Saucedo, Jenny Mann, Sarah Zaccarine,* Physical Electronics USA

Polymer electrolyte membrane fuel cells (PEMFCs) offer a promising avenue for sustainable electricity production with minimal environmental impact. However, their widespread adoption faces challenges due to durability concerns and the sluggish kinetics of the oxygen reduction reaction (ORR) at the cathode. Consequently, to advance PEMFCs, there is a pressing need for the advancement of catalyst technologies to overcome these limitations. Previous works has looked at the synthesis of extended-surface platinum-nickel (PtNi) nanowires (NWs) via atomic layer deposition (ALD) and their durability. Here we show how the composition and chemical states of the nanowires evolve after a series of post-synthetic modifications designed to maximize the longevity of these nanowires as catalysts. By combining complimentary surface analytical techniques (X-ray photoelectron spectroscopy, hard X-ray photoelectron spectroscopy, and nanoscale Auger electron spectroscopy) we develop a more complete model of the complex chemical nature of these catalysts than any single technique could by itself, accelerating the development of more durable and efficient PEMFC catalysts.

SS-ThP-17 Temperature Dependence of Surface-Catalyzed Ullmann Coupling via Activation of Highly Labile C-I, *Chamath Siribaddana, Nan Jiang,* University of Illinois Chicago

The surface-catalyzed Ullmann-coupling via activation of highly labile C-I was studied on Au(111) using metal β-diketonato molecules with scanning tunneling microscopy. Unexpectedly the C-I bonds do not dissociate upon deposition of the molecule on the Au(111) surface held at room temperature which is known to catalyze the C-I dissociation reaction under such conditions. Rather the molecules form self-assembled monolayers stabilized by halogen bonds on Au(111). Annealing this sample to 100° C or direct deposition of the molecules on a Au(111) substrate held at 100° C triggers C-I bond cleavage. However, at 100° C intact C-I bonds can be observed, as only a portion of the molecules undergo C-I dissociation. Annealing to 200° C results in complete dehalogenation of the molecules and forming two types of COFs with triangle and cross-shaped connections. The dissociated Iodine atoms are incorporated within the COF. The two kinds of COFs exhibit only short-range network order due to the irreversible nature of the C-C bond formation. This trend is observed up to annealing temperatures of 370° C and no preference is observed towards one type of COF throughout this temperature range. Annealing temperatures beyond 400° C results in the decomposition of the molecules into its ligands which form a COF different from the COFs formed by the molecule.

SS-ThP-19 Monitoring the Dynamics of Carbon-Carbon Bond Formation in Solid-Gas Heterogeneous Photoinduced Reactions, *Aakash Gupta, Keith Blackman, Alejandro Rodriguez,* Department of Physics, University of Central Florida*; Mihai Vaida,* Department of Physics and Renewable Energy and Chemical Transformations Cluster, University of Central Florida

Carbon-carbon (C-C) bond formation is paramount for a large variety of man-made chemicals such as commodity chemicals, synthetic materials, and pharmaceuticals. Monitoring the dynamics of the C-C bond formation in real time at surfaces and how this is influenced by the surface properties could be a game changer in improving the efficiency of various heterogeneous reactions.To study the dynamics of C-C bond formation, an experimental technique is employed that combines time-of-flight mass spectrometry with pump-probe spectroscopy and fast surface preparation with molecules. CH_3I and CO are used as precursor molecules. These molecules are dosed on metal oxides such as titanium dioxide and cerium oxide, on which the reactions are monitored.

The reaction is triggered by the pump laser pulse at a central wavelength of 266 nm which excites CH_3I into the dissociative A-band, which leads to the formation of CH_3 and I fragments. Subsequently, the probe laser pulse in ultraviolet spectral domain will ionize the reaction intermediates and final products, which are immediately removed from the surface by a static electric field and detected by the time-of-flight mass spectrometer. By varying the pump-probe time delay, the formation dynamics of CH_3 intermediate, as well as the reaction of CH_3 with CO, which leads to the formation CH_3CO (acetyl) and finally to CH_3COCH_3 (acetone) will be monitored. Details on CO and CH_3I partial pressure dependence as well as the influence of the surface composition and temperature will be presented.

SS-ThP-20 Transient Kinetics Study of CO Adsorption and Dissociation on a Ru (001) Surface Crystal, *Eliseo Perez Gomez,* Stony Brook University*; Anibal Boscoboinik,* Center for Functional Nanomaterials, BNL*; Sayantani Sikder,* Stony Brook University

The adsorption and dissociation of carbon monoxide (CO) on metal surfaces is a fundamental reaction with many applications in the field of surface chemistry. Particularly, this research studied the reaction between CO and a Ru (0001) single crystal. The adsorption and dissociation of the gas were investigated through the use of techniques such as infrared spectroscopy (IR) and mass spectroscopy (MS). We also employed a pulsing valve system, where controlled pulses of CO (and other reactant gases) influence the surface reaction. The effects of temperature and pressure on the

adsorption kinetics and subsequent dissociation were explored in detail, to reach a broad understanding in the transient kinetics of the reaction. By modifying various parameters, the intention is to optimize the dynamic reaction conditions. Through this comprehensive approach, we sought to contribute valuable insights into the mechanisms driving CO adsorption and dissociation, with implications for catalysis and surface science applications.

SS-ThP-21 Bimetallic Pt-Sn and Ni-Cu Catalysts for Dehydrogenation Reactions Designed for Hydrogen Storage and Transportation, *Mengxiong Qiao, Fangliang Li,* University of South Carolina; *Ali Ahsen,* Gebze Technical University, Turkey; *Donna Chen,* University of South Carolina

The use of liquid organic hydrogen carriers (LOHC) for the safe transport and storage of hydrogen requires the development of more selective catalysts for the dehydrogenation step. For example, the methylcyclohexane (MCH)-toluene pair is an attractive choice for a LOHC system, but a more selective dehydrogenation catalyst that is less prone to deactivation by fouling is needed. The bimetallic Pt-Sn and Cu-Ni systems are promising candidates for selective dehydrogenation catalysts; the addition of Sn to Pt catalysts is known to improve stability and decrease deactivation, and the addition of Cu to Ni catalysts may serve to break up the Ni ensembles that are responsible for nonselective decomposition. Model catalyst surfaces are prepared in ultrahigh vacuum (UHV) by deposition of thin films of Sn and Cu on Pt(111) and Ni(111) respectively, as well as by sequential vapor deposition of the two metals on a rutile $TiO_2(110)$ support. The surface compositions and bimetallic cluster sizes are investigated by low energy ion scattering, temperature programmed desorption with CO as a probe molecule, X-ray photoelectron spectroscopy, and scanning tunneling microscopy. Our studies have shown that Sn on Pt clusters tend to be rich in Sn due to the higher surface free energy of Pt compared to Sn, but cluster surfaces with a low concentration of Sn can also be prepared by deposition of small coverages of Sn on existing Pt clusters. In contrast, Cu on Ni clusters exhibit low Cu concentrations due to the diffusion of Cu into Ni, which is consistent with the facile alloying of Ni and Cu. A high-sensitivity recirculating loop microreactor system has been constructed for investigating the activity for MCH dehydrogenation on the bimetallic model surfaces under catalytically relevant atmospheric pressures; the microreactor is coupled directly to the UHV chamber so that the model catalysts can be transferred between the microreactor and UHV chamber without exposure to air.

SS-ThP-22 Coverage-Dependent Adsorption and Reactivity of Formic Acid on $Fe_3O_4(001)$, *Jose Ortiz-Garcia,* Pacific Northwest National Laboratory; *Marcus Sharp,* Washington State University; *Zbynek Novotny, Bruce Kay, Zdenek Dohnalek,* Pacific Northwest National Laboratory

Formic acid (FA) is a crucial intermediate in important catalytic reactions such as Fischer-Tropsch synthesis and water-gas shift. On oxide surfaces, FA generally undergoes decomposition to CO or CO_2 through decarbonylation or decarboxylation mechanisms. We study the adsorption of FA on the reconstructed $Fe_3O_4(001)$ surface, followed by stepwise annealing using a combination of scanning tunneling microscopy (STM), x-ray photoelectron spectroscopy, low-energy electron diffraction, and temperature programmed desorption (TPD). Dissociative adsorption of formic acid leads to the adsorbed formate and hydroxyl species on the surface. At low coverages, isolated formates and hydroxyls are observed. At intermediate coverages, local clustering of formate is observed, giving rise to both (1×1) and (2×1) surface periodicities. A fully saturated surface shows formates arranging predominately in the (1×1) periodicity but retains some formates in the (2×1) periodicity in agreement with prior studies.[1] Annealing the surface to 450 K induces the formation of a well-ordered surface with a (1×1) periodicity, which results in the lifting of the surface reconstruction. Stepwise annealing enables monitoring of formate reactivity and surface structure changes. Two major peaks are observed via TPD at 525 and 565 K, indicating that the formate undergoes decarbonylation to CO and H_2O, with decarboxylation to CO_2 as a minor reaction pathway. STM reveals that annealing to 550 K leads to a partial recovery of the surface reconstruction and a possible formation of single oxygen vacancy defects. Further annealing to 650 K, which leads to the conversion of all formate species, reveals the formation of pits extended along the Fe rows. This is consistent with the non-stoichiometric formic acid decarboxylation accompanied by water formation proceeding via the Mars van Krevelen mechanism. We are currently focusing on understanding the initial stages of pit formation and the role of hydroxyls in reaction mechanisms. This work underscores the significance of fundamental studies to unravel the effect of structural changes on reaction mechanisms and dynamics.

SS-ThP-23 Using Single-Layered COFs to Stabilize Single-Atom Catalysts on Model Surfaces, *Yufei Bai, David Wisman, Steven Tait,* Indiana University Bloomington

Single-atom catalysts (SACs) combine the advantages of homogeneous and heterogeneous catalysts by limiting the reaction sites to isolated single metal atoms with well-defined chemical properties. A metal-ligand coordination method to stabilize SACs has been developed by the Tait group, in which 1,10-phenanthroline-5,6-dione (PDO) was used as ligand to coordinate with metal such as Pt, Fe, and Cr. To further improve the stability of SACs and increase the metal loading, we have synthesized single-layered covalent organic frameworks (sCOFs) on model surfaces under ultra-high vacuum (UHV) conditions or under ambient conditions. These networks with high porosity and stability were used to confine single Pt atoms coordinated with ligands into sCOF pores. Under UHV conditions, the successful formation of sCOF with regular hexagonal pores on the Au(111) surface was achieved by surface-mediated Ullmann radical coupling of 1,3,5-tris-(4-bromophenyl)benzene (TBB). Further sequential deposition of PDO ligand and Pt on the TBB-sCOF surface allowed the formation of single-site Pt catalysts by coordination interaction. The scanning tunneling microscopy (STM) images show the confinement of PDO in the sCOF pores, while X-ray photoelectron spectroscopy (XPS) has proven the existence of oxidation state of Pt, which is an indication of the single atom character. Under ambient conditions, an imine-linked sCOF was formed on the highly oriented pyrolytic graphite (HOPG) surface by a solid-vapor interface mechanism which allows for a high quality sCOF with long-range order. STM characterization has shown that regular sCOF networks with few defects were formed on the HOPG surface. This sCOF is facile to prepare and can be stored stably under ambient conditions for several weeks. These systems which combine the COF and metal-ligand coordination strategy to stabilize SACs offer the possibility to achieve higher stability and greater loading in SACs.

SS-ThP-24 N-doped Graphene Synthesis through N2+ Irradiation, *Buddhika Alupothe Gedara, Prescott Evans, Zdenek Dohnalek, Zbynek Novotny,* Pacific Northwest National Laboratory

Hydrogen (H_2) is one of the most promising clean and renewable energy sources. Nevertheless, the storage of hydrogen shows poor performance due to the low gravimetric and volumetric densities. Nitrogen-doped graphene (Gr) has been identified as a potential material for H_2 storage. Here, we study the growth of Gr on a Ru(0001) surface by chemical vapor deposition (CVD) of pyridine and N-doping through N_2^+ beam irradiation using scanning tunneling microscopy (STM) and x-ray photoelectron spectroscopy (XPS). A high-quality Gr film with low N densities was obtained by pyridine CVD on Ru(0001) at 1063 K. Higher concentrations of N-dopants were introduced on the Gr/Ru(0001) through low-energy N_2^+ irradiation at 100 eV.Nitrogen can be embedded in the Gr lattice preferentially in two configurations, namely graphitic N (N substituted in the C lattice) and pyridinic N (substitutional N next to a C vacancy). Atomically resolved STM images of graphitic and pyridinic-N defects demonstrate their preferential locations within the Gr Moiré. XPS shows that coverage of up to 3.9% of pyridinic-N and 2.3% of graphitic N can be embedded into the high-quality Gr film using N_2^+irradiation at room temperature, indicating a preferential formation of pyridinic N over graphitic N. Only graphitic N was observed upon annealing the ion-irradiated Gr/Ru(0001) to 1063 K, revealing higher thermal stability of graphitic N over pyridinic N. Our current efforts center on the adsorption studies of atomic hydrogen, its interactions with N dopants, and thermally induced diffusion.

SS-ThP-25 Coverage Dependent Interaction of N-Methylaniline with Pt (111) Surface, *Bushra Ashraf, Dave Austin,* University of Central Florida; *Nils Brinkmann, Katherina Al Shamery,* Carl von Ossietzky University Oldenburg, Germany; *Talat Rahman,* University of Central Florida

The study of N-methylaniline (NMA) coverage dependent adsorption and reaction on the Pt(111) surface has gained attention because of the alkyl and aromatic amine interaction with transition metal surface.In this work, we use Density functional theory (DFT)simulations and experiment to study the structural and electronic properties of coverage dependent adsorption of NMA on Pt(111) surface. Firstly, we found that the molecule adheres to the surface by forming bonds with both the phenyl ring and the nitrogen (N) atom at the lower coverage. However, as coverage increases, a fascinating phenomenon unfolds: the phenyl ring undergoes a distinctive tilting motion away from the surface. This tilting is accompanied by a change in the incline angle, transitioning from a mere 2° at low coverage (approximately 0.02 ML) to a substantial 33° at higher coverage (around 0.17 ML). This structural transformation also brings about a variation in the

adsorption energy, shifting from -2.9 eV at low coverage to -1.5 eV at high coverage. Secondly, Bader charge analysis provided further insights into these interactions. At low coverage, the charge is sharing between the N atom and the surface Pt atom and from the surface to the carbon (C) atoms with in the phenyl ring. In contrast, at higher coverage, charge sharing primarily takes place through the N atom to the surface. This shift towards a more robust and bi-centered bonding with the surface at lower coverage indicates an increased propensity for molecular dissociation under these conditions. Finally, the analysis of the projected density of states shed more light on revealing the hybridization of the N p_z orbital with the Pt d_{z2} orbital at higher coverage. Conversely, at low coverage,hybridization of the carbon p_z orbital with the Pt d_{z2} orbital was observed, alongside Pt-N hybridization. These observations regarding molecular adsorption at different coverages indicated that, at high coverage, the molecule easily lifts off intact from the surface, while at low coverage, it tends to break into smaller fragments, consistent with experimental findings.

SS-ThP-26 Effect of an Electric Field on the Co Adsorption on Pt, *Steven Arias, Dario Stacchiola, J. Anibal Boscoboinik,* Brookhaven National Laboratory

The adsorption of carbon monoxide (CO) on platinum (Pt) has been widely studied in the literature. Pt is one of the most frequently used active metals in catalysis, with CO playing an important role in many reactions, including hydrogenation, oxidation, and car emission controls. Here, we present our preliminary progress on the study of the effect of an electric field on CO adsorption on Pt. To do this, we designed a device that can apply a direct electric field to the surface of our Pt catalyst. A layer of porous alumina was synthesized on a Pt film, to allow CO molecules to diffuse through, making the underlying Pt accessible. A layer of graphene is added on top of the porous layer to complete the device. The bottom Pt and the top layer of graphene are biased to apply an electric field that directly interacts with the Pt surface where the CO is being adsorbed. Using infrared reflective adsorption spectroscopy (IRRAS) we study the effect of such fields on CO adsorption.

SS-ThP-27 Generating Defects in Semiconductor Monolayers on Metal Surface, *Sayantan Mahapatra, Jeffrey Guest,* Argonne National Laboratory, USA

Nanoscale observation and deliberate engineering of atomic defects within semiconductor transition metal dichalcogenides (TMDs) hold significant importance for their utilization in cutting-edge quantum optics and nano-electronic devices. Here, we demonstrate a versatile approach in generating single defects on TMDs monolayers using a photon source. The newly generated defects were visualized via scanning tunneling microscopy (STM) at room temperature at the atomic level. These defects can act as single-photon emitters (SPE) and their performance remains excellent in high vacuum conditions. Furthermore, our simulations provide insights into the defect formation energies on metal surfaces compared to an insulating surface. The charge transfer between the metal and monolayer TMDs plays a significant role in generating the defects. Furthermore, simulation also sheds light on the mono- or di-chalcogen vacancies as the potential candidates for these defects, thereby providing a direct match between theory and experiment.

SS-ThP-28 Characterization of Oxygen on Rh-Based Model Catalysts, *Maxwell Gillum, Alexis Gonzalez, Elizabeth Serna-Sanchez, Allison Kerr, Stephanie Danahey, Dan Killelea,* Loyola University Chicago

The studies presented investigate the influence that surface and defect geometry have on the kinetics and reactivity of oxygen on various Rh-based model catalysts. The experiments focus on gaining structural information about the oxygen species present on the surface under various oxidative conditions utilizing scanning tunneling microscopy (STM) and low energy electron diffraction (LEED). These techniques are used in unison with temperature programmed desorption (TPD) and Meitner-auger electron spectroscopy (MAES) to identify optimal conditions for further study

SS-ThP-32 Weakly and Strongly Adsorbed H_2O Layers on Hydroxylated SiO₂ Surfaces: Dependence on H_2O Pressure at Various Temperatures, *Samantha Rau, Rebecca Hirsch, Marcel Junige,* University of Colorado Boulder; *Antonio Rotondaro, Hanna Paddubrouskaya, Kate Abel,* Tokyo Electron America, Inc.; *Steve George,* University of Colorado Boulder

Although H_2O adsorption on SiO_2 surfaces has been studied extensively, there are still many questions about the nature of the H_2O adsorbed layer. In this work, the H_2O layer thickness on flat hydroxylated SiO_2 surfaces was examined in a vacuum environment using in situ spectroscopic ellipsometry (SE). The H_2O water layer thickness was measured versus H_2O pressure at various temperatures. Complementary Fourier transform infrared (FTIR) analysis was also performed on SiO_2 powders.

Flat SiO_2 surfaces were hydroxylated using H_2O_2 plasma exposure to produce a hydrophilic surface with a water contact angle of < 10°. The in situ SE measurements were then conducted in a warm-wall vacuum chamber designed with a temperature-controlled sample stage. The H_2O layer thickness was measured versus pressure at various temperatures (Figure 1). The H_2O pressures were varied up to the saturation H_2O vapor pressure corresponding to the sample temperature. The H_2O layer thickness versus relative humidity was consistent with general expectations from the BET adsorption isotherm model.

The SE measurements showed that there were two distinct types of H_2O layers: a weakly adsorbed layer and a strongly adsorbed layer (Figure 2). The weakly adsorbed layer could be added or subtracted by increasing or removing the H_2O pressure. The strongly adsorbed layer was not lost by removing the H_2O pressure. However, the strongly adsorbed layer could be desorbed by heating the sample stage to 120°C. The SE measurements characterized the layer thicknesses for the weakly and strongly adsorbed layers versus H_2O pressure at various sample temperatures.

Using repeating H_2O exposures, the strongly adsorbed layer reached an approximate plateau at ~1 Å at various temperatures. In contrast, the weakly adsorbed layer obtained higher thicknesses at larger H_2O pressures. For example, the weakly adsorbed layer thickness was 7 Å at 92% relative humidity at 30.4°C (30 Torr). The FTIR investigations on SiO_2 powders were in qualitative agreement with the SE studies. These studies confirm the existence of a strongly adsorbed vicinal layer and a weakly adsorbed layer explained by the BET model on hydroxylated SiO_2.

SS-ThP-34 Insight into the Synergistic Effect of the Oxide–Metal Interface on Hot Electron Excitation, *Si Woo Lee,* Inha University, Republic of Korea

Understanding the role of electron transfer by energy dissipation during chemical reactions on metal catalyst surfaces is significant for elucidating the fundamental phenomena at solid−gas and solid-liquid interfaces [1]. Electronic excitation by molecular interactions between reactants and catalyst surfaces generates a flow of excited electrons with an energy of 1−3 eV; these are called hot electrons [2]. To reveal the chemically induced electronic excitations on metal catalyst surfaces, metal-semiconductor catalytic nanodiodes can be used for real-time hot electron detector [3]. In addition, recently, it was found that when the metal-oxide interface is formed, the excitation of hot electrons can be amplified [4].In this work, by employing our catalytic nanodiodes with well-defined oxide–metal interfaces [CeO₂ nanocubes (NCs)/Pt/TiO₂ Schottky nanodevices], which is the first platform for the quantitative analysis of electron transfer at interfacial sites, we observed electronic excitation under H2 oxidation at the CeO₂/Pt interface in real time. Direct measurement of the electron transfer as a function of the concentration of interfacial sites (by controlling the coverages of deposited CeO₂ on Pt) allowed us to investigate the effect of the oxide–metal interface on nonadiabatic electronic excitation during catalytic H_2 oxidation. Surprisingly, we observed that the efficiency of hot electron excitation was the highest at a specific concentration of CeO₂/Pt interfacial sites, confirming that the interface enhances hot electron excitation under exothermic catalytic reactions. Our operando techniques using Schottky nanodiodes with well-controlled oxide–metal interfaces enabled us to uncover the quantitative relationship between the nanoscale interface and hot electron excitation, thereby optimizing the catalytic performance, contributing to the rational design of future hot electron-based catalysts [5].References[1] Si Woo Lee *et al., Nano Letters,* **2023,** *23 (11),* 5373[2] Si Woo Lee *et al., Surface Science Reports,* **2021,** *76 (3),* 100532[3] Si Woo Lee *et al., ACS Catalysis,* **2019,** *9 (9),* 8424[4] Si Woo Lee *et al., Nature Communications,* **2021,** *12 (40),* 1[5] Eunji Lee *et al., ACS Catalysis,* **2024,** *14 (8),* 552

SS-ThP-35 Ab Initio Studies on Solid-Liquid Interfaces via Machine-Learned Force Fields, *Andreas Kretschmer, Markus Valtiner,* Christian Doppler Laboratory for Surface and Interface Engineering, Austria

In order to unravel the aqueous behavior at the solid liquid interface, we employ ab initio molecular dynamics simulations. To minimize finite-size artifacts of the simulation cell, but retain the chemical accuracy of ab initio simulations, we use on-the-fly machine-learned force fields as employed by the Vienna Ab Initio Simulation Package. We investigate two model systems, first we study the hydrophobic gap on graphene stacks with up to 4 layers, and second the dissolution behavior of different ionic salts. The salts are NaI, AgF, and NaCl, which all crystallize in the same NaCl structure, but have decreasing molar solubilities in water in the listed order. We first

use static density functional theory calculations to relax the individual phases separately, which is then followed by training the force fields. We compare different functionals, PBE and RPBE, both with and without Grimme D3 corrections, R2SCAN+rVV10, and vdW-DF-cx, to find the optimal compromise in the description of the two phases. The lattice parameters of graphite are best reproduced by the PBE-D3 functional, while the other functionals with dispersion treatment perform reasonably well. The PBE and RPBE functionals without Grimme corrections on the other hand lead to dramatically overestimated c axes. The lattice parameter of the ionic salts is almost exactly reproduced by the vdW-DF-cx functional, but at more than 150-fold the computational expense compared to the other functionals, while the PBE and RPBE functionals overestimate the lattice parameter slightly. The PBE-D3, RPBE-D3 and R2SCAN+rVV10 functionals on the other hand slightly underestimate the lattice parameter. In bulk water, the bond lengths and angles are overestimated by roughly 3% consistently across all functionals, only the R2SCAN+rVV10 functional performs slightly better at 2% overestimation. Each phase is first trained separately by ab-initio simulations, until the Bayesian error threshold of the forces is undercut consistently. Thus, the interactions within the phase are learned in a smaller simulation cell, saving computation time. After training the individual phases, the solid phase is joined with the liquid phase and trained together to include the interface interactions into the force field. This training regime allows efficient training of the force field that can then be applied to much larger simulation cells than the training data.

SS-ThP-36 A Highly Integrated Correlative Microscopy Platform for In-Situ AFM-SEM-EDS, *Kerim T. Arat, William K. Neils,* Quantum Design Inc.*; Stefano Spagna,* Quantum Design International

The integration of AFM and SEM techniques within a single platform implemented in a highly integrated tool offers the advantage of utilizing the complementary strengths of two different imaging modalities without the inherent complications of sample transfer. This is not only a significant improvement in time to results but also ensures high confidence in correlation accuracy and eliminates the risk of sample contamination.

In previous work, we developed a correlative microscopy platform that combines AFM and SEM [1]. These techniques can map the surface in high resolution. The trunnion stage, with up to 80° tilt capability, allows monitoring of process quality such as tip measurement or monitoring tip-sample interaction [2]. In addition to topography, the platform is able to extract electrostatic and magnetic information from the sample with electrostatic force microscopy (EFM) and magnetic force microscopy (MFM) modes. However, none of these provide the ability to determine the sample's elemental composition.

We have extended the capabilities of the correlative platform with an energy-dispersive X-ray spectrometer (EDS) to extract elemental information from the sample. The spectrometer is based on the silicon drift detector (SDD), which provides high energy resolution (< 133 eV, Mn-Kα).Its graphene-based window offers detection of elements down to carbon. The EDS elemental identification algorithm uses a background subtraction method and compares the resulting spectra to reference datasets based on the NIST database [3]. Both hardware and software integration allow correlation of elemental information with the other imaging modalities that the tool can provide where one can superimpose topography and elemental information.

Integration of EDS adds a significant analysis capability to AFM-SEM techniques applicable to a diverse range of materials such as metals, alloys, ceramics, and polymers. With this addition, researchers can obtain in-situ correlation of high-resolution, localized elemental information with high-resolution lateral and vertical topographical information, without the complications of sample transfer.

[1] A. Alipour et al., Microscopy Today 31 (2023), p. 17-22. doi: 10.1093/mictod/qaad083

[2] "FusionScope by Quantum Design – a new AFM SEM Correlative Microscopy Platform", 2024. https://fusionscope.com/ (accessed Sept. 4, 2024).

[3] D. E. Newbury and N. W. M. Ritchie, Scanning Microscopies 9236 (2014), p. 9236OH. doi: 10.1117/12.2065842

SS-ThP-37 In-Situ Characterization of Au Capping on Superconducting Nb(100), *Van Do,* Helena Lew-kiedrowska, University of Chicago*; Chi Kelly,* National Cheng Kung University (NCKU), Taiwan*; Sarah Willson, Steven Sibener,* University of Chicago

Nb is the highest temperature elemental superconductor, however, its application in particle accelerators and quantum computers are limited by growth of surface native Nb oxides. Au capping layers have been shown to prevent deleterious Nb oxidation, however, Au adsorption, growth, and morphology on Nb has not been fully investigated. This work characterizes physical deposition and subsequent anneals of sub-monolayer to monolayer converges of Au on Nb(100) using Scanning Tunneling Microscopy, X-ray and UV Photoelectron Spectroscopy, and Auger Electron Spectroscopy. Our preliminary results show Au island formation at annealing temperatures as low as 350 ℃. Additionally, Au continued to sinter, forming larger islands with increasing temperature until desorption at 900 ℃.

SS-ThP-38 Characterization of Oxidized Rhodium Surface Structures, *Elizabeth Serna-Sanchez, Dan Killelea,* Loyola University Chicago

Heterogeneously catalyzed oxidation reactions, such as the catalytic process of converting CO to CO_2, are extensively utilized for the production of modern commodities. However, there remain key questions about the atomic level details of these catalytic processes. In order to further our understanding of the process, the investigation herein will focus on characterization of the structures formed and quantification of the amount of oxygen in and on stepped Rh surfaces.A curved Rh(111) crystal will be employed, where the step with varies monotonically across the face from the (111) apex. Scanning tunneling microscopy (STM) images will help to illustrate how the behavior of oxygen will be affected by features such as surface defects and step width. Alongside the STM, other techniques such as Meitner-Auger electron spectroscopy (MAES), temperature programmed desorption (TPD), and low energy electron diffraction (LEED) will be used to identify the various species of oxygen and the structures they form on the surface.

SS-ThP-39 Investigation of Carbon Monoxide (CO) Oxidation on Rh(111) with Reflectance Absorbance Infrared Spectroscopy (RAIRS) and Temperature Program Desorption (TPD), *Alexis Gonzalez, Dan Killelea,* Loyola University Chicago

To create accurate models of catalysis, the speciation and kinetics of catalytic systems must first be experimentally determined. In previous studies, we have shown that Rh-based catalysts provided a robust model system to study oxidation reactions due to the reliability with which we can produce a limited number of oxygen species on the surface. This allowed for better control of the oxygenaceous species present in the system. By probing the reactivity of these various surface species, such as adsorbed surface oxygen and subsurface oxygen, using the CO oxidation reaction we were able to determine the influence of various oxygen species on kinetics of oxidation. Herein, we present preliminary data on how the integration of reflectance absorbance infrared spectroscopy(RAIRS) into our ultra-high vacuum (UHV) setup. IR and TPD spectra indicated that there was more carbon dioxide production on the Rh(111) surface prepared with molecular oxygen than the surface prepared with atomic oxygen. This seemingly contradicted what was expected due to the higher oxygen coverage on the surface prepared with atomic oxygen. IR spectroscopy was used concurrently with temperature programmed desorption (TPD) experiments to collect real time information about the surface composition of the crystal as the CO oxidation reaction was occurring.

Thin Films
Room Central Hall - Session TF-ThP
Thin Films Poster Session

TF-ThP-2 Surface Analysis of Nanolayers by LEIS, SIMS and XPS, *Birgit Hagenhoff,* Tascon GmbH, Germany*; Jan Tröger,* University of Münster, Germany*; Elke Tallarek, Danica Heller-Krippendorf,* Tascon GmbH, Germany

Advanced and smart materials nowadays consist of various materials featuring layers and layer systems at the nanoscale. In order to monitor the development process as well as production and customer returns, analytical techniques are required which have an information depth suited for the layered samples.

Starting with information from the outermost atomic layer using Low Energy Ion Scattering (LEIS), adding Time-of-Flight SIMS (ToF-SIMS) for the outermost 3-5 monolayers and ending with X-ray Photoelectron

Spectroscopy (XPS) for accessing up to 20 monolayers, a detailed insight can be gained into the composition of layers at the nanoscale. On the other hand, layer systems the structure of which is well known can help to better understand the performance features of the different analytical techniques.

In our ongoing studies we have compared analytical results from LEIS, ToF-SIMS and XPS for various layered systems. We will report on films produced by Atomic Layer Deposition (ALD) as well as core-shell nanoparticles. Amongst the three, XPS is the most often used technique in industry because of its power to obtain quantitative results. Our comparative data will help to put XPS data in a suited information depth perspective.

TF-ThP-3 Role of Solvent Treatment on the Structure and Thermoelectric Properties of oCVD PEDOT Films, *Ramsay Nuwayhid*, *Travis Novak, Battogtokh Jugdersuren, Xiao Liu, Jeffrey Long, Debra Rolison,* U.S. Naval Research Laboratory

Vapor-phase routes to organic conducting polymers offer many advantages over more commonly studied solution-phase methods. Conductive polymers often require functionalization to be soluble in an appropriate solvent, and techniques such as spin-coating or drop-casting are generally only suitable for relatively flat substrates. Oxidative chemical vapor deposition (oCVD) is an alternative that allows for precise control of coatings over complex 3D substrates. oCVD can produce highly conductive conjugated polymer films, notably PEDOT, but compared to solution-phase PEDOT(:PSS) films, there has been little research into optimization of these films for thermoelectric applications. In this work, we demonstrate that post-deposition treatments with common organic solvents, such as dimethyl formamide (DMF), ethylene glycol (EG), or dimethyl sulfoxide (DMSO), significantly improve the Seebeck coefficient and resulting power factor for oCVD-grown PEDOT films. Given the lack of PSS in oCVD-grown films, much of the enhancement observed in spin-coated films after solvent treatments cannot be related to removal/segregation of the PSS phase, which is a common assertion. Despite this lack of PSS, we observe Raman changes very similar to those previously seen in PEDOT:PSS films, including the disappearance of peaks previously assigned to PSS. For oCVD-grown PEDOT, we find significantly reduced Cl content after solvent treatments, which likely de-dopes the PEDOT films and subsequently enhances the Seebeck coefficient. These results not only show solvent-treatments to be effective in improving the thermoelectric properties of oCVD-grown films, but also prove that many of the phenomena attributed to PSS in spin-coated films may be related to other chemical or structural changes in the PEDOT chain.

TF-ThP-4 Development of Low-K/ High-K Multilayers for Power Capacitors, *Julie Chaussard*, *Hala Houmsi, Chloé Guérin, Aude Lefèvre,* CEA-Leti, France*; Patrice Gonon,* LTM-CNRS, France*; Vincent Jousseaume,* CEA-Leti, France

Power electronics gather many emerging applications such as electrification of transports. In power devices, voltage fluctuations can occur and damage GaN transistors, especially during switching phases. To prevent this, a snubber network can be used. It consists of a series capacitor and resistor connected in parallel to a transistor. Capacitor must have high capacitance, high breakdown voltage and thermal stability up to 150°C (operating temperature for electric vehicles). Furthermore, capacitor and resistor are usually surface-mounted devices and have disadvantages of low heat dissipation and large size. One way to miniaturize these passive components would consist in 3D integration on silicon wafers.

Today, polymer capacitors are widely used because of their low-cost manufacturing and high electric breakdown strength. However, thin films of polymer cannot be conformaly deposited into 3D structures. Also, most of polymers have low operating temperature, lower than the 150°C targeted. Among alternative non-polymeric materials, two groups stand out: high-k (with high dielectric constant but low breakdown voltage (V_{bd})) and low-k materials (higher V_{bd} than high-K materials). A strategy has to be developed to find a compromise between high dielectric constant and high breakdown voltage. A promising way is to integrate high-k/low-k multilayers into a MIM (=Metal-Insulator-Metal) capacitor.

In this work, multilayers combining an organosilicate (SiOCH) as low-k and HfO_2 as high-k were investigated. SiOCH thin films were deposited by plasma-enhanced chemical vapour deposition while HfO_2 thin films were deposited by atomic layer deposition. Chemical and physical properties of the films were studied using FTIR, ellipsometry, X-ray reflectometry and X-ray diffraction. Then, different thicknesses and stacks were fully integrated into MIM capacitors on 200 mm Si wafers for electrical characterizations. Electrical parameters such as dielectric permittivity, dielectric losses, leakage current and breakdown field were measured. It is shown that the introduction of very thin HfO_2 layer (in the 10 nm range) between SiOCH layers (50 nm thick) allow to increase the dielectric constant up to 11%. The use of more complex stack (i.e. up to 5 layers) further improves the $C*V_{bd}$ parameter. This approach combining low-k and high-k looks promising for the realization of high-voltage 3D capacitors on Si.

TF-ThP-5 The Electrical, Sensory and Photocatalytic Properties of Graphene Oxide and Polyimide Implanted by Low and Medium Energy Gold Ions, *Josef Novák,* Nuclear Physics Institute of the CAS, Czechia

In our work, we focused on the investigation of the electrical, photocatalytic and sensory properties of graphene oxide (GO) and polyimide (PI) implanted by gold energetic ions. Gold ions (Au^+) are favored for ion implantation into polymers due to several key reasons. Primarily, Au^+ possesses exceptional electrical conductivity, rendering it highly suitable for establishing conductive pathways within the polymer matrix. Additionally, gold exhibits remarkable chemical stability, thereby minimizing undesired reactions with the polymer substrate during the implantation process. The implantation of Au^+ ions is accompanied by crystallization and carbonization of the modified samples, which leads to the disruption of chemical bonds and the formation of network processes [1].]. These processes lead to the formation of conjugated systems that promote electric charge transport [2].

The organic non-conductive materials (GO, PI) were subjected to modification using low-energy Au^+ ions (20 keV) and medium-energy Au^+ ions (1.5 MeV). The ion implantation was conducted with three different ion fluences. At the lowest ion fluence (3.75×10^{12} cm^{-2}), the formation of carbon islands may occur. The second ion fluence (3.75×10^{14} cm^{-2}) induces the growth of carbon clusters and the formation of conjugated carbon bonds [2]. With the highest ion fluence used (1×10^{16} cm^{-2}), the formation of metal nanoparticles is expected to take place [3].

References

[1] V. Popok, V. Popok et al., Springer, 2019. p. 69-111

[2] J. Novak, E. Stepanovska, P. Malinsky, et al., Nucl Instrum Meth B 540, 199-209 (2023)

[3] P. Malinsky et al., Polymers 15, 1066 (2023)

TF-ThP-8 The Effects of Ultraviolet Irradiation and Mechanical Stress on Polymer-Like Hydrogenated Amorphous Carbon Thin Films, *Thomas Poché, Rajib Chowdhury, Yonatan Tesfamariam,* **Seonhee Jang**, University of Louisiana at Lafayette

Polymer-like hydrogenated amorphous carbon (a-C:H) films have found use in many applications due to their desirable material properties. Compared to other a-C:H films, are characterized by having a high H content (40-50%) as well as a significant amount of C-H sp3 bond sites, and their properties are known to be highly tunable by various post-processing methods. One such method is ultraviolet (UV) irradiation, which can remove H from the film, assist in oxygen (O) absorption, and promote graphitization. The ability to selectively tune the properties of a film at specific locations is desirable for applications such as biomedical devices and warrants further research.For this study, a-C:H films were grown onto both rigid silicon (Si) (100) and flexible indium tin oxide/polyethylene naphthalate (ITO/PEN) substrates by the plasma-enhanced chemical vapor deposition of cyclohexane (CHex, C_6H_{12}) precursor. The a-C:H films were deposited at ambient temperature of 18-19 °C with varying plasma powers from 20 to 80 W. A 275 nm UV source was applied to the a-C:H films on rigid Si for various cure times of 1 and 4 hours, and various irradiances at 0.0022 and 0.0466 W/cm2. The most extreme of these curing conditions (4 hours at 0.0466 W/cm^2) was applied to the a-C:H films on flexible ITO/PEN, prior to 10,000 cycles of repeated mechanical bending. The thickness, refractive index, extinction coefficient, and optical bandgap of the a-C:H films were measured by spectroscopic ellipsometry. The surface wettability of the films was measured by contact angle goniometry, while the surface morphology and roughness were measured by atomic force microscopy (AFM). The chemical composition and relative H content of the films was measured by Fourier-transform infrared (FTIR) spectroscopy.UV irradiation caused ablation of the film surface, decreasing the film thickness. Simultaneously, H was preferentially removed from the film while O was incorporated from the atmosphere. The films remained optically transparent and topologically smooth after the UV irradiation procedure. The surface wettability of the

films increased substantially, while the optical bandgap values decreased. The FTIR analysis supported that H removal and O incorporation occurred throughout the a-C:H films during UV irradiation. The mechanical bending procedures caused no significant changes to occur within the UV irradiated a-C:H films, indicating their potential for application in flexible electronic devices. In summary, UV irradiation plays an important role in tuning the composition, and thus the properties of polymer-like a-C:H films.

TF-ThP-9 Adoption of UV-Di for Fabricating Electrically Enhanced Amorphous In-Ga-Zn-O Thin-Film Transistors at Low Temperatures, *Giyoong Chung, Yong-Sang Kim,* Sungkyunkwan University, Korea

We investigated the electrical characteristics of sol-gel processed thin-film transistors (TFTs) and found that they are improved by the addition of UV-irradiated deionized water (DI water). The vulnerability of solution-processed metal-oxide semiconductors is significantly influenced by organic chemical-induced defects such as voids, holes, and organic residues. To address this issue, we introduced hydroxyl radicals (OH•), generated in DI water through an O3/UV process, into the In-Ga-Zn solution mixture to deposit IGZO active layers with fewer defects. The generation of hydroxyl radicals in DI water was confirmed by potassium iodide (KI)/ultraviolet-visible (UV-vis) spectroscopy analysis. The intensity of the absorbance peak at wavelengths of 290 nm and 350 nm increased with longer UV irradiation times on DI water. Additionally, we used the TG-DSC method to determine that organic materials in the IGZO solution mixture with ozonated water began to decompose at a lower temperature (121.6℃) than pristine IGZO solution mixture (144.5℃). Abrupt weight loss was also observed in the IGZO solution with ozonated water compared to pristine IGZO solution. The field-effect mobility and sub-threshold slope of the a-IGZO TFTs made with ozonated water were improved compared to the conventional process, increasing from 0.40 to 0.97 cm^2/V·s and decreasing from 0.34 to 0.29 V/dec, respectively. These results suggest that the addition of ozonated water to the sol-gel mixture is a simple method to achieve high-performance TFTs by reducing organic chemical-induced defects through low-temperature processing.

TF-ThP-10 Influence of Multi-Energy Ion Implantation of Cu and Ag Ions on the Electrical Properties of Graphene and Cyclic Olefin Copolymer Thin Films, *Eva Štěpanovská, Josef Novák,* Nuclear Physics Institute of the Czech Academy of Sciences, Czechia*; Petr Malinský,* Nuclear Physics Institute of the Czech Academy of Science, Czechia*; Vlastimil Mazánek,* University of Chemistry and Technology, Czechia*; Martin Kormunda, Luboš Vrtoch,* J. E. Purkyne University, Czechia*; Anna Macková,* Nuclear Physics Institute of the Czech Academy of Sciences, Czechia

Graphene (G) and cyclic olefin copolymer (COC) thin films with a thickness of 50 μm were subjected to multi-energy ion implantation of Cu^+ and Ag^+ ions. The ions were implanted with energies of (2.8, 2.0, 1.2) MeV and various fluences (10^{12}, 10^{13}, 10^{14}) ions/cm². Ion energy levels were chosen to create continuous layers within the organic materials, intersecting in a Gaussian distribution. Elemental changes were analyzed using Rutherford backscattering and elastic recoil detection analysis (RBS/ERDA), chemical bonds were monitored using X-ray photoelectron spectroscopy (XPS), infrared (IR) and Raman spectroscopy, and finally electrical properties were investigated using electrochemical impedance spectroscopy (EIS). With increasing ion fluence, the sheet resistance of the implanted layers decreases, indicating an increase in the material's electrical conductivity. This study provides a comprehensive insight into the changes in the microstructure and electrical properties of graphene and cyclic olefin copolymer thin films after ion implantation, which holds significant potential for applications in electronics and sensing.

TF-ThP-13 Poly(P-Phenylenediamine) by oMLD for Amine Functionalization of Polydioxanone for Biomedical Applications, *Nazifa Z. Khan, Nikhila C. Paranamana, Xiaohua Liu, Matthias J. Young,* University of Missouri-Columbia

Polydioxanone (PDO) is an aliphatic polyester with excellent biocompatibility, flexibility, and biodegradability, and has been widely used as a surgical suture. However, lack of functional groups in the backbone of PDO limits its applications to other biomedical aspects. Here, we study vapor-phase oxidative molecular layer deposition (oMLD) of an amine-containing polymer, poly(p-phenylenediamine) (PPDA), onto PDO substrates. Our goal with this is to use vapor-phase infiltration to form PPDA within PDO and provide stable surface amine groups for subsequent grafting of biomolecules. Recent work established oMLD growth of PPDA at 150 ℃. Here, a lower deposition temperature is necessary for compatibility with PDO. We study oMLD growth of PDO at 90 ℃, both onto flat silicon substrates and within the spin-coated PDO polymer. We employ *in situ*

quartz crystal microbalance (QCM) studies during oMLD growth to benchmark the deposition of PPDA at these lower temperatures. We also report *ex situ* spectroscopy and chemical analysis on flats to understand the extent of amine incorporation into PDO and the stability of this PPDA polymer in physiologically relevant solution conditions. The incorporation of amine groups onto the PDO surface will facilitate the addition of bioactive components into PDO to control cell-material interactions, therefore expanding its application in regenerative medicine.

TF-ThP-14 Tuning the Crystallinity of TiO₂ Coatings Synthesized by an Atmospheric Pressure Dielectric Barrier Discharge, *Nicolas Fosseur,* Chemistry of Surfaces, Interfaces and Nanomaterials (ChemSIN), Faculty of Sciences & 4MAT, Engineering faculty, Université Libre de Bruxelles, Brussels, Belgium*; Stephane Godet,* 4MAT, Engineering faculty, Université Libre de Bruxelles, Brussels, Belgium*; Francois Reniers,* Chemistry of Surfaces, Interfaces and Nanomaterials (ChemSIN), Faculty of Sciences, Université Libre de Bruxelles, Brussels, Belgium

Titanium dioxide (TiO_2) is a widespread semiconductor material present in numerous applications such as photovoltaic panels, various cosmetic products and batteries. Nowadays it is intensively studied for its depolluting action thanks to its photocatalytic properties. However, generating crystalline thin films using a cold plasma operating at atmospheric pressure is not trivial. This work focuses on the crystallization of anatase thin films, using a Plasma Enhanced Chemical Vapor Deposition method (PECVD). Different TiO_2 films are synthesized in an atmospheric pressure dielectric barrier discharge system, enhanced with an original heating device [1,2], and analyzed using scanning electron microscopy (SEM), X-ray diffraction (XRD), X-rays photoelectron spectroscopy (XPS) and Infrared reflection-absorption spectroscopy (IRRAS). The ultimate goal of this research is to better control the crystal size and the crystalline structure which are decisive parameters in the efficiency of the photocatalytic effect. To do so, different plasma depositions were done with a total flow of 10 slm (15% of argon flow going in the bubbler, 15 % of O_2 and 70 % of Argon carrier flow) and a deposition time of 20 minutes. By changing different parameters such as substrate temperature, power and frequency, a constant crystal size could be obtained and by increasing precursor temperature, crystal sizes ranges from 10 to 20 nm. At a larger scale, by tuning the frequency of the plasma generator, the coatings deposited exhibit different mean cauliflower-like size ranging from 570 to 975 nm, which influence the specific surface area. These preliminary results open a door on controlling more efficiently the crystal size, the crystal growth and the coating texture and density, which could help improving further photocatalytic applications.

References:

[1] A. Remy, et al. Thin Solid Films, 688, 137437 (2019).

[2] A. Remy, F. Reniers. patent EP3768048A1 (2019).

Keywords: anatase, atmospheric pressure plasma, crystal size, bubbler temperature, photocatalytic application.

TF-ThP-15 Simultaneous Nanopatterning of SiO₂ and Ru via Area-Selective Atomic Layer Deposition, *Chi Thang Nguyen, Angel Yanguas-Gil, Jeffrey W. Elam,* Argonne National Laboratory, USA

Area-selective atomic layer deposition (AS-ALD) has emerged as a promising technique for precisely controlling thin film deposition on desired areas. When combined with other fabrication methods, AS-ALD can address existing challenges in nanopatterning fabrication. In this study, ruthenium AS-ALD was integrated with an area-selective etching (ASE) process to achieve self-aligned nanopatterns. Tricarbonyl (η4-2-methylene-1,3-propanediyl)Ruthenium(II) (TRuST) and O_2 were used as novel Ruthenium precursor and reactant, respectively, for Ru AS-ALD. The bis(N,N-dimethylamino)dimethylsilane (DMADMS) served dual roles: as a precursor in SiO₂ ALD and as an inhibitor in the Ru AS-ALD process. During Ru AS-ALD, DMADMS selectively adsorbed on SiO₂ surfaces, effectively blocking Ru film growth, but not on the Ru substrate surface. Subsequently, O_3 was introduced as a counter reactant for SiO₂ ALD, reacting with DMADMS-adsorbed SiO₂ surfaces to grow ALD SiO₂ and simultaneously etching Ru from the Ru substrate surface. By controlling the selectivity of Ru using DMADMS and the O_3 exposure time, desired thicknesses of Ru and SiO₂ films were achieved, enabling controlled Ru/SiO₂ nanopatterning in a single combined AS-ALD and ASE process. The adsorption of the DMADMS

inhibitor, the selectivity and etching of Ru, and the growth of SiO_2 films were investigated using several analytical techniques including X-ray photoelectron spectroscopy (XPS), atomic force microscopy (AFM), scanning electron microscopy (SEM), in-situ spectroscopic ellipsometry (SE), and in-situ quadrupole mass spectrometry (QMS).

TF-ThP-17 Direct Growth of Molybdenum Disulfide from Metal Contacts via Atomic Layer Deposition, *John Hues, Elton Graugnard,* Boise State University

As current silicon-based transistor devices begin to approach the fundamental material scaling limits of silicon, new designs and material integration methods are required to meet the ever-increasing demand for greater computing power and memory storage densities. Molybdenum disulfide (MoS_2) is one material in the two-dimensional materials class which is a potential replacement for silicon within next generation microelectronic devices to enable further device scaling due to its high electron mobility, even when in monolayer form. High quality MoS_2 is required for integration into microelectronic devices as even small concentrations of defects can significantly impact the electrical properties of the monolayer film. Synthesis of monolayer MoS_2 which is of sufficient quality for integration into microelectronic devices while maintaining processing temperatures that are within the allowable thermal budget of back end of line processing has proven difficult. In this work we demonstrate a method of growing crystalline MoS_2 directly from contact metals via atomic layer deposition (ALD) using molybdenum hexafluoride and hydrogen sulfide as the reactants. Several different contact metals including tungsten, molybdenum, nickel, and platinum were used for blanket studies to determine the ability to deposit crystalline MoS_2 at low temperatures. Raman spectroscopy was used to examine the crystallinity of the deposited films and x-ray photoelectron spectroscopy was utilized to determine the chemical composition of the deposited films. To obtain high quality MoS_2 test structures, contact metals were patterned to template direct ALD of MoS_2. Following MoS_2 deposition the samples were again characterized using Raman spectroscopy and atomic force microscopy to determine the crystallinity and morphology of the resulting MoS_2 film.

TF-ThP-19 The Stability of Lif-Capped Fluorinated Aluminum Films When Irradiated with Electrons, *Devin Lewis, David Allred, Richard Vanfleet,* Brigham Young University

Aluminum thin films are an ideal broadband reflectors for application including space observatories. However, oxide forms on freshly-deposited Al when it is exposed to oxygen or water vapor. This oxide layer absorbs a large portion of far ultraviolet (FUV) wavelengths. In order to prevent oxidation a barrier layer layer is deposited on top of Al mirrors. To preserve high FUV reflectance it is usually a low Z metal fluoride, such as MgF_2, AlF_3 or LiF. Of the commonly used metal fluorides, LiF has the best FUV transparency. However, it is susceptible to radiation damage. Many studies have shown that the electron beam in an electron microscope (SEM or TEM) can damage halide salts such as sodium chlorides and bromides. One such process termed radiolysis. Alkali halide salts are known to be most sensitive. The halide anion disappears as does the cation. Since mirrors on space telescopes will also be exposed to the solar wind and coronal mass ejection (CME) understanding the degradation mechanism and kinetics was deemed a high priority. We have studied the radiolysis of fluoride films important to FUV optics, mainly LiF films. The first damage is a roughening of the surface and a decrease of the fluorine peak in energy dispersive x-ray analysis (EDX). Note that, lithium (Z = 3) cannot be detected by x-ray florescent techniques since its electrons are not sufficiently bound. In some cases, LiF is fully removed from the scanned region after beam exposure.

TF-ThP-20 Achieving a Low-Voltage Operation Indium Gallium Zinc Oxide Thin Film Transistor Through Optimized Crystallinity ZrO_2 Gate Insulator, *Hanseok Jeong, Soo Min Yoo,* Kyunghee University, Republic of Korea; *Minki Choe, In-Hwan Baek,* Inha University, Republic of Korea; *Woojin Jeon,* Kyunghee University, Republic of Korea

The indium gallium zinc oxide (IGZO) has been widely investigated as the active layer for the display backplane thin-film-transistor (TFT). In ultra-high-resolution displays, reducing transistor size per pixel results in submicron-scale channel lengths.[1] Consequently, the short-channel effects become a concern as TFT channel lengths decrease to the submicron scale. Novel architectures such as 3-dimensional vertical or FinFET structures would be developed. The fast-operation speed and low-voltage operation of TFTs are made possible by using the gate insulator (GI) with a high-dielectric-constant (k) value. Among many high-k materials, ZrO_2 has a high-k value (28) and a suitable band gap (5.8 eV).[2] Atomic layer deposition (ALD) has the advantages of conformal depositions,

thickness/composition controllability of thin films, and thin film quality due to its self-limiting growth behavior.

High-k materials exhibit higher dielectric constants compared to amorphous-phase SiO_2 due to their crystallinity.[3] However, high-k materials used as GI result in TFT performance degradation due to increased surface roughness caused by crystallinity, increasing surface scattering, and coulomb scattering. In the previous study, our research group controlled the crystallinity of ZrO_2 by varying the deposition temperature and optimized ZrO_2 ALD processes in Mo/ZrO_2/IGZO metal-insulator-semiconductor structures.[4] In this study, we investigated ALD-derived IGZO TFTs using an optimized ZrO_2 ALD process.

The ZrO_2 film was deposited by the thermal ALD process using Cyclopentadienyl Tris(dimethylamino)Zirconium (CpZr), and ozone (O_3). The IGZO film was deposited by thermal ALD process using STIn-7-7, trimethyl gallium (TMGa), and diethyl zinc (DEZ) precursors. O_3 was used as a reactant. The deposited film characteristics were evaluated using glancing incidence X-ray diffraction, atomic force microscope, and X-ray fluorescence spectroscopy. The ALD-derived IGZO TFTs with a bottom gate staggered structure were fabricated. The electrical properties of the TFTs were measured using a 4156C precision semiconductor parameter analyzer.

References

[1] M. Cho *et al.*, ACS Appl. Mater. Interfaces, 13, 16628-16640 (2021)

[2] J. C. Garcia et al., J. Appl. Phys., 100, 104103 (2006)

[3] L. Manchanda et al., Microelectron. Eng., 59, 351-359 (2001)

[4] M. Nam *et al.*, Adv. Mater. Interfaces, 11, 11, 2300883(2024)

TF-ThP-21 Suppressing the Interfacial Layer Formation between Metal Electrode and Insulator by Employing Molybdenum Dioxide Electrode, *Jaehyeon Yun, Seungyeon Kim, Chaeyeong Hwang, Woojin Jeon,* Kyung Hee University, Republic of Korea

Semiconductor devices, especially dynamic random-access memory (DRAM), are achieving high-density integration and remarkable technological development continuously. At the forefront of advancement in the DRAM device was the introduction of high dielectric constant (high-*k*) materials, which significantly increased its memory capacity. Especially, since the introduction of ZrO_2 as a high-*k* material, TiN electrode has been widely used as the electrode for DRAM capacitor application, owing to its crystallinity coherent with ZrO_2 [1][2]. However, due to the oxygen scavenging effect of TiN, low-*k* TiO_xN_y interfacial layer is formed between the TiN electrode and oxide. The oxygen scavenging effect generates oxygen vacancies in ZrO_2, leading to increase in leakage current. This is because the leakage current mechanism of ZrO_2 is attributed to the presence of oxygen vacancy [3]. Additionally, meeting the requirement of low leakage current for practical DRAM applications in aggressively scaled devices becomes challenging since the TiN electrode has a low work function (~4.3 eV), which reduces conduction band offset [3]. Therefore, in this work, we investigated suppressing the oxygen scavenging effect of TiN electrode using molybdenum dioxide (MoO_2) electrodes, aiming to reduce the concentration of oxygen vacancy in the ZrO_2 and leakage current.

MoO_2 is proposed as a novel oxide electrode for DRAM capacitor, owing to its high work function and excellent chemical stability [2]. To mitigate the oxygen scavenging effect of TiN and reduce leakage current, we compared TiN and MoO_2 electrodes in ZrO_2-based metal-insulator-metal (MIM) capacitors and analyzed the oxygen vacancy defects and electrical properties. Oxygen vacancy defects in ZrO_2 were investigated through AC nonlinearity in the C/C_0-V_{ac} (where C_0 represents capacitance at zero V_{ac}) [4] and XPS analysis. This revealed a reduction of defect sites induced by oxygen vacancy within ZrO_2 when introducing MoO_2 electrodes. Moreover, it should be noted that the decrease in defect sites induces a reduction in leakage current.

Reference

[1] Hwang C. S., Adv. Electron. Mater., 1, 1400056 (2015).

[2] Kim, Y. W., et al, J. Mater. Chem. C., 10, 12957 (2022).

[3] Jeon W, J. Mater. Res., 35, 775 (2020).

[4] Han, D. H., et al. IEEE Trans. Electron Devices, 68, 5753 (2021).

TF-ThP-22 Controlling the Electrical Properties of ZrO₂ Dielectric Films by Employing Sc₂O₃, *Nam Jihun, LEE Seungwoo, Choi Yoona, Jeong Jonghwan,* Kyunghee University, Republic of Korea; *Oh Hansol,* SK trichem, Republic of Korea; *Kim Hanbyul, Park Yongjoo,* SK Trichem, Republic of Korea; *Jeon Woojin,* Kyunghee University, Republic of Korea

Dynamic random-access memory (DRAM) is extensively employed in various industrial sectors as a prominent semiconductor component. Among them, there is a trend toward scaling down DRAM capacitors with MIM (metal-insulator-metal) structure to achieve high capacitance and low leakage current (<10^{-7}A/cm²) at operating voltage. However, scaling down also resulted in decreased the thickness, thereby reducing the area of capacitor and subsequently decreasing the amount of charge that can be stored. Consequently, high dielectric constant materials such as ZrO₂ and HfO₂ are employed as insulators to mitigate this issue. Hence, the conventional DRAM MIM capacitor commonly employs TiN for both top, bottom electrodes, while utilizing ZrO₂ as the insulator. ZrO₂ exists in three phases: monoclinic, tetragonal, and cubic. Among them, ZrO₂ commonly used in DRAM is manufactured via an atomic layer deposition process and exhibits a high dielectric constant (~40) in its tetragonal phase. However, there are several problems. Crystallized ZrO₂ monolayers exhibit high leakage currents due to carrier conduction paths formed by grain boundaries.[1]

Therefore, in this presentation, we demonstrate the results of employing Sc₂O₃ to improve the electrical properties of ZrO₂ dielectric film. Sc₂O₃ has a high dielectric constant (ε = 13) and a large band gap (Eg=~6 eV). [2] We expect that the wide band gap of Sc₂O₃ will serve as a barrier in the carrier conduction path. Using these experiments, we conducted two experiments via the ALD process. First, we examined the effectiveness of Sc doping into ZrO₂. Second, we precisely inserted a Sc₂O₃ monolayer between ZrO₂ insulating layers to see how it affects the performance of ZrO₂ based MIM capacitor. Moreover, we performed crystal phase analysis and evaluation of electrical properties to investigate the effect of Sc incorporation.

References:

[1] W. Jeon, J. Mater. Res, 35, 7 (2020)

[2] M. Pachecka et. al., AIP Adv.7, 105324 (2017)

TF-ThP-23 Influence of Different Oxygen Sources on the Optical Properties of HfO₂ Films Grown by Atomic Layer Deposition, *Blerina Xherahi,* Community College of Philadelphia, Philadelphia, PA 19130,USA; *Sam Azadi, David Barth, Lucas Barreto,* Singh Center for Nanotechnology, University of Pennsylvania, Philadelphia, PA 19104, USA

Hafnia (HfO₂) stands as a promising option for substituting SiO₂ on transistors due to its high dielectric constant. Furthermore, its high band gap provides transparency over a wide spectral range, which makes it applicable for optical coatings. Hafnia also presents a high index of refraction and excellent thermodynamic stability, and its orthorhombic phase exhibits a ferroelectric response. Among the different HfO₂ fabrication strategies, atomic layer deposition (ALD) is a reliable method for obtaining high-quality conformal hafnia films. Adjusting the process parameters and using different precursors can lead to variations in the resulting film properties. This work evaluates how the deposition temperature and the ALD oxygen source change the hafnia films deposited on Si(100). We use tetrakis(dimethylamido)hafnium (TDMAH) as the metal precursor, and we compare the properties of the films for two distinct oxygen precursors: H₂O and O₃. We measure the deposition rate and index of refraction using ellipsometry and correlate the results with the ALD oxygen source and deposition temperature. The results of this work provide insights for adjusting ALD deposition conditions to tune hafnia properties.

TF-ThP-24 ZnSe as Window Layer for n-CdTe Solar Cells, *Wei Wang, Vasilis Palekis, MD Zahangir, Sheikh Elahi, Chris Ferekides,* USF Tampa

ZnSe as Window Layer for n-CdTe Solar Cells

To overcome the V_OC bottleneck for traditional p-CdTe solar cells, polycrystalline n-type CdTe thin films were used as the absorber layer. Polycrystalline n-type CdTe films were deposited by the elemental vapor transport (EVT) process. The EVT process can be used to deposit CdTe films under Cd- or Te-rich conditions to facilitate extrinsic doping. Indium as n-type dopant is used to increase the CdTe conductivity. A proper p-type partner is critical to form a p-n junction with the n-CdTe absorber. A ZnSe layer was used as the p-type partner of n-CdTe solar cells. The device structure includes Glass/ITO/CdS/n-CdTe/p-ZnSe:Cu/ITO. The ZnSe layer was deposited by RF sputtering followed by the deposition of a thin Cu layer. This work investigated the effect of ZnSe as a window layer for n-CdTe solar cell, specifically: (1) the substrate temperature during ZnSe deposition; (2) Cu thickness. In addition, the effect of ZnSe as an interfacial layer for n-CdTe/p-ZnTe solar cell was studied as well. The device structures were characterized by current-voltage (J-V), spectral response (SR), and capacitance-voltage (C-V) measurements.

ZnSe thin film as an interfacial layer for n-CdTe/p-ZnTe devices causes a "kink" in the J-V curve, which is due to the large valence band offset at CdTe/ZnSe. Two substrate temperatures of depositing ZnSe thin films were studied (i.e., 250℃ and 350℃), when it was used as p-type partner of n-CdTe solar cell. The devices where the ZnSe films was deposited at 350℃ showed higher carrier collection from the SR data. Cu layers with thicknesses of 5Å and 15Å were deposited after ZnSe. Devices with larger amount of Cu exhibit lower carrier collection resulting in lower device performance.

TF-ThP-25 Understanding the Surface Chemistry of Tin Halide Perovskite Thin Films, *Mirko Prato, Antonella Treglia, Isabella Poli, Annamaria Petrozza,* Istituto Italiano di Tecnologia, Italy

Tin halide perovskites (THP - general formula: ASnX₃, A: Cs⁺, MA = CH₃NH₃⁺, FA = NH₂CHNH₂⁺; X: I⁻, Br⁻, Cl⁻) have emerged as promising alternatives to toxic lead perovskites in next-generation photovoltaics.

One of the overwhelming obstacles to improving device performance is the high carrier concentration originating from Sn vacancies, resulting in self p-doping and affecting the optoelectronic properties of the material. Simultaneously, the facile oxidation of Sn²⁺ to Sn⁴⁺ further contributes to increasing the p-doping in the bulk and non-radiative recombination centers on the surface.

One effective approach to reduce the presence of oxidized species within the material is to add reducing agents directly within the precursor solution in the form of additives. The most used and effective is SnF₂, which promotes a slower crystallization and improved film quality and effectively limits the self-p doping effect.

While the oxidation of Sn perovskites and its suppression are frequently discussed in the literature, the mechanisms involved and the role of SnF₂ in protecting the film against oxidation are still uncertain and under debate. We therefore investigated the role of tin fluoride in defining the complex surface chemistry of tin halide perovskite thin films, prepared via solution processing. We show that oxygen is found on the surface of tin perovskite thin films even if never exposed to ambient air; however, the use of SnF₂ in the precursors solution strongly affects the chemical nature of the found species. Indeed, oxygen primarily binds to tin in the form of SnO₂ only when SnF₂ is added to the precursor solution, while it is mainly due to adventitious species when SnF₂ is not used. We therefore highlight that the presence of a predominant single chemical state in the XPS Sn core level does not necessarily correspond only to Sn²⁺ species in the perovskite form but could also indicate the formation of superficial SnO₂. Finally, we show that SnF₂ does not help in avoiding nor slowing down the degradation of the perovskite film when exposed to ambient air and that oxidation occurs on the whole-grain surface. These results provide insightful guidance toward understanding oxidation in tin halide perovskites and elucidating its detrimental effect on material's properties.

TF-ThP-27 Dipole Engineering at the HfO₂/Ni Electrode Interface Using a NiOₓ Interfacial Layer, *Hansub Yoon, Keonuk Lee, Taemin Lee, Cheol Seong Hwang,* Seoul National University, South Korea

Since replacing SiO₂ to enhance transistor performance, HfO₂ has been extensively used as the dielectric layer in modern metal-oxide-semiconductor field effect transistors (MOSFETs). Unlike MOSFET with SiO₂ gate insulator (GI), where threshold voltage (V_th) control was achieved by adjusting the doping concentration of the Poly-Si gate, HfO₂-based MOSFETs have adopted metal gates to improve performance by increasing gate capacitance and preventing dopant penetration into GI.[1] For Vth control in metal-gate transistors, dipole engineering techniques have been employed. While dipole engineering offers better stability than other control methods,[2] it introduces process complexity by requiring the additional deposition of La₂O₃ for n-type and Al₂O₃ for p-type MOSFETs.[3] Such an added complexity was manageable in Fin FET (FinFET) structures. However, with the advent and adoption of gate-all-around (GAA) structures, additional stacked layers between the narrow channel nano-sheets have become a significant processing burden. This work explores alternatives to control V_th without relying on separate dipole layers to address this challenge, utilizing the NiOₓ layer, formed at the HfO₂/Ni electrode interface, as a dipole layer to regulate V_th. This approach aims to

simplify the process while maintaining effective V_{th} control, potentially reducing the overall processing complexity in GAA structures. By adjusting the annealing temperature in metal oxide semiconductor capacitor (MOSCAP) structures, the flatband voltage (V_{FB}), a parameter closely related to V_{th}, can be finely tuned. Experimental evidence suggests that this phenomenon is likely due to differences in the formation of the NiO_x layer. These findings indicate a promising approach to V_{th} control that could reduce the processing burden in semiconductor fabrication.References[1] Liu, Chun-Li, et al. "Theoretical and experimental investigation of boron diffusion in polycrystalline HfO_2 films." Appl. Phys. Lett. 81.8 (2002): 1441-1443. [2] Yoshimoto, H., et al. "Analysis of statistical variation in NBTI degradation of HfO_2/SiO_2 FETs." 2010 IEEE International Reliability Physics Symposium. IEEE, 2010.[3] Koji Kita et al., "Origin of electric dipoles formed at high-k/SiO_2 interface," Appl. Phys. Lett. 94, 132902 (2009)

TF-ThP-28 Improvement of Bias Temperature Instability in HfO2 Gate Insulator Film Through UV Treatment and Oxygen Annealing, *Taemin Park,* Seoul National University, South Korea

Bias temperature instability (BTI) is a degradation model where trapped charges within the dielectric layer lead to shifts in the threshold voltage (V_{th}) of a metal-oxide-semiconductor field effect transistors (MOSFETs). With the replacement of SiO_2 by high-k HfO_2, BTI has become a more significant reliability concern due to the higher defect state density in HfO_2 compared to SiO_2. Furthermore, as device scaling continues, the reduced dielectric thickness increases the electric field within the dielectric and the impact of hydrogen diffusion, exacerbating BTI characteristics. Therefore, understanding the BTI mechanism in HfO_2 and controlling defect states to suppress BTI degradation is crucial for high device reliability. HfO_2 gate dielectric films contain many defects originating from hydrogen and nitrogen. Hydrogen atoms within the film can escape under specific stresses, leading to the generation of positive charges,[1] while nitrogen atoms at the semiconductor-oxide interface can lower the activation energy, accelerating BTI degradation.[2] This study proposes ultra-violet (UV) photon treatment and oxygen annealing to control defect density caused by nitrogen and hydrogen defects in HfO_2 films. Initially, UV irradiation is applied to the HfO_2 film to break the hydrogen and nitrogen bonds attached to the dangling bonds within the film.[3] Subsequent oxygen annealing alters the types of atoms attaching to the dangling bonds, allowing for the control of nitrogen and hydrogen defect density within the film. Ultimately, controlling defect density aims to improve the BTI characteristics of HfO_2 films and enhance the reliability of semiconductor devices.References[1] Alam, Muhammad Ashraful, and Souvik Mahapatra. "A comprehensive model of PMOS NBTI degradation." Microelectronics Reliability 45.1 (2005): 71-81.[2] Singh, Vikram, R. Karthik, and Prem Kumar. "Study of Bias-Temperature Instability in HfO_2 sputtered Thin Films by Post Nitrogen Annealing for the Advanced CMOS Technology." Materials Today: Proceedings 4.8 (2017): 9224-9229.[3] Kim, Jaemin, et al. "Analysis of HfO_2 charge trapping layer characteristics after UV treatment." ECS Journal of Solid State Science and Technology 10.4 (2021): 044003

TF-ThP-29 Enhancement of Ferroelectric Properties of $Hf_{0.5}Zr_{0.5}O_2$ Thin Films through the Electrode Stacking Methods, *JoongChan Shin, HanSol Park, SungJae Shin, SukHyun Lee, JaeHee Song, KyungDo Kim, SeungKyu Ryoo, CheolSeong Hwang,* Seoul National University, South Korea

Ferroelectricity, characterized by spontaneous polarization that an external electric field can reverse, originates from the formation of a non-centrosymmetric crystallographic phase. $Hf_{0.5}Zr_{0.5}O_2$(HZO) thin films are recognized as promising components for next-generation semiconductor applications. Various strategies have been explored to enhance the ferroelectric properties of HZO films, including cation and anion doping and the optimization of process conditions. Particularly, it has been reported that the stress/strain applied to the HZO films significantly impacted the ferroelectric properties of HZO. Therefore, this study aimed to enhance the ferroelectricity of HZO films by controlling the stress/strain applied to the HZO films through the bilayer electrode stacking methods.

Bottom electrodes with relatively low thermal expansion coefficients, such as Tungsten (W) and Hafnium Nitride (HfN), were employed to apply tensile stress to the HZO thin films, thereby improving remanent polarization (P_r) value. TiN is usually employed as the bottom electrode for HZO films to prevent endurance degradation. When using the TiN/W, TiN/HfN bilayer as the bottom electrode, the $2P_r$ value increased by approximately 20~30 % compared to the TiN bottom electrode and demonstrated high reliability.

TF-ThP-30 Bias Stress Instability of InGaZnO Thin Film Transistors for Stackable 1capacitor-1transistor Dynamic Random Access Memory, *Hyobin Park,* Seoul National University, Republic of Korea

Recently, the demand for high-performance, low-power memory has increased with the growth of artificial intelligence and deep learning technology. The dynamic random access memory (DRAM) industry maintains the scaling trend through cell size shrink technologies to satisfy this demand. However, the two-dimensional scaling of the DRAM below 10 nm design rule is expected to be challenging due to many technical and performance challenges. Thus, it is required to adopt a stacked structure that can overcome these structural limitations. Amorphous InGaZnO (a-IGZO) has emerged as a feasible channel material for stackable DRAM due to its very low off-current and higher electron mobility compared to polycrystalline silicon.

Previous studies have mainly reported the improvement of the electrical characteristics of a-IGZO channel as a single thin film transistor (TFT). However, few reports have been made on a-IGZO TFTs' output current, threshold voltage (V_{th}) variation, and instability related to charging operation when TFT is directly connected to the capacitor.

This study implemented a planar 1T-1C DRAM structure to simulate the write/read operation of the conventional DRAM and investigated the electrical characteristics of a-IGZO TFTs during the DRAM operation process, where the TFTs have bottom-gate staggered structure using the sputtered a-IGZO channel. The TFT adopted a 20 nm-thick bottom gate with different metals and a 10 nm-thick high dielectric constant (k) dielectric film (HfO_2 and Al_2O_3) as the gate insulator. The drain electrode of the transistor was connected to the top electrode of the capacitor, and the gate insulator thin film of the transistor shared the dielectric film of the capacitor. Al_2O_3 was selected as the passivation layer, which also contributed to achieving the controllability of V_{th}[1] and stability of V_{th} under bias stress.

This work investigates whether these improvements of a-IGZO TFTs have comparable impacts under bias stress conditions caused by the charge stored in the capacitor of 1T-1C DRAM application. The findings of this study will contribute to the understanding of a-IGZO as an alternative channel material for the next DRAM transistor.

References

[1] Rha et al. "Variation in the threshold voltage of amorphous-$In_2Ga_2ZnO_7$ thin-film transistors by ultrathin Al_2O_3 passivation layer." Journal of Vacuum Science Technology B, 31, 061205 (2013).

TF-ThP-31 Growth of $BaTiO_3$ Thin Films Grown by Atomic Layer Deposition using $Ba(^iPr_3Cp)_2$ and $Ti(Me_5Cp)(OMe)_3$ Precursor on Ru Substrate, *Chansoo Kwak,* Seoul National University, South Korea

As dynamic random access memory (DRAM) capacitors continue to undergo aggressive scaling, increasing capacitance is paramount for securing sufficient sensing margins[1]. The $ZrO_2/Al_2O_3/ZrO_2$ (ZAZ) dielectric thin film prevalent in DRAM is favored for its low leakage current. However, its low dielectric constant presents a significant limitation, prompting extensive research into higher-k (dielectric constant) materials. Among these, $BaTiO_3$ (BTO) is a perovskite compound with a high k value because of the softening of phonon associated with the titanium ion motion in the crystal lattice, making the BTO highly promising for future DRAM capacitors.

BTO has traditionally been deposited using physical and chemical vapor deposition techniques, which lack sufficient conformality over the extreme three-dimensional DRAM capacitor structure. In contrast, atomic layer deposition (ALD) offers a significant advantage through its self-limiting mechanism at the atomic level, enabling the deposition of BTO thin films with excellent step coverage. This characteristic makes ALD particularly well-suited for producing BTO films that can be effectively utilized in smaller dimensions and complex three-dimensional structures.

This research examined the optimal ALD conditions for the BTO film growth on Ru substrate using the $Ba(^iPr_3Cp)_2$ and $Ti(Me_5Cp)(OMe)_3$ as the Ba- and Ti-precursors, respectively. Ru substrate was also employed to mitigate the susceptibility of high-k materials to leakage current because of its high work function. Also, this study examines the degree of crystallization according to the rapid thermal annealing (RTA) conditions. A comprehensive analysis of the dielectric constant and leakage current characteristics of the BTO thin films was conducted to evaluate their viability as dielectric materials for DRAM capacitors.

References

[1] S. W. Lee et al. "Atomic layer deposition of SrTiO3 thin films with highly enhanced growth rate for ultrahigh density capacitors." Chemistry of Materials 23.8 (2011): 2227-2236.

Undergraduate Poster Session
Room Central Hall - Session UN-ThP

Undergraduate Poster Session

UN-ThP-1 Using Fourier Smoothing to Calculate D-Parameter for Carbonaceous Samples, *Kristopher Wright, Matthew Linford,* Brigham Young University

Carbon samples reveal much about their properties through surface analysis. X-ray photoelectron spectroscopy (XPS) has proven itself a reliable approach to analyzing surfaces of all material, including carbon samples. We can use the carbon Auger peak as an important tool for characterizing the ratio of sp2 to sp3 hybridization of carbon samples. This is accomplished through determining the D-parameter, which is related to the energy difference between the first derivative minima & maxima, and which is directly proportional to the sp2:sp3 ratio of the sample. The D-parameter has many important uses, such as determining graphite versus diamond composition in a material. In the past, the characteristically noisy auger peak has made the D-parameter difficult to determine. In this poster, will be looking at various carbon samples ranging from sp3 carbon (such as diamond), polymers, and sp2 carbon samples (like HOPG) using a new approach to determining the derivative of the Auger peak via a Gauss-Hermite Filter. The Gauss-Hermite Filter convolves the data with a transfer function by utilizing Fourier analysis to break down XPS data into its components, then multiplying these by the reciprocal of the transfer function. The result is a minimalization of high frequency noise while preserving the lower frequency components that are characteristic of the signal.

UN-ThP-2 Calcium Lanthanum Sulfide - An Investigation Via X-Ray Photoelectron Spectroscopy, *Brian Butkus,* **Taylor Cook**, *Alexandros Kostogiannes, Andrew Cooper, Andrew Howe, Romain Gaume, Kathleen A. Richardson, Parag Banerjee,* University of Central Florida

Calcium lanthanum sulfides (CLS) are crucial in applications requiring high optical transmissivity in the long-wave IR regime. These ternary sulfides, forming solid solutions of CaS and La_2S_3 in a cubic Th_3P_4 phase, exhibit varying cationic vacancies depending on the Ca:La ratio to maintain stoichiometric balance and charge neutrality.

Using X-ray photoelectron spectroscopy (XPS), we analyzed the chemical and bonding states of hot pressed CLS ceramics. Our findings confirm the stoichiometry aligns with the expected Ca:La ~ 10:90 composition, revealing an intrinsic ≥10 at% oxygen impurity even under inert conditions. This suggests oxygen substitution for sulfur, particularly bonding with La, which may influence the material's optical properties as experimentally seen in the lower IR transmission of CLS and development of absorption bands in the long-wave IR regime. The interpretation and conclusions are made from data of over 30 CLS samples with varying compositions. A multivariate analysis of the composition also support the hypothesis that oxygen substitutes for sulfur in the CLS lattice.

This study highlights the persistent challenge of oxygen incorporation in CLS and suggests potential processing modifications to enhance material purity and performance.

UN-ThP-3 Avoiding Common Errors in X-ray Photoelectron Spectroscopy Data Collection and Analysis, *Braxton Kulbacki, Joshua Pinder,* Brigham Young University; *George Major,* Texas Instruments; *Matthew Linford,* Brigham Young University

X-ray photoelectron spectroscopy (XPS) is the most popular surface characterization technique because of its ability to determine the composition and chemical state of the first 5-10 nm of various materials. Although widely used, correct collection procedure, technique and reporting are not widely understood. Experts in other scientific fields use XPS, but are often not experts in XPS as well, so technical errors such as incorrect data interpretation and presentation, incorrect reporting of instrumental parameters, unjustified conclusions and unjustified peak fittings are common. Publications with these errors have made experimental reproduction difficult and have caused a reproducibility crisis. The following presentation is intended to bring awareness to common errors observed. Some common examples include: data collection, peak fitting errors, background errors, data presentation errors and data reporting errors.

UN-ThP-4 Deposition of Cobalt-Doped Zinc Oxide Nanocrystals via Successive Ionic Layer Adsorption and Reaction, *Luis Tomar, Kailong Ye, Shaohua Xie,* University of Central Florida; *Matthew Chang, Jacob Baillie,* University of Washington; *Taylor Currie, Fudong Liu, Titel Jurca,* University of Central Florida; *Daniel Gamelin,* University of Washington; *Parag Banerjee,* University of Central Florida

Transition metal doped semiconductors are highly desired due to new functionalities enabled by the dopants. For example, Co-doped ZnO has been shown to be a magnetic quantum dot [1]. These materials are typically synthesized in the form of nanoparticles [1], and the ability to synthesize these materials as high-quality thin film is desirable for their applications in optics and electronics. Successive ionic layer adsorption and reaction (SILAR) provides a simple approach to create transition metal doped semiconductors, while providing control over the film thickness and dopant concentration. SILAR works via a series of liquid-phase ionic reactions that are self-limiting, similar to atomic layer deposition [2].

This work aims to synthesize Co-doped ZnO films using a SILAR process. The approach involves adapting the mechanism of solution-based nanoparticle process into a SILAR process. While the solution process involves the rigorous mixing of the precursors to precipitate Co-ZnO nanoparticles, the SILAR process discretizes the use of these compounds into separate dip-coating steps. Thus, by simply controlling the solution concentration and number of cycles, films of various thickness are formed. The films are evaluated using ultraviolet-visible spectroscopy (UV-Vis), scanning electron microscopy, energy dispersive x-ray spectroscopy, and x-ray photoelectron spectroscopy to confirm the successful doping of the isovalent Co^{2+} in the ZnO lattice.

References:

[1] D. A. Schwartz, N. S. Norberg, Q. P. Nguyen, J. M. Parker, and D. R. Gamelin, "Magnetic Quantum Dots: Synthesis, Spectroscopy, and Magnetism of Co2+- and Ni2+-Doped ZnO Nanocrystals," *Journal of the American Chemical Society*, vol. 125, no. 43, pp. 13205–13218, Oct. 2003, doi: https://doi.org/10.1021/ja036811v.

[2] Samantha Prabath Ratnayake, J. Ren, E. Colusso, M. Guglielmi, A. Martucci, and Enrico Della Gaspera, "SILAR Deposition of Metal Oxide Nanostructured Films," *Small*, vol. 17, no. 49, Jul. 2021, doi: https://doi.org/10.1002/smll.202101666.

UN-ThP-5 Assessing and Recommending Standards to Improve Reproducibility in Thin Film Analysis; a Multi-Faceted Approach, *Jacob Crossman, Matthew Linford, Joshua Pinder,* Brigham Young University

Reproducibility is a key component of the scientific method requiring data collection to be repeatable by oneself and/or others. Also known as replication, reproducibility (or rather, a lack thereof) has established itself as a growing crisis in the scientific community—many studies are being published without providing sufficient information for an outside source to replicate and corroborate findings, thereby reducing confidence in those studies. The variety of scientific fields requiring vacuum technology, including thin film research, are not immune to the reproducibility crisis. Because thin film sciences are crucial to advancements in solar array, computer microchip, and LED technologies, it stands to reason that the scientific community should expect a high degree of transparency and reproducibility from this research. Techniques such as thin film synthesis using ALD or CVD and analysis via methods such as XPS, LEIS, or SE, must be reproducible both internally and externally. This means a researcher should be able to internally reproduce a material or measurement multiple times consistently. Additionally, should that researcher choose to publish his or her findings, he or she should provide sufficient information for an external researcher to reproduce those findings consistently and accurately. This system of reproducibility helps ensure the integrity of research. In this presentation, we pose recommendations and reminders to make sure reproducibility remains central to the research process. To ensure internal reproducibility, we recommend a thorough recording of procedures and tests for consistency. Creatively deploying physical and procedural measures, such as fitment jigs and SOPs are paramount to ensuring internal reproducibility. Externally, we suggest clarity in instrument parameter reporting (such as the tables found in certain SSS articles) and clear, complete supporting information. Any paper published should contain all the information necessary for someone else to perform the same experiment. With recommendations such as these in mind, researchers will

continue to prioritize reproducibility and increase the transparency of their research to combat the replication crisis.

UN-ThP-6 Enhancing the Selectivity of Acetaldehyde Formation Using a Copper-based Model Catalyst, *Joseph Loiselet, Ashleigh Baber,* James Madison University

Acetaldehyde is a common intermediate in many industrial chemical syntheses. Current methods of acetaldehyde formation are inefficient and wasteful, leading to low product yields and unwanted by-products. In order to improve acetaldehyde yield and minimize other products, the dry dehydrogenation and dehydration of ethanol was observed using temperature programmed desorption (TPD). These reactions occurred on flat, roughened, and oxidized Cu(111) surfaces under ultrahigh vacuum (UHV) conditions. The reaction of ethanol over each surface was studied, and the oxidized Cu(111) most readily formed acetaldehyde and hydrogen at 350 K. A second reaction pathway formed ethylene and water at 350 K. The selectivity for acetaldehyde production was maintained over 80% throughout consecutive TPDs, yet the yield decreased continuously as the surface became less oxidized. Future experiments will study the reactivity of a partially oxidized Cu(111) sample using UHV-TPD.

UN-ThP-7 Optimizing XPS Analysis with Maximum Entropy for Determination of the D Parameter, *Garrett Lewis,* Brigham Young University

In spectroscopy, the aim is to gather insights through the examination of spectra that are ideally clear of distortions and free from noise. The Maximum Entropy filter is another technique to de-noise XPS that works by preserving both high and low-order coefficients. It achieves this by utilizing the trends established by the low-order Fourier coefficients and projecting them into the white noise region (high-order coefficients). X-Ray Photoelectron Spectroscopy (XPS) is a surface analytical technique used to survey the top 5-10 nm of a sample. In sample analysis, XPS unveils the carbon Auger peak, a product of secondary electron emission upon ejection of a core-level electron from a carbon atom, subsequently filled by an electron from a higher energy level. The carbon Auger peak is pivotal in assessing the D-parameter, a ratio between sp^2 and sp^3 hybridization in carbonaceous materials such as diamond and highly oriented pyrolytic graphite (HOPG). By utilizing the maximum entropy filter, we can demonstrate its effectiveness in enhancing data quality through smoothing, thereby aiding in the determination of the D-parameter via the carbon Auger peak. This improved understanding of material characteristics enhances their potential applications.

UN-ThP-8 Copper by X-Ray Photoelectron Spectroscopy (XPS) at Pass Energies from 10 – 200 eV, *Annika Dean, Samira Jafari, Matthew Linford,* Brigham Young University

X-ray photoelectron spectroscopy (XPS) is an important analytical technique that provides chemical information about surfaces. XPS analyses of metallic copper were performed at different pass energies, ranging from 10 to 200 eV. The pass energy determines the kinetic energy at which the emitted photoelectrons pass through an analyzer and enter the detector. The pass energy determines the energy resolution of the experiment. While survey scans are generally taken at high pass energies, narrow scans are taken at lower pass energies to achieve a higher resolution. Higher resolution can aid in distinguishing between peaks that are close together, such as spin-orbit split peaks, or for identifying fine features in spectra. As expected, lower pass energies result in better resolution but lead to increased noise in spectra. Selecting an appropriate pass energy therefore includes considerations for both the spectral resolution and the desired signal-to-noise ratio.

UN-ThP-9 Structure of Benzyl Isothiocyanate Self-Assembled Monolayers on Au(111)/Mica Surfaces, *Darya Moiny, Lily Tackett, Lindsey Penland, Dmitry Ovchinnikov, Rachael Farber,* University of Kansas

Benzyl isothiocyanate (BITC) is an aromatic thiolate of biological importance and is utilized in biofunctionalization, such as the bio fabrication of nanoparticles encapsulated with BITC as a method of drug delivery. Notably, the coexistence of both the stabilizing pi-pi interactions and destabilizing electron withdrawing cyanide group can influence the packing structure and formation of the SAM of BITC. While BITC can be used to modify Au surfaces for biological applications, there is little known about the molecular packing structure of BITC self-assembled monolayers (SAM) on Au surfaces.

In this work, tapping mode atomic force microscopy (AFM) was used to investigate the relationship between solution concentration and incubation time on the molecular structure of BITC SAMs. After initial characterization of Phasis epitaxial gold, Au(111)/Mica, to determine the structural properties of the Au surface, Au(111) was incubated in a 2 mM ethanolic solution for 24 hours. AFM revealed minimal structural evolution to the Au surface, suggesting that a BITC monolayer did not form. The sample was then placed back into solution for another 41 hours, bringing the total incubation time to 65 hours. Following the prolonged incubation in BITC, a linear pattern was seen across the surface, suggesting the formation of a BITC SAM. To understand the relationship between concentration and BITC SAM formation, the solution concentration was increased by a magnitude of 10. Similar to the 2 mM preparation, there was no noticeable structural evolution following a 24-hour incubation. Incubating the Au substrate for 65 hours in the 20 mM solution did, however, result in the characteristic linear pattern seen for the 0.2 mM sample preparation.After establishing that an incubation of 65 hours was needed to form a uniform BITC SAM, the solution concentration was increased to 0.2 M. Following a 65-hour incubation, a new ring-like pattern was seen across the surface suggesting the formation of a new structure at higher BITC concentrations. Ongoing work is focused on using ultra-sharp AFM tips to investigate SAMs formed following a 65-hour incubation in a 20 mM BITC solution to resolve the exact molecular structure of the BITC SAM. In addition to continued AFM imaging,Future work will focus on imaging the BITC SAMs using ultra-high vacuum scanning tunneling microscopy (UHV-STM) and scanning tunneling spectroscopy (STS) to further investigate the structural and electronic properties of the surface of the SAM at the atomic scale.

UN-ThP-10 Computationally Enhanced Experimental Investigation of Reactivity of Isomeric Butanol on TiO₂/Au(111), *Haley Frankovich, Emily Euler, Lyssa Garber, Ava Galgano, Kendra Letchworth-Weaver, Ashleigh Baber,* James Madison University

Biofuels can be used to reduce global dependence on fossil fuels while contributing to a carbon-neutral cycle. Biobutanol has low volatility and multiple transportation options which make it an attractive alternative fuel. Understanding the fundamental thermal catalysis processes of butanol over heterogeneous model catalysts can aid in the design of more efficient catalysts. To better understand the processes in play, temperature-programmed desorption (TPD), atomic force microscopy (AFM), density functional theory (DFT), and high-performance computing are used to investigate its reaction. This study aimed to examine the reactivity of different isomers of butanol, namely 1-butanol, 2-butanol, and isobutanol, when exposed to a TiO2/Au(111) surface. TPD was used to detect products, with 1-butanol showing little reactivity and elimination products, 2-butanol showing oxidation and elimination, and isobutanol yielding all products. The selectivity of the reaction was not altered during successive desorption experiments, indicating that the model catalyst was stable without reoxidation between experiments. AFM highlighted the morphology of the surface and shows the Au(111) crystal has ~0.13ML and 0.27ML of TiO2 with predominantly 1D wire like nanoparticles. Higher coverages of TiO2 result in more particles distributed across the surface indicating that the reactivity was influenced by butanol proximity to TiO2 nanoparticles rather than differences in size or shape. DFT calculations to investigate energetic trends and provide an atomic-scale understanding of the structure of butanol adsorbed on the surface are ongoing.

UN-ThP-11 Pulsed Laser Deposition of Ruthenium Oxide Thin Films for Electrocatalytic Splitting of Water for Oxygen and Hydrogen Evolution Reactions, *Anansi Coleman, Dhananjay Kumar,* North Carolina A&T State University

Wisdom Akande, Anansi Coleman, Ikenna Chris-Okoro, Sheilah Cherono, Mengxin Liu, and Dhananjay Kumar

North Carolina Agricultural and Technical State University, Greensboro, NC 27411

This presentation reports the synthesis, structural characterization and evaluation of electrocatalytic properties of crystalline ruthenium oxide(RuO2) thin films. The films were grown using Pulsed Laser Deposition technique on a variety of single-crystal substrates, sapphire(Al2O3) and titanium dioxide(TiO2) while varying oxygen pressures from 5mTorr to 50mTorr, and substrate temperatures from 400°C to 700°C. The films were structurally characterized using x-ray diffraction, x-ray photon spectroscopy and scanning electron microscopy. Cyclic-voltammetry and Linear-sweep-voltammetry were also measured and used to evaluate the electrochemical properties during OER, with the aim of providing insights into role crystal structure and surface orientation on the electrochemical properties of the films.

UN-ThP-12 Direct Printing of Oxide Nanoparticles Via Vapor Phase Microreactor Assisted Nanomaterial Deposition (V-MAND) and Its Application, *Isaac Camp, Vinay V. Doddapaneni, Maxfield Dodge, Somayeh Pasebani, Chih-Hung Chang,* Oregon State University

Nanomaterial printing is gaining attention from the many properties nanomaterials are excellent for, such as catalysts, light absorbers/reflectors, and mechanical property modifiers compared to their bulk counter parts. Many traditional methods, such as inkjet printing and aerosol jet printing techniques, are being used to deposit and fabricate functional materials and devices. However, they require solvent dispersion of nanoparticles which can lead to carbon impurities and structural imperfections. Moreover, nanoparticle dispersion inks tend to have limited shelf-life, further limiting their applications. To address these challenges, different solventless and dry printing methods have been developed. Within this work, we developed a vapor phase microreactor assisted nanomaterial deposition (V-MAND) printing technology. This technology uses solventless or solid precursors and generates nanoparticles on-demand, transporting them to the desired surfaces from the print head. Furthermore, this V-MAND printer can be integrated into 3D printers to produce functional composites materials, such as high temperature alloys for aerospace and nuclear applications, and UV-resistant materials for food packaging applications.

UN-ThP-13 Optimizing Plasma Conditions for the Modification of Silk Fibroin Using Small and Large Molecule Precursors, *Bethany Yashkus, Mollie Corbett, Joshua Blechle,* Wilkes University

Silk materials show promise for use in biomedical applications because of their desirable mechanical properties, versatility, and accessibility. Their overall utility is limited, however, as the biological lifetime of silk materials remains uncontrolled. Plasma-enhanced chemical vapor deposition (PECVD) has previously been employed to modify silk films by altering the wettability of the surface. Significant work has been completed to explore the impact of gas composition and plasma conditions on the surface of these modified materials. Critically, the mechanism by which these modifications occur is an ongoing question due to a lack of gas-phase analyses. Here, optical emission spectroscopy (OES) is used to monitor the plasma during silk modification, with the hope of elucidating key reactive species.

Utilizing previously established conditions (Hawker, 2023) of acrylic acid and pentane precursors at 75 mTorr and 65 W revealed no observable spectral differences upon addition of silk films, providing little mechanistic insight. As such, this work will explore an expanded experimental parameter space, including pressure, power and time constraints, to probe for gas-phase reactive hydrocarbon species. Diagnostic calculations, such as relative densities and internal temperatures, will also be employed to further characterize the system. Additionally, small molecule precursor gases (namely N_2 and O_2) will be employed for direct comparison and ease of spectral analysis. Compiling diagnostic data across this expanded parameter space provides an opportunity for unparalleled insight into the mechanisms of silk fibroin surface modification.

UN-ThP-14 Epitaxial Lift-Off of Barium Hexaferrite Membranes, *Clara Jackson Jackson,* Clark Atlanta University; *Evan Li, Anna Park, Darrell Schlom,* Cornell University

Freestanding barium hexaferrite ($BaFe_{12}O_{19}$ or BaM) membranes are valuable for various technological applications, and their fabrication via Molecular-Beam Epitaxy (MBE) involves overcoming significant challenges, particularly in the epitaxial lift-off process. Initially, $\alpha\text{-}Fe_2O_3$ was chosen as the sacrificial layer for membrane detachment due to its compatibility with the BaM crystal structure. However, $\alpha\text{-}Fe_2O_3$ proved problematic due to its slow etching rate, which led to inefficient lift-off even with strong acids, jeopardizing membrane quality. To address this, the study explored alternative materials and found that ZnO, with a similar crystal structure and a much faster dissolution rate, significantly enhanced the efficiency of the lift-off process. This transition to ZnO not only improved process efficiency but also underscored the critical role of material selection in optimizing epitaxial lift-off techniques. This work advances the fabrication methods for freestanding BaM membranes and highlights the practical application of material science principles in overcoming fabrication challenges.

UN-ThP-15 Exploring the Epoxidation of Isoprene on Copper-Based Catalysts, *James Whitted,* James Madison University; *Mollie Corbett,* Wilkes University; *Ashleigh Baber,* James Madison University

Isoprene (C_5H_8) is a common greenhouse gas that forms the infamous haze observed over the Blue Ridge Mountains. It contributes to a large portion of the planet's ozone formation, and therefore finding alternative value-added uses for isoprene is critical. Isoprene is a diene, and due to its molecular structure, has both allylic hydrogen and non-allylic hydrogen sides. It is therefore a model reactant molecule for studying selective epoxidation. Atomic oxygen on Cu(111) is known to enhance the epoxidation of propylene, which contains allylic hydrogens, while Ag(110) and Ag(111) with atomic oxygen encourages the epoxidation of ethylene, which does not have allylic hydrogens. This molecule is ideal to study epoxidation reactivity on a AgCu near surface alloy (NSA), specifically for its allylic hydrogen and non-allylic hydrogen sides, which mimic propylene and ethylene. Olefins have several different reaction pathways that can be isolated through specific reaction schemes. The major reaction pathway for isoprene on oxidized Cu(111) is combustion. Creating an NSA comprised of Ag atoms on Cu(111) is expected to produce a favorable surface to form an epoxide from isoprene, while also limiting the unwanted combustion pathway. Ultra-high vacuum temperature programmed desorption (UHV-TPD) spectra were gathered on clean and partially oxidized Cu(111) and Ag/Cu(111) after dosing isoprene. As the amount of oxygen dosed on Cu(111) increased, carbon dioxide yield also increased, indicating that the combustion pathway was in full effect. To minimize overoxidation of isoprene to CO_2 under UHV, Ag was deposited on Cu(111) via physical vapor deposition. Auger electron spectroscopy was used to determine Ag coverages on the surface, post-deposition. TPD results indicate that the combustion pathway was deterred in the presence of 1 ML of Ag/Cu. Future work will focus on potential coexisting products and the molecular geometry of isoprene adsorption and packing using scanning tunneling microscopy.

UN-ThP-16 Characterizing Next-Generation SRF Materials for Accelerator Infrastructure, *Helena Lew-Kiedrowska, Van Do, Sarah Willson,* University of Chicago; *Chi Wang,* National Cheng Kung University, Taiwan; *Liana Shpani, Sadie Seddon-Stettler, Matthias Liepe,* Cornell University; *Steven Sibener,* University of Chicago

Superconducting radiofrequency (SRF) cavities are used to accelerate beams of charged particles in particle accelerators. The standard material for SRF cavities is Nb because it is the highest temperature elemental superconductor with a critical temperature (T_c) of 9.7 K.SRF performance can be further improved by growing a higher T_c metal alloy onto the Nb surface such as Nb_3Sn (T_c = 18.3 K) or by preventing the growth of a native oxide layer on Nb with capping layers of an inert metal such as Au. Previous studies have shown that anodization improves Sn incorporation for Nb_3Sn growth, and that Au capping achieves oxide passivation for Nb. In this work, we characterize anodized samples of Nb and electroplated Au on Nb samples using scanning electron microscopy and atomic force microscopy. Our results demonstrate how the underlying Nb substrate can affect metal growth on the surface: Au growth showed preferential binding in surface defects, and anodizing the Nb sample increased its surface roughness, which may explain increased Sn incorporation.

UN-ThP-17 Mitigating Hydrophobic Recovery of Oxygen Plasma-Treated PEEK, *Nicholas Shows, Mikko Mowatt, Morgan Hawker,* California State University, Fresno

Polyether ether ketone (PEEK) is a chemically inert and wear resistant thermoplastic polymer which exhibits similar elasticity and tensile properties to human cortical bone. These characteristics demonstrate why PEEK is used in orthopedic surgical procedures including cranioplasties, spinal cages, and hip arthroplasties. Despite favorable mechanical properties, PEEK is hydrophobic. Surface hydrophobicity decreases PEEK's cytocompatibility, and therefore, osseointegration. Previous research demonstrates that hydrophilic surfaces exhibit greater cytocompatibility, resulting in more favorable osseointegration. Greater surface hydrophilicity can be achieved using radio frequency (RF) oxygen plasma treatments. PEEK films treated with RF oxygen plasma exhibit a contact angle nearly 50° lower than that of native PEEK. After oxygen plasma-modification, PEEK returns to its native hydrophobic state over time through hydrophobic recovery. A hydrophobic PEEK surface will not contain osseointegrate as well as the oxygen plasma-treated PEEK immediately after plasma treatment. Prior research suggests storing various plasma-treated PEEK films in water after treatment can lessen the extent of hydrophobic recovery. Oxygen plasma-treated PEEK exhibits optimized surface hydrophilicity immediately after treatment. Strategies to mitigate the

hydrophobic recovery of RF oxygen plasma-treated PEEK remain unexplored.

This study examined the hydrophobic recovery of RF oxygen plasma-treated PEEK when stored in aqueous and ambient conditions. PEEK sheets were cut into individual films and sonicated to ensure a clean surface. PEEK films were subjected to plasma treatment in an inductively-coupled plasma reactor using an oxygen gas precursor. Optimized plasma parameters including power, pressure, and treatment times were selected based on previous literature. Plasma-modified PEEK films and untreated controls were then aged up to 30 days in ambient or aqueous conditions. Contact angle goniometry was used to analyze surface wettability of treated PEEK and untreated PEEK controls. RF oxygen plasma-treated PEEK exhibited an increasing contact angle over time in ambient conditions, indicating hydrophobic recovery occurred. RF oxygen plasma-treated PEEK did not return to its hydrophobic state when aged in aqueous conditions. Modification methods which lessen hydrophobic recovery have potential to improve the usability of PEEK in orthopedic surgical applications by improving its osseointegration.

UN-ThP-19 Deconvoluting Information-Rich Ga(I) X-Ray Adsorption Near-Edge Spectroscopy Features from First Principles, *Grace Miller,* Washington State University*; Cassie Huang,* University of California at Los Angeles*; Susannah Scott,* University of California Santa Barbara*; Jean-Sabin McEwen,* Washington State University

Due to the high demand of propylene, it is appealing to look at replacing Pt- and Cu-based catalysts for propane dehydrogenation. In this regard, an attractive alternative are Ga-based compounds. X-ray Adsorption Near-Edge Spectroscopy (XANES) contains information about the coordination environment and the oxidation state of Ga under reaction conditions. In our previous work, we deconvoluted the experimental features of Ga(III) compounds [1]. Since Ga(I) and Ga(III) compounds are both involved in propane dehydrogenation, we benchmark the spectral features of Ga(I) compounds in this work. We compare the calculations derived from structures based on *Li et al.* [2] to three additional Ga(I) structures (Ga(Si(SiMe$_3$)$_3$)$_4$,(Ga(C(SiMe$_3$)$_3$)$_4$, ((Ga$_8$Br$_8$)$_6$NEt) to further deconvolute the XANES features. Based on the literature, the XANES features with higher intensities correspond to Ga(I) oxidation states while the XANES features with lower intensities correspond to Ga(III) oxidation states. Using the CASTEP code with a Perdew-Berkman Erzenhoff (PBE) functional, we simulate the XANES from first principles. We further compare the Ga(III) features of our compounds to what has been identified previously in the literature [1]. Interestingly, two bulk Ga(I) structures did not have the high intensity feature as was identified in the other Ga(I) compounds. The study is ongoing where we are quantifying interaction energy between Ga(I) cations within these structures, where our initial results indicate that the interaction energy between them is attractive.

UN-ThP-20 Characterization and Oxidation of Curved Metal Surfaces, *Allison Kerr, Dan Killelea,* Loyola University Chicago

Due to the importance of oxide surfaces in heterogeneously catalyzed oxidation reactions, it is necessary to gain a fundamental understanding and behavior of oxygen on transition metal surfaces. Additionally, the atomic arrangement of the metal surface plays an important role in the behavior of the oxygen on the surface, which provides a need to study high defect density surfaces that are more akin to industrial catalysts. The research presented herein utilizes a curved rhodium crystal c-Rh(111) with two different well-defined defects on either side to conduct a systematic study of the influence of defect geometry on the kinetics and dynamics of different oxygen species present on the surface. Scanning tunneling microscopy (STM), low energy electron diffraction (LEED), temperature programmed desorption (TPD), and Meitner-Auger electron spectroscopy (MAES) will be used to look at the surface on an atomic scale and to observe what chemical species are on the surface after introducing oxygen into the vacuum environment.

Vacuum Technology
Room Central Hall - Session VT-ThP

Vacuum Technology Poster Session

VT-ThP-1 Surface Characterization and Vacuum Performance of AISI 1020 Low-Carbon Steel for High-Performance Vacuum Systems, *Aiman Al-Allaq,* Old Dominion University*; Md Abdullah Mamun, Matthew Poelker,* Thomas Jefferson National Accelerator Facility*; Abdelmageed Elmustafa,* Old Dominion University

The Cosmic Explorer, a next-generation gravitational wave observatory, will be very large with evacuated interferometer arms ten times longer than Advanced LIGO operating today, 40 km each. Consideration is being given to building this extremely large vacuum system using comparatively inexpensive low-carbon steel, commonly used today for natural gas delivery. But besides reduced cost, low-carbon steel offers a vacuum advantage, too. Low-carbon steel has a much lower hydrogen outgassing rate compared to stainless steel. In addition, studies performed worldwide within the gravitational wave observatory community suggest low carbon steel – particularly with a magnetite surface coating – may provide a more rapid pump down, possibly reaching acceptable vacuum conditions with only an 80 °C heat treatment. At Jefferson Lab, we plan to construct a new spin-polarized electron source using low-carbon steel, which we hope operates at a much lower pressure than our photoguns built using stainless steel. In support of this objective, we are performing studies related to water outgassing, pump down times, and ultimate pressure achieved using low-carbon steel. Some of these studies seek to understand if material surface transformations occur following different heating protocols. Small coupons made of AISI 1020 low-carbon steel were characterized using SEM, AFM, XRD, and EDS after various heat treatments. The results showed minimal oxidation up to 150 ˚C, with layered magnetite and hematite developing at higher temperatures. A steam-treated sample exhibited vertical grain orientation, while thermal oxidation favored lateral oxide colony formation. Tests on magnetite-coated and bare low-carbon steel chambers demonstrated that the magnetite-coated chamber consistently achieved lower pump down pressure and lower throughput water outgassing rates, supporting the idea that magnetite coating can improve the vacuum performance of low-carbon steel. Ongoing research at Jefferson Lab focuses on characterizing bare and magnetite-coated low-carbon steel chambers to explore their feasibility in next-generation vacuum systems, such as those required for the Cosmic Explorer project, and for spin-polarized electron guns where improved vacuum will help sustain reliable beam delivery.

VT-ThP-4 Developing an Extreme Environment Vacuum System for ITER's Ion Cyclotron Heating Antenna, *John Michael Clark, **Charles Smith III**,* Oak Ridge National Laboratory

The ITER project is designed with the goal of demonstrating the feasibility of fusion energy, and to advance the technological understanding of fusion for future commercial reactors.In order to achieve a "burning plasma", various heating methods, such as Neutral Beam, Electron Cyclotron Heating, and Ion Cyclotron Heating (ICH) are employed in the ITER fusion device. Each of these technologies require high vacuum environments to ensure safe and efficient operation; however,ICH, in particular, poses unique issues in developing a vacuum system.

The proximity of the ICH antenna, and associated vacuum pumping system of the ICH Removable Vacuum Transmission Line (RVTL) Rear Windows,to the ITER Tokamak necessitates a vacuum system that is able to withstand dynamic magnetic fields in excess of 500 mT and activation of up to 10^4Gy. Vacuum technology and hardware layouts that have become common across ITER vacuum systems are not operablein this extreme environment. To develop a functional vacuum system for the ITER ICH antenna's RVTL Rear Windows, it must be designed with hardware and an arrangement that tolerates the environment and meets pressure requirements without significant increase inevacuation time.

VT-ThP-5 Secondary Electron Yield Measurements of Vacuum Insulators, *Minh Pham, Ronald Goeke,* Sandia National Laboratories

Ceramics are commonly used for high voltage insulation in vacuum systems. The vulnerability of its high voltage standoff is a flashover of the insulator surface. The principal mechanism for this breakdown is a secondary electron emission (SEE) avalanche. In this process, some electrons striking the insulator surface produce more electrons which strike the surface again producing additional electrons. This process continues until a flashover of the insulator surface occurs and the high voltage standoff is lost. We have developed a test stand to measure SEE yields as function of incident

electron energy using very small doses of electrons to minimize surface charging of the insulators. This system utilizes a Hemispherical Grid Retarding Field Analyzer to capture all the secondary and backscatter electrons in an Ultra High Vacuum environment, ensuring an accurate measurement of SEE yield. By firing quick small pulses of electrons enables us to analyze insulating samples before the surface becomes charged which will alter the electron emission process. Results from our measurements on ceramic insulators will be

presented.

Sandia National Laboratories is a multi-mission laboratory managed and operated by National Technology and Engineering Solutions of Sandia, LLC., a wholly owned subsidiary of Honeywell International, Inc., for the U.S. Department of Energy's National Nuclear Security Administration under contract DE-NA0003525.SAND2024-07083A

VT-ThP-6 An Enhanced, High-Vacuum System and Related Testing of Unique, Prototype Sensor Hardware for the ITER-DRGA Project, *Chris Marcus, Theodore Biewer,* ORNL*; Joseph Brindley,* Gencoa, UK*; Alina Jugan,* North Carolina State University*; Christopher Klepper,* ORNL*; Patrick McCarthy,* Gencoa, UK*; **Brendan Quinlan,** ORNL*

The ITER Diagnostic Residual Gas Analyzer (DRGA) performs fusion neutral gas analyses. The ROI comprises low-amu species (1 thru 6), and includes the isotopic profiles of hydrogen and helium [1]. There are challenges in obtaining accurate measurements. First, the method sensitivity must suffice to resolve trace amounts accurately (≤1%). Second, the gas signal must be free of bias caused by the latent presence of these gases to acquire accurate measurements. For the lightest gases, backstreaming a fraction of the pumped gas load can be a source of such latency effects. This phenomena is attributed to modest inertia due to their lowest weight and smallest size. As a result, collisional effects create a reverse flow into the analysis region, which can contaminate the real-time measurement. To fully eliminate this adverse effect, a conductance-limiting device – or orifice – has been installed in the high-vacuum pumping system of the present DRGA prototype. It is intended to eliminate backstreaming by increasing the back pressure within the inter-pump volume (IPV).

An added benefit of the orifice-restricted pumping concept is that the upstream pressure increase is beneficial to the DRGA plasma cell used optical gas analysis. These sensors are attached to the IPV in the present DRGA design. The glow discharges will typically have a brighter light emission with increasing plasma cell pressure. For the DRGA, one of the glow discharge sources being evaluated for this system is a prototype made by Gencoa Limited (UK), which has been designed to exhibit satisfactory immunity to fringing fields, simulated for the tokamak environment. Also, the unique circuitry control for the input power control of the cell, when coupled with the specialized magnetic confinement of the plasma, have optimized the profile shapes of line emissions of interest for these isotopes, of which some emission lines are difficult to deconvolute.

Described herein are two ITER-DRGA related concepts: Vacuum system testing to validate elimination of light gas backstreaming and test results from using the prototype light source and a modified, Penning cathode.

This work was supported by the U.S. D.O.E. contract DE-AC05-00OR22725.

[1] C.C. Klepper et al., 2022 IEEE-TPS 50 (12) 4970

VT-ThP-7 Quantum State Specific Collision Dynamics of Vibrationally Excited Nitric Oxide at Collision Energies Over Five Orders of Magnitude, *Chatura Perera, Arthur Suits,* University of Missouri-Columbia*; Hua Guo,* University of New Mexico

Collision studies involving the open shell nitric oxide (NO) molecule have been central in many detailed investigations of molecular reaction dynamics as a prototype system for probing inelastic collisions. These processes have proven a powerful means of investigating molecular interactions, and much current effort is focused on the cold and ultracold regime where quantum phenomena are clearly manifested. Here I present our recent work on state-to-state spin-orbit changing collisions of highly vibrationally excited NO molecules prepared in single rotational and parity levels at v=10 using stimulated emission pumping (SEP). This state preparation is employed in a near-copropagating beam geometry that permits very wide tuning of the collision energy, from far above room temperature down to 2 K where we test the theoretical treatment of the attractive part of the potential and the difference potential for the first time. We have obtained differential cross sections for state-to-state collisions of NO(v=10) with Ar/Ne in spin-orbit excited manifold using velocity map imaging. Overall good agreement of the experimental results was seen with quantum mechanical close-coupling calculations done on

coupled-cluster potential energy surfaces. Probing cold collisions of NO carrying ~2 eV of vibrational excitation allows us to test state-of-the-art theory in this extreme nonequilibrium regime. The current experimental setup is now modified to permit a near-counterpropagating geometry for the molecular beams which allows us to look into really high collision energies to study chemistry in high temperature hypersonic flows. This takes us to a new direction where vibrationally inelastic processes may appear and the latest results along these experiments will also be presented.

2D Materials

Room 122 - Session 2D+EM+MN+TF-FrM

2D NEMS and Strain Engineering

Moderator: Matthias Batzill, University of South Florida

9:00am 2D+EM+MN+TF-FrM-4 Laser-Induced Strain Tuning in Monolayer Graphene Nanomechanical Resonators, *Muhammad Ashar Naveed, Sanchaya Pandit, Yanan Wang,* University of Nebraska - Lincoln

Graphene, as the paradigm-shifting two-dimensional (2D) material, has demonstrated great potential in micro-/nano-electromechanical systems (MEMS/NEMS) due to its extraordinary mechanical properties, ultimate device thicknesses, and unparalleled flexibility in integration. On the other hand, the atomic thickness and the transfer process employed in device fabrication pose challenges to achieving uniform strain over the entire device. In this work, we utilize Raman spectroscopy and investigate the strain distribution in drumhead resonators based on the mechanically exfoliated graphene monolayers suspended over patterned oxidized silicon (SiO_2/Si) substrates. Moreover, the effects of laser-induced heating and consequential strain tuning have been systematically explored by combining Raman spectroscopy and mechanical resonance measurements. This study sheds light on the strain engineering of monolayer graphene nanomechanical resonators, and the methodology developed is readily applied to other 2D materials and heterostructures.

9:15am 2D+EM+MN+TF-FrM-5 Developing 2D Snse for Piezoelectric Applications, *Jonathan Chin, Marshall Frye, Bonnie Gardner,* Georgia Institute of Technology*; Derrick Shao-Heng Liu,* Penn State University*; Maria Hilse,* Pennsylvania State University*; Ian Graham,* Georgia Institute of Technology*; Jeffery Shallenberger, Ke Wang, Mengyi Wang, Yun Kyung Shin, Nadire Nayir, Adri can Duin, Stephanie Law,* Pennsylvania State University*; Lauren Garten,* Georgia Institute of Technology

Unique functionalities can arise when 2D materials are scaled down near the monolayer limit. Tin selenide (SnSe) is one such 2D material which is centrosymmetric in bulk but becomes non-centrosymmetric when reduced to the monolayer limit, enabling piezoelectricity, and potentially, ferroelectricity. Developing 2D piezoelectric and ferroelectric materials is critical for the scaling of efficient sensors and electronics, such as ferroelectric field effect transistors. However, unlike other 2D materials, the strong interlayer bonding makes exfoliating a monolayer of SnSe challenging. Therefore, direct film growth is necessary to control the layer thickness and promote lateral growth large enough for device testing. This talk will focus on the development of processing routes to control the morphology and layering of SnSe thin films grown by molecular beam epitaxy (MBE) for piezoelectric devices. The bulk *Pnma* phase of SnSe is stabilized over a broad range of Sn:Se flux ratios from 250 – 300 °C on (100) MgO and (0001) Al_2O_3 substrates. Changing the flux ratio did not affect the SnSe film stoichiometry; increasing the flux ratio only changes the predominant crystallographic orientation. ReaxFF molecular dynamics (MD) show that the limited stoichiometric change is due to the formation of Se clusters that weakly interact with the surface of the SnSe particles. Changing the temperature, flux ratios, and flux timing had a significant impact on the morphology and orientation of the SnSe thin films. Machine learning was used to infer the critical processing parameters that are needed for creating an oriented, wafer-scale thin film. Overall, this study identifies the conditions for the growth of monolayer SnSe thin films necessary for the development of 2D piezoelectric devices.

9:30am 2D+EM+MN+TF-FrM-6 Two-Dimensional (2D) $FePS_3$ Nanoelectromechanical Resonators with Local-Gate Electrostatic Tuning, *Yunong Wang,* SM Enamul Hoque Yousuf, Xiao-Xiao Zhang, Philip X.-L. Feng, University of Florida

Nanoelectromechanical systems (NEMS) based on 2D magnetic materials are promising candidates for exploring ultrasensitive detection and magnetostrictive phenomena due to their high mechanical stiffness, high strength, and low mass. The resonance frequency of the suspended membrane resonator can be probed optically and manipulated mechanically via electrostatically induced strain. This makes electrostatic frequency tuning of the 2D magnetic NEMS resonator a promising way for exploring the novel magneto-mechanical coupling mechanism. Towards building magneto-mechanical coupling NEMS devices, we fabricated circular drumhead $FePS_3$ NEMS resonators with different cavity-diameter sizes (3um to 7um). In this work, we report on experimental demonstrations of high-performance antiferromagnet $FePS_3$ drumhead resonators with the highest frequency tuning range up to 31.62%. We further perform analytical modeling to gain insight and quantitative understanding of the frequency scaling law for $FePS_3$ drumhead resonators. Combining our experimental results and analytical modeling of the resonances, we resolved the elastic behavior of $FePS_3$, including the transition from 'membrane-like' regime to 'plate-like' regime, with built-in tension (γ) ranging from 0.1 to 2N/m. This study not only offers methods for characterizing the mechanical properties of ultrathin membranes of magnetic 2D materials but also provides important guidelines for designing high-performance magnetic NEMS resonator devices and opens possibilities for building drumhead resonator devices to exploit strain- and dynamics-engineered applications based on ultrathin magnetic 2D crystals.

9:45am 2D+EM+MN+TF-FrM-7 Tunable Phononic Frequency Combs in Atomically Thin Resonators, *S M Enamul Hoque Yousuf, Tahmid Kaisar,* University of Florida*; Jaesung Lee,* University of Central Florida*; Steven Shaw,* Florida Institute of Technology*; Philip Feng,* University of Florida

Phononic frequency comb (PnFC), the analogue of optical frequency comb in the radio frequency (RF) regime, has attracted significant research interest due to its potential applications in sensing and computing. In this abstract, we report on PnFCs generation via an atomically thin molybdenum disulfide (MoS_2) nanoelectromechanical resonator. We first measure the nonlinear mode coupling coefficient (λ) due to 1:1 internal resonance from the first-principles approach. To describe the energy exchange between the coupled modes, we employ two resonator equations with a single dispersive coupling term to model the response. The coupled mode equations are solved using the method of averaging to derive a closed form expression for the nonlinear mode coupling coefficient.To calibrate the vibration amplitude of both modes in the displacement domain, we measure the undriven thermomechanical noise.The nonlinear shift of the resonance frequency of mode 1 (f_1) that results from the dispersive coupling to mode 2 is measured as we drive mode 2 near its natural frequency (f_2). We estimate the mode coupling coefficient using our derived model.Additionally, we investigate the impact of Duffing nonlinearity on the energy cycling of the modes.

We utilize the 1:1 internal resonance to couple energy between two modes. The resonator response can be tuned from stable periodic response to quasi-periodic response by controlling external perturbation signals, such as DC gate voltage, RF drive voltage and frequency. The resonator exhibits three unique comb regions with well-defined comb structure. We observe that the periodic and quasiperiodic branches exist for a particular drive voltage and frequency, based on distinct initial conditions. Our demonstration leads the way to achieving tunable PnFCs in nanoscale devices to study nonlinear modal interactions and build ultrasensitive sensors and computing devices.

Actinides and Rare Earths

Room 123 - Session AC+MI-FrM

Actinide and Rare Earth Chemistry and Physics

Moderators: Edgar Buck, PNNL, **Krzysztof Gofryk**, Idaho National Laboratory, **Gertrud Zwicknagl**, Technical University Brauschweig

8:15am AC+MI-FrM-1 Structure, Stability, and Chemistry of Actinide Nanoparticles, *Ping Yang, Gaoxue Wang, Enrique Batista,* Los Alamos National Laboratory **INVITED**

Nanoscale materials bearing heavy elements have a wide range of applications from the nuclear fuel cycle to environment and health. Nanocrystals (NCs) with size and shape dependent properties are a thriving research field and remarkable progress has been made in the controlled synthesis and characterization of NCs composed of stable elements in the past three decades. In this context, interfacial chemistry of nano-sized materials is critical for controlling the morphology that drives their unique associated chemical and physical properties. The understanding of NCs containing f-elements is comparatively limited due to difficulties in handling them both experimentally and theoretically. In this talk, I will share some recent progress in understanding the interplay between surface energy, surfactant ligands, and the chemistry in determining the morphology of 5f-element nanoparticles. Quantum simulations provide a molecular-level picture of the relevant driving forces and dynamic properties. To push for larger lengthscale, we recently developed the density functional theory tight-binding (DFTB) parameters for actinide systems, that enabled the microsecond quantum MD simulations of actinide nanoparticle systems.

[1]G Wang, ER Batista, P Yang. *Phys Chem Chem Phys* **2018,** *20*, 17563

[2]G Wang, ER Batista, P Yang, *J. Phys Chem C,* **2019,** *123*, 30245

[3]RK Carlson, MJ Cawkwell, ER Batista, P Yang, *J. Chem. Thoery Compt***2020**, *16*, 3073

[4]NF Aguirre, J Jung, P Yang, *Phys Chem Chem Phys***2020**, *22*, 18614

[5]G Wang, ER Batista, P Yang, *Appl Sci***2020**, *10*, 4655

[6]D G Gonzalez, G Wang, ER Batista, P Yang, *Inorg Chem***2023,** *in press*

8:45am AC+MI-FrM-3 The Use of Ligand Modified Electrodes as Electrocatalysts for Actinide Redox Chemistry, *Christopher Dares,* Florida International University*; Travis Grimes,* Idaho National Laboratory*; Jeffrey McLachlan,* University of California at Berkeley*; Xiangyang Hou,* University of Utah*; Alberto Ruiz Reyes,* Florida International University **INVITED**
The lanthanides are most stable in the trivalent oxidation state, and with few exceptions, are difficult to generate in higher or lower oxidation states. In contrast the early actinides are redox active and can be generated and studied in a variety of oxidation states ranging from +7 to +2. This variety can complicate separations processes since oxidation state and can have a profound influence on ligand binding and solvent extraction. Separations schemes can also exploit the differences in binding preferences in different oxidation states to make selective extraction more efficient. In an aqueous acidic environment, the Am(IV/III) couple is at 2.6 V vs. the standard hydrogen electrode (SHE). This is nearly at the limit of what is possible in an aqueous solution where the 1-electron oxidation of water to hydroxyl radical is only about 0.3 V more positive. The subsequent potentials to generate penta- and hexavalent americium are lower though the high Am(IV/III) couple renders Am effectively redox-inert. Ligand coordination can be used to reduce the Am(IV/III) couple and/or facilitate the proton-coupled electron transfer (required to make the americyl cation). These can be organic ligands including N-donors or inorganic ligands such as lacunary polyoxometalates. Ligands anchored to metal oxide electrodes serve as good electrocatalysts to generate Am(V) or Am(VI) and operate at potentials as low as 1.6 V vs. SCE (nearly 1 V below the Am(IV/III) couple). Ligands are attached to the surface using either organic functional groups like phosphonic acids, or, through a combination of attractive interactions including hydrogen-bonding. They form well-packed monolayers on mesoporous thin layers of conductive oxides. The development of these ligand modified electrodes (LMEs) will be introduced along with characterization of their ability to adjust actinide oxidation states.

9:15am AC+MI-FrM-5 Observation of Flat Bands in Rare-Earth Based Kagome Metals, *Madhab Neupane,* University of Central Florida **INVITED**
Quantum materials with kagome lattice – comprised of corner-sharing triangles forming a hexagon in the crystal structure - have been studied as the potential playgrounds for exploring the interplay among parameters such as geometry, topology, electronic correlations, magnetic, and charge density orders. Recent report on a family of kagome metals of the form ReTi3Bi4 (Re = rare-earth) has generated interest due to the combination of highly anisotropic magnetism and a rich electronic structure. We use angle-resolved photoemission spectroscopy measurements in combination with density functional theory calculations to investigate the electronic structure of newly discovered kagome metals ReTi3Bi4. Our results reveal multiple van Hove singularities (VHSs), some of which are in the vicinity of the Fermi level. We clearly observe multiple flat bands, which originate from the destructive interference of wave functions within the Ti kagome motif. These flat bands and VHSs originate from Ti d-orbitals and are very responsive to the polarization of the incident beam. These results demonstrate that of Ti based kagome materials system is an excellent material platform for studying kagome induced flat band physics and its connection with magnetism.

9:45am AC+MI-FrM-7 Kinetics and Mechanism of Plutonium Oxycarbide Formation, *Paul Roussel,* AWE plc, UK
Plutonium is both electropositive and highly reactive, such that an oxide film of varying thickness is always present on metal samples.It is of interest from a safety point of view (reduced handling/processing) to investigate methods that either prevent or slow down the rate of corrosion reaction of the metal. Plutonium oxycarbide, $PuC_{1-x}O_x$, surface films on plutonium metal have shown the ability to slow the rate of oxidation [1]. Favart *et al*. have reported the rate of plutonium oxycarbide formation at 350 °C [2] as measured using X-ray Diffraction. In the theoretical study reported by Qiu et al. the authors proposed four different mechanisms for the formation of plutonium oxycarbide [3]. Two of the proposed mechanisms involved the reaction of a gas with plutonium sesquioxide, Pu_2O_3, and the other two involved a solid state reaction of this oxide to form plutonium oxycarbide. Using a combination X-ray Photoelectron Spectroscopy, Secondary Ion Mass Spectrometry and X-ray Diffraction the kinetics and mechanism of plutonium oxycarbide formation have been investigated and will be presented.

[1] Retardation of plutonium oxidation by a PuO surface film, D. T. Larson, D. L. Cash, J. Vac. Sci. Technol. 9, 800 (1972).

[2] Characterization of PuO/PuCO phase and its influence on the oxidation kinetics of d-plutonium, N. Favart, B. Ravat, L. Jolly, B. Oudot, L. Berlu, F. Delaunay, I. Popa, S. Chevalier, Oxid. Met., 96, 271 (2021)

[3] Thermodynamical stability of plutonium monoxide with carbon substitution, R. Qiu, X. Wang, Y. Zhang, B. Ao, K. Liu, J. Phys. Chem. C 122, 22821 (2018).

10:00am AC+MI-FrM-8 Layered *f*-Metal Zintl Phases - EuZn₂P₂ and UCu₂P₂, *LADISLAV HAVELA,* Charles University, Czech Republic*; Volodymyr Buturlim,* Idaho National Laboratory*; Oleksandra Koloskova,* Charles University, Prague, Czechia*; Dominik Legut, Jiri Prchal,* Charles University, Czech Republic*; Jindrich Kolorenc, Jiri Kastil, Martin Misek,* Institute of Physics CAS, Prague, Czechia
Zintl phases consisting of an electropositive element, cation, and covalently bonded polyanion, offer a large variability of electronic structure, bridging the gap between semiconducting and metallic behavior and offering interesting functionalities. In case of magnetic cation, properties can be further tuned by magnetic fields. Here we compare compounds based on lanthanide (Eu) and actinide (U) cations. We selected layered compounds, crystallizing in the trigonal structure $CaAl_2Si_2$, which exhibit pronounced magnetic anisotropy. $EuZn_2P_2$ is a narrow band-gap semiconductor. Antiferromagnetic ordering of Eu^{2+} moments sets in at T_N = 23 K. Rapid increase of T_N with applied pressure, which reaches 43 K at p = 9.5 GPa, can be associated with reduction of the band gap, indicated by transport properties as well as by ab-initio calculations. Ferromagnetic alignment of Eu moments, achieved in fields of several Tesla, can reduce electrical resistivity by several orders of magnitude, which is classified as Colossal Magnetoresistance Effect. At p = 18 GPa (still within the same structure type), $EuZn_2P_2$ becomes semi-metallic. The compression by hydrostatic pressure is anisotropic, with soft c-axis direction. UCu_2P_2 with a smaller unit-cell volume is semi-metallic (and probably half-metallic) at ambient conditions. Also here the magnetic order (ferromagnetic) is supported by applied pressure, reaching 290 K at 6 GPa. The situation of 5f states is dramatically different comparing with the 4f states in the Eu counterpart. The indications given by large spontaneous magnetostriction, softer a-axis direction (nearest U-U links), or extremely strong uniaxial magnetocrystalline anisotropy point to an involvement of the 5f states in bonding, i.e. delocalization, although they do not contribute to the Fermi level, located in a pseudo-gap. Tuning by composition changes is not straightforward for single crystals grown by Chemical Vapor Transport method, nevertheless certain routes have been attempted with a positive outcome and properties of doped UCu_2P_2 will be discussed.

10:30am AC+MI-FrM-10 Experimental Electronic Structure Measurements of Actinide-Containing Samples Using Scanning Tunneling Spectroscopy, *Benjamin Heiner, Miles Beaux,* Los Alamos National Laboratory
The many difficulties performing experiments on plutonium-containing samples makes the prospect of studying them using computational methods enticing. The lag in collection of experimental data using modern techniques, especially related to electronic structure, has made validating computational methods challenging. With the establishment of a scanning tunneling microscope at Los Alamos National Laboratory with the capacity to study plutonium and other radioactive samples, the ability to probe electronic structure seamlessly across the Fermi energy is now possible. In a first of its kind experiment, scanning tunneling spectroscopy data on plutonium-containing samples, especially gallium-stabilized δ-phase plutonium, has been collected. The spectra reveal a surface with semimetal characteristics instead of a computationally predicted semiconductor band gap.

LA-UR-24-24274

10:45am AC+MI-FrM-11 Unconventional Superconductivity in UBe₁₃ - Investigation via Variation of Impurity Level - and Comparison to the Conventional Superconductor LuBe₁₃, *Greg stewart, Jungsoo Kim,* University of Florida
We have prepared and characterized down to T=0.40 K three arc-melted samples each of MBe_{13}, M = Lu, U, using threedifferent purities (99.999%, 99.96%, and 99.8%) of Be but with the same high purity M (Lu or U) for all three.The measurements down to 0.40 K allow the detection of the maximum in the specific heat in all three $LuBe_{13}$samples. The resulting

superconducting properties **strongly** depend on impurity level in UBe_{13} (40% decrease in$\Delta C/T_c$, 15% decrease in $T_c$mid) while the three $LuBe_{13}$ samples exhibit significantly smaller changes (10% and 5%respectively) with purity. The comparison of properties at the first two levels of purity (99.999% vs 99.96%) iseven more disparate: 12% decrease in $T_c$mid in UBe_{13} vs no change in $LuBe_{13}$. These results are consistent withprevious results that argue for unconventional superconductivity in UBe_{13}, and are consistent with assignment of $LuBe_{13}$ as a conventional, BCS superconductor. As will be discussed in more detail, this example of comparing superconducting properties vs controlled gradations in impurity levels with two compositionally and structurally "matched" superconducting compounds (one conventional and one of to-be-determined coupling behavior) offers a new method - versus the already existing ones - for determining unconventional superconducting behavior.

11:00am AC+MI-FrM-12 Strong Magnetoelastic Interactions in HoSb Probed by High-Resolution Dilatometry and X-Ray Diffraction, *Volodymyr Buturlim,* Glenn T. Seaborg Institute, Idaho National Laboratory*; Narayan Poudel,* Idaho National Laboratory*; Dariusz Kaczorowski,* Polish Academy of Sciences, Poland*; Marcelo Jaime,* Physikalisch Technische Bundesanstalt, Germany*; Zahir Islam,* Argonne National Laboratory*; Krzysztof Gofryk,* Center for Quantum Actinide Science and Technology, Idaho National Laboratory

Rare-earth (RE) monopnictides, which crystallize in a cubic structure similar to NaCl have drawn considerable interest due to their diverse transport, magnetic, and structural properties. The non-magnetic compounds are known for the transition from topological to trivial electronic states (e.g. LaPn where Pn = Bi and As [1]). Magnetism of the compounds with long-range order brings complexity to their topological properties. However, the topological nature of these materials undergoes intense debates and investigation. HoSb is a topologically trivial semimetal, which orders antiferromagnetically below T_N = 5.7 K [2]. Application of magnetic field leads to the change of its magnetic structure from MnO-type antiferromagnetic (AFM) arrangement to HoP-type arrangement, then to ferromagnetic (FM) arrangement. There are also reports which, suggest a transition to tetragonal structure taking place at T_N [3]. The variety of the low-temperature phenomena makes HoSb a good platform to investigate the role of magnetic ordering and the strength of spin-phonon coupling on the crystal structure of this system. We will present the results of low-temperature high-resolution dilatometry as well as X-ray diffraction studies performed at static and pulsed magnetic fields. Heat capacity studies and the presence of latent heat agree with the structural distortion that occurs at T_N. The lowering of the symmetry is further supported by detailed low-temperature X-ray diffraction measurements under magnetic fields. Strong spin-lattice coupling in HoSb results in giant magnetostriction of the order of 1500 ppm. Furthermore, our detailed dilatometry studies allow us to construct a magnetic phase diagram of HoSb. We will discuss the implications of these results in the context of the strong magnetoelastic properties in HoSb and other rare-earth monopnictides.

[1] H. Y. Yang et al., Phys. Rev. B **98**, 045136 (2018).

[2] M. M. Hosen et al., Sci. Reports 2020 101 **10**, 1 (2020).

[3] F. Lévy, Phys. Kondons. Mater. **10**, 85 (1969).

11:15am AC+MI-FrM-13 Electronic Structure in a Rare-Earth-Based Intermetallic System $TbNi_3Ga_9$, *Sabin Regmi, Volodymyr Buturlim,* Idaho National Laboratory*; Binod K. Rai,* Savannah River National Laboratory*; Tomasz Durakiewicz, Krzysztof Gofryk,* Idaho National Laboratory

Rare-earth-based intermetallics provide flexibility to study the electronic, magnetic, superconducting, and topological properties by tuning the crystal structure, composition, and spin-orbit coupling. Recently, $RNi_3(Ga/Al)_9$ intermetallic materials have been studied for their richness in broad range of exotic crystal, magnetic, heavy fermion, and quantum criticality behaviors. However, momentum-resolved electronic structure studies are lacking. Here, we present results of the angle-resolved photoemission spectroscopy measurements to reveal the underlying electronic structure and topology in $TbNi_3Ga_9$, both above and below the Néel temperature. This study will open up exciting avenues towards exploration of electronic properties in the chiral family of $RNi_3(Ga/Al)_9$ materials with wide range of intriguing properties.

11:30am AC+MI-FrM-14 Catalytic Activities of Defected Actinide Dioxide AnO_2 Surface: A First Principles Study, *Shukai Yao, Gaoxue Wang, Enrique Batista, Ping Yang,* Los Alamos National Laboratory

Actinide dioxides AnO_2 play an important role as nuclear fuels in commercial nuclear reactors. Understanding the surface chemistry of AnO_2 is crucial in various aspects such as safe operations, recycling, and storage of nuclear fuels. Actinide materials have shown to be highly efficient catalyst for the activation of H_2, CO, NH_3, etc., mainly due to valent $5f$ electrons of actinides characterized by strong electron correlations and various oxides states. However, experimental studies of actinide systems are limited by their high safety requirement associated with radioactivity. In this computational study, we employed first principles electronic structure calculations based on density functional theory (DFT) to reveal the catalytic behavior of AnO_2 surface with O vacancies. We will show that O vacancies significantly change the electronic structure of AnO_2 surfaces, and act as the active sites of small molecules adsorption. As a result, defected AnO_2 surface leads to an enhanced reactivity compared to the pristine AnO_2 surface.

11:45am AC+MI-FrM-15 Thin Film Synthesis of Rare Earth and Actinide Nitrides Using Molecular Beam Epitaxy, *Keivn Vallejo, Brelon May, Zachery Cresswell, Voldymyr Buturlim, Sabin Regmi, Krzysztof Gofryk,* Idaho National Laboratory

Lanthanide- and actinide-based nitride compounds are an understudied group of materials compared to their oxide counterparts, which provide new avenues for nuclear reactor designs. Their 4f and 5f electron shell gives rise to a variety of interesting physics such as magnetism and unconventional superconductivity. Samarium nitride (SmN) has been recently identified as a material where ferromagnetic order and potential p-type superconductivity coexist. Our team will present results on the growth conditions in a molecular beam epitaxy chamber of pure and doped SmN using molecular beam epitaxy, and its electronic transport properties as a function of temperature and magnetic field. CeN and UN thin films are also explored. The presence of SmN(111) peaks on (001) substrates indicates an orientation-preference for some material systems. The electrical resistivity and magnetic susceptibility studies have shown a range of magnetic behaviors, including paramagnetic and ferromagnetic. With a potential superconductive transition around ~10 K, SmN and its doping effects on crystal structure and electronic properties are characterized.

Chemical Analysis and Imaging of Interfaces
Room 121 - Session CA-FrM

Materials, Interfaces and Metrologies for Electronics

Moderators: Alex Belianinov, Sandia National Laboratory, **Andrei Kolmakov**, National Institute of Standards and Technology (NIST)

8:15am CA-FrM-1 Surface Transfer - Modulation Doping at the Diamond-Dielectric Interface, *Aditya Deshmukh, Yu Yang, Franz Koeck, Robert Nemanich, Kevin Hatch,* Arizona State University **INVITED**

Great progress in diamond wafer technology and diamond epitaxy have inspired new concepts for diamond electronics particularly for power conversion and RF applications.However, the highactivation energy of substitutional p- and n-type dopants in diamond has limited the development of field effect transistors (FET). An alternative approach of charge transfer doping at a diamond-dielectric interface, which results in the formation of a hole accumulation layer, is not limited by thermal activation [1].However, the hole transport shows a mobility that is much lower than predicted. It is widely accepted that the low mobility is due to scattering from the near interface negative charges transferred into the dielectric layer.

Following the concept of modulation doping at heterostructure interfaces, we have proposed and demonstrated a dielectric layer configuration that results in a nearly ten-fold mobility increase for the accumulated holes at the diamond interface [2]. In this approach MoO_3 is used as the charge transfer dielectric, and Al_2O_3 is employed as the modulation doping spacer layer. The charge transfer is driven by the energy difference between the diamond valence band and the charge transfer states in the MoO_3. The thickness of the spacer layer also affects the hole accumulation layer charge density.

In this study photoemission spectroscopy is employed to measure the band alignment and band bending throughout the multi -layer structure.The relative distribution of the charge near the interface is deduced from the band diagram. These experiments and the model of Surface Transfer -

Modulation Doping demonstrates a new approach to FET channel doping for diamond field effect transistors.

[1]K. G. Crawford, I. Maini, D. A. Macdonald, and D. A. J. Moran, "Surface transfer doping of diamond: A review," Prog. Surf. Sci. 96, 100613 (2021).

[2]Yu Yang, Franz A. Koeck, Xingye Wang, and Robert J. Nemanich "Surface transfer doping of MoO3 on hydrogen terminated diamond with an Al2O3 interfacial layer," Appl. Phys. Lett. 120, 191602 (2022).

8:45am CA-FrM-3 Probing the Nanoscale: The Synergy of XPS and LEIS Analyses, *Joshua W. Pinder, Jacob Crossman,* Brigham Young University; *Stanislav Prusa, Tomas Sikola,* Brno Institute of Technology, Czechia; *Matthew Linford,* Brigham Young University

Over the past few decades, with the development of novel, advanced materials, the significance and need for surface characterization techniques has increased dramatically. These advanced materials appear in diverse sectors of the economy including in semiconductors, thin films, catalysts, batteries, fuel cells, adhesion, and for material durability. An understanding of surface and material composition often leads to improvements in material properties. In this talk, we discuss the synergy and usefulness of two important surface techniques: X-ray photoelectron spectroscopy (XPS) and low energy ion scattering (LEIS).

XPS is a mature and well-developed technique, providing both elemental and chemical state information about surfaces. However, XPS spectra do not always unambiguously identify the depths of atoms at surfaces. It is not always clear whether an atom is exposed at a surface or slightly below it. Whether an atom is exposed or not has profound implications in various fields, including in catalysis. Accordingly, LEIS, which is sensitive to the outermost atomic layer of surfaces, ideally complements XPS. Both techniques are, for the most part and for many surfaces, non-destructive.

As examples of the combined use of XPS and LEIS, we present the analyses of hydrogen-terminated, single-crystal diamond and various copper samples. First, hydrogen-terminated, single-crystal diamond is a low free energy material that can be easily cleaned. We show the reaction of hydrogen-terminated diamond with atomic oxygen and follow that oxidation by XPS and LEIS. We then reduce this surface with atomic hydrogen, again following this process with XPS and LEIS. The different functional groups that are created by oxidation and then removed by hydrogen reduction are identified and quantified by both techniques. Second, the analysis of copper highlights the extraordinary surface sensitivity of LEIS. Quantities of surface oxygen that minimally affect the XPS spectra (compared to the spectrum of the pure, unoxidized metal), very strongly alter the LEIS spectra. For example, copper metal itself is very inefficient at reionizing helium projectiles, while oxygen at the copper surface is. This difference leads to a dramatic difference in the reionization backgrounds of copper metal and oxidized copper.

For the reasons discussed in this talk, we believe that the combination of XPS and LEIS will play an increasingly important role in surface analysis.

9:00am CA-FrM-4 Capacitively and Electrically Detected Magnetic Resonance in 4H SiC MOSFET, *Artur Solodovnyk, Patrick M Lenahan,* The Pennsylvania State University

Silicon carbide MOSFETs show great potential in high-power, high-temperature applications. However, electrically active interface traps, which have a substantial impact on the device's channel-carrier mobility and threshold voltage stability are still not completely understood [1]. Several spectroscopic techniques can help identify the physical and chemical nature of such defects, among them, electrically detected magnetic resonance (EDMR)[2] and as we show in this work, capacitively detected magnetic resonance (CDMR). To the best of our knowledge, CDMR was first demonstrated in Si-based MOS devices by Brandt and coworkers [3-4]. In this work, we show that such capacitive measurements are also possible in SiC-based devices. Furthermore, we compare EDMR and CDMR measurements on the same devices at very different fields and frequencies. The line-widths and g-tensors are approximately the same for both cases. We report on EDMR and CDMR studies on 4H SiC MOSFET in capacitor configuration (gate-body). The relatively narrow line with $g\perp$= 2.0023(±0.0005) and $g_{||}$ = 2.0010(±0.0005) with the respect to the device's SiC/SiO$_2$ interface has been observed in both EDMR and CDMR. We observe close similarities at low (500 MHz, Fig. 1) and high frequency (9.784 GHz, Fig. 2) with negative bias of 3 V for both measurements. The line-width at both measured frequencies is about 6.8(±0.3) G. The measurements were carried out at room temperature.

It should be noted, that these measurements were made on devices with quite high interface trap density [5]. Thus, we feel the significance of this work, is mainly to point out the potential utility of CDMR in studies of SiC MOSFETs.

[1] Chaturvedi, M. et al. Energies 16, 1771 (2023)

[2] C. J. Cochrane et al. Appl. Phys. Lett. 100, 023509 (2012)

[3] M.S. Brandt et al. Appl. Phys. Lett. 76, 1467–1469 (2000)

[4] M.S. Brandt et al. Physica B 273-274, 1027-1030 (1999)

[5] D. J. Meyer et al. Appl. Phys. Lett. 86, 023503 (2005)

9:15am CA-FrM-5 Photoluminescence Mapping of Gallium Oxide Surfaces and Epilayers, *Matthew McCluskey,* Washington State University

Photoluminescence (PL) spectroscopy is an important method to characterize dopants and defects in gallium oxide. Features in the PL spectrum include the intrinsic UV band, blue and green bands that involve donor-acceptor pairs, and red emission due to Cr^{3+} impurities. PL mapping with excitation wavelengths as short as 266 nm reveals the spatial distribution of these features with submicron resolution. In addition to defects in the bulk, PL microscopy has revealed several specific defects on the surface. Some of these localized centers are very bright UV emitters. Raman scans of these bright emitters revealed hydrocarbon peaks, which may point toward the origin of the light emission. Homoepitaxial layers grown by metalorganic chemical vapor deposition (MOCVD) show defects that are observed via the shifts in the PL band, likely due to the strain field around a dislocation core. Damage due to high-intensity, sub-bandgap laser pulses results in a drop in the intensity of the UV band. A ring or "halo" around the damaged region is observed under 532 nm excitation, attributed to color center defects.

9:30am CA-FrM-6 Focused Ion Beam Low Energy Implantation, *Michael Titze, Chris Smyth,* Sandia National Laboratory; *Jonathan Poplawsky,* Oak Ridge National Laboratory; *Barney Doyle, Edward Bielejec,* **Alex Belianinov,** Sandia National Laboratory   **INVITED**

Ion implantation is a key capability for the semiconductor industry. As devices shrink, novel materials enter the manufacturing line, and quantum technologies transition to being more mainstream, traditional implantation methods fall short in terms of energy, ion species, and positional precision. However, lowering the implantation energy while maintaining nanometer scale spot size is a technological challenge. This presentation will show an overview of techniques at Sandia National Laboratories Ion Beam Facility that allow focused ion implants 10-200 keV range for quantum relevant applications.

Additionally new developments in sub-1 keV focused ion implants into Si and 2D devices, using a focused ion beam system, validated by atom probe tomography will be shown. We illustrate that identical results for low energy ion implants can be achieved by either lowering the column voltage, or decelerating ions using bias – while maintaining good spatial resolution. Furthermore, our data reveal that standard implant modeling approaches overestimates experimental depth by a significant margin. Finally, we discuss how our results pave a way to much lower implantation energies, while maintaining high spatial resolution.

10:00am CA-FrM-8 NIST Nanocalorimetry for In-Plasma Process Metrology Relevant to Semiconductor Fabrication, *Andrei Kolmakov, J. Trey Diulus, Feng Yi, David LaVan,* NIST-Gaithersburg

Plasma processing is among the most widely used technologies in semiconductor fabrication industry. In particular, plasma is employed for (reactive-) plasma etching, wafers cleaning, plasma-assisted chemical/physical vapor depositions and etc. However, despite variety of existing plasma diagnostics methods, there is a shortage of metrologies for *in situ* sensitive monitoring/control of the interfacial interactions relevant to semiconductor fabrication. This is particularly valid for plasma processing that relies on neutral reactive radicals and/or pulsed radicals' exposures, which are hard to detect. The current state of the art method for radials detection in research lab settings are based on catalytically activated thermocouples or quartz microbalance based etch sensors which are often too slow or not sensitive enough.

On the other hand, modern microfabricated nanocalorimeters can operate at kHz frequency domain rage and can detect fast physical and chemical (endo-)exothermal surface reactions with high sensitivity on the order of a nJ/K, including adsorption–desorption processes, interfacial reactions, chemical etching reactions all relevant to fabrication of semiconductor devices. Nanocalorimeters are small to be easily integrated to any microfabrication chambers and cheap enough to be readily modified to meet a specific process requirement.

Here we repot the pilot tests of NIST microfabricated nanocalorimeters to detect reactive radicals generated by low power (ca 20-70 W) remote (ca 10 Pa) hydrogen plasma. The setup consists of two otherwise identical sensors but one of them having Au layer exposed to vacuum. Au layer serves as a catalyst with known hydrogen recombination coefficient and the difference in heat of the recombination reactions is detected comparatively by activated and inert nanocalorimeters. The second non-activated sensor is also used to discriminate against parasitic signals such as UV-Vis radiation, ions and electrons fluxes. The setup was successfully tested and major parameters such as sensitivity and response time have been estimated and compared with existing plasma diagnostic tools.

Spectroscopic Ellipsometry
Room 116 - Session EL-FrM

Emerging Applications and Workforce Development

Moderators: Ufuk Kilic, University of Nebraska - Lincoln, **Stefan Zollner**, New Mexico State University

8:15am **EL-FrM-1 Singular Propagation States of Electromagnetic Waves in Anisotropic Media**, *Chris Sturm,* University Leipzig, Germany   **INVITED**

In optically anisotropic media, there are generally two eigenmodes for a given propagation direction, which propagate without changing their polarization. However, for certain directions, these two eigenmodes can completely degenerate, in their eigenstate and eigenvalue. In this case, only one well-defined state can propagate without changing its polarization and this direction corresponds to an exceptional point (EP) in the momentum space. In recent years, a growing interest in the fundamental physical properties of exceptional points (EP) and their use in applications has led to a significant increase in research activity in this area. The existence of such points was first reported by W. Voigt in 1902 for orthorhombic materials [1], who realized that in these materials at certain propagation directions, the propagation properties (complex refractive index) and the polarization of the two eigenmodes are simultaneously degenerated. Only a wave, either left or right circularly polarized, can propagate along such a direction without changing its state. It took almost 100 years, that the general case was discussed by Berry and Dennis in 2003 [2].

Here we present on overview on the EP in optically anisotropic materials and show that these points occur naturally in these systems [3]. In the presence of interfaces, the properties of the EP can be tuned, which is of particular of interest for technical applications [4]. Due to of the singular eigenstate at the EP, the typical used approach to describe the propagation as well as the reflection and transmission properties of an arbitrarily polarized wave at an interface by a superposition of the two eigenmodes is no longer applicable. In this case, an extension of the solution of the wave equation by a spatially dependent amplitude must be considered [3]. The results are illustrated by using the optical properties of real materials, which are used in current research, e.g., ZnO, KTP and β- Ga2O3.

[1]W. Voigt, Ann. Phys. **314**, 367 (1902).

[2]M. V. Berry and M. R. Dennis, Proc. R. Soc. London, Ser. A. **459**, 1261 (2003).

[3]Adv. Photonics Res. **5**, 2300235 (2024).

[4]S. Richter *et al.*, Phys. Rev. Lett. **123**(22) 227401 (2019).

8:45am **EL-FrM-3 Infrared-Active Phonon Modes in Variably Alloyed Bulk β-(AlXGa1-X)2O3 Determined by Mueller-Matrix Spectroscopic Ellipsometry**, *Preston Sorensen, Ian Green,* University of Nebraska - Lincoln; *Megan Stokey,* Milwaukee School of Engineering; *Akhil Mauze, Yuewei Zhang,* University of California Santa Barbara; *Jim Speck,* University of California at Santa Barbara; *Vallery Stanishev, Vanya Darakchieva,* Lund University, Sweden; *Zbigniew Galazka,* ikz berlin, Germany; *Mathias Schubert,* University of Nebraska - Lincoln

The monoclinic beta phase of gallium oxide is an ultra-wide bandgap semiconductor that has been widely studied for potential use in high power switching applications. As crystal growth methods have improved, we are able to investigate high quality $(Al_xGa_{1-x})_2O_3$ films and bulk substrates, which have been desired due to the increase in band gap with increasing Al content. Here, we study the near and mid infrared-active phonon modes of highly alloyed (x = 0.05, 0.1, 0.15, 0.2, 0.25, 0.3, and 0.35) bulk $(Al_xGa_{1-x})_2O_3$ with (100) surface orientation. We use generalized spectroscopic ellipsometry and implemented the previously described eigenpolarization model for phonon modes in monoclinic structure $(Al_xGa_{1-x})_2O_3$. We discuss the observed phonon mode parameter trends associated with alloying composition. We also investigate pseudomporhically-strained epitaxial films with x = 0.046, 0.097, and 0.163 grown on beta-phase (010) Ga_2O_3. We use our previously calculated phonon deformation potential parameter values and elastic coefficients and differentiate between strain and alloying induced phonon mode property variations as a function of Al content.

9:00am **EL-FrM-4 Predicting Perovskite Photovoltaics Performance from Spectroscopic Ellipsometry**, *Emily Amonette, Kshitiz Dolia, Yanfa Yan, Zhaoning Song, Nikolas Podraza,* University of Toledo

Complete wide band gap $FA_{0.8}Cs_{0.2}Pb(I_{0.6}Br_{0.4})_3$ perovskite photovoltaic (PV) devices are measured by spectroscopic ellipsometry in the through-the-glass configuration and analyzed to determine complex optical property spectra of the perovskite absorber properties as well as structural properties which are then used to simulate external quantum efficiency (EQE) spectra and to calculate PV device performance parameters such as short circuit current density, open circuit voltage, fill factor, and power conversion efficiency. Mapping spectroscopic ellipsometry measurements of an incomplete device are also collected from the perovskite film side to obtain layer thicknesses, perovskite band gap energies, and Urbach energies at each mapping point. These values are used to predict various PV device performance parameters such as short circuit current density, open circuit voltage, fill factor, and power conversion efficiency with the goal of increasing the accuracy of these predictions by comparing them to experimentally obtained parameters. The incomplete devices consist of glass superstrate / indium tin oxide front electrical contact / hole transport layer / perovskite absorber, while the complete devices consist of these components as well as an electron transport layer and silver back electrical contact. Simulations and calculations tend to overestimate PV device performance parameters, undermining the accuracy and usefulness of simulations. When these simulations are based on structural and optical properties obtained from spectroscopic ellipsometry measurements of incomplete perovskite films rather than complete PV devices, further inaccuracies arise as characteristics of that layer in the exposed perovskite film do not necessarily share the same of a complete, protected PV device. By comparing experimental PV performance parameters based on measured characteristics of the same devices under different assumptions in the modeling approach, the accuracy of simulated performance parameters are evaluated, and improvements in the models are implemented. The usefulness of this is apparent in situations where experimentally measuring PV device performance is unfeasible or overly tedious, as well as during intermediate steps during production.

9:15am **EL-FrM-5 Vacuum and Extreme Ultraviolet Scatterometry for Critical Dimension Metrology**, *Thomas Germer, Bryan Barnes, Stephanie Moffitt, Steven Grantham, Martin Sohn, Daniel Sunday, Eric Shirley,* National Institute of Standards and Technology (NIST)   **INVITED**

Scatterometry is often used to perform linewidth process monitoring in semiconductor manufacturing. Dimensional parameters of a periodic structure are fit to the optical signature, such as that obtained by a spectroscopic ellipsometer. The method has been typically limited to wavelengths in the near-infrared, visible, or ultraviolet, where traditional refractive optics are available for focusing and polarization control. As features are being fabricated with smaller dimensions, there is a need to employ shorter wavelengths to achieve the accuracy and precision targets. In this work, we are exploring the use of scatterometry in the vacuum and extreme ultraviolet (VUV and EUV), motivated by our finding that differentiating optical signatures should extend well into this spectral region; that compact VUV/EUV sources, such as high harmonic generation (HHG), are becoming commercially available; and that optical elements, such as phase retarders and polarizers, can be constructed using reflective optics, albeit with non-optimal attributes. In this talk, we will discuss each of these three motivations, and describe the technical challenges and opportunities that they present.

9:45am EL-FrM-7 Immersion Ellipsometry of Ultrathin Films - Breaking the Correlation between Index of Refraction and Film Thickness, *Samira Jafari,* Brigham Young University*; Blaine Johs,* Film Sense*; Matthew Linford,* Brigham Young University

The optical constants and thicknesses of ultrathin (<5 – 10 nm) films are correlated in traditional ellipsometric measurements. Accordingly, most ellipsometric measurements of these films involves assuming an index of refraction for them. This work describes the use of immersion ellipsometry to break the correlation between optical constants and film thickness, allowing both to be measured in an experiment. In immersion ellipsometry, ellipsometric data is acquired in both air and liquid ambients, and the two data sets are combined in the analysis. The measurement under liquid adds information to the analysis that breaks the correlation between the film thickness and refractive index that exists for air-only ellipsometric measurements. We describe the use of multi-wavelength immersion ellipsometry (MWIE) to sequentially measure both the thicknesses and optical constants of two ultrathin thin films: native oxide on silicon and an alkyl monolayer of chloro(dimethyl)octadecylsilane (CDMOS) on that native oxide. The average thicknesses of the native oxide and CDMOS monolayer were 1.526 ± 0.027 nm and 1.968 ± 0.057 nm, and their average indices of refraction at 633 nm were 1.519 ± 0.005 and 1.471 ± 0.004, respectively. The native oxide and CDMOS monolayer were also characterized with X-ray photoelectron spectroscopy (XPS) and contact angle goniometry. As expected, both the XPS C 1s peak and the water contact angle increase substantially after monolayer deposition. While immersion ellipsometry has been known for years, its use has been limited, probably because of a lack of awareness of the technique and/or the lack of readily available accessories for performing the experiment in many laboratories. As ultrathin films become more important, immersion ellipsometry should increase in importance as a means of characterizing them.

10:00am EL-FrM-8 Temperature Dependence of the Long-Wavelength Lattice Vibrations of NiO (111) Using Infrared Spectroscopic Ellipsometry from 25 K to 500 K, *Yoshitha Hettige, Jaden R Love, Carlos A Armenta, Atlantis K Moses, Jose Marquez, Stefan Zollner,* New Mexico State University

NiO has a cubic rock salt structure, with two optical phonon modes called transverse (TO) and longitudinal (LO). The frequency of these TO and LO modes is related to the reduced mass and the strength of the bond between the Ni^{2+} and O^{2-} ions. These vibrations can be analyzed by measuring the ellipsometric angles Ψ and Δ on an infrared ellipsometer.

A NiO (111) sample was mounted inside a Lakeshore Janis ST-400 cryostat. We measured the ellipsometric angles Ψ and Δ of NiO at room temperature at a resolution of 8 cm^{-1} from 250 to 8000 cm^{-1} on J. A. Woollam IR-VASE Mark II ellipsometer at 70° angle of incidence. Then, we cooled the NiO using liquid He and measured the ellipsometric angles Ψ and Δ between 25 and 500 K with a step size of 25 K under the same conditions. Low temperatures are achieved with a Lakeshore RCG4 recirculating helium cooler.

In our data analysis, we used one Lorentzian for the TO phonon absorption at ~400 cm^{-1} and another one for the two-phonon absorption (TO+TA) at ~560 cm^{-1}. The two edges of the reststrahlen band correspond to the TO energy (strong peak in the pseudodielectric function) and the LO energy (strong peak in the pseudoloss function). We found that the phonon energy has a redshift and increased broadening for increasing temperature due to the anharmonic decay of optical phonons. This temperature dependence of the phonon parameters are related to the self-energy of anharmonic decay. We fit the energy using the Bose-Einstein model which describes the data well. We found that the energy of the decay product is 64 meV, much larger than the TA(X) energy (16.5 meV). This unexpected result is probably because of the scattering of phonons by two magnons with an energy of about 190 meV.

10:30am EL-FrM-10 Far-Infrared Mueller Matrix Ellipsometry and Vortex Beam Spectroscopy Using Synchrotron Radiation, *Andrei Sirenko,* New Jersey Institute of Technology **INVITED**

Recent results for development of the new multi-user setup for low-temperature Ellipsometry and transmission/reflection vortex beam polarimetry in high magnetic fields will be presented. The instrument has been installed at the synchrotron radiation source – the MET beamline of NSLS-II in Brookhaven National Laboratory. This instrument is able to acquire experimental data in all three major scenarios of rotating analyzer ellipsometry (RAE), rotating compensator ellipsometry (RCE), and full-Mueller matrix ellipsometry (MM-SE) in the spectral range between 5 cm^{-1} and 10,000 cm^{-1} with the synchrotron radiation as the light source. A wide range of angles of incidence AOI between 70° and 85° is enabled by the θ-2θ goniometer. The ellipsometer has magnetic fields of up to ±7 T with a capability to switch quickly between the exact Faraday and Voigt configurations for direction of the magnetic field with respect to the sample surface. Data analysis is based on the Berreman's 4 × 4 propagation matrix formalism to calculate the Mueller matrix parameters of anisotropic samples with magnetic permeability μ different from 1. A nonlinear regression of the rotating analyzer ellipsometry and/or Mueller matrix spectra, which are usually acquired at variable angles of incidence and sample crystallographic orientations, allows extraction of dielectric constant and magnetic permeability tensors for bulk and thin-film samples.

In addition to the ellipsometric measurements, our setup is capable of producing the vortex beams of the synchrotron radiation with a distinct integer values of the orbital angular momentum (OAM). Recently we demonstrated that the vortex light with OAM can effectively couple to magnetism exhibiting dichroism in a magnetized medium. The vortex beams with various combinations of the OAM L=+/-1, +/-2, +/-3, and +/-4 and spin angular momentum S = +/-1, or conventional circular polarization, were used for studies of the magnon spectra in TbFe$_3$(BO$_3$)$_4$, h-Ni$_3$TeO$_6$, and h-Lu$_{0.6}$Sc$_{0.4}$FeO$_3$ single crystals. We observed strong vortex beam dichroism for the magnon doublets, which are split in an external magnetic field. The absorption conditions at the magnon resonances depend on the total angular momentum of light J that is determined by $J=S+L$. For the higher orders of L, the selection rules for AFM resonances dictated by L completely dominate over that for conventional circular polarization. A possibility to expand the vortex beam spectroscopy to the abroad class of the electronic systems in quantum matters will be discussed.

Parts of this work were performed in collaboration with V. Martinez, P. Marsik, L. Bugnon, C. Bernhard, V. Kiryukhin, and S.-W. Cheong.

11:00am EL-FrM-12 Infrared Dielectric Function of Thiazolothiazole Embedded Polymer Films Determined by Spectroscopic Ellipsometry, *Nuren Shuchi, Tyler Adams, Dustin Louisos, Glenn Boreman, Michael Walter, Tino Hofmann,* University of North Carolina at Charlotte

Organic photochromic polymers, whose photo-chemical and optical properties can be altered through optical stimulation, are found in diverse applications ranging from tinted lenses and smart windows to memory devices, actuators, tunable filters, and holographic gratings [1–4]. Recently, extended viologens containing the thiazolo[5,4-d]thiazole (TTz) backbone are increasingly attracting interest due to their strong fluorescence, solution-processability and reversible photochromic transition. Especially, dipyridinium thiazolo[5,4-d]thiazole viologen exhibits high-contrast, fast and reversible photochromic changes. When exposed to radiation with an energy larger than 3.1 eV, it transitions from light yellow (TTz^{2+}) to purple (TTz^{-+}) to blue (TTz^0) state due to two distinct, photo-induced single electron reductions [5]. The accurate knowledge of the complex dielectric function is essential for the design and fabrication of TTz-based optically tunable devices. The complex dielectric function of a non-photochromic TTz derivative and a photochromic TTz-embedded polymer has been determined previously in the visible and near-infrared spectral range [6,7] using spectroscopic ellipsometry.

In this presentation, we will discuss spectroscopic ellipsometry data obtained from bulk sample of photochromic thiazolo[5,4-d]thiazole embedded in polymer. The measurements were taken before and after irradiation with a 405 nm diode laser in the infrared spectral range from 500 cm^{-1} to 1800 cm^{-1}. The model dielectric functions of the thiazolothiazole embedded polymer film for its TTz^{2+} (unirradiated) and TTz^0 (irradiated) states are composed of a series of Lorentz oscillators in the measured spectral range. A comparison of the obtained complex dielectric functions for the TTz^{2+} and TTz^0 state shows that the oscillators located in the spectral ranges 500 cm^{-1}- 700 cm^{-1}, 1300 cm^{-1}- 1400 cm^{-1}, and 1500 cm^{-1}- 1700 cm^{-1} change in both amplitude and resonant frequency upon transition between the states. In addition, a resonance has been identified at approximately 1050 cm^{-1}, for which, only a change of the oscillator amplitude was observed due to the photochromic transition.

References

1. A.M. Oesterholm, *et al*., ACS Appl. Mater. Inter. **7**, 1413-1421 (2015). 2. H. Cho, and E. Kim, Macromolecules **35**, 8684-8687 (2002). 3. T. Ikeda, J.I. Mamiya, and Y. Yu, Angew. Chem., Int. Ed. **46**, 506-528 (2007). 4. C. Bertarelli, A. Bianco, R. Castagna, and G. Pariani, J. Photochem. Photobiol. C **12**, 106-125 (2011). 5. T. Adams, *et al*., Adv. Funct. Mater **31**, 2103408 (2021). 6. N. Shuchi, *et al*., Opt. Mat. Exp. **13**, 1589-1595 (2023). 7. T. Adams, *et al*., ACS Appl. Opt. Mater. *in press* (2024).

Friday Morning, November 8, 2024

11:15am **EL-FrM-13 Non-Destructive Measurement Limitations of Cavity Etched Si/SiGe Layer Superlattice Structures Using MMSE Based OCD Metrology and X-Ray Fluorescence**, *Ezra Pasikatan,* SUNY Albany CNSE*; Andrew Antonelli,* ONTO Innovation*; Nicholas Keller,* Onto Innovation*; Markus Kuhn,* Rigaku*; Satoshi Murakami,* Rigaku, Japan*; Alain Diebold,* SUNY Albany CNSE

Next generation node 3D semiconductor device structures require non-destructive metrology in order to measure key geometries for process control in high volume manufacturing. A key challenge is understanding the limitation of metrology for measuring Si/Si(1-x)Ge(x) superlattice structures, which are used in the manufacture of gate all around (GAA) transistors and future 3D DRAM memory. Nanowire test structures (NWTS) are used to measure the critical cavity etch step, where the SiGe layers in the superlattice are selectively etched to leave silicon nanowires or nanosheets.

A set of four superlattice layer NWTS were measured using Mueller matrix spectroscopic ellipsometry (MMSE) based optical critical dimension (OCD) metrology and X-ray fluorescence (XRF). Measurements were done on samples at superlattice film, anisotropic column etch, and two levels of cavity etch processing steps. X-ray diffraction (XRD) was used to determine superlattice film sample layer information for optical modeling. Limitations of MMSE based OCD modeling were explored based on contributions to measurement and model uncertainty, as well as measurability indicators. Also, matching of the non-destructive OCD and XRF based cavity etch measurements was evaluated based on a set of destructive focused ion beam (FIB) prepared transmission electron microscope (TEM) samples.

11:30am **EL-FrM-14 Elevated Temperature Spectroscopic Ellipsometry Analysis of Bulk Single-Crystal In_2O_3**, *Sema Guvenc Kilic, Ufuk Kilic,* University of Nebraska-Lincoln*; Matthew Hilfiker,* Onto Innovation*; Zbigniew Galazka,* Leibniz-Institute für Kristallzüchtung, Germany*; Mathias Schubert,* University of Nebraska-Lincoln

Transparent conductive oxides (TCOs) are materials that have a wide band gap in the ultraviolet region [1] and have been utilized in the optoelectronic industry, including solar cells, transistors, window heaters, transparent electrodes, and flat panel displays [2,3]. Among these, indium oxide (In_2O_3) is prominent due to its pronounced electron mobility and large band gap values.

In this study, we employed an in-situ spectroscopic ellipsometry (a single-rotating compensator ellipsometer, M-2000, J. A. Woollam Co., Inc.) instrument attached to a high vacuum chamber that employs a heater stage. While the angle of incidence on the sample within the chamber is at 75°, the pressure is measured to be under 6.5×10^{-5} Torr. Hence, we performed the investigation of the dielectric function properties of melt-grown bulk In_2O_3 single crystal [4] at elevated temperatures (22°C ≤ T ≤ 600°C). For each temperature value, Cauchy dispersion analysis was applied across the transparent spectrum to determine the high-frequency index of refraction. In addition, critical point model dielectric function analysis was performed to obtain the complex dielectric function and critical point transitions for selected temperature values. Ellipsometry measurements were conducted covering the spectral range from the near-infrared to the ultraviolet (300 nm to 1200 nm). Additionally, we present and discuss the room temperature wide spectral range (near-IR to vacuum ultraviolet) complex dielectric function of In_2O_3. Results indicate a pronounced temperature dependence of both the real and imaginary parts of the dielectric function, attributed to possible alterations in the electronic band structure and carrier concentration with temperature. These findings provide crucial insights into the thermal behavior of In_2O_3, aiding in the design and optimization of temperature-resilient optoelectronic devices.

References

1. Miao, L., S. Tanemura, Y. G. Cao, and G. Xu. "Spectroscopic ellipsometry study of In_2O_3 thin films." Journal of Materials Science: Materials in Electronics 20 (2009): 71-75.
2. Granqvist, C. G. "Transparent conductive electrodes for electrochromic devices: A review." Applied Physics A 57 (1993): 19-24.
3. Hamberg, Ivar, and Claes G. Granqvist. "Evaporated Sn-doped In_2O_3 films: Basic optical properties and applications to energy-efficient windows." Journal of Applied Physics 60, no. 11 (1986): R123-R160.
4. Z. Galazka, R. Uecker, R. Fornari; J. Cryst. Growth 388 (2014) 61-69.

11:45am **EL-FrM-15 Modeling Many-body Effects in Ge Using Pump-probed Femtosecond Ellipsometry**, *Carlos Armenta,* New Mexico State University*; Martin Zahradník,* ELI ERIC, Czechia*; Carola Emminger,* Leipzig University, Austria*; Shirly Espinoza,* ELI ERIC, Czechia*; Mateusz Rebarz,* ERIC ELI, Poland*; Saul Vazquez,* ELI ERIC, Mexico*; Jakob Andreasson,* ELI ERIC, Czechia*; Stefan Zollner,* New Mexico State University

This study investigates the transient dielectric function of germanium at very high electron-hole pair densities using time-resolved spectroscopic ellipsometry. By employing a pump-probe technique, we explore the evolution of the critical points E_1 and $E_1+\Delta_1$ near the L-valley as a function of delay time. We primarily focus on phase-filling singularities and many-body effects in different undoped germanium samples. Our aim is to model the behavior of the material under different carrier concentrations, analyze the impact these processes have on the material's optical properties, occurring at the temporal resolution on the order of femtoseconds.

The analysis includes modeling the dielectric function of germanium as carrier densities evolve throughout time. It addresses additional effects during electron excitation and relaxation, such as excitonic screening and acoustic phonon oscillations from energy transfer to the lattice. Experiments are conducted on bulk germanium samples oriented along various crystallographic planes. By pumping the sample with a high-power laser with 800 nm wavelength, carrier densities on the order of 10^{20} cm^{-3} were achieved. Delay times range from -10 ps to 1 ns with a 500 fs resolution. Our findings aim to enhance the understanding of germanium's optical behavior under intense laser excitation, providing insights into rapid charge carrier dynamics and their influence on the material's electronic structure.

Manufacturing Science and Technology
Room 117 - Session MS-FrM

Next Generation and Sustainable Micro-/Nano-Manufacturing
Moderators: Erica Douglas, Sandia National Laboratories, **Diane Hickey**, Department of Energy

8:15am **MS-FrM-1 DOE's Microelectronics Energy Efficiency Scaling for 2 Decades (EES2)**, *Tina Kaarsberg,* U.S. Department of Energy*; Jeffrey W. Elam,* Argonne National Lab*; S. Misra,* Sandia National Laboratory*; S. Shankar,* SLAC National Accelerator Laboratory

In response to analysis showing both slowing efficiency improvements and exponential growth in electricity use by computing and other microelectronics technologies, the United States Department of Energy (DOE) Advanced Materials and Manufacturing Technology Office (AMMTO) is leading a multi-organization effort to counter these trends with its initiative in energy efficiency scaling for two decades (EES2) for microelectronics.Similar to the "scaling" of the first few decades of microelectronics, this energy efficiency scaling would result in the biennial doubling of integrated circuits' or chips' energy efficiency. DOE's EES2 initiative aims to flatten microelectronics energy by enabling 10 biennial efficiency doublings to more than a factor of 1000 in two decades. By Earth Day 2024, 65 organizations representing industry, academia, and DOE national laboratories had signed the EES2 pledge.A key element of the pledge is an EES2 R&D Roadmap to identify "technologies to beat" that are 10 to 10,000X more energy efficient that the technologies they would replace. Version 1.0 of the EES2 roadmap is focused on enabling energy efficiency in computing by software-driven co-design across all elements of the compute stack as well as continued innovation in new non-miniaturization-related device technologies and circuit architectures.This talk will present results of version 1.0 of the roadmap highlighted with EES2-sponsored R&D. This EES2 roadmap and the R&D inspired by it is the first phase of an ongoing commitment to energy-efficient and sustainable microelectronics electricity use incomputing, communications and other emerging applications. On August 14, DOE released the draft EES2 Roadmap [https://www.energy.gov/eere/ammto/articles/doe-seeks-input-dramatically-increase-energy-efficiency-semiconductor?utm_medium=email&utm_source=govdelivery] as part of an RFI [https://eere-exchange.energy.gov/Default.aspx] . The Roadmap itself is at EES2 Roadmap Version 1.0 focused on Compute [https://eere-exchange.energy.gov/FileContent.aspx?FileID=f4234e29-cc0c-4a56-a510-86b616ab5535] . Respond to the RFI by writing to micro.electronics@ee.doe.gov [mailto:micro.electronics@ee.doe.gov] .

8:30am MS-FrM-2 An Energetically Low-Cost Future for Advanced Semiconductor Manufacturing, *John Randall, **Joshua Ballard**,* Zyvex Labs

The DOE Advanced Materials and Manufacturing Technologies Office (AMMTO) sponsored Semiconductor Industry Energy Efficiency Scaling (EES2) roadmap has identified Extreme Ultraviolet Lithography (EUV) as a significant contributor to the energy budget of advanced digital electronics [reference roadmap and Bardon and Parvais 2023]. Strikingly, EUV is so inefficient that only about 0.04% of the beam energy actually affects the resist [Shankar 2023]. Additionally, EUV – and e-beam lithography (EBL) used to make masks for EUV–are reaching their resolution limits which limits the ability to continue to make operational efficiency gains in digital electronics typical with the march of Moore's Law and Dennard scaling which posits that energy consumption scales with total device or chip area. For conventional devices, the extra precision will also allow lower voltage swings for switching to be used, which will further reduce energy consumption during usage. In the particular case of quantum devices, extreme precision in their dimensions is required; a variation of 2 nm can halve or double tunnelling rates in a quantum dot qubit, a level of precision beyond the capability of EBL or EUV.

The EES2 roadmap identifies the replacement of EUV with Nanoimprint lithography (NIL) as a key takeaway. NIL offers equal and better resolution and precision than EUV, with up to 90% lower energy costs [DNP 2023], resulting in lower costs of production.

This presentation will describe a pathway towards unprecedented resolution in nanoimprint mask fabrication. Ultrahigh-precision NIL templates are made by writing sub-nm precision patterns on Si(001) using H Depassivation Lithography (HDL), followed by selective growth via atomic layer deposition (ALD) of a hard mask such as TiO_2, which is then used as an etch mask for Reactive Ion Etching (RIE) to form a 2.5D Si template, replicating the STM pattern. This template would then be transferred into a quartz template using existing step and flash NIL processes which will be used to pattern devices. We show that sub-10 nm feature sizes and full-pitch gratings with feature radius of curvature down to 1.5 nm in the lateral dimension can be achievable. This NIL therefore addresses two AMMTO goals; atomically-precise manufacturing, and the EES2 goal of improving the energy efficiency during manufacturing and–as a fortunate side effect–during operation of digital electronics.

8:45am MS-FrM-3 Plasma Processing and the Semiconductor Supply Chain in an Era of Low GWP and/or PFAS-Free Gas Chemistries, *Eric Joseph,* IBM Research Division, T.J. Watson Research Center

Sustainability policy across the globe has become a major driver of change for the semiconductor industry and its supply chain.New net-zero emission goals and overall phase-out targets for PFAS materials are a noble cause, but an exemplary challenge to solve in a relatively short time.In this presentation, we will review the critical nature of PFAS and the widespread impact of these materials across the ecosystem.The evolution of fluorocarbon (FC) and hydrofluorocarbon (HFC) etch gas materials, a subset of PFAS which are essential in plasma processing applications, will be discussed in detail.The talk will then summarize ongoing and recent efforts to begin exploring (1) process optimization to minimize PFAS and high global-warming potential FC/HFC gas usage, (2) alternative low GWP or PFAS free material exploration and (3) capture/recovery/abatement opportunities to avoid release of these materials after use.The challenge throughout will be to satisfy all process metrics for success, which have been extensively researched over the past 50 years, and bring them towards full scale adoption industry wide which ultimately improves sustainability.

9:00am MS-FrM-4 Patterning and Etch Development of High Aspect Ratio 2.5D MIM Capacitor Structures, *Quyang Lin, Philip Nolmans, Daniel Montero Alvarez, Frederic Lazzarino, Gerald Beyer, Geert Van der Plas, Eric Beyne,* IMEC Belgium

The microelectronics industry demands smaller and more efficient chips for future-generation fabrication nodes. While most efforts of chip downscaling are focused on reducing the size of logic units, it is also important to scale capacitors accordingly to meet the design criteria of newer nodes. In this context, 2.5-D high-density metal-insulator-metal (MIM) capacitors (CAP) were proposed, offering several advantages such as high capacitance density, low parasitic impact, small form factor, and low cost [1][2]. Ref. [1] demonstrated 2.5-D MIMCAPs exhibiting 26nF/mm2 capacitance density, 3.6 times higher compared to 2D planar MIMCAP. In this work, we further scaled down 2.5-D MIMCAP by reducing the pitch, 70nF/mm2 is achieved with 10nm HfAlOx dielectric. Additionally, we pattern higher Aspect Ratio (AR) studs to effectively increase the capacitance density.

The initial design of 2.5-D MIMCAPs featured 1µm SiO2 studs with a 200nm Critical Dimension (CD) and 484nm pitch with a 5 AR [1]. Simulation results indicate that higher oxide stud enables higher capacitance density, with CD and pitch also crucial due to their role in defining the effective area and the thickness limitations of MIM layers. In this work, the development is conducted on 300mm wafers. 1-2µm oxides are deposited on top of a TaN layer. Then, the hard mask stack deposition process follows, composed of 50nm DARC and 1300nm APF. Immersion lithography is then employed to print studs with CD 200nm/Pitch 380nm. The pattern is transferred to the oxide layer, resulting in oxide studs up to 10 AR. MIMCAPs are then deposited on oxide studs (Supplement Fig. 1 and 2). Etch development becomes very challenging with such HAR and dense pitch due to the deterioration of studs: too small CD, excessive slope, and stud bending. Additionally, the thickness of APF is not supported to etch 2µm oxide, while the thicker APF is not the case because of wafer warping caused by compressive stress. To tackle these challenges, different etch investigations like gas mixture, high and low frequency powers have been conducted in various etch steps, to optimize the oxide stud CD and slope, and to understand their impact on the oxide etch rate and the selectivity to APF to enable oxide studs up to 2µm (Supplement Fig. 3 and 4).

In this work, new patterns of 2.5-D MIMCAPs are proposed, measured capacitance density is up to 70nF/mm2 on a 1µm oxide height. The formation of 2µm oxide studs of 200nm CD (10 AR) in a dense pitch of 380nm with ideal slope is ultimately achieved, promising a further substantial improvement on capacitance density. Moreover, this etch work shows the potential to achieve oxide studs with 15 AR.

9:15am MS-FrM-5 CMOS Design Pathways to Sustainable Compute Scaling, *Azeez Bhavnagarwala,* Metis Microsystems **INVITED**

In its Decadal Plan [1], the Semiconductor Research Corporation (SRC) projections of energy demand for computing versus global energy production are creating new risks - with semiconductors expected to consume nearly 25% of global energy by 2030. Computing power demands *double every two months* [2] where computational loads - in number of computations, continue to grow exponentially – driven primarily by the growth in artificial intelligence (AI) applications and training workloads. New approaches to computing, such as in-memory compute, special purpose compute engines, different AI platforms, brain inspired/neuromorphic computation etc. are identified by the SRC as necessary to support scaling of compute performance beyond barriers imposed by energy efficiency of conventional CMOS semiconductor architectures. In its Decadal Plan, the SRC asserts that *changing the computing trajectory with these innovations would be much more cost-effective than attempting to dramatically increase the world's energy supply*.

This work [3] describes alternative CMOS circuit architectures that harvest the evaluation energy of dynamic circuits - primarily used across CMOS memories and high performance CMOS arithmetic components while also engaging harvested charge to improve circuit speeds during signal development and data resolution. Harvesting circuits also self-regulate signal development by memory cells mostly eliminating the performance and energy overheads from bit cell variability seen with industry-typical circuit architectures enabling 10X improvements in the Energy-Delay metric at the component level - a 5X reduction in active energy without lowering operating voltages and a 2X improvement in circuit speed without raising operating voltages. Proposed circuit architectures do not require changes to the CMOS process, to the foundry bit cell or to the design, test and verification flows minimizing their risk and path to market. With over 70% of Accelerator chip power consumed by CMOS Memories [4], proposed circuit architectures also remove limitations on processor FMAX imposed by heat removal while also relaxing thermal constraints on the package design enabling higher semiconductor packaging efficiencies.

[1] https://www.src.org/about/decadal-plan/decadal-plan-full-report.pdf

[2] https://www.nature.com/articles/s41586-021-04362-w

[3] A Bhavnagarwala, published US Patents

[4] W Daly, Keynote at Hot Chips Conference 2023 https://hc2023.hotchips.org/assets/program/conference/day2/Keynote 2/Keynote-NVIDIA_Hardware-for-Deep-Learning.pdf [https://hc2023.hotchips.org/assets/program/conference/day2/Keynote%202/Keynote-NVIDIA_Hardware-for-Deep-Learning.pdf]

9:45am MS-FrM-7 Semiconductor Technology Needs Vacuum - How Growth in the Semiconductor Industry and Sustainable Production Can Be Achieved, *Kevin Mahler, Klaus Bergner,* VACOM, Germany

Everyone is talking about semiconductor manufacturing - but it is vacuum technology that makes it possible. In our presentation, we will highlight the role of vacuum technology as a high-tech enabler for essential key technologies in the field of semiconductor production. In particular, we will address the emerging tension between a projected market growth to $ 1 trillion in 2030, the necessary resource requirements and the increasing demands in the area of sustainability.

We then show how VACOM has implemented a sustainable vacuum mechanics production factory - far beyond the existing requirements from the semiconductor industry and politics. We highlight the role played by available resources such as air, water, sun, earth and people and how this is combined in a globally unique overall concept. The focus will be on sustainable infrastructure in production - a field of work that is sometimes underrepresented in product-related analyses and optimizations. In summary, we will show how ecological, economic and physiological possibilities can interact in a circular economy.

10:00am MS-FrM-8 High Resolution Ion Beam Imaging, Nano-Scale Analytics and Nanofabrication with Light and Heavy Ions from a Single Ion Source, *Peter Gnauck, Torsten Richter, Alexander Ost,* Raith GmbH, Germany

The liquid metal alloy ion source (LMAIS) technology has become a key component for Focused Ion Beams (FIB) nanofabrication in recent years [1]. Its remarkable beam current stability, patterning and imaging resolution, coupled with the ability to rapidly adjust the sputtering yield by switching between different ions within seconds, enable working on versatile applications using this source technology (Fig. 2).

The visualization of nanoscopic samples in 3D holds great significance across various domains, including nanotechnology, life sciences, and materials science, as it offers enhanced insights into surface and internal structures compared to traditional 2D imaging. While conventional methods for 3D volume reconstruction involve slice-wise imaging and milling of the sample with stage tilt, the usage of the LMAIS technology with light and heavy ions from a single source introduces a novel approach to obtain 3D volume information.

The GaBiLi source revolutionizes 3D imaging by alternating between imaging with Li$^+$ primary ions at high spatial resolution in secondary electron (SE) mode and fast switching to milling mode with Bi$^+$ primary ions with a high sputtering rate. Using this Mill&Image workflow the ion beam remains perpendicular to the sample surface without requiring sample tilt. The resulting collection of SE images can be assembled into a 3D stack, facilitating visualization of the sample's internal structures (Fig.1).

This FIB technology has been recently merged with a dedicated SIMS unit, combining high sensitivity, transmission and best spatial image resolution. The SIMS unit consists of key components like (i) specifically designed extractable/insertable secondary ion extraction and transfer optics ensuring maximum extraction efficiency and transmission, thereby ensuring high sensitivity, (ii) a compact floating double focusing magnetic sector mass spectrometer enabling operation in DC mode at high transmission, without performance-degrading duty cycles encountered in TOF systems, (iii) a continuous detector enabling the simultaneous detection of all masses in parallel.

This novel platform offers element imaging at the nanoscale, isotope differentiation, depth profiling and 3D chemical analysis (Fig. 3).

In this presentation, we will explore the potential for topographic 3D data with analytical surface information obtained through Secondary Ion Mass Spectrometry (SIMS), offering a forward-looking perspective on the synergistic possibilities of these capabilities and nanofabrication.

[1] K.Hoeflich et al., Appl. Phys. Rev. 10, 041311 (2023)

10:30am MS-FrM-10 Efficient 3D Printing: Investigating Wall Count as an Alternative to High Infill Density in PLA, PET-G, and PA-CF, *Devyn Fidel, Moe Rabea,* California State Polytechnic University, Pomona

An important aspect of 3D printing is using the proper slicer settings to ensure that the part printed will have the desired properties, i.e., tensile strength and print quality. While convention often highlights maximizing infill density to enhance strength, this study explores methods to achieve optimal tensile strength without resorting to 100% infill, which can be wasteful and economically inefficient—specifically, increasing the wall (or perimeter) count. Regarding slicer settings, walls refer to the number of perimeters printed concentrically around the contour of a part. Adding

more walls can offer greater strength than traditional infill structures due to the alignment of walls along the primary load-bearing axis using the same amount of material. This study compared the tensile strength of 3D-printed PLA, PET-G, and PA-CF specimens. One set of specimens had varying wall counts, and the other group had varying infill densities. The data showed that increasing wall count offers superior strength to traditional infill structures using less material.

10:45am MS-FrM-11 Sustainable Microelectronics in the Age of Ai, *Emre Salman,* Stony Brook University **INVITED**

Artificial Intelligence (AI) is increasingly pivotal in advancing the sustainability of microelectronics. It not only enhances energy efficiency through the discovery of innovative materials, devices, manufacturing technologies, but also optimizes the design automation of complex microelectronic systems. Beyond microelectronics, AI significantly contributes to environmental sustainability, notably in optimizing smart grids and advancing climate modeling to predict changing patterns more accurately. Despite these benefits, AI algorithms are executed on energy-intensive hardware platforms, predominantly housed in datacenters, which raises concerns about their environmental impact.

The energy footprint of AI hardware comprises two major elements: (1) the energy expended in the manufacturing of AI hardware, which predominantly uses advanced CMOS technologies facilitated by extreme ultraviolet (EUV) lithography, and (2) the operational energy consumption of datacenters, which includes both the computation and the cooling systems. This presentation will provide a comparative analysis of these critical components, emphasizing the significant energy demands of producing nanoscale CMOS-based integrated circuits and the substantial power used during computational tasks in datacenters.

To mitigate these challenges, the talk will explore a variety of innovative strategies and emerging technologies designed to reduce the energy footprint associated with both the manufacturing processes and the operational phases of AI hardware. The discussion will highlight recent advancements that promise greater efficiency and sustainability in the lifecycle of AI systems.

Plasma Science and Technology
Room 124 - Session PS+TF-FrM

Plasma Processes for Coatings and Thin Films

Moderators: François Reniers, Université Libre de Bruxelles, **Scott Walton**, Naval Research Laboratory

8:15am PS+TF-FrM-1 Interaction of Polycrystalline Aluminum Oxide and Sapphire Surfaces with Halogen-Containing Plasmas and Gases, *Takuya Ishihara, Hidenobu Tochigi,* Azbil corporation, Japan*; Hojun Kang,* Osaka University, Japan, Republic of Korea*; Tomoko Ito, Kazuhiro Karahashi, Satoshi Hamaguchi,* Osaka University, Japan

In semiconductor manufacturing processes such as dry etching or chemical vapor deposition, capacitance manometers are widely used as essential vacuum pressure sensors to monitor and control the pressures of process gases. These gauges must be corrosion-resistant against process gases such as halides and their radicals generated by the plasmas. The diaphragm material of the manometer is especially important because, if its surface is altered by such corrosive gases, the sensor would send imprecise output signals possibly with the zero-point drift or pressure sensitivity shift. The errors are caused by the changes in mechanical properties of the diaphragm arising from the formation of the modified surface layer. For this reason, Ni-based alloys or polycrystalline ceramics of aluminum oxide (Al_2O_3) are typically used as the diaphragm material of capacitance manometers. More recent capacitance manometers employ sapphire (single crystal α-Al_2O_3) as their diaphragm material, which is of specific interest in this study[1]. Recent studies on the interactions of polycrystalline Al_2O_3 with fluorine-containing plasmas indicated the formation of aluminum fluoride layers on Al_2O_3 exposed to such plasmas [2-6]. In this study, ion beam experiments were performed, aiming to understand the surface modification mechanisms of Ni-based alloys and polycrystalline Al_2O_3 film by fluorine-containing plasmas. With the irradiation of energetic F$^+$ and Cl$^+$ ions, it was found that the typical etching rates of Al_2O_3 are about one-half of those of Ni-based alloys. It was also found that the fluorinated layers of Al_2O_3 were thinner than those of Ni-based alloys. In addition, surfaces of sapphire samples were exposed to xenon difluoride (XeF$_2$) gases for 3 and 6 months. The sapphire surface was fluorinated over the first 3 months, but the depth of the fluorinated layer

did not increase much after 6 months. It indicates that a diaphragm made of pre-fluorinated sapphire may be able to prevent the signal shift of the manometer used under highly corrosive conditions in semiconductor manufacturing.

[1] T. Ishihara, *et al*, 35th Sensor Symposium (2018)

[2] Chen Chien-Wei, *et al*, J. Vac. Sci. Technol. A Vol.41 No.1 Page.012602-012602-9 (2023)

[3] Kim Yewon, *et al*, Appl. Surf. Sci. Vol.641 Page. Null (2023)

[4] Vos Martijn F. J., *et al*, J. Phys. Chem. C Vol.125 No.7 Page.3913-3923 (2021)

[5] Chittock Nicholas J., *et al*, Appl. Phys. Lett. Vol.117 No.16 Page.162107-162107-5 (2020)

[6] Fischer Andreas, et al, J. Vac. Sci. Technol. A. Vol.38 No.2 Page.022603-022603-7 (2020)

8:30am PS+TF-FrM-2 Development of Corrosion-Resistant, Low-ICR aC and TiN Coatings Using HIPIMS for Bipolar Plate Manufacturing for Hydrogen Fuel Cells, *Nicholas Connolly*, University of Illinois at Urbana-Champaign*; Zachary Jeckell,* University of Illinois Urbana-Champaign*; Rajib Paul, Michael Hysick,* Starfire Industries*; Md. Amzad Hossain, Brian Jurczyk, David Ruzic,* University of Illinois Urbana-Champaign

Bipolar plates (BPPs) are a critical component in proton exchange membrane fuel cells (PEMFCs) that provide conducting paths for electrons between cells, distribute and provide a barrier for reactant gases, remove waste heat, and provide stack structural integrity. Stainless steel, specifically 316L, BPPs possess high electrical and thermal conductivity, good gas impermeability, and superior mechanical properties and formability. However, stainless steel has relatively low corrosion resistance and high contact resistance in the hydrogen fuel cell stack. Additionally, to meet the Department of Energy (DOE) cost/kW target for hydrogen fuel cells, recycling of the BPPs is practically a necessity.

In order to address these challenges, we will present work on two complementary studies. The first study is deposition of conformal amorphous carbon (aC) and titanium nitride (TiN) thin films using HIPIMPS with positive cathode reversal. The interfacial contact resistance (ICR), corrosion current, and corrosion potential are reported for various aC and TiN thin films to characterize the contact resistance and corrosion resistance. The second study is etching of the previously deposited aC and TiN films in a HIPIMS system with a high-voltage cathode reversal, testing the possibility of recycling the BPP. The contact resistance and corrosion resistance are compared after the initial film deposition and then after etching of the initial film and redeposition on the same substrate.

8:45am PS+TF-FrM-3 Evolution of Graphene Nanoflake Size and Morphology in Atmospheric Pressure Microwave Plasma, *Parker Hays, Dhruval Patel, Dren Qerimi,* University of Illinois at Urbana-Champaign*; Michael Stowell,* LytEn*; David Ruzic,* University of Illinois at Urbana-Champaign

Graphene was synthesized using an atmospheric pressure microwave plasma system, employing argon/nitrogen mixtures as carrier gases and methane as the carbon precursor. This study investigates the effects of varying methane flow rates and plasma power on graphene growth, including the role of gas temperature. The process involves the decomposition and subsequent reorganization of carbon radicals into graphene sheets. To collect the synthesized graphene, tungsten carbide rods were strategically positioned at three distinct points along the plasma column.

The variations in particle diameter were systematically analyzed using Dispersive Light Scattering (DLS) and Scanning Electron Microscopy (SEM). Results indicate that particle diameter generally decreases along the plasma column until reaching a critical power threshold. Beyond this threshold, the diameter increases, particularly at the middle collection port, suggesting the presence of an optimal "Goldilocks zone" for graphene growth. This zone, located at the juncture between the bulk plasma and its afterglow, exhibits a significant temperature gradient, potentially ideal for graphene formation.

Further, an increase in methane flow rate correspondingly reduced the particle diameter across all ports, attributed to enhanced plasma quenching effects. Conversely, an escalation in plasma power led to an increase in particle diameter, likely due to the extension of the plasma field.

These findings demonstrate that manipulating methane flow rates and plasma power can significantly influence graphene particle size, optimizing growth conditions within the identified Goldilocks zone. This study provides a deeper understanding of the thermodynamic and chemical mechanisms governing graphene synthesis in microwave plasma systems, offering a pathway to tailored graphene production for advanced material applications.

9:00am PS+TF-FrM-4 Gentle Processing of Graphene and Diamond in a Low Temperature Magnetized Plasma, *Yevgeny Raitses,* Princeton Plasma Physics Laboratory*; Fang Zhao,* Fermi Lab*; Christian Pederson, Kai-Mei Fu,* University of Washington*; Arthur Dogariu,* Princeton University

In this work, we present results of the use of a low temperature plasma in applied magnetic field for graphene hydrogenation and hydrogen passivation of diamond. The chemical functionalization of two-dimensional materials is an effective method for tailoring their electronical and chemical properties with encouraging applications in energy, catalysis and electronics. Experiments on graphene hydrogenation [1] revealed that with the applied magnetic field of 10-50 Gauss, a plasma generated by a DC-RF source of non-thermal electrons at a hydrogen pressure of about 10 mtorr is capable to achieve a high (~ 36%) hydrogen coverage without damage on monolayer graphene. Plasma measurements utilizing electrostatic probes for measurements of plasma properties, optical emission spectroscopy for characterization of plasma chemical composition and two-photon absorption laser-induced fluorescence (TALIF) for measurements of absolute hydrogen density revealed that with the applied magnetic field, the plasma density and the density of hydrogen atoms are much larger than without the magnetic field. The latter explains a high converge observed in the treated 2D material [1]. In more recent experiments, the same plasma source was applied for hydrogen passivation of diamond for quantum defect charge state control [2]. Measurements indicate that in this novel plasma treatment hydrogen terminates the surface with no observable damage to diamond.

References

[1] F. Zhao, Y. Raitses, X. Yang, A.Tan, and C. G. Tully, "High hydrogen coverage on graphene via low temperature plasma" **177**, 244 (2021)

[2] C. Pederson, et al., "Optical tuning of the diamond Fermi level measured by correlated scanning probe microscopy and quantum defect spectroscopy" Phys. Rev. Mater. **8**, 036201 (2024)

9:15am PS+TF-FrM-5 A Plasma-Based Anodization Process for the Production of AlF₃ Layers, *Scott Walton, John Murphy,* US Naval Research Laboratory*; Luis Rodriguez de Marcos, Javier Del Hoyo, Manuel Quijada,* NASA*; Virginia Wheeler, Maria Sales, Mackenzie Meyer, David Boris,* US Naval Research Laboratory

Efficient ultraviolet (UV) mirrors are essential components in space observatories for UV astronomy. Aluminum mirrors with fluoride-based protective layers are commonly the baseline UV coating technology; these mirrors have been proven to be stable, reliable, and with a long flight heritage. However, despite their acceptable optical performance, it is still insufficient for future large telescopes in which several reflections are required. Recently, a readily scalable, plasma-based passivation process was developed to produce a thin AlF3 layer on the surface of aluminum. The passivation process uses an electron beam generated plasma produced in a fluorine-containing background (SF6 or NF3), to simultaneously remove the native oxide layer while promoting the formation of an AlF3 layer with a tunable thickness. Interestingly, this process has the characteristics of classic aluminum anodization – either electrochemical or plasma – where oxygen is replaced by fluorine. The process takes advantage of the ability for electron beam driven plasmas produced in electronegative gas backgrounds to generate substantial densities of negative ions, which are utilized to grow the fluoride layer. In this presentation, we will discuss the process using operating parameter studies, plasma diagnostics, and materials characterization, with an eye on understanding the growth mechanisms and the potential for better process control. This work partially supported by the Naval Research Laboratory base program.

9:30am PS+TF-FrM-6 One-Step Synthesis of Spatially Differentiated Crystalline Vanadium Oxide Coatings Using Atmospheric Pressure Dielectric Barrier Discharge, *Marie Brabant, Annaelle Demaude, David Petitjean, François Reniers,* Université libre de Bruxelles, Belgium

Initially perceived as a limitation, the presence of inconsistencies in DBDs presented obstacles to achieving uniform plasma treatments and coatings. However, recent breakthroughs in immobilizing filaments within DBDs have demonstrated effective control over these irregularities.[1,2] This

development has now enabled the deposition of innovative patterned inorganic coatings that were previously unexplored. Vanadium oxide coatings, in particular, hold promise for diverse applications, including catalysis,[3] memory compounds,[4] or as practical solutions for smart windows.[5]

This study introduces a pioneering method for locally depositing dense crystalline inorganic coatings (V_2O_5) without requiring annealing and utilizing atmospheric pressure DBDs, marking a significant advancement in the field. Vanadium oxide coatings with spatial variation were successfully deposited in a single step using an atmospheric pressure dielectric barrier discharge featuring immobilized filaments. Initial findings indicate fast deposition rates beneath the filament regions and low deposition rates between them. Moreover, differences in the oxidation states of vanadium beneath the filaments and between them were also observed, suggesting different reactivities.[6]

Through the incorporation of a patented inductive heating device into the reactor,[7,8] coupled with a pulsed signal, crystalline coatings were obtained by heating the substrate at 473 K, occasionally resulting in crystal needles measuring up to 50 μm in length. This crystallinity was confirmed by XRD analysis.

While further optimization is necessary to refine gas and reactive species distribution, this feasibility study demonstrates the potential for locally depositing crystalline coatings using a DBD with immobilized filaments and an appropriate substrate heating system, paving the way for new applications.

References :

1. A. Demaude, et al. Adv. Sci. 9, 2200237 (2022).
2. A. Demaude, et al. Plasma Chem. Plasma Process. 43, 1731 (2023).
3. I. E. Wachs, Dalton Trans., 42, 11762 (2013).
4. A. Velichko, et al. Sci. Semicond, 29 , 315–20 (2015).
5. Y. Cui, et al. Joule, 2, 1707–46 (2018).
6. M. Brabant, et al. JVST A, 42, 023008 (2024).
7. A. Remy, et al. Thin Solid Films, 688, 137437 (2019).
8. A. Remy, F. Reniers. patent EP3768048A1 (2019).

9:45am **PS+TF-FrM-7 Biofilm Decontamination in an Endoscope-Like Setup Using a Cold Atmospheric Plasma**, *Juliette Zveny,* Université libre de Bruxelles, Belgium; *François Reniers, Antoine Remy,* Université Libre de Bruxelles, Belgium; *Teo Serra,* université libre de Bruxelles, Belgium; *Amelie Bourgeois,* Erasme Hospital, Belgium; *Antoine Nonclercq, Dalila Lakhloufi, Anne Botteaux,* université libre de Bruxelles, Belgium; *Alain Delchambre,* Université Libre de Bruxelles, Belgium; *Jacques Deviere,* Erasme Hospital, Belgium

Endoscopes are essential medical devices used to detect, prevent and cure many diseases. Well-established cleaning and decontamination procedures allow them to be used safely on multiple patients every day. However, cases of cross-contamination still occur, demonstrating that the decontamination process is flawed.[1] Here, we propose a novel decontamination method using an Ar/H_2O Cold Atmospheric Plasma (CAP).

In this research, we investigate the effect of CAP not only on bacteria, but also on biofilm.Biofilm is a matrix made by bacteria to increase their resistance to external stress.[2] Pseudomonas aeruginosa biofilms were grown during 24 hours in a PTFE tube mimicking the operating channel of an endoscope before being subjected to plasma treatment. The plasma was generated in a DBD setup with the high voltage applied between a metal wire passing through the contaminated tube and a metal mesh surrounding the tube.

The decontamination process consisted of a 30 min plasma in a water-saturated argon atmosphere. The chemical activity of the discharge was optimized by the presence of water, which allowed the production of hydroxyl radicals (OH) and hydrogen peroxide (H_2O_2), powerful oxidant species. Other parameters, such as the voltage, made it possible to increase the concentration of these species without increasing the power.

Plasma treatments showed effective decontamination capacities, with no bacteria found in the tube after regrowth for various treatment times (5 to 30min). It also shows promising results in terms of biofilm destruction, with up to 79% of the original biofilm destroyed. The biofilm destruction is dependent on the position inside the tube as well as on its own humidity.

OES measurements also highlight the voltage dependency on OH radical formation and biofilm destruction.

[1] A.W. Rauwers &al, Tech. Gastrointest. Endosc. 21 (2019). https://doi.org/10.1016/j.tgie.2019.04.006.

[2] U. Beilenhoff &al, Endoscopy. 49 (2017). https://doi.org/10.1055/s-0043-120523.

10:00am **PS+TF-FrM-8 Nonthermal Plasma Jet Integrated Aerosol-Based 3D Printing with Machine Learning Optimization**, *Jinyu Yang, Yipu Du, Kaidong Song, Qiang Jiang, Yanliang Zhang, David Go,* University of Notre Dame

Aerosol-based printing has emerged as a versatile technique to fabricate functional devices with complex structures, offering high throughput and microscale resolution, along with capabilities unattainable with traditional approaches. Despite these promises, the printing of conductive films often requires post-printing sintering to remove surfactants from the nanoparticle-containing inks and promote the sintering and densification to form a continuous film with desired electrical conductivity, which conventionally demands thermal processing at elevated temperatures. Herein, we report a novel aerosol jet printing method that integrates a nonthermal, atmospheric pressure plasma jet to enable *in-situ* sintering during aerosol deposition. The impacts of various processing parameters on printing quality and *in-situ* sintering efficiency are investigated. A machine learning algorithm is incorporated to provide online, real-time defect detection and parameter control, enhancing the yield of high-quality films via automatic *in-situ* compensation whenever a region-specific anomaly is detected. Our method achieves low temperature sintering of silver nanoparticles with electrical conductivities comparable with those sintered through other plasma treatment approaches. Because the films require no post processing, the overall manufacturing time can be reduced by more than tenfold. This method holds significant potential for technological advances in printed electronics, wearable devices, and biomanufacturing.

10:30am **PS+TF-FrM-10 Fluorine Plasma Assisted Remediation of Single Crystal Diamond Surfaces**, *Michael Mathews,* National Research Council Postdoctoral Fellow at U.S. Naval Research Laboratory; *Jonathan Levine-Miles, Bradford Pate,* US Naval Research Laboratory

The extreme material properties of diamond present unique opportunities for the development of novel high-power electronic devices. Achieving these advances are, however, not without challenges. In particular, the generation of unwanted defects in diamond homoepitaxial films is known to depend on the surface preparation of the diamond seed. Most notably, the nucleation of threading dislocations from sub-surface defects of mechanically prepared diamond surfaces prevent the realization of high-quality chemical vapor deposited diamond epi-layers. Once formed, these threading dislocations propagate into the newly formed homoepitaxial layer, degrading physical properties and impacting device performance.

This work introduces a four-step process to mitigate surface preparation challenges in single crystal diamond. In the first step, an isotropic fluorine-based reactive ion etch is used to remove damaged material below the diamond surface. This yields a surface with both adsorbed and chemisorbed fluorine corresponding to one- to several monolayers of fluorine coverage with some graphitic carbon arising from ion bombardment. The second step exposes the fluorinated surface to a rapid thermal anneal designed to remove non-sp^3 carbon species. Step three is a radical-dominant etch that addresses damage from ion bombardment intrinsic to typical reactive ion etch methods, and provides further surface smoothing. This etch exploits the aggressive surface chemistry of fluorine radicals and yields a surface that has some adsorbed and significantly less chemisorbed fluorine, with no increase in sp^2 (graphitic) carbon. This surface is then exposed to the same rapid thermal anneal (Step 4) described in the second step, yielding a smoother, higher quality diamond surface. Chemical and morphological changes of the surface in each step are characterized using x-ray photoelectron spectroscopy and atomic force microscopy.

Distribution Statement A: Approved for public release, distribution is unlimited.

10:45am PS+TF-FrM-11 Noncapillary Liquid Surface Waves Generated by Self-organized Plasma Patterns, *Oles Dubrovski,* University of Notre Dame, Israel*; Jinyu Yang,* University of Notre Dame, China*; Felipe Veloso,* Pontificia Universidad Católica de Chile, Instituto de Física, Chile*; Hsueh-Chia Chang, David Go, Paul Rumbach,* University of Notre Dame

Direct current (DC) plasmas are known to self-organize into a patterned state on a resistive anode surface. This phenomenon is commonly observed in plasma-liquid interactions, where plasma will self-organize into concentric rings or spots on the liquid surface, which then move and oscillate at frequencies of ~100 – 1000 Hz [1]. We propose that a Turing-like autocatalytic reaction-diffusion mechanism drives pattern formation in the plasma, and the size (wavelength) of the pattern structures is dictated by the reaction-diffusion wavelength of plasma electrons [2]. Electro-hydrodynamic (EHD) coupling at the interface creates liquid surface waves of the same wavelength as the pattern, resulting in dynamic motion (rotation and oscillation) of the plasma pattern. Increasing the viscosity of the solution causes the pattern motion to slow down, as predicted by viscous wave theory. Interestingly, the observed characteristic frequency of the plasma-liquid waves is much slower than predicted by capillary wave theory, indicating that EHD effects dominate, and surface tension effects are negligible [3].

[1] P. Bruggeman *et al.*, J. Phys. D: Appl. Phys. 41 (2008).

[2] P. Rumbach *et al.*, PSST 28 (2019).

[3] O. Dubrovski *et al.*, Phys. Rev. Lett. (2024) –i,n press.

11:00am PS+TF-FrM-12 Dielectric Barrier Discharge Configurations for Effective Biofilm Decontamination in PTFE Tubes, *Antoine Remy, Juliette Zveny, Teo Serra, Dalila Lakhloufi, Jacques Devière, Anne Botteaux, Alain Delchambre, François Reniers, Nonclercq Antoine,* Université libre de Bruxelles, Belgium

Biofilms are extracellular protective barriers produced by bacteria, enabling their growth and proliferation in otherwise inhospitable environments. Endoscopes are particularly susceptible to bacterial contamination and biofilm development. As a result, a single endoscope that has been thoroughly decontaminated can potentially transmit disease between multiple patients. The current solution in development, single-use endoscopes, while solving the contamination problem, may lead to an expansion of the environmental and technological dependence that is already a significant concern. This study investigates the potential of cold atmospheric discharge for endoscope sterilization. The study focused on two configurations of atmospheric pressure dielectric barrier discharge (DBD), generating a plasma in a long polytetrafluoroethylene (PTFE) tube. In order to generate reactive nitrogen and oxygen species (RONS), the discharge was generated in air, helium, water-saturated argon, and water-saturated helium. The first configuration uses two discharges, one upstream from the tube and another inside it, while the second configuration generates a single discharge directly within the tube. Prior to the decontamination tests, tube samples were contaminated by 24-hour grown *Pseudomonas aeruginosa* biofilm. We employed titration with $TiOSO_4$ to quantify the production of H_2O_2, while infrared absorption spectrometry was used to analyze the presence of gaseous species, including NO, N_2O, NO_2, HNO_3, and O_3. The efficacy of the bacterial decontamination and biofilm removal was evaluated through regrowth assays of the bacteria and crystal violet assays, respectively. Among the various gases used, helium/water and argon/water were identified as the most active, demonstrating complete bacterial decontamination of the tube after a 5-minute treatment. However, the biofilm remained largely unaffected. Future research will focus on optimizing the discharge composition and duration for biofilm removal, with the aim of developing a single-step endoscope decontamination process.

11:15am PS+TF-FrM-13 Plasma Nanocoatings for Surface Passivation of Silver Nanowires, *Qingsong Yu, Yixuan Liao, Ganggang Zhao, Yun Ling, Zheng Yan,* University of Missouri-Columbia

Low-temperature plasma processing is a unique technique in thin film deposition and surface modification of various materials. Plasma deposition can produce nano-scale coatings that are highly conformal to substrate surface topography, free of voids, and have robust adhesion to various substrates, including metallic substrates. Silver Nanowires (AgNWs) have found applications in strain sensors, transparent flexible conductors, light emitting diodes, e-paper, self-healing electronic devices, liquids crystal displays, artificial skins, and solar cells [1]. The unique properties of AgNWs make them promising candidates for various technological advancements, offering advantages over traditional materials in terms of flexibility, cost-effectiveness, and optical transparency.

In this study, trimethylsilane (TMS) plasma nanocoatings with controllable thickness of 10 – 100 nm were applied onto AgNWs to examine their passivation effects and electrical conductivity stability. Our experimental results showed that application of TMS plasma nanocoatings onto AgNWs induced < 25% increase in their electrical resistance, but effectively protected them from degradation due to surface oxidation/corrosion and, as a result, significantly improved their electrical stability under various environments with different humidity levels and temperatures. It was also observed that TMS plasma nanocoating changed AgNWs surfaces from hydrophilic to hydrophobic but did not affect much in their optical transparency, which is critical for use as transparent electrodes. Detailed experimental results will be presented and discussed in the conference.

[1] A. Madeira et al., "Increasing Silver Nanowire Network Stability through Small Molecule Passivation", Nanomaterials, **2019**, 9, 899; doi:10.3390/nano9060899

Surface Science
Room 120 - Session SS+AMS+AS+CA+LS-FrM

Advanced Surface Characterization Techniques & Mort Traum Presentation

Moderator: Charles Sykes, Tufts University

8:15am SS+AMS+AS+CA+LS-FrM-1 Infrared Spectroscopy as a Surface Science Technique, *Michael Trenary,* University of Illinois - Chicago **INVITED**

Infrared spectroscopy is widely used to probe the vibrational properties of molecules in the gas, liquid, and solid phases. On the other hand, precise information on the structure and chemistry of solid surfaces, and of molecular adsorbates on solid surfaces, is best gained through use of surface science methods. These methods generally entail the use of single crystals, ultrahigh vacuum conditions, and surface sensitive techniques. Reflection absorption infrared spectroscopy (RAIRS) is a surface sensitive technique that can be used in ultrahigh vacuum to study molecular adsorption on well characterized metal single crystal samples. Unlike many other surface science methods, it can also be used under elevated gas pressures. The spectra obtained display features that are quite distinct from those of other phases of matter. For example, in the gas phase, rotational fine structure greatly complicates the appearance of the spectra but is absent in the spectra of adsorbed molecules. In the liquid phase, spectra are broadened by both static and dynamic effects often making it difficult to resolve vibrational peaks due to different chemical species. In polycrystalline molecular solids, molecules are randomly oriented relative to the electric field directions of the infrared radiation, limiting the value of the spectra as a structural probe. In contrast, when molecules adsorb on metal surfaces, they often adopt a definite orientation with respect to the surface normal. This orientation can be deduced through the surface dipole selection rule, which states that only normal modes with a component of the dynamic dipole moment oriented along the surface normal will be allowed. While IR spectroscopy in several forms has long been used to study molecular adsorption on supported transition metal catalysts, the high degree of heterogeneity of the catalyst surfaces leads to very broad peaks, with full width at half maxima (FWHM) of 10-50 cm^{-1}. In contrast, the FWHM of peaks measured with RAIRS on well-ordered metal surfaces can be quite narrow, in some cases even less than 1 cm^{-1}. When a polyatomic molecule exhibits sharp peaks throughout the mid-IR range, the advantages of performing RAIRS with a Fourier transform infrared spectrometer are most pronounced. This talk will cover the speaker's forty years of research using the technique of RAIRS to study molecular adsorbates on metal surfaces.

8:45am SS+AMS+AS+CA+LS-FrM-3 Modeling Pipeline Surface Chemistry: Reaction of Monochloramine on Iron Surfaces, *Kathryn Perrine, Subash Pandey, Olorontoba Agbelusi,* Michigan Technological University

Monochloramine (NH_2Cl), a secondary disinfectant, is utilized to treat pathogens in the municipal water system, producing fewer halogenated disinfection by-products and lasting longer than free chlorine (hypochlorite). Although a weaker oxidant, NH_2Cl has the potential to corrode the surface of pipeline materials resulting in the dissolution of unwanted species. Copper and lead pipelines have been shown to corrode in chloramine solutions, however on iron materials the surface chemistry is unexplored. Complex chemistry occurs on the surface of pipelines at solution/metal interfaces, thus providing catalytic sites for dissociation, decomposition, and degradation. Iron comprises distribution pipelines and also exists as oxides in soils in the natural environment. Redox reactions

occur on the surface of iron materials, thus initiating surface corrosion. Here, various active sites on iron are produced and known for high reactivity with nitrogen compounds. Our group employs a surface science approach to uncovering mechanisms at complex interfaces.

In this study, the reaction of monochloramine (NH_2Cl) was investigated on single crystal Fe(111) in ultra-high vacuum at the gas/solid interface using *in situ* infrared reflection absorption spectroscopy and Auger electron spectroscopy. At -160 °C, NH_2Cl molecularly adsorbs to the surface while the annealing leads to the loss of key vibrational modes, suggesting that either molecular desorption or dissociation occurs. These observations are contrasted with our findings at the solution/iron interface, where polarized modulated infrared reflection absorption spectroscopy (PM-IRRAS), ATR-FTIR, XPS, and XRD were used to assess the various regions after corrosion and their film growth. In solution, localized heterogeneous corrosion products were observed and identified, suggesting different reaction pathways exist in strongly oxidizing solutions. These findings are important for understanding the mechanism of chloramines and water disinfectants on iron interfaces relevant for water quality, material degradation, and other complex environmental processes.

9:00am SS+AMS+AS+CA+LS-FrM-4 Development of Tip-Enhanced Raman Spectroscopy for Solid-Liquid Interfaces, *Naihao Chiang,* University of Houston

Tip-enhanced Raman spectroscopy (TERS) combines the spatial resolution of scanning probe microscopy (SPM) with the chemical sensitivity of Raman spectroscopy. TERS with sub-nanometer resolution has been demonstrated under ultrahigh vacuum conditions. We aim to extend this unprecedented chemical mapping capability to interfacial studies under the solution phase. Specifically, we have developed a scanning ion-conductance microscope for TERS (SICM-TERS) capable of interrogating soft samples. In this presentation, the instrumental design will be discussed first. SICM-TERS probe fabrication and evaluation will be followed. Then, a distance-dependent SICM-TERS measurement on two-dimensional MoS_2 sheets will be used to assess the strain created by the SICM probe in close proximity. Our results demonstrate the potential of combining TERS with SICM for obtaining chemical information at interfaces, thus setting the stage for future investigation into soft materials in electrolytic environments.

9:15am SS+AMS+AS+CA+LS-FrM-5 Ion Based Pump-Probe: Probing the Dynamics Following an Ion Impact, *Lars Breuer, Lukas Kalkhoff, Ann-Sophie Meyer, Nele Junker, Leon Lasnik,* Universität Duisburg-Essen, Germany*; Yifan Yao, Andre Schleife,* University of Illinois at Urbana Champaign*; Klaus Sokolowski-Tinten, Andreas Wucher, Marika Schleberger,* Universität Duisburg-Essen, Germany

The study of ion-surface interactions is crucial for understanding material properties and their atomic-level dynamic responses. The transient nature of these interactions, occurring on ultrafast time scales, has so far limited direct experimental observation and has left the field reliant on computer simulations. Existing experimental methods, such as pump-probe techniques, have faced challenges in generating and precisely timing short, monoenergetic ion pulses essential for capturing these ultrafast phenomena.

Our group has pioneered a novel approach that overcomes these limitations by generating the world's shortest monoenergetic ion pulses in the keV regime, with a current duration of approximately 5 ps. These pulses are produced using femtosecond photoionization of a geometrically cooled gas jet, coupled with miniaturization of the ionization section.

In our experiments, we conduct ion-based pump-probe experiments observing the emission of hot electrons post-ion impact, similar to processes studied in two-photon photoemission (2PPE) experiments. Our findings not only demonstrate the feasibility of our approach and provide direct measurements of the ion pulse characteristics but also offer insights into the non-equilibrium dynamics of electronic excitation in solids following an ion impact. We can track the electronic excitation and determine the temporal evolution of a pseudo electron temperature.

This research opens new avenues for understanding the fundamental processes underlying ion-solid interactions, with significant implications for semiconductor manufacturing and materials science. Our work sets a new standard for temporal resolution in the study of ion-induced phenomena and lays the groundwork for future innovations in the field.

9:30am SS+AMS+AS+CA+LS-FrM-6 How Hot Plasmonic Heating Can Be: Phase Transition and Melting of P25 TiO₂ from Plasmonic Heating of Au Nanoparticles, *Weigang Lu, Rohil Kayastha, Blake Birmingham, Bernd Zechmann, Zhenrong Zhang,* Baylor University

Plasmonic heating has been utilized in many applications including photocatalysis, photothermal therapy, and photocuring. However, how high the temperature can be reached for the surrounding media due to the collective heating of the plasmonic nanoparticles (NPs) and the impact of the heat dissipation on the surrounding media is not clear. Herein we studied the impact of plasmonic heat generated by resonantly excited gold (Au) NPs on P25 TiO_2 nanoparticle film. Under 532 nm continuous laser irradiation at the surface of the Au-TiO_2, the surface evaporation of Au nanoparticles and phase transition of TiO_2 were observed at moderate laser power. More importantly, as high as the melting point of TiO_2 of 1830ºC is confirmed from the molten TiO_2 rutile phase. When Au/TiO_2 was irradiated with an off-resonance laser at 638 nm, no phase transformation or melting of TiO_2 was observed. The temperature calculation shows that the heating generated by Au nanoparticles is not localized. The collective heating from an ensemble of Au nanoparticles in the irradiated area produces a global temperature rise that melts TiO_2. Our results suggest that the photothermal effect could be a major mechanism in the plasmon-assisted photocatalytic reactions. The experimental observation of the high temperature of the supporting media suggests new applications for utilizing plasmonic heating, for example, additive manufacturing.

9:45am SS+AMS+AS+CA+LS-FrM-7 Kinetics and Dynamics of Recombinative Desorption of Oxygen from Silver and Rhodium Surfaces, *Dan Killelea,* Loyola University Chicago

The ability to obtain velocity distributions of molecules desorbing from surfaces with both high temporal precision and angular resolution provide newfound insight into both the kinetics and the dynamics of recombinative desorption and subsurface emergence.

I will discuss our observations of subsurface oxygen emerging from beneath Rh(111) and how the velocity distribution shifts in comparison to the thermally-dominated desorption pathways found for surface-adsorbed oxygen. In addition, it was recently discovered that decomposition of oxygenaceous surface phases on Ag(111) also exhibit pronounced shifts in the energetics of the desorbing oxygen molecules. I will discuss these observations and their potential impacts in oxidation reactions in heterogeneously catalyzed reactions over transition metal surfaces.

10:00am SS+AMS+AS+CA+LS-FrM-8 Mort Traum Award Announcement,

10:45am SS+AMS+AS+CA+LS-FrM-11 Investigation of Stannane (SnH₄) Decomposition and Sticking Coefficient on Varied Metal Surfaces in EUV Lithography Environments, *Emily Greene, Nathan Barlett, Dren Qerimi, David Ruzic,* University of Illinois at Urbana-Champaign

In the context of extreme ultraviolet (EUV) lithography, the evaporation of tin droplets frequently leads to the deposition of tin on various chamber surfaces, including collector mirrors. A prevalent method to remove this tin deposition involves hydrogen plasma etching, which transforms the deposited tin into stannane (SnH_4). This compound, existing in a gaseous state under operational conditions, can be evacuated from the chamber using a vacuum pump. However, stannane is characterized by its instability, tending to decompose and adhere to various surfaces within the chamber.

To systematically study the decomposition behavior of stannane, a specialized experimental chamber has been designed. This chamber integrates a load-lock mechanism for inserting a test tube containing liquid stannane into a loading section, which is isolated from the main vacuum chamber by a valve. Within the main chamber, a quartz crystal microbalance (QCM), regulated by a cartridge heater, measures the mass of stannane deposits. The QCM will be set to temperatures between 30-300˚C. Upon opening the valve, the stannane vaporizes and interacts with the temperature-controlled QCM, facilitating the quantitative determination of the sticking coefficient as a function of both the surface material and the temperature.

Stannane is synthesized through the reaction of $LiAlH_4$, $SnCl_4$, $C_8H_{18}O$, and $C_4H_{10}O_2$. The four chemicals are mixed in a 3-neck flask while under vacuum. The reaction produces SnH_4 which is flows through three U-tubes traps. The first trap is held at -96˚C to trap precursors, the second two traps are help at -196˚C and trap the stannane. The stannane is increasingly pure the more traps are used.

This investigation aims to understand and quantify the mechanisms of stannane deposition and decomposition, enhancing the maintenance and

efficiency of EUV lithographic systems by optimizing the cleaning protocols for tin contamination.

11:00am SS+AMS+AS+CA+LS-FrM-12 First Principles Methods for Predicting Surface Reaction Mechanisms for Chemical Functionalization of Semiconductor Surfaces, *Roberto Longo, Shyam Sridhar, Peter Ventzek,* Tokyo Electron America Inc.,

The density of semiconductor devices continues to increase, accompanied by the subsequent scaling down of the critical dimension (CD) size, which is now on the order of a few nanometers. This results in device structure changes, from two-dimensional (2D) to three-dimensional (3D) structures, because the CD size has reached its limit of reduction. To accomplish this, precise chemical modification of the required surfaces with atomic scale precision is key to obtain the desired geometric control. Precise modification implies being able to leverage knowledge of individual plasma born species and surface interactions. Unfortunately, species specific chemical interaction mechanisms in the context of reactive ions and chemical etching are still poorly understood for the full range of chemical environments at play. Once dissociated in plasma radicals, there might be a wide array of compositions. For similar atomic compositions, variations in the molecular structure of the chemical precursor can also result in significant differences as to the surface modifications and subsequent etching characteristics. The chemical nature of the surface including coverage and chemical activity add significant dimensionality to the problem of controlling plasma surface interactions in general. We divide the problem of elucidating plasma surface interactions into two major categories for practical purposes: hydrofluorocarbon driven for oxide etch and halogen driven for silicon etch. We present here semiconductor surface modeling with general characteristics and investigate the reaction mechanisms undergone by a large variety of hydrofluorocarbon molecular precursors using density-functional theory (DFT), with a focus on reactive halogen adsorption. Given the large parameter space of this problem, we describe computational approaches that efficiently and accurately generate fundamental data. Physical and chemical surface reactions and the corresponding byproducts are identified, obtaining self-limitation thresholds for each specific functionalizing chemistry. Therefore, our computational results provide valuable insights on the complex physical, chemical, and dynamic molecular and ion interactions with functionalized semiconductor surfaces, paving the road for designing tailored strategies with the desired outcome for each specific system.

11:15am SS+AMS+AS+CA+LS-FrM-13 A Model Interstellar Medium Reactivity Study: Low Energy Electron Induced Chemistry of $CH_3OH@H_2O$, *Ahmad Nawaz, Micha Asscher,* The Hebrew University of Jerusalem, Israel

The desorption kinetics for MeOH@H_2O sandwich films from Ru(0001) surfaces are investigated using temperature-programmed desorption (TPD) at ultrahigh vacuum, with a base pressure of 2×10^{-10} Torr and temperature 25K. The TPD spectra of all the prominent stable molecular products were well detected by an in-situ quadrupole mass spectrometer (QMS). However, variation of the QMS signals were observed to be lower at different exposure to the negative charges in different time interval. Further, the MeOH parent molecules decompose, upon exposure to electrons at energies of 100 eV and 6.4 eV. Molecules at m/z of 2, 28 and 44, assigned to H_2, CO and CO_2, were the most abundant products. The typical mass spectra of the parent molecules within the sandwich layer (16 ML) are shown in Figure 1. Here, the MeOH peaks appears at ~140K while the water desorption peak is at ~160K.

Thin Films
Room 115 - Session TF1+EM-FrM

Thin Films for Microelectronics III: Wide Band Gap Materials

Moderators: Mark Losego, Georgia Institute of Technology, **Virginia Wheeler**, U.S. Naval Research Laboratory

8:15am TF1+EM-FrM-1 Interlayer Engineering of Heterostructure Thermal Boundary Resistance of Power Device Heat Spreader, *Youhwan Jo, Taesoon Hwang, Kyeongjae Cho,* University of Texas at Dallas **INVITED**

The needs for high power electronic devices are expanding for diverse applications including power conversion, smart grid, renewable energy generation and storage systems. The power capacity of devices is correlated to the bandgap of the semiconductors, and the current GaN power devices are expected to evolve to more powerful devices with ultra-wide bandgap semiconductors (e.g., b-Ga2O3, diamond, AlN, c-BN) in the future. As the power capacity of a device increases, the increasing waste heat generated by the operation must be removed efficiently and maintain the device temperature sufficiently low to avoid accelerated degradation and premature failure of the devices. However, even the performance of current GaN power device is limited by the capacity of waste heat removal at the device level from the hot spots. Specifically, the thermal resistance along the heat transport pathway from the GaN device hot spots to an adjacent heat spreader (e.g., diamond or AlN) is dominated by the thermal boundary resistance (TBR) of the heterostructure interfaces. To enable the full potential performance of GaN power devices, it is critically important to optimize the GaN/diamond TBR well below the previously reported values which are larger than the classically known limit of ~3 m^2K/GW based on the diffuse mismatch model (DMM) study of phonon transport at the heterostructure interfaces. In this talk, we will discuss the role of nanoscale interlayers at the heterostructure interfaces and demonstrate that the interlayer phonon engineering can enable novel phonon transport mechanisms at nanoscale leading to TBR values lower than the classical DMM limit. We envision applying the nanophononics design of interlayers to address the thermal management challenges of high-power devices.

This work was supported by DARPA Sponsored Special Projects (DSSP) in 2021 and 2022 and is currently supported by DARPA Technologies for Heat Removal in Electronics at the Device Scale (HTREADS) program.

8:45am TF1+EM-FrM-3 Characterization of Defects in AlN Using Deep Ultraviolet Photoluminescence, *Virginia Wheeler, Neeraj Nepal, Matthew Hardy, Andrew Lang,* Naval Research Laboratory*; James Hart,* Nova Research Inc*; Brian Downey, David Meyer,* Naval Research Laboratory

AlN is being explored as an ultrawide bandgap material that offers the combined possibility of higher voltage handling and better thermal management than current semiconductor technologies such as GaN, SiC, and Si. However, realizing the full potential of this material in electronic device applications requires the ability to tailor the electrical conductivity in active AlN layers through impurity doping. Due to the large bandgap and lower formation energy of native point defects, which serves as carrier compensating centers, impurity doping in AlN has been challenging and lacking in reproducibility. Deep ultraviolet photoluminescence (DUVPL) is a crucial tool to identifying near-band edge emission and radiative point defects within ultrawide bandgap materials. In this work, we use DUVPL to identify and correlate defect and band edge emission intensities with AlN substrates and films deposited by molecular beam epitaxy (MBE) to point towards approaches to achieving electrical conductivity for device applications.

Si-doped AlN films, ~300-500 nm thick, were deposited by plasma-assisted MBE on both AlN/sapphire templates and bulk AlN substrates from different vendors using a metal modulated epitaxy approach. All AlN substrates underwent an *ex-situ* chemical clean and *in-situ* Al-absorption and desorption technique to create an abrupt, pristine, oxygen-free growth interface. Resulting films were characterized using DUVPL, x-ray diffraction (XRD), atomic force microscopy (AFM) and van der Pauw resistivity measurements. Cross-sectional transmission electron microscopy (TEM) measurements were carried out on selected samples along (10-10) and (11-20) orientations to assess the epitaxial material quality and defect density.

DUVPL measurements of MBE AlN layers, using above bandgap excitation (at 6.458 eV), show that unintentionally-doped AlN films have strong band-edge emission and no impurity bands. After Si doping, an impurity band appears near 3.67 eV related to an Al-vacancy Si-complex and the band-edge emission at 6.03 eV decreases. Van der Pauw resistivity measurements show that conductive AlN:Si films can be obtained on all substrates, but minimal changes in resistivity result from varying growth parameters further. For AlN layers grown under similar conditions, conductive AlN films have lower intensity impurity bands. Results correlating DUVPL, XRD, AFM, TEM and resistivity measurements for the full parameter space will be discussed.

9:00am TF1+EM-FrM-4 Ultrathin Tantalum Films for Silicon Carbide Schottky Barrier Diode, *Renato Beraldo, Rodrigo Reigota Cesar, José Alexandre Diniz,* Center for Semiconductor Components and Nanotechnology - CCSNano, Brazil

The first device based on SiC released was a Schottky barrier diode (SBD), and device is basically a junction of a semiconductor and a particular metal capable of providing a rectifier contact. Therefore, instead of focusing only on the work function of the elements, it is important to pay attention to the quality of the interface between metal and semiconductor, for example, inhomogeneous levels, defects, impurities and morphology, which can cause interface states and change the factor of ideality (ideal is 1). Since

then, ways of creating surface arrangements associated with better quality have been employed, including metallization techniques, annealing treatments, types of metals, geometric arrangements, and even the addition of tiny oxides, where some of these Applications can adjust SBH values and improve reliability resource results.

Among many metallization techniques, studies using ultrathin films yielded high quality junctions employing Ni onto Si and W, Ti onto SiC. So then, based on these results, the motivation of this work was the selection of tantalum to be the metal with this metallization technique, due to its low work function that could provide lower resistance of SBH and its refractory properties which could afford elevated temperature without affecting the device performance.

Initially, a double side polished SiC wafer n-type of 350 µm thick (0.015~0.028 Ω.cm) with drift layer of 3×10^{15} cm-3 dopants and 30 µm thick was selected. The samples were cleaned with 10 minutes in piranha bath and nitric acid 30% at 50 °C. After the cleaning process, 2 nm of tantalum was deposited by RF sputtering at the top of the samples to form Schottky contact and then, rapid thermal annealed performed from 500 to 700°C under 50°C intervals. Then 100 nm of aluminum was deposited by thermal evaporation to provide electric contact for test probes. To create the ohmic contact, 100 nm of nickel was deposited by sputtering without any thermal treatment. The samples were diced in 1 cm2 and followed by lithographic pattern with squares of 30 µm side.

Each device was submitted to IxV curves to check the current response, leakage current under reverse bias, SBH, and ideality factor. At Fig. 1 it is possible to verify that the annealing treatment yielded the difference among the annealing treatments. At the Fig. 1, the best result was related to the 650°C which showed lower values of leakage current and value of SBH around 0.74 eV and ideality factor of 1, resulting in a low resistance device addressed to power devices, combined with the lowest leakage current, as shown in Fig. 2.

9:15am TF1+EM-FrM-5 Plasma Enhanced Atomic Layer Deposition of Hydrogen Free In$_2$O$_3$ Thin Films with High Charge Carrier Mobility, *Sudipta Mondal*, Ian Campbell, Ageeth Bol, University of Michigan, Ann Arbor

In$_2$O$_3$ has recently emerged as an alternative channel material for field effect transistors (FETs), owing to its exceptional carrier mobility preservation even when scaled down to ultra-thin layers below 10 nm. Despite the superior performance of In$_2$O$_3$-based FETs, understanding the underlying operation mechanisms is incomplete, particularly concerning the impact of native defects and doping. Hydrogen dopants in metal oxide films are often responsible for increased Hall mobility, albeit at the detriment of device stability. Herein, we have used plasma-enhanced atomic layer deposition (PEALD) to deposit highly uniform and conformal In$_2$O$_3$ thin films. A β-diketonate indium precursor tris(2,2,6,6-tetramethyl-3,5-heptanedionato) indium-(III), which is stable over a large temperature range was used as the indium source. O$_2$ plasma was selected for oxygen incorporation instead of hydrogen-containing precursors like H$_2$O to prevent unintentional hydrogen doping, while still aiming for high carrier mobility. Saturation behaviour for the PEALD process was studied using in-situ spectroscopic ellipsometry and indicated a wide ALD window from 150°C to 500°C. Our optimized process achieves a growth rate of 0.14 Å/cycle at 150°C, and 0.29 Å/cycle at 500°C. The In$_2$O$_3$ films manifest in a polycrystalline Bixbyite cubic phase, as confirmed by grazing incidence X-ray diffraction (GIXRD). The chemical composition of the films was investigated using X-ray photoelectron spectroscopy (XPS), which revealed a rising number of oxygen vacancies with increasing deposition temperature. Diverse analytical methods, including UV-vis spectroscopy, scanning electron microscopy (SEM), and Hall measurements, were employed to elucidate the influence of oxygen vacancies on the film properties. Our n-type In$_2$O$_3$ films showed a Hall mobility value of 84.1 cm^2/V-s at a deposition temperature of 150°C, which is among the highest reported for ALD In$_2$O$_3$ thin films, making them an ideal candidate as a channel material in FET devices. Through Elastic Recoil Detection Analysis (ERDA), we have excluded the presence of hydrogen dopants by comparing the relative hydrogen concentration in the substrate and the sample, (detection limit ≥0.01 atomic %), cementing the role of oxygen vacancies as the principal contributor to the exceptional electrical behaviour in our films. Moreover, we explored post-deposition annealing in air and argon atmospheres as a strategy to modulate oxygen vacancies and, by extension, the electrical properties of the films. We observed that air annealing increases resistivity by eliminating oxygen vacancies, while vacuum annealing enhances conductivity by creating oxygen vacancies.

9:30am TF1+EM-FrM-6 Epitaxial Integration of Transition-Metal Nitrides with Cubic Gallium Nitride, *Zachery Cresswell*, *Nicole Fessler, Trent Garrett, Kevin Vallejo, Brelon May,* Idaho National Laboratory

GaN is ubiquitous in the optoelectronics industry in its thermodynamically stable wurtzite structure, but it also has a metastable zinc blende allotrope that is less explored and more difficult to synthesize. One of the potential advantages of cubic-GaN (c-GaN) is the simplified interfacial symmetry with the other cubic transition metal nitrides, which are of interest for an assortment of applications requiring high chemical and thermal stability, high hardness, superconductivity, or plasmonic properties. The shared cubic symmetry would allow for easier integration of the nitrides with a wide-bandgap semiconductor.

This work will discuss the synthesis of epitaxial c-GaN on 3C-SiC substrates and its integration with known superconducting nitrides via molecular beam epitaxy. The hexagonal-free nature of the c-GaN, and the epitaxial relationship of it and the transition metal nitrides, are confirmed via *in-situ* reflection high energy electron diffraction, *ex-situ* X-ray diffraction, photoluminescence, and transition electron microscopy. The electrical transport of the transition metal nitrides grown on c-GaN(001) is compared to growth directly on 3C-SiC(001) and c-plane hexagonal GaN. Epitaxial synthesis of cubic wide-bandgap and superconducting metallic nitrides under similar growth conditions opens a new world of possibilities in band engineering, as well as the ability to create new device structures for areas such as metamaterials, quantum computing, and condensed matter physics.

9:45am TF1+EM-FrM-7 Comparison of AlScN Thin Films Grown via Pulsed Laser Deposition and Sputtering, *John Wellington-Johnson,* Georgia Institute of Technology

Al$_x$Sc$_{1-x}$N (AlScN) is a promising material for piezoelectric micro-electro-mechanical systems (MEMS) applications, due to its high coupling coefficient ($k_t^2 > 15.5\%$) , large piezoelectric coefficient (>27 pC/N), and CMOS compatibility [1,2]. However, large variability in film crystallinity, orientation, composition, and grain morphology still limit the full potential of AlScN [2]. The majority of literature focuses on the sputtering growth on AlScN but and there is great variability in the film quality, with multiple deposition parameters influencing the resultant film composition, morphology, and crystallinity - there are limited reports on the impact of pulsed laser deposition on AlScN film quality. This presentation will compare the impact of thin film growth by sputtering and PLD to determine the impact on the resultant AlScN films' crystalline, compositional, and morphological features.

AlScN thin films were deposited on (111) platinized silicon by PLD and RF or DC sputtering. In PLD, thin films are deposited from a single stoichiometric Al$_{70}$Sc$_{30}$N target, whereas two independent AlN and Sc targets are used in sputtering. X-ray reflectivity (XRR) and diffraction (XRD) studies are used to characterize film thickness and phase. XRD scans reveal the films maintain the desired (0002) orientation over a range of temperatures and laser fluences. Compositional analysis and depth profiling reveals the nature of surface and bulk oxygen through the film, with discussions on the differing oxidation states and bonding environments of the O1s spectra, with respect to each growth method. Grain size, surface roughness, and surface morphology of the films will also be presented through SEM and AFM studies – with R$_a$ ranging from 1.3 to 5 nm. These results illustrate and compare the PLD growth of c-axis oriented AlScN thin films under CMOS conditions.

References

1. Kurz, N. *et al.* Experimental determination of the electro-acoustic properties of thin film AlScN using surface acoustic wave resonators. *Journal of Applied Physics* **126**, 075106 (2019).

2. Akiyama, M., Umeda, K., Honda, A. & Nagase, T. Influence of scandium concentration on power generation figure of merit of scandium aluminum nitride thin films. *Applied Physics Letters* **102**, 021915 (2013).

3. Perrone, A. State-of-the-Art Reactive Pulsed Laser Deposition of Nitrides. *Jpn. J. Appl. Phys.* **41**, 2163 (2002).

10:00am TF1+EM-FrM-8 Exploring the Impact of [Si-C] and [N=C] Bonds in SiCN Films by First Principles Calculation: A Study of Composition, Structure, and Properties, *Tsung-Hsuan Yang,* Tokyo Electron America, Inc.*; Gyeong Hwang,* University of Texas at Austin*; Peter Ventzek, Jianping Zhao,* Tokyo Electron America, Inc.

Silicon carbon nitride (SiCN) is a dielectric material featuring a variety of desirable properties, including thermal stability, chemical resistance, and materials strength. It has been found to have better materials properties

than silicon nitride (Si_3N_4) due to its potential for controlling the element compositions and microstructure. However, the relationship between SiCN microstructure and materials properties is not well understood. This simulation study aims to bridge the gap by correlating the bonding environment in SiCN with materials properties, specifically by investigating the effect of adding [Si-C] or [N=C] bonds to SiN film. We begin by constructing amorphous SiCN in two ways: replacing Si with C to create [N=C] bonds or replacing N with C to create [Si-C] bonds. The resulting films were annealed at 500K to optimize geometry and passivate defective sites with hydrogens. A wide range of Si, N and C compositions (e.g., Si_3N_4, SiC, $Si_2N_4C_1$) and different C bonding environments were examined. The film stability was tested, and properties such as dielectric constant, refractive index, band gap, bulk modulus, H content, and bond densities were calculated. The study successfully demonstrates how [N=C] and [Si-C] bonds modify the materials properties of SiCN film, providing guidelines for tailoring the materials properties of SiCN.

Thin Films
Room 115 - Session TF2-FrM

Thin Films: Characterization and Fundamentals

Moderators: Mark Losego, Georgia Institute of Technology, **Virginia Wheeler**, U.S. Naval Research Laboratory

10:30am **TF2-FrM-10 Variable-Angle, Spectroscopic Ellipsometry Studies of the Repeated Application of First Contact Polymers on Optical Surfaces**, *Joshua Vawdrey,* Brigham Young University*; James Hamilton,* University of Wisconsin, Platteville*; David Allred,* Brigham Young University
First Contact Polymer™ (FCP) is an adhesion-based, cleaning polymer that has been shown to remove molecular and particulate contamination from surfaces. Applying, allowing to dry, and then peeling off a layer of FCP from a contaminated surface embeds and removes contaminants. While a single peel-off has been observed to be effective at removing both particulate and molecular contaminants, the effect of consecutive fresh applications and peel-offs on the same surface has not been extensively studied. This is important since FCP is used to protect optical surface in storage. Using variable-angle, spectroscopic ellipsometric (VASE) data, modeled with J.A. Woollam Inc. software, CompleteEase, we addressed the questions: can surfaces be cleaned multiple times recovering the same clean surface each time? And what formulations are suitable for hygroscopic materials like lithium fluoride? One set of thin-film materials studied were three that are important materials in silicon microelectronics: native oxide on "bare" silicon wafer pieces, CVD silicon nitride on silicon wafers, and thermal silicon dioxide on silicon wafers. In addition, surfaces important in thin-film optics including far ultraviolet (FUV) were examined. These were metal fluoride thin films on evaporated aluminum. At each iteration in the study, we removed the layer of FCP coating each sample, measured the surface at several different spots with VASE, reapplied FCP and stored the samples for a designated time. Control samples, which received no FCP but were stored with the others, were also measured iteratively. We observed a reduction in the top-layer thickness of both silicon and CVD silicon nitride on silicon samples after cleaning impure solvent residue off the surface- We interpret this as FCP can effectively remove physisorbed materials from such surfaces yielding atomically clean surface in the absence of can be absorbed layers. We observed that the apparent native oxide layer on both FCP-coated samples and control samples increased with time. This could be due to the deposition of adventitious carbon from the environment. There is a slight increase--about an eighth of an angstrom per repeated peel-off, in the apparent top-layer thickness of the native oxide on Si samples. Cleaning fluorides proved to be more challenging. This is due to affinity of some fluorides particularly LiF to water. We determined condition under which some fluorides can be effectively cleaned without trapping water. Coatings suitable for long-term storage of fluorides are still under investigation.

10:45am **TF2-FrM-11 EnviroMETROS – A Novel Surface and Multilayer Thin Film Analysis Tool**, *Paul Dietrich, Francesca Mirabella, Stefan Boetcher, Kai Kunze, Oliver Schaff, Andreas Thissen,* SPECS Surface Nano Analysis GmbH, Germany
The new EnviroMETROS series transforms the realm of surface hybrid metrology by employing the key techniques of parallel detection angle resolved XPS (PARXPS) and multi-wavelength excitation. This method utilizes variable photon energies and emission angles operating under diverse environmental conditions for conducting chemical analyses of thin films and bulk materials. LEIS facilitates high surface sensitivity, while electronic characterization can be enhanced with UPS, IPES, and REELS.

Integrated Raman and/or IR spectroscopy provide structural information, whereas XPS mapping and SEM/SAM contribute to elemental surface maps correlated with morphology.

The relevance of ultrathin films and 2D materials in modern devices is continuously increasing, prompting a growing interest in the chemical analysis of these multilayer systems and their surfaces. A thorough characterization of stoichiometries, composition, and depth distribution of elements is crucial. The novel EnviroMETROS series serves as an ideal tool for routine analysis in this research and development field. It combines large sample and wafer handling with a photoelectron spectrometer offering variable information depth. When combined with optical and other analytical techniques, it enables depth-dependent composition analysis with unparalleled precision, reliability, and repeatability.

11:00am **TF2-FrM-12 Passivation of Indium Phosphide Substrate Evaluated by Atomic Force Microscopy**, *Fabiano Borges,* Federal Institute of Sao Paulo, Brazil*; Cassio Almeida,* PUC-Rio, LabSem, Brazil*; Audrey Silva,* Unicamp, CCS, Brazil*; Otávio Berenguel, Carlos Costa,* CNPEM, LNNano, Brazil*; Gustavo Vieira,* IEAv, Brazil*; José Diniz,* Unicamp, CCS, Brazil
Passivation involves coating a material to make it passive, i.e., less affected by the environment. In this study, passivation is achieved by depositing an aluminium oxide layer with prior surface treatment. Four surface treatments are considered: oxidation only (O), nitriding only (N), oxidation followed by nitriding (ON), and nitriding followed by oxidation (NO). An InP substrate is heated and exposed to an environment enriched with oxygen and/or nitrogen to form a thin film over the InP surface. Following this, a 20nm thick layer of aluminium oxide is deposited using atomic layer deposition (ALD). Thus, six different samples were generated for analysis: four with surface treatments, one of pure InP without any added thin film, and one of InP with only an aluminium oxide layer as the control sample for reference. This process presumably enables electricity to reliably penetrate the conducting InP below the surface while overcoming the surface states that hinder electrical conduction in the semiconducting layers. Different techniques such as Photoluminescence Spectroscopy, Atomic Force Microscopy, Electrostatic Force Microscopy, and X-ray Photoelectron Spectroscopy can be used for evaluating these treatments' effectiveness. The simplest one, analysing AFM images [1] alongside their RMS roughness values [2], reveals that samples with lower RMS roughness also possess fewer defects at their surfaces [3]. By defining the RMS roughness value of the control sample as the reference, all other values are lower: pure InP has a 15% lower RMS roughness, N has 10%, O has 20%, NO has 15%, and ON 10%. This suggests that the O sample is the smoothest and likely possesses the lowest surface defect density.

References

[1] Klapetek, P. (2006). Quantitative Data Processing in Scanning Probe Microscopy. William Andrew Publishing. 2013.
[2] Nečas, D., Klapetek, P. Gwyddion: an open-source software for SPM data analysis, Cent. Eur. J. Phys. 10(1) (2012). 181-188.
[3] Streetman, B. G., Banerjee, S. (2006). Solid state electronic devices. 6th ed. Pearson/Prentice Hall.

Acknowledgments

11:15am **TF2-FrM-13 Adsorption of Aromatic Molecules on Metal Surfaces for Area-Selective Deposition: A Dft Study**, *Matías Picuntureo,* Universidad Tecnica Federico Santa Maria, Chile*; Ilker Tezsevin, Marc Merkx,* Eindhoven University of Technology, Netherlands*; Scott Semproni, Jiun-Ruey Chen, Scott Clendenning,* Intel*; Adrie Mackus,* Eindhoven University of Technology, Netherlands*; Tania Sandoval,* Universidad Tecnica Federico Santa Maria, Chile
Area-selective deposition (ASD) is a bottom-up fabrication technique that enables the targeted growth of materials on specific regions of a patterned substrate. For applications like creating bottomless diffusion barriers in semiconductor devices, ASD allows for the selective deposition of a barrier material on the interlayer dielectric while avoiding the metal at the bottom of the trench. A key strategy in ASD involves using small molecule inhibitors (SMIs) to prevent undesired material deposition on the non-growth areas.

Friday Morning, November 8, 2024

Previous studies demonstrated the potential of aniline as an SMI for Ru and Co surfaces, where the benzene ring plays a crucial role in surface inhibition through chemical passivation and physical shielding.[1-2]

In this study, we expand on this work by investigating the adsorption of various aromatic molecules—aniline, benzaldehyde, benzene, phenol, and toluene—as potential SMI candidates on Cu(111), Ru(0001), Mo(110), and W(110) surfaces using density functional theory (DFT) calculations. We focus on (i) the differences in adsorption behavior across these metal surfaces and (ii) the effects of different substituent groups on SMI-metal interactions, employing adsorption energy decomposition and charge transfer analysis.

Our results show a strong correlation connecting the interaction energies and the charge transfer between SMIs and surfaces. Metals with higher d-band center positions exhibit more favorable interaction energies in line with the increased electron transfer from the metal to the molecule. A detailed charge transfer analysis reveals that most electron transfer is directed towards the phenyl group, underscoring its central role in adsorption. For benzaldehyde, additional electron transfer to the aldehyde group is observed, likely due to back-bonding between metal d-states and the π^* orbitals of the C=O group, leading to stronger adsorption energies. Structural deformation analysis indicates that adsorption-induced strain is effectively compensated by enhanced charge transfer in the most exothermic cases, resulting in increased interaction strength.

Overall, this study provides a fundamental understanding of SMI-metal interactions at the molecular level, offering valuable insights for optimizing ASD processes in advanced semiconductor applications.

[1]*Chem. Mater. 2020, 32, 18, 7788–7795*

[2]*J. Chem. Phys. 2024, 160, 204701*

11:30am TF2-FrM-14 In Situ Synchrotron GISAXS Studies of the Roles of Reactive and Energetic Species in Plasma-Enhanced Atomic Layer Deposition of InN, *Jeffrey Woodward, David Boris, Michael Johnson, Mackenzie Meyer,* U.S. Naval Research Laboratory; *Samantha Rosenberg,* Lockheed Martin Space – Advanced Technology Center; *Zachary Robinson,* SUNY Brockport; *Scooter Johnson,* Honeywell International; *Neeraj Nepal,* U.S. Naval Research Laboratory; *Karl Ludwig,* Boston University; *Charles Eddy,* ONR Global; *Scott Walton,* U.S. Naval Research Laboratory

The *in situ* characterization of atomic layer deposition (ALD) processes is challenged by the highly contaminating metal precursors, relatively high pressures, and harsh process environments which preclude the use of powerful electron-based techniques employed for ultrahigh vacuum growth methods.An alternative approach is to utilize hard x-ray techniques which are compatible with arbitrary pressures and allow for the placement of source and detector outside the reactor.Among such techniques, grazing incidence small-angle x-ray scattering (GISAXS) using synchrotron radiation is particularly well-suited to the study of ALD due to its exceptional surface sensitivity and ability to probe nanoscale structure in real time.[1]The application of GISAXS for the investigation of plasma-enhanced ALD (PEALD) is especially compelling when combined with *a priori* knowledge of the plasma properties, as even relatively simple plasmas may contain a broad range of species which influence the growth and resulting film properties.[2]

In this work, we investigate the growth kinetics of indium nitride (InN) PEALD using *in situ* GISAXS in a custom reactor.The InN films are grown on GaN using trimethylindium and N_2/Ar plasma as the metal precursor and reactant.Different regimes of plasma species generation are explored and are characterized by optical emission spectroscopy (OES) and Langmuir probe measurements.These plasma diagnostics are supported by modeling with the 2D Hybrid Plasma Equipment Model (HPEM), which is used to predict the fluxes of various reactive plasma species to the sample, including atomic N and metastable N_2.The growth mode is observed to be correlated to the concentration of atomic N, with high concentrations promoting island growth and low concentrations promoting layer-plus-island growth.Under conditions of high atomic N production, both the mean island radius and critical thickness for island formation are found to increase with ion flux. Furthermore, the mean InN island distance is found to change only during plasma exposure, and to continue changing with exposure even after the methylindium adlayer is believed to have fully reacted with the plasma.After identifying the low atomic N plasma condition as optimal, we then explore the influence of plasma exposure time from slightly undersaturated to optimized and excessive conditions.The InN growth mode is found to be layer-plus-island for all cases, with increased plasma exposure promoting redistribution of material from small surface features to large ones.

[1] H. Pedersen *et al.*, Cryst. Growth Des **23**, 7010-7025 (2023)
[2] J. M. Woodward *et al.*, J. Vac. Sci. Technol. A **40**, 062405 (2022)

11:45am TF2-FrM-15 Thermal Atomic Layer Deposition of Low Resistivity Metallic Films for High Aspect-Ratio Via Seed, *Dane Lindblad,* Forge Nano; *Irina Stateikina, Marc Guilmain,* MiQro Innovation Collaborative Centre (C2MI), Canada; *Sara Harris,* Forge Nano; *Xavier Gaudreau-Miron,* MiQro Innovation Collaborative Centre (C2MI), Canada; *Arrelaine Dameron, Matt Weimer,* Forge Nano

Scaling interconnects to increase device density is a critical bottle neck for a range of applications from complementary metal oxide semiconductor (CMOS) to microelectromechanical (MEMS) switches and other devices. Commonly, Cu is the interconnect metal of choice to fill vias but comes with significant challenges. A diffusion barrier is applied to ensure Cu leakage does not cause electrical breakdown between vias and a metal seed layer is required to ensure smooth and dense Cu electroplating. Uniform seed resistivity, correlated to thickness, is critical to produce low resistivity, void-free interconnects. Unfortunately, state-of-the-art processes for high quality metallic films are limited to line-of-sight techniques like chemical vapor deposition (CVD) or physical vapor deposition (PVD), limiting possible device pitch and architectures. When the aspect ratio increases above ~10:1 or there is a line-of-sight obstruction at least one of these layers are missing, resulting in insufficiently thin seed for Cu electroplating nucleation. This creates a void or thickness gradient resulting in pinch-off at the top and ultimately high line resistance or device failure. Fortunately, atomic layer deposition (ALD) can produce high density, low resistivity metal films for both Cu diffusion barrier and Cu electroplating seed applications. Here we report on a total solution using thermal ALD. Plasma enhanced ALD (PEALD) can produce quality metallic films at a reasonable thermal budget, unfortunately plasma processes have a limit to aspect ratios that can be coated conformally and have the added risk of surface plasma damage. Our all-thermal ALD solution has been demonstrated on Si vias ranging from 4:1 to 25:1 aspect ratio, an example of Cu electroplated in this solution is shown in Figure 1. First, a SiO_2 ALD film is deposited as a dielectric barrier, then a thin TiN layer is applied as a Cu diffusion barrier, followed by a low resistivity Ru film for Cu adhesion. A novel TiN thermal ALD process at 300°C has been developed alongside a high-quality Ru film with resistivity values <20 uΩ·cm which can be deposited on SiO_2, HfO_2, Pt, and TiN. When compared to PVD, the ALD stack produces dense, void free nucleation of Cu that remains well adhered to the Si via. Conversely, the PVD stack has voids at the bottom of the trench from poor adhesion of electroplated Cu and narrowing at the top from a resistivity gradient within the trench. This comparison demonstrates that the Ru seed provides sufficient adhesion for Cu electroplating and that the resistivity of the ALD Ru/TiN stack is low and consistent enough for conformal and dense Cu electroplating.

Author Index

Bold page numbers indicate presenter

Author Index

Author Index

Author Index

Author Index

Author Index

Author Index

Author Index

Author Index

Author Index

Mirabella, Francesca: EW-TuL-6, 72; TF2-FrM-11, 226
Miranda Manon, Andres: AP2+EM+PS+TF-MoA-13, 27
Misek, Martin: AC+MI-FrM-8, 212
Misicko, Tobias: CA-ThP-10, **178**
Misra, S.: MS-FrM-1, 217
Missale, Elena: 2D-ThP-18, 167
Mitchson, Gavin: NS2-MoM-13, **13**
Mitterer, Christian: SE-MoA-1, 38
Miura, Hitoshi: 2D+AP+EM+QS+SS+TF-TuM-3, 49
Miura, Makoto: PS1-MoM-1, 14
Miwa, Jill: 2D+LS+NS+SS-TuA-3, 74
Miyahara, Yoichi: NS-ThP-16, 187; NS-ThP-9, 186
Miyamoto, Junji: PS-ThP-4, **188**
Miyoshi, Masafumi: PS1-MoA-4, 32
Miyoshi, Nobuya: AP1+EM+PS+TF-TuM-1, **52**
Mkhoyan, K. Andre: EM+2D+AP+QS+TF-ThM-6, 145
Moazzeni, Alireza: CPS-MoM-1, **8**; EM+AP+TF-WeA-13, **124**
Mock, Alyssa: MI+2D+AC+TF-WeA-10, 126
Modestino, Miguel: PS2-MoA-13, 35
Moffat, W.P.: SE-MoA-15, **41**
Moffitt, Chris: 2D+LS+NS+SS-TuA-4, 74; AS-ThP-25, 173; EW-TuL-5, **72**
Moffitt, Christopher: AS-WeA-6, 120
Moffitt, Stephanie: EL-FrM-5, 215
Moher, Dillon: PS2-MoA-14, 35
Mohrhusen, Lars: SS+AMS-MoM-13, 23; SS+CA+LS-TuA-11, **89**
Moinpour, Mansour: 2D+EM+MI+QS-WeM-13, 94
Moiny, Darya: UN-ThP-9, **207**
Mokrov, Mikhail: PS-TuA-8, 85
Mol, Arjan: SE-MoM-14, 21
Molina, Nicolas: AS-ThM-8, **141**; AS-ThP-14, **171**
Molina, Nicolás: SE-MoA-13, 40
Molkenboer, Freek: VT3-MoA-14, **47**
Mondal, Mazharul Islam: AS-TuA-3, 78
Mondal, Sudipta: TF1+EM-FrM-5, **225**
Monson, Todd C.: MI+2D+AC+TF-WeA-3, 125
Montemore, Matthew M.: SS+AMS-MoM-3, 21; SS-ThP-2, 194
Montero Alvarez, Daniel: MS-FrM-4, 218
Montero, Daniel: PS1-TuM-5, **62**
Mook, William: MN2-TuM-15, 58
Moon, Kwangjin: PS-ThP-21, 191
Moore, David: EM+AIML+AP+QS+TF-WeM-1, 103
Moors, Kristof: NS-ThP-3, 185
Moretti, Federico: EM+2D+BI+QS+TF-TuA-10, 82
Morgan, David: AS-ThM-4, 140; AS-ThP-20, 172; AS-WeA-5, **120**
Morikawa, Yasuhiro: PS1-WeA-4, 127
Morin, Mathieu: NS-ThP-14, 187
Morin, Pierre: 2D-ThM-15, 137
Morozumi, Junki: PS-ThA-4, **161**
Moschandreou, Eleftherios: QS-TuM-16, 65
Moselund, Kirsten E.: EM+2D+AP+QS+TF-ThM-1, 144
Moses, Atlantis: EL-ThP-9, 180
Moses, Atlantis K: EL-FrM-8, 216
Moses, Matthew: NS-ThP-14, 187
Motoyama, Koichi: PS1-MoM-2, 14
Mou, Shin: EM+2D+AP+QS+TF-ThM-5, 145
Mounce, Andrew: MN2-TuM-15, 58
Mousa, Habeeb: AP1+EM+PS+TF-WeM-4, 98; PS-ThP-13, 190
Mowatt, Mikko: UN-ThP-17, 208

Mowbray, Duncan John: SS+2D+AMS-WeA-15, 131
Mu, Sai: MI+2D+AC+TF-WeM-3, 106
Muhowski, A.J.: QS-TuA-11, 87
Muir, Benjamin: AS-ThM-5, 140
Mukherjee, Saumya: CA-ThA-4, **158**
Mukherjee, Shagorika: EM+2D+AP+QS+TF-ThM-4, 145
Mukherjee, Shriparna: AS-WeM-5, 101
Mukhopadhyay, Kausik: 2D+EM+QS-ThA-4, 154; BI2-MoM-14, **8**
Mullapudi, Gouri Syamala Rao: EM+AP+TF-WeA-10, **123**
Müller, Christoph R.: AS-WeM-14, 102
Muller, Richard: TF2-TuM-13, 69
Mulvany, Oliver: VT2-TuA-11, 93
Mun, Junhee: PS-ThP-19, **190**
Munneke, Berend: VT2-MoA-11, 47
Munoz, Maria: NS1+2D+QS-MoA-3, 30
Murakami, Satoshi: EL-FrM-13, 217
Muray, Lawrence: VT1-TuM-1, 69
Murdin, Ben: NS2-MoM-14, 13
Murphy, John: EL2-ThA-9, **160**; PS+TF-FrM-5, 220
Murphy, Ryan A.: QS-TuA-1, 86
Murphy, Thomas E.: 2D-WeA-6, 116
Murray, Gavin: AS-ThM-4, 140
Murray, Lottie: QS1+EM+MN+PS-MoA-7, 36
Murray, Thomas: QS-TuM-6, 64
Murthy, Akshay: AS-ThP-8, 171; QS-TuM-15, 65; QS-TuM-7, **65**
Murthy, Likith Krishna Lakshmi Narashima: MN1-TuA-5, 83
Murugaiah, Anand: VT1-TuM-3, 70
Murugesan, Vijayakumar: CA-ThM-4, 142
Murugesan, Vijaykumar: AS-ThP-16, 172
Musa, Azeez O.: AP1+EM+PS+TF-MoA-7, **26**
Musavigharavi, Pariasadat: EM+AIML+AP+QS+TF-WeM-1, 103
Musick, Kevin: QS-TuM-6, 64
Mutus, Josh: AQS-SuA-10, **1**; QS-TuA-9, 87
Myers-Ward, Rachael: 2D+AP+EM+QS+SS+TF-TuM-16, 51; EM+2D+AP+QS+TF-ThM-2, 144; EM+2D+AP+QS+TF-ThM-3, **144**

— N —
Naaman, Ron: NS1-TuM-7, 60
Nagay, Bruna: BI-MoA-3, 29
Nagay, Geev: QS-TuM-15, 65
Nahm, Hyeon ho: PS-ThP-12, **189**
Nahm, Hyeon-Ho: PS-ThA-5, 161
Nakamura, Junji: SS+CA+LS-TuA-13, 89; SS+CA+LS-TuM-8, 66
Nakatani, Yusuke: AP+PS+TF-TuA-10, **77**
Nalaskowski, Jakub: QS-TuM-6, 64
Nalawade, Swapnil: AP-ThP-4, **169**
Nam, Chang-Yong: TF-WeA-12, 133
Nam, Jae Hyun: PS-ThP-2, **146**
Nam, Sang Ki: AP+PS+TF-TuA-3, 76; AP+PS+TF-TuA-4, 76; PS-ThA-8, 162
Nam, Taewook: AP1+EM+PS+TF-TuM-5, 52
Namari, Nuning: SS+CA+LS-TuA-13, 89
Namboodiri, Pradeep: QS1+EM+MN+PS-MoA-8, 36
Nanayakkara, Tharanga: QS-ThP-1, 191
Narasimha, Ganesh: AIML-WeM-17, **97**; MI+2D+AC+TF-WeM-3, 106
Narayan, Dushyant: AIML-WeM-13, 96
Nas, Ismail: VT1-TuM-3, 70
Nave, Andy: PS-ThM-17, 148
Naveed, Muhammad Ashar: 2D+EM+MN+TF-FrM-4, **211**
Navidi Kashani, Amir Hossein: SE-MoA-4, 39
Nawaz, Ahmad: SS+AMS+AS+CA+LS-FrM-13, **224**

Nayak, Ganesh: SE-MoA-4, 39
Nayir, Nadire: 2D+EM+MN+TF-FrM-5, 211
Neal, Adam: EM+2D+AP+QS+TF-ThM-5, 145
Neal, Craig: BI-ThP-14, 176
Neely, Jason: MN2-TuM-15, 58
Neils, William K.: AS-ThA-2, 156; SS-ThP-36, 200
Nejati, Siamak: TF-WeA-4, 132; TF-WeA-6, **132**
Nelin, Connie J.: AS-TuA-10, 78
Nelissen, Lisa: QS2+PS-MoA-11, 37
Nellis, W. J.: AC+MI-ThM-15, 139
Nemanich, Robert: CA-FrM-1, 213
Nemchick, Deacon: TF2-TuM-13, 69
Nemeth, Stefan: 2D-ThM-15, 137
Nemouchi, Fabrice: QS2+PS-MoA-14, 38
Nemsak, Slavomir: CA-ThM-16, **143**; LS-MoM-5, 10
Nepal, Neeraj: AP1+EM+PS+TF-WeM-2, 98; TF1+EM-FrM-3, 224; TF2-FrM-14, 227
Neumann, Christof: 2D+AP+EM+QS+SS+TF-TuM-5, 49
Neupane, Madhab: AC+MI-FrM-5, **212**; AS-TuA-3, 78
Newman, Danny: TF-WeM-8, 114
Ngo, Thong: 2D+EM+MI+QS-WeM-13, **94**
Nguyen, Chi Thang: TF-ThP-15, **202**
Nguyen, Phong: PS1-TuM-8, 63; PS-ThP-10, **189**
Nguyen, Son: AP+EM+PS+TF-MoM-7, **4**
Nguyen, Van Long: TF-WeM-8, **114**
Nguyen-Phan, Thuy-Duong: SS+CA+LS-TuM-3, 66
Ni, Guangxin: QS1+EM+MN+PS-MoA-5, **36**
Nichols, Mark: AS-WeA-10, 121
Niedbalka, David: AS-WeM-14, 102
Niemiec, Martin: BI2-MoM-13, **7**
Nikolla, Eranda: AMS2-WeA-12, 118
Nino, Edgar: TF1-TuM-4, 68
Nishizuka, Tetsuya: PS-WeM-1, 107
Niu, Yuchen: SS+AMS-MoA-14, **43**
Niu, Yuran: SS+2D+AMS-WeA-11, 130
Niverty, Sridhar: AS-WeM-8, 102
Noesges, Brenton: EM+2D+AP+QS+TF-ThM-5, 145
Nolde, Jill: EL2-ThA-9, 160
Nolmans, Philip: MS-FrM-4, 218
Nonclercq, Antoine: PS+TF-FrM-7, 221
Novák, Josef: TF-ThP-10, 202; TF-ThP-5, **201**
Novak, Travis: TF-ThP-3, 201
Novotny, Zbynek: SS-ThP-22, 198; SS-ThP-24, 198
Nunney, Tim: AS-ThM-1, 139; AS-ThM-2, 140; AS-WeM-13, 102; EW-TuL-3, **72**
Nuwal, Nakul: PS-WeM-2, 107
Nuwayhid, Ramsay: TF2-TuA-10, **91**; TF-ThP-3, **201**
Nuys, Maurice: TF1-MoM-5, 24
Nygård, Jesper: EM+2D+BI+QS+TF-TuA-3, 80
Nylander, Andreas: QS-TuM-16, 65
Nyssen, Linus: PS2-MoA-16, **35**; PS-TuA-10, 85; PS-TuA-4, 84

— O —
O'Connor, Christopher: SS+AMS-MoA-8, 42; SS-ThM-13, 149
Oehrlein, Gottlieb: PS-TuA-11, 85
Oehrlein, Gottlieb S.: PS1-MoA-9, 34
Ogaki, Takeshi: SS+2D+AMS-WeA-2, 129
Ogunbiyi, Olugbenga: 2D+EM+QS-ThA-5, 154
Ogura, Shohei: SS+AMS-MoM-4, 22
Oh, Hwan: AP1+EM+PS+TF-MoA-9, 26
Oh, Jinsu: AQS-SuA-10, 1
Oh, Youn-Jin: PS1-TuM-3, **62**
Ohta, Taisuke: 2D+LS+NS+SS-TuA-11, **75**; 2D-ThM-6, 136

Author Index

Poplawsky, Jonathan: CA-FrM-6, 214; CA-ThP-2, 177
Popov, Georgi: TF+AP-MoA-5, 44
Poudel, Narayan: AC+MI-FrM-12, 213
Powell, Michael: QS2+PS-MoA-11, 37
Powell, Tim: BI1-TuM-2, 54
Powis, Andrew: PS-WeM-7, 108
Powis, Andrew Tasman: PS-WeM-14, 109
Poynton, O.: VT4-TuM-16, 71
Prabhakaran, Venkateshkumar: AS-ThP-16, 172
Prabhu, Mahesh: SS-ThP-10, 196
Pradhan, Dhiren: EM+AIML+AP+QS+TF-WeM-1, **103**
Prager, James: PS-ThM-7, 147; PS-ThP-6, **189**; PS-ThP-7, 189
Prakash, Jai: TF2-TuA-11, **91**
Prato, Mirko: TF-ThP-25, **204**
Prchal, Jiri: AC+MI-FrM-8, 212
Prem, Priscilla: 2D-WeA-1, 116
Price, Kent: AS-ThA-8, 157; EM-ThP-6, 182
Price, Nate: QS-TuM-2, 64
Price, Patrick: CA-ThA-5, 158
Primetzhofer, Daniel: SE-MoA-3, 38
Prochazka, Pavel: SS+2D+AMS-WeM-4, 111
Provines, J.: SE-MoA-15, 41
Prozorov, Tanya: AMS2-WeA-9, **118**
Prumbs, Julia: LS-MoM-1, 10
Pruneri, Valerio: SE-MoA-12, 40
Prusa, Stanislav: CA-FrM-3, 214
Pszczulkoski, Aiden: BI-ThP-13, 176
Puggioni, Danilo: MI+2D+AC+TF-WeM-14, 107
Puig, Rafael: MN1-TuM-6, **56**
Puli, Venkata: EM+AIML+AP+QS+TF-WeM-1, 103
Pulugurtha, Markondeyaraj: SE-MoM-13, 21
Puntscher, Lena: SS+AMS-MoA-1, 41
Puretzky, Alexander: 2D+AP+EM+QS+SS+TF-TuM-4, 49; 2D+AP+EM+QS+SS+TF-TuM-8, 50; AIML-WeM-16, 97
Puydinger, Marcos: NS1-TuM-5, **59**
Pyles, Cynthia: BI1-MoM-4, 6
Pylypenko, Svitlana: AS-WeA-3, 119; AS-WeA-4, 119

— Q —

Qerimi, Dren: PS+TF-FrM-3, 220; PS-ThA-6, 162; PS-ThM-15, 148; PS-ThM-5, 146; PS-ThM-8, **147**; SS+AMS+AS+CA+LS-FrM-11, 223
Qi, Jiayuwen: AMS1-WeA-3, 118
Qiao, Mengxiong: SS-ThP-21, **198**
Qin, Fan: PS1-TuM-8, 63
Qiu, Andrew: NS-ThP-15, **187**
Qu, Chenhui: PS-WeM-5, 108
Quevedo-Lopez, Manuel A.: TF1-MoM-3, 24
Quijada, Manuel: AP1+EM+PS+TF-WeM-5, 98; AP2+EM+PS+TF-WeM-17, 100; PS+TF-FrM-5, 220
Quinlan, Brendan: VT2-MoA-5, **45**; VT2-TuA-12, 93; VT-ThP-6, **210**
Quinn, Edwin: 2D-WeA-5, 116
Quintero-Borbon, Fernando: TF1-MoM-3, 24
Quintero-Torres, Rafael: EM+2D+BI+QS+TF-TuA-5, 81

— R —

R. Love, Jaden: EM-ThP-16, 182
Rabea, Moe: MS-FrM-10, 219
Rabine, Zachary: BI-MoA-1, 28
Raboño Borbolla, Joaquin: AS-ThP-3, 170; AS-WeM-16, 103
Rack, Philip: TF2-MoM-10, **25**
Rafati, Ali: AS-ThA-5, 157
Rafique, Muhammad Shahbaz: 2D-ThM-8, 136

Ragogna, Paul: TF-WeM-13, **114**
Rahaman, Mohammad Mahafuzur: EM+AIML+AP+QS+TF-WeM-8, **104**
Rahimi, Ehsam: SE-MoM-14, 21
Rahman, Talat: AIML-WeM-14, 97; SS+AMS-MoA-2, 41; SS+AMS-MoM-14, 23; SS+CA+LS-TuM-4, 66; SS+CA+LS-TuM-5, 66; SS-ThP-25, 198
Rahman, Talat Shahnaz: SS+AMS-MoM-10, **22**
Rai, Binod K.: AC+MI-FrM-13, 213
Rai, Rajendra: NS-ThP-9, **186**
Raitses, Yevgeny: PS+TF-FrM-4, **220**; PS-ThP-9, **189**
Rajagopal, Joshya: QS1+EM+MN+PS-MoA-7, 36
Rajak, Soumyajit: SS-ThP-6, **195**
Rajapakse, Nirosha: 2D-ThP-2, **165**
Rajaraman, Swaminathan: MN1-TuA-3, 82
Rajasabai, Senthur Pandi: MI-ThP-1, 183
Ramanath, Ganpati: TF-WeM-16, 115
Ramanujam, Balaji: EL-ThP-1, 179
Ramasamy, Karthikeyan: CA-ThM-4, 142
Ramasubramanian, Suriya: SS+AMS-MoA-3, 41
Ramasubramanian, Suriya Narayanan: SS+AMS-MoA-6, **42**
Ramesh, Prashant: QS1+EM+MN+PS-MoA-7, 36
Ramis, Martí: EM+2D+AP+QS+TF-ThM-6, 145
Randall, John: MS-FrM-2, 218
Ranjan, Ravi: SS-ThP-13, **196**
Rao, Ankit: TF+EM-ThA-4, 163
Rao, Ashutosh S: NS2-MoA-15, 31
Rasel, Md Abu Jafar: EM+AP+TF-WeA-9, 123
Rashmi, Rashmi: AP+EM+PS+TF-MoM-5, 3
Rasoanarivo, Tojo: AP1+EM+PS+TF-WeM-6, **99**
Rath, David: SS+AMS-MoM-12, 23
Rau, Samantha: SS-ThP-32, **199**
Rau, Uwe: TF1-MoM-5, 24
Rauf, Shahid: PS-ThM-1, 146; PS-WeM-15, 109; PS-WeM-2, **107**; PS-WeM-7, 108
Ravichandran, Jayakanth: TF2+EM-ThM-16, 152
Ravula, Sudhir: SS+2D+AMS-WeM-17, 112
Rebar, Drew: QS-ThP-1, **191**
Rebarz, Mateusz: EL-FrM-15, 217
Rebollar, Jazline: PS-TuA-9, 85
Reddy, Kasala Prabhakar: SS+AMS-MoA-5, 42
Reddy, Rishikishore: SS+AMS-MoA-12, 43
Reece, Christian: SS-ThM-13, **149**
Reece, Duncan: TF-WeM-7, **114**
Reed, Benjamen: AS-ThP-26, 174; AS-ThP-4, **170**; AS-WeM-6, **102**
Regmi, Paras: MI+2D+AC+TF-WeM-3, 106
Regmi, Sabin: AC+MI-FrM-13, **213**; AC+MI-FrM-15, 213
Regoutz, Anna: LS-MoM-4, **10**
Reichstein, Wiebke: BI-ThP-10, 176; TF-WeA-5, 132
Reid, Brandon: QS2+PS-MoA-15, 38
Reigota Cesar, Rodrigo: NS-ThP-1, 185; TF1+EM-FrM-4, 224
Reimann, Timmy: MI+2D+AC+TF-WeA-3, 125
Reinert, Friedrich: MI+2D+AC+TF-WeM-1, 105; MI-ThP-4, 183
Reinke, Petra: 2D-ThM-5, **135**; SS+2D+AMS-WeA-11, 130
Remy, Antoine: PS+TF-FrM-12, **222**; PS+TF-FrM-7, 221
Ren, Fan: AS-ThP-5, 171; EM+AP+TF-WeA-11, 124; EM+AP+TF-WeA-9, 123; EM-ThP-7, 182

Ren, Zhuanghe: SS+CA+LS-TuA-4, **88**; SS+CA+LS-TuM-13, 67
renaud, Vincent: QS2+PS-MoA-12, 37
Renaud, Vincent: QS2+PS-MoA-13, **37**
Reniers, Francois: TF-ThP-14, 202
Reniers, François: PS+TF-FrM-12, 222; PS+TF-FrM-6, 220; PS+TF-FrM-7, 221; PS2-MoA-16, 35; PS-TuA-10, **85**; PS-TuA-4, 84
Renzas, Russ: AP2+EM+PS+TF-TuM-16, 54
Reutt-Robey, Janice: SS+AMS-MoA-14, 43
Rhallabi, Ahmed: AP1+EM+PS+TF-WeM-6, 99; PS-WeM-13, 109
Rhee, Dongjoon: EM+AIML+AP+QS+TF-WeM-17, **105**
Richardson, Christopher: QS-TuA-3, 86
Richardson, Kathleen: EM+2D+BI+QS+TF-TuA-11, 82; EM+2D+BI+QS+TF-TuA-9, 81
Richardson, Kathleen A.: UN-ThP-2, 206
Richter, Curt: NS1+2D+QS-MoA-3, 30
Richter, Daniel: QS1+VT-MoM-2, 17
Richter, Torsten: MS-FrM-8, 219
Ricker, Jacob: VT2-MoA-4, **45**
Rieth, Loren: TF+AP-MoA-9, **45**
Rindert, Viktor: EL1-ThA-5, 160
Ritala, Mikko: TF+AP-MoA-5, 44
Ritter, Sina: LS-MoM-13, 11
Roberts, Clive: BI1-TuM-2, 54
Roberts, Samuel: NS1-TuM-3, 59
Robinson, Jeremy: 2D+LS+NS+SS-TuA-11, 75
Robinson, Jeremy T.: 2D+LS+NS+SS-TuA-3, 74
Robinson, Sarah M: NS2-MoA-15, 31
Robinson, Zachary: TF2-FrM-14, 227
Rodil Posada, Sandra Elizabeth: SE-MoM-12, 20
Rodil, Sandra Elizabeth: SE-MoM-8, **20**
Rodin, Gregory: AS-ThM-8, 141
Rodriguez Bonet, Sergio: SS+AMS-MoM-6, 22
Rodriguez de Marcos, Luis: AP1+EM+PS+TF-WeM-5, 98; AP2+EM+PS+TF-WeM-17, 100; PS+TF-FrM-5, 220
Rodriguez, Alejandro: SS-ThP-19, 197
Rodriguez, Jose: SS+AMS-MoA-13, 43; SS-ThP-9, 195
Rodriguez, José A.: SS+AMS-MoA-5, 42
Rodriguez, Mark: PS-ThA-7, 162
Roe, Abigail: 2D-ThM-16, 137
Rogge, Paul: MI+2D+AC+TF-WeM-14, 107
Rohkamm, Erik: PS-ThP-17, 190
Rohnke, Marcus: AS-WeA-11, **121**
Rojas, Geoffrey: TF+EM-ThA-4, 163
Roldan Cuenya, Beatriz: SS+CA+LS-TuM-1, **65**
Rolison, Debra: TF-ThP-3, 201
Romadanov, Ivan: PS-ThP-9, 189
Romanenko, Alex: QS-TuM-7, 65
Romanenko, Alexander: QS-TuM-15, 65
ROMERO CEDILLO, Jonathan: PS-ThP-16, 190
Rommel, Marcus: QS-TuM-16, 65
Rondinelli, James: MI+2D+AC+TF-WeM-14, 107
Ronse, Kurt: PS1-MoM-6, 15
Roorda, Tycho: SS+2D+AMS-WeA-10, 130
Roqueta, Fabrice: AP1+EM+PS+TF-WeM-6, 99
Rosa, Priscilla F. S.: AC+MI-ThM-3, 138
Rosas, Debra: AC+MI-ThA-7, 155
Rosei, Federico: NSP-SuP-1, **2**
Rosen, Johanna: SE-MoM-1, **18**
Rosenberg, Samantha: TF2-FrM-14, 227
Rosenhahn, Axel: BI1-TuM-6, **55**; BI-MoA-6, **29**; BI-ThP-3, 175; BI-ThP-4, 175; BI-ThP-9, 176
Rosillo Orozco, Luis: EL1-ThA-4, 159
Rosner, Malte: 2D+LS+NS+SS-TuA-3, 74
Rosso, Kevin: AS-TuA-1, **78**
Rost, Marcel: SS-ThP-10, 196

Author Index

Author Index

Author Index

Author Index